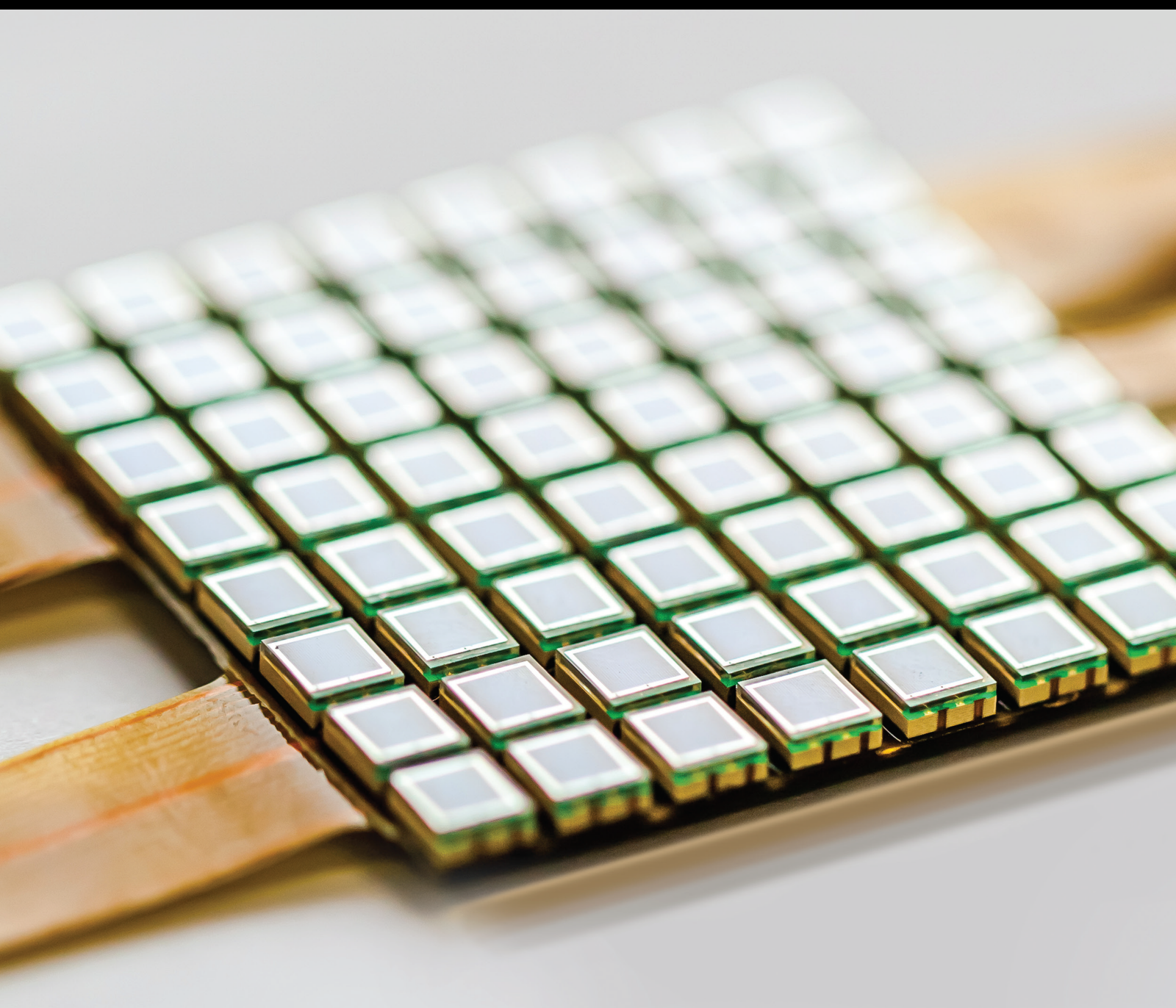


# Advanced Sensing Materials for Internet of Things Sensors

Lead Guest Editor: Wen Zeng

Guest Editors: Zhongchang Wang and Yanqiong Li





---

# **Advanced Sensing Materials for Internet of Things Sensors**

Journal of Sensors

---

**Advanced Sensing Materials for Internet  
of Things Sensors**

Lead Guest Editor: Wen Zeng

Guest Editors: Zhongchang Wang and Yanqiong Li



---




Copyright © 2023 Hindawi Limited. All rights reserved.

This is a special issue published in "Journal of Sensors." All articles are open access articles distributed under the Creative Commons Attribution License, which permits unrestricted use, distribution, and reproduction in any medium, provided the original work is properly cited.

# Chief Editor

Harith Ahmad , Malaysia

## Associate Editors

Duo Lin , China  
Fanli Meng , China  
Pietro Siciliano , Italy  
Guiyun Tian, United Kingdom

## Academic Editors

Ghufran Ahmed , Pakistan  
Constantin Apetrei, Romania  
Shonak Bansal , India  
Fernando Benito-Lopez , Spain  
Romeo Bernini , Italy  
Shekhar Bhansali, USA  
Matthew Brodie, Australia  
Ravikumar CV, India  
Belén Calvo, Spain  
Stefania Campopiano , Italy  
Binghua Cao , China  
Domenico Caputo, Italy  
Sara Casciati, Italy  
Gabriele Cazzulani , Italy  
Chi Chiu Chan, Singapore  
Sushank Chaudhary , Thailand  
Edmon Chehura , United Kingdom  
Marvin H Cheng , USA  
Lei Chu , USA  
Mario Collotta , Italy  
Marco Consales , Italy  
Jesus Corres , Spain  
Andrea Cusano, Italy  
Egidio De Benedetto , Italy  
Luca De Stefano , Italy  
Manel Del Valle , Spain  
Franz L. Dickert, Austria  
Giovanni Diraco, Italy  
Maria de Fátima Domingues , Portugal  
Nicola Donato , Italy  
Sheng Du , China  
Amir Elzwawy, Egypt  
Mauro Epifani , Italy  
Congbin Fan , China  
Lihang Feng, China  
Vittorio Ferrari , Italy  
Luca Francioso, Italy

Libo Gao , China  
Carmine Granata , Italy  
Pramod Kumar Gupta , USA  
Mohammad Haider , USA  
Agustin Herrera-May , Mexico  
María del Carmen Horrillo, Spain  
Evangelos Hristoforou , Greece  
Grazia Iadarola , Italy  
Syed K. Islam , USA  
Stephen James , United Kingdom  
Sana Ullah Jan, United Kingdom  
Bruno C. Janegitz , Brazil  
Hai-Feng Ji , USA  
Shouyong Jiang, United Kingdom  
Roshan Prakash Joseph, USA  
Niravkumar Joshi, USA  
Rajesh Kaluri , India  
Sang Sub Kim , Republic of Korea  
Dr. Rajkishor Kumar, India  
Rahul Kumar , India  
Nageswara Lalam , USA  
Antonio Lazaro , Spain  
Chengkuo Lee , Singapore  
Chenzong Li , USA  
Zhi Lian , Australia  
Rosalba Liguori , Italy  
Sangsoon Lim , Republic of Korea  
Huan Liu , China  
Jin Liu , China  
Eduard Llobet , Spain  
Jaime Lloret , Spain  
Mohamed Louzazni, Morocco  
Jesús Lozano , Spain  
Oleg Lupan , Moldova  
Leandro Maio , Italy  
Pawel Malinowski , Poland  
Carlos Marques , Portugal  
Eugenio Martinelli , Italy  
Antonio Martinez-Olmos , Spain  
Giuseppe Maruccio , Italy  
Yasuko Y. Maruo, Japan  
Zahid Mehmood , Pakistan  
Carlos Michel , Mexico  
Stephen. J. Mihailov , Canada  
Bikash Nakarmi, China

Ehsan Namaziandost , Iran  
Heinz C. Neitzert , Italy  
Sing Kiong Nguang , New Zealand  
Calogero M. Oddo , Italy  
Tinghui Ouyang, Japan  
SANDEEP KUMAR PALANISWAMY ,  
India  
Alberto J. Palma , Spain  
Davide Palumbo , Italy  
Abinash Panda , India  
Roberto Paolesse , Italy  
Akhilesh Pathak , Thailand  
Giovanni Pau , Italy  
Giorgio Pennazza , Italy  
Michele Penza , Italy  
Sivakumar Poruran, India  
Stelios Potirakis , Greece  
Biswajeet Pradhan , Malaysia  
Giuseppe Quero , Italy  
Linesh Raja , India  
Maheswar Rajagopal , India  
Valerie Renaudin , France  
Armando Ricciardi , Italy  
Christos Riziotis , Greece  
Ruthber Rodriguez Serrezuela , Colombia  
Maria Luz Rodriguez-Mendez , Spain  
Jerome Rossignol , France  
Maheswaran S, India  
Ylias Sabri , Australia  
Sourabh Sahu , India  
José P. Santos , Spain  
Sina Sareh, United Kingdom  
Isabel Sayago , Spain  
Andreas Schütze , Germany  
Praveen K. Sekhar , USA  
Sandra Sendra, Spain  
Sandeep Sharma, India  
Sunil Kumar Singh Singh , India  
Yadvendra Singh , USA  
Afaque Manzoor Soomro , Pakistan  
Vincenzo Spagnolo, Italy  
Kathiravan Srinivasan , India  
Sachin K. Srivastava , India  
Stefano Stassi , Italy

Danfeng Sun, China  
Ashok Sundramoorthy, India  
Salvatore Surdo , Italy  
Roshan Thotagamuge , Sri Lanka  
Guiyun Tian , United Kingdom  
Sri Ramulu Torati , USA  
Abdellah Touhafi , Belgium  
Hoang Vinh Tran , Vietnam  
Aitor Urrutia , Spain  
Hana Vaisocherova - Lislalova , Czech  
Republic  
Everardo Vargas-Rodriguez , Mexico  
Xavier Vilanova , Spain  
Stanislav Vitek , Czech Republic  
Luca Vollero , Italy  
Tomasz Wandowski , Poland  
Bohui Wang, China  
Qihao Weng, USA  
Penghai Wu , China  
Qiang Wu, United Kingdom  
Yuedong Xie , China  
Chen Yang , China  
Jiachen Yang , China  
Nitesh Yelve , India  
Aijun Yin, China  
Chouki Zerrouki , France

# Contents

---

**Retracted: Green Building Design Based on 5G Network and Internet of Things System**

Journal of Sensors

Retraction (1 page), Article ID 9794705, Volume 2023 (2023)

**Retracted: An Innovation and Entrepreneurship Management System for Universities Based on Cluster Analysis Theory**

Journal of Sensors

Retraction (1 page), Article ID 9873702, Volume 2023 (2023)

**Retracted: Analysis of Learning Ability of Ideological and Political Course Based on BP Neural Network and Improved  $k$ -Means Cluster Algorithm**

Journal of Sensors

Retraction (1 page), Article ID 9837089, Volume 2023 (2023)

**Retracted: Teacher Education and Management: Innovative Application of Ecological Management System of Big Data Management System**

Journal of Sensors


Retraction (1 page), Article ID 9835307, Volume 2023 (2023)

**Retracted: Construction and Effect Analysis of College Students' Physical Education Teaching Mode Based on Data Mining Algorithm**

Journal of Sensors

Retraction (1 page), Article ID 9791508, Volume 2023 (2023)

**[Retracted] Teacher Education and Management: Innovative Application of Ecological Management System of Big Data Management System**

Xiaoying Li 


Research Article (15 pages), Article ID 6048083, Volume 2022 (2022)

**Research on the Application of Hybrid Density Network Combined with Gaussian Model in Computer Music Choreography**

Li-Juan Wang 




Research Article (11 pages), Article ID 3385134, Volume 2022 (2022)

**A Forward-Looking Study on the In-Depth Development Planning of Information Technology into Teacher Education**

Chunlan Zhang 


Research Article (11 pages), Article ID 4885771, Volume 2022 (2022)

**NiO-Based Gas Sensors for Ethanol Detection: Recent Progress**

Qingting Li , Wen Zeng , and Yanqiong Li 


Review Article (19 pages), Article ID 1855493, Volume 2022 (2022)

**[Retracted] Construction and Effect Analysis of College Students' Physical Education Teaching Mode Based on Data Mining Algorithm**

Peipei Wang 

Research Article (10 pages), Article ID 1028962, Volume 2022 (2022)

**Construction and Evaluation of College Students' Psychological Quality Evaluation Model Based on Analytic Hierarchy Process**

Wei Shi 

Research Article (11 pages), Article ID 3896304, Volume 2022 (2022)

**Rural Tourism Resource Research Based on Multisensor and Geographic Information Big Data**

Lixia Wang 






Research Article (8 pages), Article ID 1670571, Volume 2022 (2022)

**Modern Clothing Design Based on Human 3D Somatosensory Technology**

Zhe Liu  and Min Luo


Research Article (11 pages), Article ID 2455103, Volume 2022 (2022)

**Stochastic Evolutionary Game Analysis on the Strategy Selection of Green Building Stakeholders from the Perspective of Supply-Demand Subject Populations**

Yaohong Yang , Jing Dai , Zhiyong Li , Ying Liu , and Yi Zeng 

Research Article (22 pages), Article ID 5354706, Volume 2022 (2022)

**Structural Assembly Analysis of Concrete Buildings with Intelligent Finite Element Analysis**

Kun Zhu , Yan Zhang, Xianyue Meng, and Zaiyong Ma

Research Article (9 pages), Article ID 6701021, Volume 2022 (2022)

**Construction of Educational Resource Metadata Management Platform Based on Service-Oriented Architecture**

Jingbin Zhang  and Tianxiang Qi 

Research Article (10 pages), Article ID 2172817, Volume 2022 (2022)

**Design of Remote Real-Time Monitoring and Control Management System for Smart Home Equipment Based on Wireless Multihop Sensor Network**

Chen Su and Wenting Chen 

Research Article (10 pages), Article ID 6228440, Volume 2022 (2022)

**Application of Temperature Compensation Combined with Neural Network in Infrared Gas Sensor**

Kangning Dong  and Jinfang Yang

Research Article (9 pages), Article ID 5063472, Volume 2022 (2022)

**Ceramic Shape Design Based on Intelligent Space Simulation Technology**


Lijian Zhang  and Guangfu Liu

Research Article (9 pages), Article ID 5251436, Volume 2022 (2022)



# Contents

## **Design of an Intelligent Sensor Teaching Experiment System and Measurement of Student Innovation Literacy**

Xiaorong Li and Qianli Xing 


Research Article (13 pages), Article ID 6128884, Volume 2022 (2022)

## **Robust Refinement of Built-in Network Information System Based on Nonparametric Density Estimation**

Qiongzhen Mei  and Fei Wang

Research Article (10 pages), Article ID 4220001, Volume 2022 (2022)

## **An Empirical Study on the Relationship between Economy and Finance in Underdeveloped Areas Based on the VAR Model**

Han Zhang  and Wenbing Jiang


Research Article (11 pages), Article ID 2224239, Volume 2022 (2022)

## **Research Progress on Humidity-Sensing Properties of Cu-Based Humidity Sensors: A Review**

Jingyu Wang  and Wen Zeng 

Review Article (29 pages), Article ID 7749890, Volume 2022 (2022)

## **A Collaborative Filtering Method for Operation Maintenance Behavior in Power Monitoring Systems**

Jinyu Wu , Wenwei Tao, Wenzhe Zhang, Zeming Jiang, and Gang Chen


Research Article (10 pages), Article ID 8277831, Volume 2022 (2022)

## **Research and Implementation of Sports Entity Simulation Based on Heterogeneous Binocular Vision**

Liang Tan  and He Gao


Research Article (12 pages), Article ID 6439660, Volume 2022 (2022)

## **Efficiency Analysis of Sports Equipment Batch Management Based on Antimetal RFID Tag**

Zhongwei Huang and Xuebin Sun 


Research Article (9 pages), Article ID 2989375, Volume 2022 (2022)

## **Application of Fine Motion Capture Method for Tai Chi Chuan Assistant Training**

Wenbo Li 


Research Article (11 pages), Article ID 1269042, Volume 2022 (2022)

## **Research on Interface Slip of Composite Reinforced Steel Truss-Concrete Test Beam and Its Calculation and Analysis Method**

Zhixiang Zhou , Xingqi Zeng, Yang Zou, Chengjun Li, Guojun Den, Liwen Zhang, and Rui Wang


Research Article (12 pages), Article ID 1987288, Volume 2022 (2022)

## **Multispectral Remote Sensing Data Analysis Based on KNNLC Algorithm and Multimedia Image**

Yingxin Sun 


Research Article (8 pages), Article ID 8692080, Volume 2022 (2022)

**Intelligent Management of Land Resources Based on Internet of Things and GIS Technology**

Hao Gong and Chen He 



Research Article (13 pages), Article ID 2216581, Volume 2022 (2022)

**The Inheritance and Future Development Direction Prediction of Opera Culture Based on Cloud Communication under the Background of Big Data**

Yufeng Yang and Ting Lei 

Research Article (9 pages), Article ID 1910766, Volume 2022 (2022)

**Sports Action Recognition and Analysis Relying on Inertial Sensors**

Yutong Liu, Zunliang Zhou, Xiaolong Qian , and Jiaming Chen 

Research Article (11 pages), Article ID 7039019, Volume 2022 (2022)

**Optimization and Application of Image Defogging Algorithm Based on Deep Learning Network**

Jianfeng Liao 


Research Article (11 pages), Article ID 7030735, Volume 2022 (2022)

**[Retracted] An Innovation and Entrepreneurship Management System for Universities Based on Cluster Analysis Theory**

Weijie Zhao  and Liang Fang

Research Article (10 pages), Article ID 4865716, Volume 2022 (2022)

**Evaluation of Sustainable Development of an Agricultural Economy Based on the DPSIR Model**

Yanan Zhang, Ying Wang, and Jinghong Wei 


Research Article (14 pages), Article ID 2591275, Volume 2022 (2022)

**Investment Strategy of Reactive Power Compensation Scheme in Wind Turbine Distribution Network Based on Optimal Allocation**

Yibing Xie  and Yang Wu


Research Article (8 pages), Article ID 7037451, Volume 2022 (2022)

**[Retracted] Green Building Design Based on 5G Network and Internet of Things System**

Meida Wang and Qingfeng Yang 

Research Article (14 pages), Article ID 7099322, Volume 2022 (2022)

**GIS-Based Urban Agglomeration Landscape Dynamic Observation and Simulation Prediction Algorithm**

Meng Liu 

Research Article (9 pages), Article ID 8117539, Volume 2022 (2022)

**Research on Garden Ecosystem Based on Monitoring Sensing Technology**

Lixia Qiang  and Jie Wang

Research Article (10 pages), Article ID 8294416, Volume 2022 (2022)

# Contents

## **Exploration on Elderly Accessible Information Interaction Design Using Fuzzy Control**

Hui Peng 








Research Article (11 pages), Article ID 5975412, Volume 2022 (2022)

## **Scenario Analysis of Water-Saving Potential in Yeast Manufacturing Industry under the Guidance of Water Intake Quota**

Yubo Zhang  and Xue Bai 


Research Article (9 pages), Article ID 8775071, Volume 2022 (2022)

## **Analysis of Water Supply-Demand Based on Socioeconomic Efficiency**

Wenyong Ren , Xue Bai , Yuetian Wang , Chaoming Liang , Siyan Huang , Zhiying Wang , and Liu Yang 

Research Article (16 pages), Article ID 3438943, Volume 2022 (2022)

## **Application Research of Deep Learning Technology in Natural Landscape Animation Design**

Lili Xu  and Lilei Wen


Research Article (10 pages), Article ID 8240900, Volume 2022 (2022)

## **Construction of Evaluation Model of Tennis Skills and Tactic Level and Application of Grey Relational Algorithm**

Ling Wang 

Research Article (11 pages), Article ID 9446175, Volume 2022 (2022)

## **Clothing Modular Design Based on Virtual 3D Technology**

Jiao Wang and Yijun Zhong 


Research Article (9 pages), Article ID 5123530, Volume 2022 (2022)

## **Big Data Analysis of Water Saving Standard Based on Bibliometrics**

Xue Bai , Meng Hao , Mengting Hu , and Liu Yang 

Research Article (9 pages), Article ID 5851114, Volume 2022 (2022)

## **Indoor Smart Design Algorithm Based on Smart Home Sensor**

Ruili Zheng 


Research Article (10 pages), Article ID 2251046, Volume 2022 (2022)

## **Application of Adaptive PID Temperature Control Algorithm under Spatial Thermal Model of ALD Reaction Chamber**

Zhenqiang Liu, Jinhui Lei , Yan Chen, Yang Xia, Jiaheng Feng, Shuaiqiang Ming, and Wa Mao


Research Article (11 pages), Article ID 1713039, Volume 2022 (2022)

## **Analysis of an Enterprise Human Resource Management Performance Evaluation Model Based on the DEA Method**

Bing Gao  and XiMeng Zhang


Research Article (11 pages), Article ID 4203768, Volume 2022 (2022)

**Research on Furniture Design Integrating Ming-Style Furniture Modeling Elements and Image Sensor Data: Taking Suitable Old Furniture as an Example**

Wei Chen 


Research Article (10 pages), Article ID 5306491, Volume 2022 (2022)

**English Pronunciation Calibration Model Based on Multimodal Acoustic Sensor**

Yurui Zhou and Guolong Zhao 

Research Article (10 pages), Article ID 2208653, Volume 2022 (2022)

**Streaming Media Music Classroom Teaching Mode and Effect Analysis Based on Audio Band Analysis Technology**

Huizhong Wang 

Research Article (15 pages), Article ID 9370782, Volume 2022 (2022)

**Athletes' State Monitoring under Data Mining and Random Forest**

Xiaolei Li 

Research Article (11 pages), Article ID 1966786, Volume 2022 (2022)

**Intelligent Design Model of Urban Landscape Space Based on Optimized BP Neural Network**

Guoping Wu, Yihua Miao, and Fang Wang 


Research Article (10 pages), Article ID 9704287, Volume 2022 (2022)

**Analysis of Ecological Environment Evaluation and Coupled and Coordinated Development of Smart Cities Based on Multisource Data**

Qianwei Ma  and Yanxia Yang


Research Article (9 pages), Article ID 5959495, Volume 2022 (2022)

**Research on the Current Situation and Countermeasures of English Listening Teaching Based on Multimedia Intelligent-Embedded Processor**

Huanping Guo 


Research Article (11 pages), Article ID 9722209, Volume 2022 (2022)

**Music Trend Prediction Based on Improved LSTM and Random Forest Algorithm**

Xiangli Liu 

Research Article (10 pages), Article ID 6450469, Volume 2022 (2022)

**[Retracted] Analysis of Learning Ability of Ideological and Political Course Based on BP Neural Network and Improved  $k$ -Means Cluster Algorithm**

Guidong Zeng 

Research Article (11 pages), Article ID 4397555, Volume 2022 (2022)

**Building a Performance Management System for Hospitals Based on Diagnosis-Related Group (DRG) Payment**

Shaolin Zhao, Yingying Gu, and Zhenju Huang 

Research Article (10 pages), Article ID 7001423, Volume 2022 (2022)

# Contents


---

## **Sports Training Intensity Information Fusion Method Based on Kinect Sensor**

Yan Huo 


Research Article (10 pages), Article ID 2095514, Volume 2022 (2022)

## **Predictive Analysis and Simulation of College Sports Performance Fused with Adaptive Federated Deep Learning Algorithm**

Wei Sun 


Research Article (11 pages), Article ID 1205622, Volume 2022 (2022)

## **Inverter Design and Droop Parallel Control Strategy Based on Virtual Impedance**

Lu Wang 

Research Article (14 pages), Article ID 9395396, Volume 2022 (2022)

## **Design of Distributed Human Resource Management System of Spark Framework Based on Fuzzy Clustering**

Qing Sun , Tao Wu, and Jia Hua


Research Article (9 pages), Article ID 4827021, Volume 2022 (2022)

## **Evaluation and Promotion of a Multidimensional Information Intelligent Speech System in Dialect Teaching**

Ya Pang 


Research Article (10 pages), Article ID 1692080, Volume 2022 (2022)

## **Analysis of the Application of Virtual Reality Technology in Football Training**

Kun Zhao and Xueying Guo 

Research Article (8 pages), Article ID 1339434, Volume 2022 (2022)

## **Design of Knitted Garment Design Model Based on Mathematical Image Theory**

Bojia Lu 



Research Article (13 pages), Article ID 3864256, Volume 2022 (2022)

## **A Real-Time Biometric Encryption Scheme Based on Fuzzy Logic for IoT**

Masoud Moradi, Masoud Moradkhani , and Mohammad Bagher Tavakoli


Research Article (15 pages), Article ID 4336822, Volume 2022 (2022)

## **Application of Cellular Automata with Improved Dynamic Analysis in Evacuation Management of Sports Events**


Jingyi Xie  and Li Zhang 

Research Article (11 pages), Article ID 8782865, Volume 2022 (2022)

## **Emotional Calculation Method of Rural Tourist Based on Improved SPCA-LSTM Algorithm**

Xi Chen 

Research Article (9 pages), Article ID 3365498, Volume 2022 (2022)



---

**A Machine-Assisted Gaze Analysis Method for Students' Psychological Evaluation**

Huiling Wang  and Yafei Shan 

Research Article (12 pages), Article ID 3206444, Volume 2022 (2022)

## *Retraction*

# **Retracted: Green Building Design Based on 5G Network and Internet of Things System**

### **Journal of Sensors**

Received 17 October 2023; Accepted 17 October 2023; Published 18 October 2023

Copyright © 2023 Journal of Sensors. This is an open access article distributed under the Creative Commons Attribution License, which permits unrestricted use, distribution, and reproduction in any medium, provided the original work is properly cited.

This article has been retracted by Hindawi following an investigation undertaken by the publisher [1]. This investigation has uncovered evidence of one or more of the following indicators of systematic manipulation of the publication process:

- (1) Discrepancies in scope
- (2) Discrepancies in the description of the research reported
- (3) Discrepancies between the availability of data and the research described
- (4) Inappropriate citations
- (5) Incoherent, meaningless and/or irrelevant content included in the article
- (6) Peer-review manipulation

The presence of these indicators undermines our confidence in the integrity of the article's content and we cannot, therefore, vouch for its reliability. Please note that this notice is intended solely to alert readers that the content of this article is unreliable. We have not investigated whether authors were aware of or involved in the systematic manipulation of the publication process.

Wiley and Hindawi regrets that the usual quality checks did not identify these issues before publication and have since put additional measures in place to safeguard research integrity.

We wish to credit our own Research Integrity and Research Publishing teams and anonymous and named external researchers and research integrity experts for contributing to this investigation.

The corresponding author, as the representative of all authors, has been given the opportunity to register their agreement or disagreement to this retraction. We have kept a record of any response received.

### **References**

- [1] M. Wang and Q. Yang, "Green Building Design Based on 5G Network and Internet of Things System," *Journal of Sensors*, vol. 2022, Article ID 7099322, 14 pages, 2022.

## *Retraction*

# **Retracted: An Innovation and Entrepreneurship Management System for Universities Based on Cluster Analysis Theory**

### **Journal of Sensors**

Received 8 August 2023; Accepted 8 August 2023; Published 9 August 2023

Copyright © 2023 Journal of Sensors. This is an open access article distributed under the Creative Commons Attribution License, which permits unrestricted use, distribution, and reproduction in any medium, provided the original work is properly cited.

This article has been retracted by Hindawi following an investigation undertaken by the publisher [1]. This investigation has uncovered evidence of one or more of the following indicators of systematic manipulation of the publication process:

- (1) Discrepancies in scope
- (2) Discrepancies in the description of the research reported
- (3) Discrepancies between the availability of data and the research described
- (4) Inappropriate citations
- (5) Incoherent, meaningless and/or irrelevant content included in the article
- (6) Peer-review manipulation

The presence of these indicators undermines our confidence in the integrity of the article's content and we cannot, therefore, vouch for its reliability. Please note that this notice is intended solely to alert readers that the content of this article is unreliable. We have not investigated whether authors were aware of or involved in the systematic manipulation of the publication process.

Wiley and Hindawi regrets that the usual quality checks did not identify these issues before publication and have since put additional measures in place to safeguard research integrity.

We wish to credit our own Research Integrity and Research Publishing teams and anonymous and named external researchers and research integrity experts for contributing to this investigation.

The corresponding author, as the representative of all authors, has been given the opportunity to register their agreement or disagreement to this retraction. We have kept a record of any response received.

### **References**

- [1] W. Zhao and L. Fang, "An Innovation and Entrepreneurship Management System for Universities Based on Cluster Analysis Theory," *Journal of Sensors*, vol. 2022, Article ID 4865716, 10 pages, 2022.



## Retraction

# Retracted: Analysis of Learning Ability of Ideological and Political Course Based on BP Neural Network and Improved $k$ -Means Cluster Algorithm

### Journal of Sensors

Received 8 August 2023; Accepted 8 August 2023; Published 9 August 2023

Copyright © 2023 Journal of Sensors. This is an open access article distributed under the Creative Commons Attribution License, which permits unrestricted use, distribution, and reproduction in any medium, provided the original work is properly cited.

This article has been retracted by Hindawi following an investigation undertaken by the publisher [1]. This investigation has uncovered evidence of one or more of the following indicators of systematic manipulation of the publication process:

- (1) Discrepancies in scope
- (2) Discrepancies in the description of the research reported
- (3) Discrepancies between the availability of data and the research described
- (4) Inappropriate citations
- (5) Incoherent, meaningless and/or irrelevant content included in the article
- (6) Peer-review manipulation

The presence of these indicators undermines our confidence in the integrity of the article's content and we cannot, therefore, vouch for its reliability. Please note that this notice is intended solely to alert readers that the content of this article is unreliable. We have not investigated whether authors were aware of or involved in the systematic manipulation of the publication process.

Wiley and Hindawi regrets that the usual quality checks did not identify these issues before publication and have since put additional measures in place to safeguard research integrity.

We wish to credit our own Research Integrity and Research Publishing teams and anonymous and named external researchers and research integrity experts for contributing to this investigation.

The corresponding author, as the representative of all authors, has been given the opportunity to register their agreement or disagreement to this retraction. We have kept a record of any response received.

### References

- [1] G. Zeng, "Analysis of Learning Ability of Ideological and Political Course Based on BP Neural Network and Improved  $k$ -Means Cluster Algorithm," *Journal of Sensors*, vol. 2022, Article ID 4397555, 11 pages, 2022.

## *Retraction*

# **Retracted: Teacher Education and Management: Innovative Application of Ecological Management System of Big Data Management System**

### **Journal of Sensors**

Received 8 August 2023; Accepted 8 August 2023; Published 9 August 2023

Copyright © 2023 Journal of Sensors. This is an open access article distributed under the Creative Commons Attribution License, which permits unrestricted use, distribution, and reproduction in any medium, provided the original work is properly cited.

This article has been retracted by Hindawi following an investigation undertaken by the publisher [1]. This investigation has uncovered evidence of one or more of the following indicators of systematic manipulation of the publication process:

- (1) Discrepancies in scope
- (2) Discrepancies in the description of the research reported
- (3) Discrepancies between the availability of data and the research described
- (4) Inappropriate citations
- (5) Incoherent, meaningless and/or irrelevant content included in the article
- (6) Peer-review manipulation

The presence of these indicators undermines our confidence in the integrity of the article's content and we cannot, therefore, vouch for its reliability. Please note that this notice is intended solely to alert readers that the content of this article is unreliable. We have not investigated whether authors were aware of or involved in the systematic manipulation of the publication process.

Wiley and Hindawi regrets that the usual quality checks did not identify these issues before publication and have since put additional measures in place to safeguard research integrity.

We wish to credit our own Research Integrity and Research Publishing teams and anonymous and named external researchers and research integrity experts for contributing to this investigation.

The corresponding author, as the representative of all authors, has been given the opportunity to register their agreement or disagreement to this retraction. We have kept a record of any response received.

### **References**

- [1] X. Li, "Teacher Education and Management: Innovative Application of Ecological Management System of Big Data Management System," *Journal of Sensors*, vol. 2022, Article ID 6048083, 15 pages, 2022.

## *Retraction*

# **Retracted: Construction and Effect Analysis of College Students' Physical Education Teaching Mode Based on Data Mining Algorithm**

### **Journal of Sensors**

Received 8 August 2023; Accepted 8 August 2023; Published 9 August 2023

Copyright © 2023 Journal of Sensors. This is an open access article distributed under the Creative Commons Attribution License, which permits unrestricted use, distribution, and reproduction in any medium, provided the original work is properly cited.

This article has been retracted by Hindawi following an investigation undertaken by the publisher [1]. This investigation has uncovered evidence of one or more of the following indicators of systematic manipulation of the publication process:

- (1) Discrepancies in scope
- (2) Discrepancies in the description of the research reported
- (3) Discrepancies between the availability of data and the research described
- (4) Inappropriate citations
- (5) Incoherent, meaningless and/or irrelevant content included in the article
- (6) Peer-review manipulation

The presence of these indicators undermines our confidence in the integrity of the article's content and we cannot, therefore, vouch for its reliability. Please note that this notice is intended solely to alert readers that the content of this article is unreliable. We have not investigated whether authors were aware of or involved in the systematic manipulation of the publication process.

In addition, our investigation has also shown that one or more of the following human-subject reporting requirements has not been met in this article: ethical approval by an Institutional Review Board (IRB) committee or equivalent, patient/participant consent to participate, and/or agreement to publish patient/participant details (where relevant).

Wiley and Hindawi regrets that the usual quality checks did not identify these issues before publication and have since put additional measures in place to safeguard research integrity.

We wish to credit our own Research Integrity and Research Publishing teams and anonymous and named external

researchers and research integrity experts for contributing to this investigation.

The corresponding author, as the representative of all authors, has been given the opportunity to register their agreement or disagreement to this retraction. We have kept a record of any response received.

### **References**

- [1] P. Wang, "Construction and Effect Analysis of College Students' Physical Education Teaching Mode Based on Data Mining Algorithm," *Journal of Sensors*, vol. 2022, Article ID 1028962, 10 pages, 2022.

## *Retraction*

# **Retracted: Teacher Education and Management: Innovative Application of Ecological Management System of Big Data Management System**

### **Journal of Sensors**

Received 8 August 2023; Accepted 8 August 2023; Published 9 August 2023

Copyright © 2023 Journal of Sensors. This is an open access article distributed under the Creative Commons Attribution License, which permits unrestricted use, distribution, and reproduction in any medium, provided the original work is properly cited.

This article has been retracted by Hindawi following an investigation undertaken by the publisher [1]. This investigation has uncovered evidence of one or more of the following indicators of systematic manipulation of the publication process:

- (1) Discrepancies in scope
- (2) Discrepancies in the description of the research reported
- (3) Discrepancies between the availability of data and the research described
- (4) Inappropriate citations
- (5) Incoherent, meaningless and/or irrelevant content included in the article
- (6) Peer-review manipulation

The presence of these indicators undermines our confidence in the integrity of the article's content and we cannot, therefore, vouch for its reliability. Please note that this notice is intended solely to alert readers that the content of this article is unreliable. We have not investigated whether authors were aware of or involved in the systematic manipulation of the publication process.

Wiley and Hindawi regrets that the usual quality checks did not identify these issues before publication and have since put additional measures in place to safeguard research integrity.

We wish to credit our own Research Integrity and Research Publishing teams and anonymous and named external researchers and research integrity experts for contributing to this investigation.

The corresponding author, as the representative of all authors, has been given the opportunity to register their agreement or disagreement to this retraction. We have kept a record of any response received.

### **References**

- [1] X. Li, "Teacher Education and Management: Innovative Application of Ecological Management System of Big Data Management System," *Journal of Sensors*, vol. 2022, Article ID 6048083, 15 pages, 2022.

## Research Article

# Teacher Education and Management: Innovative Application of Ecological Management System of Big Data Management System

**Xiaoying Li** 

*School of Public Policy and Management, School of Foreign Languages, Guangxi University, Nanning, Guangxi 530004, China*

Correspondence should be addressed to Xiaoying Li; [lixiaoyinggxu@163.com](mailto:lixiaoyinggxu@163.com)

Received 8 June 2022; Revised 15 July 2022; Accepted 26 July 2022; Published 13 September 2022

Academic Editor: Wen Zeng

Copyright © 2022 Xiaoying Li. This is an open access article distributed under the Creative Commons Attribution License, which permits unrestricted use, distribution, and reproduction in any medium, provided the original work is properly cited.

At present, with the rapid growth of China's comprehensive national power, China wants to accelerate the construction of world-class universities and world-class disciplines to match it. Therefore, the education and management of university teachers is crucial, and the current research results at home and abroad in this area are remarkable. In this paper, we will start from the innovative application of university teachers' management system and use the Oracle and SQL Server database processors commonly used in big data processing to process data. It is concluded that China's teaching force is gradually balanced; the comprehensive quality of the teaching force is improving; the academic atmosphere is more open; the fields and perspectives of academic research are richer; the distribution of teachers at all levels in China is more balanced; the comprehensive quality of our teachers is improving; the system of education and scientific research in China's universities is improving; and the ecological management system of universities is improving. In addition, in view of the current situation of education and management of teachers in China's colleges and universities, according to the results of big data analysis, we also propose (1) to improve the academic level and establish a strict institutional threshold for the college teaching profession; (2) to effectively implement the policy of freedom and equality in academic academia and improve the appointment and evaluation system of teachers and principals in higher education institutions; (3) to insist on implementing the principle of academic fairness and optimizing the teacher evaluation system; (4) to innovate and implement the incentive mechanism for teachers in colleges and universities according to the talent training characteristics of teachers' academic career ability; and (5) to establish the access system of college teachers' career development and promote academic career development and other suggestions of big data management for college teachers.

## 1. Introduction

World-class universities all have another very important and prominent business feature, that is, of course a relatively high-level professional technical faculty they have, but how to maintain a high-level faculty is a problem worth thinking about. In this regard, some universities in western developed countries have more mature experience in the management of university teachers, which is worth learning [1]. In China's university management, there are some deficiencies and defects among teachers' recruitment, assessment, promotion, and evaluation. Many unnecessary disputes and so on all originate from the lack of a perfect management system. College teachers are a highly specialized and academic group, and the academic activities of teachers determine

the popularity of colleges and universities. The core of university is high-quality academic activities. In China, the boundary between academic and administrative power is often unclear. Administrative power often interferes excessively with academic power, and academic power is not exercised effectively. This has seriously affected the personal academic creativity cultivation and personal academic motivation of some university teachers and researchers and has restricted the level of our universities' own research and innovation development capability and continuous healthy forward development. Higher education in the United States began in 1776, and after more than 200 years of development, it has borrowed the advanced management concepts of many countries' higher education institutions. After the Second World War, the quality of higher education in the

United Kingdom and the United States gradually came to the forefront of the entire world, forming a system of university faculty management that is politically, economically, and culturally compatible with that of Germany and the United States. The reasons for the growth of a group of American universities from small colleges to influential universities in the academic world are many, of which the establishment and implementation of a scientific university faculty management system is an important part [2]. Therefore, building an excellent faculty and giving it a virtuous cycle is a topic worth exploring. With the intensive development of information technology in the era of globalization, how to make efforts to adapt the school faculty management and its institutional system to the conceptual approach and development philosophy of the world's information technology advanced society and to build a highly qualified and well-structured university faculty system has increasingly become the most important practical content of today's research and exploration of higher education development. As an institution clearly different from other institutions in society, the management function of university is to provide services for teachers and professors so that they can carry out scientific research, teaching, and social service work more conveniently and effectively. Therefore, this paper attempts to analyze the concept and practice of university faculty management system in China and find out its characteristics in order to provide reference for the construction of university faculty management system in China.

Big data management system not only can store a large amount of data and form a massive data storage network system but also can analyze and process data extremely fast. A big data management system is a system that makes reasonable use of computers and network media to analyze and process various data [3]. It is gradually applied to all aspects of life with fast and convenient information processing, bringing great convenience to people's lives, updating their traditional data management concepts, providing a more novel and convenient way to store and process complex data, and greatly improving their work efficiency.

Therefore, the use of big data and management systems for our teachers' information management education training and school management can be very effective and rapid to help keep pace with the changing times of teaching, to improve the level of modern management practice ability level and research level of school teachers, to promote our country's multilevel higher education and high-level development of modernization of the research university teaching force, and to improve with the community and service satisfaction of people from all walks of life, further contributing to the improvement of the level of theoretical and scientific research abilities of our university teachers in the future, cultivating the comprehensive professional quality of our students' talents, and contributing to the high-quality development of China.

## 2. Research Background

In the management and education of teachers, foreign countries started earlier. The American scholar Burton Clark in

his book "The System of Higher Education: A Cross-National Study of Academic Organizations" focuses on the academic characteristics of colleges and universities and the rules of academic management of college organizations. Moltudal et al. point out the feasibility of faculty participation in academic management, which is conducive to motivating faculty members and can stimulate the spirit of ownership [4]. Dodo-Balu believes that teachers' own qualities and professionalism can participate in the management of the school and make it develop in a good and healthy direction, which is unattainable by other people [5]. Birnbaum (R), in his book "Models of University Operation," presents the view of the organizational model of university operation, the view of the organizational sector of university operation, and the values of equality and fair authority for the members of the school which should be the first priority for all direct participants in the decision-making bodies of the university; this is because the school is more concerned with the development of the university itself [6]. Therefore, this fair view of authority and a strong sense of responsibility make the universities run in a healthy and orderly way. As mentioned in the book, shared governance is both a concept and a form of management. Tzafilkou et al. have successively pointed out that the tenure system severely restricts and hinders the recruitment of teachers and the free internal mobility of state workforce in the country's universities, undermines the normal educational model of the society in which students are educated for continuous personal career development, exacerbates the bureaucracy that contributes to the education of some universities, and is not conducive to the creative expression of teachers outside the system [7]. There are both internal and external reasons for tenure system reform. After the 1970s, a system of tenure evaluation began to emerge as a way to promote effective development of the teaching profession, a formative evaluation that treats teachers in a developmental manner and compensates for ineffective performance [8]. A rational model would be for institutional leaders to review tenure or other alternatives to tenure and then rationally choose the appropriate institutional hiring policy. This posttenure review of the tenure system evaluation process ensures the accuracy of peer evaluation and is appropriate for performance evaluation. A major research objective of this peer review approach is also to assess the academic performance of faculty work, to promote the healthy development of young faculty levels, and to require a necessary aspect of progress in the tenure-track faculty.

The domestic study started late but progressed fast enough to keep up with the rapid development of higher education in China. By comparing the academic management of universities in China and the United States, Barros-del Río et al. pointed out that the academic management of universities is closely related to government departments and society and put forward the idea of academic management innovation by combining the operation of academic management and different cultural backgrounds [9]. They pointed out that, as far as the internal relationship of universities is concerned, teachers are the core of university academic management. Han Yanlun and Liu Huan yang

pointed out in the article “Reflections on the Ethical Construction of Academic Management System of Universities” that the important role of ethical construction in academic management system of universities includes bottom-line ethics, responsibility ethics, transaction ethics and credit ethics, cooperation ethics and sharing ethics, value ethics, and identity ethics which constitute the connotation and characteristics of the ethics of academic management system of universities [10]. The establishment of academic management system in colleges and universities needs to be based on ethics and morality, improves the system construction related to academic ethics in colleges and universities, and strengthens the status and role of institutional ethics. In addition, Tan Yuanxi and Liao Xiangyang, in their article “Analysis of Faculty Management Policies in Chinese Universities,” introduced these five basic stages of the development of the new policy of faculty salary management in Chinese universities implemented in China for more than 60 years: the foundation and adjustment period, the tortuous and turbulent period, the recovery and development period, the reform initiation period, and the reform deepening period [11]. Two kinds of thinking are proposed: the identity of state university teachers is “state cadres,” which does not reflect the special characteristics of university teachers, and also tends to lead to “officialdom,” which allows teachers to be not very precise, and schools encourage teachers to “work,” which is not conducive to the development of academics and teaching. The formulation of university teachers’ policies should fully reflect the “academic characteristics.” In addition, the macroscopic openness of the implementation of university teachers’ policies is not sufficiently grasped, the implementation guarantee is not enough, and the overall scientific understanding of the construction of the evaluation index system is not enough, which affects and restricts the assessment of the scientificity, feasibility level, and economic effectiveness of the policies. The author Geng Yiqun has written in the introduction of an article entitled “The Dilemma and the Way Out of the Tenured Professor System in American Universities” that since the late 1990s of the 20th century in the United States, social institutions such as the United States and domestic academics have raised many critical views and strong questions about the reform of the tenured university professor system in China, and some domestic universities have tried to replace the tenured professor system in the United States with a fixed contract. It is believed that China’s tenure-track university professorship system is inefficient and prone to lazy thinking of teachers, which is not conducive to attracting outstanding talents to the academic career [12]. In this article, the author of “The Dilemma of the Tenured Professorship,” J. Liu, points out that although the tenured professorship has been questioned since the 1990s, hindering faculty innovation in academia, and many other shortcomings, professors are concerned about the diversity of schools and are less susceptible to changes that would promote school reform in a more effective way [13]. The authors point out that the life of the university lies in debate, that only the outspokenness of professors makes the school face its own shortcomings and deficiencies, and that all the professorial system needs to be

protected by the freedom to express opinions rather than punish, so the tenure system serves to protect professors and thus academic freedom. In 1913, the American Association of University Professors was officially proclaimed in Johns Hopkins University. In 1915, Dewey became the first President of the United States and issued a Statement of Principles. In 1925, Dewey, in consultation with the American Association of Colleges and Universities, issued the last of Dewey’s official statements on academic freedom and tenure, making a distinction between tenure and nontenure. Tenure is a necessary measure for academic freedom, economic security, students, and society.

### 3. Basic Theory and Research Methods

#### 3.1. Basic Theories

*3.1.1. Big Data Ecomanagement System.* The big data management systems utilized today not only can store a large amount of data and form a large number of data storage network systems but also can analyze and process data extremely quickly [14]. Big data management systems are all about analyzing and processing a wide variety of data with the rational use of media such as computers and networks. It is becoming more and more popular in all aspects of life with fast and convenient digital information transmission and processing, bringing a great degree of information convenience to people’s future study and life, updating people’s traditional view of data management, providing a more innovative and convenient way to store and process a variety of data, and greatly improving people’s work efficiency. Big data management system mainly has four characteristics, such as large storage volume, rapid information processing, real and effective data results, and many types of data, as shown in Figure 1.

Big data management system can go through its own powerful information processing system to store a large amount of information. Because of its powerful system operation and processing function, it can process information and data very quickly, and unlike manual work, it is difficult for big data management system to falsify and make mistakes on data, thus ensuring the authenticity and correctness of data processing. Therefore, the use of big data management systems for ecosystem management not only improves efficiency but also instantly identifies problems in the work and finds areas for improvement in teacher management that do not match the requirements of the times [15].

*3.1.2. Teacher Education and Management.* The management responsibilities of Chinese university teachers are closely related to the academic level of teachers. The organization of higher education teachers is generally different from the general disciplinary organization of higher education schools, which is a professional and technical organization mainly composed of academic staff related to various majors and so on. The characteristics of modern university organization based on the viewpoint of the subject status of modern academic profession can be reflected in at least the following characteristics: the division of labor in

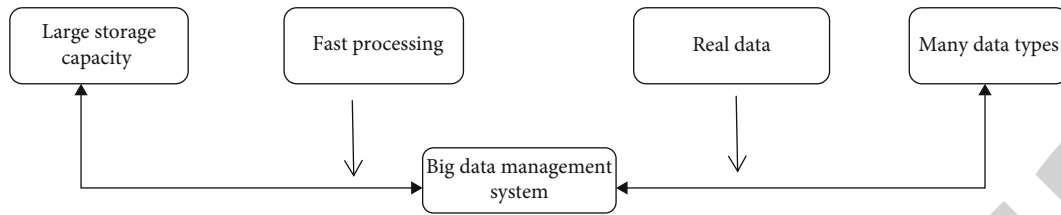


FIGURE 1: Features of big data management system.

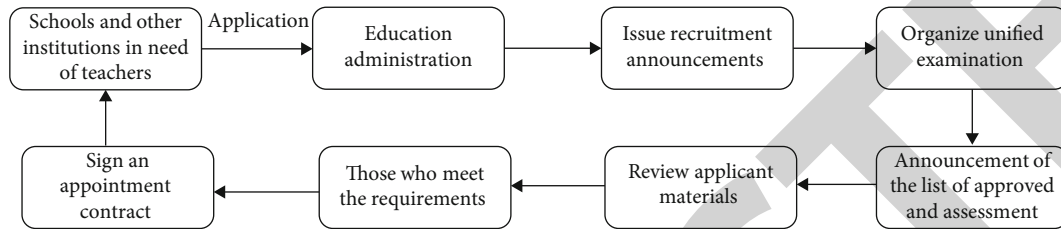


FIGURE 2: Flow chart of teacher appointment.

disciplines is the common organizational basis of all academic professions, the loose combination of disciplines is the common organizational structure characteristic of all academic professions, and the dual management authority model is the main dual organizational and management structure characteristic of modern academic professions. From the perspective of the development of contemporary academic professional norms, university teachers and their management should have several basic normative features such as modern academic standards in a more strict and systematic way, autonomy of academic process, freedom of academic activities, recognition of academic achievements, and recognition of personal reputation. Both the management of teachers and the reform of institutional structure are very important components and parts of the administrative management and reform work of Chinese university teachers. The system should be institutionally prescriptive and can be closely related to the practice of the teacher's knowledge concept in the corresponding field [16]. Therefore, an important first step in the system design and innovation of university teachers' administration is to establish a modern human-oriented system of teachers' science, i.e., to establish a "humanistic" concept system and to practice the "academic standard" education concept, and then to guide the whole process of system reform and innovation of university teachers' internal management. The further establishment, exploration, and implementation of the innovative system of teacher classification management in colleges and universities must be based on the actual basic situation of the reform of the teaching force in our country, and we must also learn extensively from the international advanced reform experience of international teachers' separation management innovation. Therefore, after the innovation of the reform basis to be on the overall principle of dynamic reform and opening up closely, fairness, democracy, competition, and interests, step by step, the theoretical innovation of the new system of university teachers' classification management in China must also adhere to the principle of people-

oriented, autonomy and freedom, scientific management, and so on [17].

In order to better strengthen the modernization of the quality of the university teaching force, as well as to cooperate with the further smooth and effective implementation of China's education policy "science and education to develop the country, talent to strengthen the country" program, universities in China have implemented a relatively strict and unified high school teacher qualification appointment methods and teaching and management assessment system. There is a strict process for teacher appointment, and the qualified candidates are finally incorporated into the teaching system, as shown in Figure 2, with a total of 8 steps, which basically ensures the basic level of China's teaching force.

In teacher appraisal, before appraising teachers, schools usually organize a meeting to promote the appraisal process and print and distribute teacher appraisal methods to individual teachers. After receiving the appraisal method, teachers should summarize the teachers' thoughts, attitudes, and responsibilities in their work, fill in information such as research achievements and awards in their work, and submit a report of their work to the management. The department will evaluate the teachers according to their individual situation and submit them to the school and the school division for review. The school and the academic department will grade and evaluate the teachers' individual work and political thought. The final overall grade of the teacher will be derived and reported to the school for acceptance. The assessment mainly includes teachers' ideology and moral character, knowledge, business ability, and performance.

Although China's teacher appraisal standards are relatively backward, these serve the cause of higher education in China for more than 40 years; after continuous historical evolution, these are also basically adapted to the basic national conditions of China and have made indelible contributions to China's higher education. China's higher education teacher appraisal process is shown in Figure 3, a total of six links.



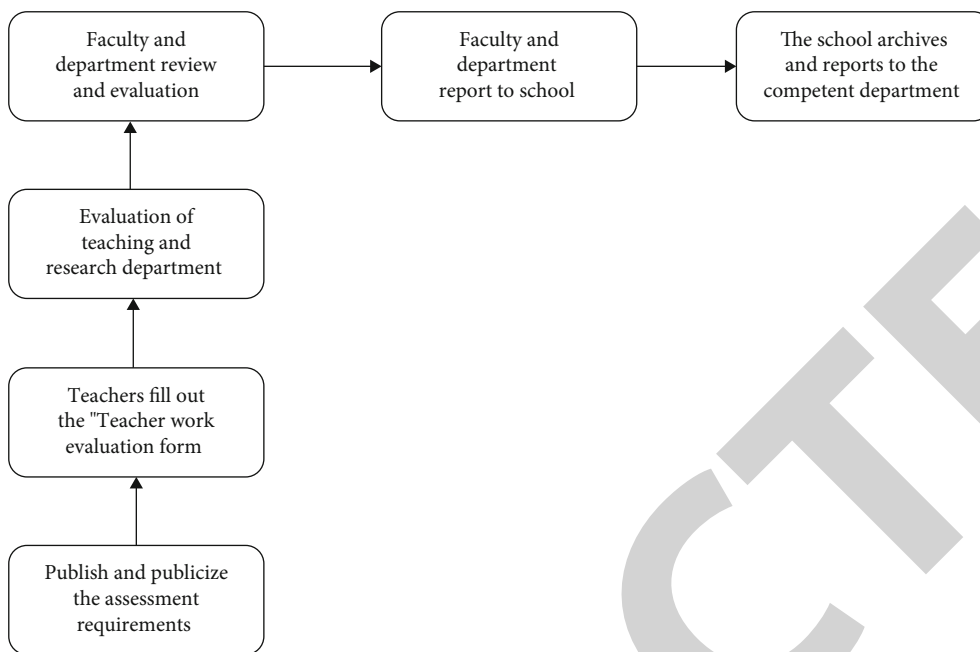


FIGURE 3: Flow chart of higher education teacher assessment in China.

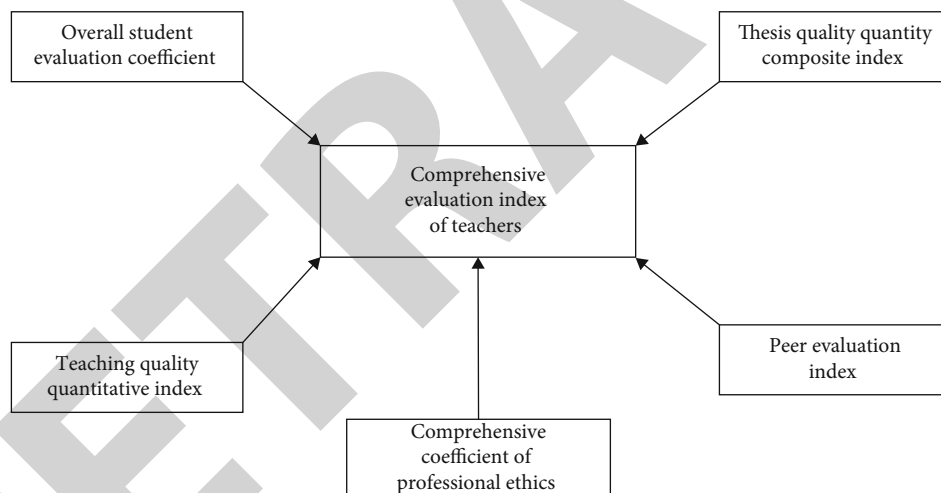


FIGURE 4: Comprehensive evaluation index of teachers.

3.1.3. *Main Formula.* To efficiently use big data to educate and manage teachers in colleges and universities, we should make comprehensive use of various analysis methods to quantify the specific indicators of teachers, specifically see the advantages and shortcomings of teachers, and better manage and educate the teachers’ team, so this paper introduces the comprehensive evaluation index of teachers to measure the comprehensive quality of teachers. The higher the index value, the higher the teacher’s evaluation and ability, as shown in Figure 4.

Teacher comprehensive evaluation index = a comprehensive index of teaching quality and quantity + b comprehensive evaluation index of students + c comprehensive index of quality and quantity of published papers + d comprehensive coefficient of teachers’ professional ethics + e peer evaluation index.

Where  $a + b + c + d + e = 1$ .

### 3.2. Research Methodology

3.2.1. *Oracle Big Data Analysis Study.* Oracle Database Management System is a relational database management system developed by the German company Oracle Software (Oracle in Chinese). It may also be another database product that Microsoft will design with the idea of distributed database as its biggest core feature. It will also be one of the most popular distributed C/S server architecture solutions or distributed B/S database architecture solutions currently used by Microsoft worldwide. Oracle database has a wide range of design aspects, such as banking, telecommunications, mobile, aviation, insurance, and e-commerce. Meanwhile, Oracle’s product is free, and we can download the installation

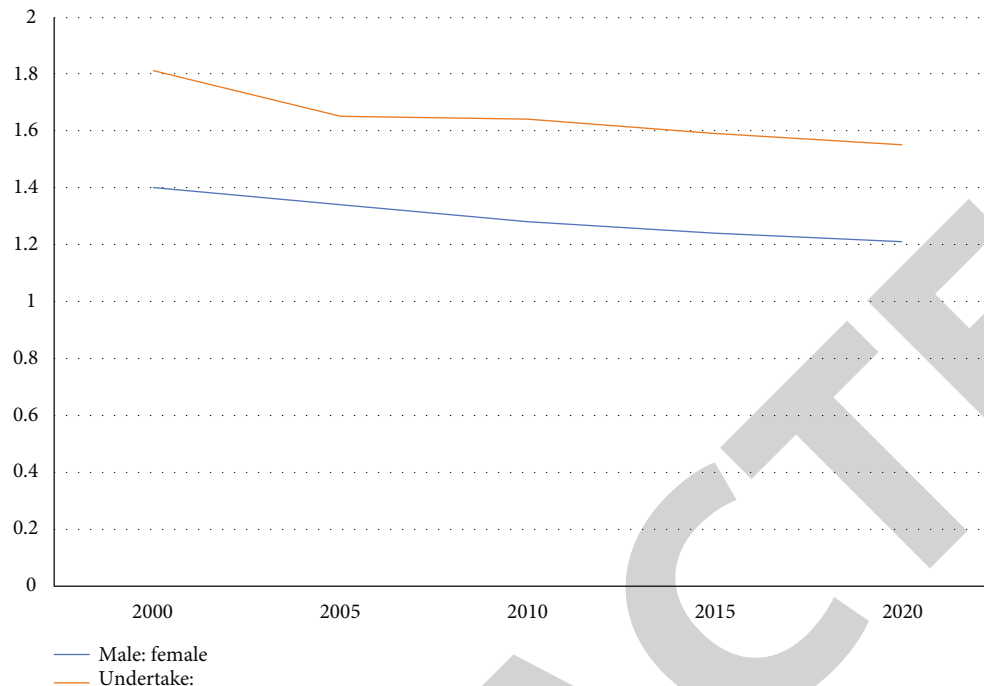


FIGURE 5: Changes of gender ratio and master's degree ratio of teachers in colleges and universities in China.

package from the official website, but its service is charged. Compared with SQL Server database, the state of “doubt” is one of the most obvious and attractive performance advantages of Oracle database parallel server model, which can achieve any one subquery decomposition into any number of subqueries and then execute subroutines on two different server CPU processors, greatly improving the performance of multiprocessing systems, which should be a data trend with a great potential competitive advantage that is growing rapidly in the coming years. Oracle database also has many other significant advantages such as complete data storage management storage capacity, large data storage capacity, long persistence time, can be shared to ensure reliability, complete related products, complete distributed management capabilities, and easy to operate [18].

In this paper, we use Oracle big data analysis to study and analyze the data of university teachers' management education system and lay the foundation of big data processing for the innovative application of big data ecological management system in this paper.

**3.2.2. SQL Server Data Analysis Research.** On the basis of today's mainstream Windows and other operating system platforms, SQL Server database as a new generation of database and analysis of the processing platform software is rapidly being widely used by various enterprise customers that are widely accepted. Unlike other current database platforms such as FoxPro and smaller databases such as Access database, SQL Server has a complete set of powerful and easy-to-use database management and service processing functions. There are engines that support development, standard database languages such as SQL, and extended feature functionality (such as replication, OLAP, and analytics). It is also

significantly ahead of the rest of the market in terms of other key features that only large database software can have to [19], such as stored procedures and triggers.

Microsoft SQL Server 2010 is based on Microsoft SQL Server 7.0, greatly extended to increase database performance, reliability, quality management, and ease of use. Microsoft SQL Server 2010 database edition is a high-performance enterprise relational database management system with high reliability, ease of use, and other characteristics.

Therefore, in this paper, SQL Server 2010 is selected for big data analysis to analyze the innovative application of teacher education management system.

## 4. Results and Discussion

**4.1. Research Results.** In this study, based on collecting data from multiple departments such as the Ministry of Education and the National Bureau of Statistics and finding relevant statistical yearbooks as reference, the results of this study were obtained by using Oracle and SQL Server to dynamically process relevant data and analyze changes in some data for up to 20 years and 6 years, respectively.

As shown in Figure 5, in the 20 years from 2000 to 2020, the ratio of male to female teachers and the ratio of master to doctor in China's colleges and universities showed a decreasing trend year by year, although the teachers with undergraduate degree and below were not considered, but it is enough to show the trend that the ratio of male to female teachers in China's colleges and universities is gradually balanced and the teachers' education is gradually improved, which further shows that the comprehensive quality of teachers is continuously improved.

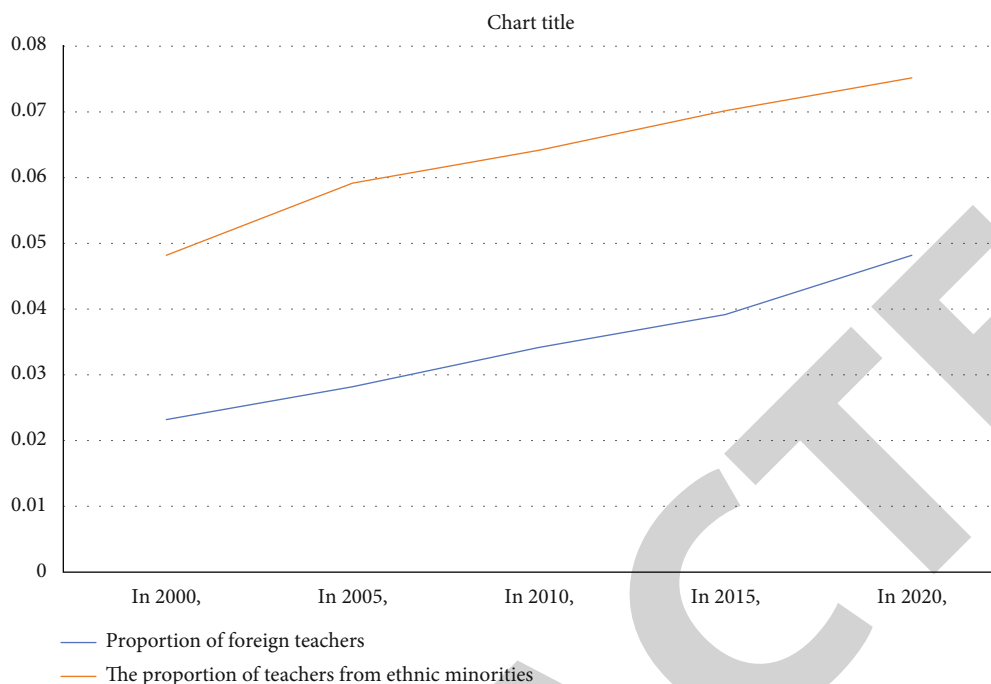


FIGURE 6: Changes in the proportion of foreign and minority teachers.

As shown in Figure 6, in the 20 years from 2000 to 2020, foreign teachers and minority teachers in China show a trend of increasing year by year. It not only shows that the increasing level of development in China attracts more foreign teachers and other high-level talents but also shows the determination of poverty alleviation identified in China and the practical implementation of minority development policies. More importantly, exchanges with foreign scholars are more common and the academic atmosphere is more open; ethnic minority scholars also enrich the fields and perspectives of academic research.

As shown in Figure 7, the total proportion of all types of teachers in one institution in China is high. Other research institutions have the lowest proportion of all types of teachers. Whether it is a bachelor's degree or independent colleges, senior high schools, or other research institutions, the structure of teachers' titles shows a relatively normal distribution structure with a middle and low on both sides [20]. The distribution of teachers at all levels in China is more balanced. In addition, the structure of teachers in China shows a distribution of the highest percentage of undergraduate and the second highest percentage of senior high school, followed by independent colleges and fewer other research institutions. It basically adapts to the rapid growth of China's development.

As shown in Figure 8, the comprehensive evaluation index of teachers in China's higher education institutions shows a trend of increasing year by year. Comprehensive evaluation index of teachers = a comprehensive index of teaching quality and quantity + b comprehensive evaluation index of students + c comprehensive index of quality and quantity of published papers + d comprehensive coefficient of teachers' professional ethics + e peer evaluation index (a + b + c + d + e = 1). It can be seen that the comprehensive

quality of teachers in China has been improving, the system of education and scientific research in China's colleges and universities has been improving, and the ecological management system of colleges and universities has been improving.

#### 4.2. Suggestions for Innovative Applications of Teacher Education and Management Systems

4.2.1. *Raising Academic Standards and Establishing a Career Entry Qualification System.* Teachers in higher education continue to engage in the academic profession of teaching first of all requires that students have undergone long-term solid training in theoretical knowledge and technical professional quality of this academic discipline and have a fairly certain high level of theoretical academic quality foundation and potential academic research development growth potential. Therefore, an improved system of access and qualifications for the education profession should be established to fully ensure the comprehensive overall quality of our teaching population.

- (1) Improve the qualification standards for practitioners in accordance with the law and strengthen the qualification legislation for access to the education profession. The revision of the professional qualification standards for teachers in colleges and universities should focus on clarifying their corresponding academic conditions and professional ethical and moral conduct requirements, highlighting in the assessment that they have the basis of disciplinary professional competence and the ability to teach and research in their disciplines, improving the accreditation standards for the admission of relevant

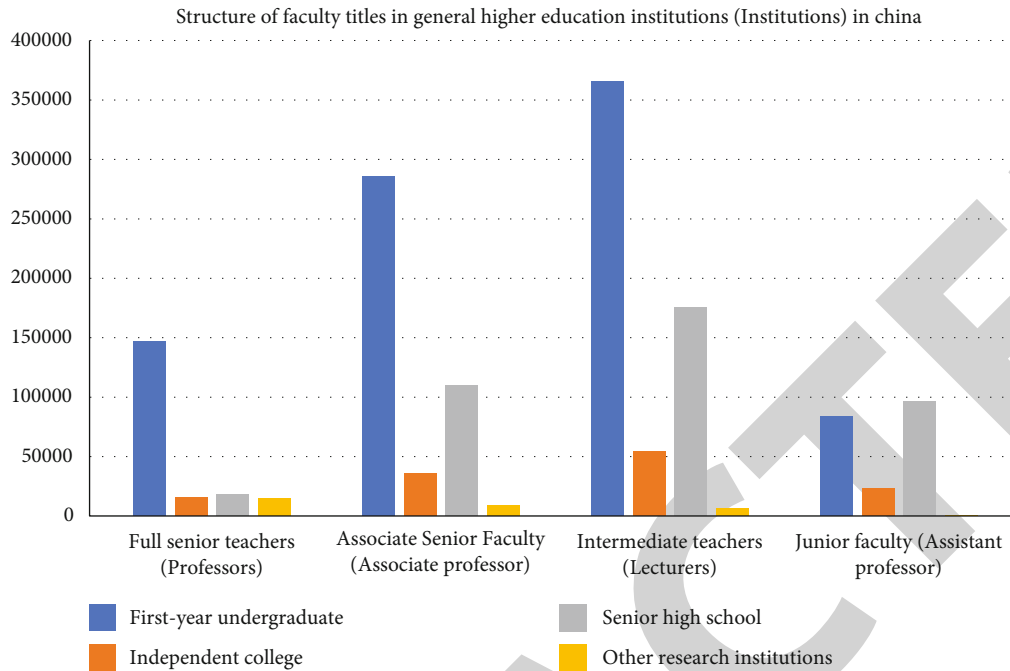


FIGURE 7: Structure of teachers' titles in general higher education institutions (agencies) in China.

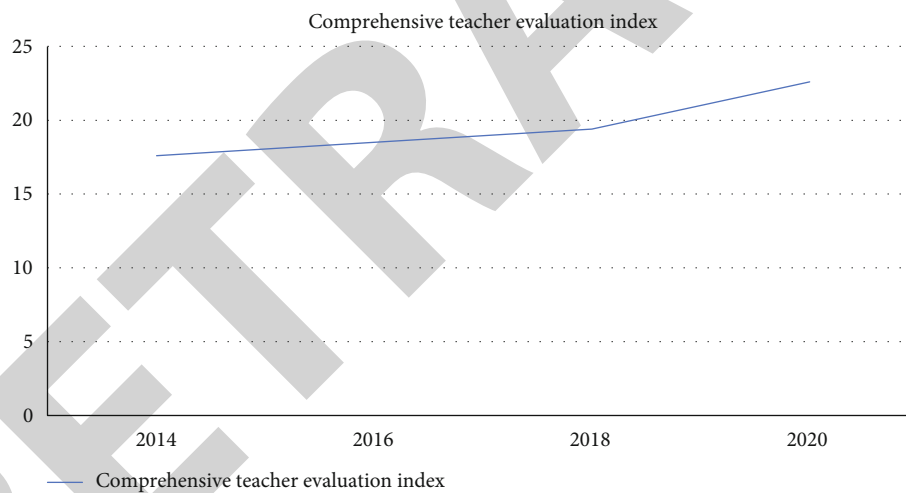


FIGURE 8: Changes in the comprehensive teacher evaluation index.

academic professionals, and ensuring the overall quality of knowledge of the general group of teachers in colleges and universities. At the same time, three different levels of professional qualification standards have been formulated and promulgated according to the needs of different historical regions, different academic types of colleges and universities, and different levels of ability development of students trained by teachers of different national academic career ladders in China. The construction of the higher education teacher qualification system is an important strategic component of the work to establish a national professional qualification system with national legal norms, and the implementation of the school teacher qualification system certifica-

tion is an important part of the work to implement the principle of unified state management of education in accordance with the law. The deficiencies of the current legislative system of access and qualification system for the professional development of teachers in higher education, etc., developed and further improved should be amended in a timely manner, and the independent legal status of the academic professional qualification system of higher education itself should be guaranteed through national legislative means

- (2) Study and establish a multilevel, time-sensitive, and highly operable assessment standard system of relevant professional qualification levels and establish

provincial professional qualification identification and implementation certification agencies. Based on the actual need situation of meeting the needs of individual lifelong development of academic career and the value concept of pursuing comprehensive lifelong development education of academic career, a set of academic professional qualification and certification career standard system with multilevel and time-effectiveness is established. Therefore, it is recommended to gradually establish academic career and certification professional standards covering several minimum levels above the college teaching career and use these minimum levels as the core qualification standards for evaluating academic career talents. At the same time, a system of regular and certified assessment and evaluation of teaching qualifications at all levels should be established, and examinations should be set for students at each level according to the level of teaching qualifications valid once (e.g., every five years). In the study validity period, you must pass the corresponding course examination of the corresponding next level of education qualification training and certification level standard by obtaining a certificate of experience and study results of teaching continuing learning education and training of a certain scale and passing the corresponding course examination of the corresponding next level of education qualification training and certification level as required, in order to successfully obtain the education continuing training teaching practice qualification. In this way, the level of development between the dual standards of qualification and certification can be interpenetrated and integrated to guide teachers and the community to encourage in-service teachers to carry out continuing in-service learning, to indicate the right direction for the in-service professional and technical development and upgrading of China's teachers, in an effort to effectively ensure the improvement of the overall quality of teachers nationwide. The establishment of institutions for the implementation of various types of professional qualification systems accreditation is a crucial legal guarantee for the effective and smooth implementation of the qualification system for teachers in higher education. For example, establish a number of professional organizations for the organization and implementation of professional qualifications within university education and a number of specialized organizations for the accreditation and implementation of external professional qualifications for university teachers—that is, several specialized accreditation committee units or accreditation bodies can be established within university teachers to jointly implement the work related to the accreditation of the university teaching qualification system, through the establishment of the development of perfect standards, fair, transparent, feasible, and fair procedures of the school teaching qualification examination and certification system to ensure the effective and smooth

implementation of the whole process of work related to the certification of the university teaching qualification system; supervisory and inspection agencies of the primary and secondary school teacher qualification training and certification work should be set up, respectively, within the universities to ensure the scientific fairness, objectivity, and scientific justice of the relevant qualification examination and certification results

*4.2.2. Follow Academic Freedom and Equality and Improve Teacher Appointment System.* Teacher appointment system management is one of the several major administrative links stipulated in the formulation of the basic system of teacher recruitment management in colleges and universities. Researchers in colleges and universities should adhere to the basic characteristics of the academic career ability of college teachers, adhere to the employment principles of following academic evaluation and free flow and peaceful flow, etc., and optimize and improve the work system of appointing college teachers to positions.

- (1) Establish a system of career “admission period” and improve the job management system. Academic career is a special profession with its own special requirements. The construction of teachers in colleges and universities is a process of “selection” and “optimization,” and a reasonable “admission period” should be set. For example, “fixed-term” appointments and “open-ended” appointments should be used as the institutional design. The setting of “entry period” of university teachers should pay attention to the following points: first, to establish a reasonable “entry period”; second, to provide professional development and equal competition opportunities for the “entry” group; third, to implement peer academic review and “developmental evaluation” in the “admission” stage; and fourth, to have corresponding regulations for the “appointment period” to protect the legitimate rights and interests of university teachers. The purpose of post management is to optimize the structure of university teachers, promote reasonable flow of academic career, and promote academic prosperity and development. According to the overall planning of the university and disciplines, the strategy of classifying posts and management is appropriately implemented so that teachers' duties are clear, each has its own role, and academic performance is maximized and most effective. By establishing a number of mobile professional staff centers and academic mobile research positions at the university, we can actively promote the social freedom and mobility of various academic professional groups, strengthen exchanges between Chinese and foreign academic workers, improve the academic level of society, and maintain the overall academic vitality of the university
- (2) The system of appointing university teachers in flexible, effective, and diversified forms is standardized

and perfected. Firstly, the flexible and efficient and diverse types of appointment system for teachers' posts and employment positions are established for various types of colleges and universities of different professional types of schools in China. In the overall design work of the appointment system, three different levels of assessment and evaluation standards and two types of appointment should be used at the same time. In order to fully promote the development of diversified academic heterogeneous research and professional diversified research of teachers' work in higher education institutions and to promote the diversified characteristic academic development of various types of university research, various types of academic career ladders responding to the characteristics of diversified development of teachers' career in China should be created by adopting some different flexible cooperation methods. Secondly, an effective labor contract system that effectively guarantees the equal development of academic interests of faculty members should be established to improve academic productivity. According to some characteristics that exist in the academic career characteristics of higher education itself, the signing of employment staff contracts by university teachers should also take two forms of signing collective contract statutes and labor contract, respectively, to clarify the division of rights and obligations of each school staff and the various rights of the individual teachers employed, to gradually promote the realization of real equality of status between the rights and obligations of the two cooperating parties, and to ensure the signing of labor dispatch contracts. In addition, the dismissal mechanism for teachers will be made clear. In addition, the effective optimization of teachers' departure and dismissal mechanism is also an important basic guarantee to promote the standardized and effective implementation of university teachers' title appointment and evaluation system, such as improving the appointment declaration system for new teachers, improving the evaluation mechanism for new teachers, broadening the channels for teachers' departure, and strengthening the guidance of public opinion

#### 4.2.3. Adhere to the Principle of Academic Fairness and Optimize the Teacher Assessment and Evaluation System.

The evaluation system of teachers in higher education should take the promotion of teachers' academic career development and teachers' self-realization as the ultimate goal of evaluation. Therefore, in order to promote the development of teachers and academic career, it is necessary to adhere to the principles of academic fairness and freedom to optimize the evaluation system of teachers in colleges and universities.

- (1) Scientifically establish the evaluation system of educational assessment to promote the overall development of their academic careers. Teachers in colleges and universities must engage in academic work of

higher education mainly according to the law, and the principle of academic evaluation freedom is its fundamental internal operation logic. The scientific establishment of the evaluation system standards of teachers' titles must all take into account the specific characteristics of academic career personnel training in colleges and universities and follow the evaluation principle of free and standardized educational academic work. On the one hand, it creates a scientific, harmonious, and fair environment atmosphere for academic education evaluation of university teachers and reflects social humanistic care. The system construction of teachers' title evaluation should pay attention to respecting the overall regular process of academic level growth and change of the teaching team and individual differences of the teaching team, respecting the historical professional achievement experience formed by contemporary college teachers themselves as high-quality intellectuals, scholar talents, and lifelong educators, and paying attention to the historical natural life, academic life value, and personal spiritual life of teacher titles. On the other hand, we should gradually change the traditional evaluation index concept and adopt the comprehensive developmental evaluation index system method. It should be highly appraised and recognized the value of teachers' academic achievements and their creation, boldly advocated and encouraged the innovative practice and academic creation of teachers' academic achievements in colleges and universities, and paid attention to the development and progress of teachers' academic potential and education in the future. But at the same time, attention should be paid to the policy principles and relative flexibility of talent evaluation work. To enable high-level creative talents to develop fully and freely, and to truly and effectively implement the "teacher-centered" philosophy. Establish an evaluation and assessment system of university professors' professional titles with the evaluation of professors' academic and professional reputation as the leading index. The lofty academic reputation of scholars themselves should be based on the general cultural recognition of the whole academic circle. The objective recognition of others' academic achievement level and innovation degree of others' academic value is the general value and affirmation of scholars' achievements of their academic professionals. Therefore, it is necessary to give full and effective play to the overall role of members of the social academic community and adhere to the principle of "academic leadership, professors conduct academic research". For example, gradually and comprehensively establish the evaluation expert reputation assessment constraint evaluation mechanism, and strengthen the standardization construction of China's evaluation and consulting expert reputation system, etc. The relative transparency of the evaluation decision-making process is increased to ensure the rationality

of the professors and experts' support to the evaluation suggestions; and set up sound cooperation mechanism with external experts cross deliberations, to improve and enrich the relevant academic standard policy and implement the professor anonymous public evaluation at regular intervals, interest withdrawal system, expert system, rotation bearer public voting system, etc., and effectively guarantee the public evaluation activities of science professor impartiality

- (2) Actively establish a multidisciplinary academic position evaluation standard system for high-level teachers. The main work of university teachers mainly involves teaching, scientific research, public welfare service, and other important academic affairs. The results of academic ability evaluation are two important objective indexes used to measure the effect of professional construction and improvement of teaching and scientific research development of a college faculty. Therefore, it is particularly necessary to establish a more diversified and scientific evaluation system of high-level academic level, respect the individual differences of knowledge of the majority of college teachers, and fully evaluate the reasonable individual demand level that satisfies the development of each high-quality teacher. The first point is to require a reasonable and systematic professional classification of teachers and students in colleges and universities, to formulate and introduce the standards of subject evaluation of corresponding disciplines, and to develop a scientific subject evaluation system. Secondly, it features a comprehensive evaluation in all aspects and from multiple perspectives. This includes faculty self-evaluation, student evaluation, evaluation by peers and other academic groups, etc., and results in a final evaluation. Finally, the scientific fairness and accuracy of the evaluation information are ensured through the feedback results of the professional information from the students' multiple perspectives. Third, in the selection of evaluation using the also need to adhere to in the process of implementation of qualitative assessment and evaluation of quantitative evaluation, the combination of individual comprehensive evaluation combined with annual team comprehensive evaluation system, the appointment process evaluation, the comprehensive evaluation of the combination of termination of employment after continue to use a combination of evaluation work of the four principles. Fourth, in the concrete implementation process, the diversification of evaluation criteria, evaluation content, and evaluation methods should be emphasized to provide development support for teachers at different stages of academic career development. Fifthly, diversified and independent academic evaluation institutions should be established to ensure the independence of academic evaluation, so as to realize scientific and fair evaluation

*4.2.4. Innovate the Incentive Mechanism for University Teachers Based on the Characteristics of Academic Profession.* The design of incentive mechanism is one of the three important practice contents in the practice of performance management of college teachers in China. University researchers should be able to innovate various incentive mechanisms for university teachers' work according to some intrinsic spiritual motivation characteristics of teachers' academic career pursuit, so as to promote the innovation and promotion of high-level academic ethics of Chinese university teachers' work and healthy professional development of university teachers.

- (1) It is necessary to strengthen the internal cultural motivation of cultivating academic professional culture and create a long-term incentive mechanism that condenses the wisdom of academic groups. As another special academic profession, competition, reputation, and group honor also constitute an important internal and external incentive mechanism of academic professional behavior. According to the analysis of the working group investigating the internal distribution of income in colleges and universities, the first consideration should be given not to merit pay and salary and welfare benefits, but to the characteristics of the work and the local academic atmosphere. The innovation of the research university teachers' incentive mechanism research should be more based on the research of the internal incentive characteristics of professional managers' behavior itself, adhering to the internal material incentive to give priority to with the internal mental factors incentive pay equal attention to; the combination of both material and spiritual principles to incentive is given priority to insist on the principle of school internal factor incentive combined with external factor incentives in colleges and universities. Based on the principle of the combination of internal factors and external factors, this paper insists on the combination of school positive incentive methods and internal negative incentive methods and gives priority to external positive incentive methods, so as to guide and stimulate young teachers' subjective enthusiasm and independent creativity in innovation to the maximum extent and promote high-level academic innovation. The group honor incentive system can be used to guide the standardized, healthy, and benign development of relevant academic organizations, promote the overall common technical progress of Chinese university teachers' profession, and effectively improve the incentive effect of academic career. It effectively overcomes certain limitations of academic organizations and their own conditions for young teachers' academic thinking innovation research and knowledge creation talent cultivation, enhances the overall cohesion among young college teachers, and strengthens the role of disciplinary synergy radiation effect within the academic professional group; also

due to the introduction of perfecting the system of competitive merit selection mechanism and quality supervision and inspection mechanism, it effectively makes up for the principal in a great extent in the sense of the quality of teaching after the end of the term of office assessment results of a certain lack. By implementing the employment system and arrangements such as the total number of quotas, it can effectively promote the overall fairness of the internal selection or appointment mechanism of researchers in the short term, promote the orderly competition of talents among the internal organizations of the university, and encourage the orderly mutual cross-collaboration of human resources among the teams of teachers in each university. Therefore, management methods such as combining individual academic award programs with collective honor award programs inside and outside the university should be considered in order to gradually adapt to the needs of work characteristics and talent demand development trends in the academic career activities of university teachers in the coming years

- (2) Pay attention to the creation of the cultural atmosphere of colleges and universities with the spirit of academic service supremacy and the academic humanistic power to promote the innovation of academic career. As a national academic organization, the university research association has relatively strong and unique university cultural characteristics. The cultural characteristics of the way teachers work in colleges and universities are also mainly reflected in their academic dimension. Therefore, strengthening the academic cultural literacy of teachers and creating a good upward social academic cultural atmosphere system in colleges and universities and an innovative environment for the development of humanistic scientific research in schools can be more effective and motivating for our college teachers. Firstly, we should actively discard some old academic culture systems that are not conducive to the development and improvement of young teachers' academic career ability. We should discard the traditional incentive mechanism of our teachers' traditional concept and culture that "seniorization of government and academia" can independently nurture college teachers and establish a scientific incentive mechanism that is really suitable for the actual needs of academic professional development of college teachers and matches the needs of self-sustainable development, correctly and reasonably. The reform of the negative academic moral incentive tendency based on the existing academic value standard of antimonetarism, materialism, and academic utilitarianism enriches the theoretical content and application of academic social incentive theory; the reform of the administrative system effectively controls and eliminates the tendency of academic moral "relationship" and abuse of academic status power

and other "rent-seeking" phenomena. The reform has effectively controlled the elimination of academic ethics "relationship" tendency and abuse of academic status and power and other "rent-seeking" phenomena to ensure the fairness of academic ethics in society. Secondly, we should make efforts to establish and develop a set of academic culture that is conducive to the comprehensive personal development of students and the pursuit of self-sustainable development of college teachers and fully play the role of research results in guiding and inspiring the front-line college teachers, for example, to create an academic culture environment similar to "open, fair, democratic and innovative", to establish a long-term incentive mechanism for teaching and research that encourages teachers' innovation and obsession with innovative academic ideas, to carry out new forms of academic culture activities such as "academic salon" essay writing, to enrich the daily academic life of university teachers and students in China, and to provide a more favorable environment for young teachers' professional growth and personal development. We also respect the general regularity of the growth of individual academic quality and pay attention to the individual differences in the development of academic talents and encourage the heterogeneous and diversified innovative development of our academic talents group

*4.2.5. Create a System for the Development of University Teachers and Promote Academic Career Development.* The teacher continuous development evaluation system is also one of the two main core content items of the teacher-training management application system research. The reform of the system of continuous development of teachers in colleges and universities should be aimed at effectively promoting the comprehensive development of contemporary college teachers' academic careers into success and their personal self-development ability as an important goal.

- (1) To gradually form a flexible and diverse effective higher education professional literacy development planning system and promote the development of Chinese teachers' professional quality toward legalization. The basic composition system of higher education teachers' talents is extremely complex and large, and the development status of each type of individual university teachers' main professional fields is significantly different in degree. Therefore, each university in different teaching type backgrounds should also have a system of policies for the development of high-level teacher professionalism of different degrees. For example, an open, flexible, diverse, and efficient mentor training mentor system, a flexible and diversified system of university-enterprise cooperative talent development programs, academic norms, a system of lifelong education development planning, and the construction of an academic sabbatical system should be



established. At the same time, according to the actual characteristics of various types of college teachers in different historical academic career stages of development, we provide free professional training, further training, academic experience exchange seminars, and other training opportunities for college teachers at all levels with corresponding levels to meet the development orientation and actual academic position development planning needs of each college teacher's own education profession. The process of legalization of the development of higher education teachers' positions is an important legal sign of the results of the construction of the professional path of higher education teachers. The main guidelines that should be followed through administrative legislation for ensuring the in-depth implementation of the strategy of professional development of highly qualified teachers are the relevant mandatory legal norms and government normative laws. At present, China has repeatedly formulated other relevant management policies, institutional designs, and reform measures to guarantee the healthy development of university teachers, but most of them have not been able to rise to the overall height of the administrative legal system, and in the process of implementing the laws, they often fail to fully play the role of guarantee that they should play due to certain practical reasons. Therefore, it is necessary to further develop a more specific and effective system of relevant legal provisions or to add some relevant institutional provisions to the existing relevant legal norms as soon as possible, so as to truly ensure the further smooth implementation of the construction of the system of guaranteeing the professional development of teachers in China.

- (2) Accelerate the construction of a new framework system for institutional development of teachers under the core goal of promoting the development of academic talents' professional specialties. Teachers in higher education are to engage in a variety of academic careers, and their educational careers and their development should undergo a relatively life-long and continuous evolutionary process. Only by being more grounded in the scientific and intrinsic value of the laws of the academic profession can the institutional system of higher education teachers ensure the development of a virtuous professional system that is truly conducive to promoting the growth of highly qualified teachers and realizing the value of contemporary teachers' subjects. For example, the design and establishment of the institutional framework should give full consideration to the maximum possible effective protection of the legitimate academic professional freedom of all university teachers themselves and truly promote the development and progress of China's university teachers as a whole; therefore, the top-level design construction and final implementation process of

the relevant institutional framework should effectively follow the mainstream value orientation of the academic professional rights of university teachers. The basic establishment of this professional qualification system framework should also further improve the basic professional competence quality and undergraduate teaching and research ability of the university teachers group in our city. In conclusion, the policy system of university teachers' management development should also take the promotion of academic career development's and professional education development reform as an important goal to help young teachers better realize academic self-actualization. In the context of internationalization, popularization, and marketization of higher education, the administrative management of university teachers is facing many serious problems and challenges in the new situation, which naturally requires us to strengthen the forward-looking research on the innovation and development of reform mechanisms and related systems for the management and development of teachers. The editor of this paper also makes a preliminary systematic discussion on the policy innovation ideas on the evaluation system of teacher administration under the new situation from the perspective of the practicality of education academic professional talent training, in order to help improve the adaptability of the current policy formulation of teacher administration assessment in colleges and universities. The reform of higher education teachers' administration and its institutional structure will be a long-term task for higher education, which requires further exploration by colleges and universities to gradually accelerate the establishment of a modernized higher education teachers' management system with distinctive Chinese working characteristics according to the current national requirements and in line with the trend of the times, in order to promote the overall health and long-term sustainable and healthy development of China's general higher education.

## 5. Conclusion

In this study on the innovative application of teacher education and management system, data processing is carried out using Oracle and SQL Server database processors commonly used for big data processing. It is concluded that China's teacher team is gradually balanced and the comprehensive quality of the teacher team is improving; the academic atmosphere is more open; the fields and perspectives of academic research are richer; the distribution of teachers at all levels in China is more balanced; the comprehensive quality of our teachers is improving; the system of education and scientific research in our universities is improving; and the ecological management system of universities is improving.

In addition, according to the results of big data analysis, the following suggestions are also put forward for the

current situation of teacher education and management in China's colleges and universities.

- (1) Improve academic level and establish a professional access qualification system

Teachers in higher education continue to engage in the academic profession of teaching firstly need that students have undergone long-term solid theoretical knowledge of this academic discipline and technical professional practice training and have a fairly certain high foundation of humanistic academic quality and potential academic professional development potential. Therefore, a system of access and qualifications for teachers in the education profession should be established and improved to fully ensure the overall professional quality of the professional teacher force. Improve qualification standards and strengthen legislation on professional access and qualifications. Establish and improve a multilevel and more timely national system of professional qualifications and certification standards, and set up professional qualification implementation agencies.

- (2) Follow academic freedom and equality, and improve the teacher appointment system

Teacher appointment system management is one of the several major administrative links stipulated in the formulation of the basic system of teacher recruitment management in colleges and universities. The academic journal of colleges and universities should be able to adhere to the actual characteristics of the nature of our academic profession, adhere to the basic academic freedom and equality and other principles of employment, and optimize the system for the appointment of college teachers' titles. The nature of academic profession is a legal profession of extremely special nature in China, with many requirements of its relative specialness. Establish a sound and flexible employment system for college teachers.

- (3) Always insist on implementing the principle of academic fairness and optimizing the assessment and evaluation method system of college teachers

The evaluation system of university teachers should take the promotion of teachers' academic career development and teachers' self-fulfillment as the ultimate goal of evaluation. Therefore, in order to promote the development of teachers and academic careers, it is necessary to optimize the evaluation system of college teachers by adhering to the principles of academic fairness and freedom. Establish an evaluation system to promote academic career development. Establish a multidisciplinary teacher academic evaluation system.

- (4) To innovate and design the incentive mechanism of college teachers according to the own characteristics of academic career group in colleges and universities

The design of incentive mechanism is one of the three important practical content links of performance manage-

ment practice of college teachers in China. University researchers should innovate and construct scientific incentive mechanism for university teachers' research according to the inherent subjective motivation characteristics of teachers' academic occupational characteristics, so as to promote the innovative transformation of high-level academic value of Chinese university teachers' research and promote the development of professional innovation. Reinforce the scientific internal motivation incentives for academic professionals and create an incentive mechanism for academic group innovation. Create a good cultural atmosphere where academic values are paramount and value the historical and humanistic environmental motivation for the flourishing of academic career in China.

- (5) Establish a development system for university teachers and promote academic career development

The teacher professional development evaluation system should be one of the three main research content systems for the development of university teachers' academic management information system. The research system of professional development of university teachers' disciplines should also be constructed with the aim of actively promoting the construction of professional development of the academic career of contemporary university teachers and the realization of self-development innovations. Formation of a system of flexible and diverse changes in the professionalism development of teachers' students legitimizes the development of professional competence of our teachers' students. The system of standards for professional development of Chinese teachers with the highest goal requirement of professionalization of the academic career of teachers should be constructed.

## Data Availability

The labeled datasets used to support the findings of this study are available from the corresponding author upon request.

## Conflicts of Interest

The author declares no competing interests.

## Acknowledgments

This work was supported by the Aba Science and Technology Bureau (19YYJSYJ0091) and the 13th Five-Year Plan of Educational Informatization Construction in Sichuan Province (Chuan Jiao Guan 2019-142).

## References

- [1] S. A. Lee, J. Mork, N. Voća et al., "A comparison of waste education in schools and colleges across five European cities," *International Journal of Sustainable Development & World Ecology*, vol. 29, no. 4, pp. 338–348, 2022.
- [2] A. I. Khalil and N. Y. Hantira, "Special education teachers' knowledge and attitudes toward the use of assistive technology

## Research Article

# Research on the Application of Hybrid Density Network Combined with Gaussian Model in Computer Music Choreography

Li-Juan Wang 

*Academy of Music, Jilin Normal University, Siping, Jilin 136000, China*

Correspondence should be addressed to Li-Juan Wang; 13134463205@163.com

Received 9 June 2022; Revised 13 July 2022; Accepted 25 July 2022; Published 12 September 2022

Academic Editor: Wen Zeng

Copyright © 2022 Li-Juan Wang. This is an open access article distributed under the Creative Commons Attribution License, which permits unrestricted use, distribution, and reproduction in any medium, provided the original work is properly cited.

Dance, as a unique form of expression, is usually accompanied by music and presented to the audience visually, improving people's cultural and spiritual lives while also strengthening their creative energy. And dance choreography is usually created by a few skilled choreographers, either individually or together, with a high level of expertise and complexity. With the introduction of motion capture technology and artificial intelligence, computers can now do autonomous choreography based on music, and science and technology are changing the way artists produce art today. Computer music choreography must solve two fundamental issues: how to create realistic and creative dance moves without relying on motion capture and manual creation and how to improve music and dance synchronization utilizing appropriate music and movement elements and matching algorithms. This article employs a hybrid density network to generate dances that fit the target music in three steps, action generation, action screening, and feature matching, to address the aforementioned two concerns.

## 1. Introduction

Color role synthesis techniques are used extensively in the creation and postretouching of virtual characters in computer games, advertisements, and film productions in recent years. Virtual character action drawing techniques are a crucial part of computer graphics because they allow virtual characters to mimic the actions of real humans. They are an extremely active research area. The invention and widespread usage of motion capture technology has secured the authenticity and safety of the action, but it is still merely a duplicate of the data. In games, animation, virtual reality, and a variety of other applications, people have a strong desire to engage with virtual characters who seem like humans. What kinds of creative activities, such as dancing, await the dance movements of virtual characters, particularly user-made dance animation, in which the animator must manually alter the position and rotation of each bone

in the model in a critical position frame? Completing this job not only takes time, but it also necessitates a high level of talent on the part of the animator, restricting the scope of virtual character dance animation [1]. As a result, a successful dance synthesis algorithm technique can be applied to a variety of sectors, such as music-assisted dance instruction, video game character movement generation, human behavior research, and virtual reality [2]. Based on the foregoing, this paper proposes a novel solution as follows: an automatic music choreography algorithm that uses dance data, a deep learning algorithm to train the training model, and a combination of filtering conditions to generate the training model automatically and intelligently to meet the expected dance movements and arrange the dance based on the matching of music and action clips. The algorithm can be modified to include unique and original dance motions, effectively replacing the traditional choreography algorithm and offering real value [3]. The algorithm is

primarily designed for 3D computer animation characters and video game roles. Animation synthesis, virtual reality, dance instruction, and other fields of interest are also important.

## 2. Related Concept Elaboration

*2.1. Research Background.* In recent years, China's economic development has accelerated, and residents' disposable income has increased year after year, propelling the rapid growth of tourism in tourist destinations. However, problems such as irregular tourism industry operation and low tourist satisfaction in tourist destinations remain fundamentally unsolved. So the direction and focus of future tourism research will be on how to establish a good tourism environment, maintain sustainable tourism development, deliver positive economic advantages, improve tourist travel experiences, and enrich the cultural life of tourist destination residents [4].

*2.2. Expressions.* Dance, as a unique form of expression, is typically accompanied by music and presented to the audience in a visual manner, enriching people's cultural and spiritual life while also encouraging their creative urge. Professional choreographers work alone or in teams to develop dance choreography that is both professional and complex. With the introduction of motion capture technology and artificial intelligence, computers can now do autonomous choreography based on music, and science and technology are changing the way artists produce art today. First is how to generate realistic dance movements without using motion capture; second is how to use appropriate music and movement features and then match algorithms to improve the synchronization of music and dance [5]. In three processes, motion creation, motion screening, and feature matching, a hybrid density network is used to generate dances that fit the target song. The dances generated in this research have improved in terms of movement coherence and realism when compared to previous investigations. Subjective user ratings suggest that the choreographic outcomes in this study match the music to a higher extent, based on the hybrid density network action generation algorithm [6]. This paper covers the steps for developing the music action dataset, the action classification premise, and the feature representation of the training data. The action generation model used in this paper's model structure, as well as parameter selections in the model training and prediction technique, is then discussed [7]. The parameter management approach and the coherence-based action filtering algorithm are described in detail when using the model for action generation, and tests are built to evaluate the algorithm and provide the experimental findings. Musical and movement components are included into the choreography. A multi-level music and movement feature matching method is developed to choreograph the generated dance motions based on the qualities of the target music. The whole music feature extraction system, including the BPM and matching algorithms, is first shown. The rhythm and intensity feature extraction technique, data segmentation and feature match-

ing algorithm, and movement connection algorithm are then described as part of the dance synthesis method [8]. The appropriate experiments are then designed to verify the choreography results, and the experiment assessment criteria are introduced, as well as the experimental outcomes.

*2.3. Research Model.* Instead of relying on the user's manual production and motion capture data, the motion generation problem must be solved in order to design an effective computer choreography algorithm that ensures that the choreography is realistic and novel enough. This chapter implements the motion generating technique based on a hybrid density network [9]. To begin, we generate the music-action dataset, categorize the data, and use features to characterize the training data. This chapter builds the action generation model from the sequence generation model outlined in Chapter 2, finishes the model's training and action generation, and performs parameter control during the action creation process [10]. This chapter chooses generated movement sequences based on coherence and gives a candidate movement library for the next choreography in order to ensure the quality of the generated movements and make them appropriate for further choreography.

In this paper, the BPMs of the corresponding music for each type of dance in the dataset are extracted, and the mean and the most values are shown in Table 1. From Table 1, the average BPM of street dance is 150.83; the average BPM of folk dance is 120.62. The maximum values of BPM for street dance and folk dance were 176.17 and 142.39, respectively, and the minimum values were 100.64 and 86.45, respectively. The skewness of BPM for both street dance and folk dance is less than 0, indicating that the distribution of these two indices is left-skewed, and the kurtosis of both is less than 3. The concomitant probability value of JB-statistic for all variables is 0.0000, which indicates that the original hypothesis of "the series obeys normal distribution" is rejected at 1% significance level for all variables of JB-test; therefore, the serial variables of BPM for street dance and folk dance do not obey normal distribution. It can be found that for both dance styles, the mean value of BPM for street dance is larger, and the mean value for folk dance is the smallest. Looking at the dance movements of each type, it can be found that the overall speed of street dance movements is faster than that of folk dance. In other words, the faster dance should have a larger mean value of BPM, which is consistent with the BPM of different dance speeds and with the intuitive audiovisual perception. However, the BPM range is not concentrated, and the feature value alone is not sufficient to describe the overall characteristics of the music.

*2.4. Objectives and Algorithm Performance.* The goals of this study are to develop a neural network-based, music-driven, and computer-automated choreography that improves the novelty and coherence of the generated dance movements, improves the harmony between the generated movements and the music, and allows users to control the generated dance results according to their preferences. The study focuses on datasets of architectural music movement.

TABLE 1: Descriptive statistical test of BPM sequences of street dance and folk dance.

Variables	Mean value	Maximum value	Minimum value	Standard deviation	Skewness	JB statistic	Probability
Street dance	150.83	176.17	100.64	0.2656	-0.6143	583.1392	0.0000
Folk dance	120.62	142.39	86.45	0.2171	-0.3720	266.8481	0.0000

Although there are some publicly available motion datasets, the majority of them are sports data, such as running and playing ball. Dance movement data that is accompanied by music is rare. Action and music data are particularly essential types of training in deep learning-based studies on the association between music and dance movements [11]. As a result, the VMD action file and WAV music file retrieved from the network and its supporting files with built-in music-dance movement dataset of 192 segments, 1057344 frames, and approximately 587 frames are used in this research. A new strategy is proposed in the generation process of actions, parameter control algorithm, and its application of consistency-based action filtering algorithm, with the goal of improving the authenticity and consistency of created actions and ensuring the consistency of action quality. The iliac bone position assesses the coherence of the action based on the rate of velocity change of each joint in neighboring frames during action production, and the average output of a Gaussian model utilizing a hybrid density network is employed as the skeleton during action filtering [12]. When compared to other control methods, the averaging method produces more realistic movements. The generated raw action data was substantially more consistent than the on-screen action data. Suggestions include integrating overall feature matching with local feature matching to create a multilevel music and activity feature matching algorithm [13], as shown in Table 1 and Figure 1.

This paper argues that the more notes a piece of music contains in an average bar, namely, the more frequent note changes, the richer the musicality of the music, and the more varied the corresponding dance movements should be. Based on this idea, this paper calculates the average duration of notes (frames) of the whole piece. The total number of frames of music signal is denoted as the total number of changing notes [14]. The specific steps of the algorithm are as follows:  $X(n)$  is obtained by CQT transformation of music signal  $X(r \circ)$ , which represents the frequency amplitude of music signal in each semitone of each frame. The frequency amplitude of the KTH semitone of music signal in  $f$  frame is represented. The stability test of each asset price is carried out by ADF unit root test.

When the target music is entered, the overall characteristics are extracted first to determine the dance style and dance speed most likely corresponding to the target music, such as BPM and the comparison table of the average duration of changing notes and the values listed in Table 2, and then, the corresponding movement generation model is selected to generate movements [15].

This paper believes that the overall speed of music should be positively correlated with the speed of movement, and the speed of movement can be measured by the speed of obvious local body parts (arms, legs, etc.) in addition to the overall movement of the whole body [16].

In addition, as can be seen from the above, the shorter the average duration of changing notes is, it means that the notes are changing, as shown in Table 2 and Figure 2.

### 3. Empirical Analysis

There are two approaches to music segmentation: one is that music structure is composed of several repeated patterns, and music can be segmented by extracting repeated patterns; another approach is to take a fixed rhythmic length of the segment as a musical segment [16]. For the first idea, the pattern of repetition may be represented by the repetition of the same passage by different instruments, so the method of structural analysis should depend on the order of the notes and should not be influenced by the timbre of the instrument or the voice. But this idea is difficult in practice [17].

This is because the timbre of each musical instrument has a basic feature, which is always composed of the keynote and its overtone (the frequency is an integer multiple of the fundamental frequency) [18]. When different musical instruments play the same note, although it is basically the same, the energy distribution of overtone is different, so it is difficult to directly extract the accurate repetition pattern in the frequency domain. Second, not all musical melodies have strict repeating patterns, and even if they do, they may be far away from each other [19]. Therefore, the length difference of music fragments after segmentation may be great, which is not conducive to the matching of subsequent action segments. For the second idea, it is actually more in line with the reality. For example, in dance teaching, music and movement are often segmented with several eight-beat rhythm lengths. The length of music fragments obtained by this segmentation method is more uniform, which is convenient for matching and choreography of subsequent music and movements. According to this idea, when music is segmented, the metronomic period is firstly extracted, the metronomic length of music  $T_{maz}$  is estimated, and music is segmented according to several lengths [20].

On the other hand, it is generally believed that for the music with faster rhythm and speed, the corresponding choreography movement changes more quickly, and the duration of music sections is also shorter in the process of choreography and dance teaching. We already know the speed marker of BPM songs; BPM is inversely proportional to the length of BPM songs [21], as shown in Table 3 and Figure 3.

*3.1. Matching Analysis.* The outputs of each synthesized dance style are pleasing to users, demonstrating that the music choreography algorithm described in this research is effective. Both types of dancing have mean values of

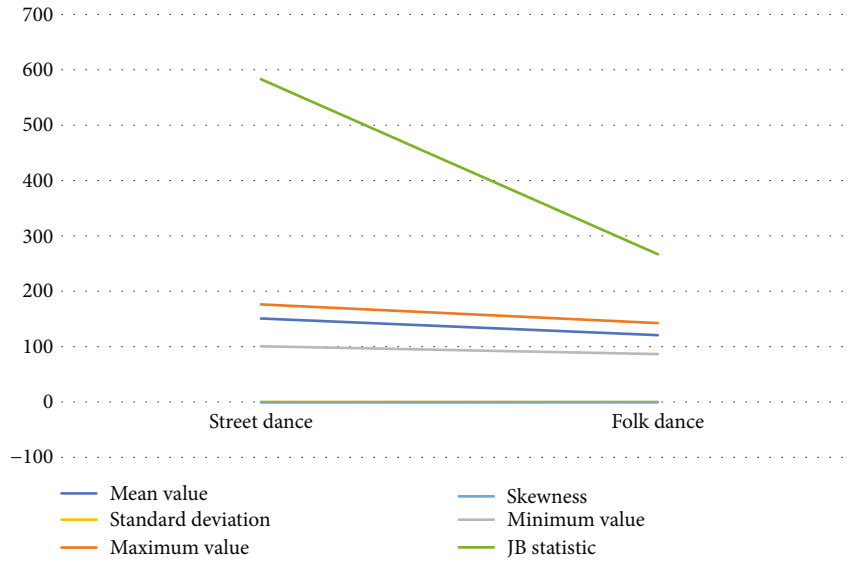


FIGURE 1: Descriptive statistical test of BPM sequences of street dance and folk dance.

TABLE 2: BPM and variation note sequential ADF unit root tests.

Variable	No intercept and no trend		With intercept		With intercept and trend	
	<i>T</i> -statistic	<i>P</i> values	<i>T</i> -statistic	<i>P</i> values	<i>T</i> -statistic	<i>P</i> values
	2.037026	0.9905	1.558638	0.5038	1.186690	0.9122
	0.311912	0.7758	1.796122	0.3829	1.619738	0.7854
	57.51557	0.0001	57.57892	0.0001	57.59223	0.0000
	75.32716	0.0001	75.32366	0.0001	75.32531	0.0001

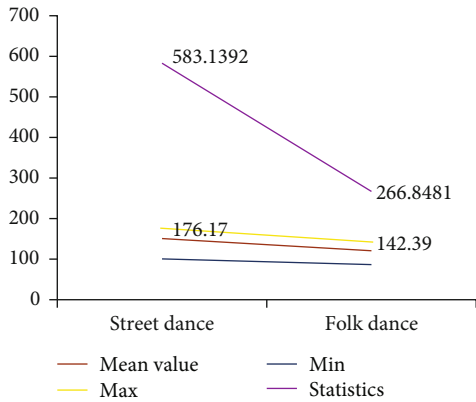


FIGURE 2: BPM and variation note sequential ADF unit root tests.

coherence, authenticity, and degree of matching with music that are higher than the score, showing that consumers are satisfied with the synthesized outcomes. The three indexes of street dance have the greatest ratings, as seen in the observation graph. The rhythm of street dance style movements is evident, and the amplitude of the movements is larger, whereas the amplitude of folk dance movements is often tiny, and it might be difficult for users to distinguish between a little movement and jitter data, affecting perception [22]. The poor synthesis findings of otaku dance compared to

street dancing are due to the greater diversity of otaku dance actions and lower concentration of actions, which makes it difficult to train and learn the action generation model in the action dataset developed in Chapter 3 of this research. Only one of the 42 users who took part in the scoring misjudged the styles of street dance and otaku dance, and the rest of the users' assessments were correct, as indicated by the optimal lag order test and cointegration test following the follow-up visit.

From the test results of maximum lag order 4, it can be seen that LR, FPE, AIC, SC, and HQ show that the optimal lag order is 3. According to the majority principle, 3 is chosen as the optimal lag order, and the VAR(3) model is established [23], as shown in Tables 4 and 5 and Figure 4.

As can be seen from Table 4, the original hypothesis of "no cointegration vector" cannot be rejected at the 10% level for either the trace statistic or the maximum eigenroot statistic, so the London Brent crude oil futures and gold future price series are not cointegrated [24].

From the JJ cointegration test, it can be seen that there is no cointegration relationship, so the VEC model cannot be established, so the VAR model should be established after smoothing the variables differentially. Since the difference variables *dlgf* and *dllco* are both smoothed, a VAR model can be established. The model is  $dlgf(t) = 0.000178 - 0.113479dlgf(t - 1) - 0.091914dlgf(t - 2) - 0.004051dllco(t - 1) + 0.005440dllco(t - 2) + \epsilon 1t$ .

TABLE 3: Comparison of choreographic changes of different dance styles.

Dance style	Music and dance matching	Coherence	Authenticity	Accuracy of style judgment
Street dance	4.39	4.18	4.15	97%
Folk dance	4.29	4.06	4.05	96%

#### 4. User Study

A multilevel choreography algorithm based on music and movement characteristics is proposed in this chapter, with the goal of improving the ensemble of music and choreographic motions. Music overall feature extraction and matching, local rhythm and intensity feature extraction and matching, and intermediate frame interpolation processes make up the algorithm. Based on the visual effect of the synthesized dance, the choreographic outcomes are visually assessed in order to analyze the algorithm's effectiveness and the effect of the synthesized dance. Experiment 6 is utilized to test if the hierarchical music and action feature matching method is effective; the dance synthesis impact is studied to see if the music and action feature matching algorithm based on rhythm and intensity features is effective [25].

Visual effects in qualitative studies can verify the algorithm's performance, but this indicator alone does not provide a complete quantitative evaluation of the trial outcomes. In the field of computer-assisted music choreography, it is difficult to scientifically and quantitatively analyze the choreographic effect, and there is no uniform objective and quantitative evaluation index, so subjective evaluation criteria are frequently used to examine the experimental results [26]. In this paper, 35 graduate students were invited to conduct a user experience study using a manual user rating method. In order to ensure that the users have certain aesthetic cognition of music and dance and sufficient musical sense and to ensure the reliability of the rating, a user ability test experiment was designed during the questionnaire survey. In the user ability test experiment, two musical dances from the training dataset were presented to the participating testers: one with music that matched the dance and the other with the same music that matched the other unmatched dance. The participants were asked to select the mismatched dance segments, and only those who selected the correct ones had enough musical sense to perceive the rhythm of the music and the movements and to judge the degree of matching the music and the movements. A novel framework for automatic music choreography is provided in this research in order to generate dance motions that are both novel and coherent and match the target music, as well as to ensure that the choreography system has appropriate robustness and generalization capacity. The framework is divided into four sections: model training and movement creation, choreography and synthesis, and dance visualization utilizing 3D character animation are the most critical steps, with model training and movement generation and choreography based on music and movement features being the most important [27], as shown in Figure 5.

In this study, we present a parameter management approach and a coherence-based motion filtering strategy to increase the authenticity and coherence of the generated motions. According to the experimental results, the mean value technique boosts the realism of the manufactured actions, and the coherence of the filtered action data is considerably improved when compared to the generated original action data. With the purpose of strengthening music and action unity and coherence, this work proposes a multi-level music and action feature matching method that combines overall feature matching with local feature matching. To match dancing movements, overall music features are used first, followed by rhythm and intensity characteristics to match local music-movement fragment features. When a control based on overall music characteristics is added to the final synthesis result, the speed and other qualities of each movement fragment are more consistent, and the entire choreography is more aesthetic [28]. In this paper, we look at the complete process of computer music choreography and propose a computer music choreography framework that provides a fresh solution to the problem. The framework includes a movement dataset construction module and a model training module.

The framework is made up of four modules: movement dataset building, model training and movement generation, dance choreography and synthesis, and 3D character animation visualization, all of which ensure the authenticity, uniqueness, and compatibility with the music of the dance fragments. Compared with the traditional algorithm, the synthesized choreographies are more novel and diverse, and the choreography system in this paper has stronger stability and generalization ability than the music-movement mapping model obtained by machine learning algorithm only. In addition, the user's requirements can be reflected in the choreography results, which makes the proposed choreography system more practical.

Although the algorithm proposed in this paper can obtain better computer music choreography effect and ensure the novelty and consistency of the choreographed movements as well as the conformity with the target music, the research on the direction of feature extraction, feature matching, and dance evaluation of music and movements is not sufficient. The shortcomings of this paper and the directions of subsequent work are mainly as follows: the existing research has less research on action high-level features, and the screening algorithm based on action features proposed in this paper mainly uses action bottom-level features. In future research, we can try to analyze the high-level features of the action; when measuring the match between local music and action, only the rhythm and intensity features of both are considered. In future studies, we can

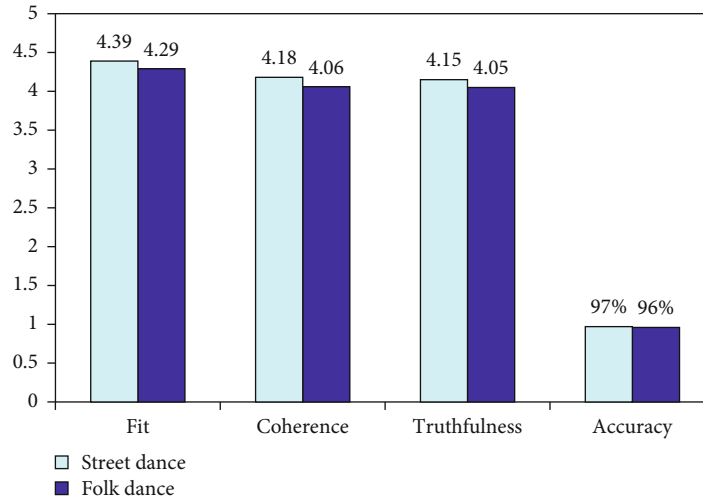


FIGURE 3: Comparison of choreographic changes of different dance styles.

TABLE 4: Optimal lag order test.

Lag	LogL	LR	FPE	AIC	SC	HQ
0	2496.306	NA	0.001263	-0.998521	-0.995912	-0.997607
1	34872.66	64713.82	$2.97e-09$	-13.95783	-13.95000	-13.95509
2	34909.9	74.41330	$2.93e-09$	-13.97114	-13.95809	-13.96657
3	34931.41	42.96391*	$2.91e-09^*$	-13.97815*	-13.95989*	-13.97175*
4	34934.62	6.403435	$2.91e-09$	-13.97783	-13.95435	-13.96960

TABLE 5: JJ cointegration test.

Original hypothesis	Trace statistic (probability)	Maximum characteristic root statistic (probability)
No covariance vector	8.424707 (0.4212)	5.976167 (0.6163)
There is at most one cointegrating vector	2.448539 (0.1176)	2.448539 (0.1176)

try to include other more abstract features common to music and movement, such as emotion and style; there is not enough research on methods to evaluate the effect of music choreography. In the existing studies, the effect of dance synthesis is often measured by visual effects, such as subjective ratings by professionals on snapshots of dance movements and synthesized dance videos. A common objective quantitative index for the assessment of the effect of music choreography has not yet been proposed, and further research is needed.

The goal of combining feature matching is to reduce the influence of the target song's overall qualities on choreography while also improving the quality, consistency, and harmony of music and movement. First, the target music's overall note density and beat per minute (BPM) of note density are extracted using a constant Q-transform for initial matching with features like movement speed, and then, local music and movement fragment data are matched using

rhythm and intensity. The multilevel feature matching algorithm is used to construct more thematic dances by synthesizing dance movement fragment sequences with more uniform features such as pace. A new solution is proposed by combining the hybrid density network-based motion creation algorithm with the multilevel music motion feature matching algorithm user control. A computer music choreography framework is designed to present a fresh notion for solving the challenge of computer music choreography. The framework, which includes a movement dataset construction module, a model training and movement generation module, a dance choreography and synthesis module, and a 3D character animation visualization module, can ensure the authenticity, novelty, and musical harmony of dance clips at the same time. Only action mapping is based on the projection model, which offers great stability and generalization ability when compared to music produced by deep neural networks. In addition, in the choreography



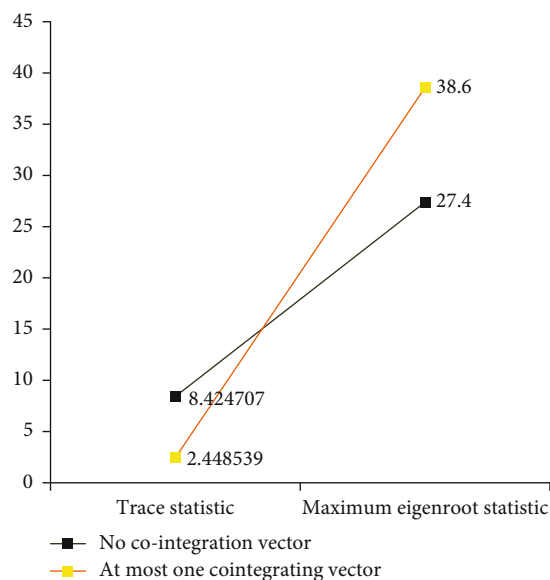


FIGURE 4: JJ cointegration test.

module, the user can control the movement speed and dance space of the local skeleton so that it can still dance with automatic computer choreography; in order to control the choreography results according to preference, this framework is more useful.

In order to improve the authenticity and diversity of computer-automated music choreography, this chapter proposes a motion generation algorithm based on a hybrid secret method degree network. First, it introduces that the construction of the music motion dataset is done by manual labeling based on the classification, and the motion data is preprocessed to obtain the feature representation of the model training data. Then, the action building is completed, and the generative model is trained to compare the effect of action generation under different training time. Then, three parameter control methods are introduced for the actions in the generation process, and the generated original actions are filtered based on the action consistency to ensure the consistency and authenticity of the validation data. The algorithm can generate sufficiently realistic and diversified dance moves, according to the findings of the experiments. The average method produces the most stable movements; as training time goes on, the human skeletal structure of the generated movements becomes more realistic, and the relative relationship between joints becomes more stable; the consistency-based movement filtering algorithm also achieves the expected effect, and the movement generation algorithm introduced in this chapter produces the best results for subsequent music and movement feasibilities, as shown in Figure 6.

The system can be divided into three phases: model training, motion generation, and music arrangement. The system uses prebuilt datasets to train the motion generation models, obtains motion generation models of different styles and speeds, and stores the models with optimal results. Before music choreography, the system uses various action

generation models to generate a certain number of action clips and builds various candidate action databases through coherence filtering. Users can choreograph music directly on this basis or generate their own candidate movements and then choreograph music. It is a flowchart for the use of model training, a flowchart for the use of action generation and screening, and a flowchart for music choreography based on a multilevel music and action feature matching algorithm. In addition, the system introduces user control in the steps of the overall music feature matching algorithm, provides a user control interface, and gives two optional methods: one is to use the system default parameters for action matching, and the other is for the user to set the local bone velocity threshold and spatial threshold of the action segment and then perform action matching. In other words, the system can adjust the matching results of music and movements according to the user's requirements for dance characteristics, thus adjusting the choreography results for targeted control according to the user's preferences. If the user wants the final choreography to have distinct movement characteristics of local body parts (arms, legs, etc.), he can set a higher bone speed threshold and order to match movement segments with bone speed greater than the threshold, as shown in Figure 7.

The feature extraction and matching algorithm of the music and action of the previous festival has obtained multiple action segments with the matching result of the target music, and the connectivity constraints are satisfied between adjacent segments. Based on this, this section will analyze the adjacent power responses to produce transition connection segments, solve the action mutation problem, and splice the action segments into a series of complete actions to complete the final dance arrangement. The action mutation discussed in this section pertains to the mutation generated by the action segment pony and its nearby actions; the segment is known as the action at the connection, and the fixed distance will cause incoherence of the immediately connected actions, impacting the dance's visual appearance. The intermediate frame interpolation algorithm is utilized in this section to interpolate  $K$  frames and action segments at the conclusion of action segment  $m$  based on the interpolation weights and to perform interpolation between the intermediate actions of  $n$  to generate the final interpolated action. This algorithm's interpolation action allows for a natural link of two action segments. Simultaneously, some of the properties of the prior action segment that ended the action are kept. The interpolated motions maintain movement continuity, but there may be unrealistic movements, such as foot sliding, and the  $K$  value should not be too high to prevent the interpolated movements from continuing too long and damaging the appearance.

We present a multilevel choreography algorithm based on music and action features in this research, with the goal of enhancing the harmony of efficient actions in music and choreography. The method includes steps for music and movement feature extraction and matching, local rhythm and intensity feature extraction, matching, and intermediate frame interpolation in order to assess the algorithm's effectiveness and the effect of the synthesized dance.

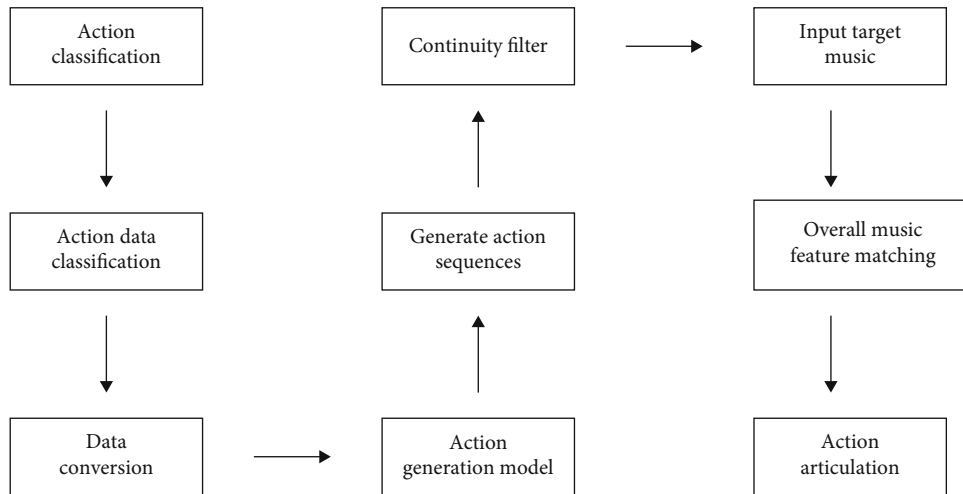


FIGURE 5: Framework of automatic music choreography system.

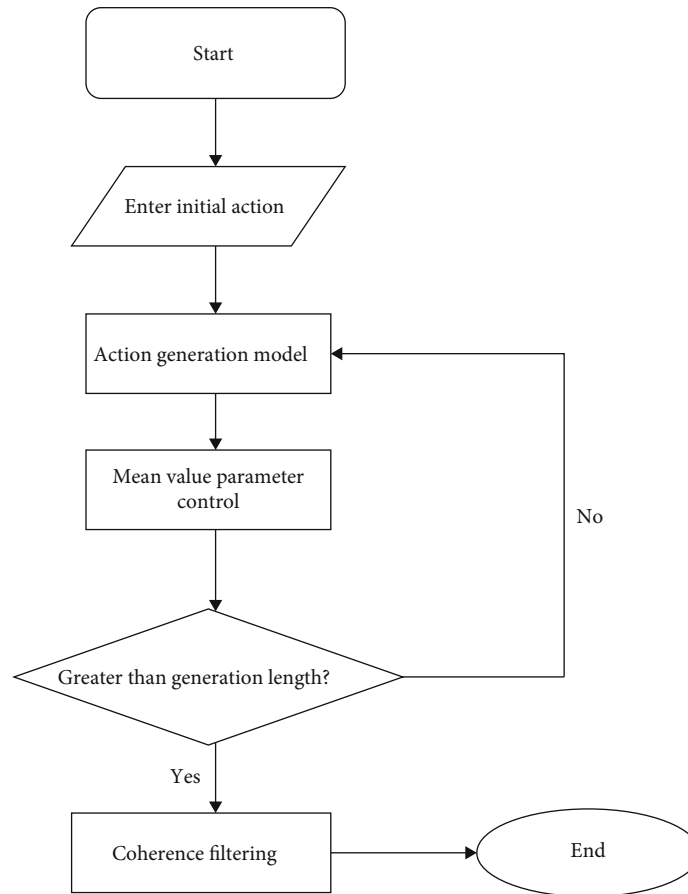


FIGURE 6: Motion generation algorithm of method degree network based on mixed secret.

The problem of computerized music choreography has been studied by previous authors and the corresponding computerized automatic sound system; music choreography system has been proposed. The systems can be broadly divided into two categories: one is based on Shirati (2006) [1] represented by traditional people designed by engineers of music and movement features and feature matching algo-

gorithms to select the target music from the constructed movement database, and the movement database usually consists of motion capture data; the other is based on Alemi (2017) [2] based on machine learning algorithms, directly constructing music dance mapping models, and generally, the mapping relationship between music and movement features is obtained through model training, so that the dance

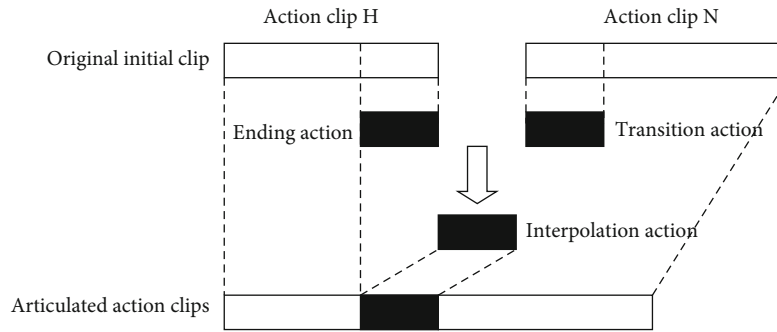


FIGURE 7: The system adjusts music and actions according to the user's requirements for dance characteristics.

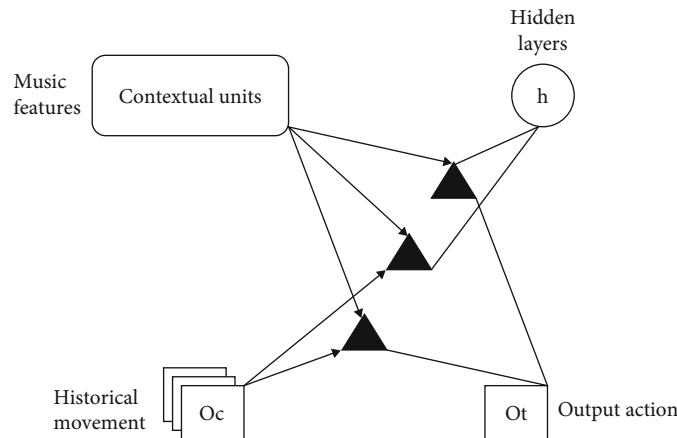


FIGURE 8: Music choreography system framework.

movements corresponding to the target music can be calculated, and the following figure shows the framework of the music choreography system, as shown in Figure 8.

In this paper, a new framework for automatic music choreography systems is investigated to address the shortcomings of previous work in order to make the generated dance movements both novel and coherent and to analyze and match them with the target music while ensuring that the choreography system has sufficient generalization capability. The framework mainly includes early dataset construction, model training, and training. The framework is divided into four parts: movement generation, choreography, synthesis, and dance visualization using 3D character animation; the core steps are model training and movement generation, as well as dance arrangement based on music and movement features.

Downscaling technical actions, Gaussian processes, Hidden Markov Models, and other machine learning-based motion generating algorithms have all been used in dance studies. Identify potential connections between musical and dance movement characteristics. High-dimensional properties of motions can be mapped to a low-dimensional space that can be utilized to capture potential correlations behind joint rotations in motion capture data using dimensionality reduction techniques. The approach, however, necessitates preparation and processing procedures such as sequence alignment and set data length, and the timeliness of the

motion data cannot be immediately examined for modeling, limiting its use to real dance movement data. Gaussian latent variable model process postvariation model can effectively summarize the changes in human cloud power, but it is not suitable for real-time model generation because of the large computational and memory resources required to overcome the limitations of these two previous models have been mentioned, but their ability to capture data changes is limited.

Music-driven dance generation should not only consider cross-modal sequence-to-sequence mapping but also emphasize the complexity of music-to-dance mapping. The relationship between music and dance movements is arbitrary, influenced by the performer's style and expertise and personality traits. In addition, the mapping relationship between music and dance changes from short-term synchronization of posture and rhythm to long-term synchronization, and the formation of dance patterns presents a complex hierarchy of temporal structures. From this perspective, the neural network has better expressive power than the HMM model. The patterns were learned using LSTM-1, and dance sequences were generated. They used six hours of contemporary dance data captured by Microsoft Kinect to train the model. The trained network can extract dance style (the expression of the dancer's movements), syntax (the language of the piece or choreography), and semantics (the general theme of the dance piece). However, the

algorithm does not provide any control over the process and results generated how to do it, and the whole process does not have any musical accompaniment. The structure of the conditional Boltzmann machine constrained Boltzmann machine (FCRBM) is suitable for controlling the properties of the generated data and allows generating operations in real time. Alemi (2017) suggests that the GrooveNet does not depend on the classification or segmentation of the audio signal FCRBM model can learn continuous cross-modal mapping from audio information to action data in an unsupervised manner. With only 23 minutes of music, FCRBM is trained using a small dataset of dance movements, and the resulting model can be independent, generating basic dance movements based on audio, and you can also learn and generate movements based on training songs. However, this does not have obvious limitations in the poor performance of unheard music and is not very practical and should propose a music-oriented dance synthesis method based on the LSTM model and autoencoder model. The model takes sound features as input and outputs the final dance composition by extracting the mapping between sound and motion features.

## 5. Main Results of the Paper

- (1) This work improves the realism and coherence of the generated motions by introducing a parameter control algorithm and a coherence-based movement filtering mechanism to the movement generating process. According to the results of the experiments, the mean value technique improves the realism of manufactured actions and improves the coherence of the filtered action data when compared to the generated original action data
- (2) This work presents a multilevel music and action feature matching method that combines overall feature matching with local feature matching in order to increase music and action unity and coherence. After the dancing motions were matched based on overall music characteristics, the local music movement fragments were matched based on rhythm and intensity. According to the trial results, adding a control based on overall music characteristics makes the pace and other features of each movement fragment in the final synthesis result more consistent and the overall choreography more aesthetic
- (3) This study examines the entire process of computer music choreography in detail and suggests a computer music choreography framework as a novel solution to the challenge. The framework is made up of four modules: movement dataset construction, model training and movement generation, dance choreography and synthesis, and 3D character animation visualization, all of which can ensure the authenticity, novelty, and musical compatibility of dance fragments at the same time. Compared with traditional algorithms, the synthesized choreography

is more novel and diverse, and the choreography system in this paper has stronger stability and generalization ability than the music-movement mapping model obtained by machine learning algorithms only. In addition, the user's requirements can be reflected in the choreography results, which makes the choreography system proposed in this paper more practical

## 6. Problems and Future Prospects

Although the algorithm proposed in this paper can obtain better computer music choreography effect and ensure the novelty and consistency of the choreographed movements and the compatibility with the target music, the research on the direction of feature extraction, feature matching, and dance evaluation of music and movements is not sufficient. The shortcomings of this paper and the subsequent future research directions are mainly as follows:

- (1) There is less research on action high-level features in the existing studies, and the action feature-based screening algorithm proposed in this paper mainly utilizes action bottom-level features. In the future research, we can try to analyze the high-level features of the action
- (2) In this paper, when considering the matching degree of local music and action, only the rhythm and intensity features of both are considered. In future studies, attempts can be made to include other more abstract common features of music and movement, such as emotion and style
- (3) This paper does not adequately examine the methods for assessing the effects of music choreography. At present, when assessing the effect of dance synthesis in existing studies, it is often measured through intuitive visual effects; for example, when assessing the effect of dance synthesis in currently available studies, it is often measured through intuitive visual effects, if professionals are invited to subjectively set music to snapshots of dance movements, synthetic dance videos, etc. The industry has not yet proposed general objective quantitative indicators to evaluate the effect of music choreography, and future research is needed

## Data Availability

The labeled datasets used to support the findings of this study are available from the corresponding author upon request.

## Conflicts of Interest

The author declares no competing interests.

## Acknowledgments

This research was supported by the Jilin Higher Education Scientific Research Project: Research on the practical reform of aesthetic education in colleges from the perspective of new media communication.

## References

- [1] A. Ns and B. Sf, "Data analysis of music preferences of web users based on social and demographic factors[J]," *Procedia Computer Science*, vol. 198, pp. 730–735, 2002.
- [2] N. N. Siphocly, A. Salem, and E. El-Horabty, "Applications of Computational Intelligence in Computer Music Composition[J]," *Egypt's Presidential Specialized Council for Education and Scientific Research*, vol. 1, 2021.
- [3] X. Yuehua and L. Wei, "Computer analysis and automatic recognition technology of music emotion," *Mathematical Problems in Engineering*, vol. 2022, Article ID 3145785, 9 pages, 2022.
- [4] Z. Xinhao, "The practice of string sound source in computer music production—take pop music production as an example," *Art and Performance Letters*, vol. 2, no. 4, 2021.
- [5] S. Gang, "Research on architecture for long-tailed genre computer intelligent classification with music information retrieval and deep learning," *Journal of Physics: Conference Series*, vol. 2033, no. 1, article 012008, 2021.
- [6] J. Xiangli, "Computer music query by humming considering subsequence matching algorithm," *Journal of Physics: Conference Series*, vol. 2037, no. 1, article 012028, 2021.
- [7] L. Maxence, "An analysis of "nyx" (2017), a computer music work by Kerry Hagan," *Computer Music Journal*, vol. 44, no. 2-3, pp. 118–132, 2020.
- [8] Y. Hong, "Research on the application of computer music software in piano rhythm teaching," *Journal of Physics: Conference Series*, vol. 1992, no. 3, article 032072, 2021.
- [9] L. Mina, "Research on the application value of orff music education system in college music education based on computer new media technology," *Journal of Physics: Conference Series*, vol. 1992, no. 3, article 032032, 2021.
- [10] X. Pan, "Research on the application of computer music software in college traditional music course," *Journal of Physics: Conference Series*, vol. 1992, no. 2, article 022178, 2021.
- [11] C. Wei, "Research on school-enterprise cooperation training model of music performance professionals in colleges and universities based on repertoire creation and computer multimedia technology," *Journal of Physics: Conference Series*, vol. 1992, no. 2, article 022033, 2021.
- [12] Y. Yunyu, "Research on the reform of vocal music teaching by computer multimedia technology," *Journal of Physics: Conference Series*, vol. 1992, no. 2, article 022089, 2021.
- [13] H. Elisabeth, "Affective brain-computer music interfaces—drivers and implications," *Frontiers in Human Neuroscience*, vol. 15, 2021.
- [14] W. Lingdan, "Application of computer music technology in college music teaching[J]," *Journal of Physics: Conference Series*, vol. 1915, no. 3, article 032073, 2021.
- [15] C. Shi, "Research on computer generation technology of fractal music," *Journal of Physics: Conference Series*, vol. 1915, no. 4, article 042015, 2021.
- [16] X. Shuai, "Research on the visualization of music stage performance based on the context of computer digital media," *Journal of Physics: Conference Series*, vol. 1915, no. 2, article 022027, 2021.
- [17] X. Ning, "Design of online popular music teaching platform based on embedded computer network and virtual reality," *Journal of Ambient Intelligence and Humanized Computing*, 2021.
- [18] L. Jie and L. Liang, "A study on the application of computer music in mass music tutoring," *Journal of Physics: Conference Series*, vol. 1865, no. 4, article 042051, 2021.
- [19] F. Yuebin, "Application of computer technology in vocal music teaching," *Journal of Physics: Conference Series*, vol. 1881, no. 2, article 022050, 2021.
- [20] L. Chuanli, W. Lizhi, and C. Libin, "Research on the application of computer technology in music creation," *Journal of Physics: Conference Series*, vol. 1883, no. 1, article 012031, 2021.
- [21] Z. Meili and H. Kewen, "Research on the application of computer music making technology in new media environment," *Journal of Physics: Conference Series*, vol. 1871, no. 1, article 012142, 2021.
- [22] R. Mihaela and C. Ciprian, "Discovering music cryptograms in the works of Viorel Munteanu through computer aided methods," *Artes. Journal of Musicology*, vol. 23, no. 1, pp. 165–173, 2021.
- [23] K. C. Tseng, "Electrophysiological correlation underlying the effects of music preference on the prefrontal cortex using a brain-computer interface," *Sensors*, vol. 21, no. 6, p. 2161, 2021.
- [24] W. Libo, "Research on the reform of music education mode in colleges and universities based on computer music technology," *Journal of Physics: Conference Series*, vol. 1744, no. 3, article 032149, 2021.
- [25] S. Rui, "Research on the application of computer multimedia music system in college music teaching," *Journal of Physics: Conference Series*, vol. 1744, no. 3, article 032214, 2021.
- [26] S. Yue, L. Yang, and S. Liu, "Application of computer technology in professional music teaching in colleges," in *Basic & Clinical Pharmacology & Toxicology*, vol. 128, WILEY, 111 RIVER ST, HOBOKEN 07030-5774, NJ USA, 2021.
- [27] I. Fujishiro and A. Kobayashi, "[Invited paper] Ambient music co-player: generating affective video in response to impromptu music performance:special section on advanced imaging and computer graphics technology," *ITE Transactions on Media Technology and Applications*, vol. 9, no. 1, pp. 2–12, 2021.
- [28] L. Ding and D. Lulu, "Application of computer music production technology and computer multimedia system in college sight-singing and ear training," *Journal of Physics: Conference Series*, vol. 1648, no. 2, article 022174, 2020.

## Research Article

# A Forward-Looking Study on the In-Depth Development Planning of Information Technology into Teacher Education

**Chunlan Zhang** 

*Department of Marxism, Zhengzhou Railway Vocational and Technical College, Zhengzhou, Henan 450052, China*

Correspondence should be addressed to Chunlan Zhang; [zhangchunlan0511@163.com](mailto:zhangchunlan0511@163.com)

Received 26 May 2022; Revised 6 July 2022; Accepted 11 July 2022; Published 28 August 2022

Academic Editor: Wen Zeng

Copyright © 2022 Chunlan Zhang. This is an open access article distributed under the Creative Commons Attribution License, which permits unrestricted use, distribution, and reproduction in any medium, provided the original work is properly cited.

Teacher professional education development is actually another type of development that crosses over into a category of teacher training development that encompasses two other types of teacher training—one of which is formal and the other is informal teacher training. The other approach to teacher professional development is quite different from the professional development of professional education. The focus of the professional development of teachers is a dynamic process of development in which teachers take the initiative, actively, and consciously pursue the direction of professional development of teachers. Therefore, how to observe and study the direction of teachers' professional development from the perspective of teachers is an urgent problem that needs to be studied and solved. The professional development of teachers should be combined with their own social and teaching lives. In addition, information technology should be integrated into teachers' daily teaching life, so that it can be used as a tool to support teachers' professional development. Information technology has gradually become a tool and a means that teachers cannot do without in their teaching lives, so it is important to study and think about it from various aspects, such as the teaching process and teachers' growth experiences, and to continuously study teachers' professional development. Therefore, it is necessary to study how information technology can be used well by teachers and used by teachers to become a useful tool in teachers' educational and teaching work from various aspects. This paper first argues that the main goal of teachers' professional development is to gradually grow into expert teachers, while the main content of teachers' professional development is to understand practical knowledge, and the specific tool used by teachers in teaching is the application of social software support that can support teachers' professional development (Romanowski and Alkhateeb, 2022). This paper envisages that information technology can be integrated into the entire teaching environment and the teaching process of teachers, as a tool and a means to make the content of teachers' teaching more concise and clear. Through the use of information technology and other tools, teachers can gradually identify what they need to improve and add to their teaching process, lay the foundation for their future development, and pave the way to become better teachers with a clearer plan for their future development.

## 1. Introduction

On April 6, 2017, four national departments, including the Ministry of Education and the National Development and Reform Commission, released a new plan, the “Plan for Universal Access to High School Education (2017-2020)” (hereinafter referred to as “the Plan”). The Plan proposes that by 2020, our country will achieve universal access to senior secondary education; it proposes that by 2020, all provinces in the country will have a gross enrollment rate of more than 90 percent in senior secondary education. And through the

unified planning and layout of educational resources, we can effectively promote the quality and balanced development of regional education, thus giving a strong impetus to the modernization of regional education. Hardware support is in place, and the software must also follow. The important goal of education reform and development is to improve the quality of education is a strategic goal to achieve now and in the very long term. To improve the quality of education, in the national education development, “Thirteenth Five-Year Plan” outline has been highlighted [1, 2]. This is an important deployment made by the party at the strategic height of building a

moderately prosperous society in all aspects. The rise and fall of the country's fortunes are tied to education; education is a major plan, teacher-oriented. This saying has been passed down since ancient times, so we can see that only with good teachers, students will receive a good education; only with good teachers, schools can do a good education to the satisfaction of the people; only with good teachers, in order to better promote the development of students. And can greatly improve the quality of education is the fundamental to the good development of teachers' own professional. That is, to improve the quality of education must improve the level of professional development of the teaching force. Since the professional development of teachers was proposed in the 1960s, people have become more and more concerned about the quality of teachers themselves and after years of theoretical research and practice to explore the professional development of teachers themselves [3]. In the 1980s, teacher professional development has become an important issue of common concern for educational researchers in many countries around the world, and it has gradually become a more important research hotspot worldwide. In China, it has also been clearly proposed to strengthen the construction of the teaching force, and in the "National Medium and Long-term Education Reform and Development Plan (2010-2020)," it is clearly proposed to gradually strengthen the construction of the domestic teaching force, which includes the construction of a high-quality teaching force, constantly improving the teachers' development. This includes building a high-quality teaching force, improving the professionalism of teachers, gradually improving the status and treatment of teachers, and improving the management system of teachers. It is also clearly stated in the outline that the qualifications of teachers should be more strictly managed, the moral character of teachers should be improved, the professional competence of teachers should be improved, the structure of teachers should be more reasonable, and the teaching staff should be energetically specialized with high quality. We also continue to improve the training system of teacher education, do a good job of teacher education training planning, and constantly optimize the teachers and improve the professional level and teaching ability of teachers in the team structure [4]. Along with the upgrading of the teaching force in the traditional sense, the professional development of teachers has not been able to keep up with the development requirements of the new situation. In the original teaching environment, it was easy for teachers to neglect their own values and to ignore the deeper aspects of their professional development, such as the meaning of self-actualization, which could cause teachers to lose themselves in passive development, while neglecting the role of teachers' professional development in promoting themselves was not conducive to long-term sustainable professional development [5]. In the current educational environment, this situation has been changed—a new view of professional development that emphasizes the importance of teachers themselves in the process of professional development and their own personal development and the realization of their own values has been gradually introduced to people. This emphasis on the self-worth of teachers is a manifestation of the "teacher," and it is believed that teachers' active participation in teaching activities is an

essential condition for their professional development [6]. Teacher-centered professional development, on the other hand, focuses on teacher development to provide quality in education and teaching, and on the other hand, it is the basis for the overall development of students. Teacher-centered professional development emphasizes the improvement of teachers' internal structures and the realization of their own self-worth. This requires not only the teachers' own efforts but also the support of the relevant teaching departments. Since school is not only a place for teachers to teach and educate but also a place for teachers to achieve professional growth and happiness, schools need to build a set of effective management models to help teachers feel the value and meaning of professional development and educational work in their educational practice, experience the creativity of education in their daily work, and gain achievement and happiness in their own development. Only when teachers find their own professional development path and become more and more interested in education, can we effectively promote the promotion of teachers' titles and the selection and development of backbone and cultivate teachers' ability to teach in high-quality classrooms, thus improving the construction of school teachers and the quality of school operation, and promoting the sustainable development of schools [7].

In the context of the new era, China's basic education development goal from "basic balance" to "quality balance," regional teaching and research to lead and drive the professional development of teachers in the region, which is of great educational significance to improve the overall level of the teaching force and improve the efficient development of local education. The traditional regional teaching and research focus on subject teaching and research, relying on experience, the research perspective is not macro, the research process is not transparent enough, a single perspective leads to the inability to form a systematic teaching research and is responsible for teaching and research management and guidance of the teaching, and research office is subordinate to the education administration, its management with certain administrative responsibilities, teaching and research managers in the exercise of power is quite strong administrative color.

It is the consensus of the government, society, experts, and scholars that teacher education must be innovative [8]. The need to improve the professionalism of teachers in the future, the need to further adopt a science education strategy, and the future trend of teacher development are strategic requirements for the professional development of the teaching profession. In recent years, many scholars have made a lot of thoughts and researches on the professionalization of the teaching profession, the improvement of teachers' professionalism and the improvement of teachers' quality, and the structural knowledge of teachers' teaching. We can see that the development of professionalization of the teaching profession is the trend, and the problem we are facing now is how to improve the professionalization of teachers. In the 21st century, China has gradually entered the world of the Internet, and the importance of information technology can be imagined, and it is obvious that it is the main trend of the development of the world and the development of the country and society [9]. The level of informationization has gradually become an

important indicator to measure the level of modernization of a country and its comprehensive national power. One of the major strategic measures to promote the integration of national economic construction and information society development in China is to actively promote the development of information society in China as a whole, to continuously improve the overall scientific and technological information literacy of our people, and to gradually cultivate high-quality information technology construction personnel, which is also a basic strategy for the development of information society construction as a modern country. The teacher education informatization project is also a major basic force to promote the development and progress of China's education informatization, from which we can find that the teacher education informatization project is actually not only both a major component of China's education informatization project but also the mainstay of the development of China's teacher education informatization project [10]. The current campus informatization construction has begun to cause the thought, education, concept, content, and methods of teachers and students in all schools. As you can imagine, if you want to achieve the continuous development of information technology in schools, training students' level of information technology, the establishment of a high-quality information technology teacher team is urgent and of the utmost importance. In the current situation, there are major problems in the process of training teachers, mainly in teacher training colleges, such as the weakness of information infrastructure and information technology resources. It can be seen that modern information technology and educational technology are not fully popular in school teaching and education, and they are not widely used in teacher education, which is difficult to adapt to the development of modern teaching.

The development of teaching and research requires innovation to ensure the professional development of teachers to keep pace with the times. The in-depth application of information technology in the field of education has brought about a great impact on the transformation of education and teaching, and regional teaching and research supported by information technology is a new requirement for reform and development and will be the new norm for teaching and research in the new era [11]. Especially in the special period of the nationwide outbreak of the epidemic at the beginning of 2020, teaching and research supported by information technology brings convenience and effectiveness to the teaching and learning work of primary and secondary schools in that period. According to the author's literature survey, although there are few studies on the integration of information technology and regional teaching and research and certain research results have been achieved, there is still a need for further research on the specific strategies of macromanagement, operational guidance, and microimplementation of regional teaching and research supported by information technology. The purpose of this study is to explore new mechanisms and models for regional teaching and research, to improve efficiency and effectiveness, to drive the professional development of teachers and the upgrading of the teaching force in the region, and to promote the quality improvement and connotation development of regional education. Information technology is an important opportunity to promote the development of teaching and

research and enhance the professional level of teachers. Information technology has entered the whole process of teachers' teaching and research and has begun to play an important role, especially in the special time of "school closure" at the beginning of 2020, when information technology-supported teaching and research plays an important role in the normal operation of education and teaching work [12]. How to face the new opportunities and challenges of teachers' teaching and research in the new era and situation requires researchers to continuously strengthen the exploration of new models and new paths for the integration of regional teaching and research with information technology. It is worth paying attention to the fact that in the research process, neither purely "only technology" nor isolated "do teaching and research." In the future, while technology is constantly changing, how to maintain innovative thinking to promote the integration of information technology and regional teaching and research development and application and how to make the effective implementation of regional teaching and research under the support of information technology and sustainable implementation, still need more and more in-depth theoretical and practical research.

## 2. Review of Domestic and International Literature

Due to the urgent needs of the current national education development and reform, the content of the new curriculum reform has become more and more extensive [13]. The modern computer technology is also a relatively new educational technology tool, which is gradually entering the society and school education, and has started to be one of the main tools for teachers to teach in the classroom and a major means to assist students to learn knowledge independently. In the course of the development of education, modern education technology, especially information technology, is being used more and more widely in the modern education process, and it is necessary to adapt to the development of education in the modern education process. It is necessary to create a solid foundation for the realization and change of the teaching methods of modern education technology. Since the 20th century, the development of teacher professionalism has become an important basis for improving the quality of education and teaching, and many countries have made the improvement of teachers' professionalism and the strengthening of the teacher education team an important breakthrough direction for improving education and teaching [14]. The British educationalists have put forward six requirements for the standard of teacher professionalism. The educator Stenhouse put forward the famous three ways of teachers' professional self-development. The teacher's own continuous learning to observe and analyze other teachers' teaching experiences, and finally, the testing of existing theories in the teaching process. The concept of teacher professionalism was explicitly introduced in American education, and it was believed that the basis for improving the quality of teaching was to establish the status of professionalism in teaching and to measure this professionalism clearly and establish clear criteria for measuring it. The emergence of professional development schools in the United States in the 20th century is considered to have



provided a great innovation in the direction of professional training and development for teachers. In recent years, some experts and educational scholars in China have also conducted systematic research on theoretical and practical aspects of classroom professional development. Professor Gu Lengjia has developed the “Action Education Research” program, which focuses on research on learning content, school-based teaching and research, school-based training, and lesson examples. Professor Ye Lan believes that teachers’ professionalism should be improved from the following aspects: improving teachers’ professional philosophy, improving teachers’ professional knowledge structure, and improving teachers’ professional competence structure. The Textbook Institute of the Capital Normal University, on the other hand, has drawn on some international examples of teacher education reform, especially the practice of teacher professional development schools in the United States, to explore a new approach to teacher professional development and set up a teacher education development school in Beijing [15]. The above content of this dissertation, therefore, systematically discusses the incorporation of information technology into teacher education and explores the impact of information education on the in-depth development planning of teacher education.

### 3. Research Methodology

**3.1. Research Methodology.** Firstly, through literature review and synthesis, we gain an in-depth understanding of the current situation of regional teaching and research under the support of information technology [16]. On the basis of identifying the research subjects, we analyze the current situation of the research subjects through questionnaires, in-depth interviews, and fieldwork, summarize experiences, analyze problems, draw on advanced experiences and practices, and propose improvement strategies for regional teaching and research under the support of information technology on this basis. The specific technical route is shown in Figure 1.

**3.2. Research Content.** This study takes District X as the main research object to understand the current implementation situation of regional teaching and research supported by information technology in District X, summarizes experiences, analyzes problems, and investigates improvement strategies for the integration application of information technology and regional teaching and research in the region under the guidance of relevant pedagogical and management theories and for different dimensions of research and analysis [17]. This paper will analyze and explore the following three parts.

Firstly, through the study of a large amount of literature to understand the current situation of research on regional teaching and research supported by information technology, we will analyze the impact on teachers’ professional development from the perspective of “teaching,” and the impact on teaching quality from the perspective of “learning” [18]. The first level is to analyze the impact on teachers’ professional development from the perspective of “teaching” and the second level is to analyze the impact on teaching quality improvement from the perspective of “learning” and to summarize the theoretical methods of integrating information technology into regional

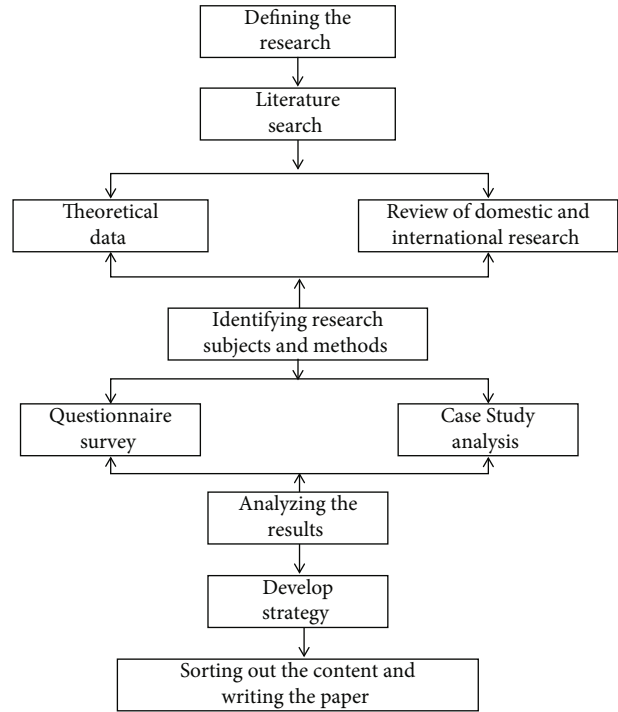


FIGURE 1: Specific technical route.

teaching and research through theoretical research on information technology and regional teaching and research.

Second, through an in-depth investigation of the “Internet +teaching and research platform” in District X, field surveys and interviews with educational administration departments, business guidance departments, and schools and teachers in District X, we understand the practice of integrating information technology and regional teaching and research in District X and analyze its experiences and problems, dissect its types, forms, and activities. We analyzed their experiences and problems; analyzed their types, forms, and activities; and constructed an effective mechanism for regional teaching and research supported by information technology [19].

Finally, we will comprehensively study and analyze the actual cases of integration of information technology and regional teaching and research, explore the effective methods of integration of information technology and regional teaching and research, extract the success factors, summarize the experiences and reflect on the problems, and provide some improvement plans or strategies for this study on the basis of case analysis and theoretical guidance.

#### 3.3. Research Methods

**3.3.1. Literature Research Method.** Through the content analysis, measurement analysis, and reading of relevant literature, we analyze the current situation of research on regional teaching and research in basic education and the role and impact of information technology in it, find the theoretical basis, organize the relevant activity data, and grasp the theoretical and practical situation more comprehensively, so as to clarify the feasibility and necessity of the research and determine the focus and direction of the research.

**3.3.2. Research Method.** In this study, a questionnaire survey will be conducted among teachers in the field of basic education in District X. Field interviews will also be conducted with administrators, business instructors, school administrators, and teachers in the field of basic education in District X to systematically understand the situation of teachers in the region with regard to regional teaching and research and the role and influence of information technology on regional teaching and research, so as to provide a clear data basis and reference for the subsequent study.

**3.3.3. Case Study Method.** This study will be conducted on existing practice cases to provide a final reference strategy for the model and strategy of combining regional teaching and research with information technology.

## 4. Results and Discussion

Educational teaching research is a feasible path to improve teaching and learning and an effective way to promote teachers' growth. Educational teaching research has an important position in the educational work as it plays the role of regulation, standardization, promotion, and enhancement [20]. Under the wave of the new round of technological reform and industrial revolution, education forms, education connotations, and education modes are facing changes with the brand of the new era, and educational research work should keep up with the times, grasp opportunities, and follow the trend based on the new situation and new tasks. Therefore, in the context of the new era, to carry out regional teaching and research with the support of information technology, to promote the overall professional development of regional teachers, and to promote the improvement of teaching standards in the region are a revolution that is bound to occur in line with the torrent of the times [21]. Based on the profound understanding of the above issues, District X has started to carry out a practical project of regional teaching and research supported by information technology since 2018.

The author conducted formal and informal interviews with administrators of the administrative department of the X District Bureau of Education and Sports, teaching and research administrators, IT administrators, and some school principals, teaching and research leaders, and some teachers at different levels in the district in order to study the practice in X District in depth, and the specific contents of the interviews were divided into administrative administrators, teaching and research personnel, and teachers according to the different interviewees. The specific content of the interviews was divided into three categories according to the interviewees: administrative staff, teaching and research staff, and teachers, mainly focusing on the conceptual thinking, institutional construction, measures, and experience of the project's implementation, and learning about the problems, difficulties, and development directions in the implementation process. In order to gain a deeper understanding of the specifics of the implementation of regional teaching and research in the district, the author conducted a questionnaire survey, which focused on the actual situation, teachers' expectations, and difficulties in

carrying out IT-supported regional teaching and research in the district [22].

When conducting the survey and interviews, based on the principle of diversity, and on the basis of active communication and discussion with the managers of the District Bureau of Education and Sports, seven schools were identified as interviewees, which included four types of schools: elementary schools, junior high schools, nine-year systems, and high schools, and the schools were located in three different regions, including town centers, rural areas, and remote villages. In the interviews, we learned about the development of teaching and research in District X, the origin and development of regional teaching and research with the support of information technology, and the current situation (Figures 2 and 3). During the survey, 400 questionnaires were distributed to teachers in the district, and 396 valid questionnaires were collected [23].

**4.1. Planning Concept of Regional Teaching and Research in District X with the Support of Information Technology.** It is a systematic project to carry out practical work from a district-wide perspective, which requires planning and guarantee at the macrolevel, as well as good guidance and overall promotion at the mesolevel, and application practice at the microlevel. In operation, different objects at different levels need to work together and pay; in content, it is necessary to consider both the overall work and the actual needs of individuals; in time, it is necessary to have both long-term development plans and short-term implementation initiatives; therefore, the X District Bureau of Education and Sports conceived and planned specific and feasible development goals, development ideas, and development stages.

**4.2. Set the Development Goals of Regional Teaching and Research Supported by Information Technology.** On the basis of definite development ideas, District X also set clear goals for the development of this work. Only under the guidance of the goals can the development direction and specific steps be more clearly defined [24]. The development goals are as follows:

- (1) Under the guidance of the administrative department of education management, take organizational guarantee as the core, fund guarantee as the basis, and establish and improve the work implementation mechanism as the key to ensure the effective development of the work
- (2) Take the lead of the teaching and research business guidance department to establish the "Internet + Teaching and research platform," with project construction as the first step and activity development as the guarantee, establish the business guidance mechanism to ensure the effective development of work
- (3) With application practice as the guiding ideology and network learning space as the platform, build research and study communities of different disciplines and projects, deepen application effects, establish long-term mechanism, and ensure the normal development of work. The ultimate goal of regional teaching and research supported by information

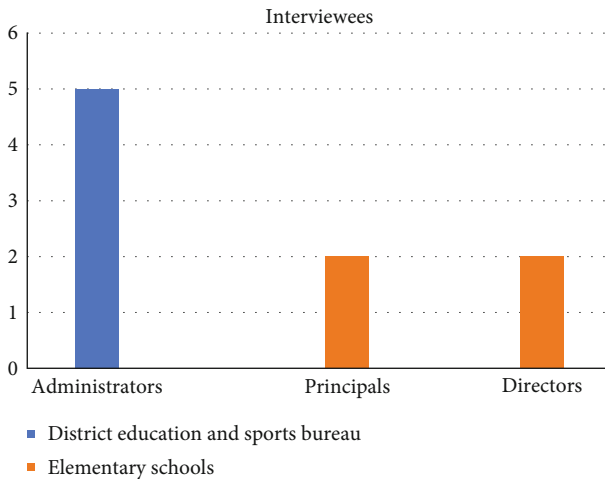


FIGURE 2: Number of interviewees.

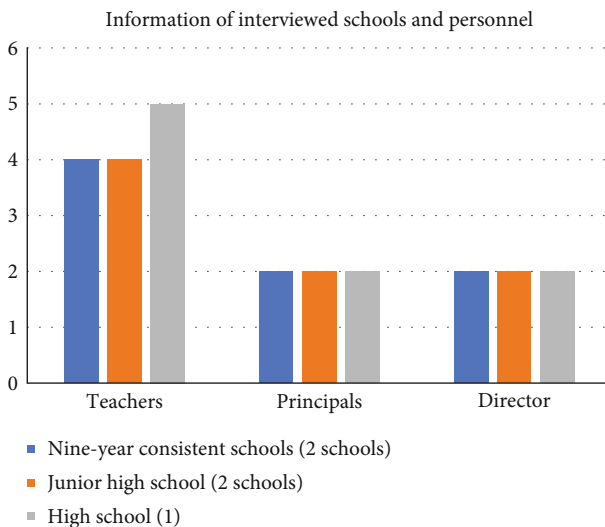


FIGURE 3: Information of interviewed schools and personnel.

technology is to effectively bring professional development and ability improvement of teachers and promote balanced development under the joint promotion of administrative guidance, business guidance, and application practice [25]

**4.3. Determine the Development Ideas of Regional Teaching and Research Supported by Information Technology.** In traditional areas of the existing research on the basis of how to apply information technology, how to better the information technology in the research into the area, giving play to the role of its application, makes a combination of both good benefit and needs to have a clear development ideas, therefore the development of the area under the information technology to support the research idea, on the basis of many research after the X area. According to the actual situation of education in this area, the development ideas of six specific operations at three levels are determined, as shown in Figure 4 [26].

**4.4. Formulate the Development Stages of Regional Teaching and Research Supported by Information Technology.** In order to better complete the work tasks and systematically carry out the work, the Education and Sports Bureau of District X formulated specific development stages according to the development ideas and goals of the work [27].

(1) The early exploration stage X area from the bureau set up a working group, the literature, collect data, to discuss work significance, background, and feasibility of writing development planning and implementation plan, to teach department lead, establish the platform based on the research of information technology, training, learning, and using the two joint as the pilot development under the information technology support intercollegiate research, sum up experience. Based on the above work, the preliminary exploration of regional teaching and research supported by information technology is completed, making practical preparations for the subsequent implementation stage

(2) Implementation and application stage

On the basis of the work carried out in the pilot schools, the implementation will be gradually promoted to the whole district. The teaching department organizes teaching and research staff, famous teachers, and backbone teachers as the core force of business guidance and carries out multiple projects and activities for in-depth research and timely summary and sharing by combining online and offline mixed methods [28].

(3) Deepening the popularization stage

On the basis of the existing work, further deepen and summarize, in the level of education administration, strengthen the administrative leadership, do a good job of job security. At the level of business guidance, overall planning and guidance should be given according to the feedback from pilot projects and popular implementation and in combination with projects and activities with more practical benefits. In the application practice level, further explore the practical experience, reflect on the deficiency, and improve the strategy and summarize the long-term mechanism of sustainable application [29].

(4) Innovative development stage

On the basis of the expected results, a scientific and comprehensive summary is carried out to further explore the depth of practice, consider the combination of new technology and new teaching and research theories, and constantly seek new development breakthroughs to improve the theoretical significance and practical benefits of the work.

**4.5. Practical Measures of Regional Teaching and Research in Area X Supported by Information Technology.** In order to ensure the smooth development of this work, the Education and Sports Bureau of District X insists on doing a good job

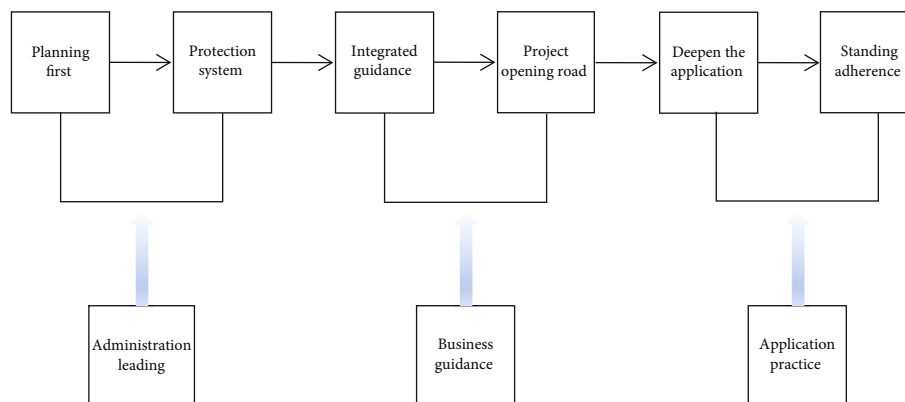


FIGURE 4: Ideas of teacher education development supported by information technology.

in administrative guidance, establishing and improving the work guarantee system and improving management efficiency.

#### 4.5.1. Operation and Promotion Mechanism Optimize Business Guidance and Promote Collaborative Development

(1) *The Teaching Department Has Established a Regional Teaching and Research Platform of “Study cloud + Workshop”.* X area of teaching according to the research department learned that teachers’ needs and their own management and guidance, and technology companies have developed the multifunction such as management, guidance, and application of “Internet +” research platform, the platform to build the two levels of four dimensions of the system platform, the first level from the education management level, and build the application system of two dimensions. In the form of “research cloud,” the whole process of teaching and research management system and the business guidance system combining school-based teaching and research with regional teaching and research are set up. The second level is from the level of teachers [30]. In the form of “workshops,” a platform for teaching and research activities is set up and a digital resource system is cobuilt and shared. The “Internet +” teaching and research platform in ZONE X has a clear structure and comprehensive functions, providing strong information support from the process management of teaching and research activities, interschool business guidance, regional research and training management, teachers’ teaching activities, teaching and research activities, exchange and discussion, and results display, etc. (Figure 5). It provides a service platform for teachers to carry out teaching and research activities within the region, across schools and across disciplines, build and share resources, exchange, and discuss, so as to comprehensively improve the level of regional teaching and research.

(2) *Create a New Teaching and Research Workshop System of “Regional+Central School+Famous Teachers”.* With the help of information technology, District X has created a new teaching and research system of “regional+central school+famous teachers.” First of all, relying on the main school of the joint school as the central school, we have built the “regional+central school+branch” form of mutual aid and collaborative teaching and research under the information

technology environment, changing the traditional offline teaching and research activities, the central school based on information technology, synchronous teaching and research activities within the joint school under the network environment, using synchronous classroom, video conference, project workshops, and other rich forms of teaching and research activities. In addition to effectively preserving resources for teaching and research activities, the center also avoids teachers’ inability to participate in activities due to long distances and time conflicts, which effectively broadens teachers’ participation. In addition, regional teaching and research workshops, school-based workshops, and master teacher workshops have been constructed, respectively, in which regional teaching and research workshops are created by the regional subject teaching and researcher, assisted by regional subject master teachers as administrators, and initiated by the teaching and research office in a task-driven manner in the region for full exchange of subject teachers and full participation in teaching and research activities. School-based workshops are created by the school’s teaching and research staff, assisted by the school’s subject teachers or grade level leaders as administrators, and led by the school’s teaching and research office in a task-driven manner for the whole school’s teachers to participate in collective teaching and research activities. Master Teacher Workshop is a teaching and research activity created freely by regional master teachers to give full play to the advantages of master teachers’ resources and promote the sharing of high-quality educational resources in the region (Figure 6).

(3) *Establishing a Regular Mechanism to Deepen Application Guidance and Lead Effective Growth.* In the process of teachers’ application practice in District X, in order to form a normal application status quo, District X has carried out a number of specific projects in pilot schools to deepen the application, so that the regional teaching and research supported by information technology can achieve its development goals.

(4) *Popularization of Online Learning Spaces.* Each teacher in District X has established his or her own online learning space, where teachers’ teaching resources and expertise can be stored and aggregated. Teachers can store all the resources needed for teaching, including courseware, audio and video, lesson plans,

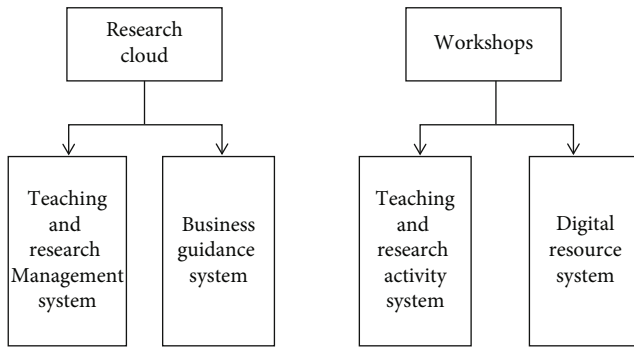


FIGURE 5: "Internet"+teaching and research activities.

and other data effectively, which effectively reflects the whole process of lesson preparation and effectively stores lesson preparation materials. It is also possible to use the recording function in the space to record the whole process of teachers' lessons, to make self-criticism and reflection after the lessons, and to communicate with other teachers on the online learning space, effectively generating, recording and sharing teachers' practical materials before, during and after the lessons.

(5) *Building Various Teacher Training Communities.* In the process of teachers' application, District X has built several teacher training communities on its "Internet+" teaching and research platform, including the training communities based on project workshops and the training communities based on online master teacher workshops.

According to the survey, teachers have generally gained more from the research on promoting teachers' professional development in the context of information technology. According to our sample survey, 27.2% of the teachers thought they were "very rewarding," 54.6% thought they were "more rewarding," 13.9% thought they were "slightly rewarding," and 13.9% thought they were "not rewarding." In addition, 88.7% of the teachers thought that the school-led education model was the most beneficial education model, and 68.3% thought that the group-based education model was the most beneficial education model. It is evident that the school's activities are effective and generally welcomed and affirmed by the teachers (Figure 7).

**4.6. Individual Teaching and Research Model Featuring Autonomy.** As mentioned above, about 1/3 of the teachers considered the individual teaching and research model featuring autonomy to be the most beneficial one.

**4.6.1. Improving Teachers' Theoretical Literacy.** The school subscribes to websites such as high school capital, middle school subject network and golden sun resource network for teaching and research groups and lesson planning groups, creating a strong atmosphere for scientific research and learning, and advocating teachers to write reading experiences and carry out online exchange activities with the recommended reading by the research textbook office and teachers' independent reading methods, so that the theoret-

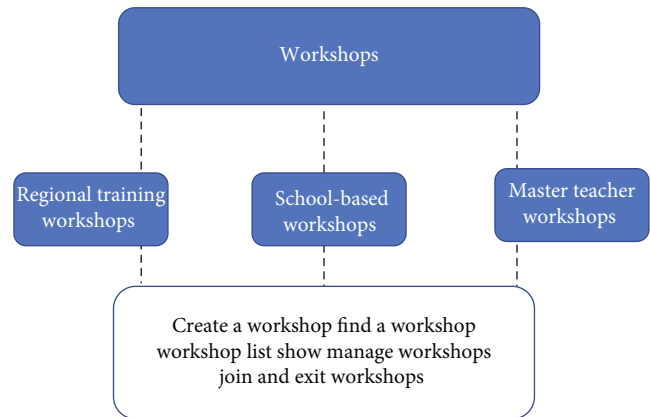


FIGURE 6: Workshop system.

ical knowledge learned online is internalized to improve teachers' professionalism.

**4.6.2. Enriched the Teaching Practice of Teachers.** We have experienced the system of teachers' postteaching reflection, requiring teachers to share on the Internet to write post-teaching notes and conduct self-reflection, reflecting on whether they have really achieved the transformation of teachers' roles, i.e., whether they have transformed from knowledge imparters into collaborators of students' learning, and facilitators reflecting on whether their teaching process has become an interactive process of codevelopment of student interaction.

**4.6.3. Improve the Ability to Teach and Research Schools Adhere to Research-Led Strategies.** The teachers are guided to establish the awareness of scientific research on problems and issues of teaching and research growth and results. The teachers are organized to carry out lesson studies around subject teaching competitions, daily teaching, etc., and to reflect and summarize carefully, so that the daily teaching work and teaching and research work and scientific research work are closely integrated to improve the teachers' teaching level and scientific research ability, and good results have been obtained so far.

**4.7. Group-Based Teaching and Research Mode.** In group-based teaching evaluation, from the survey results, about 2/3 of teachers think that the group-based teaching mode is the most beneficial teaching mode, and its main effects are reflected in the following aspects. In addition to the regular class teacher meetings held at the beginning and the end of the period, the Student Affairs Office also holds regular monthly class teacher meetings, class teacher forums, class teacher festivals, themed class meeting exchange activities, class teacher-apprentice pairing, organizing classroom teachers go out to study, subscribe learning materials for teachers, carry out teaching work reflection classroom teacher work case writing and evaluation, etc., to create a variety of learning and communication channels for young classroom teachers to guide their rapid growth to enhance the classroom management ability of young classroom

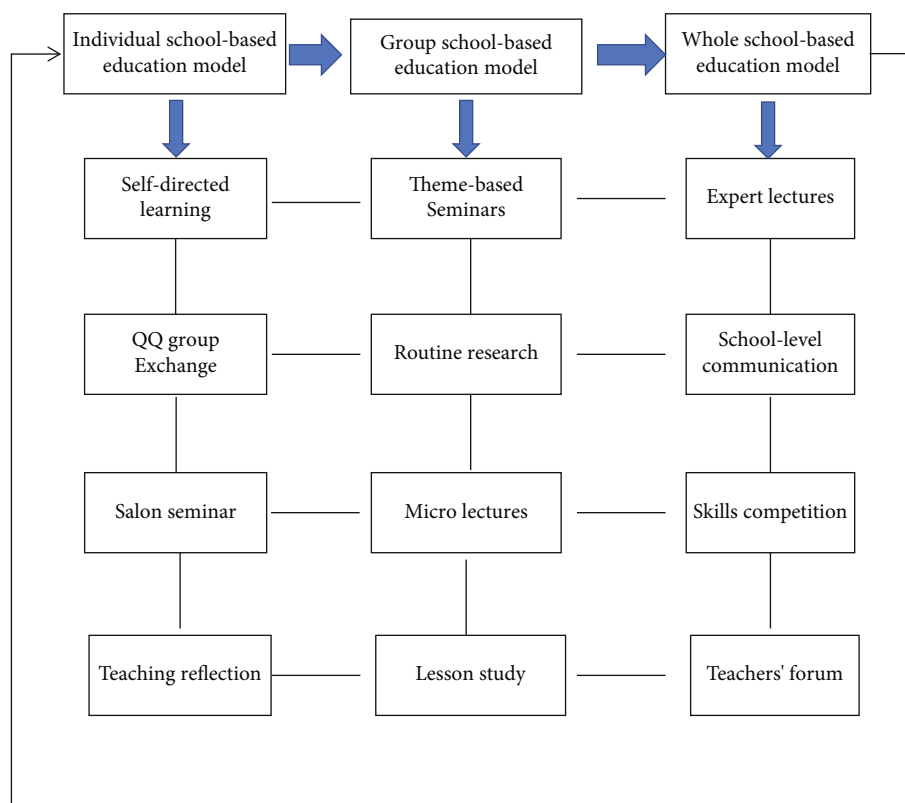


FIGURE 7: Framework of school-based teaching and research model.

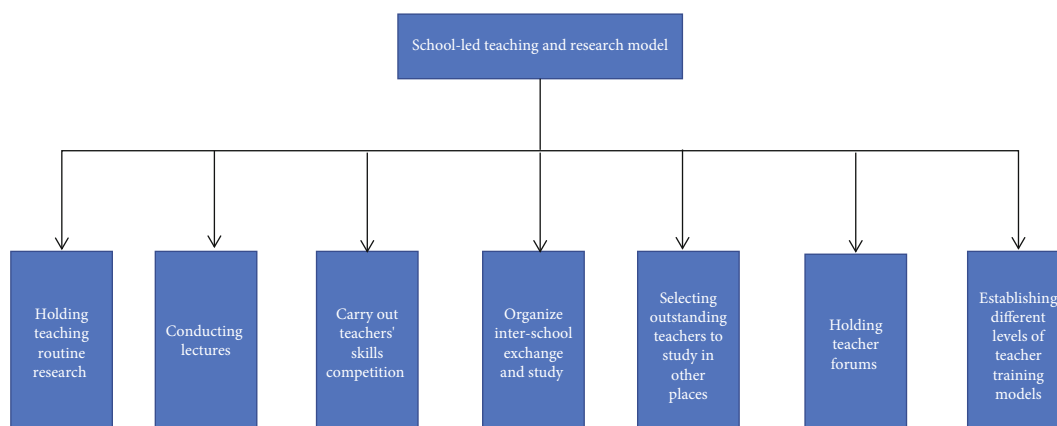


FIGURE 8: School-led teaching and research model for teacher development.

teachers to make classroom teachers clear in the classroom management of what to manage research to help classroom teachers improve their ability to learn how to manage research.

4.8. Evaluation of the Effectiveness of the School-Led Overall School-Based Teaching and Research Model. This is one of the most recognized teaching and research models, nearly 90% of teachers believe that the school-led overall teaching and research model is the most useful teaching and research model in this practical research, regular meetings are held to study the deployment of school-based teaching and research work, and a series of programs are developed to guide the

development of school-based research work, it is new teaching model to promote the development of teacher education to take the following major measures.

4.8.1. Hold Teaching Routine Research, Consolidate the Teaching Routine of Teachers. Since the implementation of the project, the school has adhered to the guidelines of routine out of efficiency, continued to deepen the teaching routine activities, through strengthening lesson preparation, lessons, grinding, listening, speaking, evaluating lessons and other aspects, forming a harmonious, positive, and progressive school culture.

**4.8.2. Offering Report Lectures to Enhance Teachers' Teaching Concepts.** We have actively conducted a series of training for teachers, carried out a series of report lectures to lead teachers in theory and guide them in practice, and offered a series of lectures and training that are close to the actual development of the school and conducive to the growth of teachers.

**4.8.3. Conducting Teacher Skill Competitions to Improve Teachers' Teaching Abilities.** Through interschool exchanges, we continue to improve the quality of classroom teaching, achieve complementary educational advantages and realize the goal of putting resources from outside the school to my use. The school builds a platform for teachers to interact and exchange ideas, invites young teachers from different schools to work together to teach classroom demonstrations, and conducts seminars after the lessons to improve teachers' teaching abilities.

**4.8.4. Organizing Interschool Exchanges and Learning to Expand Teachers' Careers.** Actively carry out interschool teaching discussion and exchange activities, and strive to expand channels, learn from all, increase the opportunities to cut and exchange with other schools, improve teachers' professional quality as much as possible, take their advantageous experiences in time management, goal management, information management, etc., and take the strengths of others to make up for their weaknesses.

**4.8.5. Selecting Outstanding Teachers to Study Offsite to Improve Their Teaching Strategies.** In order to carry out effective teaching and research, from the perspective of effectively improving teachers' professionalism, the squatting learning guidance is specially incorporated into teaching and research activities, and key teachers are sent to foreign schools to listen to lecture experience for learning, so that teachers can discover the problems that exist in their own teaching process management. What is more, it can guide and supervise the implementation of these processes, so that the teachers can benefit greatly and really promote their professional growth.

**4.8.6. Holding Teachers' Forums to Improve Teachers' Teaching Quality.** Every year, the teachers' forum is held to share teaching experience by the school's famous teachers, backbone teachers to manage the real, so that teachers can improve their teaching level in the exchange and collision to promote the improvement of teaching level.

**4.8.7. Establish Different Levels of Teacher Training Model to Promote the Development of Teachers.** In view of the weakness of teachers' teachers using a dual mentorship system to guide teachers to personal development planning, guiding teachers to grow as soon as possible under the leadership of goals and task-driven (Figure 8).

In summary, since the practical research was conducted in our school, relying solely on technology, information technology initially established your need-based research, built many professional platforms for teachers to grow and develop faster and used information technology to more standardize teachers' teaching and research activities to promote their professional development.

## 5. Conclusion

In the context of the rapid development of information technology, the full use of information technology solidly carried out a variety of teaching content for teachers to build a very large number of growth platform, teacher education development is very fast, highlighted by the teachers' view of teaching, curriculum, student view has changed significantly, followed by some new changes in the teaching curriculum: the information carried by these multimedia not only increases the knowledge information and richness, so that the teacher's classroom teaching, including not only text and voice but also graphics, images, animation, video, and other multimedia knowledge, so that the teacher's classroom is no longer a boring. And a new type of teacher-student relationship in the classroom to form the mainstream classroom, teachers often work with students to focus on life and research problems and comprehend knowledge to promote the direction of student learning change. Multimedia technology also transforms abstract knowledge into vivid images of concrete and intuitive content making it easy for students to grasp and gain knowledge more efficiently. Teachers in our school gradually have a clearer and more detailed plan for their educational and teaching development in the context of information technology.

## Data Availability

The labeled datasets used to support the findings of this study are available from the corresponding author upon request.

## Conflicts of Interest

The author declares no competing interests.

## References

- [1] M. H. Romanowski and H. Alkhateeb, "Problematizing accreditation for teacher education," *Higher Education Policy*, 2022.
- [2] E. Istiningsih, Suyatno, and Widodo, "Academic supervision to improve teachers' readiness in utilizing information and communication technology in vocational high schools," *Universal Journal of Educational Research*, vol. 8, no. 10, pp. 4365–4373, 2020.
- [3] D. Wammes, B. Slof, W. Schot, and L. Kester, "Teacher judgement accuracy of technical abilities in primary education," *International Journal of Technology and Design Education*, 2022.
- [4] E. Wildeman, M. Koopman, and D. Beijaard, "Fostering subject teachers' integrated language teaching in technical vocational education: results of a professional development program," *Teaching and Teacher Education*, vol. 112, p. 103626, 2022.
- [5] K. C. Shannon and R. Peter, "Knowledge types in initial teacher education: a multi-dimensional approach to developing data literacy and data fluency," *Learning: Research and Practice*, vol. 8, no. 1, 2022.
- [6] D. E. A. F. Ningrum, I. Rofiki, V. A. Melinda, I. H. Erfantinni, and R. O. Febriani, "Development of biotechnology textbook

- based on bioinformatics research,” *Universal Journal of Educational Research*, vol. 8, no. 11, pp. 5188–5196, 2020.
- [7] S. Karin, K. Johan, and E. Gunilla, “Finnish subject teachers’ beliefs and use of information and communication technology in Home Economics,” *Nordic Journal of Digital Literacy*, vol. 15, no. 3, pp. 202–222, 2020.
- [8] K. Ajitha Nayar and S. N. Akmar, “Technology Pedagogical Content Knowledge (TPCK) and Techno Pedagogy Integration Skill (TPIS) among pre-service science teachers- Case study of a University based ICT based teacher education curriculum,” *Journal of Education and Practice*, vol. 11, no. 6, 2020.
- [9] D. Herro, R. Visser, and M. Qian, “Teacher educators’ perspectives and practices towards the Technology Education Technology Competencies (TETCs),” *Technology, Pedagogy and Education*, vol. 30, no. 5, pp. 623–641, 2021.
- [10] K. Rowston, M. Bower, and S. Woodcock, “The impact of prior occupations and initial teacher education on post-graduate pre-service teachers’ conceptualization and realization of technology integration,” *International journal of technology and design education*, pp. 1–39, 2021.
- [11] M. Lindfors, F. Pettersson, and A. D. Olofsson, “Conditions for professional digital competence: the teacher educators’ view,” *Education Inquiry*, vol. 12, no. 4, pp. 390–409, 2021.
- [12] H. Glaser, M. Helmsing, A. K. Parker, and K. Zenkov, “Adding the “T” to the “PACK” in clinical experiences: how technology shaped our pandemic teacher education pedagogies and partnerships,” *The New Educator*, vol. 17, no. 4, pp. 353–374, 2021.
- [13] S. Massahi, D. D. Ferreira, M. H. Avngaard et al., “Hands-on project aimed at technical education: realizing a DC magnetron sputtering system. DTU Space (Denmark); bbw Hochschule (Germany),” *IDEX Health & Science LLC (United States)*, p. 11815, 2021.
- [14] F. H. Tsai, H. S. Hsiao, K. C. Yu, and K. Y. Lin, “Development and effectiveness evaluation of a STEM-based game-design project for preservice primary teacher education,” *International Journal of Technology and Design Education*, 2021.
- [15] J. Blannin, P. Redmond, A. McLeod, and F. Mayne, “Positioning the technologies curriculum: a snapshot of Australian initial teacher education programs,” *The Australian Educational Researcher*, 2021.
- [16] L. Dekeyser, M. Van Houtte, C. Maene, and P. Aj Stevens, “One does not simply track students: the relationship between teachers’ perceived public track regard and their job satisfaction in a context of rigid tracking,” *Social Psychology of Education*, vol. 24, no. 6, pp. 1433–1459, 2021.
- [17] J. D. Hendrix, Y. L. Campbell, X. Zhang, L. H. Downey, C. B. Jagger, and M. W. Schilling, “Delivery and evaluation of a food science professional development training for Mississippi career technical education teachers,” *Journal of Food Science Education*, vol. 20, no. 4, pp. 197–207, 2021.
- [18] C. Wyss, W. Bühler, F. Furrer, A. Degonda, and J. A. Hiss, “Innovative teacher education with the augmented reality device Microsoft HoloLens—results of an exploratory study and pedagogical considerations,” *Multimodal Technologies and Interaction*, vol. 5, no. 8, p. 45, 2021.
- [19] J. M. Tsarapkina, A. V. Anisimova, B. D. Gadzhimetova, A. M. Kireycheva, and A. G. Mironov, “The impact of digital education transformation on technical college teachers,” *Journal of Physics: Conference Series*, vol. 2001, no. 1, p. 012030, 2021.
- [20] G. Foster, “A case study on teacher educators’ technology professional development based on student teachers’ perspectives in Malawi,” *Journal of Interactive Media in Education*, vol. 2021, no. 1, 2021.
- [21] S. Kiyotaka, “Language teaching with video-based technology: creativity and CALL teacher education,” *Language Learning & Technology*, vol. 25, no. 2, 2021.
- [22] B. Clare, “The quality conundrum in initial teacher education,” *Teachers and Teaching*, vol. 27, no. 1-4, pp. 131–146, 2021.
- [23] S. Mudrikah, J. T. Santoso, and D. P. Astuti, “Exploring the Technological Pedagogical and Content Knowledge (TPACK) of vocational high school’s accounting teachers,” in *Proceedings of the 3rd International Conference on Economics, Business and Economic Education Science, ICE-BEES 2020*, Semarang, Indonesia, 2021.
- [24] A. C. Albina and L. P. Sumagaysay, “Employability tracer study of Information Technology Education graduates from a state university in the Philippines,” *Social Sciences & Humanities Open*, vol. 2, no. 1, article 100055, 2020.
- [25] N. A. U. Alkali, “Utilization of Information and Communication Technology (ICT) in teaching among teachers in selected public senior secondary schools in Katsina Senatorial Zone, Nigeria,” *International Journal of Business and Management*, vol. 7, no. 12, 2019.
- [26] O. N. Utkina and N. L. Yugova, “The pedagogical technique for teachers to ensure information security of the learning process in the context of the COVID-19 pandemic,” *Research Technologies of Pandemic Coronavirus Impact (RTCOV 2020)*, p. 486, 2020.
- [27] X. Zhou, H. Meng, and H. Ma, “Strategies for continuing education of elementary and middle school teachers relying on information technology,” *Science Insights Education Frontiers*, vol. 4, no. 2, 2019.
- [28] Y. Zaslavskaya Olga and N. A. Usova, “Features of teaching the use of information technologies when obtaining financial services,” *RUDN Journal of Informatization in Education*, vol. 16, no. 3, 2019.
- [29] A. Nayar and S. N. Akmar, “Technology Pedagogical Content Knowledge (TPCK) and Techno Pedagogy Integration Skill (TPIS) among pre-service science teachers-case study of a university based ICT based teacher education curriculum,” *Journal of Education and Practice*, vol. 11, no. 6, 2020.
- [30] E. C. Bernard and University of Nigeria, Nigeria, “Status of information and communication technology training and support for science and technology teacher educators in colleges of education in Southeast, Nigeria,” *IJTSRD*, vol. Volume-3, no. Issue-3, pp. 939–946, 2019.



## Review Article

# NiO-Based Gas Sensors for Ethanol Detection: Recent Progress

Qingting Li <sup>1</sup>, Wen Zeng <sup>1</sup>, and Yanqiong Li <sup>2</sup>

<sup>1</sup>College of Materials Science and Engineering, Chongqing University, Chongqing 400030, China

<sup>2</sup>School of Electronic Information & Electrical Engineering, Chongqing University of Arts and Sciences, Chongqing 400030, China

Correspondence should be addressed to Wen Zeng; [wenzeng@cqu.edu.cn](mailto:wenzeng@cqu.edu.cn) and Yanqiong Li; [702121437@qq.com](mailto:702121437@qq.com)

Received 11 June 2022; Revised 26 July 2022; Accepted 28 July 2022; Published 26 August 2022

Academic Editor: Akhilesh Pathak

Copyright © 2022 Qingting Li et al. This is an open access article distributed under the Creative Commons Attribution License, which permits unrestricted use, distribution, and reproduction in any medium, provided the original work is properly cited.

In this review, we summarized the state-of-the-art progress on the ethanol performance of NiO by means of morphology, doping, loading noble metal particles, and forming heterojunctions. We first introduced the effect of modulating NiO morphology on ethanol performance that has been reported in recent years. The morphology with large specific surface area and high porosity was considered to be the one that can bring high gas response. Then, we discussed the enhanced effect of the doping of metal cations and noble metal particle loading on the ethanol-sensitive properties of NiO. Doping ions increased the ground-state resistance and increased the oxygen defect concentration of NiO. The effects of noble metal particles on the performance of NiO included chemical sensitization and electronic sensitization. Finally, the related contents of NiO forming complexes with metal oxides and bimetallic oxides were discussed. In this section, the specific improvement mechanism was discussed first, and then, the related work of researchers in recent years was summarized. At the same time, we presented a reasonable outlook for NiO-based ethanol sensors, imagining future directions.

## 1. Introduction

Volatile organic compounds (VOCs) often appear in our lives, such as the smell of gasoline, paint, and nail polish. These VOC gases degrade air quality and even destroy the ozone layer. At the same time, these gases threaten human body [1–3]. For example, ethanol exists in laboratories, medical industries, and industrial production. When exposed to high concentrations of ethanol, humans are prone to adverse symptoms such as skin irritation and headache [4–6]. In order to prevent problems before they occur, it is essential to develop ethanol sensors to monitor ethanol concentration. In addition, ethanol sensors also play an important role in detecting drunk driving [7]. Currently, gas detection technology includes gas chromatography [8], quartz crystal microbalance [9], and TDLAS detection technology [10]. However, real-time monitoring of ethanol is achieved by chemiresistive sensors with the advantages of easy preparation, low cost, and portability [11, 12].

Metal oxide semiconductors (MOS) have special electrical conductivity, good stability, and high gas response [13–15]. ZnO [16–18], SnO<sub>2</sub> [19–21], NiO [22, 23], WO<sub>3</sub> [24–26],

In<sub>2</sub>O<sub>3</sub> [27–29], etc. are widely used in ethanol gas sensors. For instance, Jiang et al. [16] synthesized an ethanol sensor of mesoporous ZnO nanospheres, which had abundant pore structures and large specific surface area. From the ethanol gas sensing test results, it could be seen that the ZnO sensors achieved a response of 58.4 to 100 ppm ethanol at 250°C. Furthermore, this sensor could detect ppb levels of ethanol, getting a response of 1.17 at 500 ppb ethanol. For the MOS gas sensor, the resistance is used as the measured physical signal to detect the gas. When the MOS is in the air, oxygen molecules adsorb on the surface of the MOS and take electrons out. After the electrons are extracted, the carriers (electrons) of the n-type semiconductor decrease to form an electron depletion layer (EDL), while the carriers (holes) of the p-type semiconductor increase to form a hole accumulation layer (HAL). When the material comes into contact with the reducing ethanol molecules, the electrons captured by oxygen are released back into the sensitive material. The carriers of the n-type semiconductor increase, so the resistance becomes larger; the carriers of the p-type semiconductor decrease, so the resistance becomes smaller [30–32]. In addition to single metal oxides, bimetallic metal oxides have also been used as

gas sensing materials in recent years [33], including  $\text{NiCo}_2\text{O}_4$  [34],  $\text{ZnCo}_2\text{O}_4$  [35], and  $\text{LaFeO}_3$  [36]. Even though MOS possess the above advantages, high operating temperature and low selectivity are still their bottlenecks as gas sensors [37]. Among them, we often say that there is no selectivity, which means that pure MOS has only a weak gas response to the gas. It is not easy to distinguish it after mixing with other gases. Therefore, if the selectivity is not outstanding, it is considered to be nonselective. Scholars have done a lot of research to overcome these shortcomings, including doping, compounding with other materials, morphology manipulation, and UV activation [38–40]. For example, extensive experiments showed that the loading of Pd particles was important for the  $\text{H}_2$  selectivity. Because  $\text{H}_2$  adsorbs on Pd to form  $\text{PdH}_x$ , which not only increased the electrical resistance but also caused the volume expansion of the Pd host. The volume expansion of Pd enabled rapid and highly selective detection of  $\text{H}_2$ . Polyaniline had high selectivity to  $\text{NH}_3$  due to its carbon structure and special protonation/deprotonation process [41, 42]. At the same time, these modification methods can also reduce the temperature of the MOS-based gas sensors, hoping that it can make sensors work at low temperature or even room temperature. For example, ultraviolet light gives the sensor an external energy from the outside, and the energy required for the reaction is not necessarily obtained from the temperature. At the same time, the UV makes the sensitive material generate photogenerated carriers for the gas sensing reaction, which further reduces the temperature and increases the response [43]. The morphology manipulation is often used, such as the hierarchical structures. These hierarchical structures have a large number of pore structures that provide efficient gas diffusion paths, which can enhance gas response and significantly reduce operating temperature [44].

The p-type semiconductor NiO has strong oxidizing properties, excellent catalytic activity, and good electrical conductivity, so it has attracted attention in gas sensors [45, 46]. So far, more than 1,000 reports on NiO materials used in gas sensors have been published, and these reports are mainly concentrated in the past five years. For example, Li et al.'s team [47] fabricated ultrathin  $\text{Ni}(\text{OH})_2$  nanosheets directly on the substrate without using additional surfactants. The obtained NiO nanosheets had a porous structure, which was favorable for the diffusion of gas molecules. At the same time, the nanosheets provided a large surface area and crystal planes with an affinity for acetone gas. Due to these advantages, the NiO nanosheet sensor had a response value as high as 60% when detecting 100 ppb acetone gas. In addition, the NiO nanosheets exhibited a low LOD of 0.8 ppb for acetone with good stability. However, according to reports, the response of pristine NiO to ethanol was low, so the researchers modified NiO using various methods. These modifications include morphology control, doping, loading of noble metal particles, and formation of composites with n-type semiconductors. According to the survey, there have been many reports on the detection of ethanol by NiO sensors in recent years. However, the rare review on the detection of ethanol by NiO is summarized in the existing reports. Therefore, a review article is needed to systematically introduce the research basis of NiO ethanol sen-

sors, which will help scholars to quickly clarify their ideas and understand the entire research field. In addition, scholars can discover unresolved questions and think about new research directions from this review.

In this review, we will describe the influence of different modification methods on the ethanol sensitivity of NiO and summarize the development level of NiO for ethanol detection in recent years in a tabular form. We first introduced the effect of modified NiO morphology on ethanol performance that has been reported in recent years. The morphology with large specific surface area and high porosity was considered to be the structure that could bring high gas response. Then, we discussed the enhanced effect of the doping of metal cations and noble metal particle loading on the ethanol-sensitive properties of NiO. Doping ions increased the ground-state resistance and the oxygen defect concentration of NiO. The effects of noble metal particles on the performance of NiO included chemical sensitization and electronic sensitization. Finally, the related contents of NiO forming composites with metal oxides and bimetallic oxides were discussed. In this section, the specific improvement mechanism was discussed first, and then, the related work of researchers in recent years was summarized. At the same time, we presented a reasonable outlook for NiO-based ethanol sensors, imagining future directions.

## 2. Morphology

The gas response goes hand in hand with the specific surface area and porosity of the material [48, 49]. Therefore, researchers' research on topography is based on high specific surface area and porosity. During the study of the morphology, the researchers found that the grain size of the material is an important factor. When the grain size is equal to or less than twice the Debye length ( $2\lambda_D$ ), the conductance is highly influenced by each grain. So the gas response is strongly influenced by the grain size. When the grain size is larger than  $2\lambda_D$ , the relationship between the gas response and grain size gradually weakens, and the response becomes independent. But in this case, the conductivity is affected by the Schottky barrier at the grain boundaries [50]. However, compared with studies on grains, recent reports on NiO morphologies have focused on obtaining large specific surface areas and high porosity, such as NiO nanosheets [51–53] and NiO nanoflowers [54–58]. Next, the progress of NiO nanomaterials with different morphologies in ethanol sensing will be introduced.

The 2D structure of nanosheets has remarkably high specific surface area and abundant gas channels, while the spatial confinement endows 2D sensitive materials with unique properties [59–61]. The more target gas molecules attached to the metal oxides surface, the greater the resistance change of the material, that is, the higher the gas response [62]. Besides, the flexibility of 2D metal oxides enables for high compatible integration with flexible substrates, which can be applied in the field of flexible wearable sensors. Therefore, nanosheets with satisfactory sensitive properties are favored by scholars in resistive sensors. Many reports on metal oxide nanosheets have pointed out that fabricating porous surfaces on nanosheets

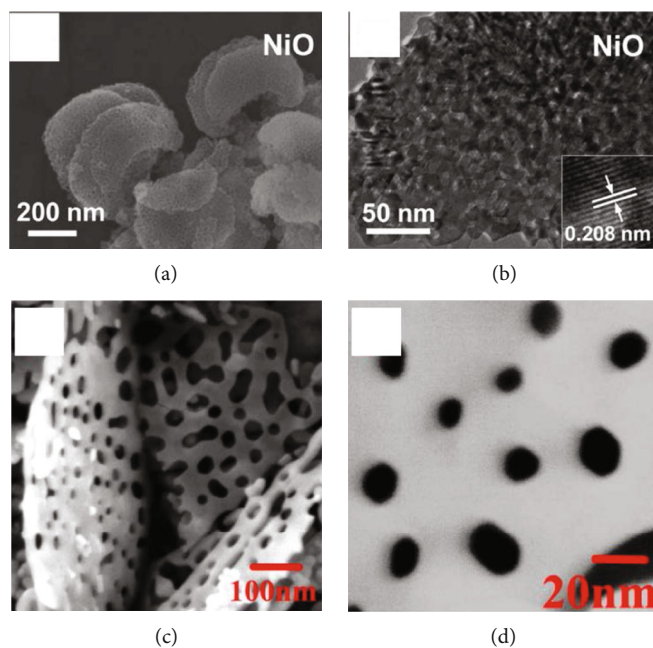


FIGURE 1: (a) SEM of crescent-shaped NiO nanoplates (reprinted/adapted by [53]). (b) HRTEM of crescent-shaped NiO nanoplates (reprinted/adapted by [53]). (c and d) SEM of NiO lotus root slice (reprinted/adapted by [52]).

could effectively improve their gas sensing properties [63]. Su et al. [53] prepared a new and unique crescent-shaped NiO nanosheet. During the calcination process, the water and gas from the NiO nanosheets were get rid of, resulting in a porous structure (as shown in Figures 1(a) and 1(b)). The steady crescent-shaped structure alleviated the accumulation of nanoparticles, and the mesopores uniformly distributed on the nanosheets improved the gas diffusion channel, making ethanol molecules easier to diffuse into NiO. The gas sensors based on crescent NiO nanosheets could rapidly detect 100 ppm ethanol at 130°C (response time and recovery time was 5 s and 20 s, respectively), with a response as high as 68.1%. At the same time, the LOD showed a low value of 200 ppb by calculation. The authors believed that the excellent ethanol sensitivity gave the credit to its steady porosity structure with tiny particle size and abundant reaction sites. Cao et al. [52] prepared a lotus root-like NiO nanosheet (as shown in Figures 1(c) and 1(d)). The average pore diameter of this lotus root structure was 15–50 nm. The specific surface area of lotus root NiO was 156.485 m<sup>2</sup>/g, which was 13 times that of ordinary NiO. Due to this unique morphology, lotus root NiO had a response of 1.51 to 80 ppm ethanol at 300°C.

The hierarchically nanoflowers structured are assembled from nanoneedles and nanosheets. This hierarchical structure is beneficial for gas adsorption and electron transport, which improves the surface reaction efficiency. At the same time, the 3D structure increases the number of its adsorption sites. This novel flower-like structure has been demonstrated to have excellent functions in photoluminescence and photocatalysis [64–66]. Zhang and Zeng [55] investigated the sensitivity of nanoflower gas sensors assembled by nanoneedles and nanosheets to ethanol (Figures 2(a) and 2(b)). Both of them showed excellent gas response to ethanol. Due to the larger specific surface area of nanosheets, which could attract more gas molecules

to react, the nanoflower sensors based on nanosheets obtained a larger gas response (the gas response of nanoneedles was 25 and nanosheets was 55). In particular, the authors mentioned that the nanoneedle-based NiO flowers could detect ethanol faster due to the lower potential energy and higher conductivity of the nanoneedles (the response/recovery time of nanoneedles was 1.7/2.2 s and nanosheets was 4.8/7 s). Nanoflowers composed of nanoneedles and nanosheets had their unique advantages, which meant that different morphologies can be synthesized according to specific needs in the future. If the sensor needed a higher response, the nanosheet flower might be a good choice; if the sensor needed to detect the target gas quickly, then the nanoneedle flower was an effective way. In addition to nanoflowers assembled from nanoneedles and nanosheets, Carbone and Tagliatesta [56] reported a granular flower assembled from particles. This granular flower was an aggregate of particles with a diameter of 10 nm (Figure 2(c)), whose surface had a great quantity of electrons that favor surface reactions. At the same time, the sturdy interparticle distance provided a stable surface for gas adsorption. NiO nanoparticles had charge/hole accumulation in short dimensions, which contained more accumulation of defects and traps. Therefore, these several factors led to the excellent ethanol sensing performance. The NiO granular flower sensor had a 35% response to 150 ppm ethanol at 200°C with a response/recovery time of 3/6 s.

It is worth noting that a lot of research have found that the hollow structure will bring a higher specific surface area and more adsorption active sites [67–69]. The interior of the hollow structure can also serve as a microreaction chamber, providing a place for gas molecules to react with sensitive materials, and a short distance for carrier transport. For the hollow structure of NiO, NiO hollow nanofibers [70] and hollow spheres [71–75] have been reported, and they have

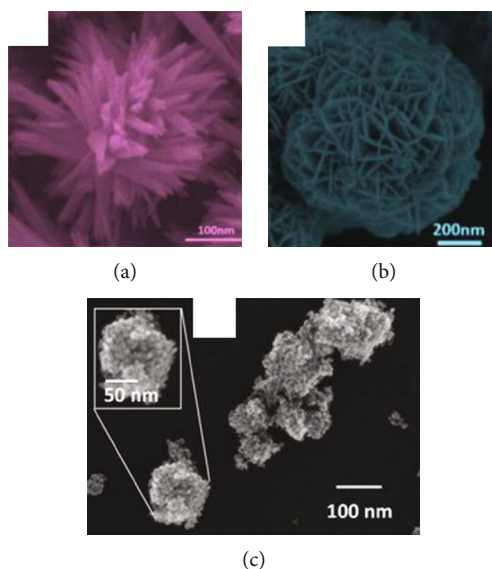


FIGURE 2: SEM of NiO nanoflower assembled from (a) nanoneedles (reprinted/adapted by [55]), (b) nanosheets (reprinted/adapted by [55]), and (c) nanoparticles [56] (open access).

obtained excellent performance in gas sensing with large specific surface area. In recent years, only NiO hollow spheres have been reported for ethanol gas sensing. Chu et al.'s team [73] used the Kirkendall effect to prepare NiO hollow nanospheres. At 240°C, the NiO hollow sphere-based sensor obtained a response of 3.1 to 800 ppm ethanol. The authors exhibited that the hollow nanostructures had enhanced surface activity, while the hollow shell layer enabled rapid diffusion of ethanol molecules and easy penetration into the interior of sensor. These properties made the hollow structure a new route to realize highly sensitive NiO ethanol sensors.

The exposed surfaces of semiconductor nanomaterials are also of interest to scholars, because different exposed surfaces lead to different surface atomic structures and properties. It has been confirmed by numerous experiments that NiO with exposed {111} facets had excellent sensitive characteristics, which owned to the 3-coordinated unsaturated Ni atoms of the {111} facets. Due to the lack of oxygen and great reducibility, the 3-coordinated Ni atoms can adsorb O<sub>2</sub>, bring free electrons, and promote the chemical reaction between oxygen species and ethanol gas [76, 77]. Furthermore, the {111} planes of NiO have a greater number of unsaturated O atoms and a higher surface energy than the usually exposed {220} planes, which is beneficial for sensitive performance [78, 79]. Liu et al. [77] prepared NiO foam structures with exposed {111} and {220} planes, and NiO with exposed {111} planes had fewer surface single-bond H groups and had higher 3-coordinated Ni atomic density. In addition, NiO with exposed {111} planes had a high Ni<sup>3+</sup>/Ni<sup>2+</sup> ratio, which was favorable for electron transport. Combining with these advantages, the NiO gas sensor with an exposed {111} surface could detect ethanol as low as 20 ppm (response value was 1.57).

In conclusion, the morphology has a significant impact on the ethanol-sensitive performance of NiO. The morphology with large specific surface area and high porosity facilitates the adsorption and transport of gas molecules. The

special advantages of the hollow structure are beneficial to the detection of ethanol gas by NiO. Meanwhile, there are a still few reports on NiO with exposed {111} facets. Therefore, the synthesis of porous hollow nanofibers and hollow spheres, as well as NiO sensors with exposed {111} planes, can be considered in future topography work. Table 1 summarizes gas performance of NiO in different morphology. However, the effect of morphology adjustment on gas response is still weak and needs to be combined with other modification methods.

### 3. Cation Doping

Doping is an essential way to enhance performance. Whether it is adding metal elements to alloys to improve their mechanical properties or adding donor and acceptor elements to dielectric ceramics to improve dielectric properties, doping is very effective [80, 81]. Doping ions are divided into high-valence ions and low-valence ions, that is, the donor ions and acceptor ions mentioned above. In improving the ethanol sensing performance of NiO, ions with a higher valence state than Ni<sup>2+</sup> are often introduced. It was found that the introduction of high-valence cations always enhanced the response by changing the ground-state resistance of NiO. As the high-valence ions replace the Ni<sup>2+</sup> sites, those generate electrons to compensate for the substitution. At the same time, the extra electrons provided by the high-valence ions recombine with the holes in the NiO valence band. These two factors cause the hole concentration decrease in NiO and the ground-state resistance increase, resulting in an enhanced response to the target gas [82–84]. Furthermore, doping induces lattice distortion and introduces more oxygen vacancy defects. When detecting ethanol, ethanol molecules are easily trapped by oxygen vacancy defects, allowing more target molecules to react with NiO, resulting in a larger gas response [85–87]. Shailja et al. [88] introduced Ga<sup>3+</sup> into NiO. The introduction of

TABLE 1: Gas performance of NiO in different morphology.

Material	Morphology	Conc. (ppm)	Operating temp (°C)	Response	Response/recovery time (s/s)	LOD (ppm)	References
NiO	Nanosheets	100	130	68.1%	5/20	0.2	[53]
NiO	Nanosheets	80	300	1.51	-/-	—	[52]
NiO	Nanosheets	50	240	11.15	4/7	1	[51]
NiO	Nanoflower	200	300	25	1.7/2.2	—	[55]
NiO	Nanoflower	200	300	55	4.8/7	—	[55]
NiO	Nanoflower	150	200	35	3/6	2.6	[56]
NiO	Nanoflower	100	190	46	-/-	—	[58]
NiO	Hollow sphere	800	240	3.1	-/-	—	[73]

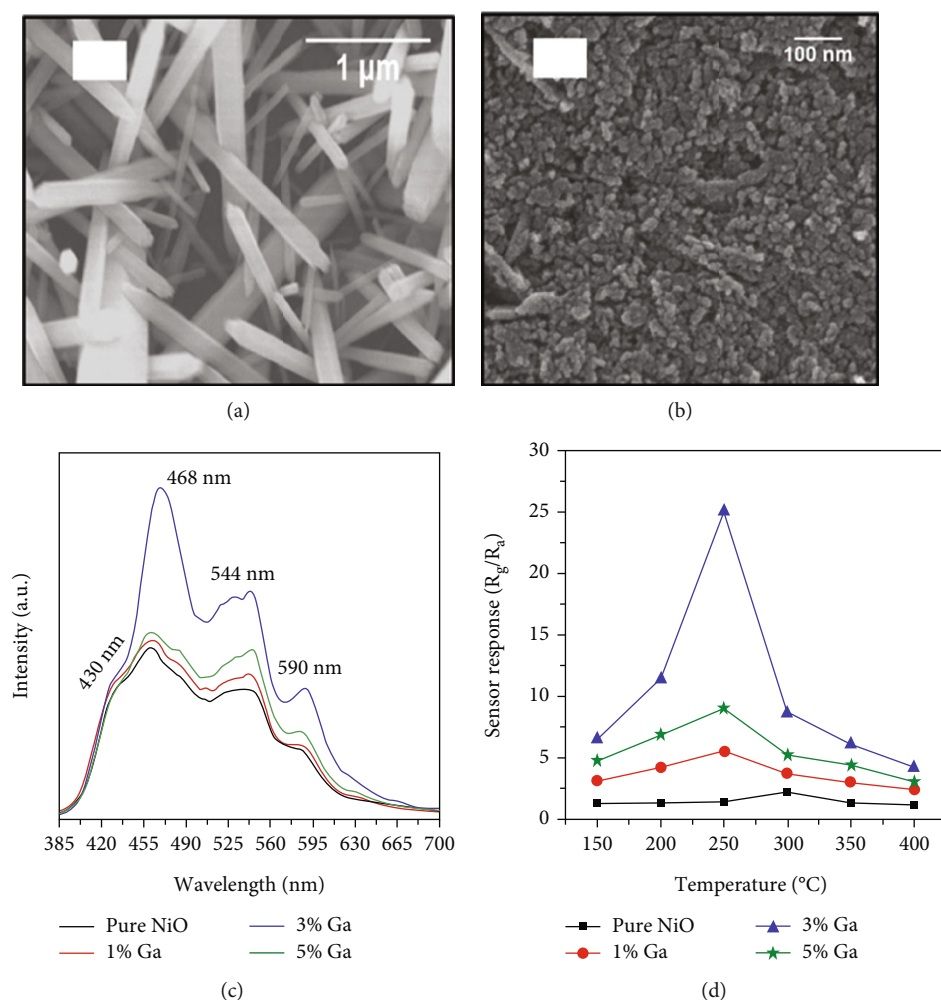


FIGURE 3: The SEM of (a) pure NiO and (b) Ga-NiO. (c) PL spectra of pure and Ga-doped NiO. (d) Gas response of pure NiO and Ga-NiO at various temperatures (reprinted/adapted by [88]).

Ga<sup>3+</sup> transformed the structure of NiO from rod to a particle (Figures 3(a) and 3(b)). The BET test showed that this morphological transformation gave Ga-NiO a higher specific surface area (135.72 m<sup>2</sup>/g). The intensity of the photoluminescence peaks of pure NiO was lower than that of Ga-NiO (Figure 3(c)), which meant that the introduction of Ga brought more defects to NiO. The sensor was tested for its ethanol-sensitive properties, and it was found that Ga-NiO had lower

operating temperature and higher gas response (300°C for pure NiO and 250°C for Ga-NiO, respectively) (Figure 3(d)). When the Ga doping level was 3%, the gas response to 50 ppm ethanol at 250°C was 25, and the response/recovery time was 8/13 s. In addition, Ga-NiO could detect ethanol down to 10 ppm.

Mahmood et al. [89] studied the gas sensing performance of mesoporous Al-doped NiO ultralong nanowires to ethanol. Al<sup>3+</sup> made NiO nanowires generate many pores, which

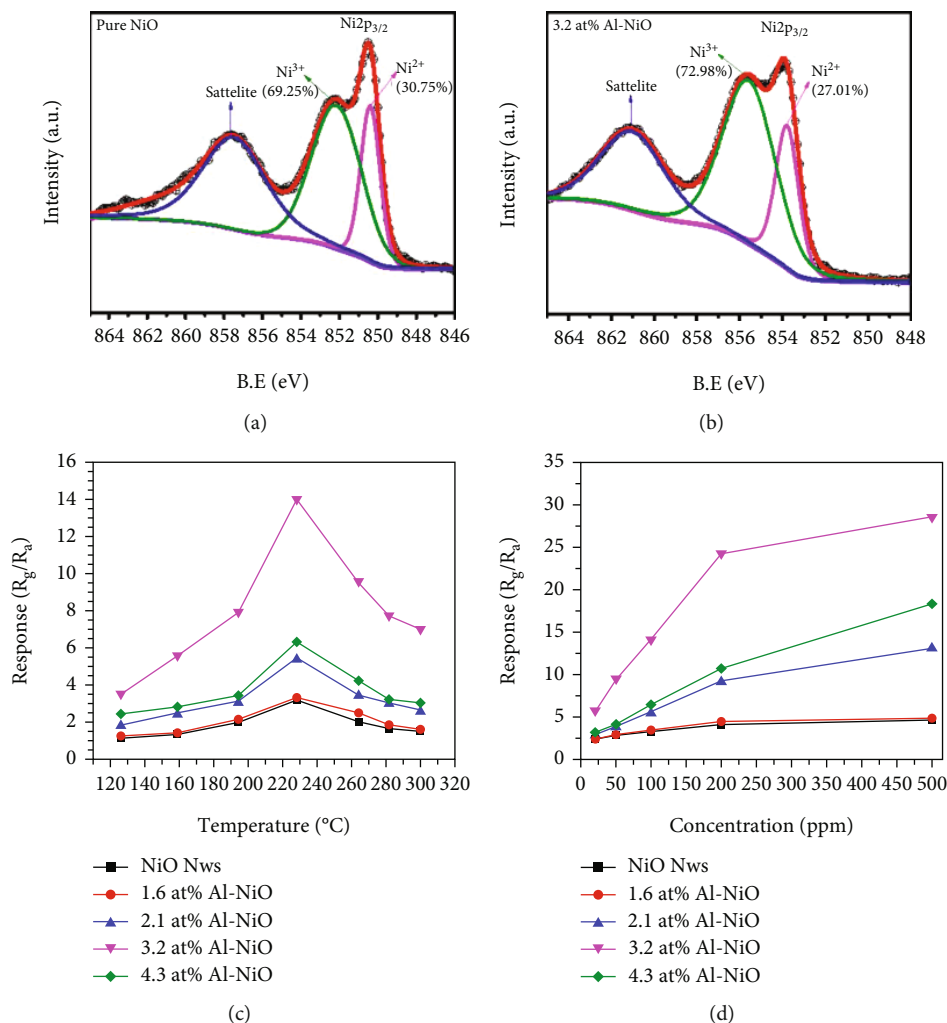


FIGURE 4: XPS spectra for Ni-2p<sub>3/2</sub> of (a) pristine NiO and (b) 3.2 at% Al-doped NiO. (c) Gas response of pure NiO and Al-NiO at various temperatures. (d) Gas response of pure NiO and Al-NiO at 228°C under the ethanol vary from 10 ppm to 500 ppm (reprinted/adapted by [89]).

brought a larger specific surface area. Owing to the smaller atomic radius of Al<sup>3+</sup> (0.54 Å for Al<sup>3+</sup> and 0.69 Å for Ni<sup>2+</sup>), Al<sup>3+</sup> was easily substituted by Ni<sup>2+</sup>, resulting in a greatly increased Ni<sup>3+</sup>/Ni<sup>2+</sup> ratio (Figures 4(a) and 4(b)). Larger Ni<sup>3+</sup>/Ni<sup>2+</sup> meant higher electronic performance, leading to better gas sensing performance. At 228°C, the sensitivity efficiency of 3.2 at% Al-NiO to 100 ppm ethanol showed 14.01, which was higher than that of undoped NiO (Figures 4(c) and 4(d)). Meanwhile, 3.2 at% Al-NiO enabled rapid detection of ethanol (response/recovery time of 73/76 s). For the enhanced sensitive performance, the authors believed that it was related to the changes in pores, oxygen species content, and carrier concentration brought about by the incorporation of Al<sup>3+</sup>.

Besides doping high-valence ions, Chen et al. [90] also introduced Li<sup>+</sup> and Zn<sup>2+</sup> into NiO. The study found that the incorporation of low-valence ions Li<sup>+</sup> and equivalent ions Zn<sup>2+</sup> accelerated the detection of ethanol molecules by NiO. The response times of Li-NiO and Zn-NiO were 11 s and 17 s, respectively, while the response time of pure NiO was 33 s. However, Zn<sup>2+</sup> hardly improved the response to

ethanol, and Li<sup>+</sup> even degraded the sensitivity of NiO. The authors believed that the Li<sup>+</sup> extracted electrons from the valence band after forming the Li-O bond, leading the original resistance to decrease. Zn<sup>2+</sup> in the same valence state hardly influenced the hole concentration, but the radius of Zn<sup>2+</sup> was quite different from that of Ni<sup>2+</sup>, so more defects were induced, which led to a slight improvement in the response of Zn<sup>2+</sup> to ethanol.

The ethanol gas sensing performance of NiO will be worsened by doping low-valence Li<sup>+</sup> alone. But there was a study reported that the gas sensing performance of NiO may be ameliorated by adding high-valence ions at the same time as adding low-valence ions. Chang et al. [91] reported the simultaneous incorporation of Sc<sup>3+</sup> and Li<sup>+</sup> into NiO nanoflowers. In addition to resulting in higher specific surface area, codoping could stabilize metastable surface oxygen vacancies (O<sub>V</sub>) in metal oxides due to Li<sup>+</sup> active sites, so Sc and Li codoping increased the O<sub>V</sub> ratio. Besides, Li<sup>+</sup> could make the bonding strength of surface oxygen weak, thereby promoting the surface redox reaction. When the doping

TABLE 2: Gas performance of doping NiO.

Material	Conc. (ppm)	Operating temp (°C)	Response	Response/recovery time (s/s)	LOD (ppb)	References
Ga-NiO	50	250	25	8/13	—	[88]
Al-NiO	100	228	14	73/76	—	[89]
Sc/Li-NiO	100	200	118.4	86/31	100	[91]
Fe-NiO	50	240	3.9	7/8	200	[92]
Mg-NiO	100	325	10.4	13/19	—	[93]

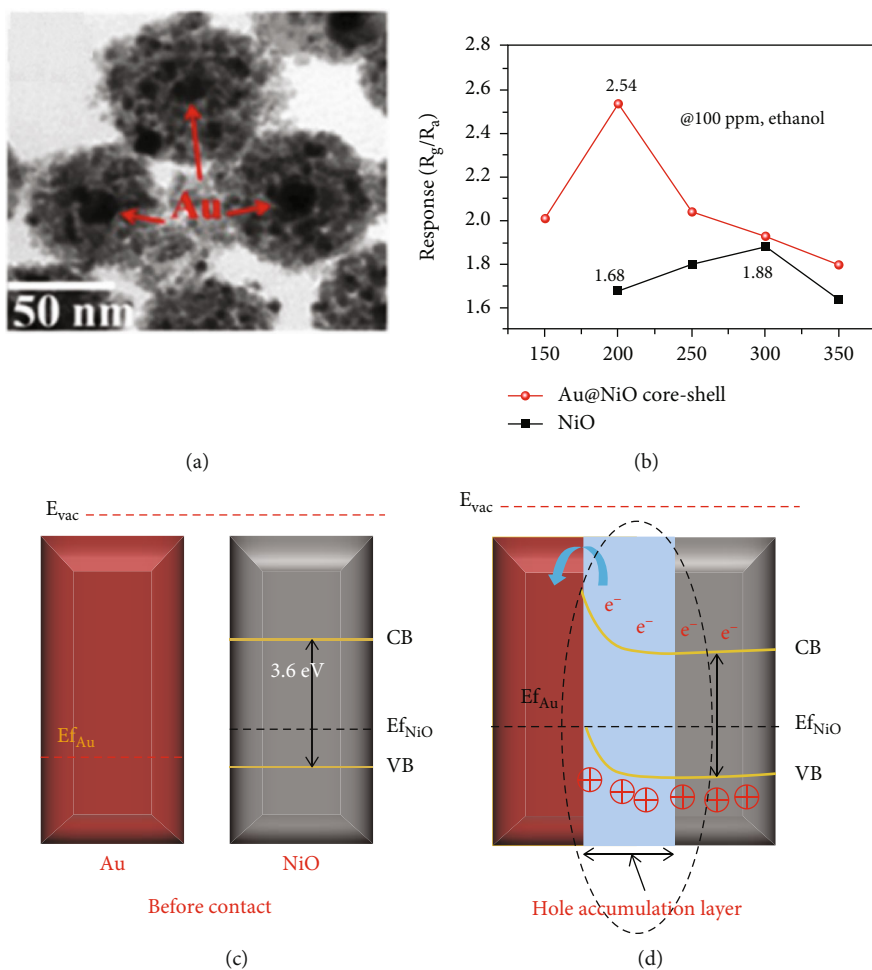


FIGURE 5: (a) The SEM of Au-NiO. (b) Gas response of NiO and Au-NiO at various temperatures. (c and d) The energy band diagram of Au-NiO before and after contact (reprinted/adapted by [95]).

amount was 2 at.% Sc and 5 at.% Li, the sensitivity to 100 ppm ethanol at 200°C was 118.4, which was 105 times higher than that of pristine NiO. Meanwhile, the response time and recovery time of the Sc/Li-NiO sensor were 86 s and 31 s. The LOD was as low as 10 ppb. According to defect characterization and first-principle calculations, the codoping of  $\text{Sc}^{3+}$  and  $\text{Li}^+$  significantly increased the stable  $\text{O}_V$  and  $\text{Ni}^{3+}$ , which greatly promoted the adsorption of ethanol molecules, resulting in an excellent gas response.

In this section, we discussed the mechanism by which cation doping enhances the performance of NiO gas sensors. NiO is mainly doped with high-valence cations, and the changes in hole concentration and defect concentration

caused by high-valence cations make NiO have better ethanol sensing performance. In particular, low-valence cations do not seem to be a method to enhance the sensitive performance of NiO. However, by doping with high-valence ions and low-valence ions, the unique properties of low-valence ions can be exerted, while high-valence ions improve the sensitivity. In the future, for the development of doping methods, we can pay more attention to high-valence/low-valence codoping. Table 2 exhibits gas performance of NiO doping by metal cation. However, the amount of ion doping is less controllable, and whether the ions successfully enter the lattice is difficult to control, while doping noble metal particles is relatively easy to control.

TABLE 3: Gas performance of NiO functional by precious metal particles.

Material	Conc. (ppm)	Operating temp ( $^{\circ}\text{C}$ )	Response	Response/recovery time (s/s)	References
Au-NiO	100	200	2.54	250/420	[95]
Au-NiO	1000	325	442%	-/-	[97]
Pt-NiO	100	200	20.85	-/-	[96]

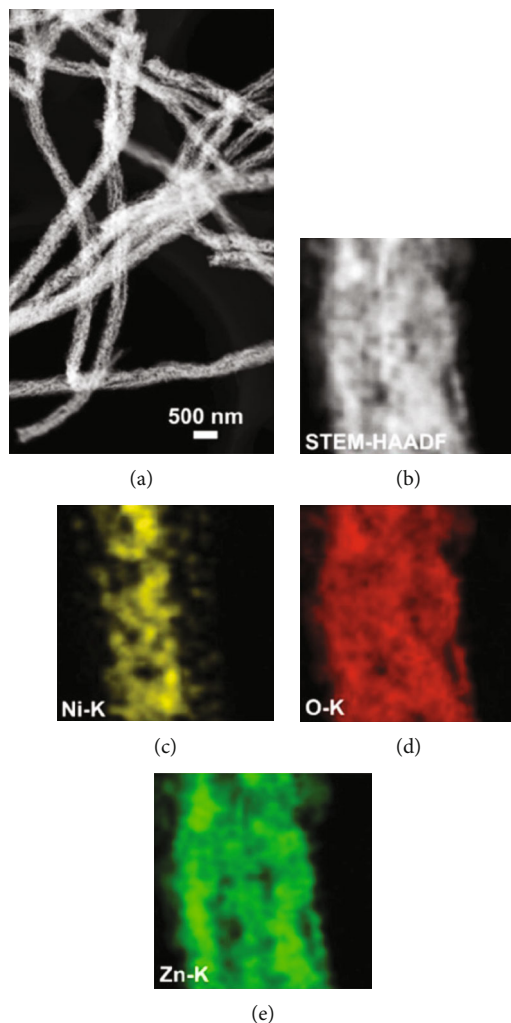


FIGURE 6: (a) TEM of NiO-ZnO. (b) HAADF-STEM image of NiO-ZnO. Elemental mapping images of (c) Ni, (d) O, and (e) Zn (reprinted/adapted by [108]).

#### 4. Precious Metal Particle Loading

Precious metal particle loading is a common way to improve sensitive properties. The improved performance of precious metal particles can be attributed to two reasons. First is chemical sensitization. Chemical sensitization exploits the catalytic properties of precious metal particles. Noble metal particles can catalyze  $\text{O}_2$  molecules to capture electrons from the valence band of NiO and dissociated into ionic species, resulting in more holes in the valence band [94]. A lower baseline resistance can result in a larger change in resistance, meaning better sensitivity. This results in a higher sensing response to ethanol gas. Second is electron sensitization. Electron sensi-

zation utilizes a change in the Fermi level. After the precious metal particles are in contact with NiO, the Fermi levels of the two are not at the same level. To reach electronic equilibrium, the Fermi level of NiO will shift, creating additional depletion layers and reducing the HAL thickness [68].

Enhanced sensitive properties are usually caused by a combination of the two. For example, Majhi et al. [95] utilized the electronic and chemical sensitization effects of Au to obtain an Au-NiO gas sensor with excellent gas sensing performance. Au particles were encapsulated inside NiO to form a core-shell structure (Figure 5(a)). The optimal operating temperature of Au-NiO was  $200^{\circ}\text{C}$ , which was  $100^{\circ}\text{C}$  lower than that of NiO (Figure 5(b)). Au-NiO obtained a 2.54 response to 100 ppm



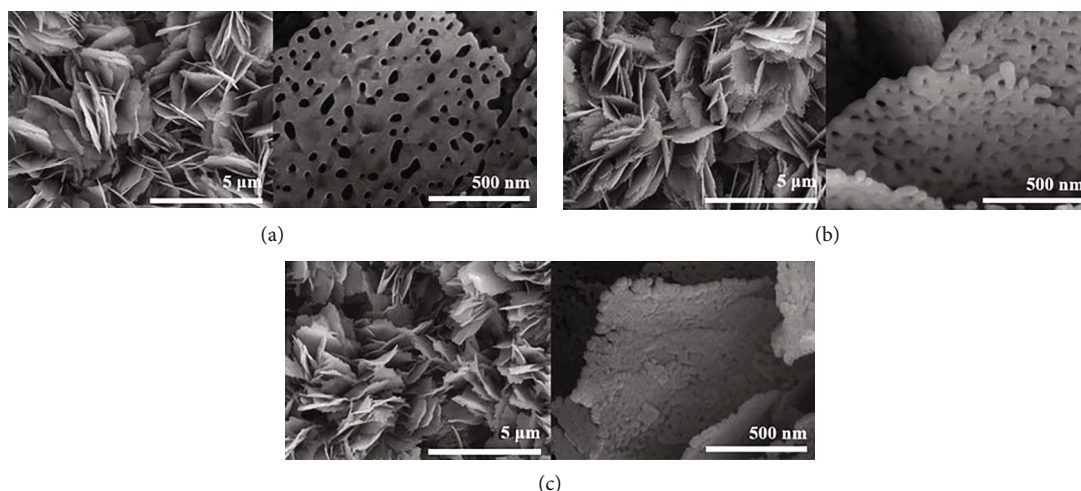


FIGURE 7: SEM of NiO/ZnO with different sputtering times [63] (open access).

ethanol at 200°C, and the response time and recovery time were 250 s and 420 s. Compared with pristine NiO, Au-NiO had a larger response and more rapid response/recovery speed. Since the Fermi levels of Au and NiO were not at the same level, Au and NiO contacted to form a Schottky junction (Figures 5(c) and 5(d)). At the same time, additional HAL was formed near the Au-NiO interface, which increased the quantity of holes in Au-NiO, resulting in a larger resistance. Fu et al. [96] synthesized Pt-NiO nanotubes by electrospinning, and the NiO nanotubes functionalized by Pt were dendriform. Due to the activation and catalytic effect of Pt on NiO, the response of 0.7% Pt-NiO nanotubes at 100 ppm ethanol and 200°C was 20.85, while pure NiO got 2.06 under the equal environment. Park et al. [97] studied the sensing performance of pristine NiO and Au-modified NiO for ethanol. The responses of NiO and Au-NiO sensors to 1000 ppm ethanol at 325°C were 273% and 442%, respectively. The author attributed the enhanced sensitive performance to the additional depletion layer and Schottky barrier formed by the Au particles, high catalytic activity, and smaller diameter of Au-NiO.

Although the chemical catalysis and electronic catalysis of precious metal particles bring excellent ethanol sensing properties to NiO, there are few reports on the modification of NiO by those in recent years. The main reason is that precious metal particles are expensive. Considering the cost, it is difficult to apply them to actual production. Table 3 is gas performance of NiO functional by precious metal particles in recent years. The Schottky barrier generated by the combination of noble metal particles and NiO is similar to PN heterojunctions, so scholars are keen to form heterojunctions to improve the ethanol-sensitive properties of NiO.

## 5. Composites

NiO, p-type semiconductor, is often combined with n-type semiconductors to form a PN heterojunction. The Fermi level of the p-type semiconductor is lower than that of the n-type semiconductor. When the two are in contact, electrons move to the p-type semiconductor and holes move to the n-type semiconductor, resulting in band bending. An

EDL is then formed in the hetero area and strongly inhibits the conduction channel. When the heterojunction contacts the target gas, electron release greatly reduces the potential barrier at the heterojunction, causing a bigger change in resistivity and a higher sensitivity [46, 98, 99].

**5.1. Metal Oxides.** In recent years, NiO has been reported to recombine with n-type semiconductors such as ZnO [63, 100–110], SnO<sub>2</sub> [67, 111–118], WO<sub>3</sub> [119–121], Fe<sub>2</sub>O<sub>3</sub> [122–124], and In<sub>2</sub>O<sub>3</sub> [125, 126].

The n-type semiconductor ZnO has received attention due to its low cost and fast response speed, which can detect a variety of gases [17, 18, 127]. Among the recent reports, NiO- and ZnO-combined sensors have the most detection of ethanol. Bai et al. [108] used electrospinning and atomic layer deposition (ALD) to design a NiO/ZnO core-shell nanotube (CSNT), in which NiO was the core and ZnO was the shell (Figure 6). There were many pores and some hollow structures in such nanotubes, which helped gas molecules to be fixed in the pore channels. NiO/ZnO CSNTs obtained a gas response of 16 for the detection of 100 ppm ethanol at 325°C, and it was much bigger than that of pristine ZnO (8.8) and pure NiO (2.5). In addition, NiO/ZnO had a shorter response time (13 s) but a longer recovery time (498 s). The nice gas sensing performance thanked to the shell thickness of NiO/ZnO close to the Debye length ( $\lambda_D$ ). In this case, a fully electron-depleted state was established and the most effective resistance modulation occurred, causing the highest gas sensing performance of NiO/ZnO. When the shell of the core-shell structure was thicker, the resistance modulation through the shell would be significantly reduced, owing to the depletion of some electron in the thick shell, thus resulting in a reduced gas response. Liang et al.'s team [63] sputter-deposited NiO onto porous ZnO nanosheets. NiO was uniformly attached to ZnO, and the addition of NiO narrowed the pore size on ZnO nanosheets (Figure 7). Due to the different work functions, a built-in electric field was formed at the NiO/ZnO heterojunction interface, which also induced band bending. The formation of the built-in electric field leads to a higher barrier height and a higher initial resistance. After exposure to ethanol

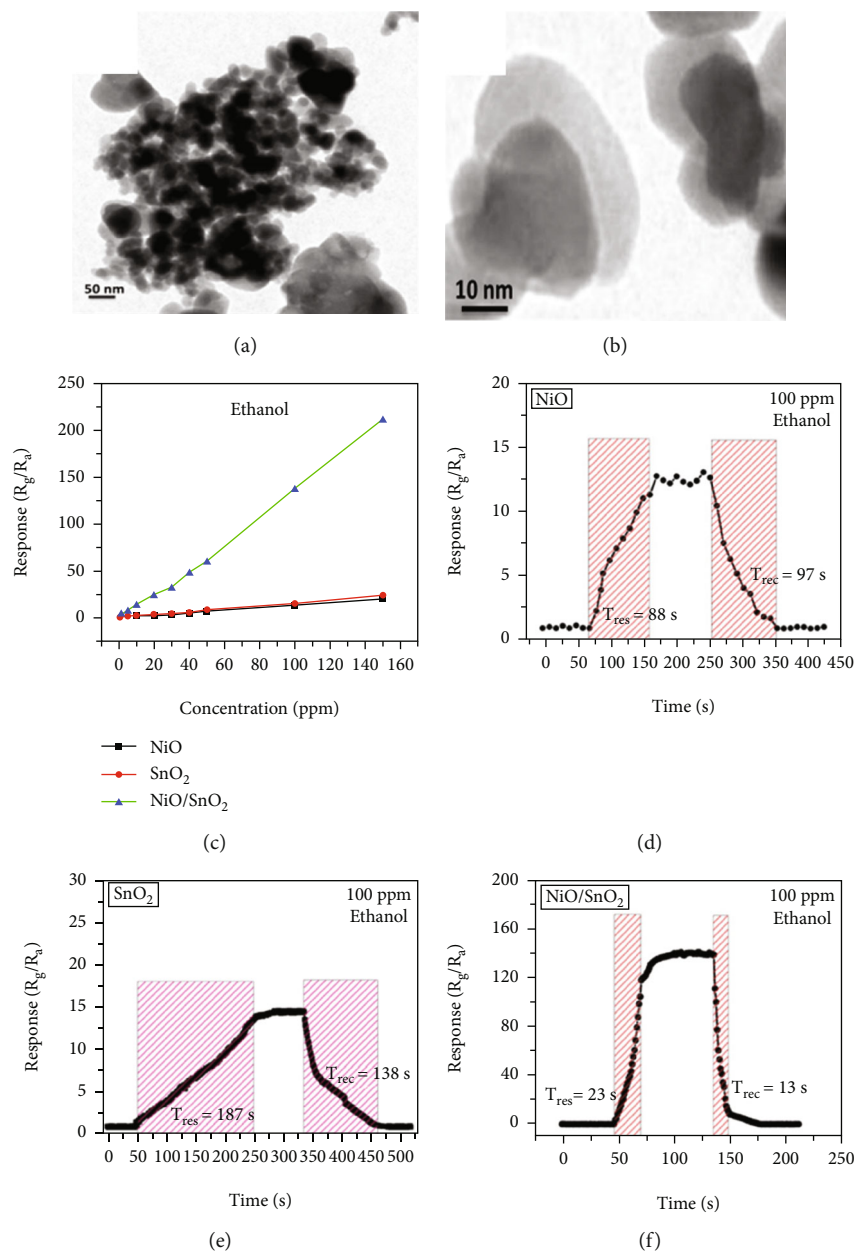


FIGURE 8: (a and b) HRTEM of NiO/SnO<sub>2</sub>. (c) Gas response of NiO, SnO<sub>2</sub>, and NiO/SnO<sub>2</sub> under various ethanol concentrations. Response and recovery curves of (d) NiO, (e) SnO<sub>2</sub>, and (f) NiO/SnO<sub>2</sub> (reprinted/adapted by [111]).

gas, electrons were released, reducing the barrier height of the depletion layer. Besides, NiO/ZnO had a distinctive porous nanosheet structure, which provided abundant surface active sites and a lot of gas diffusion channels for ethanol molecules.

There have been many reports that SnO<sub>2</sub> is easily composited with other materials to form heterostructures, which is a perfect sensitive material and is often used in ethanol gas sensors [13, 15, 128]. Jayababu et al. [111] composited NiO with SnO<sub>2</sub> to form an ethanol sensor. NiO had a semi-shielding effect on SnO<sub>2</sub> nanoparticles by HRTEM; that is, NiO partially covered SnO<sub>2</sub> (as shown in Figures 8(a) and 8(b)). Due to the PN heterostructure and catalytic activity brought by NiO, the NiO/SnO<sub>2</sub> sensors exhibited excellent sensing performance for ethanol. At RT, NiO/SnO<sub>2</sub> achieved

a response as high as 140 for ethanol, much higher than SnO<sub>2</sub> and NiO (seen in Figure 8(c)). Beyond that, NiO/SnO<sub>2</sub> showed fast response and recovery speed, with response and recovery times of 23 s and 13 s, respectively (as shown in Figures 8(d)–8(f)). Zhang et al.'s group [115] synthesized a novel NiO/SnO<sub>2</sub> vertical nanotube composite film, which consisted of 20 nm diameter NiO nanosheets attached to one-dimensional SnO<sub>2</sub> nanotubes (Figures 9(a) and 9(b)). When the molar ratio of Ni<sup>2+</sup>/Sn<sup>4+</sup> was 5%, NiO/SnO<sub>2</sub> had high adsorbed oxygen. At 250°C, it had the highest gas response to ethanol (123.7 for 1000 ppm ethanol, as shown in Figure 9(c)). Figure 9(d) is the gas response curve for five gases. NiO/SnO<sub>2</sub> has high selectivity for ethanol, which was beneficial to realize the efficient detection of ethanol. Since

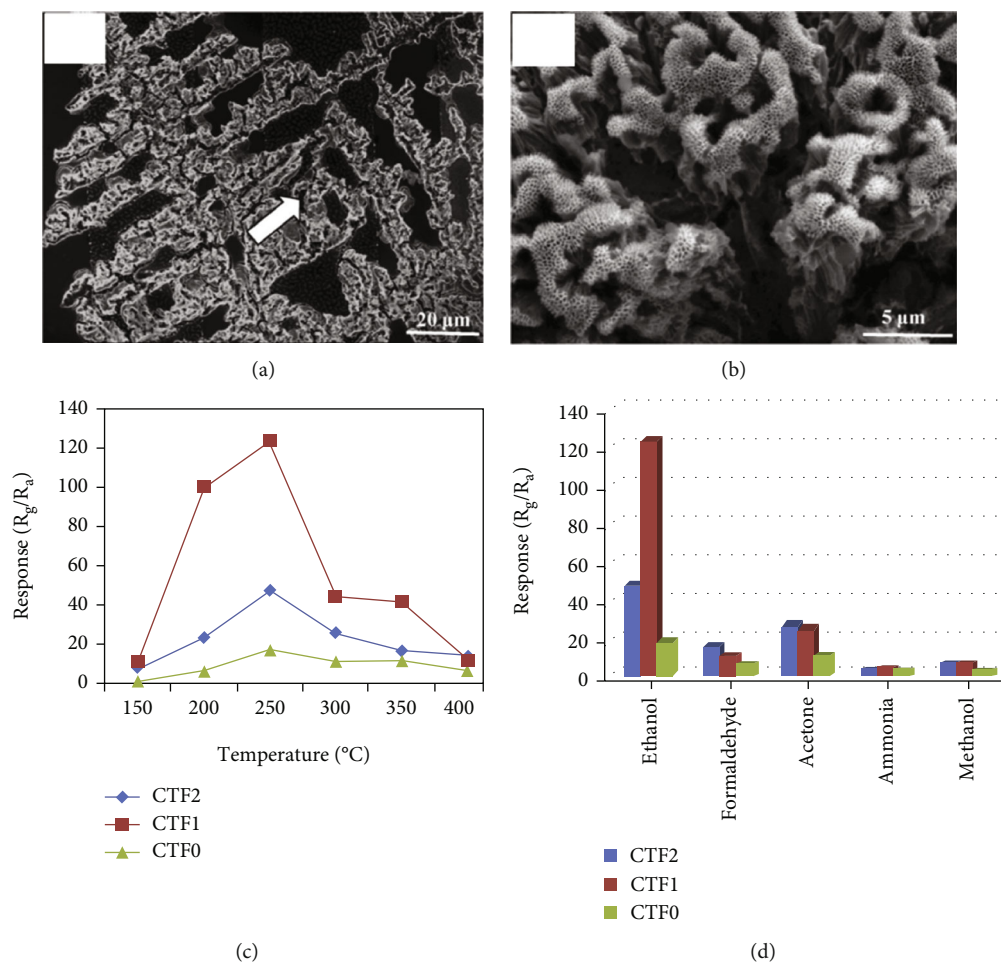


FIGURE 9: (a) SEM of NiO/SnO<sub>2</sub>. (b) Enlarged image of (a) where the white arrow points. (c) Gas response of NiO/SnO<sub>2</sub> under different temperatures. (d) Gas response of NiO/SnO<sub>2</sub> under different gases (reprinted/adapted by [115]).

SnO<sub>2</sub> nanotubes could transport electrons quickly, NiO/SnO<sub>2</sub> could rapidly detect ethanol compounds within 10 s. After the heterojunction of SnO<sub>2</sub> and NiO was formed, the band bending led to the narrowing of the electron transport channel, which increased the ground-state resistance. The higher ground-state resistance was beneficial in enhancing the gas sensing performance, so the respond value of NiO/SnO<sub>2</sub> was higher than NiO.

$\alpha$ -Fe<sub>2</sub>O<sub>3</sub>, a n-type semiconductor, has been demonstrated as an ethanol sensor due to its low cost, high stability, and environmental friendliness [129–131]. Tan et al. [124] employed microwave-assisted liquid-phase synthesis to support Fe<sub>2</sub>O<sub>3</sub> on NiO nanosheets. Owing to the enhanced sensitivity of the heterojunction pair of Fe<sub>2</sub>O<sub>3</sub> and NiO, the 1.5% Fe<sub>2</sub>O<sub>3</sub>/NiO sensor got a high response of 170.7 and an ultrafast response/recovery speed (0.5/14.6 s) to 100 ppm ethanol. In<sub>2</sub>O<sub>3</sub> has received attention in gas sensors because of its stable electrical conductivity, good chemical stability, and low cost [28, 132]. Yan et al. [125] successfully synthesized In<sub>2</sub>O<sub>3</sub>/NiO composites through electrospinning technology and ion exchange reaction. The NiO nanosheets were arranged in one dimension, and the In<sub>2</sub>O<sub>3</sub> nanoparticles were uniformly attached to them. During the detection of ethanol, the charge carriers of In<sub>2</sub>O<sub>3</sub>/NiO were conducted through the continuous NiO. The formation of the

PN junction created a thicker hole depletion layer under In<sub>2</sub>O<sub>3</sub>. Therefore, a small change in carrier concentration resulted in a larger gas response. WO<sub>3</sub> is favored in ethanol gas sensors because of its special physicochemical and electrical properties [133, 134]. Juang and Wang's team [120] found that the composite of porous NiO spheres and WO<sub>3</sub> nanoplates had a response of 155% to ethanol, which was 1.4 times that of pure WO<sub>3</sub> nanoplates. The enhanced ethanol sensitivity was attributed to the formation of the PN heterojunction. Table 4 shows gas performance of NiO/metal oxide-based composites.

**5.2. Bimetallic Oxides.** Apart from the above single metal oxides, bimetallic oxides have also been used to improve NiO materials. LaFeO<sub>3</sub> has been studied in gas sensors owing to its high electrical conductivity and good redox properties [136, 137]. Hao et al.'s team [138] modified NiO nanosheets onto porous LaFeO<sub>3</sub> microspheres and studied their ethanol sensing properties. Figures 10(a) and 10(b) are the SEM images of LaFeO<sub>3</sub> and NiO/LaFeO<sub>3</sub>. The surface of LaFeO<sub>3</sub> had abundant pore structure, and NiO nanosheets were uniformly distributed on the LaFeO<sub>3</sub> microspheres. This morphology effectively increased the contact area between the composite and ethanol. Figure 10(c) is the gas response of NiO/LaFeO<sub>3</sub> and LaFeO<sub>3</sub> under different temperatures at 10 ppm ethanol. The optimum

TABLE 4: Gas performance of NiO/metal oxide-based composites.

Material	Conc. (ppm)	Operating temp ( $^{\circ}\text{C}$ )	Response	Response/recovery time (s/s)	LOD (ppm)	References
NiO/SnO <sub>2</sub>	100	160	13.4	-/-	—	[112]
NiO/SnO <sub>2</sub>	100	RT	140	23/13	1	[111]
NiO/SnO <sub>2</sub>	100	160	23.87	57/66	—	[113]
NiO/SnO <sub>2</sub>	50	300	9	-/-	5	[114]
NiO/SnO <sub>2</sub>	1000	250	123.7	10/58	—	[115]
NiO/SnO <sub>2</sub>	1000	150	84.7	5/15	—	[116]
NiO/SnO <sub>2</sub>	100	260	153	-/-	5	[117]
NiO/SnO <sub>2</sub>	1000	320	576.5	9/34	—	[118]
NiO/SnO <sub>2</sub>	100	75	248	-/-	—	[67]
NiO/ZnO	100	260	61	-/-	—	[101]
NiO/ZnO	100	200	11.3	4/78	—	[63]
NiO/ZnO	100	350	54	-/-	—	[102]
NiO/ZnO	200	300	33	-/-	—	[103]
NiO/ZnO	250	RT	32.48%	2.7/3.6	—	[105]
NiO/ZnO	500	400	37.5	2.1/4.1	—	[106]
NiO/ZnO	100	325	16	13/498	—	[108]
NiO/ZnO	20	200	49	4/28	3	[110]
NiO/WO <sub>3</sub>	100	300	58.2	-/-	—	[119]
NiO/WO <sub>3</sub>	200	175	155%	19/20	—	[120]
NiO/WO <sub>3</sub>	200	320	10	-/-	—	[121]
NiO/Fe <sub>2</sub> O <sub>3</sub>	100	255	170.7	0.5/14.6	0.2	[124]
NiO/In <sub>2</sub> O <sub>3</sub>	100	280	4.61	-/27	—	[125]
NiO/In <sub>2</sub> O <sub>3</sub>	5	350	9.76	-/23	2	[126]
NiO/Co <sub>2</sub> O <sub>3</sub>	100	250	4.26	-/-	0.073	[135]

operating temperature of NiO/LaFeO<sub>3</sub> was 240 $^{\circ}\text{C}$ , while LaFeO<sub>3</sub> was 260 $^{\circ}\text{C}$ . It meant that NiO/LaFeO<sub>3</sub> could lower the operating temperature, which was beneficial for low temperature sensing. The response recovery curves of 10 ppm ethanol at 240 $^{\circ}\text{C}$  are shown in Figure 10(d). Both NiO/LaFeO<sub>3</sub> and LaFeO<sub>3</sub> had good reproducibility, and the response of NiO/LaFeO<sub>3</sub> was much higher than that of LaFeO<sub>3</sub>. In addition, NiO/LaFeO<sub>3</sub> had fast response and recovery speed (response time and recovery time were 2 s and 9 s, respectively). The response of NiO/LaFeO<sub>3</sub> also increased with increasing ethanol concentration and was consistently higher than that of pristine LaFeO<sub>3</sub> (Figure 10(e)). The NiO/LaFeO<sub>3</sub>-based sensors detected five different gases, as shown in Figure 10(f). The NiO/LaFeO<sub>3</sub> sensors exhibited a good selectivity to ethanol, which provided a new way to fabricate high-performance ethanol sensors. The enhanced sensing performance was ascribed to the special structure, the catalytic performance of NiO, and the electronic modulation of the Fermi level.

Haq et al. [139] used a hydrothermal method to decorate NiO nanoparticles on ZnSnO<sub>3</sub> fibers (Figure 11(a)). The gas responses of all samples at different temperatures were volcanic shape (Figure 11(b)). It was worth noting that NiO/ZnSnO<sub>3</sub> obtained the highest response at 160 $^{\circ}\text{C}$ , while NiO obtained the highest response at 200 $^{\circ}\text{C}$ . It meant that NiO/ZnSnO<sub>3</sub> obtained the highest response at 160 $^{\circ}\text{C}$ . The ZnSnO<sub>3</sub> composite could detect ethanol at lower temperatures. As in

Figure 11(c), ethanol, acetone, toluene, xylene, and benzene were detected. The NiO/ZnSnO<sub>3</sub> sensors possessed a much higher response to ethanol than other gases, with better selectivity. Figure 11(d) is the gas response of NiO/ZnSnO<sub>3</sub>, NiO, and ZnSnO<sub>3</sub> to different ethanol concentrations at 160 $^{\circ}\text{C}$ . As the ethanol concentration increased, the gas response also increased gradually. And NiO/ZnSnO<sub>3</sub> obtained the best ethanol sensing performance. The response of NiO/ZnSnO<sub>3</sub> to 20 ppm ethanol gas at 160 $^{\circ}\text{C}$  was 23.95. The enhanced sensitivity was attributed to the more oxygen content of ZnSnO<sub>3</sub> after NiO decoration. At the same time, ZnSnO<sub>3</sub> was an n-type semiconductor. The modulation effect brought by the PN heterojunction also made the resistance change of NiO/ZnSnO<sub>3</sub> larger, resulting in a higher gas response. Table 5 shows gas performance of NiO/bimetallic oxide-based composites.

In this section, we discussed the reported composites of NiO combined with MOS such as ZnO, SnO<sub>2</sub>, Fe<sub>2</sub>O<sub>3</sub>, In<sub>2</sub>O<sub>3</sub>, WO<sub>3</sub>, and bimetallic oxides LaFeO<sub>3</sub> and ZnSnO<sub>3</sub> in ethanol sensing. The combination of NiO with these oxides mainly relies on the electronic modulation brought about by the formation of PN heterojunctions. Although NiO composites have been reported, most of them are about oxides. For the future, other potential gas sensing materials, such as conducting polymers, MXene, and carbon-based materials, can also be compounded with NiO to improve the sensitive properties.

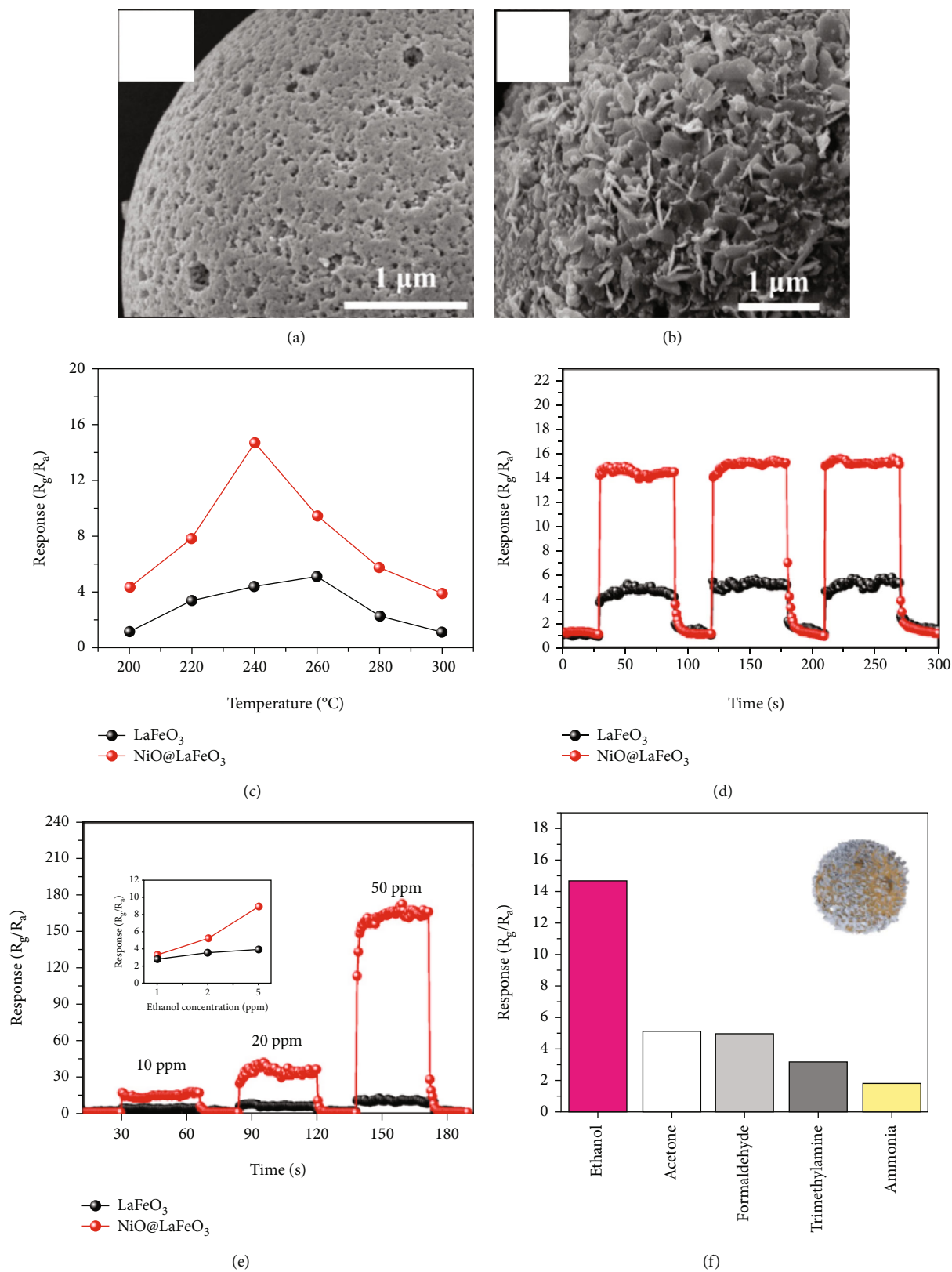


FIGURE 10: (a) SEM of  $\text{LaFeO}_3$ . (b) SEM of  $\text{NiO}/\text{LaFeO}_3$ . (c) Gas response of  $\text{NiO}/\text{LaFeO}_3$  and  $\text{LaFeO}_3$  under different temperatures at 10 ppm ethanol. (d) Response and recovery curves of  $\text{NiO}/\text{LaFeO}_3$  and  $\text{LaFeO}_3$  at 10 ppm ethanol. (e) Dynamic response curves of  $\text{NiO}/\text{LaFeO}_3$  and  $\text{LaFeO}_3$  to different ethanol concentrations at 240 °C. (f) Gas response of  $\text{NiO}/\text{LaFeO}_3$  under 10 ppm different gases (reprinted/adapted by [138]).

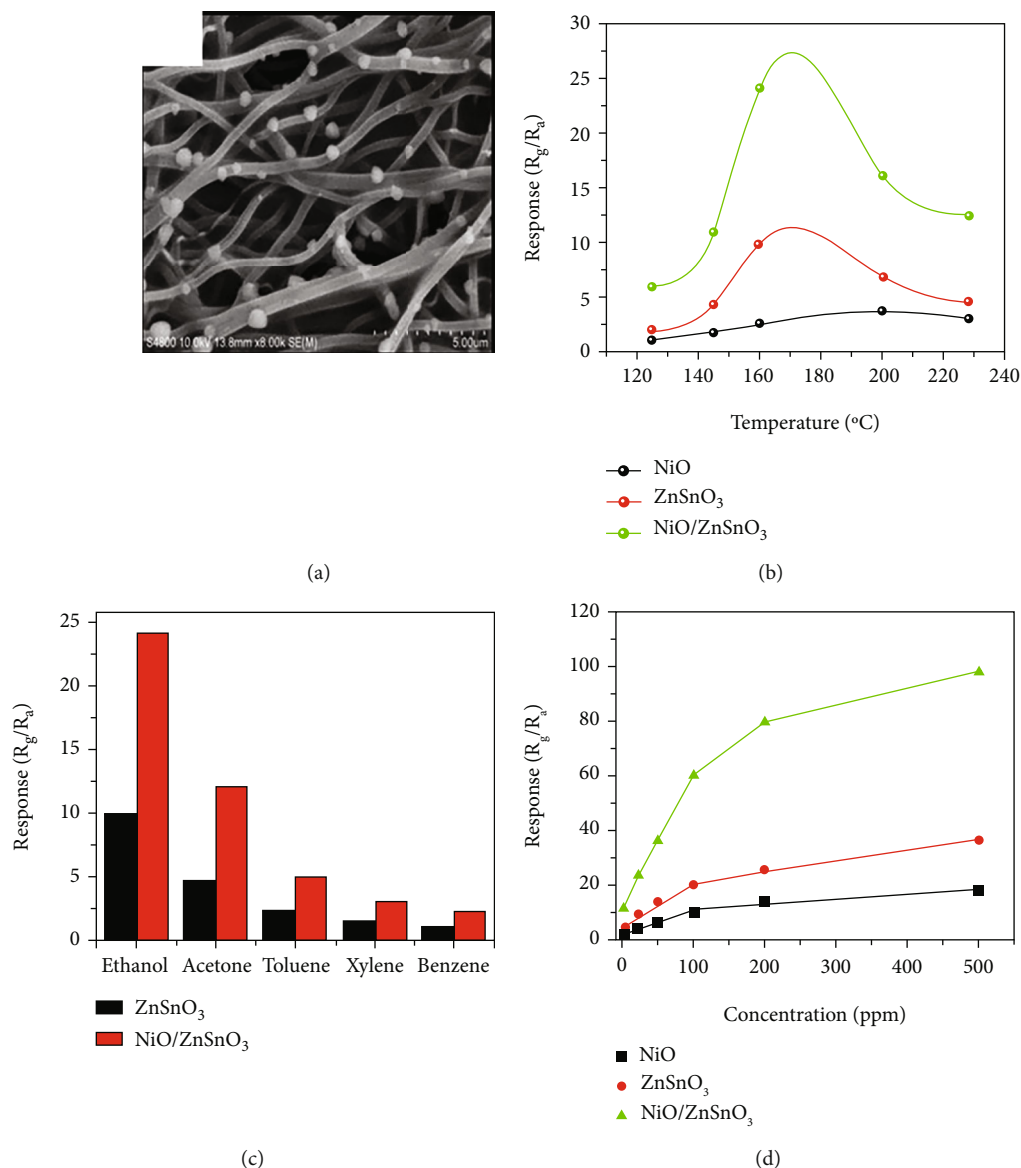


FIGURE 11: (a) SEM of NiO/ZnSnO<sub>3</sub>. (b) Gas response of NiO/ZnSnO<sub>3</sub>, NiO, and ZnSnO<sub>3</sub> under different temperatures at 20 ppm ethanol. (c) Gas response of NiO/ZnSnO<sub>3</sub> and ZnSnO<sub>3</sub> under 20 ppm different gases. (d) Gas response of NiO/ZnSnO<sub>3</sub>, NiO, and ZnSnO<sub>3</sub> to different ethanol concentrations at 160°C (reprinted/adapted by [139]).

TABLE 5: Gas performance of NiO/bimetallic oxide-based composites.

Material	Conc. (ppm)	Operating temp (°C)	Response	Response/recovery time (s/s)	LOD (ppm)	References
NiO/LaFeO <sub>3</sub>	10	240	—	2/9	—	[138]
NiO/ZnSnO <sub>3</sub>	20	160	23.95	-/-	—	[139]

## 6. Outlook

Although there have been many reports on the ethanol-sensitive performance of NiO in recent years, reports on the in-depth study of the selective mechanism of ethanol are still rare. Most of the literature addresses the fact that there is selectivity but does not discuss the ultimate mechanism of selectivity. Highly selective gas sensors are necessary in complex gas

environments, where they need to accurately identify target gases among interfering gases. The study of the mechanism of selectivity is helpful for the further development of highly selective gas sensors. In future work, researchers can further study the mechanism of ethanol selectivity to facilitate the efficient detection of ethanol in environments with interfering gases. At the same time, molecular imprinting technology is expected to be applied to improve selectivity. Molecular

imprinting is a lock-and-key technology that enables specific identification of specific gases. Combining molecular imprinting technology with resistive sensors is believed to further address the selectivity challenges of gas sensors.

## 7. Conclusion

In conclusion, this review presented an overview of NiO-based ethanol gas sensors. We first introduced the effect of modified NiO morphology on ethanol performance that has been reported in recent years. The morphology with large specific surface area and high porosity was considered to be the structure that can bring high gas response. Then, we discussed the enhanced effect of the doping of metal cations and precious metal particle loading on the ethanol-sensitive properties of NiO. Doping ions increased the ground-state resistance and increased the oxygen defect concentration of NiO. The effects of precious metal particles on the performance of NiO included chemical sensitization and electronic sensitization. Finally, the related contents of NiO forming composites with metal oxides and bimetallic oxides were discussed. In this section, the specific improvement mechanism was discussed first, and then, the related work of researchers in recent years was summarized.

## Data Availability

All data can be obtained from corresponding author Yanqiong Li.

## Conflicts of Interest

The authors declare that they have no conflicts of interest.

## Acknowledgments

This work was supported by the Graduate Research and Innovation Foundation of Chongqing, China (Grant No. CYS22003).

## References

- [1] S. Singh, J. Deb, S. Kumar, U. Sarkar, and S. Sharma, "Selective N,N-dimethylformamide vapor sensing using MoSe<sub>2</sub>/multiwalled carbon nanotube composites at room temperature," *Acs Applied Nano Materials*, vol. 5, no. 3, pp. 3913–3924, 2022.
- [2] W. Qin, R. Zhang, Z. Yuan, C. Xing, and F. Meng, "Preparation of p-LaFeO<sub>3</sub>/n-Fe<sub>2</sub>O<sub>3</sub> heterojunction composites by one-step hydrothermal method and gas sensing properties for acetone," *Ieee Transactions on Instrumentation and Measurement*, vol. 71, pp. 1–9, 2022.
- [3] B. Huang, W. Zeng, and Y. Li, "Synthesis of ZnO@ZIF-8 nanorods with enhanced response to VOCs," *Journal of the Electrochemical Society*, vol. 169, no. 4, p. 047508, 2022.
- [4] J. Fang, Z.-H. Ma, J.-J. Xue, X. Chen, R.-P. Xiao, and J.-M. Song, "Au doped In<sub>2</sub>O<sub>3</sub> nanoparticles: preparation, and their ethanol detection with high performance," *Materials Science in Semiconductor Processing*, vol. 146, p. 106701, 2022.
- [5] S. K. Rao, A. K. Priya, S. M. Kamath et al., "Unraveling the potential of Gd doping on mullite Bi<sub>2</sub>Fe<sub>4</sub>O<sub>9</sub> for fiber optic ethanol gas detection at room temperature," *Materials Chemistry and Physics*, vol. 278, p. 125646, 2022.
- [6] A. Akhtar, S. Sadaf, J. Liu et al., "Hydrothermally synthesized spherical g-C<sub>3</sub>N<sub>4</sub>-NiCo<sub>2</sub>O<sub>4</sub> nanocomposites for ppb level ethanol detection," *Journal of Alloys and Compounds*, vol. 911, p. 165048, 2022.
- [7] B. Du, Y. Zheng, J. Ye, D. Wang, C. Mao, and N. Sun, "Photoluminescence-based sensing of ethanol gas with ultrafine WO<sub>3</sub> nanorods," *Optics Letters*, vol. 47, no. 5, pp. 1145–1148, 2022.
- [8] P. Biswas, C. Zhang, Y. Chen et al., "A portable micro-gas chromatography with integrated photonic crystal slab sensors on chip," *Biosensors-Basel*, vol. 11, no. 9, p. 326, 2021.
- [9] M. B. Banerjee, S. R. Chowdhury, R. B. Roy et al., "Development of a low-cost portable gas sensing system based on molecularly imprinted quartz crystal microbalance sensor for detection of eugenol in clove oil," *Ieee Transactions on Instrumentation and Measurement*, vol. 70, pp. 1–10, 2021.
- [10] W. Qin, Z. Yuan, H. Gao, R. Zhang, and F. Meng, "Perovskite-structured LaCoO<sub>3</sub> modified ZnO gas sensor and investigation on its gas sensing mechanism by first principle," *Sensors and Actuators B-Chemical*, vol. 341, p. 130015, 2021.
- [11] K. Zhang, S. Qin, P. Tang, Y. Feng, and D. Li, "Ultra-sensitive ethanol gas sensors based on nanosheet-assembled hierarchical ZnO-In<sub>2</sub>O<sub>3</sub> heterostructures," *Journal of Hazardous Materials*, vol. 391, p. 122191, 2020.
- [12] J. van den Broek, S. Abegg, S. E. Pratsinis, and A. T. Guentner, "Highly selective detection of methanol over ethanol by a handheld gas sensor," *Nature Communications*, vol. 10, no. 1, 2019.
- [13] P. Wang, T. Song, G. Gao, K. Matras-Postolek, and P. Yang, "SnO<sub>2</sub> clusters embedded in TiO<sub>2</sub> nanosheets: heterostructures and gas sensing performance," *Sensors and Actuators B-Chemical*, vol. 357, p. 131433, 2022.
- [14] E. P. Nascimento, R. N. Araujo, H. C. T. Firmino et al., "Parallel-solution blow spun Al-SnO<sub>2</sub>/F-SnO<sub>2</sub> fibers as an efficient room temperature ethanol sensor," *Ceramics International*, vol. 48, no. 9, pp. 13163–13174, 2022.
- [15] X. Tian, H. Cao, H. Wang, J. Wang, X. Wei, and X. Wu, "Acid vapor oxidation growth of SnO<sub>2</sub> nanospheres with ultra-high sensitivity to ethanol detection at low temperature," *Journal of Alloys and Compounds*, vol. 905, p. 164229, 2022.
- [16] B. Jiang, J. Lu, W. Han et al., "Hierarchical mesoporous zinc oxide microspheres for ethanol gas sensor," *Sensors and Actuators B-Chemical*, vol. 357, p. 131333, 2022.
- [17] M. J. Ahemad, T. D. Le, D.-S. Kim, and Y.-T. Yu, "Bimetallic AgAu alloy@ZnO core-shell nanoparticles for ultra-high detection of ethanol: potential impact of alloy composition on sensing performance," *Sensors and Actuators B-Chemical*, vol. 359, p. 131595, 2022.
- [18] W. Photaram, M. Liangruksa, M. Aiempakit et al., "Design and fabrication of zinc oxide-graphene nanocomposite for gas sensing applications," *Applied Surface Science*, vol. 595, p. 153510, 2022.
- [19] R.-H. Wang, W. Wen, S. Zheng, Z. Ye, and J.-M. Wu, "Layered mesoporous SnO<sub>2</sub> for effective ethanol detection at reduced working temperature," *Sensors and Actuators B-Chemical*, vol. 362, p. 131805, 2022.

- [20] M. Pfeiffer and C. Hess, "Application of transient infrared spectroscopy to investigate the role of gold in ethanol gas sensing over Au/SnO<sub>2</sub>," *Journal of Physical Chemistry C*, vol. 126, no. 8, pp. 3980–3992, 2022.
- [21] C. Wang, R. Li, L. Feng, and J. Xu, "The SnO<sub>2</sub>/MXene composite ethanol sensor based on MEMS platform," *Chemosensors*, vol. 10, no. 3, p. 109, 2022.
- [22] X. Li, C.-X. Liu, J.-R. Zhou, Y. Ma, and S.-P. Ruan, "Study on ethanol gas sensor based on hierarchical structured NiO/Zn<sub>2</sub>SnO<sub>4</sub> nanoflowers," *Chinese Journal of Analytical Chemistry*, vol. 50, no. 4, pp. 564–573, 2022.
- [23] Z. Shao, Z. Zhao, P. Chen et al., "Enhanced ethanol response of Ti3C2TXMXene derivative coupled with NiO nanodisk," *Inorganic and Nano-Metal Chemistry*, vol. 52, pp. 1–9, 2022.
- [24] S. Singh and S. Sharma, "Temperature-based selective detection of hydrogen sulfide and ethanol with MoS<sub>2</sub>/WO<sub>3</sub> composite," *ACS Omega*, vol. 7, no. 7, pp. 6075–6085, 2022.
- [25] M. Tomic, Z. Fohlerova, I. Gracia, E. Figueras, C. Cane, and S. Vallejos, "UV-light activated APTES modified WO<sub>3-x</sub> nanowires sensitive to ethanol and nitrogen dioxide," *Sensors and Actuators B-Chemical*, vol. 328, p. 129046, 2021.
- [26] E. Spagnoli, S. Krik, B. Fabbri et al., "Development and characterization of WO<sub>3</sub> nanoflakes for selective ethanol sensing," *Sensors and Actuators B-Chemical*, vol. 347, p. 130593, 2021.
- [27] X. Li, Y. Wang, P. Cheng et al., "High-performance ethanol sensor of wrinkled microspheres by spray pyrolysis," *Sensors and Actuators B-Chemical*, vol. 344, p. 130309, 2021.
- [28] T.-T. Liang, D.-S. Kim, J.-W. Yoon, and Y.-T. Yu, "Rapid synthesis of rhombohedral In<sub>2</sub>O<sub>3</sub> nanoparticles via a microwave-assisted hydrothermal pathway and their application for conductometric ethanol sensing," *Sensors and Actuators B-Chemical*, vol. 346, p. 130578, 2021.
- [29] X. Jin, Y. Li, B. Zhang, X. Xu, G. Sun, and Y. Wang, "Temperature-dependent dual selectivity of hierarchical porous In<sub>2</sub>O<sub>3</sub> nanospheres for sensing ethanol and TEA," *Sensors and Actuators B-Chemical*, vol. 330, p. 129271, 2021.
- [30] K. Li, Y. Luo, B. Liu, H. Wang, L. Gao, and G. Duan, "Theory-guided oxygen-vacancy for enhancing H<sub>2</sub>S sensing performance of NiO," *Chemical Engineering Journal*, vol. 432, p. 134302, 2022.
- [31] M. Shoorangiz, L. Shariatifard, H. Roshan, and A. Mirzaei, "Hydrothermally synthesized flower-like vanadium oxide nanostructures for ethanol sensing studies," *Materials Science in Semiconductor Processing*, vol. 137, p. 106241, 2022.
- [32] G. Yuan, Y. Zhong, Y. Chen, Q. Zhuo, and X. Sun, "Highly sensitive and fast-response ethanol sensing of porous Co<sub>3</sub>O<sub>4</sub> hollow polyhedra via palladium reined spillover effect," *RSC Advances*, vol. 12, no. 11, pp. 6725–6731, 2022.
- [33] P. T. Moseley, "Progress in the development of semiconducting metal oxide gas sensors: a review," *Measurement Science and Technology*, vol. 28, no. 8, p. 082001, 2017.
- [34] N. Joshi, L. F. da Silva, H. Jadhav et al., "One-step approach for preparing ozone gas sensors based on hierarchical NiCo<sub>2</sub>O<sub>4</sub> structures," *RSC Advances*, vol. 6, no. 95, pp. 92655–92662, 2016.
- [35] N. Joshi, L. F. da Silva, H. S. Jadhav et al., "Yolk-shelled ZnCo<sub>2</sub>O<sub>4</sub> microspheres: surface properties and gas sensing application," *Sensors and Actuators B-Chemical*, vol. 257, pp. 906–915, 2018.
- [36] J. Yu, C. Wang, Q. Yuan, X. Yu, D. Wang, and Y. Chen, "Ag-modified porous perovskite-type LaFeO<sub>3</sub> for efficient ethanol detection," *Nanomaterials*, vol. 12, no. 10, p. 1768, 2022.
- [37] R. Malik, N. Joshi, and V. K. Tomer, "Advances in the designs and mechanisms of MoO<sub>3</sub> nanostructures for gas sensors: a holistic review," *Materials Advances*, vol. 2, no. 13, pp. 4190–4227, 2021.
- [38] N. J. Joshi, M. L. Braunger, F. M. Shimizu, A. Riul Jr., and O. N. J. M. M. de Oliveira Jr, "Insights into nano-heterostructured materials for gas sensing: a review," *Multi-functional Materials*, vol. 4, no. 3, 2021.
- [39] N. Joshi, T. Hayasaka, Y. Liu, H. Liu, O. N. Oliveira Jr., and L. Lin, "A review on chemiresistive room temperature gas sensors based on metal oxide nanostructures, graphene and 2D transition metal dichalcogenides," *Microchimica Acta*, vol. 185, no. 4, p. 213, 2018.
- [40] X. Liu, T. Ma, N. Pinna, and J. Zhang, "Two-dimensional nanostructured materials for gas sensing," *Advanced Functional Materials*, vol. 27, no. 37, 2017.
- [41] J. Zhang, X. Liu, G. Neri, and N. J. A. Pinna, "Nanostructured materials for room-temperature gas sensors," *Advanced Materials Advanced Materials*, vol. 28, no. 5, pp. 795–831, 2016.
- [42] A. Saaedi, P. Shabani, and R. Yousefi, "Study on the effects of the magneto assisted deposition on ammonia gas sensing properties of polyaniline," *Journal of Materials Science-Materials in Electronics*, vol. 30, no. 11, pp. 10765–10775, 2019.
- [43] L. Zhu and W. Zeng, "Room-temperature gas sensing of ZnO-based gas sensor: a review," *Sensors and Actuators A-Physical*, vol. 267, pp. 242–261, 2017.
- [44] Y. Wang, B. Liu, S. Xiao et al., "Low-temperature H<sub>2</sub>S detection with hierarchical Cr-doped WO<sub>3</sub> microspheres," *ACS Applied Materials & Interfaces*, vol. 8, no. 15, pp. 9674–9683, 2016.
- [45] Y. Liu, J. Bai, Y. Li et al., "Preparation of PdO-decorated NiO porous film on ceramic substrate for highly selective and sensitive H<sub>2</sub>S detection," *Ceramics International*, vol. 48, no. 4, pp. 4787–4794, 2022.
- [46] H. Liu, Z. Wang, G. Cao et al., "Construction of hollow NiO/ZnO p-n heterostructure for ultrahigh performance toluene gas sensor," *Materials Science in Semiconductor Processing*, vol. 141, p. 106435, 2022.
- [47] C. Li, P. G. Choi, K. Kim, and Y. Masuda, "High performance acetone gas sensor based on ultrathin porous NiO nano-sheet," *Sensors and Actuators B-Chemical*, vol. 367, p. 132143, 2022.
- [48] Y. Zhang, S. Han, M. Wang et al., "Electrospun Cu-doped In<sub>2</sub>O<sub>3</sub> hollow nanofibers with enhanced H<sub>2</sub>S gas sensing performance," *Journal of Advanced Ceramics*, vol. 11, no. 3, pp. 427–442, 2022.
- [49] C. Zhang, Y. Huan, Y. Li, Y. Luo, and M. Debliquy, "Low concentration isopropanol gas sensing properties of Ag nanoparticles decorated In<sub>2</sub>O<sub>3</sub> hollow spheres," *Journal of Advanced Ceramics*, vol. 11, no. 3, pp. 379–391, 2022.
- [50] T. P. Mokoena, H. C. Swart, and D. E. Motaung, "A review on recent progress of p-type nickel oxide based gas sensors: future perspectives," *Journal of Alloys and Compounds*, vol. 805, pp. 267–294, 2019.
- [51] Y. Lu, Y. H. Ma, S. Y. Ma et al., "Curly porous NiO nano-sheets with enhanced gas-sensing properties," *Materials Letters*, vol. 190, pp. 252–255, 2017.



- [52] S. Cao, L. Peng, B. Liu et al., "Hydrothermal synthesis of novel lotus-root slice NiO architectures with enhanced gas response properties," *Journal of Alloys and Compounds*, vol. 798, pp. 478–483, 2019.
- [53] C. Su, L. Zhang, Y. Han et al., "Controllable synthesis of crescent-shaped porous NiO nanoplates for conductometric ethanol gas sensors," *Sensors and Actuators B-Chemical*, vol. 296, p. 126642, 2019.
- [54] S. Liu, W. Zeng, and T. Chen, "Synthesis of hierarchical flower-like NiO and the influence of surfactant," *Physica E-Low-Dimensional Systems & Nanostructures*, vol. 85, pp. 13–18, 2017.
- [55] Y. Zhang and W. Zeng, "New insight into gas sensing performance of nanoneedle-assembled and nanosheet-assembled hierarchical NiO nanoflowers," *Materials Letters*, vol. 195, pp. 217–219, 2017.
- [56] M. Carbone and P. Tagliatesta, "NiO grained-flowers and nanoparticles for ethanol sensing," *Materials*, vol. 13, no. 8, p. 1880, 2020.
- [57] Q. Gao, W. Zeng, and R. Miao, "Synthesis of multifarious hierarchical flower-like NiO and their gas-sensing properties," *Journal of Materials Science-Materials in Electronics*, vol. 27, no. 9, pp. 9410–9416, 2016.
- [58] S. Cao, T. Han, and L. Peng, "Surfactant-free synthesis of 3D hierarchical flower-like NiO nanostructures with enhanced ethanol-sensing performance," *Journal of Materials Science-Materials in Electronics*, vol. 31, no. 20, pp. 17291–17296, 2020.
- [59] J. Wang, Q. Zhou, Z. Lu, Z. Wei, and W. Zeng, "The novel 2D honeycomb-like NiO nanoplates assembled by nanosheet arrays with excellent gas sensing performance," *Materials Letters*, vol. 255, p. 126523, 2019.
- [60] X. Chen, S. Wang, C. Su et al., "Two-dimensional Cd-doped porous Co<sub>3</sub>O<sub>4</sub> nanosheets for enhanced room-temperature NO<sub>2</sub> sensing performance," *Sensors and Actuators B-Chemical*, vol. 305, p. 127393, 2020.
- [61] J.-H. Kim, A. Mirzaei, M. Osada, H. W. Kim, and S. S. Kim, "Hydrogen sensing characteristics of Pd-decorated ultrathin ZnO nanosheets," *Sensors and Actuators B-Chemical*, vol. 329, p. 129222, 2021.
- [62] M. Kumar, V. Bhatt, J. Kim et al., "Holey engineered 2D ZnO-nanosheets architecture for supersensitive ppm level H<sub>2</sub> gas detection at room temperature," *Sensors and Actuators B-Chemical*, vol. 326, p. 128839, 2021.
- [63] Y.-C. Liang, Y.-C. Chang, and W.-C. Zhao, "Design and synthesis of novel 2D porous zinc oxide-nickel oxide composite nanosheets for detecting ethanol vapor," *Nanomaterials*, vol. 10, no. 10, p. 1989, 2020.
- [64] R. S. Ganesh, G. K. Mani, R. Elayaraja et al., "ZnO hierarchical 3D-flower like architectures and their gas sensing properties at room temperature," *Applied Surface Science*, vol. 449, pp. 314–321, 2018.
- [65] A. Das, P. M. Kumar, M. Bhagavathiachari, and R. G. Nair, "Shape selective flower-like ZnO nanostructures prepared via structure-directing reagent free methods for efficient photocatalytic performance," *Materials Science and Engineering B-Advanced Functional Solid-State Materials*, vol. 269, p. 115149, 2021.
- [66] L. Song, A. Lukianov, D. Butenko et al., "Facile synthesis of hierarchical tin oxide nanoflowers with ultra-high methanol gas sensing at low working temperature," *Nanoscale Research Letters*, vol. 14, no. 1, p. 84, 2019.
- [67] R. G. Motsoeneng, I. Kortidis, R. Rikhotso, H. C. Swart, S. S. Ray, and D. E. Motaung, "Temperature-dependent response to C<sub>3</sub>H<sub>7</sub>OH and C<sub>2</sub>H<sub>5</sub>OH vapors induced by deposition of Au nanoparticles on SnO<sub>2</sub>/NiO hollow sphere-based conductometric sensors," *Sensors and Actuators B-Chemical*, vol. 316, p. 128041, 2020.
- [68] X. Wang, F. Liu, X. Chen et al., "SnO<sub>2</sub> core-shell hollow microspheres co-modification with Au and NiO nanoparticles for acetone gas sensing," *Powder Technology*, vol. 364, pp. 159–166, 2020.
- [69] Q. Hu, Z. Wang, J. Chang, P. Wan, J. Huang, and L. Feng, "Design and preparation of hollow NiO sphere-polyaniline composite for NH<sub>3</sub> gas sensing at room temperature," *Sensors and Actuators B-Chemical*, vol. 344, p. 130179, 2021.
- [70] J. Yang, W. Han, J. Ma et al., "Sn doping effect on NiO hollow nanofibers based gas sensors about the humidity dependence for triethylamine detection," *Sensors and Actuators B-Chemical*, vol. 340, p. 129971, 2021.
- [71] W.-C. Geng, X.-R. Cao, S.-L. Xu et al., "Synthesis of hollow spherical nickel oxide and its gas-sensing properties," *Rare Metals*, vol. 40, no. 6, pp. 1622–1631, 2021.
- [72] S. Bai, H. Fu, X. Shu et al., "NiO hierarchical hollow microspheres doped Fe to enhance triethylamine sensing properties," *Materials Letters*, vol. 210, pp. 305–308, 2018.
- [73] S. Chu, C. Yang, and X. Su, "Synthesis of NiO hollow nanospheres via Kirkendall effect and their enhanced gas sensing performance," *Applied Surface Science*, vol. 492, pp. 82–88, 2019.
- [74] L. Wei, Y. Xia, and J. Meng, "A novel hollow nickel oxide sensor and gas detection performance in asphalt," *Science of Advanced Materials*, vol. 11, no. 1, pp. 56–59, 2019.
- [75] C. Kuang, W. Zeng, H. Ye, and Y. Li, "A novel approach for fabricating NiO hollow spheres for gas sensors," *Physica E-Low-Dimensional Systems & Nanostructures*, vol. 97, pp. 314–316, 2018.
- [76] B. Liu, M. Wang, S. Liu, H. Zheng, and H. Yang, "The sensing reaction on the Ni-NiO (111) surface at atomic and molecule level and migration of electron," *Sensors and Actuators B-Chemical*, vol. 273, pp. 794–803, 2018.
- [77] B. Liu, L. Wang, Y. Ma et al., "Enhanced gas-sensing properties and sensing mechanism of the foam structures assembled from NiO nanoflakes with exposed {111} facets," *Applied Surface Science*, vol. 470, pp. 596–606, 2019.
- [78] Y. Liang, Y. Yang, H. Zhou et al., "Active {111}-faceted ultrathin NiO single-crystalline porous nanosheets supported highly dispersed Pt nanoparticles for synergistic enhancement of gas sensing and photocatalytic performance," *Applied Surface Science*, vol. 471, pp. 124–133, 2019.
- [79] A. Hermawan, A. T. Hanindriyo, E. R. Ramadhan et al., "Octahedral morphology of NiO with (111) facet synthesized from the transformation of NiOHCl for the NO<sub>x</sub> detection and degradation: experiment and DFT calculation," *Inorganic Chemistry Frontiers*, vol. 7, no. 18, pp. 3431–3442, 2020.
- [80] B. Deng, J. Jiang, H. Li et al., "Enhanced piezoelectric property in Mn-doped K<sub>0.5</sub>Na<sub>0.5</sub>NbO<sub>3</sub> ceramics via cold sintering process and KMnO<sub>4</sub> solution," *Journal of the American Ceramic Society*, vol. 105, no. 9, pp. 5774–5782, 2022.
- [81] Z. Peng, L. Chen, Y. Xiang, and F. Cao, "Microstructure and electrical properties of lanthanides-doped CaBi<sub>2</sub>Nb<sub>2</sub>O<sub>9</sub> ceramics," *Materials Research Bulletin*, vol. 148, p. 111670, 2022.

- [82] C. Wang, X. Cui, J. Liu et al., "Design of superior ethanol gas sensor based on Al-doped NiO nanorod-flowers," *Acs Sensors*, vol. 1, no. 2, pp. 131–136, 2016.
- [83] L. Zhu, W. Zeng, J. Yang, and Y. Li, "Unique hierarchical Ce-doped NiO microflowers with enhanced gas sensing performance," *Materials Letters*, vol. 251, pp. 61–64, 2019.
- [84] Q. Wang, J. Bai, Q. Hu et al., "W-doped NiO as a material for selective resistive ethanol sensors," *Sensors and Actuators B-Chemical*, vol. 308, p. 127668, 2020.
- [85] J. Y. Niu, L. Wang, B. Hong et al., "Synergistic effects of  $\alpha$ -Fe<sub>2</sub>O<sub>3</sub> nanoparticles and Fe-doping on gas-sensing performance of NiO nanowires and interface mechanism," *Nanotechnology*, vol. 32, no. 48, p. 485502, 2021.
- [86] J. Wei, X. Li, Y. Han et al., "Highly improved ethanol gas-sensing performance of mesoporous nickel oxides nanowires with the stannum donor doping," *Nanotechnology*, vol. 29, no. 24, p. 245501, 2018.
- [87] M. Taeno, D. Maestre, and A. Cremades, "Fabrication and study of self-assembled NiO surface networks assisted by Sn doping," *Journal of Alloys and Compounds*, vol. 827, p. 154172, 2020.
- [88] S. Shailja, K. J. Singh, and R. C. Singh, "Highly sensitive and selective ethanol gas sensor based on Ga-doped NiO nanoparticles," *Journal of Materials Science-Materials in Electronics*, vol. 32, no. 8, pp. 11274–11290, 2021.
- [89] Z. Zhang, Z. Wen, S. Khan, N. Rahman, and L. Zhu, "Humidity sensor based on mesoporous Al-doped NiO ultralong nanowires with enhanced ethanol sensing performance," *Journal of Materials Science-Materials in Electronics*, vol. 30, no. 7, pp. 7121–7134, 2019.
- [90] H. D. Chen, K. L. Jin, J. C. Xu et al., "High-valence cations-doped mesoporous nickel oxides nanowires: nanocasting synthesis, microstructures and improved gas-sensing performance," *Sensors and Actuators B-Chemical*, vol. 296, p. 126622, 2019.
- [91] J. Chang, M. Horprathum, D. Wang et al., "Aliovalent Sc and Li co-doping boosts the performance of p-type NiO sensor," *Sensors and Actuators B-Chemical*, vol. 326, p. 128834, 2021.
- [92] X. Sun, X. Hu, Y. Wang et al., "Enhanced gas-sensing performance of Fe-doped ordered mesoporous NiO with long-range periodicity," *Journal of Physical Chemistry C*, vol. 119, no. 6, pp. 3228–3237, 2015.
- [93] Y. Zhao, J. Yan, Y. Huang et al., "Interfacial self-assembly of monolayer Mg-doped NiO honeycomb structured thin film with enhanced performance for gas sensing," *Journal of Materials Science-Materials in Electronics*, vol. 29, no. 13, pp. 11498–11508, 2018.
- [94] Y. Tang, Z. Han, Y. Qi et al., "Enhanced ppb-level formaldehyde sensing performance over Pt deposited SnO<sub>2</sub> nanospheres," *Journal of Alloys and Compounds*, vol. 899, p. 163230, 2022.
- [95] S. M. Majhi, G. K. Naik, H.-J. Lee et al., "Au@NiO core-shell nanoparticles as a p-type gas sensor: novel synthesis, characterization, and their gas sensing properties with sensing mechanism," *Sensors and Actuators B-Chemical*, vol. 268, pp. 223–231, 2018.
- [96] J. Fu, C. Zhao, J. Zhang, Y. Peng, and E. Xie, "Enhanced gas sensing performance of electrospun Pt-functionalized NiO nanotubes with chemical and electronic sensitization," *ACS Applied Materials & Interfaces*, vol. 5, no. 15, pp. 7410–7416, 2013.
- [97] S. Park, H. Kheel, G.-J. Sun, S. K. Hyun, S. E. Park, and C. Lee, "Ethanol sensing properties of Au-functionalized NiO nanoparticles," *Bulletin of the Korean Chemical Society*, vol. 37, no. 5, pp. 713–719, 2016.
- [98] S.-C. Wang, X.-H. Wang, G.-Q. Qiao et al., "NiO nanoparticles-decorated ZnO hierarchical structures for isopropanol gas sensing," *Rare Metals*, vol. 41, no. 3, pp. 960–971, 2022.
- [99] J. Zhang and J. Li, "The oxygen vacancy defect of ZnO/NiO nanomaterials improves photocatalytic performance and ammonia sensing performance," *Nanomaterials*, vol. 12, no. 3, p. 433, 2022.
- [100] H.-F. Bao, T.-T. Yue, X.-X. Zhang, Z. Dong, Y. Yan, and W. Feng, "Enhanced ethanol-sensing properties based on modified NiO-ZnO p-n heterojunction nanotubes," *Journal of Nanoscience and Nanotechnology*, vol. 20, no. 2, pp. 731–740, 2020.
- [101] L. Zhu, W. Zeng, J. Yang, and Y. Li, "Fabrication of hierarchical hollow NiO/ZnO microspheres for ethanol sensing property," *Materials Letters*, vol. 230, pp. 297–299, 2018.
- [102] L. Zhu, W. Zeng, J. Yang, and Y. Li, "One-step hydrothermal fabrication of nanosheet-assembled NiO/ZnO microflower and its ethanol sensing property," *Ceramics International*, vol. 44, no. 16, pp. 19825–19830, 2018.
- [103] L. Qiu, W. Zeng, Y. Li, and Q. Zhou, "Synthesis of nanosheet-assembled porous NiO/ZnO microflowers through a facile one-step hydrothermal approach," *Materials Letters*, vol. 256, p. 126649, 2019.
- [104] H. Chen, R. Bo, A. Shrestha et al., "NiO-ZnO nanoheterojunction networks for room-temperature volatile organic compounds sensing," *Advanced Optical Materials*, vol. 6, no. 22, p. 1800677, 2018.
- [105] S. T. Hezarjaribi and S. Nasirian, "An enhanced fast ethanol sensor based on zinc oxide/nickel oxide nanocomposite in dynamic situations," *Journal of Inorganic and Organometallic Polymers and Materials*, vol. 30, no. 10, pp. 4072–4081, 2020.
- [106] X. Deng, L. Zhang, J. Guo, Q. Chen, and J. Ma, "ZnO enhanced NiO-based gas sensors towards ethanol," *Materials Research Bulletin*, vol. 90, pp. 170–174, 2017.
- [107] C. Baratto, R. Kumar, E. Comini, M. Ferroni, and M. Campanini, "Bottle-brush-shaped heterostructures of NiO-ZnO nanowires: growth study and sensing properties," *Nanotechnology*, vol. 28, no. 46, p. 465502, 2017.
- [108] J. Bai, C. Zhao, H. Gong et al., "Debye-length controlled gas sensing performances in NiO@ZnO p-n junctional core-shell nanotubes," *Journal of Physics D-Applied Physics*, vol. 52, no. 28, p. 285103, 2019.
- [109] L. Zhou, W. Zeng, and Y. Li, "A facile one-step hydrothermal synthesis of a novel NiO/ZnO nanorod composite and its enhanced ethanol sensing property," *Materials Letters*, vol. 254, pp. 92–95, 2019.
- [110] S. Zhao, Y. Shen, Y. Xia et al., "Synthesis and gas sensing properties of NiO/ZnO heterostructured nanowires," *Journal of Alloys and Compounds*, vol. 877, p. 160189, 2021.
- [111] N. Jayababu, M. Poloju, J. Shruthi, and M. V. R. Reddy, "Semi shield driven p-n heterostructures and their role in enhancing the room temperature ethanol gas sensing performance of NiO/SnO<sub>2</sub> nanocomposites," *Ceramics International*, vol. 45, no. 12, pp. 15134–15142, 2019.
- [112] Y. Chu, H. Liu, and S. Yan, "Preparation and gas sensing properties of SnO<sub>2</sub>/NiO composite semiconductor

- nanofibers,” *Journal of Inorganic Materials*, vol. 36, no. 9, pp. 950–958, 2021.
- [113] S. U. Din, M. Ul Haq, M. Sajid et al., “Development of high-performance sensor based on NiO/SnO<sub>2</sub> heterostructures to study sensing properties towards various reducing gases,” *Nanotechnology*, vol. 31, no. 39, p. 395502, 2020.
- [114] W. Tong, Y. Wang, Y. Bian, A. Wang, N. Han, and Y. Chen, “Sensitive cross-linked SnO<sub>2</sub>:NiO networks for MEMS compatible ethanol gas sensors,” *Nanoscale Research Letters*, vol. 15, no. 1, p. 35, 2020.
- [115] L. Zhang, J. He, and W. Jiao, “Synthesis and gas sensing performance of NiO decorated SnO<sub>2</sub> vertical-standing nanotubes composite thin films,” *Sensors and Actuators B-Chemical*, vol. 281, pp. 326–334, 2019.
- [116] J. He, W. Jiao, L. Zhang, and R. Feng, “Preparation and gas-sensing performance of SnO<sub>2</sub>/NiO composite oxide synthesized by microwave-assisted liquid phase deposition,” *Particuology*, vol. 41, pp. 118–125, 2018.
- [117] G. Niu, C. Zhao, H. Gong, Z. Yang, X. Leng, and F. Wang, “NiO nanoparticle-decorated SnO<sub>2</sub> nanosheets for ethanol sensing with enhanced moisture resistance,” *Microsystems & Nanoengineering*, vol. 5, no. 1, p. 21, 2019.
- [118] G. Sun, H. Chen, Y. Li et al., “Synthesis and improved gas sensing properties of NiO-decorated SnO<sub>2</sub> microflowers assembled with porous nanorods,” *Sensors and Actuators B-Chemical*, vol. 233, pp. 180–192, 2016.
- [119] Z. Wei, Q. Zhou, J. Wang, and W. Zeng, “Hydrothermal synthesis of hierarchical WO<sub>3</sub>/NiO porous microsphere with enhanced gas sensing performances,” *Materials Letters*, vol. 264, p. 127383, 2020.
- [120] F.-R. Juang and W.-Y. Wang, “Ethanol gas sensors with nanocomposite of nickel oxide and tungsten oxide,” *IEEE Sensors Journal*, vol. 21, no. 18, pp. 19740–19752, 2021.
- [121] L. Lin, T. Liu, Y. Zhang, S. Hussain, S. Wu, and W. Zeng, “Superior ethanol-sensing performance research of WO<sub>3</sub> center dot 0.33H<sub>2</sub>O doped chrysanthemum-like NiO composite,” *Materials Letters*, vol. 108, pp. 231–234, 2013.
- [122] L. Wang, B. Hong, H. D. Chen et al., “The highly improved gas-sensing performance of  $\alpha$ -Fe<sub>2</sub>O<sub>3</sub>-decorated NiO nanowires and the interfacial effect of p-n heterojunctions,” *Journal of Materials Chemistry C*, vol. 8, no. 11, pp. 3855–3864, 2020.
- [123] S. Dong, D. Wu, W. Gao, H. Hao, G. Liu, and S. Yan, “Multidimensional templated synthesis of hierarchical Fe<sub>2</sub>O<sub>3</sub>/NiO composites and their superior ethanol sensing properties promoted by nanoscale p-n heterojunctions,” *Dalton Transactions*, vol. 49, no. 4, pp. 1300–1310, 2020.
- [124] W. Tan, J. Tan, L. Fan, Z. Yu, J. Qian, and X. Huang, “Fe<sub>2</sub>O<sub>3</sub>-loaded NiO nanosheets for fast response/recovery and high response gas sensor,” *Sensors and Actuators B-Chemical*, vol. 256, pp. 282–293, 2018.
- [125] S. Yan, W. Song, D. Wu et al., “Assembly of In<sub>2</sub>O<sub>3</sub> nanoparticles decorated NiO nanosheets heterostructures and their enhanced gas sensing characteristics,” *Journal of Alloys and Compounds*, vol. 896, p. 162887, 2022.
- [126] H.-J. Kim, H.-M. Jeong, T.-H. Kim, J.-H. Chung, Y. C. Kang, and J.-H. Lee, “Enhanced ethanol sensing characteristics of In<sub>2</sub>O<sub>3</sub>-decorated NiO hollow nanostructures via modulation of hole accumulation layers,” *ACS Applied Materials & Interfaces*, vol. 6, no. 20, pp. 18197–18204, 2014.
- [127] J. Lee, Y. Choi, B. J. Park et al., “Precise control of surface oxygen vacancies in ZnO nanoparticles for extremely high acetone sensing response,” *Journal of Advanced Ceramics*, vol. 11, no. 5, pp. 769–783, 2022.
- [128] X. Tian, H. Cao, X. Wei, J. Wang, X. Wu, and H. Wang, “Controllable acid vapor oxidation growth of complex SnO<sub>2</sub> nanostructures for ultrasensitive ethanol sensing,” *Ceramics International*, vol. 48, no. 7, pp. 9229–9238, 2022.
- [129] Y. Zhang, Z. Yang, L. Zhao, T. Fei, S. Liu, and T. Zhang, “Boosting room-temperature ppb-level NO<sub>2</sub> sensing over reduced graphene oxide by co-decoration of  $\alpha$ -Fe<sub>2</sub>O<sub>3</sub> and SnO<sub>2</sub> nanocrystals,” *Journal of Colloid and Interface Science*, vol. 612, pp. 689–700, 2022.
- [130] J. N. Mao, B. Hong, H. D. Chen et al., “Highly improved ethanol gas response of n-type  $\alpha$ -Fe<sub>2</sub>O<sub>3</sub> bunched nanowires sensor with high-valence donor-doping,” *Journal of Alloys and Compounds*, vol. 827, p. 154248, 2020.
- [131] X. Chen, R. Liang, C. Qin, Z. Ye, and L. Zhu, “Coaxial electrospinning Fe<sub>2</sub>O<sub>3</sub>@Co<sub>3</sub>O<sub>4</sub> double-shelled nanotubes for enhanced ethanol sensing performance in a wide humidity range,” *Journal of Alloys and Compounds*, vol. 891, p. 161868, 2022.
- [132] W.-H. Zhang, S.-J. Ding, Q.-S. Zhang et al., “Rare earth element-doped porous In<sub>2</sub>O<sub>3</sub> nanosheets for enhanced gas-sensing performance,” *Rare Metals*, vol. 40, no. 6, pp. 1662–1668, 2021.
- [133] H.-L. Yu, J. Wang, B. Zheng et al., “Fabrication of single crystalline WO<sub>3</sub> nano-belts based photoelectric gas sensor for detection of high concentration ethanol gas at room temperature,” *Sensors and Actuators a-Physical*, vol. 303, p. 111865, 2020.
- [134] D. Zhang, Y. Cao, J. Wu, and X. Zhang, “Tungsten trioxide nanoparticles decorated tungsten disulfide nanoheterojunction for highly sensitive ethanol gas sensing application,” *Applied Surface Science*, vol. 503, p. 144063, 2020.
- [135] J. Gao, C. Liu, S. Guo, L. Yang, Y. Yang, and K. Xu, “Heteroepitaxy growth of cobalt oxide/nickel oxide nanowire arrays on alumina substrates for enhanced ethanol sensing characteristics,” *Ceramics International*, vol. 48, no. 3, pp. 3849–3859, 2022.
- [136] P. Hao, Z. Lin, P. Song, Z. Yang, and Q. Wang, “rGO-wrapped porous LaFeO<sub>3</sub> microspheres for high-performance triethylamine gas sensors,” *Ceramics International*, vol. 46, no. 7, pp. 9363–9369, 2020.
- [137] Z. Ma, K. Yang, C. Xiao, and L. Jia, “C-doped LaFeO<sub>3</sub> porous nanostructures for highly selective detection of formaldehyde,” *Sensors and Actuators B-Chemical*, vol. 347, p. 130550, 2021.
- [138] P. Hao, G. Qiu, P. Song, Z. Yang, and Q. Wang, “Construction of porous LaFeO<sub>3</sub> microspheres decorated with NiO nanosheets for high response ethanol gas sensors,” *Applied Surface Science*, vol. 515, p. 146025, 2020.
- [139] M. Haq, Z. Zhang, X. Chen et al., “A two-step synthesis of microsphere-decorated fibers based on NiO/ZnSnO<sub>3</sub> composites towards superior ethanol sensitivity performance,” *Journal of Alloys and Compounds*, vol. 777, pp. 73–83, 2019.

## Retraction

# Retracted: Construction and Effect Analysis of College Students' Physical Education Teaching Mode Based on Data Mining Algorithm

### Journal of Sensors

Received 8 August 2023; Accepted 8 August 2023; Published 9 August 2023

Copyright © 2023 Journal of Sensors. This is an open access article distributed under the Creative Commons Attribution License, which permits unrestricted use, distribution, and reproduction in any medium, provided the original work is properly cited.

This article has been retracted by Hindawi following an investigation undertaken by the publisher [1]. This investigation has uncovered evidence of one or more of the following indicators of systematic manipulation of the publication process:

- (1) Discrepancies in scope
- (2) Discrepancies in the description of the research reported
- (3) Discrepancies between the availability of data and the research described
- (4) Inappropriate citations
- (5) Incoherent, meaningless and/or irrelevant content included in the article
- (6) Peer-review manipulation

The presence of these indicators undermines our confidence in the integrity of the article's content and we cannot, therefore, vouch for its reliability. Please note that this notice is intended solely to alert readers that the content of this article is unreliable. We have not investigated whether authors were aware of or involved in the systematic manipulation of the publication process.

In addition, our investigation has also shown that one or more of the following human-subject reporting requirements has not been met in this article: ethical approval by an Institutional Review Board (IRB) committee or equivalent, patient/participant consent to participate, and/or agreement to publish patient/participant details (where relevant).

Wiley and Hindawi regrets that the usual quality checks did not identify these issues before publication and have since put additional measures in place to safeguard research integrity.

We wish to credit our own Research Integrity and Research Publishing teams and anonymous and named external

researchers and research integrity experts for contributing to this investigation.

The corresponding author, as the representative of all authors, has been given the opportunity to register their agreement or disagreement to this retraction. We have kept a record of any response received.

### References

- [1] P. Wang, "Construction and Effect Analysis of College Students' Physical Education Teaching Mode Based on Data Mining Algorithm," *Journal of Sensors*, vol. 2022, Article ID 1028962, 10 pages, 2022.

## Research Article

# Construction and Effect Analysis of College Students' Physical Education Teaching Mode Based on Data Mining Algorithm

Peipei Wang 

Physical Education Office of Public Basic Education Department, Henan Vocational University of Science and Technology, Zhoukou, Henan Province 466000, China

Correspondence should be addressed to Peipei Wang; [wpp02083503@163.com](mailto:wpp02083503@163.com)

Received 18 April 2022; Accepted 10 June 2022; Published 4 August 2022

Academic Editor: Wen Zeng

Copyright © 2022 Peipei Wang. This is an open access article distributed under the Creative Commons Attribution License, which permits unrestricted use, distribution, and reproduction in any medium, provided the original work is properly cited.

With the wide application of computer technology, communication technology, network technology, and multimedia technology in modern education, teaching methods tend to be diversified and scientific. Based on the DM (data mining) algorithm, this paper implements a sports achievement management system. Through this system, the efficiency of inputting and counting students' achievements can be improved, and teachers can be freed from the complicated achievement management. Aiming at the problem that SVM (Support Vector Machine) is slow in training large sample sets in DM classification, a DM classification algorithm based on improved SVM, PSO\_SVM, is proposed, which applies the density of adjacent samples to the design of membership function to reduce the influence of noise points on classification. The results show that the training time of this algorithm is increased by 54.26 s and 55.69 s compared with SVM and *K*-means, respectively, and the accuracy is increased by 35.62%. The results obtained by the DM algorithm will be helpful for teachers to diagnose teaching problems and construct PET (physical education teaching) model for college students with characteristics.

## 1. Introduction

The continuous improvement of the quality of software and hardware in schools has promoted the continuous improvement and optimization of the teaching system. Based on the superiority of data, the communication between various subjects has gradually deepened, which has promoted the scientificity and rationality of school education. To a certain extent, the course results truly reflect the ability and quality of students in a certain specialty, such as music, mathematics, art, and physical education [1]. Previously, data information was only used for routine data recording and statistical classification, but now DM (data mining) technology is not only used for daily student information statistics, teaching task recording, and data storage but also used for data management. With the optimization and update of information processing technology and big data technology, educators place their hopes on the intelligent mining algorithm [2],

and DM has gradually become an effective tool for academic performance management and learning effect analysis in universities.

Nowadays, the computer network has become very popular in universities. Using DM technology to set up a university sports achievement management system can provide administrators, teachers, and students with sufficient information and quick query means, complete teachers' scoring work, and make statistics, analysis, and processing of data [3, 4]. Wang et al. used graduates' achievements as feature data, reduced the dimension of feature data by principal component analysis, and classified them by the Bayesian near *k*-nearest neighbor algorithm, namely, career direction prediction [5]. Cai et al. put forward an improved algorithm [6] after researching and analyzing ID3 algorithm and mining and analyzing the data stored in the educational administration system, so as to find out the relationship between curriculum settings and provide some data basis for the uni-

versity's achievement statistics decision-making. Moon et al., based on the Hadoop big data platform, mined the application information of information-based campus and recommended campus information for corresponding characteristic learning [7]. Nolen et al. used rough theory to excavate and analyze the correlation between the improvement of students' performance and the leading factors of active learning [8].

There are abundant teaching resources in our school, and a large amount of data can be used for reference. However, in practical application, the utilization rate of data is low, and most of the data resources are idle in the database, so they do not play their due value. In view of this, this paper studies the application of DM technology in students' multi-attribute training, with a view to effectively mine the potential rules and associations in the data related to students' training by applying proper DM technology, aiming at correctly understanding the characteristics of college students' physical education represented by Chengdu Institute of Physical Education, revealing the laws and trends of college students' physical education learning and providing reference for the research and implementation of college students' physical education learning in physical education institutes.

## 2. Related Work

*2.1. Research on the Teaching Mode of Physical Education.* Sports achievement is mainly a measure of whether there is a gap between students' physical fitness and expected goals and the means to measure this gap. It can only show the results of students' physical exercise but cannot reflect the causes of such results. Therefore, teachers have the responsibility to explain to students the significance of the test results and the reasons for the results and guide students to take appropriate exercise process to improve the test results [9].

Ding et al. used different data prediction methods, established prediction models, and made the best use of correlation analysis results and students' real achievement data to predict students' achievements in the courses currently taught by teachers [10]. Thaise et al. put forward a thousand preassumptions, intervened the students' samples, and evaluated the advantages and disadvantages of the intervention measures according to the actual teaching achievements and self-defined evaluation indicators of the intervention objects [11]. Khosravi et al. deeply understand the significance of modular teaching to the development of society and people by understanding the concept, basic characteristics and process of modular teaching [12]. According to the teaching requirements of various schools, Hu et al. divided the teaching content into several modules, combined with students' interests and employment requirements, and rationally matched the module courses [13]. The new "modular" physical education teaching structure model proposed by Li et al. is a new teaching model, which is an innovation of physical education teaching theory and plays an important role in enriching physical education teaching theory [14].

*2.2. Research on DM.* DM is a multidisciplinary field that integrates database technology, machine learning, informa-

tion retrieval, artificial intelligence, and other latest technologies.

Luo et al. applied the improved genetic algorithm to data hiding and publishing, which can better protect the privacy of original data from leaking [15]. Li et al. applied multi-objective particle swarm optimization to multiclassification [16]. Ru et al. studied the hybrid algorithm of swarm intelligence algorithm and clustering algorithm. Aiming at the shortcomings of existing clustering algorithms and particle swarm optimization algorithms, it is meaningful to improve the particle swarm optimization algorithm to optimize the clustering model and apply it to real life data mining [17]. Stamatescu et al. put forward new methods and technologies for the development of online education at home and abroad, and made positive contributions to the development of modern education [18].

Wang et al. adopted the classification method of DT (decision tree) [19], applied DM technology to students' achievement information, and constructed the DT model of professional ability, which helped teachers to gain a more accurate and efficient insight into the existing problems in the teaching process, and achieved the effect of optimizing teaching quality by using achievement information.

## 3. Research Method

*3.1. Construction of PET Mode for College Students.* In the process of PET (physical education teaching) reform, many PE educators and PET workers have done a lot of exploration and research on PET and achieved certain results. However, most teaching models teach students from the perspectives of sports techniques and learning interests, which is one-sided, ignoring the improvement of students' physical quality, and it is difficult to promote students' all-round and healthy development [20]. To construct a new modular PET structure model centered on strengthening students' physique, in order to improve students' interest in learning, enhance their physical fitness, eliminate the problems that have plagued sports workers for many years, and promote it in a large area to achieve the purpose of comprehensively improving the national physique and health.

Under the situation that the physical health of college students in China is declining day by day, how to give full play to the function of physical education, improve the effect of PET, and develop students' physical fitness in an all-round way is the top priority of contemporary college physical education research. The construction of modular teaching structure model is based on physiology and psychology, follows the law of physical quality development, and conforms to the psychological characteristics of students. The construction of the model improves the procedural and standardized degree of PET, which is convenient for PE teachers to design teaching. This method has strong operability, flexible methods, rich training means and good training effect, which can stimulate students' interest in learning and improve their physical quality. With the goal of promoting students' sports participation and social adaptability, based on the characteristics of students' physical and mental development, we design and organize the teaching content of physical education courses, divide

the modules according to the structure of students' physical quality, and practice in combination with various sports events to achieve the teaching goal.

As students' period is a period of rapid psychological and physical growth, physical education plays a vital role in the development of students' psychological and physical quality. Because physical education class is different from other indoor courses, it needs a lot of physical strength, and some students' physical abilities are weak. In addition, it is necessary to comprehensively consider the processing of all kinds of data information required by DM analysis subsystem. Compared with the traditional way of counting students' achievements by office software in teaching, big data technology pays more attention to the integration of channel data such as teaching sensors and teaching management platform. At the same time, through deep mining and analysis of the data in the database, the accurate statistical analysis results can be obtained, which can provide data support for the formulation of coaches' training plan, the monitoring of training quality and the adjustment of on-the-spot tactics.

In the process of PET, students' gender, age, and personality characteristics should also be considered. Students show different psychological characteristics at different ages. Through the influence of physical education curriculum on students' will quality, emotion, cognition, personality, and psychological characteristics, students can keep a good emotional state in physical education curriculum and control their emotions reasonably. From students with strong social adaptability to students with weak social adaptability, they should get corresponding physical exercises and enjoy the corresponding care of teachers, so that students can be fully developed.

When the system conducts DM analysis, it is necessary to analyze whether the teaching effect of teachers is related to their age, educational background, professional title, etc., which requires the system to have complete file data of participating teachers, but the above information of teachers is not needed when collecting evaluation information. It is easy to assess the grades, but how to analyze the students' grades and extract the required hidden information is also very important [21]. In all aspects, students need constant exercise in order to improve their physical quality and ability. However, teachers' neglect of PET ultimately leads to students' physical and mental health failing to develop better in sports.

In order to improve the quality of PET and make PE teachers get rid of the busy data statistics management, this paper designs a sports achievement management system based on DM technology, as shown in Figure 1.

It can be seen that users are divided into three types: physical education teachers, students, and system administrators. Firstly, it is the system presentation layer for human-computer interaction, including test project management, score management, score statistical analysis, and expansion project. Secondly, the business logic layer, as the core component of the system, contains the relevant business logic of all items in the presentation layer and completes the logic judgment and processing. Finally, the data access layer is connected with the database and documents.

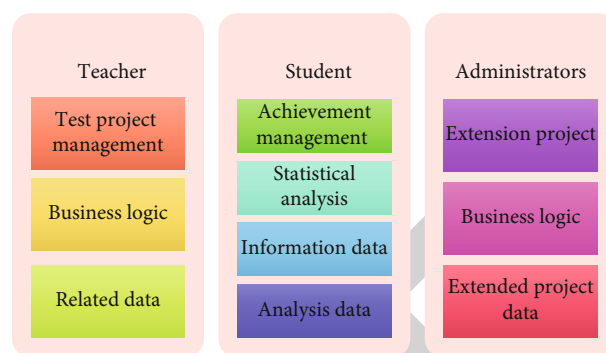


FIGURE 1: Overall system architecture.

With regard to the data of students' evaluation of teaching, further analysis and research on the data of students' evaluation of teaching by using the increasingly mature DM technology can help the teaching management departments and teachers to solve teaching problems in a targeted way. Excavate the potential correlation between the evaluation attributes in the data of teaching evaluation, find out the related factors that affect the quality of classroom teaching and the correlation between them, and put forward trend, operable and beneficial suggestions, and measures for improving the teaching level and strengthening the teaching management.

In the traditional PET evaluation, the evaluation of students is mainly based on students' sports achievements, and the evaluation of PE teachers is mainly based on personal subjective impressions, so the evaluation is incomplete and objective. At present, college PET evaluation mainly evaluates students and PE teachers by summative evaluation, which cannot reflect the situation of students and PE teachers at all stages of teaching. Manual evaluation is not only time-consuming and laborious, but also prone to errors, while intelligent evaluation is not only convenient and quick, but also accurate. Therefore, the means of college PET evaluation should be changed from traditional manual collection, statistics, and analysis to intelligent technology to collect, process, and analyze a large amount of evaluation data.

Based on the above methods and principles of functional module division, Figure 2 shows the overall functional module structure of the system. It can be seen from the figure that the sports performance management system includes five functional modules: sports test type management, test item management, performance management, performance analysis, and system management.

The data in the score management system will gradually increase with the use, and the storage will be realized by the database. At the same time, reading the requests and operations of the system will be the focus of the system development. The main technical difficulty of this process is entity identification. Accurate entity identification can reduce the redundancy of integrated data and prepare high-quality data for system DM. The flowchart is shown in Figure 3.

To complete the management of students' sports achievements, it is necessary to query, enter, delete, and export the achievements.

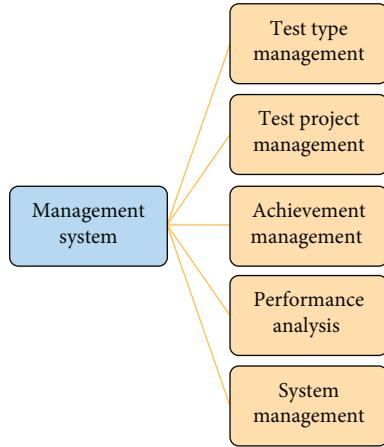


FIGURE 2: Overall functional structure of the system.

- (1) Select the score information table in the system, and insert the required new data table in the table to record the student's student ID and the corresponding score
- (2) Compare the data in the database, and judge whether the input information exists or not; if it exists, prompt the user that the input is unnecessary; if not, complete the input of the information
- (3) According to the return value in the database, judge whether the entry is successful or not. If the system displays true, the entry is successful [17]

The generation of DT is divided into two stages: learning and testing. In the DT learning stage, top-down recursion is adopted. The DT algorithm is divided into two steps: the first is tree generation. At the beginning, all the data are at the root node, and then, recursively divide the data until leaf nodes are generated. The second is tree pruning, which is to remove some data that may be noise or abnormal. After receiving the data information, the application server divides the information into two paths for transmission: one path is safely sent to teachers, students, and other types of customers through the firewall; one channel is directly received by the platform administrator to facilitate the management of PET information, maintain the safety of teaching data, and control the access qualification of users.

### 3.2. Analysis of College Students' Physical Education Learning Effect Based on DM

**3.2.1. Data Acquisition.** The collected contents include teaching data (including teacher data, student data, teaching situation data, equipment status data, and classroom status data) and information on personnel, scientific research, patents, papers, awards, and loans, which are distributed in many information points in the campus and involve all aspects of campus life. Based on the association rules generated by the Apriori algorithm, this paper analyzes the elements related to students' learning effect, that is, the favorable factors and unfavorable factors that form the cur-

rent learning effect, and helps teachers to scientifically optimize PET.

The importance of DM technology is gradually emerging. On the one hand, DM technology can discover the hidden laws of a large amount of data and the potential relationships among different data. On the other hand, DM can also make scientific predictions on the future development of things and then exert the greatest value of data. In the education industry, most of the research is aimed at students' achievement, and scholars explore the internal relationship between educational data and students' achievement through DM technology [18]. Promote the transformation of education mode, and gradually change the traditional teaching management mode into personalized teaching system.

The problem that DM has to deal with is to find out valuable hidden events in a huge database, analyze them, obtain meaningful information, and summarize useful structures. It has been found that in general or with a high probability, the smaller the tree, the stronger the prediction ability of the tree. To construct DT as small as possible, the key lies in choosing appropriate logical judgment or attribute. In the actual evaluation activities, the indicators should be flexible and adjustable. Then, preprocess the data to implement the selected DM algorithm. Finally, the results of DM are analyzed.

Data collection is the part with the largest number of participants in the whole system operation. Here, the roles of users are mainly divided into two categories: teachers and students, and the goal is to achieve complete and accurate collection of large-scale evaluation data. The steps of data acquisition are shown in Figure 4.

Through the application of DM technology, an effective PET evaluation system is established, the teaching evaluation is analyzed, and the shortcomings of PET are found, so as to change the teaching plan and improve the teaching quality. In PET evaluation, students grade the completion level of PE teachers' teaching tasks, evaluate the teaching effect of PE teachers, and put forward teaching opinions. In the stage of knowledge expression and evaluation, the useful information and association rule expression obtained in DM stage are mainly displayed to users or provided to related applications in the form of new knowledge.

Coefficient of variation refers to the coordination degree of experts. The smaller the coefficient of variation, the higher the coordination degree. If the coefficient of variation is greater than 0.25, it is considered that the degree of coordination is not high [19, 20]. The calculation formula is

$$\begin{aligned}
 V_j &= \frac{S_j}{M_j}, \\
 M_j &= \frac{1}{n} \sum_{i=1}^n X_i, \\
 S_j &= \sqrt{\frac{1}{n-1} \sum_{i=1}^n (X_i - M_j)^2},
 \end{aligned} \tag{1}$$



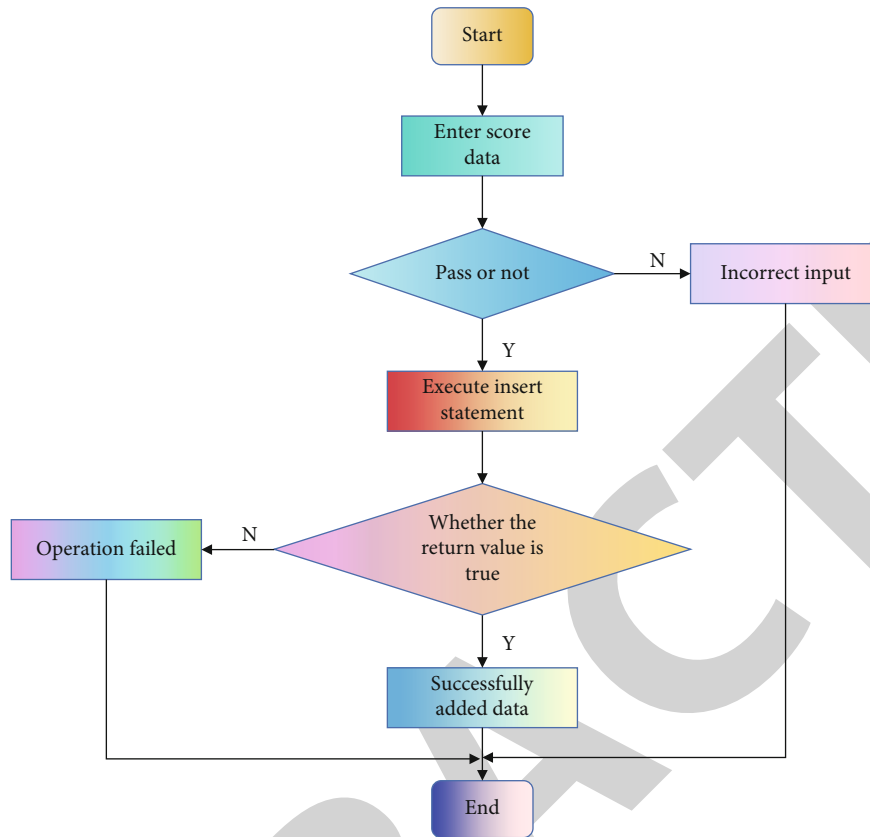


FIGURE 3: Flowchart of achievement management.

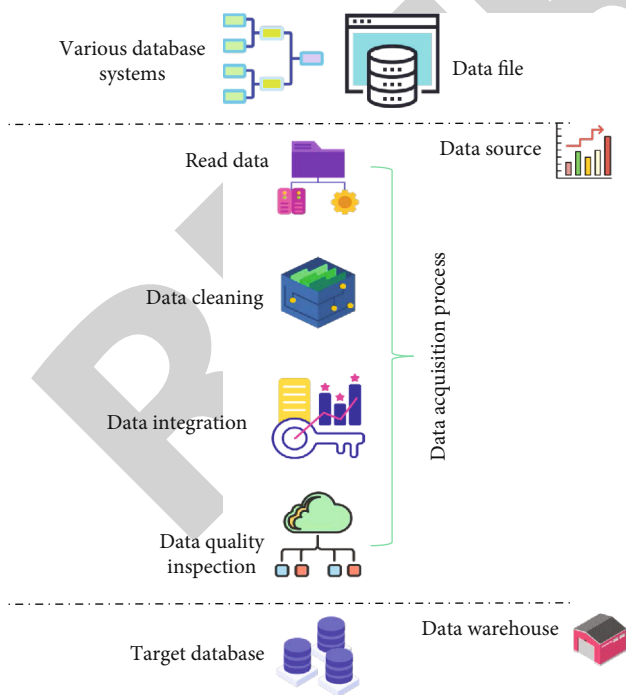


FIGURE 4: The process of data acquisition.

where  $V_j$  represents the coefficient of variation,  $S_j$  represents the standard deviation, and  $M_j$  represents the arithmetic mean.

The research of sports achievement management system based on DM university is aimed at improving the work efficiency and accuracy of physical education teachers in university, liberating them from tedious and boring work, and then improving their management level and teaching quality. Under the condition of setting test types, new test items can be added under each test type, and these test items can be modified or deleted. Similar to the test type score setting, each test item also has a certain score weight, so the system needs to set the score weight of each test item. The system can comprehensively analyze students' physique according to their achievements, including historical sports achievements, and provide valuable suggestions for improving their physique.

The users of the system are teachers, students, and system administrators. Among them, the operations that teachers can perform include test type management, test project management, grade management, grade statistical analysis, etc., while students can only participate in grade management. System administrators can perform all operations and have the maximum operating authority. The ultimate goal is to discover the potential problems in data flow in advance. These problems are various, including data flow and data processing.

The zero-level diagram of the system reflects the overall flow of data. Although it can see the specific business, it cannot clearly show the internal processing process. Therefore, the zero-layer data flow graph still needs to be decomposed. From the developer's point of view, this makes it possible to

change the business requirements, without modifying all the codes, only by adjusting the business logic, thus improving the development efficiency of the program and reducing the development cost.

**3.2.2. DM Analysis.** Among DM algorithms, the tree model is a very common algorithm, which can deal with both classification and regression problems. In most cases, it is used to deal with classification problems. DT algorithm learns from data and classifies and predicts input variables and output variables with different values in different situations. In the process of DT formation, the main components are feature selection, DT generation, and pruning. In the whole process, firstly, a feature is selected in the training set as the classification standard of the current node; then, according to the evaluation criteria, child nodes are generated from top to bottom until they are inseparable. Finally, pruning is carried out to reduce the scale of tree structure, in order to prevent DT from overfitting [21].

The ID3 algorithm uses the information gain of attributes as the criterion of node selection and considers that attributes with high information gain are good attributes. Both ID3 and C4.5 algorithms use the concept of information entropy, and the C4.5 algorithm uses information gain rate instead of information gain as the standard for determining test attributes. The branch nodes generated in this way are generated by different attributes, and each branch represents a subset of samples.

The DT algorithm can obtain DT with less instability by segmentation technology. Let  $S$  set have  $s$  sample data and  $s$  class attributes with different values:  $C_i (i = 1, 2, \dots, m)$ .

Assuming that the number of samples in class  $C_i$  is  $s_i$ , the total information entropy for this sample is

$$I(s_1, s_2, \dots, s_m) = -P_i \log_2(P_i). \quad (2)$$

The probability that the sample belongs to  $C_i$  is expressed as  $P_i$  or  $s_i/s$ .

Then, it is required that the calculated entropy value should be smaller. So for a subset  $f$  that has been given now, calculate its expected value as

$$I(f_1, f_2, \dots, f_{m_j}) = -\sum_{j=1}^n P_i \log_2(P_{ij}). \quad (3)$$

Now suppose that the coordination degree of a decision-making system such as  $S = (U, C \cup D, V, f)$ ; then,  $X \rightarrow D$  can be expressed as  $\text{CON}(X \rightarrow D)$ ; then, the decision-making coordination degree is

$$\text{CON}(X \rightarrow D) = \frac{|X \cup D|}{|X|}, \quad (4)$$

where  $|X| = \text{IND}(X)$  represents the cardinal number of  $\text{IND}(X) \subseteq U \times U$ . And  $|X \cup D|/|X|$  indicates the possibility of randomly taking out two rules with the same antecedents and successors in the decision-making system.

However, when calculating the gain of attribute information with the ID3 algorithm, logarithmic operation is used, so the computational complexity is reduced, so the original ID3 algorithm is improved accordingly.

The specific algorithm flow is as follows:

- (1) Compare the coordination degree of all attribute decisions
- (2) Calculate the information gain of attributes with similar decision coordination degree
- (3) Select the attribute with the highest degree of coordination as the split node
- (4) Recursive call is used until the conditional attribute is null, and finally DT is generated

SVM (Support Vector Machine) is a supervised machine learning algorithm; that is, it is necessary to train the training samples to obtain the optimal classification hyperplane and then classify according to the training results.

Assuming that there are  $k$  neighbor samples in the neighbor sample subset  $X_i$  of the sample, the neighbor sample density function is as follows:

$$z_i = \sum_{i \neq j}^k \frac{1}{d_{ij} + a}, \quad d_{ij} \leq e_1, i = 1, 2, \dots, \text{num}X. \quad (5)$$

Among them,  $a$  is a small penalty constant in order to process samples with the same value.

Let  $X_i = \{X_i, i = 1, 2, \dots, m\}$  be the data sample set, where the data sample  $X_i$  has the same dimension, all of which are  $d$ -dimensional vectors. The result of clustering is to find a reasonable partition  $D = \{D_1, D_2, \dots, D_k\}$ , and make the partition satisfy the following relationship:

$$\begin{aligned} X &\bigcup_{i=1}^k D_i, \\ D_i &\neq \emptyset \quad (i = 1, 2, \dots, k), \\ D_i \cap D_j &= \emptyset \quad (i, j = 1, 2, \dots, k, i \neq j). \end{aligned} \quad (6)$$

The PSO (particle swarm optimization) algorithm is widely used in practice because of its advantages of fast convergence, simplicity, and high precision. The PSO algorithm is applied to the simplified support vector of SVM to obtain a new algorithm—PSO\_SVM. The number of support vectors obtained by training SVM is the dimension of particles, and each particle has its position and velocity. The position represents the membership degree of the sample, and the velocity changes the membership value.

The location of each particle is composed of the cluster centers of  $k$  classes. Because the data sample is a  $d$ -dimensional vector, the dimension that determines the location and velocity of the particle is  $k \times d$ . The calculation steps of

individual fitness value are as follows:

$$Z_r = \frac{1}{n_r} \sum_{x_i \in C_r} x_i, \quad (7)$$

where  $n_r$  is the number of samples in cluster  $r$ .

The training sample set is processed and PSO\_SVM is trained to get the support vector set, and the average classification error of the test set is used as the fitness value of particles. The fitness function is defined as

$$\text{Fitness} = \frac{1}{M} \sum_{i=1}^M (f_i - y_i)^2, \quad (8)$$

where  $M$  is the number of samples in the test set,  $f_i$  is the predicted value, and  $y_i$  is the actual value. From the above formula, the smaller the particle fitness value, the better.

The flow of the PSO\_SVM algorithm is shown in Figure 5.

- (1) Calculate the distance between two kinds of samples and their class centers
- (2) Obtain a fuzzy candidate support vector set
- (3) Train PSO\_SVM for the subset of support vectors selected by each particle to obtain a decision function
- (4) Update the particle swarm optimization algorithm to obtain a set of new membership values
- (5) Judge whether the loop stop condition is met, ending when the adaptive value is no longer changed, and output the result; otherwise, go to step 2
- (6) The output result is used to train PSO\_SVM, and the decision function of reduced support vector is obtained, and the decision function is used for classification

#### 4. Result Analysis

Data analysis and mining are the core of the system. It is divided into two parts: one part is to make a preliminary analysis of the evaluation data by using the traditional statistical calculation method and give a quantitative result in the form of a specific score for each teacher's evaluation result. The other part is to apply DM technology to mine and analyze the collected evaluation data, discover useful knowledge hidden in the data, and extract it for schools and related teachers to learn from. Combined with the teaching data and information of the school, advanced network information technology is introduced and applied to school education management, teaching evaluation, paperless examination, teaching records, students' inductive learning, and teachers' teaching technology analysis.

The DT algorithm can dig out the potential relationship between physical measurement data and students' daily behavior habits. The association rule is to mine the associa-

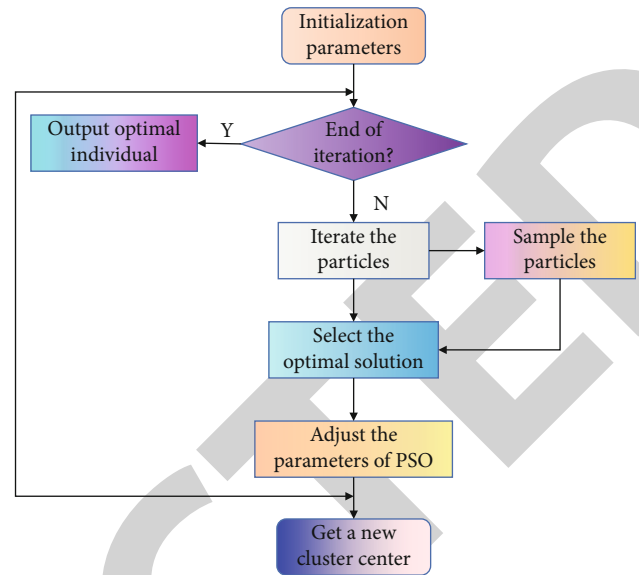


FIGURE 5: PSO\_SVM algorithm flow.

tion among factors in the physical measurement data. Based on the data information obtained after data preprocessing, the attribute of "cardiopulmonary function" in college students' physical fitness assessment table has two different values. Calculate the information profit rate of each attribute according to the formula. The calculation results are shown in Table 1.

When generating DT, the DM algorithm did not take into account the problems of data missing and noise in the actual process, so it needs pruning after generating DT. Pruning mainly simplifies the DT model by controlling the size of the tree, so as to avoid overfitting phenomenon to some extent. After the repeated branches are removed, the stability and readability of DT model are greatly improved.

The ID3 algorithm is improved and demonstrated by the degree of decision coordination, and the training sample set is tested by two different methods. Each method carries out 20 experiments on each group of data, and the average value of all experimental data is obtained by calculation, thus ensuring the universality of the experimental data. The experimental data are shown in Figures 6 and 7.

According to the above two charts, although the accuracy of the algorithm will decrease with the increase in data in the sample set, the improved algorithm is better than the original ID3 algorithm in both time and accuracy.

Endurance is divided into aerobic endurance and anaerobic endurance. In the process of physical education curriculum design, the training of endurance quality should be reasonably arranged according to the characteristics of each event. In the process of PET, different special teaching contents are different, and the intensity of stimulation to students, the development of students' physical quality, and the development of muscle groups are also different. In the process of PET, the modules corresponding to special teaching contents should be scientifically divided, and students' physical quality should be rationally developed through special exercises.

TABLE 1: Physical fitness data calculation results.

Calculation project	Diet	Work and rest	Habit	Importance of physical education
Subset expected information value	0.9332	0.9022	0.8871	0.9654
Information gain value	0.0041	0.0369	0.0805	0.0071
Split information value	0.8869	0.7748	0.9216	0.9975
Information gain rate	0.0054	0.0412	0.0884	0.0077

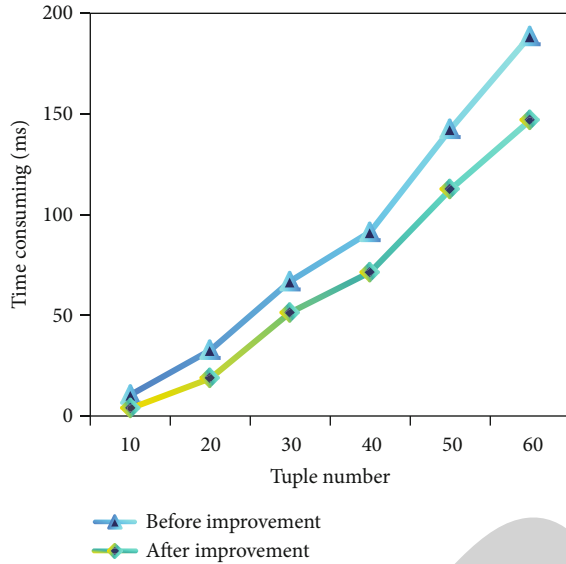


FIGURE 6: Comparison of algorithm time.

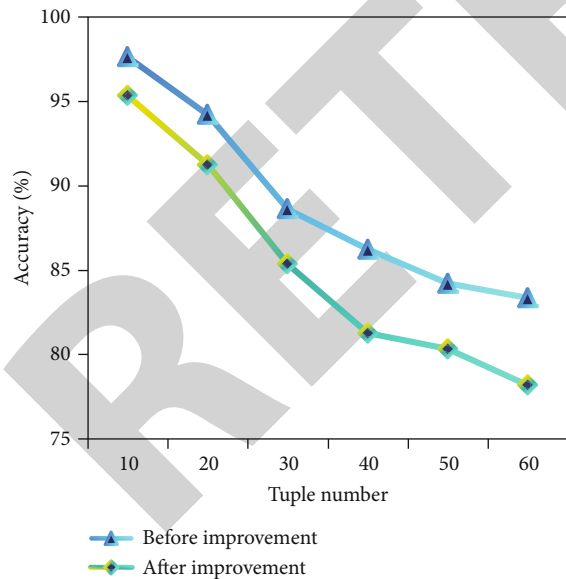


FIGURE 7: Accuracy comparison of algorithms.

Through testing the evaluation index of students' speed quality (100 m), it is found (Table 2): before and after the experiment, the average test scores of 1000 m in the control group and the experimental group are the same, both of which are 7.6 s. After the experiment, the score of the experimental group increased to  $7.2 \pm 0.6$  s, which was signifi-

cantly different from that of the same group before the experiment. The score of the control group decreased by 0.4 s and increased to  $7.1 \pm 0.7$  s. There were significant differences in the test results before and after the experiment.

During the entrance test, students' mastery of 100 m running skills is not reasonable enough, and their achievements are affected to some extent. To some extent, students' 100 m running skills are positively transferred, and their skills are developed, which is conducive to the improvement of their achievements. In addition, the special basketball practice has promoted the development of students' physical quality to a certain extent, especially their reaction speed and moving speed, thus further promoting the development of students' speed quality.

With the increasing workload and difficulty of physical education teachers, teachers need to carefully analyze the characteristics of sports events, rationally plan teaching contents, scientifically design teaching actions, constantly absorb advanced teaching ideas, blaze new trails, and strive to improve their comprehensive quality; At the same time, physical education teachers are required to have high professionalism, selfless dedication and improve their professional ethics.

With evolutionary algebra  $MaxT = 40$ , the relationship between evolutionary algebra of new algorithm PSO\_SVM and  $K$ -means algorithm and optimal fitness and interclass dispersion sum is compared. Figure 8 shows the analysis of the standard data set Iris.

It can be seen that the optimal fitness value of the new algorithm PSO\_SVM rises stepwise and reaches the optimal fitness when the evolution algebra is about 20. While the  $K$ -means algorithm has a high optimal fitness value in the first few generations of evolutionary algebra, but the fitness changes slowly in the later evolutionary algebra.

Compared with the traditional  $K$ -means algorithm, the improved PSO\_SVM algorithm can achieve smaller interclass dispersion sum, can achieve the optimal fitness value in less evolutionary algebra, and has higher accuracy of clustering results, but the stability of the algorithm needs to be further improved.

Three two kinds of data sets in the UCI database are used in this experiment. For the convenience of comparison, the parameter selection methods of the three algorithms are consistent with (1), and the training time, classification time, and classification accuracy are verified by 10 times and 50% cross-validation for the three data sets. The classification results of our algorithm and the other two algorithms are shown in Figures 9 and 10.

It can be seen that the training time and classification time of this algorithm are obviously improved. Compared

TABLE 2: Experimental results of students' 100-meter running.

Group	Experimental stage	Mean time (s)	Change value (s)
Experimental group	Before experiment	7.6 ± 0.5	0.7
	After the experiment	7.2 ± 0.6	
Control group	Before experiment	7.6 ± 0.4	0.4
	After the experiment	7.1 ± 0.7	

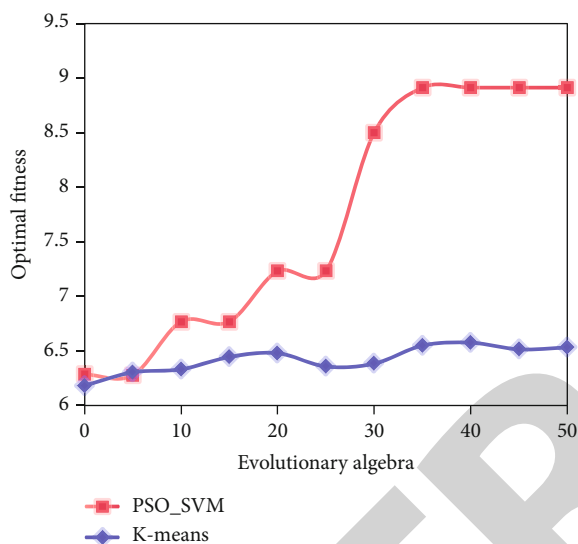


FIGURE 8: The relationship between evolution and individual optimal fitness.

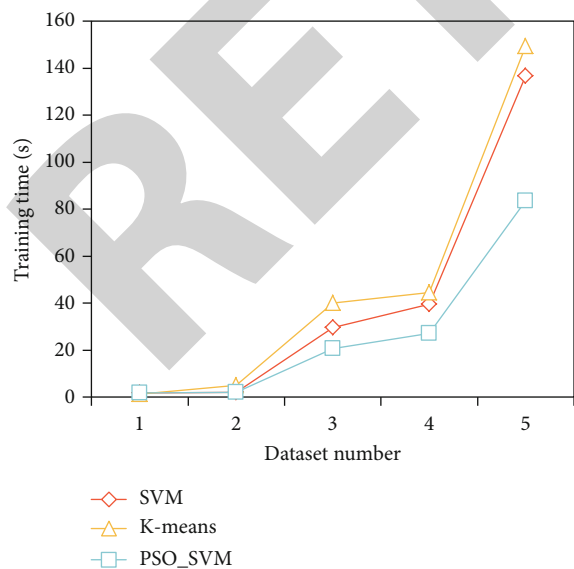


FIGURE 9: Training time.

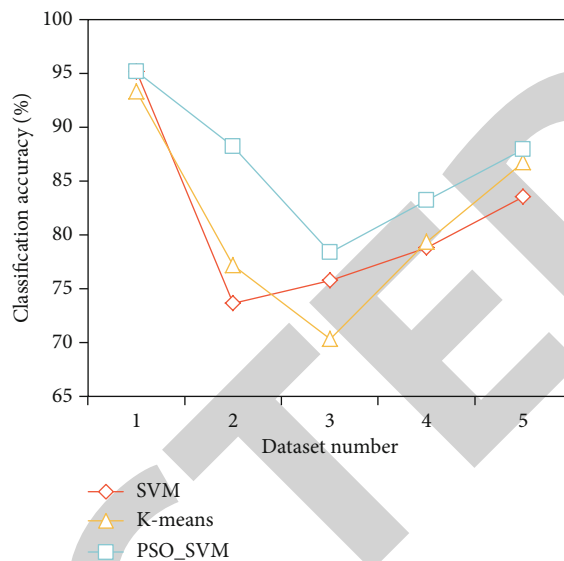


FIGURE 10: Classification accuracy.

with SVM and K-means, the training time of this algorithm is increased by 54.26s and 55.69s, respectively, and the accuracy rate is increased by 35.62%. It can be seen that the training speed is improved by reducing the number of training samples by preselecting candidate support vectors, and the classification speed is improved by using PSO to reduce support vectors.

Some data sets can achieve the best classification effect with fewer support vectors, and the accuracy of data set 4 has lost 0.08% relatively. This may be due to the fact that the support vector set obtained by training PSO\_SVM in data sets is already sparse, and there is no need for reduction. However, on the whole, the algorithm in this paper improves the training speed and classification speed while ensuring the same classification accuracy.

Appropriate exercise load means that the exercise load of teaching content in PET process should be within the range suitable for strengthening students' physique. The determination of physical education curriculum load intensity needs to be determined according to the teaching objectives, teaching contents, teaching objects, teaching environment and other factors. The new modular PET structure mode is aimed at students' individual differences, and set up different difficulty training methods to ensure that all students get full exercise; according to students' interests and hobbies, elective courses of different sports events are set up, and targeted modular design is carried out to fully arouse students' interest in learning. By effectively recording the teaching methods of physical education teachers and combining with students' academic achievements, this paper analyzes the relationship between them.

### 5. Conclusion

With the help of DM technology, in-depth research on sports industry data is not only of high scientific research value, but also of great social significance, which can greatly promote the development of sports informatization. In this

## Research Article

# Construction and Evaluation of College Students' Psychological Quality Evaluation Model Based on Analytic Hierarchy Process

Wei Shi 

Department of Mental Health Education Centre, Huanghe Jiaotong University, Jiaozuo, Henan 454950, China

Correspondence should be addressed to Wei Shi; 2017032801@zjtu.edu.cn

Received 8 April 2022; Revised 23 May 2022; Accepted 31 May 2022; Published 21 July 2022

Academic Editor: Yanqiong Li

Copyright © 2022 Wei Shi. This is an open access article distributed under the Creative Commons Attribution License, which permits unrestricted use, distribution, and reproduction in any medium, provided the original work is properly cited.

College students are a special group of society, having received university education and being at the forefront of new ideas and technologies in society. The basic psychological characteristics common to modern college students and the unique role psychological characteristics of ordinary students are the two major group factors. The basic psychological factors include cognition, personality, and social adaptive behavior. Hierarchical analysis (AHP) is a scientific method for assessing and identifying problems, correlating quantitative treatment of problems with qualitative analysis, and is well suited for semistructured or unstructured decision-making problems. This paper preliminarily studies the structure of College Students' psychological quality under the background of localization and the construction method of College Students' psychological quality evaluation model based on analytic hierarchy process. It is proposed to introduce the hierarchical analysis method into the behavioral assessment model of college students' psychological disorders as the entry point. A model was built to help college ideological and political educators determine whether college students have psychological disorders and disorders provide important insights. The results showed that the split-half reliability of this constructed method was 0.782, and the retest reliability was 0. The standard deviation of the coefficients among all the test subjects was 0.842, indicating that there is a positive correlation between the coefficients. The standard deviation of the coefficients between all test subjects was 0.842, indicating good confidence. Therefore, the model can objectively assess the psychological state of college students and realize the quantitative safety psychological assessment of college students, which is useful for reference in the implementation of teaching decisions.

## 1. Introduction

College students are the hope of social development, and their healthy growth is directly related to the future political, economic, and technological development of the country [1]. The research on the evaluation of school mental health education curriculum will directly affect how to establish the curriculum objectives of school mental health education [2], as well as a series of theoretical research and practical issues such as how to write school mental health curriculum materials, how to implement school mental health curriculum, and how to implement school mental health curriculum [3]. Their social environment and physiological age determine that the four years of college are a critical period in their life development. During this special period, college students

often face many common psychological problems, such as emotional instability and self-awareness bias [4]. With the increasing prominence of the problem of psychological disorders among college students, it has many negative effects on students themselves, their families, schools, and society [5]. If it is not effectively addressed in time, it will affect the fairness of education, the healthy growth of college students, and the stability of universities and society [6].

The AHP algorithm is a hierarchical, structured, qualitative, and quantitative decision-making method [7]. It enables the combination of qualitative and quantitative, expresses people's subjective judgments in quantitative form, and uses hierarchical structure and judgment matrix as a processing tool to systematically provide decision makers with decision results [8]. A key step in hierarchical analysis

is the construction of a decision matrix and the calculation of ranking weights for each comparison element in the decision matrix [9]. However, one of the biggest drawbacks of psychometric tests is that subjects must be truthful about their thoughts [10]. In fact, many students are reluctant to reveal their inner world to others, leading to inaccurate results [11]. Therefore, the study of the theory and methods of decision analysis is not only of theoretical importance for the development of management science, but also of practical importance for solving many complex decision problems. In particular, a quantifiable and practical measurement tool that can be used to measure psychological quality is important [12]. Cultivating college students into builders and successors of the socialist cause with Chinese characteristics requires the widest sharing and fastest development of college students' psychological quality assessment and deeper information mining in all aspects [13]. College students will inevitably face various psychological conflicts and contradictions. Without timely and effective guidance and intervention, they can lead to serious psychological disorders and tend to passivity and laziness [14]. Some students can be screened by psychological tests, but others cannot be judged. The optimal treatment period is delayed because psychologists must wait until they detect abnormal behavior before they can be sent to a psychotherapy center [15]. Therefore, it is necessary to analyze the collected information through a scientific system of early warning indicators and risk assessment models to understand the psychological state of students in time to prevent problems before they occur.

The innovation points of this paper are as follows:

- (1) It has studied the comprehensive quality assessment of college students, analyzed the current situation of comprehensive quality assessment of college students, and made a useful reference for constructing a new assessment system
- (2) The psychological assessment of college students is taken as a separate task, so that the school can understand the psychological problems of college students more intuitively and have an objective point of view in the continuous use and improvement. Students' comprehensive situational awareness in all aspects can be observed
- (3) Using the hierarchical analysis method, the corresponding index weights are set and a more detailed evaluation index system is constructed, taking into account the needs of college students at different levels of society

The research framework of this paper contains five major parts, which are arranged as follows:

The first part of this paper introduces the background and significance of the research and then introduces the main work of this paper. The second part introduces the work related to the construction of the psychological quality assessment model for college students and the application of AHP to psychological quality assessment. The third part of the paper introduces the method of constructing the hierar-

chical model and the overall design method of the psychological quality assessment model, so that the readers of this paper can have a more comprehensive understanding of the construction method of the AHP-based psychological quality assessment model for college students. The fourth part is the core of the thesis, from the theoretical analysis of AHP applied to psychological quality assessment and the group decision AHP analysis, to complete the description of AHP and its improvement analysis of psychological quality assessment. The last part of the thesis is a summary of the full work.

## 2. Related Work

*2.1. Construction of Evaluation Model of College Students' Psychological Quality.* The evaluation of school mental health education programs plays a very important role in the implementation and operation of school mental health education programs, but there are various misunderstandings and difficulties in the theoretical research and practical operation process. At this stage, there are more research results on school mental health, but they are mostly focused on educational curriculum, psychological counseling, and psychological crisis intervention programs. Few mental health education activities are available. So this paper addresses this situation and conducts a more comprehensive and in-depth theoretical research and practical discussion on the construction of the student psychological quality assessment model.

Yin defines psychological quality as "a complex whole that includes cognitive ability, needs, interests, motivation, emotions, will, personality and other non-intellectual factors in an organic way, with the development of human self-awareness as the core and the positive and social development as the unified value-oriented" [16]. Wang and Park believe that in the evaluation of mental health education curriculum, the goal oriented evaluation is not desirable, and the process oriented evaluation should be adopted [17]. Wang et al. theoretically analyzed psychological quality assessment and suggested that students' psychological qualities include positive attitudes toward life, positive self-concept, dedication and responsibility, caring and cooperation, intelligence and creativity, practice and survival, frustration tolerance, and perseverance [18]. Zala et al. developed a manual of behavioral medicine scales, such as the Anxiety Self-Assessment Scale and the Depression Self-Assessment Scale, and used the result scores of the scale questionnaire method as a basis for judgment to evaluate the psychological quality of the subjects [19]. Zala et al. suggested that psychological quality assessment could be a breakthrough in the localization movement of Chinese psychology, and that the study of psychological quality of college students could be a unique growth point in the localization of Chinese psychology [19]. The study of psychological quality of college students can be a unique growth point in the process of localization of Chinese psychology [20].

Therefore, it is important to devote to counseling students with psychological disorders or illnesses to improve their psychological tolerance, social adaptability, and

frustration tolerance, so that they can continuously adjust themselves to society, but at the same time, there is no attention to their creative ability, which to some extent curbs their thinking and ability to transform society.

**2.2. Application of AHP in Psychological Quality Evaluation.** University students are a special social group; compared with the general group, they are more youthful and energetic, with clearer life goals and higher ideal ambitions. Through the exploration and research of mental health standards, we found that many scholars in China previously used a variety of evaluation standards when conducting mental health research due to the lack of unified mental health standards for college students. Moreover, most of them refer to the mental health standards of ordinary people in the process of research, which leads to great variability of research results. Therefore, we should use AHP to construct the framework of the evaluation index system of college students' mental health education, assign weights to indicators at all levels, and derive the basic model of the evaluation index system of college students' mental health education, in an attempt to provide a realistic reference for colleges and universities to carry out the work of college students' mental health education.

Ding and Yu proposed that the evaluation system of psychological education courses includes the measurement and evaluation of psychological functions, analysis of activity results, product analysis, and analysis of introspective materials [21]. Roncaglia made a rigorous mathematical derivation of the method of finding the weighted comprehensive ranking vector under group leapfrog [22]. Power et al. proposed a statistical test method to test the consistency of judgment matrix. The key is to design "Statistics" and make assumptions about the distribution of "Statistics" [23]. Viktorenko introduced the method of using data envelopment analysis to obtain the weight ranking of judgment matrix in AHP, discussed its feasibility, and verified the wide applicability of the model through an example [24]. Pu solved the weights by geometric mean method and proposed a new consistency test method with a critical value indicator, but the method is only suitable for specific weight solving methods and has poor applicability [25].

Applying AHP, the relevant factors and their interrelationships were screened, the relative importance between the decision schemes was determined by two-by-two comparison, the judgment matrix was constructed, the importance ranking weight coefficients among the factors were solved hierarchically, and the stochastic consistency index of the judgment matrix was calculated, by which the evaluation model of psychological disorder-induced behavior of college students was constructed.

### 3. Construction Method of Evaluation Model of College Students' Psychological Quality Based on AHP

**3.1. Method for Construct Hierarchical Model.** The hierarchical model of psychological measurement refers to the use of scientific psychological test scales to collect information on

the evaluation of school mental health education programs, to measure students' mental health, and to diagnose whether the level of students' psychological development has improved and increased and what problems still exist [26]. The core aspect of constructing a two-by-two comparative judgment matrix type AHP and a good judgment matrix directly affects the objectivity of the ranking [27]. Due to the different types of information carried by the set indicators, each indicator subsystem and specific indicator items play different degrees in the process of describing a social phenomenon or social condition. Therefore, the comprehensive index value is not equal to the simple sum of the sub-indicators, but a weighted summation relationship is as follows:

$$S = \sum_{i=1}^n w_i f_i(I_i), i = 1, 2, \dots, n. \quad (1)$$

$f_i(I_i)$  denotes some measure of  $I_i$ .  $w_i$  is the weight value of each index.

Therefore, in the process of practical application of AHP, it is necessary to conduct a special study on the construction of psychometric hierarchical model in the construction of judgment matrix. The principle of application of object-oriented technology is to simulate human habits of thought as much as possible, to get as close as possible to the methods and processes of human understanding and problem solving. The systematic procedure of the hierarchical model is shown in Figure 1.

First, when applying AHP to solve problems, it is important to analyze the relationship between the various factors involved, to understand and analyze the problem under study and the specific environment in which it is located. It is mainly used to complete the self-assessment of the psychological quality of the students according to their actual situation through various self-assessment scales in the system, as well as the possibility of dialogue with the teacher in the form of messages [28]. There is a certain association between factors in the step hierarchy model. Multiple levels are formed by factors according to a certain relationship, the next level of factors is a refinement of the previous level of factors, and the previous level of factors serves as a guideline to govern the next level of related factors. When AHP decision-making evaluates a complex system or problem, what one needs to determine is the goal, the factors affecting the goal, the alternatives, etc. Among them, determining the individual factors affecting the goal is the key to decision evaluation. The absolute value is compared with the specified threshold, and the part less than or equal to the threshold is 0. The part greater than the threshold is the difference with the specified threshold, which is the soft threshold denoising. The calculation formula is as the following equation:

$$\omega\lambda = \begin{cases} [\text{sign}(\omega)](|\omega| - \lambda), & |\lambda| \geq \lambda, \\ 0, & |\omega| < \lambda. \end{cases} \quad (2)$$



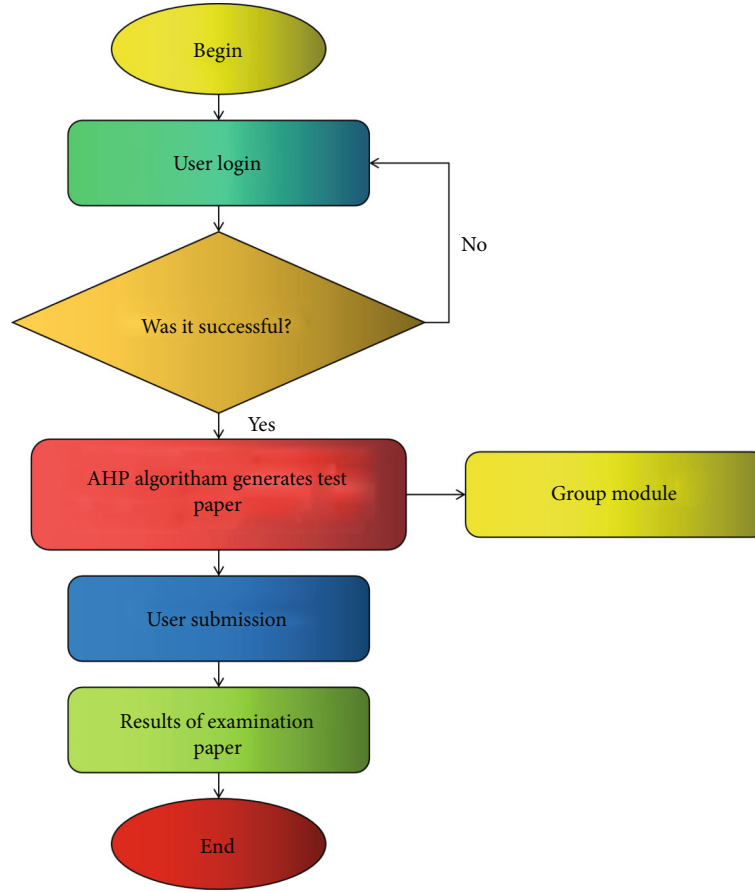


FIGURE 1: Block diagram of hierarchical model program.

Independent variable analysis can finally obtain independent components by analyzing the high-order characteristics of signals. Suppose a mixed signal  $X(k)$  is composed of  $m$  dimensional observation signal vector:

$$x(k) = [x_1(k), x_2(k), \dots, x_m(k)]^T. \quad (3)$$

Solving the relative weight of each level index subsystem or index item according to the judgment matrix is mathematically the problem of calculating the maximum eigenvalue of the judgment matrix and its corresponding eigenvector. Take the judgment matrix  $H$  as an example, that is,

$$HW = \lambda W, \quad (4)$$

where  $H$  is the judgment matrix and  $W$  is the feature vector.

Second, the problem is split and summarized to make the analysis process organized and hierarchical. The criterion layer contains each criterion that affects the goal of decision evaluation, and there are generally two relationships between the criteria: independence, in which the same layer is independent of each other and does not affect each other, and dominance, in which the factors in the upper layer dominate the relevant factors in the lower layer [29]. The credibility of the judgment matrix given by the experts

using hierarchical analysis varies due to their different knowledge levels, structures, and degree of understanding of things. Assuming that there are  $k$  experts, the expert weights are obtained using the following equation:

$$p_i = \frac{1}{1 + \partial CR_i} \quad (i = 1, 2, L, k). \quad (5)$$

In addition to the basic student management system functions, a student psychological early warning function has been added, with the help of a scientific early warning indicator system and a risk assessment model, through data analysis of the collected information. It provides timely feedback on students' study, thought, and psychological status in each semester during their school years, and improves reliable data for student work to prevent problems before they occur. Therefore, the database of this system is constructed as shown in Figure 2 below.

There are many interrelated and interacting factors within a complex system or problem [30]. These factors are intricate and not completely independent of each other, but with some simplification, the influencing factors of the model objectives can form a hierarchical structure that simplifies the decision-making in the analysis of a complex system or problem.

Finally, a hierarchical model is constructed through close collaboration between operation researchers, decision

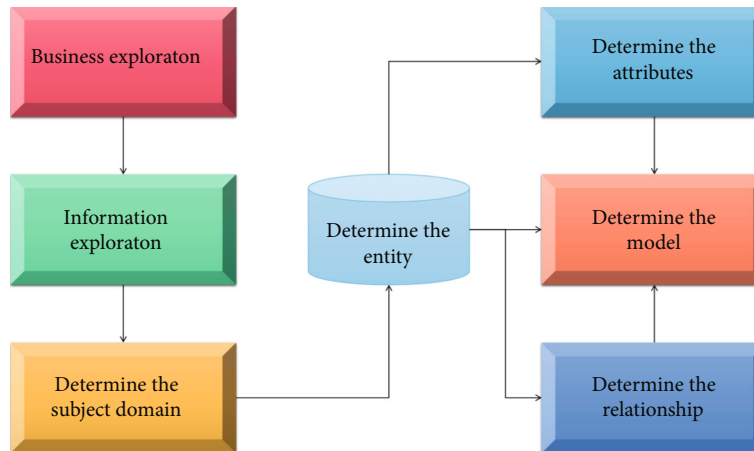


FIGURE 2: The flow chart of database construction of the system.

makers in talent assessment, and human resource practitioners. Among them, cognitive and personality factors are implicit in nature and are eventually expressed through the outward expressions of people's words, expressions, and behaviors in various activities and are observed, recognized, and understood. Through the statistical and generalization of these index elements, the structure, hierarchy, function, and contact of the evaluation system are examined comprehensively, and theories from management, psychology, and talent science are used to verify and justify, and necessary modifications and additions are made.

**3.2. Overall Design Method of Psychological Evaluation Model.** AHP is suitable for decision problems with more complex structures and multiple decision criteria that are not easily quantifiable. However, AHP also suffers from the objective fact that it cannot overcome the cross-correlations that usually exist between decision layers and between evaluation indicators. Decision makers are usually unable to quantify the specific weighting between some special factors, and the criterion level usually has a multilayer structure with a large number of influencing factors, so that decision makers cannot comprehensively and objectively determine the degree of influence of subfactors relative to the upper-level factors. Therefore, only a scientific and reasonable construction of a set of psychological quality assessment model can accurately reflect the requirements of the party and the state on the quality of college students and can play the role of correct guidance, inspection, control, and motivation.

First of all, various relevant information of students is fed back to the thinking counselor or class teacher who is responsible for managing that student in time, and at the same time, various information records are analyzed, and reports and graphs are issued. However, in the AHP assessment process, the decision maker also needs to determine the weight value of the guideline level-associated factors relative to the target level factors. Finally, the assembled results are transformed into 1~9 scales according to the inverse

transformation.

$$\begin{cases} F(x) = \frac{1}{x+1}, x \in \{0, 1, 2, \dots, 7, 8\}, \\ F(x) = -x+1, x \in \{-2, -3, -4, \dots, -7, -8\}. \end{cases} \quad (6)$$

Constructing the judgment matrix is a key step in applying AHP. The information basis of AHP is mainly the judgments given by people about the mutual importance of each element at each level, and these judgments are expressed numerically and written in the form of a matrix, i.e., judgment matrix. If the mean values of two matrices are equal, it is necessary to compare their variances:

$$\sigma_s^2 = \sum_{l=1}^k \frac{(P_{sl} - P_s)^2}{(k-1)}, \sigma_t^2 = \sum_{l=1}^k \frac{(P_{tl} - P_t)^2}{(k-1)}. \quad (7)$$

After completing the calculation of the weight vector of an element of a layer under the criterion relative to an element of the previous layer, the last is for the synthetic weight of each element relative to the total target layer, and let the ranking weight vector of the  $k-1$  elements of the  $K-1$ th layer relative to the target layer be the following:

$$\omega^{(k-1)} = \left( \omega_1^{(k-1)}, \omega_2^{(k-1)}, \dots, \omega_{k-1}^{(k-1)} \right). \quad (8)$$

The basic idea of the matrix method is to use a certain scale to represent the results of comparing two factors with each other, so as to construct a two-comparison judgment matrix. The decision problem is analyzed in detail, and all the influencing factors are derived, and then, they are grouped into different levels according to the different attributes of each influencing factor, forming an orderly progressive evaluation model layer by layer. The basic process is shown in Figure 3.

Secondly, the system uses B/S approach to implement some relevant functions and applications of psychometric analysis and early warning system. Mathematical

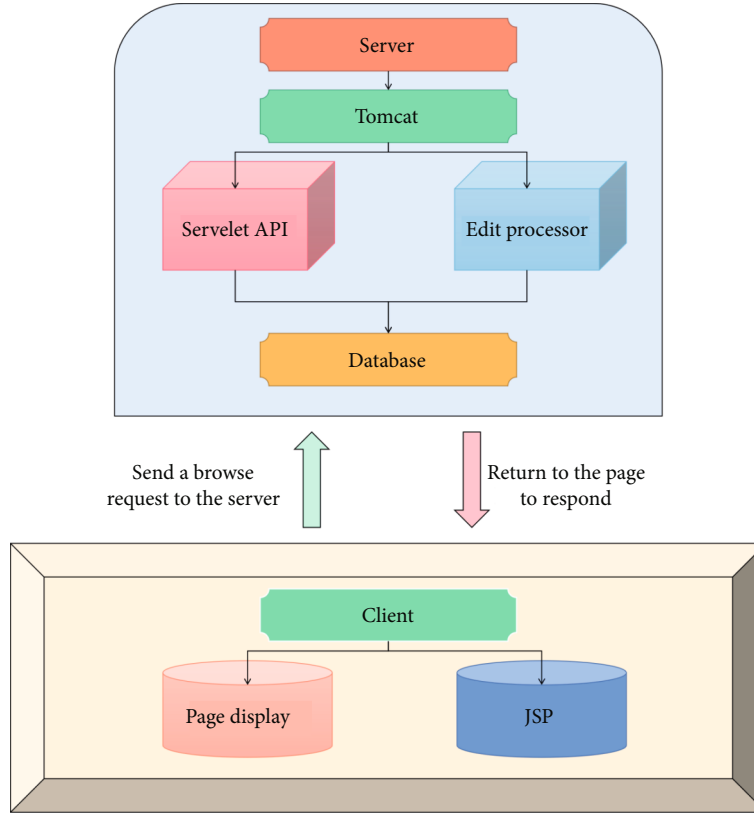


FIGURE 3: System structure realization flow chart.

transformation is generally used to transform the judgment matrix into a consistency matrix, but no consideration is given to maintaining the original judgment information of the decision maker in the improved model, which is crucial for the adjustment of the judgment matrix. Geometric averaging is performed on each row vector of the judgment matrix, and then, normalization is performed. Firstly, the product operation is performed on the elements of each row of the judgment, i.e.,

$$M_i = \left( \prod_{j=1}^n a_{ij} \right) \frac{1}{n}, \quad (9)$$

in which  $i = 1, 2, \dots, n$ . And then, normalizing

$$\omega_i = \frac{M_i}{\sum_{l=1}^n M_l}, i = 1, 2, \dots, n. \quad (10)$$

The modeling principle of diversified data collection is adopted, through multiple levels such as theoretical orientation, professional orientation, and personal orientation, while the Student Contingent Psychological Qualities Questionnaire is administered to different groups such as educational scholars, college teachers, student workers, personnel managers, and senior college students. The elements in the upper level have a dominant effect on all or some elements in the adjacent lower level, i.e., all or some elements in the

lower level are a subdivision of an element in the upper level, so that an ordered recursive assessment model can be constructed. Its output can be tabulated:

$$y = f \left( \sum_{j=1}^n w_j u_j - \theta \right) = f \left( \sum_{j=0}^n w_j u_j \right), \quad (11)$$

where  $u_j$  is the  $j$  input of sensor.

Finally, the relational database system was used to establish a database to store basic information, such as departments, counselors, class teachers, and students, as well as information of each assessment system and related assessments. The questionnaire was administered to different types of college students at the same time by using a self-assessment scale, and then, the structure of college students' actual psychological quality was constructed based on the collected information, and the actual differences between undergraduates and masters students were compared internally. It is a feed-forward network in which the input and output of each neuron are discrete values, and the output of each neuron is determined according to the threshold function after weighting and summing its input. Based on the developmental age of college students' psychological quality and the inspiration of "nearest developmental zone" theory, the actual psychological quality structure of college students is compared with the contingent psychological quality structure.

## 4. AHP of Psychological Evaluation and Its Improvement Analysis

*4.1. Theoretical Analysis of Applying AHP to Psychological Quality Evaluation.* AHP can quantify some qualitative problems that are difficult to quantify on the basis of strict mathematical operations and synthesize some quantitative and qualitative mixed problems into a unified whole for comprehensive analysis. The values of the elements in the judgment matrix reflect the decision maker's subjective perception and evaluation of the relative importance of each factor based on the objective reality. The basic idea of AHP is "decomposition before synthesis," which can be clearly seen from the steps of its use. AHP can be applied to this type of system or problem to better show its advantages, and it can also be used to analyze and evaluate more complex systems or problems. The eigenvectors and the maximum eigenroots of the judgment matrix are calculated using the eigenvalue method in order to calculate the maximum eigenroots for the total objective, taking the parameter values of 10 and 20, corresponding to the eigenvectors and eigenvalue pairs as shown in Figures 4 and 5 below.

Firstly, the factors involved in the problem are classified, and all factors are divided into target layer, criterion layer, and solution layer (also called measure layer in some literature) to find out the interrelationships and construct an ordered recursive hierarchy. The eigenvectors corresponding to the largest characteristic roots of the judgment matrix are solved first and then normalized to obtain the relative weights of the indicators in this layer corresponding to the indicators in the previous layer. A variety of extensions can also be applied, for example, data types, addition of new functions, aggregation functions, operators, procedural languages, and indexing methods. The judgment matrix constructed by the consistent matrix method is a comparison that represents the relative importance of all factors in this level against a factor in the previous level. Based on a factor of the previous level, it has a dominant relationship with the factors of the next level, and the relative importance of the factors of the next level is compared between two and two, and a certain score is assigned to it. So far, the decision maker can easily check whether the judgment matrix has order consistency and improves the judgment matrix that does not have order consistency. Among the three factors that can have an impact on the total target, bandwidth, time delay, and movement speed, bandwidth is the most important one among them, followed by the requirement for movement speed, and finally, time delay. The comparison of the weights of bandwidth, time delay, and movement speed under different scheme numbers is shown in Figure 6 below.

Secondly, the relative importance of each decision option under different criteria and total criteria is calculated by the decision maker's comparative judgment of the importance of each factor. Through expert analysis of the ratio of the influence of each two indicators on the target layer, the processing of data, and the recognition of each indicator, the judgment matrix is obtained, and then, the standardized (corresponding to the maximum eigenvalue) eigenvector of

the matrix is calculated to find out the weight of each indicator on the target, and the consistency test is performed. The weight coefficients of each indicator must be scientifically and reasonably specified according to the actual situation, so as to ensure the correct evaluation results are obtained. When it is used for two-class model classification, it is equivalent to using a hyperplane in a high-dimensional sample space, separating the two classes of samples.

Finally, the superiority ranking of the decision alternatives is derived. The server side generates the tree by receiving and analyzing the various query requests transmitted by the client, then performs data retrieval on it, and formats the results for output, and finally returns the results to the client. The experts quantify the importance of each index in this level relative to a certain index in a higher level by comparing them two by two according to the 9-scaled method in AHP, determine their corresponding importance, rank them and obtain the relative weights, and establish a judgment matrix. If the input patterns are linearly separable sets, the algorithm must converge if there exists a hyperplane that can separate them. If the input patterns are linearly indistinguishable sets, the single-layer perceptron cannot perform the correct classification.

*4.2. Group Decision AHP Analysis.* Group decision AHP is a scientific evaluation method that integrates the group decision method with AHP. This is a key step in AHP. After establishing the recursive hierarchy, the juxtaposition and subordination of the elements are determined, and the decision maker can then make a judgment for the two-comparison relationship of the elements. The group decision AHP breaks through the limitations of traditional evaluation, so that students are no longer isolated from evaluation but are provided with an opportunity to learn, so that they can judge their own progress and whether their psychological quality has been improved and developed. There is a correlation between students' psychological quality and social work, i.e., whether students take up social work or not have a certain influence on psychological quality. The comparison of the degrees of freedom and the Levin's variance of the mean difference under different characteristic values is shown in Figure 7 below.

First, multiple experts are invited to evaluate an assessment task at the same time to minimize the role of individual subjectivity, reduce the bias in the assessment results, and make the assessment results more accurate. The method of obtaining relative weight vectors using least squares is highly adaptable, and the computational effort is effectively reduced. There are many ways to divide a scale into two halves (e.g., by the difficulty of the question, by the parity of the question number, and by the content of the question), so the same scale will have different half confidence values. In this study, 100 test questions were divided into two halves according to the content of the questions and the data are shown in Table 1.

Usually there is only one element, and below the target layer is the criterion layer, which is a collection of factors that affect the target. Usually there are multiple levels of criterion layers, which means that sublevels can be established

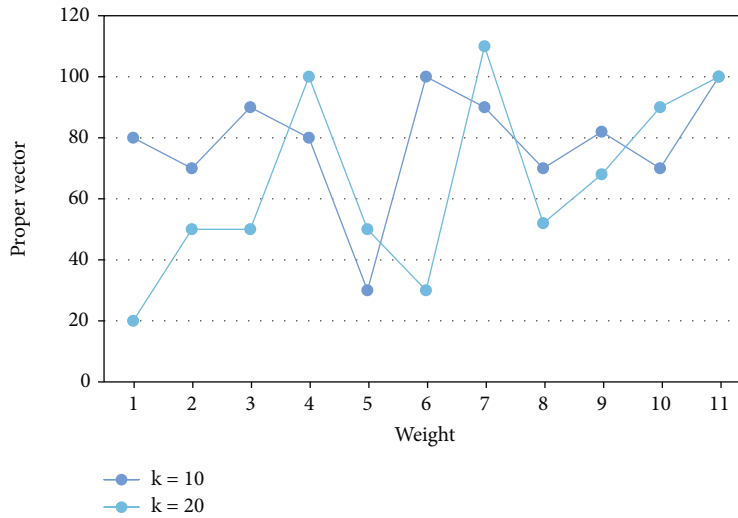


FIGURE 4: Comparison of feature vectors.

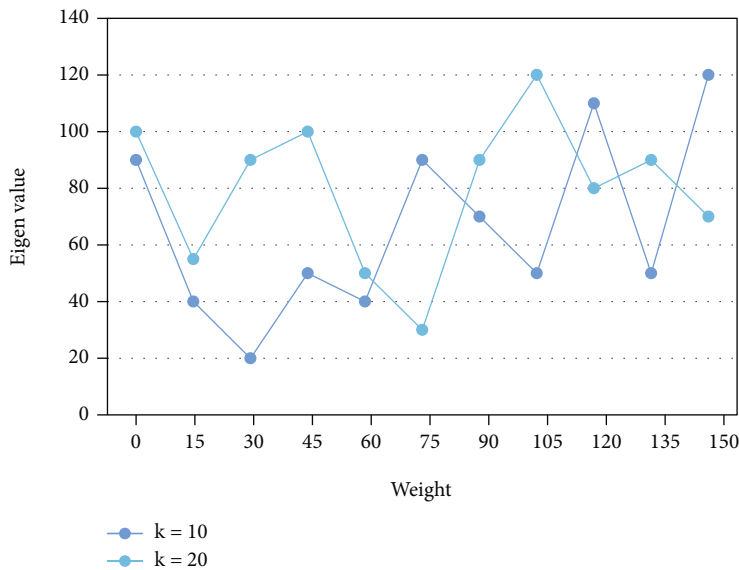


FIGURE 5: Comparison of eigenvalues.

between the criterion layers, and the sublevels are subordinated to one of the elements in the main level. Simulation data are generated through external simulation, then manual statistical calculations are performed, and the results of statistical analysis of the simulation data are compared and analyzed in the system. The consistency test is performed on the maximum eigenvalues of the judgment matrix, and if the consistency requirement is satisfied, then only the eigenvectors corresponding to the maximum eigenvalues need to be normalized, which are the final ranking weights. It is considered that there is a significant difference in the psychological quality of the investigated students who are working as social workers or not, which further indicates that whether students are working as social workers or not have a more significant effect on their psychological quality, and the Levin variance under different eigenvalues is shown specifically in Figure 8.

Second, the implementation of the group decision AHP requires a combination of the algorithm's own process and an auxiliary assessment and evaluation system. Because of the variety of split-half methods in split-half reliability and the less stable results obtained, it is relatively more accurate to use the  $\alpha$  coefficient as an estimate of the internal consistency of the scale. The results are shown in Table 2 below.

The split-half reliability of this construction method is 0.782, the test-retest reliability is 0.813, and the standard deviation of  $\alpha$  coefficient between all test objects is 0.842, which shows that this method has good reliability.

The smaller the calculation consistency index CI and CI, the greater the consistency, and vice versa. In the testing, we test the basic operations such as adding, modifying, and deleting in the system so as to ensure that the system can operate correctly. The use of 1-9 scales as the result of

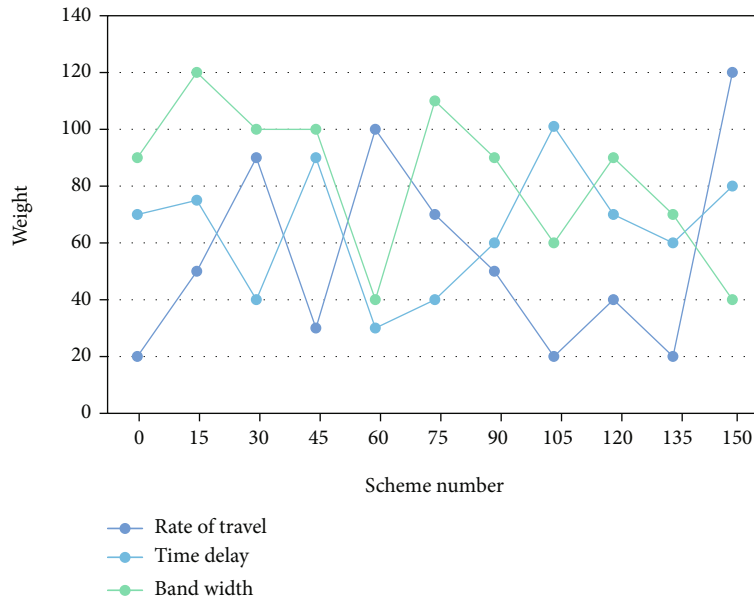


FIGURE 6: Comparison of weights of bandwidth, time delay, and moving speed.

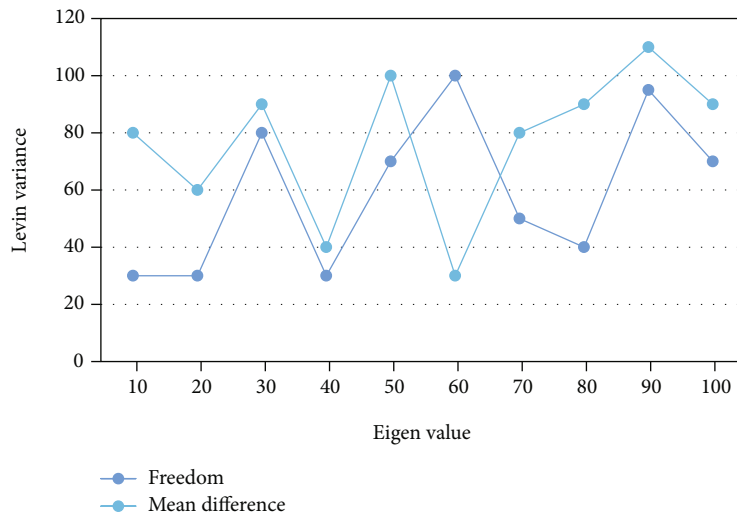


FIGURE 7: Comparison of Levin variance of freedom and mean difference under different eigenvalues.

TABLE 1: Split-half reliability with 100 topics.

	The first part	The second part
Split-half reliability value	0.562	0.498
Kehlenbach	0.44	0.38
Alpha coefficient	7.263	8.452

two-by-two factor comparison is also another reason for the deviation of the judgment matrix from consistency, and as the matrix order increases, the more difficult it is for the established judgment matrix to converge to complete consistency. Thus, when analyzing the order consistency test method of the judgment matrix, the judgment matrix of 1-9 scales is transformed into 0-1 matrix according to certain rules, thus simplifying the test method.

Finally, the data saved in the database needs to be assigned to the assessment model corresponding to the assessment task during the calculation of the method; otherwise, the calculation cannot be performed. The selection of the appropriate kernel function is the key factor, and it is necessary to apply the verified kernel function instead of the inner product according to the characteristics of the solution problem. The kernel function operation will transform the dot product operation of the high-dimensional feature space to the original space of low-dimensional features. After completing the assembly of the expert data, the upper half of the assembled matrix is converted into the full matrix, and the hierarchical single ranking and the hierarchical total ranking are performed by finding the maximum eigenvalue and the corresponding eigenvector for the full matrix to obtain the ranking results of the final solution.

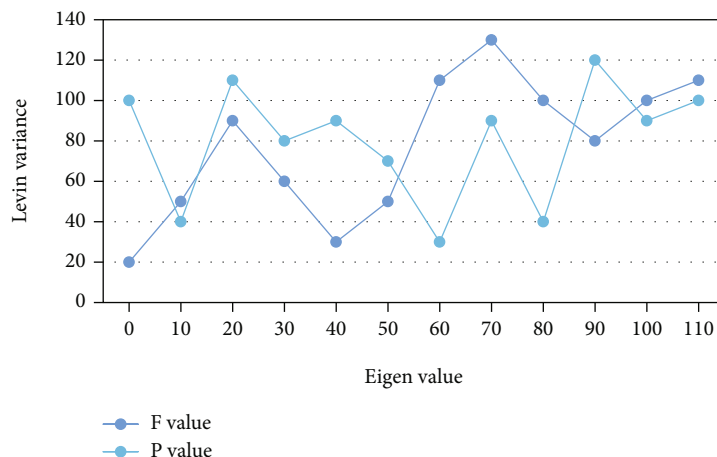


FIGURE 8: Levin variance under different eigenvalues.

TABLE 2:  $\alpha$  coefficients of different categories.

Category	Alpha coefficient of 100 questions	20 factors and the alpha coefficient of the total score	Alpha coefficient between 20 factors
Alpha coefficient	0.562	0.773	0.679
Number of factors	20	28	12

## 5. Conclusions

Modern society belongs to the era of information, and the rapid development of information technology and its popular application in all walks of life and all fields have brought radical changes to human society. Higher education has changed from elite education to mass education, and the student source of colleges and universities has become diversified and multilevel, and the problem of psychological disorders among college students has become more and more prominent. The traditional structure of psychological quality is only limited to a static form and is studied in isolation outside its “bio-ecological” environment. AHP can be used not only quantitatively but also qualitatively, combining quantitative and qualitative approaches to decision-making processes. Also, AHP can be refined in its classification, specifically in the psychological evaluation of security of a certain category of staff with commonality, and adjust parts of the evaluation model for the commonality and characteristics of a special group. The article proposes the construction method of the AHP-based psychological quality assessment model for college students, using AHP to decompose the complex target system into multilayer indicators. And by applying the theory of AHP to psychological quality assessment, the group decision AHP is studied to find the index weights of each layer, which is used to judge the relative rationality of the index system. The AHP-based psychological quality assessment model of college students can help to evaluate students’ safety psychological state quickly and

efficiently and can find out the safety psychological “shortcomings” of each student, which can be used as a reference basis for relevant departments to formulate accident prevention measures and has a certain reference effect on students’ safety.

## Data Availability

The labeled dataset used to support the findings of this study are available from the corresponding author upon request.

## Conflicts of Interest

The author declares no competing interests.

## References

- [1] W. Chan, “Correction to: analyzing ipsative data in psychological research,” *Behaviormetrika*, vol. 48, no. 1, pp. 201–201, 2021.
- [2] L. Ying, “Strategy analysis of psychological quality education in the environment of big data,” in *2017 International Conference on Smart Grid and Electrical Automation (ICSGEA)*, pp. 636–640, Changsha, China, 2017.
- [3] J. R. Kang, C. R. Lee, and D. K. Hwang, “A study on the priority of the baby boomer policy based on emotional psychology through the analytic hierarchy process,” *Korean Society for Emotion and Sensibility*, vol. 22, no. 1, pp. 77–88, 2019.
- [4] L. L. Greer, B. A. de Jong, M. E. Schouten, and J. E. Dannals, “Why and when hierarchy impacts team effectiveness: a meta-analytic integration,” *The Journal of Applied Psychology*, vol. 103, no. 6, pp. 591–613, 2018.
- [5] E. Thanassoulis, P. K. Dey, K. Petridis, I. Goniadis, and A. C. Georgiou, “Evaluating higher education teaching performance using combined analytic hierarchy process and data envelopment analysis,” *Journal of the Operational Research Society*, vol. 68, no. 4, pp. 431–445, 2017.
- [6] N. Kim, J. Park, and J. J. Choi, “Perceptual differences in core competencies between tourism industry practitioners and students using Analytic Hierarchy Process (AHP),” *Journal of Hospitality, Leisure, Sport & Tourism Education*, vol. 20, pp. 76–86, 2017.

- [7] M. Yuan and C. Li, "Research on global higher education quality based on BP neural network and analytic hierarchy process," *Computer and communication (English)*, vol. 9, no. 6, pp. 158–173, 2021.
- [8] N. F. Mahad, N. Yusof, and N. F. Ismail, "The application of fuzzy analytic hierarchy process (FAHP) approach to solve multi-criteria decision making (MCDM) problems," *Journal of Physics: Conference Series*, vol. 1358, no. 1, p. 012081, 2019.
- [9] C. Ayca and K. Hasan, "An application of fuzzy analytic hierarchy process (FAHP) for evaluating students project," *Educational Research and Reviews*, vol. 12, no. 3, pp. 120–132, 2017.
- [10] P. H. Dos Santos, S. M. Neves, D. O. Sant'Anna, C. H. de Oliveira, and H. D. Carvalho, "The analytic hierarchy process supporting decision making for sustainable development: an overview of applications," *Journal of Cleaner Production*, vol. 212, no. MAR.1, pp. 119–138, 2019.
- [11] C. Bosinski, "A proposed hierarchy of mental states," *Philosophical Studies: English version*, vol. 8, no. 9, p. 21, 2018.
- [12] M. Yang, "An evaluation-model-based research on the application of new media in student psychological health education in colleges and universities," *Revista de la Facultad de Ingenieria*, vol. 32, no. 13, pp. 856–862, 2017.
- [13] M. Strelhow, J. C. Sarriera, and F. Casas, "Evaluation of well-being in adolescence: proposal of an integrative model with hedonic and eudemonic aspects," *Child Indicators Research*, vol. 13, no. 4, pp. 1439–1452, 2020.
- [14] L. Ren and K. Hyunli, "Effects of bullying experience on psychological well-being mediated by conflict management styles and psychological empowerment among nursing students in clinical placement: a structural equation modeling approach," *Journal of Korean Academy of Nursing*, vol. 47, no. 5, pp. 700–711, 2017.
- [15] "Evaluation model of college students' mental health based on neural network," *Journal of Physics: Conference Series*, vol. 1744, no. 4, p. 042116, 2021.
- [16] X. Yin, "Prediction algorithm of young students' physical health risk factors based on deep learning," *Journal of Healthcare Engineering*, vol. 2021, no. 13, p. 8, 2021.
- [17] T. Wang and J. Park, "Design and implementation of intelligent sports training system for college students' mental health education," *Frontiers in Psychology*, vol. 12, article 634978, 2021.
- [18] T. Wang, Z. Li, Y. Ding, X. Duan, and C. Claramunt, "A psychological evaluation of a competition-based learning environment," *Current Journal of Applied Science and Technology*, vol. 29, no. 1, pp. 1–13, 2018.
- [19] D. Zala, A. Brabban, A. Stirzaker, M. R. Kartha, and P. McCrone, "The cost-effectiveness of the improving access to psychological therapies (IAPT) programme in severe mental illness: a decision analytical model using routine data," *Community Mental Health Journal*, vol. 55, no. 5, pp. 873–883, 2019.
- [20] M. P. Healey, A. Querbes, and M. Bleda, "Opportunity evaluation in organizations: a social psychological model," *Academy of Management Annual Meeting Proceedings*, vol. 2019, no. 1, p. 18937, 2019.
- [21] H. Ding and E. Yu, "Strengths-based leadership and employee psychological well-being: a moderated mediation model," *Journal of Career Development*, vol. 1, p. 089484532110188, 2021.
- [22] I. Roncaglia, "The role of wellbeing and wellness: a positive psychological model in supporting young people with ASCs," *Psychological Thought*, vol. 10, no. 1, pp. 217–226, 2017.
- [23] S. A. Power, G. Velez, A. Qadafi, and J. Tennant, "The SAGE model of social psychological research," *Perspectives on Psychological Science A Journal of the Association for Psychological Science*, vol. 13, no. 3, pp. 359–372, 2018.
- [24] S. O. Viktorenko, "Model of psychological resources of mnemonic function of students," *Bulletin of the National University of Defense of Ukraine*, vol. 58, no. 5, pp. 32–40, 2021.
- [25] Q. Pu, *Analysis of the Setback Education Mode Based on the College Student Entrepreneurial Psychological Quality Model*, pp. 395–398, 2018.
- [26] L. Zysberg, K. Verlinden, and C. Zingerle, "To have what it takes: a multi-tiered psychological resource model of first-generation college student success," *Psychology*, vol. 12, no. 10, pp. 1561–1574, 2021.
- [27] H. Chen, "Research on psychological health education of college students based on positive psychology theory," *Management science and research: Chinese and English version*, vol. 8, no. 1, p. 3, 2019.
- [28] M. Liu, "Student psychological motivation model based on quaternary data stream," *Revista de la Facultad de Ingenieria*, vol. 32, no. 7, pp. 308–316, 2017.
- [29] M. Wang, "Student psychological measurement model considering Hilbert's ecological psychological space," *Boletin Tecnico/technical Bulletin*, vol. 55, no. 9, pp. 495–502, 2017.
- [30] D. Collins and S. Winter, "Psychological models in sport psychology: a preliminary investigation," *European Journal of Sport Science*, vol. 20, pp. 1235–1244, 2020.



## Research Article

# Rural Tourism Resource Research Based on Multisensor and Geographic Information Big Data

Lixia Wang <sup>1,2</sup>

<sup>1</sup>*School of Economics and Management, China University of Mining and Technology, Xuzhou City, Jiangsu Province 221116, China*

<sup>2</sup>*Energy Economics Research Center, Henan Polytechnic University, Jiaozuo City, Henan Province 454000, China*

Correspondence should be addressed to Lixia Wang; wanglx@hpu.edu.cn

Received 28 May 2022; Accepted 24 June 2022; Published 21 July 2022

Academic Editor: Wen Zeng

Copyright © 2022 Lixia Wang. This is an open access article distributed under the Creative Commons Attribution License, which permits unrestricted use, distribution, and reproduction in any medium, provided the original work is properly cited.

With the continuous improvement of living standards, the rapid development of tourism, and increasing maturity of traveler behavior, tourism has become an essential part of people's daily life. Also, in recent years, with the continued development of economic and global integration, coordinated development has become a global trend. After more than 30 years of development and exploration, rural tourism in China is increasingly diversified. The accelerated development of a new socialist countryside and the integrated development of urban and rural areas provide important options for urban residents to escape from their habitual environment and seek leisure, comfort, and relaxation. Meanwhile, rural tourism development is based on certain resources and has a great coupling relationship with China's urban and rural development. As a result, rural tourism has long become a hot issue for academic research. However, with the continuous promotion of rural revitalization, rural tourism in China has presented some serious problems such as resource overdraft. These issues have caused serious harm to China's rural tourism resources and cultural heritage. On this basis, it is necessary to view rural tourism development from the perspective of coordinated regional development. Specifically, rural tourism resources should be characterized through a method of character selection to sort out rural development paths. At the same time, the development of regional tourism linkages for villages with shared source markets, dense location distribution, and similar landscape resources can effectively avoid regional homogeneous competition, form complementary advantages, and achieve sustainable development of regional economy, culture, and society. In addition, with the continuous development of information technology and computer technology in recent years, the construction of digital countryside has been completed. In other words, the conditions are in place to establish a rural tourism resource information platform that combines tourism information database and geospatial framework. The establishment of rural tourism resources information system will meet the information requirements of tourists and tourism management departments and lay the foundation of information technology for the development of rural tourism. Therefore, this study combines multisensor and geographic information big data technology to explore rural tourism resources. After that, based on the analysis of the evaluation results, specific regional overall linkage development strategies are proposed in four aspects: coordinating regional resources, optimizing resource allocation, integrating spatial types, and establishing regional brands. This can provide an effective strategic support for the diversified development direction of rural tourism.

## 1. Introduction

As a new force in tourism, rural tourism has emerged as a dynamic force in the rapid urbanization of cities and towns [1]. With the penetration of foreign rural tourism ideas and the subjective demand of domestic rural tourism, rural tourism in China has developed significantly. With the continuous development of rural tourism, more and more stake-

holders have started to pay attention to the past, present, and future of rural tourism [2–4]. Since 2005, there has been an explosion of research results related to rural tourism, and rural tourism has become a research hotspot in the tourism field. As a large agricultural country with a history of thousands of years of farming civilization, China has a vast territory and a large area [5]. However, due to differences in ethnicity, climate, and region, villages with diverse spatial

forms, diverse cultural components, and distinctive regional characteristics have been formed over a long period of time. Villages are seeing economic and humanistic activities based on the natural geographic environment, and they are the units of settlements with regional characteristics formed by local residents during their long lives [6]. The village is not a stable entity, but a product of the interaction between human society and ecological environment over a long period of time [7]. The landscape resources are the most obvious and vivid potential development resources of villages, which are the basis for distinguishing from other regional characteristics and forming regional personality [8].

With the continuous promotion of rural construction under the rural revitalization strategy, rural tourism development has become a proven development method for rural conservation and development [9]. As shown in Figure 1, the scenery in rural tourism is quite great. However, while rural tourism development is vigorously advocated, the phenomenon of similar models and mechanical replication of mainstream development concepts is still common [10]. In this context, a series of development problems such as one-sided villages [11], environmental pollution [12, 13], and disorderly development [14] have emerged. These problems have caused great losses to many of China's resource-rich and richly endowed villages. In addition, the rapid development of rural tourism has exacerbated the incongruous tendency to change the rural landscape while increasing economic income [15]. After all, landscape resources with local characteristics are the basic connotation of highlighting the characteristic appearance of the countryside. However, in the face of the gradual urbanization and commercialization of rural landscape, the disorderly use of rural landscape resources is the most urgent problem facing rural construction at present.

Rural landscape usually refers to the complex result of economic, social, natural, and human phenomena within a certain geographical area and is also subject to the constraints of both natural conditions and human activities. Due to the complex background of the meaning of both rural and landscape, scholars in different fields have different understanding of the concept of rural landscape [16]. From the perspective of geographical scope, rural landscape refers to the spatial landscape of human settlements and behavioral activities other than urban areas [17]. From the viewpoint of landscape composition, rural landscape is a landscape environment complex composed of rural settlement landscape, economic landscape, cultural landscape, and natural environment landscape [18]. In terms of landscape function, rural landscape has the function of providing agricultural products, maintaining ecological balance, and serving as a tourist resource [19]. What is more, from the viewpoint of landscape characteristics, rural landscape is different from urban landscape in terms of low interference, less destructive, and stronger natural attributes.

Although many scholars have studied rural tourism from different perspectives in recent years, there is still no clear and unified grounded theory on how to define the concept of rural tourism. Since rural tourism has similarities in



FIGURE 1: Scenery in rural tourism.

sustainability to agritourism and ecotourism, and the diversity of tourism product development is increasing [20], as a result, the generalization of the concept of rural tourism is worsening, and scholars are often confused about the meaning of some rural tourism concepts. In addition, the government and the tourism industry are unable to formulate targeted policies and implement management practices [21]. These factors have greatly affected and hindered the rapid development of rural tourism [22]. In addition, the topic of rural tourism development has attracted the attention of scholars in recent years and is becoming a hot topic in international rural tourism research. In the early stages of research, the focus was more on government-related factors and rural tourism hardware facilities, making the scope of research on rural tourism development relatively narrow [23]. However, in recent years, with the widespread development of rural tourism activities, a large number of scholars have begun to conduct field research and analysis. Nevertheless, there are still many imperfections in the current research on the influencing factors of rural tourism development.

What is more, quantitative research has not been carried out well compared to the current extensive qualitative research. This has not only increased the ambiguity and uncertainty of the research on the impact factors of rural tourism development but also made it difficult to concisely represent and present the complex logical relationships among the impact factors [24]. As an example, the question of who has a greater influence on rural tourism development factors remains ambiguous. After all, it is difficult to quantify and present the results of qualitative research on the extent to which the influencing factors affect each other [25]. This situation suggests that there is still much room for research and much room for improvement in the academic field of impact factors in rural tourism development. The study of impact factors is the basis for the industry's own improvement and policy formulation. As a result, there is a strong need to study the impact factors of rural tourism development based on quantitative methods.

Regional tourism linkage refers to the breaking of administrative boundaries of each tourist place within a certain geographical area. At the same time, according to the inherent correlation of tourism resources, interregional association and collaboration, with the power of regional tourism as a whole, participate in the competition and then realize the development process of common development of each tourist destination [26]. The development of tourism destinations in neighboring regions inevitably faces competition with each other, which in turn leads to the problem of common tourism products, mutual substitution, and lack of distinctive brand characteristics in each

region. Regional tourism linkage is essentially a development model that enhances the attractiveness and competitiveness of regional tourism through interregional cooperation and collaboration, bringing into play the advantages of each resource and achieving complementary advantages [27].

The Central Plains has been the main body of traditional Chinese civilization since ancient times and is one of the poles of propagation and birthplace of China's traditional civilization. The villages in close proximity to each other enjoy similar cultural and historical backgrounds due to their geographical distribution [28]. Faced with the opportunity of rural tourism development, the contradiction and conflict between the state of the heritage and the profound heritage can easily lead to vicious competition such as homogeneous development or IP competition. Regional tourism linkage is the practical part of regional linkage theory, which helps to drive regional development with tourism as the starting point, and is one of the models of regional linkage development [29]. In the context of new rural construction and the development of regional tourism linkage theory, many regions have begun to combine regional tourism linkage with rural planning practices. These initiatives are often able to maximize the development of landscape resources, maximize the value of resource utilization, and complement the advantages of the surrounding areas to achieve sustainable development [30].

Rural tourism development has become a hot topic in rural studies. Diversified ideas have emerged, but most of them remain in the microscopic perspective of single analysis and isolated development [31]. While regional tourism linkage as a new development trend has been studied to a certain extent, it is not very closely integrated with the countryside, and the relevant research base is also weak. This study provides a new theoretical basis for the development of rural tourism from a more macroscopic perspective and the linkage of resources to drive rural construction, which has certain theoretical value for rural development.

This study looks at the development of villages from a regional perspective and provides guidance on the construction status of the vast single development with no characteristics and insufficient capacity by linking resources. As a result, the status quo of isolated development and blind development of rural units in the region can be changed, and a regional synergistic development relationship can be established. This is conducive to the sustainable development of the rural ecological environment and region-wide economic growth, greatly increasing the efficiency of rural industries and farmers' income. What is more, through the development of regional tourism linkage, we can effectively get rid of the homogenization of rural development and form regional characteristic IPs, thus establishing the overall image of the region, driving the regional economy with resource linkage, and effectively stimulating the derivation of rural cultural and creative products. While driving the optimal development of cultural and creative industries, it will also deepen the

connotation of tourism, improve the income of rural tourism, and promote regional economic development.

## 2. Rural Tourism Resource System

The rural tourism resource system consists of RFID system and multisensor system, which mainly realize the data collection function. The data required to be collected include tourists' geographical location information, historical relics' location information, as well as temperature, humidity, and wind data of key areas. Among them, the location information of tourists and cultural relics can be collected by RFID system. Temperature, humidity, and wind information can be collected through a multisensor system. The overall hardware composition is shown in Figure 2.

*2.1. Multisensor System.* Multisensor network is a network system consisting of multiple sensor nodes distributed in certain specific areas according to certain coverage requirements. By connecting various types of sensors, the system transmits and summarizes the specified data information in a distributed environment to a computer management terminal by means of signals in an accurate and real-time manner. Subsequently, the management terminal is used to control and manage the wireless sensor network and related facilities, thus completing the required application services. The system collects temperature, humidity, and wind speed data of visitors through sensing devices and uses ZigBee technology to form a wireless sensor network to transmit data information.

According to the technology specified by ZigBee is a short-range, low-power wireless communication technology, mainly applicable to the field of automatic control and remote control, which can be embedded in various devices. To be specific, ZigBee defines 3 basic topologies: star topology, cluster topology, and mesh topology. The ZigBee network topology is shown in Figure 3.

Star structure is less energy consuming and simple to deploy, but less ductile. The mesh structure is more reliable but consumes more energy. Cluster structure has the advantages of both low energy consumption and good scalability and reparability. At the same time, the number of nodes and communication range are limited due to the wide range of monitoring in the scenic area and need to be deployed in key areas and remote spots of the scenic area. Therefore, a cluster type structure is chosen for the node arrangement in the scenic area weather information monitoring system.

The sensor node model consists of a processor, a sensor, a ZigBee transceiver, and a power module. The processor is divided into two parts: microcontrol unit and memory. The microcontrol unit is responsible for processing the data collected by the sensors and managing the control information, and the memory is used to store the sensors and routing information. The ZigBee transceiver is used to transmit and receive data wirelessly. The actual sensor node used in the system is mainly composed of DD219 module, sensor module, and power supply device. The hardware configuration of ZigBee sensor node is shown in Figure 4.

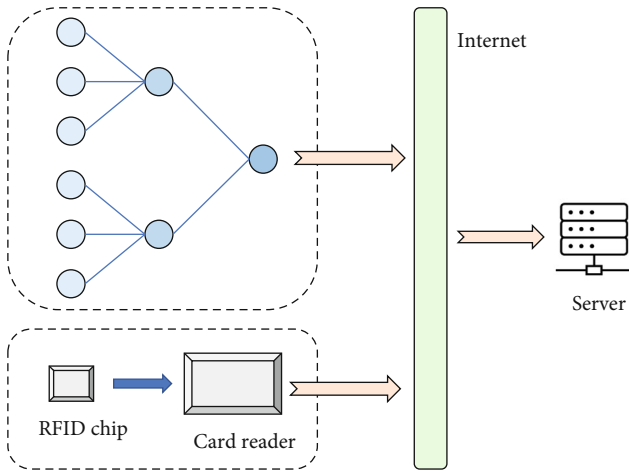


FIGURE 2: Overall hardware composition.

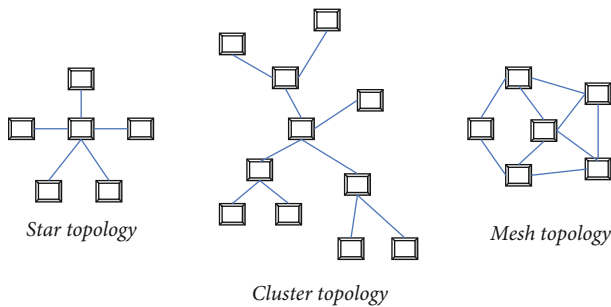


FIGURE 3: ZigBee network topology.

**2.2. RFID System.** RFID system is usually composed of several parts, such as electronic tags, readers, and application support software (Figure 5). The electronic tag has a unique electronic code; the tag stores a certain format of electronic data, often as the identification information of the item to be identified. The reader and the electronic tag can carry out data transmission according to the agreed communication protocol. Usually in the contactless mode, the reader sends out the data collection command; the electronic label parses the command according to the communication protocol and then transmits the identification data in the memory back to the reader.

The main function of RFID tags is to store the coded information of the items to be identified. Unlike bar codes, which are read passively, RFID tags must automatically or, under the prompting of an external force, actively transmit the internal data information. They are usually low-power integrated circuits with magnetic field induction coils, antennas, storage media, and controllers. Due to differences in classification standards, tags have multiple categories.

Depending on the power supply method, electronic tags can be divided into active tags and passive tags. The active tag obtains electrical power through an internally embedded battery, so it has sufficient power and high circuit stability. Its main disadvantage is that the size of the tag is larger, the production cost is higher, and the service life is limited

by the battery power. In addition, with the gradual consumption of electrical energy, the distance of signal transmission will become shorter and shorter, which eventually affects the normal operation of the RF system. Passive tags do not have internal batteries and require external energy to read properly. The more common energy-capable devices used in passive tags are coils and antennas. When the tag enters a specific working area, the antenna will receive electromagnetic waves, so the coil produces induction current, after the circuit integration to provide energy to the tag. Passive tags can be used for a long time or even permanently and are suitable for use in systems where chip information is frequently read and written. It has low production cost and long life and is lighter than active tags, also known as passive tags. The main disadvantage of passive tags is that the data reading distance is short, and the signal strength is limited by the size of the current, so a reader with high sensitivity is needed to achieve reliable reading.

As to the type of electronic chip used and the actual system function, there are significant differences in the design of the reader. The most basic function of the reader is to read the data from the electronic chip. In addition to this, the reader also requires signal state control, parity error checking, and other functions. The electronic chip contains not only the valid information to be transmitted but also specific additional data. The reader controls the reception and transmission of the data stream by means of the additional information it reads. From the technical realization aspect, the core of the RFID technology is the selection of the electronic tag, and the reader is designed according to the electronic tag. Although the reader in RFID system is much more expensive than the electronic tag, but in the actual application, the number of electronic tags is very large, and the number of readers used will be much less. The performance of the reader used in the rural tourism resource system is shown in Table 1.

The reader mainly sends RF signals of specific frequency through the antenna. When the electronic chip enters the working area of the transmitting antenna, it generates an induction current. It is then activated by the electrical energy and sends the internal coded information through the chip's built-in antenna. The system receives the carrier signal from the tag antenna and transmits it to the reader via the reader antenna, which demodulates and decodes the received signal and sends it to the server for corresponding processing. The principle of communication between the RFID reader and the electronic chip is shown in Figure 6.

In the rural tourism system, the main applications of RFID system are as follows. First, the scenic area is divided into small independent areas. In these small areas of some key location points, set RFID readers, and try to keep the role of these readers area does not interfere with each other, specifically, can use the reading method of timing polling and set the reader reading card cycle time. When a visitor carries an RFID electronic ticket through a specific area, RFID readers in that area read all the electronic ticket information within the sensing range. The collected data can then

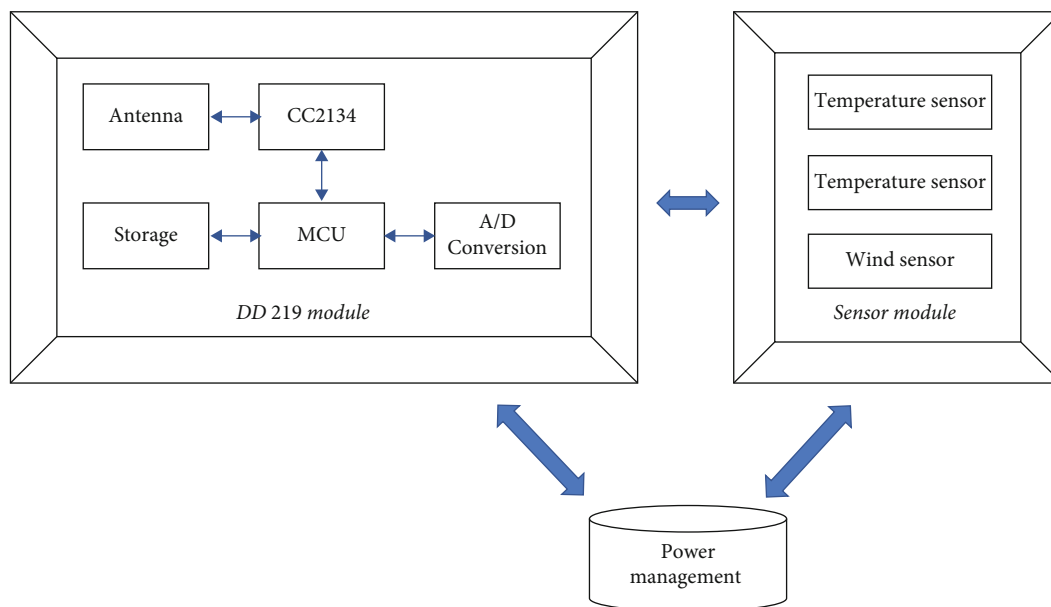


FIGURE 4: Hardware configuration of ZigBee sensor node.

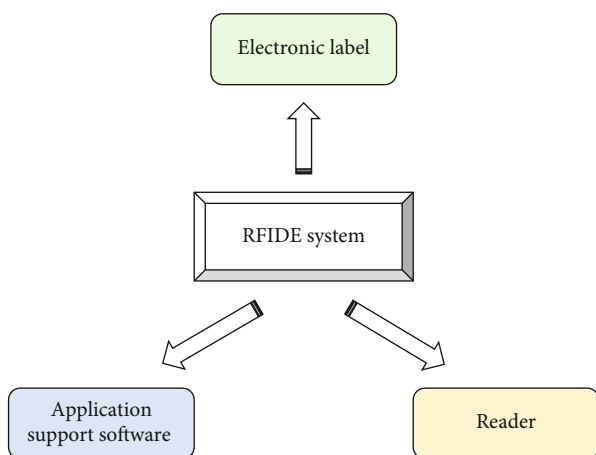


FIGURE 5: Composition of RFID system.

TABLE 1: Performance of the reader.

Parameter	Specification
Signal modulation method	GSHK
Frequency	1.65 GHz
Communication distance	10-20 m
Power	+12 V DC
Communication interface	JK234
Operating temperature	-20~60 Celsius

be sent to a data processing center for consolidation and analysis.

### 3. Geographic Information Big Data

Geographic information big data analysis is the technology required to realize online geographic information services on the Internet. The application of this technology has

important practical significance in promoting the wide application of mapping results, promoting the common construction and sharing of geographic information resources, and transforming geographic information services. In addition, the big data technology of geographic information can promote geographic information to better serve the development of tourism resources. With the rapid development of tourism industry, the demand of tourists for tourism geographic information services is getting higher and higher. The application of big data analysis technology of geographic information can solve the bottleneck problem of tourism GIS and provide authoritative geographic information service for the establishment of rural tourism resource system.

*3.1. Framework of Geographic Information Big Data.* The tourism resource management system built based on the public service platform of geographic information adopts the technology of geographic information big data to realize the design of UI layer. Then, the UI layer is designed by calling the service interface abstracted by the platform to load the data provided by the platform, such as digital line map, orthophoto map, and tourism thematic data. The digital line drawing data is mainly based on the public map data, and various public information collected is overlaid, and the content is reduced and simplified to generate tile data. It should be noted that the compiled electronic map data and its tile data need to pass the audit of the administrative department of surveying and mapping at or above the provincial level and obtain the audit number before they can be run on the Internet as public data. The framework of geographic information big data can be seen in Figure 7.

*3.2. Database Construction.* The database construction of the geographic information public service platform is the basis for the platform to provide geographic information services,

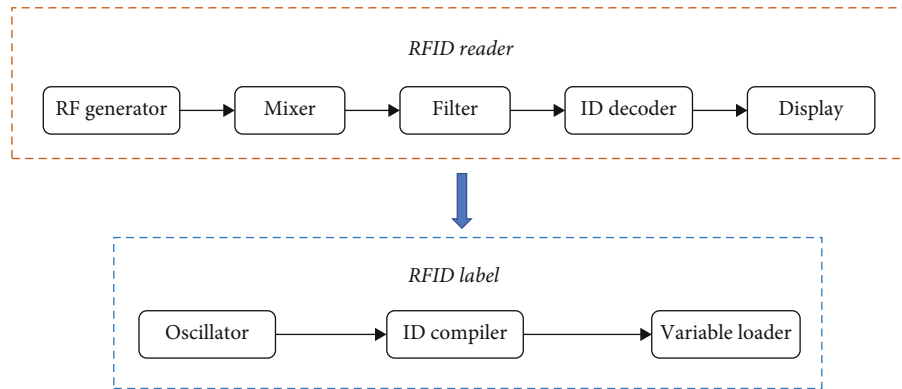


FIGURE 6: Principle of communication between RFID reader and electronic chip.

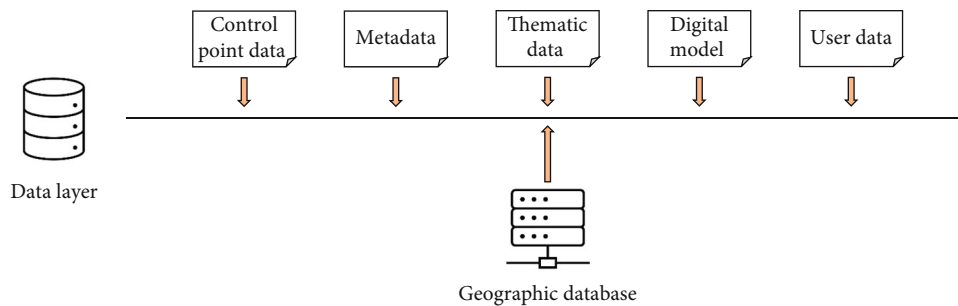


FIGURE 7: Framework of geographic information big data.

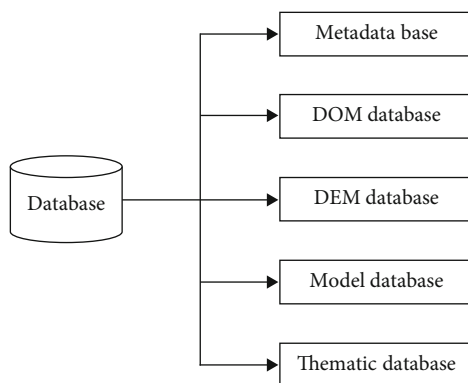


FIGURE 8: Database composition of geographic information public service platform.

which is used to store a variety of spatial data, basic mapping cattle production data, and other kinds of thematic data. The database composition of the geographic information public service platform is shown in Figure 8.

DEM and DOM data can be stored in the library, or the data can be stored in the form of files, and a file search directory can be established. DOM data are stored in two ways: in chunks and in whole chunks after fusion. Then, tiles are generated according to the rules, stored in file format, and indexed using multilevel subdirectories. The thematic database is mainly established for the geographic information data required by various thematic applications running on the geographic information public service platform. For example, the tourism-specific data applied in the tourism

resource management system based on the public service platform of geographic information studied in the thesis. Specifically, the establishment of tourism thematic database is realized by collecting and organizing relevant business data and thematic application data after conducting a large amount of market research on tourist attractions and tourists, etc.

#### 4. Conclusion

Geographic information data describe the patterns of natural events. Because of the large variety and volume of this data, it is of great importance to analyze and mine it. In this paper, we conduct a visualization study of the geographic information data in rural tourism resources in the context of digital earth and smart city advocated by the state. On this basis, this study designs and develops a tourism resource management system based on the public service platform of geographic information from the user requirements and the results of digital city construction. The system takes the public users as the target, closely combines the tourism thematic data with geospatial data, and realizes the map visualization of the traditional tourism resources with the map as the platform. Therefore, the system is able to provide different tourism services to the public users. In addition, the application of plug-in technology to the development of the tourism system provides the greatest convenience for updating, maintaining, and expanding the system later. It also provides a digital, professional, scientific, and networked management

platform for managers to improve work efficiency and decision-making.

However, the system designed in this paper is only a visual presentation, and its analysis and early warning still need to rely on human judgment. The next step of research is how to automate the analysis and early warning based on existing data to provide real intelligent help for tourism resource development and rural disaster prevention.

## Data Availability

The labeled dataset used to support the findings of this study are available from the corresponding author upon request.

## Conflicts of Interest

The author declares that there are no conflicts of interest.

## Acknowledgments

The study was supported by the “Young Backbone Teachers Support Program of Henan Polytechnic University, China (grant no. 2019XQG-13)”, by the Soft Science Project of Henan Province in 2019 (grant no. 192400410200), and by the Soft Science Project of Henan Province in 2022 (grant no. 222400410174).

## References

- [1] C. Liu, X. Dou, J. Li, and L. A. Cai, “Analyzing government role in rural tourism development: an empirical investigation from China,” *Journal of Rural Studies*, vol. 79, pp. 177–188, 2020.
- [2] A. G. Ivolga, I. I. Ryazantsev, A. G. Stroeve, Z. V. Gornostaeva, and O. V. Mandritsa, “Innovation approach to the sustainable rural tourism development,” *Research Journal of Pharmaceutical, Biological and Chemical Sciences*, vol. 9, no. 6, pp. 1588–1593, 2018.
- [3] J. J. Villanueva-Álvaro, J. Mondéjar-Jiménez, and F. J. Sáez-Martínez, “Rural tourism: development, management and sustainability in rural establishments,” *Sustainability*, vol. 9, no. 5, p. 818, 2017.
- [4] B. Cheng, K. Lu, J. Li, H. Chen, X. Luo, and M. Shafique, “Comprehensive assessment of embodied environmental impacts of buildings using normalized environmental impact factors,” *Journal of Cleaner Production*, vol. 334, p. 130083, 2022.
- [5] J. Gao and B. Wu, “Revitalizing traditional villages through rural tourism: a case study of Yuanjia Village, Shaanxi Province, China,” *Tourism Management*, vol. 63, pp. 223–233, 2017.
- [6] V. Yavas and Y. D. Ozkan-Ozen, “Logistics centers in the new industrial era: a proposed framework for logistics center 4.0,” *Transportation research part E: logistics and transportation review*, vol. 135, p. 101864, 2020.
- [7] S. Niu, A. Hu, Z. Shen, S. S. Y. Lau, and X. Gan, “Study on land use characteristics of rail transit TOD sites in new towns—taking Singapore as an example,” *Journal of Asian Architecture and Building Engineering*, vol. 18, no. 1, pp. 16–27, 2019.
- [8] B. Cheng, C. Fan, H. Fu, J. Huang, H. Chen, and X. Luo, “Measuring and computing cognitive statuses of construction workers based on electroencephalogram: a critical review,” *IEEE Transactions on Computational Social Systems*, vol. 4, pp. 1–16, 2022.
- [9] D. Hwang and W. P. Stewart, “Social capital and collective action in rural tourism,” *Journal of Travel Research*, vol. 56, no. 1, pp. 81–93, 2017.
- [10] J. Yang, R. Yang, M. H. Chen, C. H. J. Su, Y. Zhi, and J. Xi, “Effects of rural revitalization on rural tourism,” *Journal of Hospitality and Tourism Management*, vol. 47, pp. 35–45, 2021.
- [11] W. An and S. Alarcón, “How can rural tourism be sustainable? A systematic review,” *Sustainability*, vol. 12, no. 18, p. 7758, 2020.
- [12] R. Yuan, F. Guo, Y. Qian et al., “A system dynamic model for simulating the potential of prefabrication on construction waste reduction,” *Environmental Science and Pollution Research*, vol. 29, no. 9, pp. 12589–12600, 2022.
- [13] B. Cheng, J. Huang, J. Li, S. Chen, and H. Chen, “Improving contractors’ participation of resource utilization in construction and demolition waste through government incentives and punishments,” *Environmental Management*, vol. 69, pp. 1–15, 2022.
- [14] J. M. G. Martínez, J. M. M. Martín, J. A. S. Fernández, and H. Mogorrón-Guerrero, “An analysis of the stability of rural tourism as a desired condition for sustainable tourism,” *Journal of Business Research*, vol. 100, pp. 165–174, 2019.
- [15] S. Zielinski, Y. Jeong, S.-i. Kim, and C. B. Milanés, “Why community-based tourism and rural tourism in developing and developed nations are treated differently? A review,” *Sustainability*, vol. 12, no. 15, p. 5938, 2020.
- [16] M. Štastná and A. Vaishar, “Values of rural landscape: the case study Chlum u Třeboně (Bohemia),” *Land Use Policy*, vol. 97, p. 104699, 2020.
- [17] B. Csurgó and M. K. Smith, “The value of cultural ecosystem services in a rural landscape context,” *Journal of Rural Studies*, vol. 86, pp. 76–86, 2021.
- [18] P. Miller, E. Votruba-Drzal, and R. L. Coley, “Poverty and academic achievement across the urban to rural landscape: associations with community resources and stressors,” *RSF: The Russell Sage Foundation Journal of the Social Sciences*, vol. 5, no. 2, pp. 106–122, 2019.
- [19] L. E. Ridding, S. C. Watson, A. C. Newton, C. S. Rowland, and J. M. Bullock, “Ongoing, but slowing, habitat loss in a rural landscape over 85 years,” *Landscape Ecology*, vol. 35, no. 2, pp. 257–273, 2020.
- [20] M. M. Su, G. Wall, Y. Wang, and M. Jin, “Livelihood sustainability in a rural tourism destination - Hetu Town, Anhui Province, China,” *Tourism Management*, vol. 71, pp. 272–281, 2019.
- [21] D. Bozok, S. N. Kılıç, and S. S. Özdemir, “Bibliometric analysis of rural tourism on tourism literature Turizm literatüründe kırsal turizm bibliyometrik analizi,” *Journal of Human Sciences*, vol. 14, no. 1, pp. 187–202, 2017.
- [22] C. Lewis and S. D’Alessandro, “Understanding why: push-factors that drive rural tourism amongst senior travellers,” *Tourism Management Perspectives*, vol. 32, p. 100574, 2019.
- [23] R. Situmorang, T. Trilaksono, and A. Japutra, “Friend or foe? The complex relationship between indigenous people and policymakers regarding rural tourism in Indonesia,” *Journal of Hospitality and Tourism Management*, vol. 39, pp. 20–29, 2019.

- [24] A. Karali, S. Das, and H. Roy, "Forty years of the rural tourism research: reviewing the trend, pattern and future agenda," *Tourism Recreation Research*, vol. 46, pp. 1–28, 2021.
- [25] L. Dai, L. Wan, B. Xu, and B. Wu, "How to improve rural tourism development in Chinese suburban villages? Empirical findings from a quantitative analysis of eight rural tourism destinations in Beijing," *Area*, vol. 49, no. 2, pp. 156–165, 2017.
- [26] I. De Noni, A. Ganzaroli, and L. Orsi, "The impact of intra- and inter-regional knowledge collaboration and technological variety on the knowledge productivity of European regions," *Technological Forecasting and Social Change*, vol. 117, pp. 108–118, 2017.
- [27] A. Sinha, O. Driha, and D. Balsalobre-Lorente, "Tourism and inequality in per capita water availability: is the linkage sustainable?," *Environmental Science and Pollution Research*, vol. 27, no. 9, pp. 10129–10134, 2020.
- [28] K. W. H. Tsui, D. Tan, C. K. W. Chow, and S. Shi, "Regional airline capacity, tourism demand and housing prices: a case study of New Zealand," *Transport Policy*, vol. 77, pp. 8–22, 2019.
- [29] Y. Li, R. Li, W. Ruan, and C. H. Liu, "Research of the effect of tourism economic contact on the efficiency of the tourism industry," *Sustainability*, vol. 12, no. 14, p. 5652, 2020.
- [30] J. Liang and C. S. Chan, "Local cultural vicissitudes in regional tourism development: a case of Zhuhai," *Tourism Management Perspectives*, vol. 25, pp. 80–92, 2018.
- [31] M. Nosheen, J. Iqbal, and H. U. Khan, "Analyzing the linkage among CO2 emissions, economic growth, tourism, and energy consumption in the Asian economies," *Environmental Science and Pollution Research*, vol. 28, no. 13, pp. 16707–16719, 2021.



## Research Article

# Modern Clothing Design Based on Human 3D Somatosensory Technology

Zhe Liu  and Min Luo

*Fashion Art School, Hubei Institute of Fine Arts, Wuhan, 430205 Hubei, China*

Correspondence should be addressed to Zhe Liu; 20181575@hifa.edu.cn

Received 28 May 2022; Accepted 22 June 2022; Published 9 July 2022

Academic Editor: Wen Zeng

Copyright © 2022 Zhe Liu and Min Luo. This is an open access article distributed under the Creative Commons Attribution License, which permits unrestricted use, distribution, and reproduction in any medium, provided the original work is properly cited.

In the era of e-commerce, online clothing sales have grown rapidly, but the differences in clothing size and style details have brought serious problems to consumers' purchase. At present, as far as online clothing sales are concerned, the most prominent problem is that consumers cannot try on clothes online as they do in the real environment, let alone touch and feel the texture of clothing fabrics. This has seriously affected and restricted the development of online clothing sales. The after-sales service cannot keep up, which is mainly reflected in the consumer return and replacement which is not convenient, and the purchased clothing cannot be received in time and other aspects. 3D garment customization is a hot area of research at present, and there is a wide range of needs to implement a software that can be customized for users. As a depth sensing technology, it strengthens the ability of video sensors for target recognition and brings new advances in sensing and processing deep vision tasks. Aiming at this problem, this paper proposes a modern clothing design scheme based on human 3D somatosensory technology. The designed scheme focuses on the acquisition of human size data and the personalized combination process of clothing components in the process of clothing design. In the scene where the human body changes greatly or the human body moves rapidly, the real-time limb coverage of the clothing fabric is higher, and the posture matching degree is higher. Applicable clothing types and human body pose types are more abundant, with a higher sense of reality. The clothing perception model fused with profile and girth features can match the dimensional changes of key parts of the human body. Through personalized clothing design, the combination of clothing parts is used to provide more choices of clothing styles, colors, and sizes. Using this solution, the time of clothing design can be greatly shortened, and the user's satisfaction with the clothing design can be improved.

## 1. Introduction

In recent years, with the rapid development of Internet technology and the transformation of public consumption concepts and shopping methods, the e-commerce industry has grown rapidly and gradually stabilized, and apparel products are one of the most popular products in the Internet retail industry [1]. The "2016 Global Apparel B2C E-commerce Development Status" released by the Hamburg-based market research company yStats pointed out that in the huge e-commerce market, apparel sales, and consumer electronics accounted for the largest proportion. The "2015-2016 China Apparel E-commerce Industry Report" released by the China E-Commerce Research Center shows that the total

transaction volume of textile and apparel e-commerce in 2015 reached 3.71 trillion yuan, an increase of more than 25% compared with 2014, and the total transaction volume in 2016 has approached 5 trillion yuan which will continue to maintain rapid growth.

With the advent of the global economic era, the garment industry has gradually developed and expanded. It evolved from the original cold, heating, shelter, and other functions to decoration, logo, and beauty, showing the beauty of clothing, to meet people's spiritual enjoyment. When choosing clothing, consumers are not only satisfied with the same clothing, different colors, fabric and textile structure, and supporting accessories but also hope to match the clothes on the table according to their own body shape and can

customize the clothing style [2] according to their own will. Because users are not satisfied with the goods they buy, they will frequently return and exchange goods, which will directly reduce the users' shopping experience, cause cumulative and long-term impact, and even cause word-of-mouth effect, which will have a negative impact on [3] on the development of merchants, platforms, and related industries. According to Vipshop statistics, the return rate of clothing is as high as 25 percent to 30 percent. The main reason is the wrong size, poor personal experience, and do not like costume details.

Based on this background, this paper proposes a modern clothing design method based on human 3D motion sensing technology. From the user's point of view, this can achieve the "tailored" function of different human body types and design the clothing styles according to the user's expectations. Specifically, in order to realize the parameterization of the mannequin, the corresponding three-dimensional mannequin is generated in real time according to the body shape characteristics of users, so as to recommend the appropriate size and facilitate users to buy the desired clothes.

## 2. State of the Art

Based on 3D somatosensory data, the modeling of 3D data and virtual fitting technology are inseparable. First, the 3D point cloud data of the human body is obtained through the camera with the function of point cloud collection, and the distance (depth) from the image grabber to each point in the scene is an image of the pixel value that directly reflects the geometry of the visible surface of the scene. Depth images can be calculated as point cloud data after coordinate conversion, and point cloud data with rules and necessary information can also be converted into depth image data. And then, the 3D virtual modeling of the human body is performed. Then, use the different parts of the clothing design to design the clothing as a whole, and try the designed clothing on the user's virtual model [4]. Finally, according to the user's virtual model try-on effect, adjust the texture, parts, color, and other information of the designed clothing, and continue the virtual fitting until a satisfactory effect is achieved. The overall clothing design process based on human 3D somatosensory data is shown in Figure 1.

*2.1. 3D Human Body Modeling Technology.* The main methods of 3D human modeling technology are 3D modeling software modeling, image recognition method modeling, and 3D scanning equipment modeling [5].

3D modeling software simply refers to the construction of a model with 3D data in a three-dimensional virtual space, and 3D modeling is the core of 3D printing technology and the core content of 3D education. The software has the advantages of good modeling effect, strong sense of reality, and accurate data, but the production cycle is long, the realization is difficult, and professional and technical personnel are required. Image recognition method modeling is divided into two methods: image rerendering and image-

based modeling. The rerendering method only shows the rendering effect of the human body from different angles with the change of illumination and position and does not realize the three-dimensional reconstruction of the human body. Based on image modeling, the coordinates of the final 3D object are calculated from the correspondence between the extracted feature points [6]. This method requires small differences between pictures and high limitations. Image-based 3D modeling is convenient and fast, but it is often accompanied by problems such as camera positioning and tracking, calibration, image segmentation, and matching, resulting in high efficiency and robustness that cannot meet the existing requirements. The core idea of 3D scanning equipment modeling is to use scanning point cloud data or IXIB. D data for registration, surface reconstruction, and other technologies obtain the surface of the scanned object. The compact and portable depth camera can capture the color and depth information of the scanned object surface at high frequency. By actively emitting and receiving infrared light, depth data can be obtained directly, and a better interactive interface and strong practicability can be provided [7].

Kinect fusion is a three-dimensional object scanning and modeling method provided by Microsoft to Kinect developers. Its main implementation process is four steps of depth data extraction, data calibration, data fusion, and real-time rendering. Capture directly through the camera, without user interaction, in real time (GPU implementation), and easily realize 3D model reconstruction. However, because the algorithm itself depends on the depth change in the scene, it has high requirements for user actions, and it is difficult to coincide with the original position, resulting in the reconstruction of the 3D model that is not closed and only considers the rigid calibration technology, so many researchers are committed to Kinect fusion. Algorithm improvements were emerged during past years. Tong et al. proposed a 3D human reconstruction method based on multiple Kinects for the situation that the 3D model is not closed and used the turntable to calibrate the data scanned by the three Kinects to obtain complete human body point cloud data to realize the automatic scanning process. Weiss and Hirshberg[7] used a Kinect to propose a parametric human body model based on the SCAPE method, but it takes about an hour to complete the modeling process, which obviously cannot achieve rapid modeling. Zollhofer and Martinet established the correspondence between depth images and color images to achieve high-quality face models. Weise and Bouaziz used Kinect as an interactive device to build a system for capturing and tracking facial expressions in real time. Due to the difference of the Kinect distance, the acquired depth data has more or less noise, which reduces the accuracy of 3D reconstruction. Common noise reduction algorithms include Gaussian filtering, Laplace smoothing, Wiener noise reduction, and bilateral filtering.

With the rapid development of computer information technology and mechanical manufacturing technology, 3D scanning technology is widely used in different industries, which can quickly obtain a large amount of spatial point information of the target to be measured in a short period

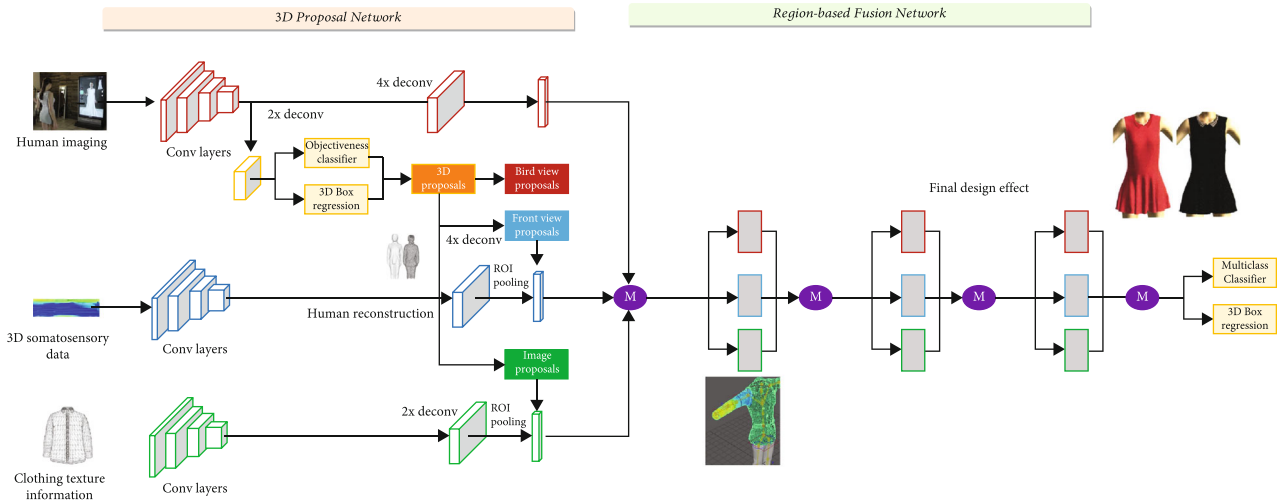


FIGURE 1: Apparel design process based on human 3D somatosensory data.

of time, establish a 3D model of the target and extract line, surface, body, and other data, obtain massive 3D point cloud data on the surface of static objects with the principle of light reflection, and adopt high-precision reverse 3D modeling and reconstruction technology. By synchronously obtaining the 3D coordinate data of the target range and digital photos, the 3D stereoscopic information of the object such as the entity or the real scene is quickly obtained, and the 3D data model is reconstructed by the computer to reproduce the real-time, changing, and real morphological characteristics of objective things, which can realize noncontact measurement and provide a new tool for rapid modeling of objects and spatial change analysis.

**2.2. Virtual Clothing Fitting.** In the early days, the virtual “fitting mirror” system with two-dimensional texture maps attracted the attention of consumers. Clothing and accessories were represented by two-dimensional maps [8]. This technical principle is simple and easy to implement, and the interaction method is intuitive and interesting, but there are often some shortcomings: (1) the standard model used in the fitting mirror is far from the body shape, and it is impossible to judge whether the clothes are suitable for you. (2) The display of clothing is often fixed in a certain posture, and real-time dynamic effects cannot be presented according to the user’s movement. (3) Clothes are closer to a flat effect, and the effects of their special decorations (such as ribbons and pleats) are difficult to display. (4) The processing of clothing photos requires significant human resources and operating costs.

In recent years, with the improvement of computer system performance, many companies have launched some 3D fitting software [9]. The 3D fitting software can see the IJ’s specific 3D image data directly from the computer, using fully automatic and interactive 3D image segmentation, quickly obtaining the target range, and creating a three-dimensional model in just a few simple steps. The MIRA-Cloth system developed by the M/RALab laboratory of the University of Geneva, Switzerland, and the C-Me and V-Stitcher systems of the American Browzwear Company are

relatively mature. The domestic three-dimensional fitting software is Hexuan C2pop software, Shanghai Quda Company (quda website deforms to the corresponding body shape according to the input body size), and Shanghai fitting company Haomaiyi (Haomaiyi website shows the same human body wearing different sizes of clothes), as shown in Figure 2.

### 3. Methodology

**3.1. 3D Somatosensory Technology.** 3D motion sensing is a deep sensing technology that allows people to use body movements directly and interact with surrounding devices or environments without the need to use any complex control devices, which enhances the ability of video sensors to recognize objects and brings new advances in perceiving and processing depth vision tasks [10]. The current mainstream 3D vision solutions include binocular stereo vision method and time-of-flight method. These technologies simulate the human vision system and promote technological development in the fields of AI and computer.

**3.1.1. Binocular Stereo Vision.** Binocular stereo vision is an important form of machine vision. It is based on the method of the principle of disparity and using the imaging equipment to obtain two images of the measured object from different positions and to obtain the 3D geometric information of the object by calculating the position deviation between the corresponding points of the image. Due to the different perspectives of the cameras, objects appear significantly different in the two images, the so-called parallax, which refers to the same point in the three-dimensional space. For the coordinate difference in the imaging of the two cameras, the closer the object is to the imaging plane, the larger the parallax, and vice versa, the smaller the parallax [11]. Three-dimensional images can be obtained through triangulation technology, which is similar to the imaging principle of human eyes. At the same time, the grayscale information of the image can also be used for encoding to reflect the effect of distance. The closer the spatial point is to the

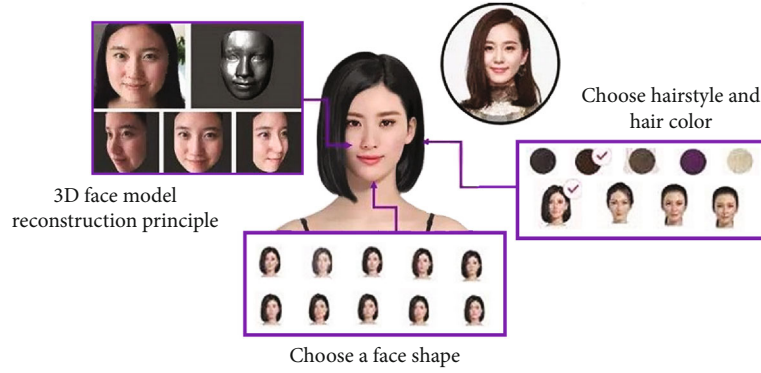


FIGURE 2: Existing virtual fitting software.

imaging plane, the brighter the grayscale value. The schematic diagram of triangulation is shown in Figure 3, and the schematic diagram of binocular stereo vision is shown in Figure 4.

According to the law of similarity of triangles, we have

$$\frac{z}{f} = \frac{x}{xl} = \frac{x-b}{xr}. \quad (1)$$

Solving the equation above, we get

$$\begin{aligned} x &= \frac{xl * b}{xl - xr}, \\ z &= \frac{b * l}{xl - xr}. \end{aligned} \quad (2)$$

Further simplification yields

$$\begin{aligned} z &= \frac{b * l}{d}, \\ x &= \frac{z * xl}{d}. \end{aligned} \quad (3)$$

According to the above formula, to solve the depth value  $z$ , it is necessary to determine the camera focal length  $f$  and the camera baseline  $b$  and also need to know the parallax  $d$  between the two camera points.

**3.1.2. Principle of 3D Registration Based on SVD Decomposition.** Three-dimensional registration is used to solve the problem of coordinate mapping from one three-dimensional coordinate system to another three-dimensional coordinate system. Usually, the SVD singular value decomposition method is used for the matching calculation of the three-dimensional point set. It is assumed that there are two three-dimensional point sets  $\{P_i\}$  and  $\{Q_j\}$ ; if the three-dimensional data points in them correspond one-to-one, there is the following conversion relationship:

$$Q_j = R \cdot P_i + T + N_i, \quad (4)$$

where  $R$  is the rotation matrix,  $T$  is the translation matrix, and  $N_i$  is the noise vector, indicating that the data points

in the point set  $\{P_i\}$  can reach the position of the corresponding data point in the point set  $\{Q_j\}$  through the transformation of rotation and translation. The matrix and  $T$  translation matrix are unknown and need to be solved by SVD singular value decomposition method. First, find the centroids of the two 3D point sets:

$$P_0 = \frac{1}{n} \sum_{i=1}^n P_i, \quad (5)$$

$$Q_0 = \frac{1}{n} \sum_{i=1}^n Q_i.$$

Calculate the correlation matrix  $H$  of two point sets using the centroid displacement vector:

$$H = \sum_{i=1}^n P_i Q_i^T. \quad (6)$$

$H$  (correlation matrix) represents the correlation of the coordinates of two point sets and performs SVD decomposition on the  $H$  matrix:

$$H = USV^T. \quad (7)$$

Matrices  $U$ ,  $S$ , and  $V$  are orthogonal matrices in the decomposition process. For matrix  $R$ , the optimal solution is

$$R = VU^T. \quad (8)$$

Verify that the optimal solution is valid: if  $\det(R) = 1$ , the matrix  $R$  is calculated correctly; otherwise, if  $\det(R) = -1$ , the  $R$  calculation is invalid. When  $R$  is calculated correctly, the translation matrix  $T$  can be calculated from  $R$ :

$$T = -R * P_0 + Q_0. \quad (9)$$

The conversion diagram of two three-dimensional point sets  $\{P_i\}$  and  $\{Q_j\}$  is shown in Figure 4:

**3.2. Human 3D Reconstruction.** Scanning reconstruction of 3D human body is one of the hot topics of research. The quality of human body model parameterization has been

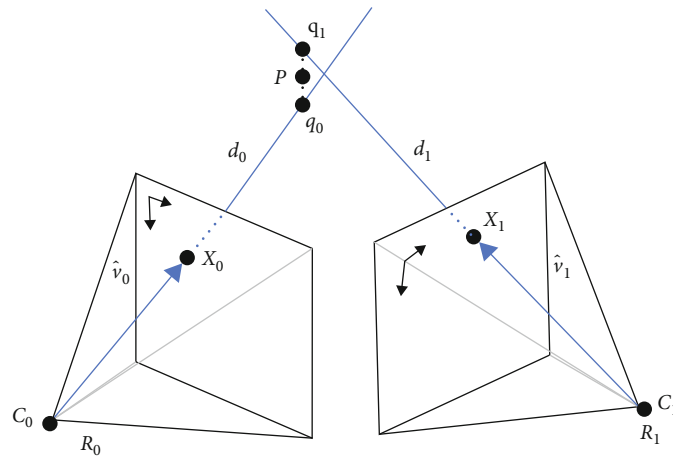


FIGURE 3: Schematic diagram of triangulation. Figure 4 Schematic diagram of binocular stereo vision.

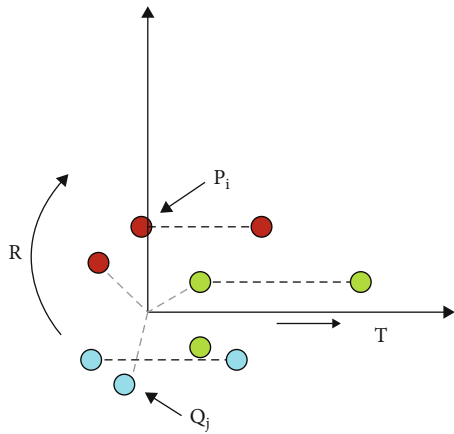


FIGURE 4: Schematic diagram of point set registration.

improved. It is directly related to whether the clothing can be properly tried on the human body and will also be a key factor for consumers to consider whether to buy the clothing [12].

3D human body reconstruction method is fast and requires no user interaction. The corresponding human body template is generated by Make Human body modeling software, and a closed and reliable 3D human body model is formed by template matching and interpolation algorithm [13]. The main steps of the algorithm are as follows:

**3.2.1. Extract Human Depth Data.** Use the cost-effective Kinect somatosensory device to extract the user's depth data, convert it into point cloud data, perform noise reduction processing on the point cloud, and calculate the normal direction of all point clouds. In addition, the depth data and infrared data are analyzed to obtain skeleton information.

Kinect is a 3D somatosensory camera developed by Microsoft, including infrared transmitters, color sensors, infrared depth sensors, and other parts, with functions such as motion capture, image recognition, microphone input, and voice recognition. Infrared data can be obtained by the

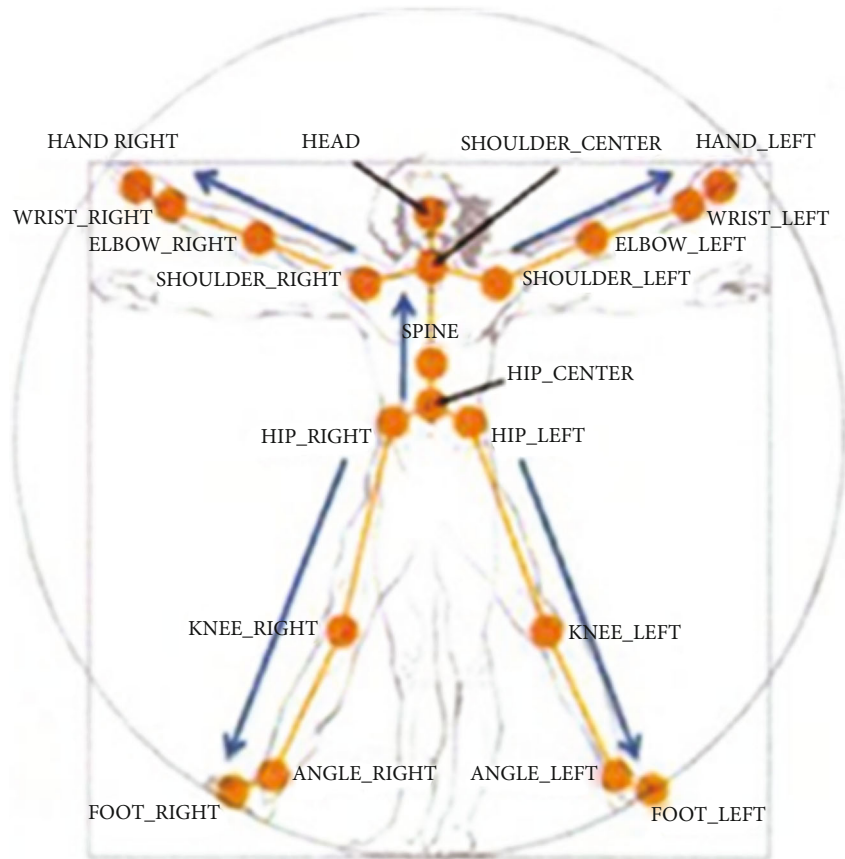
infrared transmitter and the camera, and the infrared data can be calculated and processed to obtain the depth-of-field image data.

Kinect's joint tracking system can provide users to track the joint positions of the person's skeleton, which is often used for gesture detection, user interface operation, and many other functions. The main principle of its realization is to analyze the depth data and infrared data obtained by Kinect's depth camera and infrared camera to obtain a human body model and further extract the human skeleton based on the analysis method of maximum posterior probability [14].

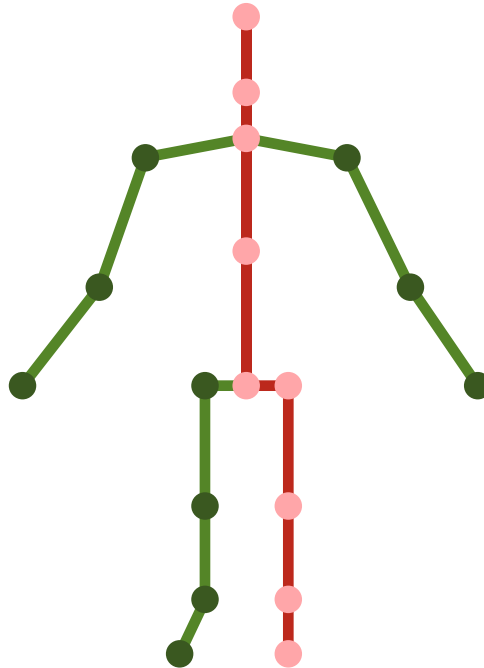
As shown in Figure 5, the Kinect skeleton consists of 23 joints and a total of 22 bones. The left side shows the details of the joints in the skeleton, and the right side shows the effect of real-time capture, all omitting the joint points showing the fingertips. Table 1 shows the numbering comparison of Kinect bone points.

**3.2.2. Data Preprocessing.** Due to the inconsistency of the coordinate system, the occlusion of surrounding objects, and the interference of noise points, the captured depth data and skeleton data often need to be preprocessed to ensure the accuracy and precision of the data and facilitate subsequent use. The noise points of the depth data are processed by the bilateral filtering algorithm; the pose (position and orientation) of the world coordinate system is calculated, and the nearest iteration method is used for calibration; the smooth filtering algorithm is used for the Kinect skeleton [15].

**3.2.3. Feature Extraction.** In order to improve the accuracy and speed of the system calculation, the human body is firstly processed into blocks; secondly, the corresponding feature points, feature lines, and contour lines are extracted from the human body data. Among them, the main characteristic points are overhead head point, laryngeal node point, acromial point, axillary point, elbow point, umbilical point, hip point, and knee point. The feature contour line is associated with the feature point, seeking the cross section parallel to the  $xoz$  plane or the  $yoZ$  plane. Finally, calculate the



(a) Skeleton name diagram



(b) Kinect human skeleton acquisition diagram

FIGURE 5: Schematic diagram of the skeleton.

circumference of the human body (waist circumference, hip circumference, bust circumference, etc.) and height information.

After obtaining the human body model, according to the linear relationship between the proportion of human body structure and height given in Table 2, we divide it

TABLE 1: The numbering comparison table of Kinect bone points.

No.	Joint type	No.	Joint type
0	Spine base	1	Spine mid
2	Neck	3	Head
4	Shoulder left	5	Elbow left
6	Wrist left	7	Hand left
8	Shoulder right	9	Elbow right

into blocks, simplify it according to the degrees of freedom, and divide the human body model into five parts: upper body, left leg, right leg, left hand, and right hand [16]. Figure 6 shows the block rendering and also shows that the block results do not depend on the pose of the human body. The algorithmic basis for the segmentation of the human body model is the position of the skeleton and the biological characteristics of the human body [17]. Firstly, the automatic alignment of human depth data and skeleton is realized by using the position of the viewing angle field of Kinect; then, according to the position of the joints in the skeleton, the setting can divide the corresponding human body. Use the center point of the hip and the horizontal scan line to separate the upper body and lower body of the human body. For arms and legs, it is carried out with the help of axillary feature points and crotch feature points. The identification of the axillary point and the cross point also adopts the method of horizontal scanning line. The left and right hands can be identified with the help of the shoulder and armpit feature points; the left and right legs can be identified with the help of the crotch and hip feature points.

**3.2.4. Human Model Reconstruction.** Realize the reconstruction of the 3D human body model matched by the feature data, and match the 3D human body model corresponding to the human body size from the human body model database [18].

**3.3. Personalized Clothing Design Based on 3D Somatosensory Technology.** In real life, user-designed products are becoming more and more mainstream, gradually replacing mass production. For consumers to buy clothing, in addition to considering the comfortable and beautiful wearing experience, they also consider the possibility of “colliding shirts.” At this stage, more and more people no longer pursue “star-like” products but care more about the personalization of clothing and their own feelings about clothing design [19]. Unlike other fashions, users prefer to change the style details of clothing according to their own preferences.

In order to facilitate the realization of modern clothing design for users, this paper proposes a method of personalized design and combination of clothing. The specific implementation process is as follows:

- (1) Design stage: the designer designs the clothing style (hand-drawn drawing), the pattern maker designs the hand-painted clothing style as a clothing model, and at the same time, the artist adjusts the position of the two-dimensional pattern and sets the stitching line on the border of the pattern

TABLE 2: Linear relationship between human body structure and height.

Project name	Linear
Height	1.00
Neck	0.84
Shoulder	0.82
Armpit	0.75
Chest circumference	0.72
Waistline	0.61
Middle hip	0.53
Crotch	0.47

- (2) Virtual fitting realization stage: automatically triangulate the two-dimensional pattern to form a uniform and unique triangular mesh; use the physical simulation method of cloth to realize the virtual fitting effect of three-dimensional clothing, and perform high-fidelity rendering of the three-dimensional clothing
- (3) Parts assembly stage: read all pattern data of parts quickly and easily, and automatically set the initial position of the pattern; realize the rapid triangulation step in the process of part assembly, reduce the total time of the part assembly process, and save each part and the main pattern. The stitching information and simulation results between them are established, and a component library is established, so that users can quickly view the simulation results

In order to realize the development of 2D pattern to 3D clothing, it is necessary to perform physical simulation on the triangulated pattern. Make the fabric conform to the laws of kinematics and display the dynamic virtual fitting effect. When an explicit integration framework is employed, the force analysis-based approach suffers from overstretching issues, whereas the position constraint-based approach to physical simulation of cloth (PBD) does not [20]. This is because the PBD method, compared with the previous explicit or implicit methods, can directly manipulate the position of the item points. When dealing with collisions, the constraints are satisfied and there will be no overstretching. In addition, the method also has the advantages of rapidity, stability, easy implementation, and strong controllability.

In the PBD method, the key point of moving particles is to ensure the conservation of linear and angular momentum. The gradient of constraint  $c$  is perpendicular to the rigid body motion of the object, since this is the direction of maximum change of the constraint. Linear and angular momentum are automatically conserved if the correction for the vertex position is chosen to be along the gradient.

$$\begin{aligned}
 C(p+\nabla p) &\approx C(p) + \nabla_p C * \nabla p = 0, \\
 \nabla p &= \lambda \nabla_p C.
 \end{aligned}
 \tag{10}$$

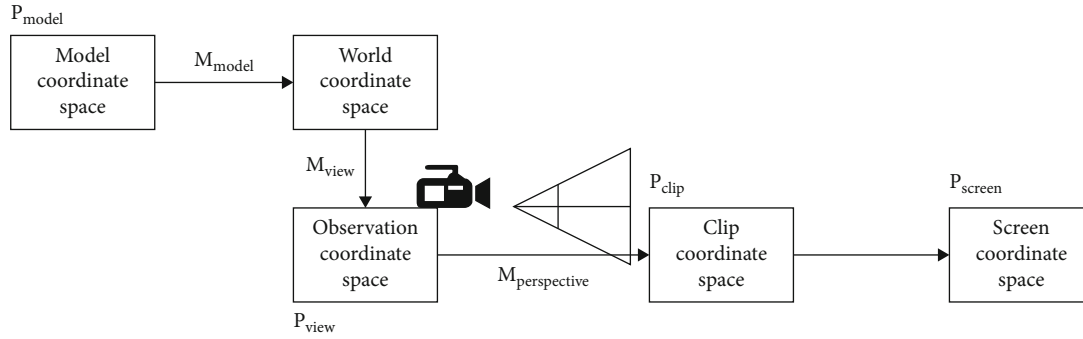


FIGURE 6: User space to screen space conversion process.

Combining the above two formulas, the following formula is obtained:

$$\nabla p = \frac{C}{|\nabla_p C|^2} \nabla_p C. \quad (11)$$

PBD adopts many constraint solving methods, such as distance constraint, bending constraint, triangle collision constraint, and volume constraint. This system mainly adopts distance constraint and bending constraint solution.

#### 4. Result Analysis and Discussion

In order to better test the performance of the clothing design method based on the human 3D somatosensory technology designed in this paper, the following test method is designed: first, the Kinect somatosensory device is used as the acquisition sensor to record the video in real time, to obtain the human somatosensory data, and to carry out three-dimensional Human reconstruction. The reconstructed three-dimensional human body model is displayed on the screen, and the specific process is shown in Figure 6. Secondly, according to the design scheme of personalized clothing, different three-dimensional effects of clothing are generated. Finally, the designed clothing is fitted with the three-dimensional human body model, and the upper body effect of the user wearing the designed clothing is displayed in real time.

During the test, the fitter faces the Kinect device and can try a variety of dynamic fitting scenarios of clothing types, such as posing any pose or turning the body. Pose changes, occlude parts of the body, etc. Finally, the image frames in the recorded video are randomly intercepted, and the try-on effect display and test evaluation are carried out.

According to the test method designed in the previous section, the specific content of the system test is as follows:

- (1) The clothing models tested include the following: short-sleeved tops, sleeveless tops, long dresses, tube top skirts, trousers, cropped trousers, five-point trousers, and other styles and types of clothing models
- (2) Test postures include the following: standing, squatting, front and rear leg raising, lateral leg raising, T-

shaped posture, arm bending posture, akimbo posture, lunge posture, and other postures

- (3) Accuracy comparison of the circumference size fitting methods of different literatures: the chest circumference, waist circumference, and hip circumference were fitted by the circumference size fitting methods of different literatures and the method in this paper, and the fitting error results were recorded
- (4) Parameter optimization of the collaborative tracking method: set the tracking error threshold  $M_0$  with different values to optimize the accuracy and real-time performance of the collaborative tracking method
- (5) Accuracy comparison of try-on methods in different literatures: compare the accuracy of try-on methods in different literatures with the collaborative tracking method in this paper, and record the results of the relative tracking error  $M$
- (6) Comparison of try-on effects of models of different body types: select models of different body types, try on clothing models of the same clothing style, and record the dynamic try-on effect in real time

This article integrates all functional modules through the Unity3d scripting feature. The Kinect data acquisition module is used to acquire two-dimensional image data, including RGB of human body areas, depth data, and skeletal features. The somatosensory measurement module used to calculate the width and circumference of the human body has also been fully utilized. Using the acquired feature data, the human body silhouette is extracted by the pixel clustering method based on the joint feature, the width size of the human body section is calculated, and the GBDT circumference calibration model is used to combine and calibrate the human body circumference size. The 3D clothing perception model building module is used to mark the dynamic feature points of clothing in the 3D clothing simulation model and integrate the circumference feature dimensions of the human body section to build a 3D clothing perception model with personalized characteristics of human bones, silhouettes, and circumferences.



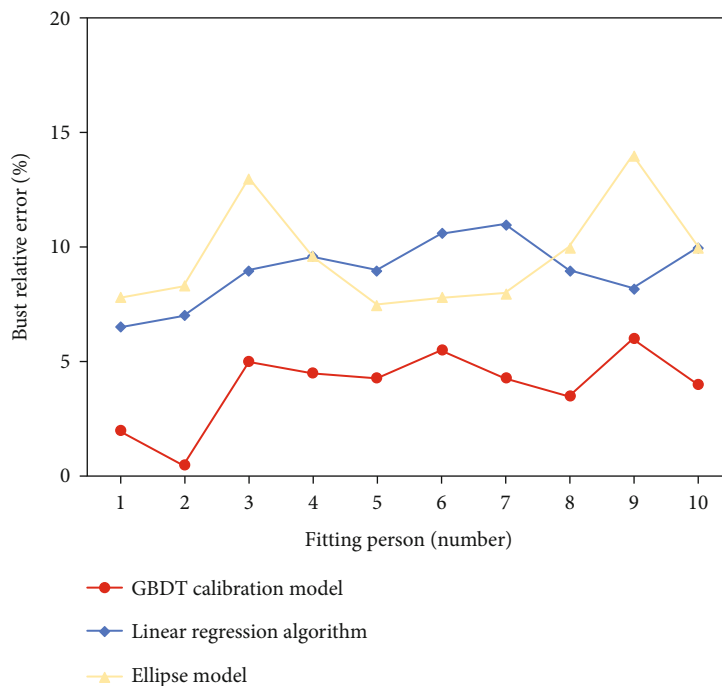


FIGURE 7: Comparison of bust size fitting results.

TABLE 3: Evaluation results of human body 3D fitting accuracy.

	GBDT calibration model	Linear regression algorithm	Ellipse model
Chest circumference	MAE: 4.2	MAE: 7.8	MAE: 8.6
	RMSE: 4.5	RMSE: 9.1	RMSE: 9.9
Waistline	MAE: 3.8	MAE: 8.3	MAE: 8.9
	RMSE: 4.1	RMSE: 8.8	RMSE: 9.2
Hip circumference	MAE: 5.1	MAE: 7.4	MAE: 8.2
	RMSE: 5.3	RMSE: 8.2	RMSE: 8.8
Mean	MAE: 4.3	MAE: 7.8	MAE: 8.5
	RMSE: 4.6	RMSE: 8.7	RMSE: 9.3

The process of forming a new set of garments after a designer provides samples of garments that have been assembled. After the designer provides the garment samples that have been assembled, the process of forming a new set of garments (including reading the stitching method of the parts from the parts library, retriangulating the parts, and fabric simulation) takes about 10 s in total. For a garment with 4 parts and four styles of each part, the approximate number of patterns is about 50, and the reading speed is about 3 s in total.

Taking the circumference size features of the human torso (chest circumference, waist circumference, and hip circumference) as an example, the accuracy of the GBDT circumference calibration model method proposed in this paper is compared with the linear regression algorithm and the ellipse model fitting method. By fitting the torso circumference of 10 fitters, each experimenter used the above three methods to calculate 3 times, respectively, and the fitting results of each method were recorded as the mean of the 3 calculations. The accuracy of the results can be calculated by combining the actual girth measurements of the 10 fitters.

Figure 7 is a comparison of the relative errors of the three methods for girth size fitting (taking bust as an example).

From the statistics of the experimental results in Table 3, it can be seen that compared with the elliptical model fitting method and the linear fitting method, the method proposed in this paper has a mean error (MAE) of 4.3 for girth fitting, and a root mean square error (RMSE) of 4.3. It is 4.6, and the overall error is smaller, so it can ensure that the clothing model more accurately matches the body structure and profile characteristics of the human body, improves the fit and personalized experience of virtual try-on, and is more conducive to clothing design and user experience feedback.

Based on the methods designed in this paper, the 3D model of the human body is generated by using the 3D somatosensory technology of the human body, and various clothing can be generated by using the component combination technology of clothing design. Finally, through the alignment and 3D registration of the 3D model and clothing, users viewing the implementation effect of the designed clothing will help to improve the efficiency of modern

clothing design. Figure 7 shows the real-time viewing effect of some garments designed by this method, and through this method, various needs and personalized solutions of users are realized.

## 5. Conclusion

By studying the architectural design of the 3D virtual try-on experience test system, the script development and integrated modulation of the module functions were completed, and a complete data collection and personalized combination of clothing components were constructed. The test software includes data collection and processing, 3D clothing perception model, clothing dynamic try-on, real-time interactive control, virtual try-on display, and other main functional architectures, with low-cost, real-time interaction design characteristics, to achieve the experience function of 3D virtual clothing dynamic try-on for real people. The key points of its implementation are as follows: on the one hand, the reconstruction effect of the human 3D model based on the Kinect depth somatosensory camera is realized. The human body model database was generated by Make Human, the depth point cloud data was captured by the Kinect depth camera, and the human body feature information (including height, circumference, feature points, and feature lines) was automatically extracted. Algorithms for matching, translation and rotation deformation algorithms are performed on the template at the same time, and mesh smoothing is performed on the deformed human model. The algorithm does not require user interaction, captures human body data in time, and implements a fast human body deformation algorithm, resulting in a uniform 3D human body mesh. At the same time, the algorithm can also be used for the user to automatically input parameters to achieve human body deformation. On the other hand, a method of clothing personalized design and combination based on 2D pattern to 3D clothing is proposed. The cloth physics simulation method of PBD is adopted, and the main principle is to use the constraint method to solve the problem. This method has many advantages such as fast, stable, easy to implement, and strong controllability. Finally, the storage structure and usage method of the clothing parts library are designed, and the free combination design method of clothing is realized.

This method has a higher degree of real-time limb coverage of clothing fabrics and a higher degree of posture matching in scenes where the human body changes greatly or the human body moves rapidly. Applicable clothing types and human posture types are more abundant (such as sideways, lunges, and akimbo), with a higher sense of reality. The clothing perception model fused with profile and girth features can match the dimensional changes of key parts of the human body. Through personalized clothing design, the combination of clothing parts is used to provide more choices of clothing styles, colors, and sizes.

## Data Availability

The labeled datasets used to support the findings of this study are available from the corresponding author upon request.

## Conflicts of Interest

The authors declare that there are no conflicts of interest.

## References

- [1] U. F. Abdurahimovna, "Methodology of training students in design and modeling of clothes using information communication technologies," *Revista Gestão Inovação e Tecnologias*, vol. 11, no. 2, pp. 749–755, 2021.
- [2] M. R. Minar and H. Ahn, "CloTH-VTON: clothing three-dimensional reconstruction for hybrid image-based virtual try-on," *IEEE Access*, vol. 11, no. 3, pp. 21–46, 2021.
- [3] Y. Zhang, "Modern digital technology assisted innovative design of Chinese knot button modeling art," in *International Conference on Applications and Techniques in Cyber Security and Intelligence*, pp. 29–48, Springer, Cham, 2021.
- [4] R. Singh and A. Shrestha, "Namuna College of Fashion Technology: pioneering in fashion and textile education in Nepal," *Textile and Fashion Education Internationalization*, vol. 11, no. 17, pp. 56–89, 2022.
- [5] Y. Shen, C. Li, and T. Zou, "Study on biomechanical response and subjective fatigue symptoms of human body wearing personal protective equipments," in *International Conference on Man-Machine-Environment System Engineering*, vol. 14no. 21, pp. 116–132, Springer, Singapore, 2022.
- [6] A. Khan, A. Nazir, A. Rehman et al., "A review of UV radiation protection on humans by textiles and clothing," *International Journal of Clothing Science and Technology*, vol. 10, no. 13, pp. 102–135, 2020.
- [7] S. Lavanya, "Clothing comfort-physiological status and psychological status," *International Journal for Modern Trends in Science and Technology*, vol. 6, no. 9S, pp. 61–67, 2020.
- [8] S. Ma, Y. Li, and X. Wang, "Research on the Ming dynasty Dao robe modeling method based on 3D simulation technology," *Journal of Physics: Conference Series*, vol. 1965, no. 1, pp. 12–40, 2021.
- [9] T. Wang and B. Gu, "Automatic recognition and 3D modeling of the neck-shoulder human shape based on 2D images," *International Journal of Clothing Science and Technology*, vol. 33, no. 5, pp. 796–810, 2021.
- [10] R. I. Eom and Y. Lee, "A three-dimensional shoulder protector based on ergonomics for workers," *International Journal of Clothing Science and Technology*, vol. 3, no. 14, pp. 256–278, 2021.
- [11] P. K. C. Kithmini, W. M. H. U. Weerakoon, A. Mediawaka, and J. D. Silva, "3D virtual clothing: an operational framework to achieve realistic 3D prototype," *Digital Fashion Innovation (DFI) e-Symposium*, vol. 11, no. 14, pp. 56–99, 2020.
- [12] M. Hatem and S. S. Shaharuddin, "A Strategy for Eco-Fashion Design Based on the Clothing Life Cycle," *International Transaction Journal of Engineering, Management, & Applied Sciences & Technologies*, vol. 11, 2020.
- [13] Q. Yang, L. Wang, and Y. Zhang, "Research on design and application based on constant temperature performance in clothing structure," *E3S Web of Conferences*, vol. 213, pp. 2–32, 2020.
- [14] W. Zhang, "Application of traditional embroidery techniques aided by image design software in modern clothing design," *Journal of Physics Conference Series*, vol. 1648, no. 3, article 032072, 2020.

- [15] B. Gu, M. K. Ahmed, Z. Zhong, and J. Jin, "3D female upper body modelling based on 2D images," *International Journal of Clothing Science and Technology*, vol. 32, no. 4, pp. 471–482, 2020.
- [16] Y. Liu, "Specialized crowd garment design model based on information technology," *Innovative Computing*, vol. 12, no. 18, pp. 250–297, 2020.
- [17] M. A. Karim, M. Moniruzzaman, M. E. Nizam, M. A. Shammi, and M. T. Hasan, "Transformative adoption of traditional 'Kantha' embroidery to modern fashion design through 'Khadi' fabric," *American Journal of Art and Design*, vol. 6, no. 1, pp. 6–12, 2021.
- [18] D. Chen, P. Cheng, S. Simatrang, and E. Joneurairatana, "Kansei engineering as a tool for the design of traditional pattern," *Autex Research Journal*, vol. 21, no. 1, pp. 125–134, 2021.
- [19] C. Bao, Y. Miao, B. Gu, K. Liu, and Z. Liu, "3D interactive garment parametric pattern-making and linkage editing based on constrained contour lines," *International Journal of Clothing Science and Technology*, vol. 15, no. 21, pp. 119–187, 2021.
- [20] S. Chen, "Exploration on the new direction of fashion design from the perspective of youth subculture—doll clothing as example," *Open Access Library Journal*, vol. 8, no. 9, pp. 1–12, 2021.

## Research Article

# Stochastic Evolutionary Game Analysis on the Strategy Selection of Green Building Stakeholders from the Perspective of Supply-Demand Subject Populations

Yaohong Yang <sup>1,2</sup>, Jing Dai <sup>1</sup>, Zhiyong Li <sup>1</sup>, Ying Liu <sup>1</sup> and Yi Zeng <sup>1</sup>

<sup>1</sup>School of Water Conservancy, North China University of Water Resources and Electric Power, Zhengzhou, Henan 450046, China

<sup>2</sup>The Henan Key Laboratory of Water Resources Conservation and Intensive Utilization in the Yellow River Basin, Zhengzhou, Henan 450046, China

Correspondence should be addressed to Yaohong Yang; [yangyaohong@ncwu.edu.cn](mailto:yangyaohong@ncwu.edu.cn)

Received 24 March 2022; Revised 24 April 2022; Accepted 3 May 2022; Published 27 June 2022

Academic Editor: Wen Zeng

Copyright © 2022 Yaohong Yang et al. This is an open access article distributed under the Creative Commons Attribution License, which permits unrestricted use, distribution, and reproduction in any medium, provided the original work is properly cited.

In construction industry, the research and development (R&D) and application of green building technologies (GBTs) are crucial to promote the development of green buildings. From the perspective of supply-demand subject populations, this paper discusses the dynamic evolution process of strategy between individuals within construction enterprise populations and between construction enterprise populations and consumer populations. Firstly, based on Moran process, the stochastic evolutionary game model of construction enterprises adopting independent innovation strategy was constructed to obtain the conditions for the dominance of independent innovation strategy. Next, the bimatrix game model of construction enterprise populations and consumer populations was constructed to obtain the equilibrium frequency of the joint strategy. Then, the influence laws of the change of parameters on game were discussed through numerical simulations. The results show that (1) reducing the cost of independent R&D cost, reducing the spillover effect coefficient, increasing the loss of technology introduction, and increasing R&D subsidies for independent innovation construction enterprises are all conducive to IIS becoming an evolutionary stable strategy. (2) The marginal effect of IIS increases with the decrease in the spillover effect coefficient, the increase in the loss of technology introduction of construction enterprises, and the increase R&D subsidies. (3) The smaller the mutation rate is, the greater the cross-price sensitivity coefficient is, the greater the green sensitivity coefficient is, the greater the probability of government active encouragement is, and the more dominant (production of green buildings, purchase of green buildings) is. Finally, relevant measures and suggestions are proposed.

## 1. Introduction

Traditional buildings produce a large amount of greenhouse gases such as carbon dioxide during construction, operation, and demolition resulting in carbon emissions from construction industry being one of the major sources of carbon emissions from global economic activities [1]. In 2017, global CO<sub>2</sub> emissions from construction accounted for nearly 40 per cent of total CO<sub>2</sub> emissions from global economic activities [2]. Carbon reduction actions in construction industry are conducive to reducing greenhouse gas emissions. Unlike traditional buildings, green buildings reduce carbon emissions and alleviate building pollution,

which can effectively respond to global climate change [3]. However, there are some problems in green building market, such as immature technology, low public willingness to purchase and imperfect management system etc. [4]. The development of green building market is jointly promoted by the strategic selection of stakeholders such as government, construction enterprises, and consumers. Focusing on GBTs, the development process of green building market is also the process of R&D and application of green building technology. Green building market development is localized [5]. The change in the number of enterprises and consumers choosing to produce and purchase green buildings affects the scale of the overall green buildings market. From the

actual situation, the construction enterprise populations and the consumer populations are two finite populations. Moreover, the two groups are in an uncertain environment of green building market, and the players' strategy selections are influenced by random factors, which may lead to strategy mutation. Therefore, it is necessary to consider the influence of random factors, strategy selection intensity, group size, and other factors on the group strategy selection process.

The development of green building is a game process between the government, construction enterprises, consumers, and other stakeholders. Most research literatures regard the government as one of the game players and analyze the impact of government policies on the strategic choice of various stakeholders, such as the impact of environmental policies on the adoption of green building technology by alliance construction enterprises composed of building material enterprises and building material developers [6]; the influence process of subsidy coefficient, market supervision intensity and other factors on the green technology innovation strategy of enterprises [7]; the impact of positive and negative policy incentives on the green transformation of PPP-BR [8]; and the influence process of different reward and punishment mechanisms on the behavior evolution of suppliers and demanders in the green building market [9].

In terms of research methods, Moran process and bimatrix analysis are commonly used. Moran process is divided into three steps: selection, reproduction, and replacement [10]. Souza et al. and Nishimura et al. introduced the Moran process based on the dominant probability into evolutionary game [11] and described the birth-and-death process of individual selection in frequency-dependent Moran process [12]. Different from the deterministic evolutionary games, the stochastic evolutionary games introduce selection intensity. According to the dependence between fitness and individual payoffs, the selection is divided into strong selection and weak selection. When the strategy has no mutation, the indicators for judging the overall evolutionary dynamics are divided into fixation probability [13] and fixation time [14]. Traulsen et al. propose an exponential mapping form suitable for strong selection and weak selection based on linear mapping form [15]. When the strategy has mutation, it is judged by average abundance. Some scholars analyzed dominant conditions for strategy to fixate when selection intensity is different [16]. The stochastic evolutionary game dynamics of bimatrix games can be described as frequency-dependent Moran process with mutation [17]. Most of the existing researches supplement and perfect the theoretical model of bimatrix game, such as introducing quantile to define the preference of stochastic payoff values and discuss the stationary distribution of the proposed birth-and-death process and the long-term equilibrium of  $2 \times 2$  bimatrix game evolution model; describing an algorithm for computing the approximate mixed Nash equilibrium in bimatrix games [18]; and proposing the expected loss averse Nash equilibrium, the optimistic loss averse Nash equilibrium, and pessimistic loss averse Nash equilibrium and their existence theorems [19]. Some scholars improve model from the perspectives of heterogeneity of learning

mechanism [20], individual emotion type [21], and ambiguity of gains [22].

To sum up, at present, most research literatures think that the construction enterprise populations or consumer populations are infinite populations, while ignoring the actual situation that the number of populations is limited, and related research has not considered the influence of random factors, populations' size, and other parameters on the strategy selection process of players. This paper analyzes the random evolution process of group strategy selection based on the R&D and application of GBTs. Among them, the R&D stage mainly analyzes the behavior evolution process within the supply-side group, and the application stage mainly analyzes the behavior evolution process of the supply-side and demand-side groups.

## 2. Materials and Methods

### 2.1. Model Parameters and Related Assumptions

*2.1.1. Model Parameters.* The model parameters are shown in Table 1.

#### 2.1.2. Basic Assumptions

(1) *Basic Assumptions of Green Building Technology in R&D Stage.*

Suppose there are  $M$  mixed and homogeneous construction enterprises in market. Each construction enterprises' R&D of GBTs can be divided into two options: independent innovation or technology introduction, respectively, denoted as  $\{\alpha_{11}, \alpha_{12}\}$ . Simplify the construction enterprise group with different strategies into two players with different strategies.

Assuming that the construction enterprises that choose the independent innovation strategies (IIS) have to pay the independent innovation cost  $C_1$ , the probability of technical R&D failure is  $f$ , and the probability of R&D success is  $1 - f$ . When technology R&D fails, independent innovation construction enterprises suffer from cost, time, and other losses is  $W_1$ . When R&D is successful, construction enterprises transfer technology patents at the probability of  $y_4$  and transfer gains  $V_2$ ; with the probability of  $1 - y_4$  chooses not to transfer, get retained earnings  $V_1$ . Enterprise independent R&D suffered time window loss is  $W_3$ . When two construction enterprises choose independent innovation, they collaborate with a probability of  $y_6$ ; the benefits of cooperation received by both construction companies choose to cooperate are  $V_4$ . Appropriate government subsidies to construction enterprises that choose independent R&D innovation which can encourage construction enterprises to carry out independent technological innovation and improve the technological development level of the construction industry. The probability of government active encouragement is  $y_3$ , and the R&D subsidies for construction enterprises that choose IIS are  $V_5$ . The construction enterprises that choose the technology introduction strategy (TIS) need to pay the cost  $C_2$ ,  $C_1 > C_2$ . Gains after technology introduction are  $V_3$ . The technology introduced by construction enterprises

TABLE 1: Model parameters.

Parameter symbol	Parameter meaning	Parameter range
$M$	Number of construction enterprises	
$\alpha$	Construction enterprise group	
$\beta$	Consumer group	
$\gamma_1$	Cross price sensitivity coefficient	0-1
$\gamma_2$	Green sensitivity coefficient of consumers	$\geq 0$
$\gamma_3$	Probability of positive encouragement by the government	
$\gamma_4$	Probability of transferring technology patents	
$\gamma_5$	Spillover effect coefficient of one party's independent innovation and the other party's technology introduction	0-1
$\gamma_6$	Cooperation probability when enterprises independently innovate	
$\gamma_7$	Spillover effect coefficient when enterprises choose technology introduction	0-1
$N, Z$	Group size	
$C_1$	Independent innovation cost	$C_1 > C_2$
$C_2$	Technology introduction cost	
$C_{g1}$	Cost of green building for construction enterprises	$C_{g1} > C_{g2}$
$C_{g2}$	Operating costs paid by consumers after purchasing green buildings	$C_{g2} > C_{b2}$
$C_{b1}$	Cost of ordinary construction of enterprises	
$C_{b2}$	Operating costs paid by consumers after purchasing ordinary buildings	
$f$	Probability of technology R&D failure	
$W_1$	Time window loss	
$W_2$	Loss of technology introduction	
$W_3$	Time window loss of independent R&D of enterprises	
$V_1$	Retained earnings	
$V_2$	Transfer income	
$V_3$	Gain from technology introduction	
$V_4$	Cooperation income	
$D_g$	Green building demand	
$D_b$	General building demand	
$V_g$	Consumers' gains from buying green buildings	
$V_b$	Consumers' gains from buying ordinary buildings	
$P_g$	Sales price of green buildings	
$P_b$	Sales price of ordinary buildings	
$G_1$	Development subsidies for construction enterprises to develop green buildings	
$G_2$	Development subsidies for consumers to buy green buildings	
$F$	Carbon tax of enterprises from producing ordinary buildings	
$h$	Green degree of construction products	$> 0$
$a$	Green building demand	$\geq 0$
$u$	Probability of strategy mutation in construction enterprise	
$v$	Probability of strategy mutation by consumers	
$r$	Market reputation gained by construction enterprises in producing green buildings	

is affected by the technology spillover effect, resulting in the loss of leading power of some industries, which is called the technology introduction loss. The loss of technology intro-

duction is  $W_2$ . The selection of technology introduction by construction enterprises is influenced by the technology spillover effect of independent R&D enterprises, which is

expressed by the spillover effect coefficient. The larger the spillover effect coefficient is, the larger the spillover effects are. The spillover effect coefficient is  $\gamma_5$  when one player innovates independently and the other player introduces technology. And the spillover effect coefficient is  $\gamma_7$  when both players choose to introduce technology.

## (2) Basic Assumptions of Green Building Technology in the Application Stage.

Denote the number of consumers and construction enterprises are finite populations, the population' size as  $Z$  and  $N$ , respectively. Consumers face two strategic choices: buying green buildings (BGB) or buying ordinary buildings (BOB). The consumer populations are denoted as  $\beta$ , and the set of feasible strategies is denoted as  $\{\beta_1, \beta_2\}$ . Consumers have a rigid demand for buildings; they will choose to buy ordinary building or green building when they do not buy the desired type of building product: green building or ordinary building. Construction enterprises have two pure strategy choices: (1) producing green building (PGB) through independent innovation or technology introduction and (2) using the original production technology to produce ordinary buildings (POB). The construction enterprise populations are denoted as  $\alpha$ , and its set of feasible strategies is denoted as  $\{\alpha_1, \alpha_2\}$ . No mixed strategies are considered [23].

Referring to the linear demand function model of product price in supply chain management research [24], the demand functions of green building and ordinary building are, respectively:

$$D_g = a - P_g + \gamma_1 P_b + \gamma_2 h, \quad (1)$$

$$D_b = \lambda a - P_b + \gamma_1 P_g. \quad (2)$$

$D_g$  and  $D_b$ , respectively, refer to the demand for green buildings and ordinary buildings.  $a$  refers to the demand for green buildings,  $a \geq 0$ . The selling price of the green building is  $P_g$ , and the selling price of the ordinary building is  $P_b$ .  $\gamma_1$  refers to the cross-price sensitivity factor,  $\gamma_1 \in (0, 1)$ . The greater the  $\gamma_1$ , the greater the competition, and the greater the impact of the selling price of its own product on demand compared to that of competing products.  $\gamma_2$  refers to the greenness sensitivity coefficient of consumers,  $\gamma_2 \geq 0$ . The larger the  $\gamma_2$ , the more sensitive the consumer is to the greenness of the building product, and the higher the consumer's green preference is; the smaller the  $\gamma_2$ , the lower the consumer's green preference.  $h$  refers to the greenness of construction products,  $h \geq 0$ .  $\lambda$  refers to the difference between the potential demand for green buildings and ordinary buildings. The demand for green buildings is greater when  $0 < \lambda < 1$ . When  $\lambda = 1$ , the demand for green buildings and ordinary buildings is equal. The demand for ordinary buildings is greater when  $\lambda > 1$ .

When construction enterprises choose to produce green buildings, it may be produced by independent innovation or technology introduction. When they choose independent R&D, it needs to pay costs on R&D; when they choose tech-

nology introduction, it needs to spend a lot of money to purchase patents, etc. These possible costs are called development costs. Construction enterprises pay development costs of  $C_{g1}$  to produce green buildings and  $C_{b1}$  to produce ordinary buildings, where  $C_{g1} > C_{b1}$ . Consumers receive the benefit  $V_g$  when they purchase green buildings, and the benefit  $V_b$  when they purchase an ordinary buildings. Running costs refers to the costs paid for heating, etc. Consumers who buy green buildings pay running costs  $C_{g2}$ , and those who buy ordinary buildings pay running costs  $C_{b2}$ , where  $C_{g2} < C_{b2}$ . To promote the development of the green building market, the government will actively encourage construction enterprises to produce green buildings and consumers to buy green buildings through subsidies and strong regulation. Suppose the probability that the government actively encourages is  $\gamma_3$ , the subsidy to construction enterprises is  $G_1$ , the subsidy to consumers is  $G_2$ , and the carbon tax  $F$  is levied on enterprises producing ordinary buildings. Construction enterprises producing green buildings will gain market reputation  $r$ .

## 2.2. Model Building

### 2.2.1. Model Building of Green Building Technology in R&D Stage.

The game payment matrix within the construction enterprise group in the R&D stage is shown in Table 2.

Suppose there are  $l$  construction enterprises within the groups of construction enterprises choosing strategy  $\alpha_{11}$  and  $M - l$  construction enterprises choosing strategy  $\alpha_{12}$ . Combined with Table 1, the expected payoffs of construction enterprises choosing  $\alpha_{11}$  and  $\alpha_{12}$  ( $E_l^{\alpha_{11}}$ ,  $E_l^{\alpha_{12}}$ ) are obtained as shown in Equations (1) and (2), where  $l = 1, 2, 3, \dots, M - 1$ .

$$E_l^{\alpha_{11}} = \frac{l-1}{M-1} \{-C_1 + (1-f)[\gamma_4 V_2 + (1-\gamma_4)V_1] - fW_1 - W_3 + \gamma_6 V_4 + \gamma_3 V_5\} + \frac{M-l}{M-1} \{-C_1 + (1-f)[\gamma_4 V_2 + (1-\gamma_4)V_1] - fW_1 - W_3 + \gamma_3 V_5\},$$

$$E_l^{\alpha_{12}} = \frac{l}{M-1} \{-C_2 + \gamma_5 V_3 - W_2\} + \frac{M-l-1}{M-1} \{-C_2 + \gamma_7 V_3 - W_2\}. \quad (3)$$

Denote selection intensity  $\omega$  as stochastic factors. The uncertain environment faced by construction enterprises is divided into two situations: expected payoffs dominated and stochastic factors dominated. Under the expected payoff dominates, the fitness is completely determined by the expected return; under the stochastic factor dominates, the expected payoffs has little effect on the fitness.

The relationship between fitness and payoff function is exponential mapping, and the fitness of construction enterprises selection  $\alpha_{11}$  and  $\alpha_{12}$  ( $f_l^{\alpha_{11}}$ ,  $f_l^{\alpha_{12}}$ ) are:

$$f_l^{\alpha_{11}} = \exp [\omega * E_l^{\alpha_{11}}], \quad (4)$$

$$f_l^{\alpha_{12}} = \exp [\omega * E_l^{\alpha_{12}}], \quad (5)$$

where  $\omega \geq 0$ . Suppose there is no mutation in game. Based on the probability transfer formula and the total probability

TABLE 2: Game payoff matrix of construction enterprise populations.

Strategy selection	IIS (y)	Construction enterprise 2	TIS (1 - y)
Construction enterprise 1	IIS (x)	$(-C_1 + (1-f)[y_2 V_2 + (1-y_4)V_1] - fW_1 - W_3 + y_6 V_4 + y_3 V_5, -C_1 + (1-f)[y_2 V_2 + (1-y_4)V_1] - fW_1 - W_3 + y_6 V_4 + y_3 V_5)$	$(-C_1 + (1-f)[y_2 V_2 + (1-y_4)V_1] - fW_1 - W_3 + y_6 V_4 + y_3 V_5, -C_1 + (1-f)[y_2 V_2 + (1-y_4)V_1] - fW_1 - W_3 + y_6 V_4 + y_3 V_5)$
	TIS (1 - x)	$(-C_2 + y_5 V_3 - W_2, -C_1 + (1-f)[y_2 V_2 + (1-y_4)V_1] - fW_1 - W_3 + y_6 V_4 + y_3 V_5)$	$(-C_1 + y_7 V_3 - W_2, -C_1 + y_7 V_3 - W_2)$



formula, the probability of  $\alpha_{11}$  and  $\alpha_{12}$  fixates ( $\rho_{\alpha_{11}}, \rho_{\alpha_{12}}$ ) are:

$$\rho_{\alpha_{11}} = \left\{ \sum_{k=0}^{M-1} \exp \left\{ \frac{\omega}{2} k(k+1) \frac{-y_6 V_4 + y_5 V_3 - y_7 V_3}{M-1} + \omega k \frac{y_6 V_4 + (M-1) \{C_1 - (1-f)[y_4 V_2 + (1-y_4)V_1] + fW_1 + W_3 - y_3 V_5 - C_2 + y_7 V_3 - W_2\}}{M-1} \right\} \right\}^{-1},$$

$$\rho_{\alpha_{12}} = \left\{ \sum_{k=0}^{M-1} \exp \left\{ \frac{\omega}{2} k(k+1) \frac{-y_6 V_4 + y_5 V_3 - y_7 V_3}{M-1} + \omega k \frac{(M-1) \{-C_1 + (1-f)[y_4 V_2 + (1-y_4)V_1] - fW_1 - W_3 + y_6 V_4 + y_3 V_5 + C_2 + W_2\} + (y_7 - My_5)V_3}{M-1} \right\} \right\}^{-1}. \quad (6)$$

After a long period of evolution, the strategy used by the player with a large fixation probability is more likely to become an evolutionary stable strategy [25]. The strategy  $\alpha_{11}$  is more likely to become evolutionary stable strategy when  $\rho_{\alpha_{11}} > \rho_{\alpha_{12}}$ ; the strategy  $\alpha_{12}$  is more likely to become evolutionary stable strategy when  $\rho_{\alpha_{11}} < \rho_{\alpha_{12}}$ .

**2.2.2. Model Building of Green Building Technology in the Application Stage.** The game payoff matrix between the construction enterprise populations and the consumer populations is shown in Table 3.

In the basic step of updating, each individual of populations  $\alpha$  interacts with each individual of populations  $\beta$  to generate payoffs. When individual  $i$  in population  $\alpha$  interacts with individual  $j$  in population  $\beta$ , the expected payoffs of individual  $i$  are  $a_{ij}$ , and that of individual  $j$  is  $b_{ij}$ . The payoff matrix is.

$$(A, B) = \begin{matrix} & \beta_1 & \beta_2 \\ \alpha_1 & (a_{11}, b_{11}) & (a_{12}, b_{12}) \\ \alpha_2 & (a_{21}, b_{21}) & (a_{22}, b_{22}) \end{matrix} \quad (7)$$

The expected benefits of each interaction of construction enterprises are  $F_{\alpha_i} = \sum_{j=1}^2 a_{ij} y_j$ ,  $i = 1, 2$ . The expected benefits of each interaction of construction enterprises are  $F_{\beta_j} = \sum_{i=1}^2 b_{ij} x_i$ ,  $j = 1, 2$ . There is an exponential mapping between the fitness and benefit functions. The fitness of the construction enterprises to adopt the strategy  $\alpha_i$  is  $f_{\alpha_i} = \exp(\delta * F_{\alpha_i})$ , and the fitness of the consumer to adopt the strategy  $\beta_j$  is  $f_{\beta_j} = \exp(\delta * F_{\beta_j})$ .  $\delta$  is the selection strength,  $\delta \geq 0$ .

### 2.3. Model Solution and Analysis

#### 2.3.1. System Analysis of Green Building Technology R&D Stage Model

(1) Under the Expected Payoff Dominates.

Under the expected payoff dominates, construction enterprises are completely rational, and their strategic selection is entirely determined by expected payoffs and is not influenced by other factors. By comparing the difference of fitness in each state, the change of the number of construc-

tion enterprises adopting a certain strategy is analyzed. Let

$$h_l = f_1^{\alpha_{11}} - f_1^{\alpha_{12}}, l = 1, 2, 3, \dots, M-1. \quad (8)$$

Take  $l=1$  and  $l=M-1$ , respectively, and substitute Equations (1)–(5) into Equation (8), we get

$$h_1 = e^{\omega * E_1^{\alpha_{11}}} - e^{\omega * E_1^{\alpha_{12}}} = e^{\omega * \{-C_1 + (1-f)[y_4 V_2 + (1-y_4)V_1] - fW_1 - W_3 + y_3 V_5\}} - e^{\omega * \{-C_2 - W_2 + \frac{1}{M-1} y_5 V_3 + \frac{M-2}{M-1} y_7 V_3\}},$$

$$h_{M-1} = e^{\omega * E_{M-1}^{\alpha_{11}}} - e^{\omega * E_{M-1}^{\alpha_{12}}} = e^{\omega * \{-C_1 + (1-f)[y_4 V_2 + (1-y_4)V_1] - fW_1 - W_3 + y_3 V_5 + \frac{M-2}{M-1} y_6 V_4\}} - e^{\omega * \{-C_2 + y_5 V_3 - W_2\}}. \quad (9)$$

The game system may have the following situations:

- (1) If  $h_1 > 0$ , selection behavior of construction enterprises supports  $\alpha_{11}$  invading  $\alpha_{12}$ ,  $\alpha_{11}$  is dominant; if  $h_{M-1} < 0$ , selection behavior supports  $\alpha_{12}$  invading  $\alpha_{11}$ ,  $\alpha_{12}$  is dominant
- (2) If  $h_1 > 0$  and  $h_{M-1} > 0$  coexist, choose favorable  $\alpha_{11}$  invading  $\alpha_{12}$ , against  $\alpha_{12}$  invading  $\alpha_{11}$ ,  $\alpha_{11}$  is superior to  $\alpha_{12}$ , and  $\alpha_{11}$  is dominant
- (3) If  $h_1 < 0$  and  $h_{M-1} < 0$  coexist,  $\alpha_{12}$  will replace  $\alpha_{11}$  as an evolutionary stable strategy
- (4) If  $h_1 < 0$  and  $h_{M-1} > 0$  coexist, choose against  $\alpha_{11}$  invading  $\alpha_{12}$ , also against  $\alpha_{12}$  invading  $\alpha_{11}$ , and selection behavior of construction enterprises against change
- (5) If  $h_1 > 0$  and  $h_{M-1} < 0$  coexist, the choice is conducive to  $\alpha_{11}$  and  $\alpha_{12}$  to invade each other, and selection behavior of construction enterprises tends to change

**Proposition 1.** Under the expected payoff dominates, for  $M \geq 2$ , there is  $h_1 > 0$ ,  $h_{M-1} > 0$ , IIS becomes an evolutionary stable strategy when  $(1-f)[y_4 V_2 + (1-y_4)V_1] + C_2 + W_2 + y_5 V_3 - C_1 - fW_1 - W_3 + y_3 V_5 - 2y_7 V_3 > 0$ .

Proposition 1 shows that when the construction enterprise populations are completely rational, its strategy

TABLE 3: Game payoff matrix for the construction enterprise populations and the consumer populations.

Strategy selection		Consumer	
		BGB ( $y$ )	BOB ( $1 - y$ )
Construction enterprise	PGB ( $x$ )	$(D_g(P_g - C_{g1} + y_3 hG_1 + r), D_g(V_g - P_g - C_{g2} + y_3 hG_2))$	$(D_b(P_g - C_{g1} + y_3 hG_1 + r), D_b(V_g - P_g - C_{g2} + y_3 hG_2))$
	POB ( $1 - x$ )	$(D_g(P_b - C_{b1} + y_3 F - r), D_g(V_b - P_b - C_{b2}))$	$(D_g(P_b - C_{b1} + y_3 F - r), D_b(V_b - P_b - C_{b2}))$

selection process is affected by parameters such as independent R&D cost, R&D failure rate, R&D failure loss, technology introduction loss, and R&D subsidies. Whether construction enterprises adopt IIS or TIS is closely related to their own income. When the profit of construction enterprises adopting IIS is greater than that of choosing TIS, construction enterprises tend to choose IIS.

(2) *Under the Stochastic Factor Dominates.*

Under the stochastic factor dominates,  $\omega \rightarrow 0$ . Construction enterprises' strategy choice is influenced by policy orientation, decision-makers' preferences, and other factors in addition to expected payoffs. By discussing the change of the ratio of two fixation probabilities, this study analyzes the change of the number of groups choosing a certain strategy.

$$\frac{\rho_{\alpha_{12}}}{\rho_{\alpha_{11}}} = \prod_{l=1}^{M-1} \exp \left[ \omega \sum_{l=1}^{M-1} (E_l^{\alpha_{12}} - E_l^{\alpha_{11}}) \right] = \exp \left\{ -\omega \left\{ \frac{M}{2} \{-2C_1 + 2(1-f)[y_4 V_2 + (1-y_4)V_1] - 2fW_1 - 2W_3 + y_6 V_4 + 2y_3 V_5 + 2C_2 - (y_5 + y_7)V_3 + 2W_2\} + \{C_1 - (1-f)[y_4 V_2 + (1-y_4)V_1] + fW_1 + W_3 - y_6 V_4 - y_3 V_5 - C_2 + y_7 V_3 - W_2\} \right\} \right. \quad (10)$$

**Proposition 2.** *Under the stochastic factor dominates, the strategy  $\alpha_{11}$  dominants when  $-C_1 + (1-f)[y_4 V_2 + (1-y_4)V_1] - fW_1 - W_3 + y_6 V_4 + C_2 + y_5 V_3 + C_2 - (y_5 + y_7)V_3 + W_2 > 0$ , IIS is more likely to become an evolutionary stable strategy.*

Proposition 2 shows that construction enterprises choosing IIS are closely related to independent R&D cost, R&D success rate, retained revenue after R&D success, transfer revenue, and R&D failure loss under the stochastic factor dominates. When the income of the enterprise choosing TIS is less than the income of IIS, the choice behavior supports IIS to invade TIS and then replaces TIS. IIS eventually becomes an evolutionary stable strategy.

Whether the situation is dominated by expected payoffs or by stochastic factors, the strategy choice of construction enterprises is related to parameters such as populations' size, cost of independent R&D, spillover effect coefficient, loss of

technology introduction, and selection intensity. Under the expected payoff dominates, the benefits of construction enterprises in IIS are greater than those in TIS, the strategy choice of construction enterprises supports the invasion and replacement of TIS by IIS, and IIS dominates. Under the stochastic factor dominates, the gain of construction enterprises in TIS is smaller than the gain in IIS, and the strategy choice of construction enterprises resists the invasion of IIS by the TIS, and the IIS prevails. There is a threshold value for the number of construction enterprises choosing a certain strategy, and the populations' strategy changes when the number of construction enterprise populations exceeds the threshold value.

**2.3.2. System Analysis of Green Building Technology Application Stage Model.** Suppose there is mutation in strategy updating process. The probability of a mutation in construction firm's strategy is  $u$  and the probability of a mutation in consumer's strategy is  $v$ . Then, discuss the evolutionary process in neutral selection and weak selection cases.

Under the neutral selection,  $\delta = 0$ . It was calculated that  $\langle x_i \rangle_0 = 1/2$ ,  $\langle y_j \rangle_0 = 1/2$ , and  $\langle x_i y_j \rangle_0 = 1/4$ . It is consistent with the results of Ohtsuki [17]. It is because the frequency of occurrence of any pair of strategy combinations of two populations under stochastic mutation conditions is expected to be the same in equilibrium.

In the case of weak selection,  $\delta \rightarrow 0$ . The equilibrium frequencies of strategies  $\alpha_1$  and strategies  $\alpha_2$  adopted by construction enterprises are:

$$\begin{aligned} \langle x_1 \rangle_\delta &= \frac{1}{2} + \frac{\delta(Z-1)(1-u)}{8(1+Zu-u)} \left[ (D_g + D_b)(P_g - C_{g1} + y_3 hG_1 + r - P_b + C_{b1} + y_3 F) + D_g r \right] + O(\delta^2), \\ \langle x_2 \rangle_\delta &= \frac{1}{2} - \frac{\delta(Z-1)(1-u)}{8(1+Zu-u)} \left[ (D_g + D_b)(P_g - C_{g1} + y_3 hG_1 + r - P_b + C_{b1} + y_3 F) + D_g r \right] + O(\delta^2). \end{aligned} \quad (11)$$

The equilibrium frequencies of consumer populations

adopting strategies  $\beta_1$  and strategies  $\beta_2$  are:

$$\begin{aligned}\langle y_1 \rangle_\delta &= \frac{1}{2} + \frac{\delta(N-1)(1-\nu)}{8(1+N\nu-\nu)} [(D_g - D_b)(V_g - P_g - C_{g2}) \\ &\quad + y_3 h G_2 + V_b - P_b - C_{b2}] + O(\delta^2), \\ \langle y_2 \rangle_\delta &= \frac{1}{2} - \frac{\delta(N-1)(1-\nu)}{8(1+N\nu-\nu)} [(D_g - D_b)(V_g - P_g - C_{g2}) \\ &\quad + y_3 h G_2 + V_b - P_b - C_{b2}] + O(\delta^2).\end{aligned}\quad (12)$$

In the bimatrix games, the distribution of joint strategies is more concerned. The equilibrium frequencies of joint strategies in different cases are shown

$$\begin{aligned}\langle x_1 y_1 \rangle_\delta &= \frac{1}{4} + \frac{\delta}{16(u+\nu)(1+Zu-u)(1+N\nu-\nu)} \\ &\quad \cdot \{(Z-1)(1-u)\{v[1+(N-1)(u+\nu)]\pi_1 + 2u\pi_2\} \\ &\quad + (N-1)(1-\nu)\{u[1+(Z-1)(u+\nu)]\pi_3 + 2v\pi_4\}\} \\ &\quad + O(\delta^2),\end{aligned}\quad (13)$$

$$\begin{aligned}\langle x_1 y_2 \rangle_\delta &= \frac{1}{4} + \frac{\delta}{16(u+\nu)(1+Zu-u)(1+N\nu-\nu)} \\ &\quad \cdot \{(Z-1)(1-u)\{v[1+(N-1)(u+\nu)]\pi_1 + 2u\pi_6\} \\ &\quad + (N-1)(1-\nu)\{u[1+(Z-1)(u+\nu)]\pi_7 - 2v\pi_4\}\} \\ &\quad + O(\delta^2),\end{aligned}\quad (14)$$

$$\begin{aligned}\langle x_2 y_1 \rangle_\delta &= \frac{1}{4} + \frac{\delta}{16(u+\nu)(1+Zu-u)(1+N\nu-\nu)} \\ &\quad \cdot \{(Z-1)(1-u)\{v[1+(N-1)(u+\nu)]\pi_9 - 2u\pi_2\} \\ &\quad + (N-1)(1-\nu)\{u[1+(Z-1)(u+\nu)]\pi_3 + 2v\pi_{12}\}\} \\ &\quad + O(\delta^2),\end{aligned}\quad (15)$$

$$\begin{aligned}\langle x_2 y_2 \rangle_\delta &= \frac{1}{4} + \frac{\delta}{16(u+\nu)(1+Zu-u)(1+N\nu-\nu)} \\ &\quad \cdot \{(Z-1)(1-u)\{v[1+(N-1)(u+\nu)]\pi_9 - 2u\pi_6\} \\ &\quad + (N-1)(1-\nu)\{u[1+(Z-1)(u+\nu)]\pi_7 - 2v\pi_{12}\}\} \\ &\quad + O(\delta^2),\end{aligned}\quad (16)$$

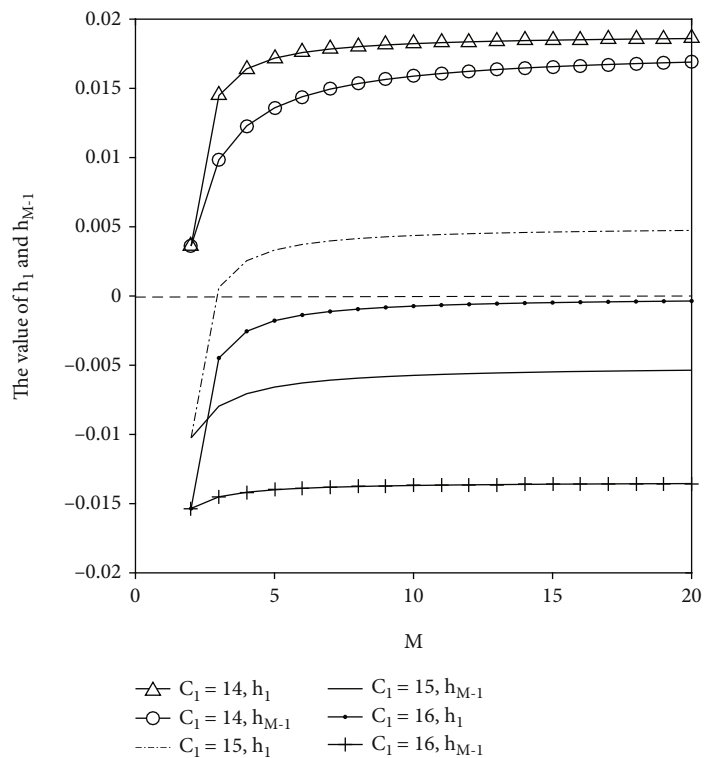
$$\begin{aligned}F) + D_g r, \quad \pi_2 &= D_g(P_g - C_{g1} + y_3 h G_1 - P_b + C_{b1} + y_3 F + 2r), \\ \pi_3 &= (D_g - D_b)(V_g - P_g - C_{g2} + y_3 h G_2 + V_b - P_b - C_{b2}), \quad \pi_4 \\ &= (D_g - D_b)(V_g - P_g - C_{g2} + y_3 h G_2), \quad \pi_6 = D_b(P_g - C_{g1} + y_3 \\ &h G_1 - P_b + C_{b1} + y_3 F + r), \quad \pi_7 = (D_b - D_g)(V_g - P_g - C_{g2} + \\ &y_3 h G_2 + V_b - P_b - C_{b2}), \quad \pi_9 = (D_g + D_b)(P_b - C_{b1} - y_3 F - r \\ &- P_g + C_{g1} - y_3 h G_1) - D_g r, \quad \pi_{12} = (D_g - D_b)(V_b - P_b - C_{b2}).\end{aligned}$$

It can be seen that the strategy selection process of construction enterprise populations and consumer populations is related to parameters such as population size, selection intensity, mutation rate, and price sensitivity coefficient. Due to the calculation formula of the equilibrium frequency of joint strategy is complex, therefore, numerical simulation is used to analyze the influence laws of population joint strategy in Section 4.3.

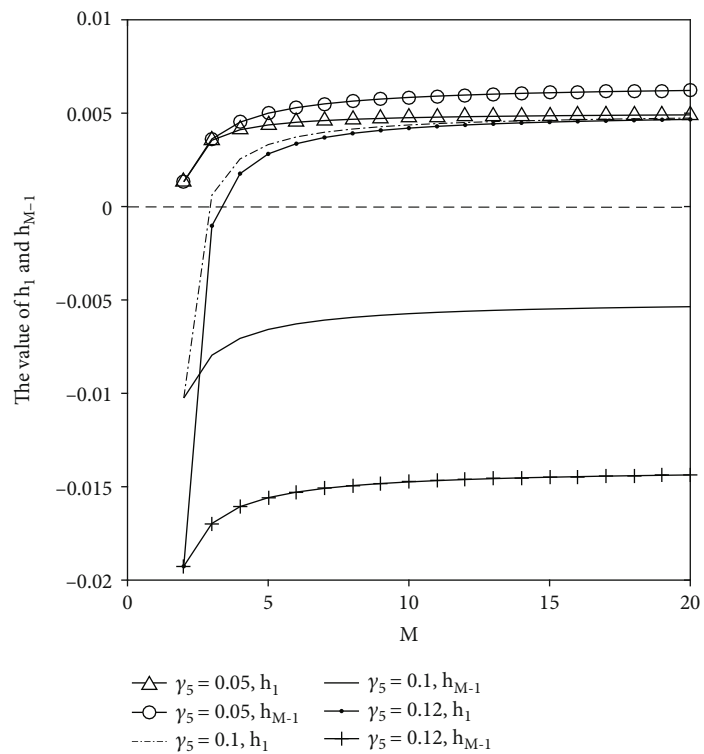
### 3. Results and Analysis

*3.1. Stochastic Evolution Analysis of Strategy Selection of Construction Enterprise Populations in the R&D Stage of Green Building Technology.* To present research results more intuitively, this paper uses numerical simulations to test the impacts of different parameter changes. The parameters are assigned: construction enterprises that choose IIS need to pay the cost of independent innovation of 15, the failure rate of technology R&D is 0.1, and suffer from R&D failure loss of 5. When the R&D is successful, the technology patent is transferred with a probability of 0.2, and the transfer gains 18; when it is not transferred, it gains self-retained earnings of 17. The probability of cooperation is 0.05 when all construction enterprises choose to innovate independently, and the gain from cooperation is 10. The probability of active government encouragement is 0.3, and the R&D subsidy for construction enterprises choosing the strategy of independent innovation is 4. Construction enterprises choosing the strategy of technology introduction need to pay the cost of technology introduction of 5, and the gain from technology introduction is 20; the loss from technology introduction after technology introduction is 1. The spillover coefficient is 0.1 when one side innovates independently and the other side introduces technology. The spillover coefficient is 0.01 when both sides choose technology introduction. Taking the group size, independent R&D cost, spillover effect coefficient, technology introduction loss, R&D subsidy, and other parameters of construction enterprises as variables, this paper analyzes the random evolution process of strategy selection of construction enterprises dominated by expected income and random factors. Under the expected payoff dominates,  $\omega = 1$ . Under the stochastic factor dominates,  $\omega = 0.0001$ .

*3.1.1. Stochastic Evolution Process Analysis of Strategy Selection of Construction Enterprises under the Expected Payoff Dominates.* The influence of the change of  $C_1$  on the evolution path under the expected payoff dominates is shown in Figure 1(a). As can be seen from Figure 1(a) that when  $h_1 < 0$ ,  $h_{M-1} < 0$ ,  $C_1 = 15$ , and  $2 \leq M \leq 4$ , the selection behavior of construction enterprises supports the invasion of IIS by TIS. When  $C_1 = 15$ , and  $M > 4$ , the selection behavior is favorable to the mutual invasion of TIS of IIS. The hybrid strategy becomes an evolutionary stable strategy. As the cost of independent R&D decreases, both curves representing  $h_1$  and  $h_{M-1}$  are located above  $h_1 = 0$  or  $h_{M-1} = 0$ . At this time,  $h_1 > 0$  and  $h_{M-1} > 0$ , IIS will replace TIS as the evolutionary stable strategy. When the cost of independent R&D increases, the two curves are located below  $h_1 =$



(a)



(b)

FIGURE 1: Continued.

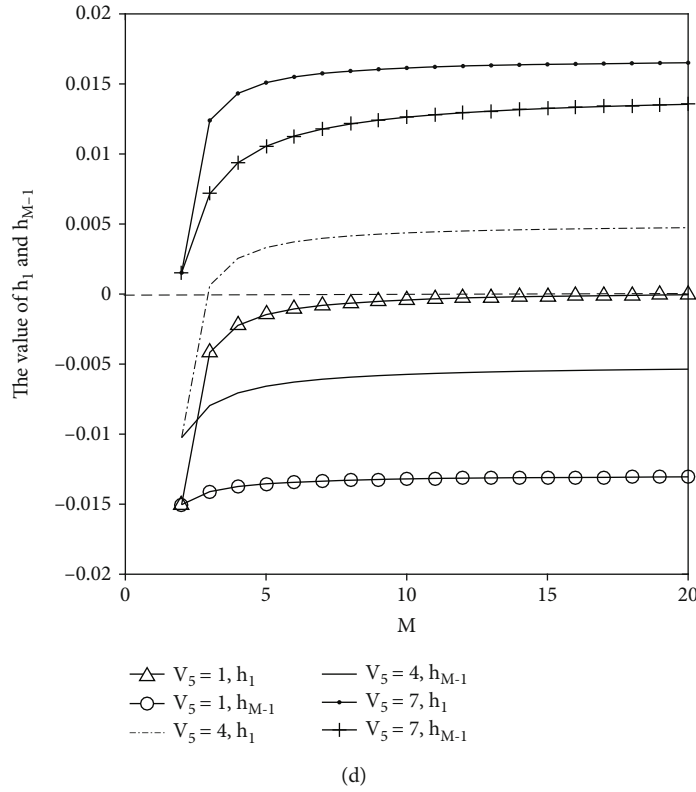
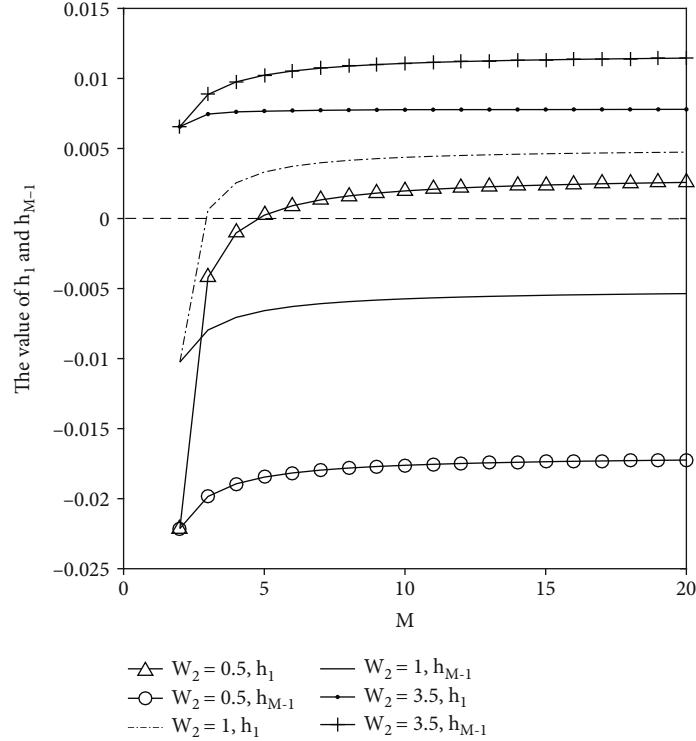


FIGURE 1: (a) Influence of the change of  $C_1$  on the evolution path under the expected payoff dominates. (b) Influence of the change of  $y_5$  on the evolution path under the expected payoff dominates. (c) Influence of the change of  $W_2$  on the evolution path under the expected payoff dominates. (d) Influence of the change of  $V_5$  on the evolution path under the expected payoff dominates.

0 or  $h_{M-1} = 0$ , and TIS replaces IIS as the evolutionary stable strategy. It indicates that the threshold value of IIS to

become evolutionary stable strategy increases. When the group's size of construction enterprises exceeds the

threshold value, some enterprises choose technology introduction, and some enterprises choose independent innovation, and a situation of two strategies coexists. When the cost of independent R&D decreases, IIS prevails and is more likely to become evolutionary stable strategy.

The influence of the change of  $\gamma_5$  on the evolution path under the expected payoff dominates is shown in Figure 1(b). As can be seen from Figure 1(b), the greater the spillover effect coefficient, the greater the threshold value of the construction enterprise group's tendency to IIS. When the group's size is less than the threshold value, the TIS is dominant; when the group's size is larger than the threshold value, the hybrid strategy is more likely to become an evolutionary stable strategy. When the spillover effect coefficient decreases,  $h_1 > 0$ ,  $h_{M-1} > 0$ , the choice behavior of construction enterprises supports IIS to replace the TIS; IIS eventually becomes evolutionarily stable strategy. The greater the spillover effect coefficient is, the stronger the negative external spillover effect is, which is prone to the situation that TIS dominates or technology introduction and independent innovation coexist.

The influence of the change of  $W_2$  on the evolution path under the expected payoff dominates is shown in Figure 1(c). As can be seen from Figure 1(c) that when the technology introduction loss of construction enterprises increases, the two curves lie above  $h_1 = 0$  or  $h_{M-1} = 0$ . The construction enterprise populations tend to choose IIS, and IIS is more likely to become evolutionary stable strategy. When the loss of technology introduction decreases, the threshold size of IIS to become an evolutionary stable strategy becomes larger, and the selection behavior of construction enterprises supports the invasion of IIS by TIS. When the populations' size is smaller than the threshold size, TIS becomes evolutionary stable strategy. When the populations' size is larger than the threshold size, the hybrid strategy becomes evolutionary stable strategy.

The influence of the change of  $V_5$  on the evolution path under the expected payoff dominates is shown in Figure 1(d). As can be seen from Figure 1(d), the government's R&D subsidies for construction enterprises affect the strategic choice of construction enterprise groups. When R&D subsidies increase,  $h_1 > 0$ ,  $h_{M-1} > 0$ , IIS is dominant. When the R&D subsidy decreases, the two curves is below  $h_1 = 0$  or  $h_{M-1} = 0$ , and TIS is dominant. When R&D subsidies decrease, with the increase of group's size, the choice behavior of construction enterprises tends to changes, and the mixed strategy is more likely to become an evolutionary stable strategy. It can be seen that the threshold scale of IIS becoming evolutionary stable strategy decreases with the increase of R&D subsidies.

*3.1.2. Stochastic Evolution Process Analysis of Strategy Selection of Construction Enterprises under the Stochastic Factor Dominates.* The influence of the change of  $C_1$  on the evolution path under the stochastic factor dominates is shown in Figure 2(a). As can be seen from Figure 2(a), in the initial state, when  $C_1 = 15$ ,  $2 \leq M \leq 6$ ,  $\rho_{\alpha 12}/\rho_{\alpha 11} > 1$ , that is,  $\rho_{\alpha 12} > \rho_{\alpha 11}$ , TIS becomes an evolutionary stable strategy. When  $M > 6$ ,  $\rho_{\alpha 12}/\rho_{\alpha 11} < 1$ , namely,  $\rho_{\alpha 12} < \rho_{\alpha 11}$ , IIS becomes

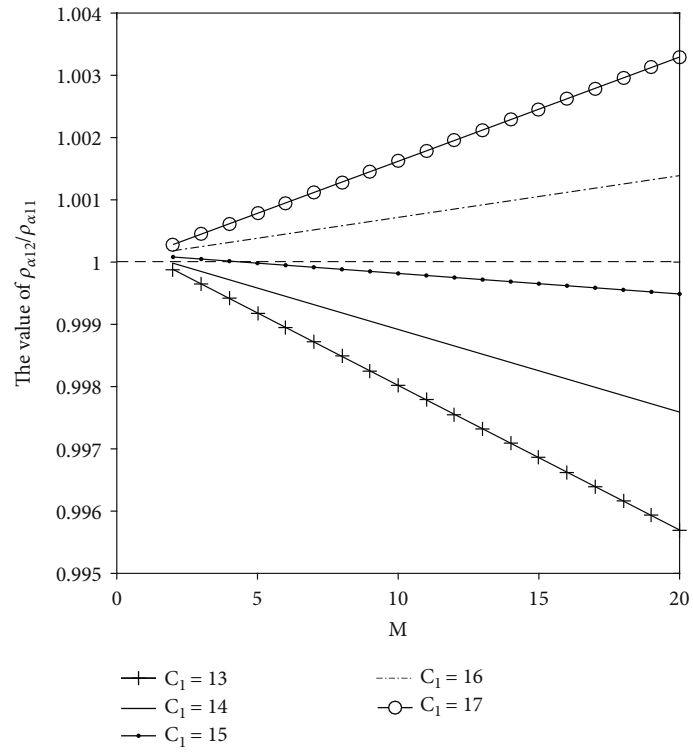
evolutionary stable strategy. When the cost of independent R&D increases, the curve representing the ratio of fixation probability is located above  $\rho_{\alpha 12}/\rho_{\alpha 11} = 1$ ,  $\rho_{\alpha 12} > \rho_{\alpha 11}$ , the TIS is more likely to become an evolutionary stable strategy. When independent R&D cost decreases,  $\rho_{\alpha 11} > \rho_{\alpha 12}$ , IIS is more likely to become evolutionary stable strategy. With the reduction of enterprises' independent R&D cost, the distance of curve distance  $\rho_{\alpha 12}/\rho_{\alpha 11} = 1$  becomes larger, and the threshold scale of IIS becomes evolutionary stable strategy which decreases, the advantage of IIS as an evolutionary stable strategy is more obvious.

The influence of the change of  $\gamma_5$  on the evolution path under the stochastic factor dominates is shown in Figure 2(b). As can be seen from Figure 2(b) that when spillover effect coefficient increases, the threshold scale of IIS becoming evolutionary stable strategy increases, and TIS is more dominant. The threshold scale of IIS becoming evolutionarily stable strategy decreases when the spillover effect coefficient decreases. The distance between curves representing fixation probability ratio and  $\rho_{\alpha 12}/\rho_{\alpha 11} = 1$  increases with the decrease of spillover effect coefficient. Construction enterprise groups are more inclined to choose technology introduction. The spillover effect coefficient increases, the marginal effect of IIS decreases, and the marginal effect of TIS increases.

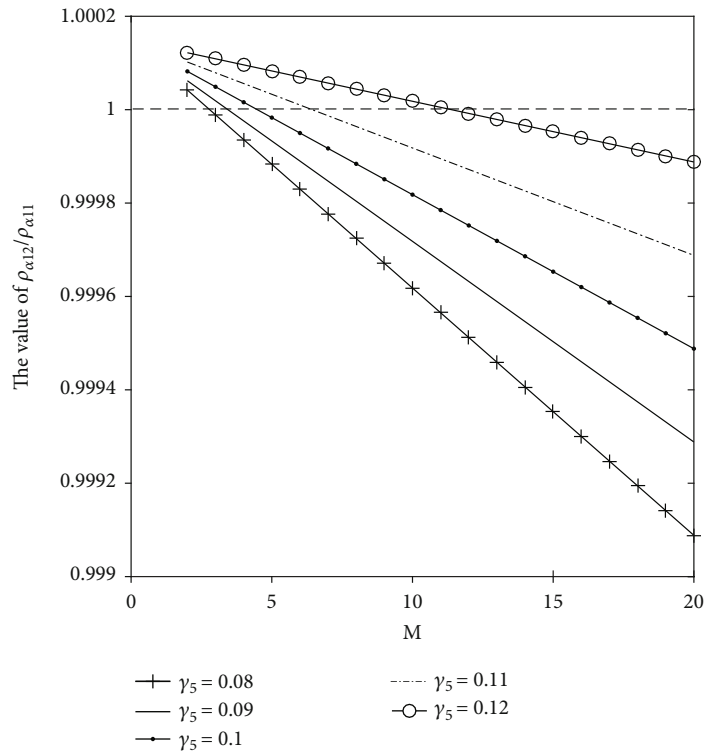
The influence of the change of  $W_2$  on the evolution path under the stochastic factor dominates is shown in Figure 2(c). As can be seen from Figure 2(c) that when the technology introduction loss decreases, TIS is dominant. When the loss of technology introduction increases, IIS gradually dominates. The threshold scale of IIS becoming evolutionary stable strategy decreases with the increase of technology introduction loss. At the same time, it is also noted that the marginal effect of IIS increases when the loss of construction enterprises choosing TIS increases.

The influence of the change of  $V_5$  on the evolution path under the stochastic factor dominates is shown in Figure 2(d). As can be seen from Figure 2(d), when the R&D subsidy is reduced, TIS is dominant; the smaller the R&D subsidy, the greater the distance between the curve representing the ratio of fixation probability and  $\rho_{\alpha 12}/\rho_{\alpha 11} = 1$ , and the more obvious the advantage of TIS is. When R&D subsidy increases, IIS gradually dominates. When the group's size of construction enterprises is constant, the greater the R&D subsidy of the government to independent innovation of construction enterprises is, the more dominant the IIS is. With the increase of group's size, the advantage of IIS becoming evolutionary stable strategy is more obvious. The threshold scale of construction enterprise groups choosing IIS to become evolutionary stable strategy decreases with the increase of R&D subsidies. Government R&D subsidies to construction enterprises increased, and the marginal effect of IIS increased.

*3.2. Stochastic Evolution Analysis of Strategy Selection of Construction Enterprise Populations in the Application Stage of Green Building Technology.* In order to describe the evolution process of the system to the ideal state more intuitively, take  $x_1 y_1$  as an example for analysis.  $x_1 y_1$  refers

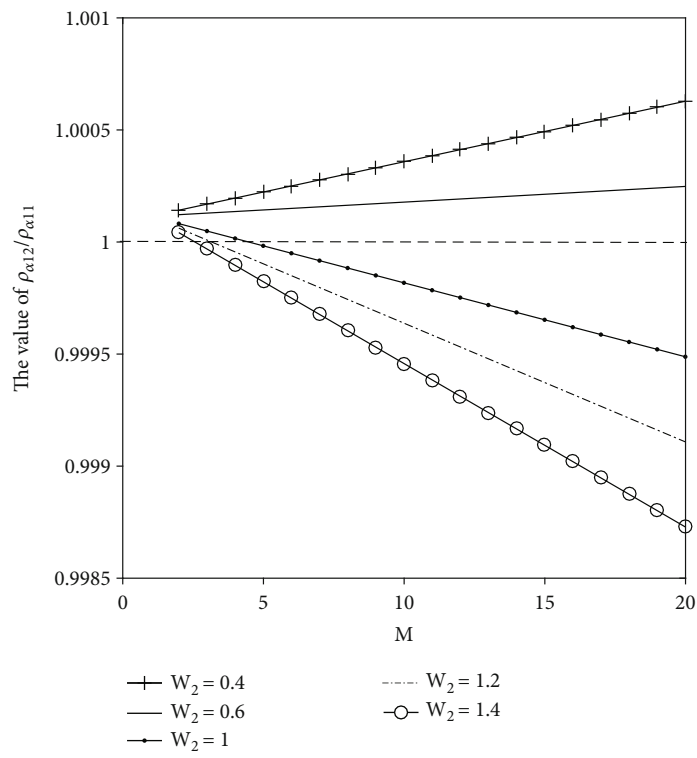


(a)

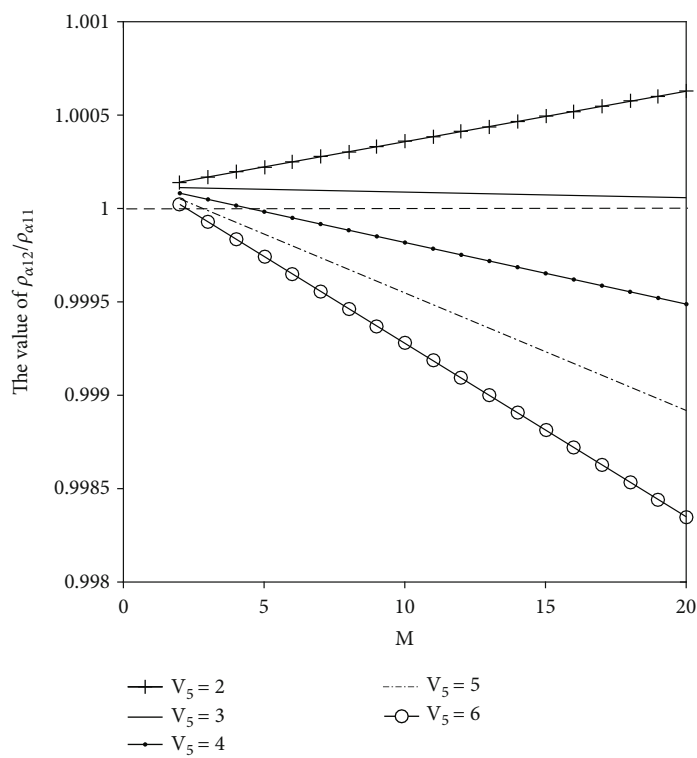


(b)

FIGURE 2: Continued.



(c)



(d)

FIGURE 2: (a) Influence of the change of  $C_1$  on the evolution path under the stochastic factor dominates. (b) Influence of the change of  $y_5$  on the evolution path under the stochastic factor dominates. (c) Influence of the change of  $W_2$  on the evolution path under the stochastic factor dominates. (d) Influence of the change of  $V_5$  on the evolution path under the stochastic factor dominates.

to the construction enterprise group choosing to produce green buildings and the consumer group choosing to buy

green buildings. The parameters are assigned: the demand for green buildings is 40, and the sales price is 35; the sales



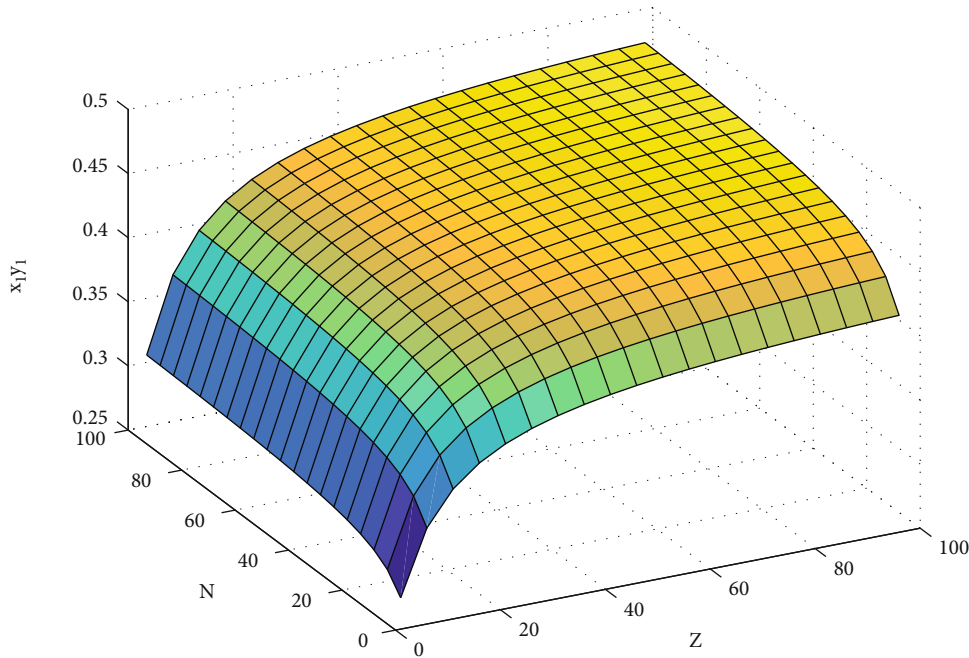


FIGURE 3: Changes in the equilibrium frequency of the joint strategy in the initial state.

price of ordinary buildings is 16. The cross price sensitivity coefficient is 0.5, the green degree sensitivity coefficient is 2.5, the green degree of building products is 3, and the potential demand difference between green buildings and ordinary buildings is 1.2. Construction enterprises need to pay 20 development costs to produce green buildings and 12 development costs to produce ordinary buildings. Consumers pay 25 for green building and 18 for ordinary building. Consumers pay 12 for green building and 21 for ordinary building. The probability of government active encouragement is 0.3, the development subsidy for construction enterprises is 20, the consumption subsidy for consumers to buy green buildings is 10, and the carbon tax is 12 for enterprises producing ordinary buildings. Construction enterprises R&D and sales of green building market reputation is 15. The probability of strategy mutation of construction enterprise groups and consumer groups is 0.1. The selection strength is 0.0001.

The change of the equalization frequency of the joint strategy in the initial state is shown in Figure 3. As can be seen from Figure 3, the equilibrium frequency of the joint strategy of (PGB, BGB) increases when the group's size of construction enterprises is certain and the group's size of consumers increases. When the consumer group's size is constant, the equilibrium frequency of the joint strategy of (PGB, BGB) increases with the increase of the construction enterprise group's size. The evolution speed of construction enterprises is greater than that of consumers. The equilibrium frequency of joint strategy increases with the increase of the scale of construction enterprise groups and consumer groups. This is because government's subsidies to construction enterprises and consumers increase the willingness of construction enterprises to produce green buildings and consumers to buy green buildings. The individual choice of

construction enterprises has changed, and then, the development of the whole group has also been affected.

*3.2.1. Analysis on the Influence of  $u$  and  $v$  Changes on the Evolution Path.* As can be seen from Figure 4, when the strategic mutation rate of the construction enterprise populations and the consumer populations is reduced, the lower bound of the equilibrium frequency of joint strategy decreases from 0.25 to 0.2, and the upper bound increases from 0.5 to 0.7. The lower bound of the equilibrium frequency of the joint strategy increases from 0.25 to 0.255, but the upper bound decreases from 0.5 to 0.28 when the mutation rates increases. It shows that the range of equilibrium frequency of the joint strategy (PGB, BGB) decreases with the increase of mutation rate. Therefore, the smaller the mutation rate is, the more dominant (PGB, BGB) is. The threshold scale of joint strategy becoming evolutionary stable strategy increases with the increase of mutation rate.

*3.2.2. Analysis on the Influence of  $y_1$  Changes on the Evolution Path.* As can be seen from Figure 5, when the cross price sensitivity coefficient decreases to 0.01, the lower bound of the equilibrium frequency of the joint strategy remains unchanged, and the upper bound decreases from 0.5 to 0.4. The lower bound of the equilibrium frequency of the joint strategy decreases from 0.25 to 0.2, and the upper bound increases from 0.5 to 0.6 when the cross-price sensitivity coefficient increases to 0.99. The equilibrium frequency of joint strategy increases with the increase of construction enterprises and consumers. The larger the price sensitivity coefficient is, the larger the threshold scale of joint strategy becoming evolutionary stable strategy is. Enterprises invest heavily in green building products in R&D and production, which leads to the price of green buildings being

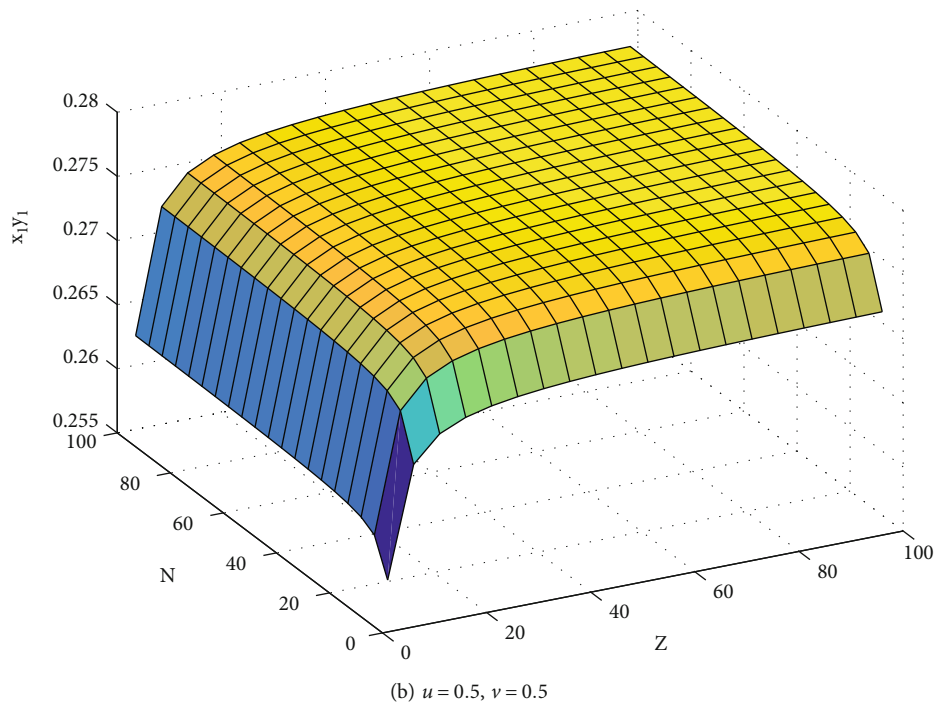
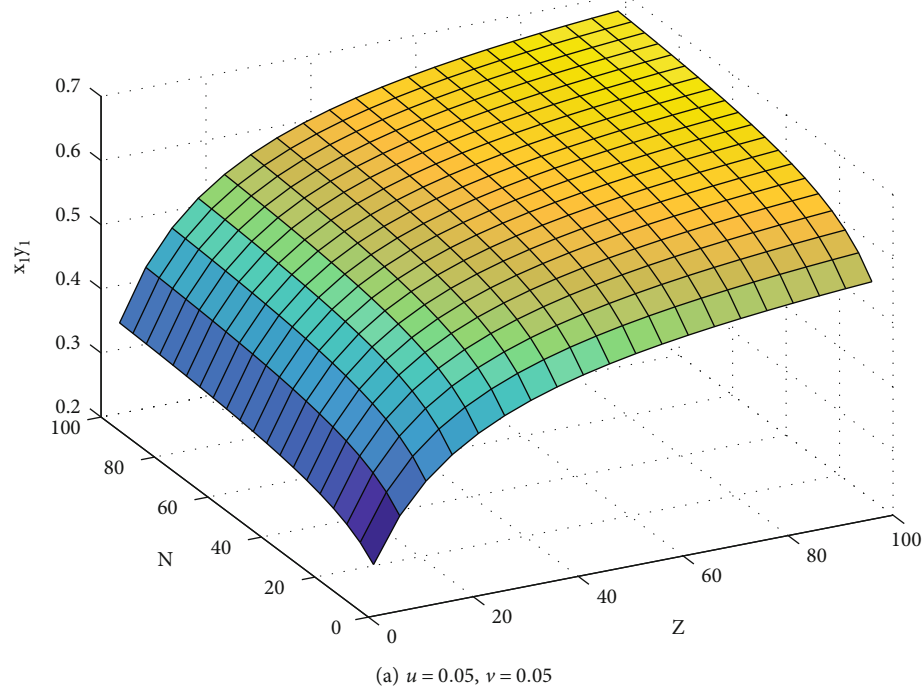


FIGURE 4: Influence of  $u$  and  $v$  changes on the evolution path.

higher than ordinary buildings, and consumers with high price sensitivity will reduce their willingness to buy green buildings. Construction enterprises that produce green buildings can reduce consumers' attention to prices through marketing strategies such as building product differentiation and building product uniqueness.

3.2.3. *Analysis on the Influence of  $\gamma_2$  Changes on the Evolution Path.* As can be seen from Figure 6, when the green sensitivity coefficient is reduced to 0.001, the con-

sumer group's size is certain; with the increase of construction enterprise group's size, the equilibrium frequency of joint strategy is reduced from 0.4 to 0.35. The equilibrium frequency of joint strategy increases slightly with the increase of construction enterprise group's size. The lower bound of the equilibrium frequency of the combined strategy decreases from 0.25 to 0.2, and the upper bound increases from 0.5 to 0.6 when the green sensitivity coefficient increases to 12. When the green sensitivity coefficient changes, the change rate of construction enterprise group

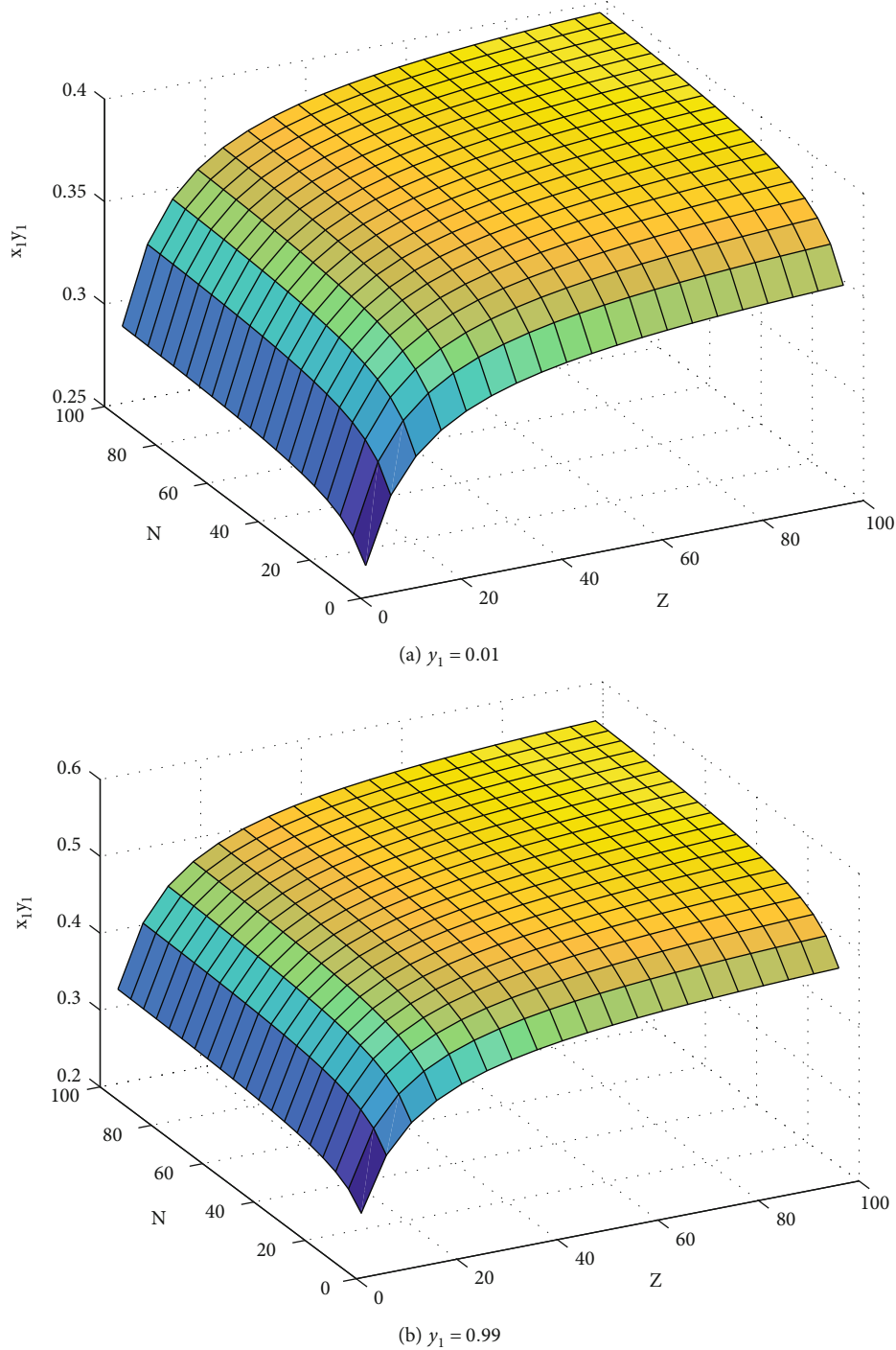


FIGURE 5: Influence of  $y_1$  changes on the evolution path.

is significantly greater than that of consumer group. The larger the green sensitivity coefficient is, the larger the threshold scale of joint strategy becoming evolutionary stable strategy is.

*3.2.4. Analysis on the Influence of  $y_3$  Changes on the Evolution Path.* As can be seen from Figure 7, when the probability of government active encouragement is reduced to 0.01, the scale of consumer groups is certain, and the frequency of joint strategy equilibrium decreases with the

increase of the scale of construction enterprises. With a certain group's size of construction enterprises, the frequency of joint strategy equilibrium increases with the increase of the group's size of consumers. The lower bound of the equilibrium frequency of the joint strategy decreases from 0.25 to 0.2, and the upper bound increases from 0.5 to 0.7 when the probability of government active encouragement increases to 0.9. The government's behavior directly affects the strategic evolution of construction enterprise groups and consumer groups. And the threshold scale of (PGB,

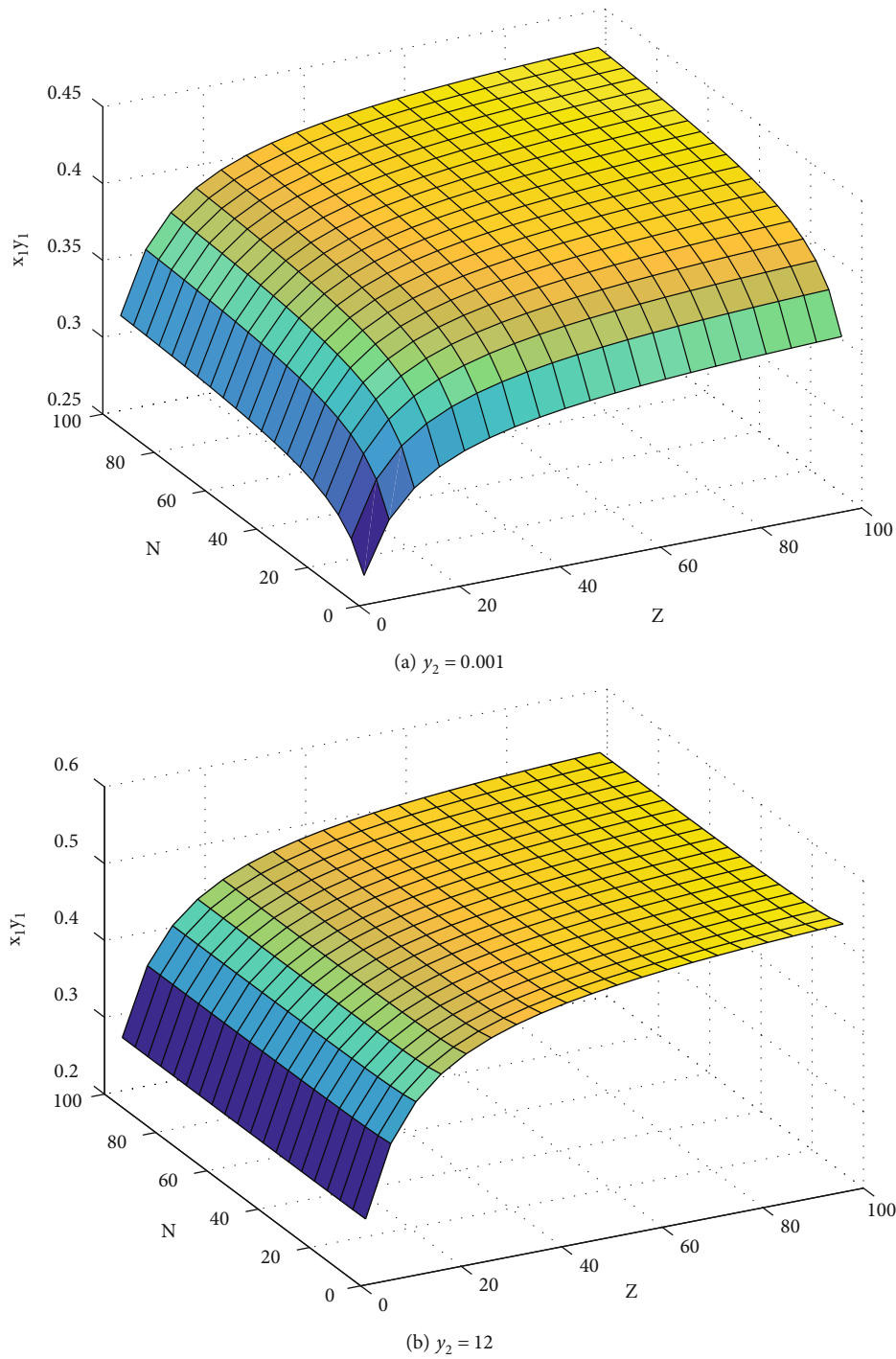


FIGURE 6: Influence of  $y_2$  changes on the evolution path.

BGB) becomes evolutionary stable strategy increases with the increase of government active encouragement's probability.

3.2.5. Analysis on the Influence of  $G_1$  and  $G_2$  changes on the Evolution Path. As can be seen from Figure 8, the equilibrium frequency of joint strategy varies with government's subsidy. The equilibrium frequency of joint strategy increases with the increase of construction enterprise's scale

and consumer group's scale when the government's subsidy increases. It shows that the government's subsidies to construction enterprise groups and consumer groups affect the group's strategy selection process. At the same time, the change of government's subsidy affects the joint strategy to become the threshold scale of evolutionary stable strategy. The greater the government's subsidy, the greater the threshold scale of coalition strategy becoming evolutionary stable strategy.

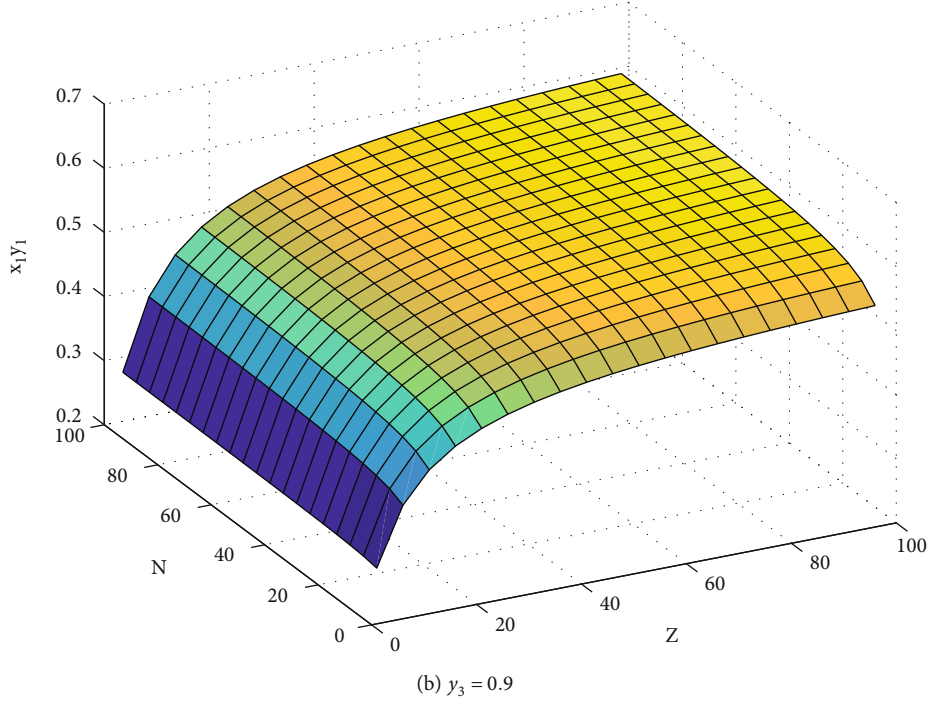
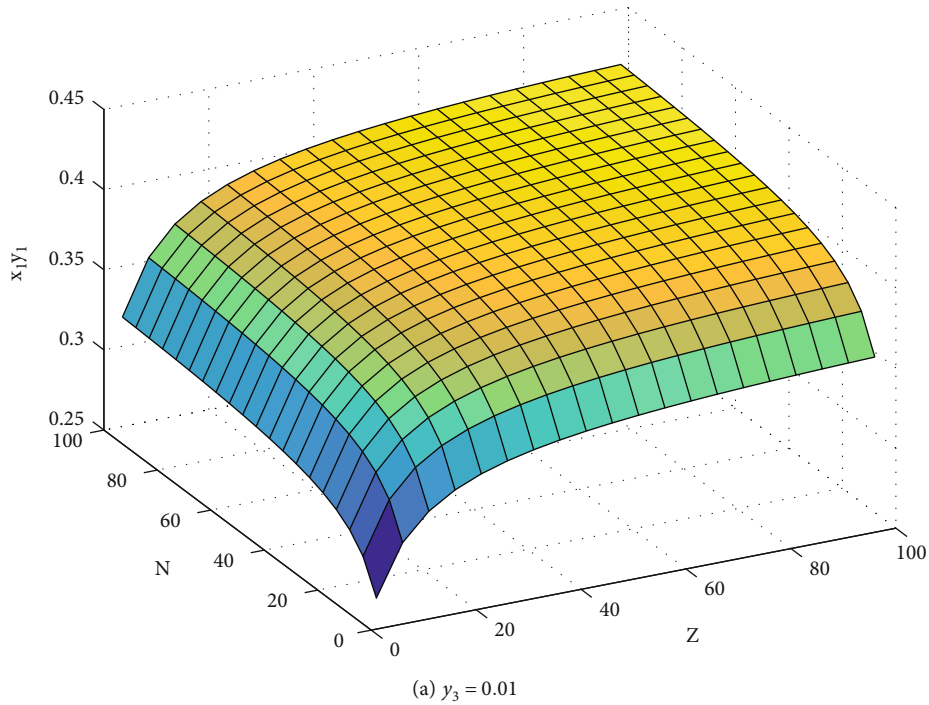


FIGURE 7: Influence of  $y_3$  changes on the evolution path.

3.2.6. *Analysis on the Influence of  $F$  and  $r$  Changes on the Evolution Path.* As can be seen from Figure 9, the carbon tax paid by construction enterprises to develop ordinary buildings decreases, the market reputation value of construction enterprises decreases, the scale of consumer groups remains unchanged, and the equilibrium frequency of joint strategies decreases significantly with the increase of the scale of construction enterprise groups. When the carbon

tax paid by construction enterprises and their market reputation value increase, the scale of consumer group remains unchanged, and the equilibrium frequency of joint strategy increases with the increase of the scale of construction enterprise group. When the scale of construction enterprise group remains unchanged, and the carbon tax and market reputation value change, the law that the equilibrium frequency of joint strategy changes with the scale of consumer group is

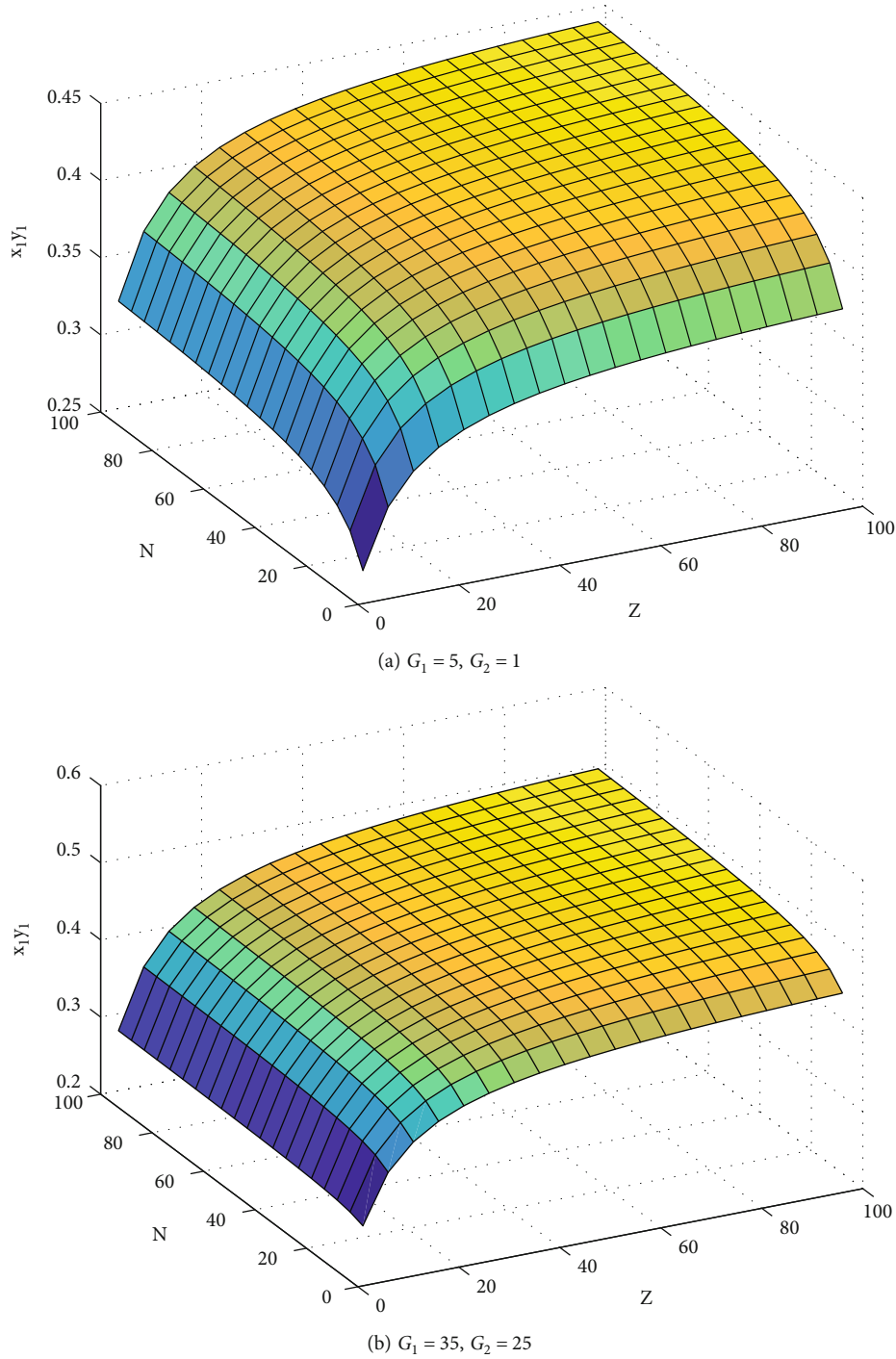


FIGURE 8: Influence of  $G_1$  and  $G_2$  changes on the evolution path.

not obvious. The threshold scale of (PGB, BGB) becomes evolutionary stable strategy increases with carbon tax and market credibility.

#### 4. Discussions and Implications

4.1. *Discussions.* This study takes the R&D and application process of green building technology as the starting point and discusses the stochastic evolution of strategy selection of construction enterprises and consumer populations from

the R&D stage and application stage, respectively, by using the methods based on Moran process analysis and bimatrix game analysis, and draws the following conclusions:

- (1) In the R&D stage of green building technology, the government can appropriately reduce the R&D cost of enterprises by providing appropriate R&D subsidies to construction enterprises and improving the success rate of independent R&D of enterprises, so as to guide enterprises to choose independent

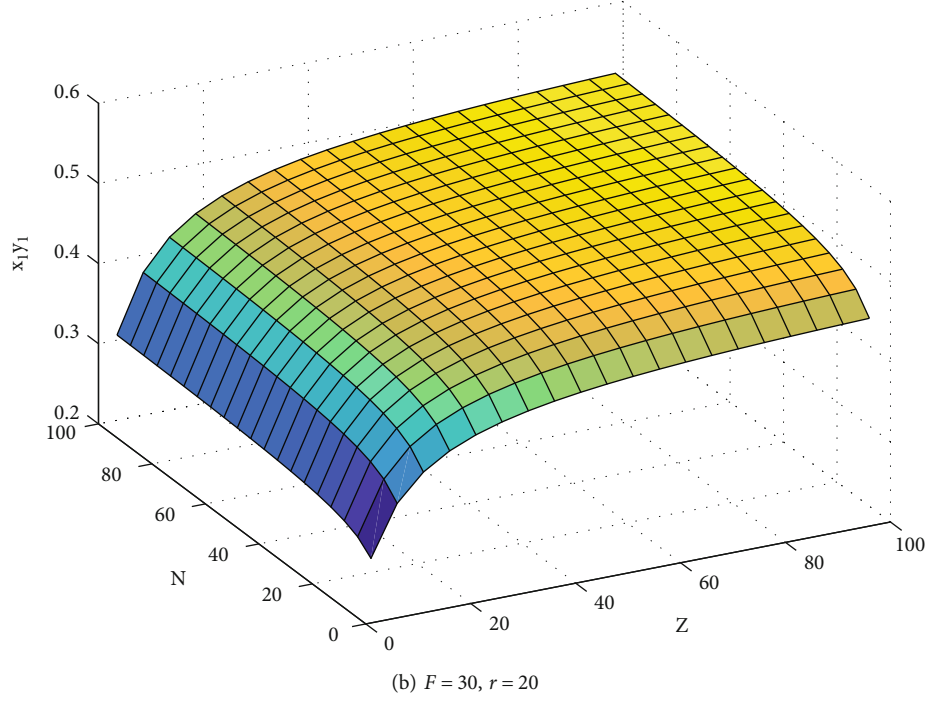
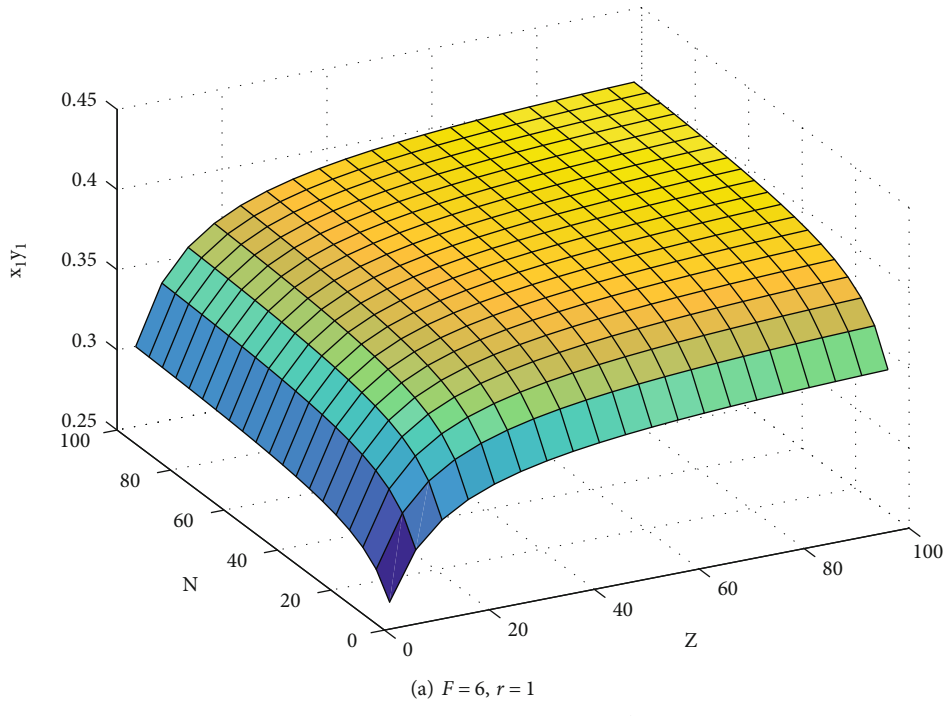


FIGURE 9: Influence of  $F$  and  $r$  changes on the evolution path.

innovation strategies, thus forms a virtuous circle through technological breakthroughs

- (2) In the application stage of green building technology, the government encourages the construction enterprise populations and consumer populations to carry out green building production and consumption with a positive attitude. For example, increasing policy publicity to improve the public's green preference and green awareness; subsidizing construction enterprises and consumers who produce and purchase green buildings; levying carbon taxes on construction enterprises who produce ordinary buildings, etc., to reduce the mutation rate of the main population strategy, increase the threshold scale of construction enterprises producing green buildings and consumers purchasing green buildings; while promoting the development of green building market through the supply side, the demand of consumers on demand sides is boosted, which in turn stimulates the expansion of production on the supply side, forming a virtuous closed loop
- (3) In the application stage of green building technology, the strategy selection process of construction enterprise groups and consumer groups is affected by the mutation rate, cross-price sensitivity coefficient, greenness sensitivity coefficient, the probability of active government encouragement, government subsidies, carbon tax, market reputation, etc. The smaller the mutation rate is, the greater the cross price sensitivity coefficient is, the greater the green degree sensitivity coefficient is, the greater the probability of government active encouragement is, and the more dominant (PGB, BGB) is

#### 4.2. Implications

- (1) The government should take the lead in improving the guidance and supervision mechanism, fully stimulate the power of construction enterprises to develop green building technology, minimize the externality of green building technology, and make up for the lack of market regulation
- (2) The government should strengthen its support for independent R&D construction enterprises. High cost and high risk of independent R&D hinder the construction enterprises to choose independent innovation strategy. The government's subsidies for independent R&D construction enterprises reduce the cost of independent R&D, improve the enthusiasm of independent R&D, and expand the threshold scale for construction enterprises to choose independent innovation strategies as evolutionary stable strategy
- (3) Construction enterprises should focus on improving their own R&D of technology. Improving the success rate of independent R&D of green building technology is the premise to promote independent R&D of

construction enterprises. Construction enterprises can improve their R&D success rate by cultivating and introducing internal high-end talents and strengthening cooperation with professional research institutions

- (4) The government should subsidize both construction enterprises and consumers. Due to the imperfect government supervision system and insufficient implementation of subsidy policy, the development of green building in China's construction market is slow. The government can increase consumers' demand for green buildings from the demand side by increasing policy propaganda and improving the public's green preferences and consumers' willingness to buy green buildings
- (5) Establish a sound carbon tax system and information platform. Information platform increases the reputation exposure of construction enterprises, which directly affects the reputation and image of enterprises. The government levies carbon tax on construction enterprises that produce ordinary buildings, drives construction enterprises to produce green buildings through strong supervision, and increases the supply of green buildings

#### Data Availability

The data used to support the findings of this study are available from the corresponding author upon request.

#### Conflicts of Interest

The authors declare no conflict of interest.

#### Acknowledgments

This work was supported by the Humanities and Social Sciences funded projects of the Ministry of Education (no.17YJCZH257): research on carbon quota allocation of enterprises based on comprehensive performance of carbon emission; support plan for scientific and technological innovation talents in Colleges and Universities of Henan Province (Humanities and Social Sciences): mechanism and efficiency of carbon water cycle in regional system; and project supported by Henan Discipline Innovation and Talent Introduction Base (no. GXJD004): intelligent water conservancy.

#### References

- [1] R. Kumanayake and H. Luo, "A tool for assessing life cycle CO<sub>2</sub> emissions of buildings in Sri Lanka," *Building and Environment*, vol. 128, pp. 272–286, 2018.
- [2] US Green Building Council, "Benefits of green building | US green building council," Accessed November 13, 2020. <https://www.usgbc.org/articles/green-building-facts,> in, 2020.
- [3] J. Zuo, R. Rameezdeen, M. Hagger, Z. Zhou, and Z. Ding, "Dust pollution control on construction sites: awareness and



- self-responsibility of managers,” *Journal of Cleaner Production*, vol. 166, pp. 312–320, 2017.
- [4] H. X. Sun, “Problems in the development of green buildings and their solutions - taking Henan Province as an example,” *Urban Problems*, vol. 6, pp. 56–58+101, 2012, (in Chinese).
- [5] W. Wang, S. Zhang, Y. Su, and X. Deng, “An empirical analysis of the factors affecting the adoption and diffusion of GBTS in the construction market,” *Sustainability*, vol. 11, no. 6, p. 1795, 2019.
- [6] Z. Yang, H. Chen, L. Mi, P. Li, and K. Qi, “Green building technologies adoption process in China: how environmental policies are reshaping the decision-making among alliance-based construction enterprises?,” *Sustainable Cities and Society*, vol. 73, article 103122, 2021.
- [7] M. Wang, Y. Li, Z. Cheng, C. Zhong, and W. Ma, “Evolution and equilibrium of a green technological innovation system: simulation of a tripartite game model,” *Journal of Cleaner Production*, vol. 278, article 123944, 2021.
- [8] X. Yang, J. Zhang, G. Q. Shen, and Y. Yan, “Incentives for green retrofits: an evolutionary game analysis on public-private-partnership reconstruction of buildings,” *Journal of Cleaner Production*, vol. 232, pp. 1076–1092, 2019.
- [9] Q. Meng, Y. Liu, Z. Li, and C. Wu, “Dynamic reward and penalty strategies of green building construction incentive: an evolutionary game theory-based analysis,” *Environmental Science and Pollution Research International*, vol. 28, no. 33, pp. 44902–44915, 2021.
- [10] A. Traulsen, J. C. Claussen, and C. Hauert, “Coevolutionary dynamics: from finite to infinite populations,” *Physical Review Letters*, vol. 95, no. 23, 2005.
- [11] E. P. de Souza, E. M. Ferreira, and A. G. M. Neves, “Fixation probabilities for the Moran process in evolutionary games with two strategies: graph shapes and large population asymptotics,” *Journal of Mathematical Biology*, vol. 78, no. 4, pp. 1033–1065, 2019.
- [12] T. Nishimura, A. Okada, and Y. Shirata, “Evolution of fairness and coalition formation in three-person ultimatum games,” *Journal of Theoretical Biology*, vol. 420, pp. 53–67, 2017.
- [13] M. A. Nowak, A. Sasaki, C. Taylor, and D. Fudenberg, “Emergence of cooperation and evolutionary stability in finite populations,” *Nature: International Weekly Journal of Science*, vol. 428, no. 6983, pp. 646–650, 2004.
- [14] P. M. Altrock and A. Traulsen, “Fixation times in evolutionary games under weak selection,” *New Journal of Physics*, vol. 11, no. 1, 2009.
- [15] A. Traulsen, N. Shresh, and M. A. Nowak, “Analytical results for individual and group selection of any intensity,” *Bulletin of Mathematical Biology*, vol. 70, no. 5, pp. 1410–1424, 2008.
- [16] X. Wang, C. Gu, J. Zhao et al., “Stochastic evolution dynamic model of Moran process with selection difference and its application,” *Systems Engineering Theory&Practice*, vol. 40, no. 5, pp. 1193–1209, 2020, (in Chinese).
- [17] H. Ohtsuki, “Stochastic evolutionary dynamics of bimatrix games,” *Journal of Theoretical Biology*, vol. 264, no. 1, pp. 136–142, 2010.
- [18] L. Gao, “An algorithm for finding approximate Nash equilibria in bimatrix games,” *Soft Computing*, vol. 25, no. 2, pp. 1181–1191, 2021.
- [19] Z. Feng and C. Tan, “Credibilistic bimatrix games with loss aversion and triangular fuzzy payoffs,” *International Journal of Fuzzy Systems*, vol. 22, no. 5, pp. 1635–1652, 2020.
- [20] Y. Zhang and X. Gao, “Stochastic evolutionary selection in heterogeneous populations for asymmetric games,” *Computational Economics*, vol. 45, no. 3, pp. 501–515, 2015.
- [21] Y. Dai, G. Zhan, Y. Ye et al., “Game dynamics of emotion evolution based on the Moran process,” *Chaos (Woodbury, N.Y.)*, vol. 31, no. 3, p. 033153, 2021.
- [22] J. Yang, D. Li, and L. Lai, “Equilibrium strategies of triangular intuitionistic fuzzy numbers bi-matrix game model and its application at considering the players’ attitude,” *Fuzzy Systems and Mathematics*, vol. 31, no. 3, pp. 79–87, 2017, (in Chinese).
- [23] C. E. Tarnita, T. Antal, and M. A. Nowak, “Mutation-selection equilibrium in games with mixed strategies,” *Journal of Theoretical Biology*, vol. 261, no. 1, pp. 50–57, 2009.
- [24] L. Xu, C. Wang, and J. Zhao, “Decision and coordination in the dual-channel supply chain considering cap- and-trade regulation,” *Journal of Cleaner Production*, vol. 197, pp. 551–561, 2018.
- [25] C. Taylor, D. Fudenberg, A. Sasaki, and M. A. Nowak, “Evolutionary game dynamics in finite populations,” *Bulletin of Mathematical Biology*, vol. 66, no. 6, pp. 1621–1644, 2004.

## Research Article

# Structural Assembly Analysis of Concrete Buildings with Intelligent Finite Element Analysis

Kun Zhu <sup>1,2,3</sup>, Yan Zhang,<sup>1</sup> Xianyue Meng,<sup>1,2,3</sup> and Zaiyong Ma<sup>1,2,3</sup>

<sup>1</sup>Changchun Institute of Technology, Changchun 130012, China

<sup>2</sup>The Key Laboratory of Earthquake Disaster Reduction for Civil Engineering in Jilin Province China, Changchun 130012, China

<sup>3</sup>Jilin Province Cold Area Residential Engineering Building Technology Research Center, Changchun 130012, China

Correspondence should be addressed to Kun Zhu; [tm\\_zk@ccit.edu.cn](mailto:tm_zk@ccit.edu.cn)

Received 29 April 2022; Accepted 3 June 2022; Published 25 June 2022

Academic Editor: Wen Zeng

Copyright © 2022 Kun Zhu et al. This is an open access article distributed under the Creative Commons Attribution License, which permits unrestricted use, distribution, and reproduction in any medium, provided the original work is properly cited.

In recent years, with the rapid development of China's construction industry, assembled buildings have become more and more common. In this context, China attaches great importance to the development of assembled buildings and has introduced a series of policies to support the promotion of assembled buildings. Assembled building technology has become relatively mature in some developed countries. From their experience, it can be learned that the construction of an assembled concrete structure technology system is the basis for the promotion of assembled concrete buildings. A factory-based production model enables prefabricated concrete elements to be produced to a good quality. The key to the technical system for the construction of assembled concrete structures is the connection of the prefabricated elements. At the same time, it is essential to consider not only the reliability of the structural performance of the assembled concrete structure but also the cost and safety of the design, production, transport, and construction processes. In fact, the safety of an assembled concrete structure depends to a large extent on whether the nodal connection technology meets the design and quality requirements. Unlike conventional cast-in-place concrete structures, the key nodes of assembled concrete structures have a greater impact on the mechanical properties of the load transfer. In other words, this influence is directly related to the design of the prefabricated elements. Hence, the mechanical properties of precast nodal joints, such as good stiffness, are essential for the structural safety of assembled buildings. In the case of assembled buildings, the correct form of nodal connection is decisive in ensuring that the connection meets the design and service requirements. In addition to this, the correct nodal connection form will ensure that the design life is maintained. The uneven quality of many prefabricated components has limited the promotion of assembled concrete structures and is a key constraint to their development. At this stage, there are no uniform standards for quality control systems and measures on site in China, and the level of technical management is not yet fully mature. What is more, the overall quality of construction personnel is not high enough, which might lead to some frequent issues with the quality of connections in the field during the actual construction process. As a result, the development of assembled concrete structures urgently requires perfect construction management standards as a guide for on-site joint construction, so as to guarantee the quality level of on-site joint construction. In order to study the force performance of assembled concrete structures, this paper establishes an analytical model for assembled concrete buildings based on the intelligent finite element method. To be specific, this research introduces artificial neural network theory into the structural analysis of assembled buildings and transports it into the finite element solution, thus forming an intelligent finite element method.

## 1. Introduction

An assembled concrete structure is a concrete structure made of prefabricated elements, which are assembled and connected [1]. To be specific, an assembled concrete structure can be fully or partially prefabricated and is a form of

industrialised building production through assembly. This type of assembled building structure has been widely used in many foreign countries. Due to its stable quality, high production efficiency, and environmental protection, assembled concrete structures are increasingly attracting the attention of real estate developers, building construction

companies, and designers in China [2]. At the same time, assembled concrete structures are not only an emerging green and energy-saving building structure but also an effective way to achieve sustainable development in housing construction [3]. The assembled building system transforms the traditional on-site work into a factory-based production system, enabling the construction of buildings to gradually enter the modernisation path of industrialisation, information technology, and intelligence [4]. As China's economic and social development and industrial transformation and upgrading accelerate, the need for modernisation of the construction industry becomes increasingly urgent and the vigorous development of assembled buildings becomes an inevitable choice [5]. As can be seen in Figure 1, from 2016 to 2021, the average annual growth rate of new construction floor area for assembled buildings in China was as high as 40%. Therefore, in order to achieve the development goal of assembled buildings, assembled concrete buildings must be the mainstay.

The assembled structure system should be viewed from two perspectives. On the one hand, assembled structures have the advantages of high production efficiency and short construction periods [6]. The combination of modern concrete construction technology and traditional assembled concrete construction technology can therefore bring the advantages of assembled construction technology into full play, thus further promoting the development of assembled construction technology [7]. On the other hand, the nodes of assembled concrete are less integral, more difficult to transport and install, and more difficult to design than cast-in-place concrete [8]. In addition to this, assembled concrete nodes have been found to be the weakest of the frame structures in the world's major earthquakes, with serious breakage of the nodes [9]. For instance, Figure 2 illustrates the seismic damage to an assembled concrete frame structure during an earthquake. For the construction of assembled concrete buildings, component design is an important part of the design phase [10]. Component design plays a key role in controlling the cost and construction cycle of an assembled building [11]. Therefore, the quality of the assembled concrete is at the heart of the design work during the component design phase. The component design is not only for laminated slabs and beams but also for beam-column nodes, beam-slab nodes, beam-beam nodes, and other nodal connections in assembled frame structures [12]. The design of assembled concrete structures involves a large number of mechanical designs and calculations. Compared to conventional structural design, the design of structural elements such as columns, beams, and slabs is more demanding, complex, and influential than traditional structural design [13].

In addition to this, component splitting is also a key aspect of component design. Usually, component manufacturers split the design drawings in order to facilitate the lifting of the components by the constructors. However, in the process of dismantling, they often neglect to verify and analyse the load-bearing properties [14]. As a result, the strength of the jointed parts is reduced in relation to the design strength during the actual dismantling process [15].

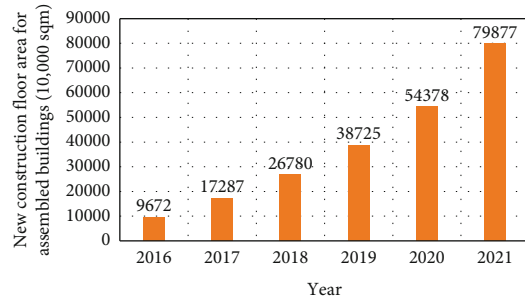


FIGURE 1: New construction floor area for assembled buildings in 2016-2021 in China.

To a certain extent, these objective factors reflect the fact that the technical system for design, dismantling, and construction in China is not yet complete, that standards and specifications are not yet comprehensive, and that the level of management needs to be improved. At the same time, there are very few design institutes that have the capacity to design mature assembly-type buildings [16]. At this stage, most design institutes are still in their infancy, and their technical systems for the design and disassembly of shaped prefabricated components are not perfect, and their experience is not yet mature. To be specific, their production capacity for shaped components does not meet the requirements of the construction site. In addition, there is a disconnect between the dismantling effect and the capacity and efficiency of the component manufacturers, which makes it difficult to produce on a rapid scale [17]. After all, component factories are more likely to disassemble simple prefabricated nodes for common applications. As a result, these problems can lead to prefabricated elements that are not fully compliant with the design requirements and can even affect the load-bearing properties of the elements.

China's concrete assembled buildings originated in the 1960s, and through independent research and foreign imports, a series of concrete assembled building systems gradually emerged. At that time, single-storey industrial buildings and multistorey frame buildings were typical types of assembled concrete buildings [18]. In the 1980s, the development of assembled concrete buildings in China reached a climax with the establishment of tens of thousands of prefabricated concrete plants throughout the country, with an annual output of 30 million sqm. In the late 1980s, the domestic construction market demand increased dramatically. However, the load-bearing capacity and ductility of domestically produced precast elements were low. Building systems using precast concrete elements did not solve the problems of waterproofing and thermal insulation well [19]. In the Tangshan earthquake, the damage to a large number of buildings using precast concrete elements revealed the lack of seismic performance of domestic assembled concrete buildings. In addition, due to the rise and promotion of commercial concrete, assembled concrete structures are gradually being replaced by cast-in-place concrete structures [3].

The fundamental reason for the decline in the development of assembled concrete buildings in China in the last



FIGURE 2: Seismic damage to an assembled concrete frame structure during an earthquake.

century was the low level of industrialisation and the lack of a mature technical system for assembled concrete structures. In addition to this, the quality control mechanism in the domestic market was not perfect [20]. From the experience of developed countries and regions, assembled concrete buildings can fully meet the safety and functional requirements of buildings and have many advantages over cast-in-place concrete buildings. In recent years, with the rapid development of China's economy and society, the demand for industrialisation of the construction industry has emerged. At the same time, the quality control mechanism of the construction market in China is gradually maturing, and the development of assembled concrete buildings has become an inevitable trend [21]. At present, China's market share of assembled buildings is relatively low, and in order to vigorously promote assembled buildings, there is an urgent need to develop a series of assembled concrete building technology systems that are in line with national conditions. In 2020, public buildings will account for 33.2% of the new construction of assembled buildings in China. In public buildings, especially schools, hospitals, and government institutions, concrete frame structures play an important role. Therefore, it is of great importance to study the technology of assembled concrete frame construction.

The structural elements of assembled concrete buildings are produced in the factory [22]. As a result, these structural elements perform better in terms of load capacity, stiffness, and ductility. The connections between prefabricated elements can be made either dry or wet, which is different from conventional monolithic cast-in-place concrete structures [23]. There are doubts in the country about the integrity of the connections, particularly in terms of their seismic performance. The damage mechanisms of frame structures under seismic action are beam-hinged, column-hinged, and mixed-hinged mechanisms (see Figure 3). The ideal damage mechanism is either the beam-hinged damage mechanism or the mixed-hinged damage mechanism, both of which are based on the formation of plastic hinges at the beam ends and first floor columns. The key to the study of the construction technology of assembled concrete frame structures is therefore the study of the seismic performance of the nodal connections.

In recent years, with the continuous development of computer technology and information technology, numerical calculation methods represented by the finite element method have been rapidly developed and widely used in construction engineering. The finite element method can effectively solve practical problems that are difficult to solve

with traditional calculation methods for assembly buildings [24]. It is worth noting, however, that although these numerical methods have successfully solved a large number of complex engineering problems and can be used to simulate the force characteristics of assembled structures by quantitative means, they must be based on a sound understanding of the material properties [25]. Only if the calculation model is sound, and the material ontology model and the calculation parameters are accurately given, can the numerical results be correct and reasonable.

The traditional method of analysing the structure of an assembled building is usually to obtain test data through some geotechnical experiments or field tests and then to analyse the test data using various data processing methods such as statistics and regression [26]. The data is then analysed using various data processing methods such as statistics and regression. The laws are then identified and fitted to the simulation using mathematical expressions. Under certain assumptions, a few material parameters are determined, the model is extended to any stress condition, and new test results are used to test and modify the model [27]. Based on this, the following problems arise. On the one hand, the complex properties of assembled building materials require complex mathematical models and a large number of material parameters to express their complex physical and mechanical properties. This makes it difficult to determine the parameters and to use the model. On the other hand, if some assumptions are made, a certain amount of error is bound to be introduced during the numerical calculations. The magnitude of this error is difficult to estimate theoretically and needs to be verified using a large number of examples. It appears that although a large number of analytical models have been proposed for the different characteristics of assembled buildings, these models are mostly simple approximations of the physical and mechanical characteristics of the building materials. In other words, it is difficult to fully express the complex nonlinear properties of assembled buildings, which has forced the application of new theories and methods to the analysis of assembled building structures.

The theory of artificial neural networks, which is based on many modern sciences such as brain neuroscience [28] and machine learning, is self-learning, self-organising, and self-adaptive. Therefore, artificial neural networks have excellent characterisation capabilities for highly nonlinear problems. This study investigates the creation and use of neural network models and how they can be applied to the finite element method to form intelligent finite element

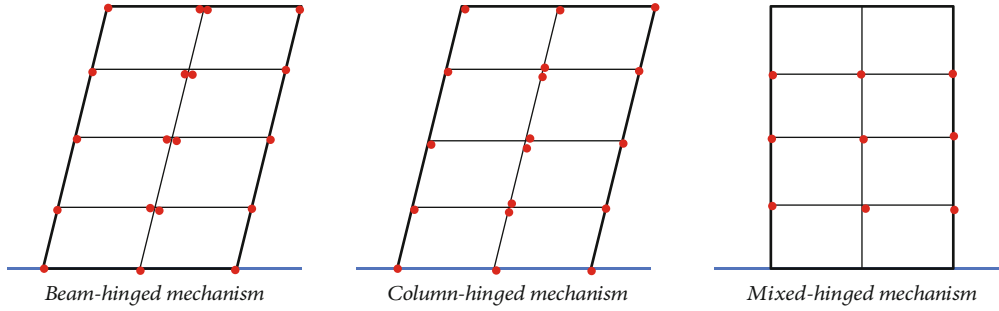


FIGURE 3: Mechanisms of damage to the frame structure.

methods. After that, this research applies the intelligent finite element method to model the building structure and analyse the assembled components to verify the accuracy of the model. At the same time, parametric analysis of the assembled frame structure is carried out to investigate the relationship between the assembled structure and the overall forces of the cast-in-place structure.

## 2. Intelligent Finite Element Analysis

The finite element method is an effective numerical calculation method that has developed rapidly in recent years. The basic idea is to discretize a continuous structure into a finite number of cells and to set a finite number of nodes in each cell, considering the continuum as a collection of many cells connected at the nodes. At the same time, the nodal values of the field functions are chosen as the fundamental unknowns and an interpolation function is assumed in each cell to represent the distribution pattern of the field functions in the cell. As a result, the variational principle in mechanics can be used to establish equations to solve the discretized finite degree of freedom problem. The cell can be designed in different geometries, allowing flexible modelling and approximation of complex solution domains. As the number of cells increases, the accuracy of the solution increases and eventually converges to an exact solution if the interpolation function meets certain requirements.

The finite element method is one of many numerical analysis methods, each with its own scope of application (see Table 1). However, in terms of the degree of application, the finite element method is the most commonly applied.

**2.1. Principle of Finite Element Analysis.** The finite element method is based on the energy principle. For different problems, the finite element method can take different forms of formulation. They are equivalent to each other and have their own scope of application. The interrelationship of the energy principles is shown in Figure 4.

In order to be able to represent cell displacements, strains, and stresses in terms of nodal displacements, certain assumptions have to be made about the in-cell displacements. This means that the distribution function of the in-cell displacements is interpolated using the cell nodal displacements, as shown in

$$v = M \times n^g, \quad (1)$$

where  $v$  refers to the displacement vector,  $M$  indicates the displacement difference matrix, and  $n^g$  is the unit node displacement vector.

From the principle of virtual work, the equilibrium equation for the unit can be derived, as shown in

$$f^g = l^g \times n^g, \quad (2)$$

where  $l^g$  refers to the stiffness matrix and  $f^g$  is the equivalent nodal force.

The Newton-Raphson method is one of the best-known methods for solving nonlinear systems of equations. For a linear equation in one element,

$$\Psi(i) = n(i)i - f = 0. \quad (3)$$

Then, the Taylor expansion of  $\Psi(i)$  at  $i_0$  is

$$\Psi(i) = \Psi(i_0) + \Psi'(i_0)(i - i_0) + o(i - i_0). \quad (4)$$

After that, removing the higher-order terms can yield

$$i = i_0 - \frac{\Psi(i_0)}{\Psi'(i_0)}. \quad (5)$$

The iterative solution process is shown in Figure 5.

**2.2. Artificial Neural Network.** The most complex and developed organ in the human body is the brain. The brain is the control centre for all human thought, the command centre for all kinds of reactions, and the material basis for higher neural activity. Scientists are constantly exploring the brain and envisaging the creation of a machine system that can mimic the brain's thinking and actions. This would replace the human brain in certain areas and reduce the amount of human work. In order to simulate the thinking and control of the human brain, a simplified mathematical model has been created based on the biological principles of the human brain, using physical and mathematical methods to simulate and abstract the biological workings of the human brain.

In terms of the transmission of information, the dendrites of a nerve cell receive signals from other nerve cells at the synapse. These signals may be either excitatory or inhibitory. The signals received by all dendrites are transmitted to the cell body for integrated processing. If the amount of excitatory signals received by a cell during a time interval

TABLE 1: Different numerical analysis methods.

Numerical analysis method	Basic principle	Solution way	Application
Finite element method	Minimum heat principle	Solving systems of equations	Inhomogeneous materials
Boundary element method	Betti's reciprocity theorem	Solving systems of equations	Small deformation materials
Discrete element method	Newton's theorem of motion	Explicit difference	Large deformation materials
Lagrangian yen method	Newton's theorem of motion	Explicit difference	Homogeneous materials

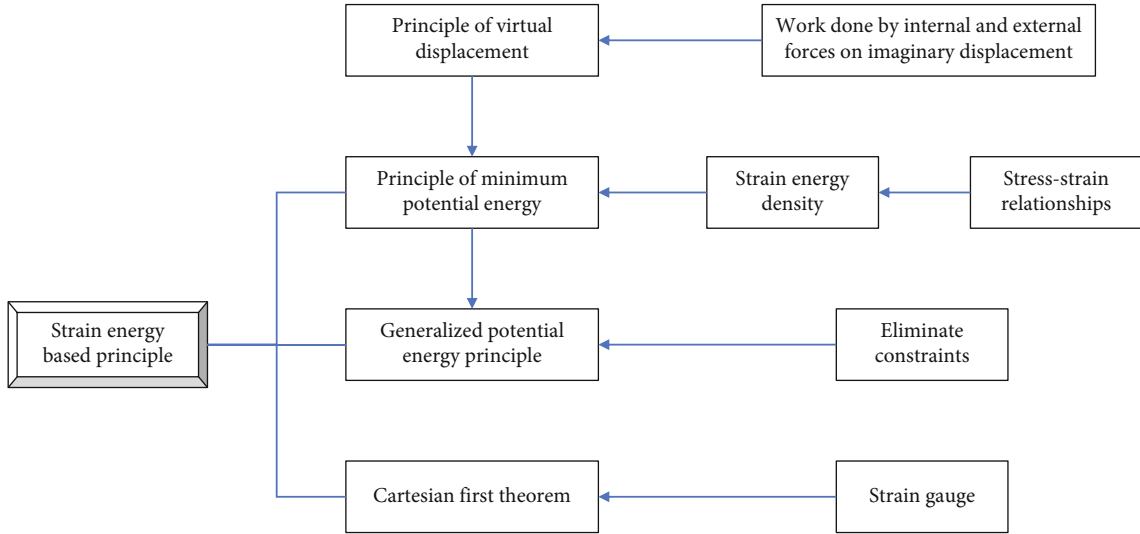


FIGURE 4: Interrelationship of the energy principles.

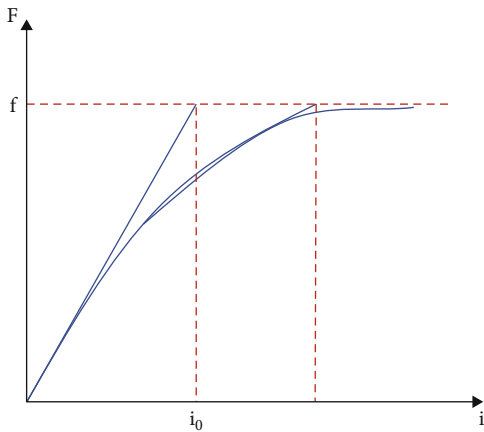


FIGURE 5: Iterative solution process.

is large enough to activate the cell, a pulse signal is generated. After that, this signal is transmitted along the axon of the cell and through the synapse to other nerve cells. By abstracting and simplifying biological neurons, artificial neuron models have been proposed, and a typical artificial neuron model is illustrated in Figure 6.

In neural network algorithms, the learning rate is defined as a constant. If it is given too low a value, the network learns slowly and the number of training sessions increases. If it is given too high, however, the training will oscillate and fail to converge. In practice, it is difficult to determine an optimal

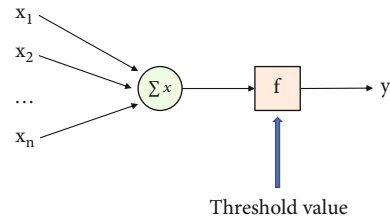


FIGURE 6: Typical artificial neuron model.

learning rate that is always appropriate in the network learning process. The adaptive learning rate method involves changing the value of the learning rate throughout the training process, depending on the actual network training situation. Thus, an adaptive learning rate adjustment system can be defined. When the weights are adjusted by the same amount twice in a row during the training process, the adjustment is too small. In this case, the learning rate can be multiplied by an adjustment factor greater than 1 to speed up the adjustment of the weights. When two consecutive weights are different, the weights are overadjusted and the learning rate should be reduced. Therefore, the learning rate can be divided by an adjustment factor greater than 1 to reduce the amount of correction to the weights, thus reducing the oscillations in the network.

2.3. *Principle of Intelligent Finite Element Analysis.* The basic idea of the intelligent finite element method is to replace the conventional instantonal model with a neural network

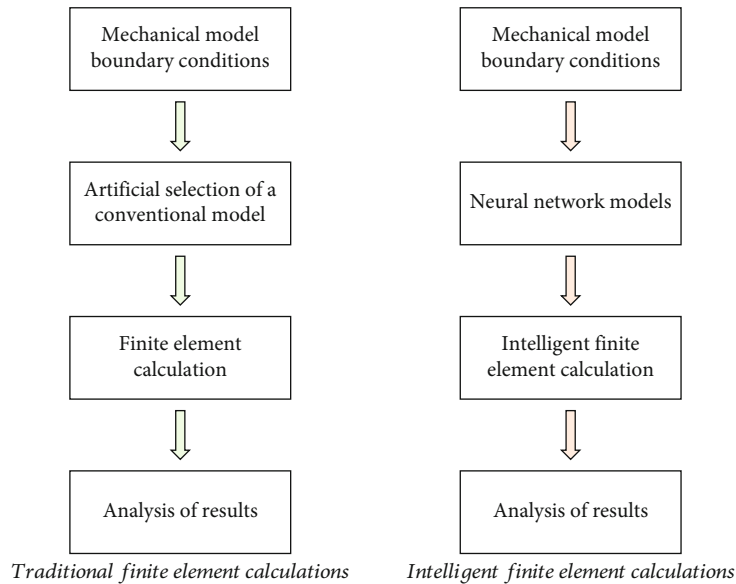


FIGURE 7: Difference between the two finite element methods.

instantonal model and use it in finite element calculations. Figure 7 shows the difference between the two finite element methods.

The adaptive intelligent finite element method calculations are carried out according to the incremental method. The stiffness matrix in each incremental step is calculated according to the conventional finite element calculation, similar to the elastoplastic nonlinear finite element method. The initial displacements of the units are solved iteratively by Newton's method, the strains are derived from the geometric equations and the stresses of the units are mapped using a trained neural network intrinsic model. As the displacements and strains in the structure are not realistic at this point, the stresses mapped by the neural network are also not realistic. The stresses mapped by the neural network are not the real stress field, and therefore, there are unbalanced forces, which are used as control criteria to iterate the solution. As the neural network, intrinsic structure model can characterise the real material intrinsic structure relationship, the reiterative solution should result in improved displacements. This cycle is repeated until the error tolerance is met. Finally, the real displacement and stress fields in the structure can be calculated. The entire solution process embeds the neural network into the finite element calculation and adaptively completes the solution, resulting in an adaptive intelligent finite element method.

### 3. Structural Assembly Analysis of Concrete Buildings

In this study, a three-dimensional nonlinear finite element analysis of the assembled concrete frame nodes was carried out using an intelligent finite element analysis method. In addition, the seismic performance of the assembled frame nodes is analysed by using interface springs to simulate the force performance of the vertical laminated surfaces of the assembled concrete joints. Based on this example, the finite

element calculation parameters applicable to the analysis of the assembled frame nodes are validated, and the experimental studies on assembled concrete conducted by other scholars are also validated. After that, a parametric analysis is carried out to compare the seismic performance of frame nodes with floor slabs with that of simple assembled beam-column nodes. This can provide some theoretical reference for the design and construction of assembled frame nodes in practical projects.

*3.1. Connection between Units.* The shear capacity of a vertical stacked beam with a vertical stack of old and new concrete at the end of the column is generally composed of three parts: the compressive shear capacity, the shear capacity of the shear key, and the shear capacity of the reinforcement pins. After treatment of the old and new concrete, the slip of the vertical laminated surface is minimal even at high shear forces. Therefore, the seismic performance of a laminated beam with a vertical laminated surface is similar to that of a cast-in-place beam.

The shear capacity of a vertical stacked beam with a vertical stack of old and new concrete at the end of the column is generally composed of three parts: the compressive shear capacity, the shear capacity of the shear key, and the shear capacity of the reinforcement pins. After treatment of the old and new concrete, the slip of the vertical laminated surface is minimal even at high shear forces. Therefore, the seismic performance of a laminated beam with a vertical laminated surface is similar to that of a cast-in-place beam. The normal force versus displacement of the nodal springs in the finite element model is shown in Figure 8.

The assembled monolithic concrete frame structure is a combination of cast-in-place columns and precast beams. The bonding strength of the old and new concrete has a significant influence on the load-bearing properties of the assembled concrete nodes. In general, the axial tensile strength of the bond is 70% of the axial tensile strength of

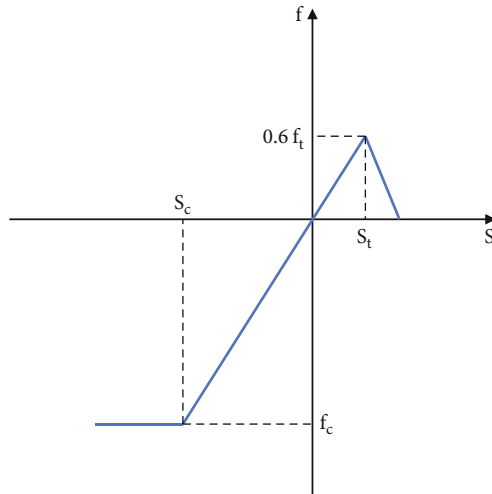


FIGURE 8: Normal force versus displacement of nodal springs in the finite element model.

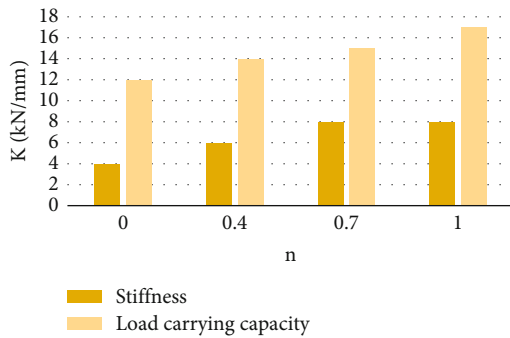


FIGURE 9: Stiffness load capacity with different tensile strength factors.

the new concrete as a whole. This indicates a reduction in strength due to the presence of the bonding surface. Within a certain range of roughness, the greater the roughness, the higher the axial tensile strength of the bond. For this reason, in general assembled concrete, the bonding surfaces of old and new concrete are made as rough and clean as possible in order to ensure that the old and new concrete work well together.

**3.2. Tensile Strength Factor of Old and New Concrete.** The tensile strength coefficients for old and new concrete range from 0 to 1. A coefficient of 1 is generally considered to approximate cast-in-place concrete construction. When 0 is taken, the tensile strength of the concrete at the joint of the old and new concrete is not considered. The results for the stiffness load capacity with different tensile strength factors are shown in Figure 9. As can be seen, when the tensile strength factor is 0, the node stiffness decreases significantly and the load-carrying capacity also decreases significantly. As the tensile strength factor increases, the node stiffness and load-carrying capacity also increase. When the tensile strength factor is 0.7-0.9, the load-displacement curve of the node does not change much and the stiffness and load-carrying capacity do not change significantly.

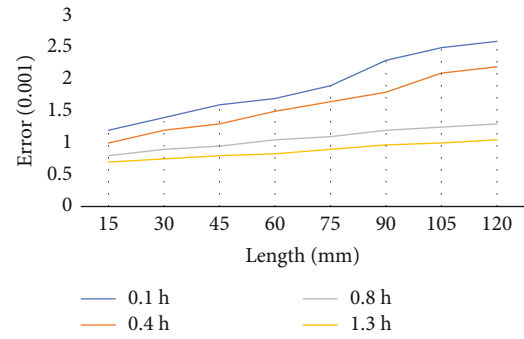


FIGURE 10: Strain diagram of the casing.

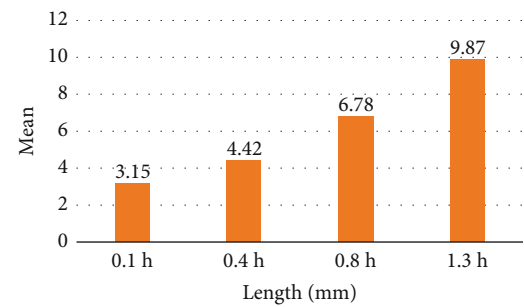


FIGURE 11: Nodal ductility for different casing lengths.

Nodal damage is the main form of damage in assembled structures, so there is an urgent need to strengthen the research on new nodes. Optimisation of the node configuration will enable the tensile strength coefficient of the old and new concrete joints to reach a level comparable to that of cast-in-place structures. At the same time, the strength performance of the nodes will not lag behind that of cast-in-place structures.

**3.3. Casing Connection Length.** Figure 10 illustrates the strain diagram of the casing, which shows the variation of the casing strain during loading of different casing lengths. As can be seen from the graph, the casing strain decreases with increasing length. When the length exceeds the height of the beam  $h$ , the casing strain does not change significantly. Therefore, the casing is within the height of the beam, which reduces the strain on the reinforcement in the casing and increases the deformation capacity of the structure.

Figure 11 shows the nodal ductility for different casing lengths. As the length of the casing increases, the ductility of the node also increases. When the length of the casing exceeds the height of the beam, the change in ductility remains more or less constant.

## 4. Conclusion

As China's technological strength continues to advance and the level of information technology in construction continues to improve, the drawbacks of traditional construction production methods are becoming more and more prominent. In the course of the development of the construction industry, modular construction will become the inevitable



development of modernised and industrialised construction in the new era. The advantages of assembled construction over traditional construction are obvious, as it not only reduces the waste of construction resources but also reduces environmental pollution. As a result, assembled buildings have begun to lead the way in the construction industry. However, a great deal of research and practical experience in engineering projects shows that China is generally late to the party in assembling buildings. Specifically, the development of assembled buildings has been slow, and standards and technical systems have been studied late. For the time being, a relatively complete set of technical standards and systems has been initially developed for the connection of assembled concrete structures. However, there are some outstanding problems with the nodal connections of assembled concrete structures in China. For example, the quality control specifications and control system are not mature enough. A reasonable form of connection for assembled concrete structures is essential to ensure structural integrity and reliability, and the nodal connection is a key technical issue in the development of assembled buildings. However, there is currently no comprehensive and complete system of standards for the nodal connections of assembled concrete structures. Therefore, this study is aimed at improving the development of assembled buildings with the help of intelligent and effective elemental methods and at promoting the rapid development of the industrialisation of construction.

Based on the findings already presented in this paper, there are several points where future work can continue in depth. Due to the limitations of the test equipment, the loading of the nodal specimens did not meet the expectations. The study of the specimens in this paper is mainly qualitative, and the seismic performance of the nodal specimens, especially the strongly connected specimens, during large displacements in the late loading period is yet to be studied.

## Data Availability

The labeled dataset used to support the findings of this study are available from the corresponding author upon request.

## Conflicts of Interest

The authors declare no competing interests.

## References

- [1] Y. Zhou, T. Chen, Y. Pei et al., "Static load test on progressive collapse resistance of fully assembled precast concrete frame structure," *Engineering Structures*, vol. 200, p. 109719, 2019.
- [2] Y. Zhou, X. Hu, Y. Pei et al., "Dynamic load test on progressive collapse resistance of fully assembled precast concrete frame structures," *Engineering Structures*, vol. 214, p. 110675, 2020.
- [3] D. Huang, J. Wei, X. Liu, P. Xiang, and S. Zhang, "Experimental study on long-term performance of steel-concrete composite bridge with an assembled concrete deck," *Construction and Building Materials*, vol. 214, pp. 606–618, 2019.
- [4] G. Wu and D. C. Feng, "Research progress on fundamental performance of precast concrete frame beam-to-column connections," *Journal of Building Structures*, vol. 39, no. 2, pp. 1–16, 2018.
- [5] B. Dal Lago, P. Negro, and A. Dal Lago, "Seismic design and performance of dry-assembled precast structures with adaptable joints," *Soil Dynamics and Earthquake Engineering*, vol. 106, pp. 182–195, 2018.
- [6] R. Yuan, F. Guo, Y. Qian et al., "A system dynamic model for simulating the potential of prefabrication on construction waste reduction," *Environmental Science and Pollution Research*, vol. 29, no. 9, pp. 12589–12600, 2022.
- [7] T. Dreher, M. R. W. Brake, B. Seeger, and M. Krack, "In situ, real-time measurements of contact pressure internal to jointed interfaces during dynamic excitation of an assembled structure," *Mechanical Systems and Signal Processing*, vol. 160, p. 107859, 2021.
- [8] X. Yang, X. Shi, R. D'arcy, N. Tirelli, and G. Zhai, "Amphiphilic polysaccharides as building blocks for self-assembled nanosystems: molecular design and application in cancer and inflammatory diseases," *Journal of Controlled Release*, vol. 272, pp. 114–144, 2018.
- [9] Z. Xue, P. Wang, A. Peng, and T. Wang, "Architectural design of self-assembled hollow superstructures," *Advanced Materials*, vol. 31, no. 38, p. 1801441, 2019.
- [10] B. Cheng, K. Lu, J. Li, H. Chen, X. Luo, and M. Shafique, "Comprehensive assessment of embodied environmental impacts of buildings using normalized environmental impact factors," *Journal of Cleaner Production*, vol. 334, p. 130083, 2022.
- [11] H. Wang, H. Zhang, K. Hou, and G. Yao, "Carbon emissions factor evaluation for assembled building during prefabricated component transportation phase," *Energy Exploration & Exploitation*, vol. 39, no. 1, pp. 385–408, 2021.
- [12] M. Pakdel, Z. Moosavi-Nejad, R. K. Kermanshahi, and H. Hosano, "Self-assembled uniform keratin nanoparticles as building blocks for nanofibrils and nanolayers derived from industrial feather waste," *Journal of Cleaner Production*, vol. 335, p. 130331, 2022.
- [13] Z. Zong, A. Hao, and P. Xing, "Halogenation regulates supra-molecular chirality at hierarchical levels of self-assembled N-terminal aromatic amino acids," *The Journal of Physical Chemistry Letters*, vol. 12, no. 4, pp. 1307–1315, 2021.
- [14] M. Sun, X. Sun, Z. Wang, S. Guo, G. Yu, and H. Yang, "Synthesis and properties of gelatin methacryloyl (GelMA) hydrogels and their recent applications in load-bearing tissue," *Polymers*, vol. 10, no. 11, p. 1290, 2018.
- [15] A. Li, F. Su, P. K. Chu, and J. Sun, "Articular cartilage inspired bilayer coating on Ti6Al4V alloy with low friction and high load-bearing properties," *Applied Surface Science*, vol. 515, p. 146065, 2020.
- [16] B. Cheng, J. Huang, J. Li, S. Chen, and H. Chen, "Improving contractors' participation of resource utilization in construction and demolition waste through government incentives and punishments," *Environmental Management*, vol. 70, pp. 1–15, 2022.
- [17] L. Xin, X. Duan, and N. Liu, "Dimerization and oligomerization of DNA-assembled building blocks for controlled multi-motion in high-order architectures," *Nature Communications*, vol. 12, no. 1, pp. 1–9, 2021.
- [18] F. Scozzese, G. Terracciano, A. Zona, G. Della Corte, A. Dall'Asta, and R. Landolfo, "Analysis of seismic non-structural damage in single-storey industrial steel buildings,"

- Soil Dynamics and Earthquake Engineering*, vol. 114, pp. 505–519, 2018.
- [19] P. K. Aninthaneni and R. P. Dhakal, “Demountable precast concrete frame–building system for seismic regions: conceptual development,” *Journal of Architectural Engineering*, vol. 23, no. 4, p. 04017024, 2017.
- [20] S. Taheri and A. Razban, “Learning-based CO<sub>2</sub> concentration prediction: application to indoor air quality control using demand-controlled ventilation,” *Building and Environment*, vol. 205, p. 108164, 2021.
- [21] L. Sanhudo, J. Rodrigues, and E. Vasconcelos Filho, “Multivariate time series clustering and forecasting for building energy analysis: application to weather data quality control,” *Journal of Building Engineering*, vol. 35, p. 101996, 2021.
- [22] C. Peng, W. He, Y. Wang, G. Li, and D. Zhai, “Optimization method for a lap-assembled parabolic concrete channel structure,” *Journal of Irrigation and Drainage Engineering*, vol. 146, no. 6, p. 04020011, 2020.
- [23] S. Navaratnam, T. Ngo, T. Gunawardena, and D. Henderson, “Performance review of prefabricated building systems and future research in Australia,” *Buildings*, vol. 9, no. 2, p. 38, 2019.
- [24] S. David Müzel, E. P. Bonhin, N. M. Guimarães, and E. S. Guidi, “Application of the finite element method in the analysis of composite materials: a review,” *Polymers*, vol. 12, no. 4, p. 818, 2020.
- [25] S. Evtiukov, E. Golov, and G. Ginzburg, “Finite element method for reconstruction of road traffic accidents,” *Transportation Research Procedia*, vol. 36, pp. 157–165, 2018.
- [26] M. Mengolini, M. F. Benedetto, and A. M. Aragón, “An engineering perspective to the virtual element method and its interplay with the standard finite element method,” *Computer Methods in Applied Mechanics and Engineering*, vol. 350, pp. 995–1023, 2019.
- [27] M. Sheikholeslami, “Finite element method for PCM solidification in existence of CuO nanoparticles,” *Journal of Molecular Liquids*, vol. 265, pp. 347–355, 2018.
- [28] Y. Qian, S. Chen, J. Li et al., “A decision-making model using machine learning for improving dispatching efficiency in Chengdu Shuangliu Airport,” *Complexity*, vol. 2020, 16 pages, 2020.

## Research Article

# Construction of Educational Resource Metadata Management Platform Based on Service-Oriented Architecture

Jingbin Zhang <sup>1</sup> and Tianxiang Qi <sup>2</sup>

<sup>1</sup>Department of Marxism, Xi'an Fanyi University, Xi'an, Shaanxi 710105, China

<sup>2</sup>Department of Social Economy and Management, Woosuk University, Wanju-gun 55338, Republic of Korea

Correspondence should be addressed to Jingbin Zhang; ruibin321@163.com

Received 15 February 2022; Revised 23 March 2022; Accepted 12 April 2022; Published 22 June 2022

Academic Editor: Wen Zeng

Copyright © 2022 Jingbin Zhang and Tianxiang Qi. This is an open access article distributed under the Creative Commons Attribution License, which permits unrestricted use, distribution, and reproduction in any medium, provided the original work is properly cited.

The existing cloud sharing system of educational resources is in the form of centralized management, which has the problems of small number of concurrent users and low score of resource retrieval results and cannot meet the current needs of implicit educational resource sharing. Therefore, a cloud sharing system of college implicit educational resources based on service architecture is proposed. At present, the sharing of educational resources mainly includes network teaching, distance education, and other methods. These schemes alleviate the sharing problem of educational data resources to a certain extent. However, the sharing and rational integrated utilization of educational application software are still under exploration, and there is no mature solution at present. At present, there is a lack of unified planning for the construction of the educational resource database of the management cadre college, and there are problems such as repeated construction, complex quantity, and nonstandard form, which directly leads to the failure of effective dissemination of resource information in the network distance education system, which is an urgent problem to be solved in the distance education system of the management cadre college. This paper first understands some domestic and foreign standardization and development of educational resources. Then, it introduces the ontology theory and the basic theory of metadata. At present, the construction of educational resource database in colleges and universities in China lacks unified planning, and there are problems such as repeated construction, complex quantity, and nonstandard form, which makes the resource information in the network distance education system unable to be shared and disseminated effectively. In order to improve the utilization of online educational resources and share the data of resource databases with different structures, a metadata management platform model of educational resources is designed. As a new architecture idea, service-oriented architecture can package existing assets and reuse existing assets. It can also minimize the impact of demand changes. This paper puts forward the process of metadata management under the service architecture and independently develops a metadata management platform suitable for the development and use of service mode. It is combined with automatic testing and continuous integration to effectively improve the data quality and development efficiency of service development.

## 1. Introduction

Nowadays, the hidden resources of colleges and universities are relatively independent, forming isolated islands of information, which cannot be shared among different colleges and universities, resulting in the waste of hidden educational resources. Each university has established a database of educational resources suitable for the use of teachers and students in the school so that teachers and students in the school can easily query and use the information [1].

Although online learning and distance education generated under the traditional education informatization model have improved the sharing and utilization of educational resources, in terms of content, educational resource service providers still provide a fixed amount of resources to learners, lacking dynamicity. Distance education realizes cross-regional and cross-school resource sharing through the network, but the services it provides are too single, ignoring the educational service resources that other educational service providers can provide [2]. For developers of resource

libraries, due to the rapid spread of educational informatization, the demand for resource sharing and resource information exchange has also increased sharply, and to achieve resource sharing and information exchange between different educational resource libraries requires a complete set of sharing and exchange specifications. Education resource libraries are complex in type and in various forms and are relatively inconsistent in data specifications. On the one hand, it is easy to cause wasted investment and repeated construction. On the other hand, each resource library is scattered and isolated, and most of them lack a description of themselves. Education when retrieving materials, workers have to find many resource libraries, which consumes a lot of time and energy [3]. One of the key factors to solve the above problems is to realize the standardization of metadata, because the metadata standard is the most important part of the current network development and the utilization of information resources. With the unlimited growth of resources, the effective management of network information will increasingly depend on the management of metadata [4].

Cloud computing is getting familiar with people gradually, which marks the emergence of a new service model and concept and also has a great impact on the field of university education, thus resulting in the university recessive education resource cloud sharing system. At present, in the process of educational informatization, we should strengthen the top-level design and give full play to the advantages of application services [5]. Based on the advantages of cloud computing in resource integration, building an educational cloud platform and improving the utilization rate of educational application services are a way to solve the above problems. Connecting the database through the network will greatly promote the exchange of educational resources among colleges and universities and also play an extremely important role in the development of modern education and new technology [6]. At present, the number of educational resource pools and the resources of each resource pool are still increasing, and with the development of network technology, the resources of educational resource pools are becoming more and more scattered, and the retrieval burden that users have to bear to obtain information is increasing day by day, making it even more difficult for users to obtain comprehensive and accurate resource information [7]. Many colleges and universities will use substandard document formats for the storage of educational resource information in the database at will because they do not understand the standards, which will bring great difficulties to retrieval, and even if they are connected to the network, it is difficult to share them. Service architecture is essentially a method of constructing distributed application systems, which provides business application functions in the form of services, so as to better assemble and reuse multiple subsystems and jointly build a resource cloud sharing system with loose coupling and high sharing [8]. How to give a standard resource description to the educational resource database, intelligently and seamlessly aggregate it, and help educators find the required resources quickly and accurately is the focus of this paper.

In the field of education, all kinds of educational websites are in full bloom. Almost every university has invested a lot of human and material resources to build its own educational resource website and try its best to improve the construction of digital campus [9]. At present, the application of educational resource management platform in domestic colleges and universities is in its infancy. Although there are some formed educational resource management platforms in the market to realize the interaction between different educational resources, there are common problems such as tight combination of modules, weak scalability, and platform related [10]. The network-based distance education mode integrates modern information technology and traditional education means, breaks the original space and time constraints, changes the original education mode by means of obtaining and using hundreds of millions of information resources on the Internet, becomes a great beneficiary in today's information age, and has been widely used in all kinds of middle schools and colleges [11]. The problems of low integration, obvious information reuse, and poor interaction of various information systems in colleges and universities are gradually emerging, which greatly affects the informatization process of college education [12]. Colleges and universities do not store educational resource information based on a unified standard, so it is impossible to establish an educational resource database that can be shared and used by all [13]. The emergence of service-oriented architecture provides a new solution for the development and integration of application systems, which can easily solve the difficulties of application system integration and expansion, so as to effectively solve the problems of tight coupling and weak scalability of educational resource management platform [14]. This paper decides to use technology to represent the metadata of educational information resources, discusses some key technologies, establishes the application model of technology-based metadata standardization in the development of educational resource database, and establishes the file-based transformation model in the standardization of educational information resources.

## 2. Related Work

Reference [15] proposed a plan to build cloud services for universities in order to improve the knowledge of computer science students in highly parallel computing practices to better cope with the emerging trend of large-scale distributed computing. Literature [16] proposed that the current construction of educational resource websites should focus on how to improve the sharing and utilization of existing resources, rather than continue to manufacture existing resources behind closed doors. Literature [17] proposes that information resources are regarded as the third national power on a par with natural resources and energy. The key and core task of national information infrastructure construction is the development and utilization of information resources. For its importance and urgency, it should be mentioned quite high to know. Reference [18] proposes that the education cloud can be regarded as taking cloud computing technology as the infrastructure, deeply merging and

integrating various educational resources and application services, and providing educational resources as services to users in the form of lease or free for users to use, to meet the needs of customers in teaching, scientific research, and daily office management. Reference [19] proposes the current typical network education resource management mode, namely, file catalog management, topic and subject website, resource management database, resource center, and distributed resource library system, and points out their basic characteristics and limitations

Literature [20] holds that all kinds of competent departments responsible for the construction of educational resources should set up resource construction expert groups, keep the original core set on the basis of the standardized norms promulgated by the state, and develop their own extended norm sets according to the scale, scope of application, and local specific conditions of resource library construction. Literature [21] points out that there is no unified standard model for educational cloud application service architecture at present. Facing the rapidly developing cloud application service, it is very necessary to design a comprehensive and effective architecture. Architecture design affects the stability, flexibility, and friendliness of cloud application software, which is of guiding significance for the implementation of educational cloud application service and solving key technical problems in the application process. Literature [22] puts forward the data model. In order to eliminate the behavior of each university building online educational resources alone, after unifying the standards, they can share these educational resources within the network. Its main core content is to formulate the relevant educational resource description standards according to different formats and types of educational resources. Literature [23] holds that as long as the business direction and content of the enterprise remain unchanged, the metadata within the enterprise is stable, and the data model composed of metadata is basically stable, while the processing method of metadata is variable. Therefore, all the output data in the system can be derived from these metadata, so as to meet the different needs of people for information systems and even data warehouses. Supporting variable processing methods with unchangeable data is the basic principle of information system engineering and the guiding ideology of information system construction. Literature [24] points out that the emergence of new technologies will always bring new inspiration and ideas to many applications, which is no exception in modern distance education. The emergence of this technology provides an effective solution for the standardization of online educational resources.

### 3. Methodology

*3.1. Metadata Management Technology.* Metadata is generally defined as data describing data. The main function of metadata is to use it as a structured information that can facilitate information retrieval, describe and interpret resources, and manage and operate information sources [25]. Metadata management is the core and basic work in enterprise data governance, and it is also the basis of enter-

prise data management. However, metadata is difficult to be parsed by computers, and it is impossible to carry out necessary interoperability and exchange through computers. Extensible markup language XML is one of the latest technologies on the Internet. The relationship between metadata and technology is reflected in the following aspects. (1) Metadata can be expressed conveniently. (2) The style language can be used to realize the transformation and display of metadata. (3) Metadata can be queried easily. (4) The industry has extensive support for technology. There are three types of metadata. The first is descriptive metadata, whose main function is to describe and identify information resources. The second is structured metadata, which is a kind of data that can store composite objects uniformly. The last one is management metadata, which is used to provide assistance for the appropriate management of a certain kind of information.

One of the great advantages of XML is that it is self-explanatory, because the structural information of the data set can be understood through the DTD and XML schema of the document. There are two main aspects about the transformation of metadata. On the one hand, metadata is converted to each other to share information, and on the other hand, it is converted to meet the output and display of various formats. The transformation method of the template is shown in Figure 1.

Template-based mapping method between XML documents and data structures in other formats, that is, embedding executable instructions in XML documents, these instructions are recognized and executed by the system during the conversion process, and the execution results are replaced to the positions where the instructions are located, thus generating the target XML documents. XML is a specification of computer-readable documents, which describes the data types and logical structure of documents in detail. One of its important features is that each user is allowed to arbitrarily mark or define labels on resources in his own webpage, and at the same time, users are allowed to nest information elements into any level, so as to ensure the uniqueness and standardization of information in his own webpage. Metadata information consists of two levels: metadata information describing the data itself and metadata information describing the relationship between data. The metadata information about the data itself mainly refers to some information only related to the data itself. If it is necessary to extract the core data elements of an educational resource, these core data elements are defined in the instruction program of the template. When the database system calls its own instruction execution program to execute the template, these data will be extracted and filled into the template. At this time, the template will become the final required corresponding XML document. Metadata is one of the important conditions to make data play a full role. It can be used for the establishment of data documents, data publishing, data browsing, data conversion, etc. It plays an important role in promoting the management, use, and sharing of data. Without metadata, the original data cannot be managed and used effectively.

*3.2. Design of Educational Resource Management Platform.* The application service architecture of education cloud

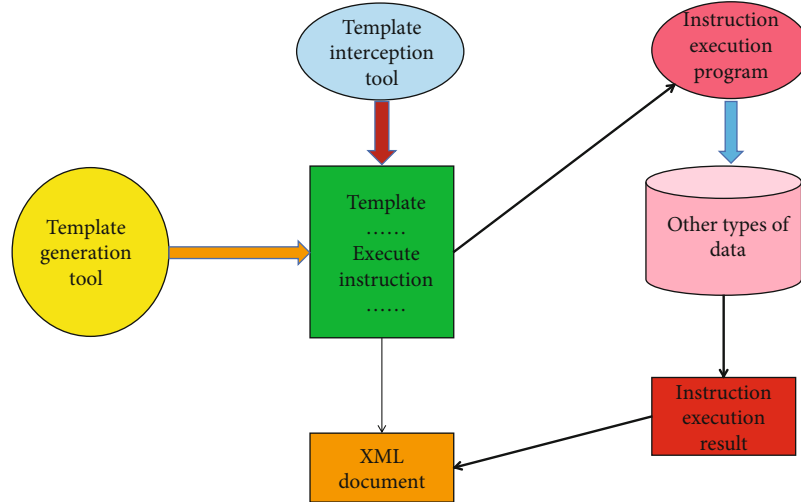


FIGURE 1: Template-based conversion method.

platform is mainly divided into three functional modules: unified identity authentication, application service management platform, and business process dynamic configuration. The scoring of resource retrieval results is the key to display the performance of the design system, and its calculation formula is

$$\text{idf}(t) = 1 + \lg \left( \frac{\text{numDocs}}{\text{docFrep} + 1} \right). \quad (1)$$

Calculate the similarity of two strings using the Dice coefficient:

$$\text{Dice}(s_1, s_2) = \frac{2 \times \text{comm}(s_1, s_2)}{\text{leng}(s_1) + \text{leng}(s_2)}. \quad (2)$$

Sort all subnets in the hardware resource by their closest distances to subnet b1 from near to far:

$$\sigma_q = \sqrt{\frac{1}{n} \sum_{i=1}^n (x_i - \mu)^2}. \quad (3)$$

Calculation formula of metadata storage lifetime:

$$T = \alpha N_s + \beta N_m. \quad (4)$$

The metadata distribution balance is measured by the metadata distribution balance, and its formula is described as

$$F_{DB} = \sqrt{\frac{1}{N-1} \sum_{i=1}^N \left( \frac{x_i}{S} - 1 \right)^2}. \quad (5)$$

The probability  $N_m$  that a metadata cache item is accessed by a new user can be calculated as

$$N_m = \frac{\sum_{i=1}^n P_i}{t}. \quad (6)$$

The purpose of the unified resource management platform is to realize the sharing of educational resources, completely break the barriers of remote and heterogeneous storage of resources, and avoid information islands. The platform uses the unified resource metadata standard to standardize resources, so as to realize the unified description and management of resource metadata. The unification of metadata provides necessary tools and links for the sharing and integration of distributed and heterogeneous educational resources. The educational resource management platform is shown in Figure 2.

The main function of the metadata editing module in the management platform is to manage the data in the system, which is mainly responsible for inputting, modifying, and deleting the data in the management platform in the form of ontology. Metadata storage module is mainly responsible for ontology-based resource pattern storage; the main function of metadata retrieval module is intelligent retrieval of ontology resources based on semantics. Read-write performance is an important index to measure the real-time efficiency of storage algorithms. It is tested by reading-write rate, as shown in Figure 3.

Enable users to write metadata at the same time. The comparison results of write data rates of this algorithm, hash storage algorithm, and random walk storage algorithm are shown in Figure 4.

At present, the popular Spring Boot architecture is used for background development, and Vue.JS is used for foreground interface development which mainly includes (1) front-end display layer, which uses Vue.JS+ browser to provide user interface; (2) access control layer, responsible for user post management, service monitoring, exception log, login authentication, and other control functions; (3) business logic layer, which provides business functions including public metadata management, database metadata management, and service interface metadata management function modules and is responsible for the input management of metadata in their respective fields; at the same time, this layer provides unified public technical components including code automatic generation, metadata check, impact

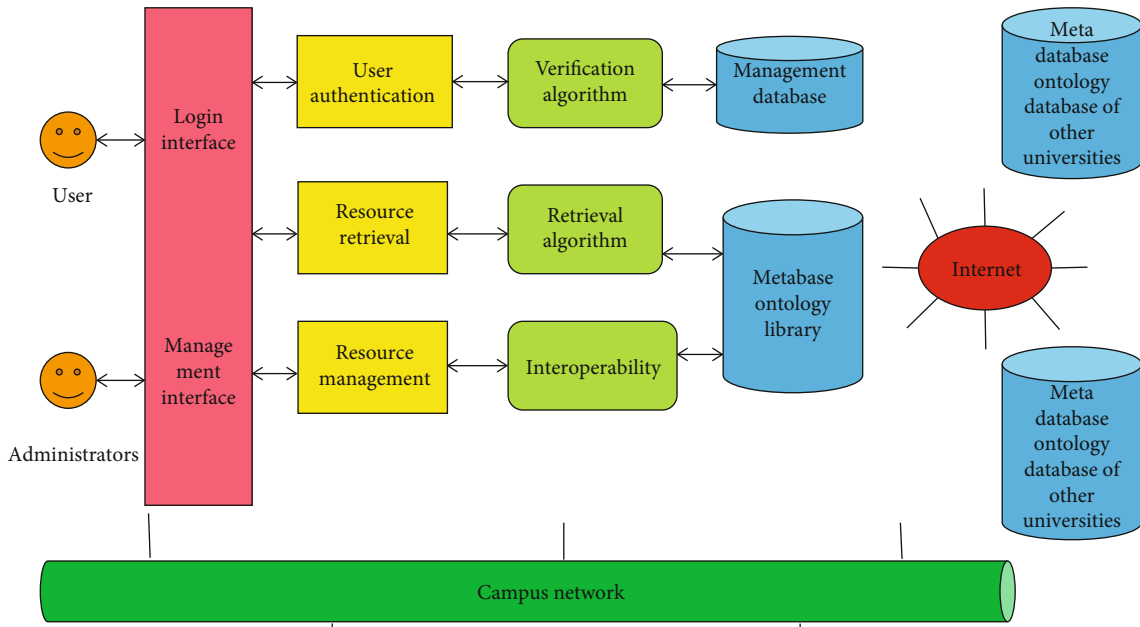


FIGURE 2: Framework of educational resource management platform.

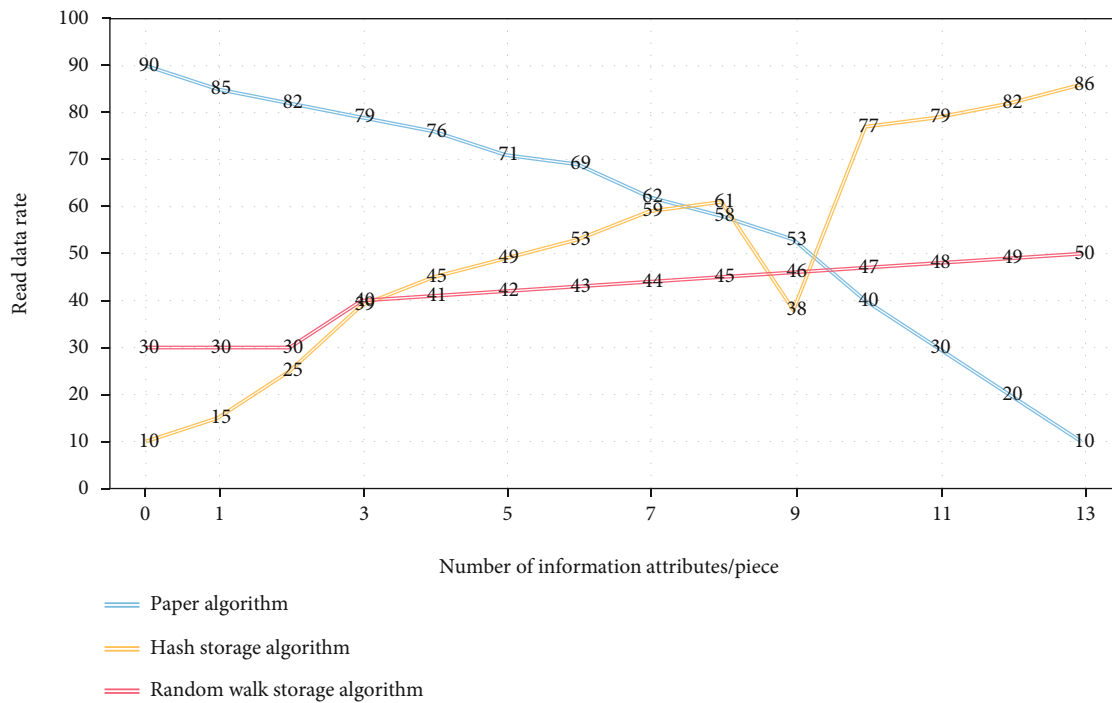


FIGURE 3: Comparison results of read rates of three algorithms.

analysis, and consanguinity analysis for unified use of upper functional modules; (4) data storage layer, which is the MySQL data and Redis cache. The performance of directory operation and file operation of our system and Gluster system based on ADSP algorithm is shown in Figure 5.

The file operation performance is shown in Figure 6.

The catalog metadata read performance is shown in Figure 7.

It can be seen from the actual demand for standardization that the demand for standards promotes the development of technical specifications, while realizing the standardization of resource attribute annotation and classification system realizes the sharing of resources, improves the interoperability of system design, and enables the sharing of educational information resources to the greatest extent, so as to ensure the efficient utilization of educational resources.

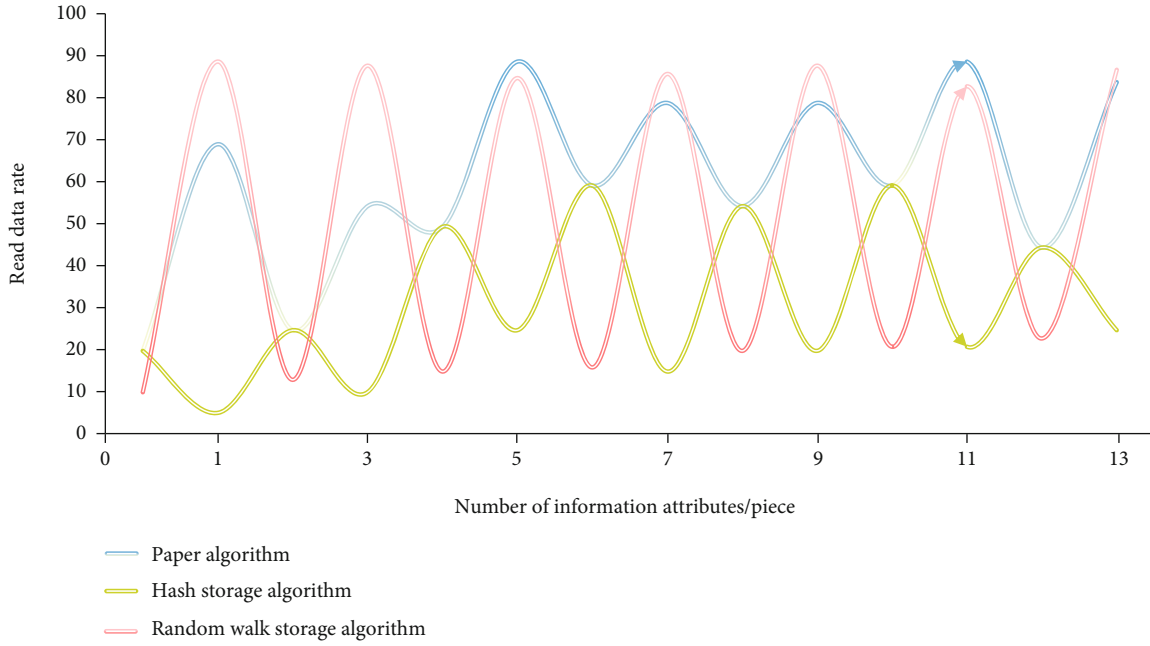


FIGURE 4: Comparison results of the write rates of the three algorithms.

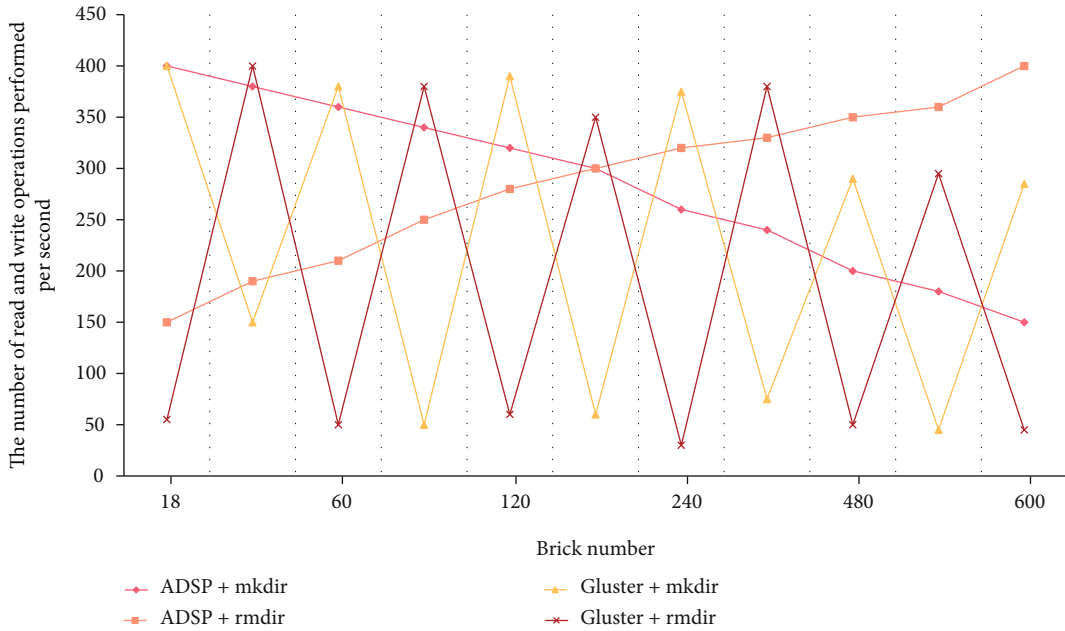


FIGURE 5: Directory metadata write performance.

The characteristics of relational database establish a series of regulations, and then use these regulations to store educational resource information knowledge in the form of ontology, and then use the rule association ability in relational database to manage data information through management ontology. In service architecture development test, the main part of automation test is the automation test of service interface, which usually requires testers to manually write cases according to the developer's interface definition. If the interface written by the developer cannot be effectively synchronized with the tester's case, the test is invalid. Realize the

data exchange between different resource databases, achieve the sharing of educational resources in a wide range, and ensure the smooth implementation of resource construction and the efficient utilization and sharing of educational resources in a regional range. Now, the development trend of metadata standards is to make their own standards more comprehensive. The educational resource metadata management platform metadata a large number of resource data collected in the field of education and distributed in different schools and creates, classifies, controls, accesses, and maintains them so that they can be stored and managed in a



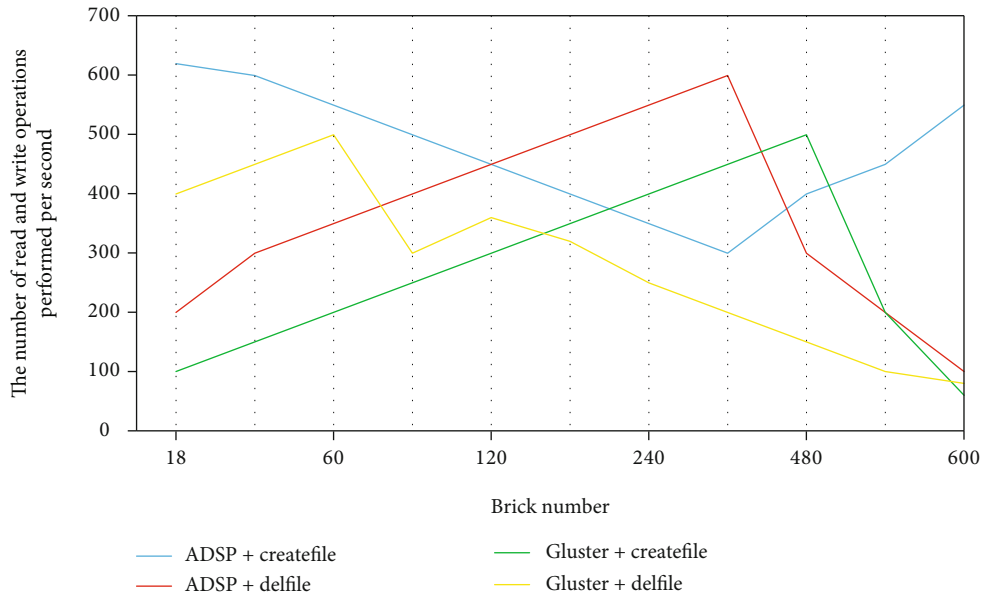


FIGURE 6: File metadata write performance.

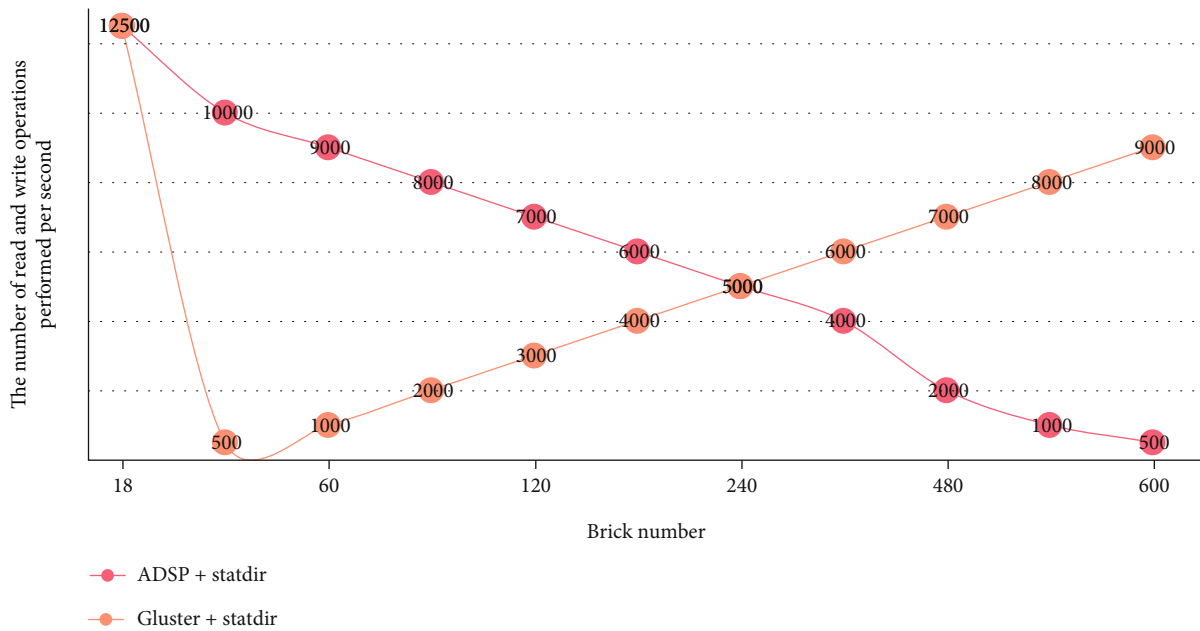


FIGURE 7: Read performance of catalog metadata.

unified and standard format. When formulating updated standards, they should not only keep up with the development of the times but also refer to each other. As a result, although it is impossible for everyone to unify their standards, they can certainly be consistent to a great extent in some specific industries so that everyone’s metadata records can be easily converted to each other. When combined with automated testing tools, the platform provides the query function of microservice interface definition. The automated testing tools automatically read the interface defined by the metadata management platform and automatically generate interface cases, which improves the efficiency of interface case writing.

#### 4. Result Analysis and Discussion

4.1. Problems with Educational Resource Banks. (1) There is too much information in resources. Originally, it is the advantage of modern distance education. For users, the greater the amount of information means more choices. (2) However, when the amount of information exceeds a certain limit, this advantage becomes a disadvantage, and users are easy to get lost in the face of the huge amount of information they retrieve. Because users use multiple systems, it is possible that users in these systems use the same password. Once the password of one system is leaked, it is

likely that other systems will also be attacked by security. (3) All user passwords are stored in the authentication system. If the authentication system is attacked and the password file is stolen by the attacker, all user information and system security will be seriously threatened. With the increase of educational resources, the heterogeneity of educational resource management platforms, and the distributed storage of educational resources in colleges and universities, the sharing of resources is a key issue for the large-scale construction and operation of educational resources. For user management, it is role-based management. Each user has a certain role, and different roles have different permissions, so different operations are carried out. Because this platform is specific to educational resources, it has its particularity, that is, the information of institutions of resources. Different users of the same role may belong to different institutions, so the available resources may be different. The research in the field of metadata description and ontology has achieved mature theories and certain achievements, but there is still a long way to go to fully realize all functions. A large amount of information redundancy has a great influence on maintaining the consistency of information. At present, a complete and easy-to-understand tool and example has not been developed. Because the network is too large, the feedback cycle of the effectiveness of development results will be longer for developers, which is not conducive to the analysis of research results

If metadata cannot be managed uniformly and a unified metamodel cannot be formed, a unified “language” cannot be formed between micro services, and data communication and interaction cannot be completed. Because of various factors such as resource form and style, each site implementing distance education repeats the resources that have been built by many other sites to a certain extent. Only the effective management of educational resources can ensure the service quality of educational resources. However, the inherent characteristics of educational resources, such as complex content, diverse forms, and wide distribution, make the management of educational resources a thorny problem. Therefore, we must define a reasonable management model in order to realize the effective management of educational resources. The information resources in the network are stored in a decentralized way, resulting in too many file formats; users are not familiar with the file format, so it is too inconvenient to call or even read out. There are also reasons for the privacy of the file. In order to ensure the security or interests of the information, the information content is encrypted or restricted, which hinders the user’s retrieval of the information. Of course, the most important point is that there are a lot of irrelevant information in the network, resulting in too long retrieval time and so on. Educational resources are a project that needs to invest a lot of human and material resources for a long time and need continuous maintenance after completion. In addition, due to the different knowledge between disciplines, nouns and terms cause heterogeneous attributes, which causes great inconvenience to the later maintenance work. Due to the characteristics of the technology itself, through the binding of the attributes of educational resources, the content-based directional

retrieval of resources can be realized, so as to improve the search efficiency on the Internet, provide a standard file exchange format, provide a standard interface for the exchange of data between different systems, and so on.

*4.2. Application and Significance of Metadata Management Platform.* The educational resources mentioned in this paper mainly refer to the data information in the network. Its main work content is to obtain the information in the network, obtain the results after logical reasoning, and provide the results to users after user retrieval. Compared with the existing system, the design system has more concurrent users and higher scores of resource retrieval results, which fully shows that the design system runs better. The overall implementation of the application service architecture of the education cloud platform first introduces the functional structure of the whole architecture, then introduces the implementation of cloud service management and application service creation in the application service architecture, and finally verifies the functions in the architecture through an implementation example. The description information of educational resources can be managed centrally. By standardizing the description information of educational resources to form a unified metadata information structure and registering the nondata information in a few resource publishing management centers, the unified management of educational resource metadata can be realized. The advantage of this is that it not only solves the phenomenon of “information island” but also does not damage the interests of resource providers. Through the centralized management of resource metadata, it solves the contradiction between centralization and decentralization, realizes the “distributed storage and centralized management” of educational resources, and achieves the effect of “one registration and sharing everywhere.” Predict the results, analyze the problems that may be encountered in the construction of each model, and find the inevitable relationship between ontology and educational resources. Finally, after clarifying the complete functions of each model, they are combined and tested to ensure the normal operation of the management platform. The application of metadata system in educational resources is shown in Figure 8.

The metadata management platform provides external metadata query functions, including service interface query, standard field query, and database script query. Therefore, metadata management can be incorporated into software development processes such as automated testing or continuous integration and called and then integrated into unified development process management. The system has the characteristics of low cost, easy realization, reliable data transmission, and low power consumption, which greatly reduces the difficulty of realizing remote monitoring, and is very convenient to install, maintain, and manage, avoiding many disadvantages of traditional remote systems in the past and representing the development trend of the system towards wireless networking. When publishing resource information, that educational resource server can generate document containing resource information according to the standard, and any authorized client can compile his own application to obtain the information. In this way, the

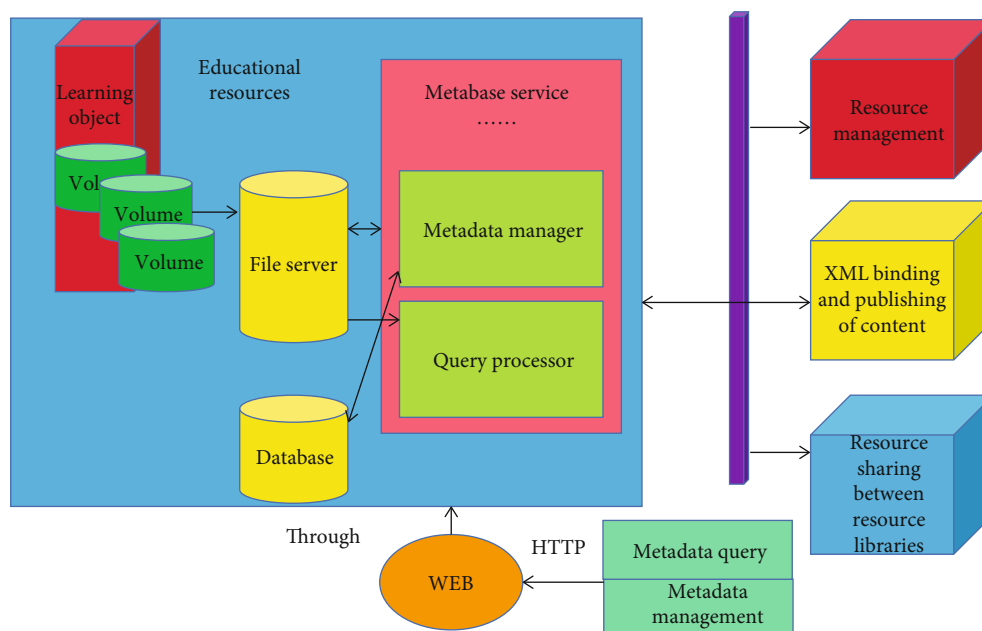


FIGURE 8: Application of metadata system in educational resource library.

established standards can be easily applied to the extraction, publication, and query of resource information. Realize the exchange of data between different resource banks, achieve the sharing of educational resources in a wide range, ensure the smooth implementation of resource construction, and make efficient use and sharing of educational resources in the region. The main advantages of building a good educational resource database are as follows: it can screen the school's teaching resources, filter out the information that is not conducive to learning in the network, and ensure the security of school educational resources. It can realize the sharing of educational resources among schools, avoid the phenomenon of repeated development, and ensure the multidirectional development of academic research by saving human and material resources. It can provide great help for students' learning so that students can obtain knowledge without the restrictions of regions, schools, and grades, ensuring the development of education in a more balanced direction and cultivating more excellent students.

## 5. Conclusion

The design direction of ontology-based educational resource metadata is to realize network sharing and integrate the resources of various colleges and universities. However, because the current implementation conditions are not mature, especially the communication conditions of various colleges and universities which are insufficient, the operation of the test system can only be carried out in a LAN, and the sharing of network knowledge cannot be realized. This paper establishes the application system of metadata system based on XML in the standardization of educational resource database. The functions are as follows: (1) effectively help demanders describe, retrieve, and process information resources; (2) provide extended applications; and (3) realize efficient search on. This paper analyzes the problems faced

in the process of educational informatization, such as uneven distribution of educational application service resources, low utilization rate of resources, and repeated development of service tools, and expounds the important role of building a reasonable application service architecture to realize scientific and reasonable educational informatization. By analyzing the current situation of the existing educational resource management platforms in colleges and universities, this paper puts forward the way of metadata sharing, standardizes the metadata of educational resources to make it meet the standards, and then uniformly registers and manages the metadata. All users' operations on resources are based on metadata, which solves the problems of distributed storage and heterogeneity of educational resources. This paper studies the management of metadata under service and develops a metadata management platform suitable for service development mode. It improves the metadata management level under the service and the design and development efficiency of the application system, improves the phenomenon of nonstandard service design, and promotes the data governance of the education platform to move forward to "consistency, standardization, openness, and sharing." It greatly improves the number of concurrent users and the score of resource retrieval results, provides a more convenient resource query channel for users and colleges, and also provides a more effective means for the development of college education.

## Data Availability

The labeled dataset used to support the findings of this study are available from the corresponding author upon request.

## Conflicts of Interest

The authors declare no competing interests.

## Authors' Contributions

Jingbin Zhang designed this study. Jingbin Zhang and Tianxiang Qi performed the experimental work and wrote the manuscript. Tianxiang Qi provided the majority of statistical analysis as well as provided the figures and tables for the manuscript. All authors read and approved the final manuscript.

## Acknowledgments

This research was supported by the Xi'an Fanyi University Online Course Construction Project in 2021 (ZK2143), the Classic Courses in Shaanxi Province (ZSK2102), the first batch of network ideological and political work research topics and practice project in Shaanxi University (2021SPWSXM-Z-8), and the Shaanxi Undergraduate and Higher Continuing Education Teaching Reform Research Project in 2021 (21BG050).

## References

- [1] J. Rao, T. Ao, K. Dai, and X. Zou, "ARCE: towards code pointer integrity on embedded processors using architecture-assisted run-time metadata management," *IEEE Computer Architecture Letters*, vol. 18, no. 2, pp. 115–118, 2019.
- [2] L. Huang, C. Zhang, and Z. Zeng, "Design of a public services platform for university management based on microservice architecture," *Microsystem Technologies*, vol. 27, no. 4, pp. 1693–1698, 2021.
- [3] Z. Zheng-Ping, P. Ren-Fang, C. Zhe, L. I. Gong-Quan, and Z. H. Guo-Sheng, "Analysis on cloud data service platform for digital oilfields," *Journal of Digital Information Management*, vol. 14, no. 6, pp. 413–422, 2016.
- [4] Y. Hara and D. Karagiannis, "Serviceology for services," in *5th International Conference, ICServ 2017, Vienna, Austria, July 12-14, 2017, Proceedings*, pp. 202–214, Vienna, Austria, 2017.
- [5] J. Wang and S. Wang, "Research on architecture design of urban comprehensive management service platform," *E3S Web of Conferences*, vol. 236, article 03023, 2021.
- [6] X. Wang and S. Li, "Design and implementation of special education school management platform based on SOA architecture," *Scientific Research Management*, vol. 42, no. 5, pp. 2084–2090, 2017.
- [7] A. Gregory, "Service-learning and social justice in architecture education: teaching students to design for the "other,"" *The International Journal of Design Education*, vol. 14, no. 1, pp. 55–71, 2020.
- [8] L. Favario and E. Masala, "A new architecture for cross-repository creation and sharing of educational resources," *International Journal of Emerging Technologies in Learning*, vol. 12, no. 2, 2017.
- [9] B. D. Valenzuela, O. G. Fragoso, R. Santaolaya, and J. Munoz, "Educational resources as learning web services, an alternative point of view to learning objects," *IEEE Latin America Transactions*, vol. 15, no. 4, pp. 711–719, 2017.
- [10] I. Lakshmi, "A competitive study on clouds computing, service orientation architecture and web services in enterprise network application," *Journal of Computer Networking, Wireless and Mobile Communications*, vol. 9, no. 1, pp. 47–62, 2019.
- [11] Z. Krajcso, "Classification and quality criteria for open educational resources in the field of foreign language learning," *Journal of Language and Cultural Education*, vol. 4, no. 1, pp. 48–59, 2016.
- [12] D. Töpfer and F. Isensee, "From «school buildings» to «school architecture» – school technicians, grand school buildings and educational architecture in Prussia and the USA in the nineteenth century," *Historia y Memoria de la Educación*, vol. 13, no. 13, p. 375, 2020.
- [13] M. Y. Parfenova, "Structural synthesis profile service-oriented it architecture," in *Educational Resources and Technology*, pp. 64–71, Moscow Witte University, 2016.
- [14] R. Nasim, H. Ullah, S. S. Rizvi et al., "A cloud-based enterprise resource planning architecture for women's education in remote areas," *Electronics*, vol. 9, no. 1758, 2020.
- [15] Z. Chen, "A distributed distribution and scheduling algorithm of educational resources based on vector space model," *International Journal of Emerging Technologies in Learning (iJET)*, vol. 14, no. 4, p. 58, 2019.
- [16] Y. Zhao and S. Shan, "Online learning support service system architecture based on location service architecture," *Mobile Information Systems*, vol. 2021, no. 7, p. 11, 2021.
- [17] K. Parthiban and R. V. Nataraj, "Exploration of service oriented architecture for online course registration," *Journal of Computational and Theoretical Nanoscience*, vol. 15, no. 5, pp. 1629–1633, 2018.
- [18] K. A. Froeschl, "Metadata management in official statistics—an IT-based methodology approach," *Austrian Journal of Statistics*, vol. 28, no. 2, p. 49, 2016.
- [19] P. Acosta-Vargas, W. Esparza, Y. Rybarczyk et al., "Educational resources accessible on the tele-rehabilitation platform," in *Advances in Intelligent Systems and Computing*, I. L. Nunes, Ed., vol. 781 of Advances in Intelligent Systems and Computing, pp. 210–220, Springer, Cham, 2019.
- [20] M. Bustos-López, G. Alor-Hernandez, J. L. Sanchez-Cervantes, M. del Pilar Salas-Zarate, and M. A. Paredes-Valverde, "EduRP: an educational resources platform based on opinion mining and semantic web," *Journal of Universal Computer Science*, vol. 24, no. 11, pp. 1515–1535, 2018.
- [21] C. B. Leng, K. M. Ali, and C. E. Hoo, "Open access repositories on open educational resources," *Asian Association of Open Universities Journal*, vol. 11, no. 1, pp. 35–49, 2016.
- [22] A. S. Sabitha, D. Mehrotra, A. Bansal, and B. K. Sharma, "A naive Bayes approach for converging learning objects with open educational resources," *Education and Information Technologies*, vol. 21, no. 6, pp. 1753–1767, 2016.
- [23] D. Linstedt, *Data Vault 2.0, Metadata Management*, 2016.
- [24] M. Walz, M. Kolodziej, and B. Madsack, "Radiologisches dosis- und metadatenmanagement," *Der Radiologe*, vol. 56, no. 12, pp. 1079–1086, 2016.
- [25] I. Staribratov, E. Angelova, and V. Arnaudova, "Education on human resources management in school with distributed platform for electronic learning dispel," *Knowledge International Journal*, vol. 28, no. 3, pp. 951–957, 2018.

## Research Article

# Design of Remote Real-Time Monitoring and Control Management System for Smart Home Equipment Based on Wireless Multihop Sensor Network

Chen Su and Wenting Chen 

Hubei University of Technology, Wuhan, Hubei 430068, China

Correspondence should be addressed to Wenting Chen; 201910980@hbut.edu.cn

Received 10 March 2022; Revised 11 May 2022; Accepted 17 May 2022; Published 8 June 2022

Academic Editor: Wen Zeng

Copyright © 2022 Chen Su and Wenting Chen. This is an open access article distributed under the Creative Commons Attribution License, which permits unrestricted use, distribution, and reproduction in any medium, provided the original work is properly cited.

With the intensification of the pace of modern urban life and the increase of work pressure, people have higher requirements for the safety and comfort of home. However, the rapid development of Internet of Things technology, wireless communication technology, embedded technology, and data fusion technology has made this desire possible, thus making intelligent and safe. Using wireless sensor network, intelligent home system can realize the real-time collection of object location and state information, remote operation of home equipment, as well as the monitoring of the information of personnel activities, etc. However, how to efficiently analyze and integrate these information to be applied to the intelligent home system is one of the problems that need to be solved; further study of the smart home system of personal behavior identifies fire monitoring and remote monitoring of mining applications. Such information collection and integration of technology and method are given based on wireless sensor network transfer of key technologies; intelligent home security monitoring system based on Bayesian networks is proposed and a card. According to the theoretical fire monitoring method, and based on the Bayesian belief network personal behavior identification model, this paper provides the theory and method for the remote safety monitoring and control in the intelligent home environment. In this paper, based on the multisensor data fusion of smart home security, real-time monitoring alarm platform is built. Through the multisensor detection module for the home fire gas human infrared monitoring, the detected data is transmitted to the data fusion center for processing; processed results are uploaded to the cloud through the Internet. When abnormal conditions occur, users can log in to the mobile phone client to view abnormal alarm results.

## 1. Introduction

At present, living environment occupies the vast majority of people's life; especially after busy work, people want to relax and enjoy from home [1]. Nowadays, with the continuous development of Internet of Things technology, embedded technology, data integration technology, and wireless communication technology, intelligent home life is no longer out of reach luxury goods. It is slowly into more and more people's family life. In enjoying the smart home that brings comfort intelligent experience at the same time, more and more people

are not only concerned about the living environment quality and comfort degree; security awareness has been strengthened [2]. Therefore, building intelligent home security early warning system in the home is of great significance to protect the personal and property safety of users. With the acceleration of social information, the relationship between people's work and life and communication and information is increasingly close. Information society is changing people's way of life and work habits at the same time but also put forward a challenge to the traditional housing. Intelligent household emphasizes person's subjective initiative, controlled by two-way

interactive way, and realizes the person and environment coordination [3, 4], to build low-carbon environmental protection and energy-saving homes.

Smart home provides a kind of intelligent residential conditions, combined with electrical home appliance control technology of wireless sensor network computer network embedded technology of wireless communication technology of computer network as a whole. Intelligent home system uses integration and automatic control technology, organic connection, and integration of each module in the home. As a whole, the wireless network transmits data to monitor the safety index in the home, and the switch control and lighting control of all kinds of household appliances can effectively make the living environment more comfortable and safe compared with the traditional residence; smart home not only provides users with a sense of security and high-quality and comfortable family life living environment, and also, from the original fixed structure into an automatic operation mechanism, by providing comprehensive information communication function, the family and the outside can maintain good information communication. With the development of China's economy and the increase of urbanization process, the number of urban population is also gradually increasing. For the city, new problems and challenges have also emerged in residential security. Household appliances in home life can bring convenience, but the hidden dangers have gradually attracted people's attention. In addition, the change of social environment also has a new impact on people's way of life, so people's demand for a perfect home security system is also more urgent. For the traditional form of civil air defense, security has been unable to meet the new needs of the times, so the concept of smart home with the fundamental purpose of providing a safe, comfortable, and convenient living environment has gradually emerged, and the safety monitoring system in smart home system has also become a key research part [5–7].

Therefore, people are constantly seeking ways to control and reduce disasters. Therefore, a reliable family security system has improved home security essentials [8]. With the development of network technology, video technology and computer technology widespread application, made from the technology Wireless remote monitoring has become possible this design of the home wireless remote monitoring system not only to the specific location of the family temperature gas concentration and vibration and other environmental indicators monitoring, can be real-time abnormal information saved in the database and can achieve sound and light alarm, but also through SMS alarm information sent to the finger [9]. At the same time, the user can also through the browser monitor the system for remote information visit to set up this kind of wireless remote monitoring system through a variety of information transmission channels and to achieve a comprehensive monitoring of the family environment, so as to provide a strong guarantee for the safety of family life and property.

Wireless sensor network (WSN) is a network composed of a large number of cheap wireline sensors. As the emerging next-generation network, WSN has changed the way of communication between human beings and the objective world and improved the ability of human beings to obtain information from the objective world.

At the same time, with the development of wireless sensor network, it will provide mankind with the most real, direct, and accurate physical information in the objective world in the next generation of Internet [10]. People can perceive the world more intuitively to obtain the corresponding information. Business week named it one of the most influential technologies of the century in its future technology report, and technology called it one of the top ten technologies that will change the world and one of the top three high-tech industries of the future. With the deepening of wireless sensor technology research, the application of wireless sensor network in smart home system has gradually become a research hotspot [11]. Intelligent home design for human is more convenient makes life more comfortable. The research of intelligent information home appliance and intelligent home system is becoming more and more important. It is of great significance to improve the quality of life of modern human beings and create a comfortable, safe, and convenient living space [12, 13].

The electrical condition monitoring system for network flow mainly adopts the access mode of single point total control and multipoint subcontrol when it is applied in smart home [14]. The choice of two working modes can be set according to the actual application needs. As shown in Figure 1, the energy-saving protection socket (PDU) based on the network flow probe is used as the main control device of the system to connect the management terminal host, the home wireless router, and the TV in the system. After the system is powered on, the subcontrol device is automatically connected to the Wi-Fi wireless network in the local area of the home through the wireless transmission module (NRF24L01), so as to realize data transmission with the master control device and the host of the management terminal [15].

Finally, the management terminal host analyzes and identifies the traffic data collected by the network traffic probe socket. Then, according to the identification results, the corresponding energy-saving protection socket is on and off control. Theoretically, the management terminal host should have low power consumption AC and DC power supply and other performance, so as to carry out power saving control and real-time feedback for household electrical appliances commonly used. It can be concluded from the above structure diagram that the application of network flow-based electric appliance status monitoring system in smart home mainly includes three parts: energy-saving protection socket (PDU) design based on network flow probe for general control, energy-saving protection socket design for subcontrol, and management terminal host system design. [16, 17].

## 2. Related Work

With the rapid development of China's economy, the increase of social floating population, the complexity of social security, burglary, and other crimes are rising, people pay more and more attention to the safety of life and property, and the traditional mechanical prevention theft has been unable to meet people's needs. Therefore, family security from civil air defense and technical defense two aspects, through the effective combination of two ways, to ensure the safety of people's lives and property [18]. In our country, the illegal invasion of

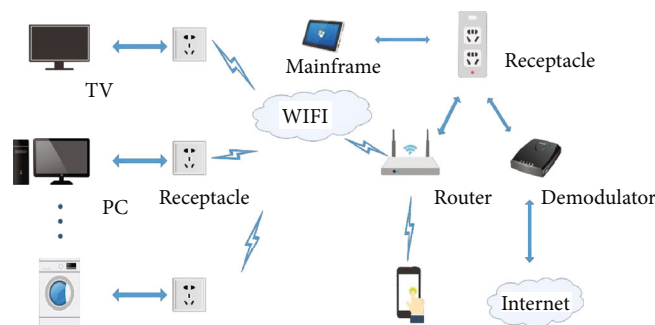


FIGURE 1: Schematic diagram of the second working mode of smart home application.

gas leakage fire alarm system is decades behind developed countries; it has experienced three stages of development; in the early few years for the early stage, our country began to start the significance on the research production of illegal invasion of leaking gas fire alarm products, and the application of it is mainly limited in special units. In the alarm product development stage, domestic manufacturers began with the large-scale imitation of foreign products and the introduction of foreign production technology; there is no real core technology. Since 2000, in order to improve the alarm products, with the accession of China, foreign enterprises began to enter the Chinese market in large numbers, bringing advanced production technology, while promoting the rapid development of the security industry and the maturity of the market in this period. China's alarm product enterprises quickly started, and some enterprises carried out technical cooperation [19]. Creating a lot of powerful businesses and even a lot of enterprises has been close to the world level; at present, security system has begun to enter all walks of life and security product brands on the market [20].

Smart home system is to adapt to the modern family's several activities to form a diversified network structure; the concept of wuya energy home is first proposed by the United States, Canada, Europe, Australia, Southeast Asia, and other economically developed countries. United Technology company applied the concept of building equipment information integration to the reconstruction of an old building in Hartford, Connecticut [21], using computer system to monitor and control the building's air conditioning, elevator lighting, and other equipment and provide voice communication, E-mail, and other information. Interest service, so far the first intelligent building, was born, opening the prologue of intelligent household development since the first intelligent building appeared in the world. The United States, Canada, Europe, Australia, Southeast Asia, and other developed countries have put forward a variety of intelligent household program. The United States, Germany, Singapore, Japan, and other countries have a wide range of applications [22]. The intelligent household in digital home and digital technology reform is an opportunity to focus on sense of luxury, comfort, and pleasure, but its energy consumption is very big and does not conform to the current worldwide low-carbon environmental protection and section derived from the concept of flow. Germany's

intelligence lives in pursuit of the development of special function pay attention to the basic functionality [23]. The South Korean government of intelligence can plot intelligent household to take a number of policy support. The provisions in the big cities such as new residential area of Seoul must have a smart home system, the new project of Korea national above the smart home system produced like Samsung and other well-known brand of smart home. The intelligent household design construction scale is the development of Japan with collectivization and is people-oriented, paying attention to function, giving consideration to future development and environmental protection, adopting a large number of new materials and new technologies, making full use of information network control and artificial intelligence technology, and realizing the modernization of housing technology [24]. The Prognostic and Health Management (PHM) technique was first proposed by the United States in the late 1990s as part of the JSF f-35 aircraft electronic equipment based military aviation field. In recent years, scholars and scientific research institutions in related fields in China are constantly exploring and developing PHM technology in military network, communication industry, construction, railway, electric power and other fields [25–27].

Although foreign remote control system has been developed relatively early, with leading technology and relatively perfect solutions [28], its configuration process is relatively cumbersome; taking the remote control system in the United States as an example, the first needs to manually select the module driver, followed by the associated module programming, but the number of modules is relatively large, it is difficult to complete its scheduled configuration in time, and the price of installing a set of remote control system abroad is very high [29]. Poor compatibility is not conducive to the widespread promotion and application of the system; international organizations need to specify a unified international standard. The United States in the end of the last century has wireless sensor network technology in military research and promotion application. Intel company is launched in the year for home care wireless sensor network system; the system will be a variety of sensors embedded in household appliances, through the wireless network [30]. The European Union pays more attention to the strategy and planning of Internet of Things technology in the future market, while the Japanese government takes the development of sensor network

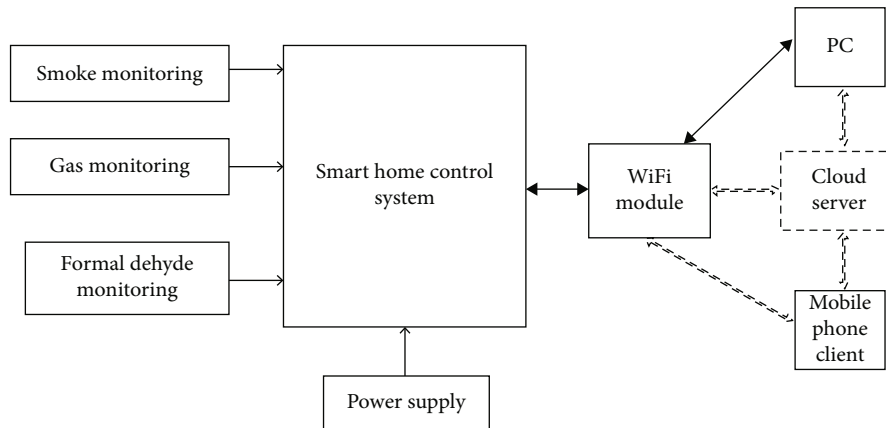


FIGURE 2: System structure block diagram.

technology as one of its key strategies, strengthening the application of Internet of Things technology in medical transportation and environmental monitoring and other fields.

The one-day Shanghai World Expo was successfully held. The scenes of smart home for better city and life were everywhere, such as various robots in the Japan pavilion, cooking robots in the Shanghai united pavilion, future urban life displayed in the future pavilion, smart connected life displayed in the cisco pavilion, smart grid and smart home life displayed in the state grid pavilion, and future low-carbon intelligent life displayed in one world. Shandong pavilion shows higher household life wisdom without one not in smart home of a better life [31]. The composition of different types of sensors, such as seismic sensors, photosensitive sensors, and image sensors, can collect corresponding data according to the needs of different applications. For example, sensor nodes such as temperature, humidity, and nuclear radiation diffusivity can be detected through continuous data acquisition events, event identification location detection and nodes control, and other operations; the processed information will be fed back to the base station, while the characteristics of wireless greatly reduce the workload in the deployment and maintenance side, which is mainly applied in the following fields [32].

Multisensor fusion technology as an emerging discipline has been put forward in the early 1980s which began as a military application, dedicated to fighting on enemy target location positioning as well as the enemy army things to collect for abroad, such as the concept of multisensor data fusion first and foremost in the military. At present, data fusion has been applied by many related links, such as marine surveillance, air defense, battlefield reconnaissance and surveillance, target acquisition, and strategic defense, in the United States, Britain, Japan, Germany, Italy, etc. At present, countries have developed some highly practical data information fusion systems in the early 20th century; the United States carried out research on sonar signals with the support of the Department of National Defense, which can be regarded as the earliest research on data fusion. In the early 20th century, the U.S. Department of Defense officially included the concept of data fusion in its white paper. After entering the 21st century, multisensor data fusion technology has been studied in the United

States as the core technical means in many fields. Compared with foreign studies, the domestic research on multisensor data fusion started relatively late at present. For multisensor data fusion, research is still in the primary stage, most still draw lessons from foreign advanced technology about this on the one hand, and there is no more for the further research of multisensor data fusion and more research on the application of data fusion technology. And at present domestic about some automation control system, large. However, with the rapid development of sensor technology and the increasing number of sensor types, China will invest more energy in the research of multisensor data fusion.

### 3. The Wireless Multihop Sensor Network-Based Smart Home Equipment Monitoring and Control Management System

*3.1. The Flow Chart of the Identification Method.* The main control chip of this system is single-chip microcomputer, through wireless sensor technology, real-time monitoring of indoor air quality index, and gas concentration, through Wi-Fi module and cloud server as communication solution; data can be sent to users' mobile APP remotely. Users can monitor indoor safety conditions in real time, such as whether there is gas leakage. The system structure block diagram is shown in Figure 2.

The positive and negative terminals of the 3.3V power module are, respectively, connected with the single-chip microcomputer and the sensor module and the VCC and GND pins of the ESP8266 communication module for power supply, which just serve as a Wi-Fi transmission. The output ports of the sensor module are, respectively, connected with the ports of single-chip microcomputer 14, 15, and 16 to transmit the monitoring signal to single-chip microcomputer 12 and 13 for identification. Pin Nos. (TX and RX) are, respectively, connected to RXD and TXD pins of ESP8266 module for data communication. Single-chip microcomputer and ESP8266 module are connected to download and debug PC firmware through USB to serial port. The client is identified and configured to communicate with the cloud server through Wi-Fi or



the Internet. The mobile client displays the transmitted data through the APP of the cloud server, and the PC displays the data through the web page of the cloud server.

**3.2. Multisensor Data Fusion Security Algorithm Model.** Generally speaking, the occurrence of abnormal events in the family is accidental, so no amount of security sample data can completely contain every abnormal situation in the home, especially the occurrence of fire in the security of smart home; the occurrence of fire is a complex process, and there are many uncertainties. Therefore, it is necessary to use the adaptive and self-learning characteristics of neural network to solve the problem of such accidental events. There are many structure types of neural network. In view of the complexity and uncertainty existing in the security of smart home, this paper selects the relatively mature BP neural network algorithm to fuse the data information collected by the security detection module:

$$f(x) = \frac{1}{1 + e^{-x}}. \quad (1)$$

The input of neuron of the  $j$ th hidden layer is

$$u_j^I = \sum_{i=1}^J (\omega_{ij} x_{mi} - \theta_j). \quad (2)$$

The output is

$$v_j^I = f(u_j^I). \quad (3)$$

Then, the input of neuron of the  $k$ th output layer is

$$u_k^K = \sum_{j=1}^J (\omega_{jk} v_j^I - \theta_k). \quad (4)$$

The output is

$$y_{mk} = v_k^K = f(u_k^K). \quad (5)$$

The output error of neuron of the  $k$ th output layer is

$$e_{\{mk\}}(n) = t_{\{mk\}}(n) - y_{\{mk\}}(n). \quad (6)$$

The sum of error energy of the system output layer is

$$E(n) = \frac{1}{2} \sum_{k=1}^K e_{mk}^2(n). \quad (7)$$

Then, the propagation of neural network error is opposite to the forward propagation process of neural network system signal, which is propagated from back to front. Therefore, in the error correction process of neural network system, the system will correct the weight and deviation from back to front. In the BP neural network algorithm, the error energy of the expected output is positively correlated with the partial derivative of the weight of the hidden layer and the output layer, i.e.,

$$\frac{\partial E(n)}{\partial \omega_{jk}(n)} = \frac{\partial E(n)}{\partial e_{mk}(n)} \cdot \frac{\partial e_{mk}(n)}{\partial y_{mk}(n)} \cdot \frac{\partial y_{mk}(n)}{\partial u_k^K(n)} \cdot \frac{\partial u_k^K(n)}{\partial \omega_{jk}(n)}. \quad (8)$$

According to the definition of the system and all known relations,

$$\begin{aligned} \frac{\partial E(n)}{\partial e_{mk}(n)} &= e_{mk}(n), \\ \frac{\partial e_{mk}(n)}{\partial y_{mk}(n)} &= -1, \\ \frac{\partial y_{mk}(n)}{\partial u_k^K(n)} &= f'(u_k^K(n)), \\ \frac{\partial u_k^K(n)}{\partial \omega_{jk}(n)} &= v_j^I(n). \end{aligned} \quad (9)$$

Accordingly, there are

$$\frac{\partial E(n)}{\partial \omega_{jk}(n)} = -e_{jk}(n) \cdot f'(u_k^K(n)) \cdot v_j^I(n). \quad (10)$$

## 4. Experimental Results and Analysis

**4.1. Introduction to Experimental Data Set.** The intelligent gateway is not only the outside network and network communication bridge but also the center of the data fusion processing with node collected by the abnormal data that needs to be transmitted to the intelligent gateway to analyze fusion processing data fusion center. Therefore, the data acquisition system of the intelligent data fusion center is very necessary. Therefore, the data acquisition system in this paper is transmitted to the intelligent gateway from the node end of the perception layer to ensure the integrity and availability of data.

Intelligent security gateway data fusion center receives the data acquisition end after the transfer of data information, gateway nodes need to perceive the information fusion processing the data collected, it is involved in the intelligent gateway platform for the design of the data fusion algorithm, and already in the third chapter is data fusion algorithm for security detection system. The model is introduced in detail. The system uses the method of combining BP neural network algorithm and fuzzy logic reasoning algorithm to fuse the data from the sensing node end. The BP neural network is the main judgment basis, and fuzzy logic reasoning is used for auxiliary judgment.

**4.2. Experimental Results Analysis.** The ESP8266 series wireless modules support standard IEEE802.11b/G/N protocol and complete TCP/IP stack; users can use this series of modules to add functionality to the existing devices or build separate network control systems. This system uses ESP8266-12F wireless communication module, which is an ultralow power Wi-Fi single-chip solution with the microprocessor core inside the Wi-Fi and microcontroller chip. ESP8266 has two usage schemes: one is to use the internal processor directly and through I/O. In addition, the ESP8266 module can be connected to a single-chip microcomputer and can

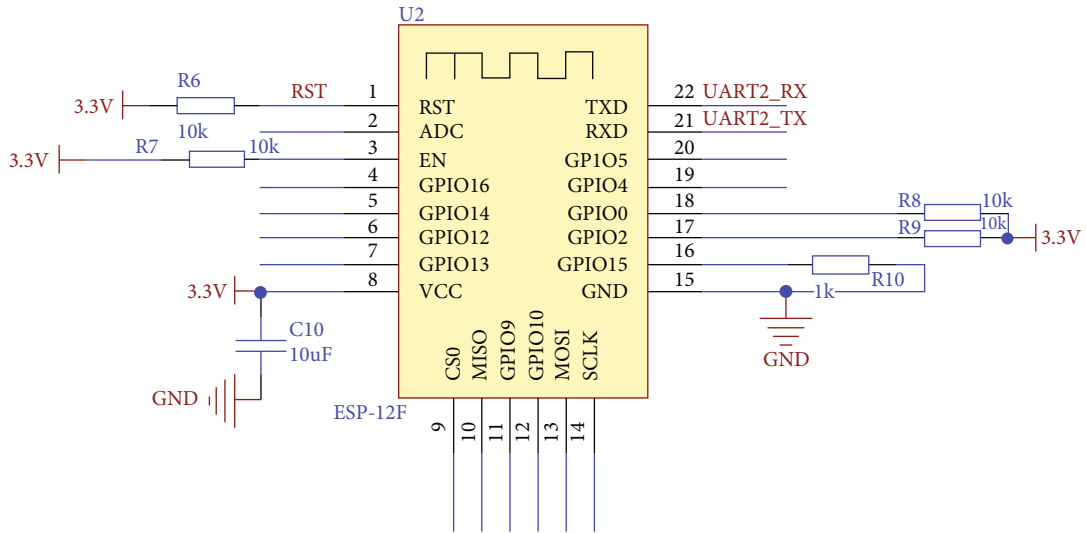


FIGURE 3: ESP8266 module schematic diagram.

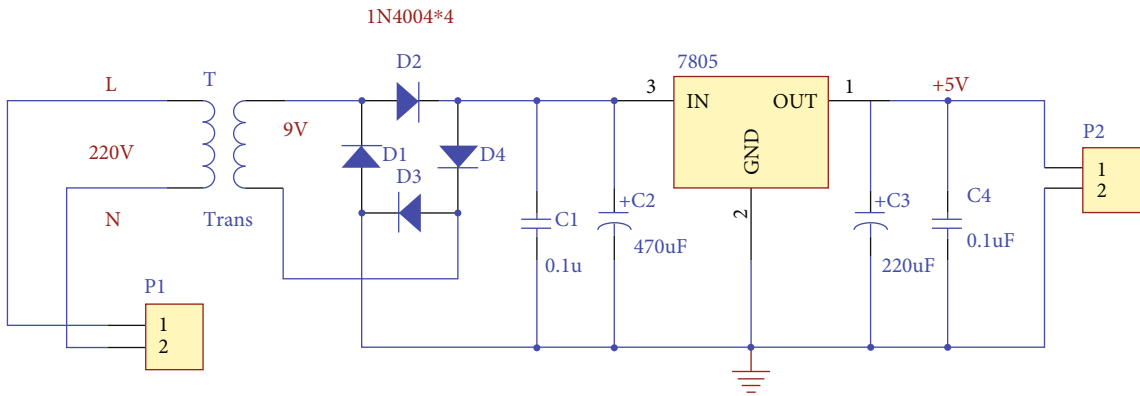


FIGURE 4: 5 V power output.

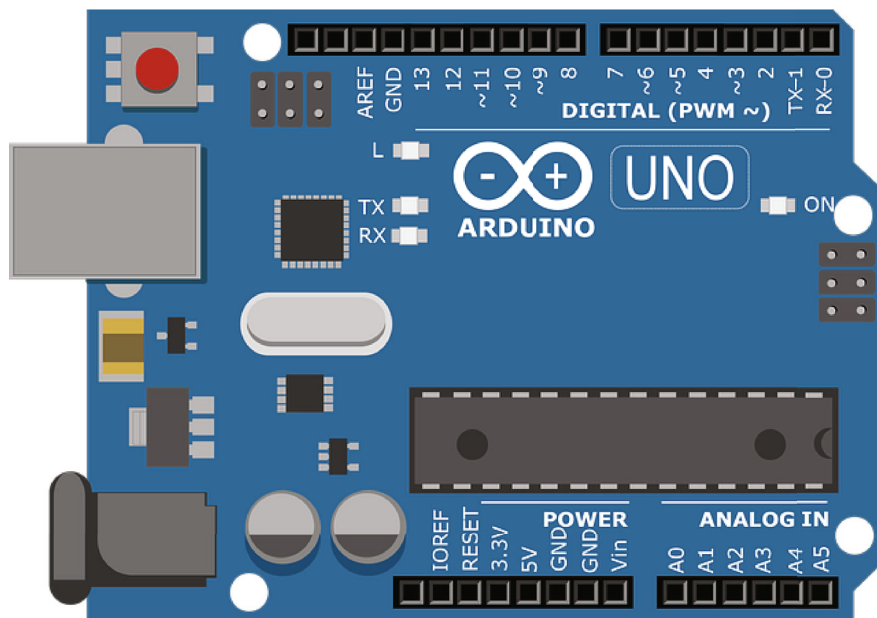


FIGURE 5: Arduino UNO control board experimental platform physical picture.

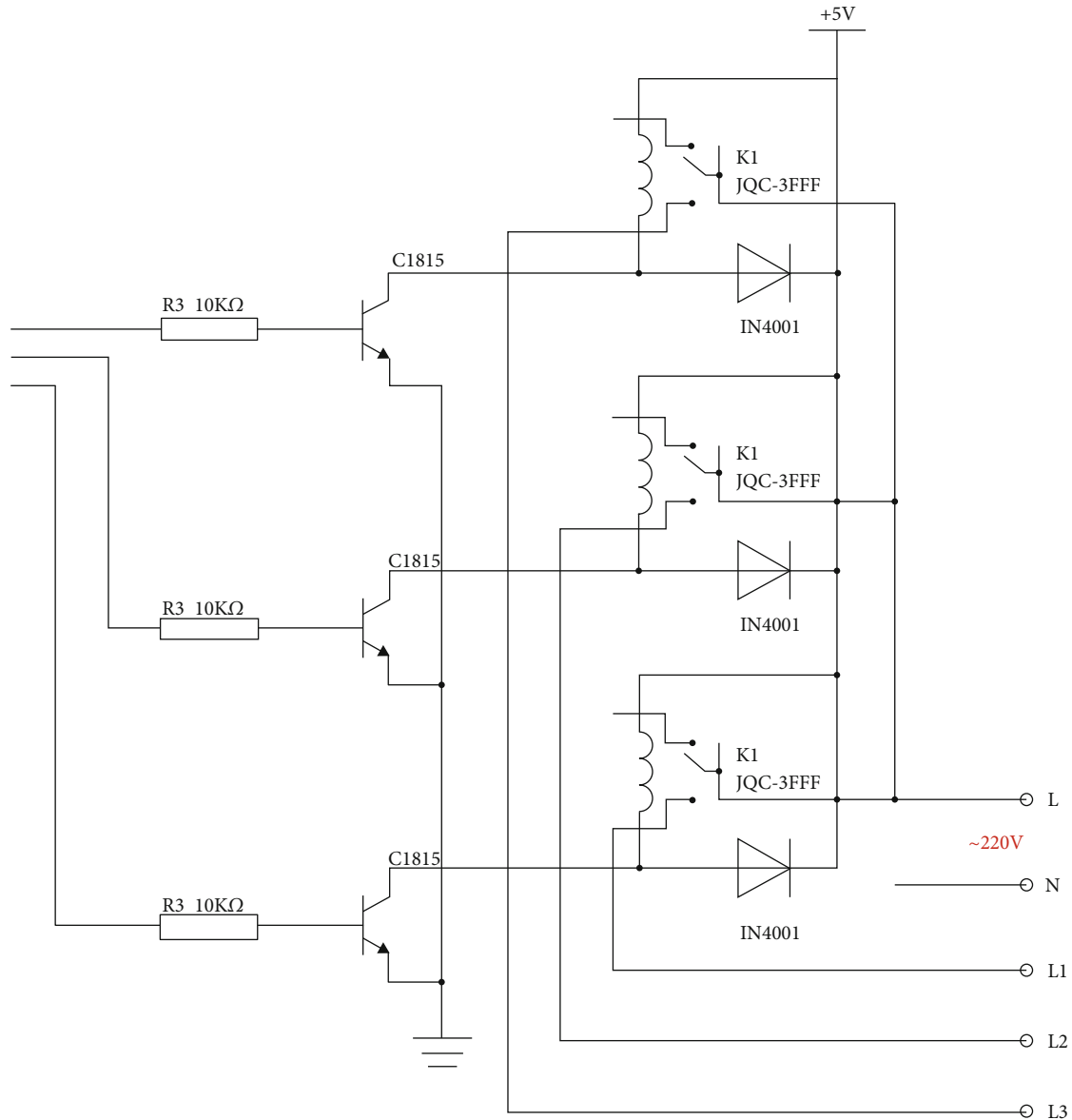


FIGURE 6: Circuit schematic diagram of relay switching module (three-way control).

be used for network-related tasks. It operates using AT commands and communicates with an external MCU through a serial port. The solution is fast and stable but relatively high cost. The ESP8266 wireless module has the following features: (1) ultrasmall 802.11b/g/N Wi-Fi SOC module; (2) low power 32 CPU, which can double the application processor; (3) main frequency up to 160 MHz; (4) Built in 10 bit high-precision ADC; (5) support the UART/GPIO IIC/PWM/ADC/HSPI interface; (6) integrated Wi-Fi MAC/BB/RF/PA/LNA; (7) support a variety of sleep mode and deep sleep current to 20  $\mu$ a; (8) embedded lwIP protocol stack; (9) STA/AP/STA+AP working mode; (10) Smart Config/Air Kiss one-click network configuration; (11) serial port rate up to 4 Mbps; (12) universal AT instruction quick start; (13) SDK support secondary development; and (14) support for serial port local upgrade and remote firmware upgrade (FOTA). The principle diagram of ESP8266 MCU is shown

in Figure 3, from which we know that ESP8266 module consists of multiple subsystems, and they work together to finish the monitoring task.

The system provides a stable DC 3.3 V for the microcontroller and its control of the peripheral circuit in the design of power supply. The voltage of 220 V AC passes through the transformer voltage changing bridge rectifier circuit, rectifier, and filter, and the capacitor passes through the three-terminal voltage stabilizer (7805) to obtain +5 V voltage, which is then stabilized to 3.3 V by the voltage regulator chip LM1117 to supply power to the single-chip microcomputer and other modules. The circuit diagram is shown in Figure 4. It can be seen that circuit diagram consists of multiple subsystems, and they work together to finish the monitoring task.

The main control chip of this system is STM32F103CBT6 microcontroller. With the cloud server as a communication solution, the data can be sent remotely to the user's mobile

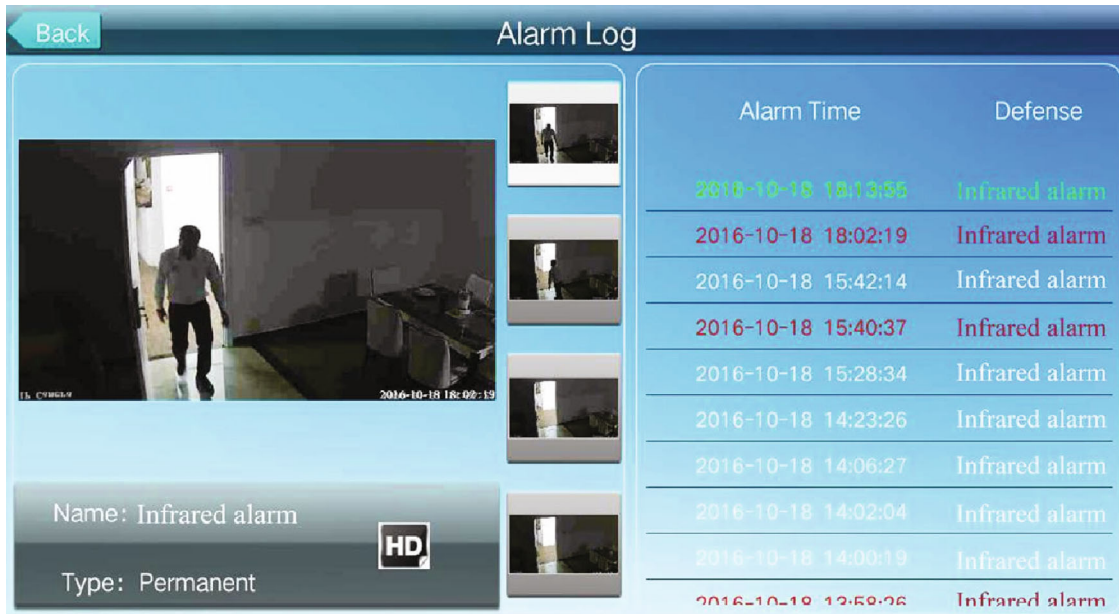


FIGURE 7: Infrared sensing measurement of human body.

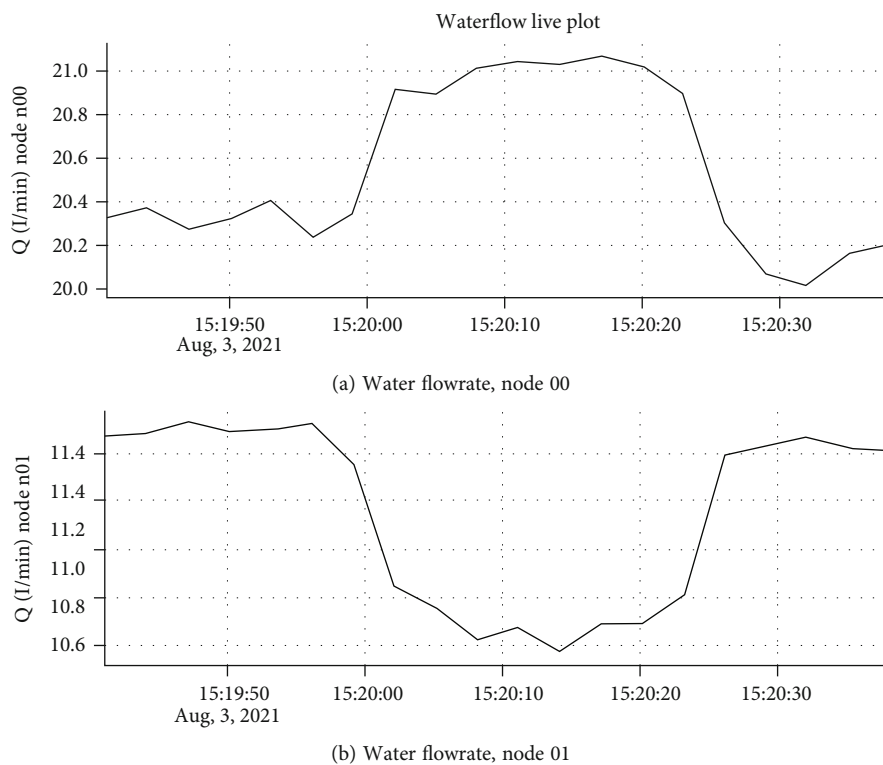


FIGURE 8: Water leakage monitoring alarm subsystem test results.

APP and the user can monitor the indoor security situation in real time. Arduino is the ancestor of open source sensor experimental platform. It is a collection of open source hardware middleware products and provides rich open source interface, compatible with a variety of generic sensor actuators on the market, and other programming methods are rel-

atively easy; you just need to simply master similar JAVA C language in function implementation related functions, and you can realize the program writing program is also very simple, only universal USB. In practical application, Arduino is most widely used in the field of smart home, as a unified access platform for sensors and actuators. Arduino can solve

problems such as heterogeneity of different sensors. It greatly reduces the development cost and improves the feasibility of smart home applications. In addition, Arduino has also been widely used in the field of robot environmental monitoring. The actual figure of the Arduino UNO control board experimental platform is shown in Figure 5. It can be seen from Figure 5 that Arduino UNO consists of multiple subsystems, and they work together to finish the monitoring task.

In this paper, JQC-3FF relay is designed to realize switching control of energy-saving socket power supply. PC0~PC3 pin output control signal of MCU drives the control end of relay. Corresponding relay module can also be configured according to the actual application situation to achieve multi-channel control. In order to ensure that the control signal output by MCU can drive the relay module normally, the triode should be connected to amplify the control signal. At the same time, a continuing-current protection diode is also designed below the relay to prevent the reverse induction current generated by the relay coil from damaging the triode and other original devices, as shown in Figure 6.

Human infrared perception test is mainly used to detect illegal entry of aliens. For example, when aliens steal, human infrared detectors are arranged in each main position of the home to carry out real-time monitoring. As shown in Figure 7, when someone enters, the system will set a screenshot of the person and provide relevant records.

The test results of water leakage monitoring and alarm subsystem are shown in Figure 8. The relationship between the probability of water leakage and time can be seen from the figure. Generally speaking, around 3:20 PM, the peak period of water leakage is detected quickly.

## 5. Conclusions

Nowadays, with the continuous improvement of people's living standards, in the pursuit of a comfortable, stable, and intelligent home life at the same time, people are more and more concerned about their personal and property safety. Therefore, this paper designed a set of intelligent home security scheme based on multisensor data fusion and proposed a neural network. The data fusion method combining complex and fuzzy logic reasoning is found to have certain reliability and feasibility through experimental simulation and actual testing. Compared with traditional security detection methods, the multisensor data fusion method has high detection accuracy and seldom has false alarm or missing alarm.

This kind of home system is a complex system engineering, involving communication computer automation architecture and other fields of technology. A lot of programs have been put forward, and the process of improving the home system research is very difficult. In this paper, there are many things needed to improve the place; the follow-up should focus on one concrete application and complete the various modules organically unified together, forming a transition of the prototype system. Although the system in this paper has more innovations and better application effects, how to use wireless sensor network to process big data in home furnishing is a subject worth studying in the future.

## Data Availability

The data used to support the findings of this study are available from the corresponding author upon request.

## Conflicts of Interest

The authors declare that they have no known competing financial interests or personal relationships that could have appeared to influence the work reported in this paper.

## References

- [1] B. Rahmadya, Z. Zaini, and M. Muharam, "IoT: a mobile application and multi-hop communication in wireless sensor network for water monitoring," *International Journal of Interactive Mobile Technologies*, vol. 14, no. 11, p. 6393, 2020.
- [2] H. Wang, "Sustainable data analysis framework of smart city based on wireless sensor network," *International Journal of Networking and Virtual Organisations*, vol. 25, no. 2, pp. 114–133, 2021.
- [3] J. Liu, Z. Zhao, J. Ji, and M. Hu, "Research and application of wireless sensor network technology in power transmission and distribution system," *Intelligent and Converged Networks*, vol. 1, no. 2, pp. 199–220, 2020.
- [4] Y. Cui, L. Zhang, Y. Hou, and G. Tian, "Design of intelligent home pension service platform based on machine learning and wireless sensor network," *Journal of Intelligent & Fuzzy Systems*, vol. 40, no. 2, pp. 2529–2540, 2021.
- [5] X. Zhu, "Complex event detection for commodity distribution Internet of Things model incorporating radio frequency identification and wireless sensor network," *Future Generation Computer Systems*, vol. 125, pp. 100–111, 2021.
- [6] M. Lewandowski and B. Płaczek, "Data transmission reduction in wireless sensor network for spatial event detection," *Sensors*, vol. 21, no. 21, p. 7256, 2021.
- [7] J. Jiang, H. Wang, X. Mu, and S. Guan, "Logistics industry monitoring system based on wireless sensor network platform," *Computer Communications*, vol. 155, pp. 58–65, 2020.
- [8] M. Kostrzewski, L. Filina-Dawidowicz, and S. Walusiak, "Modern technologies development in logistics centers: the case study of Poland," *Transportation Research Procedia*, vol. 55, pp. 268–275, 2021.
- [9] H. Zongjian, "Application of intelligent sensor technology in steady state operation of power system," *Converter*, vol. 17, no. 1, pp. 9–15, 2021.
- [10] M. U. Younus and S. W. Kim, "Proposition and real-time implementation of an energy-aware routing protocol for a software defined wireless sensor network," *Sensors*, vol. 19, no. 12, p. 2739, 2019.
- [11] J. Zhao and G. Li, "Study on real-time wearable sport health device based on body sensor networks," *Computer Communications*, vol. 154, pp. 40–47, 2020.
- [12] C. Zhou, X. Luo, T. Huang, and T. Zhou, "Function matching of terminal modules of intelligent furniture for elderly based on wireless sensor network," *IEEE Access*, vol. 8, pp. 132481–132488, 2020.
- [13] F. Tian, X. Long, and W. Liao, "Design of Smart home system based on basic radio frequency wireless sensor network," *International Journal of Online Engineering*, vol. 14, no. 4, pp. 126–136, 2018.

- [14] T. Kim and W. Chiu, "Consumer acceptance of sports wearable technology: the role of technology readiness," *International Journal of Sports Marketing and Sponsorship*, vol. 14, pp. 57–89, 2018.
- [15] P. Devan, F. A. Hussin, R. Ibrahim, K. Bingi, and F. A. Khanda, "A survey on the application of WirelessHART for industrial process monitoring and control," *Sensors*, vol. 21, no. 15, p. 4951, 2021.
- [16] T. Mahmood, J. Li, Y. Pei et al., "An intelligent fault detection approach based on reinforcement learning system in wireless sensor network," *The Journal of Supercomputing*, vol. 78, no. 3, pp. 3646–3675, 2022.
- [17] J. Yang and W. Lv, "Optimization of sports training systems based on wireless sensor networks algorithms," *IEEE Sensors Journal*, vol. 21, no. 22, pp. 25075–25082, 2021.
- [18] R. K. Saini, M. K. Saini, and R. Sharma, "Requirements of applications of wireless sensor networks for the Internet of Things," in *Internet of Things for Agriculture 4.0*, pp. 241–254, Apple Academic Press, 2021.
- [19] M. Faheem, R. A. Butt, B. Raza, M. W. Ashraf, M. A. Ngadi, and V. C. Gungor, "A multi-channel distributed routing scheme for smart grid real-time critical event monitoring applications in the perspective of Industry 4.0," *International Journal of Ad Hoc and Ubiquitous Computing*, vol. 32, no. 4, pp. 236–256, 2019.
- [20] W. Fang, W. Zhang, W. Chen, Y. Liu, and C. Tang, "TMSRS: trust management-based secure routing scheme in industrial wireless sensor network with fog computing," *Wireless Networks*, vol. 26, no. 5, pp. 3169–3182, 2020.
- [21] M. T. Arefin, M. H. Ali, and A. K. M. F. Haque, "Node mobility optimization in multi-hop WBAN using genetic algorithm," *International Journal of Computer Science and Information Security*, vol. 19, no. 3, pp. 1432–1445, 2021.
- [22] O. Lawal, J. Odiete, and O. Oyediran, "Wireless sensor network: a framework for power and temperature monitoring utility system," *Networking and Mobile Computing*, vol. 34, no. 1, pp. 1–18, 2019.
- [23] M. Yan, P. Liu, R. Zhao et al., "Field microclimate monitoring system based on wireless sensor network," *Journal of Intelligent & Fuzzy Systems*, vol. 35, no. 2, pp. 1325–1337, 2018.
- [24] A. Yang, C. Zhang, Y. Chen, Y. Zhuansun, and H. Liu, "Security and privacy of smart home systems based on the internet of things and stereo matching algorithms," *IEEE Internet of Things Journal*, vol. 7, no. 4, pp. 2521–2530, 2020.
- [25] F. Muzafarov and A. Eshmuradov, "Wireless sensor network based monitoring system for precision agriculture in Uzbekistan," *Telkomnika*, vol. 17, no. 3, pp. 1071–1080, 2019.
- [26] Z. Dong, "Research on grid connected control method of single phase inverter based on wireless sensor network," *International Journal of Wireless Information Networks*, vol. 29, pp. 193–202, 2022.
- [27] X. Li, H. Liu, W. Wang, Y. Zheng, H. Lv, and Z. Lv, "Big data analysis of the Internet of Things in the digital twins of smart city based on deep learning," *Future Generation Computer Systems*, vol. 128, pp. 167–177, 2022.
- [28] G. Shanthi and M. Sundarambal, "FSO-PSO based multihop clustering in WSN for efficient medical building management system," *Cluster Computing*, vol. 22, no. S5, pp. 12157–12168, 2019.
- [29] J. Zhang, "Real-time detection of energy consumption of IoT network nodes based on artificial intelligence," *Computer Communications*, vol. 153, no. 2, pp. 188–195, 2020.
- [30] D. L. Mythri and J. N. Kuriti, "A brief review on wireless sensor network technologies," *System*, vol. 12, no. 3, pp. 313–335, 2019.
- [31] G. Yang and H. Liang, "A smart wireless paging sensor network for elderly care application using LoRaWAN," *IEEE Sensors Journal*, vol. 18, no. 22, pp. 9441–9448, 2018.
- [32] M. Abdelhafidh, M. Fourati, L. C. Fourati, and A. Chouaya, "Wireless sensor network monitoring system: architecture, applications and future directions," *International Journal of Communication Networks and Distributed Systems*, vol. 23, no. 4, pp. 413–451, 2019.

## Research Article

# Application of Temperature Compensation Combined with Neural Network in Infrared Gas Sensor

Kangning Dong<sup>1</sup> and Jinfang Yang<sup>2</sup>

<sup>1</sup>College of Mechanical Engineering, University of Science and Technology Beijing, Beijing 100083, China

<sup>2</sup>The Suited (Beijing) Science and Technology Development, Ltd., Beijing 100083, China

Correspondence should be addressed to Kangning Dong; b20100344@xs.ustb.edu.cn

Received 28 March 2022; Revised 21 April 2022; Accepted 28 April 2022; Published 7 June 2022

Academic Editor: Wen Zeng

Copyright © 2022 Kangning Dong and Jinfang Yang. This is an open access article distributed under the Creative Commons Attribution License, which permits unrestricted use, distribution, and reproduction in any medium, provided the original work is properly cited.

Due to the state of the gas to be measured, the detection mechanism of the pyroelectric detector and the temperature drift of the peripheral circuit components and the detection of the ambient temperature will interfere with the measurement accuracy of the nondispersive infrared gas sensor from many aspects. This paper proposes a temperature compensation method based on the BP neural network. The compensation function of the gas sensor is realized by programming the various functional parameters in the neural network through the program provided in the Matlab neural network toolbox. Experimental simulation results show that the proposed method effectively reduces the influence of external temperature on the gas sensor output and improves its accuracy and stability.

## 1. Introduction

Influenced by the state of the gas to be measured, the detection mechanism of the pyroelectric detector and the temperature drift of the peripheral circuit components and the detection of the ambient temperature will interfere with the measurement accuracy of the nondispersive infrared gas sensor from many aspects. Gas sensor temperature compensation is generally divided into hardware compensation and software compensation; the main idea of hardware compensation is through the external equipment of gas sensor chamber temperature in dynamic balance, so as to avoid the measurement error caused by detection of environmental temperature change; representative is Yongquan et al. for a gas sensor accurate temperature control method and device, through real-time detection of the current ambient temperature, to correct the temperature target using the temperature control module [1]. However, due to the drift of electronic components and the precision of component welding, the measurement circuit of hardware compensation is often of low reliability and high cost. The main idea of software compensation is to fit the gas sensor according to the temperature experiment results to correct the nonlinear

effects of the least squares method, interpolation method, polynomial method, and the validity of the infrared gas sensor. This paper tries to use BP neural network to compensate the gas sensor for temperature.

## 2. States of the Art

The research on infrared gas sensor emerged in the 1970s. After decades of development, it has a relatively mature technology and is widely used in air pollutant monitoring, automobile exhaust composition analysis, mine gas monitoring and special gas concentration detection, and other fields of [2]. Representatives are the following: SM-SF6 SF6 gas sensor of SmartGas, measuring range of 0~1000 ppm, detection accuracy of  $\pm 2\%$  FS, resolution of 1 ppm, and pre-heating time of 30s, and CozIR CO<sub>2</sub> gas sensor of GSS, measuring range of 0~5%, with warm compensation function. Detection accuracy can reach  $\pm 0.03\%$  FS, repetitive error less than 1.7% Fs and S8 CO<sub>2</sub> gas transmitter of SenseAir 0~2000 ppm and  $\pm 1.2\%$ . TIF SF6 can set seven leakage concentration; detection accuracy can reach 3g/year. In year 2010, Xiaodong of Zhengzhou University conducted a study based on the design of the infrared absorption type CO<sub>2</sub>

concentration analyzer. Using the ATmega128 microcontroller as the control core, the measurement range is ranging from 0 to 5%. Relative error is less than 2% [3]. In 2011, Jing of Fudan University studied on the key technology of NDIR portable gas sensor. We propose a novel MEMS microenrichator based on silicate-1 molecular sieve material. Midinfrared hollow fiber is introduced as the gas chamber of NDIR portable gas sensor, effectively improving the system signal-to-noise ratio. The lower detection limit can reach 5 ppm [4]. In 2014, Harbin Institute of Technology conducted research on gas concentration detection alarm device based on NDIR technology. A quadratic polynomial fitting curve was used for the calibration. The measurement range is ranging from 0 to 5%. The detection accuracy can reach  $\pm 0.05\%$  FS [5]. In 2016, Lili of the University of Science and Technology of China conducted a study on the key technology of aircraft fire alarm detection based on CO<sub>2</sub> gas concentration detection. The temperature compensation model was established by using the polynomial partial least squares method and by low temperature (4°C), room temperature (25°C), and high temperature (40°C). The measurement range is from 0 to 1000 ml/m<sup>3</sup> etc. [6].

With the continuous improvement of modern gas detection means, the detection results of gas sensors are becoming more and more accurate.

This is due to the following two factors: first, the gas sensor materials, the performance of the sensor accuracy, and the optimization and development of the gas sensor detection model, especially the application of machine learning algorithm to the sensor modeling analysis, replacing the traditional simple controller AD sampling data conversion process. The sensor detection model input is no longer limited to a single variable. Therefore, establishing a suitable measurement model for the gas sensor is helpful to improve the stability of the detection system.

The Slovenian Joseph Stefan Institute was the first to attempt to use neural networks in short-term air pollution prediction and to predict SO pollution around Slovenian thermal power plants, proving that the method can reduce the peak of pollutant concentrations in critical meteorological conditions [7]. The University of Arizona has developed a portable, low-power, battery-powered hydrogen detection system. The system has a wide hydrogen detection range, and a dual set point of sound and flashing alarms, and a direct readout of the hydrogen concentration ppm [8].

Sudan Qaboos University of Oman has proposed O<sub>3</sub> sensor modeling using neural networks in the lower atmosphere to predict the relationship between tropospheric O<sub>3</sub> concentration and meteorological conditions and various air quality parameters. The results show that artificial neural network (ANN) is an effective method for modeling air pollution [9]. Huazhong University of Science and Technology proposed a fiber hydrogen sensor based on BP artificial neural network, which uses the neural network to eliminate the internal and external effects of light source fluctuations, light loss, and optical fiber beam jitter, and the accuracy of the sensor was improved to 0.1% [10].

Southeast University designed a hydrogen concentration detector based on LPC2104 controller for the thermal con-

ductivity hydrogen sensor TCS208F, analyzed the hardware circuit and software design of the system, and applied it to the hydrogen purity detection of Changzhou Halipu Company [11]. Nanjing University of Information Engineering adopts the improved genetic algorithm to optimize the back-propagation neural network algorithm and realize the temperature compensation of the HMP45D humidity sensor. Compared with the measured data under multitemperature conditions, it is found that the improved measurement system improves the compensation accuracy somewhat, and the convergence rate is also faster [12].

Nanjing University of Science and Technology designed a multisensor hydrogen leakage detection system, through the experimental test analyzed the temperature on the sensitivity and response characteristics of metal oxide hydrogen sensor, and through the concentration measurement sensor and reference sensor resistance rate difference, reduce the environmental temperature interference to the measurement results [13].

New methods for simulation and digital hardware and software for detecting hydrogen concentrations are proposed by Amir Kabir University of Technology in Iran. With the advantages of MEMS technology, the digital and analog circuits of the MEMS hydrogen analyzer can calculate the conductivity between the heating power loss and the temperature difference between the sensor and the environment, thus realizing the measurement of hydrogen concentration with a maximum accuracy error of about 0.2% [14].

In 2016, Lamamra and Rechem proposed an artificial neural network (ANN) modeling method for the metal oxide gas sensor TGS2610 and optimized it through genetic algorithm. The comparative results of ANN model and experimental data showed good consistency, which verified the reliability of this model [15]. China University of Mining and Technology has developed a new MEMS gas sensor based on neural network temperature compensation. In view of the problem that the new thermal conductivity gas sensor is greatly affected by temperature, BP neural network, and RBF neural network, China University of Mining and Technology has developed a new MEMS gas sensor based on neural network temperature compensation, so that high and low temperature can meet the requirements of the system [16].

Nanjing University of Information and Engineering studied the temperature and humidity sensor compensation algorithm based on BP neural network. The BP neural network is improved by the artificial fish swarm algorithm, and the BP neural network is improved by the simplified particle swarm algorithm, respectively, which can reduce the interference of environmental factors to the sensor measurement results to a certain extent [17]. Shandong University developed a hydrogen measuring instrument for the containment of nuclear power plants, analyzed the influence of pressure, temperature, and humidity factors on the measurement results of the thermal conductivity probe, and compensated the temperature and humidity digital according to the fitting formula of the measurement data, and the calibration accuracy can also meet the design requirements [18]. The hydrogen detection system using the temperature monitor is designed by the Tuxi University of Technology.



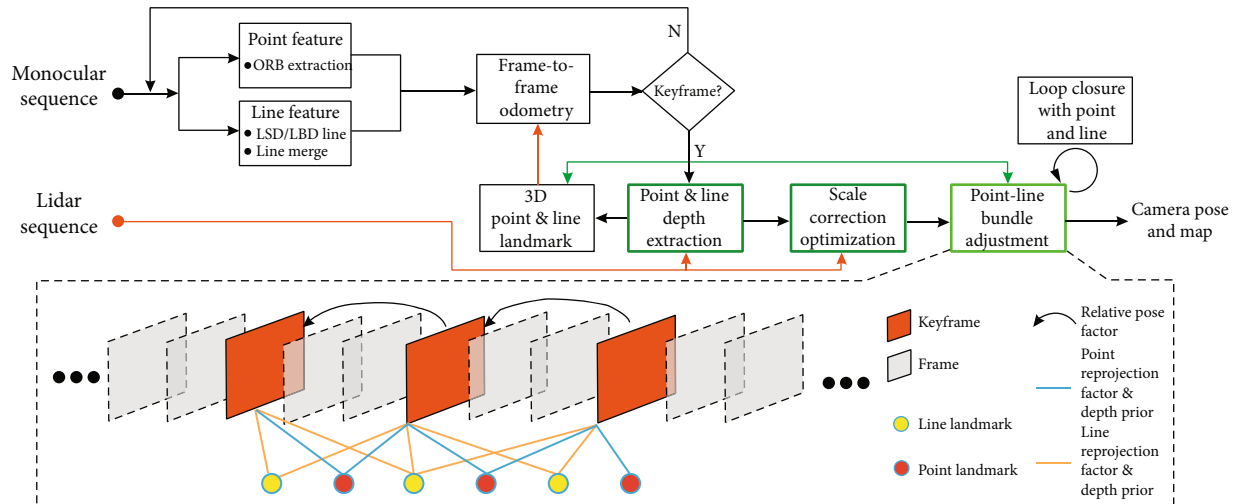


FIGURE 1: Measurement method in gas sensor with BP neural network.

The structure diagram of the hydrogen detection system based on the temperature monitor is specially used for the high concentration of hydrogen measurement in hydrogen fuel cells. Based on the neural network algorithm, to measure the H<sub>2</sub> concentration in a wide dynamic range by learning the solid temperature in a hydrogen-containing gas, the system can measure hydrogen in the range of 40% to 100% [19]. From the above studies, we can see that using the appropriate algorithm for modeling can effectively improve the gas sensor accuracy. From the above studies, we can see that using the appropriate algorithm for modeling can effectively improve the gas sensor accuracy. This paper presents a gas sensor temperature measurement method incorporating BP neural network compensation. This method effectively reduces the influence of external temperature on the gas sensor output and effectively improves the accuracy and stability of the sensor. The overall method is shown in the following Figure 1.

### 3. Methodologies

**3.1. BP Neural Network.** Multilayer feedforward artificial neural network (or multilayer perceptron, MLP) using the error back propagation algorithm (BP: Error Back-propagation Algorithm) is called BP neural network or BP neural network model. Neural network has obvious characteristics.

**3.1.1. Distributed Information Storage Mode.** Neural network stores information in the form of the state of the various processors themselves and the connections between them. One information is not stored in one place but is distributed throughout the network by content. Instead of storing only one external information, it stores parts of multiple information. The entire network processes multiple information before it is stored throughout the network, so it is a distributed storage mode.

**3.1.2. Massively Parallel Processing.** The storage and processing of neural network information are combined; that is, the

storage of information is now in the distribution of neurons' interconnection and is mainly processed in large parallel distribution, which is superior to the modern digital computer with serial discrete symbol processing.

**3.1.3. Self-Learning and Adaptability.** The direct connection weights of each layer of the neural network have a certain tunability. The network can determine the weights of the network through training and learning, showing a strong adaptability to the environment and the self-learning ability of external things.

**3.1.4. Strong Robustness and Fault Tolerance.** The distributed information storage mode of neural network makes it have strong fault tolerance and associative memory function, so that if a certain part of the information is lost or damaged, the network can still restore the original complete information, and the system can still run.

According to statistics, in all neural network applications, BP neural network accounted for more than 80%. BP neural network is favored by many industries because of its good nonlinear approximation ability and its ease of use. The back propagation (BP algorithm) used by the BP neural network is the most mature and widely used tutor learning algorithm in the feedforward neural network. The application of pattern recognition, image processing, information processing, intelligent control, fault detection, enterprise management, market analysis, and other aspects has achieved remarkable results.

**3.2. The BP Neural Network Structure.** The BP neural network [20–24] is a multilayer feedforward network trained by the error backpropagation algorithm, which is usually used to classify and predict the data. The most important part of BP neural network is the learning part of its weight and threshold. Generally, the learning process is divided into two parts. One part is the forward transmission process; that is, the input sample is transmitted from the input layer layer by layer to the output layer. The other part is the error reverse transmission process; that is, if the actual output of

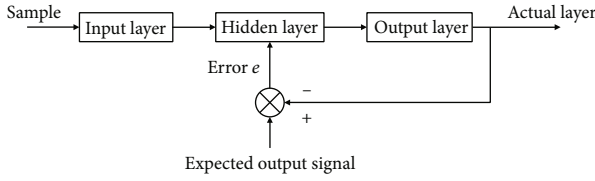


FIGURE 2: Basic structure of the BP network.

the output layer is not the desired output, the error is an adjustment signal layer by layer, processing the connection weight matrix between neurons to reduce the error. After a repeated learning process, the error is finally reduced within the initially set range. The BP neural network is composed of the input layer, the output layer, and the intermediate layer between the two. The middle layer can be a single layer or a multilayer, because the middle layer is not connected to the external environment, so it is also called the hidden layer. The layers are connected between the input layer, the hidden layer, and the output layer, but not between the individual nodes of the single layer. The structural diagram of the BP neural network is shown in Figure 2. The input layer mainly sends the training samples to the network, while the hidden layer and the output layer mainly train the sample data. The parameters obtained by the network training samples are stored in the weights between the neuron and the threshold of each neuron.

### 3.3. The BP Neural Network Training Process

**3.3.1. Forward Propagation.** The input sample is processed from the input layer layer by layer and then transmitted to the output layer, and the state of each layer only affects the state of the next layer. The output layer compares the actual output with the desired output, and if the actual output does not equal the desired output, it enters the backpropagation process. Figure 3 is a flow chart of the BP neural network algorithm.

There are  $n$  input layer nodes,  $q$  hidden layer nodes, and  $m$  output layer nodes, the weights between input layer and hidden layer are  $v_{ki}$ , and the transfer function of hidden layer is  $f_1(\cdot)$ . The weight between the hidden layer and the output layer is  $w_{kj}$ , and the transfer function of the output layer is  $f_2(\cdot)$  [25]; then, hide the layer node output  $w_{ki}f_2$ .

$$z_k = f_1 \left( \sum_{i=0}^n v_{ki} x_i \right), \quad k = 1, 2, \dots, q. \quad (1)$$

Output layer node output:

$$y_j = f_2 \left( \sum_{k=0}^q w_{jk} z_k \right), \quad j = 1, 2, \dots, m. \quad (2)$$

In this way, the BP network completes the approximate mapping of the  $n$ -dimensional space vectors to the  $m$ -dimensional space.

**3.3.2. Back Propagation.** First, the error function is defined with  $p$  learning samples, with  $x_1, x_2, \dots$ . For the  $x_p$  representation, the  $p$ th sample that enters the network gets the output  $y_j^p$ ,  $j = 1, 2, \dots, m$ , using the squared error function:

$$E_p = \frac{1}{2} \sum_{j=1}^m (t_j^p - y_j^p)^2. \quad (3)$$

The expected output is given in the formula for  $t_j^p$ .

For the  $p$  samples, the global error is

$$E = \frac{1}{2} \sum_{p=1}^P \sum_{j=1}^M (t_j^p - y_j^p)^2 = \sum_{p=1}^P E_p. \quad (4)$$

For backpropagation, the error signal is transmitted back by the original forward propagation path, and the weight coefficient of each neuron in each hidden layer is constantly modified, so that the global error signal  $E$  tends to be minimized. During the learning process, the standard BP algorithm uses a unified learning speed for all the weights, and the length of each step is proportional to its directional slope. The updated basic weight formula [26] is

$$W_{jk}(n) = -\eta (\partial E / \partial W_{jk}). \quad (5)$$

In the formula,  $W_{jk}$  is the step length parameter (learning rate);  $\partial E$  is the  $n$ th weight correction; and  $\partial W_{jk}$  is the negative gradient of error squares.

Since BP only uses local gradient information, the value must be small, thus making the algorithm skip the minimum value, which leads to slower learning convergence speed. In order to speed up the convergence speed, the common method is to add the momentum factor, whose weight update formula is as follows:

$$W_{jk}(n) = -\frac{\partial E}{\partial W_{jk}(n)} + \mu W_{jk}(n-1). \quad (6)$$

In the formula,  $\mu$  is the momentum factor used to dampen local oscillations. In order to meet the requirements of accelerating training speed and avoid local minimum value, the method to improve BP algorithm is proposed:

- (1) Different learning rate is used for each weight and represented by the exponential decay function ( $k$ ). This allows the learning rate to increase faster in flatter regions than in steeper regions
- (2) In the learning process, the learning rate can be adaptively adjusted according to the gradient information of the error function  $E$ , to improve the generalization ability of the network and improve the network convergence performance [27]

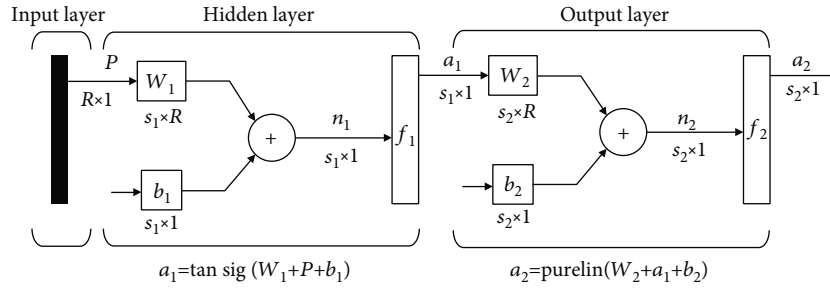


FIGURE 3: Flow chart of the BP neural network algorithm.

- (3) The momentum term is used in the algorithm, and the momentum term, like the learning rate, also changes
- (4) In order to avoid too large learning rate or momentum, set the upper limit
- (5) Parameters and probability  $P$  are used to control the memory and recovery of the network learning process; that is, if the number of error increases is greater, the learning rate and momentum coefficient will be reduced, and the best point will be searched to learn again. In order to avoid fluctuations, the search is carried out randomly in the way of probability  $P$

3.4. *Hybrid PSO-BP Neural Network.* Since the initial weights and thresholds of the BP neural network are randomly generated, when the selection of the two is inappropriate, problems such as slow network convergence and local minimum may occur. For this problem, this paper further uses the PSO algorithm to optimize the BP neural network, reduce the influence of the initial value on the prediction results of the BP neural network, and improve the network convergence speed and prediction accuracy. When the PSO algorithm is used to optimize the BP neural network, the degree of the particle search results is usually determined by the fitness value, which can be based on the mean squared error function.

And the formula is

$$\text{fitness} = \frac{1}{n} \sum_{t=1}^n \sum_{p=1}^q \left[ Y_p(i) - \hat{Y}_p(i) \right]^2, \quad (7)$$

where  $n$  is the number of network learning samples and  $Y_p(i)$  is the expected output value of neurons in the network output layer. The process of optimizing the BP neural network by the PSO algorithm is shown in Figure 4. When the fitness value meets the accuracy requirements or the number of iterations reaches the set upper limit, the best speed and position of the PSO algorithm in finding the particle in the solution space are taken as the weight and threshold of the BP neural network, and the PSO-BP hybrid neural network prediction model is established.

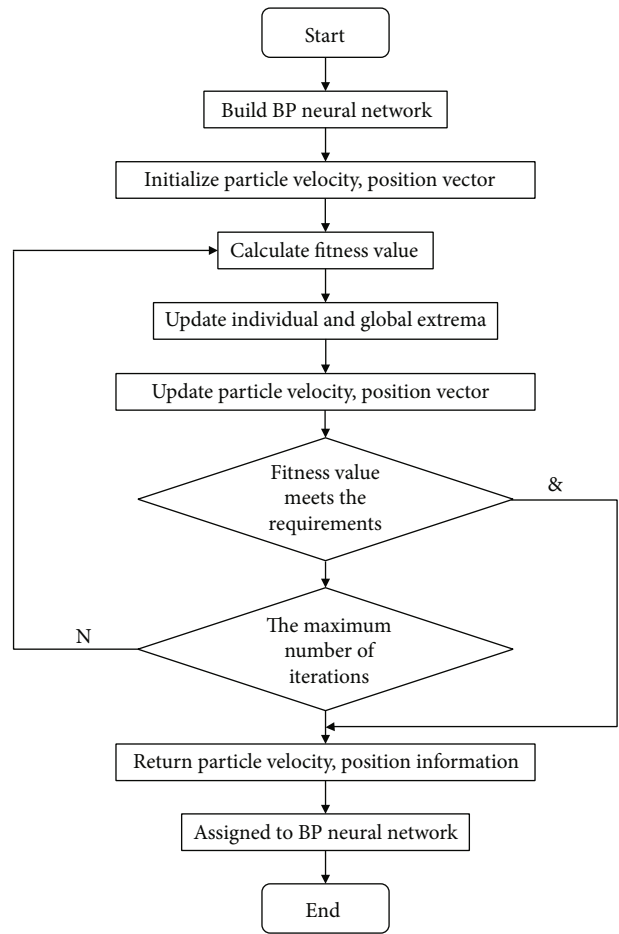


FIGURE 4: Optimizing the BP neural network flow.

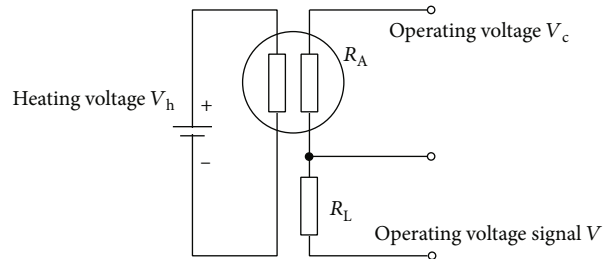


FIGURE 5: Basic test circuit.

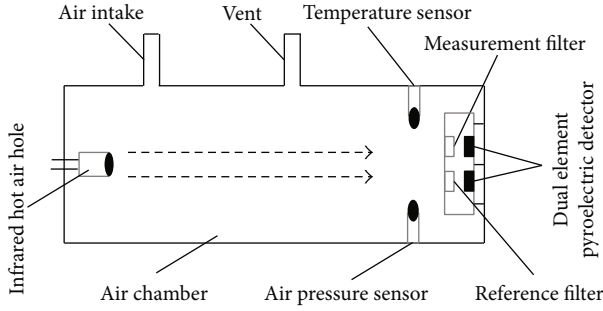


FIGURE 6: Schematic diagram of the gas sensor.

## 4. Result Analysis and Discussion

**4.1. Basic Test Circuit.** The basic test circuit is shown in Figure 5. In the figure,  $V_c$  is the working voltage,  $V_h$  is the heating voltage, the output voltage  $V$  is the amount to be measured, and the sensitivity  $S$  is  $V0/Vg$ , where  $V0$  and  $Vg$  are the output voltage of the sensor in the air and the measured gas, respectively.

**4.2. Gas Sensor Test Calibration Data.** The use of BP neural network for temperature compensation is because of the basic characteristics of the neural network, so that the sensor has a complex nonlinear mapping, self-organization, self-learning, and reasoning capabilities [28]. Only the sample needs to be trained to simulate the intrinsic relationship of input and output. The input amount of the BP neural network is the sensitivity  $S$ . Under the influence of temperature, the sensitivity  $S$  of the gas will change, and the output is the concentration  $C'$ , requiring the output  $C'$  of the neural network to approximate the calibrated target amount  $C$ , so as to achieve the temperature compensation of the concentration  $C$ . To meet the above requirements, the neural network should be first trained, and the training samples are provided by the experimental data calibrated by the laboratory. The sensor used in the experiment is an ethanol sensor with tin dioxide as a sensitive material. The schematic diagram of the sensor is shown in Figure 6, the heating voltage is 4 V, and the calibration results are shown in Table 1.

To better converge the neural network, [29] the experimental data were first normalized before feeding the sample data into the network. The formula is as follows:

$$\bar{S}_{i,m} = \frac{S_{i,m} - S_{i,\min}}{S_{i,\max} - S_{i,\min}}, \quad (8)$$

$$\bar{C}_m = \frac{C_m - C_{\min}}{C_{\max} - C_{\min}}, \quad (9)$$

where  $S_{i,m}$  and  $C_m$  are the normalized values of the input and output of neural network;  $S_{i,m}$  and  $C_m$  are the input and output of  $m$ - $m$  sample;  $S_{i,\max}$  and  $S_{i,\min}$  are the maximum and minimum calibration values of voltage sensitivity measured in group  $i$  experiment; and  $C_{\max}$  and  $C_{\min}$  are the maxi-

TABLE 1: Sensor input and output calibration values at different ambient temperatures.

C on concentration $C/(\text{g}\cdot\text{m}^{-3})$	Sensitivity $S$			
	18°C	20°C	22°C	24°C
0.500	3.465	3.776	3.987	4.182
1.000	4.107	4.316	4.432	4.692
1.500	4.507	4.664	5.404	5.486
2.000	5.601	5.704	6.008	6.137
2.500	6.328	6.528	6.554	7.281
3.000	7.208	7.693	7.803	8.161

TABLE 2: The normalized NN input-output samples

(a)							
$m$	$\bar{C}_m$	$\bar{S}_{i,m}$		$m$	$\bar{C}_m$	$\bar{S}_{i,m}$	
		18°C				20°C	
1	0	0		1	0	0	
2	0.2	0.172		2	0.2	0.138	
3	0.4	0.278		3	0.4	0.227	
4	0.6	0.571		4	0.6	0.492	
5	0.8	0.765		5	0.8	0.703	
6	1	1		6	1	1	

(b)							
$m$	$\bar{C}_m$	$\bar{S}_{i,m}$		$m$	$\bar{C}_m$	$\bar{S}_{i,m}$	
		22°C				24°C	
1	0	0		1	0	0	
2	0.2	0.117		2	0.2	0.053	
3	0.4	0.371		3	0.4	0.328	
4	0.6	0.53		4	0.6	0.49	
5	0.8	0.672		5	0.8	0.779	
6	1	1		6	1	1	

imum and minimum calibration values of concentration. After normalizing the data, the data shown in Table 2 are available.

**4.3. Simulation Studies and Results.** The data were processed for [30] using the BP Neural Net toolbox for Matlab2012. Data processing in the Matlab environment is mainly divided into two parts: constructing the BP neural network and integrating the samples and obtaining the structure coefficient. The detailed process is shown in Figure 7.

The BP algorithm is used to process the samples. One node is selected for the input layer, and six nodes are selected [31] for the hidden layer. The number of hidden layers is not fixed, and the output layer selects one node. The range of the input vector is  $[0,1]$ , the implicit layer adopts the losig function, the output layer adopts the purelin function, and the network training function is trainlm [32–34]. The training error was set to 0.0001, and the

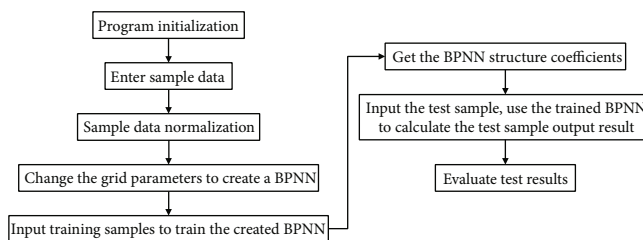


FIGURE 7: Matlab environment data processing process.

TABLE 3: Output results after the training period.

C on centration C/(g•m <sup>-3</sup> )	Sensitivity S			
	18°C	20°C	22°C	24°C
1.000	0.204 7	0.199 6	0.199 6	0.196 3
1.500	0.403	0.396 7	0.399 5	0.400 6
2.000	0.600 1	0.601 7	0.599 8	0.598 5
2.500	0.799 7	0.801 8	0.799	0.799 4
3.000	1	1	1	1

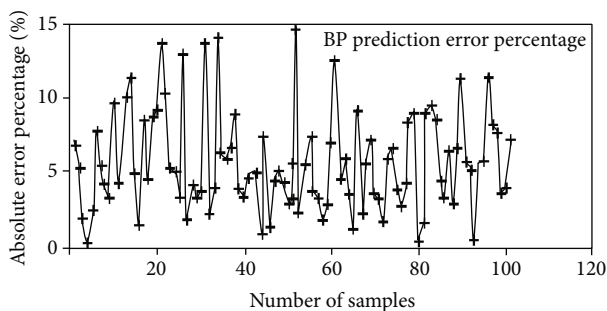


FIGURE 8: Percent absolute error of BP neural networks

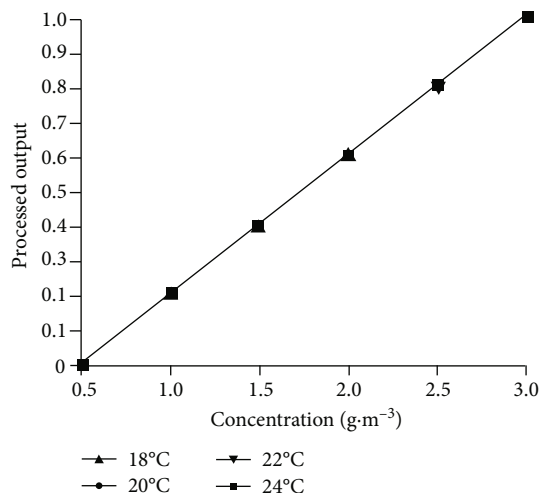


FIGURE 9: Working curve after compensation.

training number was set to the maximum 3000. The data in Table 3 can be obtained by processing the trained network data of Table 2. The percent absolute error of the BP neural network prediction is shown in Figure 8.

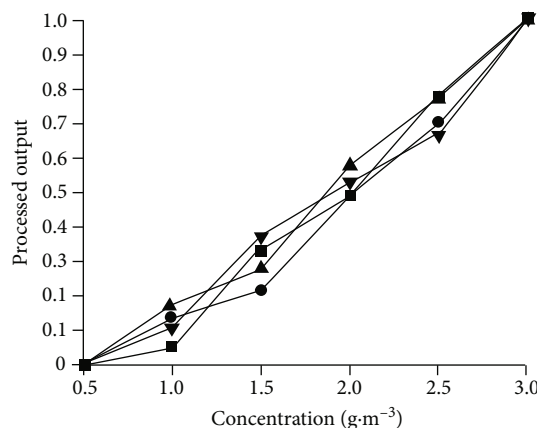


FIGURE 10: Working curve before compensation.

4.4. Analysis of the Algorithm Compensation Effect. Through the Matlab drawing function, writing the corresponding program to simulate each temperature point before compensation and after compensation, it can be found that Figure 9 (working curve at different temperatures after compensation) is better overlapping than Figure 10 (working curve before compensation), effectively reducing the impact of external temperature on the output.

### 5. Conclusions

With the development of automation level, the application of gas sensor is more and more extensive in all kinds of control systems of automation equipment. Among them, the application of infrared gas sensor is particularly prominent, but the infrared gas sensor will be affected by the temperature, resulting in zero-point drift and sensitivity drift. Because temperature is the most important interference amount of the sensor system, it is extremely important to compensate the sensor temperature in practical application. To improve the measurement accuracy and improve the error output characteristics caused by the temperature change of the sensor, measures must be taken to correct the temperature error. Experts and scholars take temperature compensation as an important way to improve the accuracy of gas sensors, and there are a lot of researches, regarding the maturity and development of computer algorithms. It is a new trend to predict temperature compensation based on mature models. In this paper, an ethanol sensor with tin dioxide as a sensitive material is an example.

Based on the BP neural network method, through the programs provided in the Matlab Neural Network toolbox, various function parameters in the neural network are programmed to realize the compensation function of the gas sensor. By comparing the working curve diagram before and after the compensation, it is found that this method effectively reduces the influence of the external temperature on the gas sensor output at all temperature levels and effectively improves the accuracy and stability of the sensor.

## Data Availability

The labeled datasets used to support the findings of this study are available from the corresponding author upon request.

## Conflicts of Interest

The authors declare no competing interests.

## Acknowledgments

This work is supported by the University of Science and Technology Beijing.

## References

- [1] C. Yongquan, L. Youqing, and J. Tao, *A Precise Thermostatic Control Method and Device for Gas Sensor*, 2016, China: CN105388937A.
- [2] T. Yasuda, S. Yonemura, and A. Tani, "Comparison of the characteristics of small commercial NDIR CO<sub>2</sub> sensor models and development of a portable CO<sub>2</sub> measurement device," *Sensors*, vol. 12, no. 3, pp. 3641–3655, 2012.
- [3] W. Xiaodong, *Based on the Infrared Absorption Type CO<sub>2</sub> Concentration Analyzer Design*, Zhengzhou University, 2010.
- [4] P. Jing, *Research on Key Technologies of NDIR Portable Gas Sensor*, Fudan University, 2011.
- [5] original bright, *Gas Concentration Detection and Alarm Device Based on NDIR Technology*, Harbin Institute of Technology, 2014.
- [6] F. Lili, *Research on Key Technology of Aircraft Fire Detection in CO<sub>2</sub> Gas Concentration Monitoring Based on NDIR*, China University of Technology, 2016.
- [7] M. Boznar, M. Lesjak, and P. Mlakar, "A neural network-based method for short-term predictions of ambient SO<sub>2</sub> concentrations in highly polluted industrial areas of complex terrain," *Atmospheric environment. Part B. urban atmosphere*, vol. 27, no. 2, pp. 221–230, 1993.
- [8] D. L. Hetherington, R. W. Grant, K. L. Hughes et al., "A portable low-power hydrogen gas sensor system for wide range H<sub>2</sub>/sub 2/detection," in *In Proceedings of 1994 37th Midwest Symposium on Circuits and Systems*, vol. 1, pp. 199–201, Lafayette, LA, USA, 1994, August.
- [9] S. A. Abdul-Wahab and S. M. Al-Alawi, "Assessment and prediction of tropospheric ozone concentration levels using artificial neural networks," *Environmental Modelling & Software*, vol. 17, no. 3, pp. 219–228, 2002.
- [10] G. Zhang, L. Cui, and Y. Chen, "A novel reflective optical fiber bundle hydrogen sensor based on BP network," in *In 2008 Fourth International Conference on Natural Computation*, vol. 5, pp. 376–380, Jinan, China, 2008, October.
- [11] Q. X. Zeng, Q. Wang, and H. W. Wang, "Design of hydrogen concentration detector based on thermal conductivity sensor," *Measurement & Control Technology*, vol. 27, no. 4, pp. 10–12, 2008.
- [12] P. Jiwei, L. Wenhua, X. Hongyan, and W. Xiangjuan, "Temperature compensation of the humidity sensor based on a modified GA-BP neural network," *Chinese Journal of Scientific Instrument*, vol. 34, no. 1, pp. 153–160, 2013.
- [13] Y. Luo, *Research on Hydrogen Leakage Detection Technology Based on Multiple Sensors*, Nanjing: Nanjing University of Science and Technology, 2013.
- [14] Y. Rajabzadeh and M. Mozafari, "Design and implementation of a digital analyzer for MEMS hydrogen concentration sensor," in *In The 3rd Conference on Thermal Power Plants*, pp. 1–5, Tehran, Iran, 2011, October.
- [15] K. Lamamra and D. Rechem, "Artificial neural network modelling of a gas sensor for liquefied petroleum gas detection," in *In 2016 8th International Conference on Modelling, Identification and Control (ICMIC)*, pp. 163–168, Algiers, Algeria, 2016, November.
- [16] Jinlei, *Development of a Novel MEMS Gas Sensor Based on Neural Network Temperature Compensation*, Xuzhou: China University of Mining and Technology, 2017.
- [17] M. Guo, *Research on Temperature and humidity Sensor Compensation algorithm Based on BP Neural Network*, Nanjing: Nanjing University of Information and Engineering, 2018.
- [18] D. Jiang, *Based on Containment High Reliability Hydrogen Gauge under Severe Accidents*, Jinan: Shandong University, 2018.
- [19] B. Harkinezhad, A. Soleimani, and F. Hossein-Babaei, "Hydrogen level detection via thermal conductivity measurement using temporal temperature monitoring," in *In 2019 27th Iranian Conference on Electrical Engineering (ICEE)*, pp. 408–411, Yazd, Iran, 2019, April.
- [20] Z. Yaofeng, S. Icai, and X. Xiaohui, "Temperature compensation [1] of the pressure sensor based on the artificial neural network," *Electronic Journal*, vol. 36, no. 2, pp. 358–361, 2008.
- [21] L. Survilo, I. Buksa, A. Gaidukovs, and V. Shendryk, "Analysis of questionnaire results in the use of BP and ND in public administration," *Applied Computer Systems*, vol. 16, no. 1, 2015.
- [22] G. He, C. Huang, L. Guo, G. Sun, and D. Zhang, "Identification and adjustment of guide rail geometric errors based on BP neural network," *Measurement Science Review*, vol. 17, no. 3, p. 135, 2017.
- [23] W. Jiquan, *The Theory of BP Neural Network and Its Application in Agricultural Mechanization*, Shenyang Agricultural University, 2011.
- [24] T. P. Liu, M. F. Kao, T. R. Jang et al., "New application of bio-electrical impedance analysis by the back propagation artificial neural network mathematically predictive model of tissue composition in the lower limbs of elderly people," *International Journal of Gerontology*, vol. 6, no. 1, pp. 20–26, 2012.
- [25] X. Hongyan, P. Jiwei, L. Wenhua, W. Xu, and W. Xiangjuan, "A fusion algorithm for the temperature compensation of a humidity sensor," *Journal of Sensing Technology*, vol. 25, no. 12, pp. 1711–1716, 2012.
- [26] Z. Hefang and X. Jingyun, "A BP neural network algorithm for pressure sensor temperature compensation," *Journal of Xi'an Polytechnic University*, vol. 33, no. 2, pp. 163–167, 2013.

- [27] S. Yanmei, M. Fengjuan, and T. Bairui, "Application of the PSO-based BP neural network in pressure sensor temperature compensation," *Journal of Sensing Technology*, vol. 27, no. 3, pp. 342–346, 2014.
- [28] M. Yanjing, N. Wang, T. Ming, and Y. Yang, "Application of wavelet neural network in pressure sensor temperature compensation," *Journal of Shaanxi University of Science and Technology (Natural Science edition)*, vol. 27, no. 2, pp. 84-87–84-91, 2009.
- [29] Z. Peng, C. Ming, Q. Bo, and P. He, "The temperature compensation of the vibrator tube pressure sensor based on the BP neural network," *Journal of Sensing Technology*, vol. 6, no. 10, pp. 2213–2217, 2007.
- [30] Z. Kaili, *Neural network model and its MATLAB simulation program design*, Tsinghua University Press, 2005.
- [31] Z. Xuejun, "Capacitive pressure sensor temperature-compensated RBF neural network," *Sensor Technology*, vol. 10, no. 5, pp. 9–11, 2001.
- [32] S. Mukherjee and S. K. Nayar, "Automatic generation of RBF networks using wavelets," *Pattern Recognition*, vol. 29, no. 8, pp. 1369–1383, 1996.
- [33] H. Yubin, D. Jingyi, and M. Wang, *Neural Network*, vol. 17-39, Xidian University Press, Xi'an, 2007.
- [34] R. Lippmann, "An introduction to computing with neural nets," in *IEEE Assp magazine*, pp. 4–22, North-Holland Publishing Co, 1987.

## Research Article

# Ceramic Shape Design Based on Intelligent Space Simulation Technology

Lijian Zhang  and Guangfu Liu

*School of Ceramics, Pingdingshan University, Henan Key Laboratory of Research for Central Plains Ancient Ceramics, Pingdingshan, Henan 467000, China*

Correspondence should be addressed to Lijian Zhang; 4346@pdsu.edu.cn

Received 11 March 2022; Revised 21 April 2022; Accepted 29 April 2022; Published 2 June 2022

Academic Editor: Wen Zeng

Copyright © 2022 Lijian Zhang and Guangfu Liu. This is an open access article distributed under the Creative Commons Attribution License, which permits unrestricted use, distribution, and reproduction in any medium, provided the original work is properly cited.

With the development of the times, intelligent space simulation technology has gradually emerged in the design of ceramic forms, and the development of modern ceramics has gradually transformed into artistic development. The development of ceramics must conform to the design trend, adjust the rhythm, and seek development opportunities. Organic design opens up a green channel for ceramics and integrates into the lives of today's people. This paper mainly discusses the external form of ceramics and studies from two levels of curve form and bionic form. Through the intelligent space simulation technology, the shape design of ceramics is studied, and the optimal shape of ceramics is obtained, which enables people to have a better understanding of ceramic art.

## 1. Introduction

Ceramic is an ancient and traditional product. The historical value and cultural value carried by ceramics are immeasurable. During the development of ceramics, the design of ceramics is constantly changing, expanding, and enriching. The development of ceramics must conform to the design trend, adjust the pace, and seek development opportunities [1]. The organic design concept pays attention to balance and coordination. In the complex material life, people constantly seek the balance between things, which is a dynamic balance relationship. The combination of modern ceramic design and intelligent space simulation technology, under the pressure of high energy consumption of materials and resources, and intelligent space simulation technology has opened up a green channel for ceramics, allowing ceramic art to be integrated into people's lives, so that ceramic art can be produced in people's daily life [2].

In the classification of ceramic product design, in terms of its design nature, it can be divided into the improved design and innovative design. The so-called improved ceramic product design is based on the use of the original

ceramic product, improving the design in some aspects of the ceramic product to make the ceramic product easier to use, easy to use or easy to process and manufacture [3]. However, because its nature is to improve on the basis of existing ceramic products, it does not make a leap over the main functions and properties of ceramic products, so it is difficult to achieve breakthrough results, which is an increase in "quantity" and "quality." The core of an innovative ceramic product design is to redefine the way users use it and then reorganize the internal factors of ceramic product design, that is, there are breakthrough changes in the use purpose, material, structure, shape, etc. of ceramic products. Redefining the way users use ceramic products is the basis of innovative ceramic product design. Once the use purpose, operation method, and use environment of ceramic products are redefined, the internal factors of ceramic products must be recombined [4]. This is exactly what innovative ceramic products are fundamentals of product design. The form of ceramic products is the realistic basis for the formation of ceramic products, and it is also the precondition for the realization of the material and spiritual functions of ceramic products. When consumers choose and use ceramic



products, they often judge their use methods through the information conveyed by the visual or tactile forms of ceramic products [5]. For example, the shape and structure of the teapot handle suggest how people pick up and pour the teapot; the shape of the plate in the tableware indicates that it is used for dishes with less soup. All of these, without the need for textual explanation, show that the form can accurately reflect the operation mode and function of the ceramic product.

After the advent of the industrial age, science and technology developed rapidly. People's observation and understanding of nature are more in-depth and thorough, and they have experienced a cognitive process from the outside to the inside, from the macro to the micro [6]. The study of biological forms and structures in nature has gradually formed a professional discipline—bionics. Under the guidance of bionics, the designer combines nature and human needs, uses a variety of craftsmanship, highlights the concern for human nature and emotion, combines practicality and artistry, and makes ceramics a naturalistic spirit and humanistic care. Modern ceramics pay more attention to the extraction of balance and rhythm in natural forms and elevate bionic design from figurative to abstract, so as to design porcelain works that can better serve people's material and spiritual life [7]. The reason why daily-use ceramic products can exist in life for a long time and is welcomed by people is that it has its use value, conforms to functional utility, and is closely related to people's lives. The design of daily-use ceramic products has specific functional attributes. Its material characteristics and processing methods must meet the requirements of people's use and, at the same time, adapt to people's aesthetic habits, thus forming unique aesthetic characteristics. As an important part of daily life, it is the most common and common aesthetic object for consumers. Consumers choose, purchase, and use under the control and adjustment of certain psychological laws. Therefore, the design of daily-use ceramic products is inseparable from the analysis and research of consumer psychology. This paper discusses the application of intelligent space simulation technology in the shape design of ceramic products, hoping to let more people understand the art of ceramics and promote its inheritance and development.

## 2. Form Design of Ceramic Products

**2.1. Curve Shape Design of Ceramics.** Because of the intense loneliness that the increasingly competitive environment makes, people begin to understand themselves and go back to square one. The importance of products that are closely related to nature depends on the recognition of the values of health and well-being in nature. Therefore, all philosophies and attitudes about human life have tended to pay attention to nature. Designers capture inspiration from nature, look for the source of various life, and, through their own refining and processing, consciously shape works of art, giving ceramic works of art a new soul. Design should respect nature. The relationship between nature and design is like blood and veins. It is inseparable. It is a link between nature and life. Under the trend of people seeking a more

natural and primitive way of life, and under the trend of the times when the relationship between design and natural life is increasingly close, bionic design and ceramics are combined with each other, and the concept of bionic design came into being. Biomimetic design, as the point of convergence between human social production activities and nature, has achieved a high degree of unity between human society and nature and is gradually becoming a bright spot in the development of ceramic design.

As one of the morphological visual languages, from the perspective of graphic composition, the curve is the smallest unit of artistic form, and it is applied to product design with its various natural forms. The current curvilinear form is one of the characteristics of organic forms, and ceramics have a strong plastic shape, which can well show and express organic forms. A flattening curve is a sphere formed by a uniform rotation of concentric circles and uniform external thrust. Its line form depends on the shape, and the shape depends on the material characteristics of the object itself. Under the influence of the process characteristics, the shape and structure of the ceramic itself present the expression of a flattened curve, forming the basic modeling structure of the sphere, which is the expression of the flattened curve. Kitajun adopts the concept of organic design in many design fields. Native Japanese handicrafts pursue the harmonious coexistence of materials, shapes, technologies, and nature in nature. This is a work of art with a life attitude formed under natural conditions. Sacchetti et al. extracted many oriental elements into their own product creation, forming their own unique style [8].

**2.2. Three Dimensional Surface Design of Ceramics.** The three-dimensional surface is a geometric body surrounded by a curved surface or a curved surface and a plane. From the perspective of the shape of the ceramic product, the three-dimensional surface is the combination of the curved surface and the plane projection that makes up the curved surface. The works of British ceramist Tina Vlassopoulos are one of the representatives of the organic form of ceramic design [9]. In the pottery works designed by the author, the colors used are basically a combination of simplicity and nature, and the morphological structure is more soft [10]. The series of vases he created fully display the lines of ceramics through the overall shape. And in the author's other pottery works, most of them are based on lines to construct unique ceramic works. There is also the work "Toot" by Vlassopoulos as shown in Figure 1(a). The neck of the bottle is inclined and curved, the belly of the bottle is protruding, and the outside of the Taiping mouth is still in a protruding state. The shape has a large tortuous transformation, forming an S-curve. When designing ceramic works, Vlassopoulos transformed the S-curve into a three-dimensional structure, making the curve more three-dimensional [11]. The outer contour lines of the bottle are also very fine and smooth, which can echo with the overall structure of the bottle. This ceramic product design perfectly demonstrates the organic language form in ceramic design. The overall shape of the plate is like a soft white petal, with three undulating arcs that expand naturally. In order to



FIGURE 1: Some works displayed.

ensure the area of the plate, the three petals are deformed and designed to be easy for people to grasp, so that while ensuring the function of use, it also shows an organic sense. In a series of ceramic jewelry created by Jack Booth, we fully feel the charm of ceramic materials. Unlike most of the popular ceramics in Jingdezhen, Jack Booth tries to highlight white porcelain. The market-oriented design of Jingdezhen ceramic ornaments is based on the color of the ceramic itself, but Jack Booth uses subtraction and just uses simple geometric shapes to assist the ceramics [12, 13]. For the material [14, 15], there is also a classic design—today's necklace, with a semicircular geometric design and adjustable cotton rope; when worn, the pure white ceramic surface occupies the core of the chest, while the large ceramic surface and the conspicuous white porcelain color, concise and lively, highlight the original sense of ceramic simplicity. The shape of this ceramic ornament is not a simple and sensual mechanical geometry but is inspired by the organic forms of nature. The white porcelain bracelet made of tree trunks is naturally expressed by cylinders and large faces [16]. The cylindrical shape itself has a curved feel, rather than a straight cylindrical shape, and the wavy bracelet is also naturally designed as shown in Figure 1(b). When Jake Booth expresses the sense of wavy curve, he abstracts the design elements but retains the natural meaning and forms an image form. In this ceramic jewelry design, the iconic design vocabulary is composed of bright colors, large-scale block shapes, and simple and soft lines, creating a highly recognizable fashion design style, which is a relatively successful ceramic jewelry. In a case, the designer hopes to reflect today's fashion theme through a simple and organic modern expression: ecological, organic, capable, and orderly.

### 3. Intelligent Space Simulation Technology

The advantages and disadvantages of the simulation platform are mainly reflected in two aspects. One is the interactivity of the platform. The interactivity of the platform is essentially reflected in the modeling process in the simulation foundation [17]. In the modeling process, good interactivity is service-oriented. The basic requirements of users are the external requirements of the simulation platform; the second is that the quality of the simulation engine directly determines the usability and main value of the simulation platform, that is, the internal requirements of the simulation platform [18–21]. There are basically two realization methods for the modeling means based on modern simulation: (1) graphical modeling represented by UML (Unified

Modeling Language) and (2) scripted modeling based on scripting language. Today, most simulations generally use graphical modeling, which can provide users with a good sense of interactive experience. However, for some complex batch simulations, the interaction of simulation is not the focus, but the pursuit of simulation solutions for large-scale data. Therefore, both aspects are indispensable. The core and top priority of the simulation foundation that the simulation engine mainly completes the execution and scheduling of the simulation tasks and the solution of the solver in the entire simulation process. In terms of practical applications, the simulation platform shown in Figure 2 can reduce the entry threshold and capital investment for building computing clusters for users who need high-performance simulation functions. Users with simulation requirements are not required to use any system. They only need to have a browser locally, and they can access the high-performance simulation function through the web anytime and anywhere to complete any simulation tasks required. Service-oriented is the overall architecture of the entire simulation platform, that is, the platform's construction idea is based on service-oriented, including the construction and implementation of the entire simulation is also based on a service-oriented concept [22–25].

EVS is the explained variance, which refers to the variance score of the model, and  $R^2$  is the coefficient of determination or goodness of fit. The two calculation formulas are as follows:

$$EVS = 1 - \frac{\text{Var}(X_i - \bar{X}_i)}{\text{Var}(X_i)}, \quad (1)$$

$$R^2 = 1 - \frac{\sum(X - \hat{X})}{\sum(X - \bar{X})}, \quad (2)$$

where  $\text{Var}$  is the variance,  $X_i$  is the actual value, and  $\bar{X}_i$  is the mean.

MSE is the mean square error, which represents the expectation of the error variance:

$$MSE = \frac{1}{n} \sum_{i=1}^n (X - \hat{X})^2, \quad (3)$$

where  $X$  is the actual value and  $\hat{X}$  is the predicted value.

MAE is the mean absolute error, RMSE is the root mean square error, and MAPE is the mean absolute percent error, as follows:

$$MAE = \frac{1}{n} \sum_{i=1}^n |\hat{Y} - Y|, \quad (4)$$

$$RMSE = \sqrt{\frac{1}{n} \sum_{i=1}^n (\hat{Y} - Y)^2}, \quad (5)$$

$$MAPE = \frac{1}{n} \sum_{i=1}^n \left| \frac{\hat{Y} - Y}{Y} * 100 \right|. \quad (6)$$

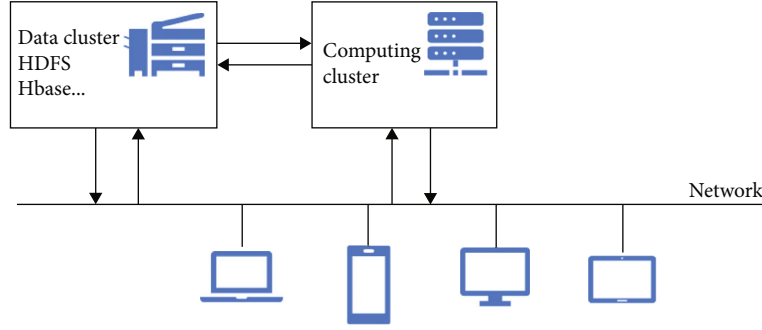


FIGURE 2: Physical structure of the simulation platform.

In the above formula,  $Y$  is the actual value and  $\hat{Y}$  is the predicted value.

Among them, the occlusion angle algorithm is

$$SVF = \cos^2 \beta \left( \frac{\alpha}{360} \right), \quad (7)$$

where  $\beta$  is the height of the occlusion angle and  $\alpha$  is the azimuth.

The spatial orientation is calculated as follows:

$$\vec{x} = (x, y)^T, \vec{x}_1 = (x_1, y_1)^T. \quad (8)$$

Then, (8) can be obtained by a two-dimensional change:

$$\begin{bmatrix} x \\ y \end{bmatrix} = \mu \begin{bmatrix} \cos \alpha & -\sin \alpha \\ \sin \alpha & \cos \alpha \end{bmatrix} \begin{bmatrix} x_1 \\ y_1 \end{bmatrix} + \begin{bmatrix} S_1 \\ S_2 \end{bmatrix}. \quad (9)$$

Among them,  $x$  and  $y$  are the coordinate values,  $\mu$  is the scaling coefficient,  $\alpha$  is the rotation coefficient, and  $S$  is the translation value.

The hardware environment of the cloud platform is composed of a private cloud composed of several servers, disk arrays, graphics workstations, and various terminal computers, as shown in Figure 3, and is connected to each other through gigabit switches to form a LAN (local area network) network environment; graphics workstations and terminal computers in the network are formed. Various simulation services and simulation resources provided by the cloud server can be accessed through Gigabit Ethernet. Supported by their corresponding system software, the servers and disk arrays of the cloud platform are divided into two parts: computing clusters and data clusters according to different functions, which, respectively, carry related services such as simulation scientific computing services and database cluster cloud management [26–28]. The computer terminals of ordinary users carry the interactive functions of simulation task deduction and the functions of visual display and interaction of simulation results, as shown in Figure 4; they exchange data with computing clusters and data clusters through network switches and constitute the entire cloud-based task deduction and virtual experiment platform.

By extracting and tracking the shape contour of the pre-processed image, a digitized shape contour curve is obtained,

which is expressed as an ordered set of integers on the plane, and the form is as follows:

$$C = \{c_i | 1 \leq i \leq N, c_i \in R^2\}, \quad (10)$$

$$P = \{p_i | 1 \leq i \leq N, p_i \in R^2\}. \quad (11)$$

Among them,  $N$  is the number of points on the curve, the  $i$ th point is  $c_i$ , the approximate point is  $p_i$ , and  $R$  is a set of real numbers.

Usually, the compression rate CR is used to represent the amount of information, as follows:

$$CR = \frac{N_C}{N_p}. \quad (12)$$

$N_C$  is the number of points on the shape curve and  $N_p$  is the number of approximate vertices. The global error squared sums ISE and CR give the graphics quality FOM:

$$FOM = \frac{CR}{ISE}. \quad (13)$$

#### 4. Application of Intelligent Space Simulation Technology in Ceramic Form Design

The basic simulation software on the platform can realize interactive drag-and-drop simulation model modeling. Users only need to drag and drop the model modules provided in the platform and then combine and connect the existing basic modules according to the user's own modeling and simulation tasks [29]. Then, after a simple interactive operation in the software, the drag-and-drop model can be simulated according to the user's imagination. In the user-oriented interactive simulation interface, the focus should be placed on the realization of the interface and the experience of human-computer interaction [30–32]. Therefore, as shown in Figure 5, in the process of designing and developing the simulation interactive interface, the part displayed to the user should be enhanced, and the implementation of specific functions related to simulation should be placed in the simulator. This part can be bound in one-to-one correspondence with the actual operation of the user's simulation

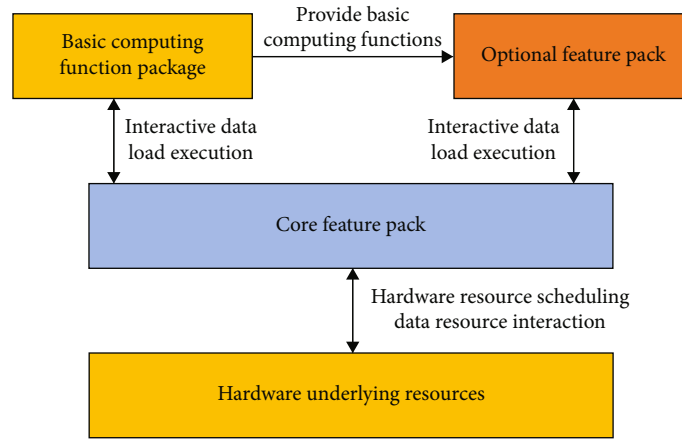


FIGURE 3: Overall architecture diagram.

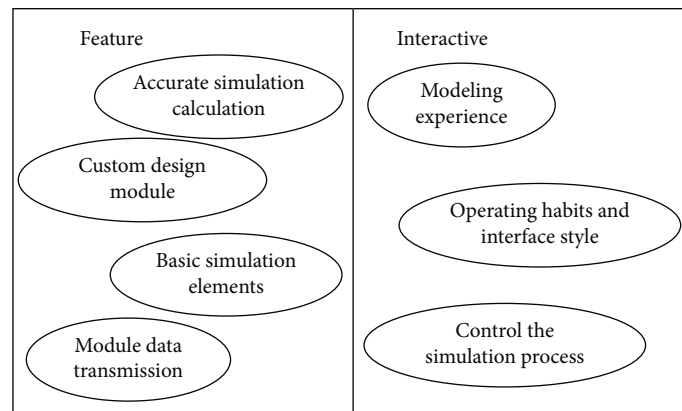


FIGURE 4: Requirement diagram of interactive interface function package.

modeling by using the interface of the specific simulation function exposed in the simulator.

Since ancient times, nature has been the source of various scientific and technological principles and major inventions of mankind. The biological world has a wide variety of animals, plants, and substances. In the long evolutionary process, in order to survive and develop, they have gradually acquired the ability to adapt to changes in nature. Humans live in nature and are “neighbors” with the creatures around them. The various strange abilities of these creatures attract people to imagine and imitate. Designers use their observation, thinking, and design abilities to gain insight into the subtle changes in the natural world and begin to imitate creatures and express it in their ceramic works. From the human face pattern constructed by the ancient primitive people to the bull-shaped lamp and the chicken-head pot, from the fish-shaped pattern in the primitive period to the persimmon-shaped cup, melon-shaped pot, lotus-leaf plate, tree-head-shaped pen holder, etc. in modern ceramic works, a large number of floral patterns and geometric forms have emerged in handicrafts. From three-color silk camels to shadow celadon horses and the simulation of petal shapes, from the true reproduction of nature to the various imagery expressions based on nature, from the bionic of external forms transplanted to the variant of the internal structure,

the bionic design is undoubtedly the protagonist throughout the ceramic art, as evaluated in Figure 6. In the figure, the abscissa represents the number of times and the ordinate represents the percentage, in which the proportion of the space value, artistic value, and design value fluctuates significantly. Flowers, plants, animals, shells, fossils, and water patterns are undoubtedly the most common and vivid forms of objects in ceramic works. From the development of naive and vivid imitation to the realistic reproduction of mature techniques, from the comprehensive expression of all aspects to the ultimate play of individual factors, the bionic design shows the harmonious unity of artistic design and natural life in diversity. Here, the author studies the appearance of bionic morphological design in ceramics from two perspectives.

A concrete form means that a substance has a certain specific form. The figurative form depends on the specific form, and its visual attributes are visible, tactile, detailed, and not abstract, reflecting the essential attributes of specific things. Figurative forms in nature refer to specific images in nature, unrefined prototypes, such as rocks, water marks, animals, and plants. Except for some that show strong rules and sequences, most forms show free, vivid, and irregular. In ceramic design, the concept of figurative generally refers to the form of objective existence. Through the thinking,

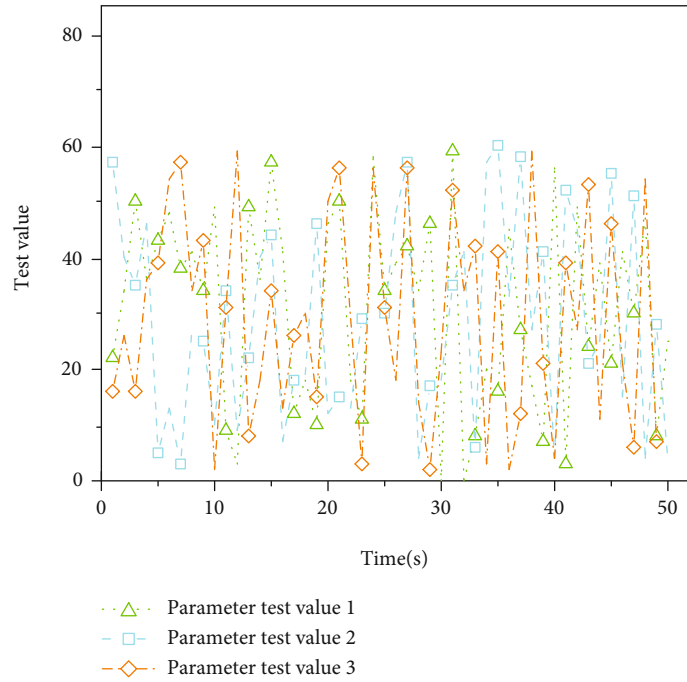


FIGURE 5: Multiparameter test results.

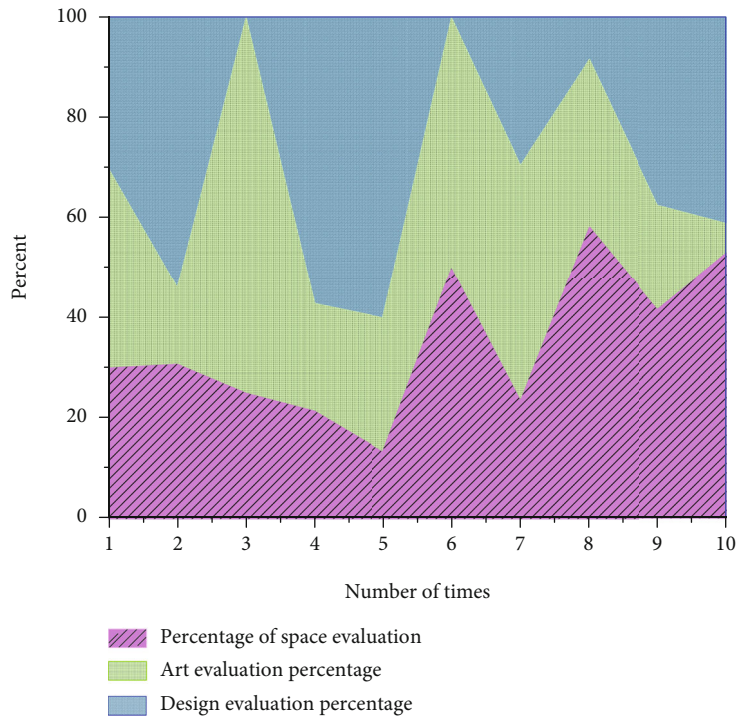


FIGURE 6: Multiangle evaluation results.

methods, and means of design, such as the use of refining, processing, and organization, the ceramic works have the characteristic modeling form of figurative form, such as characters and animals and plants. From the concept of design, it retains the characteristics, individuality, and typicality of natural forms, but after the works are released, it

is no longer a simple simulation of the original form of nature, but the generalization and sublimation of biological forms as shown in Figure 7.

Natural creatures are vivid and natural, and designers constantly dig out their various charms of life to express their subjective intentions and convey various artistic

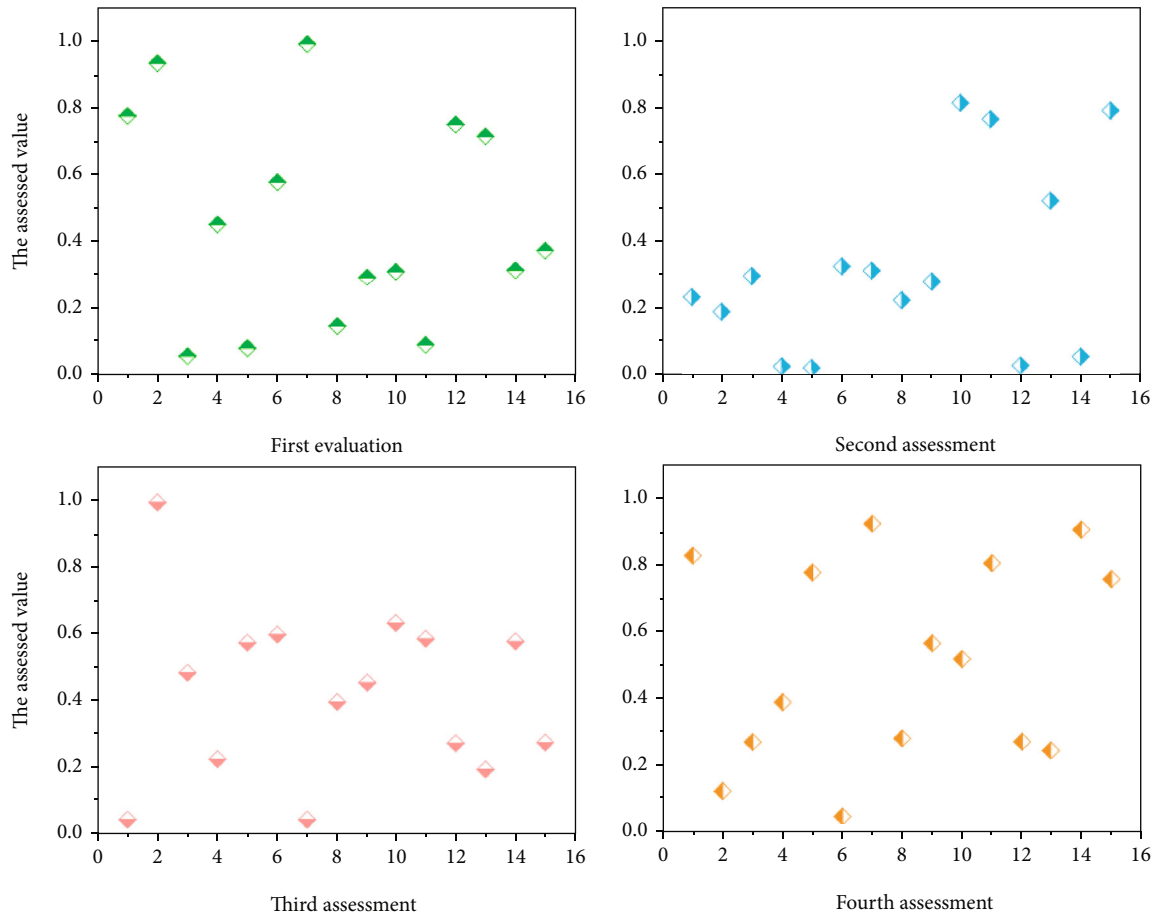


FIGURE 7: Different test values of space simulation.

feelings to people. The artistic appeal of ceramic works is increased by simulating the representation of the figures and spirits. The characters in the bionic design are used as the medium to connect life and art, as well as ceramics and life, which is the meeting point of nature and art. In fact, the shape and function are mutually influencing and interrelated, and the two are inseparable and interactive. The bionic design of the ceramic shape creates a rich aesthetic effect and also creates a functional beauty that serves people—visually pleasing functional beauty and comfortable functional beauty. There is no doubt that ceramics are utensils with certain practical functions. Generally speaking, bionic modeling is limited by its functions in simulating natural objects. It must be an extension based on utensil modeling that satisfies and adapts to its modeling functions. The “natural form” formed. Under certain special conditions, people often think of looking for them in nature. Something to replace the lacking items, such as using a bamboo tube to cook rice, or using an ostrich egg shell instead of a bowl, etc., so there is egg-shaped tableware. As long as we always have a unique vision and rich associations about everything around us, inspiration sometimes bursts out in this accident. The bionic ceramic works functionalize the shape of the leaf, but it is not a simple and rigid simulation. The designer starts from the perspective of bionic design, as shown in Figure 8, adding personal design elements, thus enhancing the formal

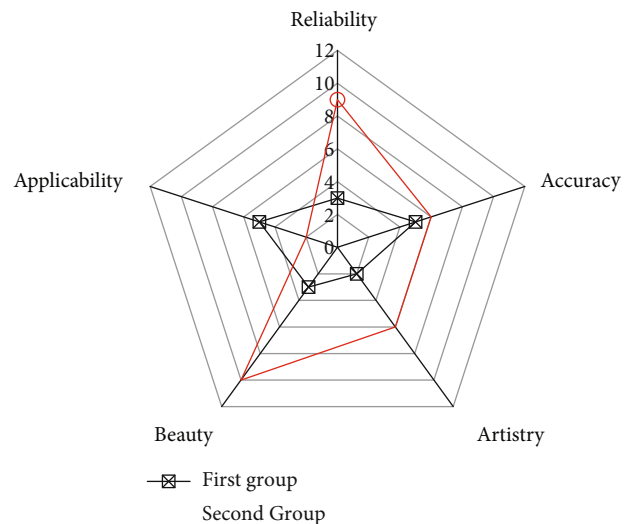


FIGURE 8: Multidimensional evaluation scoring chart.

beauty of the entire ceramic vessel, vividly. Without losing the sense of rhythm, the color matching is also just right. As the second group, the bionic design of functional space is due to other design methods.

Ceramic art culture has a long history. As a comprehensive artistic phenomenon that entrusts people's pursuit and shaping of beauty, it not only provides material services for human life in function but also meets people's aesthetic needs spiritually. In a sense, ceramics has become an artistic medium that can enrich and satisfy human emotional needs, and the human breath and emotional temperature it carries go beyond its physical form. Natural form bionics has a natural advantage in building an emotional bridge between man and nature. The bionic design of the form of ceramics is conducive to awakening the natural desire in the depths of human beings, so that the soul can escape from the steel forest in the industrial age and return to the most primitive and simple natural spiritual home. We use the ceramic form bionic design to communicate the emotional communication between man and nature, build a more harmonious relationship between man and nature by conveying the beauty of nature, and, at the same time, use the bionic design of the natural form to continuously enrich the design level to meet the spiritual needs of modern human beings. Ceramic art is the artistic carrier of human material and spiritual needs. To explore the cultural connotation and design principles of natural form language in ceramic form design is not only the inheritance and continuation of traditional natural spirit and ceramic culture but also for the further construction of human, ceramic, and ceramic art. The harmonious relationship in nature provides a reference. The in-depth discussion on the bionic design of ceramic form broadens the space and dimension of ceramic form design, which is conducive to the emotional injection of ceramic artworks, so as to transcend the material body and bloom with life, thus becoming a spiritual carrier for emotional communication between humans and nature.

## 5. Conclusion

The mystery of nature can never be explored. It is our inexhaustible and inexhaustible driving force for design. For us, the form of natural objects is just a starting point for design. The key is to form a bionic form to form reconstruction. The ceramic works are perfectly presented. This process is a peculiar and arduous adventure road for the designer, which is mixed with adventure and excitement, joy and pain, which reflects the struggle and running-in between man and nature. The form design of ceramic products should consider the following elements of use behavior: First, ceramic products require full grasp of ergonomic principles, as well as the user's psychology and behavior in the process of form design, so that the designed product conforms to the user's use habit and psychology. When designing the form of a ceramic product, the most important thing is to consider which body parts the user uses to use the product. For example, when designing a ceramic tea set, it is necessary to consider whether the structural characteristics of the tea set are consistent with the user object, and whether the handle design of the tea set is suitable for the hand shape characteristics of the user; the handling of the handle is not ergonomic, and it will make it difficult to handle when holding it. People have a feeling of being too heavy or strenuous;

too large a cover is difficult to grasp, and too small makes the fingers tense. Secondly, in the process of user operation of ceramic products, it is necessary to consider whether the product is smooth and convenient to use, and its shape should be suitable for user operation, whether the shape of the surface is suitable for use actions such as grasping, pinching, and rotating. When designing the shape, it is also necessary to consider the specific actions of people when using ceramic products. For example, people in Fujian, Guangdong, Taiwan, and other regions like to drink "Kung Fu tea." Therefore, the capacity of the tea set is smaller. In ethnic minority areas such as Mongolia and Tibet, large-capacity tea bowls are generally preferred due to the dry climate and the habit of drinking milk tea or butter tea. This requires that the form of ceramic products can meet various operating actions. The shape design of ceramic products is for the purpose of being convenient for people to use, so it must first make people feel satisfied and satisfied physically, and then make people feel happy spiritually. Again, the shape of the ceramic product should conform to the sequence of operations. When setting the form of a ceramic product, to ensure the correct operation of the user, two aspects of information must be provided from the design: the operating device and the operating sequence, and the combination of the ceramic product components must conform to the operating logic. "Slanted" teapot is designed according to the order in which the tea is brewed. When using it to make tea, you should first put the tea leaves on the inner partition and place the teapot lying down. The table top is at an angle, and some of the tea leaves leave the water. After the tea is completely brewed, the teapot is erected, and the tea leaves are no longer in contact with the tea water. In addition, the environmental factors used are more complex, and different environments used require ceramic products to be considered in terms of shape processing, material selection, and even color to meet the needs of users.

## Data Availability

The data used to support the findings of this study are available from the corresponding author upon request.

## Conflicts of Interest

The authors declare that they have no known competing financial interests or personal relationships that could have appeared to influence the work reported in this paper.

## References

- [1] L. D. Petrenko, "Green trend in global energy development: tendencies and opportunities," *International Journal of Energy Economics and Policy*, vol. 11, no. 5, pp. 1–7, 2021.
- [2] N. Chen, J. Zhang, I. Amp, C. E. Faculty, and S. J. University, "Research on the design of ceramic tea set under the combination of fractal idear and traditional wintersweet culture," *Art and Design*, vol. 11, no. 5, pp. 117–119, 2017.
- [3] G. N. Papulova and M. Y. Kvasnikov, "Development of compositions of pigmented colored lead-free glazes for improving

- ceramic product design,” *Glass and Ceramics*, vol. 78, no. 3–4, pp. 129–132, 2021.
- [4] B. Fonseca, M. S. Coelho, C. Bueno, C. E. Fontana, A. S. De Martin, and D. G. P. Rocha, “Assessment of extrusion and postoperative pain of a bioceramic and resin-based root canal sealer,” *European Journal of Dentistry*, vol. 13, no. 3, pp. 343–348, 2019.
- [5] I. Belboula, C. L. Ackermann, J. P. Mathieu, and C. Cuny, “Consumers’ responses to product design: using a semantic priming task to assess automatic understanding of product positioning,” *International Journal of Market Research*, vol. 61, no. 2, pp. 140–156, 2019.
- [6] T. F. Rodriguez, *Methods and arrangements involving substrate marking*, 2015, U.S. Patent 9,898,793.
- [7] P. Costanzo, M. Nardi, and M. Oliverio, “Similarity and competition between Biginelli and Hantzsch reactions: an opportunity for modern medicinal chemistry,” *European Journal of Organic Chemistry*, vol. 2020, no. 26, pp. 3954–3964, 2020.
- [8] A. Sacchetti, B. Bachmann, K. Lffel, U. M. Künzi, and B. Paoli, “Neural networks to solve partial differential equations: a comparison with finite elements,” vol. 10, pp. 32271–32279, 2022.
- [9] P. Wolniewicz, “Representatives of the family Actinostromatidae (Stromatoporoidea) in the Devonian of southern Poland and their ecological significance,” *Geologos*, vol. 22, no. 3, pp. 227–249, 2016.
- [10] S. Gielen and J. Magueijo, “Quantum analysis of the recent cosmological bounce in comoving Hubble length,” 2022, <http://arxiv.org/abs/2201.03596>.
- [11] V. Keswani, M. Lease, and K. Kenthapadi, “Designing closed human-in-the-loop deferral pipelines,” 2022, <http://arxiv.org/abs/2202.04718>.
- [12] O. O. Akinola and I. A. Adekunle, “Developing market-oriented politics in Nigeria: a review of the 2019 presidential election,” *Working Papers*, vol. 28, no. 1, pp. 73–94, 2022.
- [13] A. Ferreira, “Reconsidering the merit of market-oriented planning innovations: critical insights on transferable development rights from Coimbra, Portugal,” *Land Use Policy*, vol. 99, p. 104977, 2020.
- [14] J. Wu, H. Ma, N. Wood et al., “Early development of Jingdezhen ceramic glazes,” *Archaeometry*, vol. 62, no. 3, pp. 550–562, 2020.
- [15] B. Ysa, M. Zhou, Y. Zhang et al., “Poisonous delicacy: market-oriented surveys of the consumption of rhododendron flowers in Yunnan, China,” *Journal of Ethnopharmacology*, vol. 265, 2021.
- [16] A. Jivnescu, “Effects of simulated gastric acid exposure on surface topography, mechanical and optical features of commercial CAD/CAM ceramic blocks,” *Applied Sciences*, vol. 11, no. 18, p. 8703, 2021.
- [17] T. Smethurst, ““We put our hands on the trigger with him”: guilt and perpetration in Spec OPS: the line,” *Criticism*, vol. 59, no. 2, p. 201, 2017.
- [18] E. V. Muravyova, A. V. Utkin, and B. M. Valiullin, “Determining the vulnerability of educational institutions in terms of the requirements of the program “my city to prepare,”” *IOP Conference Series: Materials Science and Engineering*, vol. 962, no. 4, p. 042019(10pp), 2020.
- [19] J. Mao, “On the basic requirements and problems of piano performance technology,” *Arts Studies and Criticism*, vol. 1, no. 1, 2020.
- [20] Z. Ye, K. Pang, Y. Du, G. Zhao, S. Huang, and M. Zhang, “Simulation analysis of the tensile mechanical properties of a hydraulic strain clamp-conductor system,” *Advances in Materials Science and Engineering*, vol. 2020, 19 pages, 2020.
- [21] H. Ji, G. Song, X. Huang, J. Li, W. Pei, and W. Xiao, “Precision hot forging forming experiment and numerical simulation of a railway wagon bogie adapter,” *The International Journal of Advanced Manufacturing Technology*, vol. 120, no. 1–2, pp. 907–925, 2022.
- [22] E. Hustad and D. H. Olsen, “Creating a sustainable digital infrastructure: the role of service-oriented architecture,” *Procedia Computer Science*, vol. 181, no. 1, pp. 597–604, 2021.
- [23] L. Mendoza-Pitti, H. Calderon-Gomez, M. Vargas-Lombardo, J. M. Gomez-Pulido, and J. L. Castillo-Sequera, “Towards a service-oriented architecture for the energy efficiency of buildings: a systematic review,” *IEEE Access*, vol. 9, pp. 26119–26137, 2021.
- [24] J. Dreher and J. Thiel, “Star architecture projects and the geographies of innovation across the construction supply chain: the case of the Elbphilharmonie,” *European Planning Studies*, vol. 30, no. 1, pp. 105–120, 2022.
- [25] I. Leon, “Use of flat interwoven wooden strips in architecture and construction. Simulation and optimization using 3D digital models,” *Sustainability*, vol. 13, no. 11, p. 6383, 2021.
- [26] K. Al-Zoubi and G. Wainer, “Mobile experimentation using modelling and simulation in the Fog/Cloud,” *Journal of Simulation*, vol. 5, pp. 1–22, 2021.
- [27] F. Mahmood, F. Z. Khan, M. Ahmed, I. Ahmad, and B. B. Gupta, “Green Cloud Net++: simulation framework for energy efficient and secure, green job scheduling in geographically distributed data centers,” *Transactions on Emerging Telecommunications Technologies*, vol. 33, no. 4, 2022.
- [28] D. W. Lee, “Simulation and optimization for a closed-loop vessel dispatching problem in the Middle East considering various uncertainties,” *Applied Sciences*, vol. 11, no. 20, p. 9626, 2021.
- [29] L. Henderick, R. Blomme, M. Minjauw et al., “Plasma-enhanced atomic layer deposition of nickel and cobalt phosphate for lithium ion batteries,” *Dalton Transactions*, vol. 51, no. 5, pp. 2059–2067, 2022.
- [30] R. Butleris, “Extending drag-and-drop actions-based model-to-model transformations with natural language processing,” *Applied Sciences*, vol. 10, no. 19, p. 6835, 2020.
- [31] H. Holz and D. Meurers, “Interaction styles in context: comparing drag-and-drop, point-and-touch, and touch in a mobile spelling game,” *International Journal of Human-Computer Interaction*, vol. 37, no. 9, pp. 835–850, 2021.
- [32] I. S. Frydas, M. Kermenidou, O. Tsave, A. Salifoglou, and D. A. Sarigiannis, “Unraveling the blood transcriptome after real-life exposure of Wistar-rats to PM2.5, PM1 and water-soluble metals in the ambient air,” *Toxicology Reports*, vol. 2020, no. 7, pp. 1469–1479, 2020.



## Research Article

# Design of an Intelligent Sensor Teaching Experiment System and Measurement of Student Innovation Literacy

**Xiaorong Li and Qianli Xing** 

*Yancheng Institute of Technology, Yancheng, Jiangsu 224051, China*

Correspondence should be addressed to Qianli Xing; [xql@ycit.edu.cn](mailto:xql@ycit.edu.cn)

Received 6 April 2022; Accepted 17 May 2022; Published 2 June 2022

Academic Editor: Wen Zeng

Copyright © 2022 Xiaorong Li and Qianli Xing. This is an open access article distributed under the Creative Commons Attribution License, which permits unrestricted use, distribution, and reproduction in any medium, provided the original work is properly cited.

Most of the experimental teaching links adopt experimental teaching, and few of them are taught through experimental simulation system. The intelligent sensor teaching experimental simulation system is a simulation measurement software system compiled by access and LabVIEW software to assist the use of sensor measurement and virtual instrument practical teaching platform, which realizes the network teaching of experimental links and carries out exploratory work. It has important practical significance for the modernization of experimental links. At the same time, the intelligent sensor experimental system can effectively improve the problems of students' low learning motivation and poor learning effect in the learning process and finally let students participate in the construction of sensor teaching experimental system, improve students' learning interest and enthusiasm, and cultivate students' autonomous learning and innovation ability. Through the establishment of intelligent sensor teaching simulation system, this paper successfully improves students' innovative literacy in teaching level, scientific research practice, teaching content, teaching methods, and intelligent lectures and greatly improves students' learning enthusiasm, learning efficiency, and teaching quality.

## 1. Introduction

The “sensor” course is a vital professional technology course in electronics, electrical automation technology, computer applications, and so on [1]. At this stage, colleges and universities usually provide sensors and related courses for students majoring in science and technology. Many colleges offer a specific course in the senior year called “Sensor Principles and Applications” [2–3]. There are some contradictions between learning and career development for senior undergraduate students: on the one hand, students need these courses to improve their knowledge structure, enhance their professional knowledge and skills, and develop the ability to apply their knowledge in practice; on the other hand, students at this stage are under pressure to study for graduate school, find a job, and travel abroad for English exams, among other things [4–5]. As a result, students are frequently unmotivated to pursue professional courses, and the learning effect is minimal. The learning impact is likewise quite poor, and both teachers and students

have expressed their dissatisfaction [6]. A university has made certain adjustments to the teaching material, particularly to increase the experimental teaching connection, and altered the experimental teaching content, in order to boost students' motivation and teaching quality. For example, in the experimental teaching link the virtual instrument development tool LabVIEW is introduced, which allows students to autonomously design hardware and software systems and use software simulation and hardware circuits to create sensor data acquisition and control systems [7–8]. At the same time, students may exercise their practical and practical abilities, the capacity to evaluate and solve issues, and the ability of autonomous learning and creativity [9] and enhance their overall quality through experimental instructional content and the independent learning process [10–11].

This article covers classroom theoretical teaching content innovation, as well as the reform and practice of experimental teaching content in the “sensors” course [12–13]. The content of the paper has been implemented in the actual

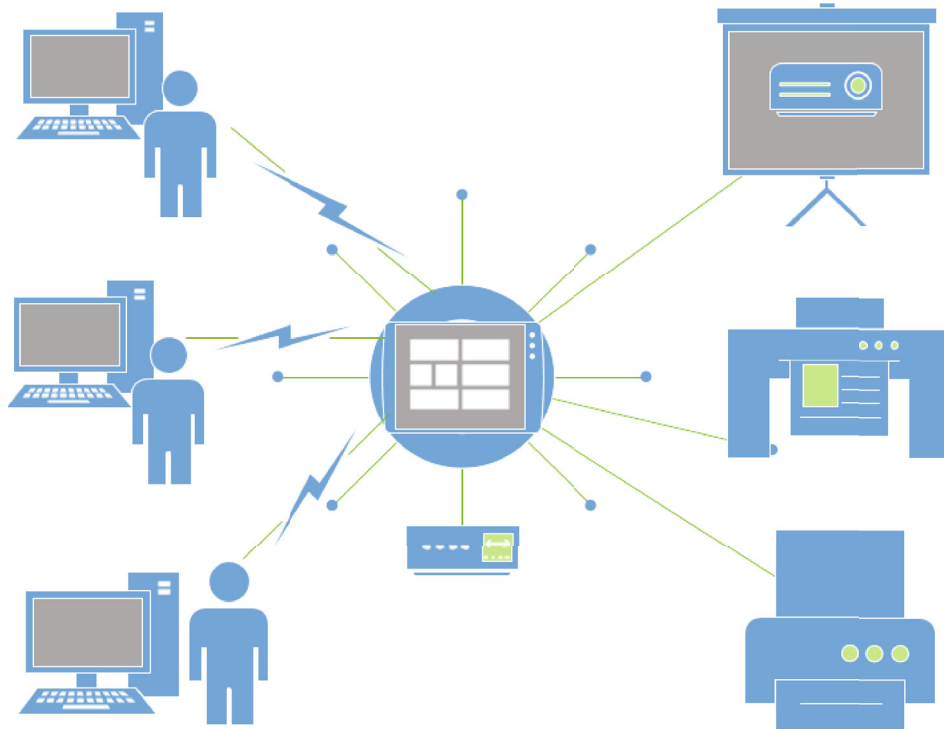


FIGURE 1: Conceptual structure diagram of intelligent sensor teaching experiment system.

teaching process of a university, which can significantly improve students' learning enthusiasm, and is expected to achieve good teaching results [14–15]. Relevant experience can also be used as a reference for similar courses [16–17]. The design concept diagram of an intelligent sensor teaching experiment system is shown in Figure 1.

Based on the establishment of an intelligent sensing teaching simulation system, it was incorporated into the evaluation system of students' innovative literacy [18]. Taking the innovative ability of students in 10 colleges and universities as an example, a more complete and diversified evaluation system of college students' innovative literacy is obtained.

## 2. Classroom Theory Teaching Content Innovation

Sensor technology is one of the cornerstones of today's information technology age, and it should be given the same respect as computer and Internet technology [19–20]. With the development of wireless sensor networks, the Internet of Things, and other fields, today's information society has experienced a wave of computer and Internet technology. At present, sensor technology has become a hot spot in the field of science, technology, and industry, and variety of sensor technology have developed very rapidly. The existing "sensor" course has problems: the teaching content is somewhat old, and new sensor technology and development are less engaged [21]. At the same time, pure sensor principal teaching is rather monotonous, and students are bored. Students do not have a strong desire to study. Therefore, the content of classroom teaching has been adjusted.

*2.1. Acquiring New Sensor Technology Expertise.* New sensor technology information is added to the teaching content to ensure that students learn as much as possible about the cutting-edge development of sensors [22–23]. Some emerging sensor technology applications and the most recent sensing materials and devices are incorporated into the curriculum, such as Internet of Things (IoT) technology, which connects items to the Internet for information exchange and communication according to agreed protocols in order to achieve intelligent identification, positioning, and navigation [24]. Another example is a wireless sensing network, which is a multihop self-organizing network comprised of a large number of low-cost small sensor nodes distributed in the monitoring environment [25].

*2.2. Schedule Classroom Discussions.* Encourage students to actively participate in learning by organizing classroom discussions. The classroom discussion primarily consists of two aspects: first, for a specific sensor taught in class, let students use such sensors to complete an after-class homework, through the class to find the corresponding information, design a sensor application circuit and system, and then the teacher arranged a special discussion session, allowing students to introduce their design and communicate with other students[26–27]; and for a specific sensor taught in class, let students use such sensors to complete an after-class homework, through the class to find the corresponding information [28]. Second, for current market popular sensor technology, such as various MEMS (micro electro mechanical systems) sensors in smart phones, CCD (charge coupled device) sensors in digital cameras, fiber optic sensors, and fingerprint sensors in the field of security, online

information such as technical indicators, technical advantages, and market share, and make a presentation report in the classroom, students can learn a lot of knowledge independently during the entire process[29–31].

### 3. The Design of Experimental Teaching Content

Experimental teaching sessions are very important for the learning of sensors. In the early experimental teaching process, we mainly use CSY sensor system experimental instrument to provide students with some verification experiments [32], in which students operate according to the experimental instruction tutorial to test the characteristics of various sensors and understand the working principle of sensors. The advantage of this experimental teaching is that it combines the classroom content and deepens the understanding of the working principle and characteristics of sensors. Its disadvantage is that students' participation is more passive and lack of innovative experimental content. In addition, the cost of the experimental system is higher, some parts are easy to be damaged, the cost of renewal and maintenance is higher, and there are usually more students and less instruments.

National Instruments (NI) launched LabVIEW, a virtual instrument development platform that offers a graphical programming language development environment with strong functionalities and a user-friendly development environment [33]. Environment that supports numerous bus and data connection interfaces, as well as sophisticated graphical control components and software panels, and powerful data and signal processing function features created a sensor experiment platform based on LabVIEW + serial communication + microcontroller, and students worked in groups to perform software and hardware simulations on this platform. Students must check the data, build their own sensor data acquisition and control system, collaborate to complete the design scheme, hardware circuit, and software system, and finally write a comprehensive experimental report.

This experimental process increases students' interest in learning while also allowing them to master sensing device selection, data acquisition, and processing skills, prompting students to actively participate in the experimental process. In order to complete the experiments, the students must conduct independent data inquiry, analysis, and discussion. This can help students gain a better understanding of the theoretical knowledge they have learned while also cultivating their own. It also develops students' broad application skills and teamwork spirit. Furthermore, the structure of the design is adaptable, making it simple to update and expand. Because the design is adaptable and easy to update and expand, the development cost is low, and it is suitable for students to complete the design and practice independently. It is appropriate for students to design and practice independently.

### 4. Experimental Teaching Platform Based on LabVIEW

This sensor experimental platform consists of several modules, including sensors, an analog-to-digital conversion chip,

and a microcontroller to form the front-end data acquisition system (analog temperature acquisition). The digital-to-analog conversion chip will transform the sensor signal into a digital signal into the microcontroller, followed by the sensor signal to the upper computer (PC) via the communication system, which here uses a serial communication interface. LabVIEW is used to write the upper computer data processing system program, which can perform functions such as real-time dynamic temperature displayed, data storage and alarm temperature setting, and temperature analysis and processing. The interface of the experimental simulation system is shown in Figure 2, which is composed of buttons, diagrams, and other elements.

This system can be broken down into several experiments such as hardware design, software design, software simulation, hardware simulation, and circuit board development, and students complete each experimental session in turn. The specific content of each experimental session is as follows: hardware design is to design the front-end acquisition system, back-end control system, and communication interface circuit in the circuit design software (such as Proteus). Students have studied circuit development and design in previous courses and are very familiar with circuit design software, so they can complete the experiment relatively smoothly.

The software design includes the lower computer microcontroller program and the upper computer LabVIEW program. The LabVIEW platform provides students with a graphical development environment that can be mastered quickly and conveniently. The system completes the functions of data reception, processing, display, and storage and forms the control signal to the microcontroller. LabVIEW platform provides students with rich development interfaces and functional modules, and students can complete various sensor data processing functions on this platform.

The software simulation is performed fully on the computer and is invoked jointly by many development tools (Proteus, Keil, LabVIEW, and so on) to mimic communication between the upper and bottom computers through the virtual serial connection. The hardware simulation is based on the software simulation, and the microcontroller experiment box is used to construct the lower computer system and complete the system's operations. After all of the preceding simulation steps have been completed successfully, you may design the circuit board, acquire the necessary components, solder the circuit board, and lastly connect the PC for debugging and operating. Students with a higher learning interest and stronger hands-on ability can complete the experimental contents in the hardware simulation and PC debugging sessions independently, and the specific functions and modules in the system can be redesigned by students, and after the software simulation is successful, then enter the hardware simulation and PC debugging. The system structure has strong adaptability, and students can complete the above experimental courses in the order most suitable for their own needs. After that, students may construct their own system, replacing and extending some of the modules, as well as adding new ones. Furthermore, the overall development cost of the system is modest and does not place undue stress on instructors and laboratories.

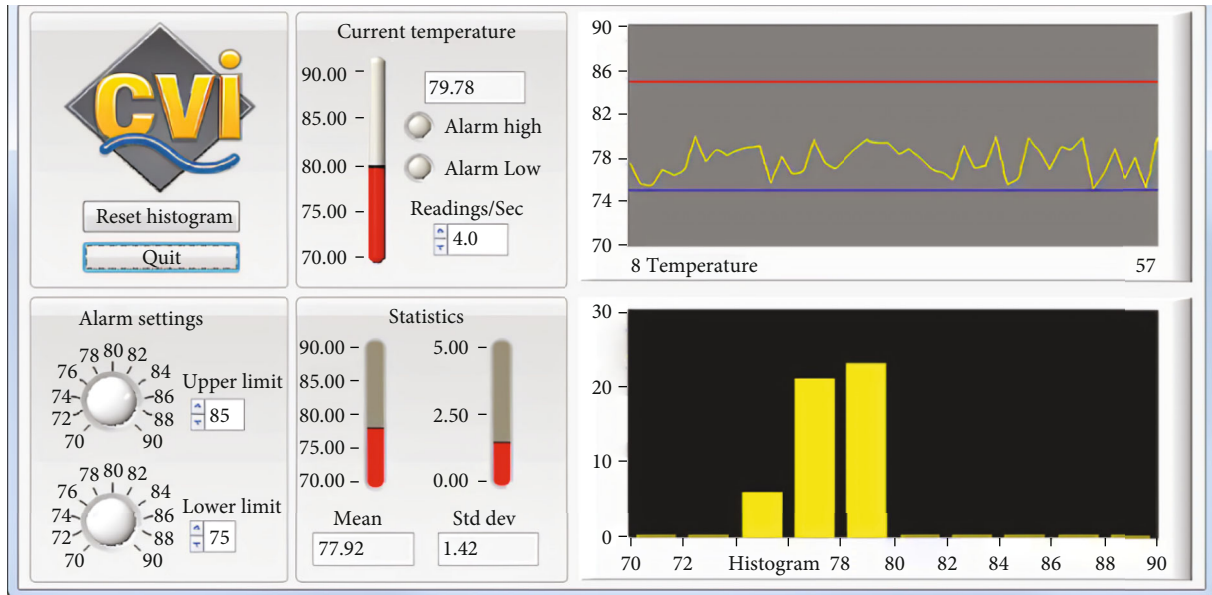


FIGURE 2: The experimental teaching platform based on virtual instruments.

## 5. Establishment of Evaluation System for Students' Innovative Ability

So far, the experimental simulation system introduced by it has only been used for sensor teaching. On the one hand, students can complete science and technology courses more effectively, comprehensively, and realistically. On the other hand, it can effectively shorten the learning cost, reduce the resistance in the learning process, and improve the teaching effect. On this basis, the undergraduate teaching is effectively connected with the research study and innovation ability training of college students, and an evaluation system for innovation literacy of college students is established. The evaluation system is described below.

Firstly, in order to establish each indicator item, an effective screening and combination was conducted through a thorough literature search, based on facts and curriculum design, and according to the specific requirements of the assessment of college students' innovation ability. Secondly, for each indicator, there is a relatively scientific and standardized definition that encapsulates the explanation and description of its definition as well as specific operational and assessment instructions. Each of these indicators has a graded description at the same time. Thirdly, according to the comprehensive scoring method, i.e., the correlation analysis of the indicator items is conducted first, then standardized, and finally the weights of each indicator are determined through expert meetings. Finally, the indicator system used the classification weight setting method; i.e., the specific classification registration of the indicators was set according to the weight proxy, level by level, and the total value of each level weight was 100%. Therefore, the weighted weighting analysis is then used to quantify effectively. The specific setting of the evaluation system of students' innovation ability is shown in Table 1.

## 6. Case and Discussion

Taking 10 innovative universities as an example, a multifaceted evaluation of the possible teaching of intelligent sensors around the innovation ability is conducted. The analysis is carried out by considering the three aspects of the school's teaching philosophy, teaching level, and research and practice ability. According to the evaluation system, it is divided into level I, level II, and level III. The evaluation results of intelligent sensor teaching system are organically combined with the evaluation of students' innovation ability.

*6.1. Evaluation of Teaching Concept.* According to the sample survey of students from the existing 10 schools, students scored the 10 universities on school orientation, training objectives, and teaching status around the educational philosophy. The idea of running a school is out of 100 points. For the major category of school orientation, it was determined whether the school considers innovation as a category for cultivating talents. The results of school orientation scores are shown in Figure 3. Among them, school orientation accounted for 20%, and all 10 schools scored more than 10 points for school orientation, with the school with the highest school orientation score basically reaching 17 points. On the other hand, cultivation goals, the main goal of the school for the development of students, innovation is one of the main factors of its goals. 10 schools have a score of more than 20% of the cultivation goals, and the college with the highest cultivation goals has a goal score of more than 28 points.

For the broad category of educational philosophy, specific measures for schools to implement innovative education were identified. As shown in Figure 4, the educational philosophy accounted for 30%, and all 10 schools scored more than 20 points for school orientation, with the college with the highest educational philosophy score close to 30

TABLE 1: Evaluation system of students' innovation ability.

Weight	Weight	Second-level indicators	Third-level indicators	Best-in-class description	
Educational philosophy 100	0.1	School orientation 50	School orientation 20	Research-oriented or innovative universities, which have scientific plans and can be implemented with notes, are more distinctive	
			Training objectives 30	Emphasis is placed on the all-round development of students, with the cultivation of innovative spirit and practical and self-learning ability	
		Educational philosophy 50	Educational philosophy 30	With advanced educational concepts, education cultivates students as the main body, has a strong sense of quality, and has a clear concept of innovation ability training	
			Teaching status 20	Make teaching work the most important central work in higher education	
Subtotal marks					
Education and teaching 100	0.5	Culture mode 35	Professional settings 10	Wide caliber training, large-scale enrollment, to achieve cross-disciplinary integration	
			General education 10	General education is more numerous and more diverse, cultivating students' complete knowledge and sound personality	
			Credit 15	Under the guidance of teachers, according to the needs of interest and personalized development, flexible choice of learning content, time, and method	
		Course teaching 40	Curriculum system 15	Establish a multidimensional curriculum structure with functional courses as the backbone, and strengthen the practicality and selectivity of courses	
			Teaching content 15	The implementation of a scientific practice course is combined with the teaching of professors	
		Teaching mode 25	Teaching methods 10	Relying on the completion of intelligent sensor teaching experiments, students learn independently and cooperate, and teachers provide guidance	
Subtotal marks			Intelligent teaching 15	Many courses use intelligent sensor teaching technology to guide students to use hardware and software tools to learn	
			Open trials	Experimental design 30	Using the intelligent sensor teaching system, a more autonomous and diverse experimental course is designed to comprehensively evaluate the students' experimental ability
				Laboratories are open 10	The lab is open for a long time, making the most of the spare time so that the intelligent sensor system covers every student
				Base construction 15	In the innovation base, we provide students with a good intelligent sensor teaching test system
Scientific research practice 100	0.4	Scientific research activities 45	Project funding 15	Adequate funding for student courses	
			Scientific research system 15	Mature innovation management mechanism and evaluation system, covering resource allocation, policy support, process supervision, results acceptance, etc.	
		Social 15	Practical training 15	There is a stable off-campus practice base, which can better reproduce the teaching results of the intelligent sensor	
			Subtotal marks		
Score					

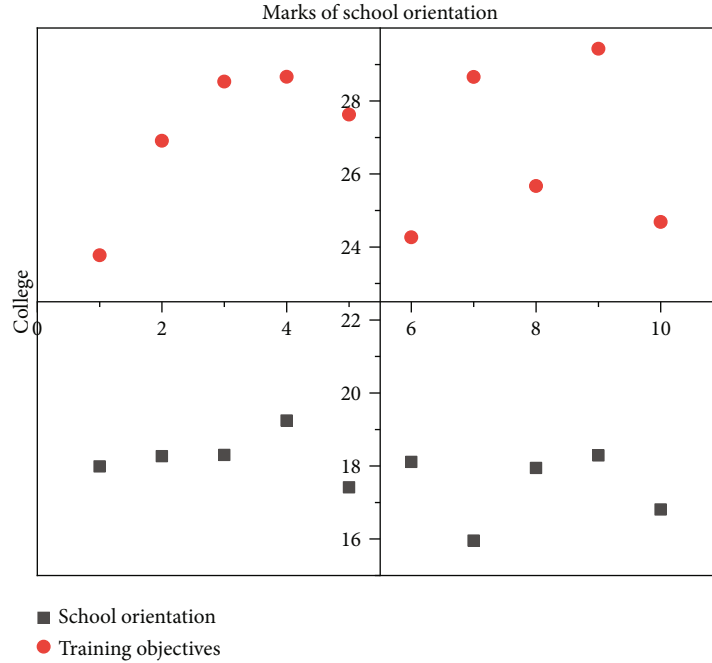


FIGURE 3: Marks of school orientation.

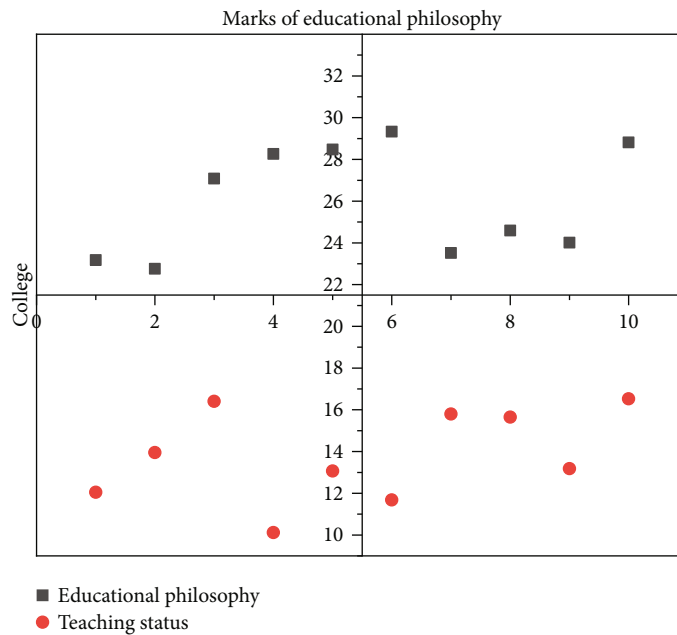


FIGURE 4: Marks of educational philosophy.

points. On the other hand, the educational means accounted for 20%, and all 10 schools under the educational means scored more than 10 points, with the college with the highest educational means score scoring 16 points.

6.2. Evaluation of Education and Teaching. According to the analysis results of the sample survey of students in 10 existing schools, students scored 10 schools around the evaluation of education and teaching in three categories: training mode, curriculum teaching, and teaching mode. Seven

aspects of curriculum system, teaching content, teaching methods, and intelligent teaching.

For the large category of cultivation mode, it was determined to include the intelligent sensor teaching system, which is mainly divided into three parts: professional setting, general education, and credit system. The results are shown in Figure 5; among them, professional setting and general education accounted for a smaller 10%, and the scores of all 10 universities were greater than 5 points less than 10 points. The credit system, on the other hand, can include

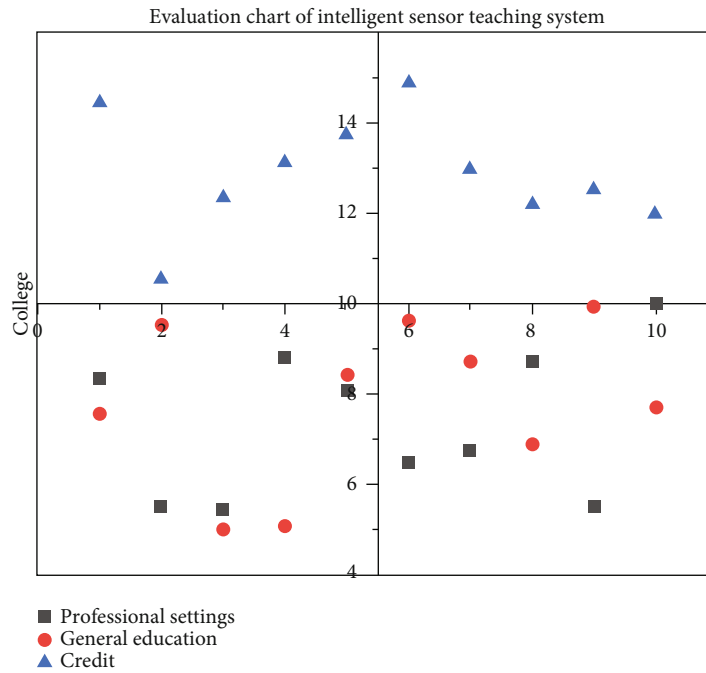


FIGURE 5: Evaluation chart of intelligent sensor teaching system.

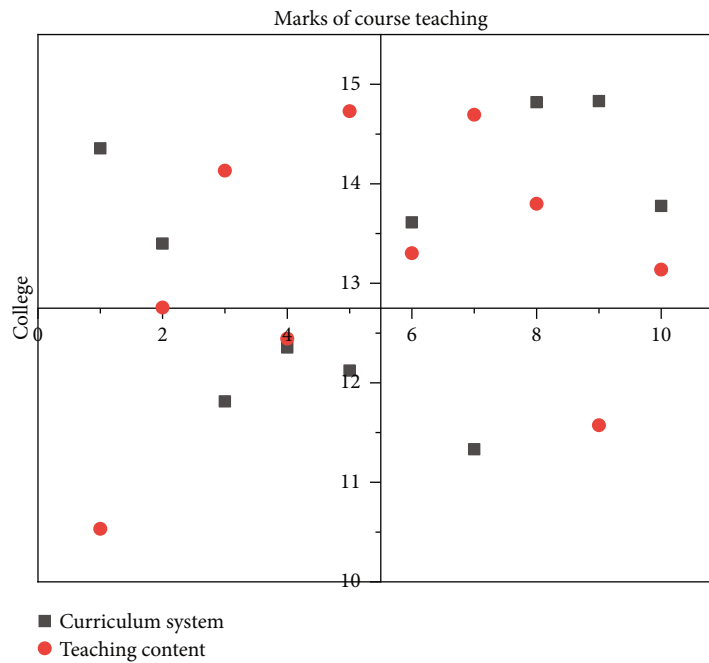


FIGURE 6: Marks of course teaching.

specific innovative courses, accounting for 15%, and the scores of all 10 colleges and universities are greater than 10, and the score of the college with the best implementation of the credit system is 15.

For the large category of curriculum and teaching, it is mainly divided into two parts: curriculum system and educational content, both of which should be planned into the intelligent sensor teaching system. The results of course teaching results after inclusion are shown in Figure 6, where

the abscissa represents the university and the ordinate represents the score. On the whole, the trend of course system and teaching content is good. Curriculum system and educational content both account for 15%; 10 universities in these two scores are greater than 10 points, where the highest score of the curriculum system is 15 points, and the highest score of the teaching content scores 14.5 points. For the large category of teaching models, it is mainly divided into two parts: teaching methods and intelligent delivery. As shown

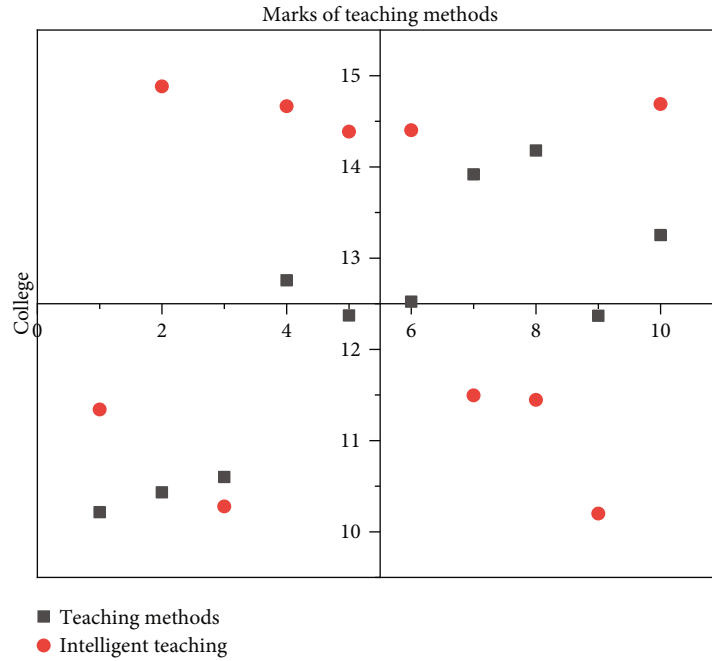


FIGURE 7: Marks of teaching methods.

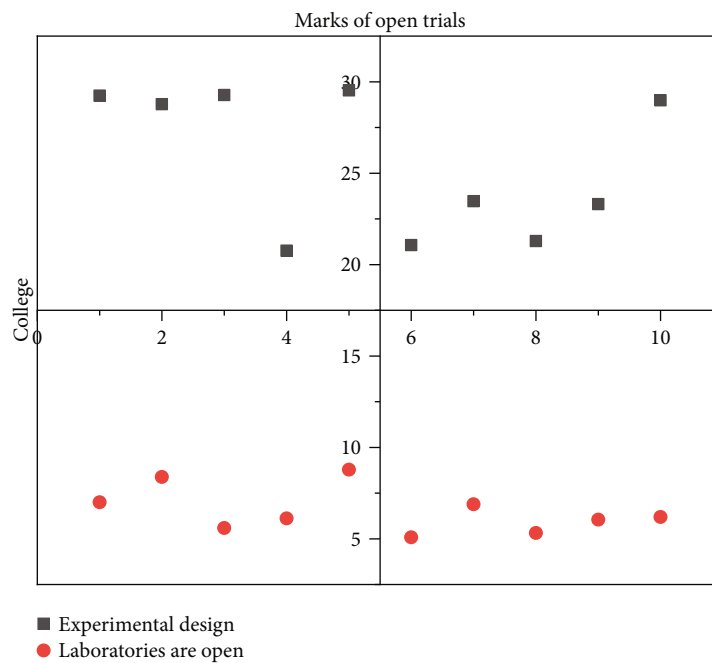


FIGURE 8: Marks of open trials.

in Figure 7, among them, teaching method accounts for 15%, and teaching method itself covers the application of smart sensor teaching system, and all 10 universities have scored more than 10 points in this item, and the highest university has 14 points. On the other hand, intelligent teaching itself can be narrowly understood as intelligent sensor teaching system, and this part accounts for 15%, and all 10 universities have scored more than 10 points in this item, and the highest university can even reach a full score of 15 points.

6.3. *Evaluation of Education and Teaching.* According to the results of the analysis of a sample of students from the existing 10 schools, the students scored 10 schools around the research practice on the three categories of open experiments, research activities, social practice, experimental design, laboratory opening, base construction, project funding, research system, practical training, 6 major categories. In the open design category, the intelligent sensor teaching system itself is the main part of the experimental design. As shown in Figure 8, the



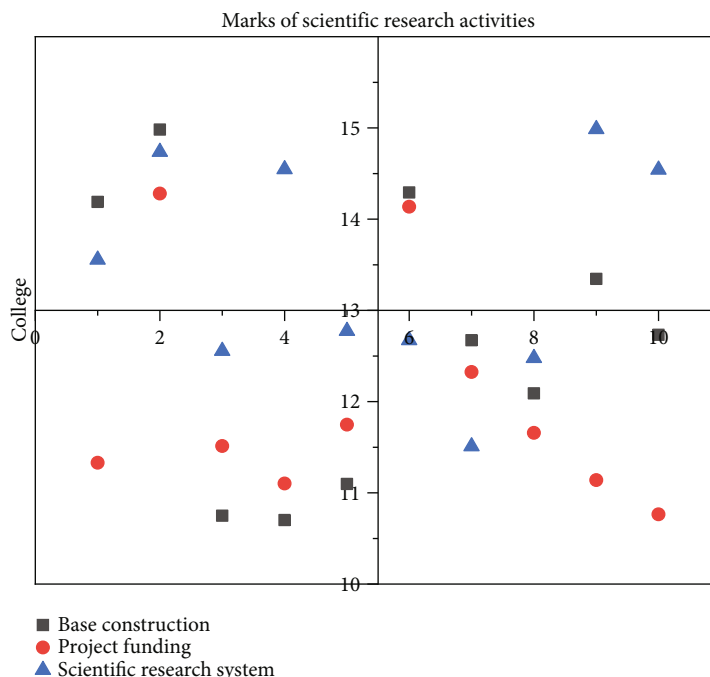


FIGURE 9: Marks of scientific research activities.

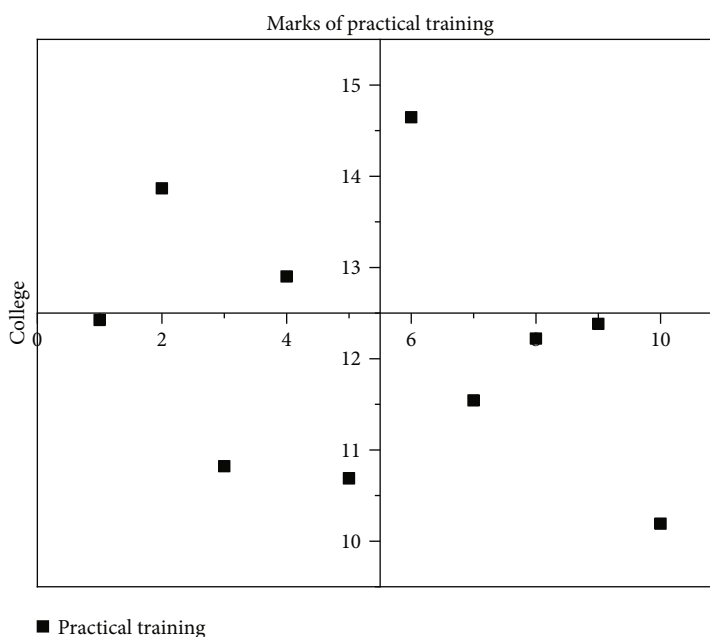


FIGURE 10: Marks of practical training.

score of experimental design accounts for about 30%, the scores of 10 universities are more than 20, and the highest score is 39. On the other hand, the degree of openness of the laboratory, accounting for 10%, sufficient open time helps students to improve their self-learning and innovation ability, with the highest score of 10 points in the university.

In the broad category of research activities, there are three main parts, base construction, project funding, and research system. The study is shown in Figure 9. The percentage of these

three research activities is all 15%, and all three provide infrastructure, financial support, and evaluation system for intelligent sensor teaching system. 10 universities have three scores of 10 or more, and the highest scores are 15, 14, and 15, respectively.

The last major category is social practice. The intelligent sensor teaching system is essentially a simulation system, and the use of learning in a stable off-campus internship base can deepen and consolidate this piece of knowledge. The results are shown in Figure 10. The percentage of this

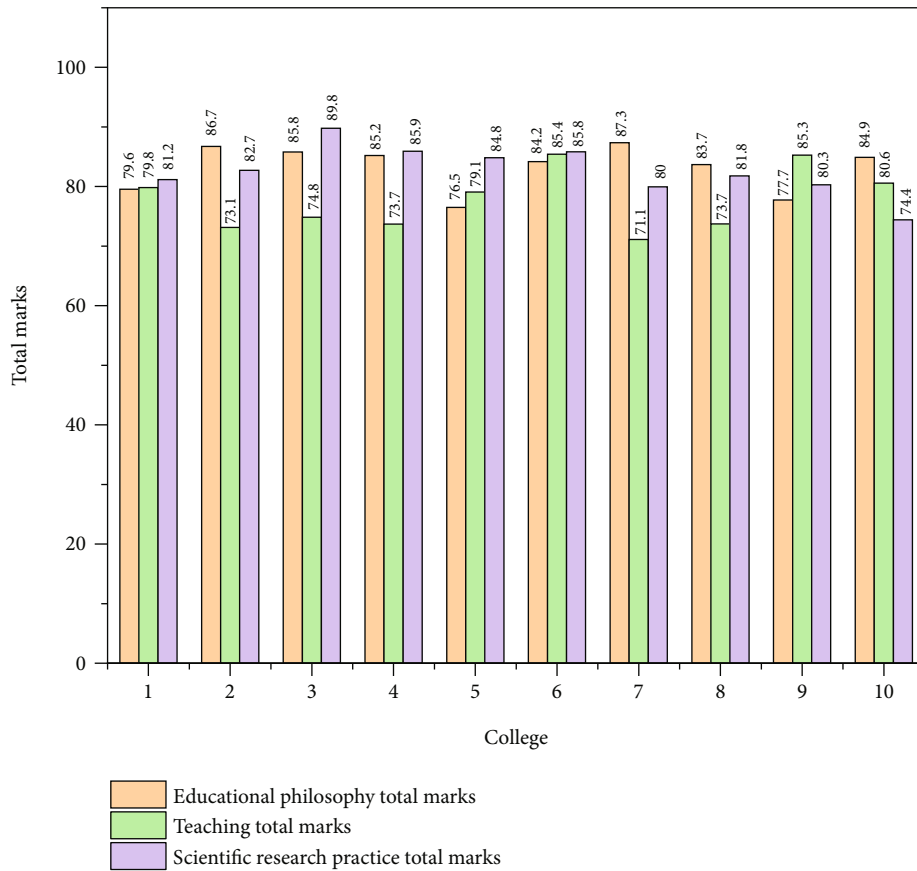


FIGURE 11: Total marks of educational concept, teaching level, and research practice.

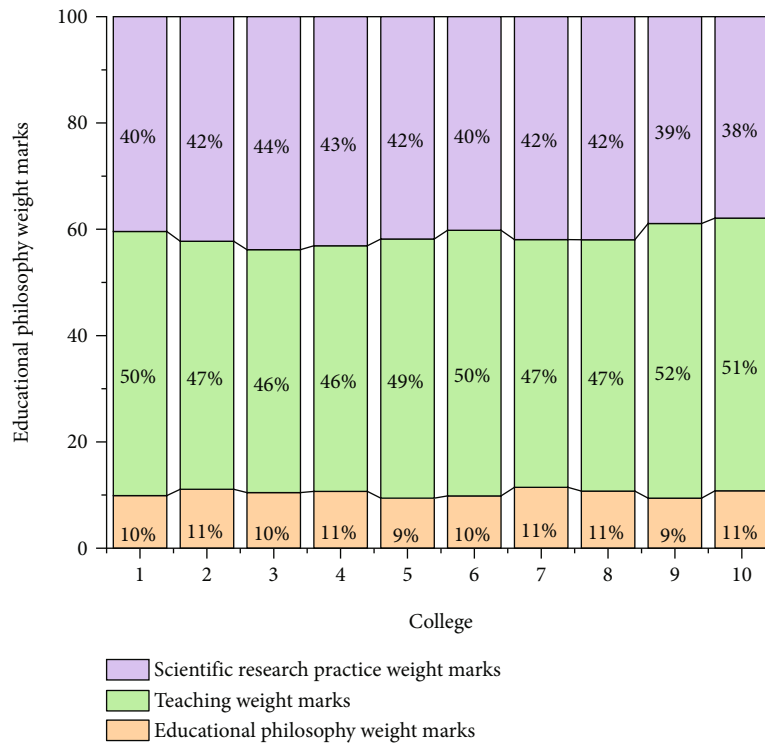


FIGURE 12: Total marks of weight percentage of educational concept, teaching level, and research practice.

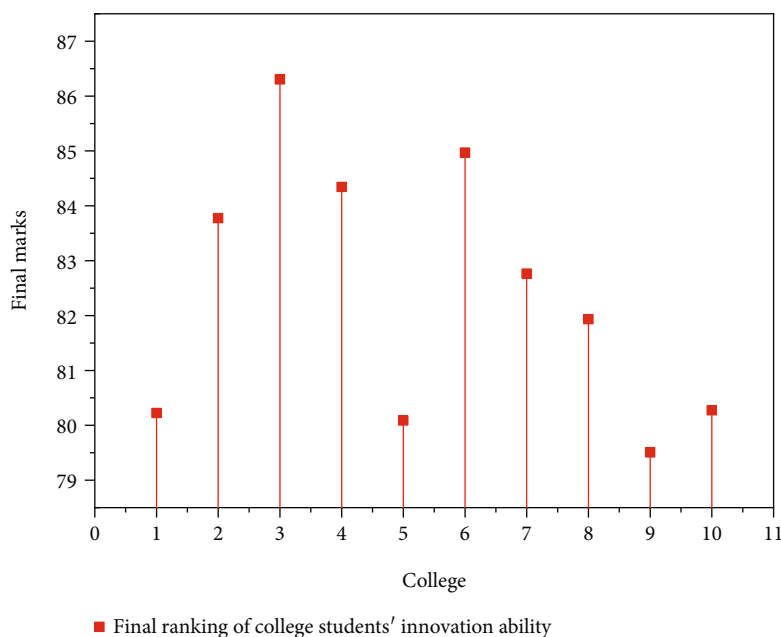


FIGURE 13: Innovation literacy ranking of students from the 10 universities.

part is 15%, and the highest score of the university scores more than 14.5 points.

**6.4. Total Evaluation of Student Innovation Literacy.** The three parts of educational philosophy, teaching level, and research practice, which evaluate the educational level of school students, were weighted and integrated according to the ratio of, 0.1 : 0.5 : 0.4, to obtain the total score of the assessment of students' innovative quality in 10 universities, which also reflects the highly relevant degree of implementation of the intelligent sensor teaching experiment simulation system.

It is expressed by the evaluation of three parts: educational philosophy, teaching level, and scientific research practice; the result is shown in Figure 11. It can be found that the scores of all colleges and universities exceed 70 points in each of them, while the average score reaches 80 points. The highest scores of educational philosophies, teaching level, and research practice are 87.3, 89.8, and 89.8, respectively, which are all close to 90. It also shows that teaching level and research practice are more important for the comprehensive assessment of students' innovation literacy in each university, compared with educational philosophy.

In terms of percentage share, according to the established ratio of 0.1 : 0.5 : 0.4 and weighted integration, the results are shown in Figure 12. Their share is basically stable, and a part of the more prominent universities, the score of research practice can reach 44%, and the share of educational average can reach more than 52%. At the same time, the average score of educational philosophy will not account for more than 11%.

Integrating the innovation literacy of students from the 10 universities can be obtained, the results are shown in Figure 13. It can be found that the highest score is 86.5, and there is only one college with a score lower than 80. From the figure, it can be found that the degree of implementation of intelligent sensor teaching experiment simula-

tion system in each university is relatively close, and the innovation literacy of students in each university is concentrated in the range of 80 to 85 points. At the same time, 85 points is a threshold, and only one college has students' innovation ability significantly more than 86.5 points.

## 7. Conclusion

This article describes the reform of several theoretical teaching components and student literacy evaluation in the course "sensors," as well as the incorporation of the LabVIEW virtual instrument creation platform into the experimental teaching. Based on the establishment of intelligent sensor teaching simulation system, it is incorporated into the evaluation system for evaluating students' innovation literacy; the innovation ability of students in 10 colleges and universities is achieved.

Students can strengthen their comprehension of the theoretical information they have studied via independent analysis and mutual debate, as well as build their comprehensive application ability and teamwork spirit. It has been demonstrated that incorporating the aforementioned teaching materials and approaches into the actual teaching process dramatically increased students' learning passion, learning efficiency, and teaching quality.

Intelligent sensor teaching simulation system has a great promotion effect on improving students' innovative literacy, mainly reflected in the improvement of teaching level and research practice. For teaching level, the successful application of the system is mainly reflected in teaching content, teaching methods, and intelligent lecture areas. For research realization, the successful application of the system is mainly reflected in the laboratory construction, incentive construction, and project funding. In short, through the intelligent sensor teaching simulation system, students' innovation ability has been greatly developed.

## Data Availability

The data used to support the findings of this study are available from the corresponding author upon request.

## Conflicts of Interest

The authors declare that they have no known competing financial interests or personal relationships that could have appeared to influence the work reported in this paper.

## References

- [1] Y. Gang, Z. H. Jia, and L. J. Wang, "Study and design of wireless data communication experiment teaching system based on GPRS," *Advances in Intelligent & Soft Computing*, vol. 108, pp. 527–534, 2011.
- [2] D. Chen, X. Kong, and Q. Wei, "Design and development of psychological virtual simulation experiment teaching system," *Computer Applications in Engineering Education*, vol. 29, no. 2, pp. 481–490, 2020.
- [3] Z. Zhuang, P. Xi, H. Shiliang, S. Xu, and A. Jing, "Design and implementation of data structure experiment instruction assistant system based on NAO robot," *Electronics World*, vol. 5, p. 2534, 2018.
- [4] S. G. Kim and S. G. Baek, "The longitudinal relationships between undergraduate students' competencies and educational satisfaction according to academic disciplines," *Asia Pacific Education Review*, vol. 21, no. 4, pp. 573–587, 2020.
- [5] H. I. Lin, "Design of an intelligent robotic precise assembly system for rapid teaching and admittance control," *Robotics and Computer-Integrated Manufacturing*, vol. 64, no. 9, article 101946, 2020.
- [6] X. Zhang, Y. N. Yang, and B. Liu, "Direct current charger hardware platform design," *Electronics World*, vol. 5, no. 4, pp. 1–10, 2018.
- [7] G. Karalekas, S. Vologiannidis, and J. Kalomiros, "Europa: a case study for teaching sensors, data acquisition and robotics via a ROS-based educational robot," *Sensors*, vol. 20, no. 9, p. 2469, 2020.
- [8] J. Hui, Y. Zhou, M. Oubibi, W. di, L. Zhang, and S. Zhang, "Research on art teaching practice supported by virtual reality (VR) technology in the primary schools," *Sustainability*, vol. 14, no. 3, p. 1246, 2022.
- [9] M. Fitriawanati, M. Sintawati, and E. Retnowati, "Analysis toward relationship between mathematical literacy and creative thinking abilities of students," *Journal of Physics Conference Series*, vol. 1521, no. 3, p. 032104, 2020.
- [10] Y. S. Yang and S. S. Yeh, "Manipulator point teaching system design integrated with image processing and iterative learning control," *Journal of Intelligent & Robotic Systems*, vol. 96, no. 3–4, pp. 477–492, 2019.
- [11] Z. Hao, P. M. Kumar, and R. Samuel, "Internet of things framework in athletics physical teaching system and health monitoring," *International Journal on Artificial Intelligence Tools*, vol. 30, no. 6n08, article 2140016, 2021.
- [12] M. Federer and A. Herrmann, "Comprehensibility of system models during test design: a controlled experiment comparing UML activity diagrams and state machines," *Software Quality Journal*, vol. 27, no. 1, pp. 125–147, 2019.
- [13] Y. Shi, W. Zhang, Z. Yao et al., "Design of a hybrid indoor location system based on multi-sensor fusion for robot navigation," *Sensors*, vol. 18, no. 10, p. 3581, 2018.
- [14] E. C. Callo and A. D. Yazon, "Exploring the factors influencing the readiness of faculty and students on online teaching and learning as an alternative delivery mode for the new normal," *Universal Journal of Educational Research*, vol. 8, no. 8, pp. 3509–3518, 2020.
- [15] M. Metz, "Pedagogical content knowledge for teaching critical language awareness: the importance of valuing student knowledge," *Urban Education*, vol. 56, no. 9, pp. 1456–1484, 2021.
- [16] J. Tomkin and M. West, "STEM courses are harder: evaluating inter-course grading disparities with a calibrated GPA model," *International Journal of STEM Education*, vol. 9, no. 1, pp. 73–101, 2022.
- [17] H. Kim, C. Sui, K. Cai, B. Sen, and J. Fan, "Notice of retraction: An efficient high-speed channel modeling method based on optimized design-of-experiment (DoE) for artificial neural network training," *IEEE Transactions on Electromagnetic Compatibility*, vol. 60, no. 6, pp. 1648–1654, 2018.
- [18] N. Butchart, J. A. Anstey, K. Hamilton et al., "Overview of experiment design and comparison of models participating in phase 1 of the SPARC quasi-biennial oscillation initiative (QBOi)," *Geoscientific Model Development Discussions*, vol. 11, no. 3, pp. 1009–1032, 2018.
- [19] Q. Liu, "Intelligent environmental monitoring system based on multi-sensor data technology," *International Journal of Ambient Computing and Intelligence (IJACI)*, vol. 11, no. 4, pp. 57–71, 2020.
- [20] S. Chen, M. Xuan, J. Xin et al., "Design and experiment of dual micro-vibration isolation system for optical satellite flywheel," *International Journal of Mechanical Sciences*, vol. 179, article 105592, 2020.
- [21] S. N. Wei, J. Dong, Y. H. Wei, Q. Z. Wan, and H. N. University, "Teaching exploring and research of flipped classroom teaching mixed mode in course of sensor and testing technology," *Education Modernization*, vol. 8, pp. 21–25, 2019.
- [22] Y. Zhao, Z. J. Jiang, S. M. Liu, and J. Q. Zhao, "Exploratory experimental teaching design in the teaching practice of polymer physics experiment—with the case study from "preparation and performance research of halogen-free flame retardant epoxy resin"," *Polymer Bulletin*, vol. 5, pp. 11–19, 2019.
- [23] C. Kroustalli and S. Xinogalos, "Studying the effects of teaching programming to lower secondary school students with a serious game: a case study with Python and CodeCombat," *Education and Information Technologies*, vol. 26, no. 5, pp. 6069–6095, 2021.
- [24] A. Ebadat, P. E. Valenzuela, C. R. Rojas, and B. Wahlberg, "Model predictive control oriented experiment design for system identification: a graph theoretical approach," *Journal of Process Control*, vol. 52, pp. 75–84, 2017.
- [25] J. Jiang, X. Zhang, W. G. Xiu, B. I. Dong-Yun, and H. Liu, "Design of portable intelligent wireless FDR sensor system based on mobile phone APP," *Environmental Technology*, vol. 45, pp. 62–70, 2017.
- [26] M. Lin, L.I Ji-Bin, Y. Wang et al., "Design and exploration of comprehensive experiment in teaching polymer physical experiment," *Polymer Bulletin*, vol. 9, pp. 15–21, 2018.
- [27] L. Zhang, X. Zeng, L. I. Chun-Hai et al., "Teaching design and practice of food microbiology experiment based on working

- process orientation,” *Journal of Microbiology*, vol. 10, pp. 1–11, 2019.
- [28] Z. He and E. Doss, “Correlation of design parameters with performance for electrostatic precipitator. Part II. Design of experiment based on 3D FEM simulation,” *Applied Mathematical Modelling*, vol. 57, no. 5, pp. 656–669, 2018.
- [29] I. Resin and A. Ki, “Design of experiment approach to optimize hydrophobic fabric treatments,” *Polymers*, vol. 12, no. 9, 2020.
- [30] D. Laneri, M. Marcotullio, and A. Neri, “A design of experiment approach for ionic liquid-based extraction of toxic components-minimized essential oil from *Myristica fragrans* Houtt. fruits,” *Molecules*, vol. 23, no. 11, 2018.
- [31] A. Shahzad, N. Ahmad, Z. Ali et al., “Statistical analysis of yarn to metal frictional coefficient of cotton spun yarn using Taguchi design of experiment,” *The Journal of Strain Analysis for Engineering Design*, vol. 53, no. 7, pp. 485–493, 2018.
- [32] K. Wang, L. Zhang, Y. Le, S. Zheng, B. Han, and Y. Jiang, “Optimized differential self-inductance displacement sensor for magnetic bearings: design, analysis and experiment,” *IEEE Sensors Journal*, vol. 17, no. 14, pp. 4378–4387, 2017.
- [33] S. Sivaranjani, S. Velmurugan, K. Kathiresan, M. Karthik, and M. Suresh, “Visualization of virtual environment through lab VIEW platform,” *Materials Today: Proceedings*, vol. 45, no. 2, pp. 2306–2312, 2020.

## Research Article

# Robust Refinement of Built-in Network Information System Based on Nonparametric Density Estimation

Qiongzhen Mei<sup>1</sup>  and Fei Wang<sup>2</sup>

<sup>1</sup>College of Artificial Intelligence, Chongqing Creation Vocational College, Yongchuan, Chongqing 402160, China

<sup>2</sup>College of Automotive Engineering, Chongqing Creation Vocational College, Yongchuan, Chongqing 402160, China

Correspondence should be addressed to Qiongzhen Mei; [meiqongzheng1@163.com](mailto:meiqongzheng1@163.com)

Received 22 March 2022; Revised 22 April 2022; Accepted 9 May 2022; Published 31 May 2022

Academic Editor: Wen Zeng

Copyright © 2022 Qiongzhen Mei and Fei Wang. This is an open access article distributed under the Creative Commons Attribution License, which permits unrestricted use, distribution, and reproduction in any medium, provided the original work is properly cited.

In the research process of robustness refinement solution of built-in information systems for electronic networks, there are too many factors related to robustness in the current system robustness design, and different factors have different influences on robustness. In stochastic programming problems, uncertain variables usually obey a certain probability distribution, but in real decision-making, these determined distributions are often unknown or we only know part of the information of the distributions, and distributed robust refinement solution is just an effective solution to solve uncertain problems. The robustness measurement solution of information systems for electronic networks is analyzed. The robust refinement of information system is deeply studied by nonparametric density estimation solution, which is based on the strict robustness requirements put forward by users. Based on the research results of interdependent network theory and aiming at “improving the robustness of electronic information system,” this paper makes an in-depth study on the robustness refinement strategy of power information system. The comparison between the companies that adopted the robust refinement of built-in information systems for electronic networks based on nonparametric density estimation and the companies that did not adopt it shows that the refinement rate of the companies that adopted it in the first three years was 82%, while that of the companies that did not adopt it was only 57%, and the overall misjudgment rate was 43%. Therefore, it is proved that using the proposed reliability refinement solution to optimize, the embedded system can improve the service life, modeling accuracy, and availability of the system and has certain practicability.

## 1. Introduction

With the continuous rise of China’s network technology level, the built-in information systems for electronic networks have entered a rapid development, and it also makes its role in application construction more prominent. [1]. Vigorously promoting informatization is a strategic measure of China’s overall modernization drive and an urgent need and inevitable choice for building an innovative country [2]. Nonparametric density estimation is an important direction of modern statistics development in recent years, which has changed the development pattern of traditional statistics [3]. For the system of network operation platform, built-in information systems for electronic networks are essential. As an index, robustness can measure the ability

of network electronic information system to maintain normal operation under pressure environment or abnormal input environment. [4]. The nonparametric density estimation solution does not need to assume the parameter form of point sample distribution in advance, and can estimate the probability density function accurately and robustly only from the sampled data itself, which provides a new solution for the analysis and modeling of unknown distribution point samples [5].

For multiobjective refinement problems, the existing research mainly focuses on searching high-quality solutions, and many multiobjective refinement algorithms based on Pareto optimal set are proposed, but the research on multiobjective robust refinement solutions is relatively less [6]. For example, in the part processing system, the machine

cannot process in strict accordance with the specified specifications, and there are often certain errors, which require that the design parameters can meet a certain tolerance [7]. In some special cases, sufficient conditions are provided to ensure the uniqueness of the robust solution and the continuity of the data on the undisturbed problem [8]. The research of complex network theory in power system mainly focuses on the actual power network, which can be obtained through the geographical wiring diagram of power network. Some studies directly use the topology diagram of IEEE node system as the research object [9]. Driven by technological progress and external demand, the function of embedded system continues to expand, the scale of the system is becoming larger and more complex, and the defect and failure rate of the system are also increasing.

The nonparametric density estimation is a developing field with a short history. People are still unfamiliar with it and lack of understanding of it. Its application in practice, especially in the economic field, is less, and its application field needs to be further expanded [10]. However, as a new thing, people are relatively unfamiliar with the nonparametric density estimation solution compared with the traditional parametric solution and lack in-depth understanding of it. There are still many areas worthy of improvement in the specific application of combining with other algorithms, and the application field needs to be further expanded [11]. Due to the complexity of the research object, it is necessary to carry out comprehensive research of multidisciplinary, such as computer science, management science, system science, information science, and cybernetics [12]. Not only that many control systems have a lot of noise and interference, which cannot be accurately expressed in the model, so the control system must have a little anti-interference ability, that is to say, but also it has certain robustness [13]. To study robustness, it is necessary to fully understand the influencing factors of system robustness, identify the operating mechanism of the system in essence, and then explain the external behavior characteristics of the system [14]. At this time, if we want to use nonparametric statistical solutions, the only remedy is to increase the sample size and use large samples to make up for the losses caused by using nonparametric statistical solutions [15]. Sometimes, the solution of the refinement problem is very sensitive to the parameters. When the parameters are slightly disturbed, the solution of the problem will fluctuate greatly, which makes it no longer the solution of the problem or even highly infeasible, which is of great significance in practical problems.

The innovation of this paper:

- (1) The principle of nonparametric discriminant analysis based on nonparametric density estimation is introduced in detail, which makes the application of nonparametric discriminant solution reasonable
- (2) The application of nonparametric density estimation solution can calculate the density value of arbitrarily distributed difference matching samples at the test sample points in the feature space

- (3) The electronic information system must keep advancing and developing, so as to gain advantages in the fierce market competition environment. Information resources are one of the important components of enterprise management information system. Using component solution to complete the analysis and design of information resources of electronic information system greatly enhances the reusability of electronic information system

The research framework of this paper includes five parts, and the specific arrangements are as follows: the first chapter introduces the research background and significance and then introduces the main work of this paper. Chapter 2 focuses on the current status of research related to nonparametric density estimation and robust reinforcement of embedded information system. Chapter 3 proposes a specific solution and implementation of robust reinforcement of embedded information system design. In Chapter 4, the nonparametric density discrimination is analyzed in detail. The fifth chapter is the summary of the full text.

## 2. Related Work

*2.1. Nonparametric Density Estimation.* Because nonparametric estimation does not assume the mathematical form of unknown density function, it is difficult to expect to get deep small sample properties. Although this solution is accurate, real, and relatively simple, when the system structure is huge, its closed-loop structure will become very complicated correspondingly, resulting in unstable reliability. Samples within a certain distance play the same role. Intuitively, it can be imagined that for estimating the density function, the close samples seem to play a greater role than the far samples.

Therefore, nonparametric density estimation is only an effective tool for point sample analysis or modeling in many cases. Many specific problems need to be combined with other algorithms or processing solutions to be solved. It is proved that the linear feedback system with single gain and infinite gain has good stability [16]. Chao et al. focused on a robust refinement solution for embedded information systems based on Markov algorithm. The histogram density estimation solution is used to model the moving target color features, but the weight kernel function related to the pixel position features is also introduced in the modeling process, which improves the accuracy of density estimation and suppresses the influence of interference and deformation on the tracking accuracy to a certain extent [17]. Garroppo et al. proved the estimated point-by-point strong phase coincidence speed problem in robust optimal design of networked information systems by building a stochastic response model and Markov time chains for networked information systems [18]. Andregiovanni et al. focused on the application of nonparametric estimation; first, construct the model of network electronic information system and sample from the known probability distribution of network electronic information system [19].

**2.2. On Robust Refinement of Embedded Web Information Systems.** Nyikes et al. first proposed a convex programming model, then solved this problem through an auxiliary linear programming model, and finally applied this model to an inexact linear programming problem. Until 1990s, robust refinement attracted extensive attention of scholars [20]. Rodrigues et al. proposed a solution to improve the system reliability by connecting the system with its cross-linked physical equipment [21]. The whole system is truly connected with its cross-linked physical equipment to form a closed-loop structure to increase the reliability of the system. Sun et al. aimed at analyzing the growth and evolution mechanism of information systems and at the same time built the generation and evolution model of small-world information systems. By analyzing the correlation between network topology and information flow characteristics, it was finally verified that small-world characteristics are the result of long-term refinement evolution of information systems [22]. Gramacki and Gramacki believe that robust refinement is a modeling solution combined with computational tools, which is mainly used to deal with the refinement problems with uncertain data and the real data only belong to some uncertain sets [23]. Chauveau et al. proposed a robust refinement solution of built-in information systems for electronic networks based on simulated annealing algorithm [24]. This solution calculates the global optimal solution of the objective function of the built-in information systems for electronic networks according to the mapping characteristics of the probability sudden jump characteristics of the built-in information systems for electronic networks in the solution space and realizes the robustness refinement of the built-in information systems for electronic networks. Trentin discusses the robustness refinement solution of built-in information systems for electronic networks based on branch and bound algorithm [25].

Aiming at the above problems, a robust refinement solution of built-in information systems for electronic networks based on nonparametric density estimation is proposed. Thus, the robustness refinement design of built-in information systems for electronic networks is realized, which has high application value [26]. In the development and management of large-scale Internet software system, the robust refinement of built-in information systems for electronic networks with obvious self-organization characteristics of complex system is a subversive innovation of traditional structured information system.

### 3. Embedded Information System Refinement

**3.1. Solution of Failure Probability of Built-in Information Systems for Electronic Networks.** The word “robustness” comes from Latin, meaning robustness [27]. In engineering refinement design, there are two kinds of parameters: design parameters and environmental parameters. The design parameters change during the refinement process, and the objective refinement is realized by their changes. The satisfaction of performance is subjectively determined by the expectations of designers and users, so the measurement index of robustness is not unique, which means that robust-

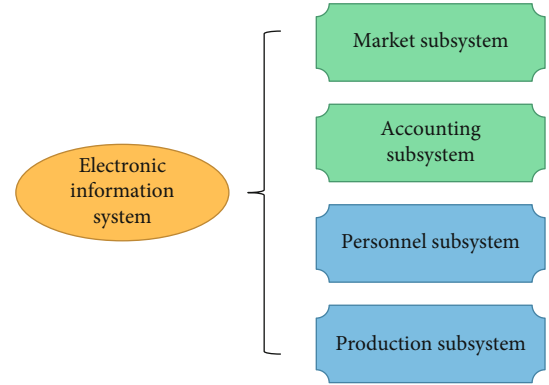


FIGURE 1: Structure diagram of internal management system of electronic information system.

ness analysis is a necessary link in the process of information system design and operation [28]. For stable systems, the real part of eigenvalues is greater than zero, so only  $P \underline{\Delta} W_c(\infty)$  needs to be considered. That is to say,  $(A, B)$  is a controllable state if and only if it is a controllable matrix:

$$P \underline{\Delta} \int_0^{\infty} e^{A\tau} B B^T e^{A^T \tau} d\tau. \quad (1)$$

The value of environmental parameters is generally given in advance and fixed in the refinement process [29]. Although the theorem only gives the sufficient conditions for the robust stability of the system, it also satisfies the necessary conditions. Because the robustness of the two types of parameters needs to be considered, for convenience, these two types of parameters are not distinguished, which are collectively referred to as the parameters of the refinement problem. The use of information technology gradually rises from the management of operation level to the management of decision-making level. Enterprise management is based on the decision-making system model. The internal management system structure of electronic information system is shown in Figure 1.

Firstly, the failure modes of built-in information systems for electronic networks are divided into single limit state and multilimit state. The topological integrity of the network after being attacked is higher than that of the initial network, which indicates that the recovery speed of the system from the failure state is faster. Obviously, the solution of failure probability of built-in information systems for electronic networks can effectively improve the ability to resist cascading failures. For incomplete controllable multi-input-multioutput continuous-time linear time-invariant systems

$$\begin{aligned} x &= Ax + Bu, \\ y &= Cx. \end{aligned} \quad (2)$$

We assume that users have fully understood the essence of the problem and clearly know the disturbance amplitude and disturbance range of each parameter. On this basis, a strict robustness requirement is given. The input to the controller is  $r - y_m$ ,  $y_m = y + n$  is the measurement output, and it is the measurement noise, so the input to the object  $G$  is



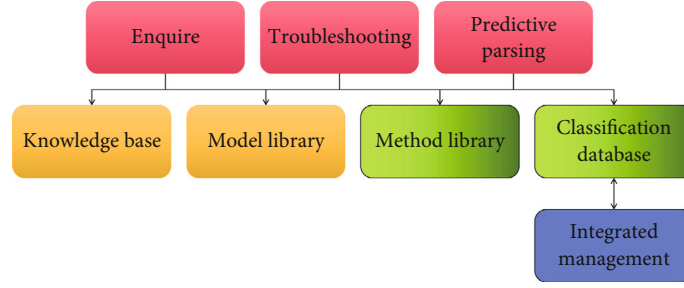


FIGURE 2: Robustness improvement process.

$$u = K(s)(r - y - n). \quad (3)$$

The algebraic connectivity is used to measure the robustness of the network, and the system robustness is improved by optimizing the component-level network structure and ensuring the rapid propagation of the best behavior model. The promotion process is shown in Figure 2.

Secondly, random sampling cannot accurately reflect the situation of each point in the neighborhood. For the robust solution obtained by this measurement solution, the variation of the function value of the point disturbed by the parameter may fall outside the specified variation range in practical application. Therefore, the failure probability of built-in information systems for electronic networks in two states is calculated, and the robustness refinement function of built-in information systems for electronic networks is given based on the obtained failure probability. The influence of configured physical nodes on the robustness refinement of electronic information system is related to the relative power load of neighbor nodes in the physical layer. When there are small power load nodes in the adjacent nodes of the physical nodes, it can greatly improve the robustness of the information system.  $S$  is the system output, while  $n$  is the closed-loop transfer function from the reference signal to the system output. From  $S + T = I$

$$\begin{aligned} |1 - \sigma(S)| \leq \sigma(T) \leq 1 + \sigma(S), \\ |1 - \sigma(T)| \leq \sigma(S) \leq 1 + \sigma(T). \end{aligned} \quad (4)$$

The failure mode consists of single limit state and multi-limit state. When the failure factors in the failure mode of the system are all connected in series and each failure factor contains common variables, this failure mode is defined as a single limit state. The traditional solution includes solving the overall refinement problem and making all decisions at the same time. With the increase of the number of variables and constraints, the problem may soon become difficult. However, the solution of built-in information systems for electronic networks failure probability mainly strips the code of embedded electronic information system software, then tests it with digital platform, and then improves the reliability in a targeted way. Therefore, how to define an appropriate image problem under the framework of image space analysis so that it can be equivalent to robust correspondence problem and contain uncertain parameters is very important.

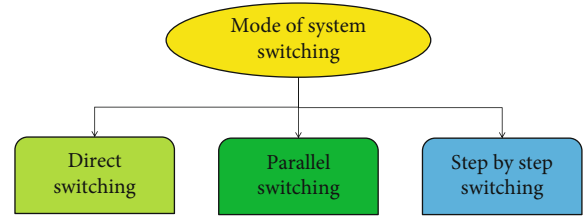


FIGURE 3: System switching mode.

**3.2. Robustness Refinement Solution of Built-in Information Systems for Electronic Networks.** Integrating the combination of chaos optimization and particle swarm optimization is based on determining the robustness refinement objective function of built-in information systems for electronic networks [30]. The information network is composed of information communication equipment and communication lines. Among them, information communication equipment includes computing equipment (computer, server, and embedded computing equipment) and data acquisition equipment (sensor, PMU, and embedded data acquisition equipment). In the process of system switching and delivery, make a system switching plan, control the progress of work, check the quality of work, and timely coordinate all aspects to ensure the successful switching and delivery of the system. There are usually three ways to switch and deliver the system, as shown in Figure 3.

Firstly, the robust refinement area of embedded electronic information system is dynamically analyzed with the help of robust refinement function. The purpose of computer programming is to realize the management mode and business application proposed in system analysis and design. The calculation of embedded electronic information system is mainly composed of operating system and application program. It needs to make up for the differences in hardware in the calculation, provide a unified system interface for the application program, and complete the control of memory management and task scheduling. Assuming a multivariable system  $P(S)$ , find a stable controller  $K(s)$  so that the transfer function  $T_{ZW}$  of the closed-loop system, that is, the transfer function from input  $Z$  to output  $e$ , satisfies the following relationship:

$$\frac{1}{F_M(T_{ZW}(j\omega))} < 1. \quad (5)$$

According to the robustness function of built-in information systems for electronic networks, the robust refinement area of built-in information systems for electronic networks is dynamically searched, and the robustness refinement objective function value of built-in information systems for electronic networks is calculated. The solution of the above problem involves the nonconvex refinement problem of  $\Delta$ , which cannot be calculated by the standard nonlinear gradient descent solution, because the convergence of the algorithm cannot be guaranteed. However, because  $\mu$  has an upper bound,  $F_M$  can be calculated by the following formula:

$$\frac{1}{F_M(T_{ZW})} = \mu(T_{ZW}) \leq \inf \|DT_{ZW}D - 1\|. \quad (6)$$

Among them, data aggregation preprocesses the data obtained from various data sources and then stores the data in the database. Data analysis is to further process data and produce valuable information by using tools such as stream computing and data mining.

Secondly, the global refinement is carried out by calculating the robustness refinement objective function value of built-in information systems for electronic networks. This refinement work may be realized through certain test solutions. The test solution of any product is general if you already know the functions that the product should have and if you can test whether each function can be used normally. Using the separation theory or the principle of definite equation, the solution of this problem can be understood as finding a simple state feedback law:

$$u(t) = -K_r x(t), \quad (7)$$

where  $K_r$  is the constant matrix.

Due to the limited capacity of the embedded system's own ROM, the system's application programs need to complete specific application tasks based on EOS. However, the embedded electronic information system itself has no independent development capability, and users must carry out secondary development through a set of development tools and environment, which will also lead to the decline of system reliability. In the context-aware design and production, based on the massive data collected by sensors, platforms, and websites, it automatically evaluates and analyzes the operation status of enterprises and provides improved solutions for product design, resource allocation, preventive maintenance, and supply chain management of enterprises. The sensor obtains the output of the sensor by performing proportional, integral, and differential operations on the error signal and weighting the results, which is the control value of the controlled object. The mathematical description of the sensor is

$$u(t) = Kp \left[ e(t) + \frac{1}{T_i} \int e(t) dt + T_d \frac{de(t)}{dt} \right], \quad (8)$$

where  $u(t)$  is the controller output;  $e(t) = r(t) - c(t)$  is the

system error signal;  $r(t)$  is the system input quantity; and  $c(t)$  is the system output.

Based on the value of robustness refinement objective function of built-in information systems for electronic networks, the speed and position of update particles are calculated. Regardless of its internal structure and processing process, give it appropriate inlet parameters to see whether its outlet parameters are correct or whether the corresponding functions are realized. The built-in information systems for electronic networks discussed in this paper is a multi-input-multioutput linear time invariant system, which is expressed in state space as follows:

$$P \begin{cases} x = Ax + B_w w + Bu \\ y = Cx + D_w w \\ z = C_z x + D_{zw} w + D_z u \end{cases}, \quad (9)$$

where  $u \in R^{n_u}$  is the control input vector;  $w$  is the external input vector;  $y \in R^{n_y}$  is the measure of the output vector; and  $z$  is the output signals related to the performance of the control system.

If you know the internal working process of the product, you can test whether the internal actions of the product are carried out normally according to the specifications.

## 4. Nonparametric Density Discriminant Analysis

**4.1. K-Nearest Neighbor Discriminant Analysis.** The so-called discriminant analysis is a statistical analysis solution that establishes a discriminant criterion according to the observed data of a batch of samples, which are known to be different types of research objects, and then discriminates and classifies the unknown types of samples. This solution realizes the direct intelligent control of the embedded electronic information system by adding a control module to the embedded electronic information system and increases the reliability of the system. If the kernel function is uniformly distributed, the final probability density is estimated as the proportion of the number of sample points falling into a form to the number of all sample points. Figure 4 lists the expressions and function curves of some one-dimensional kernel functions.

According to different node configuration strategies, physical nodes are added to reduce the load; then, information nodes are added; and edges are added according to the principle of topological similarity. In the theory of nonlinear dynamics, the attributes or characteristics of the system are represented by state variables, and the change of state variables reflects the operating rules of the system. If we calculate the difference between the eigenvectors of the pixel samples at the corresponding positions of the two window matching primitives, it can be known from the compatibility constraint that all the difference eigenvectors should be zero vectors in an ideal situation. When carrying out robustness refinement activities, it is necessary to consider the differences of the action intensity of each element on the system,

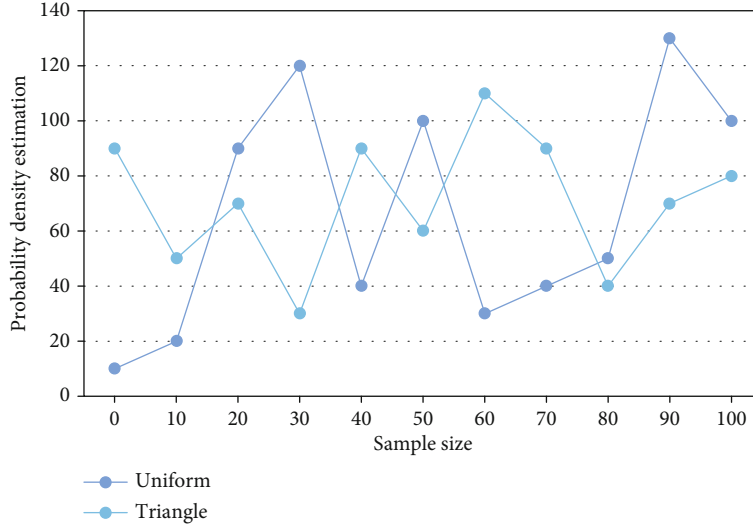


FIGURE 4: One-dimensional kernel function curve.

TABLE 1: Coupling strength of each node.

Variable	$ M_{xi} $	$ R \max (x_i) $	$d(x_1)$	$x_i$
$p_1$	0.421	17	0.3	$t_1$
$p_2$	0.413	13	0.4	$t_2$
$p_3$	0.501	15	0.1	$t_3$
$p_4$	0.623	14	0.6	$t_4$
$p_5$	0.459	16	0.5	$t_5$
$p_6$	0.437	13	0.4	$t_6$

which is conducive to taking control measures more carefully and clearly in priority subconsciously. Table 1 shows the coupling strength of each node.

First of all, both the positive and wrong judgment rates indicate a good judgment effect, and the latter indicates a good judgment effect. Therefore, we can estimate the probability density function  $p$  by estimating probability  $P$ . Because the electronic information system contains many connected by nonlinear interaction relations, it can be deduced that its operation model is a multidimensional logical mapping. Parameters  $\alpha_{i1}$  and  $\alpha_{i2}$ , respectively, represent the change rate of technical level and management level when the technical system and organizational system operate independently and the input is constant. Consider how the singular value of the auxiliary sensitivity function  $T(s)$  determines the stability margin of the multivariable multiplicative disturbance  $\Delta_M$ . It is found that when  $k_n$  is an even number, it is judged as other, indicating that the sample mixing is serious. At this time,  $k_n$  can only take odd numbers, and finally, the discriminant function of  $k_n = 1$  is established. The greater the value of  $\alpha_{i1}$ , the more technical system investment, the same as  $\alpha_{i2}$ . The same analysis can also be made for the additive uncertainty  $\Delta_M$ , and the results are similar to those of  $\Delta_{A(s)}$ . The kernel density estimation can be regarded as the sum of the windows centered on each

observation sample point, while the smooth kernel estimation is the sum of the smooth “bulges” placed at the observation points, as shown in Figure 5.

Secondly, the chaos factor is used to identify the main failure modes of the built-in information systems for electronic networks, and the robustness of the system structure is analyzed to calculate whether each particle meets its constraint conditions. In each step, firstly, the power loads of all physical nodes are recalculated, and the nodes are sorted according to the load from large to small. Let the candidate solution be and the corresponding objective function vector of  $x$  is  $f(x)$ . In the process of implementation, due to the influence of environment or other inevitable factors, it is impossible for the implementer to implement strictly according to its specified quantity  $x$ . Therefore, when the number of samples  $n$  tends to infinity, the distribution becomes steep (the variance becomes smaller), and we can get a good estimate of the probability  $P$  from the proportion of samples falling into the region  $R$ . And find out all the dependent nodes of these nodes as neighbors of the newly configured information nodes. In the process of robust refinement design of built-in information systems for electronic networks, the remaining 70% of the population is randomly generated in the searched space. The larger the value of the probability density function at the sample of the test point, the more concentrated the distribution of all sample points near the point. To characterize the robustness of a solution, we should know the disturbance distribution of parameters in advance, including the disturbance distribution and joint disturbance distribution of each parameter near the solution. Therefore, by changing the value of this register, the smaller phase error can be corrected, and the larger phase error can be realized by anti-aliasing filter. Let  $\{x_n\}$  be the generated sequence and  $x_0$  be a limit point. If every  $\xi \in f(x)$  is continuously differentiable and  $X$  is a convex function, then  $x_0$  is the optimal solution.

The results show that the company that adopted the robust refinement of built-in information systems for

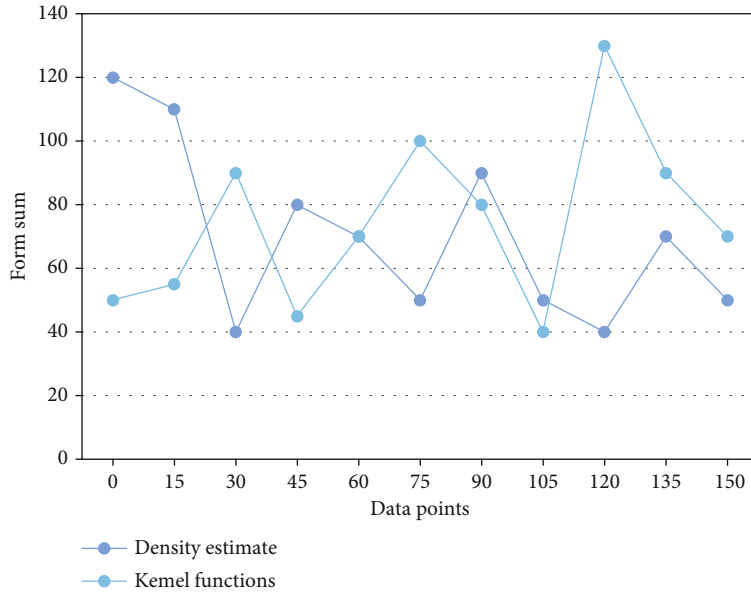


FIGURE 5: Schematic diagram of kernel density estimation.

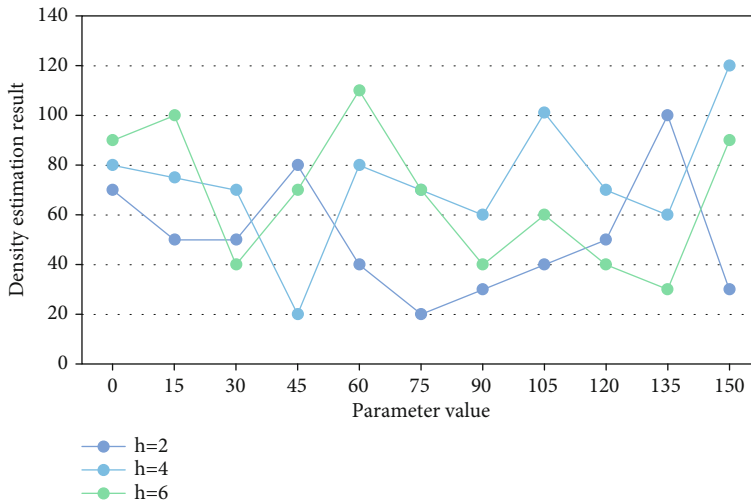


FIGURE 6: Kernel density estimation results under different bandwidth.

electronic networks based on nonparametric density estimation achieved a refinement rate of 82% in the first three years, while the company that did not adopt it achieved a refinement rate of only 57%, and the overall error rate was 43%. To sum up, it can be explained that the robust refinement principle of built-in information systems for electronic networks effectively completes the robust refinement design of the system.

**4.2. Bayes Discriminant Analysis.** The traditional Bayesian discriminant solution specifies that the population follows the normal distribution, but in practical application, especially some economic problems, the population does not meet the normal distribution at all. Therefore, in the Bayesian discriminant solution, it is not assumed that the population satisfies any distribution; of course, it does not satisfy the normal distribution, but directly estimates the probabil-

TABLE 2: Parameter results calculated by Bayes solution.

$\varepsilon$	Optimal value	Optimal solution	Iter
1	$x^* = (0, 0, 0, 0, 0, 0.1, 0, 0)$	2.156	4
0.1	$x^* = (0, 0, 0, 0, 0.2, 0.3, 0, 0)$	3.261	4
0.01	$x^* = (0, 0, 0, 0, 0.4, 0.5, 0, 0)$	4.895	4
0.001	$x^* = (0, 0, 0, 0, 0.6, 0.7, 0, 0)$	5.732	4
0.0001	$x^* = (0, 0, 0, 0, 0.8, 0.9, 0, 0)$	6.573	4
0.00001	$x^* = (0, 0, 0, 0, 1, 1.1, 0, 0)$	7.648	4

ity density of various types in the population through the nonparametric density estimation solution, which forms the nonparametric discriminant solution. In embedded system, computer system is generally embedded into the whole application system as an intelligent control component. It is

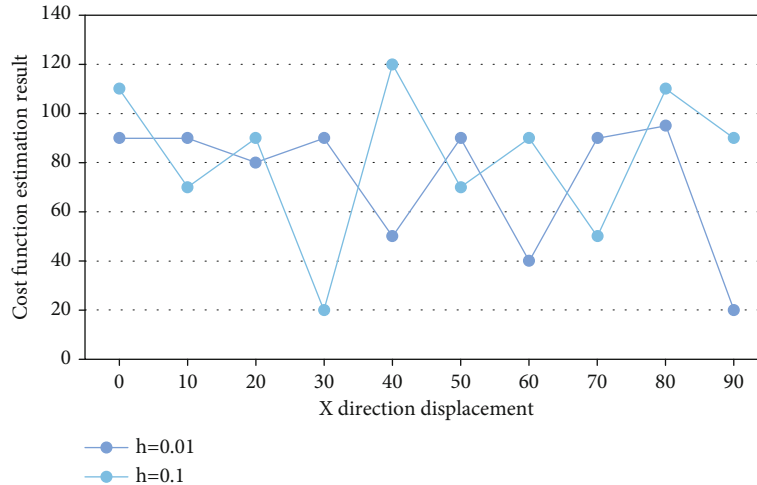


FIGURE 7: Relationship curve between bandwidth and cost function.

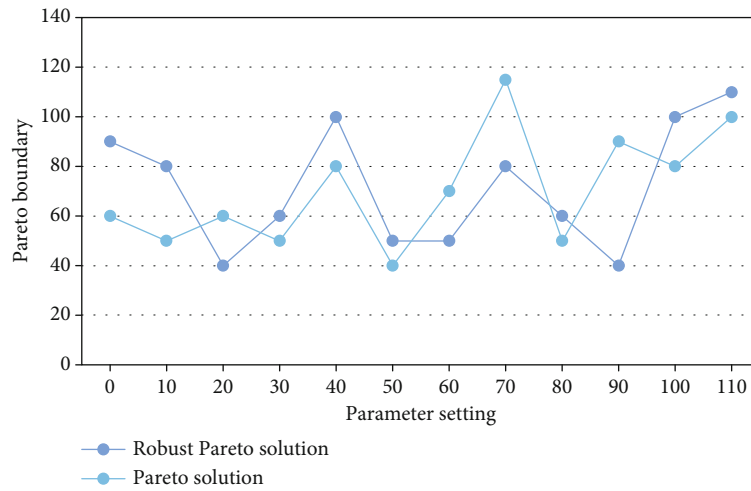


FIGURE 8: Pareto boundary simulation results.

the control center of the whole system. It is mainly used to control the information processing component and user interface of the system. The task of discriminant analysis is to establish a discriminant function according to the mastered sample data and then judge which population it comes from for a given new observation. It can be divided into two population discrimination and multipopulation discrimination. Figure 6 shows the density estimation results obtained when the Gaussian kernel function is also selected and the bandwidth is 2, 4, and 6, respectively.

First of all, if you know something, it can be divided into  $k$  population:  $G_1, \dots, G_2, G_k$ , the characteristics of this thing are described by  $p$  indicators. Before analysis, samples in each population have been observed. The specified range of a function variation and the radius of a spherical neighborhood with parameter variation are determined in advance. The robustness refinement area of built-in information systems for electronic networks is dynamically searched by using the acquisition function, and the global optimal solution of robustness design of built-in information systems for electronic networks is carried out by calculating the

robustness refinement objective function of built-in information systems for electronic networks. When  $f_n = 5\%$ , the proportion of physical nodes with power load above 800 in the original physical layer and its four strategies was 15%, 24%, 36%, 22%, and 50%, respectively. With the increase of the proportion of configuration nodes, the digitized voltage and current values are sent to each calculation unit to obtain various power parameters, and these parameters are saved in the corresponding registers. Next, Table 2 shows the experimental results that the proportion of physical nodes is 15%, 24%, 36%, 22%, and 50%, respectively, and the power parameters are calculated in Bayes solution.

If the system has a stable controller and satisfies the frequency constraint, the function must be able to find at least one such global optimal solution. After getting the global optimal solution, we try to get the similarity relationship between the reference matching window and the target matching window by analyzing the distribution of the set in the feature space. The fault density function of embedded electronic information system is optimized to reduce the number of system faults. In the process of cost function

refinement, the choice of bandwidth will affect the shape of the relationship curve between parameter values and cost function values and then affect the solution of quasi-Newton refinement process. Figure 7 shows two sets of laser scanning data obtained at two adjacent times.

Secondly, the estimated prior probability and density function are substituted into the discrimination rules to obtain the posterior probability for comparison.  $H_\infty$  theory is used for the preliminary design of the system, and then, the appropriate criteria are selected according to the results of the preliminary design. Finally, Pareto boundary theory is used to complete the final system design. Figure 8 shows the Pareto boundary obtained by running under the same parameter setting and the Pareto boundary meeting the user's robustness requirements.

The failure modes of built-in information systems for electronic networks are divided into single limit state and multilimit state, and the failure probability of built-in information systems for electronic networks in these two states is calculated. The failure rate of embedded electronic information system is defined as the probability that the embedded system will fail in a certain period of time; that is, the ratio of the number of failed devices in a unit period of time to the devices still works normally at the moment after the system works until the moment. The reason is that the technical level and the management level gradually consume limited resources in the evolution process, and when the consumption reaches a certain level, there will be a self-restraint effect. For each candidate solution, a certain number of points are randomly sampled in a spherical neighborhood with a given radius. If the number of points whose function value does not exceed the specified range is not lower than a given threshold compared with the number of all sampling points, the candidate solution is considered to be robust.

## 5. Conclusions

When using the current algorithm to optimize the robustness of the system, it is difficult to determine the global optimal solution of the system, and there is a problem of large refinement design error. However, while improving the automation level, social production efficiency, and user experience, informatization also brings many hidden dangers to the security of intelligent system. The commonly used multiobjective refinement control algorithms include linear programming, genetic algorithm, evolutionary algorithm, and neural network refinement. The failure of the information system may affect the other party's network, resulting in cascading failure propagation, which seriously affects the safe operation of the electronic information system. Driven by the competing development of probability theory and statistics and the trend of overlapping applications, various application studies based on nonparametric density estimation and statistical analysis have been proposed and developed and gradually show good application performance.

Therefore, in this paper, nonparametric density estimation is used as a means to analyze point samples, and the solutions of failure probability and robustness refinement

of built-in information systems for electronic networks are studied, respectively. Compared with traditional solutions, the reliability refinement solution proposed in this paper can improve the service life, availability and efficiency of embedded system to a certain extent, and it has certain reference value. The interaction threshold condition determined by model analysis and corresponding algorithm is the key to robust operation, which can provide reference for system planning, design and operation and maintenance management. In addition, for multi-input and multioutput systems, multiobjective control system design is carried out by using multichannel design idea, and robust refinement of built-in information systems for electronic networks based on nonparametric density estimation is more simple and effective.

## Data Availability

The labeled dataset used to support the findings of this study are available from the corresponding author upon request.

## Conflicts of Interest

The author declares no competing interests.

## Acknowledgments

This research supported by Natural Science Foundation of Yongchuan District, Chongqing (No.2020nb0504).

## References

- [1] P. Yang, X. Zhou, and J. Jia, "Research on robust design and optimization of embedded network electronic information system," *Journal of Physics Conference Series*, vol. 1550, no. 3, article 032119, 2020.
- [2] Z. Gao and H. Lu, "WITHDRAWN: design of robust pole configuration controller based on embedded network distributed single input system," *Microprocessors and Microsystems*, vol. 6, article 104066, 2021.
- [3] Y. Yuan, Z. Li, and B. Huang, "Robust optimization under correlated uncertainty: formulations and computational study," *Computers & Chemical Engineering*, vol. 85, no. Feb.2, pp. 58–71, 2016.
- [4] T. Nagler and C. Czado, "Evading the curse of dimensionality in nonparametric density estimation with simplified vine copulas," *Journal of Multivariate Analysis*, vol. 151, pp. 69–89, 2016.
- [5] K. Ji, M. Ling, Y. Zhang, and L. Shi, "An artificial neural network model of LRU-cache misses on out-of-order embedded processors," *Microprocessors and Microsystems*, vol. 50, pp. 66–79, 2017.
- [6] C. Maschio and D. J. Schiozer, "Probabilistic history matching using discrete Latin Hypercube sampling and nonparametric density estimation," *Journal of Petroleum Science & Engineering*, vol. 147, pp. 98–115, 2016.
- [7] B. Xia, Z. Ni, T. Li, Q. Li, and Q. Zhou, "VRer: context-based venue recommendation using embedded space ranking SVM in location-based social network," *Expert Systems with Applications*, vol. 83, pp. 18–29, 2017.

- [8] Q. Du and H. Huang, "Application strategy of computer network technology in electronic information engineering," *International Technology Management*, vol. 4, p. 3, 2017.
- [9] Q. Zhang, T. Han, G. Tang, J. Chen, and K. Y. Hashimoto, "SAW characteristics of AlN/SiO<sub>2</sub>/3C-SiC layered structure with embedded electrodes," *IEEE Transactions on Ultrasonics Ferroelectrics and Frequency Control*, vol. 63, no. 10, pp. 1608–1612, 2016.
- [10] D. Bertsimas, I. Dunning, and M. Lubin, "Reformulation versus cutting-planes for robust optimization," *Computational Management Science*, vol. 13, no. 2, pp. 195–217, 2016.
- [11] O. Djedidi, M. A. Djeziri, and N. K. M'Sirdi, "Data-driven approach for feature drift detection in embedded electronic devices<sup>3</sup>," *IFAC-Papers OnLine*, vol. 51, no. 24, pp. 1024–1029, 2018.
- [12] B. Hu and L. Wu, "Robust SCUC considering continuous/discrete uncertainties and quick-start units: a two-stage robust optimization with mixed-integer recourse," *IEEE Transactions on Power Systems*, vol. 31, no. 2, pp. 1407–1419, 2016.
- [13] Q. Hu, S. Xie, S. Lin, S. Wang, and P. S. Yu, "Clustering embedded approaches for efficient information network inference," *Data Science & Engineering*, vol. 1, no. 1, pp. 29–40, 2016.
- [14] R. Chaure and N. A. Pande, "Design and implementation of ethernet based embedded network controller using ARM 7 (LPC 2148) processor," in *2016 World Conference on Futuristic Trends in Research and Innovation for Social Welfare (Startup Conclave)*, pp. 1–4, Coimbatore, India, 2016.
- [15] X. Bai and Y. Liu, "Robust optimization of supply chain network design in fuzzy decision system," *Journal of Intelligent Manufacturing*, vol. 27, no. 6, pp. 1131–1149, 2016.
- [16] H. Xu, Y. Liu, and H. Sun, "Distributionally robust optimization with matrix moment constraints: Lagrange duality and cutting plane methods," *Mathematical Programming*, vol. 169, no. 2, pp. 489–529, 2018.
- [17] N. Chao and F. You, "Adaptive robust optimization with minimax regret criterion: multiobjective optimization framework and computational algorithm for planning and scheduling under uncertainty," *Computers & Chemical Engineering*, vol. 108, no. jan. 4, pp. 425–447, 2018.
- [18] F. D'Andreagiovanni, R. G. Garroppo, and M. G. Scutellà, "Green design of wireless local area networks by multiband robust optimization," *Electronic Notes in Discrete Mathematics*, vol. 64, pp. 225–234, 2018.
- [19] A. Yucheng, "Study on human resource information system based on Java language," *Electronic Design Engineering*, vol. 27, no. 2, pp. 25–28, 2019, 33.
- [20] Z. Nyikes, Z. Nemeth, and A. Kerti, "The electronic information security aspects of the administration system," in *2016 IEEE 11th International Symposium on Applied Computational Intelligence and Informatics (SACI)*, pp. 327–332, Timisoara, Romania, 2016.
- [21] G. S. Rodrigues, D. J. Nott, and S. A. Sisson, "Functional regression approximate Bayesian computation for Gaussian process density estimation," *Computational Statistics & Data Analysis*, vol. 103, pp. 229–241, 2016.
- [22] J. Qin, B. J. Harding, and L. Waldrop, "Nonparametric H density estimation based on regularized nonlinear inversion of the Lyman alpha emission in planetary atmospheres," *Journal of Geophysical Research: Space Physics*, vol. 123, no. 10, pp. 8641–8648, 2018.
- [23] A. Gramacki and J. Gramacki, "FFT-based fast bandwidth selector for multivariate kernel density estimation," *Computational Statistics & Data Analysis*, vol. 106, pp. 27–45, 2017.
- [24] D. Chauveau and V. Hoang, "Nonparametric mixture models with conditionally independent multivariate component densities," *Computational Statistics & Data Analysis*, vol. 103, pp. 1–16, 2016.
- [25] M. C. Edwards, R. Meyer, and N. Christensen, "Statistics and computing Bayesian nonparametric spectral density estimation using b-spline priors," *Statistics and Computing*, vol. 29, no. 1, pp. 67–78, 2019.
- [26] E. Trentin, "Soft-constrained neural networks for nonparametric density estimation," *Neural Processing Letters*, vol. 48, no. 2, pp. 915–932, 2018.
- [27] P. Carbone, D. Petri, and K. Barbe, "Nonparametric probability density estimation via interpolation filtering," *IEEE Transactions on Instrumentation and Measurement*, vol. 66, no. 4, pp. 681–690, 2017.
- [28] N. Hu, B. Duan, H. Cao, and Y. Zong, "Robust optimization with convex model considering bounded constraints on performance variation," *Structural and Multidisciplinary Optimization*, vol. 56, no. 1, pp. 59–69, 2017.
- [29] B. Jia and S. R. Gunn, "Sparse deep neural network optimization for embedded intelligence," *International Journal of Artificial Intelligence Tools*, vol. 29, no. 3n04, article 2060002, 2020.
- [30] Y. He and M. Li, "Human resource management structure of communication enterprise based on microprocessor system and embedded network," *Microprocessors and Microsystems*, vol. 81, article 103749, 2021.

## Research Article

# An Empirical Study on the Relationship between Economy and Finance in Underdeveloped Areas Based on the VAR Model

Han Zhang <sup>1</sup> and Wenbing Jiang<sup>2</sup>

<sup>1</sup>College of Management, Wuzhou University, 543003, China

<sup>2</sup>City Faculty of Economics, Lanzhou City University, 730070, China

Correspondence should be addressed to Han Zhang; [han.zhang@my.jru.edu](mailto:han.zhang@my.jru.edu)

Received 26 February 2022; Revised 22 April 2022; Accepted 28 April 2022; Published 29 May 2022

Academic Editor: Wen Zeng

Copyright © 2022 Han Zhang and Wenbing Jiang. This is an open access article distributed under the Creative Commons Attribution License, which permits unrestricted use, distribution, and reproduction in any medium, provided the original work is properly cited.

In recent years, the level of local economic, social, and financial development had been greatly improved. However, due to the large gap between regions, the economic and financial industries in underdeveloped regions restricted the further development of the whole national economy to a great extent. It was known from the existing research that economic development was inseparable from the support of the financial industry, but the role of the financial industry in the process of regional economic development had not attracted attention. Therefore, from the perspective of economic development in underdeveloped areas, this paper put forward relevant assumptions by analyzing the relationship between economic growth and financial factors. In view of the development of financial industry in underdeveloped areas, this paper mainly analyzed from three aspects: banking, securities, and insurance, and selected corresponding indicators to observe the changes of banking, security, market and insurance market. Vector autoregressive model and vector error correction model were used to carry out cointegration test and Granger causality test for financial and economic-related indicators in underdeveloped areas. According to the impulse response function and variance decomposition results, this paper analyzed the dynamic relationship between financial development and economic growth, as well as the disturbance and duration of financial factors on economic development. The empirical results showed that the VAR model can better analyze the relationship between financial growth and economic growth, as well as the role of financial factors in the process of economic development. This study can provide reference for formulating financial development policies suitable for economic development.

## 1. Introduction

For a long time, one of the macropolicy objectives of governments and central banks is to maintain moderate inflation and macroeconomic stability. However, under the background that the financial system plays an increasingly important role in the whole macroeconomy, central banks gradually ensure the coordinated development of the financial market and real economy: on the one hand, it requires the financial system to operate normally and stably. On the other hand, the financial system can effectively resist the negative impact of external instability on the domestic financial system [1–3]. Therefore, ensuring and promoting financial stability have gradually become one of the important objectives of the central bank to control the stability of the

macroenvironment [4]. Since the 1990s, some international financial organizations and central banks have begun to build a financial stability monitoring system to evaluate the stable operation of finance and warn of the potential risks of the financial environment [5–8]. At the beginning of the founding of China, China's financial system was more administrative planning system, which meant that China's unstable factors and financial risks were small. First, the planned economic system monitored the financial system strictly, which made it difficult to produce greater financial risks and instability in China. Secondly, the administrative planning system of the financial system makes it difficult for foreign financial risks to affect the domestic financial market and reduce external financial risks. However, with the reform and opening up, in the process of marketization



and internationalization of China's financial system, the unstable factors and even the impact of financial risks caused by the original imperfect financial system in the process of financial development are becoming more and more prominent [9]. In addition, due to the internationalization of the development of the financial system, speculative international hot money and financial risks of other countries are more likely to affect China's financial system, which further increases the risk of the domestic financial system. Therefore, it is urgent to build a financial stability evaluation and monitoring system suitable for China's national conditions.

However, for every country, this may also be the trigger for its economic downturn. Economic globalization makes countries interact more frequently, have closer relations, and strengthen economic interdependence [10]. It promotes rapid economic development. Economic globalization makes countries more and more open to the outside world, and some uncertain factors are injected into the domestic financial system more or less, even financial risks that affect the global economic situation. The currency crisis in the 1990s soon spread to the whole of Asia. At the same time, the share of total financial volume in GDP is increasing day by day, and the role of the financial industry in the process of economic development is becoming increasingly prominent. If the finance is done well, one move will make the whole game live [11–14]. But the reality is that compared with the rapid economic development, the development of the financial industry is slightly slow, and its role in promoting the economy has not been brought into full play. Therefore, the theoretical and empirical research on the relationship between the two, the action mechanism between finance and economy, and the contribution of finance to the economy has certain guiding significance and reference value for enriching the financial and economic theory and giving better play to the promoting role of finance in the process of economic growth. It also has corresponding practical guiding significance for the further improvement of China's current financial market and the transformation of economic development mode [15]. Financial growth will promote economic growth to a certain extent, which can also activate people's investment and wealth management boom. To a certain extent, it will promote the growth of the national economy, which is a favorable thing.

Financial development is a key variable affecting economic growth, which has been affirmed by most economists [16]. On the premise of recognizing the importance of financial development, the discussion on the contribution of financial development to economic growth has gradually become the forefront and core of economic research. The existing theoretical and empirical studies show that the financial industry plays a great role in mobilizing social savings, promoting the optimal allocation of resources, reducing transaction costs, disseminating effective market information, giving full play to the information advantages of professional organizations, reducing economic losses caused by information asymmetry, and dispersing market risks. However, for a region or a city, it is still unclear what role financial development plays in economic growth [17].

Therefore, we must start from reality and test it through practice. The level of financial development and economic development across the country is different, and the gap is quite large, and the role of financial development in promoting economic growth is also different [18]. To study the relationship between financial development and economic growth, the conclusion may have no practical guiding significance. Therefore, to draw a practical guiding conclusion according to the relationship between financial development and economic growth, we must make an empirical analysis for a specific region [19].

Considering the influence of population and price factors, this paper selects the per capita real GDP growth rate as the index to measure economic growth and adds the control variable of per capita fixed asset investment in the whole society to ensure the comprehensiveness and reliability of the test results. At the same time, in order to analyze the role of finance in the process of economic growth, this paper studies the deposit and loan balance of financial institutions at the end of the year. In addition to the stock market, the research on the security market also brings the financing amount of the bond market into the security market, so as to ensure that the financing amount of the security market will not be omitted. The research results of this paper not only have certain reference significance for other regions but also provide reference for the economic development of underdeveloped regions in China to formulate corresponding financial policies.

## 2. Related Works

Focusing on the role of financial market in economic growth, scholars and research institutions have conducted a series of empirical studies on financial and economic development in different regions. At the same time, different analysis methods are used to pay close attention to the relationship between them. Regional governments and economists also attach great importance to the specific relationship between the two. Some scholars have carried out relevant research on the relationship between financial development and economic growth. For example, through the research, it is found that economic growth stimulates financial development to a certain extent, while financial development promotes economic growth. At the same time, there is a certain interaction mechanism between the two. The different roles played by various departments of the financial industry in the process of economic development have become the focus of many scholars.

The process of financial development is mainly reflected in the sustained growth of financial aggregate and the innovation and optimization of financial structure. Among them, the total financial volume mainly reflects the overall development of the financial industry and the improvement of the financial market in a country or region. Generally, it has a positive correlation with the local economic development level. In areas with high economic development levels, the overall situation of financial industry development is naturally better; on the contrary, it is worse. The financial structure mainly reflects the specific situation of the

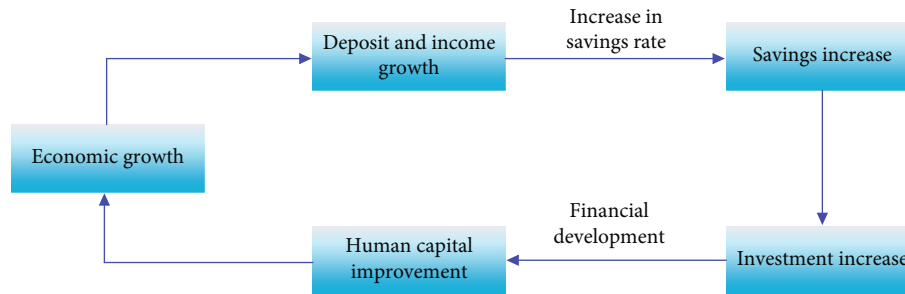


FIGURE 1: Relationship between financial development and economic growth.

composition, scale, and operation of each part of the total financial volume. The financial structure of a region will change with the change of financial aggregate, which is also related to the internal mechanism in the process of financial development. The total amount of financial development and the optimization of financial structure can be understood as different stages of the development of the same thing. Financial aggregate is the primary stage of the development of the financial industry because it more reflects a continuous accumulation process of financial assets and the basis of financial structure optimization. The optimization of financial structure is increasingly enriched and improved based on the continuous increase of the total financial volume in the early stage because the change of financial structure always occurs when the various components of the total financial volume change, which can be regarded as the advanced stage of financial development. From this, we can know that there is a dialectical and interdependent relationship between the continuous growth of financial aggregate and the continuous optimization of financial structure [20–23]. A large number of practical research results show that vector autoregressive (VAR) model is a special algorithm to deal with financial factors. It can not only better integrate financial influencing factors but also mine the factors affecting the relationship between finance and economic growth. As shown in Figure 1, the balanced development of regional economy plays a fundamental role in building a socialist harmonious society.

From the perspective of economic theory, the improvement of financial industry is an important driving force of economic growth. In order to realize the balanced development of regional economy, we must pay attention to the role of financial industry. As an underdeveloped region, the existing financial system has not been improved and its role in promoting economic development has not been effectively played. In the context of this rise, the corresponding discussion on the relationship between finance and economy plays a corresponding guiding role in promoting the reform of the financial system, giving full play to the role of the financial industry in economic development and realizing “leapfrog development”. As can be seen from Figure 1, there is a certain degree of interaction between finance and economic growth, and the financial industry can promote economic growth. Economic growth can also promote the vigorous development of the financial industry.

According to the above analysis, it can be clear whether the region should focus on financial development or economic growth in its future development. The research shows that the relevant policies issued by local governments to promote economic development have important guiding significance. Compared with other surrounding areas, underdeveloped areas have certain similarities in financial and economic development. In the choice of economic growth indicators, domestic scholars either choose GDP or per capita real GDP. However, there are many factors affecting economic growth. In addition to the financial industry, population, investment, and price factors will also affect economic growth.

### 3. Research Assumption and Model Construction

**3.1. Research Assumption.** The financial structure of most regions is dominated by banks, and the banking system plays a leading role in economic growth. In the security market, the development of stock and bond markets is relatively slow, and they have not played their due role, and their driving role in the economy has not yet appeared. As a social stabilizer, the insurance market also plays a certain role in the process of economic development.

From existing research, most regional financial intermediaries are mainly large state-owned banks, which account for a high proportion of the whole financial intermediaries, and their service subjects are relatively single [24]. They mainly provide relevant services for some large state-owned enterprises, which leads to difficulties in financing for some private enterprises other than state-owned enterprises. It is difficult for them to finance through these banks, weakening the allocation function of the financial market, which will weaken the role of the banking industry in promoting the economy to some extent. Although such financial institutions as securities, insurance, trust, and leasing can provide loan support to some small and private enterprises, their development speed and level are far from those of banking financial institutions. This situation not only hurts the further development and improvement of the financial market but also leads to the uneven distribution of the financial structure, making banking financial institutions face higher financial risks. The service demand of the financial industry has the characteristics of complexity, multilevel, and diversity. Simple large-scale banking financial institutions are unable to meet the diversified

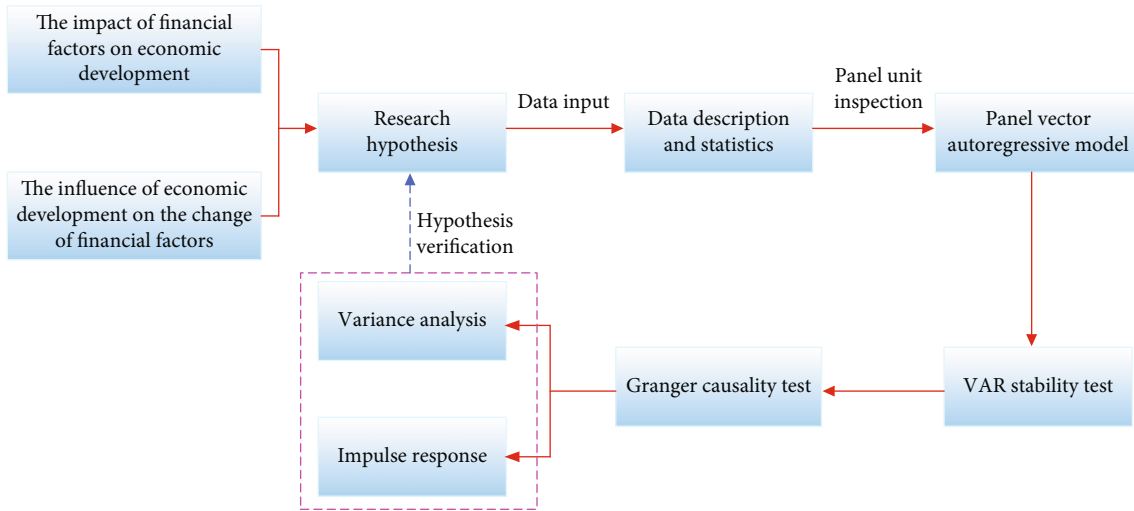


FIGURE 2: Flow chart of research assumption and model testing technology.

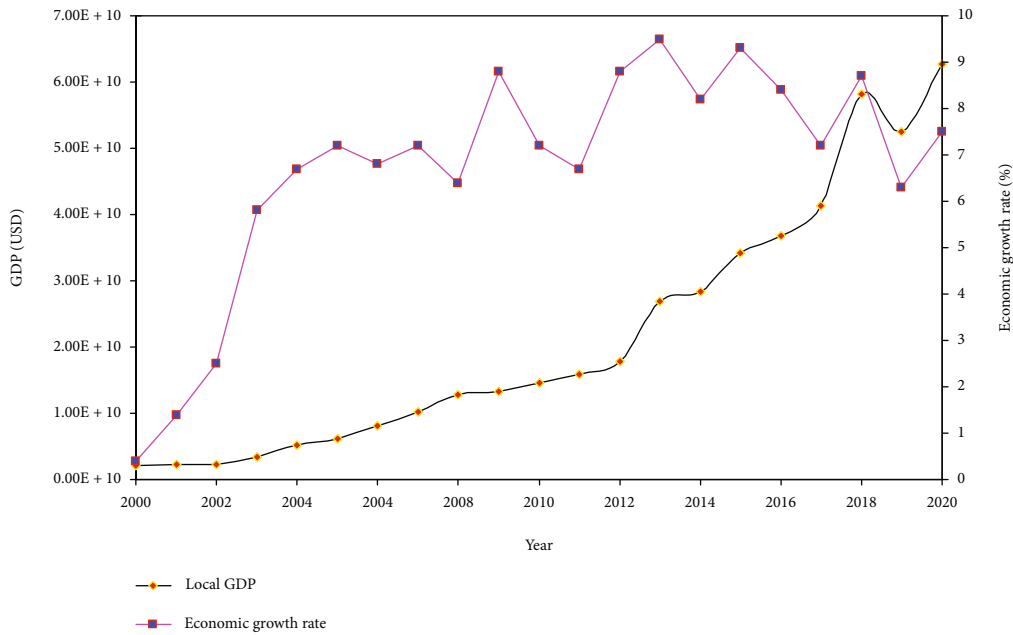


FIGURE 3: Relationship between GDP and economic growth rate in the past 20 years.

financial needs of all kinds of personnel [25, 26]. Therefore, this requires us to pay attention to the diversified development of financial institutions and pay more attention to the development of non-state-owned and nonbank financial institutions, which can not only enrich the current state of financial structure but also alleviate the current problems that are difficult to meet the diversified financial service needs of all kinds of personnel, to promote benign competition among financial institutions, reduce financial risks, improve the competitiveness of financial institutions, and give better play to their role in economic development.

The research shows that the insurance market has a certain impact on the stability of enterprise operation and the healthy development of people’s life [27]. In economic and social development, insurance plays an important role in

reducing social disasters and promoting economic development. However, there is still a big gap between regions with different levels of economic development, and there are still problems in the development of insurance market in some regions. For example, it is difficult for insurance varieties to meet the diversified needs of the people, and the use level of funds in the insurance market is not high. The total number of talents in the insurance market is insufficient, and there is a lack of corresponding high-quality management talents and professional and technical talents. Therefore, the integrity and market order of the insurance market need to be improved and further standardized.

In the current financial market, the potential of the security market to promote economic growth has gradually exceeded the traditional financial intermediary. In terms of

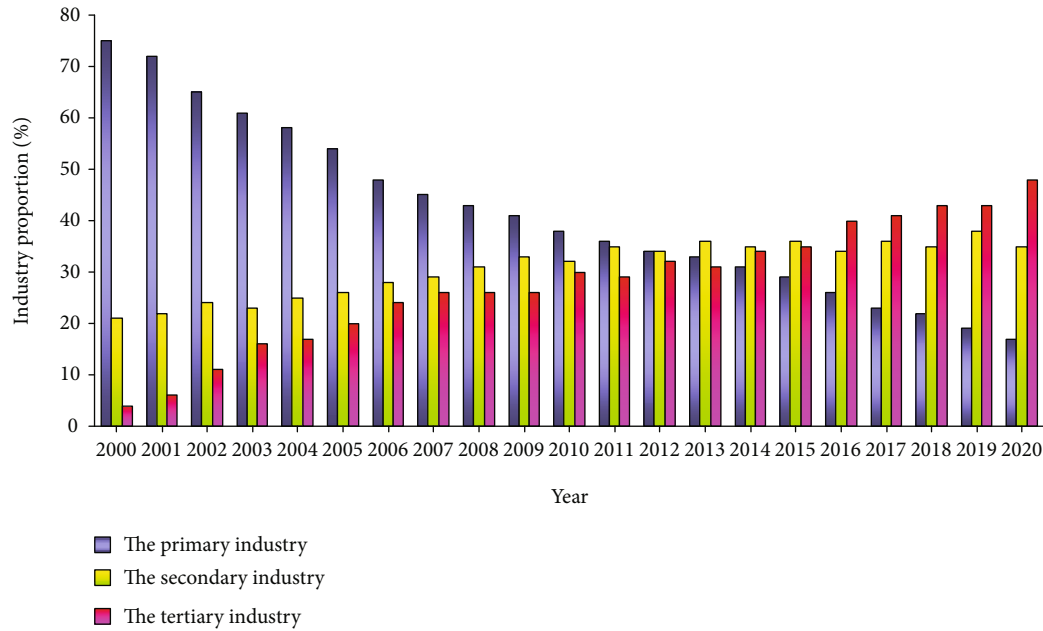


FIGURE 4: Development trends of the three major industries in the past 20 years.

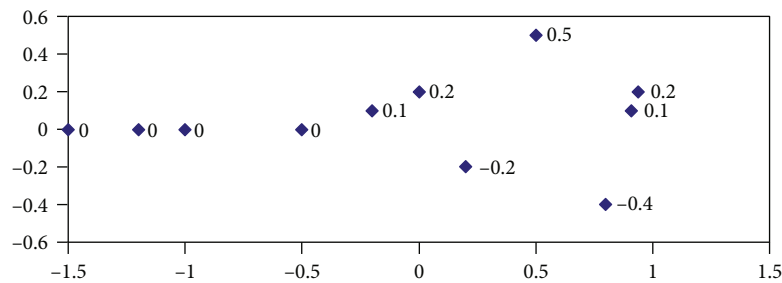


FIGURE 5: Model stationarity test.

the number of listed companies and the amount of stock and bond financing, the development of the security market is relatively low [28, 29]. Due to the complexity of financial demand and financial services, relying solely on formal state-owned financial institutions cannot fully meet the needs of all kinds of investors. Only by relying on various special state-owned and non-state-owned financial institutions can we provide all-round financial services. In order to ensure the long-term development of economy and society, the separate business model of banking, securities, and insurance has changed the traditional concept of “emphasizing banks, neglecting the stock market and weak insurance.” It can not only promote the relationship between direct financing and indirect financing but also give play to the role of insurance and security institutions in promoting the economy, and its contribution to economic development is greater than that of traditional banking [30].

From the research progress on the relationship between financial development and economic growth at home and abroad, as well as the research results on the relationship between financial elements and economic growth, this paper puts forward the following research hypotheses:

*Hypothesis 1.* Financial development in underdeveloped areas has a significant impact on economic development. When other conditions remain unchanged, there is a certain positive correlation between them.

*Hypothesis 2.* Financial factors in underdeveloped areas have a certain impact on economic development and change. When other conditions remain unchanged, there is a certain mutual restriction relationship between various elements of finance and economic growth.

*3.2. Model Construction.* In order to effectively analyze various factors affecting the relationship between finance and economic growth, this paper uses the vector autoregressive (VAR) model. The cointegration test, impulse response function analysis, and variance decomposition are all carried out based on the vector autoregressive model. The VAR model is a generalization of the AR model, in which each endogenous variable is a lagged function of other endogenous variables. It is an unstructured model based on the statistical properties of data.

Most economic variables with a strong trend, such as GDP, are unstable variables. When the time series is

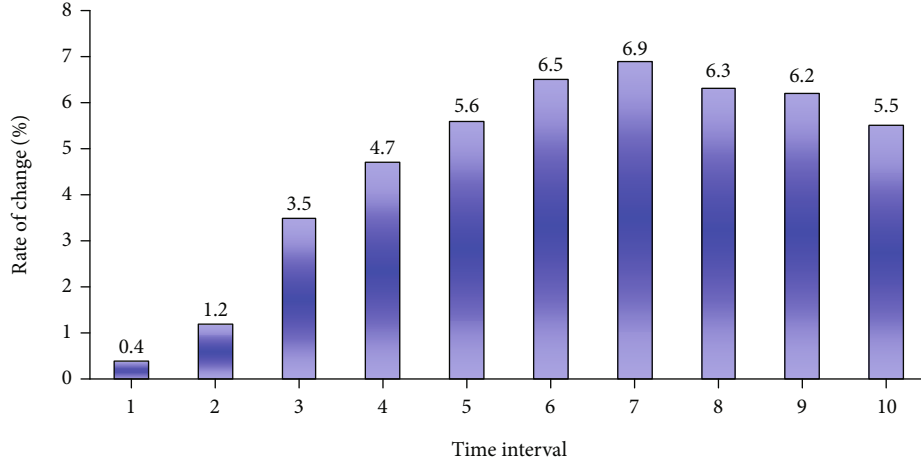


FIGURE 6: Effect of LnFIR on the change of LnRGDP impulse response function.

nonstationary variables, the direct use of OLS regression will often lead to pseudoregression. If pseudoregression occurs, even if the results we get are significant, it has no significance. Therefore, we must test the stationarity of the variables before regression, unit root test. The unit root tests commonly used are the DF test, ADF test, and PP test. In this paper, the ADF test is used to test the stationarity of variables [31, 32].

$$\Delta X_t = a + b_t + rX_{t-1} + \sum_{i=1}^k r_i \Delta X_{t-i} + \varepsilon_i, \quad (1)$$

where  $\Delta X_t$  is the  $k$  dimension column vector of endogenous variables,  $\Delta X_{t-i}$  denotes a vector of lagged endogenous variables, and  $\Delta X_{t-i}$  represents the hysteresis order of the exogenous variable.  $\Delta X_{t-i}$  shows a vector composed of  $k$ -dimensional random error terms, which can be correlated with each other simultaneity but not with their respective lag terms and variables on the right side of the equation.

ADF test uses  $t$  statistic to test and gives the critical value of  $t$  statistic at 1%, 5%, and 10% test level under different samples. If the test  $t$  statistic is less than the critical value, reject the original hypothesis, otherwise, accept the original hypothesis. If the original hypothesis is accepted, it means that sequence  $X$  contains the unit root; that is,  $X_t$  is nonstationary. If the original hypothesis is rejected, then  $X_t$  has no unit root and is a stationary sequence.

$$\begin{aligned} a_{t+1} &= a_t + u_t, \\ \sigma_t^2 &= \gamma \exp(h_t). \end{aligned} \quad (2)$$

If the coefficient changes, it can catch the coefficient that does not change linearly, such as gradual or structural change. Because  $a_t$  is free to change under random walk, this assumption means that time-varying parameters can capture not only real changes but also the possibility of nonreal changes.

The Bayesian theorem is as follows:

$$\pi\left(\frac{\theta}{y}\right) = \frac{f(y|\theta)\pi(\theta)}{\int f(y|\theta)\pi(\theta)d\theta}. \quad (3)$$

The starting point can be selected as follows:

$$\begin{aligned} \theta^{(0)} &= (\theta_1^{(0)}, \dots, \theta_p^{(0)}), \\ \theta^{(i)} &= (\theta_1^{(i)}, \dots, \theta_p^{(i)}). \end{aligned} \quad (4)$$

The conditional posterior density function of  $\beta$  is shown as follows:

$$\begin{aligned} g(\beta) &= \pi\left(\frac{\beta}{\gamma, a, h, y}\right) \times \exp\left\{-\frac{1}{2}(\beta - \beta_0)' B_0^{-1}(\beta - \beta_0)\right\} \\ &\times \left\{-\frac{\sum_{t=1}^n (y_t - x_t' \beta - z_t' a)^2}{2\gamma e^{ht}}\right\} \\ &\times \exp\left\{-\frac{1}{2}(\beta - \hat{\beta})' \hat{\beta}^{-1}(\beta - \hat{\beta})\right\}, \end{aligned} \quad (5)$$

where  $\hat{\beta}$  is expressed as follows:

$$\begin{aligned} \hat{\beta} &= \left(B_0^{-1} + \sum_{t=1}^n \frac{x_t \hat{y}_t}{\gamma e^{ht}}\right)^{-1}, \\ \hat{\beta} &= \hat{\beta} \left(B_0^{-1} \beta_0 + \sum_{t=1}^n \frac{x_t \hat{y}_t}{\gamma e^{ht}}\right). \end{aligned} \quad (6)$$

VAR model can be expressed as follows:

$$\begin{aligned} A y_t &= F_1 y_1 + \dots + F_s y_{t-s} + u_t, \quad t = s = 1, 2, \dots, n, \\ y_t &= B_1 y_1 + \dots + B_s y_{t-s} + A^{-1} \sum \varepsilon_t, \quad \varepsilon_t \in N(0, I_k). \end{aligned} \quad (7)$$

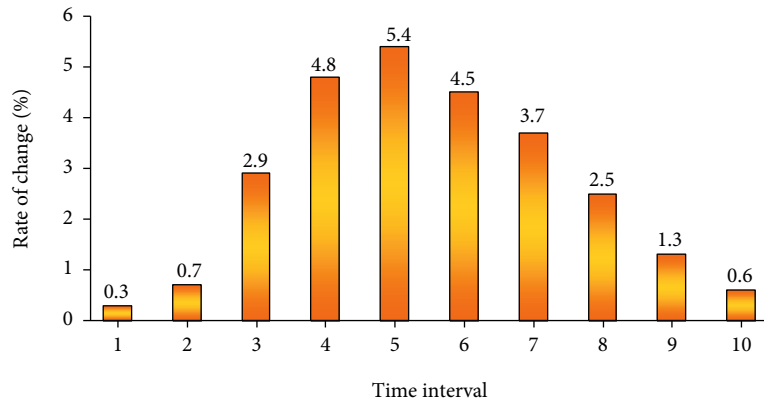


FIGURE 7: Effect of LnFL/FS on the change of LnRGDP impulse response function.

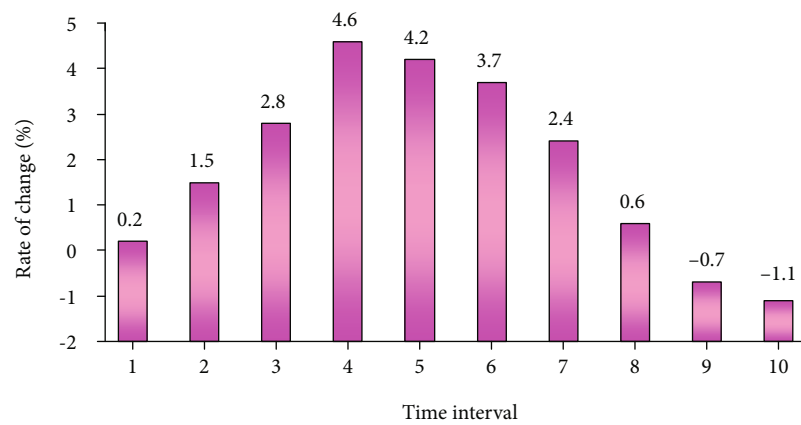


FIGURE 8: Effect of R on the change of LnRGDP impulse response function.

The model can be rewritten as follows:

$$y_t = X_t \beta_t + A^{-1} \sum \varepsilon_t. \quad (8)$$

All parameters and coefficients in the above formula do not change with time. If all parameters and coefficients are allowed to change with time, they can be changed to the following form:

$$y_t = X_t \beta_t + A^{-1} \sum \varepsilon_t, \quad t = s + 1, \dots, n. \quad (9)$$

When an endogenous variable in the model is disturbed by a standard deviation, the impulse response function can not only calculate the changes of other endogenous variables of the system but also predict the impact on these variables [33–36]. Variance decomposition (VD) mainly studies the influence and contribution of each structural impact on other endogenous variables (basically measured by variance) in the system, that is, to study the contribution degree of each new interest's impact to other endogenous variables in the system and then know the relative size of the change effect of each new interest in endogenous variables [37–40]. The impulse response function can reflect the changing relationship between finance and economic growth from a certain angle, as well as the region with relatively

large fluctuations. Through the variance, we can get the factors that lead to the error between the predicted value and the actual value of the VAR model, which provides a basis for financial practitioners to explore the source of error and solve problems.

As shown in Figure 2, the research assumption and model testing technology flow chart of this paper is given.

## 4. Demonstration and Analysis

**4.1. Sample Selection.** Aiming at the development of financial industry in underdeveloped areas, this paper mainly analyzes from three aspects: banking, securities, and insurance, and selects corresponding indicators to observe the changes of banking, security market, and insurance market. Among them, the development of the banking industry is mainly expressed by the level of bank loans and bank deposits, the development of the security market is reflected by the sum of bond and stock financing, and the development level of the insurance market is measured by the depth of insurance.

According to the existing research, the economy of underdeveloped areas is growing rapidly, the level of social development is improving day by day, the total economic volume is expanding, and the industrial structure is becoming more and more reasonable, but the economic development is still

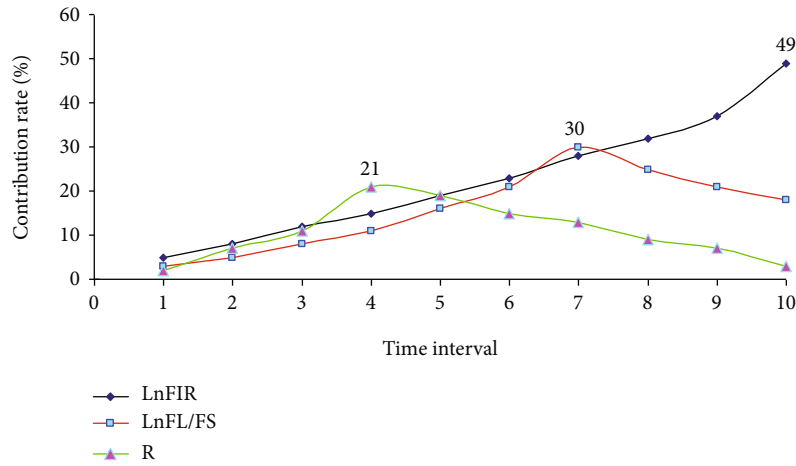


FIGURE 9: Comparison results of contribution rate changes of different factors in LnRGDP changes.

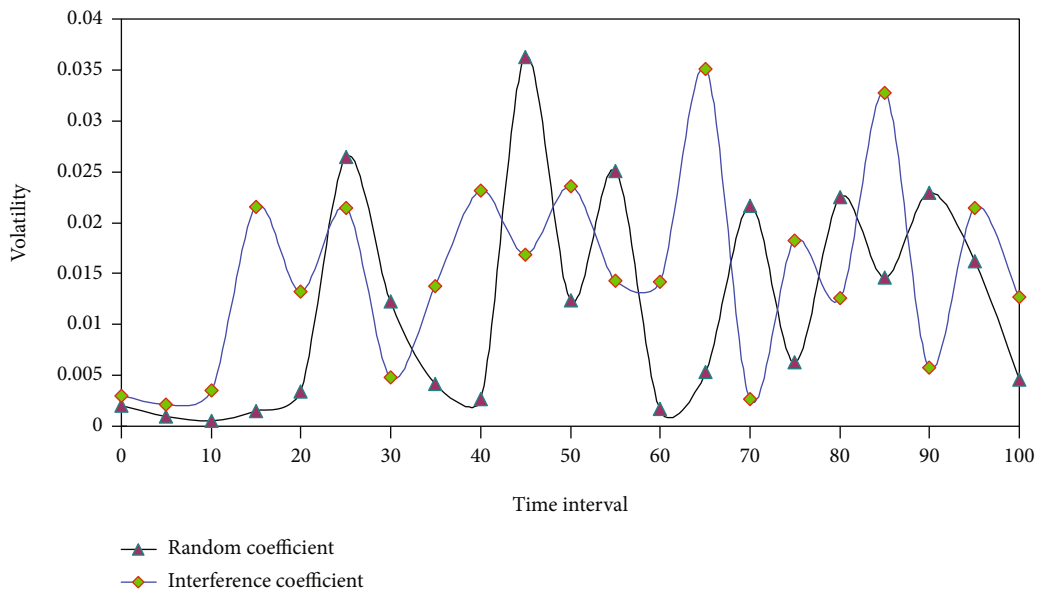


FIGURE 10: Influence of model coefficients on the change of LnRGDP impulse response function.

relatively extensive, and there are still many problems in the industrial structure [41–43]. At present, investment is still the first driving force driving economic growth, and the proportion of service industry is far lower than that in developed regions. Therefore, the goal of economic development is to adjust the industrial structure and realize the common development of urban and rural areas while maintaining the total growth.

**4.2. Data Description and Statistics.** As shown in Figure 3, it reflects the change trend of real GDP and economic growth rate in underdeveloped areas. Although the economic growth rate continues to rise, there is no obvious linear relationship between GDP growth and economic growth rate. As shown in Figure 4, the development trend of the three major industries from 2000 to 2020 is described. With the passage of time, the secondary industry and the tertiary

industry show a good state of development and occupy the main position of economic growth, while the primary industry shows a declining trend. Therefore, with the development of the financial industry, we can know the impact of the financial industry on the economic changes of different industries and also show the close relationship between economic growth and finance.

In the VAR model, if the value is less than 1, it means that the VAR model has better adaptability to the research object. This also shows that this model has good adaptability in the financial field. The stationarity test of the VAR model was carried out. As shown in Figure 5, there is no root greater than 1 in this VAR model, so it is a stable system. The results obtained by VAR analysis are valid.

**4.3. Model Test and Result Analysis.** Considering the lack of stability of the VAR model, this paper selects the impulse

response test of LnRGDP and tests the impulse response function. Among them, the influencing factors mainly include LnFIR, LnFL/FS, and R. In order to explore the influence of different factors on LnRGDP, we can observe the results of pulse test in different time periods. As shown in Figure 6, it reflects the influence of LnFIR on the change of LnRGDP.

It can be seen from Figure 6 that the value of financial impulse response function continues to rise over time, but it will gradually decline when the impulse value reaches a certain peak. Because the second derivative of financial impulse response function is less than zero, it shows a certain downward change after rising rapidly over time, but the downward trend is relatively slow. From this, we can know that the relationship between financial development and economic growth is not a simple linear change. In the long run or short term, the improvement of financial relevance has a positive impact on the growth of per capita GDP.

In order to test the influence of LnFL/FS on LnRGDP, the corresponding results are obtained through the impulse response experiment of LnRGDP, as shown in Figure 7.

From the action relationship of LnFL/FS on LnRGDP reflected in Figure 7, when LnFL/FS rises, LnRGDP first rises at a certain degree of uniform rate, and the driving effect of the fourth stage on LnRGDP is the largest. However, with the passage of time, the impact of LnFL/FS on LnRGDP shows a downward trend and has almost no impact on LnRGDP in the eighth stage, indicating that LnFL/FS will have a certain reaction to LnRGDP in the later stage. This shows that the loan deposit ratio can effectively promote the change of LnRGDP in theory, but only controlling LnFL/FS within a reasonable range is conducive to the development of LnRGDP.

Finally, in order to test the influence of R on LnRGDP, the corresponding results are obtained through the impulse response experiment of LnRGDP, as shown in Figure 8.

According to the relationship between R and LnRGDP reflected in Figure 8, when R increases, LnRGDP first increases rapidly and then decreases. With the passage of time, the positive effect of R on LnRGDP showed a downward trend. Whether in the long term or short term, interest rate has a positive impact on LnRGDP to a certain extent. However, when the value of LnRGDP is negative, the impact of R on LnRGDP will be negatively correlated. Therefore, although R can promote LnRGDP to some extent, it is necessary to deal with the stable relationship between finance and economic growth.

In order to reflect the role of different factors in the change of LnRGDP, the variance decomposition of LnRGDP can be carried out and the corresponding comparison results can be obtained, as shown in Figure 9.

From the comparison results in Figure 9, without considering the contribution rate of LnRGDP itself, the contribution of LnFIR to LnRGDP is the largest and increases with the passage of time, reaching 49% in the 10th cycle. LnFL/FS and R also contribute significantly to LnRGDP. The contribution rate of LnFL/FS to LnRGDP reached the maximum in phase 7, accounting for 30%, while the contribution rate of R to LnRGDP reached the maximum in phase 4, accounting for 21%.

In order to test the influence of correlation coefficient in the VAR model on the change of LnRGDP impulse response function, the random coefficient and interference coefficient in the model are tested. As shown in Figure 10, it reflects the influence of different coefficients on the change of LnRGDP impulse response function over time.

Because the correlation coefficient in the VAR model is estimated based on sample data, it generally does not change with time. From the influence results of different coefficients on the change of impulse response function reflected in Figure 10, it can be seen that with the passage of time, the random coefficient and interference coefficient in the model have an impact on the impulse response function to a certain extent. Therefore, the impulse response function will fluctuate with time, but it will not have a great impact on the test of relevant indicators.

From the above empirical analysis results, we should put the development of capital market before the banking industry, strengthen the financing of security market, give full play to the important role of security market in the rational allocation of existing social resources, and better promote economic growth. The development of financial institutions should not only expand the scale but also focus on improving efficiency and giving better play to the role of banks in economic development. At the same time, we will strengthen cooperation and complementarity among banking, securities, and insurance businesses; coordinate the healthy development of the three; and provide more perfect and diversified financial services for the people. Strengthen the construction of relevant laws, regulations, and systems to provide legal and policy support for the development of financial markets. Improve the service and supervision level of financial markets and financial intermediaries, give better play to the resource allocation function of financial markets, and promote economic development.

In addition, from the empirical results, we can see that in the current financial market, the potential of the security market to promote economic growth has gradually exceeded the traditional financial intermediary. In terms of the number of listed companies and the amount of stock and bond financing, the development of the security market is relatively slow. Due to the complexity of financial demand and financial services, relying solely on formal state-owned financial institutions cannot fully meet the needs of all kinds of investors. The empirical analysis further shows the importance of the VAR model in financial services. In order to realize a comprehensive financial service model, we must consider all kinds of financial industries, whether state-owned enterprises or non-state-owned enterprises.

## 5. Conclusion

Although some studies have shown that financial development has a certain impact on economic growth, the research on the relationship between financial factors and economic growth in underdeveloped areas is not clear enough. On the basis of summarizing the connotation of the relationship between financial development and economic growth, this paper analyzes the interaction mechanism between financial



development and economic growth. In order to further explore the internal relationship between financial development and economic growth in underdeveloped areas, this paper proposes to use the vector autoregressive model and error correction model to study the relationship between financial factors and economic growth in underdeveloped areas. Using the VAR model, financial development, financial stability, and economic growth are brought into the unified equation, and the dynamic relationship between the three is analyzed. By selecting relevant indicators, this paper tests and analyzes the impulse response function and variance decomposition that affect the relationship between financial factors and economic development. Empirical analysis and results show that in a short period of time, the impact of financial development on economic growth is small and not obvious enough. In the long run, the impact of financial development on economic growth has undergone structural changes. At the same time, economic growth also has a certain positive impact on financial development, and this impact will become more and more significant with the passage of time. Through the above research and analysis, it can be seen that the VAR method can better reflect the relationship between various factors of finance and economic growth. This research has a certain reference value for financial practitioners.

## Data Availability

The data used to support the findings of this study are available from the corresponding author upon request.

## Conflicts of Interest

The authors declare that they have no known competing financial interests or personal relationships that could have appeared to influence the work reported in this paper.

## References

- [1] L. Kogan, D. Papanikolaou, A. Seru, and N. Stoffman, "Technological innovation, resource allocation, and growth," *The Quarterly Journal of Economics*, vol. 132, no. 2, pp. 665–712, 2017.
- [2] R. P. Pradhan, M. B. Arvin, and S. Bahmani, "Are innovation and financial development causative factors in economic growth? Evidence from a panel granger causality test," *Technological Forecasting and Social Change*, vol. 132, no. 12, pp. 130–142, 2018.
- [3] R. P. Pradhan, M. B. Arvin, J. H. Hall, and M. Nair, "Innovation, financial development and economic growth in Eurozone countries," *Applied Economics Letters*, vol. 23, no. 16, pp. 1141–1144, 2016.
- [4] Q. Ji, H. Marfatia, and R. Gupta, "Information spillover across international real estate investment trusts: evidence from an entropy-based network analysis," *The North American Journal of Economics and Finance*, vol. 46, no. 13, pp. 103–113, 2018.
- [5] A. Jreisat, "Productivity growth of the Australian real estate investment trusts," *Electronic Journal of Applied Statistical Analysis*, vol. 11, no. 1, pp. 58–73, 2018.
- [6] C. Alexiou, S. Vogiazas, and J. G. Nellis, "Reassessing the relationship between the financial sector and economic growth: dynamic panel evidence," *International Journal of Finance & Economics*, vol. 23, no. 2, pp. 155–173, 2018.
- [7] K. E. Maskus, S. Milani, and R. Neumann, "The impact of patent protection and financial development on industrial R&D," *Research Policy*, vol. 48, no. 1, pp. 355–370, 2019.
- [8] A. Alam, M. Uddin, and H. Yazdifar, "Financing behaviour of R&D; investment in the emerging markets: the role of alliance and financial system," *R & D Management*, vol. 49, no. 1, pp. 21–32, 2019.
- [9] S. Qian and H. Renyong, "Knowledge forms and enterprise innovation performance," *International Journal of Knowledge Management*, vol. 13, no. 3, pp. 55–70, 2017.
- [10] H. T. Yang and P. X. Yang, "Study on the influence of openness, relational network and knowledge sharing on enterprises' innovation performance," *Industrial Engineering and Management*, vol. 20, no. 2, pp. 68–73, 2015.
- [11] C. Ma and Z. Liu, "Effects of M&As on innovation performance: empirical evidence from Chinese listed manufacturing enterprises," *Technology Analysis & Strategic Management*, vol. 29, no. 8, pp. 960–972, 2017.
- [12] S. Ren, A. B. Eisingerich, and H.-T. Tsai, "How do marketing, research and development capabilities, and degree of internationalization synergistically affect the innovation performance of small and medium-sized enterprises (SMEs)? A panel data study of Chinese SMEs," *International Business Review*, vol. 24, no. 4, pp. 642–651, 2015.
- [13] J. Wu, C. Wang, J. Hong, P. Piperopoulos, and S. Zhuo, "Internationalization and innovation performance of emerging market enterprises: the role of host-country institutional development," *Journal of World Business*, vol. 51, no. 2, pp. 251–263, 2016.
- [14] T. C. Kuo and S. Smith, "A systematic review of technologies involving eco-innovation for enterprises moving towards sustainability," *Journal of Cleaner Production*, vol. 192, no. 21, pp. 207–220, 2018.
- [15] S. Yin and B. Li, "A stochastic differential game of low carbon technology sharing in collaborative innovation system of superior enterprises and inferior enterprises under uncertain environment," *Open Mathematics*, vol. 16, no. 1, pp. 607–622, 2018.
- [16] J. St-Pierre, O. Sakka, and M. Bahri, "External financing, export intensity and inter-organizational collaborations: evidence from Canadian SMEs," *Journal of Small Business Management*, vol. 56, no. 12, pp. 68–87, 2018.
- [17] C. Corsi and A. Prencipe, "Improving the external financing in independent high-tech SMEs," *Journal of Small Business and Enterprise Development*, vol. 24, no. 4, pp. 689–715, 2017.
- [18] M. Meuleman and W. De Maeseneire, "Do R&D subsidies affect SMEs' access to external financing?," *Research Policy*, vol. 41, no. 3, pp. 580–591, 2012.
- [19] Y. Jin and S. Zhang, "Credit rationing in small and micro enterprises: a theoretical analysis," *Sustainability*, vol. 11, no. 5, pp. 1330–1442, 2019.
- [20] D. Dohse, R. K. Goel, and M. A. Nelson, "Female owners versus female managers: who is better at introducing innovations," *The Journal of Technology Transfer*, vol. 44, no. 2, pp. 520–539, 2019.
- [21] D. Acemoglu, U. Akcigit, H. Alp, N. Bloom, and W. Kerr, "Innovation, reallocation, and growth," *American Economic Review*, vol. 108, no. 11, pp. 3450–3491, 2018.

- [22] P. Boeing, "The allocation and effectiveness of China's R&D subsidies - evidence from listed firms," *Research Policy*, vol. 45, no. 9, pp. 1774–1789, 2016.
- [23] J. Burchardt, U. Hommel, D. S. Kamuriwo, and C. Billitteri, "Venture capital contracting in theory and practice: implications for entrepreneurship research," *Entrepreneurship Theory and Practice*, vol. 40, no. 1, pp. 25–48, 2016.
- [24] R. A. Cole and T. Sokolyk, "Debt financing, survival, and growth of start-up firms," *Journal of Corporate Finance*, vol. 50, pp. 609–625, 2018.
- [25] R. Cole, D. Cumming, and D. Li, "Do banks or VCs spur small firm growth?," *Journal of International Financial Markets, Institutions and Money*, vol. 41, pp. 60–72, 2016.
- [26] S. Durguner, "Do borrower-lender relationships still matter for small business loans?," *Journal of International Financial Markets, Institutions and Money*, vol. 50, pp. 98–118, 2017.
- [27] S. T. Howell, "Financing innovation: evidence from R&D grants," *American Economic Review*, vol. 107, no. 4, pp. 1136–1164, 2017.
- [28] M. Marino, S. Lhuillery, P. Parrotta, and D. Sala, "Additional-ity or crowding-out? An overall evaluation of public R&D subsidy on private R&D expenditure," *Research Policy*, vol. 45, no. 9, pp. 1715–1730, 2016.
- [29] A. Assaf, A. N. Berger, and R. A. Rinam, "Does efficiency help banks survive and thrive during financial crises?," *Journal of Banking and Finance*, vol. 106, no. 7, pp. 445–470, 2019.
- [30] O. Badunenko and S. C. Kumbhakar, "Economies of scale, technical change and persistent and time-varying cost efficiency in Indian banking: Do ownership, regulation and heterogeneity matter?," *European Journal of Operational Research*, vol. 260, no. 2, pp. 789–803, 2017.
- [31] C. Curi, A. Lozano-Vivas, and V. Zelenyuk, "Foreign bank diversification and efficiency prior to and during the financial crisis: does one business model fit all?," *Journal of Banking and Finance*, vol. 61, no. 1, pp. S22–S35, 2015.
- [32] F. Mergaerts and V. R. Vander, "Business models and bank performance: a long-term perspective," *Journal of Financial Stability*, vol. 22, no. 2, pp. 57–75, 2016.
- [33] M. M. Cornett, O. Erhemjamts, and H. Tehranian, "Greed or good deeds: an examination of the relation between corporate social responsibility and the financial performance of U.S. commercial banks around the financial crisis," *Journal of Banking and Finance*, vol. 70, no. 9, pp. 137–159, 2016.
- [34] A. Novak, D. Bennett, and T. Klietnik, "Product decision-making information systems, real-time sensor networks, and artificial intelligence-driven big data analytics in sustainable Industry 4.0," *Economics, Management, and Financial Markets*, vol. 16, no. 2, pp. 62–72, 2021.
- [35] M. D. Amore and A. Minichilli, "Local political uncertainty, family control, and investment behavior," *Journal of Financial and Quantitative Analysis*, vol. 53, no. 4, pp. 1781–1804, 2018.
- [36] H. An, Y. Chen, and D. Luo, "Political uncertainty and corporate investment: evidence from China," *Journal of Corporation Finance*, vol. 36, no. 11, pp. 174–189, 2016.
- [37] G. Golak, A. Durnev, and Y. Qian, "Political uncertainty and IPO activity: evidence from U.S. gubernatorial elections," *Journal of Financial and Quantitative Analysis*, vol. 52, no. 6, pp. 2523–2564, 2017.
- [38] C. E. Jens, "Political uncertainty and investment: causal evidence from U.S. gubernatorial elections," *Journal of Financial Economics*, vol. 124, no. 3, pp. 563–579, 2017.
- [39] B. Kelly, E. Pastor, and P. Veronesi, "The price of political uncertainty: theory and evidence from the option market," *The Journal of Finance*, vol. 71, no. 5, pp. 2417–2480, 2016.
- [40] D. Luo, K. C. Chen, and L. Wu, "Political uncertainty and firm risk in China," *Review of Development Finance*, vol. 7, no. 2, pp. 85–94, 2017.
- [41] G. Shen and B. Chen, "Zombie firms and over-capacity in Chinese manufacturing," *China Economic Review*, vol. 44, no. 44, pp. 327–342, 2017.
- [42] K. Imai, "A panel study of zombie SMEs in Japan: identification, borrowing and investment behavior," *Journal of the Japanese and International Economies*, vol. 39, pp. 91–107, 2016.
- [43] S. Urionabarrenetxea, J. Domingo, L. San-Jose, and J. Retolaza, "Living with zombie companies: do we know where the threat lies?," *European Management Journal*, vol. 36, no. 3, pp. 408–420, 2018.

## Review Article

# Research Progress on Humidity-Sensing Properties of Cu-Based Humidity Sensors: A Review

Jingyu Wang  and Wen Zeng 

*College of Materials Science and Engineering, Chongqing University, Chongqing 400030, China*

Correspondence should be addressed to Wen Zeng; [wenzeng@cqu.edu.cn](mailto:wenzeng@cqu.edu.cn)

Received 10 March 2022; Revised 15 April 2022; Accepted 4 May 2022; Published 25 May 2022

Academic Editor: Alberto J. Palma

Copyright © 2022 Jingyu Wang and Wen Zeng. This is an open access article distributed under the Creative Commons Attribution License, which permits unrestricted use, distribution, and reproduction in any medium, provided the original work is properly cited.

Novel humidity sensors based on semiconducting metal oxides with good humidity-sensing properties have attracted extensive attention, which due to their high sensitivity at room temperature, high safety, low hysteresis, and long-term stability. As a typical p-type semiconductor metal oxide, CuO is considered to be a high-performance moisture-sensitive material; however, with the development of production, the complex working environment has put forward higher requirements for its humidity sensitivity, especially sensitivity and stability. In this regard, workers around the world are working to improve the moisture-sensing properties of sensing elements. In this review, the humidity-sensing properties of CuO-based moisture-sensitive materials are comprehensively summarized, focusing on effective measures to improve the moisture-sensing properties of CuO-based moisture-sensitive materials, including surface modification and nanocomposites. The future research of semiconducting metal oxide humidity-sensitive materials is also prospected.

## 1. Introduction

As the source of life, water plays an important role that cannot be ignored in the production process of human daily life. It is also one of several basic substances that constitute the human body. Among the vast majority of substances used by human beings, water exists [1], and even low levels can affect the properties of the material. Therefore, before conducting the experimental operation, we need to measure the water content in the operating environment to avoid its influence on the experimental results. Importantly, the word “humidity” is usually expressed as the amount of water vapor in the atmosphere [2].

Humidity sensor is used to measure ambient humidity and is an important device widely used in our production and experimental process [3]. It can effectively monitor ambient humidity to improve human comfort. In addition, humidity sensors can also be used in medical, construction, biological, environmental monitoring, and other fields [4–7]. In order to prevent humidity from interfering with the measurement results, the humidity value of the experi-

mental environment should be carefully measured and controlled by a humidity sensor [8].

The performance of the humidity sensor determines that only those materials with high sensitivity, rapid response, nontoxicity, and easy processing have the potential to become humidity-sensitive materials. Different types of humidity sensors have been developed using a variety of materials with good humidity sensitivity, among which the most distinctive ones are semiconductor metal oxides [9] and organic polymer materials [10], in addition, carbon-based materials, and it has also gradually become a research hotspot in humidity-sensitive materials [11]. And their composite materials [12] even show better humidity-sensitive properties than individual materials in some aspects. The new humidity sensor based on semiconductor metal oxide not only has high sensitivity but also can effectively detect humidity value in a wide range of humidity. With these advantages, the humidity sensor based on semiconductor metal oxide has gradually become the most popular in the field of humidity sensing [13, 14]. For this type of humidity sensor, the sensing mechanism is explained as the change in

the resistance of the sensing element, which is now accepted by most people, and it is believed that when the humidity-sensitive material is exposed to the atmosphere, the surface of the material is exposed to water vapor. A physicochemical reaction causes the impedance of the material to change.

Among many semiconducting metal oxides, CuO has many unique physical and chemical properties, and it is nontoxic and easy to prepare, relatively stable in properties, and low in production cost [15]. For applications in humidity sensing, CuO is also the most popular material among several copper-based metal oxides [16]. It is worth mentioning that, compared with copper oxide, the two materials, Cu<sub>2</sub>O and Cu<sub>2</sub>O<sub>3</sub>, are less stable and difficult to prepare, so they have great limitations in the application of humidity-sensitive materials. As a typical p-type metal oxide, CuO has a monoclinic structure with a narrow bandgap of only 1.2 eV [17, 18]. These properties make CuO widely concerned and applied in photothermal [19] and photoconductive fields [20]. In addition, studies have shown that copper oxides exposed to different gas atmospheres remain stable and exhibit relatively low changes in base resistivity, indicating that the application of copper oxides can effectively reduce the material cost in humidity-sensing elements [21].

Cuprous oxide (Cu<sub>2</sub>O) is also one of the typical p-type semiconductor metal oxide materials. Although both are copper oxides [22], there are still many differences between Cu<sub>2</sub>O and CuO, especially in terms of structure and performance. First, copper oxide is a black metal, but cuprous oxide is red; secondly, the structure of copper oxide is more complex, which is a monoclinic crystal structure. In this regard, the structure of cuprous oxide is much simpler, which is a typical cubic structure; in addition, cuprous oxide has a complete Cu 3d shell, and its direct bandgap is higher than that of copper oxide, which is 2.17 eV [23, 24]. In contrast, copper oxide has a very narrow bandgap (1.2 eV), which is fully capable of absorbing near-infrared light [25]. Recent reports claim that cuprous oxide has inferior electrical conductivity compared to cupric oxide but occupies a certain advantage in carrier mobility [26]. However, based on the principle of semiconductor metal oxide humidity sensor, it is clear that copper oxide with higher conductivity is more suitable as a humidity-sensitive material.

Although CuO and Cu<sub>2</sub>O, two copper-based semiconductor metal oxides, have great differences in properties, they also have similarities in performance. For example, both of them have relatively low bandgap energy and excellent activation and catalytic performance. Both materials are nontoxic and easy-to-produce safe materials [27–30], which are widely used in optoelectronics, humidity sensing, and batteries and various in the catalytic process. In recent years, the synthesis and preparation of CuO and Cu<sub>2</sub>O and the optimization and improvement of their nanostructured surface morphology have been extensively studied, and tremendous progress has been made [27, 28, 31–33]. However, copper oxide has gained greater attention and more in-depth research in the field of humidity sensing due to its better stability.

CuO is a typical chemical resistance sensing material, and its humidity sensing is mainly controlled by the change

in the resistance of the humidity-sensing material itself when water and water derivatives (water vapor) contact and react with its surface [35]. In a humid atmosphere, water molecules in the environment will be adsorbed to the surface of the CuO material. Adsorption can be divided into physical adsorption and chemical adsorption [36]. When the relative humidity is low, the surface of CuO is lightly covered by water vapor molecules, chemical adsorption occurs, and the charge transfer is ensured by the hopping of protons (hydrogen ions) between the hydroxyl groups adsorbed in the chemical adsorption layer. The chemical adsorption layer that has been formed will continue to adsorb water molecules and then form physical adsorption. The water molecules form a physical layer on the hydroxyl group through hydrogen bonds (Figure 1), and a large number of water molecules are ionized into hydronium ions (H<sub>3</sub>O<sup>+</sup>). According to Grotthuss's Transport mechanism, it is between hydronium ions and water molecules. When the relative humidity is high, hydrogen ion exchange is a process in which protons (hydrogen ions) hop between adjacent water molecules, creating conduction, increasing ionic conductance, and reducing impedance values [37]. Therefore, it is due to the change in sensor resistance that humidity detection is achieved. There is no doubt that the adsorption of water vapor occurs on the surface of the copper oxide humidity sensor, so any factor that affects the apparent morphology of the material will significantly affect the impedance of the material. At present, the research of humidity sensor based on copper oxide has made great progress, and its humidity-sensitive performance shows outstanding advantages in response speed, selectivity [34, 38], etc. In particular, the selectivity of copper oxide to humidity is better than that of the commonly used metal oxide SnO<sub>2</sub>. Under high humidity conditions, copper oxide shows high sensitivity to humidity [39]. The influence of other interfering gases in the ambient atmosphere on the copper oxide-based humidity sensor is basically negligible, and under low humidity conditions, gases such as H<sub>2</sub>S will react with oxygen on the surface of the material, releasing electrons to reduce the resistance of the material [40]. Therefore, copper oxide-based humidity sensors can detect NH<sub>3</sub> and H<sub>2</sub>S at low humidity levels [41, 42].

In the past ten years, more than 900 papers have been published on the humidity-sensing performance of copper oxide, and the number of papers has been increasing year by year (Figure 2). In the preparation of copper oxide humidity-sensitive materials, in addition to the traditional hydrothermal method and chemical deposition method [43], some new methods such as biosynthesis and microwave-assisted chemical solution synthesis have gradually attracted the attention of researchers [16, 44]. However, only a few reports describe the introduction of synthetic strategies for CuO nanostructures and their related applications [28, 31, 33]. Quite a few of these papers focus only on the production and fabrication of one-dimensional copper oxide nanostructures [27, 28, 31]. However, with the continuous development of production and processing technology and the increasingly complex production and experimental environment, the demand for the performance of humidity

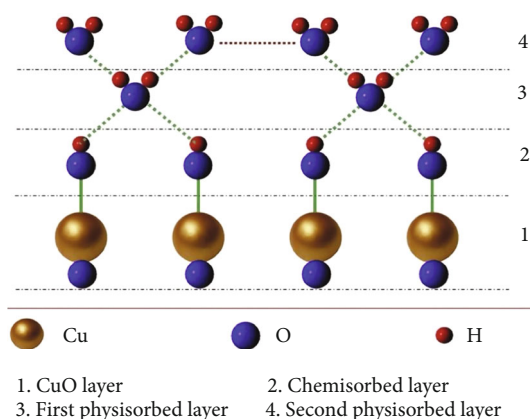


FIGURE 1: Schematic diagram of the humidity-sensing mechanism of CuO [34].

sensors is gradually increasing. The existing copper oxide humidity sensor urgently needs to be further improved and improved in some humidity-sensitive properties, especially the sensitivity and stability of humidity sensing [45, 46].

As far as we know, the performance of the humidity sensor depends to some extent on the surface topography of the humidity-sensitive material, including the size, the number of defects, and the specific surface area [47]. In addition, the working temperature is also an important factor. This temperature affects the electron migration rate inside the humidity-sensitive material and controls the electrical conductivity of the material [48]. The optimal operating temperature of traditional copper oxide-based humidity sensors is usually between 120 and 150 degrees Celsius [49]. But such humidity sensors also have good humidity sensitivity at room temperature. Operating in a high temperature environment limits the wide application of such humidity sensors, because high temperature operation means energy loss and waste, which is seriously inconsistent with the concept of energy conservation and emission reduction in today's society. High temperature environments can also affect the stability of the humidity sensor, resulting in deviations in the measurement results. In addition, the copper oxide-based humidity sensor that operates at room temperature does not require an additional heating device, which reduces power consumption, and also makes the sensor smaller and easier to carry. Therefore, according to the current development trend, copper oxide-based humidity sensors with good humidity sensitivity at room temperature are more in line with the needs of production and life in today's society [50].

In addition to the working ambient temperature, other gases in the atmosphere are also one of the main reasons that affect the performance of the humidity sensor [51], especially gases like  $\text{NH}_3$  and  $\text{H}_2\text{S}$ . They can be adsorbed on the surface of the copper oxide humidity-sensitive material and react with the molecular sites of oxygen to limit the normal adsorption of water vapor [52]. Therefore, when studying the humidity-sensitive properties of materials at room temperature, the interference of other gases needs to be considered, which requires the material to have good selectivity to humidity [53]. Fortunately, copper oxide-based humidity-

sensing materials have good selectivity to humidity. Under high humidity conditions, the effect of interfering gases on the sensor is basically negligible. Under low humidity conditions, most organic volatile gases do not affect the measurement of humidity by copper oxide-based sensors [34]. In short, the biggest challenge for the further development of the current copper oxide-based humidity sensor is how to improve its sensitivity and response speed.

Although many articles have reported improving the sensitivity and response speed of copper oxide-based humidity sensors to a certain extent so far, this has not fully met the needs of the work. Perillo et al. [54] synthesized copper oxide nanofilms on silicon wafers by the continuous ionic layer adsorption reaction method (SILAR), and the fabricated sensors exhibited good response and recovery time at room temperature. Hsu et al. [55] synthesized high-density  $\text{CuO}/\text{Cu}_2\text{O}$  composite nanowires by heating oxidation method, which effectively improved the sensitivity of the sensor to humidity. Much work has been done to improve the humidity sensitivity of the sensor, including surface modification based on copper oxide nanomaterials and doping of various additives with different properties, and the enhancement mechanisms of these two technologies are different, which will be explained in detail in Sections 2 and 3 below.

But to the best of our knowledge, substantial progress has been made in extensive research on CuO-based humidity sensors, and reviews on this related topic are lacking. In this paper, the humidity-sensing properties of copper oxide-based humidity sensors are summarized, and the effective strategies and mechanisms to improve the humidity-sensing performance of copper oxide-based sensing elements are discussed. We hope to provide some inspiration for future research on semiconductor-based metal oxide humidity sensors.

## 2. Surface Modification

At present, the materials of humidity sensors are mostly nanomaterials, because the size of nanomaterials is smaller, which is conducive to the current research direction of miniaturization of humidity sensors. In addition, nanomaterials have more prominent physical and chemical properties than ordinary bulk materials. Usually, nanomaterials have a large specific surface area, which makes a considerable part of atoms located on the surface of the material [56–58], fully in contact with the outside atmosphere, and the specific surface area of nanomaterials is closely related to its size.

Obviously, the nanostructured copper oxide is smaller in size, which makes its specific surface area much higher than that of ordinary copper oxide bulk material. In addition, the surface of copper oxide nanomaterials has more active centers, which fully shows the great advantages as humidity-sensitive materials. It has been found that the grain size of copper oxide nanostructures is an important factor affecting its moisture-sensing properties [34]. In recent years, how to reduce the grain size of copper oxide nanostructures has become the goal of many scientific

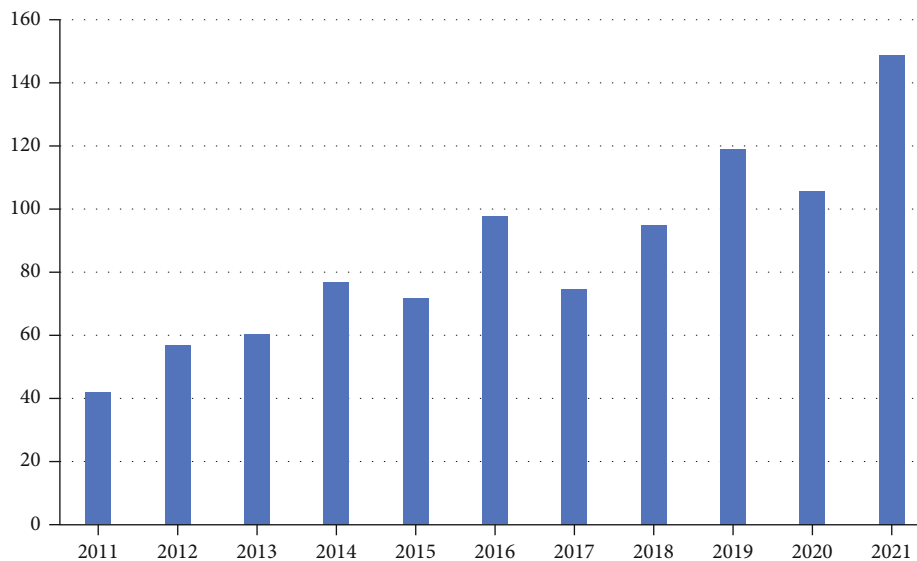


FIGURE 2: Number of papers on CuO-based humidity sensing.

experiments. But it is worth mentioning that the grain size cannot be reduced indefinitely; van der Waals force is an important factor to promote particle aggregation, and its size is inversely proportional to the grain size [59]. This means that if the particle size is blindly reduced, although the size and specific surface area of the material are effectively improved, the thermal stability of the material will be seriously reduced, and the resistance of the gas diffusion process between particles will also increase, which will affect the material's moisture-sensitive properties [60]. In addition to the size of the grains, the surface morphology of the copper oxide nanostructures also affects the humidity-sensing properties of the sensing element. In reality, there are always some defects and pores on the surface of nanomaterials. The morphology and structure of these regions are different, and the diffusion ability of water vapor molecules in these regions is also different. Different copper oxide nanostructures have large differences in their spatial structure and surface area, and these properties will lead to different diffusion capabilities of water vapor during the adsorption and desorption processes on the surface of copper oxide.

In general, the nucleation and growth process of copper oxide nanostructures are controlled by adjusting the parameters of material preparation and synthesis [61], which in turn affects the surface morphology of nanostructures, such as increasing the surface porosity and increasing the grain size [62], so as to obtain copper oxide nanostructured materials with good moisture-sensitive properties. In particular, some complex structural materials are composed of basic one-dimensional nanostructures, such as nanorods and nanofibers. Its complex layered structure can effectively improve the electron mobility of the material, thereby effectively reducing the impedance of the humidity sensor [28, 63, 64].

So far, researchers around the world have designed and synthesized CuO nanostructures with various morphologies

through various methods to realize CuO-based humidity sensors.

Malook et al. [34] reported that CuO nanoparticles were prepared by decomposing basic copper carbonate (BCC) at high temperature (Figure 3), which has a large specific surface area (56.25 m<sup>2</sup>/g). Its average pore size is 32-37 nm. At 293 K, the RC response of the humidity-sensitive material varies with frequency and relative humidity as shown in Figure 4(a). Expose the sensor to moisture and notice a sudden drop in resistance. A graphical representation of the resistive and capacitive responses of moisture-sensitive materials as a function of applied frequency was also investigated (Figure 4(b)). It was found that the effect of frequency on the resistance and capacitance response dominates at low humidity levels. However, at higher humidity, the effect of frequency on the moisture-sensitive materials' resistive response is negligible. The humidity sensor has a good response/recovery speed, which indicates that the sensitivity of the humidity sensor with mesoporous copper oxide particles is better (Figure 4(c)). Even after 30 days of alternating exposure to a higher humidity environment (90%RH) and an indoor humidity environment, the sensor still maintained a good sensing behavior with little change in the dynamic response curve (Figure 4(d)). In addition, the authors also studied the humidity selectivity of copper oxide nanoparticles. By detecting the response of the sensor to different interfering gases (H<sub>2</sub>S and NH<sub>3</sub>) in different humidity environments, it was found that under high humidity conditions, interfering gases have little effect on the sensor, and it shows that this material has good selectivity to humidity.

Rupashree and colleagues [65] selected green tea extract as the raw material and synthesized a new type of moisture-sensitive material by sintering (Figures 5(a) and 5(b)) with a particle size of 64.5 nm, and CuO NPs achieved an optimal 99% (7-97% relative humidity). It may be due to the increase in grain size, which leads to the change of the surface

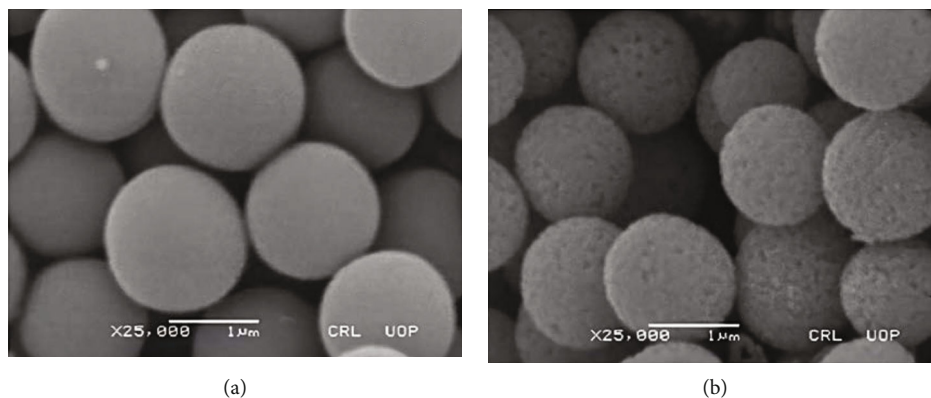


FIGURE 3: SEM micrograph of (a) basic copper carbonate and (b) calcined CuO [34].

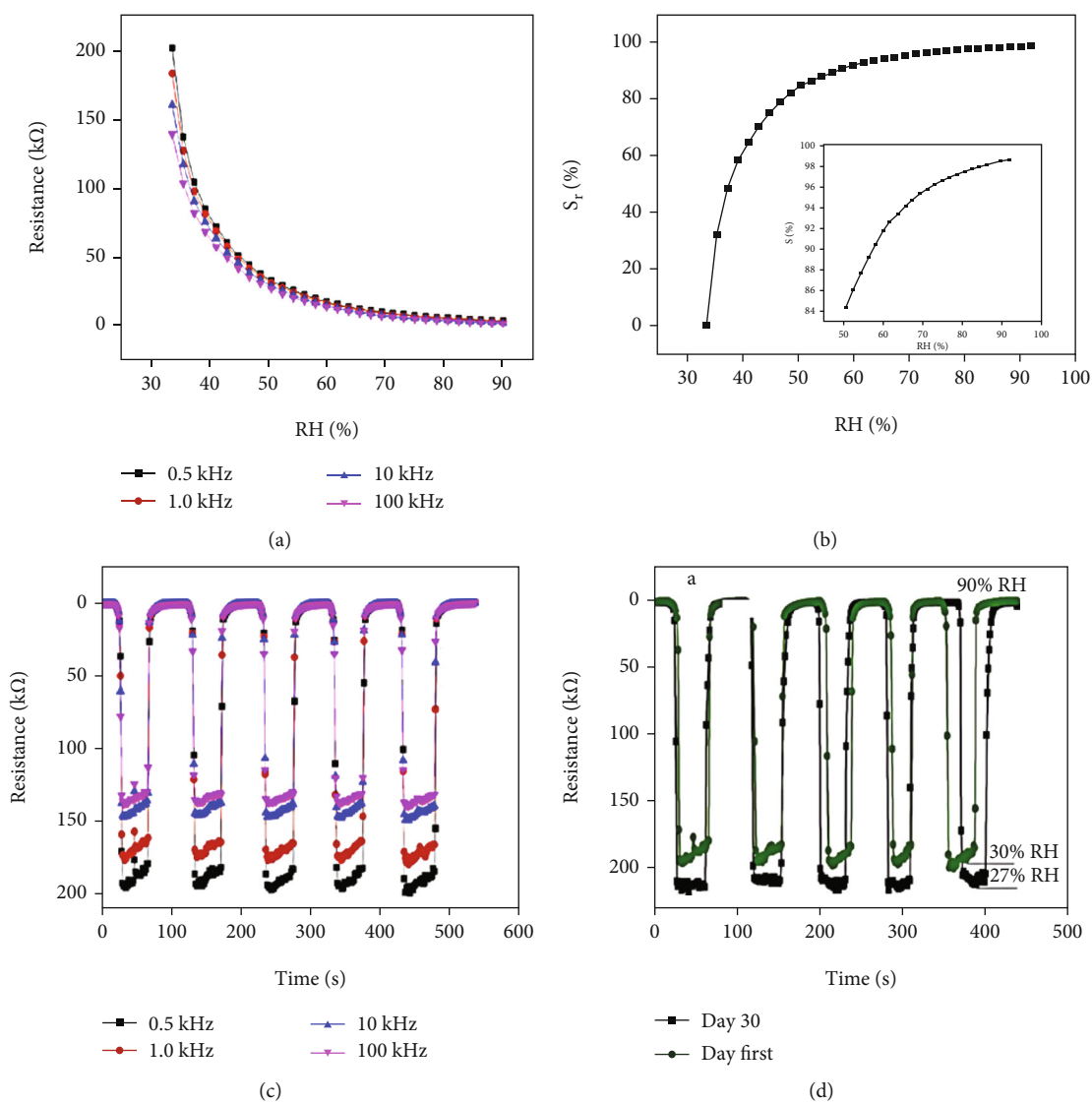


FIGURE 4: (a) Graph of the change of resistance with humidity at different frequencies (CuO-based sensor). (b) Copper oxide-based humidity sensor resistance sensitivity change graph with humidity (18-22°C). (c) Resistive dynamic response to humidity under a CuO-based humidity sensor (18-22°C). (d) Comparative resistive dynamic response of CuO-based sensor towards humidity on day first and after 30 days [34].

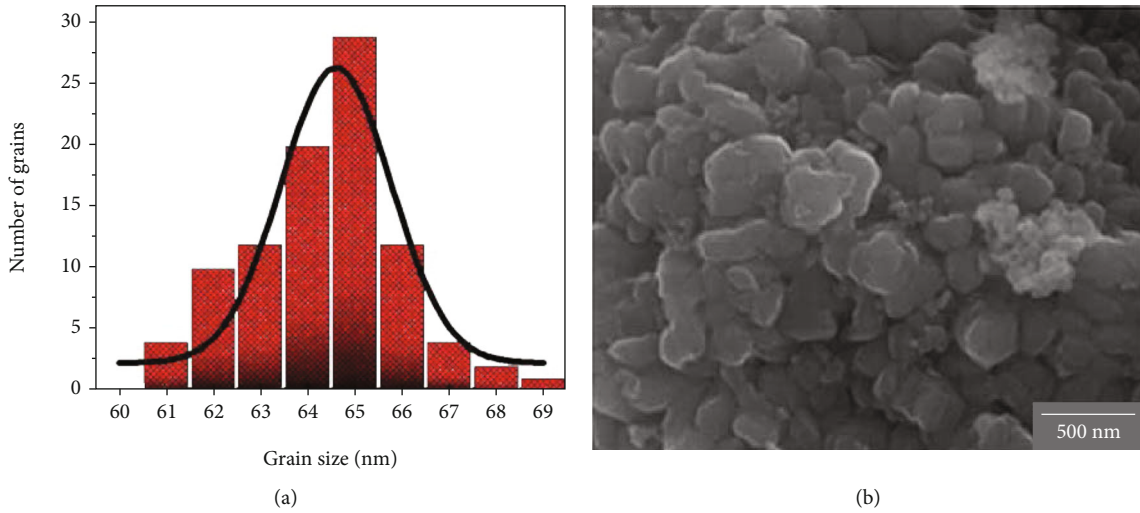


FIGURE 5: (a) Histograms for grain size. (b) SEM image of CuO NPs [65].

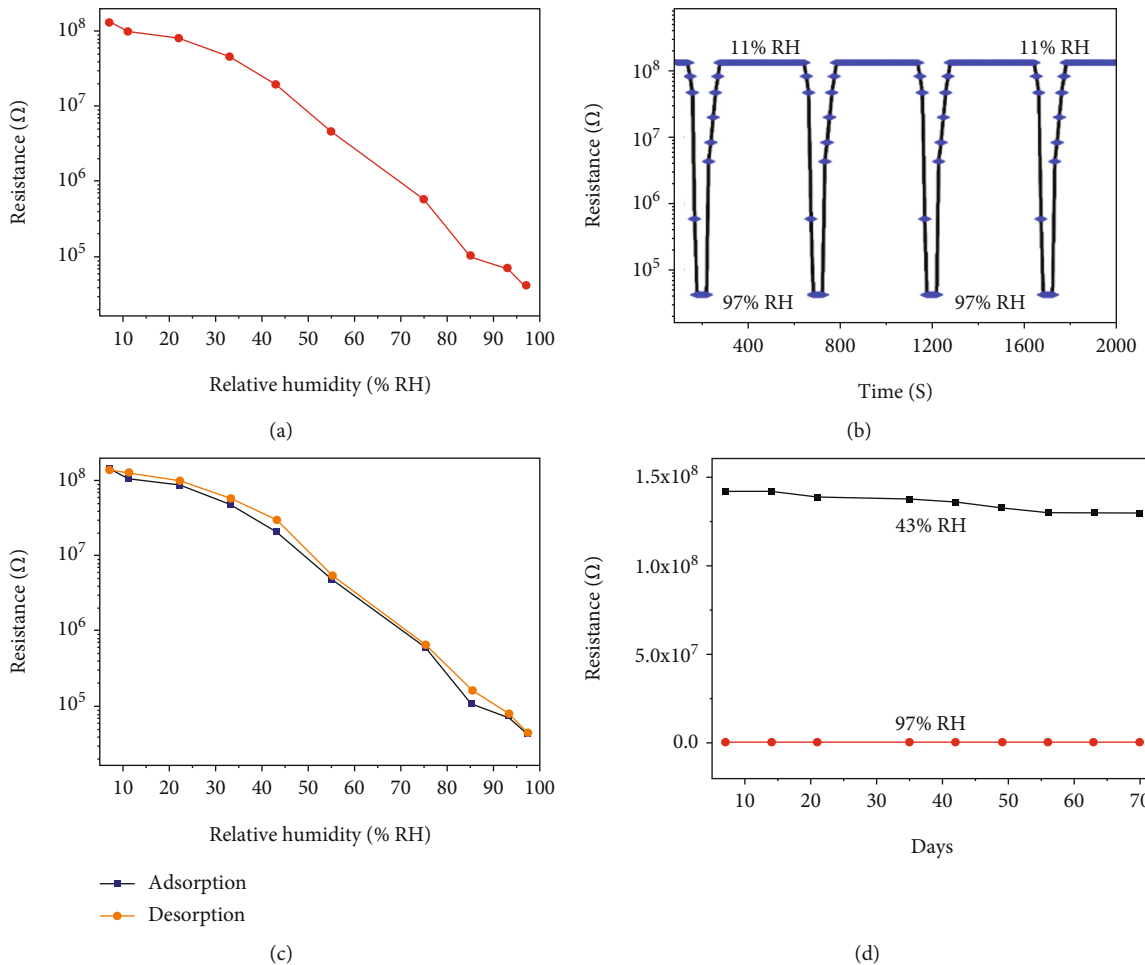


FIGURE 6: (a) Graph of resistance-humidity function (CuO NPs). (b) The timing behavior of the CuO NPs. (c) The humidity hysteresis of CuO NPs. (d) The humidity stability of the CuO NPs [65].

morphology of the moisture-sensitive material, allows more water vapor to adsorb on the surface of the moisture-sensitive material and condense in the capillary pores, and enhances the electrical conductivity of moisture-sensitive

materials. Its response time was 22 seconds, and recovery time was 31 seconds (Figure 6(b)). Over a two-month period, CuO NPs showed minimal hysteresis and good stability (Figures 6(c) and 6(d)), and the moisture-sensitive



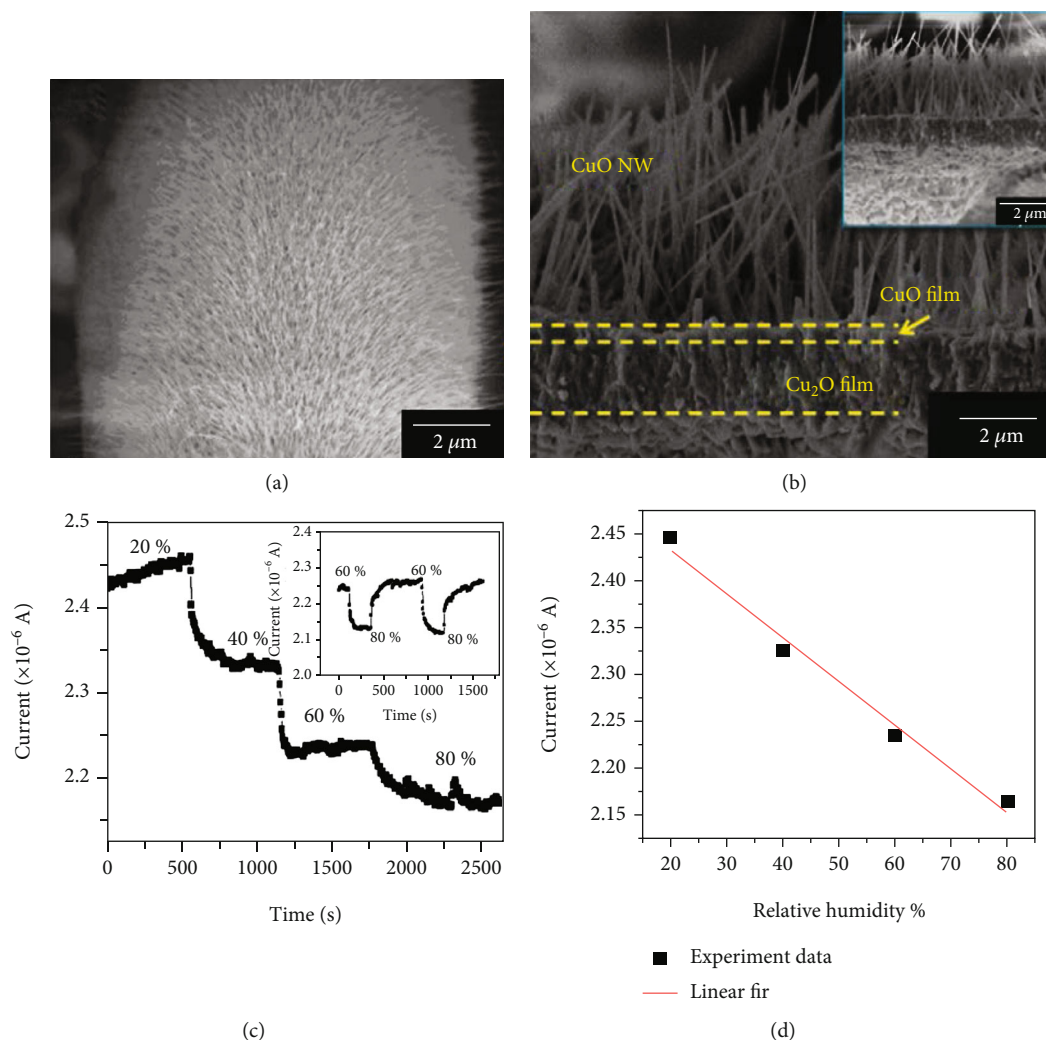


FIGURE 7: (a) Top-view. (b) Cross-sectional FESEM images of the thermally treated sample. (c) Graph of current versus time and inset the reproducible sensing response. (d) Measured current as a function of RH [8].

materials based on green synthetic copper oxide nanoparticles are more stable and more sensitive at lower humidity.

Wang et al. [8] reported that Cu wires can be transformed by thermal annealing into CuO/Cu<sub>2</sub>O/Cu core-shell trilayers covered with high-density CuO nanowires (Figures 7(a) and 7(b)), average length is 2-5 μm, and average diameter is 50 nm. During the high temperature treatment, Cu atoms diffuse into the outer layer of the material and oxidize to form a Cu<sub>2</sub>O layer and then further oxidized to CuO, forming a CuO/Cu<sub>2</sub>O/Cu core-shell three-layer structure. By studying the growth mechanism of copper oxide nanowires, it is found that the shape of copper oxide nanowires is affected by experimental parameters, including temperature and time, which similarly affects their sensing performance. The currents of the humidity-sensing materials measured in different humidity environments are shown in Figure 7(d). In addition, the sensing characteristics of the fabricated device are not only stable but also reproducible (Figure 7(c)), which has the potential for application in humidity-sensing devices.

Hsueh et al. [3] fabricated CuO nanowires (NWs) on glass substrates (Figures 8(a) and 8(b)), and it was found that with the increase of the initial thickness of the copper film after oxidation, the length of the copper oxide nanowires also increased, respectively (Figure 8(c)), and the resistance of the samples (80°C) when we increased the RH from 20% to 90% increased from  $0.55 \times 10^6$  to  $0.62 \times 10^6 \Omega$  (Figures 9(a) and 9(b)), which mainly because the adsorbed oxygen ions take away the electrons on the surface of the humidity-sensitive material, leading to the accumulation of holes on the surface of CuO. And the trapped electrons would follow the mechanism leaving holes, oxygen ions react with hydrogen ions generated by water vapor dissociation to form hydroxyl groups [66, 67], this liberates the electrons previously taken away by oxygen ions, and this part of the electrons will neutralize the vacancies on the surface of the moisture-sensitive material, thereby reducing the number of surface vacancies, thereby increasing the resistance of the CuO NW surface layer [68]. The authors fabricated a humidity sensor based on CuO NWs, and during the measurement process, the low hysteresis

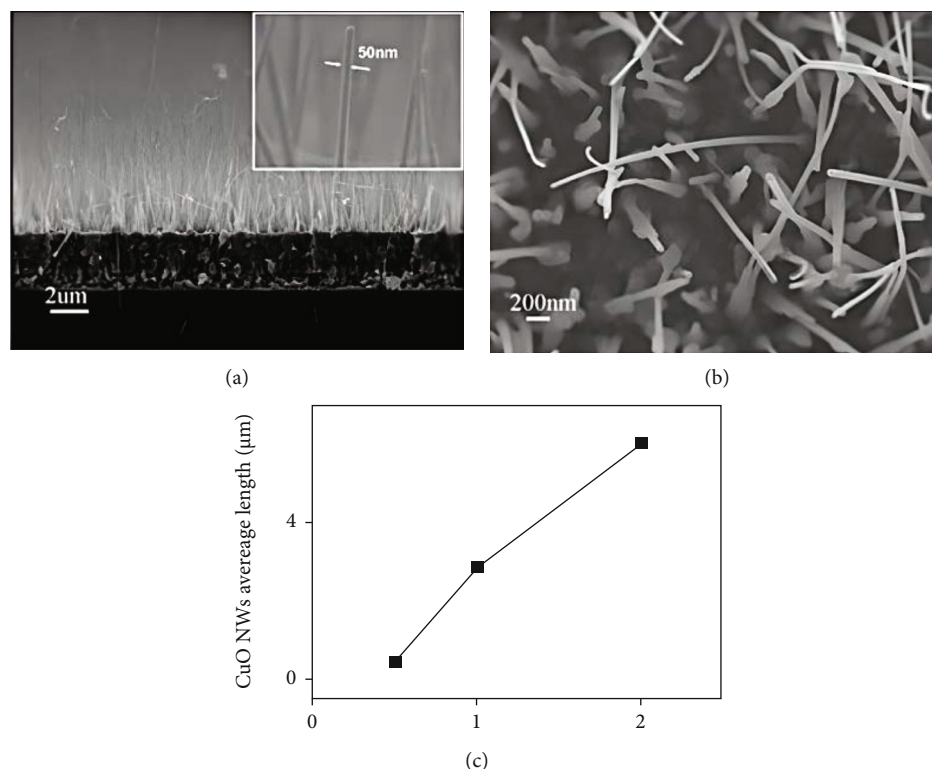


FIGURE 8: (a) Cross-sectional and (b) top-view SEM images of the thermally treated sample. (c) Average length of CuO NWs as a function of initial copper film thickness [3].

(Figure 9(c)) and stability (Figure 9(d)) of the humidity sensor were confirmed.

Xu et al. [69] prepared copper oxide nanomaterials with special structures by a two-step electrochemical deposition method (Figures 10(a)–10(d)). Scanning electron microscopy images found that the CuO honeycombs consisted of well-oriented nanowires with high surface volume ratio. This material has a honeycomb-like structure, and its unique surface structure and high porosity can improve the adsorption of water vapor molecules on the surface of the material. The authors and collaborators prepared  $\text{Cu}(\text{OH})_2$  in KOH solution and further heated to synthesize the target material. The prepared CuO honeycomb was peeled off the substrate by a rapid annealing process, and a CuO humidity sensor was prepared. From 12 to 97% humidity, the sensor impedance changes significantly with increasing humidity, the sensitivity factor  $S_f = 130$  and the resistance at 12% and 97% relative humidity are  $3 \times 10^6 \Omega$  and  $2.3 \times 10^4 \Omega$ , respectively (Figure 10(e)), and the sensor resistance remained stable during the measurement lasting one week (Figure 10(f)).

Gu and coworkers [70] reported the preparation of CuO nanosheets of different sizes using different concentrations of NaOH solutions (Figures 11(a)–11(c)). In the performance test, it was found that the copper oxide nanosheet with the smallest size has the highest sensitivity in the humidity range of 11.3–97.3% (Figures 12(a) and 12(b)), has the best low humidity hysteresis characteristics (Figure 12(c)), and has the fastest response time (32 s), but the recovery time was longer (22 s) (Figure 12(d)).

The authors attribute the excellent humidity-sensing performance of CuO nanosheets with a length of  $1 \mu\text{m}$  to their largest specific surface area, which enables a larger area of the sensor-sensing interface and higher activity, both for chemisorption at low humidity levels, or physical adsorption behind. Small-sized copper oxide nanosheets have larger specific surface area, and their adsorption capacity is stronger. So the sensitivity of the humidity sensor will increase with the decrease of the copper oxide nanosheets, but at the same time, the stronger the adsorption capacity of the surface of the material, the tighter the binding with water molecules, which will cause the water molecules to suffer greater resistance during the desorption process and seriously affect the recovery time of the moisture-sensitive material.

We summarize some reports on the humidity-sensing properties of pure CuO with different morphologies, including nanoparticles, nanowires, and nanosheets, and details are shown in Table 1. The increased specific surface area of the copper oxide nanostructures enhances the adsorption capacity of water vapor in the outer layer of the material, thereby improving the sensitivity of the humidity sensor. We found that the surface modification of pure copper oxide increases the defect density on the surface of the material, and changing its nanostructure can improve the sensitivity and response speed of the copper oxide-based humidity sensor to a certain extent, and the working stability of the product has also been proved. However, in general, copper oxides with different nanostructures show poor room temperature sensitivity; in other words, only surface modification of pure

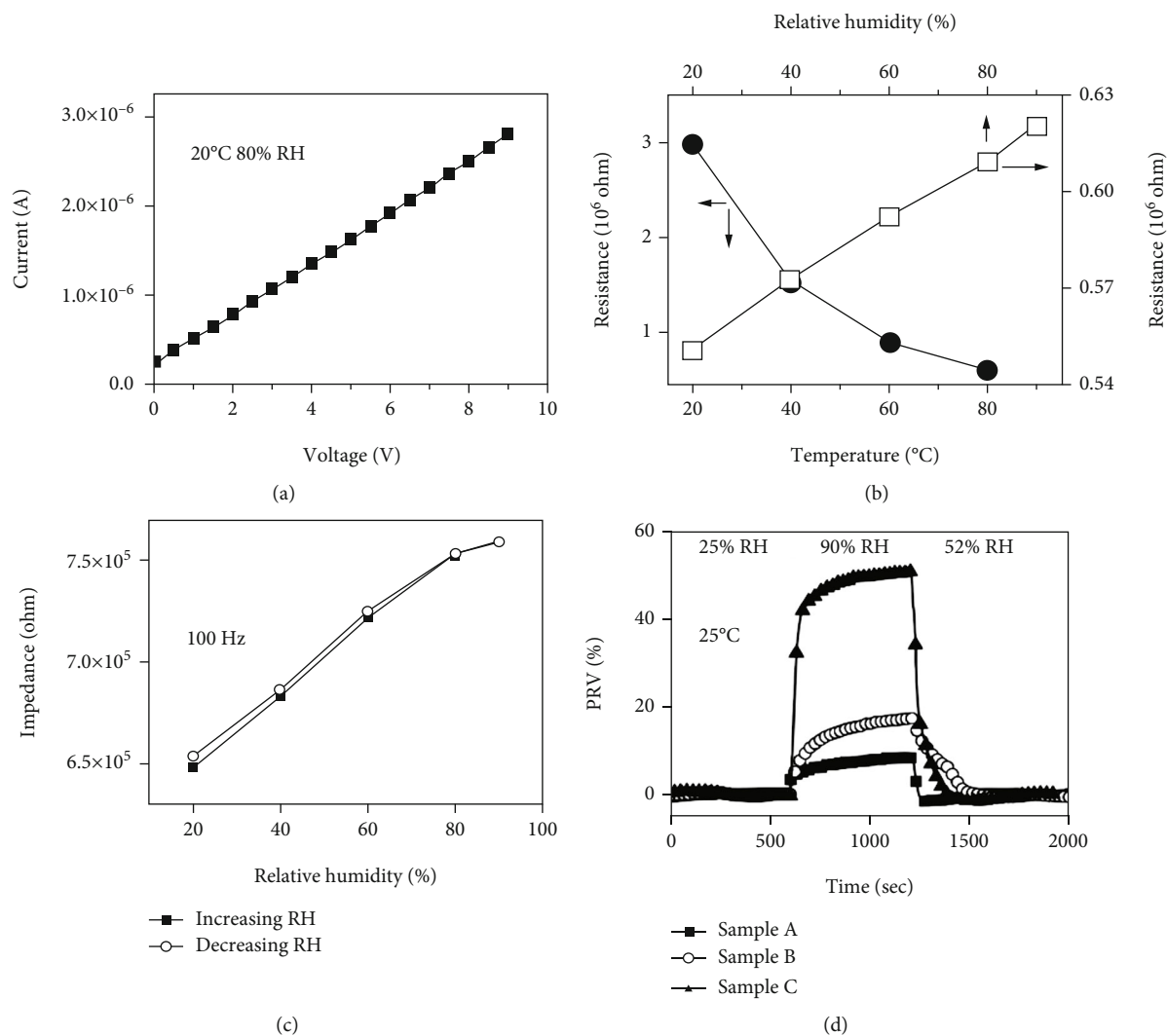


FIGURE 9: (a) I-V characteristics of sample C measured at 25°C, 80%RH. (b) Sample impedance as a function of time, temperature with 5 V applied bias. (c) Hysteresis of CuO NW samples (1 V applied bias and 80°C). (d) Dynamic response of three humidity sensors at room temperature (5 V applied bias) [3].

copper oxide materials can only improve their humidity-sensitive properties to a certain extent, and we need to find more suitable method to further improve the sensitivity and response speed of the sensor.

### 3. Additive Doping

At present, the attention of many researchers has been attracted by the field of nanometers. Many materials based on nanometer size will have special properties [74]. The further improvement of the physicochemical properties of nanomaterials depends on the synthesis of nanoparticles with different structures and properties and the ability to obtain the desired performance [75]. Nanocomposites are a new topic in the field of materials. By compounding different or the same type of nanoparticles to obtain expected properties [8, 76], it is also possible to dope pure copper oxide nanostructures by doping additives (mainly organic polymers, metal oxides, and carbon-based materials) as

secondary components to improve the moisture-sensing properties of copper oxide, as Table 2.

**3.1. Organic Polymer Doping.** Organic polymers include polypyrrole (PPy) [88], polyvinylpyrrolidone (PVP) [89], polyethylene oxide (PEO) [90], polyvinyl alcohol (PVA) [91], polyaniline (PANI) [92], cellulose acetate (CA) [93], and polyethyleneimine (PEI) [94]. As sensing materials, they have low cost, high sensitivity, small hysteresis, and low response short time and easy to prepare and process [95], and they can also operate at room temperature, and the advantages of using polymeric materials as humidity sensors have been widely reported [96, 97].

Copper oxide and organic polymers are doped together to form hybrid nanocomposites; this mechanism of enhanced sensing performance can be attributed to the heterojunction of organic polymers forming vacancy-electron depletion layers on the surface of copper oxide materials, electrons, and vacancies in copper oxide materials and organic polymers will migrate. This process will cause the energy band to bend,

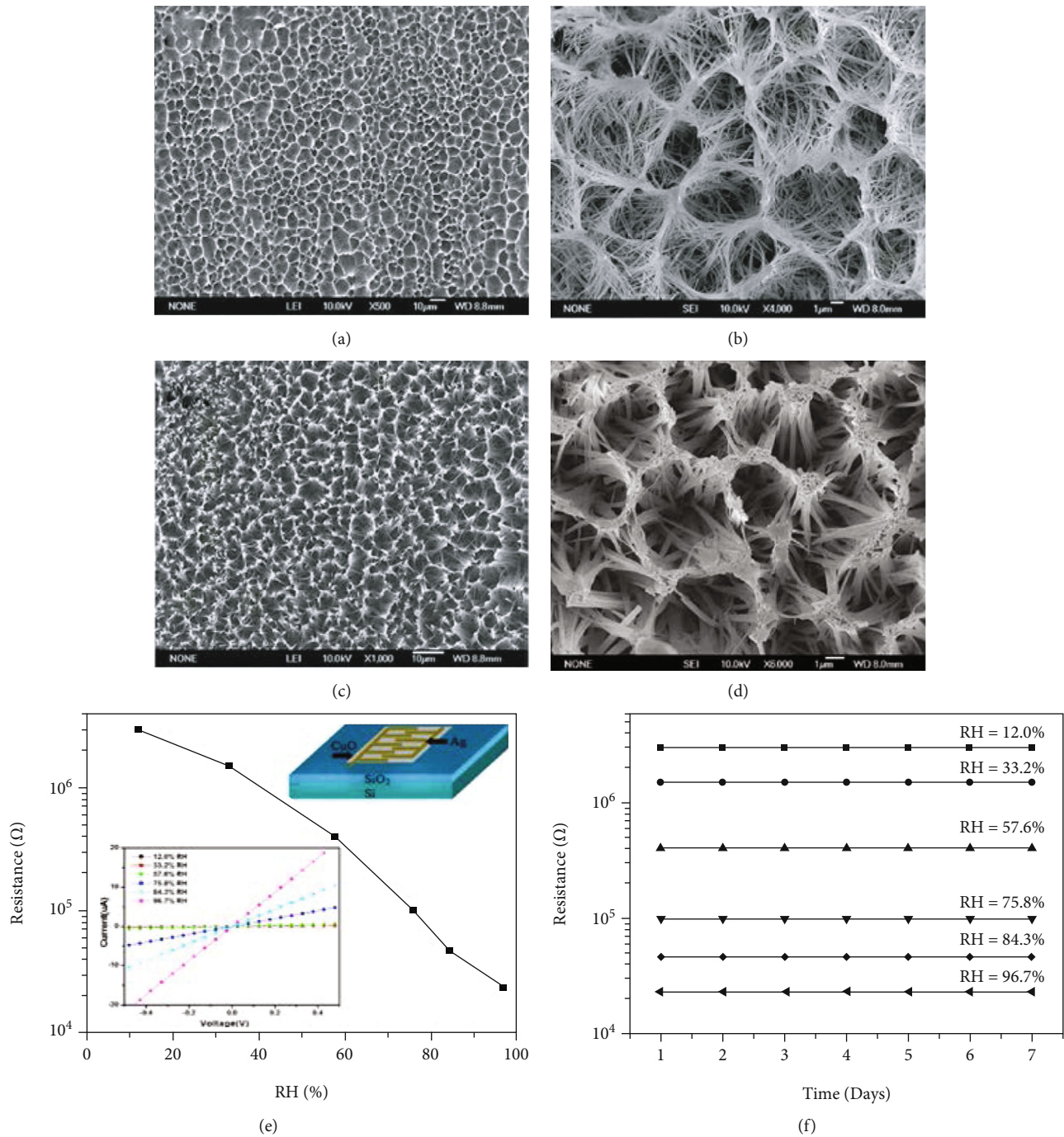


FIGURE 10: SEM images of CuO honeycombs via two-step electrochemical deposition at different voltage for 4 h: (a, b)  $E = 3$  V and (c, d)  $E = 5$  V. (e) The impedance versus humidity plot of CuO honeycombs (25°C). The insets show schematic illustration (upper-right) and the corresponding I-V curves (lower-left) of a CuO honeycomb-based humidity sensor. (f) Resistance variations with time for the CuO sample at various RH levels [69].

and eventually, the Fermi level will reach a new equilibrium state, thereby forming a heterojunction at the interface where the copper oxide and the polymer come into contact. the current across the heterojunction barrier is known to be exponentially related to the junction barrier height [15]. Therefore, the conductivity of the heterojunction is very sensitive to small changes in the junction barrier height. When the moisture-sensitive material is in contact with water vapor in the atmo-

sphere, the water vapor will be adsorbed on the surface of the material, and the width of the depletion layer will change, resulting in a change in the height of the potential barrier [96]. The conductivity of the material is unusually sensitive to the barrier height, so this approach would be effective in increasing the sensor's moderate sensitivity.

Polyvinylpyrrolidone (PVP) is a hydrophilic polymer with good sensing properties. It is a conjugated polymer that

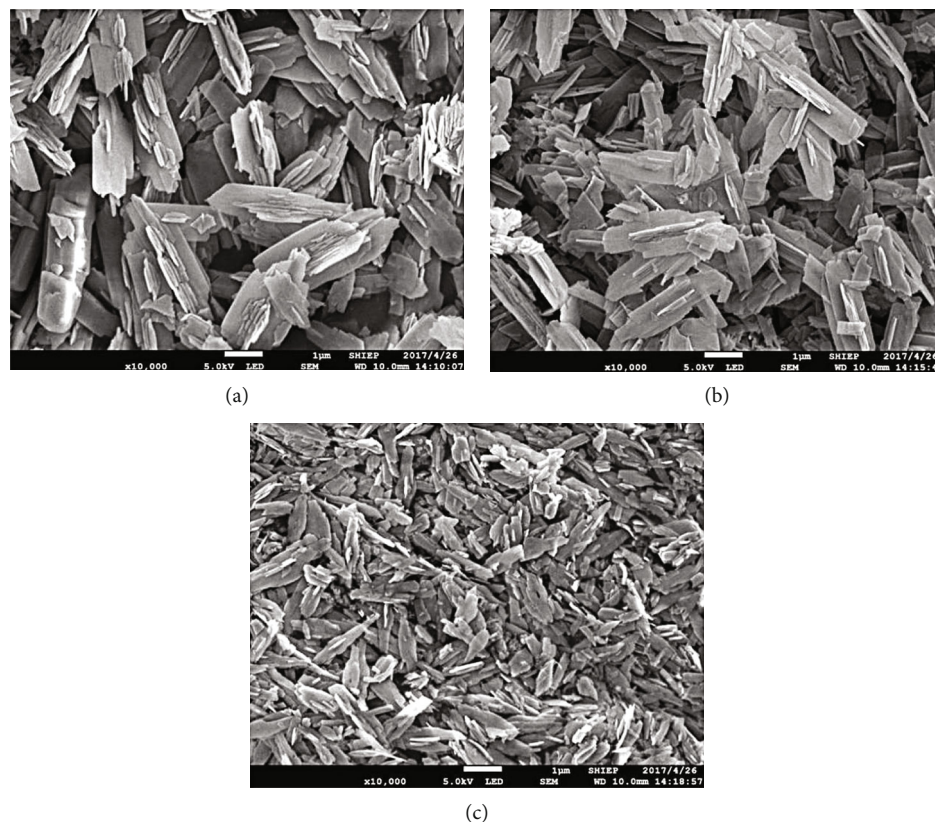


FIGURE 11: SEM micrographs of CuO nanosheets prepared with different concentrations of NaOH: (a) 0.5 mol/l (sample 1), (b) 0.125 mol/l (sample 2), and (c) 0.05 mol/l (sample 3) [70].

is soluble in water and still maintains relatively good properties at high temperatures [89]. Therefore, polyvinylpyrrolidone is suitable as a hydrophilic polymer to be doped into copper oxide to prepare nanocomposites to improve the humidity-sensitive properties of pure copper oxide, and its thermal stability can effectively reduce the operating temperature of copper oxide sensors. Conductivity can also be complementary to copper oxide. Khan et al. [15] reported the preparation of polyvinylpyrrolidone (PVP)/CuO composites with a dense structure by polymerization (Figure 13(a)). The authors found that the SEM micrographs showed that the copper oxide particles distorted and destroyed the PVP. The smooth structure makes the PVP surface rough, and the rough surface makes it easier for the water vapor in the environment to adsorb on the surface of the composite material, thus enhancing the sensing performance of the thin film. The authors fabricated PVP/CuO nanocomposite by a simple drop method the humidity sensor of the material, and it is observed that the PVP/CuO composite material has superior resistance response in the humidity range of 25–95%RH (Figure 13(b)), and the sensitivity is high. The response/recovery times at room temperature are 35 seconds and 12 seconds, respectively. The response-recovery behavior is better than that of the pure copper oxide sensor, with a hysteresis of only 2.1% (Figure 13(c)), while showing good stability over 60 days of repeated detection (Figure 13(d)).

In another experiment, Ahmad and coworkers [77] successfully prepared nanomaterials composed of polyethylene

oxide (PEO), oxidized multiwalled carbon nanotubes (MWCNT), and copper oxide (CuO) by electrospinning. The composite nanofibers composed of particles (Figures 14(a) and 14(b)), copper oxide, and carbon nanotubes were filled into polyethylene oxide as fillers (PEO–CuO–MWCNT: 1% and PEO–CuO–MWCNT: 3%). A digital LCR meter was used to measure the capacitance and resistance of the material at different relative humidity levels, and the moisture sensing properties of the composite nanomaterials were investigated. Scanning electron micrographs showed that the composites exhibited fine fibers with smooth surfaces, which indicated that the fillers in the polymer matrix were uniformly dispersed. Experiments show that PEO–CuO–MWCNT: 1% and PEO–CuO–MWCNT: 3% exhibit high sensitivity to humidity in the humidity range of 30–90% at 25°C (Figures 14(c) and 14(d)). Both materials exhibit fast response and recovery rates (Figures 14(e) and 14(f)).

Similar to polyethylene oxide (PEO), polyvinyl alcohol (PVA) also has good hydrophilicity, no harm, and excellent thermal stability [98], which makes it suitable for use in biotechnology and sensing field as promising candidates [99]. Hashim et al. [78] synthesized a nanocomposite film of polyvinyl alcohol-polyethylene oxide and copper oxide (PVA–PEO–CuO) nanoparticles by a casting method. The study found that the PVA–PEO–CuO nanocomposite film showed good sensitivity in the humidity range of 30–70%. The authors believe that in environments with low relative

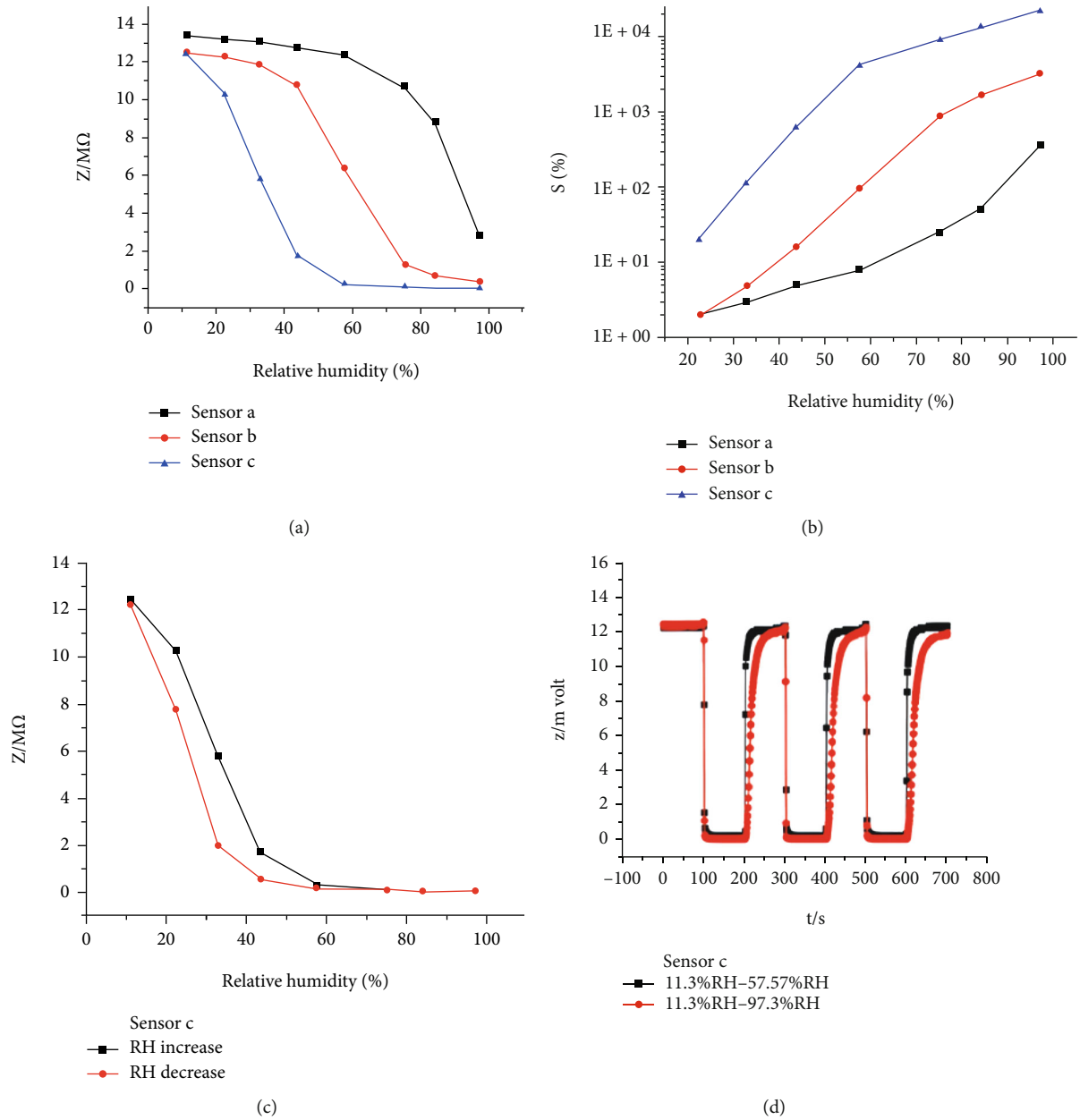


FIGURE 12: (a) Impedance changes of CuO nanosheets of different sizes with humidity. (b) Sensitivity of CuO nanosheets of different sizes varies with humidity. (c) Hysteresis characteristic of CuO sensors at different RH ( $1 \mu\text{m}$ ). (d) The response/recovery behavior and repeatability of CuO sensors ( $1 \mu\text{m}$ ) [70].

humidity, polymer chains curl and the migration of copper oxide particles is restricted. As the humidity increases, the material absorbs the water molecules to unfold and align, reducing the hopping resistance of charge carriers, thereby enhancing the sensing response of the composite.

Hashim et al. [78] chose polyaniline (PANI) with good electrical conductivity as the doped polymer material. Polyaniline itself is relatively stable, low cost, and easy to produce [100, 101]. At the same time, the combination of copper oxide and polyaniline also optimized the adsorption performance of polyaniline [102] and can also effectively address the limitations of poor processability and insufficient mechanical properties of PANI. The authors and colleagues

[79] reported the synthesis of polyaniline-copper oxide nanocomposites (CuO/PANI) using ammonium persulfate as the polymerization agent by a chemical oxidative polymerization route (Figure 15(a)). According to the experiments, the electrical resistance of the composite changes significantly with increasing humidity (Figure 15(b)). This shows that the CuO/PANI composite has a good response to humidity changes and further explains the sensing mechanism (Figure 15(c)). The material exhibits regular repeatability at room temperature with a response and recovery time of 40 and 55 seconds, respectively (Figure 15(d)), while the material also has a good response intensity (Figure 15(e)) and showed sufficient stability in the six-month test.

TABLE 1: Moisture-sensitive properties of copper oxide nanostructures with different morphologies.

Morphology	Synthesis method	$T_{opt}$ (°C)	Humidity range	Humidity-sensitive properties				Ref.
				Response time (s)	Recovery time (s)	Hysteresis	Response	
Mesoporous particles	Thermal decomposition	25	33-90%RH	~1	11	NA	NA	[34]
	Biosynthesis	25	7-97%RH	22	31	NA	99%	[65]
Nanoparticles	Microwave-assisted chemical solution	25	25-95%RH	NA	NA	NA	99%	[71]
	Thermal annealing	25	20-80%RH	~98	~98	NA	NA	[8]
Nanowire	Deposition	25	20-90%RH	NA	NA	<1.5%	NA	[3]
	Two-step electrochemical deposition	25	12-97%RH	NA	NA	NA	130	[32]
Nanosheets	Hydrothermal	25	11.3- 97.3%RH	32	22	NA	NA	[70]
	Spin-spray	25	20-90%RH	2.1	2.8	4%	170%	[72]
Nanorods	Hydrothermal	25	30-85%	NA	NA	NA	82.03%	[73]
Nanofilm	SILAR	25	20-80%	130	320	5%	NA	[54]

Note:  $T_{opt}$ : operating temperature; NA: not available.

TABLE 2: Humidity-sensing properties of dopants/CuO.

Dopant	Synthesis method	$T_{opt}$ (°C)	Humidity range	Humidity-sensitive properties				Ref.
				Response time (s)	Recovery time (s)	Hysteresis	Sensitivity	
PVP	Polymerization	26.85	25-95 RH	35	12	2.1%	NA	[15]
PEO	Electrospinning	25	30-90%RH	20	11	NA	53837.6%	[77]
PVA	Casting	25	30-70%RH	NA	NA	NA	NA	[78]
PANI	Chemical oxidative polymerization	25	10-95%RH	40	55	NA	70%	[79]
CA	Instrument-less novel technology	25	0-90%RH	13	17	NA	3.8 MΩ/%RH	[80]
Chitosan	Magnetic stirrer	25	20-95%RH	20	50	NA	-0.72to -2.1%RH	[81]
O-B-EG- B	Organic surfactant template	30	5-83.8%RH	180	160	NA	1.25%-7.9%	[82]
ZnO	Solid-state reaction	25	10-95%RH	NA	NA	±4%	29.95 MΩ/ %RH	[83]
	Hydrothermal	25	30-90%RH	6	7	21%	6045 ± 731	[84]
TiO <sub>2</sub>	Microwave-assisted synthesis	25	10-98%RH	162	428	NA	3.4%	[85]
Cu <sub>2</sub> O	Heated oxidation	25	35-98%RH	NA	NA	NA	-10.0%	[55]
rGO	Microwave-assisted hydrothermal	25	11-98%RH	2	17	NA	NA	[86]
MWCNT	Electrospinning	25	30-90%RH	3	22	NA	3798.2%	[77]
KCl	WEE	25	11-95%RH	40	50	4%RH	NA	[87]

Note:  $T_{opt}$ : operating temperature; NA: not available.

Chani and colleagues [80] first introduced a new instrument-free technique to fabricate a smart humidity sensor based on cellulose acetate-copper oxide (CA-CuO) nanocomposites. The SEM images were compared (Figures 16(a) and 16(b)). The authors found that thin-film composites have higher porosity than granular composites, and the porosity is favorable for the adsorption of water vapor, which in turn improves the moisture-sensing perfor-

mance. For granular materials, the surface porosity is low. The reason given by the authors is related to the manufacturing pressure of granular material processing. The humidity sensor based on the CA-CuO nanocomposite film has obvious changes in its capacitance and resistance between 0 and 90%RH (Figure 16(c)) and shows very little lag in experiments (Figure 16(d)). It is possibly due to higher porosity and smaller thickness of the material, which

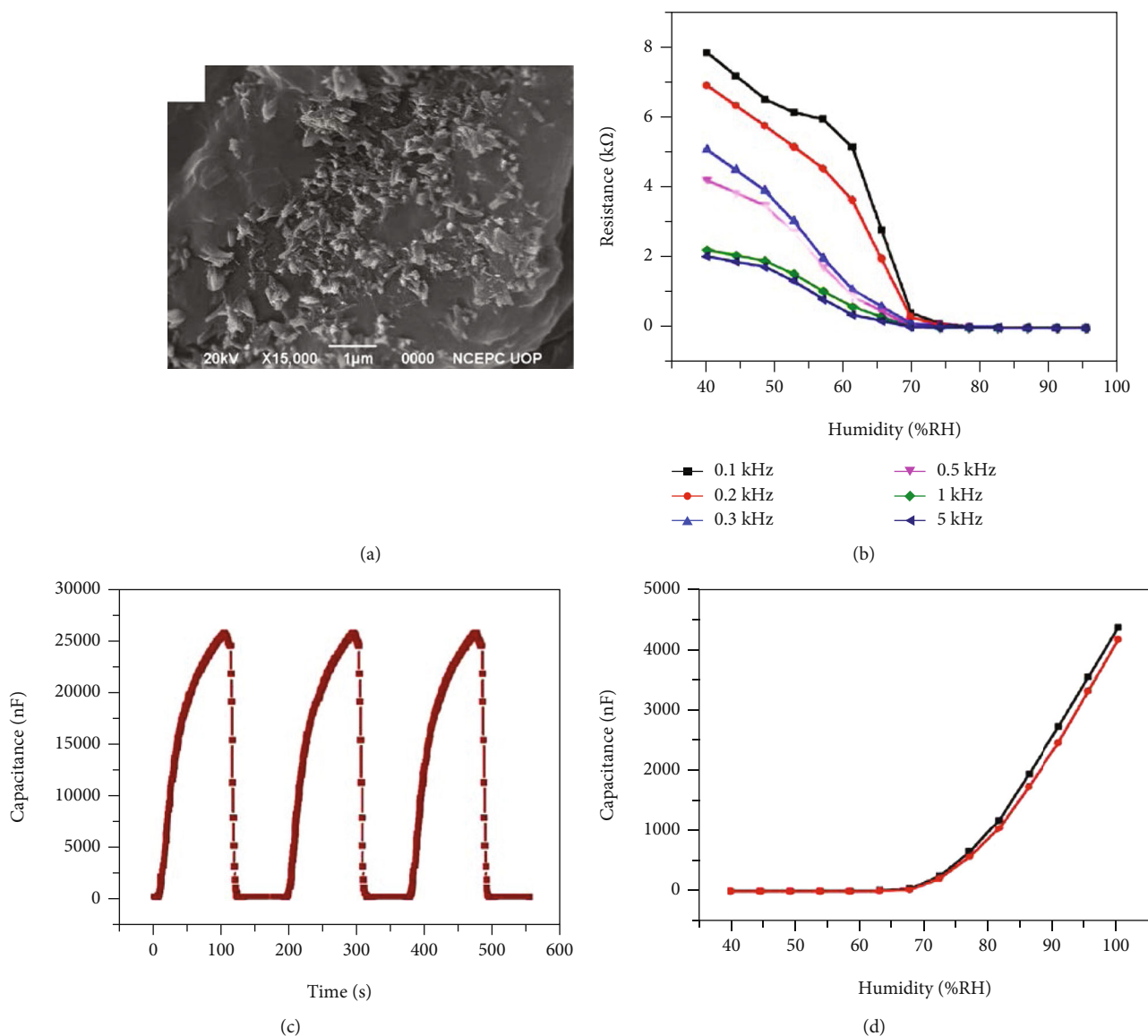


FIGURE 13: (a) SEM micrograph of PVP/CuO nanocomposite. (b) Resistance variation with different %RH at different frequencies of PVP/CuO nanocomposite. (c) Response and recovery curve of PVP/CuO nanocomposite sensors. (d) Hysteresis curve of PVP/CuO nanocomposite sensors at 100 Hz [15].

illustrates that the problem of large hysteresis in hydrophobic polymer-based sensors is further improved.

The results show that by doping organic polymers into copper oxide to form a heterojunction, the sensitivity and response speed of the sensor to humidity can be effectively improved, and the product also has good stability at room temperature. It has the potential to further explore new moisture-sensitive materials.

**3.2. Metal Oxide Doping.** In addition to organic polymers, the coupling of semiconducting metal oxides ZnO [83, 84], TiO<sub>2</sub> [85], SnO<sub>2</sub> [103], In<sub>2</sub>O<sub>3</sub> [104], and Fe<sub>3</sub>O<sub>4</sub> and Cu<sub>2</sub>O [81] into copper oxide can also significantly enhance its sensing performance. After careful summary investigations, we found that the resulting nanocomposites after coupling significantly improved the humidity-sensing behavior. More specifically, the effect of semiconducting metal oxides on the

humidity-sensitive properties of CuO-based humidity sensors is mainly because of the formation of heterojunctions with vacancy-electron depletion layers between CuO and semiconducting metal oxides [105, 106]. As far as we know, CuO is a typical p-type material, and the metal oxide compound doped with it is usually an n-type semiconductor. Because of the carrier concentration gradient, the free electrons in the n-type metal oxide usually migrate to the p-type copper oxide with vacancies as the main carriers. At the same time, the vacancies in the copper oxide will gradually diffuse to the n-type copper oxide. In semiconducting metal oxides, the energy band bends and the Fermi level finally reaches a new equilibrium, thereby forming a heterojunction at the interface between the two. The tunneling current across the heterojunction barrier is exponentially related to the junction barrier height [107]. Therefore, the conductivity is very sensitive to the small change of the



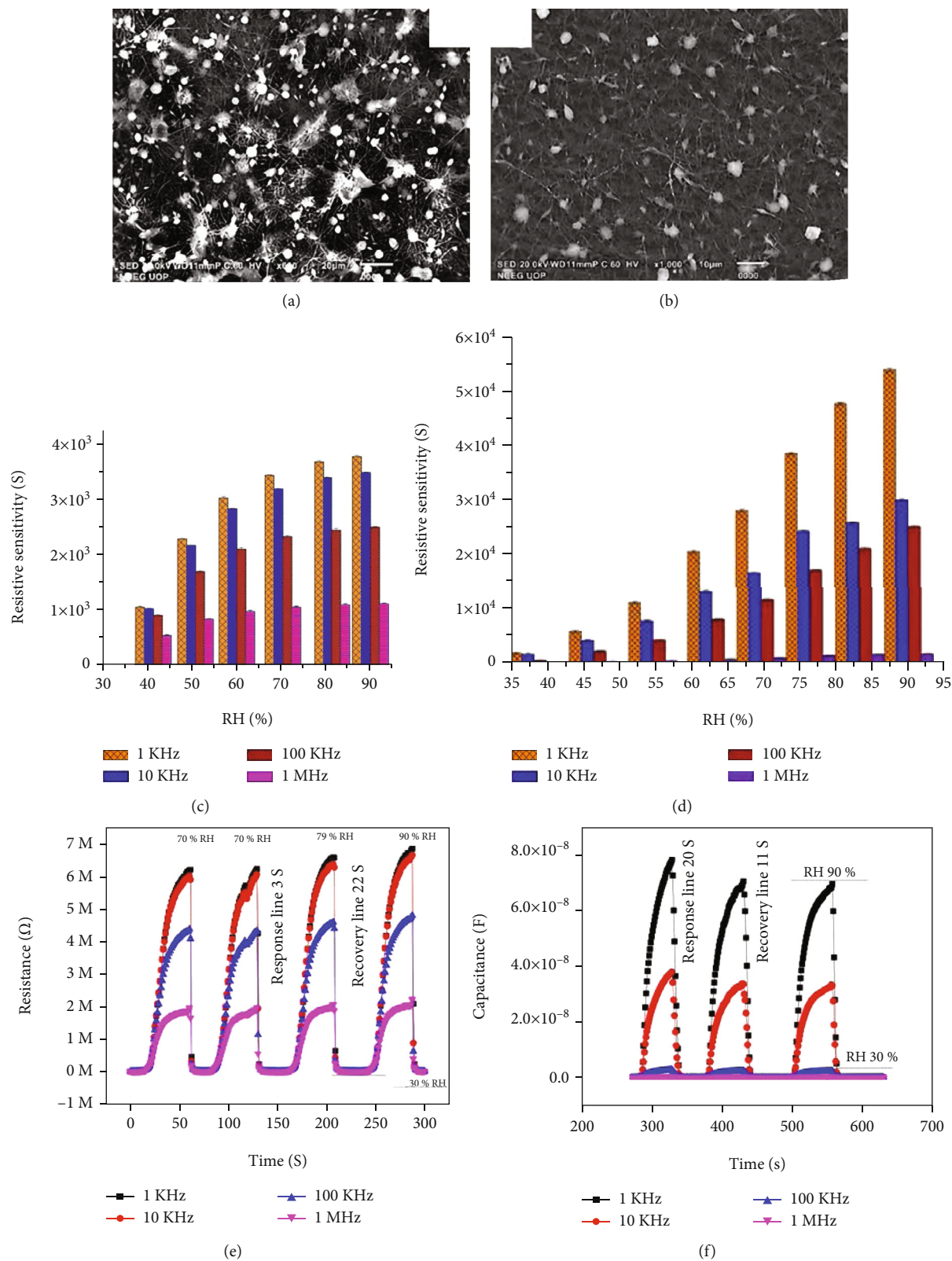


FIGURE 14: SEM micrographs of PEO-CuO-MWCNT: (a) 1% and (b) 3% nanofibers. Resistivity Sensitivity of PEO-CuO-MWCNT: (c) 1% and (d) 3% nanocomposite at different %RH. Resistivity response/recovery time for PEO-CuO-MWCNT: (e) 1% and (f) 3% nanocomposites [77].

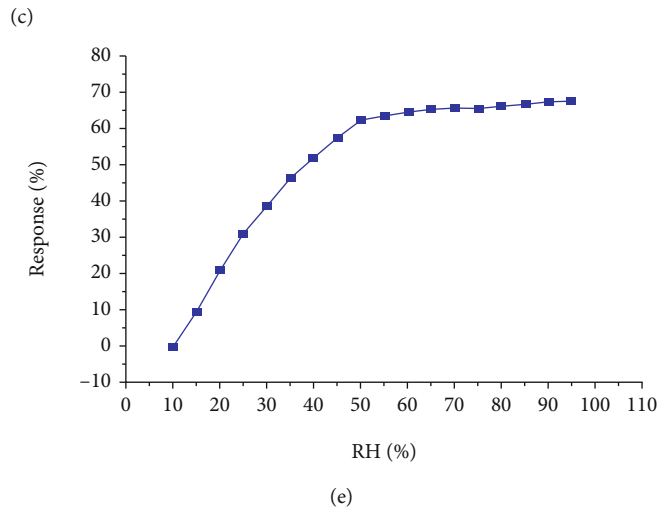
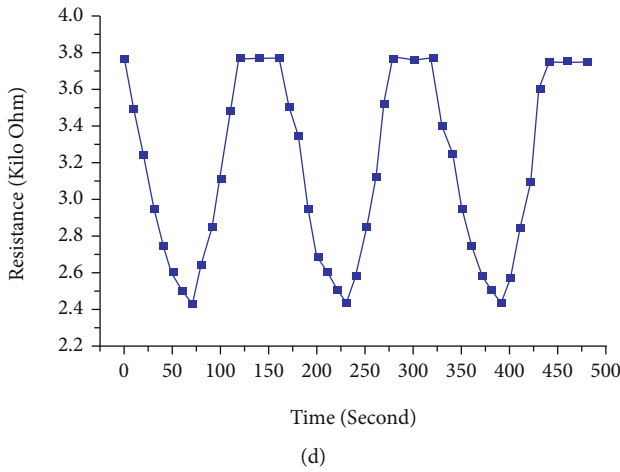
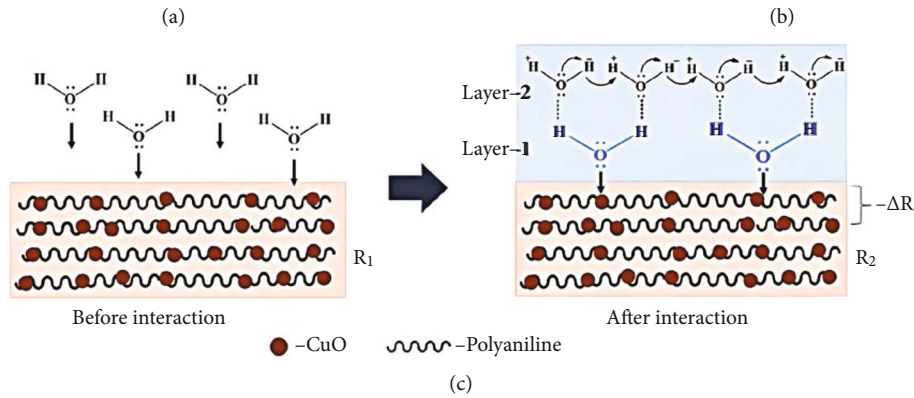
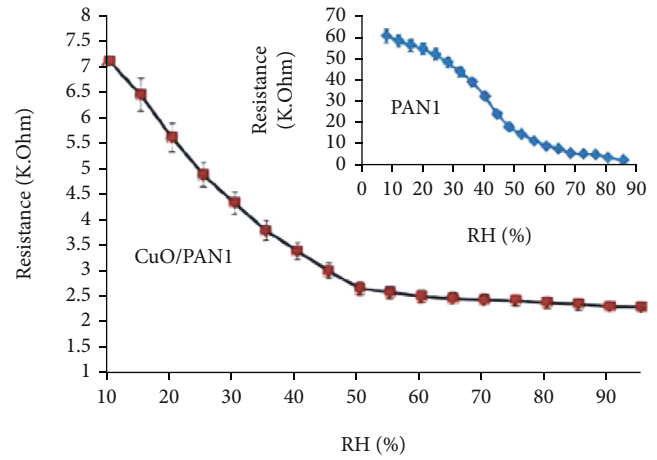
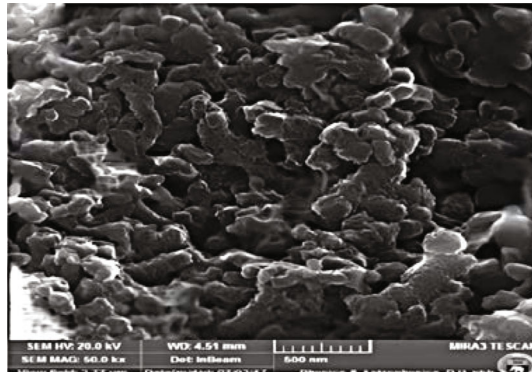


FIGURE 15: (a) SEM image of CuO/PANI. (b) CuO/PANI impedance as a function of humidity; the inset shows the variation trend of pure PANI impedance as a function of humidity. (c) Schematic illustration of sensing mechanism over CuO/PANI nanocomposite. (d) Change in resistance of CuO/PANI nanocomposite with time at 60%RH. (e) Percentage sensing response of CuO/PANI at different relative humidity [78].

junction barrier. Heterogeneous contacts of p-type and n-type semiconductors are humidity sensors acting through the contact interface [108–111], in such a sensor, and as the p-n junction is gradually exposed to the outside atmosphere, the water vapor in the environment gradually penetrates into the heterojunction interface, which also changes the electrical properties of the heterojunction [112].

ZnO, a typical n-type semiconductor with a wide band-gap of 3.37 eV, is abundant in nature [113]. It has stable

physical and chemical properties, low dielectric constant, nontoxic, and low cost [114]. Generally, the combination of narrow bandgap semiconductor and wide bandgap semiconductor will improve its sensing performance. Rajput et al. [83] reported the preparation of CuO–ZnO nanocomposites. It was found that between 10% and 95%RH, with the increase of copper oxide content, the resistance of the nanocomposite changed more significantly, and its humidity-sensitive performance and sensitivity were better

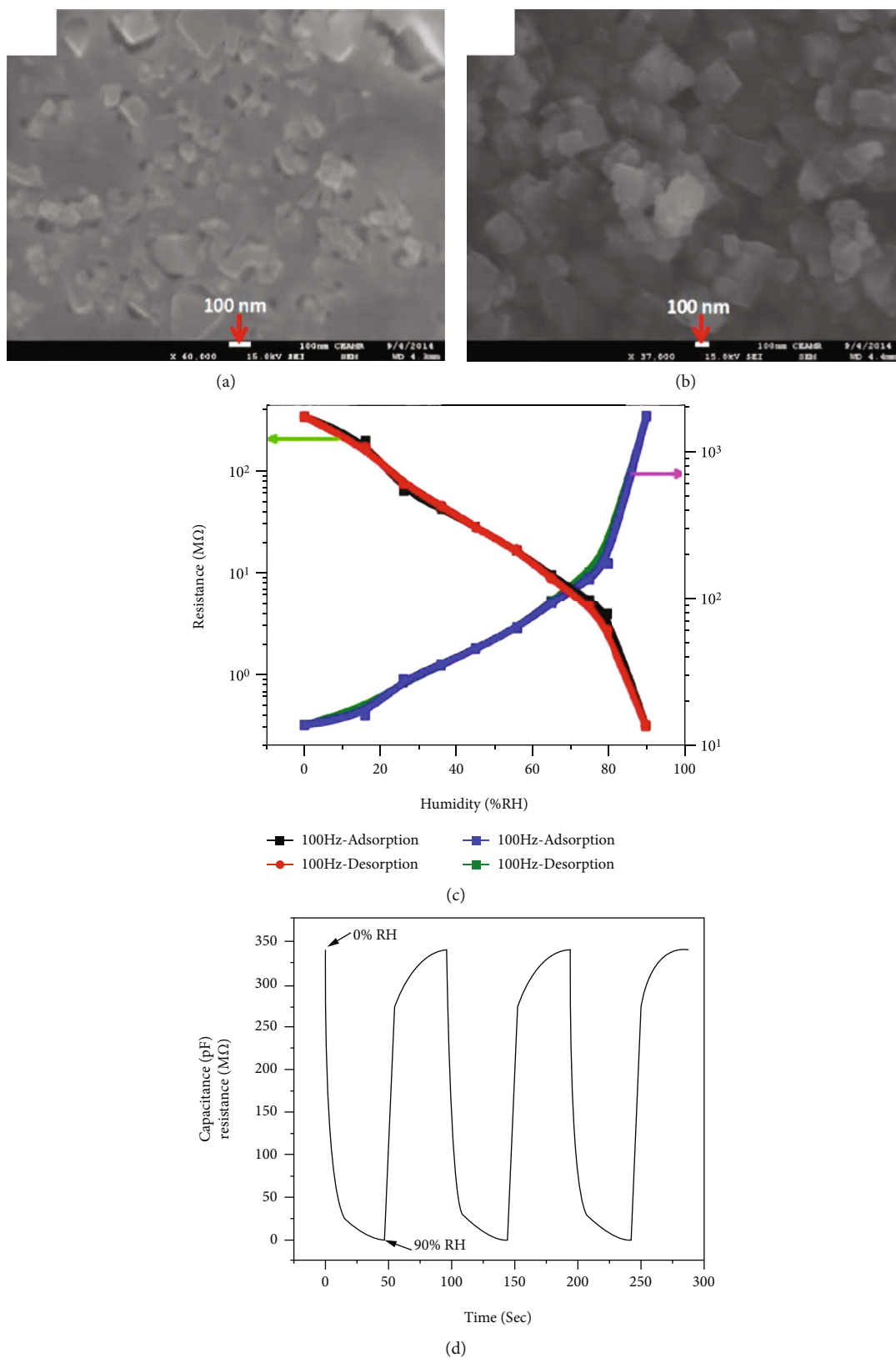


FIGURE 16: Surface morphologies of the (a) CA-CuO nanocomposite films and (b) pellets. (c) Capacitance and resistance-humidity relationships of CA-CuO humidity sensors. (d) Response-recovery behavior of the CA-CuO nanocomposite-based film sensors [80].

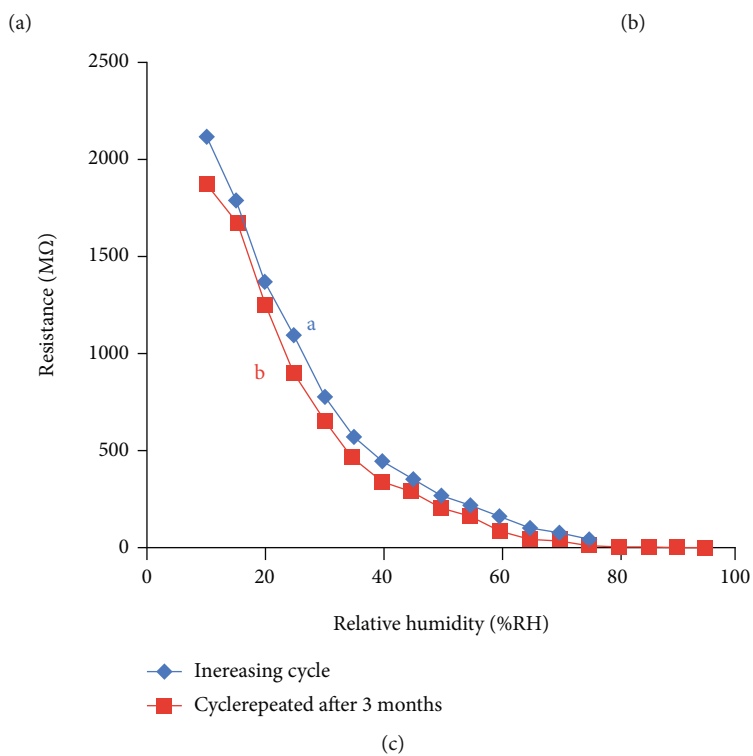
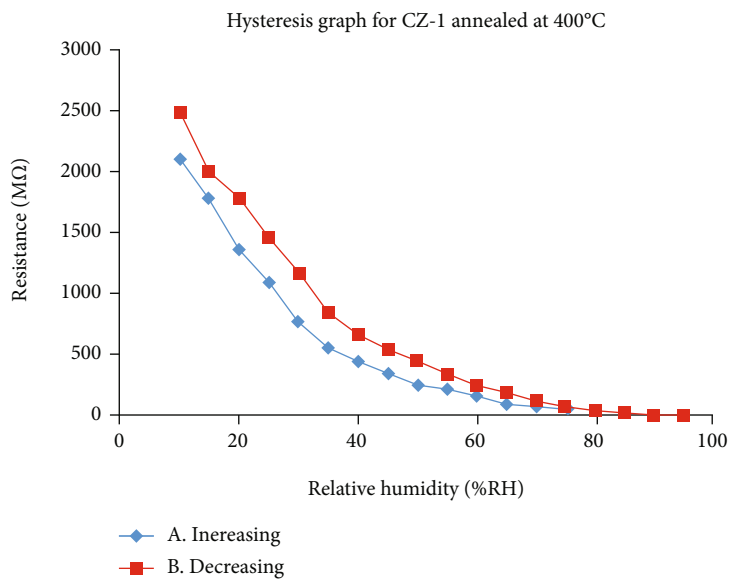
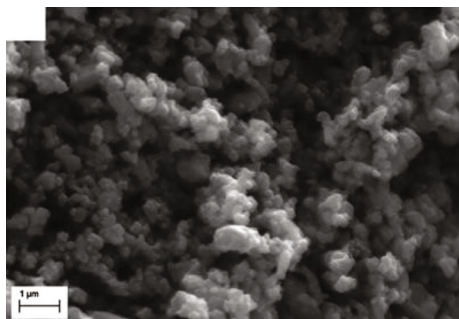


FIGURE 17: Continued.

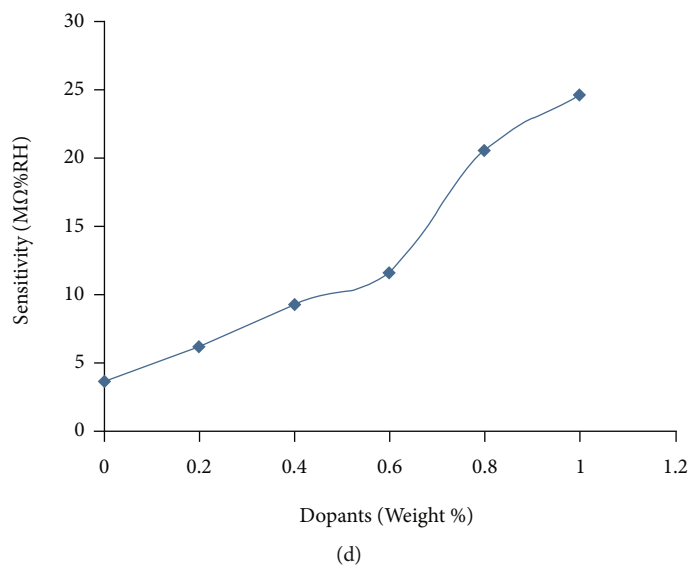


FIGURE 17: (a) Scanning electron micrograph of sample CZ-1 (1.0% by weight of CuO in ZnO). (b) Variation in resistance with change in %RH for sample CZ-1: (A) increasing cycle and (B) decreasing cycle. (c) Variation in resistance with change in %RH for sample CZ-1 for annealing temperature 400°C: (A) increasing cycle and (B) repeated cycle after 3 months. (d) Variation in sensitivity with wt% of CuO in ZnO [83].

(Figure 17(d)). Figure 17(a) is a scanning electron microscope photograph of 1.0% by weight of CuO in ZnO. The calculated sample exhibits good hysteresis with a minimum hysteresis of  $\pm 4\%$  (Figure 17(b)). The experimental results were reproducible across different operating cycles, with an aging of  $\pm 4\%$  after three months (Figure 17(c)).

In another experiment, Zainelabdin and colleagues [84] reported the preparation of copper oxide nanomaterials with special morphologies on ZnO nanorods (NRs) by a hydrothermal method. During the hydrothermal treatment, the surface of the ZnO nanorods was eroded and hydroxylated, which promotes CuO nanostructure growth through directional attachment. After four hours of hydrothermal treatment, the surface of ZnO nanorods was completely covered by CuO nanostructures, and ZnO was completely chemically dissolved at this time (Figures 18(a)–18(c)). According to the experiments, the humidity sensor based on ZnO/CuO nanocoral shows good linearity and sensitivity between 30% and 90%RH (Figure 18(d)), and the sensitivity factor 32Sf (referred to as R30%/R90%) was found to be 6045 ( $\pm 731$ ). Using the same process to fabricate four different sensors, the measured standard deviation was 12%, which the authors attribute to the different densities of ZnO nanorods and/or CuO nanostructures. Importantly, the sensor exhibited a high hysteresis of 21%, indicating the presence of a reactive reaction that affects water desorption from nanocoral voids, which requires further experimental investigation.

Similar to zinc oxide, TiO<sub>2</sub> is also an n-type semiconductor material with a bandgap of 3.2 eV [115]. Ashok et al. [85] reported the synthesis of CuO/TiO<sub>2</sub> nanocomposites using EMISE (1-ethyl-3-methyl-imidazolium-ethylsulfate). It was found by scanning electron microscopy that the nanocomposites presented a nanotube-like structure, and with the increase of copper oxide content in the composites, the lon-

ger the nanotubes were, the longer the nanotubes were. When the mass percentage of copper oxide is 8%, the length of the resulting nanotubes is 36 nm (Figure 19(a)). Within the humidity range given in the experiment, it can be observed that the resistance of the CT-8 sample changes most significantly and has good sensitivity at 300 K (Figures 19(b) and 19(c)). The response and recovery time are measured as 162 and 428 seconds. The authors attribute the sensitivity of the sensing element to the nanocomposite tube structure of CuO/TiO<sub>2</sub>, and it enhances the diffusion of water.

Besides cupric oxide, cuprous oxide is also one of the earliest typical p-type materials [116]. As mentioned in the first section, the crystal structure of cuprous oxide is cubic with a narrow direct bandgap ( $=2.1$  eV), and although the conductivity is lower than that of copper oxide, it has higher carrier mobility. Hsu et al. [55] reported the preparation of Cu<sub>2</sub>O/CuO nanomaterials on Cu through-silicon vias by thermal oxidation. It is observed that the RH response of the sensing element increases with increasing humidity, as explained by the authors when water molecules displace O<sup>2-</sup> and liberate electrons from oxygen ions, which reduces the vacancy concentration in the outer layer of the nanowire, and the electrical conductivity declines.

**3.3. Carbon-Based Material Doping.** Some carbon-based materials with good properties and easy mass production, such as reduced graphene oxide (rGO) [86] and carbon nanotubes (CNT) [77], are doped as the second component to improve the humidity sensitivity of copper oxide characteristic.

Graphene is a unique two-dimensional carbon structure, and it not only has excellent electronic performance [117], but also has excellent stability [118]. In addition, graphene is nontoxic and rich in raw materials, making it a hot and

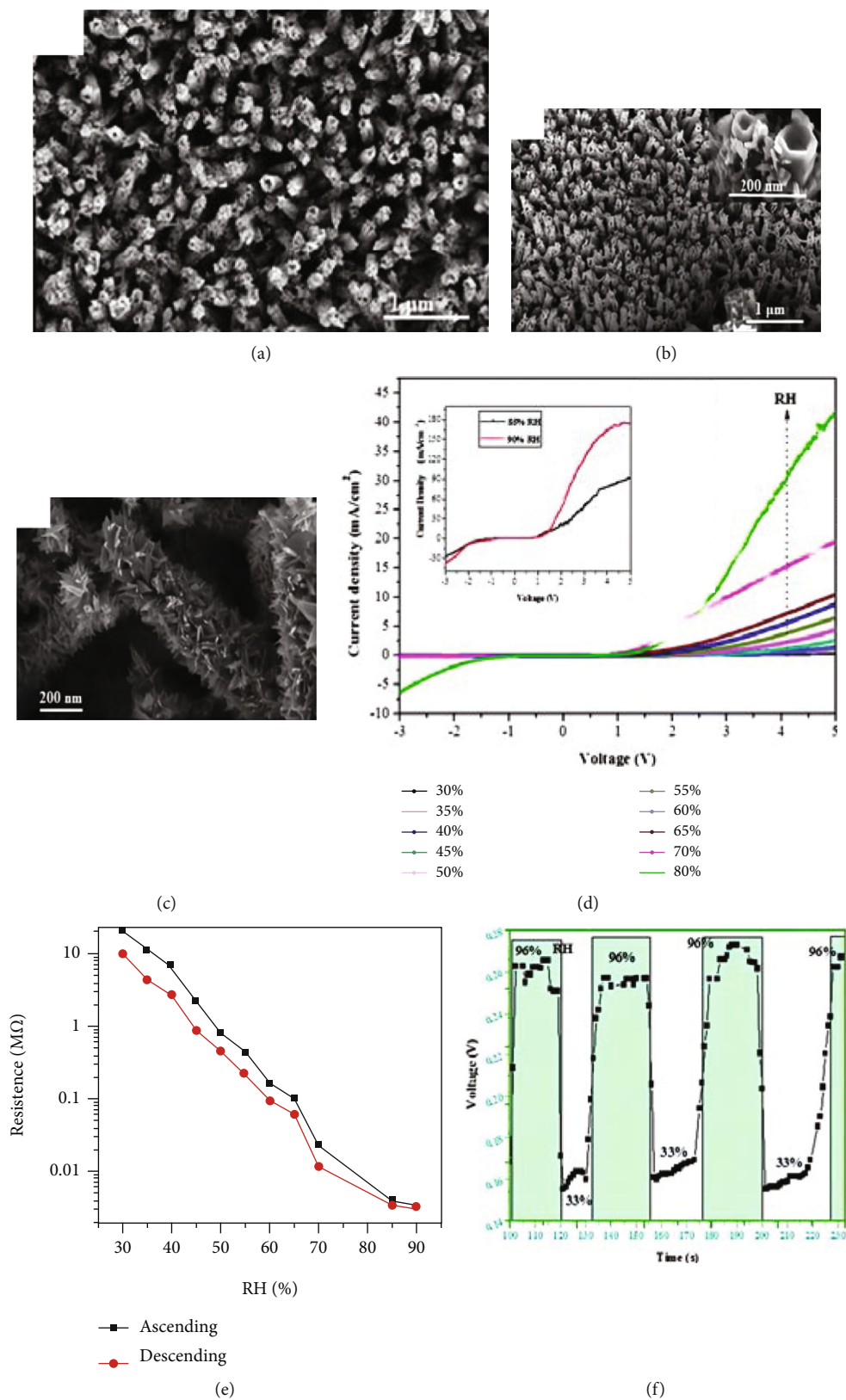
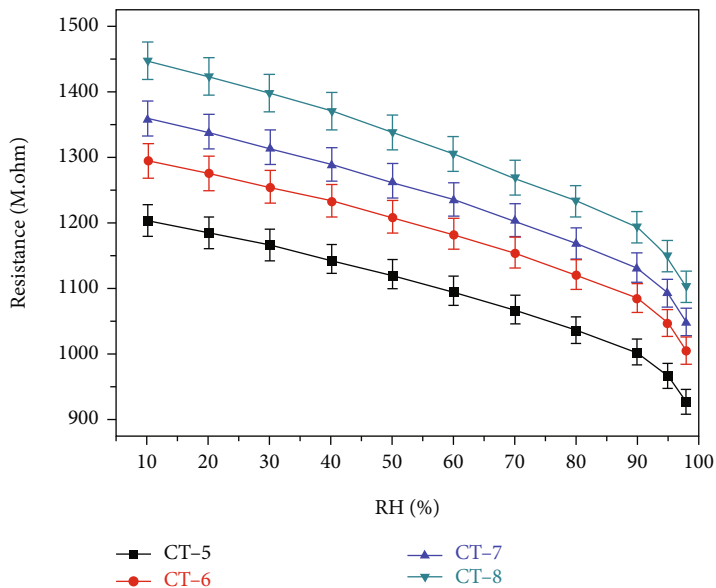
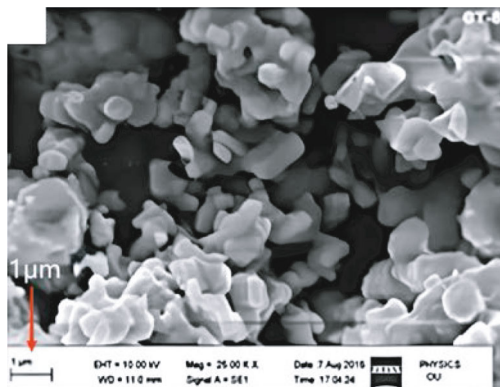
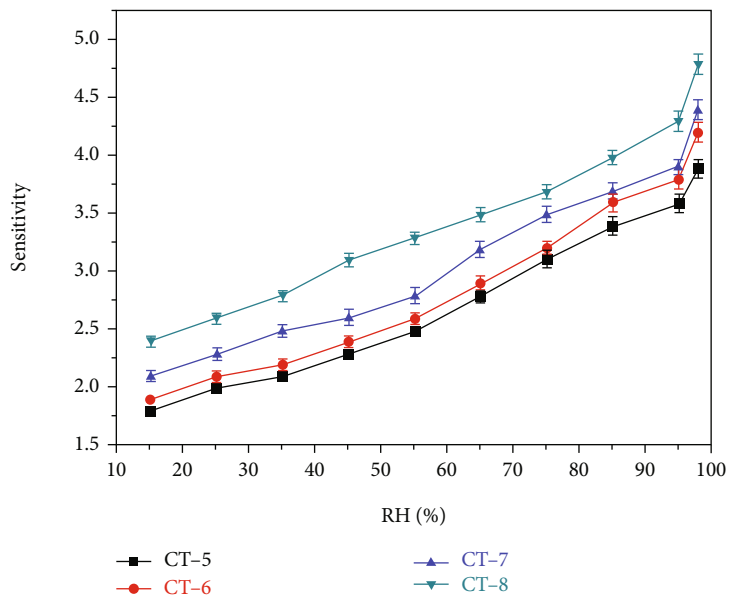


FIGURE 18: (a, b) Top and side views of the highly branched nanocorals. (c) Single CuO/ZnO nanocorals after hydrothermal growth for 4 h. (d) Current density–voltage characteristics of a typical nanocoral sensor at a different relative humidity (RH); the inset shows the J–V characteristics of the sensor at 85 and 90%RH. (e) DC resistance of a typical nanocoral sensor with increasing humidity and recovery cycle (ascending and descending). (f) Dynamic response of the nanocoral sensor when switched between 96% and 32%RH [84].



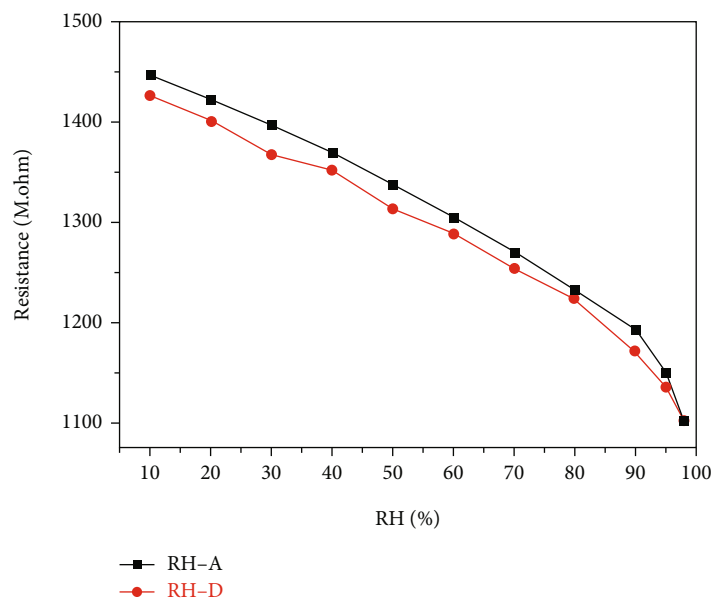
(a)

(b)



(c)

FIGURE 19: Continued.



(d)

FIGURE 19: (a) SEM images of CuO/TiO<sub>2</sub> CT-8 (8.0% by weight of CuO in TiO<sub>2</sub>) nanocomposites. (b) Resistance w.r.t. relative humidity. (c) Sensitivity w.r.t. relative humidity. (d) Hysteresis curve of CT-8 [85].

popular material in many fields [119]. So far, among the several graphene preparation methods known, chemical or thermal reduction of graphene oxide is less costly, which best meets the needs of practical applications [120–123].

Wang and colleagues [86] reported the synthesis of reduced graphene oxide- (rGO-) modified sea urchin-like CuO nanostructures (Figures 20(a) and 20(b)). Experimental observations show that the change of material impedance with humidity conforms to the general law of humidity sensing (Figure 20(d)). Sea urchin-like composite nanomaterials exhibit fast response (2 s) and recovery time (17 s) (Figure 20(c)), which is faster than the copper oxide humidity sensor. In addition, the repeatability of the composite material is also better. In the article, the author introduces the Schottky junction theory to explain the change in the sensor impedance. He believes that the reduced graphene oxide with good conductivity and CuO forms a Schottky junction, which increases the normal impedance of the composite material. As humidity increases, water molecules replace oxygen ions to release electrons, while attracting electrons to the surface. Under low humidity, the transport of charges is achieved by a hopping mechanism, and with the injection of electrons, the hole barrier is lowered, which will reduce the impedance in the Schottky junction. Under high humidity conditions, electrons are transported through the Grotthuss mechanism, and proton migration becomes easier, not only the surface impedance of copper oxide decreases, but also the impedance in the Schottky junction is greatly reduced. Therefore, the composite material exhibits a high response speed to humidity under high humidity conditions.

Ahmad [77] et al. reported that they prepared nanocomposites made of polyethylene oxide (PEO), oxidized multi-walled carbon nanotubes (MWCNT), and copper oxide

(CuO) by electrospinning fiber. Among them, MWCNT and CuO are filled into polyethylene oxide as fillers. The data show that this composite exhibits a good response to humidity.

**3.4. Doping with Other Inorganic Substances.** In the selection of copper oxide doping materials, inorganic compounds such as potassium chloride (KCl) [87] and sulfuric acid (H<sub>2</sub>SO<sub>4</sub>) [124] are occasionally used to improve the moisture-sensitive properties of composites. When water vapor is adsorbed on the outer layer of the sensing element, such inorganic substances can be effectively dissolved into the adsorbed water and dissociated into an ionic state under the action of local charge density and strong electrostatic field. These ions can act as carriers to transfer charge carriers, thereby reducing the impedance of the sensing element [125, 126].

Qi et al. [87] reported the preparation of composite nanoparticles (KCZ/CZNs) using KCl-doped Cu-Zn/CuO-ZnO (CZ/CZNs). Through experiments, it was found between 11 and 95%RH; KCZ/CZNs showed a better linear correlation (Figure 21(a)), indicating that doping of KCl optimizes the impedance-humidity linearity. The response and recovery speed of the material has also been reliably verified (Figure 21(b)), with small hysteresis (Figure 21(c)) and shows good stability in the 60-day experiment.

In another experiment, Rahim et al. [124] recently reported the preparation of polyaniline and copper oxide-(PANI-CuO-) doped sulfuric acid (H<sub>2</sub>SO<sub>4</sub>) composites. The doped composite has higher conductivity, exhibits good response/recovery speed in experiments, and has excellent stability.

In general, doping copper oxide with additives increases the carrier density in the moisture-sensing material, which



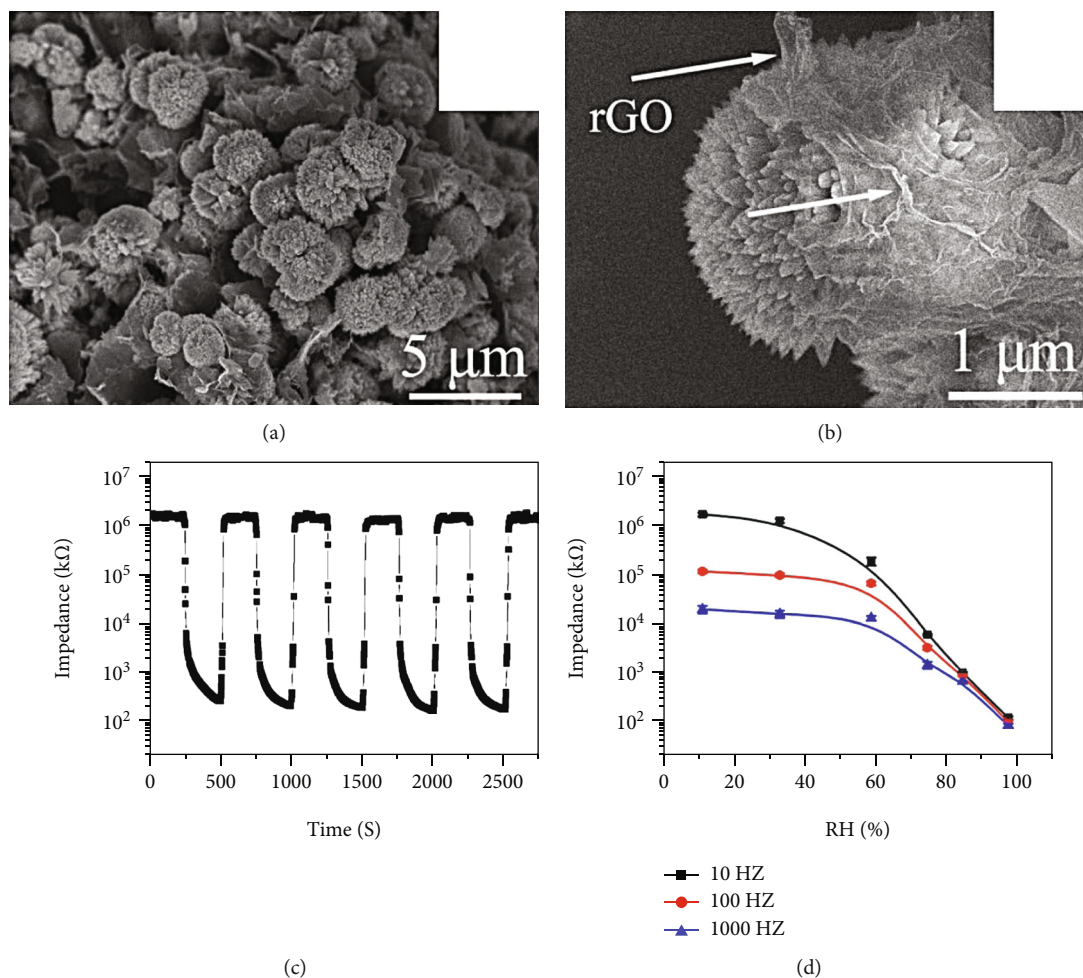


FIGURE 20: (a, b) SEM images of CuO/rGO composites. (c) Response and recovery properties of the sensors fabricated with the CuO/rGO composites. The curves were measured between 11% and 98%RH at 25°C. (d) Impedances of the sensors based on the CuO/rGO composites under different RHs measured at different frequencies [86].

makes the adsorption process of water vapor easier, and also reduces the activation energy of the sensing reaction on the surface of the material. As a result, the sensitivity and response speed of copper oxide-based humidity-sensing materials at room temperature are improved. Compared with the surface modification of pure copper oxide materials, in general, doping additives can effectively improve the humidity-sensing performance of sensors. Among them, the strengthening effect of metal oxides is the most significant.

#### 4. Conclusions

To sum up, we found that doping organic polymers, metal oxides, and carbon-based materials is an efficacious way to achieve breakthroughs in the performance of CuO-based humidity-sensing elements, especially the doping of organic polymers and metal oxides. Through doping, the contact site of the additive with the copper oxide will form a heterojunction, which can effectively improve the sensitivity of copper oxide-based humidity-sensing elements, which points out the direction for the development of higher-performance

copper oxide-based humidity sensors in the future, and even humidity sensors of other semiconductor metal oxides. It must be pointed out that doping organic polymers and metal oxides also increase the difficulty and cost of sensor fabrication. Apart from that, with the enhancement of water adsorption on the sensing element outer layer, the desorption process becomes difficult. Therefore, such a well-balanced connection between the sensitivity and hysteresis of the moisture-sensitive materials becomes crucial.

#### 5. Outlook

There is no doubt that the current humidity sensor is developing rapidly in the direction of miniaturization and high efficiency. However, the complex and changeable working environment has become a major challenge for the current humidity sensor application, which urgently requires us in the performance of sensing elements, including its sensitivity, response speed, hysteresis and stability have been further improved. In recent years, promising results have been achieved in improving the humidity-sensing performance of copper oxide-based humidity

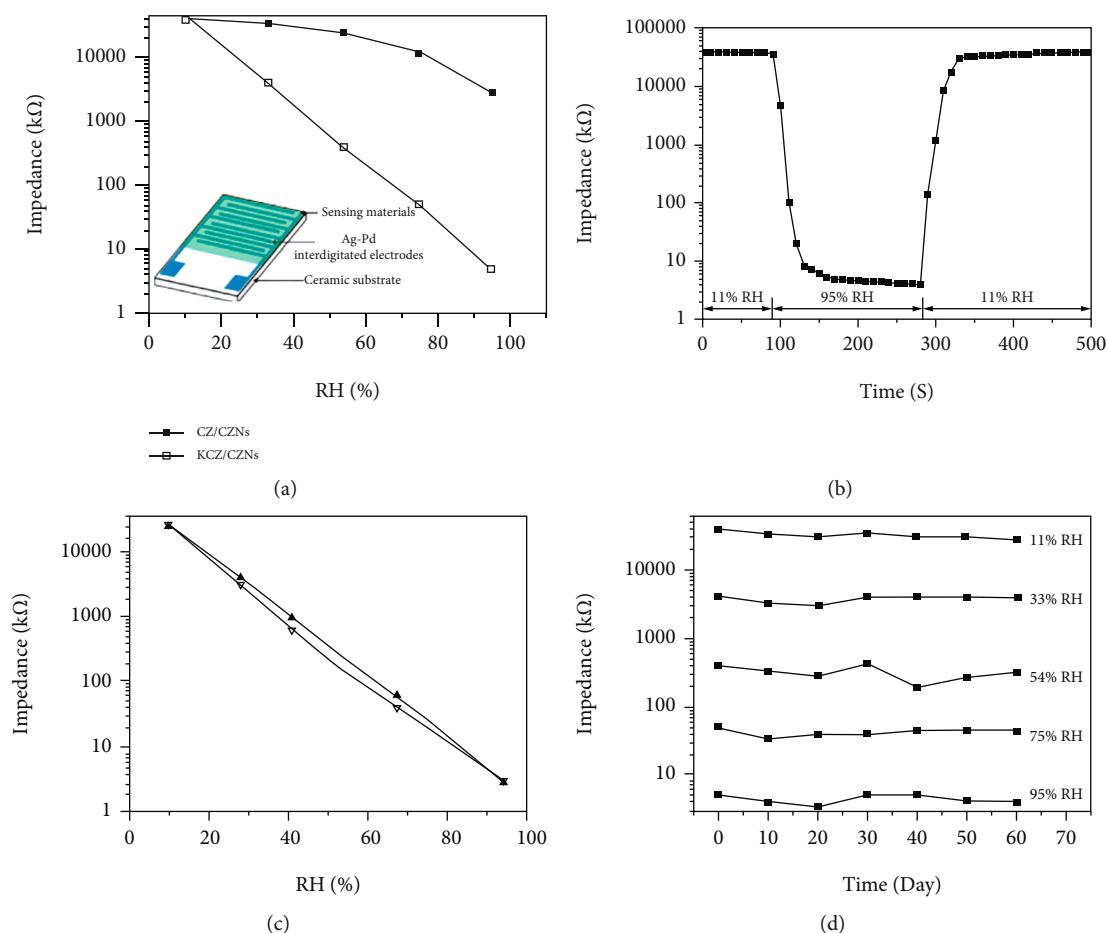


FIGURE 21: (a) The dependence of impedance on RH for pure and KCl-doped Cu–Zn/CuO–ZnO nanoparticles measured at 1 V, 100 Hz, and the inset shows the structure of the humidity sensor applied in our measurement. (b) Response of KCl-doped Cu–Zn/CuO–ZnO nanoparticles measured at 1 V, 100 Hz. (c) Hysteresis of KCl-doped Cu–Zn/CuO–ZnO nanoparticles measured at 1 V, 100 Hz. (d) Long-term stability of KCl-doped Cu–Zn/CuO–ZnO nanoparticles measured at 1 V, 100 Hz [87].

sensors. Fortunately, by modifying the surface of copper oxide and doping with different additives, considerable results have been achieved in improving the humidity sensitivity, especially the sensitivity, of copper oxide-based humidity sensors. Grain size, specific surface area, surface defects, and porosity are the main factors that affect the moisture-sensing properties of pure copper oxide. Smaller nanometer size enables the material to have a larger specific surface area, which increases the material's exposure to the atmosphere. Surface defects facilitate the adsorption of water vapor on the outer layer of the material, and the larger porosity can promote the condensation of water molecules. However, simple surface modification can only improve the humidity-sensitive properties of copper oxide to a certain extent, and it is difficult to make further performance improvements.

Nowadays, how to further ameliorate the humidity sensitivity of copper oxide-based moisture-sensitive materials is still a daunting challenge. Although many achievements have been made in bettering the performance of copper oxide-based moisture-sensitive materials, the performance of some humidity sensors, especially the sensitivity and stability, still cannot meet the needs of harsh environments,

which requires further research. On the surface morphology modification of pure CuO, novel nanostructures can be synthesized by optimizing the structure and improving the process parameters, such as high-density nanofibers with a shell-core three-layer structure, which have better stability. In addition, doping additives are also effective measures to improve the humidity-sensing properties of copper oxide-based humidity-sensing materials. According to our previous detailed report, we found a considerable part of previous research on metal oxide doping has concentrated on n-type semiconducting metal oxides, in order to form a p-n junction with copper oxide, but there are few reports on p-type semiconductor metal oxides, which may be a good research direction and deserve further exploration. In fact, for improving the humidity-sensing properties of humidity-sensing materials, there have been experiments using a synergistic idea of combining multiple optimization strategies to further modify the surface morphology on the basis of doping additives, but there are still few reports. Finally, we sincerely hope that our work can contribute to the improvement of the humidity-sensing performance of copper oxide and even other kinds of semiconductor metal oxide humidity sensors.

## Data Availability

All data can be obtained through contacting Pro. Wen Zeng.

## Conflicts of Interest

The authors declare that they have no conflicts of interest.

## References

- [1] T. A. Blank, L. P. Eksperiandova, and K. N. Belikov, "Recent trends of ceramic humidity sensors development: a review," *Sensors and Actuators B-Chemical*, vol. 228, pp. 416–442, 2016.
- [2] X. F. Li, Z. Zhuang, D. Qi, and C. J. Zhao, "High sensitive and fast response humidity sensor based on polymer composite nanofibers for breath monitoring and non-contact sensing," *Sensors and Actuators B-Chemical*, vol. 330, p. 129239, 2021.
- [3] H. T. Hsueh, T. J. Hsueh, S. J. Chang et al., "CuO nanowire-based humidity sensors prepared on glass substrate," *Sensors and Actuators B-Chemical*, vol. 156, no. 2, pp. 906–911, 2011.
- [4] L. T. Chen, C. Y. Lee, and W. H. Cheng, "MEMS-based humidity sensor with integrated temperature compensation mechanism," *Sensors and Actuators a-Physical*, vol. 147, no. 2, pp. 522–528, 2008.
- [5] T. L. Yeo, T. Sun, and K. T. V. Grattan, "Fibre-optic sensor technologies for humidity and moisture measurement," *Sensors and Actuators a-Physical*, vol. 144, no. 2, pp. 280–295, 2008.
- [6] P. G. Su and C. P. Wang, "Flexible humidity sensor based on TiO<sub>2</sub> nanoparticles-polypyrrole-poly 3-(methacrylamino)-propyl trimethyl ammonium chloride composite materials," *Sensors and Actuators B-Chemical*, vol. 129, no. 2, pp. 538–543, 2008.
- [7] A. Vijayan, M. Fuke, R. Hawaldar, M. Kulkarni, D. Amalnerkar, and R. C. Aiyer, "Optical fibre based humidity sensor using Co-polyaniline clad," *Sensors and Actuators B-Chemical*, vol. 129, no. 1, pp. 106–112, 2008.
- [8] S. B. Wang, C. H. Hsiao, S. J. Chang et al., "CuO nanowire-based humidity sensor," *IEEE Sensors Journal*, vol. 12, no. 6, pp. 1884–1888, 2012.
- [9] A. Dey, "Semiconductor metal oxide gas sensors: a review," *Materials Science and Engineering B-Advanced Functional Solid-State Materials*, vol. 229, pp. 206–217, 2018.
- [10] T. G. Kang, J. K. Park, G. H. Yun, H. H. Choi, H. J. Lee, and J. G. Yook, "A real-time humidity sensor based on a microwave oscillator with conducting polymer PEDOT:PSS film," *Sensors and Actuators B-Chemical*, vol. 282, pp. 145–151, 2019.
- [11] Z. H. Duan, Y. D. Jiang, Q. Huang et al., "Paper and carbon ink enabled low-cost, eco-friendly, flexible, multifunctional pressure and humidity sensors," *Smart Materials and Structures*, vol. 30, no. 5, p. 055012, 2021.
- [12] D. Z. Zhang, H. Y. Chang, P. Li, R. H. Liu, and Q. Z. Xue, "Fabrication and characterization of an ultrasensitive humidity sensor based on metal oxide/graphene hybrid nanocomposite," *Sensors and Actuators B-Chemical*, vol. 225, pp. 233–240, 2016.
- [13] Z. H. Duan, Y. D. Jiang, M. G. Yan et al., "Facile, flexible, cost-saving, and environment-friendly paper-based humidity sensor for multifunctional applications," *ACS applied materials & interfaces*, vol. 11, pp. 21840–21849, 2019.
- [14] Q. N. Zhao, Z. Yuan, Z. H. Duan et al., "An ingenious strategy for improving humidity sensing properties of multi-walled carbon nanotubes via poly-L-lysine modification," *Sensors and Actuators B-Chemical*, vol. 289, pp. 182–185, 2019.
- [15] H. U. Khan, M. Tariq, M. T. Shah et al., "The efficacy of polyvinylpyrrolidone (PVP)/CuO nanocomposite as an appropriate room temperature humidity sensing material: fabrication of highly sensitive capacitive resistive type humidity sensor," *Journal of Materials Science-Materials in Electronics*, vol. 31, no. 10, pp. 7698–7707, 2020.
- [16] A. Rydosz, "The use of copper oxide thin films in gas-sensing applications," *Coatings*, vol. 8, no. 12, p. 425, 2018.
- [17] A. E. Rakhshani, "Preparation, characteristics and photovoltaic properties of cuprous oxide—a review," *Solid-State Electronics*, vol. 29, no. 1, pp. 7–17, 1986.
- [18] B. Balamurugan and B. R. Mehta, "Optical and structural properties of nanocrystalline copper oxide thin films prepared by activated reactive evaporation," *Thin Solid Films*, vol. 396, no. 1–2, pp. 90–96, 2001.
- [19] D. X. Li, X. J. Zeng, Z. P. Li et al., "Progress and perspectives in dielectric energy storage ceramics," *Journal of Advanced Ceramics*, vol. 10, no. 4, pp. 675–703, 2021.
- [20] A. H. MacDonald, "Superconductivity - copper oxides get charged up," *Nature*, vol. 414, no. 6862, pp. 409–410, 2001.
- [21] A. Mirzaei, K. Janghorban, B. Hashemi, and G. Neri, "Metal-core@metal oxide-shell nanomaterials for gas-sensing applications: a review," *Journal of Nanoparticle Research*, vol. 17, no. 9, 2015.
- [22] D. P. Singh, N. R. Neti, A. S. K. Sinha, and O. N. Srivastava, "Growth of different nanostructures of Cu<sub>2</sub>O (nanowires, nanowires, and nanocubes) by simple electrolysis based oxidation of copper," *Journal of Physical Chemistry C*, vol. 111, no. 4, pp. 1638–1645, 2007.
- [23] W. Y. Ching, Y. N. Xu, and K. W. Wong, "Ground-state and optical-properties of Cu<sub>2</sub>O and CuO crystals," *Physical Review B*, vol. 40, no. 11, pp. 7684–7695, 1989.
- [24] T. Ito, H. Yamaguchi, K. Okabe, and T. Masumi, "Single-crystal growth and characterization of Cu<sub>2</sub>O and CuO," *Journal of Materials Science*, vol. 33, pp. 3555–3566, 1998.
- [25] J. Ghijsen, L. H. Tjeng, J. Vanelp et al., "Electronic-structure of Cu<sub>2</sub>O and CuO," *Physical Review B*, vol. 38, no. 16, pp. 11322–11330, 1988.
- [26] A. H. Jayatissa, K. Guo, and A. C. Jayasuriya, "Fabrication of cuprous and cupric oxide thin films by heat treatment," *Applied Surface Science*, vol. 255, no. 23, pp. 9474–9479, 2009.
- [27] A. Ghosh, D. J. Late, L. S. Panchakarla, A. Govindaraj, and C. N. R. Rao, "NO<sub>2</sub> and humidity sensing characteristics of few-layer graphenes," *Journal of Experimental Nanoscience*, vol. 4, no. 4, pp. 313–322, 2009.
- [28] Y. Li, X. Y. Yang, Y. Feng, Z. Y. Yuan, and B. L. Su, "One-dimensional metal oxide nanotubes, nanowires, nanoribbons, and nanorods: synthesis, characterizations, properties and applications," *Critical Reviews in Solid State and Materials Sciences*, vol. 37, no. 1, pp. 1–74, 2012.
- [29] G. Filipic and U. Cvelbar, "Copper oxide nanowires: a review of growth," *Nanotechnology*, vol. 23, no. 19, p. 194001, 2012.
- [30] J. C. Park, J. Kim, H. Kwon, and H. Song, "Gram-scale synthesis of Cu<sub>2</sub>O nanocubes and subsequent oxidation to

- CuO hollow nanostructures for lithium-ion battery anode materials,” *Advanced Materials*, vol. 21, no. 7, pp. 803–807, 2009.
- [31] L. Debbichi, M. C. M. de Lucas, J. F. Pierson, and P. Kruger, “Vibrational properties of CuO and Cu<sub>4</sub>O<sub>3</sub> from first-principles calculations, and Raman and infrared spectroscopy,” *Journal of Physical Chemistry C*, vol. 116, no. 18, pp. 10232–10237, 2012.
- [32] D. P. Singh and N. Ali, “Synthesis of TiO<sub>2</sub> and CuO nanotubes and nanowires,” *Science of Advanced Materials*, vol. 2, no. 3, pp. 295–335, 2010.
- [33] P. Lignier, R. Bellabarba, and R. P. Tooze, “Scalable strategies for the synthesis of well-defined copper metal and oxide nanocrystals,” *Chemical Society Reviews*, vol. 41, no. 5, pp. 1708–1720, 2012.
- [34] K. Malook, H. Khan, M. Ali, and H. Ihsan Ul, “Investigation of room temperature humidity sensing performance of mesoporous CuO particles,” *Materials Science in Semiconductor Processing*, vol. 113, p. 105021, 2020.
- [35] S. Anandam and S. H. Yang, “Emergent methods to synthesize and characterize semiconductor CuO nanoparticles with various morphologies - an overview,” *Journal of Experimental Nanoscience*, vol. 2, no. 1-2, pp. 23–56, 2007.
- [36] D. J. Late, Y. K. Huang, B. Liu et al., “Sensing behavior of atomically thin-layered MoS<sub>2</sub> transistors,” *ACS Nano*, vol. 7, no. 6, pp. 4879–4891, 2013.
- [37] P. M. Faia, C. S. Furtado, and A. J. Ferreira, “Humidity sensing properties of a thick-film titania prepared by a slow spinning process,” *Sensors and Actuators B-Chemical*, vol. 101, no. 1-2, pp. 183–190, 2004.
- [38] B. Aarti, S. Bhadauria, A. Nanoti et al., “[Cu<sub>3</sub>(BTC)<sub>2</sub>]-polyethyleneimine: an efficient MOF composite for effective CO<sub>2</sub> separation,” *Rsc Advances*, vol. 6, no. 95, pp. 93003–93009, 2016.
- [39] X. H. Liu, T. T. Ma, N. Pinna, and J. Zhang, “Two-dimensional nanostructured materials for gas sensing,” *Advanced Functional Materials*, vol. 27, no. 37, 2017.
- [40] J. S. Miao, C. Chen, and J. Y. S. Lin, “Humidity independent hydrogen sulfide sensing response achieved with monolayer film of CuO nanosheets,” *Sensors and Actuators B-Chemical*, vol. 309, p. 127785, 2020.
- [41] S. H. Li, L. L. Xie, M. He et al., “Metal-organic frameworks-derived bamboo-like CuO/In<sub>2</sub>O<sub>3</sub> heterostructure for high-performance H<sub>2</sub>S gas sensor with low operating temperature,” *Sensors and Actuators B-Chemical*, vol. 310, p. 127828, 2020.
- [42] M. M. Sivalingam, J. A. Olmos-Asar, E. Vinoth et al., “Copper oxide nanorod/reduced graphene oxide composites for NH<sub>3</sub> sensing,” *Acs Applied Nano Materials*, vol. 4, no. 12, pp. 12977–12985, 2021.
- [43] Y. C. Huan, K. D. Wu, C. J. Li, H. L. Liao, M. Debligny, and C. Zhang, “Micro-nano structured functional coatings deposited by liquid plasma spraying,” *Journal of Advanced Ceramics*, vol. 9, no. 5, pp. 517–534, 2020.
- [44] Y. Li, Y. L. Lu, K. D. Wu, D. Z. Zhang, M. Debligny, and C. Zhang, “Microwave-assisted hydrothermal synthesis of copper oxide-based gas-sensitive nanostructures,” *Rare Metals*, vol. 40, no. 6, pp. 1477–1493, 2021.
- [45] A. Kapic, A. Tsiro, P. G. Verdini, and S. Carrara, “Humidity sensors for high energy physics applications: a review,” *IEEE Sensors Journal*, vol. 20, no. 18, pp. 10335–10344, 2020.
- [46] D. Barmpakos and G. Kaltsas, “A review on humidity, temperature and strain printed sensors-current trends and future perspectives,” *Sensors*, vol. 21, no. 3, p. 739, 2021.
- [47] Z. Chen and C. Lu, “Humidity sensors: a review of materials and mechanisms,” *Sensor Letters*, vol. 3, no. 4, pp. 274–295, 2005.
- [48] Y. Li, “Temperature and humidity sensors based on luminescent metal-organic frameworks,” *Polyhedron*, vol. 179, p. 114413, 2020.
- [49] L. Yin, H. B. Wang, L. Li, H. Li, D. L. Chen, and R. Zhang, “Microwave-assisted preparation of hierarchical CuO@rGO nanostructures and their enhanced low-temperature H<sub>2</sub>S-sensing performance,” *Applied Surface Science*, vol. 476, pp. 107–114, 2019.
- [50] J. Zhang, X. H. Liu, G. Neri, and N. Pinna, “Nanostructured materials for room-temperature gas sensors,” *Advanced Materials*, vol. 28, no. 5, pp. 795–831, 2016.
- [51] J. J. Yang, C. J. Gao, H. Yang, X. C. Wang, and J. F. Jia, “High selectivity of a CuO modified hollow SnO<sub>2</sub> nanofiber gas sensor to H<sub>2</sub>S at low temperature,” *European Physical Journal-Applied Physics*, vol. 79, no. 3, p. 30101, 2017.
- [52] X. Liu, B. S. Du, Y. Sun et al., “Sensitive room temperature photoluminescence-based sensing of H<sub>2</sub>S with novel CuO-ZnO nanorods,” *ACS Applied Materials & Interfaces*, vol. 8, no. 25, pp. 16379–16385, 2016.
- [53] N. Chen, D. Y. Deng, Y. X. Li et al., “The xylene sensing performance of WO<sub>3</sub> decorated anatase TiO<sub>2</sub> nanoparticles as a sensing material for a gas sensor at a low operating temperature,” *RSC Advances*, vol. 6, no. 55, pp. 49692–49701, 2016.
- [54] P. M. Perillo and D. F. Rodriguez, “Humidity sensor using CuO nanorices thin film,” *Anales De La Asociacion Fisica Argentina*, vol. 32, no. 3, pp. 76–82, 2022.
- [55] C. L. Hsu, J. Y. Tsai, and T. J. Hsueh, “Ethanol gas and humidity sensors of CuO/Cu<sub>2</sub>O composite nanowires based on a Cu through-silicon via approach,” *Sensors and Actuators B-Chemical*, vol. 224, pp. 95–102, 2016.
- [56] S. Hong, J. Shin, Y. Hong et al., “Humidity-sensitive field effect transistor with In<sub>2</sub>O<sub>3</sub> nanoparticles as a sensing layer,” *Journal of Nanoscience and Nanotechnology*, vol. 19, no. 10, pp. 6656–6662, 2019.
- [57] Y. D. Zhu, Y. Y. Wang, G. T. Duan et al., “In situ growth of porous ZnO nanosheet-built network film as high-performance gas sensor,” *Sensors and Actuators B-Chemical*, vol. 221, pp. 350–356, 2015.
- [58] H. Kim, S. Park, Y. Park, D. Choi, B. Yoo, and C. S. Lee, “Fabrication of a semi-transparent flexible humidity sensor using kinetically sprayed cupric oxide film,” *Sensors and Actuators B-Chemical*, vol. 274, pp. 331–337, 2018.
- [59] Z. J. Yu, Y. J. Yang, K. W. Mao, Y. Feng, Q. B. Wen, and R. Riedel, “Single-source-precursor synthesis and phase evolution of SiC-TaC-C ceramic nanocomposites containing core-shell structured TaC@C nanoparticles,” *Journal of Advanced Ceramics*, vol. 9, no. 3, pp. 320–328, 2020.
- [60] D. Liu, H. H. Liu, S. S. Ning, and Y. H. Chu, “Chrysanthemum-like high-entropy diboride nanoflowers: a new class of high-entropy nanomaterials,” *Journal of Advanced Ceramics*, vol. 9, no. 3, pp. 339–348, 2020.
- [61] W. W. Guo, T. M. Liu, H. J. Zhang et al., “Gas-sensing performance enhancement in ZnO nanostructures by hierarchical morphology,” *Sensors and Actuators B-Chemical*, vol. 166-167, pp. 492–499, 2012.

- [62] L. Zhu and W. Zeng, "A novel coral rock-like ZnO and its gas sensing," *Materials Letters*, vol. 209, pp. 244–246, 2017.
- [63] Z. W. Chen, Z. Jiao, D. Y. Pan et al., "Recent advances in manganese oxide nanocrystals: fabrication, characterization, and microstructure," *Chemical Reviews*, vol. 112, no. 7, pp. 3833–3855, 2012.
- [64] R. H. Sui and P. Charpentier, "Synthesis of metal oxide nanostructures by direct sol-gel chemistry in supercritical fluids," *Chemical Reviews*, vol. 112, no. 6, pp. 3057–3082, 2012.
- [65] M. P. Rupashree, K. Soppin, S. Pratibha, and B. Chethan, "Cost effective photocatalytic and humidity sensing performance of green tea mediated copper oxide nanoparticles," *Inorganic Chemistry Communications*, vol. 134, p. 108974, 2021.
- [66] C. Wang, X. Q. Fu, X. Y. Xue, Y. G. Wang, and T. H. Wang, "Surface accumulation conduction controlled sensing characteristic of p-type CuO nanorods induced by oxygen adsorption," *Nanotechnology*, vol. 18, no. 14, p. 145506, 2007.
- [67] D. D. Li, J. Hu, R. Q. Wu, and J. G. Lu, "Conductometric chemical sensor based on individual CuO nanowires," *Nanotechnology*, vol. 21, no. 48, p. 485502, 2010.
- [68] P. Chauhan, S. Annapoorni, and S. K. Trikha, "Humidity-sensing properties of nanocrystalline haematite thin films prepared by sol-gel processing," *Thin Solid Films*, vol. 346, no. 1-2, pp. 266–268, 1999.
- [69] J. W. Xu, K. Yu, J. Wu et al., "Synthesis, field emission and humidity sensing characteristics of honeycomb-like CuO," *Journal of Physics D-Applied Physics*, vol. 42, no. 7, p. 075417, 2009.
- [70] Y. Gu, H. N. Jiang, Z. Ye et al., "Impact of size on humidity sensing property of copper oxide nanoparticles," *Electronic Materials Letters*, vol. 16, no. 1, pp. 61–71, 2020.
- [71] P. Krcmar, I. Kuritka, J. Maslik et al., "Fully inkjet-printed CuO sensor on flexible polymer substrate for alcohol vapours and humidity sensing at room temperature," *Sensors*, vol. 19, no. 14, p. 3068, 2019.
- [72] R. Nitta, H. E. Lin, Y. Kubota, T. Kishi, T. Yano, and N. Matsushita, "CuO nanostructure-based flexible humidity sensors fabricated on PET substrates by spin-spray method," *Applied Surface Science*, vol. 572, p. 151352, 2022.
- [73] B. R. Bade, S. R. Rondiya, Y. V. Hase et al., "Hydrothermally synthesized CuO nanostructures and their application in humidity sensing," in *4th International Conference on Emerging Technologies - Micro to Nano (ETMN)*, Savitribai Phule Pune Univ, Pune, India, 2021.
- [74] T. L. da Silva, F. P. de Araujo, E. C. D. da Silva, M. B. Furtini, and J. A. Osajima, "Degradation of poly(ethylene oxide) films using crystal violet," *Materials Research-Ibero-American Journal of Materials*, vol. 20, pp. 869–872, 2017.
- [75] M. Joulazadeh, A. H. Navarchian, and M. Niroomand, "A comparative study on humidity sensing performances of polyaniline and polypyrrole nanostructures," *Advances in Polymer Technology*, vol. 33, no. S1, 2014.
- [76] A. Hashim and A. Hadi, "Novel pressure sensors made from nanocomposites (biodegradable polymers-metal oxide nanoparticles): fabrication and characterization, Ukrainian," *Journal of Physics*, vol. 63, pp. 754–758, 2018.
- [77] W. Ahmad, B. Jabbar, I. Ahmad et al., "Highly sensitive humidity sensors based on polyethylene oxide/CuO/multi walled carbon nanotubes composite nanofibers," *Materials*, vol. 14, no. 4, p. 1037, 2021.
- [78] A. Hashim, Y. Al-Khafaji, and A. Hadi, "Synthesis and characterization of flexible resistive humidity sensors based on PVA/PEO/CuO nanocomposites," *Transactions on Electrical and Electronic Materials*, vol. 20, no. 6, pp. 530–536, 2019.
- [79] P. Singh and S. K. Shukla, "Structurally optimized cupric oxide/polyaniline nanocomposites for efficient humidity sensing," *Surfaces and Interfaces*, vol. 18, p. 100410, 2020.
- [80] M. T. S. Chani, K. S. Karimov, S. B. Khan, and A. M. Asiri, "Fabrication and investigation of cellulose acetate-copper oxide nano-composite based humidity sensors," *Sensors and Actuators a-Physical*, vol. 246, pp. 58–65, 2016.
- [81] M. T. S. Chani, "Impedimetric sensing of temperature and humidity by using organic-inorganic nanocomposites composed of chitosan and a CuO-Fe<sub>3</sub>O<sub>4</sub> nanopowder," *Microchimica Acta*, vol. 184, no. 7, pp. 2349–2356, 2017.
- [82] C. H. Yuan, Y. T. Xu, Y. M. Deng, N. N. Jiang, N. He, and L. Z. Dai, "CuO based inorganic-organic hybrid nanowires: a new type of highly sensitive humidity sensor," *Nanotechnology*, vol. 21, no. 41, p. 415501, 2010.
- [83] V. B. Rajput and N. K. Pandey, "Moisture sensing studies of CuO-ZnO nanocomposites," *International Journal of Applied Ceramic Technology*, vol. 14, no. 1, pp. 77–83, 2017.
- [84] A. Zainelabdin, G. Amin, S. Zaman et al., "CuO/ZnO nanocorals synthesis via hydrothermal technique: growth mechanism and their application as humidity sensor," *Journal of Materials Chemistry*, vol. 22, no. 23, pp. 11583–11590, 2012.
- [85] C. H. Ashok and K. V. Rao, "Microwave-assisted synthesis of CuO/TiO<sub>2</sub> nanocomposite for humidity sensor application," *Journal of Materials Science-Materials in Electronics*, vol. 27, no. 8, pp. 8816–8825, 2016.
- [86] Z. Y. Wang, Y. Xiao, X. B. Cui et al., "Humidity-sensing properties of Urchinlike CuO nanostructures modified by reduced graphene oxide," *ACS Applied Materials & Interfaces*, vol. 6, no. 6, pp. 3888–3895, 2014.
- [87] Q. Qi, T. Zhang, Y. Zeng, and H. B. Yang, "Humidity sensing properties of KCl-doped Cu-Zn/CuO-ZnO nanoparticles," *Sensors and Actuators B-Chemical*, vol. 137, no. 1, pp. 21–26, 2009.
- [88] M. Das and S. Roy, "Polypyrrole and associated hybrid nanocomposites as chemiresistive gas sensors: a comprehensive review," *Materials Science in Semiconductor Processing*, vol. 121, p. 105332, 2021.
- [89] N. Ruecha, R. Rangkupan, N. Rodthongkum, and O. Chailapakul, "Novel paper-based cholesterol biosensor using graphene/polyvinylpyrrolidone/polyaniline nanocomposite," *Biosensors & Bioelectronics*, vol. 52, pp. 13–19, 2014.
- [90] P. S. More, S. S. Patil, and S. S. Borwar, "Intercalative nanocomposites poly (ethylene oxide)/Cu for LPG sensing application," *Digest Journal of Nanomaterials and Biostructures*, vol. 5, pp. 107–111, 2010.
- [91] M. R. Yang and K. S. Chen, "Humidity sensors using polyvinyl alcohol mixed with electrolytes," *Sensors and Actuators B-Chemical*, vol. 49, no. 3, pp. 240–247, 1998.
- [92] M. T. S. Chani, K. S. Karimov, F. A. Khalid, and S. A. Moiz, "Polyaniline based impedance humidity sensors," *Solid State Sciences*, vol. 18, pp. 78–82, 2013.

- [93] V. Ducere, A. Bernes, and C. Lacabanne, "A capacitive humidity sensor using cross-linked cellulose acetate butyrate," *Sensors and Actuators B-Chemical*, vol. 106, no. 1, pp. 331–334, 2005.
- [94] X. F. Wang, B. Ding, J. Y. Yu, and M. R. Wang, "Highly sensitive humidity sensors based on electro-spinning/netting a polyamide 6 nano-fiber/net modified by polyethyleneimine," *Journal of Materials Chemistry*, vol. 21, no. 40, pp. 16231–16238, 2011.
- [95] Y. L. Wang, Y. Q. Liu, F. Zou, C. Jiang, C. B. Mou, and T. Y. Wang, "Humidity sensor based on a long-period fiber grating coated with polymer composite film," *Sensors*, vol. 19, no. 10, 2019.
- [96] H. Farahani, R. Wagiran, and M. N. Hamidon, "Humidity sensors principle, mechanism, and fabrication technologies: a comprehensive review," *Sensors*, vol. 14, no. 5, pp. 7881–7939, 2014.
- [97] K. Ke, L. Yue, H. Q. Shao, M. B. Yang, W. Yang, and I. Manas-Zloczower, "Boosting electrical and piezoresistive properties of polymer nanocomposites via hybrid carbon fillers: a review," *Carbon*, vol. 173, pp. 1020–1040, 2021.
- [98] T. S. Gaaz, A. B. Sulong, M. N. Akhtar, A. A. H. Kadhum, A. B. Mohamad, and A. A. Al-Amiery, "Properties and applications of polyvinyl alcohol, halloysite nanotubes and their nanocomposites," *Molecules*, vol. 20, no. 12, pp. 22833–22847, 2015.
- [99] M. I. Baker, S. P. Walsh, Z. Schwartz, and B. D. Boyan, "A review of polyvinyl alcohol and its uses in cartilage and orthopedic applications," *Journal of Biomedical Materials Research Part B-Applied Biomaterials*, vol. 100B, no. 5, pp. 1451–1457, 2012.
- [100] F. Zhao, Y. Shi, L. J. Pan, and G. H. Yu, "Multifunctional nanostructured conductive polymer gels: synthesis, properties, and applications," *Accounts of Chemical Research*, vol. 50, no. 7, pp. 1734–1743, 2017.
- [101] P. Singh and S. K. Shukla, "Advances in polyaniline-based nanocomposites," *Journal of Materials Science*, vol. 55, no. 4, pp. 1331–1365, 2020.
- [102] V. G. Bairi, B. A. Warford, S. E. Bourdo, A. S. Biris, and T. Viswanathan, "Synthesis and characterization of tannin-sulfonic acid doped polyaniline-metal oxide nanocomposites," *Journal of Applied Polymer Science*, vol. 124, no. 4, pp. 3320–3328, 2012.
- [103] B. C. Yadav, P. Sharma, and P. K. Khanna, "Morphological and humidity sensing characteristics of SnO<sub>2</sub>-CuO, SnO<sub>2</sub>-Fe<sub>2</sub>O<sub>3</sub> and SnO<sub>2</sub>-Sb<sub>2</sub>O<sub>3</sub> nanocomposites," *Bulletin of Materials Science*, vol. 34, no. 4, pp. 689–698, 2011.
- [104] Y. J. Sun, Z. T. Zhao, K. Suematsu et al., "Rapid and stable detection of carbon monoxide in changing humidity atmospheres using clustered In<sub>2</sub>O<sub>3</sub>/CuO nanospheres," *Acs Sensors*, vol. 5, no. 4, pp. 1040–1049, 2020.
- [105] Y. Ushio, M. Miyayama, and H. Yanagida, "Fabrication of thin-film CuO/ZnO heterojunction and its humidity-sensing properties," *Sensors and Actuators B-Chemical*, vol. 12, no. 2, pp. 135–139, 1993.
- [106] H. L. Tai, Z. H. Duan, Y. Wang, S. Wang, and Y. D. Jiang, "Paper-based sensors for gas, humidity, and strain detections: a review," *Acs Applied Materials & Interfaces*, vol. 12, no. 28, pp. 31037–31053, 2020.
- [107] L. Y. Zhu, H. Li, Z. R. Liu, P. F. Xia, Y. H. Xie, and D. H. Xiong, "Synthesis of the 0D/3D CuO/ZnO heterojunction with enhanced photocatalytic activity," *Journal of Physical Chemistry C*, vol. 122, no. 17, pp. 9531–9539, 2018.
- [108] B. K. Meyer, A. Polity, D. Reppin et al., "Binary copper oxide semiconductors: from materials towards devices," *Physica Status Solidi B-Basic Solid State Physics*, vol. 249, no. 8, pp. 1487–1509, 2012.
- [109] A. Mirzaei, S. S. Kim, and H. W. Kim, "Resistance-based H<sub>2</sub>S gas sensors using metal oxide nanostructures: a review of recent advances," *Journal of Hazardous Materials*, vol. 357, pp. 314–331, 2018.
- [110] R. P. Wijesundera, M. Hidaka, K. Koga, J. Y. Choi, and N. E. Sung, "Structural and electronic properties of electrodeposited heterojunction of CuO/Cu<sub>2</sub>O," *Ceramics-Silikaty*, vol. 54, pp. 19–25, 2010.
- [111] Y. Hu, X. H. Zhou, Q. Han, Q. X. Cao, and Y. X. Huang, "Sensing properties of CuO-ZnO heterojunction gas sensors," *Materials Science and Engineering B-Solid State Materials for Advanced Technology*, vol. 99, no. 1-3, pp. 41–43, 2003.
- [112] A. S. Ismail, M. H. Mamat, M. F. Malek et al., "Heterogeneous SnO<sub>2</sub>/ZnO nanoparticulate film: facile synthesis and humidity sensing capability," *Materials Science in Semiconductor Processing*, vol. 81, pp. 127–138, 2018.
- [113] S. Park, D. Lee, B. Kwak, H. S. Lee, S. Lee, and B. Yoo, "Synthesis of self-bridged ZnO nanowires and their humidity sensing properties," *Sensors and Actuators B-Chemical*, vol. 268, pp. 293–298, 2018.
- [114] F. S. Tsai and S. J. Wang, "Enhanced sensing performance of relative humidity sensors using laterally grown ZnO nanosheets," *Sensors and Actuators B-Chemical*, vol. 193, pp. 280–287, 2014.
- [115] W. D. Lin, C. T. Liao, T. C. Chang, S. H. Chen, and R. J. Wu, "Humidity sensing properties of novel graphene/TiO<sub>2</sub> composites by sol-gel process," *Sensors and Actuators B-Chemical*, vol. 209, pp. 555–561, 2015.
- [116] N. K. Pandey, K. Tiwari, A. Tripathi, A. Roy, A. Rai, and P. Awasthi, "Relative humidity sensing properties of Cu<sub>2</sub>O doped ZnO nanocomposite," in *International Conference on Transport and Optical Properties of Nanomaterials (ICTOPON 2009)*, pp. 463–466, Allahabad, India, 2009.
- [117] T. Fu, J. Zhu, M. Zhuo et al., "Humidity sensors based on graphene/SnO<sub>x</sub>/CF nanocomposites," *Journal of Materials Chemistry C*, vol. 2, no. 24, pp. 4861–4866, 2014.
- [118] Y. J. Huang and C. L. Wan, "Controllable fabrication and multifunctional applications of graphene/ceramic composites," *Journal of Advanced Ceramics*, vol. 9, no. 3, pp. 271–291, 2020.
- [119] C. Lv, C. Hu, J. H. Luo et al., "Recent advances in graphene-based humidity sensors," *Nanomaterials*, vol. 9, no. 3, p. 422, 2019.
- [120] G. L. Li, Y. H. Xia, Y. L. Tian et al., "Review-recent developments on graphene-based electrochemical sensors toward nitrite," *Journal of the Electrochemical Society*, vol. 166, no. 12, pp. B881–B895, 2019.
- [121] S. Karthick, H. S. Lee, S. J. Kwon, R. Natarajan, and V. Saraswathy, "Standardization, calibration, and evaluation of tantalum-nano rGO-SnO<sub>2</sub> composite as a possible candidate material in humidity sensors," *Sensors*, vol. 16, no. 12, p. 2079, 2016.
- [122] M. S. Tsai, P. G. Su, and C. J. Lu, "Fabrication of a highly sensitive flexible humidity sensor based on Pt/polythiophene/

- reduced graphene oxide ternary nanocomposite films using a simple one-pot method,” *Sensors and Actuators B-Chemical*, vol. 324, p. 128728, 2020.
- [123] Z. H. Duan, Q. N. Zhao, C. Z. Li et al., “Enhanced positive humidity sensitive behavior of p-reduced graphene oxide decorated with n-WS<sub>2</sub> nanoparticles,” *Rare Metals*, vol. 40, no. 7, pp. 1762–1767, 2021.
- [124] M. Rahim, A. Shah, S. Bilal, I. Rahim, and R. Ullah, “Highly efficient humidity sensor based on sulfuric acid doped polyaniline-copper oxide composites,” *Iranian Journal of Science and Technology Transaction a-Science*, vol. 45, no. 6, pp. 1981–1991, 2021.
- [125] Q. Qi, Y. L. Feng, T. Zhang, X. J. Zheng, and G. Y. Lu, “Influence of crystallographic structure on the humidity sensing properties of KCl-doped TiO<sub>2</sub> nanofibers,” *Sensors and Actuators B-Chemical*, vol. 139, no. 2, pp. 611–617, 2009.
- [126] Q. Qi, T. Zhang, and L. J. Wang, “Improved and excellent humidity sensitivities based on KCl-doped TiO(2) electrospun nanofibers,” *Applied Physics Letters*, vol. 93, no. 2, p. 023105, 2008.

## Research Article

# A Collaborative Filtering Method for Operation Maintenance Behavior in Power Monitoring Systems

Jinyu Wu , Wenwei Tao, Wenzhe Zhang, Zeming Jiang, and Gang Chen

China Southern Power Grid Co., Ltd., Huangpu District, Guangzhou, Guangdong 510623, China

Correspondence should be addressed to Jinyu Wu; wujinyu0301@163.com

Received 7 March 2022; Revised 12 April 2022; Accepted 18 April 2022; Published 20 May 2022

Academic Editor: Wen Zeng

Copyright © 2022 Jinyu Wu et al. This is an open access article distributed under the Creative Commons Attribution License, which permits unrestricted use, distribution, and reproduction in any medium, provided the original work is properly cited.

As an important part of power infrastructure, a power monitoring system provides real-time data acquisition, state detection, and remote control of power equipment for the power grid and can deal with sudden anomalies in time. The operation and maintenance of the power monitoring system are very important to ensure the stable operation of power grid. The current mainstream remote operation and maintenance mode has internal threats such as misoperation of operation and maintenance personnel or malicious damage caused by attackers stealing operation and maintenance authority. Meanwhile, the existing operation and maintenance audit has the problems of high human resource cost and limited supervision of operation and maintenance personnel. To solve this problem, this paper proposes a collaborative filtering method for operation and maintenance behavior of power monitoring system called CFomb. Exploiting a keyword matching algorithm, CFomb determines the power resources accessed by operation and maintenance users from multiple operation instructions and extracts operation and maintenance behaviors. Referring to the collaborative filtering idea, the feature matrix decomposition scheme is introduced to train the access probability model based on the historical normal behavior of multiple operation and maintenance users, which provides a basis for real-time prediction of the access behavior probability of target operation and maintenance users. The OTSU binarization technique is used to determine the probability threshold of abnormal operation and maintenance behaviors, identify abnormal behaviors through threshold comparison, and send real-time alarms to operation and maintenance audit. The simulation experiment results show that the method in this paper can effectively identify the abnormal behavior of operation and maintenance users, reduce the overhead of manual audit, and help improve the power monitoring system's ability to respond to internal threats of operation and maintenance.

## 1. Introduction

As an important part of power infrastructure, the power monitoring system provides reliability support for the stable operation of power grid. In order to ensure the normal operation of the power operation system, it is necessary to carry out routine operation and maintenance for the system function, related equipment, hardware and software, and other internal resources, to deal with emergencies and abnormalities in time. The power monitoring system is distributed and deployed in different power stations, power distribution stations, and dispatching centers at all levels. Therefore, in case of employing on-site operation and maintenance, on the one hand, it will be difficult to deal with the emergencies anywhere in the system; on the other hand, it will be hard to

control the operation and maintenance of power monitoring system. As a result, the operation and maintenance platform of power monitoring system needs to realize both remote and centralized operation and maintenance management.

The current typical operation and maintenance platform of the power monitoring system is generally built based on bastion host [1–3], whose technology can manage operation and maintenance accounts and assets uniformly and set the buffer to allow the assets of the power monitoring system to realize remote operation and maintenance without direct exposure to the outside. The administrator of bastion can configure the access strategy of operation and maintenance users. When logging in to the power monitoring system with fortress machine technology to implement operation and maintenance, the operation and maintenance personnel can record



the operation and maintenance process of operation and maintenance personnel in real time, and the auditors can audit the operation and maintenance process of operation and maintenance personnel according to the audit rules, so as to achieve the supervision of operation and maintenance personnel. In addition, the bastion can isolate the internal resources of the power monitoring system from external exposure, centralize the identity of operation and maintenance users, and achieve centralized access control of operation and maintenance work. However, the remote operation and maintenance mode of the bastion host power monitoring system neglects the protection against internal threats, resulting in the high human resource cost of security audit.

To solve this problem, this paper proposes a collaborative filtering method (CFomb) for the operation and maintenance behaviors of power monitoring system. Exploiting keyword matching algorithm, CFomb determines the power resources accessed by operation and maintenance users from multiple operation instructions and extracts operation and maintenance behaviors; by reference to the collaborative filtering idea of the recommended system, the feature matrix decomposition scheme is introduced to train the access probability model based on the historical normal behavior of multiple operation and maintenance users, which provides a basis for real-time prediction about the access behavior probability of operation and maintenance users; OTSU binarization technique is used to determine the probability threshold of abnormal operation and maintenance behaviors, identify abnormal behaviors through threshold comparison, and send real-time alarms to operation and maintenance audit. Finally, the behavior that multiple operation and maintenance users of the power monitoring system access multiple power resources was simulated, and an experiment was carried out. The experimental results show that the methods proposed in this paper can help build a behavior probability prediction model for users and resources based on user behavior patterns and determine whether random behavior of users is abnormal in accordance with the thresholds generated automatically.

The overall structure of the paper is shown in Figure 1.

## 2. Related Work

Various information security issues are introduced in the informatization development of the power industry. Among others, the internal threats of information system, as a hot issue in the research on current general information system security, have drawn increasing attention [4–7]. In terms of internal threat recognition methods, the traditional way was to audit the historical access logs of operation and maintenance users and detect the internal attacks that occurred by afterward examination. For example, Liu et al. [8] proposed the Log2vec method to detect the abnormal behavior of system. Based on the log information, this method extracts multiple factors, such as the sequential relationship between user behavior sequences within a day, the relationship between behavior sequences on different dates, and the behavior topology relationship of resource access by users, to carry out behavior modeling; the logging behavior is trans-

formed into a vector using graph neural networks; the behavior vector is separated from abnormal behavior with the clustering algorithm, and then the insiders responsible for the abnormal behavior are traced. Gu and Guo [9] proposed an internal threat detection method based on role abnormal behavior mining, which mines the role abnormal behaviors using the sequence pattern and carries out pattern matching with KMP algorithm to recognize abnormal users. However, these methods require studying the historical data offline, failing to analyze new data in real time and to locate the malicious behaviors in real time. Therefore, it is difficult to avoid the losses caused by internal threats.

Rashid et al. [10] simulated the weekly normal behaviors of each user using the hidden Markov model and then applied them to the detection of the significant deviation between abnormal behaviors and normal behaviors. Happa [11] used the EM algorithm to train a GMM for the behaviors of each user in the first month, to simulate the normal behaviors of the user. The trained GMM is applied to computing the likelihood of input observations to indicate the possibility of the input. If the likelihood is smaller than the threshold, the observation will be detected as abnormal.

However, the above methods merely consider modeling the normal behaviors of users using the sequential features of a single user's behaviors, failing to consider the correlation between user behaviors. As recommendation systems analyze and model user behavior data, they predict and recommend products that users do not use but are likely to be interested in. Collaborative filtering algorithm is a key algorithm in recommendation systems. Collaborative filtering can use user behaviors similar to those of the target user to infer the target user's preference for a specific product and then make recommendations accordingly based on this preference. Therefore, by reference to the collaborative filtering idea, in the abnormal behavior detection of internal threats on the operation and maintenance platform of the power monitoring system, this paper not only considers the historical longitudinal features of operation and maintenance users but also integrates the transverse impacts among similar operation and maintenance users.

Compared with the existing work, the main innovations of this paper are as follows.

- (1) The introduction of the feature matrix decomposition method to train the access probability model, which is simple to compute, easy to obtain training data, and does not require complex processing, can be applied to more power monitoring system O&M scenarios
- (2) Combining collaborative filtering idea and OTSU binarization method to achieve probability prediction of real-time access behavior of O&M users and adaptive selection of probability threshold of abnormal O&M behavior, supporting more efficient and safe development of power monitoring system O&M
- (3) Simulation experiments are carried out based on the OTSU access behavior dataset for power monitoring system multiple O&M users to access multiple power

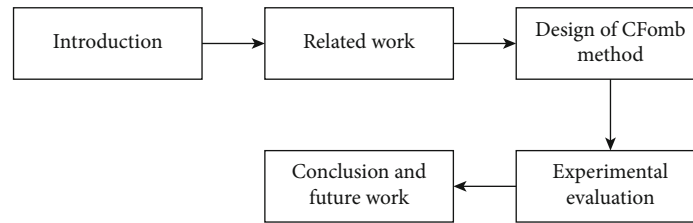


FIGURE 1: The overall structure of the paper.

resources behavior, and the results show that the proposed method can effectively identify the abnormal behavior of power monitoring system O&M users and can reduce the cost of human O&M audit

### 3. Design of the CFomb Method

**3.1. Overall Design of the CFomb Method.** The overall architecture of the CFomb method is shown in Figure 2. The method mainly consists of three modules, i.e., operation and maintenance behavior extraction, behavior analysis, and behavior alarm. The operation and maintenance behavior extraction module and the behavior alarm module are deployed in the bastion host on the operation and maintenance platform of the power monitoring system, while the computation nodes of the behavior analysis module can be deployed separately. In the CFomb method, the operation and maintenance behavior extraction module provides real-time behavior input for the behavior analysis module, which recognizes abnormal behavior and outputs abnormal behavior alarm information to the behavior alarm module, while the behavior alarm module displays the alarm information to the auditor and feeds back to the behavior analysis module.

**3.2. Extraction of Operation and Maintenance Behaviors.** As the processing object of the CFomb method, the description of an operation and maintenance behavior requires defining the specific operation and maintenance users and objects.

The operation and maintenance user can be a user with the operation and maintenance permission for the server of the power operating system. The user may carry out operation and maintenance based on the server of the power monitoring system within the preset time in accordance with the requirements of operation and maintenance [12]. When an operation and maintenance user carries out the operation and maintenance, the user needs to determine the target power resources to be accessed firstly and then input the corresponding operating instruction into the operation and maintenance platform of power monitoring system based on the determined target power resources. The operation and maintenance platform will obtain the corresponding operating instruction and determine the target power resources in accordance with the operating instruction, so that the target operation and maintenance user can smoothly carry out the corresponding operation and maintenance.

The operation and maintenance users and the power resources shall have unique identification information on

the operation and maintenance platform of the power monitoring system. In CFomb method, the operation and maintenance behavior extraction module inserts the instruction extraction points into the bastion host to extract the real-time operation and maintenance instructions of operation and maintenance users. Through comparing and analyzing the instructions and keyword database of operation and maintenance objects, the module determines the operation and maintenance users and the resource objects accessed and outputs the operation and maintenance behaviors. For each instruction input by users, the algorithm indicated in Algorithm 1 is called to extract the user behavior in the instruction. As the input of the behavior analysis module, the behavior information output is used to recognize the current abnormal behavior of a user.

**3.3. Analysis of Operation and Maintenance Behaviors.** As the core of CFomb method, the behavior analysis module needs to collect the historical access records of users to construct the behavior matrix and obtains the user model and resource model via behavior matrix decomposition. When the behavior analysis module obtains the real-time behavior information input of the behavior extraction module, it can extract the corresponding features from the user model and resource model, predict the probability of occurrence of such behavior, and determine whether the behavior is normal or abnormal based on the probability threshold classification. In addition, the behavior buffer will continuously record user behavior and take it as the training set adjustment information of follow-up iterative training to update the learning model.

**3.3.1. Construct the Training Set.** Stemming from the statistics on historical behaviors of operation and maintenance users, the training set employs the frequency of resource access by users to describe the probability of resource access by users. Since the scope of historical access behavior and resource access by users is limited, the training set merely contains the information of resource access frequency of a few users.

The training set is represented in the form of frequency matrix  $P_{M \times N}$  of  $M$  rows and  $N$  columns, among which the number of matrix row  $M$  represents the total quantity of users on the operation and maintenance platform, while the number of matrix column  $N$  represents the total quantity of resources on the operation and maintenance platform, and the behavior space (i.e., the scale of frequency matrix) is  $M \times N$ . Since the training set is a sparse matrix, it can be stored in the form of triple  $(i, j, p_{i,j})$ , among which  $p_{i,j}$

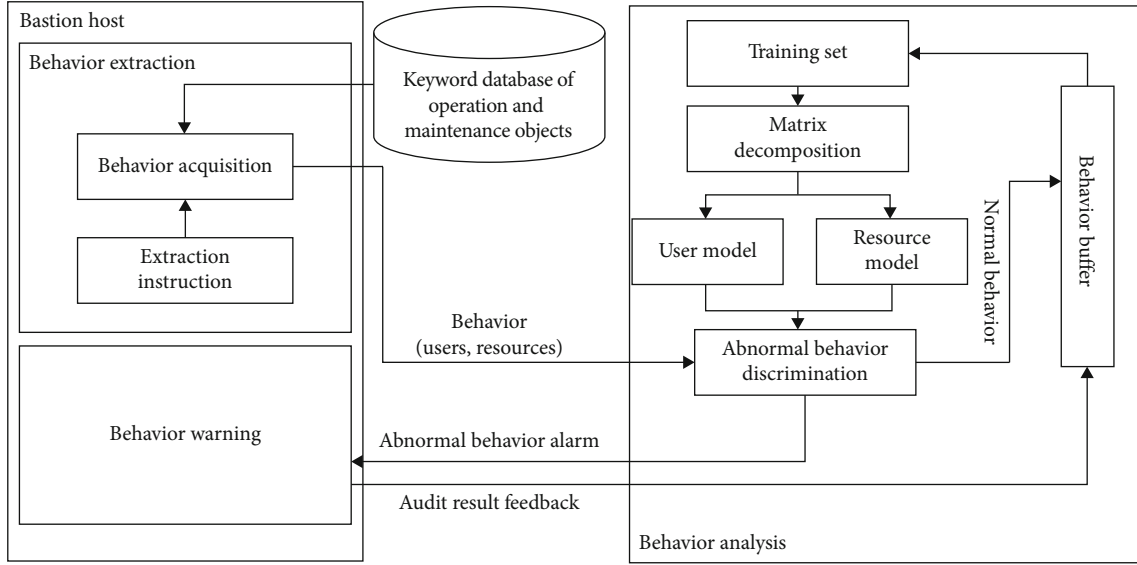


FIGURE 2: Architecture of CFomb.

**Input:** a real-time operating instruction character string  $I$  of a user, the current user id  $user\_id$ , and resource keyword database  $source\_db$

**Output:** behavior information  $\{user\_id, source\_id\}$  containing user id and resource id

```

1 Divide instruction  $I$  into multiple words
2 for word in each words. /*Traverse the words in the instruction*/
3   use the word to query the keyword database to obtain the resource id  $source\_id$ 
4   if (successful query)
5     output the behavior information  $\{user\_id, source\_id\}$ 
6   end if
7 end for

```

ALGORITHM 1: Workflow of operation and maintenance behavior extraction algorithm.

represents the element ( $1 \leq i \leq M, 1 \leq j \leq N$ ) in the  $i$ th row and the  $j$ th column.

Based on the statistics on the historical behaviors of operation and maintenance users, the construction of the training set is updated continuously with the new access behavior of operation and maintenance users. If the record on user behaviors is unavailable in the initial construction stage of operation and maintenance platform, it is necessary to collect the user behaviors for a period of time before enabling the CFomb method for the follow-up work.

**3.3.2. Matrix Decomposition.** With the aim of predicting the probability of random behavior in behavior space, the CFomb method introduces the collaborative filtering algorithm based on matrix decomposition and carries out matrix decomposition of the training set to construct the feature model of users and resources [13]. The user model represents the matrix  $X_{M \times K}$  of  $M$  rows and  $K$  columns, the resource model represents the matrix  $Y_{N \times K}$  of  $N$  rows and  $K$  columns, among which  $K$  represents the implied feature dimension, whose value is much smaller than any one of  $M$  and  $N$ .

Matrices  $X_{M \times K}$  and  $Y_{N \times K}$  represent the feature distribution of  $M$  users and  $N$  resources in  $K$  dimensional feature

space. The  $i$ th column in matrix  $X$  and the  $j$ th column in matrix  $Y$  represent the  $K$  dimensional eigenvector of user  $i$  and resource  $j$ , respectively. The similarity of these  $M + N$  eigenvectors can be obtained through inner product computation, which includes similarity between users and resources, similarity among users, and similarity among resources. Among these, the similarity between users and resources represents the prediction of the probability of resource access by users.

Therefore, the user model and resource model obtained by the matrix decomposition algorithm shall guarantee that the product of matrix  $X$  and matrix  $Y$  approaches, as much as possible, the frequency matrix  $P$  indicated in the training set, i.e., frequency matrix  $P$  can be represented by  $X$  and  $Y$  in the form of the following formula.

$$P_{M \times N} \approx X_{M \times K}(Y_{N \times K})^T. \quad (1)$$

For the user  $i$  and the resource  $j$  designated randomly in the behavior space, the  $i$ th column and the  $j$ th column can be taken, respectively, in the user model matrix  $X$  and the resource model matrix  $Y$  to obtain  $K$  dimensional column vectors  $X_i$  and  $Y_j$ . Therefore, the predictive value of the

```

Input: Behavior frequency matrix  $P_{M \times N}$  of resource access by users
Output: User matrix  $X_{M \times X}$  and resource matrix  $Y_{N \times k}$ 
1 Construct the loss function  $Loss$ 
2 Randomly initialize user model  $X$  and resource model  $Y$ 
3 while ( $Loss$  does not converge)
4     for  $i$  from 1 to  $M$ 
5         for  $j$  from 1 to  $N$ 
6             if ( $p_{i,j}$  is recorded in the training set)
7                  $e = X_i Y_j - p_{i,j}$  /* Predictive value of model- Corresponding value of training set */
8             end if
9  $x_{i,j} = x_{i,j-2} * \alpha + (e * y_{i,j} + \lambda * x_{i,j}) / \alpha$  /*  $\alpha$  represents the learning rate */
10  $y_{i,j} = y_{i,j-2} * \alpha + (e * x_{i,j} + \lambda * y_{i,j}) / \alpha$  /*  $\alpha$  represents the regular terms */
11 end for
12 end for
13 Output  $X_i$  and  $Y_j$  as user matrix  $X_{M \times k}$  and resource matrix  $Y_{N \times k}$ 

```

ALGORITHM 2: Workflow of computing user and resource models by alternating least squares method.

```

Input: Set  $S$  of all probability prediction values of behavior space
Output: Abnormal behavior discrimination threshold  $T$ 
1 Obtain the behavior probability set  $S$ 
2  $maxScore = 0$ 
3 for  $t = \min(S)$  to  $\max(S)$  by  $0.0001$  /*  $t$  represents the candidate threshold, traverse all the probabilities between  $\min(S)$  and  $\max(S)$ , with an increased step size of  $0.001$  ( $0.1\%$ ) */
4  $S_1 = \{s | s \in S, s \leq t\}$   $S_2 = \{s | s \in S, s > t\}$ 
5 Obtain the mean values of  $m_1, m_2$  in  $S_1$  and  $S_2$ 
6 Obtain ratios  $p_1$  and  $p_2$  of  $S_1$  and  $S_2$  in  $S$ 
7 Obtain the between-cluster variance  $s^2$  of  $S_1$  and  $S_2$  with Formula (6)
8 if ( $maxScore < s^2$ )
9      $T = t$ 
10 end if
11 end for
12 Output the final threshold  $T$ 

```

ALGORITHM 3: The workflow of calculating abnormal behavior discrimination threshold  $T$  based on OTSU.

element in the  $i$ th row and the  $j$ th column of matrix  $P$  can be obtained by Formula (2). In the formula,  $\hat{p}_{i,j}$  represents the estimated value of the element  $p_{i,j}$  in the  $i$ th row and the  $j$ th column of the frequency matrix  $P$  by user model  $X$  and resource model  $Y$ .

$$p_{i,j} \approx \hat{p}_{i,j} = X_i Y_j^T. \quad (2)$$

For the decomposition of matrices, the CFomb method employs ALS (alternating least squares).

First, the loss function is constructed as formula (3), among which  $P_0$  represents the set of numbers of rows and columns corresponding to the recorded users and resources.  $\lambda$  represents the coefficient of regular terms for preventing overfitting.

$$Loss = \sum_{(i,j) \in P_0} (p_{i,j} - X_i Y_j^T)^2 + \lambda \sum_{i=1}^M \|X_i\|^2 + \lambda \sum_{j=1}^N \|Y_j\|^2. \quad (3)$$

Formulas (4) and (5) represent the gradient descent iteration formulas for this loss function.

$$X_i = X_i - 2\alpha \left[ \sum_{j=1}^N (X_i Y_j^T - p_{i,j}) Y_j + \lambda X_i \right], \quad (4)$$

$$Y_j = Y_j - 2\alpha \left[ \sum_{i=1}^M (X_i Y_j^T - p_{i,j}) X_i + \lambda Y_j \right]. \quad (5)$$

The algorithm that computes user model  $X$  and resource model  $Y$  by ALS is shown in Algorithm 2.

**3.3.3. Abnormal Behavior Recognition.** The abnormal behavior recognition by the CFomb method is divided into two steps: the first step is to quickly predict the probability of real-time behavior, and the second step is to discriminate whether the current behavior is abnormal based on the abnormal threshold.

The user model  $X$  and resource model  $Y$  can be obtained by the matrix decomposition method provided in 3.3.2. For

**Input:** User model  $X$ , resource model  $Y$ , abnormal behavior discrimination threshold  $T$ , and the extracted user behavior information  $i$  and  $j$  (User  $i$  accesses Resource  $j$ )

**Output:** 1 / 0; 1 indicates the normal behavior, and 0 the abnormal behavior

- 1 Extract vector  $X_i$  in the  $i$ th column of user model and vector  $Y_j$  in the  $j$ th column of resource model
- 2  $p = X_i(Y_j)T$  / \*  $p$  represents the prediction probability, which is obtained by computing the inner product of vectors  $X_i$  and  $Y_j$  \* /
- 3 if ( $p > T$ )
- 4 Output 1
- 5 else
- 6 Output 0
- 7 end if

ALGORITHM 4: The workflow of abnormal behavior recognition algorithm.

**Input:** The extracted user behavior information  $i$  and  $j$  (user  $i$  accesses resource  $j$ ), the audit  $tag$ , and the BUFFER\_SIZE

**Output:** update the training set

- 1 Obtain the behavior information  $i, j$
- 2 Set the default integration ratio as  $alpha=1$
- 3 if ( $tag=1$ ) / \* audit feedback enters the buffer \* /
- 4  $alpha = BUFFER\_SIZE$
- 5 end if
- 6  $action[i][j] += alpha$  / \* statistics on behaviors in the buffer \* /
- 7  $user[i] += alpha$  / \* update the amount of user behavior \* /
- 8 if ( $user[i] > BUFFER\_SIZE$ )
- 9 Employ Formula (7) to update the information corresponding to user  $i$  in the training set
- 10  $user(i)=0$
- 11  $action[i][j]=0$
- 12 end if

ALGORITHM 5: The workflow of O&amp;M behavior buffer.

the behavior that random user  $i$  accesses random resource  $j$ , the eigenvector of user  $i$  can be obtained by extracting the  $i$ th column of  $X$ , and that of resource  $j$  can be obtained by extracting the  $j$ th column of  $Y$ . The inner product of these two eigenvectors represents the probability prediction of such behavior.

The recognition of abnormal behavior can be completed by determining the abnormal behavior discrimination threshold after the behavior prediction probability is obtained. The CFomb method has introduced the OTSU algorithm to adaptively determine the abnormal behavior discrimination threshold.

First, the statistics on the prediction probability of all behaviors can be made in behavior space via user model and resource model. The prediction probability of abnormal behavior will be concentrated in the lower probability interval, while that of normal behavior will be concentrated in the higher probability interval. If an existing probability threshold  $T$  divides the behavior into two maximum sets of between-cluster variance  $\sigma^2$  in the behavior space, the threshold  $T$  can be taken as the probability threshold for abnormal behavior discrimination.

Formula (6) provides the computation of between-cluster variance in operation and maintenance behavior in the CFomb method.

$$\sigma^2 = p_1 \cdot p_2 \cdot (m_1 - m_2)^2. \quad (6)$$

In the formula,  $p_1$  represents the proportion of behaviors with a prediction probability not more than the threshold  $T$  in the behavior space,  $p_2$  represents the proportion of behaviors with a prediction probability above the threshold  $T$  in the behavior space,  $m_1$  represents the mean probability of behaviors with a prediction probability not more than threshold  $T$ , and  $m_2$  represents the mean probability of behaviors with a prediction probability above the threshold  $T$ .

The specific algorithm steps for computing threshold  $T$  based on OTSU algorithm are shown in Algorithm 3.

Furthermore, the real-time operation and maintenance behavior can be realized in accordance with operation and maintenance user model  $X$ , power resource model  $Y$ , and abnormal behavior discrimination threshold  $T$ , with the specific algorithm shown in Algorithm 4.

**3.3.4. Construction of Behavior Buffer.** The CFomb method will continuously collect the behavior information of users during operation. In order to implement the dynamic adjustments to the user model and resource model, the CFomb method designs a behavior buffer in the behavior analysis module for receiving the behavior information of operation and maintenance users and feeding back new operation and maintenance user behaviors to the training model, thereby adjusting the user model and resource model.

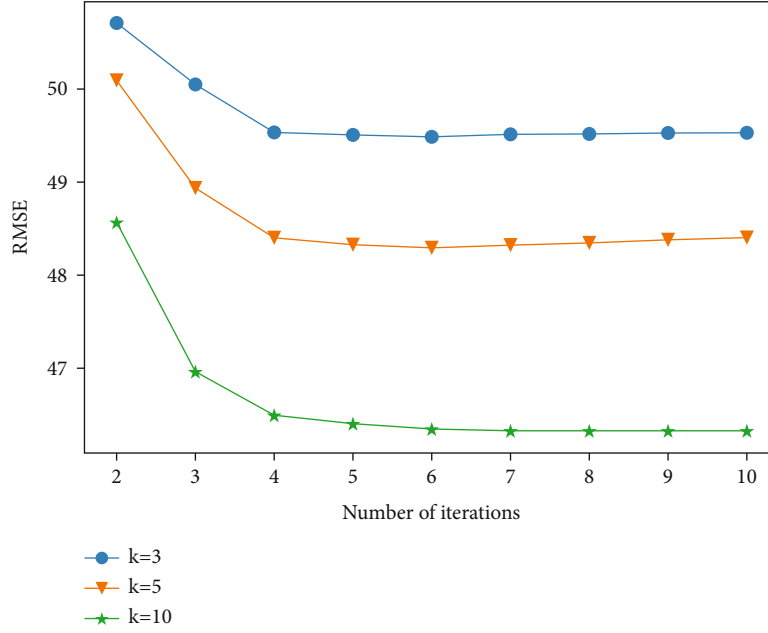


FIGURE 3: RMSE curve of the model with different values of  $k$ .

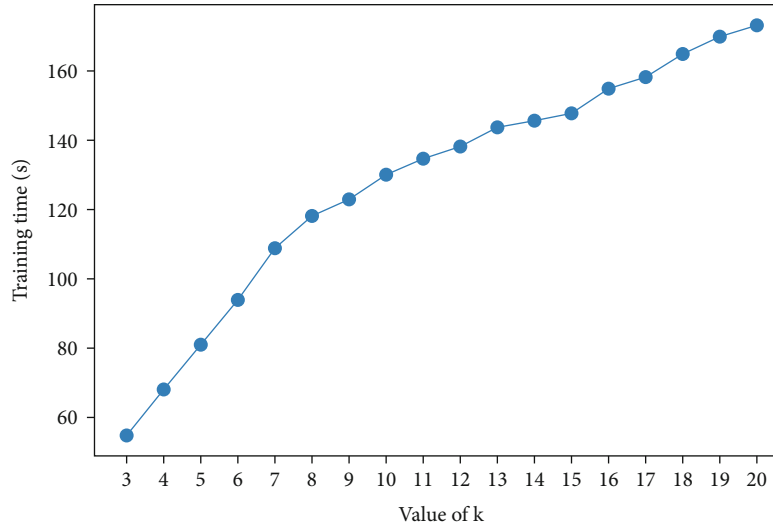


FIGURE 4: Training time curve under different values of  $k$ .

The behavior information to be written in the behavior buffer will be stored in the form of triple  $(i, j, \text{action}_{i,j})$ , indicating that the number of times stored in the buffer for accessing resource  $j$  by an operation and maintenance user  $i$  is  $\text{action}_{i,j}$ . Moreover, the behavior buffer maintains a counting sequence  $\text{times}_i$ , in which  $1 \leq i \leq M$ , indicating that  $\text{times}_i$  behavior information of the  $i$ th operation and maintenance user is recorded in the buffer. Formula (7) represents the computational formula in which the access behavior of an operation and maintenance user  $i$  to resource  $j$  in the behavior buffer is integrated into the training set.

$$p_{i,j} = (1 - w)p_{i,j} + w \cdot \frac{\text{buffer}_{i,j}}{\text{times}_i}, \quad (7)$$

where  $w$  ( $0 < w < 1$ ) represents the writing weight of user buffer. The higher the writing weight, the higher the change rate of training set. The specific values will not be specified in this paper. Algorithm 5 provides the workflow of operation and maintenance behavior buffer.

## 4. Experimental Evaluation

**4.1. Data Preparation.** In order to verify the recognition efficiency of the CFomb method on the users' abnormal behaviors of access to the resources on the operation and maintenance platform of power monitoring system, the behavior of resource access by operation and maintenance users is simulated under the background of operation and maintenance [14–15], and the dataset of resource access by

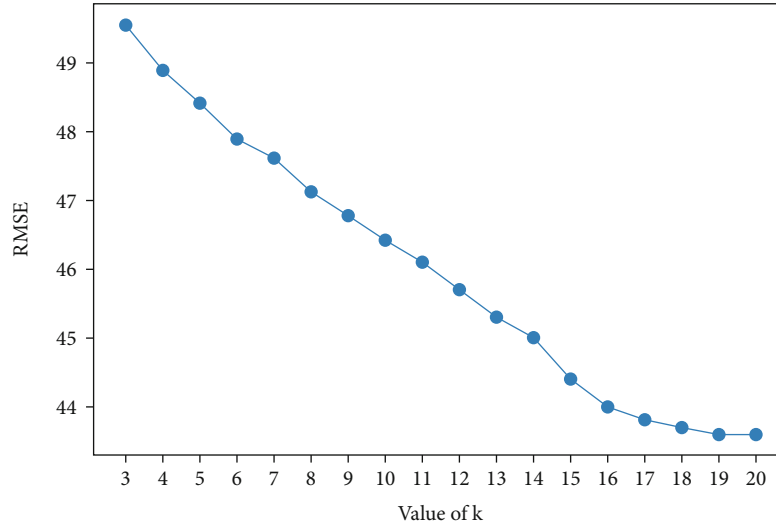
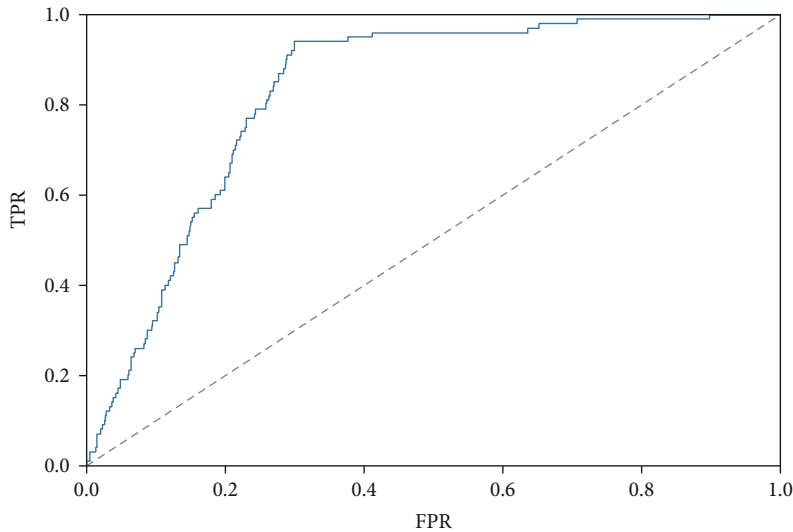
FIGURE 5: RMSE under different values of  $k$ .

FIGURE 6: ROC curve of the test case.

TABLE 1: Abnormal behavior identification confusion matrix.

	Recognition		Total
	Abnormal	Normal	
Actual			
Abnormal	94 (TP)	6 (FN)	100
Normal	1,513 (FP)	3,487 (TN)	5,000
Total	1,607	3,493	5,100

operation and maintenance users is generated, based on which the recognition capability of the CFomb method on abnormal behaviors is verified. The dataset was obtained from the internal network data of China Southern Power Grid Corporation, which contains a total of 107,670 records on 1,170 users' access to 7,455 resources. Moreover, 1,759 access records are generated by simulating the malicious user access behavior to verify the recognition effect.

**4.2. Influence of Feature Dimension on Model Training.** In the implementation of the algorithm of user behavior matrix decomposition, it is necessary to first determine the values of feature dimension  $k$  in user model and resource model. The value of  $k$  represents the dimension describing the features of users and resources when predicting the probability of resource access by users, which affects the prediction accuracy of the training model, model size, and training time. In order to verify the influence of  $k$  on the prediction accuracy of training model, the predictive RMSE of model for 2 to 10 rounds of training is recorded, respectively, when the values of  $k$  are 3, 5, and 10, and the RMSE decline curve was drawn. The experimental results are shown in Figure 3. It is obvious that the larger the value of  $k$  in the training model is, the smaller the model error is; and all the training models converge to the steady state after the fifth round.

In order to further determine the influence of the values of  $k$  on model training, the number of training times is set as 5, and the training time and RMSE with the value of  $k$  ranging from 3 to 20 are recorded, as shown in Figures 4 and 5, respectively. It can be seen that when the value of  $k$  ranges from 3 to 20, the increase in training time and the decline in RMSE are linear and variable.

Since it is necessary to continuously update the training set to implement iterative training in the context of operation and maintenance and quickly output model on the premise of ensuring the accuracy of the training model. The value of  $k$  in this experiment is set as 10.

**4.3. Threshold Sensitivity Analysis Based on the Test Set.** The user model and resource model are obtained via the training on the behavior dataset in 4.2. Through the models, the probability prediction on all behaviors in behavior space can be implemented. In order to realize the abnormal behavior recognition, the abnormal behavior discrimination threshold shall be determined. In order to verify whether the probability prediction value of user behaviors obtained from the training model can distinguish the normal behavior from the malicious behavior, 100 malicious access behaviors and 5,000 normal behaviors are extracted to form a test set to test the training model.

In the experiment, the probabilities of all behaviors in the test set in the user model and the resource model are predicted, and the sensitivity of the data in dataset on the prediction probability threshold is verified using ROC (receiver operating characteristic) curve in combination with the tags indicating whether the behaviors are abnormal. The ROC curve can depict the relationship between false positive rate (FPR) and true positive rate (TPR) when test data classify the abnormal behaviors at different thresholds. TPR is the proportion of correctly identified positive data to the total positive data, i.e., the recall rate, while FPR indicates the percentage of negative data predicted to be positive when the actual value is negative. The specific formulas (8) and (9) of FPR and TPR are as follows:

$$\text{TPR} = \frac{\text{TP}}{\text{TP} + \text{FN}}, \quad (8)$$

$$\text{FPR} = \frac{\text{FP}}{\text{FP} + \text{TN}}. \quad (9)$$

In the formula, TP, FP, TN, and FN represent true positive, false positive, true negative, and false negative, respectively. Since it is generally assumed that behaviors equal to or lower than the probability threshold are abnormal, the behaviors lower than the threshold are determined as positive in this experiment [16, 17].

The ROC curve of test set data in this experiment is shown in Figure 6. The threshold sensitivity of data in test set can be represented by AUC (area under the curve) [18, 19], and the AUC of the test data is 82.80%. The ROC curve indicates that the probability threshold has a certain capability to classify normal and abnormal behaviors in the data of test set [20–22]. However, a higher accuracy rate of abnormal

behavior recognition will be accompanied by FPR increase to some extent [23–25].

**4.4. Recognition Effect of Abnormal Operation and Maintenance Behavior.** In practical application, it is necessary to adaptively generate the abnormal behavior discrimination threshold in accordance with the probability distribution in behavior space; therefore, the CFomb applies the OTSU algorithm to the computation of the abnormal behavior discrimination threshold. In the experiment, the probabilities of all behaviors in behavior space are calculated, and the threshold of 0.0927 is obtained with the OTSU algorithm.

Afterward, the effect of abnormal behavior recognition proposed in this paper is further tested at the threshold of 0.0927. There are a total of 5,100 behavior records in the experiment. The confusion table (as shown in Table 1) is obtained based on the statistics on recognition results, with the corresponding TPR and FPR of 94% and 30.26%, respectively. The data indicates that 94% of malicious behaviors are recognized at the threshold of 0.0927, with 30.26% of normal behaviors determined as abnormal behaviors. Moreover, of all the behaviors, 31.51% are determined as normal behaviors, indicating that CFomb can exclude 68.49% of behavior records in manual audits, which significantly reduces the workload of security audit.

## 5. Conclusion and Future Work

Based on the matrix decomposition collaborative filtering method, this paper proposes the CFomb-based abnormal behavior collaborative filtering method under the background of internal attacks against the operation and maintenance platform of the power monitoring system. This method obtains a user model and resource model via training in global data access by users, combined with collaborative filtering idea and OTSU binarization method to realize the probability prediction of real-time access behavior of O&M users and adaptive selection of probability threshold of abnormal O&M behavior to support more efficient and safe development of power monitoring system O&M. The experiment indicates that the recognition effect is obvious, which can effectively prevent internal threats to the operation and maintenance platform of the power monitoring system and significantly reduce the workload of manual audits. The method proposed in this paper overcomes the inefficiency of traditional methods and provides new ideas for the operation and maintenance mode of power monitoring systems. Due to the limitation of the data in the training set, the probability prediction model has certain errors. Based on this paper, we will lower the misjudgment rate in the future in combination with other behavior features of operation and maintenance users as well as the feedback iteration of operation and maintenance personnel on the training model, to further study more effective methods for recognizing abnormal behaviors.



## Data Availability

The labeled dataset used to support the findings of this study are available from the corresponding author upon request.

## Conflicts of Interest

The authors declare no competing interests.

## References

- [1] M. S. LiQ, S. Zhang, M. Wu, J. Zhang, and M. Taleby, "Safety risk monitoring of cyber-physical power systems based on ensemble learning algorithm," *Access*, vol. 7, pp. 24788–24805, 2019.
- [2] H. Shi, "Design and application of operation and maintenance security management and control system based on bastion machine technology," *China Management Information*, vol. 19, no. 24, pp. 44–45, 2016.
- [3] W. Zheng, H. Chen, and P. Wu, "Demand and application scenario design of online operation and maintenance audit platform for power monitoring system," *Network Security Technology and Application*, vol. 2020, no. 11, pp. 134–135, 2020.
- [4] H. Wu, "Analysis of preventive measures for network information security of electric power enterprises information system," *Engineering*, vol. 2018, no. 12, p. 73, 2018.
- [5] G. Yang, J. Ma, A. Yu, and D. Meng, "Research on insider threat detection," *Journal of Information Security*, vol. 1, no. 3, pp. 21–36, 2016.
- [6] S. Yuan and X. Wu, "Deep learning for insider threat detection: review, challenges and opportunities," *Computers & Security*, vol. 104, p. 102221, 2021.
- [7] H. Peng, *Research on Insider Threat Detection Method Based on User Behavior*, Beijing Jiaotong University, Beijing, 2019.
- [8] F. Liu, Y. Wen, D. Zhang, X. Jiang, and D. Meng, "Log 2vec: a heterogeneous graph embedding based approach for detecting cyber threats within enterprise," in *the 2019 ACM SIGSAC Conference. ACM*, 2019.
- [9] G. Zhaojun and G. Jingxuan, "An insider threat detection method based on character abnormal behavior mining," *Computer Engineering and Design*, vol. 41, no. 10, pp. 2740–2746, 2020.
- [10] T. Rashid, I. Agrafiotis, and J. R. C. Nurse, "A new take on detecting insider threats: exploring the use of hidden Markov models," in *Proceedings of the 8th ACM CCS International workshop on managing insider security threats*, pp. 47–56, 2016.
- [11] J. Happa, "Insider-threat detection using Gaussian mixture models and sensitivity profiles," *Computers & Security*, vol. 77, pp. 838–859, 2018.
- [12] Z. Khan, S. Zubair, K. Imran, R. Ahmad, S. A. Butt, and N. I. Chaudhary, "A new users rating-trend based collaborative denoising auto-encoder for top-N recommender systems," *IEEE Access*, vol. 7, pp. 141287–141310, 2019.
- [13] W. Wang, J. Chen, J. Wang, J. Chen, J. Liu, and Z. Gong, "Trust-enhanced collaborative filtering for personalized point of interests recommendation," *IEEE Transactions on Industrial Informatics*, vol. 16, no. 9, pp. 6124–6132, 2020.
- [14] C. Zhang and C. Wang, "Probabilistic matrix factorization recommendation of self-attention mechanism convolutional neural networks with item auxiliary information," *IEEE Access*, vol. 8, pp. 208311–208321, 2020.
- [15] Y. Zhang, Y. Wang, and S. Wang, "Improvement of collaborative filtering recommendation algorithm based on intuitionistic fuzzy reasoning under missing data," *IEEE Access*, vol. 8, pp. 51324–51332, 2020.
- [16] J. Chen, J. Han, X. Meng, Y. Li, and H. Li, "Graph convolutional network combined with semantic feature guidance for deep clustering," *Tsinghua Science and Technology*, vol. 27, no. 5, pp. 855–868, 2022.
- [17] M. Heydarian, T. Doyle, and R. Samavi, "MLCM: multi-label confusion matrix," *Access*, vol. 10, pp. 19083–19095, 2022.
- [18] S. Zhang and M. Abdel-Aty, "Real-time pedestrian conflict prediction model at the signal cycle level using machine learning models," *IEEE Open Journal of Intelligent Transportation Systems*, vol. 3, pp. 176–186, 2022.
- [19] S. Lin, P. Rouse, Y. Wang, and F. Zhang, "A statistical model to detect DRG outliers," *IEEE Access*, vol. 10, pp. 28717–28724, 2022.
- [20] Z. Huang and D. Chen, "A breast cancer diagnosis method based on VIM feature selection and hierarchical clustering random forest algorithm," *IEEE Access*, vol. 10, pp. 3284–3293, 2022.
- [21] M. Wu, L. Tan, and N. Xiong, "A structure fidelity approach for big data collection in wireless sensor networks," *Sensors*, vol. 15, no. 1, pp. 248–273, 2015.
- [22] S. Huang, A. Liu, S. Zhang, T. Wang, and N. N. Xiong, "BD-VTE: a novel baseline data based verifiable trust evaluation scheme for smart network systems," *IEEE Transactions on Network Science and Engineering*, vol. 8, no. 3, pp. 2087–2105, 2021.
- [23] H. Li, J. Liu, K. Wu, Z. Yang, R. Liu, and N. Xiong, "Spatio-temporal vessel trajectory clustering based on data mapping and density," *IEEE Access*, vol. 6, pp. 58939–58954, 2018.
- [24] K. Gao, F. Han, P. Dong, N. Xiong, and R. du, "Connected vehicle as a mobile sensor for real time queue length at signalized intersections," *Sensors*, vol. 19, no. 9, p. 2059, 2019.
- [25] P. Yang, N. Xiong, and J. Ren, "Data security and privacy protection for cloud storage: a survey," *IEEE Access*, vol. 8, pp. 131723–131740, 2020.

## Research Article

# Research and Implementation of Sports Entity Simulation Based on Heterogeneous Binocular Vision

Liang Tan <sup>1,2</sup> and He Gao<sup>3</sup>

<sup>1</sup>College of Marxism, Jilin Sport University, Changchun, Jilin 130022, China

<sup>2</sup>College of Physical Education, National Taiwan Sport University, Taoyuan, Taiwan 333325, China

<sup>3</sup>College of Architecture & Planning, Jilin Jianzhu University, Changchun, Jilin 130118, China

Correspondence should be addressed to Liang Tan; 0333@jlsu.edu.cn

Received 25 February 2022; Revised 18 March 2022; Accepted 28 March 2022; Published 16 May 2022

Academic Editor: Wen Zeng

Copyright © 2022 Liang Tan and He Gao. This is an open access article distributed under the Creative Commons Attribution License, which permits unrestricted use, distribution, and reproduction in any medium, provided the original work is properly cited.

To study the value of heterogeneous binocular vision in the detection of sports targets, a Zynq-based joint software and hardware design method is proposed, and a mobile object detection system for binocular vision is developed based on it. This paper introduces the relevant technologies and theories used in the system design. First, the basic principles and various modules of the binocular stereo vision process are introduced, including camera tuning, stereo correction, stereo tuning, and telescope stereo vision. Based on the depth information, a method to detect and measure motor targets was developed. Finally, combined with the improved mobile target detection algorithm, the real-time methodology research and algorithm design to determine the target range are completed. The performance of the moving target detection system based on binocular stereo vision and the moving target detection and ranging algorithm are tested and analyzed. We know that the front and rear width of the moving target (the person tested in this paper) is at least 10 cm, while the error value of the ranging algorithm in this paper is within 6 meters, and the average error is less than 10 cm. According to the characteristics of binocular stereo vision, the farther the viewing angle is, the smaller the parallax value of the left and right image pixels will be. Therefore, the insignificant change of depth information will bring some errors to the ranging algorithm. The greater the measurement error is, the lower the percentage deviation of the measurement result is within 2%. It also shows that the target ranging algorithm in this paper can ensure good accuracy within a certain distance. Through this method, we can obtain the accurate data of moving objects in sports competition, so as to improve the training method of athletes and improve the competition results.

## 1. Introduction

The modern Olympic movement has gone through a glorious history of more than 100 years. While the athletes have won a star-studded medal in the struggle and competition, they have also shown the infinite charm of sports to the world. Through the analysis of the evolution process of Olympic sports performance, the author found that the improvement of almost all sports performance has decreased over time, and even some sports, such as the men's 100 m sports performance, even increased by 1% or 2%. It is very difficult, because human beings rely on their own instinctive power to challenge their own physiological limit, which is close to the limit level. Therefore, only from the perspective

of sports technology, in order to improve or make breakthroughs in sports performance, two changes must be completed in sports technology research methodology, that is, from the traditional one based mainly on human eye observation to one based on high-precision motion capture and analysis. The transformation of the technical measurement method of human movement is from the empirical method based on too much emotion to the human movement analysis method based on the programmed human movement simulation and simulation. As early as 2000, the Institute of Sports Science of the General Administration of Sports of the People's Republic of my country and the Institute of Computer Science of the Chinese Academy of Sciences have successfully developed a series of advanced sports (such as

diving and weightlifting) and quasiadvantage projects (such as gymnastics and trampoline) The “digital three-dimensional human motion simulation system” based on computer virtual simulation technology of intellectual property rights and applying it to the preparations for the Athens Olympic Games not only ensures the absolute advantage of Chinese athletes in diving but also helps the first-generation trampoline athletes in my country. The Olympics won a bronze medal. In the future, China will invest huge human, material, and financial resources in the research and application of sports virtual reality technology based on three-dimensional simulation of sports technology.

Among the many means of human access to information, vision occupies an absolutely important position, and computer vision is to use computers to understand human visual process, in order to replace some difficult tasks with machines [1]. Computer vision is a very complex process. It captures the same scene through two precalibrated cameras and then restores the depth information by calculating the parallax of binocular images on the same spatial point in the same scene and the principle of triangulation. At present, the binocular vision system designed by binocular vision theory has been widely used in aerospace, industrial detection, robotics, automatic driving, and other fields [2]. In recent years, with the deepening of the theoretical research of binocular vision, people’s understanding of the binocular vision system is also deepening. The current research shows that the binocular vision system is not only suitable for indoor scenes but also suitable for outdoor scenes. In the outdoor scene, the depth information of the outdoor scene can be reconstructed through high-resolution binocular camera and appropriate matching algorithm, which greatly enriches the application scene of the binocular vision system. In addition, with the increasing demand for high-performance and low-power computing, there have been many advances in the field of processor architecture. Multicore and multithreaded computing have been widely used in various applications, and heterogeneous multicore processing has gradually emerged in various fields. The multicore processor can greatly improve the computing performance on the premise of limiting the power consumption, and the isomerization of the computing core can make the computing mode of the algorithm not simple serial, but more parallelization, which further shortens the running time of the algorithm. Therefore, the heterogeneous multicore processor has been widely concerned and studied by various industries since its birth. For example, the accelerated processing unit produced by AMD company integrates the traditional CPU periphery with GPU core, which greatly improves the parallel computing ability on the premise of limiting power consumption. The performance of the traditional FPGA processor produced by Zynq company is greatly improved. The number of CPU cores of Xeon series processors produced by Intel company has reached 16, and through the vectorization expansion of CPU instructions, it can also provide powerful parallel computing power; NVIDIA has directly extended GPU to the field of general computing and developed its own CUDA (Compute Unified Device Architecture) programming architecture. Rapid progress is

taking place in the field of high-performance processors and will have a far-reaching impact on traditional computing methods. In this context, the application of heterogeneous multicore processors in the binocular vision system can not only solve the problem of low real-time performance of the algorithm but also effectively control the power consumption. Therefore, binocular stereo vision is also widely used in visual navigation, target detection and tracking, target measurement, target recognition, and 3D scene perception. Figure 1 is a real-time moving target detection system.

## 2. Literature Review

At present, in competitive sports, the research hotspots of sports technology in various countries focus on two fields: video analysis of sports technology and 3D virtual simulation of sports technology. Among them, the three-dimensional simulation of sports technology is to reproduce the subtle links of the technical movements of elite athletes through computer virtual reality technology. The training intention of the coaches, the organization plan of the manager, and the training process of the athletes achieve the interpretation, analysis, and prediction of the sports system, organization, and evaluation of an experimental technology science. As far as the research and application status of 3D simulation of sports technology in the world is concerned, China is in a relatively leading position, which is mainly due to the national system of my country’s sports competition and management system. To solve this research problem, Fang and others put forward the idea of cost aggregation of bidirectional adaptive weight, which reduces the complexity of cost aggregation, which makes the cost aggregation process of binocular matching the most time-consuming can be completed quickly, and then improves the real-time performance of the matching algorithm [3]. Boulaouche and others proposed the idea of using GPU to accelerate the SGM algorithm based on mutual information in parallel. By using mutual information matching cost and semiglobal optimization method, the edge blur of parallax image caused by low matching accuracy of the local matching algorithm is solved. At the same time, the powerful parallel computing ability of GPU is used, further improving the real-time performance of the semiglobal matching algorithm based on mutual information [4]. GUR and others implemented an adaptive window matching algorithm based on FPGA. The algorithm makes full use of the parallelism and pipelined execution characteristics of FPGA, which not only improves the real-time performance of the algorithm but also reduces the system power consumption. Its disadvantages are long development cycle and poor maintainability of the algorithm [5]. Guo and others evaluated the performance of binocular matching algorithm on various common multicore processors and pointed out that the parallel acceleration effect of GPU on binocular matching algorithm is better than that of DSP and FPGA [6]. Moghaddas and others proposed a sensor method combining radar depth and binocular vision depth, which realizes object segmentation in high-speed environment and has high accuracy and robustness. There are steps of identifying and locating targets [7]. Karray and

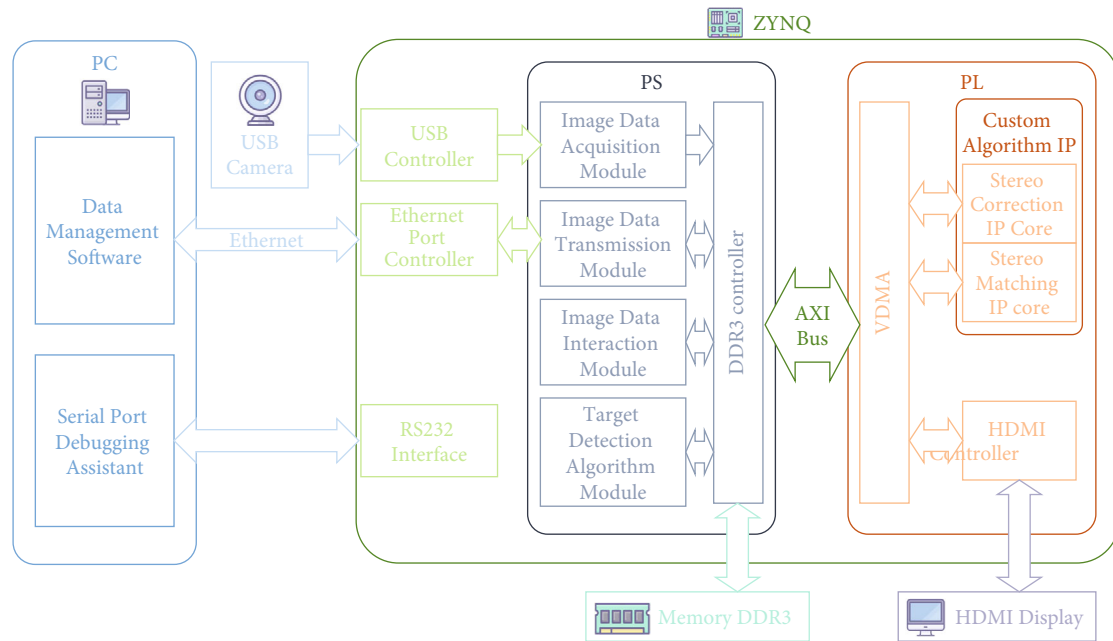


FIGURE 1: Real time moving target detection system.

others proposed LBP (local binary pattern) feature for target detection and face recognition. This method has good effect and simple calculation and is widely used in the field of machine vision [8]. Bieze and others proposed SIFT (scale invariant feature transformation) algorithm on ICCV to extract local features. It uses the found extreme points in space to extract scale, position, and rotation invariants [9]. Sun and others proposed Haar-like feature, which can be used by Lianhart and others to calculate the pixel sum of regional image, which greatly improves the efficiency [10]. Wang and others proposed the hog (direction amplitude histogram) algorithm to extract features. It describes the features through the histogram of statistical image edges and detects pedestrians combined with SVM. This method has strong robustness to illumination changes and improves the recognition accuracy [11]. Jiang and others proposed the surf (accelerated robust feature) feature detection algorithm, which absorbs the advantages of sift and uses the Hessian algorithm to detect key points several times faster than sift [1]. Panda and others proposed DPM (variable component model) target detection algorithm, which improved hog and added multicomponent strategy to describe the target through the relationship between components. The DPM algorithm has become an important part of human behavior and posture classifier [12]. On the current research basis, with the popularity of artificial intelligence all over the world, the science and technology industry also began to develop in the direction of intelligence and digitization. This paper in the aspect of target detection, we should not only find the position of the target in the image but also classify the target objects. This requires the cooperation of target detection and object classification algorithms. In this paper, SSD deep learning neural network combined with mobile net is selected for target detection. Mobile net, as a lightweight clas-

sification algorithm, can quickly and accurately extract the characteristics of target objects. SSD, as a one-step target detection algorithm, can output the position of target objects efficiently and accurately. The combination of the two greatly improves the accuracy of target detection.

### 3. Method

**3.1. Binocular Stereo Vision.** The essence of binocular stereo vision is to use two identical cameras to capture two images of the same scene from two perspectives and use the triangulation principle to calculate the position difference between the corresponding pixels of the two images to obtain the parallax map containing the three-dimensional information of the scene [13]. Figure 2 shows the flow of the whole binocular stereo vision technology. Camera data acquisition is the data source of the system, which provides data basis for subsequent processing modules [14]. The application of three-dimensional scene mainly uses the ranging principle of binocular stereo vision and parallax map to complete the application of visual navigation and positioning, object noncontact measurement, and so on. In this paper, it is moving target detection and real-time ranging. Next, it mainly introduces the important part of binocular stereo vision technology.

**3.1.1. Camera Calibration.** The camera setting is to establish a relationship between the pixels of the image and the actual image location point. The goal is to obtain the camera's internal parameters, external parameters, and distortion parameters, so as to lay the foundation for the use of the stereoscopic editing module and the following 3D scenarios. The imaging principle of the aperture camera determines the transition process between the four coordinate systems.

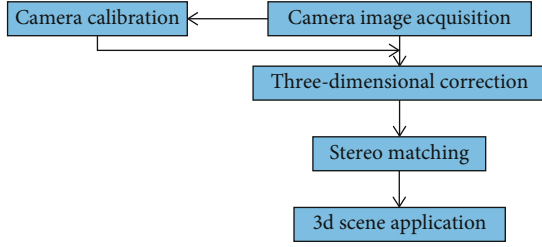


FIGURE 2: General flow of binocular stereographic techniques.

Assuming that the coordinate of a point in the world coordinate system is  $[x_w, y_w, z_w]^T$  and the imaging point in the image pixel coordinate system is  $[u, v]^T$ , the conversion relationship of the point from the world coordinate system to the image pixel coordinate system is

$$s \begin{bmatrix} u \\ v \\ 1 \end{bmatrix} = \begin{bmatrix} f_x & 0 & u_0 & 0 \\ 0 & f_y & v_0 & 0 \\ 0 & 0 & 1 & 0 \end{bmatrix} \cdot \begin{bmatrix} RT \\ 01 \end{bmatrix} \begin{bmatrix} x_w \\ y_w \\ z_w \\ 1 \end{bmatrix}. \quad (1)$$

Here,  $R$  is an orthogonal rotation matrix, and  $T$  is a translation matrix. They are used to determine the positional relationship between the global and camera frames and the relative position of the telescope camera. The parameters required to define the two matrices are called external parameters.  $u_0$  and  $v_0$  represent the position coordinate of the center of the virtual imaging plane in the image pixel coordinate system.  $f_x$  represents the projection of the focal length in the  $X$  direction in the image physical coordinate system, and  $f_y$  represents the projection in the  $Y$  direction.  $f_x, f_y, u_0,$  and  $v_0$  are the internal parameters of the camera. Internal parameters indicate how to convert 3D camera coordinates into 2D image coordinates inside the camera. Therefore, internal parameters are only related to the camera itself. Another internal parameter of the camera is distortion parameter. Distortion is the distortion and change caused by the camera in order to collect more image data under limited viewing angle. It generally includes radial distortion and tangential distortion. A total of five parameters need to be determined.

Among the calibration methods, the calibration method is simple and mature. In the process of calibration, only one chess and card grid panel needs to be used as the calibration board. By fixing the camera, let the calibration plate move at different positions and angles to collect the image of the camera [15]. Different equations are established according to the key points on the calibration board, and then the values of relevant parameters are obtained by closed-form solution and maximum likelihood estimation method.

**3.1.2. Stereo Correction.** The first step of stereo correction is image correction, which uses the camera distortion parameters to remove the distortion of the image. In stereo correc-

tion, the most mature method is Bouguet's stereo correction algorithm. The principle of this algorithm is the epipolar correction method. The principle of this method is briefly introduced below.

Due to the epipolar geometry of the corresponding pixels of the binocular image, under the epipolar constraint, for the feature points on the imaging plane, the matching points on the other imaging plane must be on the corresponding epipolar line. The function of binocular stereo correction is to make strict line correspondence between the two corrected images by using the geometric relationship of the opposite level and keep the epipolar lines of the two images on the same horizontal line, so that a corresponding pair of pixel points can be found on the same line of the two images [16]. When calculating the image parallax to find the corresponding point of the pixel point, it only needs to carry out linear search in this line, to speed up the calculation speed, and to reduce the false matching rate.

**3.1.3. Stereo Matching.** Its purpose is to match the corresponding pixel points in the binocular image after stereo correction, calculate the difference of  $u$  coordinates of these corresponding points in the image pixel coordinate system in the left and right images, obtain the difference of corresponding points, and finally combine the difference of all pixel points to form a parallax map.

Stereo matching algorithms are complex and diverse. The research on stereo matching algorithms is also a hot research direction in binocular stereo vision technology. In these three categories, researchers have proposed a variety of stereo matching methods. The most commonly used is region-based matching. Its principle is to establish a region block window centered on the pixel to be matched in the reference image and then find a pixel in another image, so that the region blocks window of the same size created with it as the center and the region block window in the reference image meet the similarity under certain threshold conditions.

**3.1.4. Principle of Binocular Stereo Vision Ranging.** According to the principle of similar triangle, the depth information  $Z$  can be deduced:

$$\frac{|x_l - x_r'|}{B} = \frac{f}{Z} \Rightarrow Z = \frac{fB}{d}, \quad (2)$$

where  $B$  represents the distance between the optical centers of binocular cameras, also known as the camera baseline distance. The parallax value  $D$  of the target point  $P$  can be obtained through the stereo matching algorithm, and the depth information of the point  $P$ , that is, the distance value, can be obtained by bringing its value into equation (2).

**3.2. Software and Hardware Collaborative Design.** Zynq is a chip combining software and hardware. Software and hardware collaborative design aims at the system requirements. In the design process, software and hardware interact to achieve the purpose of efficient work of the system. In the early development of software and hardware system,

hardware and software development were divided into two independent parts. Generally, the hardware is designed first, and then the software is designed on the hardware platform. Due to the lack of clear understanding of software and hardware architecture and implementation mechanism in the design process, the design results are often blind. As a result, the whole system design needs to rely on the designer's development experience, and the design time and cost are greatly improved. Moreover, in the process of repeated modification, it often deviates from the original design requirements in some aspects. Compared with the disadvantages of the traditional independent design of software and hardware architecture, the software and hardware collaborative design method excavates the correlation between the system software and hardware as much as possible by comprehensively analyzing the functions [17]. Divide the software and hardware reasonably, then complete the software and hardware data interaction in a correct way, and finally generate the hardware and software architecture of the system through hardware comprehensive simulation and software compilation and testing.

In the design process, the functional requirements of the system are analyzed from the description of the target system. Considering the existing resources, algorithm complexity, and cost and time of system development, the software and hardware of the system are divided reasonably, make clear which module is implemented by hardware and which module is implemented by software, and design the software and hardware interaction interface. Secondly, the software and hardware of the system are developed synchronously, including the synthesis and simulation of hardware modules, the compilation and testing of software modules, and the interactive design of software and hardware interfaces. Finally, the integrated hardware is integrated with the compiled software, and the simulation test of the system is carried out to detect whether the system meets the performance requirements. Otherwise, it is necessary to redivide the software and hardware. With the increasing development and maturity of programmable devices, excellent embedded systems are inseparable from the architecture method of software and hardware collaborative design.

**3.3. Traditional Sports Object Detection Algorithm.** By analyzing the sequence of video or continuous image frames, determine whether each frame has a forward target, that is, moving the target; then decompose the corresponding front-end target attribute, i.e., the detection of the moving target is completed. Based on the presence of relative motion between the detected phenomenon and the camera, the motion target detection algorithm can be divided into static background detection and motion background detection [18].

**3.3.1. Frame Difference Method.** The frame difference method uses the principle of strong correlation between adjacent frames of image sequence to separate moving targets through the differences between image frame sequences. Its essence is to calculate the difference of pixel values between two or more adjacent frames in image sequence

and set the corresponding threshold to divide the foreground region and background region.

Assuming that the  $k$ -th frame image in the continuous image sequence is represented as  $f_k(x, y)$ , the  $K$ - $T$  frame image is represented as  $f_{k-t}(x, y)$ ,  $T$  represents the interval of the differential frame, and the difference  $D_k(x, y)$  of the two frame images can be described by formula (3):

$$D_k(X, y) = |f_k(X, y) - f_{k-t}(x, y)|. \quad (3)$$

Then, the  $D_k(x, y)$  is binarized, and the result is shown in equation (3). By analyzing the  $M_k(x, y)$  value to distinguish the front scenic spot,

$$M_k(x, y) = 1, D_k(x, y) > T, \quad (4)$$

$$M_k(x, y) = 0, D_k(x, y) \leq T. \quad (5)$$

The moving target can be extracted from the background by binarization of all pixels of the target image. The flow chart is used to describe the frame difference method, as shown in Figure 3.

In Figure 3 that after the image difference is calculated through equations (3) and (4) and binarized, some methods in morphology (such as filtering) need to be used to attenuate the noise in the binarized image. Because the moving target obtained by frame difference method may have some holes, it also needs connectivity processing, which finally determines the moving target.

The algorithm of frame difference method has low complexity, can better adapt to the background environment with slow change, and has high real-time performance. However, the detection accuracy of the algorithm is not high. When the color of the target is like the background, it cannot effectively detect the moving target; moreover, the algorithm is prone to false detection. For example, when checking fast-moving targets, it is easy to detect multiple moving targets or treat the background as moving targets.

**3.3.2. Background Subtraction Method.** Background subtraction is the most used basic method in moving target detection. Its essence is to establish a background model to represent the detection scene; then, the pixels of each subsequent frame are subtracted from the corresponding pixels in the background, and the ones with large changes in the operation results are regarded as the front scenic spots, and vice versa. The core of the background subtraction method is the establishment of the background model, which should reflect the realistic changes of the scene as much as possible. Because the real scene cannot be static, the factors such as illumination, water wave, and the change of leaves all increase the difficulty of background modeling, and the background model needs to be updated constantly. There are many modeling methods for different application environments. Figure 4 shows the working flow chart of background subtraction method for primary target detection.

By analyzing the flow of Figure 4, the algorithm first needs to obtain a frame of image in the image sequence and attenuate the image noise through simple preprocessing

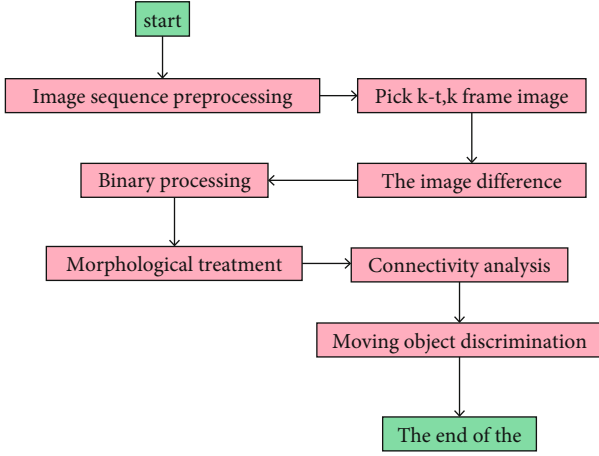


FIGURE 3: Workflow of the frame difference method.

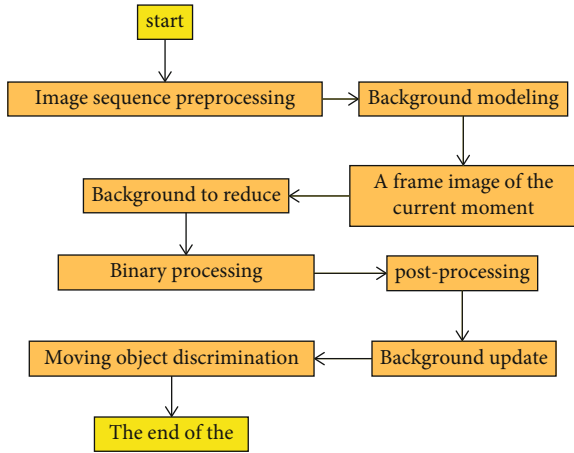


FIGURE 4: Workflow of the background subtraction method.

and then carry out background modeling according to a certain background modeling principle. If a frame image at time  $t$  is selected as  $F(x, y, t)$ , assuming that the image after background modeling at this time is  $B(x, y, t)$ , the background of the image is subtracted to obtain the difference between the image and the background. By comparing with the threshold  $T$  selected in a specific environment scene, the binarized image  $I(x, y, t)$  is obtained. The expression is as follows:

$$\begin{aligned} I(x, y, t) &= 1 |F(x, y, t) - B(x, y, t)| > T, \\ I(x, y, t) &= 0 |F(x, y, t) - B(x, y, t)| \leq T. \end{aligned} \quad (6)$$

The binary image has highlighted the foreground target. In order to eliminate noise, it is also necessary to carry out morphological filtering such as frame difference method and target connectivity analysis. Because the background model is not one layer invariant, corresponding algorithms need to be adopted to update the background model and finally determine the moving target.

It has little computation and is easy to implement and performs well in obtaining the foreground area when the scene changes slightly; however, the algorithm is sensitive to illumination changes and vulnerable to background fluctuations. The effect of this method also depends on the establishment and updating of the background model. At present, the commonly used background updating methods include Gaussian mixture modeling and vibe model updating. Due to the large amount of calculation and high complexity of Gaussian mixture modeling, it is not suitable for the moving target detection system with high real-time requirements; so, it will not be described in detail here.

**3.3.3. Vibe Algorithm.** The Vibe algorithm is a pixel-level video background modeling algorithm. The algorithm stores a sample set of all pixels in an image, and each sample set is the pixel value before the pixel and the pixel value of the neighbors; then, compare the new range with the value in the sample set to determine whether the point is a background point and update the sample value of the pixel and its field points with a certain probability. The algorithm has no limited requirements for the detection environment. It estimates the background model through random sampling to simulate the random volatility of the real environment. By adjusting the time secondary sampling factor, a few new sample values are used to replace the changes of all sample values, considering the detection accuracy and computational complexity.

For any pixel  $v(x, y)$  in the selected image, the algorithm randomly selects the pixel values  $v_i(x, y)$  of  $N$  neighborhood points as sample values and stores them in the background sample set  $M(x, y)$  of the pixel. The result is shown in formula (7). Finally, the sample values of all pixels in the image are collected to initialize the background model.

$$M(x, y) = \{v_1(x, y), v_2(x, y), \dots, v_N(x, y)\}. \quad (7)$$

Positive image detection is as follows: starting from the second frame of the video image sequence, go through each pixel of the new frame image in  $v(x, y)$  to modify the pixel sample set:

$$D(x, y) = (d_1(x, y), d_2(x, y), \dots, d_N(x, y)), \quad (8)$$

where  $D(x, y)$  represents the set of differences between the value of the current pixel  $v(x, y)$  and all sample values in the pixel sample set  $M(x, y)$ :

$$d_i(x, y) = v(x, y) - v_i(x, y). \quad (9)$$

Before foreground detection, the threshold  $r$  is to judge whether the pixel is close to the historical sample value, and the threshold  $T$  is to judge whether it is the front scenic spot need to be set in advance; then, traverse all elements  $d_i(x, y)$  in  $D(x, y)$  and compare its size with the threshold  $R$ ; count the number of  $d_i(x, y)$  as  $N_f$ . If  $N_f > T$ , this point is the front scenic spot. According to the experimental test results, the three main parameters in the detection process

are generally set as follows: the number of sample sets  $N = 20$ , the threshold  $R = 20$ , and the threshold  $T = 2$ .

Background model updating is as follows: while detecting the foreground, the background model needs to be updated constantly so that the model can adapt to the changing scene. The update method determines that the update strategy of the vibe algorithm includes three attributes: memoryless update strategy, time sampling update strategy, and spatial domain update strategy. First, whether the sample values are replaced in the sample set of the background model is independent of time. Secondly, the algorithm reduces the update frequency of the sample value in the background and its neighbor sample value through the time secondary sampling mechanism. Third, for the pixel to be updated, a pixel will be randomly selected in its neighborhood to update the selected sample pixel value with the newly selected pixel [19].

According to the understanding of the basic principle of the vibe algorithm, the algorithm process is simple, has strong randomness in time and space, and can effectively adapt to environmental changes. The vibe algorithm is more stable than the frame difference method and background subtraction method and is not easy to be affected by illumination and scene mutation; at the same time, the algorithm has low complexity and small amount of calculation, which is easy to implement on embedded devices [20]. Through the test of the data set, it is found that if the scenes in frame are all background, the detection effect will perform well, but if there are moving objects in the first frame, the phenomenon of “ghost” will occur, or the sudden movement of stationary targets in the process of moving target detection will also produce the phenomenon of “ghost.” Secondly, the detection of moving target by the vibe algorithm is usually incomplete, resulting in that the moving target is not a connected region in the detection effect. These two problems will have an adverse impact on the target ranging module of the moving target detection system: “ghost” phenomenon will lead to multiple target areas, resulting in false detection and blank ranging. If the target detection is incomplete, there will be multiple subregions and multiple inaccurate distance information. In view of these two shortcomings of the vibe algorithm, this paper improves it according to the depth information obtained by binocular stereo vision technology [21].

### 3.4. Improved Vibe Algorithm Based on Depth Information

**3.4.1. Correction of “Ghost” Phenomenon.** If the frame image used to initialize the background model happens to have a moving target, it will be regarded as the background. Similarly, when the target is forbidden to move suddenly during the detection process, such a “ghost” phenomenon will also appear. Considering that the depth information of pixels in this area will increase suddenly after the target moves, combined with this feature, when the algorithm initializes the background model, the depth information of each pixel will also be stored in the sample set. In a new frame of image detection, the difference value of depth information will be increased, and the result information is stored in the matrix  $D$ :

$$\begin{aligned} \text{Mat}D(x, y) &= 1 | \text{depth}_s(x, y) - \text{depth}(x, y) | > D, \\ \text{Mat}D(x, y) &= 0 | \text{depth}_s(x, y) - \text{depth}(x, y) | \leq D, \end{aligned} \quad (10)$$

where  $\text{depth}$  represents the  $\text{depth}_s(x, y)$  information in the pixel sample set,  $\text{depth}_s$  represents the  $\text{depth}_s(x, y)$  information of the current pixel, and  $D$  represents the differential threshold of the depth information. It is necessary to correct the point as a background point and reinitialize the background model.

**3.4.2. Correction of Incomplete Target Detection.** This phenomenon is usually caused by the complexity and variability of the scene or moving target. There is also some noise interference, which makes isolated noise points and connected noise areas appear in the image data. Considering that the depth information of pixels in the moving target area is similar, there will not be too much mutation.

First, you need to define eight field value sets  $s(x, y)$  of any pixel  $(x, y)$ :

$$\begin{aligned} S(x, y) &= \{ (x-1, y-1), (x, y-1), (x+1, y-1), (x-1, y-1) \\ &\quad \cdot (x+1, y), (x+1, y-1), (x, y+1), (x+1, y+1) \}. \end{aligned} \quad (11)$$

Then, the depth information of the pixel  $(x, y)$  and the depth information of the field value are differentiated:

$$| \text{depth}(x, y) - \text{depth}_i(x, y) | \leq F, \quad (12)$$

where  $\text{depth}(x, y)$  represents the depth information of the pixel,  $\text{depth}_i(x, y)$  represents the depth information of the neighborhood of the pixel, and  $f$  represents the difference threshold of the depth information between the two. If the current pixel point is the front scenic spot and its neighborhood point satisfies formula (12), its neighborhood point is also corrected as the front scenic spot.

**3.5. Target Ranging Algorithm.** We know that moving object detection with distance information can effectively improve the safety of pedestrians and vehicles in road traffic. However, the common target ranging is usually to detect the feature points of moving targets and express the target distance through the single depth information of feature points. This method is simple and easy, but the selection of feature points often cannot fully include all the information of the target. The target is a moving region, and several key feature points cannot be used to describe the distance information of the region. To solve this problem, this paper analyzes the depth information of the moving target area, classifies, discards all the depth values in the area, and finally calculates the mean value of the selected value to represent the real-time distance of the moving target.

Through the improved vibe algorithm described in the previous section, the region of the moving target can be accurately obtained, and then the moving target can be framed with a rectangle by using the simple method in openCV, considering that the depth information of all pixels in the moving target contour should have certain similarity,



even the same value. After removing the moving target in the rectangular area, the background is the background. The depth information of the background points has similar similarity, and their values must be much larger than all pixels in the moving target contour; moreover, the number of depth values of foreground targets in the detection area should be much greater than the number of depth values in the background. According to these characteristics, this paper classifies and discards the depth information in the rectangular box.

Suppose that the starting pixel of the rectangular box is  $(u_0, v_0)$  and the ending pixel is  $(u_i, v_i)$ , define the maximum distance as Max, divide the distance value from 0 to Max into equal intervals, totaling  $n$  segments, and the interval of each segment is  $d$ ; Then, the depth value of each interval  $(k, k + d)$  is statistically summed:

$$S_i = \sum_{(x,y)=(u_0,v_0)}^{(x,y)=(u_i,v_i)} \text{depth}(x, y) \text{depth}(x, y) \in (k, k + d), \quad (13)$$

where  $S_i$  represents the sum of the depth values of each interval,  $\text{depth}(x, y)$  represents the depth value of pixels  $(x, y)$ ,  $k = 0, d, 2d \dots \text{MAX}-d$ . At the same time, count the number of depth values in the interval  $(k, k + d)$ :

$$C_i = \sum_{(x,y)=(u_0,v_0)}^{(x,y)=(u_i,v_i)} 1 \text{depth}(x, y) \in (k, k + d), \quad (14)$$

where  $C_i$  represents the sum of the number of depth values of each interval. Then, put the  $S_i$  and  $C_i$  of each interval into the set, respectively:

$$\begin{aligned} \text{ConA} &= \{S_1, S_2, \dots, S_N\}, \\ \text{ConB} &= \{C_1, C_2, \dots, C_N\}. \end{aligned} \quad (15)$$

After the completion of statistics, calculate the percentage of each element in the set con B in the sum of elements in the whole set. Select the element  $C_i$  with the highest percentage value and find the corresponding  $S_i$  in the set con A according to the index value  $I$ . Finally, the mean  $S_i/C_i$  is obtained. The distance of the moving target obtained by this algorithm can effectively avoid the deviation caused by the method of estimating the distance by local feature points and has a certain accuracy in the test system.

## 4. Results and Analysis

Due to the bandwidth limitation of USB2.0 interface of development board, the system cannot meet the real-time data acquisition of camera. In order to meet the test requirements, the system test adopts USB3.0 interface of PC, and the collected data is quickly transferred to the installed hardware card through PCIe interface, which can avoid data delay and detection target and improve the accuracy of the test system algorithm. Ethernet port transmits data to PC through UDP transmission thread for later storage and

TABLE 1: System hardware resource consumption.

Resource	Utilization	Available
LUT	182789	218601
FF	171530	437201
BRAM	485	544
DSP	267	901

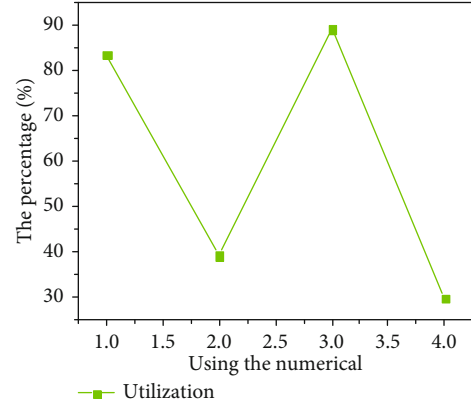


FIGURE 5: System referral resource utilization.

TABLE 2: Time of complex algorithms.

Platform	Stereo correction	Stereo matching	Total
CPU	0.230 s	29.752 s	29.982
Zynq	0.00472 + 0.00351		0.00823 s

application; PCIe interface is used for high-speed transmission of data collected by camera. Based on this experimental platform, the following first introduces the environment construction and performance test of the system, and then introduces the result test and data analysis of the moving target detection and ranging algorithm of the system.

**4.1. System Construction and Performance Test.** First, the mobile target detection system implements the PL logic design section through the Xilinx Vivado development toolkit, which can process and encapsulate the IP kernel. Using this tool, we can complete the design of the specific IP kernel design in the system, the hardware path between the IP cores, and verify that the design is optimal and correct with the help of hardware simulation. As shown in Table 1 and Figure 5, the main resources spent on the system hardware are as follows.

As can be seen from Table 1 and Figure 5, the main resource consumption of the development board is within the available range and can meet the system operation requirements. The PL part realizes the stereo correction and stereo matching algorithm through the parallel acceleration of FPGA to improve the processing speed of the system.

TABLE 3: Comparison results of system processing frame rate.

Design architecture	Device	Resolving power	Hardware resource	Frame rate
Design of embedded real-time	XC7Z045	640*480	182933 LUTS, 143223 FFS, 100 DSPs, 138 BRAMs	101
This paper	XC7Z045	640*480	182796 LUTS, 171526 FFS, 268 DSPs, 485 BRAMs	121.42

TABLE 4: Frame rate of image processing with different resolutions.

Resolving power	640*480	1280*720	1280*960	1920*1080
Frame rate	121.426	66.725	54.959	36.560

To obtain a speed comparison between the hardware and software design architecture (fpga100 MHz, arm667 MHz) and simple CPU (2.50 GHz), the processing times were checked and collected using a telescope image test at 640 \* 480 resolution. Two complex algorithms are multiple stereo corrections and stereo tunings. The PS part calls the system clock according to the program instructions and calculates the software development time through the jet lag. Table 2 shows the average time to develop the test package. It can be seen that a simple CPU takes almost half a minute to develop the two algorithms, while the Zynq system develops the two algorithms in parallel according to the collaborative design method of the architecture. Logical control of the PS part takes only 0.00473 seconds, while the algorithm development of the PL part takes only 0.00350 seconds.

This paper compares the system architecture with the embedded real-time design stereo vision system architecture only for the processing time of complex algorithms. The comparison results are shown in Table 3. Although the embedded real-time design stereo vision system architecture has low hardware resource consumption, however, the image frame rate is slightly lower than the architecture method proposed in this paper. Moreover, the system in this paper also reflects the human-computer interaction performance, while the embedded real-time design stereo vision system does not reflect any human-computer interaction performance.

The development board does not support the rapid transmission of high-resolution camera and cannot test the best effect of the overall system. Therefore, the acquisition end is changed to store atlas with different resolutions in the startup card. The system carries out actual test by reading these atlantes and controls the interactive work such as system startup and resolution change through buttons on the GUI. In PS coding, the method of calling system time through program instructions calculates the time difference before receiving data from PL. The test results are shown in Table 4 and Figure 6:

It can be seen from the table and figure that when processing images with a resolution of 640 \* 480, the frame rate of the system can reach 121.44 frames/s. The real-time effect can be achieved by displaying the processing results through HDMI display and GUI, if the system is applied to vehicle safe driving.

4.2. *Application Algorithm Test and Result Analysis.* Disparity map information technology can meet many application

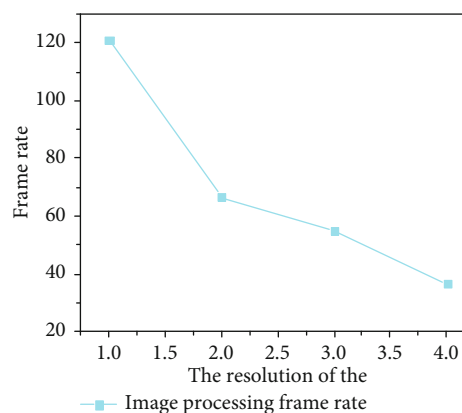


FIGURE 6: Frame rate diagram of image processing with different resolutions.

requirements in 3D scene perception. In order to detect the sports entity target, this paper completes the application of moving target detection. The ZC706 hardware development board selected for the system adopts a low-level manual system with low processing ability and low real-time of the application algorithm. Therefore, the effect of the system application algorithm is tested on the computer [22].

In this paper, the video with image resolution of 640 \* 480 is sampled and tested in indoor lighting environment and outdoor brightness uniform environment, respectively. First, build the system test platform correctly. Then, with the help of the ruler, let the target walk parallel to the camera angle at the fixed actual distance point and collect and process the video to ensure that the camera captures the moving target at the same distance. Finally, the system test distance of each frame image is recorded.

In order to minimize the measurement error, the measurement values of all frame images from frame 100 to frame 300 in the measurement video of each distance point are counted in this paper. Then, compare these measured values and select the target value with the largest number of measured distance values as the system measurement value of the moving target. Based on this statistical method, the indoor environment and outdoor environment are measured and counted, respectively. The statistical results are shown in Figures 7–14:

Because the camera height setting of the system platform is different when it is built indoors and outdoors, this paper

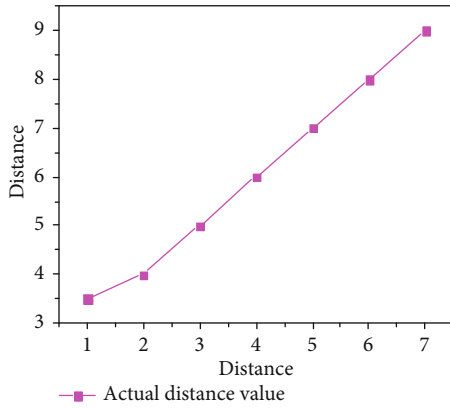


FIGURE 7: Actual value of indoor moving target ranging.

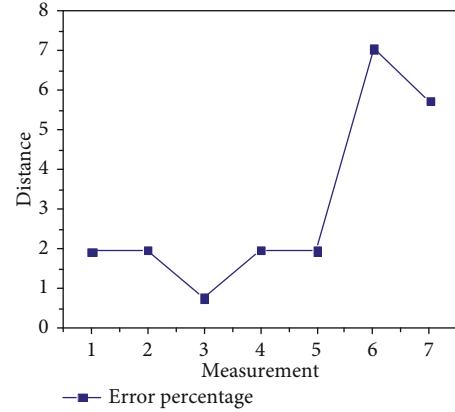


FIGURE 10: Indoor moving target ranging error percentage.

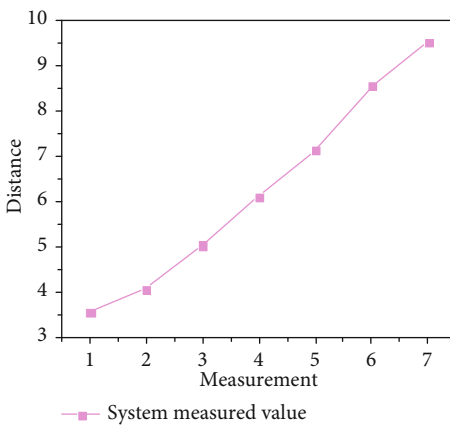


FIGURE 8: Measured values of the indoor moving target ranging system.

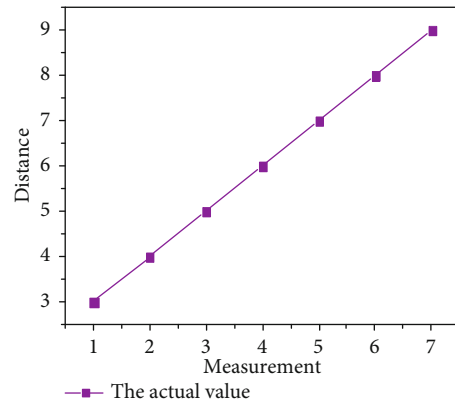


FIGURE 11: Actual value of outdoor moving target ranging.



FIGURE 9: Indoor moving target ranging error value.

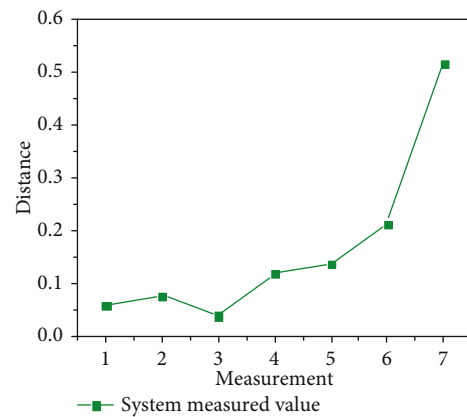


FIGURE 12: Measured values of the outdoor moving target ranging system.

takes the ability to see the whole contour of the moving target as the standard for distance measurement; so, the starting point of indoor ranging is 3.5 m, and the starting point of outdoor ranging is 3 M. Moreover, the moving target has become small and blurred beyond 9 meters; so, the measurement ends at 9 meters. From the comparison of Figures 7–14, in this article, you can see that the indoor

and outdoor performance is slightly different for the target algorithms. We know that the moving object (the person tested in this document) is at least 10 cm wide, but the algorithm error specified in this document is within 6 m, and the average error is less than 10. From the stereo visual characteristics of the binocular, the farther the perspective, the smaller the pixel parallax of the left and right images.

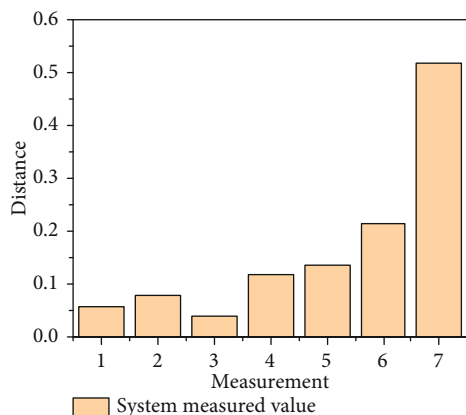


FIGURE 13: Ranging error value of outdoor moving target.

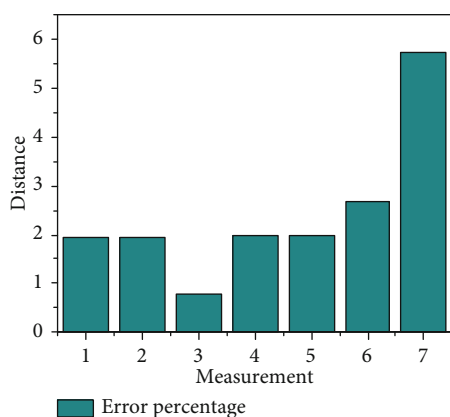


FIGURE 14: Percentage of ranging error of outdoor moving target.

Therefore, small changes in depth information can all lead to some algorithmic errors. It can be seen that the higher the measurement error, the smaller the measurement deviation is less than 2%; it also shows that the target distance algorithm can provide good accuracy within a certain distance.

## 5. Conclusion

This paper presents the research and implementations of various binocular-based moving object modeling. To detect objects of moving objects, we complete a program to detect moving targets and determine real-time distances based on the traditional vibration algorithm and scaling stereo visual information. The ZC706 hardware development board selected for the system implementation adopts a low-level manual system, with low processing ability and low real-time performance of the application algorithm. Therefore, the effect of the system application algorithm is tested on the computer. This paper presents a software and hardware codesign method for the moving target detection system. Combine the respective advantages of software and hardware to divide the software and hardware of the system module and then design efficient and accurate data control and transmission between software and hardware; finally,

combined with the specific algorithm and logic control of binocular stereo vision technology and moving target detection technology, the software and hardware of the system are realized. In the test and analysis of the real-time performance of the system, the processing speed of the system decreases linearly with the increase of image resolution. In the future development of science and technology, people's requirements for image quality are gradually improved, and there is a great demand for high-resolution images. Therefore, the system can be further optimized in the architecture design and binocular stereo vision algorithm, such as increasing the bandwidth of data transmission interface under high resolution in the architecture, to reasonably reduce the complexity of the algorithm when ensuring the accuracy of the algorithm. Through this method, we can obtain the accurate data of athletes in sports competition. Through data analysis, we can improve the athlete training method, so as to improve the competition performance. The experiment shows that this method can be effectively applied to sports training.

## Data Availability

The labeled dataset used to support the findings of this study are available from the corresponding author upon request.

## Conflicts of Interest

The authors declare no competing interests.

## Acknowledgments

This work is supported by the National Social Fund of China, A Study of Entertainment Culture in Tang Dynasty (18CTY016).

## References

- [1] S. Jiang, P. Lin, Y. Chen, and C. Tian, "Research on heterogeneous fiber grating spectrum separation based on transfer matrix and adaptive algorithm," *Optical Engineering*, vol. 58, no. 9, p. 1, 2019.
- [2] W. Song, M. Xu, and Y. Dolma, "Design and implementation of beach sports big data analysis system based on computer technology," *Journal of Coastal Research*, vol. 94, no. sp1, p. 327, 2019.
- [3] Z. Fang, H. Gao, and Z. Ma, "Prediction and evaluation of groundwater environmental impact based on numerical simulation model," *Journal of Coastal Research*, vol. 115, no. sp1, p. 286, 2020.
- [4] T. Boulaouche, D. E. Kherroub, K. Khimeche, and M. Belbachir, "Green strategy for the synthesis of polyurethane by a heterogeneous catalyst based on activated clay," *Research on Chemical Intermediates*, vol. 45, no. 6, pp. 3585–3600, 2019.
- [5] S. Gur, G. N. Frantziskonis, S. Pannala, and C. S. Daw, "Application of wavelet-based methods for accelerating multi-time-scale simulation of bistable heterogeneous catalysis," *Industrial & Engineering Chemistry Research*, vol. 56, no. 9, pp. 2393–2406, 2017.

- [6] Y. Guo, Z. Lu, Q. Wang et al., "Detecting density dependence from spatial patterns in a heterogeneous subtropical forest of Central China," *Canadian Journal of Forest Research*, vol. 45, no. 6, pp. 710–720, 2015.
- [7] M. Moghaddas and A. Davoodnia, "Atom-economy click synthesis of tetrahydrobenzo [b] pyrans using carbon-based solid acid as a novel, highly efficient and reusable heterogeneous catalyst," *Research on Chemical Intermediates*, vol. 41, no. 7, pp. 4373–4386, 2015.
- [8] S. Karray, "Modeling brand advertising with heterogeneous consumer response: channel implications," *Annals of Operations Research*, vol. 233, no. 1, pp. 181–199, 2015.
- [9] T. M. Bieze, A. Kruszewski, B. Carrez, and C. Duriez, "Design, implementation, and control of a deformable manipulator robot based on a compliant spine," *The International Journal of Robotics Research*, vol. 39, no. 14, pp. 1604–1619, 2020.
- [10] Y. Sun and X. Zhao, "Research and implementation of license plate recognition based on android platform," *MATEC Web of Conferences*, vol. 309, no. 15, article 03034, 2020.
- [11] M. Wang, H. Zhang, Q. Hu, D. Liu, and H. Lammer, "\*\* Research and implementation of a non-supporting 3D printing method based on 5-axis dynamic slice algorithm\*\*," *Robotics and Computer-Integrated Manufacturing*, vol. 57, pp. 496–505, 2019.
- [12] A. R. Panda, D. Mishra, and H. K. Ratha, "Fpga implementation of software defined radio-based flight termination system," *IEEE Transactions on Industrial Informatics*, vol. 11, no. 1, pp. 74–82, 2015.
- [13] H. Li, "Research and implementation of art animation system based on video stream," *Revista de la Facultad de Ingenieria*, vol. 32, no. 6, pp. 153–161, 2017.
- [14] L. Li, "Research and implementation of fast image processing algorithm based on fpg," *Revista de la Facultad de Ingenieria*, vol. 32, no. 3, pp. 749–756, 2017.
- [15] Y. Peng, X. Liu, G. Yu, W. Wang, and J. Wang, "Research and implementation of localization algorithm based on zigbee technology," *Boletin Tecnico/Technical Bulletin*, vol. 55, no. 4, pp. 9–15, 2017.
- [16] W. Fang, "Research and implementation of key technologies of digital forensics based on cloud computing," *Boletin Tecnico/Technical Bulletin*, vol. 55, no. 6, pp. 572–579, 2017.
- [17] Y. Liu, "Research on heterogeneous data fusion algorithm based on iot," *Revista de la Facultad de Ingenieria*, vol. 32, no. 4, pp. 549–556, 2017.
- [18] D. Ou, L. Chen, L. Shi, X. He, and D. Dong, "Research on speed-guidance control model and implementation method for tramcars based on signal priority at intersections," *Tiedao Xuebao/Journal of the China Railway Society*, vol. 39, no. 6, pp. 80–86, 2017.
- [19] Y. C. Song, J. Xiong, L. I. Xian-Wang, and X. H. Chen, "Integration for heterogeneous manufacturing information systems based on semantic entity," *International Journal of Smart Home*, vol. 10, no. 9, pp. 31–44, 2016.
- [20] L. Proskuryakova, D. Meissner, and P. Rudnik, "The use of technology platforms as a policy tool to address research challenges and technology transfer," *Journal of Technology Transfer*, vol. 42, no. 1, pp. 206–227, 2017.
- [21] X. Lin, J. Wang, and C. Lin, "Research on 3d reconstruction in binocular stereo vision based on feature point matching method," *Paper Asia*, vol. 2, no. 1, pp. 21–25, 2019.
- [22] X. Yang, M. Zhao, L. Shi, Z. Chen, and M. Zheng, "Research and implementation of fast algorithm for intra prediction mode selection oriented to hardware," *Journal of Computer-Aided Design and Computer Graphics*, vol. 31, no. 1, p. 158, 2019.

## Research Article

# Efficiency Analysis of Sports Equipment Batch Management Based on Antimetal RFID Tag

Zhongwei Huang<sup>1</sup> and Xuebin Sun <sup>2</sup>

<sup>1</sup>School of Physical Education, Jiamusi University, Jiamusi, Heilongjiang 154000, China

<sup>2</sup>School of Physical Education in Main Campus, Zhengzhou University, Zhengzhou, Henan 450001, China

Correspondence should be addressed to Xuebin Sun; [mizunosxb@zzu.edu.cn](mailto:mizunosxb@zzu.edu.cn)

Received 9 March 2022; Revised 18 April 2022; Accepted 25 April 2022; Published 13 May 2022

Academic Editor: Wen Zeng

Copyright © 2022 Zhongwei Huang and Xuebin Sun. This is an open access article distributed under the Creative Commons Attribution License, which permits unrestricted use, distribution, and reproduction in any medium, provided the original work is properly cited.

Based on the antimetal RFID tag model, a sports equipment batch management system is established. The establishment process of the model and system is discussed in detail, and the principle of metal-resistant RFID tag is revealed. Then, the antimetal RFID tag sports equipment batch management system is applied to colleges, middle schools, and primary schools, and the use of teachers and students on the efficiency of sports equipment batch management is studied, highlighting the advantages of the management system. In general, the antimetal RFID tag sports equipment batch management system has timeliness, universality, and reliability. It can adapt to the sports equipment management of different schools, improve its management efficiency, and play a positive role in the development of modern school sports.

## 1. Introduction

Sports equipment is the carrier of sports development. Physical education in colleges must rely on a large number of sports equipment for support, which can achieve better teaching results. In the vigorous development stage of college sports, more teaching projects must be completed with the help of sports equipment. In physical education, colleges should not only provide sports equipment but also manage sports equipment, so as to provide better serve physical education [1, 2].

Sports equipment can be defined as all kinds of equipment used in various sports. Sports equipment is obviously closely related to the sports needs of human beings at all stages. Sports equipment mainly comes from two aspects. On the one hand, it is the evolution of some equipment in people's long-term production labor and social struggle, and on the other hand, it comes from all kinds of equipment

formed in people's long-term entertainment [3–5]. For example, some throwing events mainly come from human long-term war practice, and ball games mainly come from human daily entertainment. The origin of different sports equipment is different, and the diversified sources have created the rich and colorful content of sports.

At present, all kinds of equipment can realize intelligent management. Using the system for system management can facilitate the management of equipment in the process of physical education teaching; especially at present, the management of sports equipment is directly related to the improvement of physical education quality [6]. The state pays special attention to the physical education of teenagers, and the sports equipment management system is mainly a comprehensive information service platform created for sports managers. The main purpose is to obtain a series of information of equipment and obtain the use of equipment through specific instructions. The development of the

system is conducive to expand the development path of school physical education and promote the modern development of management system [7].

In the management of sports equipment, it mainly aims at the secondment management and return management of sports equipment. In the system business process, users can query the actual situation of their returned equipment through the system. The equipment manager mainly counts the equipment and understands the performance of the equipment and inquires about the use of users' equipment. In the management of sports equipment, the most important thing is to manage the borrowing process and return process, as well as the borrowing approval and management process [8–10].

The functional performance requirements of the sports equipment management system need to ensure beauty and cleanliness. At the same time, it should be convenient, fast, easy to operate, able to enter data, ensure a clear user direction and user group, and facilitate user authentication. For example, the implementation of three algorithm steps can be set. Under Windows OS, to ensure the stable operation and powerful function of the system, it also needs strong fault tolerance, emphasizes the expandability and function of the system, and emphasizes the maintainability, development, and portability of the system [11, 12]. It supports keyboard input and mouse operation, which can realize man-machine interactive processing. At the same time, it can also output relevant sports data in combination with the printer to ensure the stable operation of the system.

On the whole, the sports management department assists with the support of the sports equipment management system, helps the department to have time to perform tasks on the job, and provides good data support for the construction of the sports equipment management department.

Internet of things (IOT) is a project that extends and extends its client to any information exchange and network communication based on Internet applications, which is one of the important components of modern information industry [13]. RFID (radio frequency identification) is not only an automatic identification technology but also a key part of the Internet of things technology, which completes noncontact automatic identification by using radio frequency signals for data and energy transmission. The RFID system generally includes tag and reader, and the tag is used to identify the object. The reader reads the information stored on the tag through radio frequency signal and then completes the identification of the object [14]. Compared with the two-dimensional code technology widely used at present, RFID has the advantages of fast reading rate, long reading distance, large information capacity, and high security performance. In addition, it is supported for fast reading and writing, no need for manual attendance, and no need for manual visualization. Through information sharing in the form of Internet, RFID technology can realize the sharing and tracking of relevant item information all over the world [15–17]. Therefore, it can be said that RFID is the cornerstone of the Internet of things.

RFID technology has a large number of applications and great development prospects in many fields such as com-

modity management, transportation and production, manufacturing, and commerce [18]. At present, the main applications of RFID include access control, product tracking, logistics management, intelligent shelf, anticounterfeiting security, and medical device management. RFID is the important foundation of Internet plus and Internet of things. Its development needs to keep pace with the rapid development of Internet plus and Internet of things. Although RFID technology is developing rapidly, it is not mature enough [19]. At this stage, there are two main problems: firstly, the cost of labels. Although the cost of ordinary labels is relatively low, for special applications, such as labels applied to metals and specific forms of goods, the cost is high, and a single identification cannot be completed for all goods. Secondly, the tag performance cannot meet the application requirements of specific size and form, which also hinders the popularization of RFID technology [20].

In practical applications, metal objects are common application carriers. According to the antenna theory, the metal object or surface has a great influence on the antenna. When the ordinary tag antenna is pasted on the metal surface, the reading distance becomes shorter or even cannot be read. Metal-resistant RFID tag refers to RFID tag specially designed for metal environment.

At present, there are two main implementation methods of antimetal labels: ordinary labels add additional materials or structures to form antimetal labels and design tag antennas with specific structures and forms. Adding additional materials or structures to ordinary tags to form antimetal tags mainly includes the following methods: adjusting the distance between the tag antenna and the metal surface, adding absorbing materials between the tag antenna and the metal, and adopting structures such as electromagnetic band gap structure EBG and artificial magnetic conductor AMC [21, 22]. These methods mainly study the external environment of the tag, while the metal resistance of the label is realized by changing the external environment of the label. However, this method has many problems in practical application, and its performance and size may not meet the actual needs. The design of tag antenna with specific structure and form mainly includes the design of microstrip antenna and PIFA antenna. These antennas have metal floor, which can effectively reduce the influence of metal surface on them. This way is to study the structural performance of the antenna itself and ignore the influence of the external metal of the tag antenna [23]. Generally, the so-called design of antimetal tag antenna refers to this specially designed tag antenna form.

For the design of antimetal tag antenna, the antimetal performance of tag antenna should be stable, and the performance changes little on metal carriers of different sizes. Reading distance is the most direct performance identification of the tag antenna. The tag needs to have a long recognition distance and a large recognition range, which requires the tag antenna to have high gain and wide lobe width to facilitate the reading of the tag.

Albrecher et al. [24] studied that the input impedance of ordinary tag antenna by the metal environment, which further affected the reading distance of tag antenna, would

cause some damage to the management of sports equipment. By studying the influence of metal sports equipment of different sizes on the performance of folded dipole antenna, Rodean and Morar [25] pointed out the influence of the size of metal plate of sports equipment on the width of main lobe of antenna and the influence of the distance between metal plate and antenna on the number of main lobe of antenna and found the management method of metal sports equipment. Bogusaw and Elbieta [26] studied the management of sports equipment under different antennas through the budget of wireless link and obtained the antimetal RFID tag, which was helpful to improve the management efficiency of sports equipment. Based on the above research, Patra et al. [27] summarized and analyzed the influence of metal sports equipment on the impedance, transmission coefficient application, and directivity of tag antenna through simulation and experiment and obtained the best management mode of sports equipment.

Based on the antimetal RFID tag, the optimum parameters of the antenna are obtained by this method, and the influence of impedance data on the properties of metal materials is studied. Then, the optimal number of antimetal RFID antennas is obtained. Through the study of the influence of antenna impedance on metal equipment, the corresponding RFID model is established. Then, for the problems existing in the batch management of sports equipment, the batch management behavior of sports equipment is studied in detail based on the antimetal RFID tag model. The results show that the antimetal RFID tag is helpful to improve the efficiency of batch management of sports equipment, which provides a certain model algorithm and experimental data support for the batch management of sports equipment.

## 2. Model Establishment Based on Antimetal RFID Tag

Antimetal RFID antenna is mainly composed of three parts: base plate, dielectric substrate, and radiation patch. The radiation patch can be divided into two parts. The first part digs out a rectangular slot, and the second part inserts a metal patch smaller than the rectangular slot in the middle of the rectangular slot and finally forms an annular slot hole.

When the antenna is bent, the electric field of the microstrip line to the ground has a vector in the tangent direction, which can be equivalent to a capacitor connected in series with the antenna, resulting in the shift of the frequency to high frequency. In order to reduce this effect, the metal coverage area of the antenna can be reduced; that is, the value of series capacitance can be reduced by digging out a rectangular slot. However, this method also increases the flow path of the current on the antenna surface, that is, increases the inductance [28]. In order to weaken this effect, insert a metal patch in the middle of the rectangular slot, and the metal patch is coupled at the upper and lower ends to generate reverse current, which reduces the inductance of the patch antenna and causes the effect of frequency rise.

Therefore, when the antenna is bent, the frequency will rise due to the series capacitance, but the phenomenon of

the shift of the resonant frequency to the high frequency is slowed down due to the excavation of the rectangular groove, and then the effect of the intermediate metal patch is further used to make the antenna resonant frequency shift very small.

In this design, the antimetal RFID antenna adopts the inductive coupling feed structure, which has the advantages of quickly eliminating interference and collecting signals, and can obtain the required information more accurately, and the inductive coupling matching uses the ring resonator to form the feed structure to provide high inductive impedance and then coupled to the radiator. The size of the ring can adjust the reactance, and the coupling strength between the ring and the radiator can adjust the resistance [29]. So, the method is easier in matching design.

The input impedance at the feed of the feed ring is expressed by equation (1):

$$Z_{in} = Z_{loop} + \frac{(2\pi f M)^2}{Z_{rb}}, \quad (1)$$

where  $Z_{loop}$ ,  $M$ , and  $Z_{rb}$  are the input impedance of the feed ring, the mutual inductance between the feed ring and the radiator, and the input impedance of the radiator, respectively. Antenna input impedance is the resistance in the process of antenna input, which reflects the influence of external environment on antenna signal. Based on equation (1), the resistance  $R_{in}$  and reactance  $X_{in}$  of antenna input impedance can be expressed as equations (2) and (3):

$$R_{in}(f_0) = \frac{(2\pi f M)^2}{R_{rb}(f_0)}, \quad (2)$$

$$X_{in}(f_0) = 2\pi f_0 L_{loop}, \quad (3)$$

where  $f_0$  is the working frequency of the antenna, which is the speed at which the antenna receives the signal, reflecting the overall working capacity of the antenna. The higher the working frequency of the antenna is, the better the ability of the antenna to receive signals. According to equation (2), the input resistance of the antenna is determined by the mutual inductance between the feed ring and the radiator, and its size can be adjusted by adjusting the size of the feed ring and the distance between the feed ring and the radiator. For the antenna input reactance, due to the size of the feed ring, such as length, width, and height, it will affect the resistance of the reactance. In addition, mutual inductance effect and radiation effect will affect the input reactance of the antenna. Therefore, it is mainly affected by the size of the feed ring, as shown in equation (4):

$$L_{loop} = 0.4 (L_L + W_L) \ln \left[ \frac{2L_L W_L}{s(L_L + W_L)} \right] (\mu H), \quad (4)$$

where  $L_L$  is the length of the feeder loop,  $W_L$  is the width of the feeder loop, and  $s$  is the line width of the feeder loop.

For a rectangular radiating patch, after considering the short edge effect, which is caused by the difference and



synergy of some energy or information in the rectangular radiation patch, the actual length  $L$  of the radiating element is shown in equation (5):

$$L = \frac{c}{2f\sqrt{\epsilon_{\text{eff}}}} 2\Delta L, \quad (5)$$

where  $c$  is the free space wavelength with a value of  $3.0 \times 10^8$  m/s,  $\epsilon_{\text{eff}}$  is the effective dielectric constant, which is 1.0054,  $\Delta L$  is the equivalent radiation gap length, and it can be expressed by equations (6) and (7), respectively:

$$\Delta L = \frac{(\epsilon_{\text{eff}} + 0.3) ((W/h) + 0.264)}{(\epsilon_{\text{eff}} - 0.258) ((W/h) + 0.8)}, \quad (6)$$

$$\epsilon_{\text{eff}} = \frac{\epsilon_r + 1}{2} + \frac{\epsilon_r - 1}{2} \left[ 1 + 12 \frac{h}{W} \right]^{1/2}, \quad (7)$$

where  $\epsilon_r$  is the relative permittivity of the medium,  $h$  is the thickness of the medium, which refers to the material composition of the antenna, and the thickness of the medium represents the signal receiving ability of the antenna.  $W$  is the width of the rectangular patch.

The inductive coupling feeding is used to make the working frequency of the antimetal RFID antenna conjugate with the chip impedance at 915 MHz. At this time, the substrate  $\text{ise}_r = 3.9$ , and the dielectric loss tangent  $\tan \delta = 0.003$ . The thickness  $h$  of the medium is 1.5 mm, which meets the low profile requirement of the antimetal RFID antenna. When the antimetal RFID antenna is miniaturized, it not only helps to eliminate the interference of metal substances but also has the advantage of receiving signals quickly. What is more, the width  $W$  of the radiation patch is 10 mm, which can meet the miniaturization of the antimetal RFID antenna size.

### 3. Establishment of the Sports Equipment Batch Management System Based on Antimetal RFID Tags

**3.1. System Framework.** The sports equipment batch management system based on antimetal RFID tags is designed with an antimetal RFID frame structure. The C language program is used to design the antimetal RFID management mode, which has good openness and can effectively meet the remote needs of users. The system based on the antimetal RFID management mode is divided into three layers: user interface layer, business logic layer, database layer, and system layered structure. The specific system structure diagram is shown in Figure 1.

From this, it can be seen that in the middle layer, the work completed by the system roughly includes three items: setting business development rules, accessing relevant data, and verifying the legality of business and data. In general, there is no direct interaction between the client and the database. The connection between the two depends on the support of the middle layer, and they complete the data interaction task through the intermediary. The middle layer

has a large amount of data, and the browser of the client can access and communicate well, so as to generate the database. Under the whole structure of the antimetal RFID management system, the browser is the main standard configuration of the client, the web server adopts the standard configuration of the application program, and the database server performs the work of processing related data.

Based on the antimetal RFID management frame structure, the design of the sports equipment batch management system in this paper includes five levels: (1) the network hardware support layer, which provides a networked communication environment to the system users with the help of the campus network, (2) database server layer, centralized and unified management of sports equipment data recorded in the system, (3) system tool library, including each functional module that the system should have, (4) application layer, calling each functional module to play a role of the self-service borrowing and returning system, and (5) user layer, the system user accesses the application program in the server through the browser.

**3.2. System Function Modules.** Combined with the current situation of sports equipment management in a school and the overall goal of system design, the sports equipment management system is divided into two major sub-modules: the front-end functional module and the back-end functional module. Specifically, the front-end module includes three functions of equipment preborrowing, account viewing, and information modification. The back-end module involves two functions of equipment borrowing and returning management and user management. The system function module is showed in Figure 2.

**3.3. Database Design.** In the design of the whole sports equipment management system, the database design is extremely important. The database collects and processes the data. After analyzing it by software, the transformation of data and signal can be realized, so as to promote the smooth implementation of the antimetal RFID label management system framework. Supported by the application of database technology, the very rich data in the system can be reasonably organized and stored, which reduces the redundancy of the data and realizes the data sharing function to ensure the efficiency and security of data processing.

The function modules in the system are designed with rich data fields and types, and their function is to establish the association of applications in each link of the system. Every business in the system will involve more than (or equal to) one data table, which highlights the importance of table structure design and master-slave table design in the database. Analyzing the system requirements, the categories of database tables should be specifically divided based on different functions. As the basic content of database development, database requirement analysis involves three parts: structure analysis, data definition analysis, and integrity analysis.

There are many types of data analysis, including business data, maintenance data, and user data, which can provide favorable conditions for the organization, management,

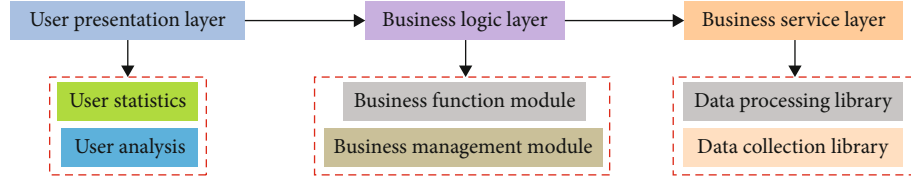


FIGURE 1: Sports equipment batch management system based on antimetal RFID tag.

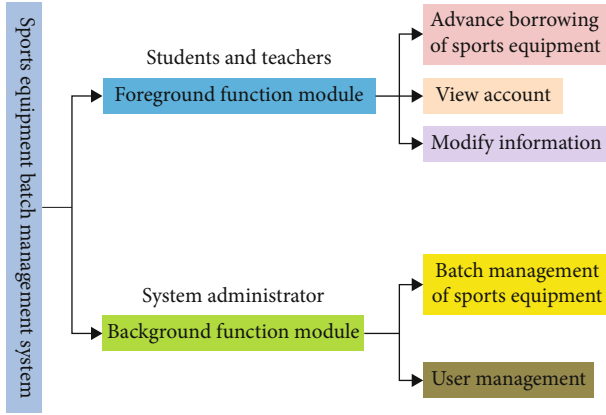


FIGURE 2: Function module of the sports equipment batch management system based on antimetal RFID tag.

and safe storage of system data, ensure the accuracy of the association between tables, and provide strong support for the operation and maintenance of the database.

#### 4. Simulation Results and Analysis

In the antimetal RFID test system, the antenna return loss reflects the signal loss caused by some external reasons in the process of receiving the signal by the antimetal RFID tag. So, the definition of antenna return loss ( $S_{11}$ ) is shown in equation (8):

$$S_{11} = -20, \quad (8)$$

where  $Z_{\text{chip}}$  is the chip impedance, and  $Z_{\text{ant}}^*$  is the conjugate of antenna input impedance. The return loss diagram of metal-resistant RFID tag is shown in Figure 3. It can be seen that when in the plane structure, the working frequency of the antenna will have an adverse impact on the return loss rate and show a fluctuating trend. When the working frequency reaches 0.25 Hz, the lowest return loss rate of the antimetal RFID tag is about -20 dB. Then, with the increase of working frequency, the return loss rate increases gradually. In general, the return loss rate of the antenna-resistant to metal RFID tag is comprehensive, and the maximum benefit of the antenna can be well observed.

The power reflection coefficient is expressed as the ratio of the reflected wave power ( $P_{\text{rfl}}$ ) of the tag antenna to the incident wave power ( $P_{\text{tag}}$ ), as shown in equation (9):

$$\frac{P_{\text{rfl}}}{P_{\text{tag}}} = \left[ \frac{Z_{\text{chip}} - Z_{\text{ant}}^*}{Z_{\text{chip}} + Z_{\text{ant}}^*} \right]^2. \quad (9)$$

Power transmission coefficient ( $\beta$ ) represents the size of the incident wave power transmitted to the label chip, as shown in equation (10):

$$\beta = 1 - \frac{P_{\text{rfl}}}{P_{\text{tag}}}. \quad (10)$$

The power transmission coefficient can reflect the ability of incoming and outgoing radiation to be accepted by the antimetal RFID tag, and the power reflection coefficient is the ability lost by the antimetal RFID tag. In order to measure the reading performance of metal-resistant RFID tags and facilitate recording the behavior of tags under different bending angles, the maximum reading distance  $d$  can be defined for comparison, and the unit is m. The larger the maximum reading distance  $d$ , the stronger the reading performance of antimetal RFID tag and the better the acceptance ability of antenna, as shown in equation (11):

$$d_{\text{tag}} = \frac{\alpha}{4\pi} \sqrt{\frac{G_r P_{\text{EIRP}}}{P_{\text{ir}}}}, \quad (11)$$

where  $P_{\text{EIRP}}$  is the equivalent isotropic power of the transmitter of the reader and here is 3.28 W.  $P_{\text{ir}}$  is the sensitivity of the tag chip, where the value is -18 dBm.  $G_r$  is the simulation of the antimetal RFID tag antenna gain.

Figure 4 shows the variation of power reflection coefficient and power transmission coefficient of antimetal RFID tag antenna with working frequency. It can be seen that with the increase of the operating frequency, the power reflection coefficient of the antimetal RFID tag antenna shows a trend of first increasing and then decreasing. When the frequency is 20 Hz, the value of the power reflection coefficient is the largest. The power transfer coefficient gradually decreases, and at 10 Hz, the power transfer coefficient is close to zero. The above results show that metal substances will not affect the normal use of the antimetal RFID tag antenna, the sensitivity is low, the antenna performance is good, the application range is wide, and it has good application potential.

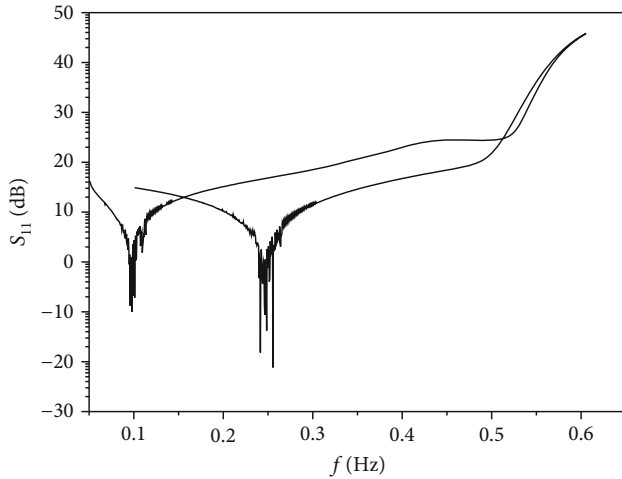


FIGURE 3: Return loss diagram of metal-resistant RFID tag.

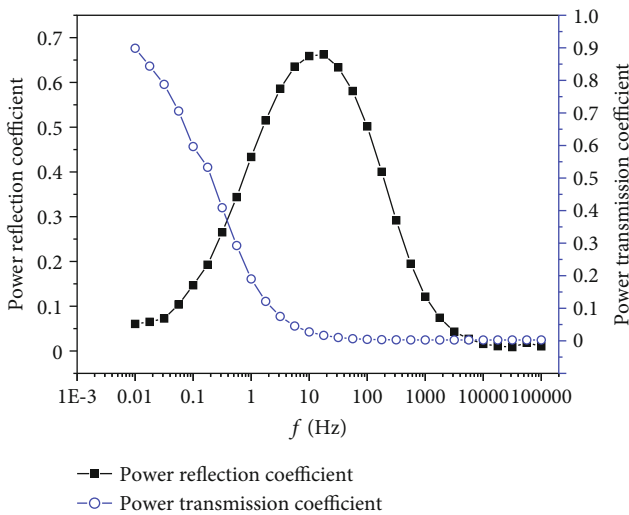


FIGURE 4: Variation of power reflection coefficient and power transmission coefficient of antimetal RFID tag antenna with working frequency.

## 5. Application of Antimetal RFID Tag in Batch Management of Sports Equipment

**5.1. Application of Antimetal RFID Tag in Batch Management of Sports Equipment.** There are two factors in the development of physical exercise activities. In addition to the sports equipment, the sports ground is also a very important factor. Therefore, improving the sports ground and supporting facilities also has a very positive practical significance for improving the application of sports equipment. On the basis of fully understanding the actual situation of the sports ground, managers need to make reasonable arrangements for the limited venues to ensure that the sports ground can fully meet the exercise needs of different people. On this basis, corresponding supporting facilities should be set around the sports ground, so as to effectively improve the utilization rate of the sports ground. In addition, with the increase of the capacity of sports venues, the overall uti-

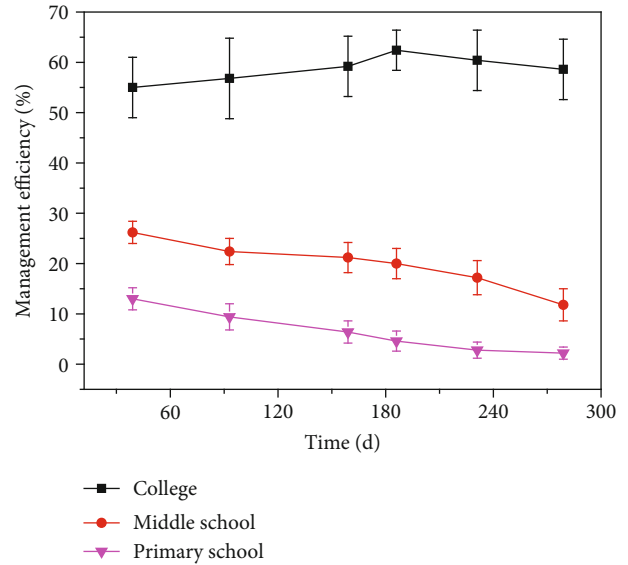


FIGURE 5: Analysis of batch management of sports equipment based on metal RFID tag between different schools.

lization efficiency of sports equipment will be improved accordingly. Antimetal RFID tags can build a management platform. Based on this platform, sports equipment can be managed in batches.

According to the management of sports equipment in various schools, this paper discusses the application analysis in colleges, middle schools, and primary schools. Figure 5 is the analysis of batch management of sports equipment based on metal RFID tag between different schools. It can be seen that with the increase of application time, the management efficiency of sports equipment in primary and secondary schools gradually decreases, and the management efficiency of sports equipment in primary schools is the lowest. The management efficiency of sports equipment in colleges shows a gradual upward trend with the increase of application time. The main reason may be that college students have enough time and love sports. Therefore, with the increase of time, the management efficiency of sports equipment increases gradually. For primary and middle school students, their curriculum tasks are heavy, and they can rarely participate in sports; so, the management efficiency of sports equipment is low.

**5.2. Application Effect of Antimetal RFID Tag in Batch Management of Sports Equipment.** Modern people's pace of life is speeding up, and they also strive to be efficient in the process of participating in physical exercise. Therefore, for some large-scale sports equipment, due to the relatively complex lending procedures and high return difficulty, most people tend to stay away and have low utilization efficiency. In view of this situation, in order to effectively improve the utilization rate of equipment, the relevant responsible personnel of the gymnasium can try to provide some simple equipment for the personnel participating in physical exercise, which can effectively achieve the purpose of exercise on the one hand and effectively improve the overall exercise efficiency of the personnel participating in physical exercise

on the other hand. For example, in the exercise of waist strength, large-scale sports equipment was used to achieve the goal of exercise in the past. However, due to the relatively large floor area of these sports equipment, it is difficult to meet people's growing sports needs. In view of this situation, the gymnasium can try to add some simple equipment such as hula hoops and fitness balls. In this way, it can not only effectively meet people's sports needs but also have a very positive practical significance for improving the utilization rate of sports equipment.

Figure 6 shows the utilization rate of different sports equipment among different schools. It can be seen that college students prefer basketball, followed by volleyball and badminton, and finally football. For middle school students, the utilization rate of tennis is the highest, and that of football is the lowest. The use of primary and secondary school students is similar, but also, they prefer volleyball to football. In short, no matter what kind of students, the students do not like football. The above results require that when using the antimetal RFID tag sports equipment batch management system, we should carry out classified management according to the students' hobbies, so as to improve the efficiency of sports equipment batch management and promote the wide application of sports equipment.

**5.3. Satisfaction Analysis of Antimetal RFID Tags between Different Schools in Batch Management of Sports Equipment.** In the sports equipment management system, the authority of teachers should be granted the ability of the management system. In the specific design process, teachers can be divided into several types, such as system management teachers, sports equipment management teachers, and sports equipment management responsible teachers. The teacher management system is responsible for system registration and borrowing and returning equipment. This link is the core of managing the main database. The second is the class form. The class form is the statistics of students in each class in the school and the form filled by students in the class taught by teachers. When students in a class need to use sports equipment, they should show personal information data, such as student ID card. After the teacher determines the student identity and class, they can borrow sports equipment uniformly. When the borrower returns the equipment, the administrator changes and records the real situation again. For the return record form, when the teacher or student is returning it, the system can automatically update it and mix and analyze the record form at the same time. The system can also query the students or teachers who have not returned the equipment and even remind the teachers to replace the equipment in time in the process of actual use.

The degree of satisfaction of antimetal RFID tags between different schools in batch management of sports equipment is shown in Figure 7. It can be seen that for students, college students are the most satisfied with this management system, followed by middle school students, and primary school students are the least satisfied. For teachers, it is consistent with the satisfaction of students; that is, university teachers are most satisfied with the management sys-

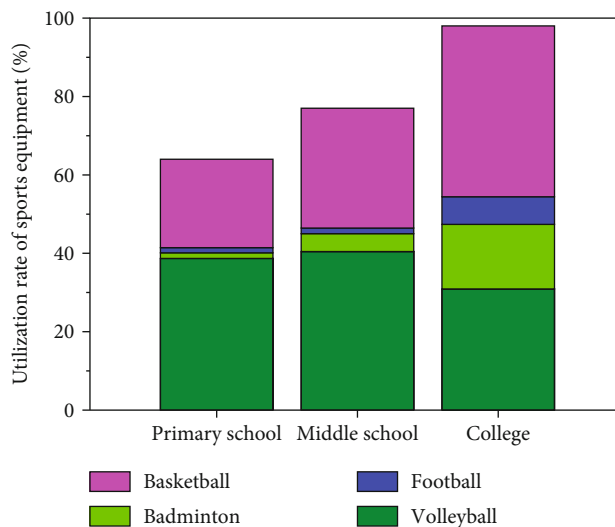


FIGURE 6: Utilization rate of different sports equipment among different schools.

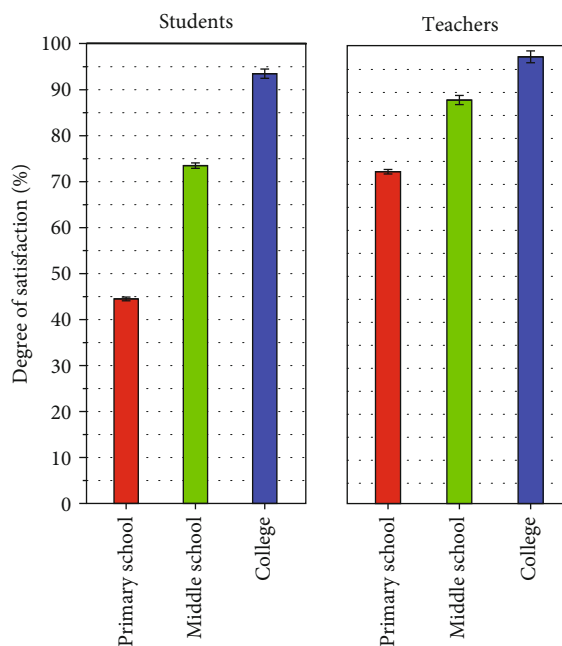


FIGURE 7: Degree of satisfaction of antimetal RFID tags between different schools in batch management of sports equipment.

tem, and primary school teachers are the least satisfied. However, it is worth noting that compared with students, the satisfaction of teachers in similar schools is higher than that of students. The main reason may be that college students are adults, have the ability to distinguish right from wrong and autonomous learning, and can well adapt to the management system of sports equipment. However, middle school students are not familiar with this system and have heavy studies; so, their satisfaction with it is low. For primary school students, their autonomous learning ability needs to be strengthened, and they are young; so, it is difficult to adapt to such scientific and technological sports

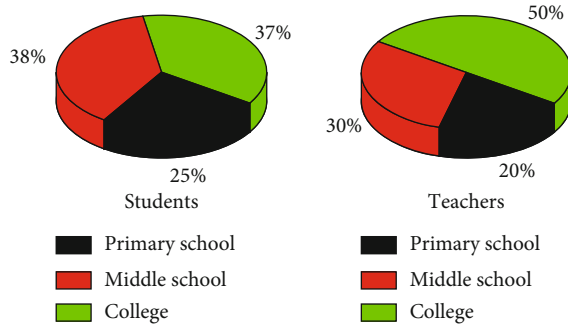


FIGURE 8: Proportion of satisfaction of teachers and students in batch management of sports equipment in different schools.

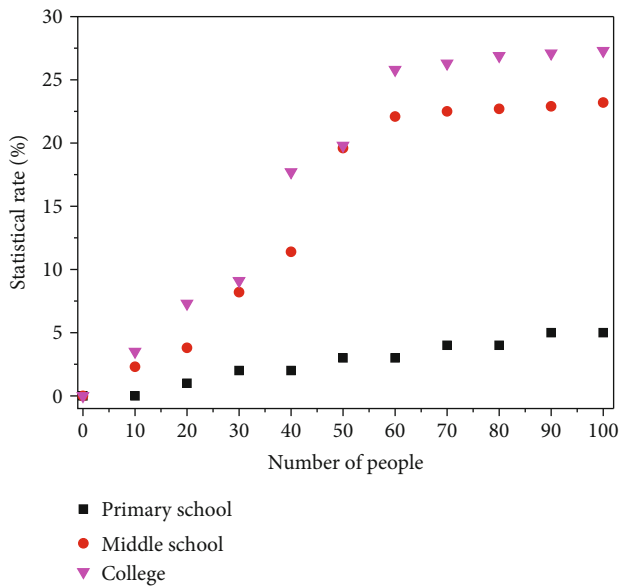


FIGURE 9: Statistical rate of antimetal RFID tags between different schools in batch management of sports equipment.

equipment management systems. Although teachers can quickly adapt to this management system, due to the different learning ability and cooperation ability among students, the satisfaction of teachers is different. Because teachers are managers of sports equipment and students are users, their different identities lead to different satisfaction.

Figure 8 shows the proportion of satisfaction of teachers and students in batch management of sports equipment in different schools. For students, middle school students account for the largest proportion, followed by college students and finally primary school students, but there is little difference between the three, and the data are very close. For teachers, the proportion of university teachers is the highest, up to 50%, followed by middle school teachers and primary school teachers. In general, the proportion of students' and teachers' satisfaction is different among different schools, which also reflects the applicability and universality of antimetal RFID tags in the batch management of sports equipment.

5.4. *Statistical Results of Antimetal RFID Tags between Different Schools in Batch Management of Sports Equipment.* Because it is the study of sports equipment management between different schools, in the analysis, we should focus on the differences between different schools, so as to provide experimental support for the popular application of sports equipment. Figure 9 shows the statistical rate of antimetal RFID tags between different schools in batch management of sports equipment. It can be seen that with the increase of the number of students, the statistical rates of primary school students are low, and the statistical rates of middle school students and college students gradually increase and then tend to be stable. The main reason is that middle school students and college students have established a safety guarantee system to correct the problems found in the system, eliminate them in management, and eliminate them in action. We should always adhere to the principle that the expansion of sports facilities is not only the safety of teachers and students but also the safety of students. Form a professional safety management and inspection team to investigate possible hidden dangers and improve the use safety of sports equipment. At the same time, we should also mobilize the majority of students to screen the possible problems, increase the manpower in safety protection, and reduce the possible damage.

## 6. Conclusion

The sports equipment batch management system based on antimetal RFID tag is mainly to ensure the standardization and rationalization of sports equipment management and effectively improve the batch management efficiency of sports equipment by building an effective management information system. This paper discusses the model establishment process of antimetal RFID tag and analyzes the framework of the sports equipment batch management system based on antimetal RFID tag in detail. Then, apply the antimetal RFID tag sports equipment batch management system to colleges, middle schools, and primary schools, study the application of the batch management system, and realize independent management, which provides some ideas and research methods for building an intelligent modern education environment.

## Data Availability

The data used to support the findings of this study are available from the corresponding author upon request.

## Conflicts of Interest

The authors declare that they have no known competing financial interests or personal relationships that could have appeared to influence the work reported in this paper.

## References

- [1] N. Zhang, H. Zhu, X. Li, G. Gao, and Z. Qi, "UHF pure near-field RFID reader antenna based on CSRR," *IET Microwaves Antennas & Propagation*, vol. 14, no. 7, pp. 634–642, 2020.

- [2] S. R. Lee, E. H. Lim, F. L. Bong, and B. K. Chung, "High-efficient compact folded-patch antenna fed by T-shaped L-probe for on-metal UHF RFID tag design," *IEEE Transactions on Antennas and Propagation*, vol. 68, no. 1, pp. 152–160, 2020.
- [3] Y. Xu, L. Dong, H. Wang, X. Xie, and P. Wang, "Surface crack detection and monitoring in metal structure using RFID tag," *Sensor Review*, vol. 40, no. 1, pp. 81–88, 2020.
- [4] F. Deng, K. Wen, H. Zeng, and Z. Xie, "Novel metal-oxide arrester monitoring technology based on RFID sensor and mind evolutionary computation," *Electric Power Systems Research*, vol. 192, p. 106859, 2021.
- [5] G. Masella, N. V. Prokof'ev, and G. Pupillo, "Anti-drude metal of bosons," *Nature Communications*, vol. 13, no. 1, pp. 1–7, 2021.
- [6] Y. H. Lee, C. W. Moh, E. H. Lim, F. L. Bong, and B. K. Chung, "Miniature folded patch with differential coplanar feedline for metal mountable UHF RFID tag," *IEEE Journal of Radio Frequency Identification*, vol. 4, no. 2, pp. 93–100, 2020.
- [7] L. J. Gortschacher, F. Amtmann, U. Muehlmann, E. Merlin, P. Priller, and J. Grosinger, "Passive HF RFID repeater for communicating with tags in metal housings," *IEEE Antennas and Wireless Propagation Letters*, vol. 19, no. 9, pp. 1625–1629, 2020.
- [8] X. Li, G. Gao, H. Zhu, Q. Li, N. Zhang, and Z. Qi, "UHF RFID tag antenna based on the DLS-EBG structure for metallic objects," *IET Microwaves, Antennas & Propagation*, vol. 14, no. 7, pp. 567–572, 2020.
- [9] S. R. Lee, W. H. Ng, E. H. Lim, F. L. Bong, and B. K. Chung, "Compact magnetic loop antenna for omnidirectional on-metal UHF tag design," *IEEE Transactions on Antennas and Propagation*, vol. 68, no. 2, pp. 765–772, 2020.
- [10] N. Ripin, E. H. Lim, F. L. Bong, and B. K. Chung, "Miniature folded dipolar patch with embedded AMC for metal mountable tag design," *Transactions on Antennas and Propagation*, vol. 68, no. 5, pp. 3525–3533, 2020.
- [11] Z. Zhou, C. Qian, and W. Yuan, "Self-healing, anti-freezing, adhesive and remoldable hydrogel sensor with ion-liquid metal dual conductivity for biomimetic skin," *Composites Science and Technology*, vol. 203, p. 108608, 2021.
- [12] Z. C. Wang, N. V. Tkachenko, L. Qiao et al., "All-metal  $\sigma$ -antiaromaticity in dimeric cluster anion  $\{[\text{CuGe}_9\text{Mes}]_2\}^{4-}$ ," *Chemical Communications*, vol. 56, no. 48, pp. 6583–6586, 2020.
- [13] A. Mazinghi and A. Freni, "2-Dipoles circularly-polarized antenna integrated in lamp holder for fixed RFID reader," *IEEE Access*, vol. 8, pp. 84134–84140, 2020.
- [14] M. H. Hassan, B. Sievert, J. T. Svejda et al., "OAM mode order conversion and clutter rejection with OAM-coded RFID tags," *IEEE Access*, vol. 8, pp. 218729–218738, 2020.
- [15] P. Sen, S. Kantareddy, R. Bhattacharyya, S. E. Sarma, and J. E. Siegel, "Low-cost diaper wetness detection using hydrogel-based RFID tags," *IEEE Sensors Journal*, vol. 20, no. 6, pp. 3293–3302, 2020.
- [16] Y. T. Chang, S. Lee, and H. K. Park, "Efficiency analysis of major cruise lines," *Tourism Management*, vol. 58, pp. 78–88, 2017.
- [17] N. Agrawal, "An integrated benchmarking efficiency analysis of the Indian banking industry using data envelopment analysis," *International Journal of Process Management and Benchmarking*, vol. 11, no. 5, pp. 671–692, 2021.
- [18] W. Vereycken, S. Riaño, T. Van Gerven, and K. Binnemans, "Continuous counter-current ionic liquid metathesis in mixer-settlers: efficiency analysis and comparison with batch operation," vol. 10, no. 2, pp. 946–955, 2022.
- [19] L. Yu, X. Zhao, X. Gao et al., "Effect of natural factors and management practices on agricultural water use efficiency under drought: a meta-analysis of global drylands," *Journal of Hydrology*, vol. 594, no. 3, p. 125977, 2021.
- [20] P. Li, Z. Cao, R. Zhao, G. Li, M. Yu, and S. Zhang, "The kinetics and efficiency of batch ball grinding with cemented tungsten carbide balls," *Advanced Powder Technology*, vol. 31, no. 6, pp. 2412–2420, 2020.
- [21] A. Saavedra-Nieves and M. G. Fiestras-Janeiro, "Analysis of the impact of DMUs on the overall efficiency in the event of a merger," *Expert Systems with Applications*, vol. 195, p. 116571, 2022.
- [22] Y. Kozmenkov, M. Jobst, S. Kliem, K. Kosowski, F. Schaefer, and P. Wilhelm, "The efficiency of sequential accident management measures for a German PWR under prolonged SBO conditions," *Nuclear Engineering and Design*, vol. 363, p. 110663, 2020.
- [23] C. R. BrunoThibault and S. Khalloufi, "A mathematical tool for estimating the efficiency of pore formation during dehydration," *Journal of Food Engineering*, vol. 323, p. 110981, 2022.
- [24] H. Albrecher, M. Bladt, and E. Vatamidou, "Efficient simulation of ruin probabilities when claims are mixtures of heavy and light tails," *Methodology and Computing in Applied Probability*, vol. 23, no. 4, pp. 1237–1255, 2021.
- [25] I. Rodean and D. Morar, "Live operating and efficiency of equipment's management," in *2017 12th International Conference on Live Maintenance*, pp. 1–6, Strasbourg, France, April 2017.
- [26] C. Bogusaw and C. Elbieta, "Efficiency and equity – the Swedish economy in comparison to other countries at the beginning of the 21st century," *International Journal of Management and Economics*, vol. 57, no. 3, pp. 255–267, 2021.
- [27] K. Patra, A. Sengupta, A. Boda et al., "Mechanism unravelling for highly efficient and selective  $99\text{TcO}_4$ -sequestration utilising crown ether based solvent system from nuclear liquid waste: experimental and computational investigations," *RSC Advances*, vol. 12, no. 6, pp. 3216–3226, 2022.
- [28] Y. Tan and D. Despotis, "Investigation of efficiency in the UK hotel industry: a network data envelopment analysis approach," *International Journal of Contemporary Hospitality Management*, vol. 33, no. 3, pp. 1080–1104, 2021.
- [29] C. B. Lvarez and P. Adhikari, "Management accounting practices and efficiency in a Colombian multi-utility conglomerate," *Journal of Accounting in Emerging Economies*, vol. 11, no. 5, pp. 714–734, 2021.

## Research Article

# Application of Fine Motion Capture Method for Tai Chi Chuan Assistant Training

Wenbo Li <sup>1,2</sup>

<sup>1</sup>Chinese Wushu Academy, Beijing Sport University, Beijing 100084, China

<sup>2</sup>Department of Physical Education, China University of Geosciences (Beijing), Beijing 100083, China

Correspondence should be addressed to Wenbo Li; 2019010017@cugb.edu.cn

Received 26 February 2022; Revised 13 April 2022; Accepted 26 April 2022; Published 13 May 2022

Academic Editor: Yanqiong Li

Copyright © 2022 Wenbo Li. This is an open access article distributed under the Creative Commons Attribution License, which permits unrestricted use, distribution, and reproduction in any medium, provided the original work is properly cited.

Tai Chi Chuan is an important part of Chinese wushu and is the product of the Chinese civilization; it contains abundant philosophy sense. Tai Chi Chuan has experienced a long historical process of development; in the process of development and change numerous for brief, to the rough, now widely process of Tai Chi Chuan for its style is easy to learn and has a strong role of strengthening the body while widely popular among the people of all ages. The existing Tai Chi Chuan training methods have not satisfied people's pursuit of spiritual life that has more and more high request, therefore urgently needs to study new and efficient Tai Chi Chuan training method. In this paper, the characteristics and development history of the Tai Chi Chuan development were analyzed. In order to overcome difficulties in training, at present, the research on application of AI technology with fine motion capture method auxiliary taijiquan training is aimed at, which can further improve the social mass to understand Tai Chi Chuan, and guide people to exercise more scientifically, improve the body quality, training effect, and enrich the spiritual and cultural life.

## 1. Introduction

With the continuous development of our social economy, the quality of people's living standard continues to improve; the pursuit of health also is rising, so more and more social masses choose through sports to improve their physical quality and health level. Tai Chi Chuan is a training sport chosen by a lot of people. It is a fist of the traditional martial arts in China, through the scientific exercise, it can improve human body functions, and has a positive effect to improve people's health level.

The schemes of Tai Chi Chuan training are shown in Figure 1. It shows that Tai Chi Chuan is a traditional sport, which with the function of curing not ill, adjusting body and mind, and the rich national cultural charm. Therefore, it is widely popular with the masses.

Tai Chi Chuan is one of China traditional martial arts and has been listed as world nonmaterial cultural heritage. It is a blend of traditional Chinese Confucianism, Taoist philosophy of Tai Chi, and dialectical thought of Yin and Yang; sets the temperament; strengthens physical health care; and

combats against a variety of functions and combined with the five element changes of Yin and Yang of medicine and Chinese medicine meridian. There were many different taijiquan factions in the history; there are reference and inheritance relationship among the various factions; each Tai Chi Chuan factions made outstanding contribution for the development of China's traditional culture. Tai Chi Chuan not only contains martial arts and philosophy but it also absorbs the traditional medicine meridian, qi, and blood, such as guiding theory. It conforms to the ancient Chinese medicine of traditional Chinese medicine and physical knowledge, to Tai Chi Chuan physical activity for a long time, can have very good training effect, and makes the person body quality enhances unceasingly. Many scholars around the world have done lots of research works on the development status and training methods of Tai Chi Chuan course, which will promote the Tai Chi Chuan movement conducted in-depth, and achieved fruitful research results. Li et al. [1–3] studied the Tai Chi Chuan training effect on the well-being of the elderly, and the study results shown that Tai Chi Chuan training can promote the exchanges



FIGURE 1: Diagram of Tai Chi Chuan training.

and promote the physical training and literacy of old people in a certain extent, to let them in a larger extent and improve the well-being. Jiménez-Martín et al. [4] studied the influence of three different modalities Tai Chi Chuan to people body of clinical cases and found that most common forms used in the research design associated with TCC correspond to those linked to the sports modality of this activity, while the forms associated with the therapeutic modality are scarcely present. Domestic and foreign relevant scholars [5–10] carried out much research work about assistant training method for Tai Chi Chuan movement; the research work on the dissemination and promotion of Tai Chi Chuan has played a positive role. With the development of competitive sports, many scholars studied the difference training methods between the traditional Tai Chi Chuan and competitive Tai Chi Chuan, and some reasonable training suggestions were made out for competitive Tai Chi Chuan and traditional Tai Chi Chuan training, respectively, for Tai Chi to adapt to different people playing a promoting role.

The cultural connotation, characteristics, and the development of Tai Chi Chuan and the shortage of its common training methods are studied in this paper, in order to a better support training and improve training efficiency and effectiveness; a method about fine motion capture Tai Chi Chuan assistant training is researched by combining with AI technology. It can improve the training efficiency and effectiveness for Tai Chi Chuan training, and for Tai Chi Chuan, better promotion also plays a positive role.

## 2. Related Works

**2.1. Development History of Tai Chi Chuan.** Tai Chi Chuan is one of Chinese martial arts, and in the form of a genre [1, 11–13], it draws on many other martial arts genre theory and technology of the essence. Before the warring states period, the taijiquan theory has formed the basis of the theoretical system; many technical elements about Tai Chi Chuan have been derived. In the late Ming dynasty, the complete concept of Tai Chi Chuan, its theory, and technology architecture began to appear. Several important genres of Tai Chi Chuan are widely popular both at home and abroad from Qing dynasty derivation and are developed gradually. The theory system of Tai Chi Chuan was the complete form in Ming dynasty and to early Qing period. In Qing dynasty, the first development peak time of Tai Chi Chuan appeared, and the major genres of Tai Chi Chuan

began to appear in this period. In 1950s, Tai Chi Chuan started from family local area, widely to the society. Such as the soft boxing club, Wu-dang Tai Chi Chuan. In advance Tai Chi Chuan, Spring Tai Chi Chuan club was established in Shanghai, YongNian Tai Chi Chuan club was established in Beijing. These clubs supported the public to learn Tai Chi Chuan [14–18] and the famous Tai Chi Chuan agencies. During this period, much research works about Tai Chi Chuan have been carried out, and some of the academic scientific insights are actively advocating Tai Chi Chuan. Among them, the more representative includes Tang Hao, Xu Zhedong, etc.; they devote a great deal of energy to study the history of Tai Chi Chuan.

After the founding of new China, Tai Chi Chuan gets unprecedented development; it becomes the real service for mass sports fitness method and mass towards the world and makes the Chinese nation excellent culture shared by all over the world. In the 1950s, China's national sports commission sports department of the martial arts division organized a number of Tai Chi Chuan experts to choreographing the 24 types of simplified Tai Chi Chuan.

Today, Tai Chi Chuan has become a kind of fitness exercise, which has a wide influence and attracts people to participate in worldwide. As its participation and influence is big, international cultural experts call it "the world's fitness brand."

**2.2. Characteristics of Tai Chi Chuan.** Tai Chi Chuan [19–22] is a blend of Chinese traditional philosophy, ethics, art, and aesthetics, keeping in good health, literature, painting, calligraphy, music, dance, drama, and many other cultural factors.

The movement characteristic of Tai Chi Chuan is a unique sport of waist axis of limb flexion and rotation speed of uniform circular motion, which is different from other sports. The waist as the axis of limb flexion and rotation speed of uniform circle movement is the main part of the taijiquan movement; it plays a major role in the Tai Chi Chuan movement. By seizing the individuality movement characteristic of Tai Chi Chuan, its characteristic is easy soft, round living nature, hips, and continuous, clear, flexibility, spiral wound. These dynamic image is driving from the waist to the limb extremely slow to fast, and "virtual and real" two kinds of motion process cycle of uniform circle movement of speed. It is the symbol of Tai Chi Chuan.

**2.3. Main Training Method and Content of Tai Chi Chuan.** The systematic training for Tai Chi Chuan can be divided into five stages [22–25]; they are learning shelf, fixing shelf, kneading shelf, along shelf, and opening shelf. Through the five stages of training, you will be able to systematically master authentic Tai Chi Chuan.

The first stage is learning the shelf (understand rules, skilled routine). Learn shelf stage is the early stages of practice of Tai Chi Chuan. At this stage, you need to master the basic action of simple. The basic action includes fixed step hand silk action and skilled cooperate gait coordination practice. After these preliminary exercises, you will understand the basic movements, footwork, hand type, and step



type of Tai Chi Chuan and get the basic characteristics and style of Tai Chi Chuan. This stage must be conscientious and a recruit type to practice and do not rush. After a period of practice, repeated practice makes the routine more skilled and strengthens memory. Then, to do it in a relaxation, soft, natural, and easy state, and get rid of its frozen, which you can finally achieve more skilled, drill down naturally.

The second stage is fixing shelf (master requirement, embody characteristics). After completing the first stage Tai Chi Chuan training and a period of practice to action after skilled, you can get into the second stage. This stage is about fixing shelf training for Tai Chi Chuan; in this stage, you need according to the requirements of Tai Chi Chuan for each part and complete set of shelves to correct generally; the relatively obvious common faults should be corrected and demonstrate the basic movement characteristics of Tai Chi Chuan.

The third stage is kneading shelf (adjust the posture to accurate). In the third stage, when training each set of Tai Chi Chuan boxing, you should put each part of your body in right place in accordance with Tai Chi Chuan standard action, make sure each part of your body meets the requirements. At this stage, you should make sure each set of Tai Chi Chuan boxing stretch generous gestures, and make sure your posture is unbiased, center of gravity is accurate.

The fourth stage is alonging the shelf (along with nature, highlight style). In the fourth stage, along the shelf is based on the stage of kneading shelf to make sure that each set frame of Tai Chi Chuan boxing is according to the requirements of the flowing, continuous runs throughout. Exercise style of this period requires to do “fast and not random, slow and do not come loose, light and not superficial, sink and not frozen.” Conform to the boxing theory of up and down parts in the whole, waist as the axis, successively permeate, and achieve hand-eye step posture of coordination and pneumatic power full reunion realm.

The fifth stage is opening shelf (usage is clear, change freely). Based on the four stages of Tai Chi Chuan basic training, your set of Tai Chi Chuan can reach a certain level. And then, you can get into the fifth stage (opening shelf stage); at this stage, you need to analyze each posture movement apart based on posture standard specification and basic skills of solid, which is not only to learning but also to knowing why to do like this. It is to understand the intention of each movement, know that every boxing potential of meaning and its change in different situations, know each usage of flexibility, make sure what you can really grasp, and improve your practical combat level.

**2.4. Main Problems in Tai Chi Chuan Training.** Through consulting relevant data and investigation questionnaire, we found that the current social masses give supportive to practice Tai Chi Chuan generally; due to it helps in improving the quality of the human body and reducing body problems caused by long bow sitting such as lumbar disc of office workers and students. But learning and training Tai Chi Chuan are restricted by time, place, and training cost and can not to the public scope of better promotion. Now, the following problems exist in Tai Chi Chuan training learners.

**2.4.1. Lack of Teaching Resources.** At present, although the Tai Chi Chuan is welcomed by the masses, but there are a relatively small number of professional Tai Chi Chuan coaches, and their teaching levels of the good and bad are intermingled. It is very bad to the popularization of Tai Chi Chuan promotion.

Network video teaching for Tai Chi Chuan is also in a process of development, but this way is lack of the interaction communication between teaching staff and students; students are easy to form withdrawn action. In addition, the Tai Chi Chuan training venues are one of the main problems of restricting its propulsion; the professional Tai Chi Chuan teaching and training are seldom on the market.

**2.4.2. Trainees Learn Quickly but Lack of Capability.** In the fierce competition in the Tai Chi Chuan athletic field, performance is the only measure. Coaches and athletes all hope get a good result as early as possible, which will lead lack of enough attention and patience to athletes' skill training process usually. The spoil things type of enthusiasm training by excessive is formed, which has violated the law of development of sports training and physical, and causing athlete has a lot of injuries. Basic skills are the foundation of all the sports, if the basic skills are not practiced well enough, and it is impossible to improve technology level. Without basic skill for protection, the technical main point is difficult to accurately, and exercise levels cannot reflect in action.

### 3. Assistant Training Research

**3.1. Introduction about Assistant Training Method.** With the rapid development of computer technology [26–29], the motion capture technology and other fields of science and technology are gradually applied to physical education teaching. The Tai Chi Chuan teaching activities have very strong practicality and motion capture technology applied to Tai Chi Chuan training, can be used as a proper complement to traditional teaching, are used to overcome the shortage of the traditional training methods, and promote efficiency of Tai Chi Chuan teaching.

Rapid popularization and development of computer network technology have made it possible to apply technology to Tai Chi Chuan teaching. Through the combination of motion capture technology and traditional teaching can make up inherent defects of traditional teaching methods and forms. Fine motion capture technology is a technology to collect changes of human body movement and space displacement by sensor devices and transformed them into digital model.

In recent years, this technology has been widely applied to many fields and got very good development in the assistant training teaching. An assistant training system can observe student training position from multiple visual based on motion capture technology and with analyzing the movement parameters that got by sensor devices, which can provide more scientific, more intuitive, and reliable training advice for students. It can improve the learning efficiency and achieve the goal of assistant training.

**3.2. Tai Chi Chuan Assistant Training Method.** In this paper, we study the application of AI technology, and using fine motion capture assistant method for Tai Chi Chuan training, the technical process diagram is shown in Figure 2.

As shown in Figure 2, we can see that teaching video library and AI study and analysis algorithm are the difficult points, in the process of the fine motion capture method for Tai Chi Chun assistant training. Thus, determining what is the Tai Chi Chun standard action and how to evaluate students training are the focus in the study of this paper.

**3.3. Assistant Training System Design.** According to Section 3.2 of the Tai Chi Chuan assistant training analysis, through access to sports training assistant system design of related data, questionnaire survey, and market research to the social populace, Tai Chi Chuan assistant training system should have as follows: (1) AI autonomous learning ability of Tai Chi Chuan for standard action learning and phonetic explanation, (2) fine motion capture for students training action and expression, and (3) according to the accumulation of autonomous learning, trainees' training movements should be evaluated by assistant training system; if it needs to improve, some corresponding opinions and action demonstration should be put forward, otherwise will this action as examples of autonomous learning, etc.

The main functions and the main components of the Tai Chi Chuan fine motion capture assistant training system are shown in Figure 3.

Figure 3 shows the main functions and main components of the fine motion capture assistant training system for Tai Chi Chuan. We can see that the main functions of fine motion capture assistant training system are self-learning Tai Chi Chun teaching method, capturing trainers' training movements, reading and evaluation training movement, giving suggestions for improvement, human-machine interaction, etc., while its main components of fine motion capture assistant training system are equitable wearing equipment, motion capture camera, CPU for computing processing, screen for human-machine interaction, etc. By the way, the assistant training system should also small, easy to carry and convenient erection of use, etc.

The main function modules and functions of Tai chi assistant training system are shown as Figure 4.

Figure 4 shows that the Tai Chi Chuan assistant training system based on fine motion capture mainly contains four function modules; they are self-learning module, motion acquisition module, and test scoring module. Self-learning module can learn teaching video of Tai chi Chuan standard movements in the database autonomously. Motion acquisition module can collect the movements of trainee training Tai Chi Chuan, then filtering, noise reduction, and storage the physical parameters. Test scoring module can match physical parameters of students to the physical parameters in the database automatically and compared with the teaching video database standard action to get student training function of action points. Improvement proposal module can put forward concrete suggestions on promotion of student training actions according to the first three modules of data accumulation condition.

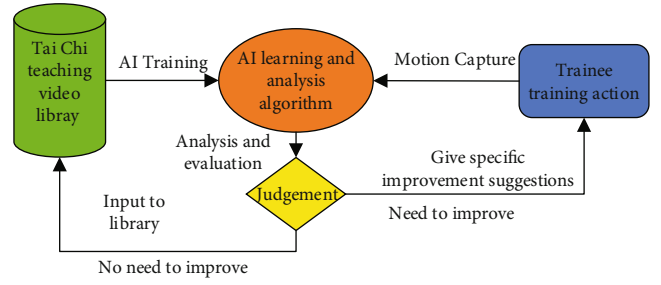


FIGURE 2: Schematic diagram of Tai Chi Chun assistant training.

Among them, to ensure the objective evaluation system of assistant training system is correct, the Tai Chi Chuan teaching video material should cover each age stage from 28 to 65 years old, cover height from 155 to 195 mm, and male and female faculty ratio of 1:1. Teaching video data requirements are shown as follows:

$$\begin{cases} \text{age} = [18, 65], \\ H = [150, 195], \\ \text{male} : \text{female} = 1 : 1. \end{cases} \quad (1)$$

For more detailed, better capture the trainees' Tai Chi Chuan training action and action evaluation work, structure diagram of human body is established according to the characters of the human body structure as shown in Figure 5(a).

Figure 5(b) is the human body structure simplified model. The black nodes in the figure represent each key moving part of the human body, respectively; the specific relations of them are shown in Table 1.

In order to describe trainees' movements of Tai Chi Chuan training more scientifically and precisely, the human body structure is simplified into the 13 nodes. The degrees of freedom at each node have a different direction, mainly including before and after, left, right, and rotation. And the testing body geometry center is set as the origin of coordinates, and a three-dimensional space rectangular coordinate system is established. The X axis is pointing to the human body in front, the Y axis is pointing to the opposite direction of gravity, and Z axis is pointing to the left side of the body. Each point location can be expressed by vector  $\mathbf{a}$ ,  $\mathbf{b}$ , ...,  $\mathbf{n}$ , respectively.

$$\mathbf{a} = [A_x A_y A_z A_\theta], \quad (2)$$

$$\mathbf{b} = [B_x B_y B_z B_\theta], \quad (3)$$

$$\mathbf{c} = [C_x C_y C_z C_\theta]. \quad (4)$$

The vector formulas (2), (3), and (4) represent the positions of the 3 key nodes shown in 0(b) in the space coordinate system, and the remaining 10 key node positions can be obtained using the same method. Each element in a vector represents the key node in the three-dimensional space coordinate X, Y, and Z coordinate values and the rotation angle value of the node. A matrix of  $13 \times 4\mathbf{R}_t$  can be

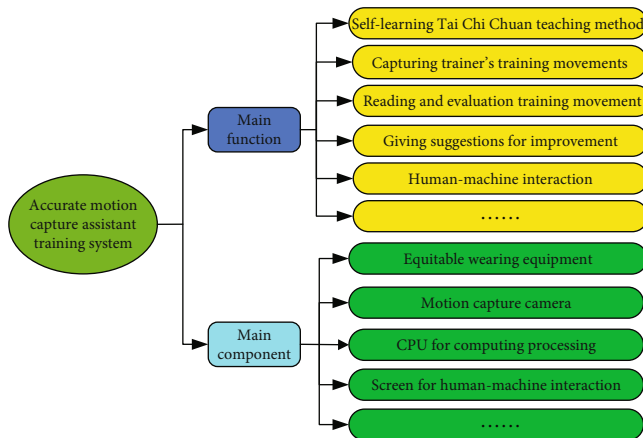


FIGURE 3: The main function and composition of fine motion capture assistant training system.

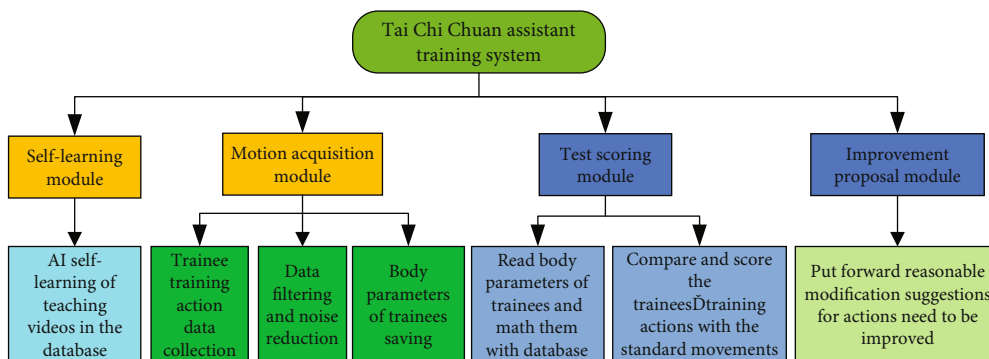


FIGURE 4: Tai Chi Chuan assistant training system.

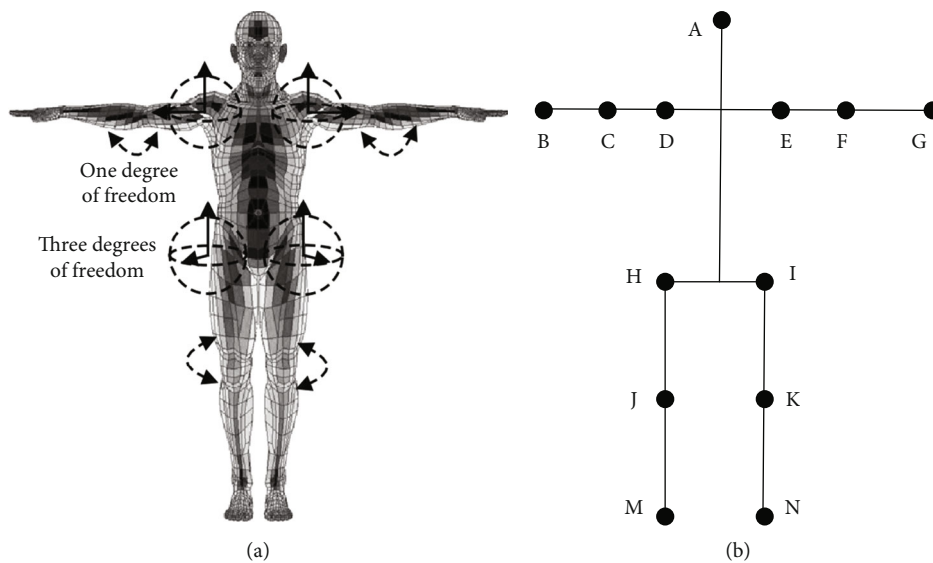


FIGURE 5: Model for the human body.

TABLE 1: The specific relations of each node and the key points.

Node number	Body part	Node number	Body part	Node number	Body part
A	Head	E	Left shoulder	I	Left hip joint
B	Right hand end	F	Left elbow	J	Right knee
C	Right elbow	G	Left hand end	K	Left knee
D	Right shoulder	H	Right hip joint	M	Right foot
N	Left foot				

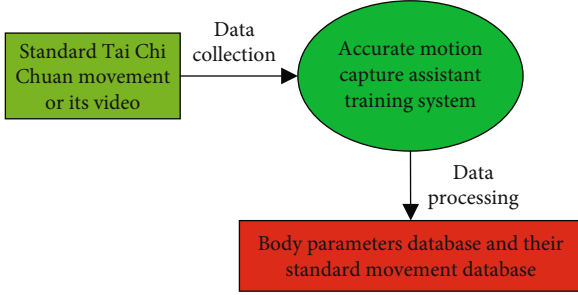


FIGURE 6: Diagram of standard action read process.

established according to the position of each node vector of the human body, which can describe the state of position in the process of training Tai Chi Chuan.

$$\mathbf{R}_t = \begin{bmatrix} A_x & A_y & A_z & A_\theta \\ B_x & B_y & B_z & B_\theta \\ C_x & C_y & C_z & C_\theta \\ \vdots & \vdots & \vdots & \vdots \\ N_x & N_y & N_z & N_\theta \end{bmatrix}. \quad (5)$$

Tai Chi Chuan fine motion capture assistant training system can get and store the parameters of body position for real-time and storing trainees' physical parameters (such as height, weight, arm, and leg length), which will be used in action of training students after the assessment and put forward relevant suggestions for improvement.

Tai Chi Chuan fine motion capture assistant training system for the basic process of autonomous learning Tai Chi standard action is shown in Figure 6.

Tai Chi Chuan precision motion capture auxiliary training system based on a lot of different ages, different genders, and different height personnel demo video standard Tai Chi Chuan movement, by reading the related parameter data are collected for autonomous learning, and the corresponding data processing of faculty body parameter database of library and corresponding Tai Chi Chuan as a standard action.

The flow diagram of trainees' training movement evaluation based on Tai Chi Chuan fine motion capture assistant training system is shown in Figure 7.

Figure 7 shows the Tai Chi Chuan assistant training system for training evaluation process. As shown in Figure 7, we know that Tai Chi Chuan fine motion capture assistant training system can be get the data that parameters matching

of Tai Chi Chuan standard action database and establish the training of personnel human motion state matrix  $\mathbf{R}_{t0}$ , based on the physical parameters and standard each act and faculty body as shown as follows:

$$\mathbf{R}_{t0} = \begin{bmatrix} A_{x0} & A_{y0} & A_{z0} & A_{\theta0} \\ B_{x0} & B_{y0} & B_{z0} & B_{\theta0} \\ C_{x0} & C_{y0} & C_{z0} & C_{\theta0} \\ \vdots & \vdots & \vdots & \vdots \\ N_{x0} & N_{y0} & N_{z0} & N_{\theta0} \end{bmatrix}. \quad (6)$$

Reading the body parameters of trainee, match the faculty body parameters in the database, and get the state of human body in the process of Tai Chi Chuan training as shown in formula (5).

State of the human body parameters in the process of training Tai Chi Chuan of trainees is similar compared to standard action and get the state parameter error, and some corresponding suggestions for improvement are put forward. The process formula of similarity comparison is shown as follows:

$$\begin{aligned} \Delta \mathbf{R}_t &= \mathbf{R}_t - \mathbf{R}_{t0} \\ &= \begin{bmatrix} A_x & A_y & A_z & A_\theta \\ B_x & B_y & B_z & B_\theta \\ C_x & C_y & C_z & C_\theta \\ \vdots & \vdots & \vdots & \vdots \\ N_x & N_y & N_z & N_\theta \end{bmatrix} - \begin{bmatrix} A_{x0} & A_{y0} & A_{z0} & A_{\theta0} \\ B_{x0} & B_{y0} & B_{z0} & B_{\theta0} \\ C_{x0} & C_{y0} & C_{z0} & C_{\theta0} \\ \vdots & \vdots & \vdots & \vdots \\ N_{x0} & N_{y0} & N_{z0} & N_{\theta0} \end{bmatrix} \\ &= \begin{bmatrix} \Delta A_x & \Delta A_y & \Delta A_z & \Delta A_\theta \\ \Delta B_x & \Delta B_y & \Delta B_z & \Delta B_\theta \\ \Delta C_x & \Delta C_y & \Delta C_z & \Delta C_\theta \\ \vdots & \vdots & \vdots & \vdots \\ \Delta N_x & \Delta N_y & \Delta N_z & \Delta N_\theta \end{bmatrix}. \end{aligned} \quad (7)$$

$\Delta \mathbf{R}_t$  is the parameter error value matrix of the human body movement state parameters and standard action state,

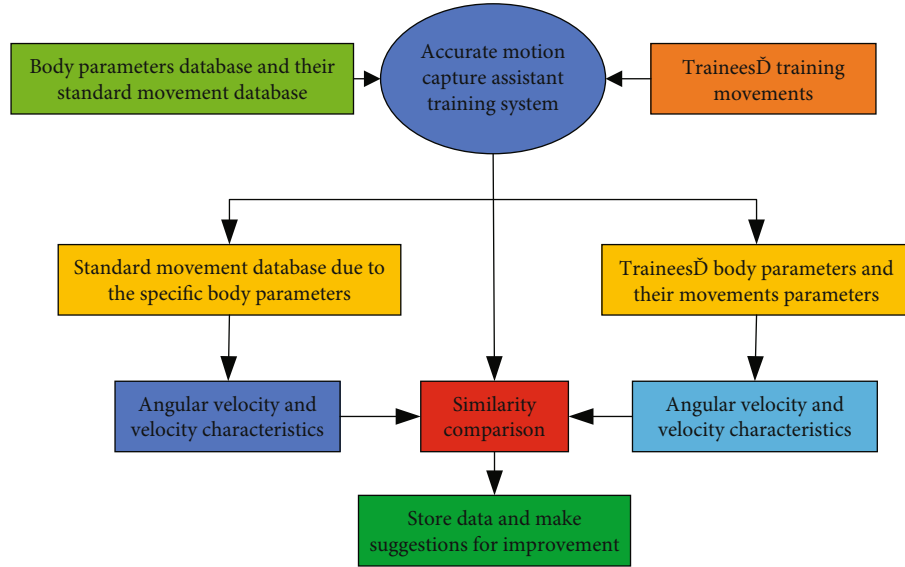


FIGURE 7: Flow diagram of Tai Chi Chuan training evaluation.

in the process of the Tai Chi Chuan training. The smaller error of the absolute value of matrix element indicates the movements more standard; suggestions for improvement are also based on the error value matrix.

In the process of practicing Tai Chi Chuan, the rating action is based on movement deviation to determine the amplitude and the need to action according to the deviation dimensionless as follows:

$$\Delta \mathbf{R} = \frac{\Delta \mathbf{R}_t}{\mathbf{R}_{t_0}} = \frac{\begin{bmatrix} \Delta A_x & \Delta A_y & \Delta A_z & \Delta A_\theta \\ \Delta B_x & \Delta B_y & \Delta B_z & \Delta B_\theta \\ \Delta C_x & \Delta C_y & \Delta C_z & \Delta C_\theta \\ \vdots & \vdots & \vdots & \vdots \\ \Delta N_x & \Delta N_y & \Delta N_z & \Delta N_\theta \end{bmatrix}}{\begin{bmatrix} A_{x0} & A_{y0} & A_{z0} & A_{\theta0} \\ B_{x0} & B_{y0} & B_{z0} & B_{\theta0} \\ C_{x0} & C_{y0} & C_{z0} & C_{\theta0} \\ \vdots & \vdots & \vdots & \vdots \\ N_{x0} & N_{y0} & N_{z0} & N_{\theta0} \end{bmatrix}} \cdot \begin{bmatrix} \frac{\Delta A_x}{A_{x0}} & \frac{\Delta A_y}{A_{y0}} & \frac{\Delta A_z}{A_{z0}} & \frac{\Delta A_\theta}{A_{\theta0}} \\ \frac{\Delta B_x}{B_{x0}} & \frac{\Delta B_y}{B_{y0}} & \frac{\Delta B_z}{B_{z0}} & \frac{\Delta B_\theta}{B_{\theta0}} \\ \frac{\Delta C_x}{C_{x0}} & \frac{\Delta C_y}{C_{y0}} & \frac{\Delta C_z}{C_{z0}} & \frac{\Delta C_\theta}{C_{\theta0}} \\ \vdots & \vdots & \vdots & \vdots \\ \frac{\Delta N_x}{N_{x0}} & \frac{\Delta N_y}{N_{y0}} & \frac{\Delta N_z}{N_{z0}} & \frac{\Delta N_\theta}{N_{\theta0}} \end{bmatrix}. \quad (8)$$

Based on the action of different dimensionless shown in equation (8),  $\mathbf{f}(\mathbf{R})$  is the movement differences during a complete set of Tai Chi Chuan training, which can be obtained on the basis of the  $\Delta \mathbf{R}$  get students Tai Chi Chuan exercise of and time integral; calculation process is shown as follows:

$$\mathbf{f}(\mathbf{R}) = \int \Delta \mathbf{R}(t) dt. \quad (9)$$

$\Delta \mathbf{R}(t)$  is the action deviation in the process of students to practice Tai Chi Chuan in real time.

The whole process of Tai Chi Chuan training can be digital output by fine Tai Chi Chuan motion capture assistant training system, which is shown as follows:

$$F_{\text{out}} = \sum_{t=0}^T f(\mathbf{R}). \quad (10)$$

$T$  is the whole time of trainee to complete a whole set of action.

For application of AI intelligent algorithm to rate the motion of the students to practice Tai Chi Chuan, the specific process is shown as follows:

$$S = \mathbf{W} \times \mathbf{f}(\mathbf{R}) + \mathbf{b}. \quad (11)$$

$S$  is the output scores value,  $\mathbf{W}$  is the weight matrix, and  $\mathbf{b}$  is for bias. Application of equation (11) is for trainees to practice Tai Chi Chuan movement difference filtering and score.

**3.4. Results and Analysis.** Tai Chi Chuan trainees according to age are divided into 20~30 years old, 30~40 years old, 40~50, 50~60 years old, aged 60~70, and 70~80, six groups in this paper. According to the Tai Chi Chuan fine motion

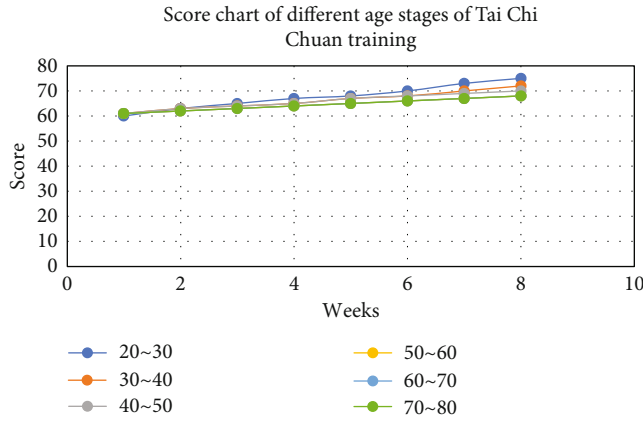


FIGURE 8: Score chart of different age stages of Tai Chi Chuan training.

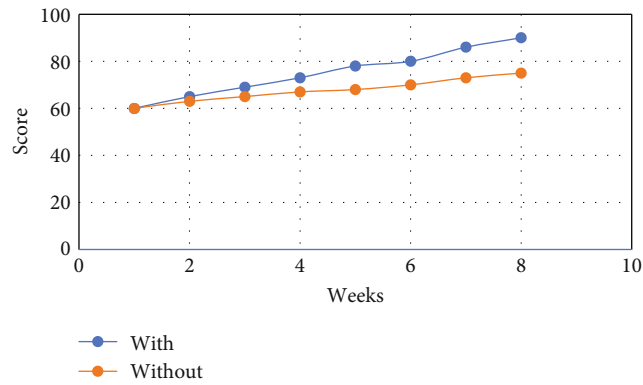


FIGURE 9: Score comparison with and without assistant training system.

capture assistant training system studied in Section 3.3, its grading evaluation module is adopted to study and statistic the various age groups under the condition of without assistant training system in 8 weeks.

Tai Chi practitioners of different age groups of Tai Chi Chuan movement score are to adopt large sample statistical average calculated.

$$E(S) = \frac{1}{n} \sum_{i=1}^n S_i. \quad (12)$$

$S_i$  is a certain age group within the sample in the  $i$ th Tai Chi Chuan action score value of the trainer.

And six Tai Chi Chuan trainees' groups' Tai Chi Chuan training scores are in Figure 8, respectively.

Figure 8 shows that the training scores that improve speed of Tai Chi Chuan training of different age groups in the eight-week training process with the Tai Chi Chuan fine motion capture assistant training system score are different. And the smaller the age of the trainee and the stronger ability to learn, the faster speed to improve the score.

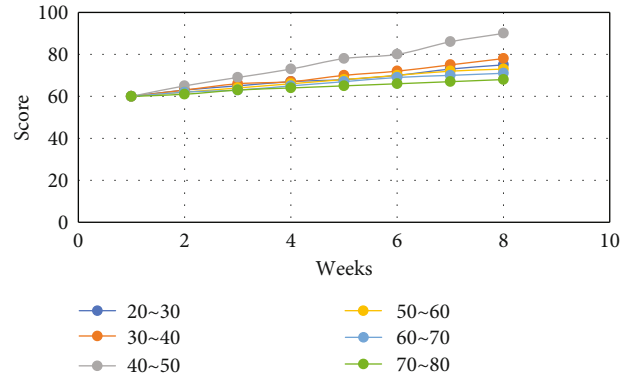


FIGURE 10: Score chart of different age stages of Tai Chi Chuan training.

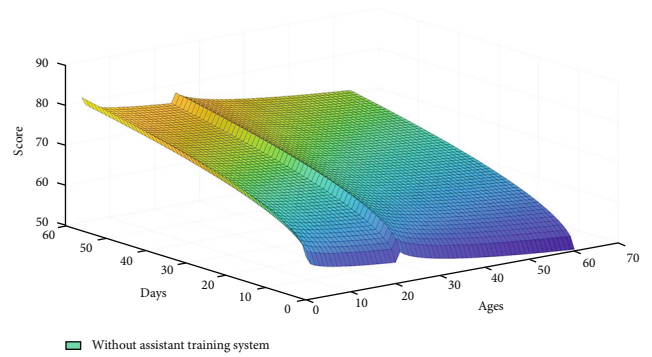


FIGURE 11: Score prediction for all age groups without assistant training system during different training time.

Figure 9 shows the score comparison of the 20~30 years old Tai Chi Chuan trainees with and without the Tai Chi Chuan fine motion capture assistant training system in eight weeks.

Figure 9 shows that the Tai Chi Chuan fine motion capture assistant training system studied in this paper to improve the Tai Chi Chuan training scores of 20~30 years old groups have significant effect; it can help improve the Tai Chi students withdrawn actions and improve the training efficiency.

Figure 10 shows the training scores of 20~30 years old, 30~40 years old, 40~50, 50~60 years old, aged 60~70, and 70~80, six groups of Tai Chi Chuan trainees with the Tai Chi Chuan fine motion capture assistant training system in eight weeks.

Contrast Figures 8 and 10, it shows that the Tai Chi Chuan fine motion capture assistant training system for different ages of learners to improve the efficiency of Tai Chi Chuan training has a great help, and 40~50 learners improve the most significant effect.

According to a large number of different age levels of Tai Chi Chuan training score values, AI intelligent algorithm is applied to deal with data and fitting and to predict the presence of fine Tai Chi Chuan motion capture assistant training system for different age groups of Tai Chi Chuan training

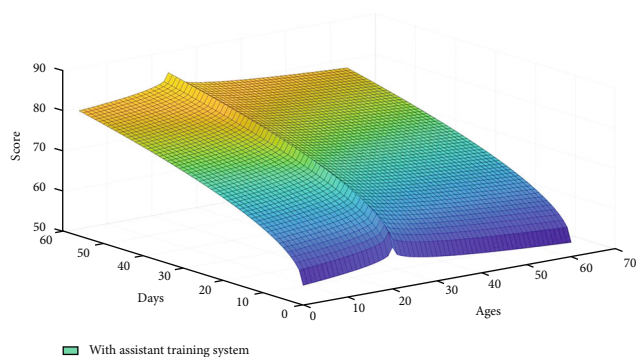


FIGURE 12: Score prediction for all age groups with assistant training system during different training time.

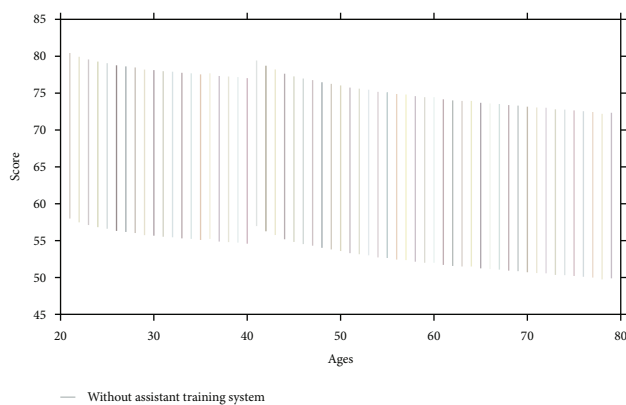


FIGURE 13: Score prediction for all age groups without assistant training system.

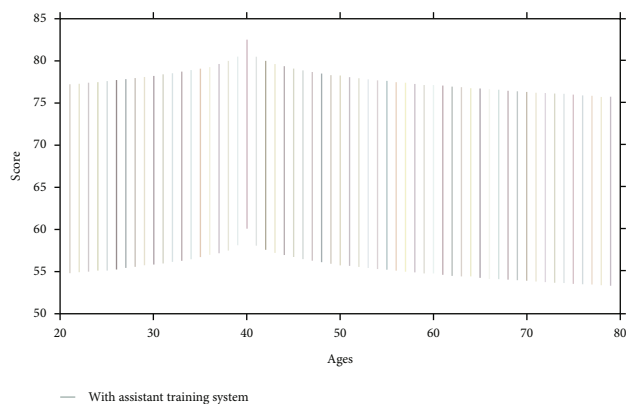


FIGURE 14: Score prediction for all age groups with assistant training system.

effect, which is shown in Figures 11–16. The data of Figures 11–16 are obtained from different age levels of taijiquan training in different training period for tracking.

Figures 11 and 12 show the training score improvement of different age stages of Tai Chi Chuan trainees in 8 weeks. The main difference is that the Tai Chi Chuan fine motion assistant training system is used to guide the training or not.

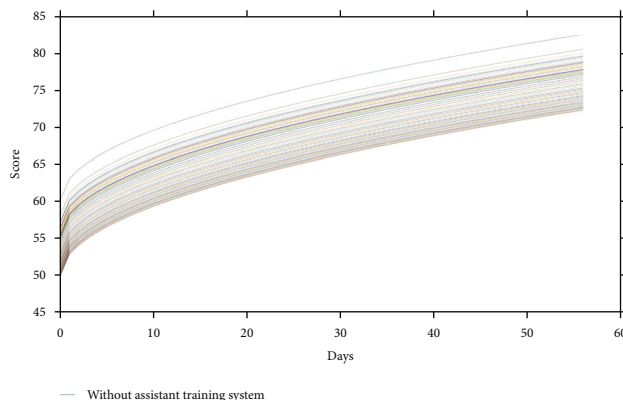


FIGURE 15: The score prediction without assistant training system in 8 weeks.

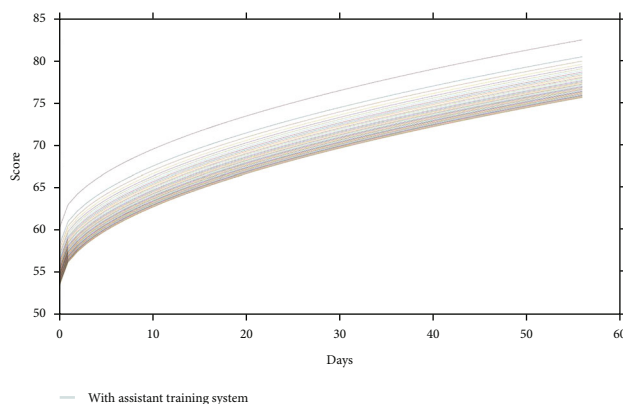


FIGURE 16: The score prediction with assistant training system in 8 weeks.

By comparing Figures 11 and 12, we can know that the Tai Chi Chuan auxiliary training system have a positive effect to the training of all age groups. While it has different improve effect to different age stages of training, and its effect to years groups around 30 is the most obvious.

### 4. Conclusions

Aiming at solving the problems existing in the Tai Chi Chuan training, a Tai Chi Chuan fine motion capture assistant training system is studied and designed. And it is used to help Tai Chi Chuan trainees improving their training quality and efficiency in this paper. Firstly, the development situation at home and abroad and the research status of Tai Chi Chuan are introduced in this paper. Secondly, the main training methods and contents of Tai Chi Chuan are learned shelf, fixed shelf, knead shelf, along shelf, and open shelf, which is conducted by analyzing and summarizing the research states of Tai Chi Chuan. Thirdly, the main contradictions existing in current training for Tai Chi Chuan are analyzed in detail. Fourthly, aiming at the existing problem of Tai Chi Chuan training, the assistant taijiquan training

system based on fine motion capture is studied this paper, and the system has the ability of autonomous learning, trainees' training assessment and modification suggestions, and other functions, which can improve the efficiency of people training effectively. It also plays a positive role in overcoming the current main problems of Tai Chi Chuan training and has the promotion of Tai Chi Chuan. Fifthly, the Tai Chi Chuan fine motion capture assistant training system for different age groups of Tai Chi Chuan trainees to improve their training quality and effect has a positive effect. Besides, the assistant training system studied in this paper can be applied to assist other sports training, according to the specific content of the training to modify built-in algorithm.

### Data Availability

The labeled datasets used to support the findings of this study are available from the corresponding author upon request.

### Conflicts of Interest

The authors declare no competing interests.

### Acknowledgments

This study is sponsored by the China University of Geosciences (Beijing).

### References

- [1] L. Liangtao, S. Cheng, G. Wang, G. Duan, and Y. Zhang, "Tai chi chuan exercises improve functional outcomes and quality of life in patients with primary total knee arthroplasty due to knee osteoarthritis," *Complementary Therapies in Clinical Practice*, vol. 35, no. 1, pp. 121–125, 2019.
- [2] M. R. Solloway, S. L. Taylor, P. G. Shekelle et al., "An evidence map of the effect of Tai Chi on health outcomes," *Systematic Reviews*, vol. 5, no. 1, p. 126, 2016.
- [3] J. Burschka, P. Kuhn, U. Menge, and P. Oschmann, "Research on Tai Chi as a sport in health care," *The challenge of complex interventions, Sportwissenschaft*, vol. 43, no. 1, pp. 181–196, 2013.
- [4] P. J. Jiménez-Martín, H. Liu, and A. M. Ortega, "The importance of differentiating the three modalities of Tai Chi Chuan practice in clinical trials - a critical review," *European Journal of Integrative Medicine*, vol. 17, no. 1, pp. 45–55, 2018.
- [5] Q. Zhu, H. Lingyan, L. Jingxian et al., "Effect of Taijiquan practice versus wellness education on knee proprioception in patients with knee osteoarthritis: a randomized controlled trial," *Journal of Traditional Chinese Medicine*, vol. 37, no. 6, pp. 774–781, 2017.
- [6] T. Uslu, E. Gezgin, S. Özbek, D. Güzin, F. C. Can, and L. Çetin, "Utilization of low cost motion capture cameras for virtual navigation procedures: performance evaluation for surgical navigation," *Measurement*, vol. 181, no. 109624, pp. 1–14, 2021.
- [7] C. Zhuo, J. Zhu, P. Yufeng, J. Li, and J. Ge, "Thermophoretic enhancement for fine ash particle capture in a corrugated falling-film channel," *International Journal of Heat and Mass Transfer*, vol. 179, p. 121645, 2021.
- [8] H. Yasin and S. Hayat, "DeepSegment: segmentation of motion capture data using deep convolutional neural network," *Image and Vision Computing*, vol. 109, p. 104147, 2021.
- [9] J. Ziegler, A. Reiter, H. Gattringer, and A. Müller, "Simultaneous identification of human body model parameters and gait trajectory from 3D motion capture data," *Medical Engineering & Physics*, vol. 84, no. 1, pp. 193–202, 2020.
- [10] M. Sarabzadeh, B. B. Azari, and M. Helalizadeh, "The effect of six weeks of Tai Chi Chuan training on the motor skills of children with autism spectrum disorder," *Journal of Bodywork and Movement Therapies*, vol. 23, no. 2, pp. 284–290, 2019.
- [11] E. Azimzadeh, M. A. Hosseini, K. Nourozi, and P. M. Davidson, "Effect of Tai Chi Chuan on balance in women with multiple sclerosis," *Complementary Therapies in Clinical Practice*, vol. 21, no. 1, pp. 57–60, 2015.
- [12] M. L. Moy, P. M. Wayne, D. Litrownik et al., "Long-term exercise after pulmonary rehabilitation (LEAP): design and rationale of a randomized controlled trial of tai chi," *Contemporary Clinical Trials*, vol. 45, pp. 458–467, 2015.
- [13] D. Qi, N. M. Wong, R. Shao et al., "Qigong exercise enhances cognitive functions in the elderly via an interleukin-6-hippocampus pathway: a randomized active-controlled trial," *Brain, Behavior, and Immunity*, vol. 95, no. 1, pp. 381–390, 2021.
- [14] D. Barsasella, M. F. Liu, S. Malwade et al., "Effects of virtual reality sessions on the quality of life, happiness, and functional fitness among the older people: a randomized controlled trial from Taiwan," *Computer Methods and Programs in Biomedicine*, vol. 200, no. 105892, p. 105892, 2021.
- [15] S. Lu and S. Wang, "Intelligent monitoring of Taijiquan exercise based on fuzzy control theory," *Microprocessors and Microsystems*, vol. 82, p. 103859, 2021.
- [16] J. Pelssers, E. Hurkmans, J. Scheerder et al., "Acting one's age in physical exercise: do perceived age norms explain autonomous motivation among older adults," *Journal of Aging & Physical Activity*, vol. 26, no. 4, pp. 521–529, 2018.
- [17] Y. López-Benavente, J. Arnau-Sánchez, T. Ros-Sánchez, M. Lidón-Cerezuela, A. Serrano-Noguera, and M. Medina-Abellán, "Difficulties and motivations for physical exercise in women older than 65 years. A qualitative study," *Revista Latino-Americana de Enfermagem*, vol. 26, no. 1, pp. 1–15, 2018.
- [18] E. M. McMahon, P. Corcoran, G. O'Regan et al., "Physical activity in European adolescents and associations with anxiety, depression and well-being," *European Child & Adolescent Psychiatry*, vol. 26, no. 1, pp. 111–122, 2017.
- [19] Z. Haili, Z. Haijun, and X. Guo, "Experimental study on Taijiquan exercise improving university students' cognitive function," *Cognitive Systems Research*, vol. 52, no. 1, pp. 591–595, 2018.
- [20] L. Xinke and D. Guobin, "Analyzing the role of taijiquan meditation exercise in the mental health management system," *Aggression and Violent Behavior*, vol. 1, p. 101604, 2021.
- [21] M. Theeboom, D. Zhu, and J. Vertonghen, "Wushu belongs to the world. But the gold goes to China...: the international development of the Chinese martial arts," *International Review for the Sociology of Sport*, vol. 52, no. 1, pp. 3–23, 2017.
- [22] A. Alsubiheen, J. Petrofsky, N. Daher, E. Lohman, E. Balbas, and H. Lee, "Tai Chi with mental imagery theory improves



- soleus H-reflex and nerve conduction velocity in patients with type 2 diabetes complement,” *Complementary Therapies in Medicine*, vol. 31, no. 1, pp. 59–64, 2017.
- [23] S. Y. Cetin, S. Erel, and U. Bas Aslan, “The effect of Tai Chi on balance and functional mobility in children with congenital sensorineural hearing loss,” *Disability and rehabilitation*, vol. 42, no. 12, pp. 1736–1743, 2020.
- [24] R. Loomes, L. Hull, and W. P. L. Mandy, “What is the male-to-female ratio in autism spectrum disorder? A systematic review and meta-analysis,” *American Academy of Child and Adolescent Psychiatry*, vol. 56, no. 6, pp. 466–474, 2017.
- [25] J. B. Mistry, R. D. Elmallah, A. Bhave et al., “Rehabilitative guidelines after total knee arthroplasty: a review,” *The Journal of Knee Surgery*, vol. 29, no. 3, pp. 201–217, 2016.
- [26] R. Cabeza, M. Albert, S. Belleville et al., “Maintenance, reserve and compensation: the cognitive neuroscience of healthy ageing,” *Nature Reviews. Neuroscience*, vol. 19, no. 11, pp. 701–710, 2018.
- [27] J. M. Burnfield, G. M. Cesar, T. W. Buster, S. L. Irons, and C. A. Nelson, “Kinematic and muscle demand similarities between motor-assisted elliptical training and walking: implications for pediatric gait rehabilitation,” *Gait & Posture*, vol. 51, no. 1, pp. 194–200, 2017.
- [28] J. Liu, X. Q. Wang, J. J. Zheng et al., “Effects of Tai Chi versus proprioception exercise program on neuromuscular function of the ankle in elderly people: a randomized controlled trial,” *Evidence-based Complementary and Alternative Medicine*, vol. 2012, Article ID 265486, 8 pages, 2012.
- [29] Y. C. Guo, P. X. Qiu, T. G. Liu, and J. Q. Tai, “Tai Ji Quan: an overview of its history, health benefits, and cultural value,” *Journal of Sport and Health Science*, vol. 3, no. 1, pp. 3–8, 2014.

## Research Article

# Research on Interface Slip of Composite Reinforced Steel Truss-Concrete Test Beam and Its Calculation and Analysis Method

Zhixiang Zhou <sup>1,2,3</sup> Xingqi Zeng,<sup>1,2</sup> Yang Zou,<sup>1,2</sup> Chengjun Li,<sup>4</sup> Guojun Den,<sup>5</sup> Liwen Zhang,<sup>1,2</sup> and Rui Wang<sup>6</sup>

<sup>1</sup>State Key Laboratory of Mountain Bridge and Tunnel Engineering, Chongqing 400074, China

<sup>2</sup>School of Civil Engineering, Chongqing Jiaotong University, Chongqing 400074, China

<sup>3</sup>College of Civil and Transportation Engineering, Shenzhen University, Shenzhen, Guangdong 518060, China

<sup>4</sup>Department of Road and Bridge Engineering, Sichuan Vocational and Technical College of Communications, Chengdu, Sichuan 611130, China

<sup>5</sup>Bridge and Structure Engineering Research Institute, China Merchants Chongqing Communications Technology Research & Design Institute Co., Ltd., Chongqing 400067, China

<sup>6</sup>Department of Transportation and Municipal Engineering, Sichuan College of Architectural Technology, Deyang, Sichuan 618000, China

Correspondence should be addressed to Zhixiang Zhou; zhixiangzhou@szu.edu.cn

Received 24 February 2022; Revised 23 March 2022; Accepted 9 April 2022; Published 12 May 2022

Academic Editor: Wen Zeng

Copyright © 2022 Zhixiang Zhou et al. This is an open access article distributed under the Creative Commons Attribution License, which permits unrestricted use, distribution, and reproduction in any medium, provided the original work is properly cited.

In this study, a model of test beam in negative moment area is designed, and the slip characteristics of test beam under overlimit static load and variable amplitude cyclic load are studied, respectively. By constructing the relationship between shear stiffness and slip parameters of the test beam, the deformation calculation method of the test beam under different fatigue cycles is derived, and the accuracy of the calculation model is verified by experiments. The results show that the maximum slip value (0.038 mm) of static load after 10,000 times of limited fatigue load is increased by 58.3% compared with that before overlimit fatigue load is applied (0.024 mm). When the fatigue cycle is 0-2 million times, the total slip is between 0.019 and 0.026 mm and the residual slip percentage is between 4.17 and 8.33%. The maximum residual values are 0.022 mm, 0.027 mm, and 0.028 mm after 1.5 times, 2 times, and 3 times of overload and variable amplitude fatigue loads, respectively, and the slip values have no obvious fluctuation, all of which show good working performance. The average value of the ratio between the deformation value and the measured value of composite beams is 0.89, and the standard deviation is 4.86%. When the fatigue loading times are more than 2.8 million, the ratio between the calculated value and the measured value is less than 0.85, so the adaptability of the calculation model has certain limitations. On the whole, the calculation model proposed in this study fully considers the factors such as the stiffness and fatigue loading times of composite beams, and the error between the calculated results and the measured results is within 5%, with high accuracy, which can be used as a reference for the actual design.

## 1. Introduction

Steel-concrete composite beam is a new type of member with good mechanical performance, which is formed by connecting steel beam and concrete slab through different shear connection structures. It has the mechanical characteristics of steel structure and concrete structure and is widely used

in bridge structure design [1, 2]. Steel-concrete composite beam bridge deck has good ductility and seismic performance. Steel truss girder and concrete bridge deck are mainly connected by various shear keys, and their structural forms include deck composite bridge, half-through composite bridge, and through composite bridge [3]. For bridge design, the main function of steel-concrete composite beam

bridge deck is to bear the dynamic load of vehicles, so it is particularly important to carry out the fatigue design of steel truss-concrete composite beam reasonably [4, 5].

In the study of fatigue cycle characteristics of test beams, foreign scholars have carried out a lot of research [6, 7]. Gattesco et al. have found that the traditional load-fatigue life calculation method has good adaptability only when the assembly structure is in an elastic state, but for composite beams with shear connection structure under low cycle fatigue load, the relative slip between steel and concrete will cause inelastic deformation of the connectors [8]. In recent years, domestic scholars have also carried out a large number of researches on the slip characteristics between steel plates and concrete. Zhou et al. have studied the static and fatigue mechanical characteristics of steel-concrete composite bridge deck, and, respectively, adopted the combination method of converted section and stiffness reduction and then put forward the deflection calculation formula of composite beams [9]. Through multiple fatigue tests on composite beams with partial shear connection structures, it is found that the fatigue stiffness calculation method is only based on the fitting of test data and the adaptability of the model has yet to be investigated [10]. In addition, a new calculation model was developed for the deformation behavior of steel-concrete composite beams under fatigue loading, taking into account the cross-sectional stiffness, peeling performance, load amplitude, and load ratio of the composite beam [11, 12]. Jianjun has carried out many fatigue tests on composite beams with partial shear connections and deduced the calculation method of fatigue stiffness, but it is only based on the fitting of test data, so the adaptability of the model needs to be studied [10]. Nie and Wang studied the deformation behavior of steel-concrete composite beams under fatigue load and deduced their parallel calculation model. The proposed model considered the cross-sectional stiffness of composite beams, stress performance of studs, load amplitude, load ratio, and other factors [11]. Composite beams are prone to fatigue failure when subjected to repeated vehicle loads [12]. Fatigue load will increase the slip at the interface between concrete and steel beam, and the increase of slip will reduce the stiffness of composite beam [13, 14]. Therefore, in the actual design of steel-concrete composite beams, if only the stiffness of composite beams subjected to fatigue load is calculated according to the static method, the final deformation value of composite beams will be smaller than the actual value, which makes the design of composite beams unsafe [15].

In this study, based on Tsing Qi Chung Bridge of Guangzhou-Foshan-Zhaoqing Expressway, a test beam model with negative moment area is designed. Firstly, the interface slip characteristics of fabricated steel truss-concrete test beams are studied, and the slip characteristics of test beams under overlimit static load and variable amplitude cyclic load are tested, respectively. Secondly, based on the existing calculation and analysis method of interface residual slip of test beam under fatigue load, the deformation calculation method of test beam under different fatigue cycles is deduced by constructing the relationship between shear stiffness and slip parameters. Finally, the accuracy of

the calculation model is verified by experiments, which provides theoretical guidance for the engineering application of new fabricated steel truss-concrete test beam.

## 2. Materials and Methods

*2.1. Design of Test Beam.* A variable cross-section test beam with negative moment (as shown in Figure 1) is designed and manufactured. The total length of test beam is 8.55 m, and its overall height is 1.44 m; the height of steel truss is 1.3 m, the height of concrete bridge slab is 0.14 m, the width of top slab of concrete bridge slab is 0.7 m, the width of bottom slab of concrete bridge slab is 0.26 m, and the spacing between steel web members is 0.22 m. The cube compressive strength of the concrete specimen was 71.39 MPa, the axial compressive strength was 47.6 MPa, the splitting tensile strength was 4.2 MPa, the modulus of elasticity of the concrete was 44796 MPa, and the modulus of elasticity of the steel was 210055 MPa. The top chord of steel truss beam is connected with the bottom slab of concrete by PCSS new shear key, and all joints of truss are connected by submerged arc welding. The test beam is designed refers to 4.3.7 of the general specification for design of highway bridges and culverts D60-2015 [16]. Fatigue load I (lane load model) is adopted, and the lane load is taken as 0.7 times, and multi-lane reduction is considered at the same time. In this experiment, the Midas/civil software is used to build the finite element model of Qingqiyong Bridge. The whole bridge has 3958 nodes and 4811 units. When the surface stress of bridge deck is 3.6 MPa, the load of test beam is 154 kN. When the surface stress of bridge deck is 4.8 MPa, the load of test beam is 220 kN. Therefore, the upper and lower limit of fatigue load in normal use stage are 154 kN and 220 kN, respectively.

### 2.2. Slip Characteristic Test of Test Beam

- (1) *Loading Schemes under Different Fatigue Loads.* Bridges are often subjected to overload during actual operation. Firstly, the test beam is subjected to 10,000 times of overlimit cyclic loading, and the change rule between slip and load is discussed. After 10,000 times of overlimit cyclic loading, the test beam is subjected to constant amplitude cyclic loading for 2 million times, and static loading test is carried out after reaching a certain number of cycles. When the test beam has not been damaged under 2 million constant amplitude cyclic loads, the slip-load variation law of the test beam under variable amplitude cyclic loads is discussed by keeping the lower limit of fatigue load unchanged and increasing the upper limit of fatigue load. At first, 2 million times of fatigue cyclic loading with 154 kN-220 kN are carried out, and then, 1.5 times (154 kN-244 kN) vehicle overload after 500,000 times, 2 times (154 kN-272 kN) vehicle overload after 300,000 times, and 3 times (154 kN-320 kN) vehicle overload after 300,000 times are carried out, respectively. The American MTS equipment is used to load the test

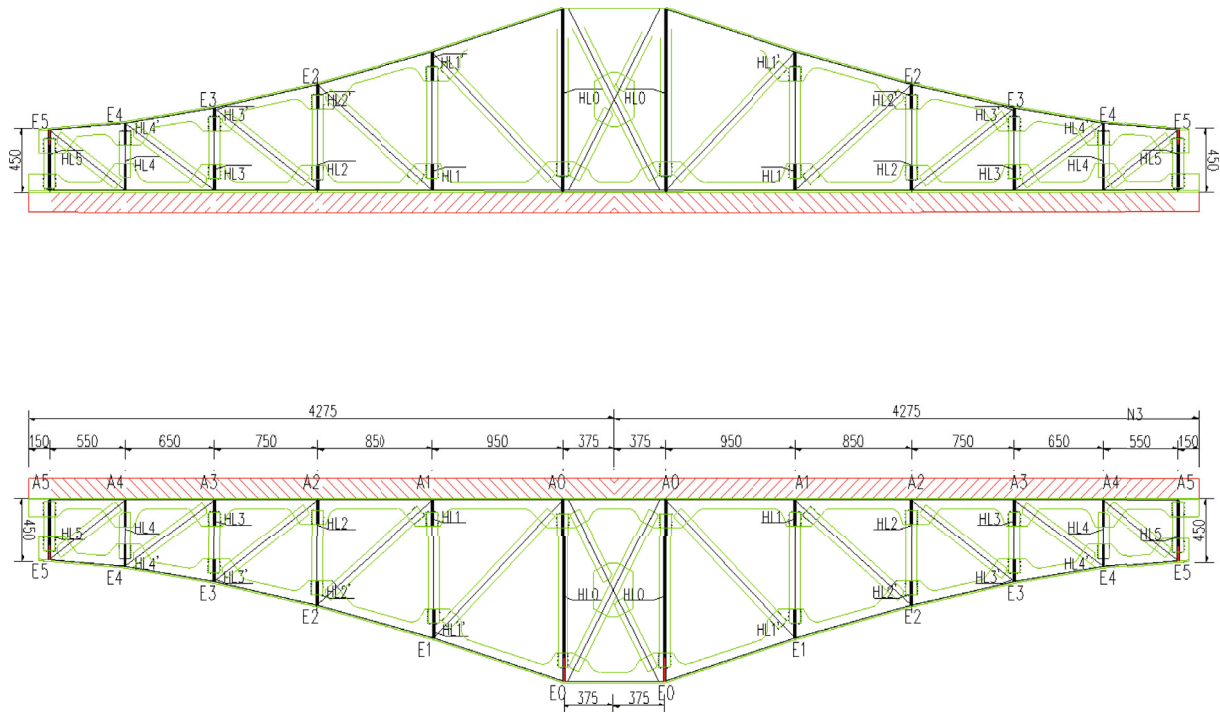


FIGURE 1: Elevation layout and size design of variable cross-section test beam in negative moment area.

beam, and JM3812 static strain test and analysis system is used to test the deflection distribution of the test beam after different fatigue loading times.

- (2) *Test Scheme of Slip Distribution.* In this test, a slip measuring point is, respectively, arranged in the middle of 1#-9# steel plates to obtain the change law of slip and load between steel plate and concrete. The specific test scheme is as follows: 10 deflection measurement points were arranged at the support position, quarter point position, and midspan position of the combined beam. Firstly, a plexiglass sheet is pasted on the concrete plate, and then, a steel seat is installed at the outer edge of the upper chord of the steel truss 2.5 cm away from the plexiglass sheet, so that the dial indicator passes through the reserved hole of the seat and abuts against the plexiglass sheet. Finally, the slip distribution between steel and concrete under different loading tonnage can be measured by the degree of dial indicator (the arrangement of measuring points is shown in Figure 2 below).

### 3. Results and Discussion

*3.1. Slip Test Results of Test Beam under Overlimit Static Load.* Figure 3 is the load-slip curves of No. 1 concrete slab before the application of overlimit fatigue load and after the overlimit fatigue load is applied for 10,000 times. It can be seen that the two curves show similar development trends. When the load is less than 36 t, the slip value generally shows a linear increase trend with the increase of load. When the load is further increased to 47 t, the slip growth slows down, because the stud is in a state of combined bend-

ing and shear stress, and there are tension side void zone and compression bonding zone between stud and concrete, so stud is in the stage of elastic-plastic deformation. When the load starts to decrease, the slip recovery lags behind, showing a trend of slow first and then accelerated decline. Further comparison shows that the maximum slip value is 0.024 mm when the load reaches 47 t during the static load before the overlimit fatigue load is applied. However, during the static load test after 10,000 times of overlimit fatigue loading, the increase rate is smaller than that before loading. When the load reaches 47 t, the maximum slip value is 0.038 mm, which increases by 58.3%. By comparison, it can be seen that the slip value between steel plate and concrete increases with the increase of fatigue load times. Under the same load, the slip value in the static load stage before the test is less than that in the static load stage after 10,000 overlimit fatigue loads. On the other hand, under the action of repeated load, the concrete near the stud will increase the void displacement between the stud and the concrete, resulting in the total slip amount of static load after 10,000 fatigue cycles under the same load is greater than the slip amount of static load before the test, which also indicates that the test beam has accumulated damage after the overlimit fatigue load [17, 18].

#### *3.2. Slip Test Results of Test Beam under Variable Amplitude Cyclic Load*

*3.2.1. Static Load Slip Test Results after 2 Million Fatigue.* After 10,000 times, 50,000 times, 100,000 times, 500,000 times, 1 million times, 1.5 million times, and 2 million times of fatigue loading, the static load-slip curve of 2 million times of fatigue is obtained (as shown in Figure 4(a)). It

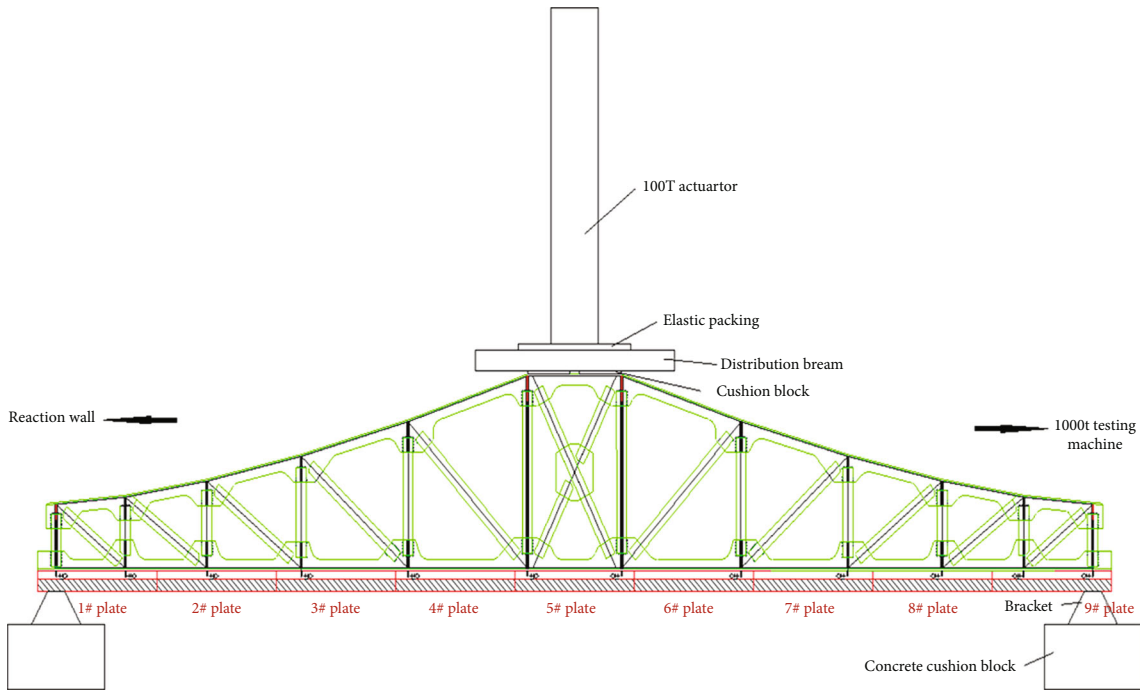


FIGURE 2: Schematic diagram of test layout of slip table.

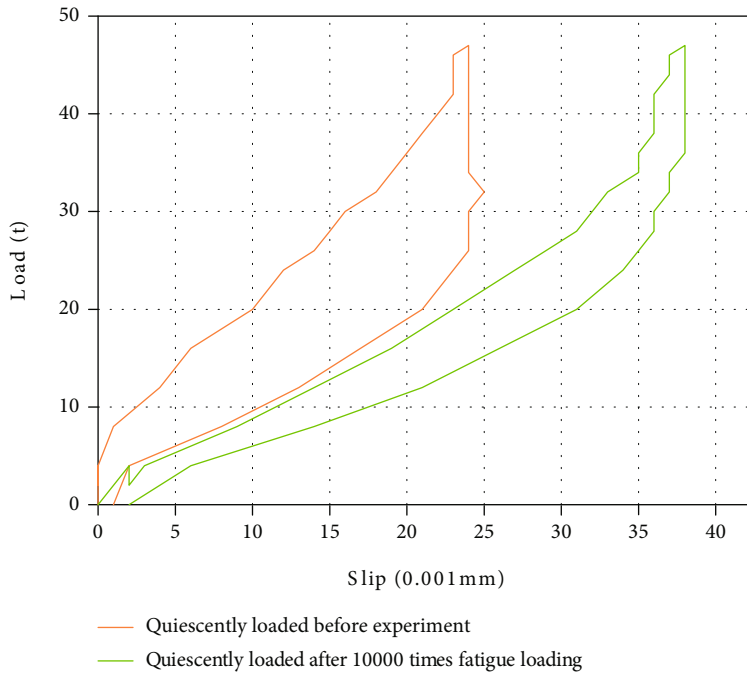
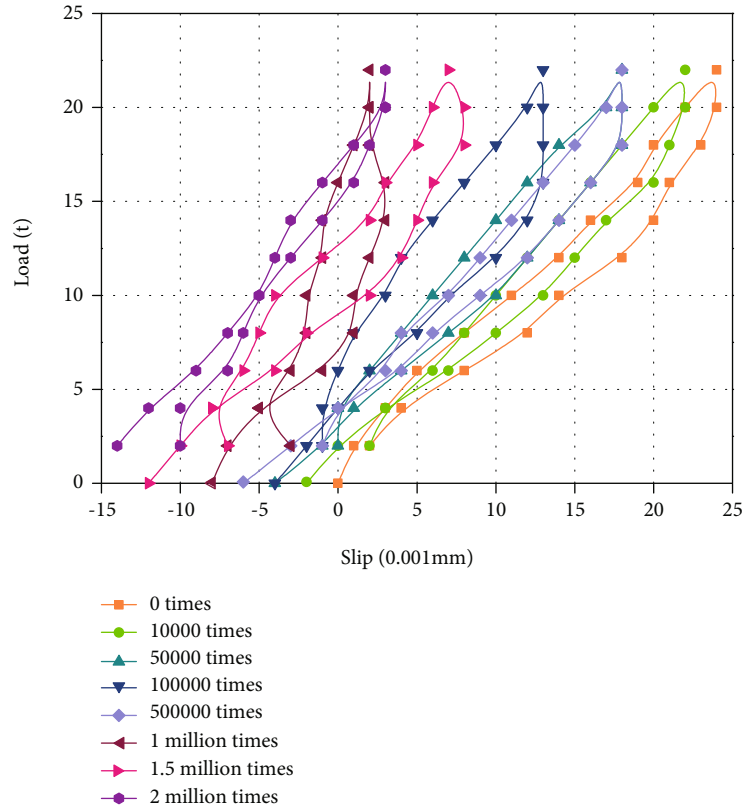


FIGURE 3: Load-slip curve of concrete slab before overlimit fatigue load is applied and after overlimit fatigue load is applied 10,000 times.

can be seen from the figure that the static load curves after different fatigue loadings show an increasing trend as the load increases. When the load begins to decrease, the slip value first decreases slowly and then decreases rapidly. On the other hand, with the increase of cyclic fatigue loading times, the residual slip value is negative, which is mainly due to the relative displacement between steel truss and concrete after 10,000 times of overlimit loading, and the slip

slowly recovers after fatigue loading. When the fatigue loading times are less than 500,000, the average residual slip is 0.001 mm, while when the fatigue loading times are 500,000-2 million, the average residual slip is 0.003 mm, which indicates that the residual slip will increase with the increase of fatigue loading times, but the increase is not obvious. Generally speaking, the residual slip of the test beam is small after 2 million times of fatigue from 154 kN to 220 kN,



(a)



(b)

FIGURE 4: (a) Static load-slip curve and the (b) relationship between slip and fatigue loading times after 2 million fatigue times.

which indicates that the combined test beam has better elastic performance. Figure 4(b) shows the change of total slip and residual slip percentage of the test beam under different fatigue loading times. It can be seen from the figure that with the increase of fatigue loading times, both the total slip and

residual slip percentage show a trend of first decreasing, then increasing, and then decreasing. The total slip is between 0.019 and 0.026 mm, and the residual slip percentage is between 4.17 and 8.33%. When the fatigue loading times are 500,000 times, the residual slip percentage reaches the

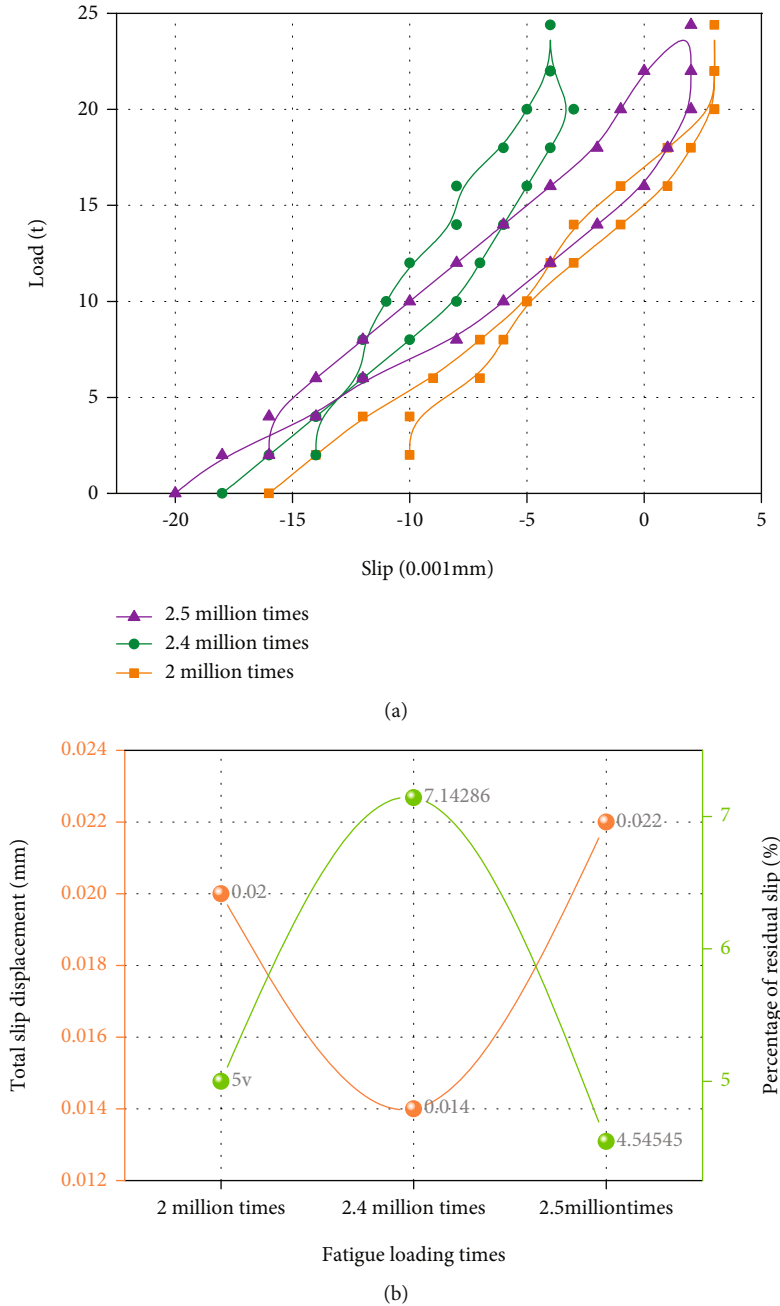
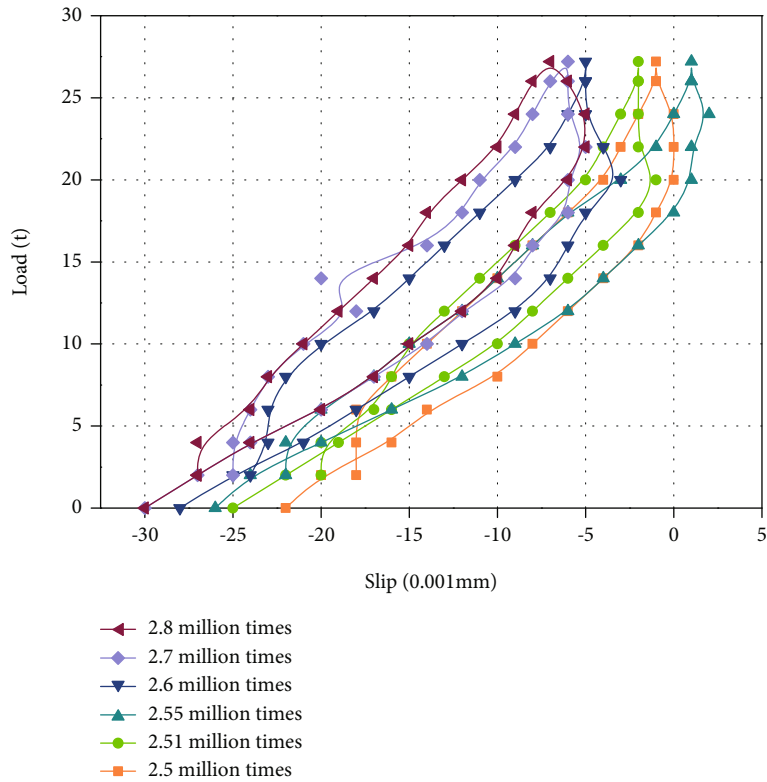


FIGURE 5: (a) Static load-slip curve and the (b) relationship between slip and fatigue loading times after 2.5 million (1.5 times overload) fatigue times.

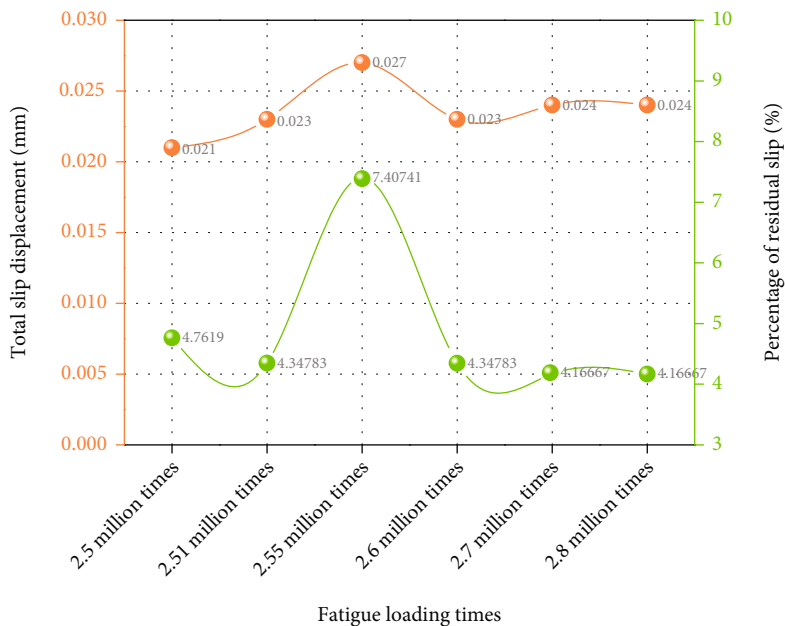
maximum value (8.33%). Overall, the maximum slip of the test beam is relatively stable, indicating that the test beam is still in elastic working state after 2 million fatigue loads

**3.2.2. Slip Test Results of Static Load after 1.5 Times Overload Fatigue.** Figure 5(a) shows the static load-slip curve of the test beam after static load cycling after 2 million, 2.4 million, and 2.5 million fatigue loads, respectively. It can be seen from the figure that the residual slip value is negative after 2 million, 2.4 million, and 2.5 million cyclic fatigue loads, and the average residual slip increases with the increase of cyclic fatigue loads. Figure 5(b) shows the relationship

between the maximum slip of concrete slab and fatigue loading times. It can be seen from the figure that when the load reaches 244 kN, the slip value between concrete slab and steel truss shows a trend of first decreasing and then increasing, ranging from 0.014 mm to 0.022 mm. However, with the increase of fatigue loading times, the percentage of residual slip first increases and then decreases. When the loading times are 2.4 million times, the percentage of residual slip reaches the maximum of 7.14%. Generally speaking, after 1.5 times overload loading, the maximum slip fluctuation of the test beam is not obvious, showing good working performance



(a)



(b)

FIGURE 6: (a) Static load-slip curve and the (b) relationship between slip and fatigue loading times after 2.8 million (2 times overload) fatigue times.

3.2.3. Slip Test Results of Static Load after 2 Times Overload Fatigue. Figure 6(a) shows the static load-slip curve of the test beams after static load cycle and after 2.5 million, 2.51 million, 2.55 million, 2.6 million, 2.7 million, and 2.8 million fatigue loading, respectively, under the action of 2 times overload and variable amplitude fatigue load. It can be seen

from the figure that the residual slip values are negative after different cyclic fatigue loads, and the average residual slip value increases with the increase of cyclic fatigue load times, but the increase is not obvious. Figure 6(b) shows the relationship between the maximum slip and the fatigue loading times of concrete slab. It can be seen from the figure that



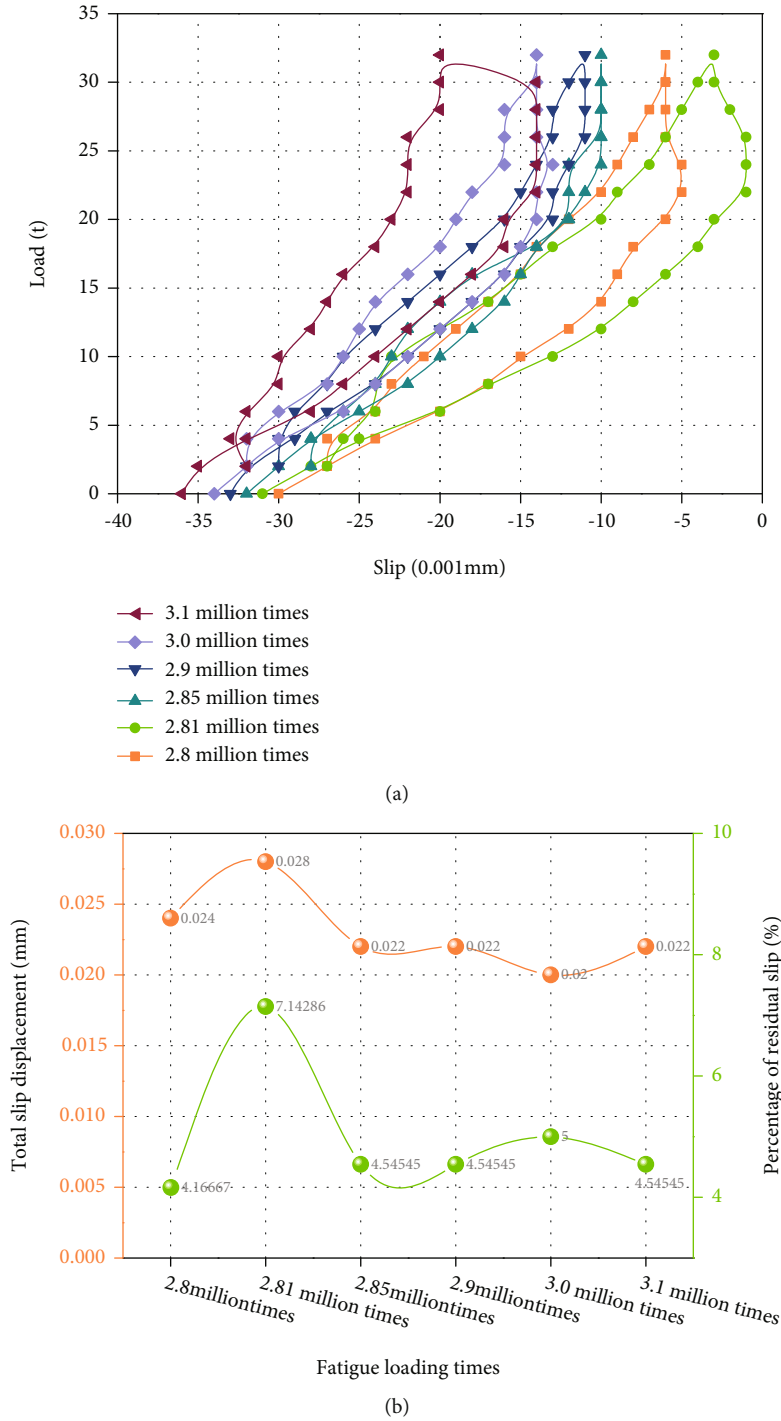


FIGURE 7: (a) Static load-slip curve and the (b) relationship between slip and fatigue loading times after 3.1 million (3 times overload) fatigue times.

when the load reaches 272 kN, the slip value between concrete slab and steel truss is increased first and then decreased and finally reaches a stable trend, with the slip value between 0.021 mm and 0.027 mm, while the residual slip percentage decreases slightly and then decreases rapidly with the increase of fatigue loading times. When the loading times are 2.55 million, the maximum residual slip percentage is 7.40%. Generally speaking, the maximum slip and residual

slip percentage of the test beam are not obvious after 2 times of overload loading, showing good working performance

*3.2.4. Slip Test Results of Static Load after 3 Times Overload Fatigue.* Figure 7(a) shows the static load-slip curve of the test beam after static load cycling and after fatigue loading of 2.8 million times, 2.81 million times, 2.85 million times, 2.9 million times, 3 million times, and 3.1 million times,

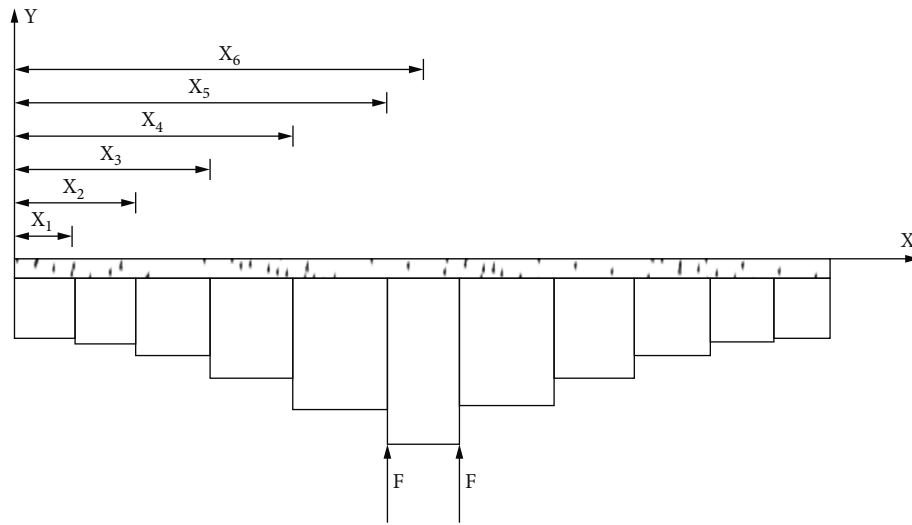


FIGURE 8: Simplified model of steel truss-concrete test beam.

respectively. It can be seen from the figure that the residual slip value is negative after different cyclic fatigue loads, and the average residual slip increases with the increase of cyclic fatigue loads. When the fatigue cycle is more than 3 million times, the average residual slip increases obviously. Figure 7 (b) shows the relationship between the maximum slip of concrete slab and fatigue loading times. It can be seen that when the load reaches 320 kN, the slip value and residual slip percentage between concrete slab and steel truss show a trend of first increasing and then decreasing and finally reaching a stable level. The slip value ranges from 0.020 mm to 0.028 mm, and when the loading times are 2.81 million times, the residual slip percentage reaches the maximum of 7.14%. Generally speaking, after 3 times overload loading, the fluctuation of maximum slip and residual slip percentage is not obvious, and it still shows good working performance

### 3.3. Deformation Theory Calculation and Experimental Verification of Test Beam under Fatigue Load

**3.3.1. Theoretical Calculation of Test Beam Deflection.** According to the existing research results [19–21], the mid-span deflection  $f$  of the test beam under fatigue load is a function of fatigue load cycle times  $n$ , and the general expression is

$$f = f_c + f_s, \quad (1)$$

where  $f$  is the total deflection of the test beam and  $f_c$  and  $f_s$  are the deflection due to static load and the residual deflection in the span of the combined beam after  $n$  cycles of fatigue loading, respectively.

In this study, the influence of slip between concrete slab and steel truss is fully considered. Firstly, the relationship between shear stiffness  $J$  and slip parameter  $W$  of test beam is established, and the following assumptions are made: (a) The shear stiffness of shear connectors is assumed to be constant, that is, the longitudinal shear at the interface between

concrete slab and steel truss is proportional to the relative slip, and the shear stiffness of shear connectors is uniformly distributed along the truss span. (b) Because the slip deformation between steel and concrete is very small, the shear deformation between concrete slab and steel frame can be ignored. It is assumed that both concrete slab and steel truss conform to Bernoulli theory. (c) Ignoring the effect of lifting on the interaction between concrete slab and steel truss, it is assumed that the section angles of concrete slab and steel truss are equal and the deformation is coordinated. (d) Ignoring friction between concrete slab and steel truss, it is assumed that the longitudinal shear force at the interface between concrete slab and steel truss is only borne by shear connectors.

$$J = \frac{K}{m} W, \quad (2)$$

where  $J$  is the longitudinal shear force,  $K$  is the shear stiffness of shear keys,  $m$  is the spacing of connectors, and  $W$  is the slip.

To solve the slip parameter  $W$ , the steel truss test beam is simplified (the simplified model is shown in Figure 8 below), and half of it is calculated according to its symmetrical structure and loading characteristics.

For  $0 \leq x \leq x_5$ , take any section for analysis, and when  $x_1 \leq x \leq x_2$ , the expression of slip parameter  $W_1$  at the interface between concrete and steel truss is obtained:

$$W_1 = C_{21} e^{\sqrt{\beta_2} x} + C_{22} e^{-\sqrt{\beta_2} x} - \frac{\alpha_2}{\beta_2} x, \quad (3)$$

where  $W_1$  is the slip parameter of the interface between concrete and steel truss and  $\alpha_2$  and  $\beta_2$  are the parameters of  $x_1 - x_2$  section.

TABLE 1: Values of  $\alpha$  and  $\beta$  and equivalent plate thickness of steel truss-concrete test beams in each section.

Parameters	$0-x_1$	$x_1-x_2$	$x_2-x_3$	$x_3-x_4$	$x_4-x_5$	$x_5-x_6$
$\alpha$	0.0167	0.0151	0.0118	0.0084	0.0060	0.0045
$\beta$	4.3591	4.3830	3.8526	3.2075	2.7048	2.4563
Equivalent plate thickness	4.39	2.48	1.35	1.15	0.96	0

TABLE 2: Comparison of deflection calculation results and measured results of steel truss-concrete test beam.

Sample number	Loading times (10,000 times)	Deflection measured values-left site (mm)	Deflection calculation (mm)	Deflection calculation/deflection measured values
	0	1.20	1.10	0.92
	1	1.25	1.15	0.92
	1.5	1.25	1.17	0.94
	3	1.25	1.14	0.91
	5	1.27	1.07	0.84
	5.5	1.25	1.13	0.9
	10	1.30	1.22	0.94
Combination beam with 2 million cyclic loads	20	1.25	1.18	0.94
	50	1.22	1.21	0.99
	80	1.20	1.15	0.96
	100	1.23	1.18	0.96
	120	1.23	1.06	0.86
	140	1.18	1.04	0.88
	160	1.36	1.23	0.9
	180	1.30	1.12	0.86
	200	1.30	1.05	0.81
	200	1.75	1.52	0.87
	210	1.70	1.61	0.95
Combination beam with 2.5 million cyclic loads	220	1.70	1.58	0.93
	230	1.75	1.57	0.9
	240	1.65	1.62	0.98
	250	1.75	1.66	0.95
	250	2.40	1.97	0.82
	251	2.38	2.05	0.86
Combination beam with 2.8 million cyclic loads	255	2.35	2.02	0.86
	260	2.42	2.15	0.89
	270	2.38	1.99	0.84
	280	2.31	2.09	0.9
	280	3.20	2.77	0.87
	281	3.15	2.65	0.84
Combination beam with 3.1 million cyclic loads	285	3.25	2.70	0.83
	290	3.25	2.73	0.84
	300	3.30	2.80	0.85
	310	3.10	2.60	0.84
Statistical result			Mean	0.89
			SD (%)	4.86%

When  $x_5 \leq x \leq x_6$ , the expression of slip parameter  $W_2$  at the interface between concrete and steel truss is obtained:

$$W_2 = C_{61}e^{\sqrt{\beta_6}x} + C_{62}e^{-\sqrt{\beta_6}x} - \frac{\alpha_6}{\beta_6}x + \frac{\gamma_6}{\beta_6}, \quad (4)$$

where  $W_2$  is the slip parameter of the interface between concrete and steel truss and  $\alpha_6$  and  $\beta_6$  are the parameters of  $x_5 - x_6$  section.

Combining equation (3) with equation (4), we can know from the boundary conditions that  $W(x=0) = 0$  and  $W'(x=x_6) = 0$ ; also,  $x_0 = 0$ , and the total expression of slip parameter  $W_{i1}(x)$  is derived:

$$W_{i1}(x) = \begin{cases} C_{i1}e^{\sqrt{\beta_i}x} + C_{i2}e^{-\sqrt{\beta_i}x} - \frac{\alpha_2}{\beta_2}x, & x_{i-1} \leq x \leq x_i (i = 1, 2, 3, 4, 5), \\ C_{i1}e^{\sqrt{\beta_i}x} + C_{i2}e^{-\sqrt{\beta_i}x} - \frac{\alpha_6}{\beta_6}x + \frac{\gamma_6}{\beta_6}, & x_5 \leq x \leq x_6. \end{cases} \quad (5)$$

Among them, the values of  $\alpha$  and  $\beta$  in each section of the test beam are obtained from the following Table 1:

Since the slip and relative slip strain between the steel and concrete at the fulcrum are all 0, the parameters  $C_{i1}$  and  $C_{i2}$  are further solved according to the boundary conditions; then, the expression of the section curvature  $\varphi$  is derived:

$$\varphi = \int_{x_0}^{x_5} \frac{1}{EI} \left( V + \frac{K}{m} W(h_c + h_s) \right) dx + c_1. \quad (6)$$

The relationship between curvature and bending moment is

$$\frac{M_s}{E_s I_s} = \frac{M_c}{E_c I_c} = \varphi. \quad (7)$$

Incorporating formula (7) into the final derivation, the expression of the total deflection  $f$  in the middle span of the steel-concrete test beam after  $n$  fatigue load cycles is obtained:

$$f = \int_0^l \frac{M_{ci} \bar{M}}{\sum_{i=1}^n E_{ci} I_{ci}} ds + \int_0^l \frac{M_{si} \bar{M}}{\sum_{i=1}^n E_{si} I_{si}} ds. \quad (8)$$

**3.3.2. Test Verification.** The above calculation method is used to calculate the midspan deflection value of the test beam under fatigue loading of 154-220 kN for 0-2 million times, fatigue loading of 154-244 kN for 500,000 times, fatigue loading of 154-272 kN for 300,000 times, and fatigue loading of 154-320 kN for 300,000 times, respectively, and the comparison with the actual measured value is shown in Table 2. It can be seen from Table 2 that the average value of the ratio between the deformation value and the measured value of composite beams is 0.89, and the standard deviation is 4.86%. In addition, it can be found that with the increase of fatigue loading times, the calculation accuracy of the model decreases gradually. When the fatigue loading times

are more than 2.8 million times, the ratio of the calculated value to the measured value is less than 0.85, and the calculation results are unsafe, so the adaptability of the calculation model has certain limitations. Generally speaking, the calculation model proposed in this study fully considers the stiffness and fatigue loading times of composite beams. Compared with the measured results, the error is within 5%, so the accuracy is high, which can be used as a reference for practical design

## 4. Conclusion

- (1) The slip test results of test beam under the overlimit static load show that the load-slip curve of the static load before and after the overlimit fatigue load is applied for 10,000 times shows a trend of linear growth first and then slows down. When the ultimate load is reached, the maximum slip values of the two are 0.024 mm and 0.038 mm, respectively, and the maximum slip value of the static load after the overlimit fatigue load is applied for 10,000 times is increased by 58.3% compared with that before the overlimit fatigue load is applied
- (2) The slip test results of test beam under variable amplitude cyclic loading show that when the fatigue cycle is 0-2 million times, the total slip and the residual slip percentage first decrease, then increase, and then decrease. The residual slip increases with the increase of the number of fatigue loading, with the total slip amount between 0.019 and 0.026 mm and the residual slip percentage between 4.17 and 8.33%. When the loading times are 500,000, the residual slip percentage reaches the maximum value (8.33%).
- (3) The test results under overload variable amplitude fatigue loads show that the maximum residual values are 0.022 mm (the maximum residual slip percentage was 7.14%), 0.027 mm (the maximum residual slip percentage was 7.40%), and 0.028 mm (the maximum residual slip percentage was 7.14%) after 1.5 times, 2 times, and 3 times of overload and variable amplitude fatigue loads, respectively, and the slip values have no obvious fluctuation, all of which show good working performance
- (4) Fully considering the factors of shear stiffness and fatigue cycles, the deformation calculation model of the test beam is deduced. The average value of the ratio between the deformation value and the measured value of composite beams is 0.89, and the standard deviation is 4.86%. The error between the calculation results and the measured results is less than 5%, with high accuracy

## Data Availability

The labeled dataset used to support the findings of this study is available from the corresponding author upon request.

## Conflicts of Interest

The authors declare no competing interests.

## Acknowledgments

This research was supported by the National Natural Science Foundation of China Youth Science Foundation Project (No. 52008066), Science and Technology Projects in TAR (XZ202001ZY0054G), State Key Laboratory of Mountain Bridge and Tunnel Engineering (No. SKLBT-2110), Research Project of education and teaching reform in Chongqing Jiaotong University, and the application of basic research projects of the Ministry of Communications (No. 2013 319814 040).

## References

- [1] M. Safa, M. Shariati, Z. Ibrahim, A. Togholi, and D. Petkovic, "Potential of adaptive neuro fuzzy inference system for evaluating the factors affecting steel-concrete composite beam's shear strength," *Steel & Composite Structures*, vol. 21, no. 3, pp. 679–688, 2016.
- [2] C. Amadio, C. Bedon, M. Fasan, and M. R. Pecce, "Refined numerical modelling for the structural assessment of steel-concrete composite beam-to-column joints under seismic loads," *Engineering Structures*, vol. 138, pp. 394–409, 2017.
- [3] M. A. Uddin, M. A. Alzara, N. Mohammad, and A. Yosri, "Convergence studies of finite element model for analysis of steel-concrete composite beam using a higher-order beam theory," *Structure*, vol. 27, pp. 2025–2033, 2020.
- [4] X. Li and B. Glisic, "Evaluating early-age shrinkage effects in steel concrete composite beam-like structures," *Steel Construction*, vol. 10, no. 1, pp. 47–53, 2017.
- [5] W. Salvatore, O. S. Bursi, and D. Lucchesi, "Design, testing and analysis of high ductile partial-strength steel-concrete composite beam-to-column joints," *Computers & Structures*, vol. 83, no. 28-30, pp. 2334–2352, 2005.
- [6] A. Benavent, E. Castro, and A. Gallego, "Evaluation of low-cycle fatigue damage in RC exterior beam-column subassemblages by acoustic emission," *Construction & Building Materials*, vol. 24, no. 10, pp. 1830–1842, 2010.
- [7] B. Cermelj, P. Moze, and F. Sinur, "On the prediction of low-cycle fatigue in steel welded beam-to-column joints," *Journal of Constructional Steel Research*, vol. 117, pp. 49–63, 2016.
- [8] N. Gattesco, E. Giuriani, and A. Gubana, "Low-cycle fatigue test on stud shear connectors," *Journal of Structural Engineering*, vol. 123, no. 2, pp. 145–150, 1997.
- [9] X. W. Zhou, Y. Yang, X. D. Huo, and J. Y. Xue, "Experiment on bearing capacity of composite beam with steel plate-concrete composite bridge decks," *Journal of Guangxi University*, vol. 36, no. 4, pp. 547–555, 2016.
- [10] L. I. Jianjun, *Experimental study on the fatigue of steel-concrete composite beams*, Tsinghua University, Beijing, 2002.
- [11] J. G. Nie and Y. H. Wang, "Deflection of a composite steel-concrete beam subjected to a fatigue load," *Journal of Tsinghua University*, vol. 49, no. 12, pp. 1915–1920, 2009.
- [12] J. Vaara, M. Vantanen, P. Kamarainen, J. Kemppainen, and T. Frondelius, "Bayesian analysis of critical fatigue failure sources," *International Journal of Fatigue*, vol. 130, article 105282, 2020.
- [13] T. Hozjan, M. Saje, S. Srpi, and I. Planinc, "Fire analysis of steel-concrete composite beam with interlayer slip," *Computers & Structures*, vol. 89, no. 1-2, pp. 189–200, 2011.
- [14] S. F. Jiang, X. Zeng, and D. Zhou, "Novel two-node linear composite beam element with both interface slip and shear deformation into consideration: formulation and validation," *International Journal of Mechanical Sciences*, vol. 85, pp. 110–119, 2014.
- [15] H. Wang and E. Zhu, "Dynamic response analysis of monorail steel-concrete composite beam-train interaction system considering slip effect," *Engineering Structures*, vol. 160, pp. 257–269, 2018.
- [16] Y. C. Kuang, J. R. Feng, Z. W. Yu, and X. J. Liu, "Experimental study and analysis of the structural behavior of steel-concrete composite beam after shear connector corrosion," *Applied Mechanics & Materials*, vol. 578-579, pp. 1522–1530, 2014.
- [17] H. R. Valipour and M. A. Bradford, "A steel-concrete composite beam element with material nonlinearities and partial shear interaction," *Finite Elements in Analysis & Design*, vol. 45, no. 12, pp. 966–972, 2009.
- [18] Y. Hao, "Study on the influence simulation of steel-concrete composite beam sliding," *Boletin Tecnico/Technical Bulletin*, vol. 55, no. 20, pp. 16–21, 2017.
- [19] M. Nijgh, I. A. Girbacea, and M. Veljkovic, "Elastic behaviour of a tapered steel-concrete composite beam optimized for reuse," *Engineering Structures*, vol. 183, pp. 366–374, 2019.
- [20] X. Zeng, S. F. Jiang, and D. Zhou, "Effect of shear connector layout on the behavior of steel-concrete composite beams with interface slip," *Applied Sciences*, vol. 9, no. 1, 2019.
- [21] Y. Zhang, B. Chen, A. Liu et al., "Experimental study on shear behavior of high strength bolt connection in prefabricated steel-concrete composite beam," *Composites*, vol. 159, pp. 481–489, 2019.

## Research Article

# Multispectral Remote Sensing Data Analysis Based on KNNLC Algorithm and Multimedia Image

Yingxin Sun 

Department of Information Engineering, Changchun College of Electronic Technology, 130000, China

Correspondence should be addressed to Yingxin Sun; 201615991118@stu.yznu.edu.cn

Received 18 February 2022; Revised 31 March 2022; Accepted 20 April 2022; Published 11 May 2022

Academic Editor: Wen Zeng

Copyright © 2022 Yingxin Sun. This is an open access article distributed under the Creative Commons Attribution License, which permits unrestricted use, distribution, and reproduction in any medium, provided the original work is properly cited.

In order to combine multimedia imagery and multispectral remote sensing data to analyze information, preprocessing becomes a necessary part of it. It is found that the KNN algorithm is one of the classic algorithms of data mining. As one of the most important branches in the field of data analysis, it is widely used in many fields such as classification, regression, missing value filling, and machine learning. As a lazy algorithm, this method requires no prior statistical knowledge and no additional data to train description rules and is easy to implement. However, the algorithm inevitably has many problems, such as how to determine the appropriate  $K$  value, the unsatisfactory effect of data processing for some special distributions, and the unacceptable computational complexity of high-dimensional data. In order to solve these shortcomings, the researchers proposed the KNNLC algorithm. Then, taking the classification experiment as an example, through the comparison of the experimental results on different data sets, it is proved that the average level of the classification performance of the KNNLC algorithm is better than the classic KNN classification algorithm. The KNNLC algorithm shows better performance in most cases, with an accuracy rate of 2 to 5 percentage points higher. An improved algorithm is proposed for the nearest neighbor selection strategy of the traditional KNN algorithm. First, in theory, combined with the theory of sparse coding and locally constrained linear coding, the classical KNN algorithm is improved, and the KNNLC algorithm is proposed. The comparison of the experimental results on the data set proves that the average level of the KNNLC algorithm is better than the classical KNN classification algorithm in terms of classification performance.

## 1. Introduction

Remote sensing image fusion is a technology that combines multisource remote sensing images through advanced image processing. It makes full use of the different characteristics of a variety of data, so that the image has a higher spectral and spatial resolution at the same time, and improves the vision of the image. The effect and accuracy of image feature recognition and classification accuracy are shown in Figure 1 [1]. Remote sensing image fusion is a hot research topic in the international remote sensing community in recent years. In the method of image fusion, there are some classic algorithms, such as HIS transformation method, COS transformation method, HIS transformation method, and HSV transformation method. In recent years, with the introduction of wavelet transform into the field of image processing, image fusion methods based on wavelet transform have attracted people's

attention. The fusion of SPOT panchromatic image and multispectral image based on 2-ary and 3-ary wavelet is studied, respectively. However, these two algorithms simply replace low-resolution images with high-resolution remote sensing images for low-frequency components after wavelet decomposition, without considering the loss of image features; although the feature-based binary wavelet image is studied fusion, but without considering the resolution of the image to be fused, the fusion effect is not very good [2]. Based on the in-depth study of wavelet transform fusion method, a new fusion method is proposed, a feature-based multiband wavelet fusion. The fusion results of SPOT image and TM5, 4, 3 image, SPOT panchromatic image, and SPOT multispectral band image are given and compared with other fusion methods [3]. The experimental results show that the method in this paper has obvious advantages compared with other fusion methods. Although the KNN algorithm has a good effect on applications

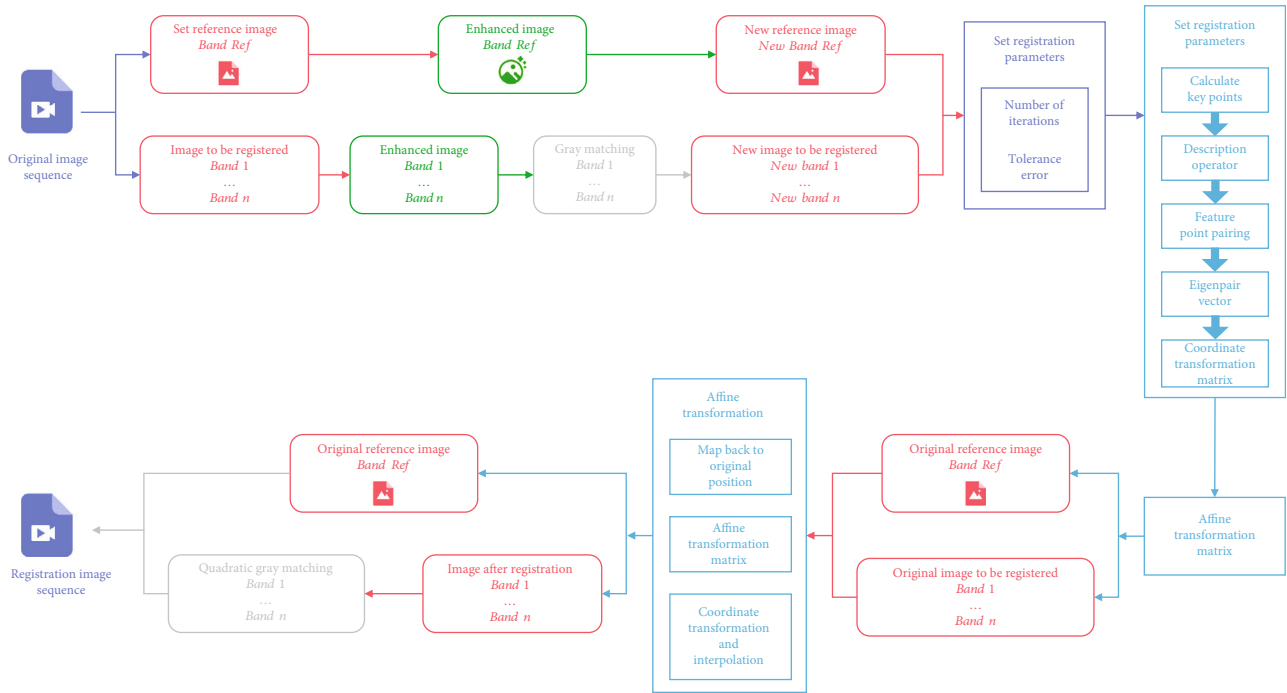


FIGURE 1: Data analysis flow chart of multispectral remote sensing image.

such as classification and prediction in many data sets, it inevitably produces many problems that need to be solved, such as the high time complexity and space complexity of the algorithm, and the  $K$  value. The processing effect is not ideal for some special distributed data and the computational complexity of high dimensional data is unacceptable. These shortcomings must be solved for a mature algorithm. Therefore, experts and scholars who are interested in this direction have done a lot of research and obtained many optimization algorithms.

## 2. Literature Review

Jin, R. et al. systematically analyzed the effects of traditional spectral parameters and two-band normalization and ratio vegetation index under different observation angles in estimating wheat leaf nitrogen content (LNC), thereby establishing a multiangle quantitative monitoring of wheat canopy leaf nitrogen content model [4]. Du, JH et al. found that the canopy reflectance and the coefficient of determination of 40 conventional spectral vegetation indices and LNC decreased with the increase of the observation angle, regardless of the forward or backward observation direction, and reached the maximum at  $-20^\circ$  in the backward direction value [5]. RI-1dB and EVI-1 have the closest relationship with LNC at  $-20^\circ$  backward and vertical angle, respectively. The areas with good correlation between the ND and SR parameters of the original spectral reflectance combination of the two bands and LNC are mainly concentrated in the blue-red light band, the green-red band, and the red-side red band combination range. This sensitive area varies with the spectrum observation. The angle is different. The new Multi-Angle Vegetation Index (MAVI), which uses the combination of sensitive spectral parameters and observation angles, can better estimate LNC. After indepen-

dent data testing at different years, the MAViR model is most sensitive to leaf nitrogen content. By systematically analyzing the angular sensitivity characteristics of different wavebands and spectral parameters, Fang, X. et al. studied the quantitative relationship between suitable characteristic parameters extracted by different spectral analysis techniques and the nitrogen content of leaves. The results show that the correlation between spectral vegetation index and leaf nitrogen content is better than that of vertical and forward observation angles in the backward observation angle. The red edge parameters mND705, GND (750, 550), NDRE, and RI-1dB are compared with LNC. The relationship is the closest, but the difference is large under different experimental factors, especially when the leaf nitrogen content is high ( $>4.5\%$ ), the spectral parameters tend to be saturated [6]. Yang, FC and others found that the newly constructed angle insensitive parameter (AIVI) reduces the influence of different test factors. In the range of  $-10^\circ \sim 40^\circ$  observation angle, AIVI can establish a unified and stable monitoring model, and it has been independently tested. According to the data test, it is the best to construct a monitoring model of wheat canopy leaf nitrogen content based on AIVI, which has strong angle adaptability [7]. Ren, J. et al. found that the inversion accuracy of wheat leaf nitrogen content based on FA-BPNN analysis was significantly higher than that of conventional spectral parameters under different observation angles [8]. Therefore, both the new vegetation index AIVI and FA-BPNN can reliably monitor the nitrogen content of wheat leaves under different experimental conditions. By comparing the relationship between various spectral analysis methods and LAI under different observation angles, the appropriate band sensitive to changes in LAI can be extracted, and the observation angle; thus, a quantitative monitoring model for wheat LAI was established. The results show that different

spectral analysis methods are more suitable for monitoring LAI (leaf area index) near the vertical angle. The spectral reflectance and the correlation between spectral parameters and LAI (leaf area index) in the backward observation direction are higher than those in the forward observation direction. Li, J. et al. found that the two-band ratio (SR) and normalized index (ND) under different observation angles did not show outstanding monitoring advantages, but the SR effect was better than the ND method [9]. Using factor analysis technology, it is found that the load of the green light band decreases with the increase of the observation angle in the first factor and increases with the increase of the observation angle in the second factor. After independent test data in different years, the wheat LAI (leaf area index) monitoring model established with the spectral parameter  $VI_{opt}$  as a variable has good test results and can be used for accurate estimation of wheat LAI (leaf area index). Torra, V. et al. analyzed and compared the saturation, angle sensitivity, and variety sensitivity of commonly used vegetation indices for estimating LAI (leaf area index). The results of wide-angle adaptability show that the accuracy of LAI (leaf area index) estimation of spectral parameters is better for erect varieties than for discrete varieties. Nonperpendicular observation angles did not significantly improve the ability of spectral parameters to estimate LAI (leaf area index) [10]. Except for EVI and TVI, the spectral parameters NDVI, SAVI, OSAVI, MSAVI, WDRVI, MTVI, and mND705 all tend to be saturated when LAI is greater than 4. KA Zweig et al. found that the angle reduction coefficient  $K_f$  constructed based on green light and near-infrared bands is closely related to LAI (leaf area index). The product of VIs and  $K_f$  effectively alleviates the saturation and variety sensitivity of LAI (leaf area index) estimation at different observation angles, and significantly improves the monitoring accuracy and adaptability of LAI (leaf area index) [11]. V., Subramaniaswam et al. found that in the above-mentioned spectral parameters, except for WDRVI, EVI, and TVI, the other spectral parameters and the  $K_f$  product established a unified monitoring model at all observation angles. The prediction model based on mND705 and OSAVI spectral parameters is more accurate and reliable [12]. The effects of various spectral processing methods to estimate chlorophyll density were analyzed by integrating spectral data from different observation angles, and a multi-angle remote sensing monitoring model for wheat leaf pigment density was established. The results show that the spectral reflectance that has a good correlation with chlorophyll density is mainly concentrated in the red edge and the near-infrared region (720–900 nm). The spectral parameters VOG1, RI-1dB, NDRE, SDR/SDB, and DD are closely related to the chlorophyll density. The sensitive bands of the normalized and ratio vegetation index of the two bands in the backward observation direction are mainly concentrated in the red area, and in the forward observation direction, they are mainly concentrated in the blue and red light areas. Research by Hu, J. et al. found that the first factor of the FA-BPNN model is mainly concentrated in the blue and red bands under different observation angles, and the second factor is mainly concentrated in the near-infrared region. Backward observation close to the vertical observation angle is beneficial to improve the prediction accuracy of chlorophyll density. The spectral parameters SDR/SDB, DD, ND (720, 760), and

ND (732, 738) are the most effective for monitoring wheat chlorophyll density [13]. K nearest neighbors (KNN for short) is an extension of the nearest neighbor method and is a lazy learning method based on instance statistical classification. As one of the classic algorithms for classifiers and machine learning, KNN's earliest related papers are nearest neighbor pattern classification published by Cover<sup>TM</sup> and Hart<sup>PE</sup> of Stanford University in 1967. In order to improve the KNN algorithm, the number of nearest neighbors is set to  $K$ . The mathematical model of the theory has been developed, opening the door to various improved studies based on nearest neighbor theory.

### 3. Methods

**3.1. KNN Algorithm.** The basic idea of KNN: For an input test sample with no assigned label, first compare the features or attributes of the test sample with the corresponding features or attributes of all training samples with existing labels; then find the  $K$  nearest samples from the training samples, and then sort the labels of these training samples in descending order, and the label corresponding to the first position in the sequence is the label of the test sample. First, for a given data set, if any data in the set has a class label, then this set is called a training sample set, and the data in it is called a training sample; conversely, if the class label of the data is unknown, it is called the test sample, and the collection is called the test sample set.

The working principle of the KNN classification algorithm is to use a similarity measure to compare each attribute or feature of the test sample with the attributes or features corresponding to all training samples in the training sample set, and arrange the test samples corresponding to the similarity in descending order. According to this, the first  $K$  most similar (measured nearest) training samples ( $K$  nearest neighbors) can be found in the training set. Generally,  $K$  is selected as an integer not greater than 20. Finally, sort the number of occurrences of the class labels of the  $K$  training samples in descending order, and the label corresponding to the first place in the sequence is the class label of the test sample [14, 15]. First, for a given data set, if any data in the set has a class label, Figure 2 is a classic example of the KNN classification process. In Figure 2, the training sample includes two types of triangles (Angle) and squares (Square). For the sake of simplicity and clarity of description, we use  $T$  and  $S$  to represent their numbers, respectively. The dots in the figure are test samples, and  $K$  is the number of training samples closest to the test sample, that is, the number of nearest neighbors. When  $K=3$ ,  $T=2$ ,  $S=1$ , and  $T > S$  in the small circle in the dotted line as shown in the figure. According to the principle described above, the test sample is assigned to the triangle type at this time. When  $K=5$  is adjusted,  $T=2$ ,  $S=3$ , and  $T < S$  within the large dashed circle in the figure; at this time, the test sample label is judged to be a square. Figure 3 is a flowchart of KNN classification. The specific steps involved in calculating the similarity measurement, selecting the nearest neighbor, and classifying when executing the algorithm will be described in detail later. The flow of the algorithm is described as follows: Supposing that there are  $m$  samples in the training set, and the



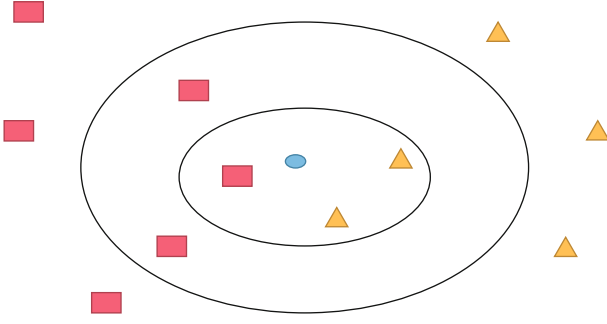


FIGURE 2: An example of KNN algorithm.

number of attributes of each sample is  $n$ , then the training set can be recorded as

$T = \{X_i = (x_{i1}, x_{i2}, \dots, x_{in}) | i = 1, 2, \dots, m\}$ . The set consisting of the class label of each sample in the set can be denoted as  $L = \{C_i | i = 1, 2, \dots, m\}$ . The test sample set is denoted as  $S = \{S_i = (s_{i1}, s_{i2}, \dots, s_{in}) | i = 1, 2, \dots, a\}$ , where  $a$  is the number of test samples [16, 17]. Then, KNN classification calculation, where  $a$  is the number of test samples. The KNN classification algorithm can be described in Figure 2.

Simply put, the similarity between the test sample and each training sample in the KNN algorithm is measured by calculating the distance. For different data, using an appropriate distance metric is the premise to obtain a good data processing effect. The distance metrics commonly used in the KNN algorithm are Euclidean Distance, Manhattan Distance, MinKowsKi Distance, and Hamming Distance. Given training samples  $X = (x_1, x_2, \dots, x_n)$  and test samples  $S = (s_1, s_2, \dots, s_n)$ , then the distance  $\text{dist}(X, S)$  between them is calculated with the following formula.

See formula (1) for Euclidean distance:

$$\text{dist}(X, S) = \sqrt{\sum_{i=1}^n (x_i - s_i)^2}. \quad (1)$$

See formula (2) for Mahalanobis distance:

$$\text{dist}(X, S) = \sqrt{\sum_{i=1}^n |x_i - s_i|}. \quad (2)$$

See formula (3) for Ming's distance:

$$\text{dist}(X, S) = \left( \sum_{i=1}^n (|x_i - s_i|^q) \right)^{1/q}. \quad (3)$$

The Hamming distance is shown in formula (4):

$$\text{dist}(X, S) = \sum_{i=1}^n |x_i - s_i|. \quad (4)$$

Minmax normalization is the most common data normalization processing method. The principle of this method is to use a mapping function to project attributes or eigenvalues into the

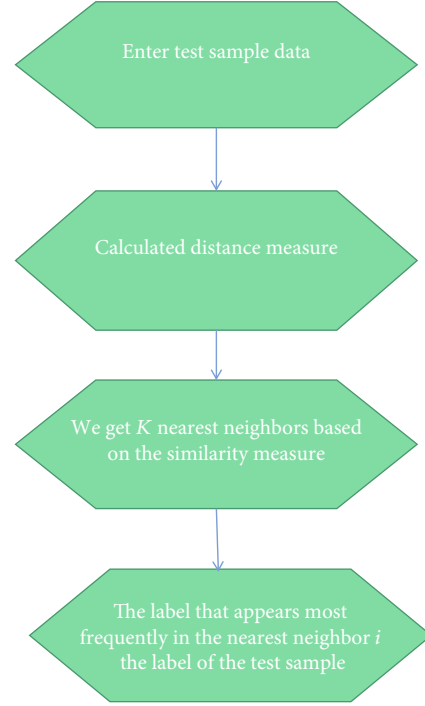


FIGURE 3: KNN algorithm flow chart.

[0,1] interval. Minmax normalization can be expressed by the following formula (5):

$$a' = \frac{a - \min_F}{\max_F - \min_F}. \quad (5)$$

Among them,  $a$  is the original value,  $a'$  is the value mapped in the [0,1] interval, and  $\min_F$  and  $\max_F$  are the lower and upper bounds of the values belonging to the same attribute or feature, respectively. There are many commonly used normalization methods, but the basic principles are similar. For example, the form introduced below is shown in formula (6):

$$a'_{ij} = \frac{a_{ij}}{\sqrt{\sum_{i=1}^{m+1} \sum_{j=1}^n a_{ij}^2}}. \quad (6)$$

The rules of this voting mechanism will also be used in this study. The mathematical representation of the most frequent rule is shown in Equation (7):

$$C_S = \arg \max_{x \in N} \sum I(v = C_x). \quad (7)$$

Since attributes naturally have such distribution characteristics, in the algorithm, in order to make the processing results better reflect the objective facts, weights are generally assigned to each attribute. In the KNN algorithm, the weighting formula of the label can be used as formula (8) form representation:

$$C_s = \arg \max_{x \in N} \sum w_i \times I(v = C_x). \quad (8)$$

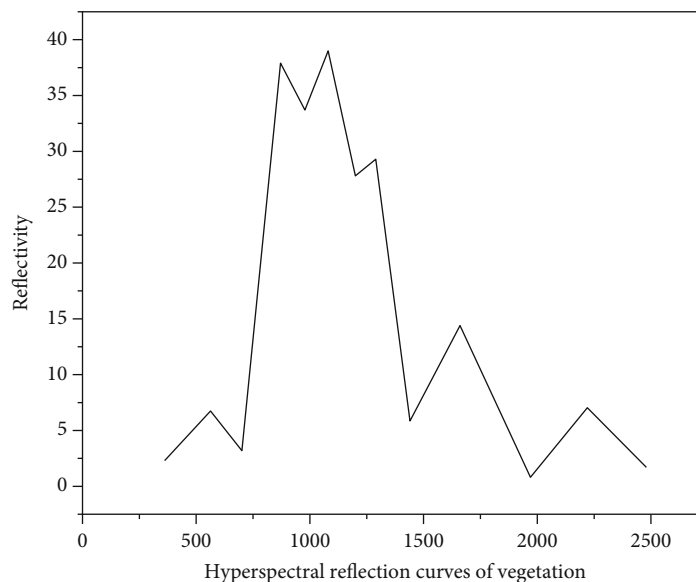


FIGURE 4: The main peak and valley characteristics of the vegetation hyperspectral reflectance curve.

Among the many weighting methods, the weighting method based on the reciprocal similarity is the most classic, and it is also used consistently by the KNN algorithm. Its mathematical expression is shown in Equation (9):

$$w_i = \frac{1}{\text{dist}(X, S)^P}. \quad (9)$$

Among them,  $P$  is the weighted power exponent, usually taken as  $P=2$ , see formula (10):

$$w_i = \frac{1}{\text{dist}(X, S)^2}. \quad (10)$$

**3.2. Data Analysis and Utilization.** A Locally Constrained Linear Coding Based on Related Research (Locality-constrained Linear Coding, LLC) to improve the classic KNN algorithm. Multiangle remote sensing data has the characteristics of rich information and large amount of data. The selection of spectral absorption characteristic parameters, sensitive angles, and optimal calculation methods are important issues in the study of hyperspectral remote sensing. In addition to the data processing methods commonly used in conventional vertical remote sensing, this study also adopted normalization (ND), ratio (SR), and neural network (BP) analysis methods. The specific methods are as follows: Figure 4 shows typical reflections of vegetation spectral curves, which form absorption valleys at 455 (blue light), 680 (red light), 980, 1200, and 1468 nm, and reflection peaks at 550 (green light), 1090, 1285, 1685, and 2200 nm [18, 19].

Factor analysis is a statistical method for extracting common factors from multiple variables for the purpose of dimensionality reduction. Factor analysis can make factor variables more interpretable through rotation, as shown in Figure 5. Use SPSS software to perform factor analysis on the standardized spectrum data, select the critical factor

numbers whose cumulative contribution rate exceeds 99%, and output the factor data. The BPNN model is provided by Matlab's Neural Network Toolbox. The network is divided into an input layer, a hidden layer, and an output layer. In this study, the input vector is  $I$  and the learning goal is  $T$ . The input layer is a comprehensive factor with a large contribution rate obtained after factor analysis: the number of neurons in the middle layer is the number of comprehensive factors, and the activation function of the middle hidden layer is "TANSIG"; the neurons in the output layer are 1, and the activation function is "PURELN"; the training function uses the TRAINLM function [20, 21].

## 4. Results and Analysis

In the classification experiment, we select 4 typical sample sets from the UCI data set as experimental materials. The basic situation of the sample data is shown in Table 1. Among them, Australian and Magic are data sets with only two labels, respectively, and the experiments on them belong to the binary classification experiment, while the experiments on the two data sets of Mpgdata and Ins belong to the case of multiple classification [21–23]. In the four data sets, Iris is a common data set prone to overfitting. The sample is quoted only to show the feasibility of the algorithm and the degree of improvement compared with the more classic algorithms. Its classification effect is obviously difficult to reach in practice. However, the amount of data in the Magic data set is relatively large. Although it is not as good as the big data standard, it is still not general. From this, the potential of the improved algorithm in processing high-capacity data sets compared to traditional algorithms can be seen.

For algorithm classification performance, regardless of the sample size and the number of label classes, the establishment of the corresponding confusion matrix (confusion matrix) is a relatively common and objective evaluation method [24, 25]. The following briefly introduces the confusion matrix. In the

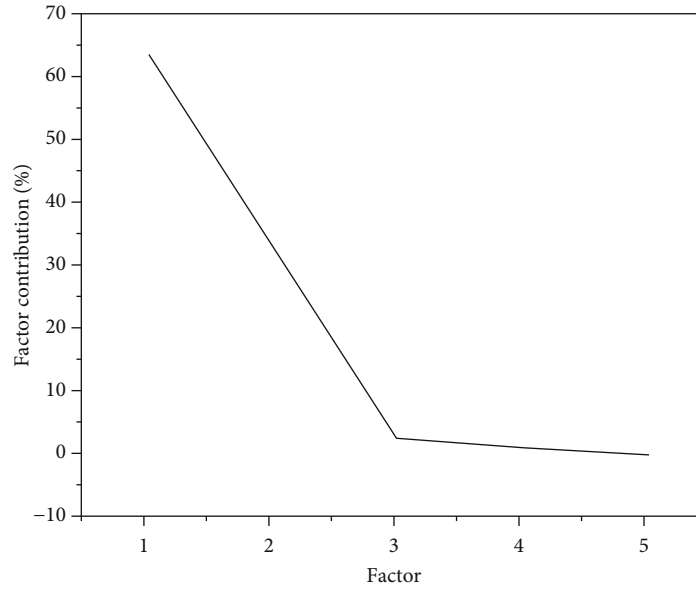


FIGURE 5: Factor contribution degree after t400-900nm band rotation.

TABLE 1: Basic situation of experimental materials.

Data set	Number of instances	Number of attributes
Inis	150	4
Mpgdata	390	7
Australian	690	14
Magic	19020	10

TABLE 2: Confusion matrix.

Predicted class Actual class	Positive	Negative
Positive	TP	FP
Negative	FN	TN

TABLE 3: Accuracy comparison of two classification algorithms (mean  $\pm$  standard deviation).

Data set	KNNLC	KNN
Iris	0.9667 $\pm$ 0.0470	0.9400 $\pm$ 0.0857
Mpg data	0.8000 $\pm$ 0.0551	0.7769 $\pm$ 0.0745
Australian	0.8464 $\pm$ 0.0445	0.7928 $\pm$ 0.0305
Magic	0.8220 $\pm$ 0.0055	0.8002 $\pm$ 0.0088

classification problem, due to the difference between the predicted result and the objective facts, the final result has four possibilities, namely, TP (true positive), FP (false positive), FN (false negative), and TN (true negative). They, respectively, represent the four possibilities of pairing between the sample and the label, and the corresponding confusion matrix is shown in Table 2.

Table 2 shows a quantitative comparison of the two algorithms on the four data sets. The use of the mean  $\pm$  standard

deviation makes the results more accurate. For classification algorithms, accuracy is often one of the most concerned evaluation criteria. Compared with the classic KNN classification algorithm, the KNNLC algorithm shows better performance in most cases, with an accuracy rate of 2 to 5 percentage points higher [26]. Absolutely, the classic algorithm is classic because of its extensive effectiveness. For data with different distributions, the adaptability of classic algorithms may be more common. For the classification of Mpgdata data sets, sometimes the effect of improved algorithms is not satisfying. It shows that the KNNLC algorithm is sensitive to specific distributed data and needs further improvement. The results on high-capacity sample data sets show that to a certain extent, the KNNLC algorithm may be more suitable for processing high-dimensional data, and its classification accuracy and stability are significantly better than the classic KNN algorithm. On the whole, in the classification problem, the KNNLC classification algorithm has better performance than the classic KNN classification algorithm, and the higher the data dimension, the more obvious this advantage. In fact, this is because KNNLC uses local coding to obtain neighbor samples, which meets the expectations of theoretical research, as shown in Table 3.

Table 3 shows the quantitative comparison of the experiments of the two algorithms on the four data sets, respectively, using the form of mean  $\pm$  standard deviation to make the results more accurate. For classification algorithms, accuracy is often one of the most concerned evaluation criteria. As can be seen from the above table, compared to the classic KNN classification algorithm, the KNNLC algorithm shows better performance in most cases, with an accuracy rate of 2 to 5 percentage points higher.

## 5. Conclusion

Research on the improvement of KNN algorithm and its application in the field of image processing. This article mainly

discusses and improves the traditional KNN algorithm and the mean filtering algorithm from the perspective of the nearest neighbor selection strategy. Therefore, in the process of obtaining the neighbors, the neighbors with higher similarity can be captured. At the same time, based on this idea, the template selection of the mean filter is regarded as the neighbor selection, and the membership function is combined to obtain a more effective filter template, and experiments have proved the advantages of the improved algorithm [27]. Aiming at the problem that traditional KNN algorithm is sensitive to data distribution, combined with sparse coding and LLC theory, using the nearest neighbor selection strategy of local coding, KNNLC algorithm is proposed, which improves the effect of classic KNN algorithm. Through experiments on multiple representative data sets, it is proved that the KNNLC algorithm has great advantages and potential compared with the classic KNN algorithm in classification performance. The KNNLC algorithm shows better performance in most cases, with an accuracy rate of 2 to 5 percentage points higher.

## Data Availability

The data used to support the findings of this study are available from the corresponding author upon request.

## Conflicts of Interest

The authors declare no conflicts of interest.

## References

- [1] Y. Liang, C. Sun, J. Jiang, X. Liu, and Y. Xie, "An efficiency-improved clustering algorithm based on KNN under ultradense network," *IEEE Access*, vol. 8, pp. 43796–43805, 2020.
- [2] H. Guo, Y. Li, Y. Li, L. Xiao, and J. Li, "BPSO-Adaboost-KNN ensemble learning algorithm for multi-class imbalanced data classification," *Engineering Applications of Artificial Intelligence*, vol. 49, pp. 176–193, 2016.
- [3] K. Wang, X. Yu, Q. Xiong, Q. Zhu, and L. Zhao, "Learning to improve WLAN indoor positioning accuracy based on DBSCAN-KRF algorithm from RSS fingerprint data," *IEEE Access*, vol. 7, pp. 72308–72315, 2019.
- [4] R. Jin, Y. Wang, C. Niu, and W. Song, "A novel high precision and low consumption indoor positioning algorithm for internet of things," *IEEE Access*, vol. 7, pp. 86874–86883, 2019.
- [5] J. H. Du, "Automatic text classification algorithm based on gauss improved convolutional neural network," *Journal of Computational Science*, vol. 21, pp. 195–200, 2017.
- [6] X. Fang, Z. Jiang, L. Nan, and L. Chen, "Optimal weighted k-nearest neighbour algorithm for wireless sensor network fingerprint localisation in noisy environment," *IET Communications*, vol. 12, no. 10, pp. 1171–1177, 2018.
- [7] F. C. Yang, B. Tseng, C. Y. Lin, Y. J. Yu, A. Linacre, and C. I. Lee, "Population inference based on mitochondrial dna control region data by the nearest neighbors algorithm," *International Journal of Legal Medicine*, vol. 135, no. 4, pp. 1191–1199, 2021.
- [8] J. Ren, Y. Wang, C. Niu, W. Song, and S. Huang, "A novel clustering algorithm for wi-fi indoor positioning," *IEEE Access*, vol. 7, pp. 122428–122434, 2019.
- [9] J. Li, "An improved K-nearest neighbor algorithm using tree structure and pruning technology," *Intelligent Automation and Soft Computing*, vol. 25, no. 1, pp. 1–15, 2019.
- [10] V. Torra, Y. Narukawa, A. Honda, and S. Inoue, "Modeling decisions for artificial intelligence," *14th International Conference, MDAI 2017*, 2017, pp. 77–88, Kitakyushu, Japan, 2017.
- [11] K. A. Zweig, O. Deussen, and T. D. Krafft, "Algorithmen und meinungsbildung," *Informatik-Spektrum*, vol. 40, no. 4, pp. 318–326, 2017.
- [12] V. Subramaniaswam and R. Logesh, "Adaptive KNN based recommender system through mining of user preferences," *Wireless Personal Communications*, vol. 97, no. 2, pp. 2229–2247, 2017.
- [13] J. Hu, Y. Li, W. X. Yan, J. Y. Yang, H. B. Shen, and D. J. Yu, "KNN-based dynamic query-driven sample rescaling strategy for class imbalance learning," *Neurocomputing*, vol. 191, pp. 363–373, 2016.
- [14] S. Yin, H. Zheng, S. Xu, H. Rong, and N. Zhang, "A text classification algorithm based on feature library projection," *Journal of Central South University*, vol. 48, no. 7, pp. 1782–1789, 2017.
- [15] C. Yücelba, "A new approach: information gain algorithm-based k-nearest neighbors hybrid diagnostic system for Parkinson's disease," *Physical and Engineering Sciences in Medicine*, vol. 44, no. 2, pp. 511–524, 2021.
- [16] Z. Qin, T. Kirubarajan, and Y. Liang, "Application of an efficient graph-based partitioning algorithm for extended target tracking using gm-phd filter," *IEEE Transactions on Aerospace and Electronic Systems*, vol. 56, no. 6, pp. 4451–4466, 2020.
- [17] H. Sun, X. Liu, Q. Deng, W. Jiang, and Y. Ha, "Efficient FPGA implementation of K-nearest-neighbor search algorithm for 3D LIDAR localization and mapping in smart vehicles," *Circuits and Systems II: Express Briefs, IEEE Transactions on*, vol. 67, no. 9, pp. 1644–1648, 2020.
- [18] N. Bhaskar and P. M. Kumar, "Optimal processing of nearest-neighbor user queries in crowdsourcing based on the whale optimization algorithm," *Soft Computing*, vol. 24, no. 17, pp. 13037–13050, 2020.
- [19] D. A. Adeniyi, Z. Wei, and Y. Yang, "Personalised news filtering and recommendation system using Chi-square statistics-based K-nearest neighbour ((SB)-s-2-KNN) model," *Enterprise Information Systems*, vol. 11, no. 6–10, pp. 1283–1316, 2017.
- [20] H. J. Cho and J. Chae, "A safe exit algorithm for moving k nearest neighbor queries in directed and dynamic spatial networks," *Journal of Information Science and Engineering*, vol. 32, no. 4, pp. 969–993, 2016.
- [21] B. Aiazzi, L. Alparone, S. Baronti, R. Carlà, A. Garzelli, and L. Santurri, "Sensitivity of pansharpening methods to temporal and instrumental changes between multispectral and panchromatic data sets," *IEEE Transactions on Geoscience & Remote Sensing*, vol. 55, no. 1, pp. 308–319, 2017.
- [22] U. K. Ghosh, K. K. Naik, and M. P. Kesari, "Digital image processing of multispectral aster imagery for delineation of alteration and related clay minerals in sakoli belt: Maharashtra – a case study," *Journal of the Geological Society of India*, vol. 88, no. 4, pp. 464–470, 2016.
- [23] Q. Xie, X. Chen, L. Li, K. Rao, L. Tao, and C. Ma, "Image fusion based on kernel estimation and data envelopment analysis," *International Journal of Information Technology & Decision Making*, vol. 18, no. 2, pp. 487–515, 2019.

- [24] L. Chen, X. Zhang, and H. Ma, "Sparse representation over shared coefficients in multispectral pansharpening," *Tsinghua Science and Technology*, vol. 23, no. 3, pp. 315–322, 2018.
- [25] C. Han, H. Zhang, C. Gao, C. Jiang, N. Sang, and L. Zhang, "A remote sensing image fusion method based on the analysis sparse model," *IEEE Journal of Selected Topics in Applied Earth Observations & Remote Sensing*, vol. 9, no. 1, pp. 439–453, 2016.
- [26] D. Stevic, I. Hut, N. Dojcinovic, and J. Jokovic, "Automated identification of land cover type using multispectral satellite images," *Energy & Buildings*, vol. 115, pp. 131–137, 2016.
- [27] I. Kotaridis and M. Lazaridou, "Remote sensing image segmentation advances: a meta-analysis," *ISPRS Journal of Photogrammetry and Remote Sensing*, vol. 173, no. 3, pp. 309–322, 2021.

## Research Article

# Intelligent Management of Land Resources Based on Internet of Things and GIS Technology

Hao Gong<sup>1</sup> and Chen He<sup>2</sup> 

<sup>1</sup>School of Land Science & Technology, China University of Geosciences (Beijing), Beijing 100083, China

<sup>2</sup>Faculty of Accounting, Hubei University of Economics, Wuhan 430205, China

Correspondence should be addressed to Chen He; 00001678@hbue.edu.cn

Received 17 March 2022; Revised 13 April 2022; Accepted 19 April 2022; Published 11 May 2022

Academic Editor: Wen Zeng

Copyright © 2022 Hao Gong and Chen He. This is an open access article distributed under the Creative Commons Attribution License, which permits unrestricted use, distribution, and reproduction in any medium, provided the original work is properly cited.

In order to improve the effect of land resource management, this paper combines the Internet of Things technology and GIS technology to build an intelligent management system for gradient resources to improve the efficiency of land resource management. Aiming at the hybrid intelligent model of wetland resource remote sensing monitoring technology, this paper analyzes and studies the remote sensing image processing theory. Moreover, this paper studies in detail remote sensing image restoration, TM image reflectivity simulation imaging, image enhancement technology, optimal band selection based on the characteristics of wetland resources, expert decision analysis, deep mining of image data, knowledge reasoning, and decision tree analysis to form a theoretical support system for a hybrid intelligent classification model for wetland resources. The research shows that the intelligent management system of land resources based on the Internet of Things and GIS technology has a good effect in the collection and processing of land resource information and can effectively improve the management efficiency of land resources.

## 1. Introduction

China has a vast territory and abundant resources in absolute quantity, but the per capita quantity is insufficient. Moreover, the natural resources, ecological and environmental conditions, and social and economic development vary greatly from place to place, and the stages of development and the problems existing in the development are also different. If we do not consider the characteristics and differences of regions and use the same standard to measure the development of various regions, it will be difficult for the evaluation to be objective and fair. At the same time, when the same policy is used to guide the development of various regions, the measures are often lacking in pertinence and effectiveness. In addition, with the rapid increase of the population, on the one hand, the area of arable land in China has dropped sharply, the land has been degraded, and the land reserve resources are seriously insufficient. On the other hand, extensive land use, low utilization rate, and low output rate make the situation of land resources increasingly severe

and the contradiction between man and land increasingly prominent.

The research on comprehensive land carrying capacity has its own characteristics: first, the research on comprehensive land carrying capacity is a systematic perspective on regional land, grain, population, and social development. It involves many aspects and is affected by many factors, of which nature and humanity are the two most important ones. Natural factors include the quantity and quality of land resources, regional climatic conditions and water resources, etc.; human factors include population status, the level of social and economic development, the rationality of technological level resource utilization, etc. These factors together affect the level of carrying capacity of land resources makes it an intricate system. Secondly, while the research on comprehensive land carrying capacity has been improved with the development of science and technology and some natural processes, it does not mean that it can develop permanently and unrestrictedly. It is constrained by two aspects: the absolute limit of the productivity of land resources and

the relative limit over a certain period of time. The former refers to the ultimate source of productivity of land resources—solar radiation energy is limited per unit area; especially, the conversion rate of solar energy cannot exceed a certain limit, thus stipulating the limit of productivity of land resources. In the foreseeable future, it is impossible for the development of science and technology to break through the limit of land productivity, such as the level of grain yield per unit. The limit of land production capacity determines the limit of land carrying capacity, which has far-reaching significance for objectively grasping the regional resource-population problem.

The “comprehensive” study of comprehensive land carrying capacity includes two meanings [1]. On the one hand, for the carrier, the land should not be limited to cultivated land but should be a generalized land including garden land, forest land, pasture land, urban settlements and industrial and mining land, water area, transportation land, and unused land. On the other hand is the question of what to carry, that is, carrying substance. Land problems are caused by human social and economic activities. The goal of land use is to coordinate human social and economic activities with the corresponding environment and to protect and improve the land resources for human survival and development. Therefore, the bearing object should be various social and economic activities of human beings, such as the city scale, economic output value, transportation scale, land pollution capacity, etc., not only the bearing population size and population consumption pressure, which forms the “comprehensive carrying capacity of land.” The comprehensive carrying capacity of land refers to the maximum population and urban development scale that the land resources can bear on the basis of the foreseeable level of technological, economic and social development, the principle of sustainable development, and the premise of maintaining the benign development of the human ecological environment under the current development stage [2]. That is to say, the size of the comprehensive land carrying capacity is not only a reflection of the characteristics of the natural geographical environment but also depends on the development level of human society, economy, and technology; the effective use of land resources by humans; and the improvement of the ecological environment [3].

This paper combines the Internet of Things technology and GIS technology to build an intelligent management system for gradient resources, improve the efficiency of land resource management, and effectively promote the progress and development of intelligent land management technology.

## 2. Related Work

Literature [4] establishes a real estate database management system, which integrates the decentralized management of land registers and other information, which greatly improves work efficiency; in the application research of basic farmland management information system, literature [5] uses MapGIS secondary. The development library SDK builds a permanent basic farmland database and uses C++ language to design and implement a basic farmland demarcation system. Based on the MapGIS9 platform, Yang Weibin of Xiamen University adopts a combination of C/S and B/S architecture

to solve the possible defects of the basic farmland management information system. Literature [6] developed the basic farmland management information system of Ninghua County based on ArcGIS Engine components and C# as the development language. Literature [7] used Oracle as the database management platform and ArcSDE as the spatial database search engine, participated in the design and establishment of the basic farmland management information system in Sichuan Province, and used ArcGIS Server and WebService technology to enable the public to conduct related business queries on the browser side. These attempts in basic farmland information management have provided effective advanced experience for the system construction of farmland protection [8]. However, a large part of the region has not established a comprehensive and effective basic farmland information system, and we still need to explore and work together [9]. The use of UML language and CASE tools is the trend of GIS software development [10]. Literature [11] studies and summarizes the development process of cadastral information system by adopting the object-oriented GIS development method and combining with UML. Literature [12] describes the land change process realized by drawing lines with the mouse using UML and realizes the land change subsystem in the land management information system by means of secondary development. These studies reflect the application of UML technology in land information management software development from different angles and meet the needs of software system development in GIS projects. On the basis of the above practice, further research is carried out in combination with the characteristics of permanent basic farmland data and applications. The theoretical technology of geographic information system has gone through the process of desktop geographic information system, client/server mode in local area network, and WebGIS [13]. At present, the land information system is still in the stage of continuous development and generally shows the following development trends: (1) The integration with remote sensing system (RS), global positioning system (GPS), and other technologies needs to be strengthened. Surveying and mapping technologies such as RS and GPS can provide strong technical support for the real-time collection of large-area land use information and achieve high precision and automation of ground data collection [14]. (2) Modern land management information systems not only care about the distribution area, and it is a research direction of land management information system [15]. (3) With the help of artificial intelligence theory and expert system technology enables computers to use expert knowledge to simulate human brain thinking for reasoning, which can greatly improve work efficiency, and its applications in cartography, spatial decision support, and intelligent data processing need to be further deepened [16]. (4) With the advent of the era of big data and the rapid development of network technology, the use of the Internet to publish spatial data and provide users with the functions of spatial data browsing, query, and making thematic maps and analysis has become an inevitable trend in the development of land information systems [17]. Literature [18] proposes to build a “land and resources cloud”

technology system and create an “Internet + land and resources service” model, which is to make full use of advanced concepts and technologies such as cloud computing and big data to achieve unified deployment of services and comprehensive data sharing.

### 3. Remote Sensing Image Processing Based on Internet of Things and GIS

After the GCP ground control point selection is completed, the pixel coordinates  $(x, y)$  should be converted into image coordinates that are related to the reference coordinates  $(X, Y)$  through a mathematical model. The selected coordinate change function (mathematical correction model) is a polynomial correction model, and commonly used image correction functions include polynomial, Legendre polynomial, and collinear correction. Because the polynomial principle is intuitive, the calculation is simple, and it has better accuracy; the polynomial correction method is generally chosen. In this study, a quadratic polynomial function is used to perform precise geometric correction. The formula is as follows:

$$\begin{aligned} x &= a_0 + a_1X + a_2Y + a_3X^2 + a_4XY + a_5Y^2, \\ y &= b_0 + b_1X + b_2Y + b_3X^2 + b_4XY + b_5Y^2. \end{aligned} \quad (1)$$

Polynomial coefficients (conversion parameters) are obtained by least squares regression. According to the root mean square error formula ( $\text{RMS}_{\text{error}}$ ), the difference between the estimated coordinates and the original coordinates is obtained.

$$\text{RMS}_{\text{error}} = \sqrt{(x' - x)^2 + (y' - y)^2}, \quad (2)$$

That is, by calculating the root mean square error of each control point, the ground control points with larger errors can be checked, and the accumulated overall root mean square error can be obtained, so as to obtain the accuracy of coordinate change.

The absorptivity and reflectivity of an object vary with the temperature of the object and the wavelength of incident radiant energy, so we define the monochromatic reflectance and monochromatic absorptivity of an object as [19]:

$$\alpha(\lambda) = \frac{E_a(\lambda)}{E}, \quad (3)$$

$$\rho(\lambda) = \frac{E_r(\lambda)}{E}. \quad (4)$$

In the formula,  $a(\lambda)$  is the monochromatic absorptivity of light with wavelength  $\lambda$ ,  $\rho(\lambda)$  is the monochromatic reflectance of light with wavelength  $\lambda$ ,  $E_a(\lambda)$  is the energy absorbed by light with wavelength  $\lambda$  incident on the surface of an opaque object,  $E_r(\lambda)$  is the energy reflected by the light with wavelength  $\lambda$  incident on the surface of an opaque object, and  $E$  is the total incident energy.

We use the TM data to make the principle of simulated reflectivity image, and the energy carried by the color light of different bands and the weight  $W_i$  of the total energy are shown in the table. From this, we can obtain the total reflected energy:

$$E\rho = \sum_{i=1}^5 W_i TM_i + W_7 TM_7. \quad (5)$$

In the formula,  $E\rho$  is the total reflected energy,  $K_i$  is the weight of the  $i$ -th band in the total energy,  $TM_i$  is the remote sensing data of the  $i$ -th band,  $W_7$  is the weight of the seventh band in the total energy, and  $TM_7$  is the remote sensing data of the seventh band.

From Wien's displacement theorem  $\lambda \max = 2897/T$ , it can be known that with the increase of temperature, the peak value of radiant emission shifts to the short-wave direction. When the surface temperature is  $-60^\circ\text{C}$ , the wavelength peak of the surface radiation is  $13.6\ \mu\text{m}$ , and when the surface temperature is  $60^\circ\text{C}$ , the wavelength peak of the surface radiation is  $8.7\ \mu\text{m}$ . The surface temperature is generally between  $-60^\circ\text{C}$  and  $60^\circ\text{C}$ , and the radiated wavelength peak falls within the wavelength range of TM6. Therefore, the relative value of the energy lost by the earth due to long-wave radiation can be represented by TM6.

The surface of the earth with the size of each pixel receives the light energy of the sun as  $E_0$ , then:

$$E = E_a + E_p, \quad (6)$$

$$a + p = 1. \quad (7)$$

The energy change of a pixel on the earth's surface (expressed as a temperature difference change) is  $E_\Delta$ , and the scattered energy is  $E_e$ , then:

$$E_\Delta = E - E_e - E_p. \quad (8)$$

That is,

$$E - E_\Delta = E_e + E_p. \quad (9)$$

Since the relative value of the energy lost by the earth due to long-wave radiation can be represented by  $TM_6$ , formula (7) can be written as follows:

$$E - E_\Delta = TM_6 + E_p. \quad (10)$$

We set:

$$P_{\text{sim}}(\lambda) = \frac{E_r(\lambda)}{E - E_\Delta} = \frac{E_r(\lambda)}{TM_6 + E_p}. \quad (11)$$

In a very small time, the temperature difference change of the surface can be ignored; that is,  $E_\Delta = 0$ , and formula (9) can be transformed into:



$$P_{\text{sim}}(\lambda) = \frac{E_r(\lambda)}{E} = \frac{E_r(\lambda)}{E_{tm_6} + E_\rho}. \quad (12)$$

Since  $E_\Delta$  is not strictly equal to 0, we call  $P_{\text{sim}}$  as the monochromatic reflectance. Through the different energy values of different bands, the monochromatic reflectance data of each band in the TM band can be obtained, and the synthesized color map is called the simulated reflectance map.

The first step in band combination is to select a band by numerical evaluation according to the amount of information contained in each band of a remote sensing image. Through analysis, it can be determined which parts or which bands (i.e., band subsets) contain the amount of information. The standard deviation of each band reflects the total dispersion of the gray value and the average value of each pixel in the image and to a certain extent reflects the amount of information in each band. The larger the value, the greater the amount of information contained. The amount of ground object information contained in each band of a TM image is generally measured by the radiation quantization level covered by the band image, that is, the range of brightness values or brightness difference (maximum brightness value-minimum brightness value).

The standard deviation formula is

$$S = \frac{1}{MN} \sqrt{\sum_m \sum_n (A_{ij} - A_0)^2}. \quad (13)$$

An image is  $A_{ij}$ , ( $i = 1, 2, 3, \dots, j = 1, 2, 3, \dots$ ), its image matrix size is  $M \times N$ , and  $A_0$  represents the average gray value of the whole image. The brightness difference reflects the degree of change in the gray value, and its magnitude is equal to the maximum brightness value minus the minimum brightness value, and the formula is  $f_{\text{range}}(i, j) = f_{\text{max}}(i, j) - f_{\text{min}}(i, j)$ . The mean vector represents the average reflection intensity of the objects in the image.

$$f = \frac{\sum_{i=0}^{M-1} \sum_{j=0}^{N-1} f(i, j)}{MN}. \quad (14)$$

The correlation coefficient between the bands reflects the degree of information overlap between the two bands. If the correlation coefficient between the two bands is large, it means that their information overlap is high. Therefore, two channels with high correlation can be combined into one or one of the channels can be taken as one. The formula for the correlation coefficient between the bands is as follows:

$$R = \frac{S_{ij}^2}{S_{ij} S_j}. \quad (15)$$

In the formula,  $S_{ij} = \text{COV}(i, j) = (1/N) \sum_{k=1}^n (X_{ik} - \bar{X}_i)(Y_{jk} - \bar{Y}_j)$ .

Among them,  $i, j$  is the number of bands 1, 2, 3, 4, 5, and 7, and  $S_{ij}$  is the covariance between the  $i$ -th band and the  $j$ -th band,  $\bar{x}_i$  is the spectral gray mean value of the  $i$ -th band,  $\bar{x}$  is the gray value of the  $k$ -th pixel in the  $i$ -th band, and  $Y_{jk}$  is the

gray-scale value of the  $k$ -th pixel in the  $j$ -th band.  $\bar{Y}_j$  is the spectral gray mean value of the  $j$ -th band;  $k = 1, 2, 3, \dots, n$  is the number of pixels in the experimental sample area. The larger the  $R$ , the greater the information overlap between the bands. The calculation of the band correlation coefficient matrix is relatively simple, and the general image processing software has this function. The analysis of the correlation coefficient becomes the basis of the band selection, and the calculation of the correlation coefficient is also necessary for the optimal index method.

Because the larger the standard deviation of the image data, the larger the amount of information it contains, and the smaller the correlation coefficient between the bands, which indicates that the independence of the image data in each band is higher and the information redundancy is smaller. Therefore, the concept of the optimal index (OIF) proposed by Chavez in the United States can also be used.

$$\text{OIF} = \frac{\sum_{i=1}^3 S_i}{\sum_{r=1}^3 R_{ij}}. \quad (16)$$

Among them,  $S_i$  is the standard deviation of the  $i$ -th band, and  $S_{ij}$  is the correlation coefficient of the  $i$  and  $j$  bands. The larger the OIF, the greater the information content of the corresponding combined image. The OIF values are arranged from large to small, and the band corresponding to the largest OIF value is the best band combination. This method is currently the most commonly used band selection method. Moreover, the calculation method is simple, easy to operate, and closer to the principle of band selection.

The joint entropy represents the information amount of the combination of multiple bands, and the combined band with the largest joint entropy is the best band in the sense of "the largest amount of information." However, the joint entropy method requires a considerable amount of calculation and is generally not easy to operate. When computing, we need to write a program to implement it.

The entropy of an 8bit image  $X$  is

$$H(x) = - \sum_{i=0}^{255} p_i \log p_i \text{ (Bit)}. \quad (17)$$

In the formula,  $p_i$  is the probability that the gray value of the image pixel is  $i$ . Similarly, the joint entropy of 2-3 images is as follows:

$$H(x_1, x_2) = - \sum_{i_1, i_2=0}^{255} p_{i_1} p_{i_2} \log p_{i_1, i_2}, \quad (18)$$

$$H(x_1, x_2, x_3) = - \sum_{i_1, i_2, i_3=0}^{255} p_{i_1, i_2, i_3} \log p_{i_1, i_2, i_3}.$$

In the formula,  $P_{i_1}, P_{i_2}, P_{i_3}$  represents that the gray value of the pixel in the image  $X_1$  is  $i_1$ ; the gray value of the pixel with the same name in the image  $X_2$  is  $i_2$ , and the gray value of the pixel with the same name in the image  $X_3$  is the joint

probability of  $i$ . Generally speaking, the larger  $H(x)$  and  $H(x_1, x_2, x_3)$ , the richer the information contained in the image (or group of images). Using entropy and joint entropy, bands and band combinations with a large amount of information can be obtained.

The learning process of BP algorithm consists of two aspects: forward propagation and back propagation. In the forward propagation process, the input pattern is processed layer by layer from the input layer through the hidden layer and finally transmitted to the output layer. The output state of each layer of neurons only affects the input state of the next layer of neurons. If the expected output cannot be obtained in the output layer, backpropagation is performed, the error signal is returned along the original path, and the weights and thresholds between neurons in each layer are corrected to make the error meet the requirements. For the BP algorithm, the commonly used network error is the mean square error function, which is defined as follows:

$$E_p = \frac{1}{2} \sum_{j=1}^N (t_{pj} - o_{pj})^2. \quad (19)$$

Among them,  $E_p$  is the error of the  $p$ -th network vector,  $t_{pj}$  is the expected value of the  $j$ -th output neuron, and  $o_{pj}$  is the actual value of the  $j$ -th output neuron.

The central idea of the BP algorithm is to adjust the weights to minimize the total error of the network; that is, the mean square error  $E_p$  between the expected value and the output value of the neural network tends to be the smallest. The negative gradient of the error function of the weights points in the direction in which the error function decreases the fastest. If the algorithm moves along this vector in the weight space, it will eventually reach a minimum, at which point the gradient is zero. The weight adjustment formula is mathematically described as follows:

$$\Delta_p W_{ji} \propto - \frac{\partial E_p}{\partial w_{ji}}. \quad (20)$$

In the formula,  $\Delta_p W_{ji}$  represents the change of the weight between the source neuron  $i$  in the  $L-1$  layer and the destination neuron  $j$  in the  $L$  layer. This change in the weights causes the gradient to change in the direction of reducing the error in the weight space.

The goal of the entire BP algorithm is to determine how to adjust each weight to make the network converge. Formula (3) describes the relationship that each weight  $w_{ij}$  will change in the direction of the negative gradient where the local error decreases most rapidly. Converting it into an expression suitable for computer implementation, the differential equation required by the BP algorithm can be obtained:

$$\Delta_p w_{jt} = \eta \delta_{pj} O_{pi}. \quad (21)$$

In the formula,  $\eta$  is the learning rate,  $\delta_{pj}$  is the error signal of the neuron  $j$  in the  $L$  layer, and  $O_{pj}$  is the output of the neuron  $i$  in the  $L-1$  layer.

The error signal can be expressed as follows:

$$\text{For output neurons: } \delta_{pj} = (t_{pj} - O_{pj}) O_{pj} (1 - O_{pj}).$$

$$\text{For hidden layer neurons: } \delta_{pj} = O_{pj} (1 - O_{pj}) \sum_k \delta_{pk} \omega_{kj}.$$

In the formula,  $O_{pj}$  represents the output of neuron  $j$  in layer  $L$ ,  $O_{pi}$  represents the output of neuron  $i$  in layer  $L-1$ , and  $\delta_{pk}$  represents the error signal of neuron  $k$  in layer  $L+1$ .

According to the above description, the whole BP learning algorithm can be described as follows:

(1) The algorithm randomly gives the input layer unit to the hidden layer unit, the hidden layer unit to the output layer unit, the threshold value of the hidden layer unit, and the threshold value of the output layer unit. Generally, a small random number within  $(-1, +1)$  is assigned

(2) The algorithm performs the following operations on  $(x_k, y_k)$  ( $k = 1, 2, \dots, m$ ) for the sample pattern

(2-1) The algorithm sends the value of  $x_k$  to the input layer unit and calculates the new activation value of the hidden layer unit of the network.

$$O_{pj}^{(1)} = f_j \left( \text{net}_{pj}^{(1)} \right) j = 1, 2, \dots, M. \quad (22)$$

(2-2) The algorithm calculates the activation value of the output layer unit.

$$O_{pj}^{(2)} = f_j \left( \text{net}_{pj}^{(2)} \right) j = 1, 2, \dots, N. \quad (23)$$

(2-3) The algorithm calculates the output layer unit and the generalization error.

$$\delta_{pj}^{(2)} = O_{pj}^{(2)} \left( 1 - O_{pj}^{(2)} \right) \left( t_{pj} - O_{pj}^{(2)} \right) j = 1, 2, \dots, N. \quad (24)$$

(2-4) The algorithm calculates the training error of the hidden layer unit.

$$\delta_{pj}^{(1)} = O_{pj}^{(1)} \left( 1 - O_{pj}^{(1)} \right) \sum_{k=1}^N \delta_{pk}^{(2)} \omega_{kj} j = 1, 2, \dots, M. \quad (25)$$

(2-5) The algorithm adjusts the connection weight from the hidden layer to the output layer.

$$\Delta w_{ij} = \eta O_{pj}^{(1)} \delta_{pj}^{(2)} \eta \text{ is the learning rate, } 0 < \eta < 1.$$

(2-6) The algorithm adjusts the connection weight from the input layer to the hidden layer.

$$\Delta w_{kj} = \eta A_k \delta_{pj}^{(1)}. \quad (26)$$

(2-7) The algorithm adjusts the threshold from the output layer to the hidden layer.

$$\Delta r_j = \eta \delta_{pj}^{(2)}. \quad (27)$$

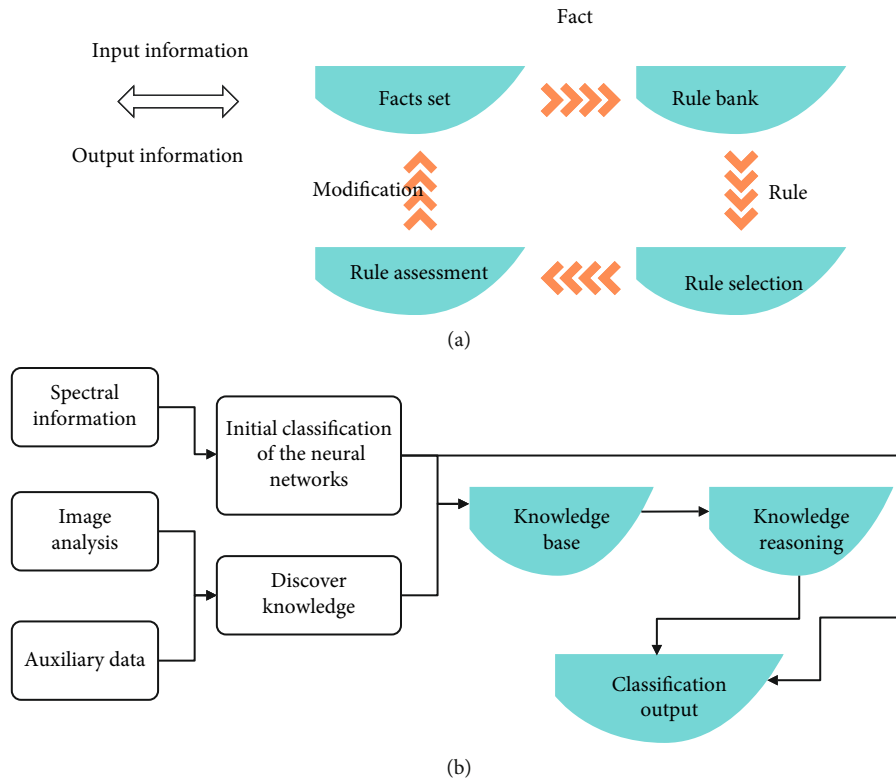


FIGURE 1: Data flow and basic idea of hybrid AI system: (a) data flow in the rules; (b) rule discovery.

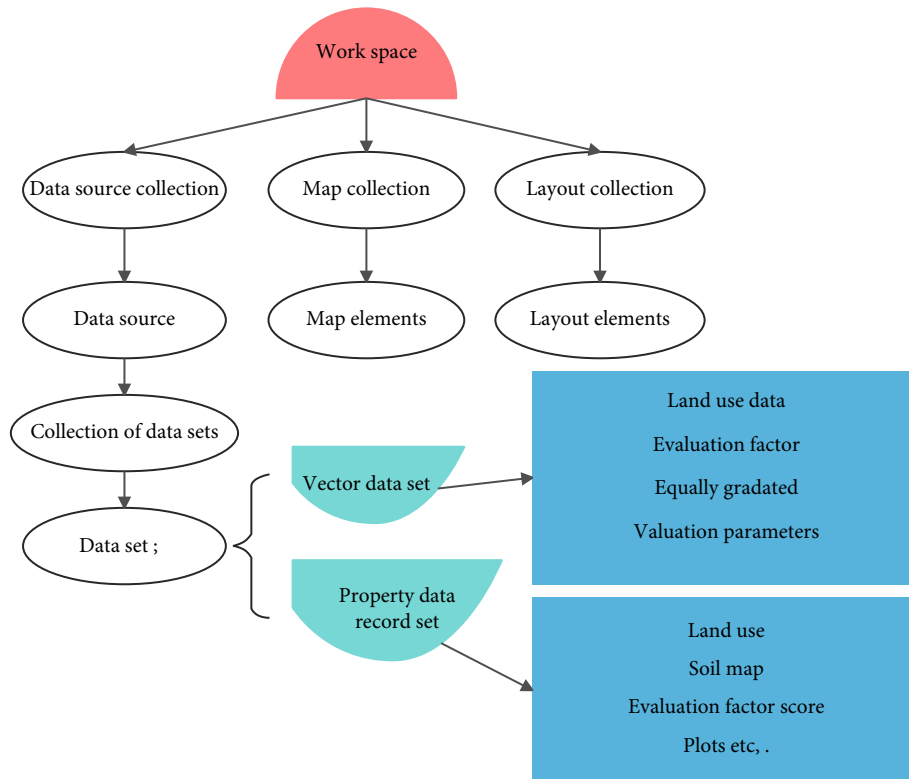


FIGURE 2: The structure frame of the data mining library.

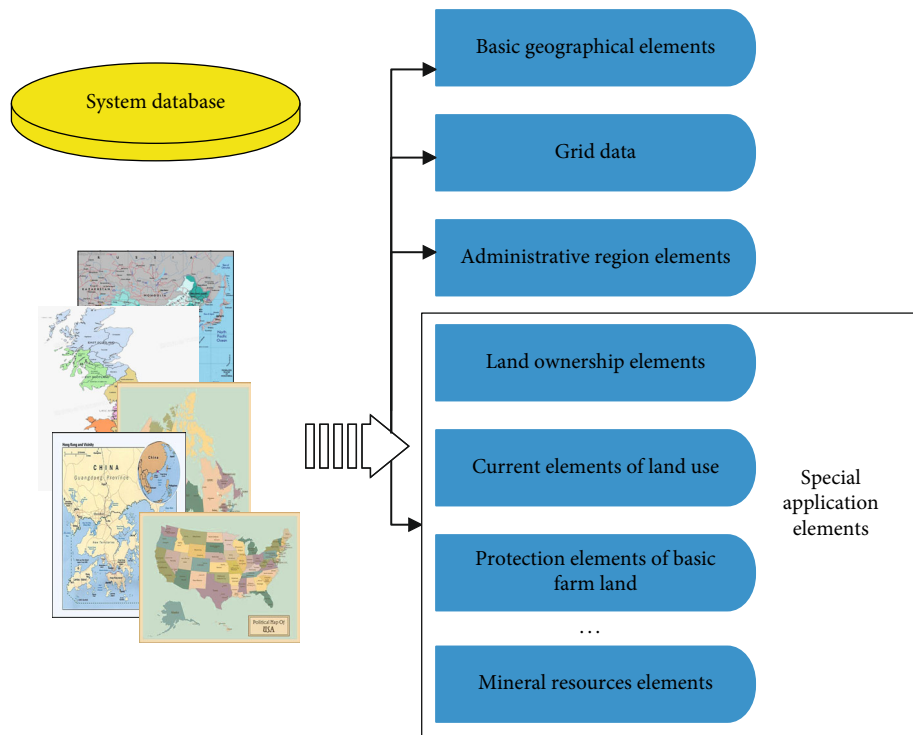


FIGURE 3: System data frame.

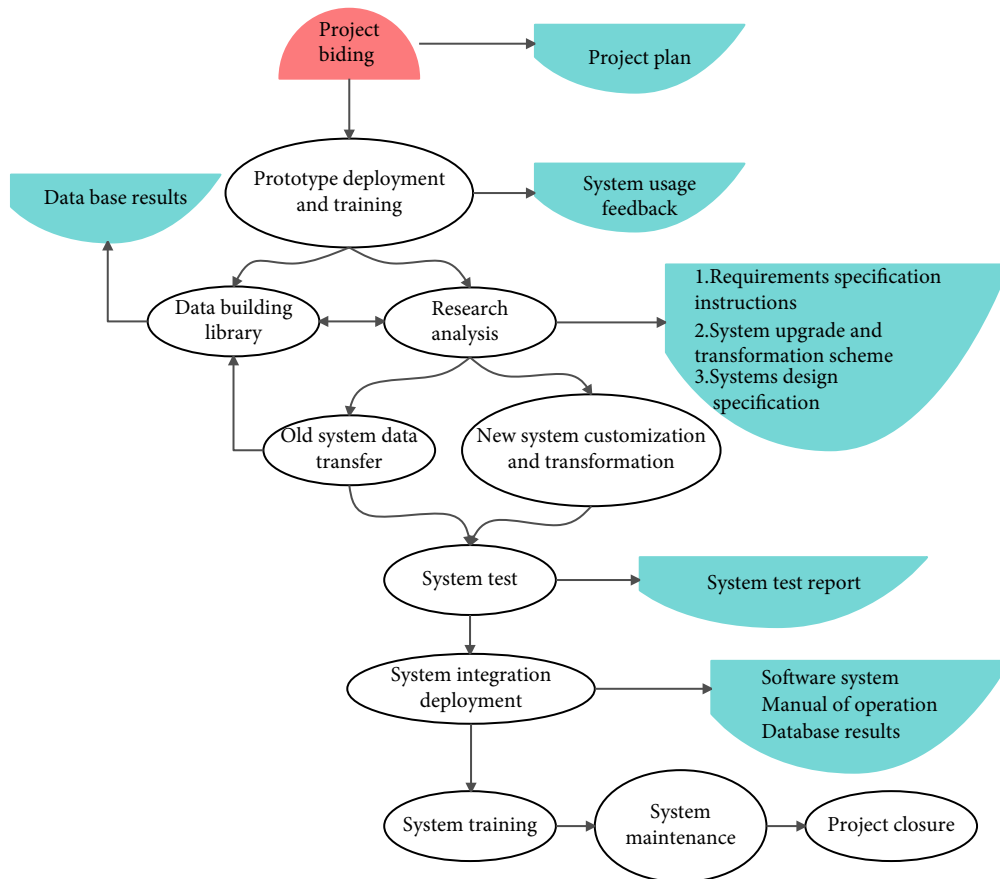


FIGURE 4: Implementation of the system.

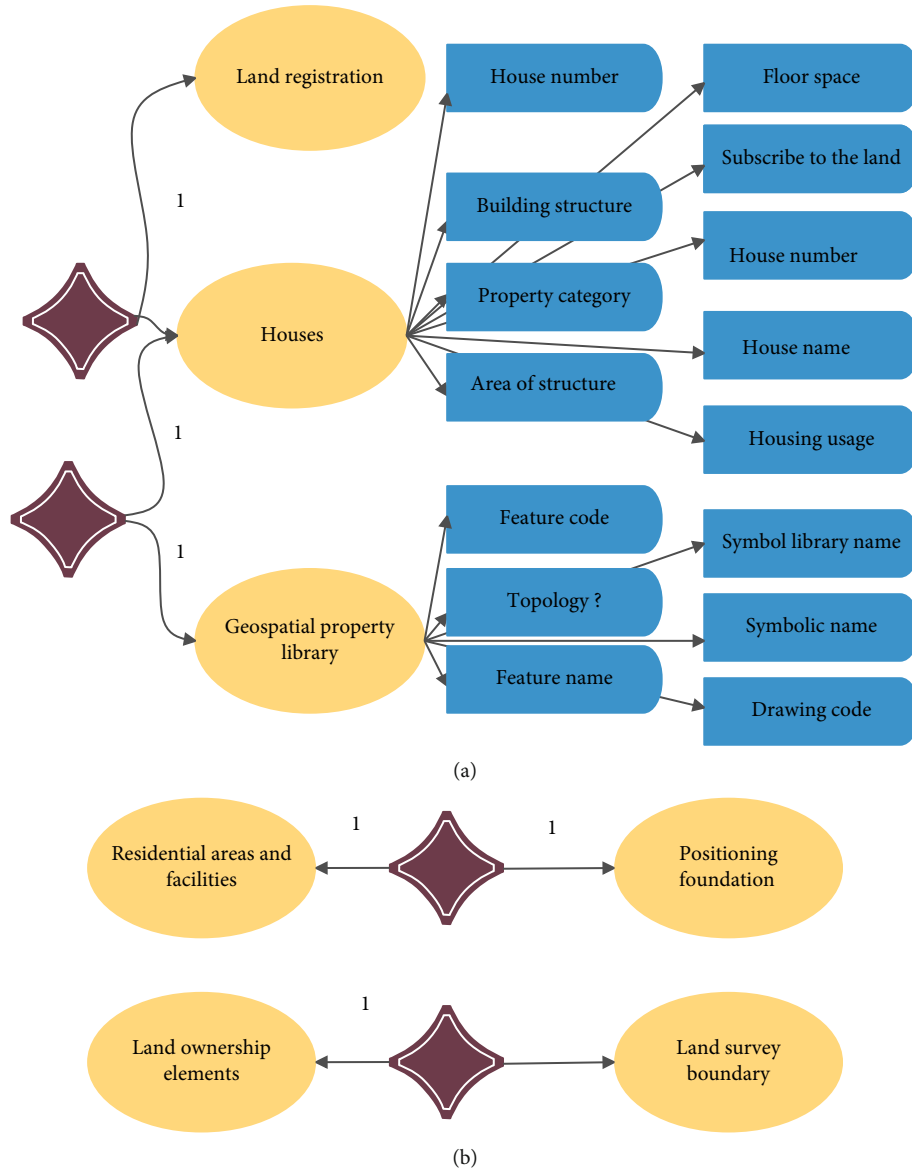


FIGURE 5: The design of the database E-R mode: (a) ER model of land registry business; (b) ER model of the underlying geography.

(2-8) The algorithm adjusts the threshold of the hidden layer unit.

$$\Delta\theta_j = \eta\delta_{pj}^{(1)}. \quad (28)$$

(3) The algorithm judges whether the error meets the requirements. If the requirements are satisfied, the algorithm executes step 5, otherwise, executes step 4

(4) The algorithm judges whether the maximum number of iterations is exceeded. If it exceeds, it means that the training fails, and step 5 is performed; otherwise, it returns to step 2

(5) The algorithm ends

The shape and size of a feature is one of the important signs to identify a feature. The description of the shape includes regular geometric shapes, such as rectangle, square, rhombus, diagonal, circle, ellipse, and pentagon, as well as some irregular geometric figures. The shape soil of the mea-

surement object is the perimeter  $P$  and area  $A$  of the base-inch object, and its shape index  $K$  is defined as follows:

$$K = \sqrt{\frac{A}{P}}. \quad (29)$$

The shapes of various types of objects are summarized into the following types.

3.1. *Round*. For areas of equal area, a circle has the shortest perimeter, and an object that has the shape of a circle will have the largest area/perimeter ratio. For any circular object, it is not difficult to derive the following relationship:

$$\sqrt{\frac{A}{P}} = \frac{1}{2\sqrt{P}} > \frac{1}{4}. \quad (30)$$

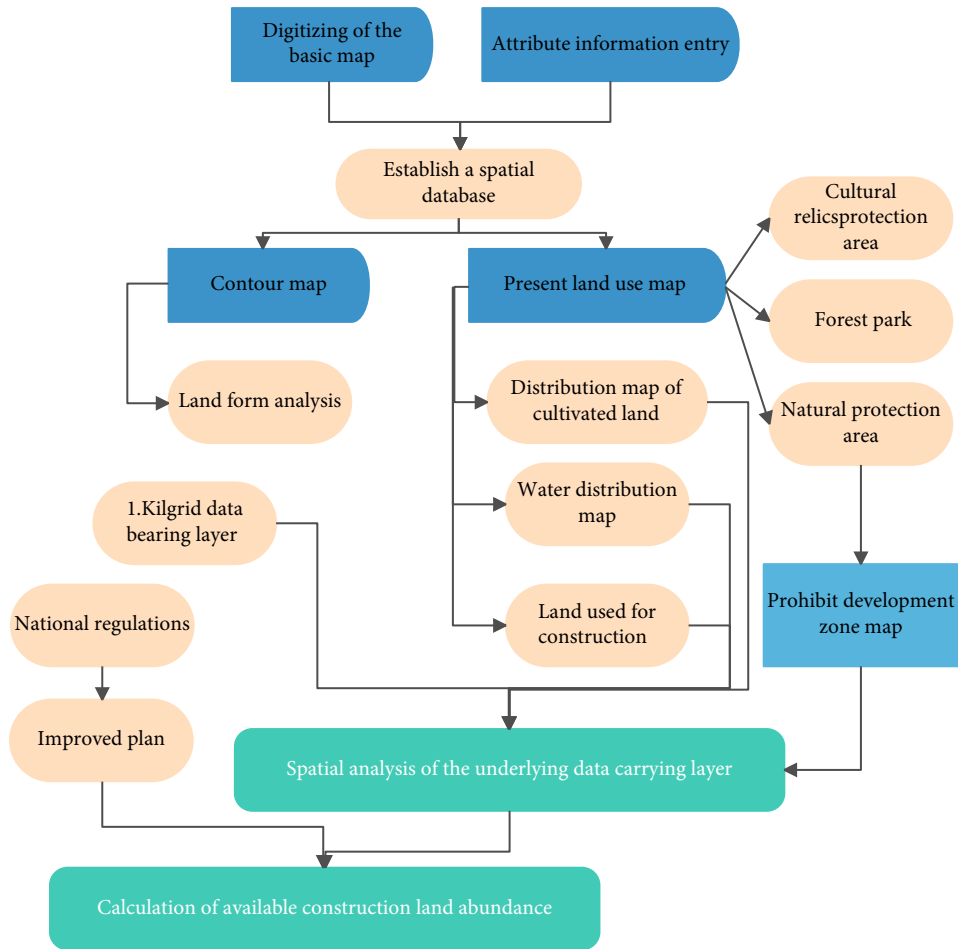


FIGURE 6: Basic work flow chart.

3.2. *Square*. Square objects can share the following relationships:

$$\sqrt{\frac{A}{P}} = \frac{1}{4}. \quad (31)$$

The shape index of a square is smaller than that of a circle.

3.3. *Rectangle*. If the long side of the rectangle is  $k$  times the short side, it can have the following relationship:

$$\sqrt{\frac{A}{P}} = \sqrt{\frac{k}{2}}(k+1) < \frac{1}{4}. \quad (32)$$

3.4. *Linear Objects*. Linear objects have small shape index values, and such objects include roads, rivers, and airports.

3.5. *Irregular Objects*. The more complex the shape of this type of object, the smaller its shape index. For some objects that share obvious shapes, it is the most effective method to

use shape information to identify them. The shape index  $K$  can be used as an important indicator to measure the shape of an object. A complex or long object always has a smaller shape index value. Conversely, a simple or round object has a larger shape index value.

The area of an object can also be used as another important shape indicator to identify some different types of objects. For example, the shape index of a lake and a reservoir may be similar, but the area of a lake is much larger than that of a reservoir, and they can be completely distinguished based on the area index.

After the knowledge is expressed in an appropriate way, it is necessary to study the reasoning mechanism for using the knowledge. Reasoning is the thinking process of drawing a new judgment from a known judgment according to a given principle. In the remote sensing image knowledge inference system, rule inference and rule expression use production rules to describe the solution to the problem. This kind of rule-based inference is also called production inference. At the same time, roughly speaking, production reasoning is the reasoning engine selects the rules from the rule base and applies the rules. When these selected rules are applied, they perform the actions of the concluding part of the rules and thus lead to the addition, deletion, modification, etc. of the

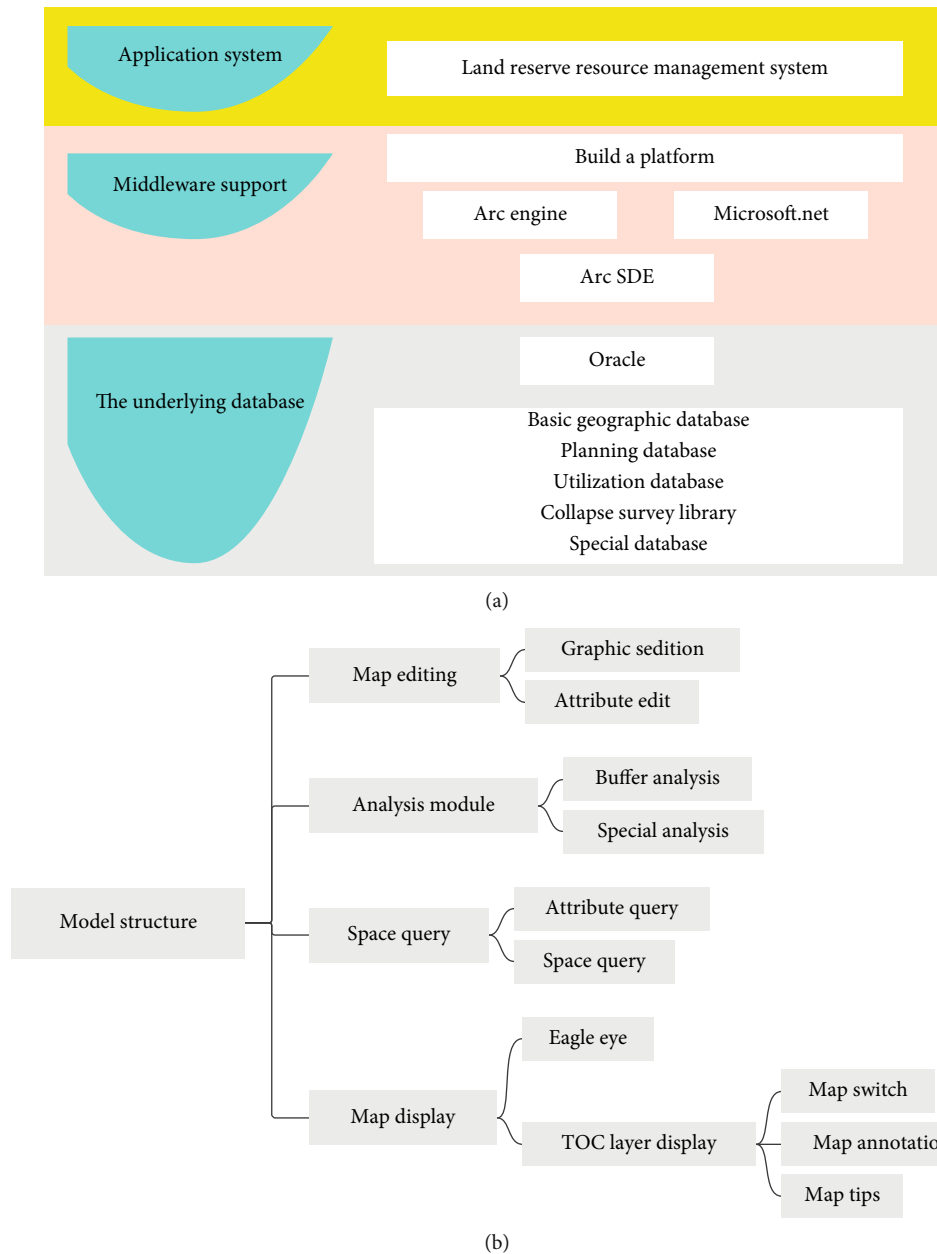


FIGURE 7: Intelligent management system of land resources based on Internet of Things and GIS technology: (a) structure diagram of land reserve resource management system; (b) schematic diagram of the overall structure of the frame.

facts in the fact base. Figure 1(a) is a schematic diagram of the changes of rules and facts in the working process of the inference engine, and the direction of the arrow indicates the direction of data flow. Figure 1(b) is the rule discovery.

In the object-oriented knowledge representation, the operation of the object is contained in the object; that is, the reasoning is distributed in each object. Rules represent the way and strategy of reasoning and are used to represent the experience of experts in the specific application of knowledge. During inference, when the fact expression is consistent with the conditional expression of the rule in the knowledge base, inference can be generated according to the rule, and the credibility value given by the expert can be obtained.

#### 4. Intelligent Management of Land Resources Based on Internet of Things and GIS Technology

The design of the system database mainly adopts the top-down design scheme and the object-oriented programming idea. The top layer is the workspace, which includes three parts: data source set, map set, and layout set. Map set and layout set are mainly used for map output of spatial data, and they are composed of map elements and layout elements, respectively. Moreover, the data source set can derive subclass data source, the data source is composed of the data set, and the data set is a subclass of the data set, which

TABLE 1: The effect of intelligent treatment of land resources.

Number	Information processing	Number	Information processing	Number	Information processing	Number	Information processing
1	86.112	19	90.639	37	91.603	55	90.024
2	85.688	20	91.070	38	90.174	56	91.803
3	87.955	21	86.180	39	84.736	57	84.129
4	92.038	22	84.174	40	92.911	58	86.351
5	86.368	23	84.961	41	91.897	59	89.671
6	89.744	24	84.884	42	84.434	60	88.926
7	89.109	25	92.701	43	84.671	61	86.935
8	90.527	26	90.730	44	84.217	62	92.007
9	86.701	27	89.684	45	89.516	63	88.405
10	85.062	28	86.349	46	85.361	64	92.278
11	91.437	29	92.040	47	89.637	65	87.194
12	91.564	30	85.535	48	87.674	66	88.478
13	85.800	31	87.064	49	88.757	67	86.047
14	89.195	32	91.311	50	91.295	68	90.638
15	92.765	33	91.022	51	84.898	69	89.595
16	91.210	34	92.832	52	87.312	70	89.139
17	85.537	35	85.918	53	86.181	71	92.262
18	90.494	36	84.648	54	90.821	72	89.216

TABLE 2: The effect of land resource management.

Number	Land management	Number	Land management	Number	Land management	Number	Land management
1	83.101	19	82.675	37	81.887	55	83.482
2	80.579	20	83.033	38	86.298	56	80.108
3	81.242	21	80.846	39	85.034	57	80.538
4	87.008	22	83.737	40	83.202	58	82.808
5	85.425	23	84.360	41	80.487	59	83.085
6	86.776	24	83.579	42	82.218	60	86.631
7	86.118	25	85.664	43	81.450	61	85.964
8	81.128	26	80.772	44	81.636	62	85.311
9	86.674	27	85.902	45	85.149	63	82.297
10	83.050	28	84.112	46	82.483	64	85.543
11	84.867	29	87.334	47	80.371	65	82.051
12	86.532	30	81.800	48	83.378	66	85.295
13	81.277	31	84.093	49	83.510	67	81.233
14	80.343	32	81.997	50	83.546	68	81.354
15	82.522	33	85.829	51	86.196	69	87.817
16	86.037	34	80.677	52	83.581	70	87.873
17	81.763	35	82.276	53	82.413	71	81.881
18	82.962	36	82.831	54	81.405	72	81.550

includes the vector data set attribute data record set. Its structural frame is shown in Figure 2.

The data can be logically divided into spatial data, image data, attribute data, public configuration data, and document data. Spatial databases are divided into two categories. One is basic geographic data, administrative area data, and image

data, which are provided to other applications as shared data. The other category is each thematic application elements as shown in Figure 3.

The implementation strategy that goes hand in hand with prototype trial, database building, and software customization and transformation is specified. The implementation scheme



of intelligent management of land resources based on the Internet of Things and GIS technology is shown in Figure 4.

The design of the database E-R model is shown in Figure 5, in which Figure 5(a) is the ER model of the land registration business, and Figure 5(b) is the basic geographic ER model.

The construction land resource evaluation study is based on the workflow shown in Figure 6.

This system uses the current land survey data, planning data, and agricultural special data as the analysis data; uses C# as the development front-end; and is designed and developed based on ArcGIS Engine. The system structure is shown in Figure 7(a), and the framework generally includes five parts: map display, query module, analysis module, and land evaluation, as shown in Figure 7(b).

On the basis of the above research, the intelligent management system of land resources based on the Internet of Things and GIS technology proposed in this paper is evaluated, and the effect of intelligent processing of land resources and the effect of land resource management are counted, and the results shown in Tables 1 and 2 are obtained.

From the above research, it can be seen that the intelligent land resource management system based on the Internet of Things and GIS technology has a good effect in the collection and processing of land resource information and can effectively improve the management efficiency of land resources.

## 5. Conclusion

According to the resource and environmental carrying capacity, existing development density, and development potential of different regions, this paper considers the future population distribution, economic layout, land use, and urbanization pattern and divides the land space into four main functional areas: optimized development, key development, restricted development, and prohibited development. Moreover, this paper clarifies the main function, guides the development direction, regulates the development order, controls the development intensity, adjusts the development policy, and gradually forms a new pattern of spatial development in which population, economy, resources, and environment are coordinated. The main functional area is the product of implementing the scientific concept of development, and the proposal of the main functional area plan is also a new breakthrough in promoting the coordinated development of the region, and it is the regional embodiment of the sustainable development strategy. This paper combines the Internet of Things technology and GIS technology to build an intelligent management system for gradient resources. The research shows that the intelligent management system of land resources based on the Internet of Things and GIS technology has a good effect in the collection and processing of land resource information and can effectively improve the management efficiency of land resources.

## Data Availability

The labeled dataset used to support the findings of this study are available from the corresponding author upon request.

## Conflicts of Interest

The authors declare no competing interests.

## Acknowledgments

This study is sponsored by the National Social Science Foundation Project “The Research on Social Capital, CEO Power and Enterprise Resource Allocation along with its Economic Consequences” (Serial Number: 20CGL011).

## References

- [1] A. Farahbakhsh and M. A. Forghani, “Sustainable location and route planning with GIS for waste sorting centers, case study: Kerman, Iran,” *Waste Management & Research*, vol. 37, no. 3, pp. 287–300, 2019.
- [2] K. S. Sahitya and C. Prasad, “Modelling structural interdependent parameters of an urban road network using GIS,” *Spatial Information Research*, vol. 28, no. 3, pp. 327–334, 2020.
- [3] M. A. Dereli, “Monitoring and prediction of urban expansion using multilayer perceptron neural network by remote sensing and GIS technologies: a case study from Istanbul Metropolitan City,” *Fresenius Environmental Bulletin*, vol. 27, no. 12a, pp. 9336–9344, 2018.
- [4] T. C. M. Guerreiro, J. Kirner Providelo, C. S. Pitombo, R. Antonio Rodrigues Ramos, and A. N. Rodrigues da Silva, “Data-mining, GIS and multicriteria analysis in a comprehensive method for bicycle network planning and design,” *International Journal of Sustainable Transportation*, vol. 12, no. 3, pp. 179–191, 2018.
- [5] G. Carpentieri and F. Favo, “The end-use electric energy consumption in urban areas: a GIS-based methodology. An application in the city of Naples,” *TeMA-Journal of Land Use, Mobility and Environment*, vol. 10, no. 2, pp. 139–156, 2017.
- [6] J. France-Mensah, W. J. O’Brien, N. Khwaja, and L. C. Bussell, “GIS-based visualization of integrated highway maintenance and construction planning: a case study of Fort Worth, Texas,” *Visualization in Engineering*, vol. 5, no. 1, pp. 1–17, 2017.
- [7] K. A. Baba, D. Lal, and A. Bello, “Application of remote sensing and GIS techniques in urban planning, development and management (A case study of Allahabad District, India),” *International Journal of Scientific & Engineering Research*, vol. 10, no. 6, pp. 1127–1134, 2019.
- [8] S. Teixeira, “Qualitative geographic information systems (GIS): an untapped research approach for social work,” *Qualitative Social Work*, vol. 17, no. 1, pp. 9–23, 2018.
- [9] E. Khayambashi, “Promoting urban spatial and social development, through strategic planning of GIS,” *Socio-Spatial Studies*, vol. 2, no. 4, pp. 66–80, 2018.
- [10] G. Lü, M. Batty, J. Strobl, H. Lin, A. X. Zhu, and M. Chen, “Reflections and speculations on the progress in geographic information systems (GIS): a geographic perspective,” *International Journal of Geographical Information Science*, vol. 33, no. 2, pp. 346–367, 2019.
- [11] T. R. Alrobaee, “Measuring spatial justice indices in the traditional Islamic cities by using GIS, An-Najaf Holy City, Iraq a case study,” *Journal of Geoinformatics & Environmental Research*, vol. 2, no. 1, pp. 01–13, 2021.
- [12] M. R. Meenar, “Using participatory and mixed-methods approaches in GIS to develop a Place-Based Food Insecurity

- and Vulnerability Index[J],” *Environment and Planning A*, vol. 49, no. 5, pp. 1181–1205, 2017.
- [13] J. J. Giesekeing, “Operating anew: queering GIS with good enough software,” *The Canadian Geographer/Le Géographe Canadien*, vol. 62, no. 1, pp. 55–66, 2018.
- [14] M. Giannopoulou, A. Roukouni, and K. Lykostratis, “Exploring the benefits of urban green roofs: a GIS approach applied to a Greek city,” *CES Working Papers*, vol. 11, no. 1, pp. 55–72, 2019.
- [15] A. T. N. Dang and L. Kumar, “Application of remote sensing and GIS-based hydrological modelling for flood risk analysis: a case study of District 8, Ho Chi Minh city, Vietnam,” *Geomatics, Natural Hazards and Risk*, vol. 8, no. 2, pp. 1792–1811, 2017.
- [16] S. K. Yadav and S. L. Borana, “Monitoring and temporal study of mining area of Jodhpur City using remote sensing and GIS,” *International Research Journal of Engineering and Technology (IRJET)*, vol. 4, no. 10, pp. 1732–1736, 2017.
- [17] W. Chen, G. Zhai, C. Fan, W. Jin, and Y. Xie, “A planning framework based on system theory and GIS for urban emergency shelter system: a case of Guangzhou, China,” *Human and Ecological Risk Assessment: An International Journal*, vol. 23, no. 3, pp. 441–456, 2017.
- [18] S. Abdullahi and B. Pradhan, “Land use change modeling and the effect of compact city paradigms: integration of GIS-based cellular automata and weights-of-evidence techniques,” *Environmental Earth Sciences*, vol. 77, no. 6, pp. 1–15, 2018.
- [19] N. Alghais and D. Pullar, “Modelling future impacts of urban development in Kuwait with the use of ABM and GIS,” *Transactions in GIS*, vol. 22, no. 1, pp. 20–42, 2018.

## Research Article

# The Inheritance and Future Development Direction Prediction of Opera Culture Based on Cloud Communication under the Background of Big Data

Yufeng Yang<sup>1</sup> and Ting Lei<sup>2</sup> 

<sup>1</sup>School of Humanities and Education, Xijing University, Xi'an, Shaanxi 710123, China

<sup>2</sup>College of International Cooperation, Xi'an International University, Xi'an, Shaanxi 710077, China

Correspondence should be addressed to Ting Lei; [leiting@xaiu.edu.cn](mailto:leiting@xaiu.edu.cn)

Received 21 January 2022; Revised 2 March 2022; Accepted 18 March 2022; Published 10 May 2022

Academic Editor: Wen Zeng

Copyright © 2022 Yufeng Yang and Ting Lei. This is an open access article distributed under the Creative Commons Attribution License, which permits unrestricted use, distribution, and reproduction in any medium, provided the original work is properly cited.

In the digital economy era, digital technologies such as cloud computing, big data, artificial intelligence, mobile Internet, and Internet of Things are becoming the new foundation of social operation and industry innovation. In order to achieve creative transformation and innovative development of traditional opera culture and art, there is a need to actively embrace the new digital technologies of the Internet. From the perspective of big data, according to the development status of Chinese opera art, this paper examines the limitations of traditional means to protect and develop opera art and puts forward the inheritance of opera culture and the prediction of future development direction based on cloud communication. This paper demonstrates the matrix system and inheritance development direction of Kunqu Opera culture to realize cloud communication. The main conclusions of this paper are as follows: firstly, promoting the overall digitalization of Kunqu Opera culture is the inevitable choice to realize the inheritance and development of Kunqu Opera; secondly, it is scientific and feasible to promote the overall digitalization and inheritance of Kunqu Opera culture. Thirdly, promoting the research and planning of cloud-spread opera should be promoted to become a national cultural strategy.

## 1. Introduction

Opera art is a combination of Chinese excellent music, dance, poetry, and other artistic elements. It is the cultural symbol and life memory of a nation and a region and the cultural root of people's homesickness. As a unique Chinese excellent traditional culture, it adds confidence and pride to the hearts of the Chinese people and the Chinese nation and is also the foundation and source of national cultural strength and cultural industry development [1]. Print media, mainly represented by newspapers and magazines, expanded the exhibition space of opera performances to thousands of households, and three-dimensional media such as radio, film, and television also joined in, attracting new and old audiences to the stage of opera performances from thousands of households. Internet, big data [2], cloud computing [3], artificial intelligence, and other new technologies and

new applications are rapidly influencing and changing our society [4], changing our way of life, work, and study. However, at present, the operation of real society and the cognition and research of virtual space boundaries of the Internet are becoming increasingly vague.

Promoting cloud dissemination of opera is an inevitable choice for China's traditional culture and opera industry to meet the challenges of the Internet age. At present, the Internet has not only brought about the great development of productivity but also caused great changes in industrial structure and cultural inheritance methods and paths. How to deal with and integrate the Internet in culture and opera determines the foundation, framework, and rules of inheritance and operation of culture and opera. With the continuous progress of the times, the development of traditional culture cannot be limited to theatres. Audiences need operas, and operas need audiences even more. Nowadays,

marketability is a prominent feature of the cultural industry, and the theme of the market is the audience. If the opera wants to develop, it must be reformed to face the market [5, 6]. The era of electronic media is an era surrounded by all kinds of information such as words, images, audio, and videos, and it is also the home of new media. People can pick up mobile new media such as mobile phones and tablets at hand at any time to look at information around the world. Its timeliness, interactivity, mobility, cloud storage, and integration of multimedia push information dissemination to a new stage [7]. In the current society and information age, the traditional opera art has been impacted by itself and the outside world, and people's aesthetic style has changed. Under the environment that the opera has not fully adapted to the rapid development of media, its spread has shown obvious decline. However, as an important part of Chinese traditional culture and an important carrier of communication, the inheritance and development of opera cannot be ignored. The research on the communication of opera culture in the current audio-visual media environment will highlight its significance and value [8, 9].

In the era of digital economy, people cannot refuse the convenience brought by smart phones, and opera culture and art have naturally entered the era of digital communication. Cloud communication of opera is an inevitable move for opera culture and art to actively embrace the new digital technology of the Internet [10]. In the era of big data, data has penetrated into every industry and business function, which has led to earth-shaking changes in all walks of life. However, the research and exploration on the field of opera art are still in its infancy. In view of the current development situation of traditional Chinese opera, this paper analyzes from the perspective of communication and studies the exploration of communication content, media, and audience in the process of communication. Relying on the current audio-visual media, this paper innovates communication content, unblocks communication channels, and broadens audience groups, so as to achieve effective and extensive communication of traditional Chinese opera. Take Kunqu Opera, the representative work of national intangible cultural heritage, as an example to carry out the research of this topic.

## 2. Related Work

Opera art is the unique "cultural heritage" and "civilized memory" of the Chinese nation, with a long historical tradition, a profound realistic foundation, and a sustainable future [11]. Document [12] puts forward the status and protection of opera as an intangible cultural heritage, and document [13] describes the current situation of opera in the process of urbanization and makes an in-depth analysis. Literature [14] summarizes and discusses the survival dilemma and internal and external reasons of traditional Chinese operas and puts forward new ideas and paths. However, more research focuses on the transmission of performing arts, the popularization of award-winning plays and representative plays, the inheritance of talents, the publicity of news media, etc. Literature [15] adapts Sichuan Opera from

the similarities of action and dialogue design between Sichuan Opera and animation to realize the organic integration of opera and animation. Literature [16] said: "Facing the world of economic globalization, communication globalization and cultural diversity and diversity, the way to maintain traditional cultural genes is to look at the world and keep pace with the times." Literature [17] points out that the regulation and modeling design of Sichuan Opera Theater has a strong era, and the concept of Sichuan Opera's inheritance and development in each era also determines the choice of acoustic and optical technologies that should be considered in theater performance design in this era, and these performance field designs can also promote the innovation and development of Sichuan Opera. Literature [18] uses mobile terminal animation to subtly spread and inherit traditional culture and to make colorful description and nuanced penetration.

Literature [19] also integrates traditional culture into Internet products, forming a picture of the existence of traditional culture in the new era. Literature [20] puts forward the research direction of "organic integration of traditional culture and digital media," and France has in-depth practical and related theoretical research on promoting the traditional cultural communication of digital media. Literature [21] holds that "the new media represented by TV and Internet have destroyed the traditional aesthetic sense of opera, such as the aesthetic rules of virtual assumption stylization of opera. He believes that opera can only be shaped and developed if it returns to the countryside." Literature [22] holds that the spread of traditional culture needs not only the traditional media but also the assistance of new media platforms, which is of great significance to the spread of traditional culture and the realization of the Chinese dream. In literature [23], after an empirical analysis of the opera websites, it is found that "Opera websites are mostly independent survival types, with outstanding personalized characteristics and distinctive public welfare color." It needs to be clearly recognized that although the Xiqu website has its own space for rapid development, it is not the mainstream of website development. From the perspective of drama, this paper sorts out the concept, characteristics, and communication period of drama films. In literature [24], from the perspective of communication, this paper expounds the influence of electronic media on opera communication and puts forward constructive communication ideas from the aspects of basic ways of communication, etc.

## 3. Research Method

*3.1. Cloud Communication of Traditional Opera Cultural Heritage.* Based on the cloud communication supported by big data technology, artificial intelligence technology, mobile Internet technology, and cloud computing technology, through the multidimensional and multistate fusion organization of these communication forms, the borderless and borderless communication under the information society ecology can be realized.

With the gradual maturity of big data technology, its great value in scientific research, economy, society, and

other aspects has become increasingly apparent. Therefore, it has attracted great attention from the government, academia, business circles, and literary and art circles. All parties are scrambling to seize the strategic high point in this field and apply it to different industries and departments. However, the research on opera art by big data has just started.

Although the exhibition space of opera culture and art is stage-centered, it is not the only display carrier of opera culture and art. Modern media integration is to make full use of media carriers to comprehensively integrate different media, such as radio, television, and newspapers, which have something in common but are complementary, in terms of manpower, content, and publicity. With the help of the Internet-based mode of media communication platform and driven by the power of the masses, traditional opera culture and art can quickly attract attention and quickly understand the opinions and suggestions of the audience. Providing a better shooting experience and a lower use threshold can enable users to reinterpret and spread traditional opera culture easily and easily and can promote the audience's perception of the fragmentation of opera culture and art to further explore the whole.

Opera breeds in the soil of new media, which is bound to shape a new paradigm suitable for opera according to the survival rules of new media and form a virtuous circle of opera. Make full use of mobile terminal applications to spread opera, and combine many advantages of WeChat official account, such as multimedia presentation, instant interactive communication, and longer service arrival time, with traditional opera culture. Unlike the previous theater linear communication, it changes the single linear social network in which opera culture only stays in the personal carrier but cannot spread, and pays more attention to the feedback of the audience.

Compared with traditional theater stage performances, cloud communication has its unique advantages. First, the network communication mode determines its wide audience and fast speed, far exceeding the narrow theater capacity and interpersonal communication mode of word of mouth. Second, it can meet people's demand for opera appreciation anytime, anywhere. It can be based on any platform, any terminal, any time, any place, any way, any node, and other limitations, breaking the shackles of time, space, and place of traditional theater opera dissemination.

Although the network teaching of Kunqu Opera is different from the general school network course, under the top-level design strategy of promoting digital data inheritance, the network and platform system of network teaching of Kunqu Opera has become a strong support for the government to support this cultural cause, because the platform support and resource support needed by network teaching of Kunqu Opera need more powerful information means and network technology. In order to build a simulation and synchronous teaching experience platform, support the participatory interactive teaching of virtual and realistic technologies, support the specific expression language and artistic image of Kunqu Opera to communicate with learners in spirit, and support and meet the needs of learners with different cognitive levels (see Figure 1).

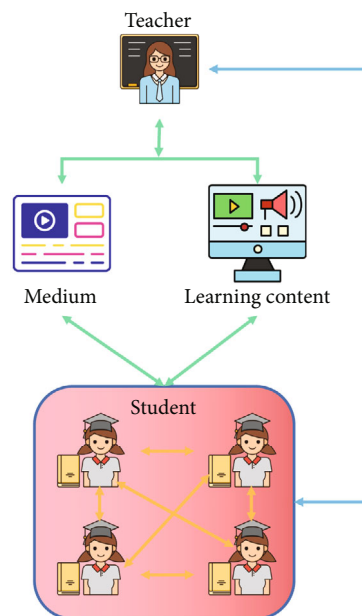


FIGURE 1: Topology diagram suitable for network teaching platform architecture of Kunqu Opera.

Innovating the new network teaching mode of Kunqu Opera, starting from the infrastructure of network teaching, carry out the popularization activities of traditional opera education in primary and secondary schools, bring the popularization teaching of traditional opera into the category of characteristic education in primary and secondary schools, and establish a number of demonstration bases for traditional opera teaching. Develop traditional opera teaching materials of various operas; explore new modes of digital, remote, and networked teaching; and form a reserve of traditional opera teaching materials with various styles and characteristics.

From the form of drama communication, drama communication is a present and nonreplicable form of acceptance, while network communication is nonpresent and replicable. This change not only did not weaken the original characteristics of opera but also enhanced the communication effect of opera because of the marriage with digitalization. While the Internet has changed the traditional concept of drama watching, on the one hand, it is necessary to guide the audience reasonably and actively expand the drama watching space outside the Internet on the other. Use the Internet as a front to promote opera and national quintessence, not only to capture the hearts of young people but also to promote opera and national quintessence for foreign friends.

What cannot be underestimated is that the extended dissemination of opera has become the main way of communication nowadays, and it has effectively changed the audience's viewing habits, which has brought about a new situation in the amount of information spread, the spread surface, the interaction between communication and audience, etc. Cloud classroom solves the problem that traditional learning and training are limited in places, hardware, software, teachers, distance, resources, etc. Any person or

institution can incite and promote an educational revolution by renting space and technical services. Any educator who has expertise in learning and teaching can preach and dispel doubts to audiences distributed in various regions, ethnic groups, and cultures through the cloud classroom, with thousands of students at the same time.

*3.2. Prediction of the Development Direction of Opera Culture under the Background of Big Data.* In the Internet age, the “enabling organization” supported by digital technology refers to a platform that can endow social production elements with stronger production and communication capabilities. The core of “Internet Plus” is empowerment; that is, with the help of digital platform, the relatively independent production elements are optimized and integrated, and a new production system and communication chain are formed in the interrelated and interactive scene. The core value of big data lies in the analysis of data. Through big data analysis technologies such as cloud computing, the multidimensional, scientific, and reasonable integration and induction of opera-related data scattered on the network, new media, and other platforms can fully tap the huge value contained in the data. Big data analysis technology can quickly realize data processing. In the traditional ranking statistics system of opera publications and box office, research institutions or literary and art units may spend several weeks sorting out, counting, and analyzing.

Using big data analysis and judgment may be the solution for the troupe to explore, create, and select scripts [9]. In the protection of traditional opera cultural heritage, protecting its “original ecology” is often emphasized repeatedly. When creating new plays, on the one hand, strive to maintain the true character and essence of traditional opera, such as aria, tunes, and operas. On the other hand, according to the results of audience feedback value analysis, audience hobby analysis, and communication behavior analysis based on big data platform, the model is established by using various parameters, and then, the rational data conclusion is obtained by careful data analysis. With the help of people’s favorite modern art elements and traditional art elements, the opera is packaged and transformed, and the aesthetic principles of tradition and modernity are effectively reconciled, so as to successfully realize the promotion and inheritance of opera in contemporary society.

Developing creative products of opera culture is a new way to protect and develop traditional opera art. Traditional opera costumes, props, and various decorative patterns are treasures of Chinese traditional art. Excavate the artistic resources of opera; collect various opera props, masks, and decorative patterns; excavate various artistic symbols in the patterns; and sort them out to create the library of opera patterns, basic elements, and common symbols. Apply the decorative patterns seen in various traditional operas to different characters, and apply them to contemporary art forms such as TV, movies, animation, publishing, games, and cartoons. Through cultural and creative products, the information of opera culture is actively integrated into people’s daily life, which arouses people’s concern and love for opera art.

Consider that a recommendation system includes several users and commodities, and each user has purchased some commodities. The value of element  $a_{ij}$  in the user-commodity relationship matrix is shown in the following formula:

$$a_{ij} = \begin{cases} 1 & u_j \text{ has chosen product } o_i, \\ 0 & u_j \text{ commodity } o_i \text{ has not been selected.} \end{cases} \quad (1)$$

If user  $u_i$  selects commodity  $o_j$ , the commodity obtains an initial resource of one unit, otherwise the initial resource of the commodity  $o_j$  is zero. Compared with different users, the initial resources of the same commodity have different values.

The weight  $s_{kij}$  represents the similarity between the user  $u_i$  and the target user  $u_j$  with respect to the commodity  $o_k$ , and its calculation formula is as follows:

$$s_{kij} = \frac{a_{ki} \text{sim}(u_i, u_j)}{\sum_{i=1}^m a_{ki} \text{sim}(u_i, u_j)}, \quad (2)$$

in which  $\text{sim}(u_i, u_j)$  represents the similarity of user  $u_i, u_j$ ;  $m$  represents the number of users in the system;  $a_{ki}$  represents the selection relationship between commodity  $o_k$  and user  $u_i$ ; and  $\sum_{i=1}^m a_{ki} \text{sim}(u_i, u_j)$  represents the sum of the similarity between all users who have selected the product  $o_k$  and the target user  $u_j$  in the system.

$s_{kij}$  also satisfies the following equation:

$$\sum_{i=1}^m s_{kij} = 1. \quad (3)$$

That is, the sum of the relative similarities between all users who have selected product  $o_k$  and the target users is 0, which can ensure that the total amount of resources in the bipartite graph remains unchanged.

The initial resources of commodity nodes in the commodity set flow to each user node in the user set. At this time, the calculation formula of resources owned by user node  $u_l$  is

$$f(u_l) = \sum_{i=1}^n \frac{a_{il} f(o_i)}{k(o_i)}. \quad (4)$$

The resources on the user  $u_l$  come from  $n$  nodes in the commodity collection.

$w_{ij}$  integrates the contribution rate of the initial resources of node  $o_j$  to the final resources of node  $o_i$  in these two rounds of resource flows. Let the matrix  $W = \{w_{ij}\}_{n \times n}$ ; then, the resource flow process of the above two rounds can be expressed as

$$f' = Wf, \quad (5)$$

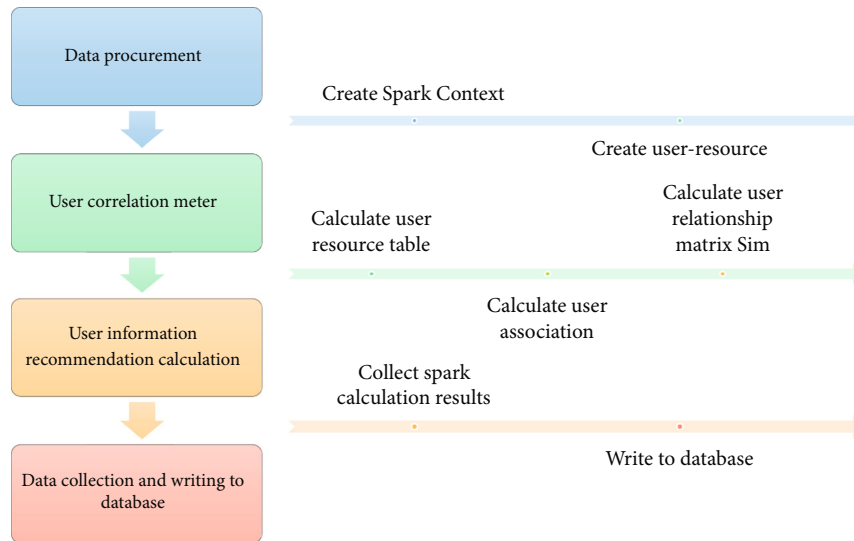


FIGURE 2: Implementation process of big data engine.

where  $f$  corresponds to the  $n$ -dimensional initial resource vectors of  $n$  commodities in commodity set  $o$  and  $f'$  is the final resource vector of these  $n$  commodities. Set the final resource value of the commodities that the target user has already purchased in vector  $f'$  to zero, and then, select  $L$  commodities with the largest resource value as the recommendation list made by the system for the target user.

User similarity can be calculated by cosine similarity formula:

$$\text{Sim}(\text{user}_1, \text{user}_2) = \frac{|\text{items of}(\text{user}_1) \cap \text{items of}(\text{user}_2)|}{\sqrt{|\text{items of}(\text{user}_1)| * |\text{items of}(\text{user}_2)|}}. \quad (6)$$

The information recommendation process is to find the product information to be recommended through the established correlation matrix  $\text{Sim}$ . The formula for calculating user  $u_1$  interest in information resource  $i_1$  is

$$\text{interest}(u_1, u_2) = \sum_{u_i \in (\text{reluser}(u_1, N) \cap \text{itemsuser}(i_1))} \text{Sim}(u_1, u_i) \times (u_i, i_1). \quad (7)$$

Among them,  $\text{reluser}(u_1, N)$  represents the set of  $N$  other users related to user  $u_1$ , and such filtering can reduce the scale of calculation.  $\text{Itemsuser}(i_1)$  refers to the set of users interested in  $i_1$  resources, which can be obtained through the inverted list.

The core of big data engine lies in the implementation of recommendation algorithm, and the user-based collaborative filtering recommendation algorithm is written by using Scala language to call Spark RDD-related interfaces. The flow is shown in Figure 2.

The implementation process of big data engine takes the user information recommendation function as an example, and its overall process includes the following four stages:

preparation stage (resource loading and data acquisition), user relevance calculation, user information recommendation calculation, and ending stage (data collection and writing into database).

#### 4. Result Analysis and Discussion

What are the attitudes and demands of audiences of opera and new media? In order to illustrate the problem with data, this paper uses questionnaires to prove it. Refine the data, collect 5~10 people from each group, and then, convert the results into percentages (Figure 3).

As can be seen from Figure 3, most of the new media are used by young people, but a considerable number of middle-aged people are using it. Secondly, on the issue of the inheritance of Kunqu Opera, people at all stages have reached a consensus. Young people think that the combination of Kunqu Opera and new media is a promising thing.

Building a three-dimensional communication channel of opera culture based on new media can attract the wide attention of the audience. The new media communication of Kunqu cultural heritage needs to attach importance to and link the Internet platform of Kunqu culture at all levels, which provides a good opportunity for the communication of Kunqu cultural heritage through various intelligent terminals such as smart phones and tablets.

With the maturity and continuous innovation of Internet technology, the presentation and application of new media are becoming more and more diversified. Under the background that the policy environment and entrepreneurial environment encouraging the development of Internet content are becoming more and more perfect, the evolution of new media forms and contents, on the one hand, the video community applications with small videos and short videos as the main bearing forms are increasing obviously; on the other hand, the video live broadcast industry is also developing extremely rapidly, and various live broadcast platforms, live broadcast communities, and other nonmedia

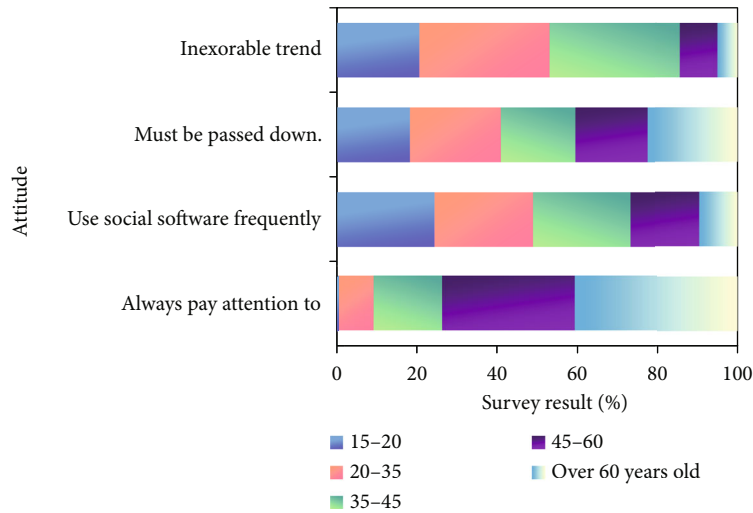


FIGURE 3: Questionnaire on the inheritance and promotion of Kunqu Opera in the new media era.

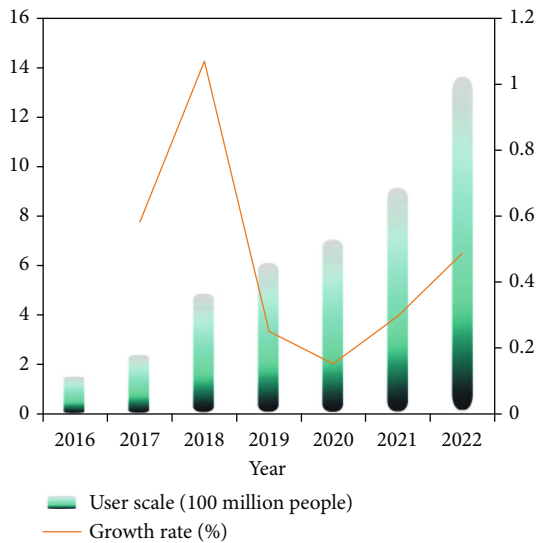


FIGURE 4: The scale and forecast of short video users in China.

platforms are growing into new self-media carriers. Figure 4 shows the statistics of short video user value research.

Figure 4 shows that the growth trend of short video users in China is obvious and the demand is clear. The new spread of Chinese traditional culture is also attracting more attention from young people with its own innovations and attempts.

Opera WeChat official account is loved by opera lovers because it pays attention to the standardization of content and the diversity of communication modes in the push process. To a great extent, the WeChat account of opera meets the aesthetic needs of the audience. While spreading opera knowledge, it conveys cultural positive energy and caters to the audience’s emotions in terms of text expression. Through investigation, the authors found that 89% of subscribers said that opera stories, celebrity anecdotes, and so on can attract and mobilize emotions, arouse inner excite-

ment and waves, and greatly stimulate interest in WeChat official account (Figure 5).

In the era of new media, relying on the spread of WeChat official account, it injects fresh blood into the opera culture, makes it integrate with the times, and glows with new and stronger vitality. For today’s opera circles and media workers, they should not only create operas and interpret the essence of operas but also learn to make full use of the thinking of new media to expand the influence and communication power of operas, so that operas can meet the aesthetic needs of audiences to the maximum extent and promote excellent national culture.

63.2% people think that the development of the Internet has led to the decrease of the audience of opera, 46.55% people think that the opera itself is too old, and 35.71% people know that the opera is too mild, lacking in freshness and excitement. As for the reasons why teenagers do not like opera, 64.33% of the respondents said they are really not interested, because they are too procrastinating and old, 49.32% of the respondents said they could not understand it, and 23.28% of the respondents felt that they did not have time to enjoy it (Figure 6).

The integration of big data engine and digital platform adopts the way of database integration. The platform database is used, and the actual research and comparison are made on the selection of data engine. Select the most commonly used centralized database storage engine in MySQL 5.6.17 for research and testing. The final statistics are as follows in Figure 7.

The full application of online new media is manifested not only in the full sharing of online resources but also on the basis that resources can be found at any time. It is also manifested in the drama taking the initiative to find its own position in online new media, making full use of the platform to publicize itself, publishing the latest drama information, making it convenient for everyone to know the performance information of the drama, publishing advertisements, letting everyone know the existence of the



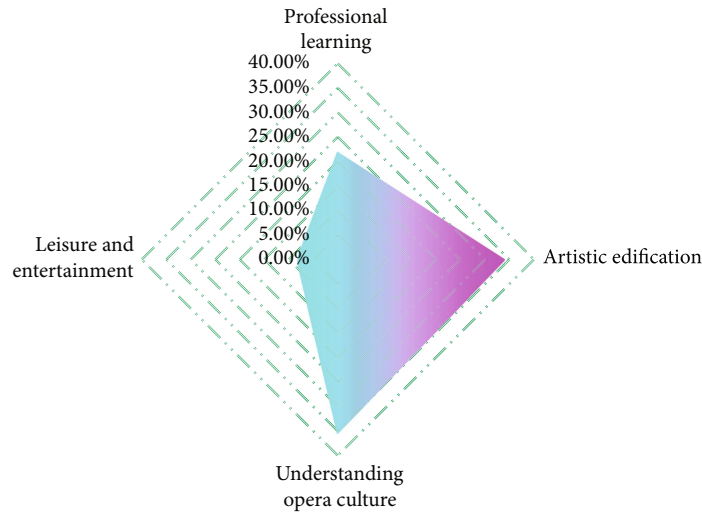


FIGURE 5: Investigation on the audience motivation of the opera WeChat official account.

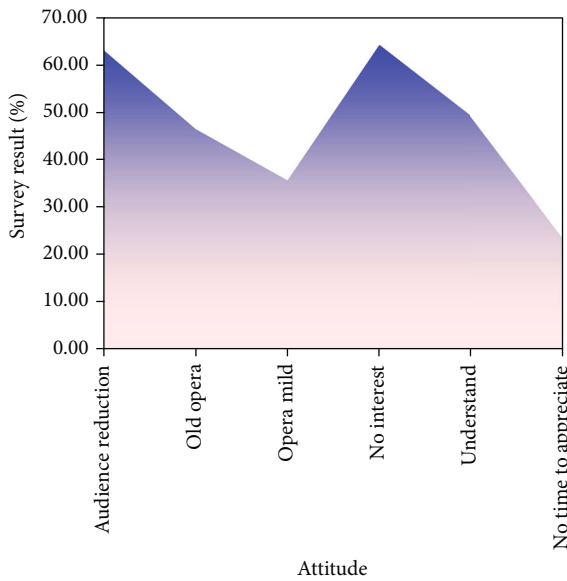


FIGURE 6: What aspects of opera are respondents interested in?

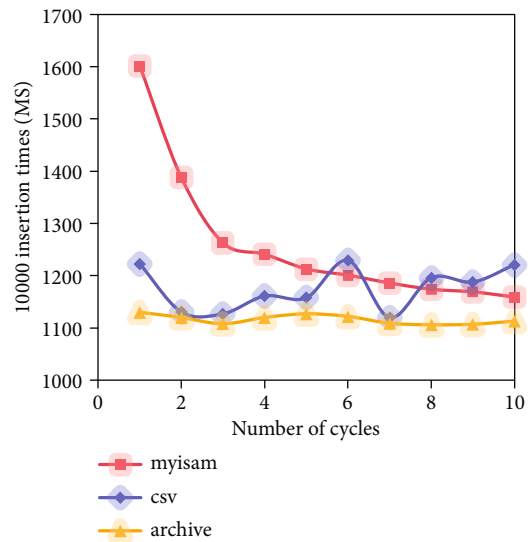


FIGURE 7: Time-consuming situation of MySQL storage engine continuously inserting ten thousand pieces of data.

online drama platform, and letting everyone pay attention to this information, thus forming influence.

The simulation experiments of UB\_CF (user-based collaborative filtering algorithm), WB\_R (WB\_R, web-based recommendation algorithm) and UB\_NR (user-based network recommendation algorithm) proposed in this paper are carried out, respectively. Figure 8 is the result chart of prediction accuracy of recommendation algorithm.

It can be seen from the figure that the average absolute error of UB\_CF is the smallest. Although the prediction accuracy of UB\_NR improved in this paper is higher than UB\_CF, it is lower than that of the traditional recommendation algorithm based on network structure. It can be seen that UB\_NR has greatly improved the prediction accuracy compared with the recommendation algorithm based on network structure and narrowed the gap between the recom-

mendation algorithm based on network structure and collaborative filtering algorithm in prediction accuracy index.

Figure 9 is an experimental result diagram of the ranking accuracy of the recommendation algorithm.

It can be seen from the figure that UB\_NR has the highest promotion index value among the three algorithms, which indicates that compared with the original recommendation algorithm based on network structure, the improved UB\_NR in this paper has increased the ranking accuracy by 8.66%.

Chinese traditional culture is the outstanding artistic creation achievement created and precipitated by the Chinese nation in the long historical development process for thousands of years. Opera culture is not an exhibit in a museum, but a movable work of art. To inherit opera culture, fundamentally innovate the concept of opera in the

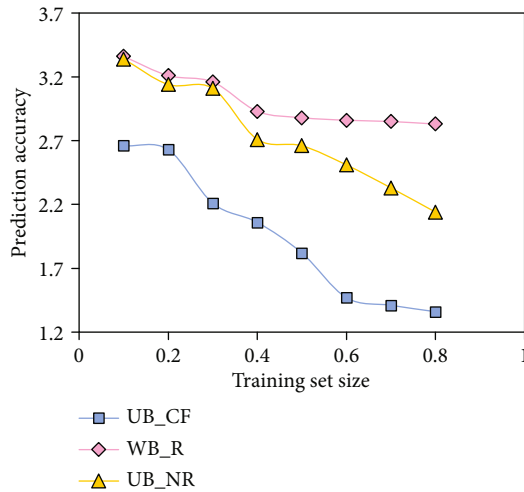


FIGURE 8: Simulation results of recommendation algorithm.

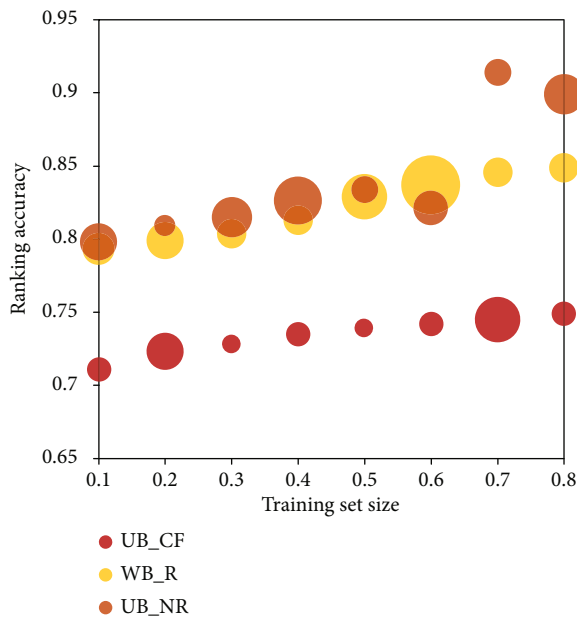


FIGURE 9: Experimental results of ranking accuracy of recommendation algorithm.

current media environment. The development and inheritance of opera cannot just stay on the glory of the past but should actively carry out independent innovation to meet the aesthetic needs of people under the current popular culture and reflect the current aesthetic tendency of young people on the basis of retaining the basic creative concept of opera.

Today, with the development of the information age, the sudden rise of new media has to be paid close attention to by us. Its effective and rapid communication mode is an opportunity that cannot be ignored in the process of opera communication. In the face of the current media opportunities, opera should be fully prepared and boldly innovated to meet the aesthetic needs of young people, and at the same time, the classic traditional plays should be retained. Let the audience have more choices in the new media environment.

## 5. Conclusion

The protection and inheritance of opera art based on big data technology are an active protection. Through the deep integration of opera art and science and technology, the opera culture will be full of vigor and vitality. Under the background of digital economy, traditional opera culture and art need to adapt to new development and changes, improve innovation ability, replace context and reconstruct scenes on the premise of maintaining excellent tradition, and realize the innovative development of cloud-based opera. The use of new media communication technology and communication methods, with rapid and massive information dissemination, will further meet people's spiritual and cultural needs and enhance people's cultural quality and cultural connotation, and at the same time, it is also the actual needs and strong wishes of the general public. Because of the comprehensive implantation of information technology and cloud communication means, the Kunqu Opera culture will make the inheritance elements and development means of Kunqu show a young state, which will help to rejuvenate the youth of Kunqu Opera and promote the healthy realization of digital inheritance of Kunqu Opera culture.

## Data Availability

The labeled dataset used to support the findings of this study is available from the corresponding author upon request.

## Conflicts of Interest

The authors declare no competing interests.

## Acknowledgments

This research was supported by Scientific Research Projects of Shaanxi Provincial Department of Education (18JK1193).

## References

- [1] X. Wang, "Spiritual inheritance: a case study of Henan opera," *Contemporary Educational Research*, vol. 5, no. 9, p. 5, 2021.
- [2] W. Liu, "Research on the application of multimedia elements in visual communication art under the Internet background," *Mobile Information Systems*, vol. 2021, 10 pages, 2021.
- [3] J. G. Peritz, "Orpheus's civilising song, or, the politics of voice in late enlightenment Italy," *Cambridge Opera Journal*, vol. 31, no. 2-3, pp. 1-24, 2019.
- [4] N. Vilknor, "The opera and the omnibus: material culture, urbanism and Boieldieu's *La dame blanche*," *Cambridge Opera Journal*, vol. 32, no. 1, pp. 90-114, 2020.
- [5] J. Zhou, "Statistical research on the development of rural tourism economy industry under the background of big data," *Mobile Information Systems*, vol. 2021, 11 pages, 2021.
- [6] Y. Wang and X. Hu, "Wuju opera cultural creative products and research on visual image under VR technology," *Access*, vol. 8, pp. 161862-161871, 2020.
- [7] X. Wang and Y. Ping, "Enabling original Chinese opera to go global - China national opera house of cultural interviews of

- the five-year endeavor,” *Cultural exchange between China and foreign countries: English version*, vol. 11, p. 4, 2017.
- [8] P. Bhatt, B. Sedani, and N. Kotak, “Designing and simulation of 30Gbps FSO communication link under different atmospheric and cloud conditions,” *International Journal of Engineering Trends and Technology*, vol. 69, no. 5, pp. 228–234, 2021.
- [9] F. Jiao, “Peking opera costumes: a display of history, culture, and fine craftsmanship,” *China Today*, vol. 69, no. 3, pp. 72–75, 2020.
- [10] J. Feng, “Peking opera costumes: a display of history, culture, and fine craftsmanship,” *China today: English version*, vol. 69, no. 3, p. 4, 2020.
- [11] Y. Gao, Y. Wu, Z. Cui, H. Chen, and W. Yang, “Robust design for turning and climbing angle-constrained UAV communication under malicious jamming,” *IEEE Communications Letters*, vol. 25, no. 2, pp. 584–588, 2021.
- [12] “None Tibetan opera: inscribed on the representative list of the intangible cultural heritage of humanity in 2009,” *China and Africa: English version*, vol. 2, pp. 60–61, 2020.
- [13] X. Yu, F. Jiang, J. Du, and D. Gong, “A user-based cross domain collaborative filtering algorithm based on a linear decomposition model,” *Access*, vol. 5, pp. 27582–27589, 2017.
- [14] G. Qiao, X. Liu, L. Ma, S. Mazhar, and Y. Zhao, “Residual Doppler effect analysis of the FBMC/OQAM communication system in underwater acoustic channel,” *IEEE Communications Letters*, vol. 25, no. 9, pp. 3090–3093, 2021.
- [15] D. Margaritis, A. Kobusinska, D. Spiliotopoulos, and C. Vassilakis, “An adaptive social network-aware collaborative filtering algorithm for improved rating prediction accuracy,” *Access*, vol. 8, pp. 68301–68310, 2020.
- [16] X. Yu, F. Jiang, J. Du, and D. Gong, “A cross-domain collaborative filtering algorithm with expanding user and item features via the latent factor space of auxiliary domains,” *Pattern Recognition*, vol. 94, pp. 96–109, 2019.
- [17] C. Cai, C. Zhe, J. Luo, H. Pu, M. Hu, and R. Zheng, “Boosting chirp signal based aerial acoustic communication under dynamic channel conditions,” *IEEE Transactions on Mobile Computing*, vol. PP(99):1-1, p. 1, 2021.
- [18] C. Tong, J. Qi, Y. Lian, J. Niu, and J. J. P. C. Rodrigues, “Time-TrustSVD: a collaborative filtering model integrating time, trust and rating information,” *Future Generation Computer Systems*, vol. 93, pp. 933–941, 2019.
- [19] H. Xu, “Empirical study on theories and techniques of adolescent physical health promotion under the background of big data,” *Mobile Information Systems*, vol. 2021, 13 pages, 2021.
- [20] A. H. Sodhro, Z. Luo, G. H. Sodhro, M. Muzamal, J. J. P. C. Rodrigues, and V. H. C. de Albuquerque, “Artificial intelligence based QoS optimization for multimedia communication in IoV systems,” *Future Generation Computer Systems*, vol. 95, pp. 667–680, 2019.
- [21] X.-d. Yin, “Dynamic data driven big data cooperative control scheme with virtual visualization for mobile multimedia communication,” *Cluster Computing*, vol. 22, no. S1, pp. 1541–1548, 2019.
- [22] S. Xu, X. Wang, and M. Huang, “Modular and deep QoE/QoS mapping for multimedia services over satellite networks,” *International Journal of Communication Systems*, vol. 31, no. 17, 2018.
- [23] A. A. Vasiliev, Y. V. Pechatnova, and Y. V. Pechatnova, “Legal and environmental problems of personal data protection under commercialization of big data,” *Ukrainian Journal of Ecology*, vol. 10, no. 5, pp. 133–135, 2020.
- [24] G. K. Audhya, S. C. Ghosh, and B. P. Sinha, “Lower bound on bandwidth and channel assignment algorithm for multimedia communication in cellular networks,” *IEEE Transactions on Mobile Computing*, vol. 18, no. 8, pp. 1816–1830, 2019.

## Research Article

# Sports Action Recognition and Analysis Relying on Inertial Sensors

Yutong Liu,<sup>1</sup> Zunliang Zhou,<sup>1</sup> Xiaolong Qian ,<sup>2</sup> and Jiaming Chen <sup>1</sup>

<sup>1</sup>Physical Education Department, Northeastern University, Shenyang, 110819 Liaoning, China

<sup>2</sup>College of Information Science and Engineering, Northeastern University, Shenyang, 110819 Liaoning, China

Correspondence should be addressed to Xiaolong Qian; 1971203@stu.neu.edu.cn and Jiaming Chen; 2001275@stu.neu.edu.cn

Received 7 March 2022; Revised 8 April 2022; Accepted 15 April 2022; Published 9 May 2022

Academic Editor: Wen Zeng

Copyright © 2022 Yutong Liu et al. This is an open access article distributed under the Creative Commons Attribution License, which permits unrestricted use, distribution, and reproduction in any medium, provided the original work is properly cited.

The process of sports action recognition involves not only the change of motion speed but also the change of motion attitude, so it is necessary to carry out coordinate system transformation and attitude behavior recognition in combination with the actual situation, and inertial sensors play an important role in this process. Moreover, this paper combines inertial sensors to construct a sports action recognition and analysis system. In addition, based on the STA/LTA-AIC vibration wave picking method, an improved STA/LTA-AIC method based on wavelet packet decomposition is proposed to automatically identify the first arrival of vibration waves. Through the experimental research, it can be seen that the sports action recognition system based on an inertial sensor proposed in this paper has a good performance in sports action feature recognition.

## 1. Introduction

In a real environment or an indoor obstacle environment, the user's walking speed is difficult to control. Regarding sensor signals, gait recognition by spatial angle sensor data is rarely involved in previous studies. The reason for this is that studies typically use sensors attached to the waist or smart handheld devices placed in a trouser pocket. The body part involved in this type of equipment is basically unable to measure the angle change of the leg, so it can only be analyzed through acceleration data. The study measured the angle change of each part of the whole leg. This method can indeed better reflect the gait stage, but it still remains at the laboratory level due to the need for a large number of customized sensor equipment. Moreover, it is still worth exploring using the built-in angle sensor of ordinary wearable smart devices to measure gait.

Special attention is required regarding the use of spatial angle sensor data in wearable devices. The space angle definition of these devices usually adopts the Euler angle system, which may cause the problem of Gimbal lock. The universal lock is a problem that occurs when the dynamic Euler angle

is used to represent the rotation of a three-dimensional object; that is, when the axis is rotated to coincide with the axis, the degree of freedom is lost. Specifically, when an Euler angle is rotated beyond 180 degrees, it will jump to a position of -180 degrees. In recent years, the use of portable mobile devices for object motion behavior monitoring is one of the most popular researches in the field of mobile computing in recent years, and the corresponding motion behavior monitoring applications have also become a popular and popular category of various application software.

When the interactive behavior occurs in multiple different time and place contexts, by observing the interaction patterns in different contexts, the design content can be brought into the user's different contexts [1]. When users move from one context to another, the multidimensional cognitive content of the context is generated, including context location, user subject, interaction behavior, interaction barriers, and interaction guidance, which are all extremely important concerns. Multidimensional context is a multianalysis of the acquisition results of historical contexts. The information of these contexts can be obtained from observation or extracted from user interviews or contextual

storyboards [2]. By analyzing the content of different contextual dimensions, according to the relevant data of these historical contexts, the designers in the current context are provided with the context construction requirements [3].

This paper combines inertial sensors to construct a sports action recognition and analysis system and builds an intelligent system, which provides a reference for subsequent sports action recognition and analysis.

## 2. Related Work

When discussing various statistical properties of stochastic resonances, there are mainly the Langevin equation or the corresponding Fock-Planck equation in theory. Under the condition of adiabatic approximation, the literature [4] studied the SR effect of the two-state model of the bistable system and obtained the adiabatic approximation theory, but this theory has some shortcomings, it is only suitable for modulation signals with very small frequency and amplitude, and the transition probability formula it gives cannot predict the higher harmonics in the output spectrum. In order to better describe the output behavior of the bistable system, the literature [5] proposed the linear response theory of stochastic resonance, so that the SR effect can be better predicted theoretically. Reference [6] proposed the residence time distribution theory. The eigenvalue theory proposed in [7] is also known as the Fock theory. The eigenvalue theory does not require the assumptions made by the adiabatic approximation theory but regards the signal as a weak disturbance, and according to the Fock-Planck equation, it obtains the probability distribution and asymptotic spectral density of the system. Reference [8] conducted such an experiment. First, a modulation signal with a fixed frequency and amplitude was input to the trigger, and a noise signal with variable intensity was superimposed on this basis. Reference [9] made an experiment on an optical system: the bistable state in the system is the clockwise and counterclockwise motion of the laser modes in the bidirectional ring laser, and the stochastic resonance has been further proved in this experiment, and also, the study of stochastic resonance has entered a new stage. For the Langevin equation, people generally conduct a comprehensive experimental study through the electronic circuit simulation method. Chinese scholars Qin Guangrong, Hu Gang, and others have proved some theories and predictions through experiments related to electronic circuits. At the same time, they have given the differences between theories and experiments, obtained the scope of application of adiabatic approximation theory and linear response theory, and pointed out stochastic resonance: research direction and application prospect [10]. At the same time as the in-depth study of stochastic resonance mechanism, the research on signal detection and processing using stochastic resonance is also vigorously carried out. It has applications in electromechanical equipment fault detection, biomedicine, signal detection under the background of ocean noise, and image information enhancement. For a long time, the related application research of stochastic resonance in the field of signal detection has mainly focused on the traditional bistable system [11]. Reference [12] men-

tioned that the phenomenon of stochastic resonance was found in the underdamped monostable system, which subverted the previously recognized stochastic resonance must have three elements (nonlinear system with bistable or multistable, noise, and input signal). Subsequent researches on stochastic resonance in monostable systems have continued to progress. Reference [13] studied the stochastic resonance caused by multiplicative noise and additive noise in a monostable system. Due to the action of multiplicative noise, a potential barrier appeared in the monostable potential well, which essentially transformed the monostable system into a bistable system. The literature [14] studies the stochastic resonance phenomenon generated by the monostable system composed of the monostable potential function as a piecewise linear function; the literature [15] studies the stochastic resonance phenomenon in the single-mode nonlinear optical system; according to the analysis of the monostable system, this paper deduces the general conclusion that the system will have stochastic resonance if there is an inflection point in the monostable function. Is there no inflection point in the monostable function and no stochastic resonance? The answer is no. The monostable function given in the literature [16] has no potential barrier, and there is no inflection point in the case of the paper. The system appears stochastic resonance phenomenon under the action of additive noise and driving signal, which the author considers to be a new type of stochastic resonance.

In previous studies, step symmetry was used to measure gait symmetry (gait symmetry) [17]. Step symmetry is defined as the ratio of step regularity to stride regularity. By calculating the autocorrelation coefficient of the VT axis acceleration signal data, the time period difference with the most significant autocorrelation can be found [18]. If the sensor is fixed on the subject's waist in the experiment, each peak corresponds to a step. At this time, since the step and the stride appear in a time series in a cross, the peak corresponding to the step regularity and the peak corresponding to the stride regularity also appear in a cross. By looking for the difference between the two peaks, the symmetry of left and right foot movements can be illustrated [19]. The calculation method of step regularity can also be obtained in the study, which is to find the peak value in the autocorrelation coefficient. Step regularity reflects whether the stride is regular and uniform in the whole walking cycle.

Although gait features can be extended in the gait stage, because the sensor data is susceptible to noise interference, research on the gait stage is mostly carried out with high-cost laboratory equipment, such as the motion capture device Vicon. Some studies have attempted to classify gait stages using acceleration sensors at the waist of the human body [20]. This is a very bold and worthwhile attempt, but due to the noise processing involved in filtering and the division of stages too detailed, the accuracy is still open to question. The research accuracy of acceleration sensor data for the gait stage tends to be low, mainly because the acceleration sensor captures the acceleration data of body buffering or shaking. The meaning of this data is not clear enough, the angle data is easier to capture, it is easier to find characteristic points in the signal, and it is more consistent with the various definitions of the gait cycle [21].

### 3. Sports Action Recognition and Analysis Relying on Inertial Sensors

The Short-Term Average/Long-Term Average (STA/LTA) method is one of the commonly used automatic pick-up methods for vibration waves. The principle of the STA/LTA method is to use the ratio of STA (average value in a short time window of the signal) to LTA (average value in a long time window of the signal) to represent the change in the energy or amplitude of the sports signal and to predict the first arrival time of the sports vibration wave. Averages in short time windows are more sensitive to rapid fluctuations in time series amplitude, while averages in long time windows reflect only background noise. Therefore, when the sports signal comes, the variation of the average value in the short-term window (STA) will always be greater than the variation of the average value in the long-term window (LTA), and the STA/LTA also increases significantly. When the ratio of STA to LTA is greater than a preset threshold, it is determined that a sports event occurs. At this time, the mutation point of the ratio is the first arrival point of the sports signal, and the time point of the mutation is the first arrival time of the sports signal. The schematic diagram of the STA/LTA method is shown in Figure 1.

According to different calculation methods, the calculation methods of STA and LTA can be divided into two types: recursion and standard. The calculation formulas are shown in formulas (1) and (2), respectively:

Recursive STA/LTA are

$$STA_t = STA_{t-1} + \frac{f_c(t) - STA_{t-1}}{N_{Sta}}, \quad (1)$$

$$LTA_t = LTA_{t-1} + \frac{f_c(t - N_{Lta} - 1) - LTA_{t-1}}{N_{Lta}}. \quad (2)$$

Standard STA/LTA are

$$STA_t = STA_{t-1} + \frac{f_c(t) - f_c(t - N_{Sta})}{N_{Sta}},$$

$$LTA_t = LTA_{t-1} + \frac{f_c(t - N_{Sta} - 1) - f_c(t - N_{Sta} - N_{Lta} - 1)}{N_{Lta}}. \quad (3)$$

In the above formula,  $STA_t$  is the average value of the signal in the short time window at time  $t$ ,  $LTA_t$  is the average value of the signal in the long time window at time  $t$ , and  $f_c(t)$  is the characteristic function value of the signal at time  $t$ .  $N_{Sta}$  and  $N_{Lta}$  are the number of recorded sample points included in the short-term average time window and the long-term average time window, respectively.

When using the STA/LTA method to process sports signals, the stability and accuracy of the results obtained will be affected by many factors, such as the selection of feature functions, the size of the time window, and the setting of the trigger threshold.

The selection of the characteristic function directly affects the accuracy of the vibration wave pickup. The

long-short time window mean ratio method is used to identify the vibration wave and vibration wave. The more common characteristic functions are as follows:

$$\begin{aligned} f_c(t) &= |Y(t)|, \\ f_c(t) &= Y(t)^2, \\ f_c(t) &= Y(t) - Y(t-1), \\ f_c(t) &= Y(t)^2 - Y(t-1)Y(t+1). \end{aligned} \quad (4)$$

The calculation process of the mean ratio method of long and short time windows is fast and simple, and it can better carry out vibration wave pickup experiments in the environment of large-scale propagation paths and high signal-to-noise ratio. However, when the initial fluctuation is not obvious and the environmental noise is large, the pickup effect of the vibration wave is not good, and it is easy to produce large errors. The selection of the length of the time window also directly affects the accuracy of the automatic pickup of vibration waves, and the length of the short time window can be obtained from the above STA/LTA calculation formula.

In order to more clearly confirm the optimal threshold, this paper introduces the parameter  $Q$  to represent the perceptual quality of the early warning system, where  $Q$  is the ratio of the accuracy rate to the false alarm rate. According to the experimental results in Table 1, Figure 2(b) plots the numerical variation of the ratio  $Q$  of the accuracy rate to the false alarm rate under different thresholds. The larger the value of  $Q$ , the higher the accuracy and the better the effect of the early warning system.

Figure 2(a) shows that the accuracy and false alarm rate of the STA/LTA method change with the threshold  $R$ . It can be seen from this figure that the accuracy rate increases with the increase of the threshold and the false alarm rate decreases with the increase of the threshold  $R$ . When the optimal threshold point is reached, the false alarm rate increases continuously with the increase of the threshold  $R$ , which indicates that the threshold is set too high, and some vibration events that meet the requirements are ignored and not identified. Combining with Figures 2(a) and 2(b), we can find that in the experimental environment of this paper, when the threshold  $R$  is equal to 2, the vibration recognition accuracy is the highest, so the threshold size of the STA/LTA method involved in this paper is set to 2.

**3.1. Setting of Long and Short Time Windows.** The short time window (STA) is mainly used to obtain a time window for sports signals, so the shorter the short time window, the more advantageous it is for the acquisition of sports signals in a short period, and the long time window (LTA) is used to measure the time window. STA/LTA can automatically adjust the acuity of the sports signal according to the noise level in the background environment. It is necessary to find the optimal choice of long time window and short time window in this experimental environment. This paper uses a fixed long time window size to analyze the picking results corresponding to different short time windows and uses a

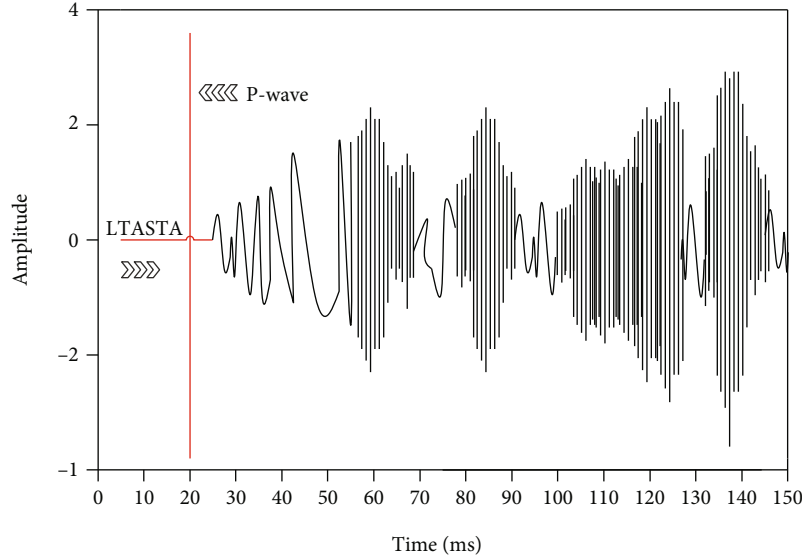


FIGURE 1: Vibration wave of STA/LTA method.

TABLE 1: Recognition effect of sports action feature of sports action recognition system based on inertial sensor.

Number	Sports recognition	Number	Sports recognition	Number	Sports recognition
1	92.19	17	92.24	33	93.76
2	88.46	18	93.99	34	90.78
3	88.47	19	93.47	35	92.30
4	90.29	20	90.51	36	93.83
5	88.91	21	89.51	37	92.92
6	90.54	22	91.91	38	92.85
7	92.38	23	90.03	39	88.22
8	91.98	24	88.06	40	92.23
9	93.66	25	90.74	41	92.90
10	89.41	26	91.55	42	87.30
11	93.15	27	88.00	43	88.11
12	93.89	28	88.36	44	90.15
13	90.56	29	89.34	45	89.40
14	90.78	30	87.02	46	92.22
15	90.76	31	89.12	47	88.98
16	87.95	32	87.26	48	89.61

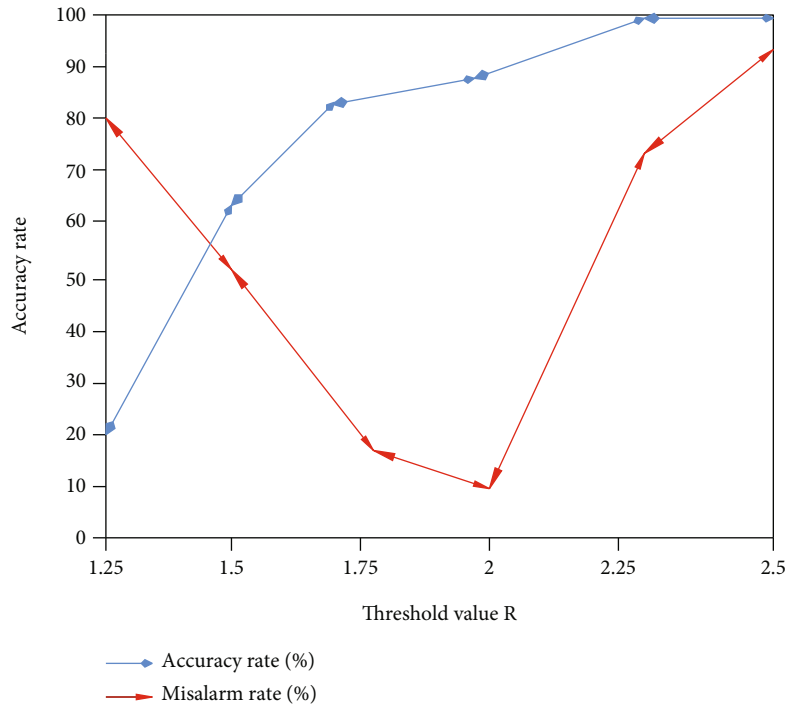
fixed short time window size to analyze the picking results corresponding to different long time windows and determines the size of the long and short time windows. It is obtained that the accuracy rate reaches the highest when the short-time window size is 0.2 s and the long-time window size is 2 s. Therefore, the short-time window size in this paper is set to 0.2 s, and the long-time window size is set to 2 s.

When processing the data using the  $|Y(t)|$  and  $Y^2(t)$  characteristic functions, it only reflects the change in the amplitude of the vibration wave in sports, and cannot highlight the change in frequency. Although  $Y(t) - Y(t-1)$  can reflect the changes of amplitude and frequency, the recognition effect is poor in the background of low signal-to-noise ratio. Based on the low

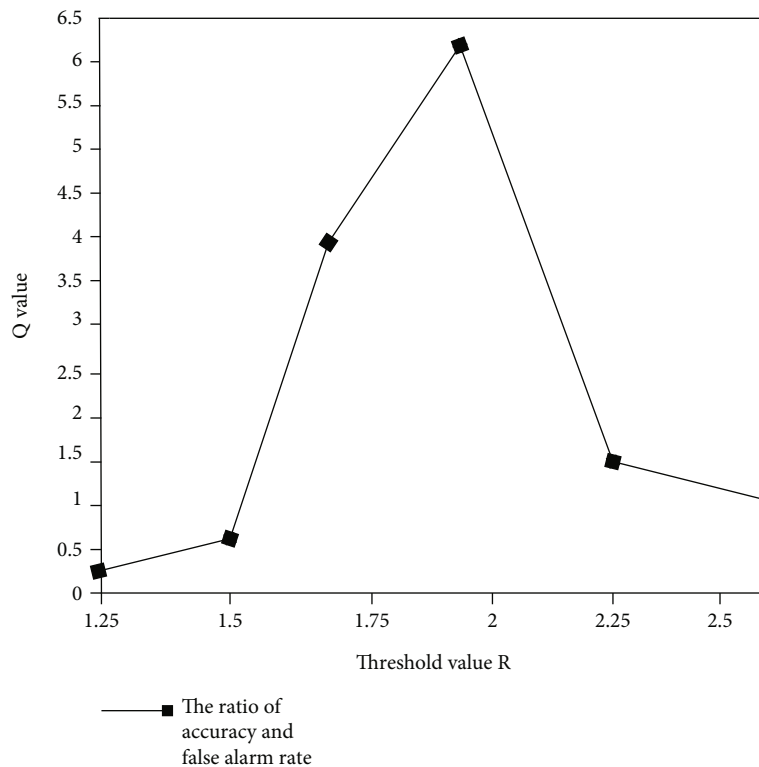
signal-to-noise ratio of the data collected by the inertial sensor,  $Y(t)^2 - Y(t-1)Y(t+1)$  is used as the feature function of this paper to characterize the data, and the result after characterizing the data is shown in Figure 3.

After the sample data is processed by the feature function, the abnormal vibration waveform features can be significantly amplified under the condition that the signal-to-noise ratio is relatively low. Therefore, after the sample data is characterized by the feature function  $Y(t)^2 - Y(t-1)Y(t+1)$ , the pick-up rate of the STA/LTA algorithm can be effectively improved.

The Akaike Information Criterion (AIC), also known as the minimum information criterion, is used to measure the estimated model complexity and the goodness of the model's



(a) Accuracy rate and false alarm rate under different thresholds



(b) The ratio of the accuracy rate to the false alarm rate under different thresholds

FIGURE 2: Accuracy rate, false alarm rate, and ratio of accuracy to false alarm rate under different thresholds.

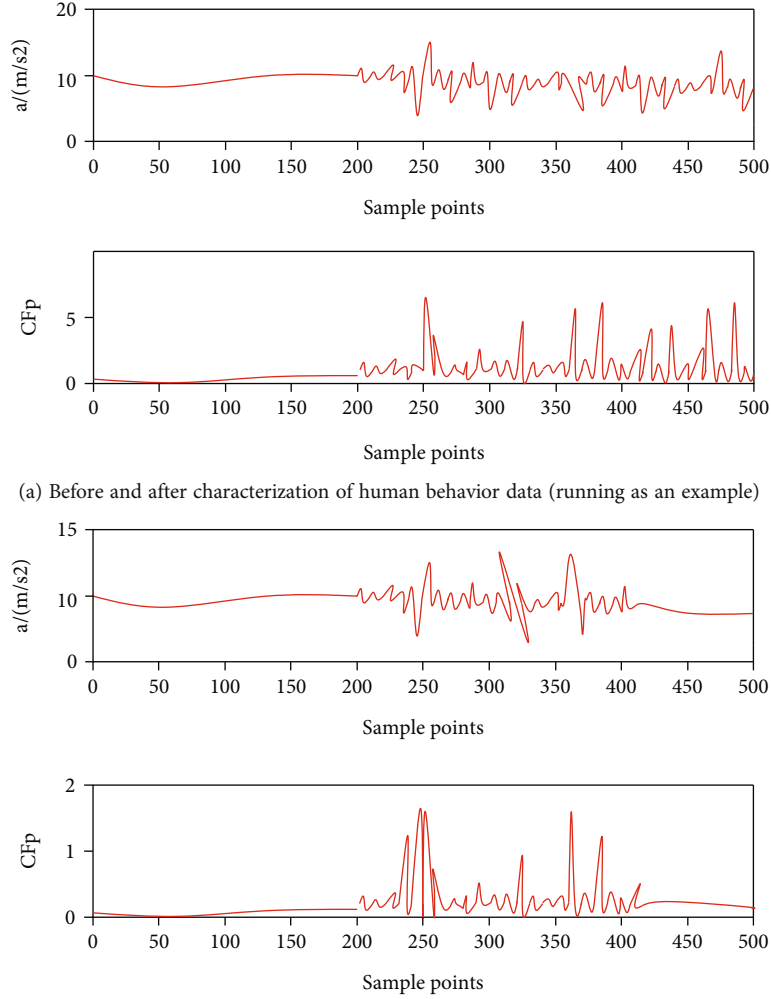
fitting data. The basic expression of AIC is shown in

$$AIC = 2k - 2 \ln(\text{likelihood function}). \quad (5)$$

Among them,  $k$  is the number of parameters.

The basic principle of using the AIC method to identify sports vibration waves is that the point corresponding to the minimum point of the AIC curve is the optimal dividing point between the sports signal and the background environmental noise. The AIC curve of the sports signal is solved in





(b) Before and after characterization of simulated sports data

FIGURE 3: Results after data characterization processing.

the corresponding time window, and the minimum point corresponding to the curve is the point where the vibration wave reaches. The basic schematic diagram of the AIC algorithm is shown in Figure 4.

Its expression is shown in

$$\text{AIC} = C - 2 \log(L). \quad (6)$$

Among them,  $C$  is a constant and  $L$  is the maximum likelihood function.

The sports signal recording can be divided into two steady-state process sequences (sports signal and noise), and the first arrival of the vibration wave is used as the dividing line to distinguish the two steady-state processes of the sports signal and noise, which means that the minimum point of AIC is the vibration wave. At that time, in the boundary point of the two steady-state processes, the arithmetic expression of AR-AIC is shown in

$$\text{AIC}(K) = (K - N) \log(\sigma_{1,\max}^2) + (M - N - K) \log(\sigma_{2,\max}^2) + C. \quad (7)$$

In the above formula,  $N$  is the order of fitting the autoregressive model data,  $M$  is the length of the sports data,  $\sigma_{1,\max}^2$  and  $\sigma_{2,\max}^2$  are the variance of the data fitting in the two time intervals, and  $C$  is a constant.

The expression of VAR-AIC is shown in

$$\text{AIC}(K) = K \times \log\{\text{var}(x[1, K])\} + (M - K - 1) \log\{\text{var}(x[K + 1, M])\}. \quad (8)$$

Among them,  $K$  includes all the sample points of the input sports signal  $x$ , which is the corresponding serial number of the sample points in the selected time window, and  $\text{var}(x[1, K])$  and  $\text{var}(x[K + 1, M])$  are the variances of two different time series. At this moment, the minimum value of the AIC curve is the first arrival point of the vibration wave.

Through the analysis of the experimental results of using the STA/LTA method and the AIC method alone to pick up the first arrival time of the vibration wave, the AIC method alone has a large deviation from the real arrival time of the vibration wave. The AIC method has a

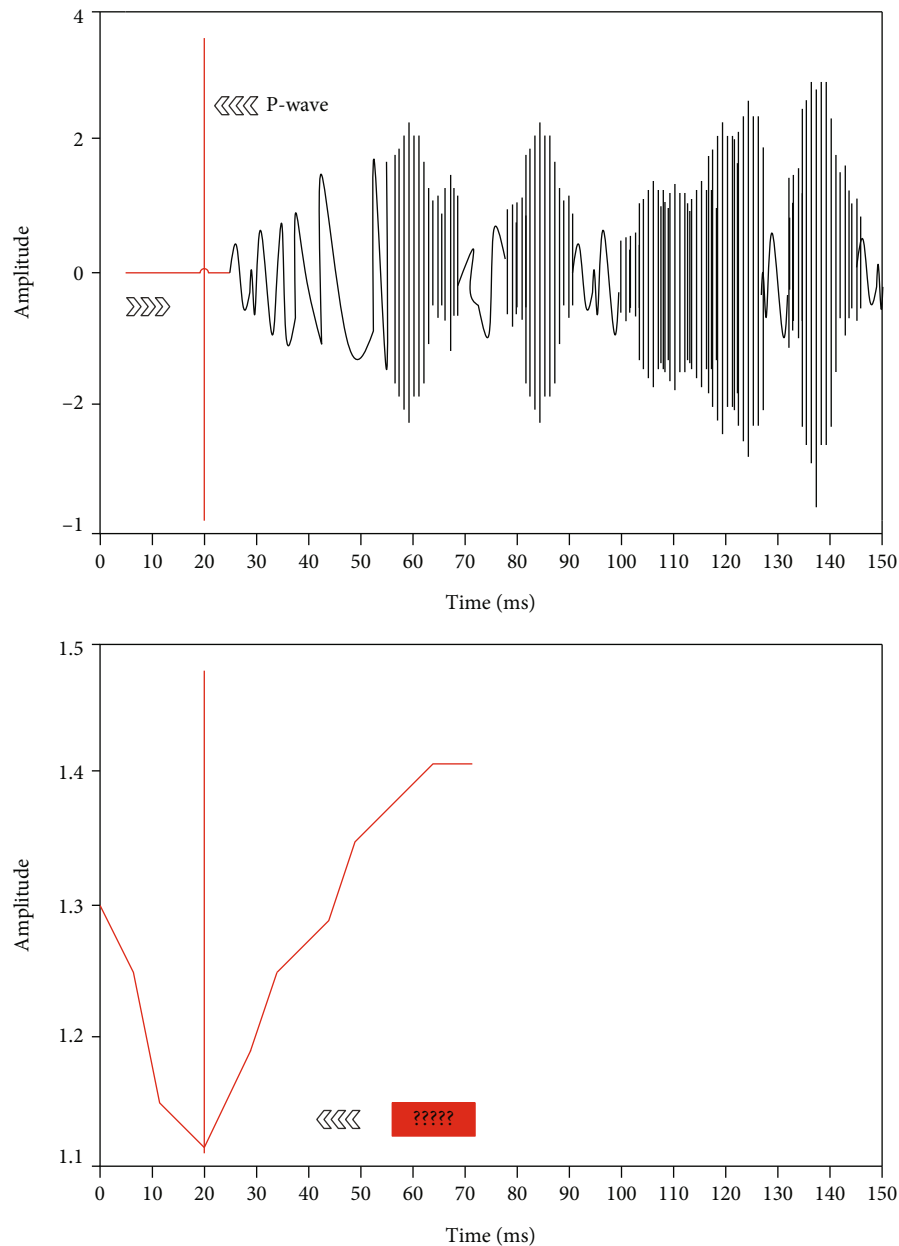


FIGURE 4: Schematic diagram of AIC method when picking up.

smaller deviation but also has a larger pickup error. At present, the STA/LTA-AIC comprehensive method is widely used. The specific steps of using this method in this paper are as follows:

- (Step 1) It uses the characteristic function determined.
- (Step 2) It uses the STA/LTA calculation formula to calculate the value of STA/LTA, and the obtained ratio is compared with the previously set threshold  $R$ . When the ratio is larger than the threshold  $R$ , the algorithm proceeds to the next step, and when it is smaller than the threshold  $R$ , the algorithm ends.

- (Step 3) The algorithm uses the AIC criterion within the time window of 2 s before and after to calculate the corresponding AIC curve.

The minimum value of the curve is the arrival time of the vibration wave.

Figure 5 is the flow chart of the STA/LTA-AIC integrated method to pick up the vibration wave when the vibration wave arrives.

Traditional vibration signal analysis and processing generally use windowed Fourier analysis. This method is an analysis method in which the window function does not change, so it cannot explain the characteristics of vibration signals such as short duration, frequency domain time

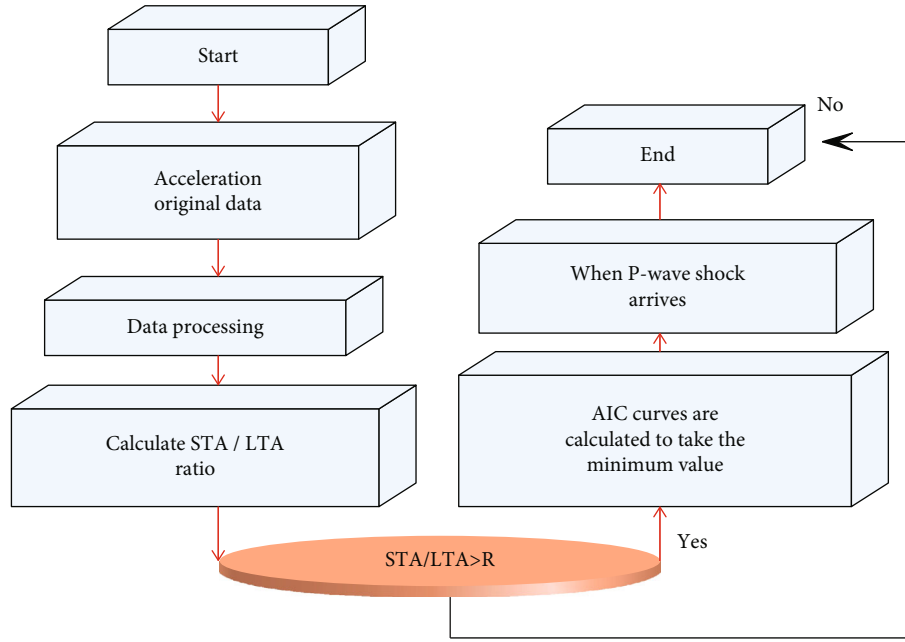


FIGURE 5: Flow chart of the STA/LTA-AIC method for picking up the vibration wave when the vibration wave arrives.

domain localization, and nonstationarity. Wavelet analysis is a time-domain localized analysis method with variable shape but constant window area. In this method, only the low-frequency signal is decomposed and decomposed again, and the high-frequency signal is not decomposed again, and the frequency resolution will decrease as the frequency increases. The transformation formula is as follows:

$$c_{2n}^{k+1} = I_0(c_n^k), c_{2n+1}^{k+1} = I_1(c_n^k). \quad (9)$$

Among them,  $c_n^k = \{c_n^k, j\}_{j \in \mathbb{Z}}$ ,  $c_{2n}^{k+1} = \{c_{2n,j}^{k+1}\}_{j \in \mathbb{Z}}$ ,  $c_{2n+1}^{k+1} = \{c_{2n+1,j}^{k+1}\}_{j \in \mathbb{Z}}$ , and the expressions of operators  $I_0$  and  $I_1$  such as formula (10) are

$$I_0\{S_k\}(j) = \sum_{k \in \mathbb{Z}} S_k d_{k-2j}, I_1\{S_k\}(j) = \sum_{k \in \mathbb{Z}} S_k g_{k-2j}. \quad (10)$$

Wavelet packet analysis divides the frequency bands at multiple levels and decomposes each frequency band again after decomposing and obtains more detailed signal decomposition than wavelet transform. In the first decomposition of the wavelet packet, two parts of high frequency and low frequency are obtained, and the two parts are decomposed simultaneously in the second decomposition. Moreover, two sequences are obtained after each decomposition. The wavelet packet decomposition tree is shown in Figure 6.

The original sports signal is regarded as the decomposition transformation  $c_0^0$  of the scale zero node  $(0, 0)$ , that is,  $\{c_{0,j}^0\}_{j \in \mathbb{Z}}$ . The algorithm performs wavelet packet decomposition transformation on the zero node  $(0, 0)$  through formula (10) to obtain two nodes  $(1, 0)$  and  $(1, 1)$  with a scale of 1. The corresponding coefficients are  $c_0^1$  and  $c_1^1$ , which, respectively, include

the low-frequency and high-frequency parts of the original sports signal. Following this rule, the coefficient corresponding to a node of scale  $k$  is denoted  $c_0^k, c_1^k, \dots, c_{2^k-1}^k$ .

The wavelet packet avoids the disadvantage that the local performance of the spectrum is deteriorated due to the increase of the scale of the wavelet transform and can analyze the sports signal more accurately. Therefore, this paper proposes the method of wavelet packet decomposition and reconstruction to decompose and reconstruct abnormal vibration signals.

Based on the STA/LTA-AIC vibration wave picking method, this paper proposes an improved STA/LTA-AIC method based on wavelet packet decomposition to automatically identify the first arrival of vibration waves. The basic idea of the method is as follows:

- (Step 1) The algorithm uses the STA/LTA method to roughly pick up the picked original signal and compares the STA/LTA ratio with the threshold  $R$  set in Section 2. When the ratio is greater than the threshold  $R$ , the algorithm proceeds to the next step, and when the ratio is less than the threshold  $R$ , the algorithm ends the experimental step.
- (Step 2) The algorithm decomposes the original vibration signal with three-scale wavelet packet and reconstructs the original vibration signal using the decomposed coefficients.
- (Step 3) The algorithm then calculates the AIC curve of the reconstructed signal in the time window of  $t \pm 2s$  under the three scales according to formula (8) and then superimposes the AIC curves of the three scales, and the minimum value

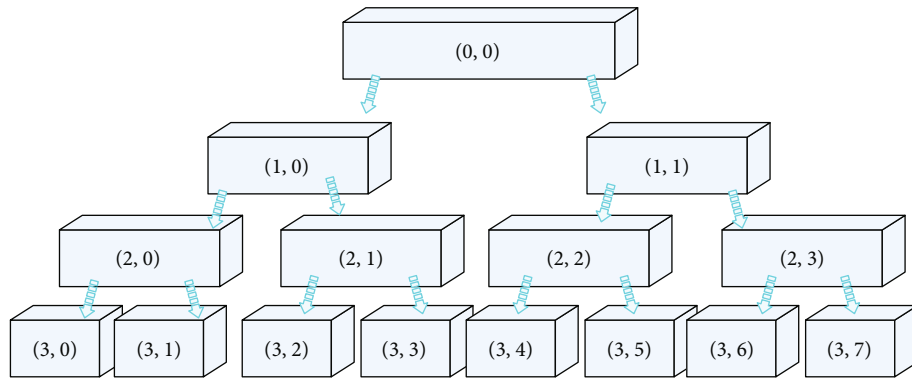


FIGURE 6: Wavelet packet decomposition tree.

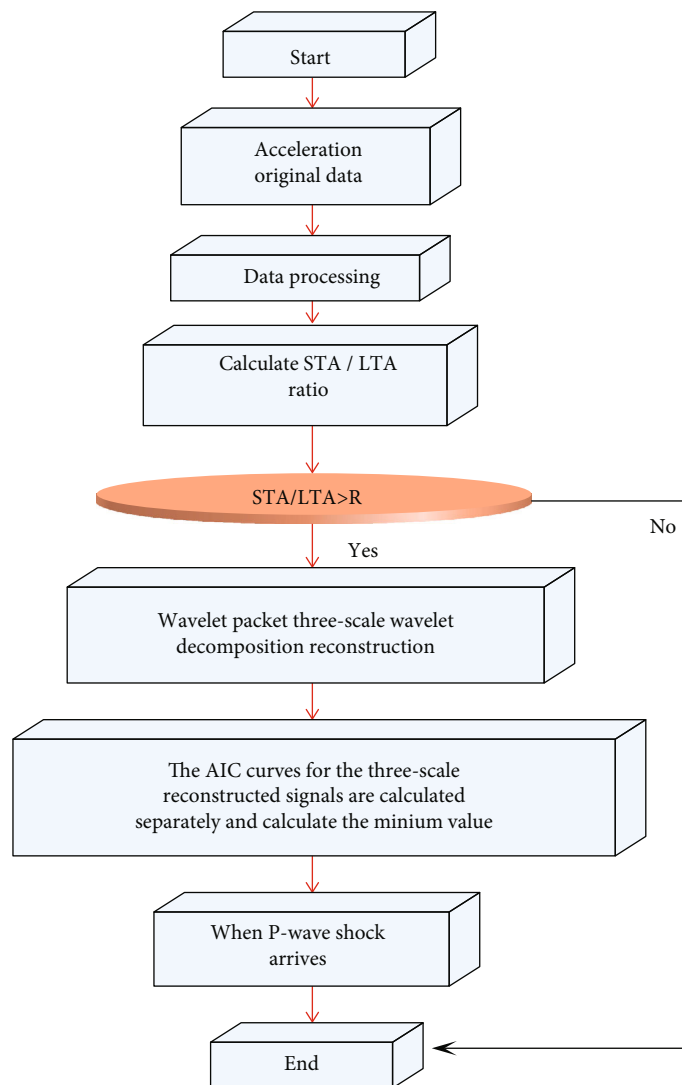


FIGURE 7: Flow chart of picking up vibration wave at the first arrival based on wavelet packet.

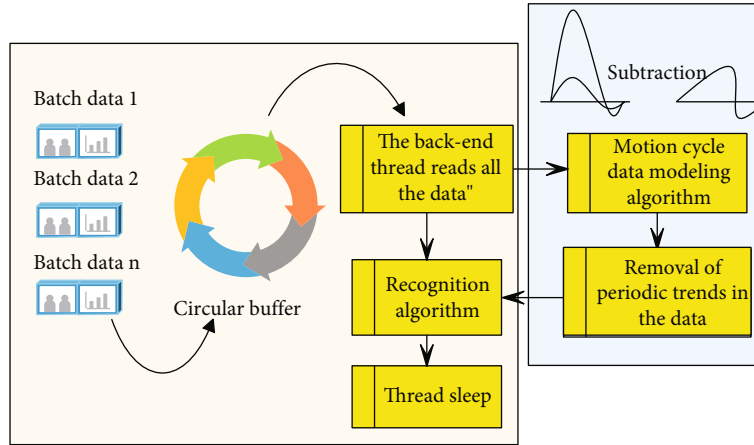


FIGURE 8: Sports action recognition process based on inertial sensors.

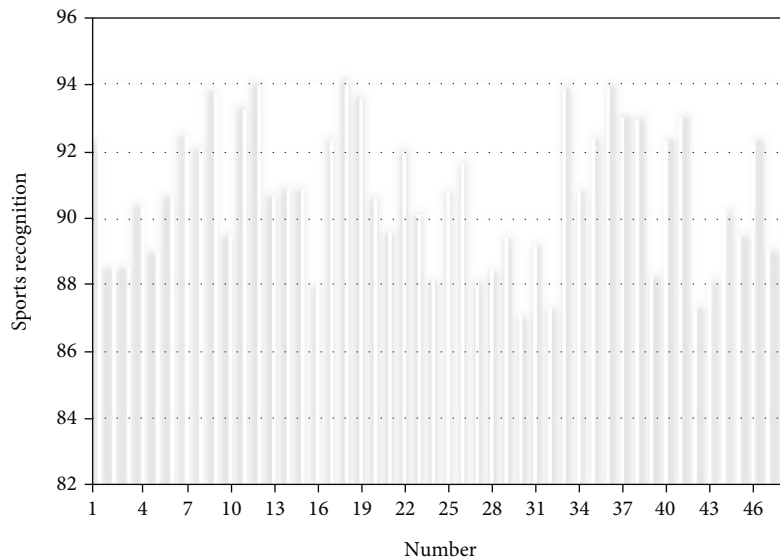


FIGURE 9: Intuitive statistics of sports action feature recognition effect of inertial sensor-based sports action recognition system.

obtained is the arrival time of the vibrational wave.

Figure 7 is the flow chart obtained when the STA/LTA-AIC method based on wavelet packet decomposition proposed in this paper is used to pick up the first arrival of the vibration wave.

#### 4. Sports Action Recognition and Analysis System Based on an Inertial Sensor

The intelligent sports action recognition system uses motion sensor (including acceleration sensor and angular velocity sensor) data for learning and judgment. Action sensors are susceptible to noise, especially shaking when the body is in motion. For the operation of sports recognition, recognition using angle sensor data is another path. The data from the angle sensor is easier to process and characterize. In addition, another way to improve sports recognition is by adding a filter model of the user's motion

state to the data processing model. Figure 8 shows an inertial sensor-based sports motion recognition technique. The sports action recognition technology directly performs gesture recognition based on the data in the data buffer. Through the additional process, the data in the buffer is first processed, the motion cycle data is extracted, and the motion data is modeled. Moreover, by means of signal subtraction or filtering, the interference of the motion state to gesture recognition can be reduced, and the recognition accuracy can be improved.

On the basis of the above analysis, the sports action recognition system based on inertial sensor proposed in this paper is verified, the sports action recognition effect is counted, combined with multiple sets of data for comparative analysis, and the statistical test results are shown in the following Table 1 and Figure 9.

From the above research, it can be seen that the sports action recognition system based on inertial sensor proposed in this paper has a good performance in sports action feature recognition.

## 5. Conclusion

Previous studies mostly used speed as a variable to analyze the impact of movement speed on the use of smart devices. However, the real situation is more detailed and specific. When a user moves in a certain motion state, his body shakes, and visual and cognitive resources are scattered. In particular, motion causes instability of the device screen, making the use of smartwatches difficult. Furthermore, they refine the study of specific gait conditions and the impact of specific phases of the stride on performance. In addition, in previous studies, the preferred walking speed was used as the setting to control the movement state. This method can quantitatively measure the movement state, but it is only applicable to the experimental environment on the treadmill. In this paper, the inertial sensor is used to construct a sports action recognition and analysis system, and an intelligent system is constructed. Through experimental research, it can be seen that the sports action recognition system based on inertial sensors proposed in this paper has a good performance in sports action feature recognition.

## Data Availability

The labeled dataset used to support the findings of this study is available from the corresponding authors upon request.

## Conflicts of Interest

The authors declare no competing interests.

## Acknowledgments

This study is sponsored by Northeastern University.

## References

- [1] A. Martínez-González, M. Villamizar, O. Canévet, and J. M. Odobez, "Efficient convolutional neural networks for depth-based multi-person pose estimation," *IEEE Transactions on Circuits and Systems for Video Technology*, vol. 30, no. 11, pp. 4207–4221, 2019.
- [2] M. Li, Z. Zhou, and X. Liu, "Multi-person pose estimation using bounding box constraint and LSTM," *IEEE Transactions on Multimedia*, vol. 21, no. 10, pp. 2653–2663, 2019.
- [3] J. Xu, K. Tasaka, and M. Yamaguchi, "Fast and accurate whole-body pose estimation in the wild and its applications," *ITE Transactions on Media Technology and Applications*, vol. 9, no. 1, pp. 63–70, 2021.
- [4] G. Szűcs and B. Tamás, "Body part extraction and pose estimation method in rowing videos," *Journal of Computing and Information Technology*, vol. 26, no. 1, pp. 29–43, 2018.
- [5] R. Gu, G. Wang, Z. Jiang, and J. N. Hwang, "Multi-person hierarchical 3d pose estimation in natural videos," *IEEE Transactions on Circuits and Systems for Video Technology*, vol. 30, no. 11, pp. 4245–4257, 2019.
- [6] M. Nasr, H. Ayman, N. Ebrahim, R. Osama, N. Mosaad, and A. Mounir, "Realtime multi-person 2D pose estimation," *International Journal of Advanced Networking and Applications*, vol. 11, no. 6, pp. 4501–4508, 2020.
- [7] N. T. Thành and P. T. Công, "An evaluation of pose estimation in video of traditional martial arts presentation," *Journal of Research and Development on Information and Communication Technology*, vol. 2019, no. 2, pp. 114–126, 2019.
- [8] I. Petrov, V. Shakhuro, and A. Konushin, "Deep probabilistic human pose estimation," *IET Computer Vision*, vol. 12, no. 5, pp. 578–585, 2018.
- [9] G. Hua, L. Li, and S. Liu, "Multipath affinity stacked—hour-glass networks for human pose estimation," *Frontiers of Computer Science*, vol. 14, no. 4, pp. 1–12, 2020.
- [10] K. Aso, D. H. Hwang, and H. Koike, "Portable 3D human pose estimation for human-human interaction using a chest-mounted fisheye camera," in *Augmented Humans Conference 2021*, pp. 116–120, Finland, Feb 2021.
- [11] D. Mehta, S. Sridhar, O. Sotnychenko et al., "Vnect: real-time 3d human pose estimation with a single rgb camera," *ACM Transactions on Graphics (TOG)*, vol. 36, no. 4, pp. 1–14, 2017.
- [12] S. Liu, Y. Li, and G. Hua, "Human pose estimation in video via structured space learning and halfway temporal evaluation," *IEEE Transactions on Circuits and Systems for Video Technology*, vol. 29, no. 7, pp. 2029–2038, 2019.
- [13] S. Ershadi-Nasab, E. Noury, S. Kasaei, and E. Sanaei, "Multiple human 3d pose estimation from multiview images," *Multimedia Tools and Applications*, vol. 77, no. 12, pp. 15573–15601, 2018.
- [14] X. Nie, J. Feng, J. Xing, S. Xiao, and S. Yan, "Hierarchical contextual refinement networks for human pose estimation," *IEEE Transactions on Image Processing*, vol. 28, no. 2, pp. 924–936, 2019.
- [15] Y. Nie, J. Lee, S. Yoon, and D. S. Park, "A multi-stage convolution machine with scaling and dilation for human pose estimation," *KSII Transactions on Internet and Information Systems (TIIS)*, vol. 13, no. 6, pp. 3182–3198, 2019.
- [16] A. Zarkeshev and C. Csiszár, "Rescue method based on V2X communication and human pose estimation," *Periodica Polytechnica Civil Engineering*, vol. 63, no. 4, pp. 1139–1146, 2015.
- [17] W. McNally, A. Wong, and J. McPhee, "Action recognition using deep convolutional neural networks and compressed spatio-temporal pose encodings," *Journal of Computational Vision and Imaging Systems*, vol. 4, no. 1, pp. 3–3, 2018.
- [18] R. G. Díaz, F. Laamarti, and A. El Saddik, "DTCoach: your digital twin coach on the edge during COVID-19 and beyond," *IEEE Instrumentation & Measurement Magazine*, vol. 24, no. 6, pp. 22–28, 2021.
- [19] A. Bakshi, D. Sheikh, Y. Ansari, C. Sharma, and H. Naik, "Pose estimate based yoga instructor," *International Journal of Recent Advances in Multidisciplinary Topics*, vol. 2, no. 2, pp. 70–73, 2021.
- [20] S. L. Colyer, M. Evans, D. P. Cosker, and A. I. Salo, "A review of the evolution of vision-based motion analysis and the integration of advanced computer vision methods towards developing a markerless system," *Sports Medicine-Open*, vol. 4, no. 1, pp. 1–15, 2018.
- [21] I. Sárándi, T. Linder, K. O. Arras, and B. Leibe, "Metrabs: metric-scale truncation-robust heatmaps for absolute 3d human pose estimation," *IEEE Transactions on Biometrics, Behavior, and Identity Science*, vol. 3, no. 1, pp. 16–30, 2021.

## Research Article

# Optimization and Application of Image Defogging Algorithm Based on Deep Learning Network

Jianfeng Liao 

*Department of Computer, Wenhua University, Wuhan, Hubei 430074, China*

Correspondence should be addressed to Jianfeng Liao; [jazz9812@163.com](mailto:jazz9812@163.com)

Received 25 February 2022; Revised 18 March 2022; Accepted 20 April 2022; Published 9 May 2022

Academic Editor: Wen Zeng

Copyright © 2022 Jianfeng Liao. This is an open access article distributed under the Creative Commons Attribution License, which permits unrestricted use, distribution, and reproduction in any medium, provided the original work is properly cited.

In the foggy environment, the images collected outdoors are prone to problems, such as low contrast and loss of details. In order to solve this problem, this paper proposes an algorithm based on multiscale parallel-depth separable convolutional neural network (MSP-DSCNN) to remove fog from foggy images and improve image quality. The multiscale feature extraction module extracts texture feature details from fog images at different scales and extracts high-dimensional and low-dimensional features from fog images by using parallel depth and shallow channels. In order to further optimize the network model, a split convolution method is proposed, which can split the feature graph into two categories, one is the main feature and the other is the secondary feature. The key information is extracted from the main features with high complexity, and the compensation information is extracted from the minor features with low complexity. Experiments show that compared with other algorithms, the model constructed in this paper has obvious advantages in defogging effect, natural color of restored images, good detail retention, and dominant indicators. It effectively solves the problems of incomplete haze, color offset, and poor visibility of detail maintenance in the current image.

## 1. Introduction

Intelligent equipment such as video surveillance plays an important role in the application of computer vision system. Because of the existence of fog and haze, the quality of images collected by imaging equipment is seriously degraded, and the target object cannot be well monitored, which brings great inconvenience to the visual system [1–3]. Therefore, image defogging has very important practical significance, research value, and practical value.

The visibility of fog image decreases evidently, due to the existence of fog. There are two main reasons to produce foggy images: first, the reflected light of the object is absorbed and scattered by suspended particles in the atmosphere, resulting in the attenuation of reflected light energy and the reduction of image brightness and contrast. Second, much of the ambient light, such as sunlight, is scattered by scattering materials in the atmosphere to form a bright background [4]. In various applications based on computer vision, input foggy images may lead to system performance degradation or even errors [5–8].

In recent years, image defogging has attracted extensive attention. Based on the atmospheric scattering model [9], many single-image defogging methods have been developed. The key idea shared by most methods is to adopt various image priors, such as dark channel priors [10] and color attenuation priors [11]. Literature [12] estimated the local aerial components of the image and then used the multiscale fusion method to restore the fog-free image. In reference [13], the transmission image is estimated by using per-pixel alpha mixing method by estimating the light source region and nonlight source region, respectively; thus, they are effectively mixed, since the distance between different things and the camera in foggy images has different transmission coefficients and the assumption of each close cluster in fog-free images. Literature [14] makes each cluster to become a line in RGB space in foggy images, and the algorithm can use these lines to recover depth maps and fog-free images. These methods are not ideal when dealing with foggy images under complex imaging conditions.

In order to improve the shortcomings of traditional algorithms, deep learn-based defogging methods develop rapidly

and become the mainstream direction of image defogging. The method uses convolutional neural network (CNN) to train the required features by constructing an end-to-end Network architecture.

Literature [15] built a Dehaze-Net defogging network based on deep CNN to train the transmittance, and recovered fog-free images with the help of atmospheric scattering model, which achieved good results, especially in the sky area. However, this network is constructed with a priori or assumption in traditional methods, which has certain limitations. The end-to-end gated fusion defogging network GFN proposed in literature [16] realizes the final defogging through a series of operations such as white balance, contrast enhancement, and gamma correction, but the network implementation process is quite complicated. AOD network proposed in literature [17] integrates transmittance and atmospheric light into a unified parameter  $K$ , training through the formula of deformed atmospheric scattering model, changes the previous methods of training atmospheric light and transmittance separately. However, due to the small number of network layers and limited accuracy, good defogging effect cannot always be achieved. Literature [18] proposed a feature attention network FFA-NET combining channel attention and pixel attention mechanism since different channel features contain completely different weighted information and fog concentration distribution on different image pixels is also different. Because this network only considers the difference between images with fog and images without fog, and does not start from the overall style of the image. Although it has a good effect on the composite image, there are still serious details on loss and incomplete removal of fog in the real scene. Literature [19] found through the statistics of different color channels of many foggy images that foggy areas are mainly concentrated in the brightness channel of Ycbr color space. Therefore, the atmospheric lighting priori is proposed and the AIPNet fog removal network is built. The image quality is improved to a certain extent, but there are still incomplete feature extraction and residual fog in some restored images.

Based on the above traditional methods and the shortcomings of existing networks, in this paper, an image defogging model based on multiscale parallel-deep split convolution neural network (MSP-DSCNN) is proposed. This model draws on the idea of multiscale information extraction [20] in target detection [21]. In the network training stage, convolution of different sizes is used to check the input image for convolution operation; then, the extracted features are fused. And then, the fused feature images are put into deep channel and shallow channel, respectively, for learning. In order to further optimize the network model, a split convolution operation is proposed, which divides the feature graph into two categories, namely, primary concern feature and secondary concern feature, simplifying the process of defogging and highlighting the importance of features.

In the study of fogging image removal, the main innovations of this paper are as follows.

- (1) The multiscale feature extraction module is used to extract image feature information from different scales

- (2) The parallel deep and shallow channels are proposed to extract high- and low-dimensional features from foggy images, respectively
- (3) A split convolution operation is proposed to further reduce the number of network parameters, accelerate the reasoning speed of the model, and improve the model's defogging accuracy

This paper consists of the following four main parts.

- (1) The first part is the introduction
- (2) The second part is the image defogging model
- (3) The third part is the experiment and analysis
- (4) The fourth part is the conclusion

Besides, there are also abstract and references.

## 2. Image Defogging Model

*2.1. Problem Description.* Assume that the foggy image is  $I$ , the fogged image is  $J$ , and the foggy noise image in the foggy image is  $Q$ . Equation (1) can be obtained as follows.

$$I = J + Q, \quad (1)$$

$$F(I) = J. \quad (2)$$

In the traditional convolutional neural network, the foggy image  $I$  is taken as the network input, and the mapping model formula (2) from  $I$  to  $J$  is directly learned by training the model. However, it is very difficult to train the model in such a direct way of learning network mapping, and the precision of defogging is not high. Therefore, this paper uses residual learning strategy to reduce the difficulty of network learning. The outputs and inputs of the network form a large residual unit.

The actual mapping that the network learns is shown in Formula (3), that is, the network learns the image  $Q$  of fog noise distribution in the image.

$$R(I) = I - J. \quad (3)$$

The residual learning method can transform the haze removal image mapping obtained by direct learning into the fog noise distribution in the haze image, which reduces the difficulty of network learning and improves the model's fog removal accuracy.

*2.2. Multiscale Feature Extraction Module.* In the convolutional neural network, the receptive field is the mapping region on the input image corresponding to the output image of each layer in the convolutional neural network. The larger the receptive field, the larger the area of input image to focus on. In the image input stage, three convolution kernels of different scales ( $1 \times 1$ ,  $3 \times 3$ , and  $5 \times 5$ ) were used for feature extraction. A large convolution check should have a larger receptive field, which can extract



features in a large range. Small convolution kernel can extract small range of detail features.

The feature fusion method of parallel superposition [22] is used to fuse all feature maps together as the input of depth channel, see Figure 1. ReLU layer is the activation function layer. The purpose is to improve the nonlinearity of the model, as shown in Equation (4).

$$\text{ReLU}(i) = \text{Max}(0, i). \quad (4)$$

In actual model training, a  $5 \times 5$  convolution kernel with a cavity step of 2 is used. The number of model parameters remained unchanged while expanding the receptive field.

**2.3. Deep and Shallow Channel Parallel Method.** This paper uses parallel depth and shallow channels to extract feature information of different dimensions from foggy images. The shallow channel is composed of 6 layers of neural network, which is mainly used to extract low-dimensional feature information.

The deep channel is composed of 16 layers neural network, which is used to extract high-dimensional feature information. The feature fusion method of parallel superposition is used to merge the depth and shallow channel information.

**2.4. Split Convolution Operation.** To further optimize the network model, a split convolution operation is proposed, as shown in Figure 2. Feature maps of the same layer proposed from the image often have similar results and feature redundancy. Therefore, in accordance with the principle of bisection, the feature graph of each layer is divided into two parts for independent convolution operation. Group convolution with a convolution kernel size of  $3 \times 3$  and group number of 2 was used to conduct group convolution operation on some feature graphs to obtain the main features of interest. Meanwhile, for the remaining feature graphs, point convolution operation with convolution kernel size of  $1 \times 1$  is used to obtain the features of secondary concern. Then, the global average pooling operation is carried out on the feature graph  $P_c$  by using Equation (5) to generate the initial weight value of each channel [23–25] and obtain  $S_1$  and  $S_2$ , respectively, where  $B$  and  $M$  represent the height and width of the feature map, respectively.

$$S_c = F(P_c) = \frac{1}{B \times M} \sum_{x=1}^B \sum_{y=1}^M P_c(x, y), c \in \{1, 2\}. \quad (5)$$

In order to dynamically adjust the weight of each channel, the generated  $S_1$  and  $S_2$  are stacked together and passed to the full connection layer. Then, *Softmax* function is used to regenerate the main and secondary attention features, and the weight  $\alpha$  and  $\beta$  of each channel, as shown in Equation (6).

$$\alpha = \frac{e^{S_1}}{e^{S_1} + e^{S_2}} \beta = 1 - \alpha. \quad (6)$$

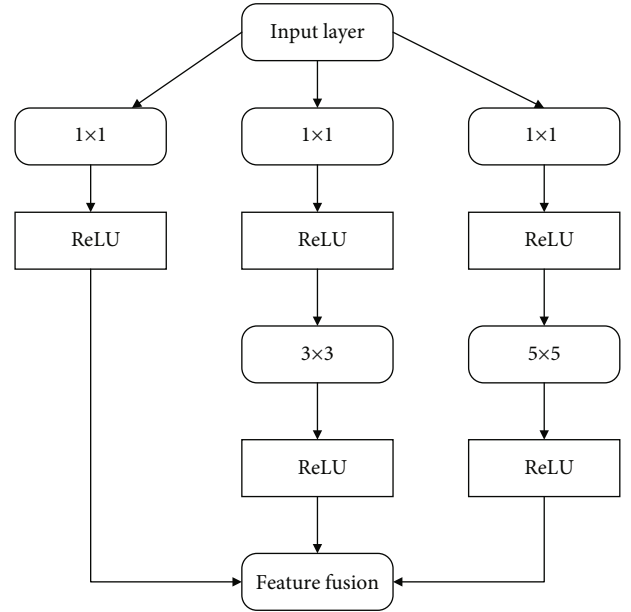


FIGURE 1: Multiscale feature extraction diagram.

The network output after deconvolution is shown in Equation (7).

$$J = \alpha \cdot P_1 + \beta \cdot P_2. \quad (7)$$

**2.5. Overall Structure of MSP-DSCNN Model.** As shown in Figure 3, the overall framework of model MSP-DSCNN consists of four parts. In the initial stage of the network, a multi-feature extraction module is used to extract the detail features of the foggy images at multiple scales by using convolution kernels of different sizes. The upper part of the model is *Sconv Block* module, where *Sconv* is separable convolution operation and *BN* is batch regularization. The shallow channel module consists of 6 layers of networks. Each separable convolution operation is followed by a *BN* and *ReLU*. The deep channel module consists of 16 layers of networks. In order to reduce the difficulty of network learning, residual network is first used to directly transfer the features of the first layer of separable convolution processing to the fifth, ninth, and thirteenth layers. Then, the feature fusion module of parallel superposition is used to merge the information extracted from depth channel. Finally, a layer of convolution operation is used to transform the feature graph into the output image of the first layer. In order to reduce the learning difficulty of the whole network, the whole network is composed of a large residual unit. The input and output form a subtraction operation. In this way, the network can directly learn the fog noise distribution in the fog image, instead of directly learning the clean image.

This paper uses mean square error as the loss function of the model, as shown in Equation (8), where  $R(I_x)$  represents the residual image block obtained from network learning and  $I_x - J_y$  represents the actual residual image block, that is, the label.

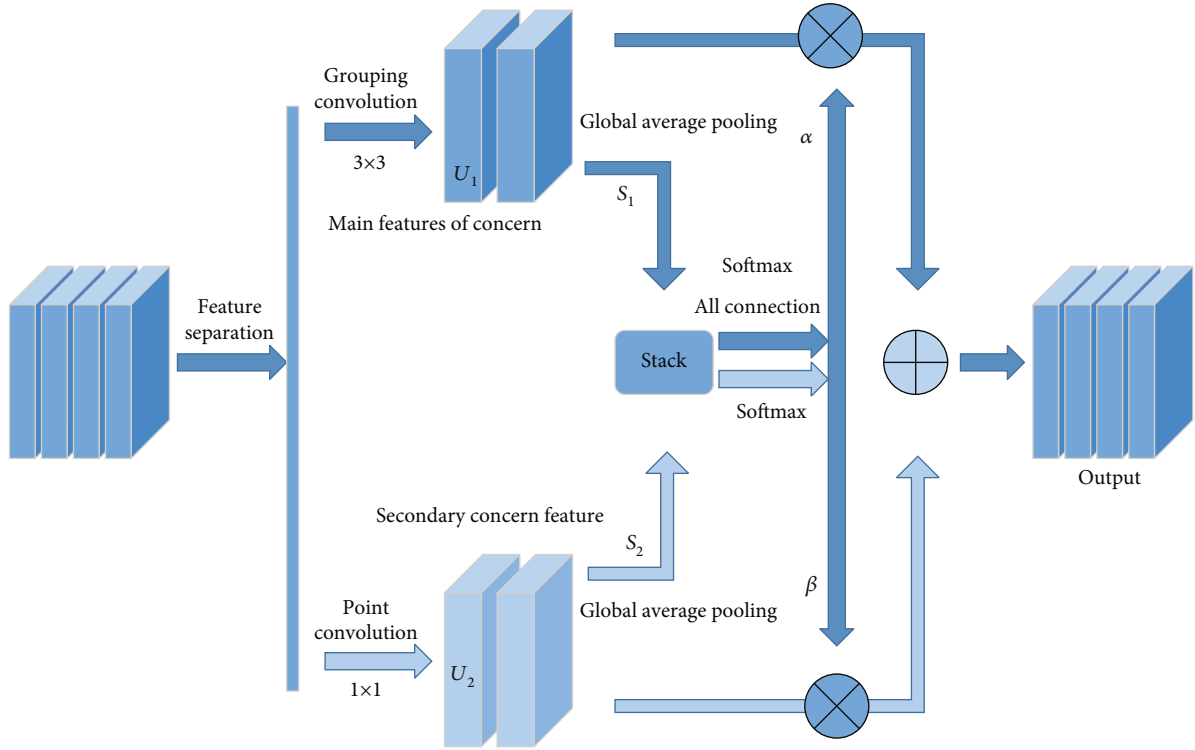


FIGURE 2: Split convolution operation.

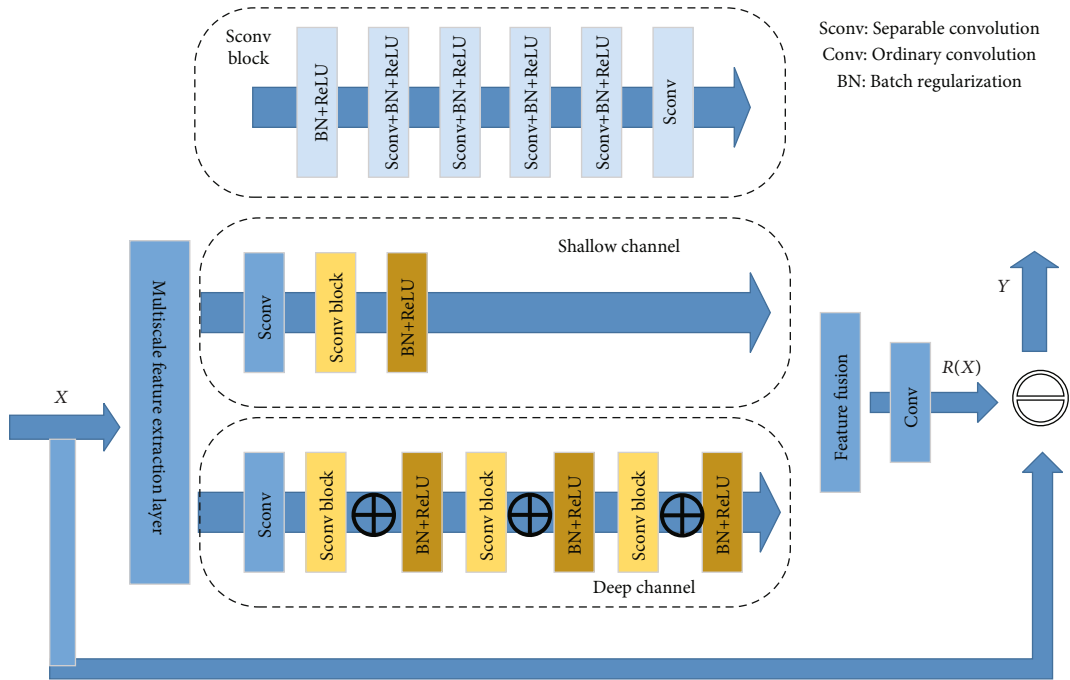


FIGURE 3: MSP-DSCNN model.

$$\text{Loss\_MSE} = \frac{1}{T} \sum_{x=1}^T \|R(I_x) - (I_x - J_x)\|_2^2. \quad (8)$$

The convolution kernel size and the number of output channels of each layer of model MSP-DSCNN are shown

in Table 1. The first layer is the multifeature extraction layer, which consists of 48  $1 \times 1$  convolutional kernels, 64  $3 \times 3$  convolutional kernels, and 32  $5 \times 5$  (cavity step 2) convolutional kernels. In depth channel, separable convolution operation is used first. The main feature is 2, 38 convolution operations with a size of  $3 \times 3$ . Secondary features 26

convolution kernels of  $1 \times 1$  size are used for feature completion operation. Then, 64 feature layers of each depth channel are superimposed together in parallel. After the convolution layer of the last layer 1 output channel, the residual image block is obtained.

### 3. Experiment and Analysis

In order to verify the effectiveness and rationality of the proposed network, quantitative evaluation of its defogging effect on synthetic images and real images is made in this paper, and the results are more convincing by comparing with the current advanced algorithms from two aspects of visual effect and objective data.

*3.1. Experimental Settings and Data Sets.* The network implementation in this paper is based on Pytorch framework. Use M2000GPU in Ubuntu environment to train defogging network. Set the initial learning rate to experience value 0.0001 and batch size to 32. The momentum decay exponents of Adam optimizer are, respectively,  $\beta_1 = 0.899$  and  $\beta_2 = 0.999$ . The number of iterations is 40, and the training time for one iteration is 32 minutes. Finally, the size of the trained network model is 1608 KB.

The training network of RESIDE (Realistic Single Image Dehazing) [26] is used in this paper. RE-SIDE Images are selected from NYU2 [27] depth data set. By randomly selecting atmospheric light  $A$  ( $A \in (0.8, 1.0)$ ) and scattering coefficient  $\beta$  ( $\beta \in (0.5, 1.5)$ ), different foggy images are synthesized. It includes Indoor Training Set (ITS), Outdoor Training Set (OTS), and Synthetic Objective Testing Set (SOTS), the ITS data set in RESIDE as the training set and SOTS as the test set. The training set (ITS) includes 1399 clear images and 13990 foggy images with different fog concentrations. The test set SOTS includes 500 indoor foggy images and 500 outdoor foggy images. In addition, in order to better verify the effectiveness and practicability of the proposed network, fog images with rich colors in the real environment are selected for testing.

In terms of quantitative evaluation of network performance, this paper selects some representative algorithms in the field of defogging for comparison, including traditional algorithm [28] based on physical model and algorithm [29] based on literature. Literature [28] algorithm, and literature [30] algorithm based on deep learning.

#### 3.2. Quantitative Evaluation of Synthetic Image Data Sets

*3.2.1. Subjective Evaluation.* The network was evaluated from both subjective and objective aspects on the synthetic image data set SOTS, and one indoor image and one outdoor image were randomly selected for effect evaluation. The defogging effect of each algorithm is shown in Figures 4 and 5. The image obtained by the method in reference [28] is completely defogged, but the overall image is darker than the renderings of other algorithms, and the sky region is seriously distorted due to the limitations of dark channels, as shown in Figure 5. In addition, the estimation of transmittance at the edge mutation is inaccurate, leading to the occurrence of halo and block effect at the edge of the

TABLE 1: Network structure parameters of model MSP-DSCNN.

Convolution layer	Convolution kernel	Output channel
Level 1	$1 \times 1, 3 \times 3, 5 \times 5$	48, 64, 32
Shallow channel	Grouping convolution: $3 \times 3$	38
2~5 layers	Point convolution: $1 \times 1$	26
Deep channel	Grouping convolution: $3 \times 3$	38
Layer 2~13	Point convolution: $1 \times 1$	26
Feature fusion layer	None	$64 \times 2$
The 15th floor	$3 \times 3$	1

restored image. As shown in Figure 5, there is halation around the roof. The image obtained by the method of literature [29] has natural color, especially the sky area, but there are problems of incomplete defogging and serious loss of details. In Figure 4, there is obvious residual fog in the background wall area. And in Figure 5, the details of the lawn are blurred. Compared with the algorithm in reference [28], the algorithm in reference [28] has improved color bias in sky region, but some images have problems of incomplete defogging and color oversaturation. The fourth image in Figure 4 and the fog removal effect in Figure 5 are poor. The image obtained by the method in reference [30] has good color fidelity and thorough defogging. However, due to the shallow network structure, the feature extraction is not very rich, and the detail recovery of the remote area is poor, as shown in Figure 5. For the fog-free image obtained by the algorithm in literature [28], the indoor image has a good defogging effect and the restored image has a natural color, while the outdoor image is not completely defogged, but the sky area has a natural color and no obvious color deviation, as shown in Figure 4. Comparing with the previous classical algorithms, the algorithm presented in this paper has a significant effect on defogging, with good details and no obvious distortion, color deviation, and other problems. The color of defogging images is natural and has good performance in both indoor and outdoor images.

*3.2.2. Objective Evaluation.* Objective evaluation indexes adopt Structural Similarity Index Measurement (SSIM) and Peak Signal to Noise Ratio (PSNR), which are uniformly used in deep learning. Among them, the structural similarity SSIM is used to measure the similarity degree of two images, and the value range is [0,1]. The peak signal to noise ratio (PSNR) is used to represent the ratio of useful signal to noise in an image, and the larger the better. The corresponding mathematical expressions of the two indicators are shown in Formula (9) and Formula (10), respectively.

$$\text{SSIM}(x, y) = \frac{(2\mu_x\mu_y + c_0)(\sigma_{xy} + c_1)}{(\mu_x^2 + \mu_y^2 + c_0)(\sigma_x^2 + \sigma_y^2 + c_1)}, \quad (9)$$



FIGURE 4: Comparison of fogging effect of various algorithms in indoor synthetic hazy image.

where  $\mu_x$  and  $\mu_y$  are the mean values of images  $x$  and  $y$ ,  $\sigma_x$  and  $\sigma_y$  are the standard deviations of the two images,  $\sigma_{xy}$  is the covariance of the two images, and  $c_0$  and  $c_1$  are constants.

$$\text{PSNR} = 101a \frac{\text{MAX}^2}{\text{MSE}}, \quad (10)$$

where MSE is the minimum mean square error of the image after defogging and the clear image and MAX is generally 255. Objective indicators on SOTS are shown in Table 2 (data are mean values). The pictures obtained by the network processing proposed in this paper. SSIM index is ahead of other algorithms, PSNR index is better than most algorithms, and good results are obtained. The validity of the proposed network is verified.

### 3.3. Quantitative Evaluation of Real Image Data Sets

**3.3.1. Subjective Evaluation.** In order to further confirm the practical value of the proposed network, this paper conducts an experimental evaluation on its effect images in real

scenes, and the defogging effect of each algorithm is shown in Figure 6. You can see that the algorithm in literature [28] has a good defogging effect on images with rich close-range, but due to the misestimation of transmittance caused using the minimum filter, the recovered image is prone to halo at the edge, and the inaccurate estimation of atmospheric light leads to serious distortion of the defogging image in the distant area with the sky. Compared with other algorithms, both the algorithm in literature [29] and the algorithm in literature [28] have problems such as incomplete defogging and serious detail loss. The algorithm in literature [30] has a remarkable effect of defogging, especially in the sky area, where the color is restored to nature. However, the degree of defogging in some images is too large, resulting in the loss of some pixels and darkening of images. Compared with other algorithms, the effect picture of the algorithm in this paper is completely defogged, the details are maintained well, and the scene is clear and natural.

**3.3.2. Objective Evaluation.** Objective evaluation adopts the unreferenced image quality evaluation method often used

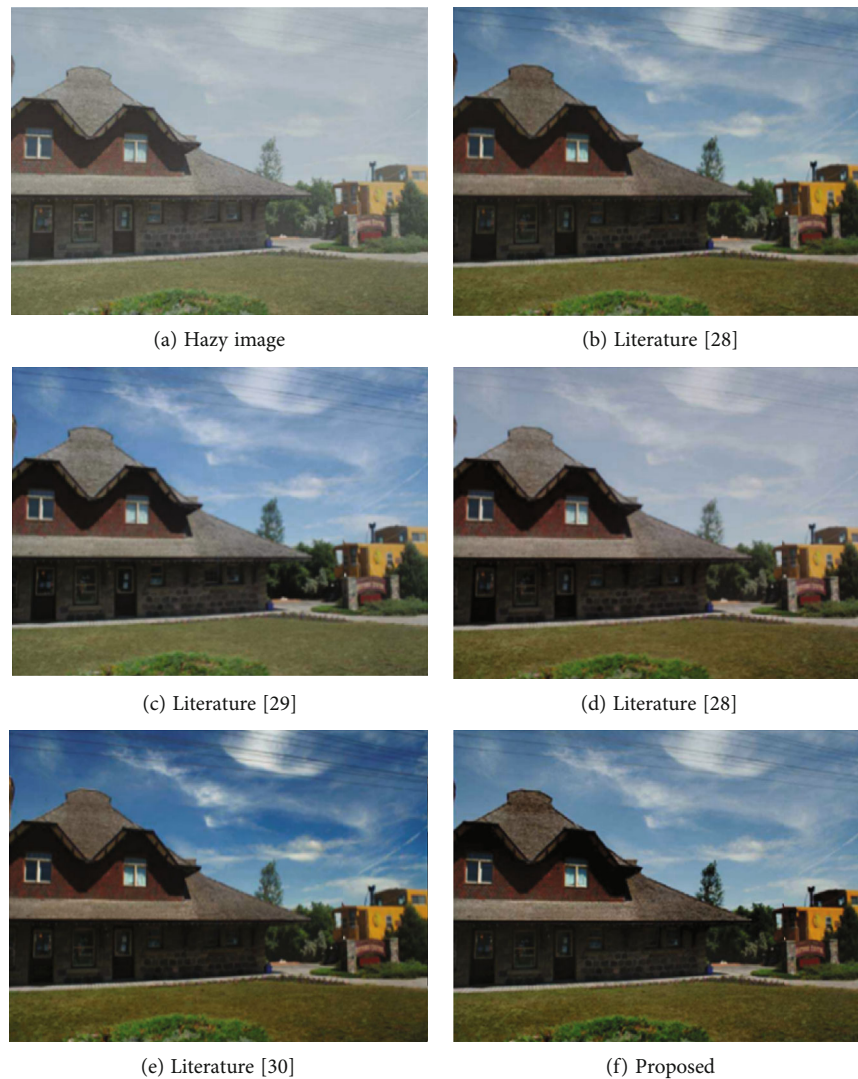


FIGURE 5: Comparison of restoration effects of various algorithms in outdoor synthetic hazy image.

TABLE 2: SOTS data set evaluation indicators.

Items		Literature [28]	Literature [29]	Literature [28]	Literature [30]	Proposed
Indoor	SSIM	0.804	0.817	0.796	0.821	0.898
	PSNR	16.887	26.331	24.647	24.269	26.967
Outdoor	SSIM	0.791	0.840	0.796	0.859	0.954
	PSNR	16.175	22.302	19.429	20.208	26.863

in the field of real scene defogging [31], whose evaluation indexes include the number of saturated pixels  $m$ , the number of visible edge sets  $E$ , the average gradient  $R$ , and the running time  $T$  (unit is second). The smaller the number of saturated pixels and the running time, the better the performance of the algorithm. The larger the value of visible edge set  $e$  and mean gradient  $R$ , the better the algorithm is.

Each index in each algorithm is shown in Table 3 (the data in the table is the mean value).

As it can be seen from Table 3, the network proposed in this paper performs well in the number of saturated pixels and the running time, and has a leading advantage in the number of visible edge sets and the mean gradient. Comparing with other algorithms, the proposed network improves the number of visible edge sets by 20.6% and the average gradient by 20.9%.

**3.4. Ablation Experiment.** In order to further verify the contribution of the proposed modules to the result of fog



FIGURE 6: Comparison of fog removal effects of various algorithms in real scenes.

TABLE 3: Evaluation indicators of real scenes.

Items	Literature [28]	Literature [29]	Literature [28]	Literature [30]	Proposed
$m$	0.0008	0.03	0.0189	0.0022	0.001
$e$	5.5273	6.8498	5.9726	6.4361	7.4745
$r$	1.259	1.3359	1.394	1.6454	1.6989
$t/s$	1.6562	2.843	2.1151	1.0774	1.1270

removal, an image in the SOTS data set was randomly selected for the ablation experiment as follows.

It mainly includes the following steps.

- (1) Only the features (LF) in a wide range of foggy images are extracted to reconstruct the original image
- (2) Only a small range of detail features (DF) of foggy images are extracted to reconstruct the original image
- (3) Large range of features and small range of detail features work together

It can be seen from the comparison diagram in Figure 7.

The large range feature image only retains some global features and loses a lot of details. The detail information of small range detail feature image increases obviously, but there are problems of incomplete defogging and color deviation. In contrast, the image under the joint action of the two features not only retains the color of the original image but also has obvious details, and which is more thoroughly defogged. Each image index is shown in Table 4.

As it can be seen from Table 4, the SSIM and PSNR of the image obtained under the combined action of the two features were significantly improved.

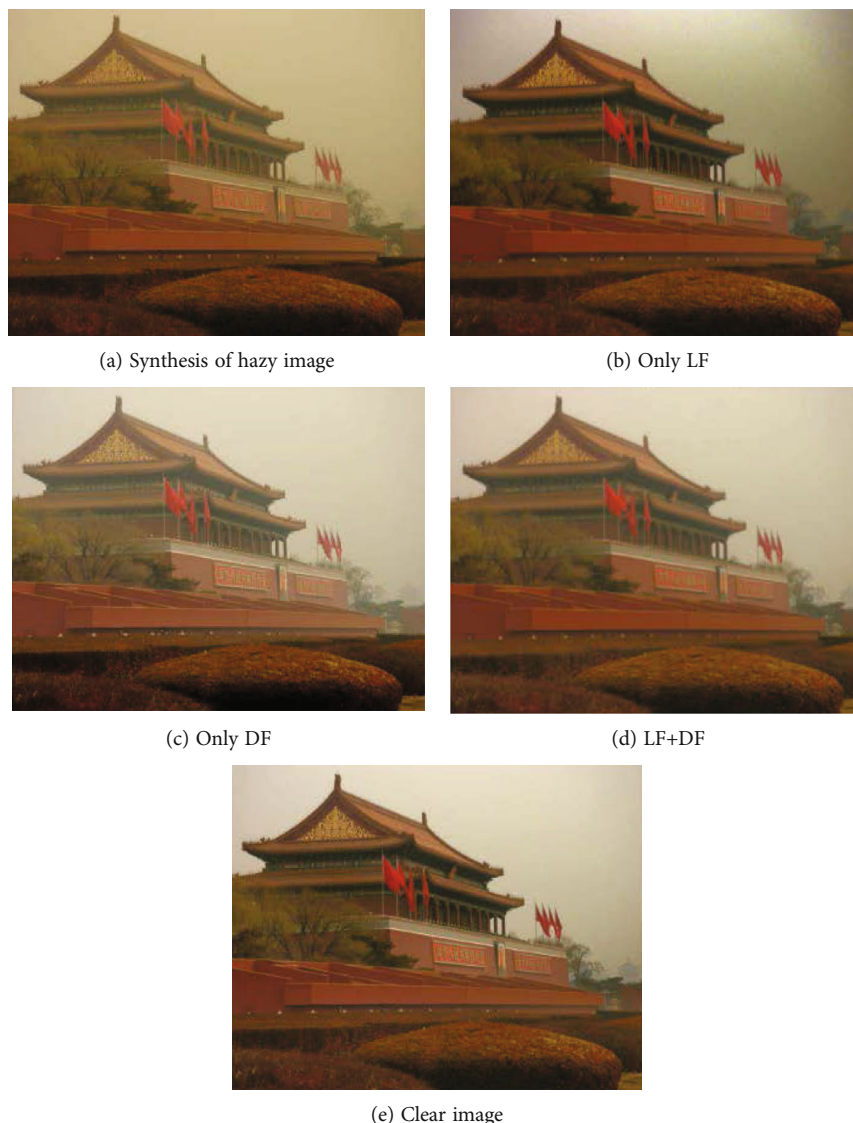


FIGURE 7: Comparison of ablation results.

TABLE 4: Comparison of evaluation indexes in SOTS data set.

Items	Only LF	Only DF	LF+DF
SSIM	0.8028	0.8735	0.9574
PSNR	16.9104	17.9054	24.7789

#### 4. Conclusion

In order to keep details as much as possible while defogging the image, a multiscale parallel-depth separable convolutional neural network (MSP-DSCNN) was designed in this paper. By comparing the experimental results, compared with other comparison algorithms, model MSP-DSCNN has better performance in both subjective visual effect and objective evaluation indicators. At the same time, the network ablation experiment proves that the proposed multiscale feature extraction module and the parallel strategy of

shallow and deep channels have a good effect of haze removal and high image fidelity. Comparing with other algorithms, the algorithm has distinct advantages and effectively solves the problems such as incomplete defogging of the current image, poor color offset, detail retention, and reduced visibility. The accuracy and accuracy of fog removal have also been further improved. The split convolution operation further reduces the number of parameters in the network model, improves the feature redundancy of traditional convolutional neural network, and accelerates the training and convergence speed of the network. The overall experiment shows that the model MSP-DSCNN can finish the image defogging task faster and better. However, since the restoration module of the network essentially relies on the atmospheric scattering model, some restored images still have shortcomings in detail preservation and color fidelity of sky area. Therefore, improving the accuracy of the defogging model will be the focus of further research in the future.

## Data Availability

The labeled data set used to support the findings of this study is available from the corresponding author upon request.

## Conflicts of Interest

The author declares no competing interests.

## Acknowledgments

This work is supported by the Wenhua University.

## References

- [1] J. Liu, Q. Gao, Z. Tang et al., "Online monitoring of flotation froth bubble-size distributions via multiscale deblurring and multistage jumping feature-fused full convolutional networks," *IEEE Transactions on Instrumentation and Measurement*, vol. 69, no. 12, pp. 9618–9633, 2020.
- [2] Z. H. Arif, M. A. Mahmoud, K. H. Abdulkareem et al., "Comprehensive review of machine learning (ML) in image defogging: taxonomy of concepts, scenes, feature extraction, and classification techniques," *IET Image Processing*, vol. 16, no. 2, pp. 289–310, 2022.
- [3] P. Martinez, M. Al-Hussein, and R. Ahmad, "A scientometric analysis and critical review of computer vision applications for construction," *Automation in Construction*, vol. 107, p. 102947, 2019.
- [4] W. Lou, Y. Li, G. Yang, C. Chen, H. Yang, and T. Yu, "Integrating haze density features for fast nighttime image dehazing," *IEEE Access*, vol. 8, pp. 113318–113330, 2020.
- [5] Q. K. Tran and S. Song, "Computer vision in precipitation nowcasting: applying image quality assessment metrics for training deep neural networks," *Atmosphere*, vol. 10, no. 5, p. 244, 2019.
- [6] Y. Pei, Y. Huang, Q. Zou, X. Zhang, and S. Wang, "Effects of image degradation and degradation removal to cnn-based image classification," *IEEE Transactions on Pattern Analysis and Machine Intelligence*, vol. 43, no. 4, pp. 1239–1253, 2019.
- [7] S. Zhang, F. He, W. Ren, and J. Yao, "Joint learning of image detail and transmission map for single image dehazing," *The Visual Computer*, vol. 36, no. 2, pp. 305–316, 2020.
- [8] D. Chen, M. He, Q. Fan et al., "Gated context aggregation network for image dehazing and deraining," in *2019 IEEE winter conference on applications of computer vision*, pp. 1375–1383, Waikoloa, HI, USA, Jan. 2019.
- [9] S. He, Z. Chen, F. Wang, and M. Wang, "Integrated image defogging network based on improved atmospheric scattering model and attention feature fusion," *Earth Science Informatics*, vol. 14, no. 4, pp. 2037–2048, 2021.
- [10] T. Dong, G. Zhao, J. Wu, Y. Ye, and Y. Shen, "Efficient traffic video dehazing using adaptive dark channel prior and spatial-temporal correlations," *Sensors*, vol. 19, no. 7, p. 1593, 2019.
- [11] S. Kuanar, D. Mahapatra, M. Bilas, and K. R. Rao, "Multi-path dilated convolution network for haze and glow removal in nighttime images," *The Visual Computer*, vol. 38, no. 3, pp. 1121–1134, 2021.
- [12] X. Liu, C. Liu, H. Lan, and L. Xie, "Dehaze enhancement algorithm based on retinex theory for aerial images combined with dark channel," *Open Access Library Journal*, vol. 7, no. 4, pp. 1–12, 2020.
- [13] M. N. Mat Nor, I. D. Rupenthal, C. R. Green, and M. L. Acosta, "Differential action of connexin hemichannel and pannexin channel therapeutics for potential treatment of retinal diseases," *International Journal of Molecular Sciences*, vol. 22, no. 4, p. 1755, 2021.
- [14] M. Ju, C. Ding, C. A. Guo, W. Ren, and D. Tao, "IDRLP: image dehazing using region line prior," *IEEE Transactions on Image Processing*, vol. 30, pp. 9043–9057, 2021.
- [15] J. Du, J. Zhang, Z. Zhang, W. Tan, S. Song, and H. Zhou, "RCA-NET: image recovery network with channel attention group for image dehazing," in *International Conference on Smart Multimedia*, pp. 330–337, Springer, Cham, 2020.
- [16] Y. Liu, H. Al-Shehari, and J. Min, "Improved multi-feature fusion approach based on end-to-end convolutional neural network for dehazing," in *IEEE International Conference on Software Engineering and Artificial Intelligence*, pp. 75–81, Xiamen, China, June 2021.
- [17] L. She, H. K. Zhang, Z. Li, G. de Leeuw, and B. Huang, "Himawari-8 aerosol optical depth (AOD) retrieval using a deep neural network trained using AERONET observations," *Remote Sensing*, vol. 12, no. 24, p. 4125, 2020.
- [18] X. Qin, Z. Wang, Y. Bai, X. Xie, and H. Jia, "FFA-Net: feature fusion attention network for single image dehazing," *Proceedings of the AAAI Conference on Artificial Intelligence*, vol. 34, no. 7, pp. 11908–11915, 2020.
- [19] S. Bianco, L. Celona, F. Piccoli, and R. Schettini, "High-resolution single image dehazing using encoder-decoder architecture," in *Proceedings of the IEEE/CVF Conference on Computer Vision and Pattern Recognition Workshops*, Long Beach, USA, 2019.
- [20] Y. Li, S. Meng, and D. Liang, "Multi-scale information extraction residual network for 3D point clouds classification," in *Chinese Automation Congress*, pp. 636–640, Shanghai, China, Nov. 2020.
- [21] M. Ju, H. Luo, Z. Wang, Hui, and Chang, "The application of improved YOLO V3 in multi-scale target detection," *Applied Sciences*, vol. 9, no. 18, p. 3775, 2019.
- [22] R. Yang, Y. Wang, Y. Xu, L. Qiu, and Q. Li, "Pedestrian detection under parallel feature fusion based on Choquet integral," *Symmetry*, vol. 13, no. 2, p. 250, 2021.
- [23] S. Zhang, W. Huang, and C. Zhang, "Three-channel convolutional neural networks for vegetable leaf disease recognition," *Cognitive Systems Research*, vol. 53, pp. 31–41, 2019.
- [24] K. Chitsaz, M. Hajabdollahi, N. Karimi, S. Samavi, and S. Shirani, "Acceleration of convolutional neural network using FFT-based split convolutions," vol. 12621, 2020 <http://arxiv.org/abs/2003.12621>.
- [25] C. Yuan, Y. Wu, X. Qin et al., "An effective image classification method for shallow densely connected convolution networks through squeezing and splitting techniques," *Applied Intelligence*, vol. 49, no. 10, pp. 3570–3586, 2019.
- [26] Y. Qu, Y. Chen, J. Huang, and Y. Xie, "Enhanced pix 2pix dehazing network," in *Proceedings of the IEEE/CVF Conference on Computer Vision and Pattern Recognition*, pp. 8160–8168, Long Beach, USA, 2019.
- [27] J. J. J. Condon, L. Oakden-Rayner, K. A. Hall et al., *Replication of an open-access deep learning system for screening mammography: Reduced performance mitigated by retraining on local data*, medRxiv, 2021.



- [28] W. Liang, J. Long, K. C. Li, J. Xu, N. Ma, and X. Lei, "A fast defogging image recognition algorithm based on bilateral hybrid filtering," *ACM Transactions on Multimedia Computing, Communications, And Applications*, vol. 17, no. 2, pp. 1–16, 2021.
- [29] N. Hassan, S. Ullah, N. Bhatti, H. Mahmood, and M. Zia, "A cascaded approach for image defogging based on physical and enhancement models," *Signal, Image and Video Processing*, vol. 14, no. 5, pp. 867–875, 2020.
- [30] R. Q. Ma, X. R. Shen, and S. J. Zhang, "Single image defogging algorithm based on conditional generative adversarial network," *Mathematical Problems in Engineering*, vol. 2020, 8 pages, 2020.
- [31] K. Hu, Y. Zhang, F. Lu, Z. Deng, and Y. Liu, "An underwater image enhancement algorithm based on MSR parameter optimization," *Journal of Marine Science and Engineering*, vol. 8, no. 10, p. 741, 2020.

## *Retraction*

# **Retracted: An Innovation and Entrepreneurship Management System for Universities Based on Cluster Analysis Theory**

### **Journal of Sensors**

Received 8 August 2023; Accepted 8 August 2023; Published 9 August 2023

Copyright © 2023 Journal of Sensors. This is an open access article distributed under the Creative Commons Attribution License, which permits unrestricted use, distribution, and reproduction in any medium, provided the original work is properly cited.

This article has been retracted by Hindawi following an investigation undertaken by the publisher [1]. This investigation has uncovered evidence of one or more of the following indicators of systematic manipulation of the publication process:

- (1) Discrepancies in scope
- (2) Discrepancies in the description of the research reported
- (3) Discrepancies between the availability of data and the research described
- (4) Inappropriate citations
- (5) Incoherent, meaningless and/or irrelevant content included in the article
- (6) Peer-review manipulation

The presence of these indicators undermines our confidence in the integrity of the article's content and we cannot, therefore, vouch for its reliability. Please note that this notice is intended solely to alert readers that the content of this article is unreliable. We have not investigated whether authors were aware of or involved in the systematic manipulation of the publication process.

Wiley and Hindawi regrets that the usual quality checks did not identify these issues before publication and have since put additional measures in place to safeguard research integrity.

We wish to credit our own Research Integrity and Research Publishing teams and anonymous and named external researchers and research integrity experts for contributing to this investigation.

The corresponding author, as the representative of all authors, has been given the opportunity to register their agreement or disagreement to this retraction. We have kept a record of any response received.

### **References**

- [1] W. Zhao and L. Fang, "An Innovation and Entrepreneurship Management System for Universities Based on Cluster Analysis Theory," *Journal of Sensors*, vol. 2022, Article ID 4865716, 10 pages, 2022.

## Research Article

# An Innovation and Entrepreneurship Management System for Universities Based on Cluster Analysis Theory

Weijie Zhao  and Liang Fang

*College of Innovation and Entrepreneurship, Pingdingshan University, Pingdingshan 467000, China*

Correspondence should be addressed to Weijie Zhao; 2135@pdsu.edu.cn

Received 26 February 2022; Revised 31 March 2022; Accepted 4 April 2022; Published 9 May 2022

Academic Editor: Wen Zeng

Copyright © 2022 Weijie Zhao and Liang Fang. This is an open access article distributed under the Creative Commons Attribution License, which permits unrestricted use, distribution, and reproduction in any medium, provided the original work is properly cited.

With the development of the market economy and changes in the demand for talents in the market, the cultivation of innovation and entrepreneurship (IAE) among university students has been emphasized, and how to improve the quality of IAE education and promote the overall development of university students has become a key concern of university teachers. Therefore, the design and implementation of the IAE project management system should be explored in the study, starting from the IAE education of university students. The thesis addresses the current situation and characteristics of IAE development of university students and develops a WEB system applicable to the project management of IAE for university students at this stage. Cluster analysis is a mathematical statistical method for grouping and categorising similar data. The design of a classification system based on university innovation and entrepreneurship data proposes a new definition of outlier index for outliers detected in real time, combined with the concept of  $CBLOF(t)$ . On this basis, the system also implements the monitoring function for abnormal data, thus serving as system optimisation and fault warning. The system implements the main functions such as login, registration, project release, project declaration, and management.

## 1. Introduction

To date, the majority of universities do not have a system for the declaration and management of innovative projects [1] for the students, and the declaration of projects mainly relies on manual registration and approval by special personnel, which is inefficient and not easy to manage. Therefore, it is urgent to develop an efficient and stable project declaration system [2]. The development of an innovative project declaration system will gradually move from the original single and simple to diversified and intelligent. The future innovation project declaration system for university students will be an efficient and stable information management system built on the basis of the Internet and supported by a database [3].

An analysis of the IAE project practice reveals that it plays a key role in cultivating the innovation, entrepreneurship, and practical ability of university students [4] and that after China proposed to implement IAE education for university students in the field of higher education, many

schools have made corresponding practical exploration in this regard [5], creating idealized conditions for the cultivation of IAE ability of university students. However, it must be clearly noted that in order to give play to the important role of innovative and entrepreneurial educational practices of students [6], universities must promote the improvement of the technical level of educational practices with the help of scientific management. It is therefore essential to analyse the project management aspects of student IAE to ensure that scientific management can free student managers from the tedium of management, improve management efficiency and level, and strive to provide diversified services to the student community [7–9].

The IAE management system can create certain convenience for the management, and the analysis of the management system shows that the IAE project management platform system for students is mainly an information management system for university students to participate in IAE projects [10]. The system is designed with B/S architecture and MVC model, which can provide support for students

to participate in IAE project management and implement information audit and management of relevant information, which has strong practical significance for the management of university students' IAE projects at present [11]. Therefore, it is necessary to strengthen the exploration of the management platform system in view of the basic situation of the management of the IAE projects of college students in China, so as to the platform system and promote the stable development of the IAE practice activities of college students.

The focus of university students' IAE project management is to analyse the current problems on the basis of a comprehensive understanding of the project management characteristics and then to clarify the problems that exist in it. The work is then combined with different business requirements to complete UML modelling and determine scientific and reasonable measures for authority control [12]. In general, the comprehensive promotion of university students' IAE project management can enhance the adaptability of university students to society, cultivate their entrepreneurial ability, and cultivate high-level entrepreneurial development talents for the country [13].

A systematic study of the construction of the IAE system for students reveals that the B/S architecture is introduced in the design and planning of the system, which can meet the needs of project management and promote the realization of diversified functions of the system [14]. With the support of the system, assessment experts and relevant instructors can have a comprehensive grasp of the project's operation and provide effective guidance, as well as facilitate students' access to their own IAE practices [15]. In planning the management platform system, it is necessary to promote the convenience of operation, but also to have the stability of functions, to ensure the accuracy and safety of data, so in the design and planning of the system, it must be analysed from multiple perspectives, to improve the management system, to develop the information backup and statistical analysis functions with the support of modern tools, and to ensure that it can be combined with the participation of students in IAE. The system should be designed and planned from multiple perspectives, and the management system should be improved [16], and the information backup and statistical analysis functions should be developed with the support of modern tools, so as to ensure the effective education and management of university students in the context of their participation in IAE education, to provide a corresponding platform for university students to participate in IAE education and practice, and to ensure that the basic work can be done well and the comprehensive development of university students' IAE education can be improved. In this way, reform and innovation of IAE education for university students can be carried out [17], and the comprehensive work level will be improved comprehensively, which will play a good role in promoting the implementation of IAE education for university students. Based on the theory of cluster analysis, this paper adopts the weighted K-means algorithm based on Euclidean distance, establishes a clustering model by analyzing a large amount of normal historical data, and then, according to the actual operation, succes-

sively proposes the definition of the outlier index of parameter points within the cluster and the definition of the outlier index of abnormal parameter points outside the cluster and proposes a university innovation and entrepreneurship project management system based on this model.

## 2. Analysis of Basic System Requirements

According to the characteristics of the management of entrepreneurship for the Department of Innovation [18, 19], there are four roles involved in the system. The main functions are shown in Figure 1.

The system adopts an object-oriented approach [20], abandoning the traditional approach the development, instead of making full use database design tables based on the Java code corresponding to the entities written and the mapping files of the entity objects. This approach reduces the need to write cumbersome SQL statements to build the tables directly. The use of reverse engineering to generate the corresponding database tables from the entity objects' Javabeans and their corresponding mapping files (xml files) [21] reduces data redundancy.

The supervisor provides guidance to the student leader and analyses the student leader's project in the context of the actual situation and provides appropriate guidance. In general, the supervisor has the function of reviewing the project declaration, the midterm check, and the closing of the project. The EMS is based on the real needs of the development and management of student IAE projects. The system is used to ensure that students and teachers are involved in the process of each project, to guarantee the effective implementation of student entrepreneurship projects, to give full play to the important role of student IAE projects, and to promote the overall improvement of the quality of personnel training.

*2.1. Entity Object Design.* Based on a comprehensive analysis of the entity objects required by the system and their relationships, eight entity objects were identified, these are the administrator entity, the project application entity, the project applicant entity, the project reviewer entity, the new project entity, the old project entity, the project issuer entity, and the project executor entity.

In the proposed management system, there are 26 database tables, for the project declaration, and project evaluation modules are the core of the system, and there is a close relationship between project declaration and project evaluation. In the study, a variety of different database tables are discussed, and in this study, the identity information table and the project information table are selected for specific analysis. The administrator is able to keep up-to-date information about the student innovation and entrepreneurship projects in the management system. In general, their main job responsibility is to follow the realistic needs of student entrepreneurship, the output of the declaration plan and the evaluation plan, the information on the projects, etc., on the platform, thus ensuring that a scientific evaluation plan is developed. It is the focus centre of the whole system and can exchange information on the front page module

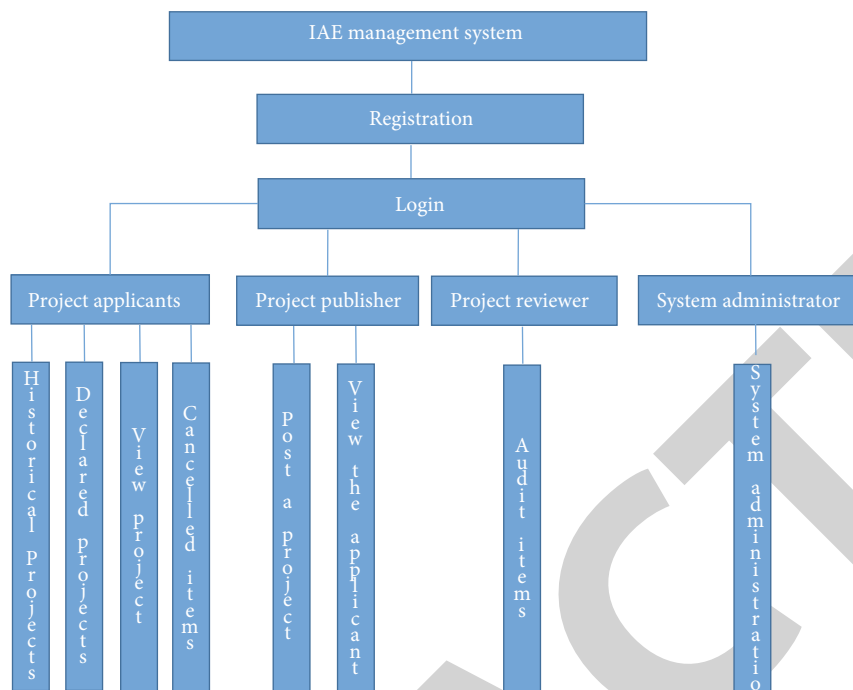


FIGURE 1: Functional diagram of system roles.

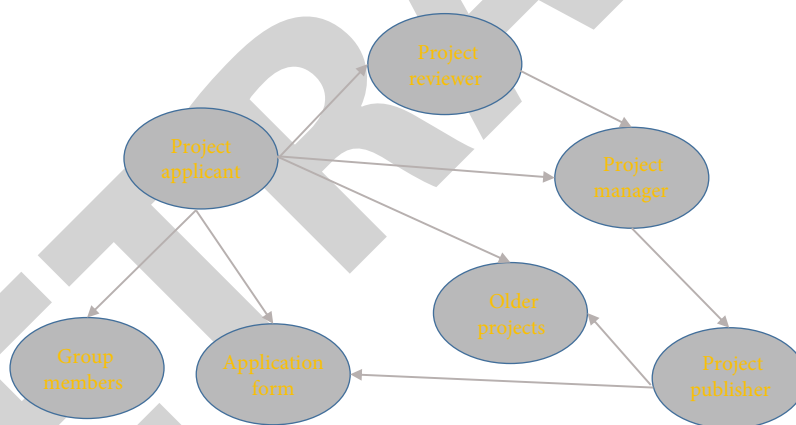


FIGURE 2: Interentity correlations.

[22]. The relationship between the various entities is shown in Figure 2.

### 3. Cluster Analysis Theory

The so-called cluster analysis algorithm works on the principle that for all vectors in an  $m$ -dimensional space  $R$ , the algorithm clusters each vector and achieves a category of vectors by minimising the distance between each vector and the centre of the cluster [23, 24]. That is, the greater the intraclass correlation, the better, and the smaller the interclass correlation, the better. As an unguided learning problem, the purpose of clustering is to obtain some intrinsic

data pattern by dividing the original set of objects into similar groups or clusters.

**3.1. Introduction to Clustering Algorithms.** There are many kinds of clustering algorithms, such as hierarchy-based, division-based, and density-based algorithms [25]. In this paper, the most common and reliable division-based K-means algorithm is used for analysis. The K-means algorithm divides  $n$  vectors  $x_i (i = 1, 2, \dots, n)$  into  $k$  classes  $G_i (i = 1, 2, \dots, k)$  and find the cluster centres of each class so that the objective function of the nonsimilarity (or distance) index is minimized. When the metric between the vector  $x_i$  and the corresponding cluster centre  $C_i$  in the  $i$ -th class  $G_i$  is chosen as the Euclidean distance, the objective function

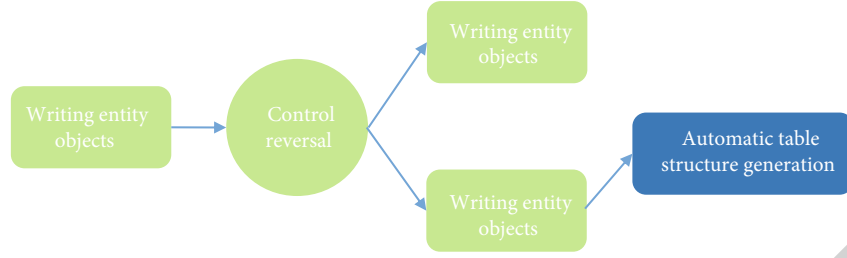


FIGURE 3: Generating data tables using control reversal reverse engineering.

can be defined as

$$J = \sum_k^{i=1} J_i = \sum_k^{i=1} \sum_{l, x_l \in G_i} x_l - c_i^2. \quad (1)$$

Here,  $J_i = \sum_{l, x_l \in G_i} x_l - c_i^2$  is the objective function  $G_i$  within the class, the apparent  $J$  size of which depends on the  $G_i$  shape of the cluster centre  $c_i$ , and the  $J$  smaller the cluster, the better the clustering.

The basic idea of the K-means algorithm is as follows.

- (1) First,  $k$  vectors are randomly selected as the centres of each class
- (2) Let  $U$  be a 2-dimensional subordination matrix of  $c * n$ . If the  $j$ rd vector  $x_j$  belongs to class  $i$ , then the element  $u_{ij}$  in matrix  $U$  is 1; otherwise, it is 0; i.e.,

$$u_{ij} = \begin{cases} 1 & \text{For each } k \neq j \text{ and } \|x_j - c_i\| \leq \|x_j - c_k\| \\ 0 & \text{others} \end{cases} \quad (2)$$

- (3) Based  $u_{ij}$  on the value of the calculated objective function, stop if it is less than a threshold or if the difference between two consecutive times is less than a threshold
- (4)  $u_{ij}$  Calculate the centre  $G_i$  of each cluster according to  $C_i: c_i = \sum_{l, x_l \in G_i} x_l / |G_i|$ ,  $|G_i|$  being the number of elements in the cluster. Then, return to (2)

The system entity object to database table relationship analysis and implementation entity object to relational table implementation process is shown in Figure 3.

**3.2. Weighted Clustering Algorithms.** The K-means algorithm has its limitations in that it takes into account all factors in the clustering analysis and assumes that these factors have an equal effect on distance. Relying equally on similarity measures for all attributes can be misleading [26, 27]; one effective way of overcoming this dimensionality trap can be achieved by assigning weights to each attribute, so that different attributes can achieve optimal results in the clustering

TABLE 1: Comparison of the parameters of the 4 clusters.

Serial number	Central value	Radius	Percent
Cluster 1	0.52,0.63	0.32	0.62
Cluster 2	0.17,0.21	0.06	0.04
Cluster 3	0.21,0.56	0.17	0.21
Cluster 4	0.32,0.41	0.23	0.13

process based on their own weights. In terms of the Euclidean space from a data perspective, adding weights is equivalent to lengthening the axes corresponding to the attributes of interest and shortening the axes corresponding to the attributes with smaller weights.

To this end, the objective function should be  $\|x_l - c\|_i^2$  replaced by  $\sum_{k=1}^{i=1} (w_j(x_{lj} - c_{ij}))^2$  an objective function that  $J$  also depends on the weights  $w_j$ , the size of which can be determined by experienced staff using expert scoring methods to determine the importance of the equipment parameters for production optimisation and fault warning, thus solving the ‘‘dimensional trap’’ problem.

**3.3. Concepts and Definitions of Outlier Indices.** To date, there is no formal and generally accepted definition of an outlier. More recent findings are given in the relevant literature [28, 29]. To first give an example to illustrate this basic idea, consider the two-dimensional data set in Figure 1, where it can be found that there are four cluster centres, of which  $C_1$  and  $C_3$  are outliers. Since outliers are defined as data that are not inside any large cluster, here clusters  $C_2$  and  $C_4$  are to have the vast majority of the data and  $C_1$  and  $C_3$  are not part of clusters  $C_2$  and  $C_4$ , so they are outliers. In order to show the physical characteristics of outlier data, an index is designed for each identified outlier data object, called  $CBLOF(t)$ , some concepts are given below, and the absolute value of  $C$  is used to indicate the number of data points in  $C$ .

**Definition 1.** Let  $A_1, \dots, A_m$  denote a series of data points whose value domain is  $D_1, \dots, D_m$  such that the result of clustering the database  $D$  is denoted  $C = \{C_1, C_2, \dots, C_k\}$ ; here,  $C_i \cap C_j \neq \Phi$  and  $C_1 \cup C_2 \cup \dots \cup C_k = D$ , by the number of clusters  $k$ .

**Definition 2.** Suppose  $C = \{C_1, C_2, \dots, C_k\}$  is the order of the clusters:  $|C_1| \geq |C_2| \geq \dots \geq |C_k|$ , given two numerical

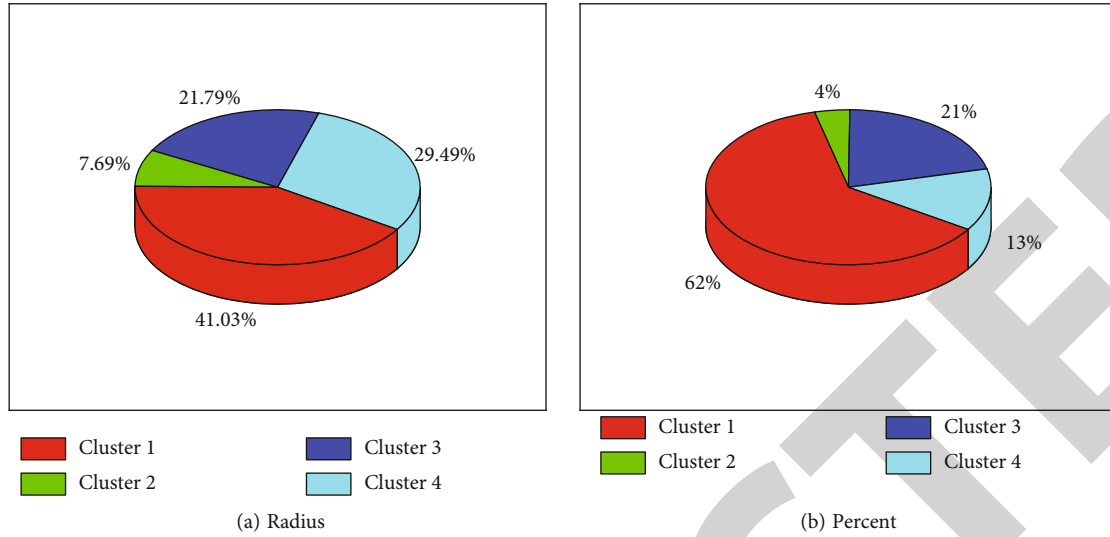


FIGURE 4: Comparison of pie charts of radii and percentages of clusters.

parameters:  $\alpha$  and  $\beta$ ; we let  $b$  be the boundary of the size cluster, then

$$\begin{cases} (|C_1| + |C_2| + \dots + |C_b|) \geq |D| \cdot \alpha, \\ |C_b|/|C_{b+1}| \geq \beta. \end{cases} \quad (3)$$

The first part of equation (3) takes into account that the vast majority of data points in a data set are not outliers, so that a cluster that contains the vast majority of data points is a large cluster. The second part of equation (3) takes into account that the main difference between large and small clusters is the number of data points within the cluster, e.g., set  $\beta$  to 5, and then, any cluster in LC is 5 times larger than in SC [30].

*Definition 3.* Putting the above analysis together, assuming that  $C = \{C_1, C_2, \dots, C_k\}$  is the order of clustering:  $|C_1| \geq |C_2| \geq \dots \geq |C_k|$ , and consistent in the definitions of  $p_{ij}(t)$ ,  $\alpha$ ,  $\beta$ ,  $b$ , LC, and SC and setting the number of clusters in LC to  $n$ , the resulting outlier index for any data point  $t$  is

$$CBLOF(t) = |C_i| \cdot \min(\text{distance}(t, C_j)), \quad (4)$$

where  $t \in C_i$ ,  $C_i \in SC$ ,  $C_j \in LC$ ,  $j = 1$  to  $b$ .

According to Definition 3, the outlier index of a data point is determined by the size of the cluster in which it is located and the distance of this data point from the edge of its nearest large cluster.

#### 4. System Design and Implementation

The process of using clustering models to guide production optimisation has been implemented in the previous work. The basic process is as follows: the clustering model is trained with a large amount of historical data of normal operation, and then, the corresponding actual data of the field operation is collected and put into the clusters of aggre-

gation; if it is not included in any of the clusters, it means that it is an abnormality, and an alarm should be prompted to the staff to check the equipment, which serves as an early warning function. The detected anomalies belonging to any of the clusters mean that the equipment is operating normally and can be further explored in order to optimise the equipment.

*4.1. Raw Data Preprocessing.* Since the units of the parameters used in the design of the system vary considerably between orders of magnitude, the data must first be processed to make them dimensionless, and the standardised metric used in this paper is

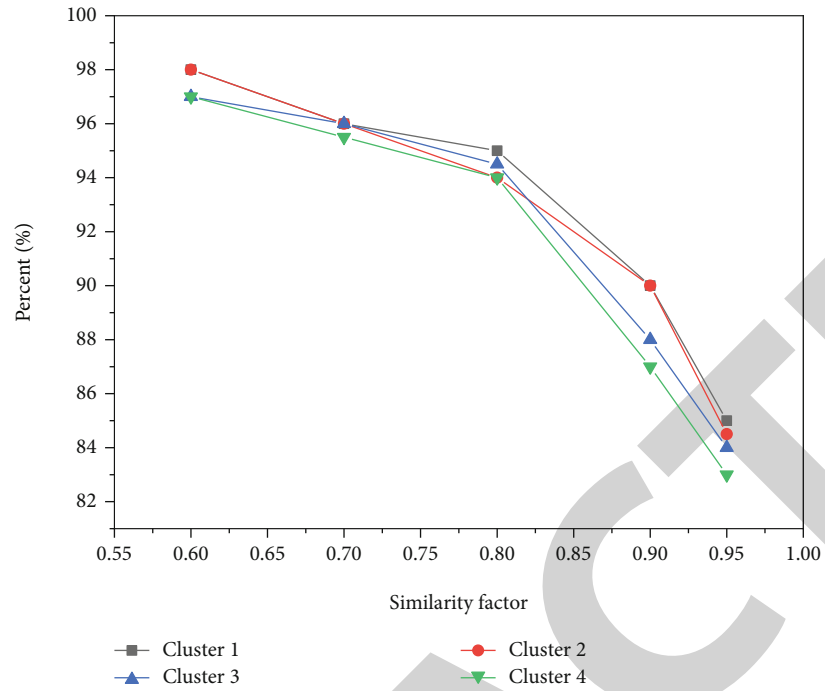
$$x_{if} = \frac{z_{if} - h_f}{S_f}, \quad (5)$$

where  $z_{if}$  is an actual parameter,  $h_f$  is the mean  $z_{if}$  of  $n$ , and  $S_f$  is the mean standard deviation.

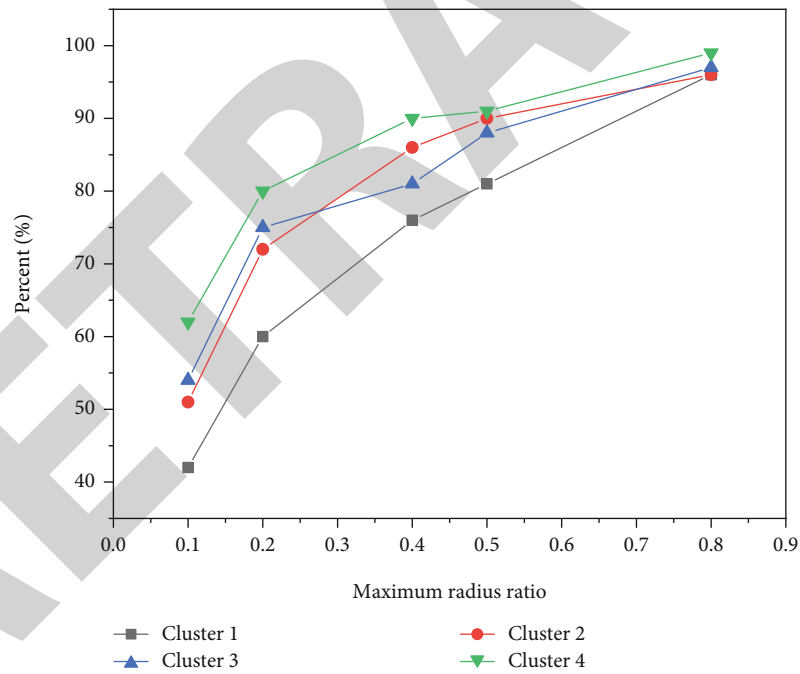
$$S_f = \frac{1}{n} \sum_{i=1}^n |z_{if} - h_f|. \quad (6)$$

*4.2. Analysis of the Off-Kernel Indices of the Parameter Points within Clusters.* Using IAE at the Shanghai Jiaotong University as the application context, five years of relevant actual production data were collected, the data were processed with standardised metric values and stored in a database, and the corresponding parameters were trained to form a clustering model using a weighted K-mean algorithm. The similarity of the actual parameters within the clusters to the cluster centres was then analysed.

The similarity between the other parameters within the cluster and the central parameter is calculated using the correlation coefficient method and the Euclidean distance, respectively; the Euclidean distance has been described earlier, and the following equations are used for the correlation



(a) Similarity factor



(b) Maximum radius ratio

FIGURE 5: Ratio of the number of parameter points to the total number of clusters at different degrees of similarity.

TABLE 2: Relationship between anomalous parameter points and clustering models.

Exceptional parameter points	Cluster 1	Cluster 2	Cluster 3	Cluster 4
1	0.65	0.51	0.75	0.58
2	0.62	0.49	0.69	0.61
3	0.59	0.41	0.71	0.56
4	0.63	0.45	0.72	0.52



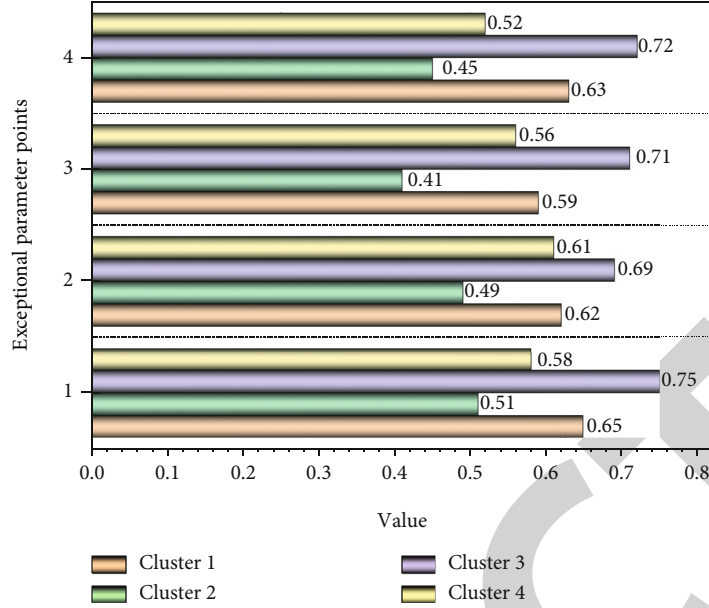


FIGURE 6: Comparison effect of anomalous parameter points for the four clustering models.

TABLE 3: Clustering accuracy data for the four clusters.

Category	Cluster 1	Cluster 2	Cluster 3	Cluster 4
Experiment 1	89.56	95.86	93.42	85.32
Experiment 2	90.24	95.32	94.21	84.68

coefficient method.

$$r_{ij} = \frac{\sum_{m=1}^{k-1} (x_{ik} - \bar{x}_i)(x_{jk} - \bar{x}_j)}{\sqrt{\sum_{m=1}^{k-1} (x_{ik} - \bar{x}_i)^2} \times \sqrt{\sum_{m=1}^{k-1} (x_{jk} - \bar{x}_j)^2}}, \quad (7)$$

where  $\bar{x}_i = 1/m \sum_{m=1}^{k-1} x_{ik}$  and  $\bar{x}_j = 1/m \sum_{m=1}^{k-1} x_{jk}$ . When  $x_j$  is the cluster centre,  $r_{ij}$  is the similarity measure between the other parameters and the centre parameter. A total of 20,000 points were collected, and all data were clustered into 4 clusters; the results of which are shown in Table 1.

A pie chart of the radii and percentages of the four clusters is given in Figure 4.

Then, the ratio of the number of equipment parameters to the number of parameters in the whole cluster was obtained for different correlation coefficients, and the ratio of the number of parameters in this point to the number of parameters in the whole cluster was obtained for different ratios of the distance from the parameter point to the centre of the cluster to the maximum radius, and the ratio was obtained in Figure 2(b). From Figure 2(a), it can be seen that the correlation with the central parameter is greater than 0.8 in more than 90% of the cases, while the proportion below 0.6 is less than 3%. Similar results are obtained for the other equipment parameters; the same analysis is also reflected in Figure 2(b). Examining these four clusters, the data points within 20% of the maximum radius each already account for more than 50% of all data points. This indicates that

the equipment has been operating in a performance optimised condition for a long time and that once the equipment parameters have deviated from the optimised condition, the staff immediately call back to bring them back to the optimised condition, so that a large proportion of the parameters are close to the centre of the cluster and a small proportion are far from the centre. The above results show that the magnitude of the dispersion of these data is related not only to the similarity of this point to the central point but also to the proportion of the points occupied, such that the kernel dispersion index of the parameter points within the cluster can be defined as

$$\text{SCAF}(t) = \begin{cases} r(t, C_j) \sqrt{p/|C_j|}, \\ (1 - d(t, C_j))/r_j \sqrt{p/|C_j|}, \end{cases} \quad (8)$$

where  $p$  represents the number of device parameter points at point  $t$ .

The curve of where the data points are located and the error detection parameters in the system at this time is shown in Figure 5. Cluster 1 represents a normal and good operating condition of the system; cluster 2 is an over-adjusted state with a low error rate and a good system; clusters 3 and 4 are the result of the system not being retuned in time, and clusters 3 and 4 also show that the marginal values (points with large dispersion) of the clusters are of poor error quality.

With the above analysis, after training the clustering model with a large amount of historical data of normal operation, when monitoring the operating conditions of the equipment in real time, when a real-time parameter point is within a cluster, this model can not only indicate in which cluster it is but also know the off-kernel index of the parameter point.

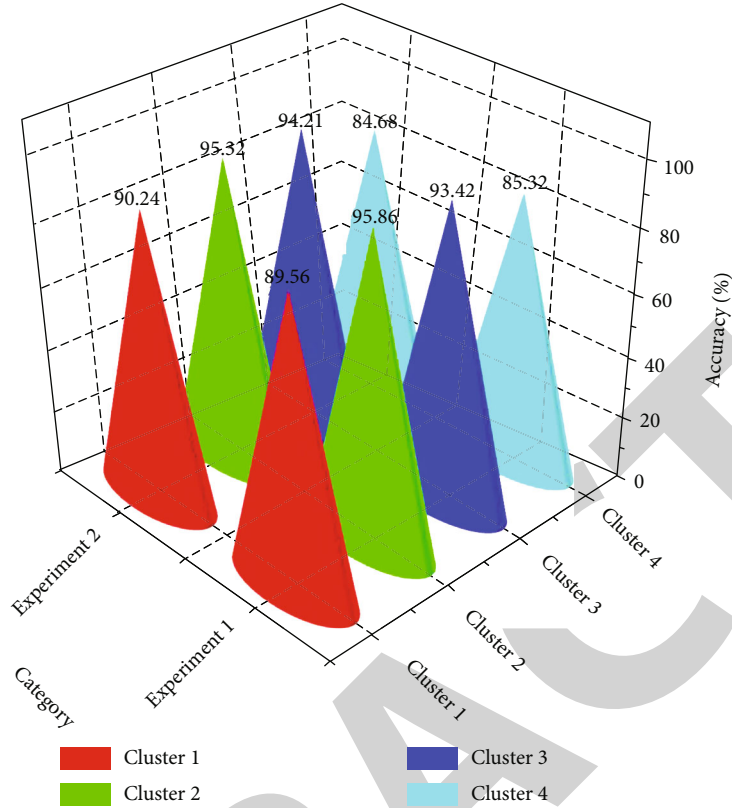


FIGURE 7: Comparison of clustering accuracy data for the four clusters in the two sets of experiments.

**4.3. Analysis of Outlier Indices for Anomalous Parameter Points Outside Clusters.** When the monitored real-time parameter point was outside the cluster, it was an anomaly. In order to be able to analyse the extent of the outliers of the anomaly, the outlier index  $CBLOF(t)$  was first calculated using equation (3), and the propane content of the dry gas at this point was checked. As shown in Table 2, the outlier index 1 for the outlier point was larger than for the outlier point 2, but the propane content was not high at this time. The analysis shows that if outlier a is closer to a cluster with fewer parameter points and further away from a cluster with more and outlier b is closer to a cluster with more parameter points and further away from a cluster with fewer,  $CBLOF(b) > CBLOF(a)$  is calculated, but in reality, outlier a may be more outlier than outlier b. The outlier index of an outlier is related not only to the distance of this outlier from the nearest cluster but also to the distance between this cluster and other clusters and the number of clusters within it. Also taking into account the weighted nature of clustering, a new definition of outliers for anomalous parameter points is obtained.

$$NCF(t) = \sum_k^{j=1} \sqrt{\frac{|c_j|}{N}} \cdot \min(\text{distance}(t, c_j)). \quad (9)$$

When a parameter point is not in a cluster, a new outlier index can be used to analyse it, which gives insight into the

system operation and provides a basis for monitoring the system operation in an optimised state.

Point pairs of anomalous parameters for four of the clustering models are shown in Figure 6.

Two sets of experiments were conducted using cluster analysis theory to cluster 20,000 data points from four clusters, and the detailed data distribution of cluster accuracy for the four clusters is given in Table 3.

The comparative effect of the clustering accuracy data for the four clusters in the two sets of experiments is given in Figure 7.

## 5. Conclusion

The design and implementation of the IAE project management system is mainly based on the real demand for the development and management of university students' IAE projects, to achieve coordinated management with the power of the system, thus ensuring that the teacher and student groups can participate in each project process, reducing the management workload and improving the comprehensive effect of management. Cluster analysis itself is a method of grouping data based on a certain similarity measure, and this paper adopts the weighted K-means algorithm based on the Euclidean distance to establish a clustering model by analysing a large amount of normal historical data and then, according to the actual operation, successively proposes the definition of the off-kernel index of parameter points within clusters and the definition of anomalous parameter points

outside clusters. The definition of the outlier index of the parameter points within the cluster and the definition of the outlier index of the abnormal parameter points outside the cluster were then proposed according to the actual operation. The management system proposed in this paper can monitor the historical data of the system running in an optimised state, thus enabling the effective implementation of the innovation and entrepreneurship project, but due to the many uncontrollable factors in the actual operation, further development of the system is necessary to make the innovation and entrepreneurship project management system practically useful.

## Data Availability

The data used to support the findings of this study are available from the corresponding author upon request.

## Conflicts of Interest

The authors declare that they have no known competing financial interests or personal relationships that could have appeared to influence the work reported in this paper.

## References

- [1] C. Jiang, W. Liu, and J. Zhang, "Risk assessment of generation and transmission systems considering wind power penetration," *Transactions of China Electrotechnical Society*, vol. 29, pp. 260–270, 2014.
- [2] M. Abdelrahem and R. Kennel, "Fault-ride through strategy for permanent-magnet synchronous generators in variable-speed wind turbines," *Energies*, vol. 9, no. 12, pp. 1066–1070, 2016.
- [3] M. Cao, Y. Qiu, Y. Feng, H. Wang, and D. Li, "Study of wind turbine fault diagnosis based on unscented Kalman filter and SCADA data," *Energies*, vol. 9, no. 10, p. 847, 2016.
- [4] S. J. Watson, B. J. Xiang, W. Yang, P. J. Tavner, and C. J. Crabtree, "Condition monitoring of the power output of wind turbine generators using wavelets," *IEEE Transactions on Energy Conversion*, vol. 25, no. 3, pp. 715–721, 2010.
- [5] Z. Radoslaw, B. Walter, and B. Tomasz, "Diagnostics of bearings in presence of strong operating conditions non-stationarity—a procedure of load-dependent features processing with application to wind turbine bearings," *Mechanical Systems and Signal Processing*, vol. 46, no. 1, pp. 16–27, 2014.
- [6] Z. Hameed, Y. S. Hong, Y. M. Cho, S. H. Ahn, and C. K. Song, "Condition monitoring and fault detection of wind turbines and related algorithms: a review," *Renewable and Sustainable Energy Reviews*, vol. 13, no. 1, pp. 1–39, 2009.
- [7] X. Y. Zhang, X. P. Zhang, and B. P. Su, "Vibrant fault diagnosis for hydro-turbine generating unit using minmax kernel K-means clustering algorithm," *Power System Protection and Control*, vol. 43, no. 5, pp. 27–34, 2015.
- [8] Z. Johanyák and O. Papp, "A hybrid algorithm for parameter tuning in fuzzy model identification," *Acta Polytechnica Hungarica*, vol. 9, no. 6, pp. 153–165, 2012.
- [9] R. Precup, R. David, E. Petriu, S. Preitl, and M. B. Rădac, "Novel adaptive charged system search algorithm for optimal tuning of fuzzy controllers," *Expert Systems with Applications*, vol. 41, no. 4, pp. 1168–1175, 2014.
- [10] M. Kiran and O. Findik, "A directed artificial bee colony algorithm," *Applied Soft Computing*, vol. 26, pp. 454–462, 2015.
- [11] I. P. Solos, I. X. Tassopoulos, and G. N. Beligiannis, "Optimizing shift scheduling for tank trucks using an effective stochastic variable neighbourhood approach," *International Journal of Artificial Intelligence*, vol. 14, pp. 1–26, 2016.
- [12] Q. Zhou, W. Sun, Y. Zhang, H. J. Ren, C. X. Sun, and J. Y. Deng, "A new method to obtain load density based on improved ANFIS," *Power System Protection and Control*, vol. 39, pp. 29–34, 2011.
- [13] O. Dragomir, F. Dragomir, and V. Stefan, "Adaptive neuro-fuzzy inference systems as a strategy for predicting and controlling the energy produced from renewable sources," *Energies*, vol. 8, no. 11, pp. 13047–13061, 2015.
- [14] A. Ahmed, S. Jun, M. Senior, and J. Yan, "Modeling and simulation of an adaptive neuro-fuzzy inference system (ANFIS) for mobile learning," *IEEE Transactions on Learning Technologies*, vol. 5, no. 3, pp. 226–237, 2012.
- [15] B. Chen, P. Matthews, and P. Tavner, "Automated on-line fault prognosis for wind turbine pitch systems using supervisory control and data acquisition," *IET Renewable Power Generation*, vol. 9, no. 5, pp. 503–513, 2015.
- [16] E. Lapira, D. D. Brisset, H. Ardakani, and J. Lee, "Wind turbine performance assessment using multi-regime modeling approach," *Renewable Energy*, vol. 45, pp. 86–95, 2012.
- [17] X. Zheng, M. Li, J. Wang, H. Ren, and Y. Fu, "Operational conditions classification of offshore wind turbines based on kernel principal analysis optimized by PSO," *Power System Protection and Control*, vol. 44, pp. 28–35, 2016.
- [18] Y. Li and R. Fang, "Reliability assessment for wind turbine based on weighted degree of improved grey incidence," *Power Syst Prot Control*, vol. 43, pp. 12–69, 2015.
- [19] Z. Yin, B. Han, and S. Xie, "An Improved Grey Correlation Algorithm and Its Application for Diesel Fault Prediction," in *2015 Sixth International Conference on Intelligent Control and Information Processing (ICICIP)*, pp. 412–416, Wuhan, China, 2015.
- [20] Y. Kong and M. Jing, "Research of the classification method based on confusion matrixes and ensemble learning," *Computer Engineering & Science*, vol. 34, no. 6, pp. 111–117, 2012.
- [21] M. Bilal, M. Ullah, and H. Ullah, "Chemometric data analysis with autoencoder neural network," *Electronic Imaging*, vol. 31, no. 1, pp. 679-1–679-6, 2019.
- [22] S. Chatterjee and A. S. Hadi, "Estimation of the underlying structure of systematic risk with the use of principal component analysis and factor analysis," *Contaduría y Administración*, vol. 59, no. 3, pp. 197–234, 2014.
- [23] R. L. de Guevara Cortés, S. T. Porras, and E. M. Moreno, "Extraction of the underlying structure of systematic risk from non-Gaussian multivariate financial time series using independent component analysis: evidence from the Mexican stock exchange," *Computación y Sistemas*, vol. 22, no. 4, 2018.
- [24] R. Ladrón de Guevara Cortés, S. Torra Porras, and E. Monte Moreno, "Neural networks principal component analysis for estimating the generative multifactor model of returns under a statistical approach to the arbitrage pricing theory. Evidence from the Mexican stock exchange," *Computación y Sistemas*, vol. 23, no. 2, 2019.
- [25] K. Imajo, K. Minami, K. Ito, and K. Nakagawa, "Deep portfolio optimization via distributional prediction of residual factors," 2020, arXiv:2012.07245.

## Research Article

# Evaluation of Sustainable Development of an Agricultural Economy Based on the DPSIR Model

Yanan Zhang, Ying Wang, and Jinghong Wei 

*College of Economics and Management, Hebei Agricultural University, Baoding, Hebei 071000, China*

Correspondence should be addressed to Jinghong Wei; [caiwuguanli@hebau.edu.cn](mailto:caiwuguanli@hebau.edu.cn)

Received 24 January 2022; Revised 14 March 2022; Accepted 1 April 2022; Published 30 April 2022

Academic Editor: Yanqiong Li

Copyright © 2022 Yanan Zhang et al. This is an open access article distributed under the Creative Commons Attribution License, which permits unrestricted use, distribution, and reproduction in any medium, provided the original work is properly cited.

With today's rapid economic growth, the role of agriculture in production and life has come to the forefront. Many problems in China's agricultural economy have seriously constrained the vitality of Chinese agriculture. Therefore, it is necessary to further strengthen the study of an agricultural economy, inject new impetus into an agricultural development, develop targeted solutions, and lay a solid foundation for the sustainable development of China's agricultural economy. Therefore, in this paper, based on the theory of sustainable development of an agricultural economy, this paper constructs a sustainable agricultural development index system in Jiangsu province from five aspects of the DPSIR model: driving force, pressure, state, impact and response and uses principal component analysis to make a comprehensive evaluation of the level of sustainable agricultural development in Jiangsu province from 2010 to 2016. The analysis results show that Jiangsu's agricultural economy is overall better and steadily improving, and it has made a huge leap in the seven-year period from 2010 to 2016, showing better sustainability. We found that the state subsystem exposed some social problems after analyzing the subsystem, and if relevant measures are not taken in time to solve the emerged problems, it will affect the other subsystems and the sustainability of the agricultural economy.

## 1. Introduction

As the material basis for human survival and development, natural resources play an important role as energy sources and spatial carriers in social and economic development, and play an irreplaceable role [1–4]. However, with the growth of population and the acceleration of urbanization, some problems limit the sustainable development of agriculture, such as the reduction of arable land area and quality, groundwater over-exploitation and deterioration of an agricultural ecological environment [5–8]. The sustainable development of an agricultural economy is a development that ensures the regenerative function of natural resources as much as possible and poses no harm to natural resources while satisfying the people of the present [9, 10]. This will not only affect the conservation of natural resources for future generations but will also lead the country to evolve in a more rational and harmonious direction [1, 11–13]. Vigorously promoting sustainable agricultural development is not only an inevitable requirement for transforming an

agricultural development model and building modern agriculture but also an inevitable choice for realizing the “five-in-one” strategic layout and building a beautiful countryside [14, 15].

In terms of sustainable use of regional resources, some problems limit kinds of evaluation methods and conceptual models in the international arena [16–21]. In the process of implementing sustainable development strategy, people must deal with the balance of the four factors of “society, economy, resources and environment,” of which resources are an important supporting factor, resources originate from the environment, the environment breeds resources, resources themselves are a component of the environment, and some factors in the environment are also resources. Therefore, resources are more important, and when resources are depleted, the environment will be completely deteriorated. In recent years, domestic and foreign experts and scholars often use the DPSIR model to analyze the problem of sustainable development of agricultural resources and economy, are an evaluation model proposed by OECD in 1993, and were

first adopted by the European Environment Agency to assess the environment [22–24]. Next, we analyze the sustainable development of the agricultural economy in Jiangsu Province (as shown in Figure 1) as an example. Jiangsu is located in the north-south climate transition zone, ecological types and agricultural production conditions are unique, known as the “land of fish and rice.” Jiangsu is the largest japonica rice producing province in the south of China and is also a national advantageous area for the production of high-quality weak-grained wheat, corn, peanuts, oilseed rape, and a variety of mixed grains, mixed beans, and other special grain crops throughout the province and wild herbs more than a thousand kinds. Luoma Lake is located in the north of Jiangsu Province, spanning Xuzhou and Suqian. The lake is 27 kilometers long, with a maximum width of 20 kilometers, and a water area of 296 square kilometers (corresponding water level 21.81 meters). Hongze Lake, the water surface area is 1597 square kilometers, the average water depth is 1.9 m, the maximum water depth is 4.5 m, and the volume is 3.04 billion cubic meters. The lake has a length of 65 kilometers and an average width of 24.4 kilometers. The water level in flood season or flood year can be as high as 15.5 m, and the area can be expanded to 3500 square kilometers. The waters of the whole lake are composed of Chengzi Lake Bay, Lihe Lake Bay, and Huaihe Lake Bay. Gaoyou Lake is 48 kilometers long and 28 kilometers wide. The general elevation of the bottom of the lake is 4.5 meters. When the water level is 6 meters, the water area is 700 square kilometers; when the water level is 5.70 meters, the area is 650 square kilometers; when the water level is 9 meters, the water area is 780 square kilometers. Taihu Lake is located on the southern edge of the Yangtze River Delta, known as Zhenze and Lize in ancient times, is one of the five largest freshwater lakes in China, ranking third [1, 2], bounded by  $30^{\circ}55'40'' \sim 31^{\circ}32'58''$  north latitude and  $119^{\circ}52'32'' \sim 120^{\circ}36'10''$  east longitude, located in the south of Jiangsu Province, bordered by Jiangsu Wuxi to the north, Zhejiang Huzhou to the south, Jiangsu Changzhou and Jiangsu Yixing to the west, and Jiangsu Suzhou to the east.

## 2. DPSIR Conceptual Model

In the DPSIR [25–28] conceptual model as shown in Table 1 and Figure 2, “Driving Force” refers to the core factor that dominates the development and direction of an agricultural system and determines its fundamental fate, and is the fundamental force and essential cause [29, 30].

We can see from Table 2, in the process of assessing the sustainable development of Jiangsu’s agricultural economy, that Driving Force is the main influencing factor and has become the leading driver of Jiangsu’s sustainable agricultural economy. The common driving factors are as follows: population growth, urbanization, market changes, economic growth, and other factors. The growth of China’s population will drive consumer demand and a broader market for related agricultural products. On the other hand, urbanization will reduce the number of farmers, which in turn leads to the reduction of an agricultural land, bringing it close to

the land red line, which has a serious negative impact on an agricultural development. Market changes, as a direct influence, can have a significant impact on agriculture directly.

Some problems limit factors that affect market prices and agricultural production materials, such as harvest, weather, supply, and demand. This can lead to a series of price reactions that can have particularly severe effects on the structure and scale of production in agriculture. Economic growth, on the other hand, stimulates the consumption of the relevant agricultural products. Therefore, to summarize, we combine an agricultural GDP per capita and price index of agricultural production materials as economic indicators in this study and Engel’s coefficient, natural population growth rate, and urbanization rate as social drivers.

This set of indicators puts a series of “pressures” on the sustainability of agriculture, as shown in Table 3, which are reflected in the overconsumption of natural resources, including energy and minerals, which in turn has a strong social impact on agricultural systems. Examples include environmental damage, overexploitation of resources, and adaptive imbalance of ecosystems. Combined with the above analysis, we use indicators such as value added in agriculture per 10,000 Yuan, electricity per 10,000 Yuan, water per 10,000 Yuan, and water resources development and utilization rate to reflect the metrics of socioeconomic drivers of pressure on agriculture. In addition, we also consider the overexploitation and utilization of natural resources such as water and soil resources and labor resources by the secondary and tertiary industries, as well as the competition among them as an influencing factor, and the competitive intensity of such influencing factors can be reflected by the land competition index and water competition index. Similarly, the rural labor force is more likely to be attracted by the wage level of secondary and tertiary industries, which is the income of an agricultural production; thus, the competition intensity of secondary and tertiary industries on rural labor resources can be reflected by the index of per capita income difference between urban and rural residents. The resource competition index refers to the ratio of industrial and an agricultural output value per unit of resources (including water resources and land resources). The income difference index between urban and rural residents is expressed by the ratio of urban residents’ disposable income to rural residents’ per capita disposable income.

The “state” refers to the state of resource utilization, an agricultural productivity, as shown in Table 4, management efficiency, and living standards of rural people as well as the state of the agricultural environment, etc. of the entire agricultural system under the action of driving forces and pressures, among which the state of agricultural resources is expressed by the reclamation index (land area land area), water resources per unit area of land for an agricultural use, natural disasters. The rate of disaster, forest greening rate (the sum of actual forest area and orchard area at the end of the year and the ratio of the city’s land area), and other indicators to indicate an agricultural production efficiency and management level with indicators such as replanting index, an agricultural land productivity (total



FIGURE 1: Jiangsu Province map.

TABLE 1: Composition of subsystems of Jiangsu agricultural system and their weights.

Target layer	Jiangsu agricultural system				
System layer	Driving force subsystem ( <i>D</i> )	Pressure system ( <i>P</i> )	Status system ( <i>S</i> )	Impact system ( <i>I</i> )	Response system ( <i>R</i> )
Weights	0.2284	0.2028	0.2246	0.1394	0.2049

output value of plantation per unit of land area), and an agricultural labor productivity (total output value of agriculture per unit of an agricultural labor) with rural per capita disposable income to indicate the standard of living of farmers with a unit area of pesticides.

“Impact” refers to the impact of the system formed by the structure of the agricultural industry on human produc-

tion and life as shown in Table 5. It is used to describe the change in the state of the environment caused by various social factors and reflects the final result of the state change, for example, vegetation cover, etc.

“Response” refers to the integration of an agricultural industry structure and consumption structure. To achieve sustainable development of an agricultural industry and

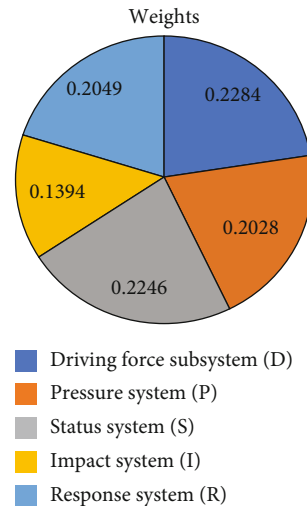


FIGURE 2: Rate of weights.

TABLE 2: Indicators of the driving force subsystem.

System layer	Drive system (D)				
Abbreviations	D1	D2	D3	D4	D5
Indicator layer	An agricultural value added per capita	An agricultural production materials price index	Engel system	Natural population growth rate	Urbanization rate
Unit	Yuan/person	%	Yuan/yuan	‰	%

protection of an agricultural environment, as shown in Table 6, human production and life are inseparable from the state of an agricultural system.

Therefore, the model has a clear causal relationship among the factors, is able to monitor the continuous feedback mechanism among the indicators, is an effective way to find the causal chain between human activities and environmental impacts, and thus is generally recognized and applied. In conclusion, the DPSIR conceptual model provides clear ideas to help select relevant elements and indicators, organize data, or information, can ensure that key elements and information are not overlooked, and helps to systematically analyze environmental or sustainable development issues, as shown in Figure 3.

The DPSIR model describes a causal chain between the origins and outcomes of environmental problems, which suggests that social problems are considering, as shown in Figure 3, and economic and demographic development act as long-term drivers of environmental stress, resulting in changes in ecological status. This causal chain shown that social, economic, and demographic developments act as long-term drivers on the environment, thus exerting pressures on the badlands and causing changes in the ecological state, resulting in various impacts on the ecological environment, such as arable land resources; these impacts lead to human responses to changes in the ecological state, which in turn act on the social, economic, and demographic complex system or directly on the environmental pressures, state, and impacts. These impacts drive human responses to changes in the state of the ecosystem, which in turn act

on the complex system of social, economic, and demographic factors or directly on environmental pressures, states, and impacts. In the DPSIR model as a whole, the drivers, pressures, states, and impacts describe the objective state of each factor in the environment, and the responses are the measures taken to keep the ecological environment in harmony and sustainable development. The cause-and-effect relationship among the five components of the DPSIR model is not only static but also reflects a dynamic mechanism. For example, the relationship between driving forces and pressures generated through human socioeconomic activities is a relationship between a technical ecoefficiency function and a use function, with more driving forces utilized while generating less pressure indicating high ecoefficiency. Similarly, the relationship between impacts on humans or ecosystems and the state of the environment depends on the carrying capacity between these systems. Whether society responds to impacts depends on how those impacts are perceived and evaluated, the results of social responses to drivers depend on the effectiveness of the response.

### 3. Evaluation Methodology

The principal component analysis method was chosen for its factor analysis, and the formula was calculated as follows.

$$U_i = \sum_{j=1}^n M_{ij}Z_{ij}, i = 1, 2, 3, 4, \dots, n, \quad (1)$$

TABLE 3: Indicators of the pressure subsystem.

System layer Abbreviations	Pressure system ( <i>P</i> )					
	P1	P2	P3	P4	P5	P6
Indicator layer	Water consumption of an agricultural value added in ten thousand yuan	Energy consumption of 10,000 yuan of an agricultural value added	Electricity consumption of 10,000 RMB of an agricultural value added	An agricultural water resources development utilization rate	Competition index of resources (water and land resources)	Urban and rural residents per capita income gap index
Unit	Yuan/person	%	Yuan/yuan	‰	%	/



TABLE 4: Indicators of the state subsystem.

System layer	Abbreviations	Indicator layer	Unit
State system (S)	S1	Cultivation index	%
	S2	Amount of water used for agriculture per unit area of cultivated land	m <sup>3</sup> /hm <sup>2</sup>
	S3	Natural disaster incidence	%
	S4	Forest greening rate	%
	S5	Replanting index	/
	S6	An agricultural land productivity million yuan	Million yuan/hm <sup>2</sup>
	S7	An agricultural labor productivity	10,000 yuan/person
	S8	Per capita disposable income of rural residents	Yuan
	S9	Amount of fertilizer applied per unit area	kg/hm <sup>2</sup>
	S10	Pesticide use per unit area	kg/hm <sup>2</sup>

TABLE 5: Indicators of the state subsystem.

System layer	Abbreviations	Indicator layer	Unit
Impact system (I)	I1	Rural arable land area per capita	hm <sup>2</sup> /person
	I2	Grain yield per unit area	kg/hm <sup>2</sup>
	I3	Grain possession per capita	kg/person
	I4	Meat intake per capita	kg/person
	I5	Vegetables per capita	kg/person

TABLE 6: Indicators of the response subsystem.

System layer	Abbreviations	Indicator layer	Unit
Response system (R)	R1	The proportion of expenditure on local financial allocations for science and technology	%
	R2	Expenditure on agriculture, forestry, and water affairs	%
	R3	Percentage of local financial expenditure on environmental protection	%
	R4	Labor quality	
	R5	Soil erosion control rate (proportion of area under control)	%
	R6	Proportion of water-saving irrigation area	%

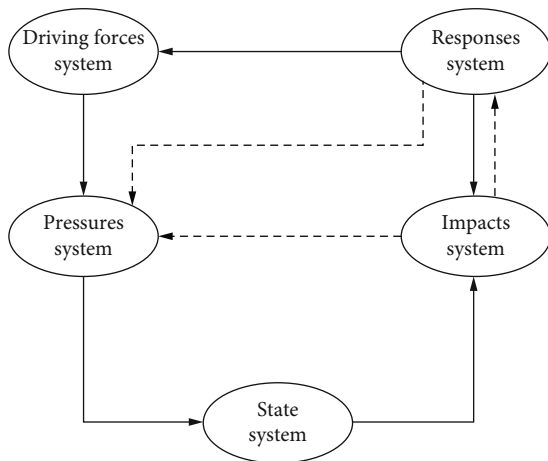


FIGURE 3: DPSIR analytical model affecting sustainable agricultural development.

$$U_A = \sum_{i=1}^n U_i V_i, i = 1, 2, 3, 4, \dots, n. \quad (2)$$

Therefore, the Jiangsu Agricultural Economic Sustainability Index AESDI – LYG can be calculated as follows.

$$\text{AESDI} - \text{LYG} = \sum_{i=1}^n W_i U_i, i = D, P, S, I, R. \quad (3)$$

The meanings of the parameters are shown in Table 7.

## 4. Experimental Results

4.1. *Analysis of Subsystem.* We can see initial eigenvalue from Figure 4. First, we have to analyze the various indicators of this subsystem and the five indicators listed by the author on its principal component analysis, and we can see this data from the histogram. Because too much data will affect the calculation, so we follow the contribution rate

TABLE 7: Parameters and meaning.

Parameters	Meaning
$U_i$	Is the systematic value that is not multiplied by the contribution margin
$Z_{ij}$	Standardized data for the $j$ -th factor and indicator extracted by system $i$
$M_{ij}$	Contribution of the $j$ -th factor of system $i$
$n$	Is the total number of extracted factors for system $i$
$U_A$	The system value of the requested system, the sustainability index of each system layer $i$
$V_i$	The contribution of a principal component of system $i$
AESDI – LYG	Reflecting the low level and strong capacity of sustainable development of Jiangsu's agricultural economy
$U_i$	Is the system value of system layer $i$ , i.e., the sustainability index of each system
$W_i$	$i$ system layer weights on the target layer

Data from the “Jiangsu Statistical Yearbook” and the statistical information of enterprises, agricultural bureaus, show parks in each county (township and township) within Jiangsu.

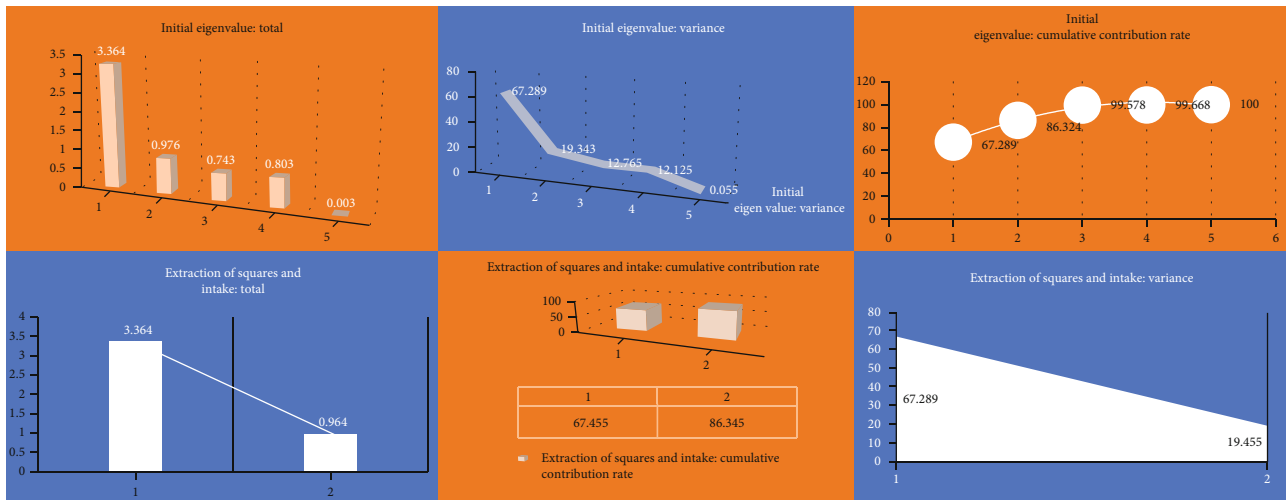


FIGURE 4: Initial eigenvalue.

greater than 85% to extract the main influence components and then get the expression of the driving force subsystem as

$$F_1 = 0.53ZD_1 - 0.36ZD_2 - 0.49ZD_3 - 0.27ZD_4 + 0.53ZD_5, \quad (4)$$

$$F_2 = 0.15ZD_1 - 0.18ZD_2 - 0.43ZD_3 - 0.87ZD_4 - 0.02ZD_5, \quad (5)$$

$$Q_1 = \frac{\lambda_1}{\lambda_1 + \lambda_2} F_1, \quad (6)$$

$$Q_2 = \frac{\lambda_2}{\lambda_1 + \lambda_2}. \quad (7)$$

Combining equations (5) and (6), we can calculate the following values:

$$U_{D1} = Q_1 F_1, \quad (8)$$

$$U_{D2} = Q_2 F_2. \quad (9)$$

Combining and summing them gives the following values:

$$U_D = U_{D1} + U_{D2}, \quad (10)$$

$$U_P = U_{P1} + U_{P2}, \quad (11)$$

$$U_S = U_{S1} + U_{S2}, \quad (12)$$

$$U_I = U_{I1} + U_{I2}, \quad (13)$$

$$U_R = U_{R1} + U_{R2}. \quad (14)$$

$ZD_i$  is the standardized data calculated by the  $Z$ -Score method under the driver system,  $U_D$  is the sustainability index of the Jiangsu agricultural driver subsystem, and  $F_1$  represents the proportion of the eigenvalues corresponding to each principal component to the sum of the total eigenvalues of the extracted principal components to calculate the driver system values as weights.

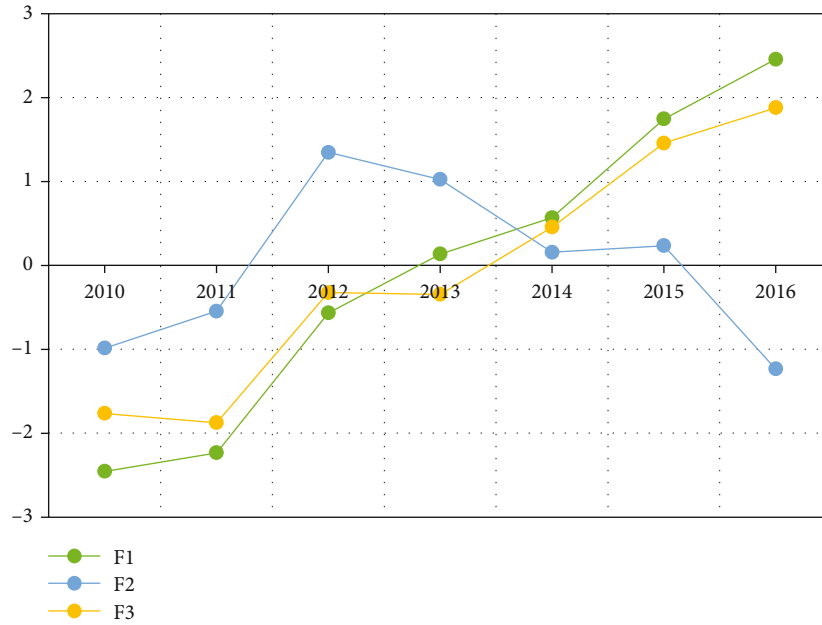


FIGURE 5: The comprehensive index.

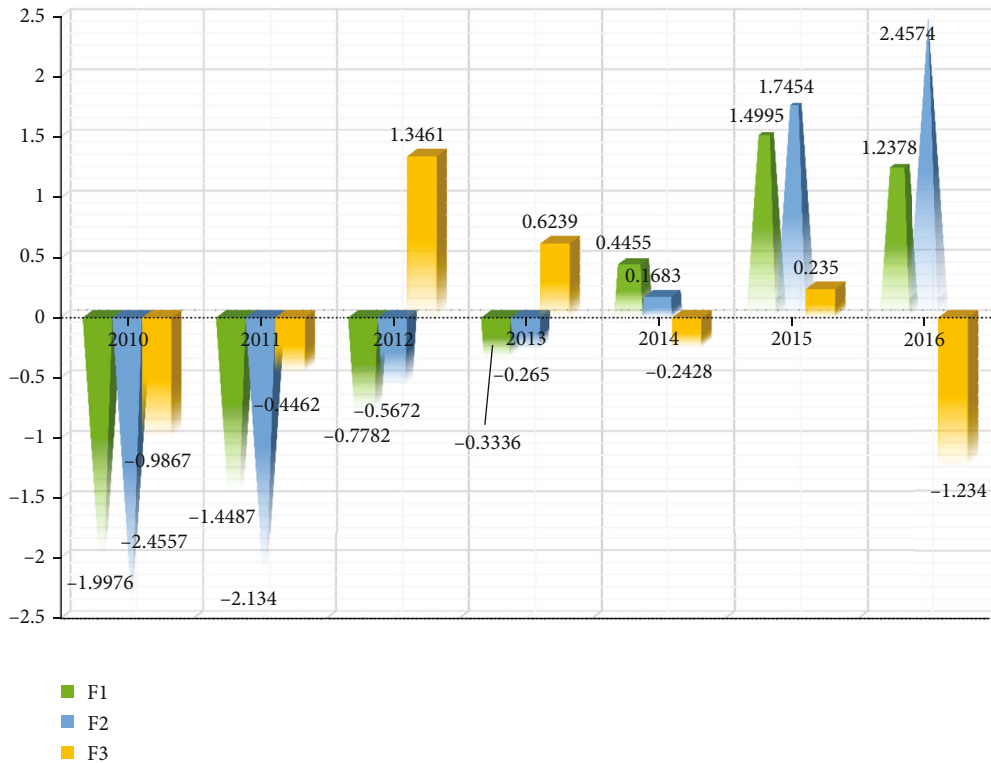


FIGURE 6: The comprehensive index of the pressure system.

From Figure 5, we can know that the comprehensive index of sustainable development  $U_D$  jumped from -1.7654 in 2010 to 1.8778 in 2016, which is a huge progress and a rapid improvement of sustainable development, which indicates that the excessive driving force causes the whole system

to show a strong vitality. Specifically, the driving force subsystem includes a total of five basic indicators, mainly economic indicators, among which the indicators of an agricultural GDP per capita and urbanization rate have been growing rapidly in recent years, while the Engel coefficient

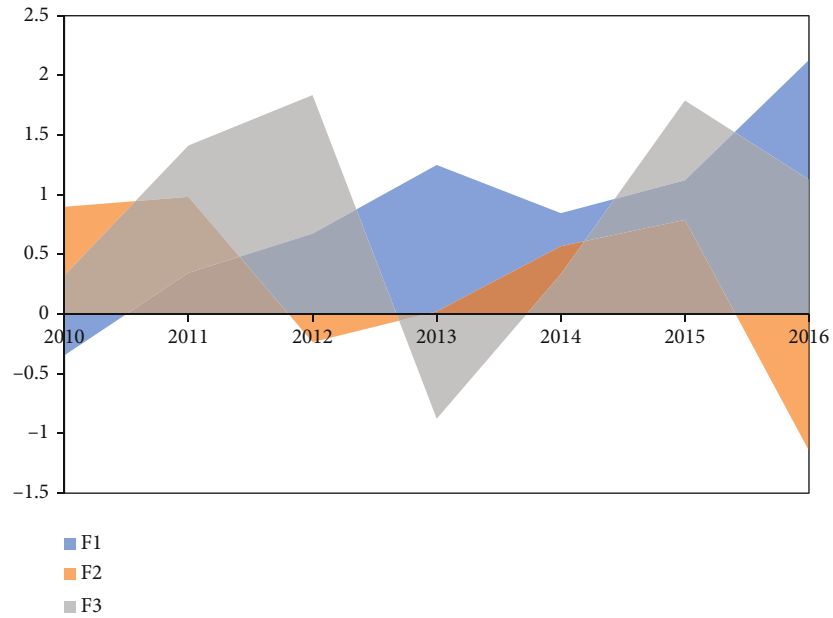


FIGURE 7: The comprehensive index of the state system.

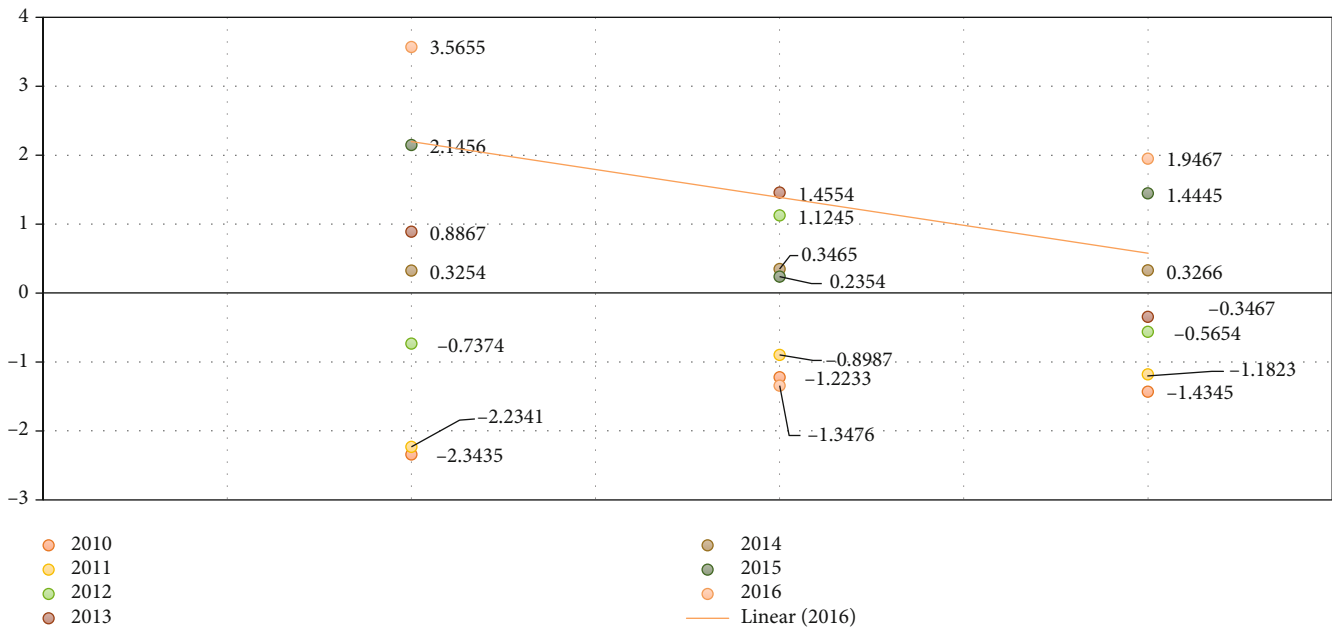


FIGURE 8: The comprehensive index of the impact system.

has been on a decreasing trend, indicating that the level of economic and social development in rural Jiangsu has been steadily improving, urbanization has been developing rapidly, and the scale of an agricultural economy has been growing.

The stress subsystem contains six underlying indicators, and we initially analyzed these six relevant indicators. The results of the principal component analysis were extracted from the two main principal components for the analysis, and the total variance contribution rate was 94.212% cumulatively. As can be seen in Figure 6, the  $U_D$  value showed an

overall increasing trend, with the highest value in 2015, followed by a fall of about 0.25. This indicates that some factors have appeared to interfere with the composite value, which may be related to resource and energy consumption, such as water consumption, electricity consumption, and energy consumption, and objective causes should be found and corrected in time for him to not have the problem of declining year after year, so as to maintain sustainable development efforts. It indicates that the way of crude growth of Jiangsu agriculture, which is mainly resource consumption, is gradually changing, while the competition index of water

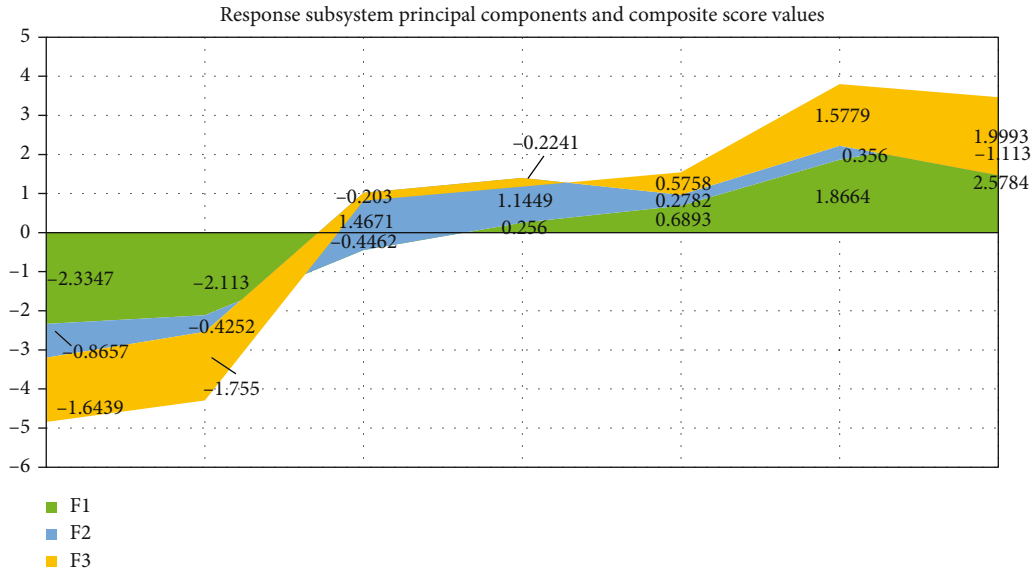


FIGURE 9: The comprehensive index of the response system.

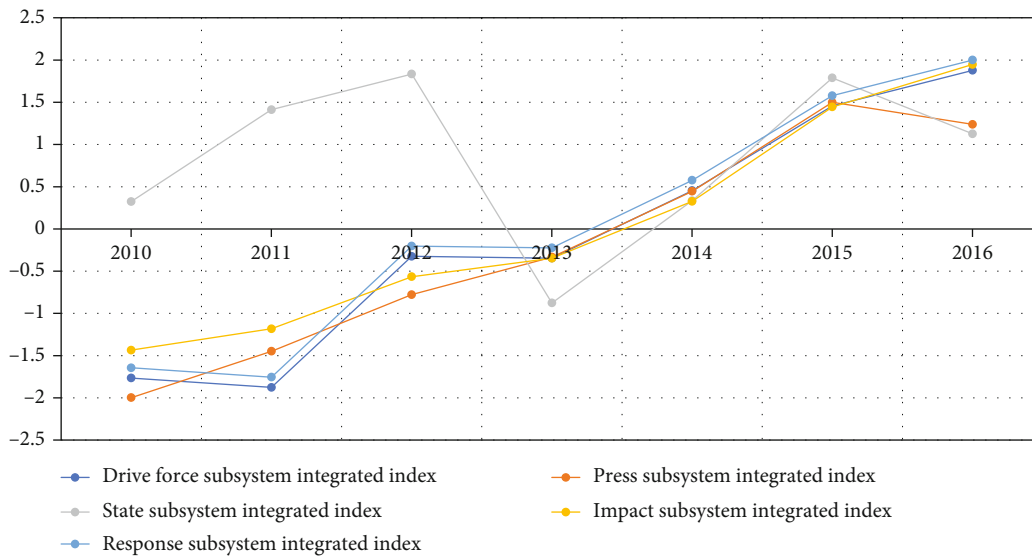


FIGURE 10: The comprehensive index of the whole subsystem.

and soil resources, which reflects the competition between secondary and tertiary industries and agriculture in resource utilization, and the index of per capita income gap between urban and rural residents have an upward trend, but the magnitude is not large; thus, the overall result is that the value of the pressure subsystem is in a downward trend.

The state subsystem contains far more basic indicators than other indicators, which is since the state subsystem is influenced by so many factors, and various dimensions and types of factors can affect it from all angles. After analyzing its principal components, it is found that the total variance contribution is 91.3245% accumulated by extracting 3 principal components. Based on the Figure 7, we can see that the combined parameters of the state subsystem are positive except for 2013. However, its data trend is very unstable,

showing a stable upward trend in the first three years and a particularly high volatility in the latter years, which hides the deep-seated reasons behind. For example, resource status, the average amount of water per acre of arable land for an agricultural use, forest greening rate, an agricultural land productivity, replanting index, an agricultural labor productivity, fertilizer and pesticide carrying capacity per unit area, etc. all have a strong influence on it.

The impact subsystem contains five base indicators, which are lower than the state subsystem and the response subsystem. This is because the state subsystem is influenced by so many factors, and various levels and types of factors can affect it from all angles. The factors influencing the state subsystem mainly include rural per capita arable land area, grain yield per unit area, per capita grain share, per capita

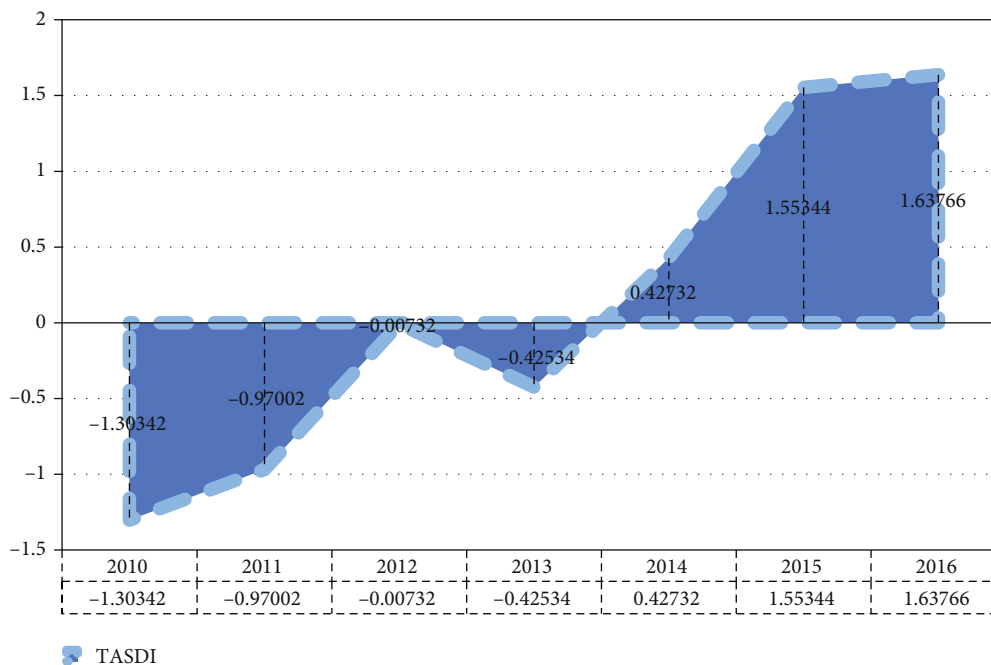


FIGURE 11: The comprehensive index of the TASDI system.

meat share, and per capita vegetable share. We can see experiments from Figure 8. After analyzing its principal components, it was found that 2 principal components were extracted, and the total variance contribution was 93.1435% cumulatively. Through the histogram, we can see that the impact subsystem sustainability index of the sustainable development system of Jiangsu agricultural economy is in a situation of steadily increasing, the trend, from -1.4345 in 2010 to 1.9467 in 2016, indicating that the state of the sustainable development system of agriculture in Jiangsu is relatively strong for the changes generated by the ecosystem, and the resource environment, etc. achieve better self-healing ability.

The response subsystem sustainability index ( $U_R$ ) analysis processed the seven basic indicators contained in the response subsystem of Jiangsu agricultural economy by principal component analysis, and a total of three principal components were extracted, whose total variance contribution rate was 91.8% cumulatively. The base indicators are lower than the state subsystem and more than the other subsystems. This is because the response subsystem is affected by so many factors, and various levels and types of factors can affect it from all angles. As can be seen from Figure 9, the overall trend of the UR of the response subsystem value of Jiangsu agriculture in the seven years from 2010 to 2016 is increasing, from -1.6439 in 2010 to 1.9993, indicating that Jiangsu modern-type agriculture has a stronger ability to adjust to the current economic and social development, wasteful consumption of agricultural resources, pollution of the agricultural ecology and environment, and the sustainable development of agriculture to external pressure. The adjustment mechanism of sustainable agricultural development to external pressure is gradually improving. Specifically, the seven basic indicators contained in the Jiangsu

agricultural response subsystem mainly reflect some measures taken by Jiangsu in the process of promoting sustainable agricultural development, which have played a role and achieved some better results.

*4.2. Analysis of Jiangsu Agricultural Sustainable Development Level Composite Index (TASDI).* The sustainable development values of the five major systems were calculated using the linear weighting method to obtain the Jiangsu Agricultural Sustainable Development Index (TASDI). The smaller the value of TASDI, the lower the level of sustainable agricultural development; the larger the value, the higher the level of sustainable agricultural development. The calculated results of the comprehensive evaluation of the sustainable development of agriculture in Jiangsu from 2007 to 2013 are shown in Figure 10.

Through the measurement and analysis of the five indices, it is generally clear that the level and development trend of Jiangsu's agricultural economic sustainability has been increasing over the seven-year period from 2010 to 2016, and although it remained stable in 2012-2013, it began to rise steadily again in 2014. This indicates that Jiangsu's agricultural economic sustainability has been steadily enhanced by all system junctions except the state subsystem under the premise of comprehensive socioeconomic development. The state subsystem, however, shows great variability. The combined parameters of the state subsystem are positive except for 2013, but its data trend is very unstable, showing a steady upward trend in the first three years and particularly high volatility in the latter years, which hides a deep-seated reason behind. In the process, the majority of construction indicators show a steady trend toward improvement. However, the various levels of sustainable development of an agricultural economy are

still unbalanced, and some of the indicators are not completed satisfactorily, such as the increase of natural population growth rate, the low rate of water quality compliance of drinking water sources, and the decrease of degraded land restoration rate. At present, the comprehensive index of ecological sustainable development in Jiangsu is high and in a high state of sustainable development, we can see experiments from Figure 11.

Therefore, in the future, the relevant construction should be promoted in a comprehensive and coordinated manner while paying more attention to the construction of weak links, adhering to the scientific concept of development as the leader, conscientiously implementing the “Jiangsu An agricultural Economy Sustainable Construction Master Plan,” actively promoting the relevant We should adhere to the scientific development concept, conscientiously implement the “Master Plan for Sustainable Construction of Jiangsu An agricultural Economy,” actively promote relevant infrastructure construction, strive to change the economic growth model, and increase efforts to coordinate an agricultural economic development and an agricultural environmental protection.

## 5. Conclusions and Recommendations

In general, from 2010 to 2016, the comprehensive score of Jiangsu’s agricultural economic sustainability has increased year by year, from -1.30342 in 2010 to 1.63766 in 2013, it only started to be a value greater than 0 in 2014, and the overall agricultural sustainability has improved significantly. From the evaluation score, among the five systems of the DPSIR model, the best development status and trend is the Jiangsu agricultural response subsystem, followed by the impact subsystem, which is the pressure subsystem, then the driver subsystem, and the pressure subsystem, and the response subsystem is ranked last. Specifically, first, compared with other subsystems, the overall pressure subsystem of Jiangsu agricultural economy is steadily increasing, indicating that the pressure on the development of Jiangsu agricultural economy is gradually increasing, thus hindering the sustainable development of Jiangsu agricultural economy; second, the steady improvement of Jiangsu agricultural economy, the speed of urbanization, and the growing scale of the economy have led to the good development of the driving force system of Jiangsu agriculture, which promote the benign development of its sustainability; third, the overall development of the state subsystem of Jiangsu’s agricultural economy has a tendency to fluctuate drastically, indicating that despite the pressure of rapid economic and social development, accelerated urbanization, resource consumption, and resource competition, the state subsystems of society, resources, and environment under Jiangsu’s agricultural economy have received drastic impacts, which seriously restrict the sustainability of the system; fourth, the response of Jiangsu’s agricultural economy subsystem, indicating that to achieve and promote the sustainable development of Jiangsu’s agricultural economy, corresponding measures must be taken to increase the intensity of an agricultural investment and investment in an agricultural scientific

research, transform the development model of an agricultural production, intensively use agricultural resources, and protect and improve the agricultural ecological environment; fifth, the development of the five subsystems of Jiangsu’s agricultural economy sustainable development system is still uneven, the level of Jiangsu’s agricultural economy sustainable development. In general, the level of sustainable development of Jiangsu agricultural economy has shown a clear and steady upward trend. Through the evaluation and analysis of the sustainable development of Jiangsu’s agricultural economy from 2010 to 2016, the overall comprehensive index of Jiangsu’s agricultural economy has maintained a steady growth, and the sustainable development of agriculture is in a good trend, but there is still room for significant improvement. To achieve sustainable agricultural development, given the actual sustainable agricultural development in Jiangsu and the problems in the utilization of resources, it is recommended that first of all, it is necessary to strengthen organizational leadership, strengthen the implementation of responsibilities, continue to introduce a series of favorable policies and measures for Jiangsu’s agricultural economy and ecological environmental protection, and establish a long-term management mechanism, and while coordinating an agricultural production, it is necessary to pay more attention to the environmental protection of agricultural resources. We need to increase the protection of arable land, water, forest, wetland, and other resources, develop green, ecological, recycling, and water-saving agriculture, and improve the efficiency of an agricultural resource utilization and the benefits of an agricultural ecological environment. Secondly, we need to improve the monitoring system, strengthen the publicity and guidance, to ecological environmental protection, an agricultural input reduction, resource recycling, and an agricultural ecological restoration as a means to strengthen scientific and technological support, increase investment to promote the comprehensive prevention and control of an agricultural surface pollution, focusing on the implementation of eight projects, and strive to achieve the city’s “one control, two reduction, three basic” goal, and effectively improve the rural ecological environment to enhance the sustainable development of the agricultural economy of Jiangsu. Finally, the construction of Jiangsu beautiful countryside has an opportunity to fully explore the ecological and economic value of the countryside, the ecological advantages effectively into development advantages, and the rural energy saving and emission reduction work into the ecological village and new rural construction assessment system, at the same time, to cultivate the concept of rural green consumption, supply-side reform to promote the rural ecological environment governance, to provide strong support for rural ecological environment governance, and to ultimately achieve sustainable agricultural development.

## Data Availability

The data used to support the findings of this study are available from the corresponding author upon request.

## Conflicts of Interest

The authors declare that they have no known competing financial interests or personal relationships that could have appeared to influence the work reported in this paper.

## Acknowledgments

This work was supported by Social Science Fund: Risk Assessment of Corn Industry Chain under the Background of Agricultural Supply-side Reform HB18GL055.

## References

- [1] M. Kaur, K. Hewage, and R. Sadiq, "Investigating the impacts of urban densification on buried water infrastructure through DPSIR framework," *Journal of Cleaner Production*, vol. 259, article 120897, 2020.
- [2] A. Agramont, N. van Cauwenbergh, A. van Griesven, and M. Craps, "Integrating spatial and social characteristics in the DPSIR framework for the sustainable management of river basins: case study of the Katari River basin, Bolivia," *Water International*, vol. 47, no. 1, pp. 8–29, 2022.
- [3] A. Anandhi, K. R. Douglas-Mankin, P. Srivastava et al., "DPSIR-ESA vulnerability assessment (DEVA) framework: synthesis, foundational overview, and expert case studies," *Transactions of the ASABE*, vol. 63, no. 3, pp. 741–752, 2020.
- [4] F. Bagordo, D. Migoni, T. Grassi et al., "Using the DPSIR framework to identify factors influencing the quality of groundwater in Grecia Salentina (Puglia, Italy)," *RENDICONTI LINCEI-SCIENZE FISICHE E NATURALI*, vol. 27, no. 1, pp. 113–125, 2016.
- [5] S. Bell, "DPSIR = A Problem Structuring Method? An exploration from the Imagine approach," *European Journal of Operational Research*, vol. 222, no. 2, pp. 350–360, 2012.
- [6] E. D. Bidone and L. D. Lacerda, "The use of DPSIR framework to evaluate sustainability in coastal areas. Case study: Guanabara Bay basin, Rio de Janeiro, Brazil," *REGIONAL ENVIRONMENTAL CHANGE*, vol. 4, no. 1, pp. 5–16, 2004.
- [7] T. Duan, J. Feng, Y. Zhou, X. Chang, and Y. Li, "Systematic evaluation of management measure effects on the water environment based on the DPSIR-Tapio decoupling model: a case study in the Chaohu Lake watershed, China," *Science of the Total Environment*, vol. 801, article 149528, 2021.
- [8] S. H. Yee, P. Bradley, W. S. Fisher et al., "Integrating Human Health and Environmental Health into the DPSIR Framework: A Tool to Identify Research Opportunities for Sustainable and Healthy Communities," *ECOHEALTH*, vol. 9, no. 4, pp. 411–426, 2012.
- [9] M. Ehara, K. Hyakumura, R. Sato et al., "Addressing maladaptive coping strategies of local communities to changes in ecosystem service provisions using the DPSIR framework," *Ecological Economics*, vol. 149, pp. 226–238, 2018.
- [10] S. F. Hansen and A. Baun, "DPSIR and stakeholder analysis of the use of Nanosilver," *NanoEthics*, vol. 9, no. 3, pp. 297–319, 2015.
- [11] A. P. Karageorgis, V. Kapsimalis, A. Kontogianni, M. Skourtos, K. R. Turner, and W. Salomons, "Impact of 100-year human interventions on the deltaic coastal zone of the Inner Thermaikos Gulf (Greece): A DPSIR framework analysis," *ENVIRONMENTAL MANAGEMENT*, vol. 38, no. 2, pp. 304–315, 2006.
- [12] M. Pirvu and M. Petrovici, "DPSIR conceptual framework role: a case study regarding the threats and conservation measures for caddisflies (Insecta: Trichoptera) in Romania," *KNOWLEDGE AND MANAGEMENT OF AQUATIC ECOSYSTEMS*, no. 411, 2013.
- [13] S. X. Shi and P. S. Tong, "EVALUATION SYSTEM AND SPATIAL DISTRIBUTION PATTERN OF ECOLOGICAL CITY CONSTRUCTION-BASED ON DPSIR-TOPSIS MODEL," *Applied Ecology and Environmental Research*, vol. 17, no. 1, pp. 601–616, 2019.
- [14] P. Kuldna, K. Peterson, H. Poltimäe, and J. Luig, "An application of DPSIR framework to identify issues of pollinator loss," *Ecological Economics*, vol. 69, no. 1, pp. 32–42, 2009.
- [15] R. Kyere-Boateng and M. V. Marek, "Analysis of the social-ecological causes of deforestation and Forest degradation in Ghana: application of the DPSIR framework," *Forests*, vol. 12, no. 4, p. 409, 2021.
- [16] N. T. Skoulikidis, "The environmental state of rivers in the Balkans-A review within the DPSIR framework," *SCIENCE OF THE TOTAL ENVIRONMENT*, vol. 407, no. 8, pp. 2501–2516, 2009.
- [17] J. H. Spangenberg, J. M. Douguet, J. Settele, and K. L. Heong, "Escaping the lock-in of continuous insecticide spraying in rice: developing an integrated ecological and socio-political DPSIR analysis," *Ecological Modelling*, vol. 295, pp. 188–195, 2015.
- [18] K. Swangjang and P. Kornpiphat, "Does ecotourism in a mangrove area at Klong Kone, Thailand, conform to sustainable tourism? A case study using SWOT and DPSIR," *Environment, Development and Sustainability*, vol. 23, no. 11, pp. 15960–15985, 2021.
- [19] B. Wang, F. Yu, Y. G. Teng, G. Z. Cao, D. Zhao, and M. Y. Zhao, "A SEEC model based on the DPSIR framework approach for watershed ecological security risk assessment: a case study in Northwest China," *WATER*, vol. 14, no. 1, 2022.
- [20] C. Wang, A. Y. Qu, P. F. Wang, and J. Hou, "Estuarine ecosystem health assessment based on the DPSIR framework: a case of the Yangtze estuary, China," *Journal of Coastal Research*, vol. 165, pp. 1236–1241, 2013.
- [21] W. Q. Wang, Y. H. Sun, and J. Wu, "Environmental warning system based on the DPSIR model: a practical and concise method for environmental assessment," *SUSTAINABILITY*, vol. 10, no. 6, 2018.
- [22] T. Ladi, A. Mahmoudpour, and A. Sharifi, "Assessing environmental impacts of transportation sector by integrating DPSIR framework and X-Matrix," *Transport Policy*, vol. 10, no. 1, pp. 434–443, 2022.
- [23] X. Liu, H. T. Liu, J. C. Chen, T. W. Liu, and Z. L. Deng, "Evaluating the sustainability of marine industrial parks based on the DPSIR framework," *JOURNAL OF CLEANER PRODUCTION*, vol. 188, pp. 158–170, 2018.
- [24] Y. B. Liu, W. Y. Du, N. C. Chen, and X. L. Wang, "Construction and evaluation of the integrated perception ecological environment indicator (IPEEI) based on the DPSIR framework for smart sustainable cities," *SUSTAINABILITY*, vol. 12, no. 17, 2020.
- [25] M. Malmir, S. Javadi, A. Moridi, A. Neshat, and B. Razdar, "A new combined framework for sustainable development using the DPSIR approach and numerical modeling," *Geoscience Frontiers*, vol. 12, no. 4, article 101169, 2021.



- [26] M. Masoudi and E. Amiri, "A new model for Hazard evaluation of vegetation degradation using Dpsir framework, a case study: Sadra region, Iran," *Polish Journal of Ecology*, vol. 63, no. 1, pp. 1–9, 2015.
- [27] M. N. Miranda, A. M. T. Silva, and M. F. R. Pereira, "Microplastics in the environment: a DPSIR analysis with focus on the responses," *Science of the Total Environment*, vol. 718, article 134968, 2020.
- [28] H. Mueller, D. P. Hamilton, and G. J. Doole, "Response lags and environmental dynamics of restoration efforts for Lake Rotorua, New Zealand," *Environmental Research Letters*, vol. 10, no. 7, 2015.
- [29] B. J. Palmer, T. R. Hill, G. K. McGregor, and A. W. Paterson, "An assessment of coastal development and land use change using the DPSIR framework: case studies from the eastern cape, South Africa," *Coastal Management*, vol. 39, no. 2, pp. 158–174, 2011.
- [30] N. Pirrone, G. Trombino, S. Cinnirella, A. Algieri, G. Bendoricchio, and L. Palmeri, "The Driver-Pressure-State-Impact-Response (DPSIR) approach for integrated catchment-coastal zone management: preliminary application to the Po catchment-Adriatic Sea coastal zone system," *REGIONAL ENVIRONMENTAL CHANGE*, vol. 5, no. 2-3, pp. 111–137, 2005.

## Research Article

# Investment Strategy of Reactive Power Compensation Scheme in Wind Turbine Distribution Network Based on Optimal Allocation

Yibing Xie  and Yang Wu

Qingdao Vocational and Technical College of Hotel Management, Qingdao, Shandong 266100, China

Correspondence should be addressed to Yibing Xie; [jdgcxxy@qchm.edu.cn](mailto:jdgcxxy@qchm.edu.cn)

Received 14 February 2022; Revised 2 March 2022; Accepted 10 March 2022; Published 27 April 2022

Academic Editor: Wen Zeng

Copyright © 2022 Yibing Xie and Yang Wu. This is an open access article distributed under the Creative Commons Attribution License, which permits unrestricted use, distribution, and reproduction in any medium, provided the original work is properly cited.

The development and application of new energy have been paid more and more attention by governments of various countries since the 21st century. It is of practical engineering significance to study reactive power compensation of wind turbine distribution network. In view of the problems of poor grid quality and increased active power loss caused by a large amount of reactive power transmission during the operation of wind farms, based on the improved genetic algorithm, aiming at the minimum compensation capacity and the minimum voltage deviation of load nodes, a multiobjective optimization scheme of reactive power in wind farms is proposed, and an example is analyzed in Matlab. The results verify the effectiveness of the improved genetic algorithm in reactive power optimization of wind motor.

## 1. Introduction

Energy consumption, as the focus of all countries in the world in the new era and new stage, not only promotes the rapid development of global economy and continuous innovation in the field of science and technology but also triggers a series of energy security challenges [1–5]. A series of energy security challenges, such as resource competition among countries, global energy shortages, and environmental pollution caused by excessive use of fossil energy, have caused problems for countries all over the world and seriously threatened humanity's survival and development. Since the twenty-first century, China's overall national strength has grown, as has its energy consumption for social development and scientific and technological innovation [6]. In recent years, research shows that China has surpassed the United States and become the world's largest energy consumer. Although China is rich in total resource storage, there are great drawbacks in energy consumption structure, mainly reflected in low per capita resource reserves, unbalanced regional distribution of energy, high utilization rate of nonrenewable resources such as coal and oil in the energy system, etc. Figure 1 shows the appearance of wind motor.

To avoid the potential consequences of energy consumption, the United Nations places a high value on energy consumption and other issues [7–11] and makes an extremely harsh appeal: before the twenty-second century, all countries must reduce greenhouse gas emissions to zero. As one of the five permanent members of the United Nations Security Council, China has fulfilled its responsibilities and responded to the call of the United Nations with practical actions. At the APEC meeting held in Beijing, China promised that relevant departments should do a good job of supervision and strictly control the emissions of greenhouse gases from various factories; at the same time, the proportion of nonfossil energy in total energy consumption increased to about 20%, and the carbon dioxide emission per unit GDP decreased by 60%–65% compared with that in 2005. Later, at the G20 meeting in Hangzhou, China declared that in the second half of this century, it is necessary to fulfill the requirements of the United Nations and reduce greenhouse gas emissions to zero. In order to realize China's commitment on energy consumption, various types of factories must be reformed, and the energy consumption will gradually transform from fossil energy to renewable clean energy such as wind power, hydropower, and photovoltaic.

At present, all countries in the world have realized the importance of renewable energy. Wind energy resources have been widely used because of its large energy storage, wide distribution, and green and clean energy in the world. According to the prediction of the Global Wind Energy Council (GWEC), by 2030, the annual new market of wind power will reach 145 GW, and the cumulative market will reach 2110 GW. By 2050, the annual new market will reach 208 GW, and the accumulated market capacity will reach 5806 GW [2].

Reactive power optimization (RPO) of a power system refers to a special optimal power flow problem that seeks the ideal reactive power flow distribution that satisfies definite physical and safety restrictions under the condition that the active output power of the generator set is decided, so that the power grid operation cost (minimum loss) or voltage quality is the highest.

In order to better save energy and reduce emissions, expand the installed capacity of wind power, and solve the problems of voltage exceeding limit, reactive power surplus, and waste of electric energy caused by wind turbines; it has become an important research topic.

## 2. Related Work

Reactive power optimization (RPO) of a power system refers to a special optimal power flow problem that seeks the optimal reactive power flow distribution that satisfies certain physical and safety constraints under the condition that the active output power of the generator set is determined, so that the power grid operation cost (minimum loss) or voltage quality is the highest [12, 13]. RPO is the most commonly used measure for the system to adjust the node voltage balance and maintain all kinds of equipment in a stable working state [14]. By changing the number of reactance/capacitor switching groups, OLTC tap position, adjusting generator output, etc., the goal of not exceeding the limit of node voltage and minimizing the cost of equipment operation and inspection is achieved [15].

*2.1. Fan in Reactive Power Optimization.* The introduction of distributed generation will alter the security and stability of the distribution network. Experiment results in recent years show that energy nodes and capacity factor of distributed generation are closely related to the power system's safety performance index [16–18]. The location of distributed generation needs to consider various factors, such as energy richness of installation location, distance from urban area, and economic cost. The selection of suitable installation location and the determination of installed capacity can solve a series of problems caused by the access of distributed generation to distribution network and promote the popularization of distributed generation. Therefore, it is of great significance to rationally plan the installation position and determine the installed capacity of distributed generation for reactive power and voltage regulation of power system [19]. Figure 2 shows a general configuration of an OWF network.



FIGURE 1: Appearance of wind motor.

Scholars in the United States and abroad have conducted extensive research on the location and capacity determination of DG. The selection of DG nodes in this manner not only consumes a significant amount of planner time but also introduces some human factors into the problem of distributed generation location and capacity determination. In general, planners are more willing to select the planning model of the unknown distributed generation access points to be selected, i.e., to find a group of DG access points to be selected from the DG location model using a mathematical method. The notion of equivalent net loss incremental rate calculates the iterative rate using a sensitivity analysis method and sorts it to determine the best DG installation position.

*2.2. Reactive Power Optimization Model and Optimization Algorithm.* Carpentier, a French electrical engineer, developed an early mathematical model of reactive power optimization through rigorous mathematical deduction and introduced a series of equality and inequality constraints such as upper and lower voltage limits, line power limits, and reactive power compensation limits, as well as traditional intelligent methods to solve the optimal power flow problem [20]. Literature [21] proposes to control wind farms with DFIG units by hierarchical voltage control mode. The upper layer is reactive power optimization of distribution network considering global economic cost, and the lower layer carries out DFIG automatic voltage control according to the control results of the upper layer. The literature [16] established a computational formula of reactive power optimization that begins with a comprehensive cost analysis of the distribution network, in which the influence of equipment operation times was considered, and the wide range of tool times was reduced to adjustment cost, as well as the loss cost and adjustment cost. A two-population particle swarm optimization algorithm is proposed, which effectively solves the control variable optimization problem via special coding.

In reference [18], a reactive power optimization model based on equipment action cost is established according to the control requirements of the actual regional power network. In this model, not only the switching changes of OLTC in adjacent periods are considered, but also the constraints of capacitor switching times are considered in combination with the actual operation principle of variable capacitors. The improved hybrid intelligent algorithm is used to effectively solve the reactive power optimization model.

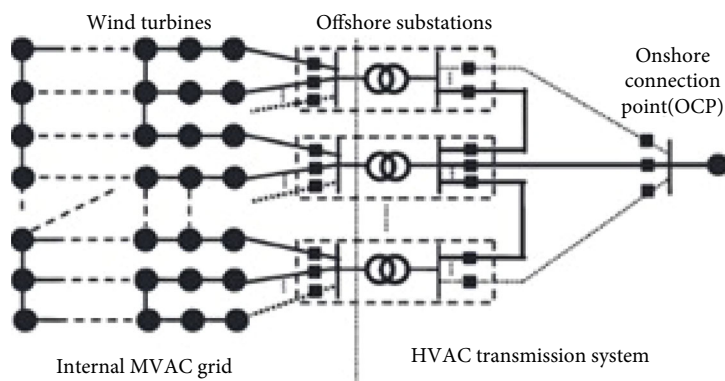


FIGURE 2: General configuration of an OWF network.

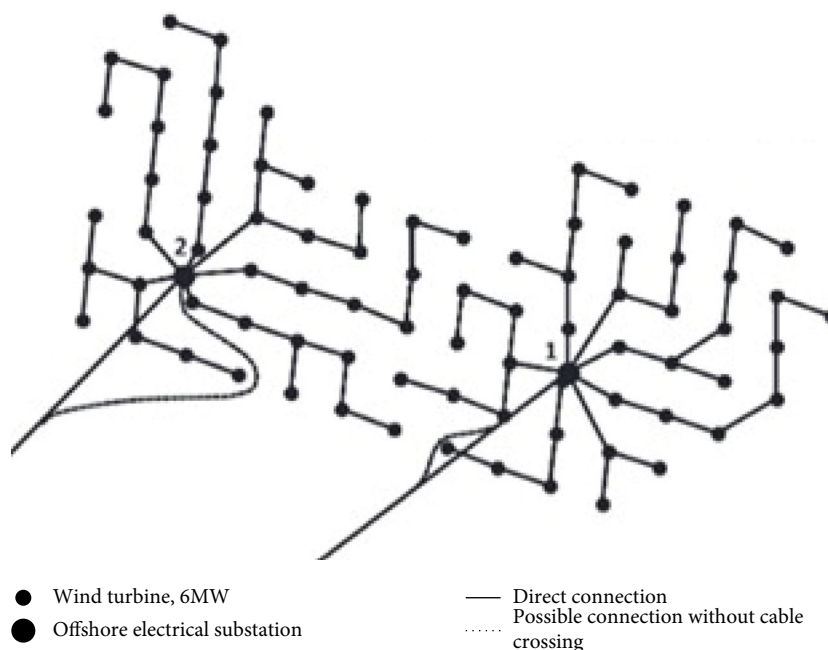


FIGURE 3: Optimal connection topology of the wind farm network.

**2.3. Intelligent Optimization Algorithm.** Conventional optimization algorithms have high requirements on the accuracy of mathematical models and cannot solve the problem of multiextremum. And the processing of discrete variables is poor, and most reactive power compensation equipment are discrete variables, so it is difficult for them to meet the requirements of real-time state control of complex power systems. In recent years, the intelligent optimization algorithm has been continuously developed, gradually replacing the conventional optimization algorithm, and applied to solving reactive power optimization problems [15]. Simulated annealing algorithm belongs to a probabilistic algorithm, which effectively solves the difficulty that the calculation process easily falls into local optimum by giving the search process a time-varying probability jump which eventually tends to zero. In the iterative process of the algorithm, the regression of the optimization results may occur, and the convergence speed is slow [12].

### 3. Improved Genetic Algorithm

The first step in the search for genetic algorithm optimization is to accomplish the mapping of individuals from phenotype to genotype using reasonable coding operations and then form the first generation population [8, 9]. The superiority of the first people is closely related to the algorithm's optimization efficiency and solution convergence. Although a population of random individuals can better reflect all of the information in the sample space, it will lose the initial population's superiority [10]. Figure 3 shows the proposed optimal connection topology of the wind farm network.

**3.1. Adaptive Crossover Operator.** Crossover operation is an important way to produce excellent individuals, which promotes the evolution from feasible solution to optimal solution. If the initial crossover rate of iteration is still adopted

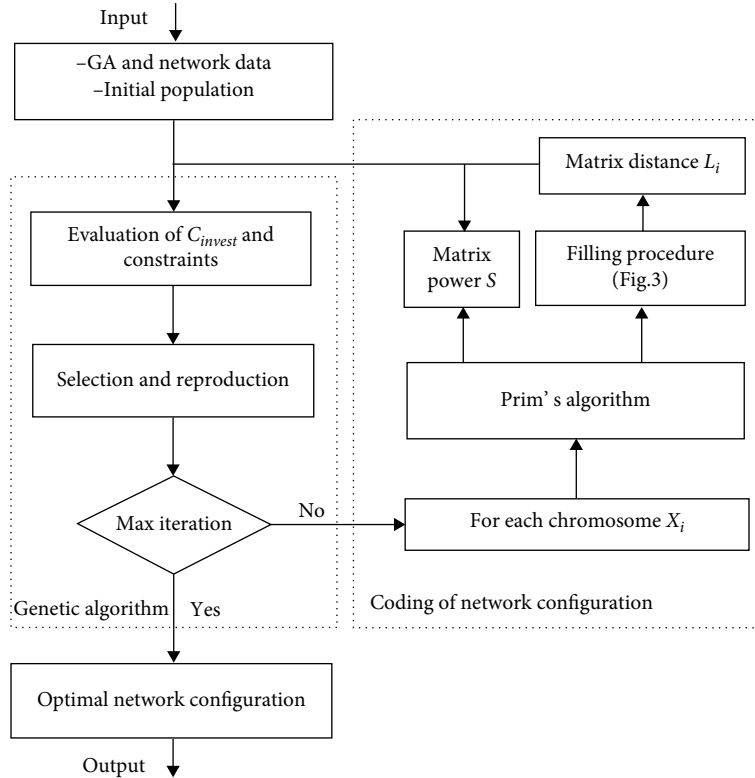


FIGURE 4: Reactive power optimization algorithm flow.

at this time, the proportion of excellent individuals in contemporary population will be reduced, which will increase the convergence difficulty of the algorithm and affect the quality of the solution.

Therefore, this paper adopts the adaptive crossover operator which changes with the evolution of population, namely,

$$P_c = P_{c1} - \frac{(P_{c1} - P_{cmin})d}{D}, \quad (1)$$

in which  $P_{c1}$  is the initial crossover rate,  $d$  represents the current population evolution times,  $D$  represents the maximum population evolution times, and  $P_{cmin}$  is the minimum population crossover rate.

In this paper, when using genetic algorithm to solve the problem, triple convergence criterion is adopted:

- (1) Reaching the maximum number of evolutions
- (2) The difference of the optimal solution of successive generations of genetic algorithm is smaller than the preset small positive number
- (3) The fitness value of the objective function is less than the preset small positive number

In this paper, the triple convergence criterion is applied to enhance the efficiency of the algorithm and the quality of the solution.

**3.2. Reactive Power Optimization Algorithm Flow.** The genetic algorithm operates with only an arbitrary initialization population and gradually evolves the population into an increasingly optimal region in the search space through selection, heredity, crossover, mutation, and other operations, in order to find the best solution to the problem. The genetic algorithm is continued to improve in this paper as follows:

- (1) The initial population selection adopts the method of uniform distribution sampling, which avoids the generation of infeasible solutions by random methods. The solution space is evenly divided into  $n$  subspaces, the same number of  $M$  chromosomes are selected in each subspace, and the  $m * n$  chromosomes are used as the initial population
- (2) The coding improvement adopts the combination of binary coding and floating-point coding to reduce the search space of the system. The switching state of reactive power compensation device is selected as the control variable in wind farm reactive power optimization, which is expressed by integer. The switching amount of reactive power of reactive power compensation device, the position of on load transformer tap, and the terminal voltage of wind turbine generator are selected as control variables, which are expressed by floating-point numbers

Figure 4 shows the proposed reactive power optimization algorithm flow.

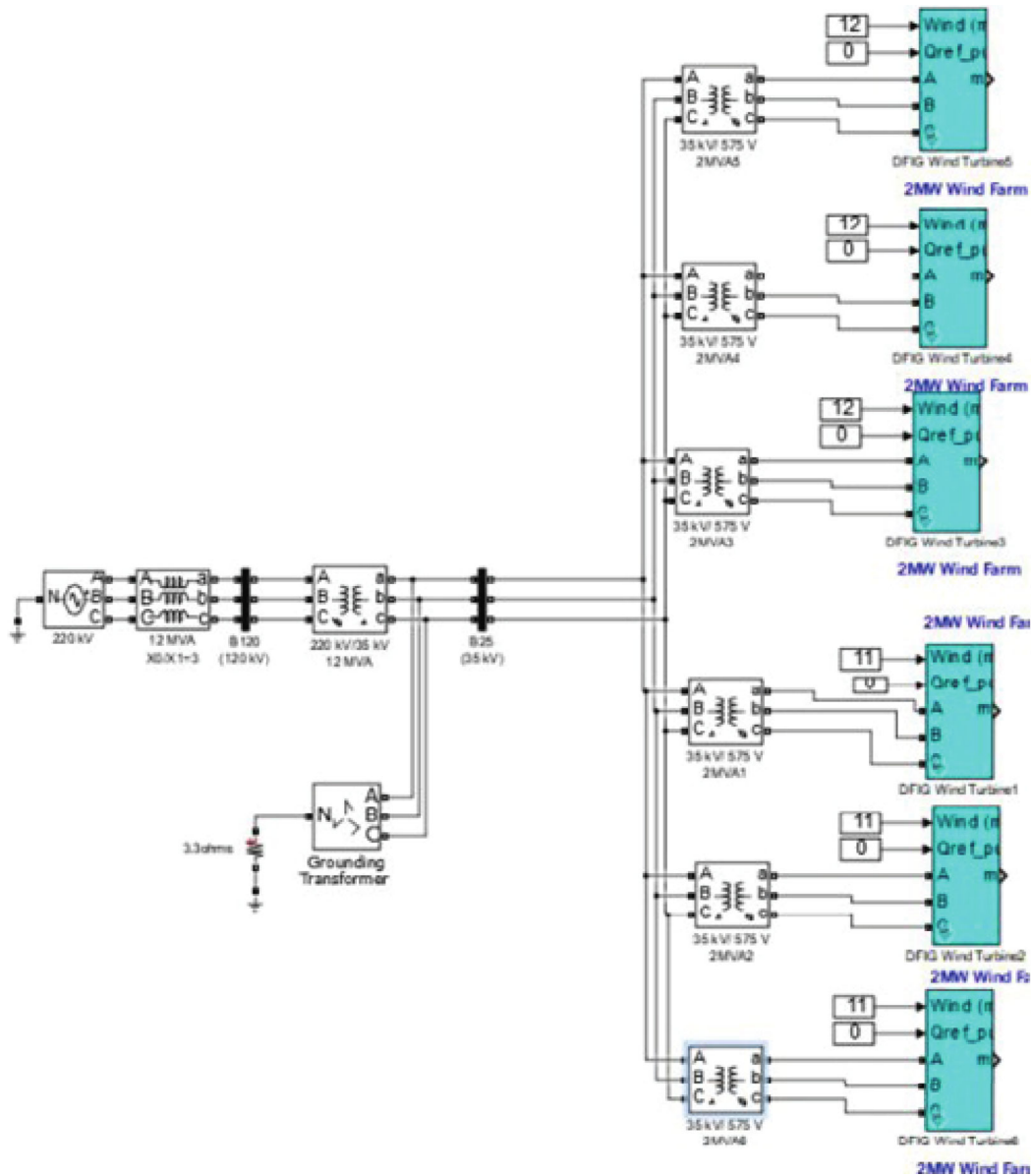


FIGURE 5: An example model diagram of the offshore wind farm.

TABLE 1: Voltage stable modal value of each node of the offshore wind farm.

Node number	Voltage stable mode value	Node number	Voltage stable mode value	Node number	Voltage stable mode value
One	0.01124	Six	0.00925	11	0.00126
Two	0.01003	Seven	0.00829	12	0.01093
Three	0.00745	Eight	0.01017	13	0.00982
Four	0.01367	Nine	0.01218	14	0.00871
Five	0.01136	10	0.00698	15	0.00115

#### 4. Experiment and Analysis

The wind power simulation equivalent model is established in Matlab, and the whole offshore wind farm is treated with equivalent modeling scheme. See Figure 2 for the model. In this paper, the reference capacity of the system is 100 MVA, the transformer capacity of wind turbine genera-

tor set is 20 MVA, and the transformer capacity of offshore booster station is 80 MVA. Node 15 is identified as the balance node, and the remaining nodes are all designated as PQ nodes. The amount of reactive power demand compensation is greatest whenever the wind turbine is running, when the output is at full load, so the offshore wind farm set in this paper is in the case of 100 percent output state.

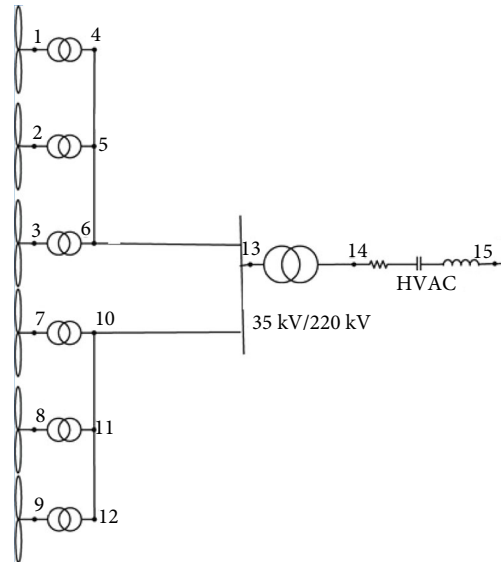


FIGURE 6: Node number and wiring diagram of the offshore wind farm.

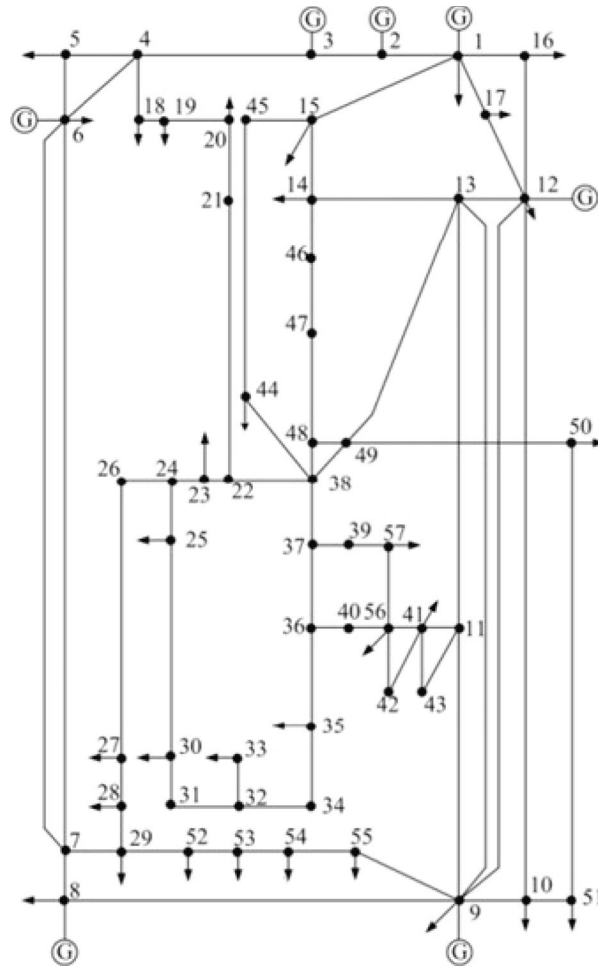


FIGURE 7: Node system diagram.

TABLE 2: Parameter setting of the improved genetic algorithm.

Encoding	The population size	Crossover operation	Crossover probability	Mutation probability	Optimal front-end individual coefficient	Maximum iteration
Real integer mixed encoding	100	New mutation operator	0.9	0.01	0.2	50

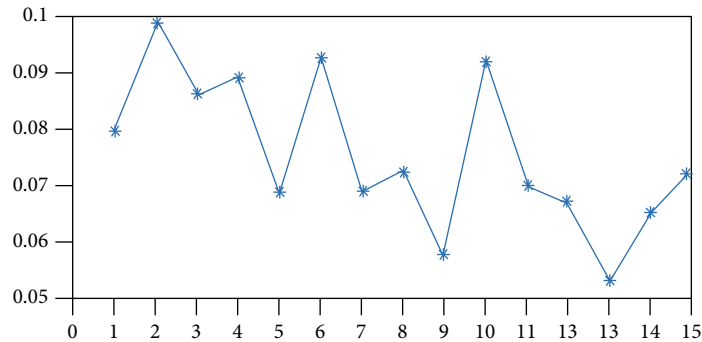


FIGURE 8: Voltage deviation diagram of load node.

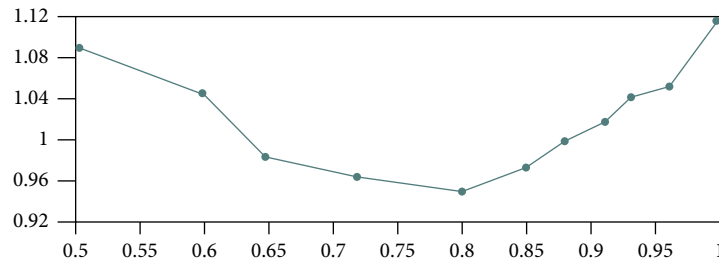


FIGURE 9: F minimum under different weight coefficients.

The schematic diagram of offshore wind farm example model is shown in Figure 5. The technique described in Chapter 4 is used to perform the voltage stability mode shapes of each node of an offshore wind farm, and the voltage stability modal values of each node are solved as shown in Table 1 below. Figures 6 and 7 show the node system diagram and node number with wiring diagram of the offshore wind farm.

Select the point in Figure 3 with the smallest steady-state voltage modal value as the offshore wind farm's reactive power compensation point; then, compare the quantitative value of each node in Table 1, and the voltage stability modal values of nodes 11 and 15 are the smallest, which can be used as power factor correction nodes. Using the improved fast nondominated sorting genetic algorithm with elite strategy, the Pareto optimal solution with the least power factor correction capacity and the least voltage deviation of load nodes is obtained. The genetic algorithm's parameter settings are shown in Table 2.

Comparing the data in Table 1, the voltage stability modal values of node numbers 11 and 15 are the smallest, which can be used as reactive power compensation points. The improved genetic algorithm is used to solve the Pareto optimal solution with the minimum reactive power compen-

sation capacity and the minimum voltage deviation of load nodes. The Pareto solution is shown in Table 2, and the voltage deviation diagram of load nodes is shown in Figure 8.

Fuzzy weight method is used to optimize the objective function. From an economic point of view, firstly, the reactive power optimization goal of at least 1F of reactive power compensation capacity of wind turbine is considered and given the maximum fuzzy weight, and secondly, the reactive power optimization goal of at least 2F of voltage deviation of load node of wind turbine is considered. From the above Table 2, it can be seen that the optimal solutions of voltage deviation of load nodes are in line with the requirement that the absolute value of positive and negative voltage deviation should not exceed 10% of the nominal voltage in Technical Provisions for Wind Farm Access to Power Grid. According to the priority of objective function considered in this paper, the experimental results under different specific gravities are compared and weighed, as shown in Figure 9.

## 5. Conclusion

In this paper, an investment strategy based on genetic algorithm is proposed, and an improved reactive power optimization scheme is proposed for wind turbines. The



effectiveness of the new algorithm in reactive power optimization of wind farms is tested in a simulation example of wind turbines, and the optimization results show good performance in voltage quality, active power loss, and node voltage deviation of wind turbines. However, the problem of complex current collection network in wind turbine has not been considered in this paper, and whether reactive power optimization of wind turbine can adapt to this scheme needs further study.

## Data Availability

The labeled dataset used to support the findings of this study is available from the corresponding author upon request.

## Conflicts of Interest

The authors declare no competing interests.

## References

- [1] W. Huang and W. Zhang, "Research on distributed wind power reactive voltage coordinated control strategy connected to distribution network," in *2021 4th International Conference on Energy, Electrical and Power Engineering (CEEPE)*, pp. 529–534, IEEE, Chongqing, China., April 2021.
- [2] A. Eid, S. Kamel, and L. Abualigah, "Marine predators algorithm for optimal allocation of active and reactive power resources in distribution networks," *Neural Computing and Applications*, vol. 33, no. 21, pp. 14327–14355, 2021.
- [3] J. Hao, S. Luo, and L. Pan, "Computer-aided intelligent design using deep multi-objective cooperative optimization algorithm," *Future Generation Computer Systems*, vol. 124, pp. 49–53, 2021.
- [4] K. Suvarchala, T. Yuvaraj, and P. Balamurugan, "A brief review on optimal allocation of distributed generation in distribution network," in *2018 4th International Conference on Electrical Energy Systems (ICEES)*, pp. 391–396, IEEE, Chennai, India., Feb 2018.
- [5] C. K. Das, O. Bass, T. S. Mahmoud, G. Kothapalli, M. A. S. Masoum, and N. Mousavi, "An optimal allocation and sizing strategy of distributed energy storage systems to improve performance of distribution networks," *Journal of Energy Storage*, vol. 26, article 100847, 2019.
- [6] V. A. Morais, J. L. Afonso, A. S. Carvalho, and A. P. Martins, "New reactive power compensation strategies for railway infrastructure capacity increasing," *Energies*, vol. 13, no. 17, p. 4379, 2020.
- [7] K. Mehmood, Z. Li, M. F. Tahir, and K. M. Cheema, "Fast excitation control strategy for typical magnetically controllable reactor for reactive power compensation," *International Journal of Electrical Power & Energy Systems*, vol. 129, article 106757, 2021.
- [8] X. Ding, R. Yao, X. Zhai, C. Li, and H. Dong, "An adaptive compensation droop control strategy for reactive power sharing in islanded microgrid," *Electrical Engineering*, vol. 102, no. 1, pp. 267–278, 2020.
- [9] A. Dhaneria, "Grid connected PV system with reactive power compensation for the grid," in *2020 IEEE Power & Energy Society Innovative Smart Grid Technologies Conference (ISGT)*, pp. 1–5, IEEE, Washington, USA., Feb 2020.
- [10] M. Wang, H. Yi, Z. Yang et al., "Comprehensive control of voltage quality in distribution network based on reactive power optimization," *IEEE 9th International Power Electronics and Motion Control Conference (IPEMC2020-ECCE Asia)*, 2020, IEEE, Nanjing, China., 2020.
- [11] N. Karmakar and B. Bhattacharyya, "Optimal reactive power planning in power transmission network using sensitivity based bi-level strategy," *Sustainable Energy, Grids and Networks*, vol. 23, article 100383, 2020.
- [12] W. Yang, L. Chen, Z. Deng, X. Xu, and C. Zhou, "A multi-period scheduling strategy for ADN considering the reactive power adjustment ability of DES," *International Journal of Electrical Power & Energy Systems*, vol. 121, article 106095, 2020.
- [13] O. D. Montoya and W. Gil-González, "Dynamic active and reactive power compensation in distribution networks with batteries: a day-ahead economic dispatch approach," *Computers & Electrical Engineering*, vol. 85, article 106710, 2020.
- [14] S. Tamalouzt, Y. Belkhier, Y. Sahri et al., "Enhanced direct reactive power control-based multi-level inverter for DFIG wind system under variable speeds," *Sustainability*, vol. 13, no. 16, p. 9060, 2021.
- [15] F. Chen, H. Deng, and Z. Shao, "Decentralised control method of battery energy storage systems for SoC balancing and reactive power sharing," *IET Generation, Transmission & Distribution*, vol. 14, no. 18, pp. 3702–3709, 2020.
- [16] M. L. Kolhe and M. Rasul, "3-phase grid-connected building integrated photovoltaic system with reactive power control capability," *Renewable Energy*, vol. 154, pp. 1065–1075, 2020.
- [17] X. Tang, Z. Huang, and M. Zhang, "An auxiliary unit with selective harmonic suppression and inherent reactive power compensation for civil distribution networks," *International Journal of Electrical Power & Energy Systems*, vol. 124, article 106323, 2021.
- [18] Y. Tao and W. Yue, "Multi objective reactive power optimization of distribution network with distributed generation power uncertainty," *Journal Of Physics: Conference Series*, vol. 2023, no. 1, article 012041, 2021.
- [19] Y. Muhammad, R. Khan, M. A. Z. Raja, F. Ullah, N. I. Chaudhary, and Y. He, "Solution of optimal reactive power dispatch with FACTS devices: a survey," *Energy Reports*, vol. 6, pp. 2211–2229, 2020.
- [20] B. K. Jha, A. Singh, A. Kumar, R. K. Misra, and D. Singh, "Phase unbalance and PAR constrained optimal active and reactive power scheduling of virtual power plants (VPPs)," *International Journal of Electrical Power & Energy Systems*, vol. 125, article 106443, 2021.
- [21] B. Kelkoul and A. Boumediene, "Stability analysis and study between classical sliding mode control (SMC) and super twisting algorithm (STA) for doubly fed induction generator (DFIG) under wind turbine," *Energy*, vol. 214, article 118871, 2021.

## *Retraction*

# **Retracted: Green Building Design Based on 5G Network and Internet of Things System**

### **Journal of Sensors**

Received 17 October 2023; Accepted 17 October 2023; Published 18 October 2023

Copyright © 2023 Journal of Sensors. This is an open access article distributed under the Creative Commons Attribution License, which permits unrestricted use, distribution, and reproduction in any medium, provided the original work is properly cited.

This article has been retracted by Hindawi following an investigation undertaken by the publisher [1]. This investigation has uncovered evidence of one or more of the following indicators of systematic manipulation of the publication process:

- (1) Discrepancies in scope
- (2) Discrepancies in the description of the research reported
- (3) Discrepancies between the availability of data and the research described
- (4) Inappropriate citations
- (5) Incoherent, meaningless and/or irrelevant content included in the article
- (6) Peer-review manipulation

The presence of these indicators undermines our confidence in the integrity of the article's content and we cannot, therefore, vouch for its reliability. Please note that this notice is intended solely to alert readers that the content of this article is unreliable. We have not investigated whether authors were aware of or involved in the systematic manipulation of the publication process.

Wiley and Hindawi regrets that the usual quality checks did not identify these issues before publication and have since put additional measures in place to safeguard research integrity.

We wish to credit our own Research Integrity and Research Publishing teams and anonymous and named external researchers and research integrity experts for contributing to this investigation.

The corresponding author, as the representative of all authors, has been given the opportunity to register their agreement or disagreement to this retraction. We have kept a record of any response received.

### **References**

- [1] M. Wang and Q. Yang, "Green Building Design Based on 5G Network and Internet of Things System," *Journal of Sensors*, vol. 2022, Article ID 7099322, 14 pages, 2022.

## Research Article

# Green Building Design Based on 5G Network and Internet of Things System

Meida Wang<sup>1</sup> and Qingfeng Yang<sup>2</sup> 

<sup>1</sup>Department of Construction Engineering and Mechanics, Yanshan University, Qinhuangdao 066004, China

<sup>2</sup>School of Architectural Arts, Hebei University of Architecture, Zhangjiakou 075000, China

Correspondence should be addressed to Qingfeng Yang; [yqf1106@hebiace.edu.cn](mailto:yqf1106@hebiace.edu.cn)

Received 16 February 2022; Revised 10 March 2022; Accepted 16 March 2022; Published 25 April 2022

Academic Editor: Yanqiong Li

Copyright © 2022 Meida Wang and Qingfeng Yang. This is an open access article distributed under the Creative Commons Attribution License, which permits unrestricted use, distribution, and reproduction in any medium, provided the original work is properly cited.

An information-based and intelligent comprehensive energy consumption management system should not only collect, manage, and analyze energy consumption data but also monitor the environmental data inside the building, to manage and display the real energy consumption and internal environmental quality more effectively and reliably. In order to solve this problem, the design and construction of the front-end hardware of the energy consumption management system are proposed, mainly including the design of data acquisition node and data centralization end. The design of data acquisition node includes the selection of DSP controller, wireless communication module, and data acquisition module and the design of main circuit and peripheral circuits. The design of data centralization end includes the selection of its high-performance processor and the transplantation of Linux operating system. This paper only introduces the design and research of lighting control algorithm and applies fuzzy control algorithm to intelligent lighting. The fuzzy control system is introduced, and a fuzzy controller based on intelligent lighting is created. The fuzzy control rule table and fuzzy control query table of the intelligent lighting system are obtained through the fuzzy control algorithm. According to the basic rules of light intensity control, when the indoor light intensity is greater than the set value of light intensity, the LED lamps are turned off, so when  $e < 0$ , the LED lamp is off and the PWM output value is 0. Therefore, when designing the fuzzy controller of intelligent lighting system, the basic domain of illumination intensity error  $E$  is  $[0500]$ , excluding the case that the indoor illumination intensity is greater than the set value of illumination intensity.

## 1. Introduction

As we all know, the global environmental and resource problems have become increasingly prominent and contradictory. Countries have begun to actively seek ways to protect the environment and save energy. Due to the needs of social development and people's life, lighting is carried out every day. The global energy consumed by lighting is huge one day. If countries can eliminate waste in lighting power consumption, then the energy consumed for power generation will be reduced, and the environmental problems caused by power generation can be effectively controlled [1]. Therefore, countries around the world began to advocate and focus on the development of intelligent lighting projects. As shown in Figure 1, people began to get involved in the

field of intelligent lighting. The direct benefits brought by intelligent lighting made people realize that intelligent lighting can not only bring higher living comfort but also protect the environment and save energy, which has been widely promoted by all walks of life. Intelligent lighting has developed rapidly in the field of global lighting, and countries have opened the era of intelligent lighting. In order to meet the international development trend and according to the actual situation of China, the research and development of intelligent lighting industry can bring many benefits to China, that is, it can improve the lighting quality, provide a lighting environment beneficial to people's life, save electric energy, and protect the environment, to truly reduce the energy consumption index and meet people's growing needs [2]. However, according to the current research,

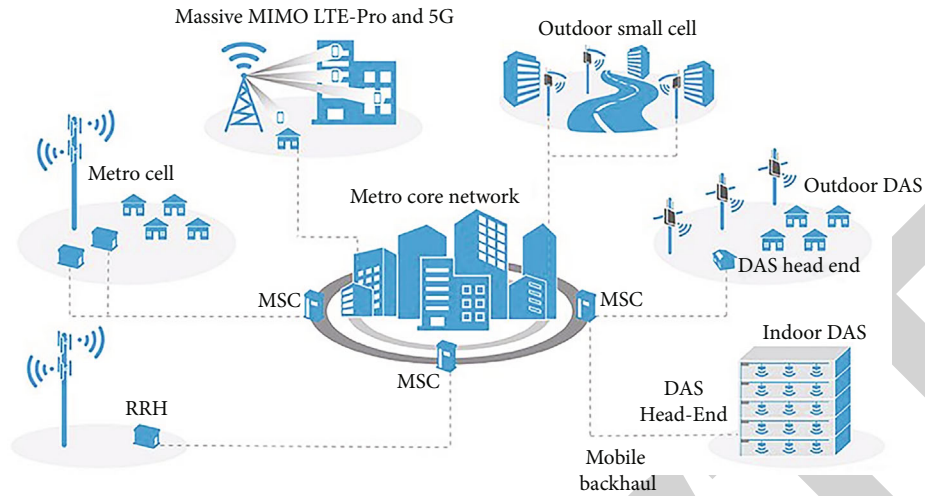


FIGURE 1: Development of intelligent lighting project.

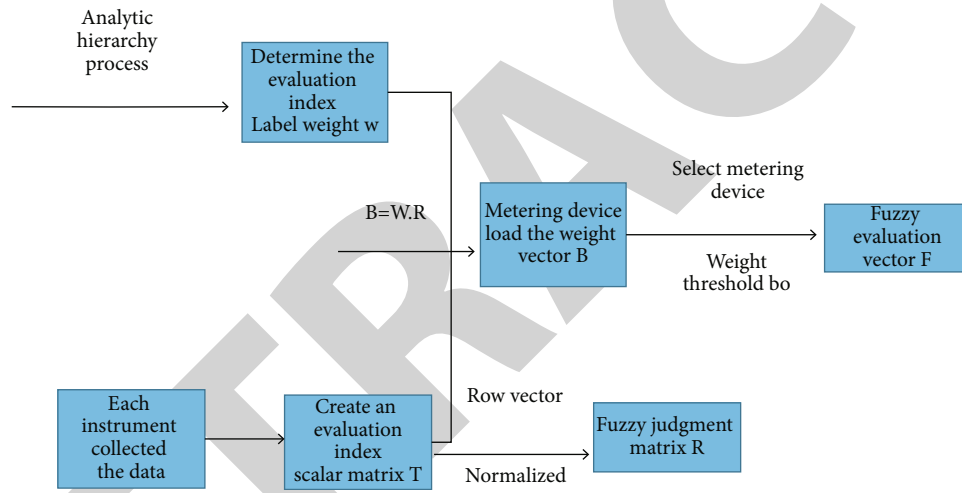


FIGURE 2: Flowchart of fuzzy estimation.

people's research on intelligent lighting mostly focuses on commercial lighting and office lighting, excessively pursuing people's comfort and economic benefits in indoor lighting, ignoring that the power consumption of urban road lighting is also very huge and the lighting quality and effect of urban roads also need to be improved. With the rapid development of the Internet of things and semiconductor electronic devices, people's demand for urban lighting is no longer limited to traditional memory, but only limited to the goal of brand lighting. With the emergence of intelligent lighting, more and more people hope that it can realize networking function (i.e., networking), intelligent function (i.e., intellectualization), and saving function (i.e., energy saving) and apply the above three functions to street lamps, meet people's demand for urban road lighting, and realize energy conservation and environmental protection. Compared with traditional road lighting, street lamps with intelligent lighting system have obvious advantages. Computers are used as the control platform to process relevant information, and wireless communication technology is used to transmit

information wirelessly; the perfect combination of the two technologies can remotely control the lighting lamps, which not only reduces the workload of managers but also can monitor, manage, and maintain the lighting situation in real time. According to the data fed back from the on-site environment, it can automatically adjust the LED lamps intelligently and provide lighting according to the actual situation of the site, to truly save electricity and protect the environment [3]. However, at present, the research of street lamp lighting in intelligent lighting is still missing or imperfect. The existing intelligent lighting street lamps are uniformly controlled on and off by the terminal, and there is a lack of design of single street lamp control. In addition, the existing street lamps are kept on for a long time during the night, and the lighting on demand is not achieved. If a street lamp breaks down, the street lamp cannot alarm the computer terminal by itself. The administrator cannot know the light and dark state of the street lamp at the first time, nor can he determine which street lamp has a problem through the computer terminal, which is not convenient

for people to manage the street lamp. If the above problems can be properly solved, it will undoubtedly bring new color and impact to people's night traffic, save more electric energy on modern urban road lighting, effectively reduce energy consumption, and improve environmental problems through power generation. Therefore, the research on LED intelligent lighting system based on Internet of things will bring more benefits to the country and people [4].

## 2. Literature Review

Liu and others used a BP neural network to create visual patterns of light entering a room. The inputs of the BP neural network model include the vertical illuminance of natural light, the height and azimuth of the sun, the temperature of outdoor environment, the distance between the illuminance prediction point and the window, the reflectivity of indoor wall, and the number and orientation of windows. The output is the illuminance value of the target point. Finally, the accurate control of the illuminance of the target point is realized. This method successfully solves the trouble caused by the cumbersome layout of indoor illuminance sensors in the use of natural light [5]. Tikhomirova and others took an office building in Dubai as the research object, designed an office building indoor lighting control system with building energy consumption monitoring function from the aspects of energy utilization and residents' health, and evaluated the impact of natural light used for indoor lighting on indoor lighting and temperature energy consumption, realizing the coordinated control of natural light and artificial light source [6]. Rohimi and others investigated the light comfort of office buildings. The results show that when the natural light is completely blocked, the comfort of indoor personnel is very weak and the office efficiency is low [7]. Chen and others analyzed the research results of indoor light environment and light comfort in recent years and put forward the evaluation index of light comfort, which provides a theoretical basis for the design of buildings [8]. Hassan et al. propose an improved research algorithm to improve the energy consumption of lighting. Manage lighting control systems to reduce lighting consumption through extreme value detection. The hardware of the system is designed, and the practicability and effectiveness of the control method are verified by using the hardware platform [9]. Yousuf and others invented an intelligent lighting control system, which supports intelligent heterogeneous lighting technology. Using ZigBee technology, a wireless sensor and actuator network is constructed to collect information such as natural illumination and indoor personnel activities and change the light intensity through server control to meet visual comfort [10]. Liu and others proposed an intelligent LED lighting control system based on fuzzy logic control theory [11]. The system can be divided into two modes. In the automatic mode, the light changes with the person's position, and the light intensity can also be controlled according to the natural light intensity. In manual mode, people can manually adjust the light intensity by using an application on a Bluetooth-enabled smartphone. In addition, the application also adds various lighting effects to users.

Users can create and use different scene modes by using their mobile phone. On the premise of not affecting users' visual comfort, they can reduce energy consumption by adjusting lights and related control systems. As China pays more and more attention to building energy conservation, national experts and scholars are also studying the rational use of natural light. Combining natural lighting with artificial lighting, the quantitative model of comfort evaluation index is established, the corresponding lighting control algorithm is studied, and a double fuzzy controller is established. The main fuzzy controller controls the opening angle with the external solar altitude angle and sky light mode as inputs to achieve rapid response. In order to improve the control accuracy, the angle fine adjustment is carried out by taking the opening angle and illumination deviation value as the input from the fuzzy controller. Under the environment of MATLAB and Dialux, based on different sky light modes and solar altitude angle, the comfort of light environment before and after light supplement as well as the energy-saving effect of only artificial lighting and natural daylighting is compared. It is proved that the proposed control method can achieve good lighting effect, and the energy-saving effect is 47% compared with the traditional method. The intelligent model of indoor illumination based on constant illumination is constructed by Leonard et al. Huang and others used the control idea of "daylight control" for the light environment of office space, combined natural light with artificial light supplement in the daytime, conducted experimental research on the energy-saving design of office lighting control system, and realized "green lighting" [12]. Durgalakshmi and others established an intelligent lighting model based on personnel displacement. The mathematical formula used in the model described the relationship between personnel position, artificial lighting equipment, and natural light and output the model using particle swarm optimization algorithm based on penalty function to find out the optimal combination of equipment dimming [13]. Chen and others established an expert system to control the indoor lighting control system combined with natural light and established an optimization model based on improved particle swarm optimization algorithm, realized the method of finding the best brightness combination of lamps in the shortest time, and achieved the lowest total energy consumption of lamps [14].

## 3. Method

In the communication process of the Internet of things, the accuracy and efficiency of information interaction are the most critical. In the building energy consumption management system, the selection of appropriate wireless communication mode is the primary problem, and many factors such as networking structure, communication distance, and economic cost need to be considered. At present, mature, stable, and widely used wireless communication technologies are within the scope of selection, such as UWB, Wi-Fi, ZigBee, GSM, and Bluetooth. UWB technology is a mature wireless communication mode under IEEE 802.15.3a standard. It uses wireless carrier communication technology with

TABLE 1: Scale of relative quantized value.

Factor $I$ versus factor $j$	Quantized value
Equally important	1
Slightly important	3
More important	5
Strongly important	7
Extremely important	9
Judge intermediate value	2.4.6.8

TABLE 2: Order correspondence.

Order	1	2	3	4	5	6	7	8	9
R	0	0	0.6	0.9	1.1	1.2	1.3	1.4	1.5

frequency bandwidth above 1 GHz. However, as a point-to-point communication network, it cannot meet the needs of one-to-many networking, so it does not have the conditions for application in large-scale building energy consumption acquisition system. Both Wi-Fi and ZigBee networks have the characteristics of reliable transmission and simple networking. ZigBee can complete multinode wireless networking and is widely used in various industries, making its development relatively simple, low cost, and short R&D cycle. It is the preferred wireless communication mode of the system; GSM network has fast communication speed and good stability, but at the same time, it has the characteristics of relying on communication operators. In Bluetooth wireless networking, one device can form a one-to-many network with up to seven subordinate devices at the same time, which cannot meet the networking requirements of many data acquisition nodes [15]. Based on the comparison of the characteristics of the above commonly used wireless communication technologies, GSM and ZigBee wireless communication networks can be selected and applied to the wireless communication under different environmental conditions in the large-scale building energy consumption acquisition system. The layout of energy consumption acquisition nodes should generally follow the methods of expanding the layout area, ensuring the layout density, no dead corner, and no blind area. However, due to the limitations of cost and productivity and the low annual utilization rate of some areas in the building, the reference value of energy consumption data is low. Therefore, in order to determine the specific layout of energy consumption data acquisition nodes, whether to install acquisition nodes is determined according to the importance of different areas in large buildings, that is, the importance of different areas is solved by using the method of weight analysis, to obtain the node layout. The specific process is shown in Figure 2. Analytic hierarchy process (AHP) is a decision-making method proposed by Thomas L. Saaty, a professor at the University of Pittsburgh, in the 1970s. It combines qualitative judgment and quantitative analysis to decompose the problem into multiple different constituent factors according to the nature of the problem and the objectives to be

achieved. According to the correlation and influence between the factors and the subordinate relationship, the factors are gathered and combined according to different levels to form a multilevel analysis structure model, so as to finally make the problem boil down to the determination of the weight of the lowest level (schemes and measures for decision-making) relative to the highest level (ultimate goal) or the arrangement of the order of advantages and disadvantages. Therefore, the weight of different regions can be determined by analytic hierarchy process, to judge whether to set acquisition nodes. The specific steps are as follows [16–18].

- (1) The hierarchical structure model is established to compare the decision-making objectives, considerations, and decision-making objects. The comparison results are expressed by relative quantitative values, as shown in Table 1, and the judgment matrix  $A$

$$A = (a_{ij})_{n \times n}, \quad (1)$$

where  $a_{ij} > 0$ ,  $a_{ij} = 1/a_{ji}$ ,  $n$  is the number of weight evaluation factors.

- (2) Normalize the columns of judgment matrix  $A$

$$\bar{a}_{ij} = \frac{a_{ij}}{\sum_{k=1}^n a_{ik}}. \quad (2)$$

- (3) Find the sum  $\bar{w}_i$  of the elements in each row of the judgment matrix  $A$

$$\bar{w}_i = \sum_{j=1}^n \bar{a}_{ij}. \quad (3)$$

- (4) Normalize  $\bar{w}_i$  to obtain  $w = \{w_1, w_2, \dots, w_i\}$

$$w_i = \frac{\bar{w}_i}{\sum_{i=1}^n \bar{w}_i}. \quad (4)$$

- (5) Consistency of inspection results

The consistency test index is  $CI = \lambda_{\max} - n / n - 1$ , where  $\lambda_{\max}$  is the maximum characteristic root of  $A$ . Refer to the order in Table 2 to obtain the average random consistency index RI.

Then, the consistency ratio  $CR = CI/RI$ .

When  $CR < 0.1$ , the consistency is satisfied, otherwise matrix  $A$  is corrected.

(6) Establish judgment factor matrix  $t$

$$T = \begin{bmatrix} t_{11} & \cdots & t_{1m} \\ \cdots & \cdots & \cdots \\ t_{n1} & \cdots & t_{nm} \end{bmatrix}, \quad (5)$$

where matrix  $T$  is the  $n \times m$  order matrix;  $n$  is the number of judgment factors,  $m$  is the location label of the collection node layout, and then  $t_{nm}$  represents the weight value of the  $n$ th judgment factor corresponding to position  $m$ , which is determined according to the actual object situation.

(7) Calculation of comprehensive judgment matrix

Normalize the vectors of each row of the judgment factor matrix  $t$  to obtain the comprehensive judgment matrix  $R$ :

$$R = \begin{bmatrix} r_{11} & \cdots & r_{1m} \\ \cdots & \cdots & \cdots \\ r_{n1} & \cdots & r_{nm} \end{bmatrix}. \quad (6)$$

(8) Calculate the installation weight vector of acquisition node

$$B = w \cdot R = (b_1, b_2, \cdots, b_m), \quad (7)$$

where  $w$  is the weight vector of judgment factors;  $b_1, b_2, \cdots, b_m$  is the weight of the layout position of each acquisition node.

(9) Establish fuzzy judgment vector

$$F_i = \begin{cases} 0, & b_i < b_o, \\ 1, & b_i > b_o, \end{cases} \quad (8)$$

$$F = \{F_1, F_2, \cdots, F_i\}. \quad (9)$$

Among them,  $F_i$  is the optimization result of the installation position weight of acquisition node  $i$ ,  $b_i$  is the installation position weight of acquisition node  $i$ ,  $0 < i < m$ , and  $b_o$  is the weight threshold, which is taken according to the actual situation of the object. Then,  $b_i > b_o$ , that is, when  $F_i$  is taken as 1, the position has high weight, and the acquisition node needs to be installed;  $b_i < b_o$ . If 0 is taken, the metering device does not need to be installed.  $F$  in equation (9) is the fuzzy evaluation vector.

The weight of each node can be determined according to the above node distribution method [19, 20].

The data centralization end is responsible for summarizing the data collected by multiple data collection nodes and uploading it to the data management terminal. The application object of this subject is large public buildings, so the

data centralization system is installed in each area. Its structural framework is shown in Figure 3.

The work of the data centralization end includes receiving, sending and analyzing data information, and connecting with the data terminal by using TCP/IP and gateway. Ordinary DSP controller is difficult to realize complex functions, so the main control part of the data centralization end selects Exynos 4412 dual core processor produced by Samsung company. The processor has powerful functions. By running Linux system in the processor, a large number of complex functions can be realized. In addition to the wireless communication module, an Ethernet card is also connected to the processor port to realize the rapid reflection of various instructions transmitted by wireless communication and TCP/IP protocol and analyze and process the data packets sent by the acquisition terminal and management terminal in time. At the same time, it is also equipped with synchronous dynamic random access memory (SDRAM), NAND flash memory, and SD expansion card slot to store data, so as to improve the cache processing ability of the system for a large amount of data. Fuzzy controller includes four parts: fuzzification, fuzzy reasoning, knowledge base, and clarity. The schematic diagram of fuzzy controller is shown in Figure 4.

The work of the data centralization end includes the reception, transmission and analysis of data information, and the connection with the data terminal by using TCP/IP and gateway. It is difficult for the ordinary DSP controller to realize complex functions, so the main control part of the data centralization end selects the Exynos 4412 dual core processor produced by Samsung. The processor has powerful functions. By running Linux system in the processor, a large number of complex functions can be realized. In addition to the wireless communication module, an Ethernet card is also connected to the processor port to realize the rapid reflection of various instructions transmitted by wireless communication and TCP/IP protocol and analyze and process the data packets sent by the acquisition terminal and management terminal in time. At the same time, it is also equipped with synchronous dynamic random access memory (SDRAM), NAND flash memory, and SD expansion card slot to store data, so as to improve the cache processing ability of the system for a large amount of data [21, 22].

Fuzzy control has the following basic operations.

### 3.1. Fuzzification Operation.

$$x = Fz(x_o), \quad (10)$$

where  $x_o$  is the clarity of the input,  $x$  is the fuzzy set, and  $Fz$  is the fuzzier.

### 3.2. Sentence Connection Operation.

$$R = \text{also}(R_1, R_2, \cdots, R_n), \quad (11)$$

where  $R_i, i = 1, 2, 3, \cdots, n$ ; numbers represent the fuzzy implication represented by this provision; also represents the combinatorial operation of all relationships.

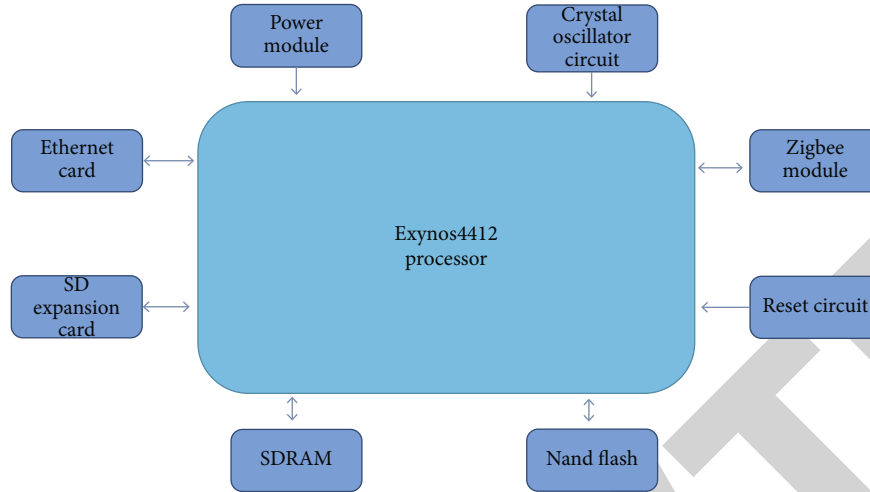


FIGURE 3: Structural block diagram of data centralization terminal.

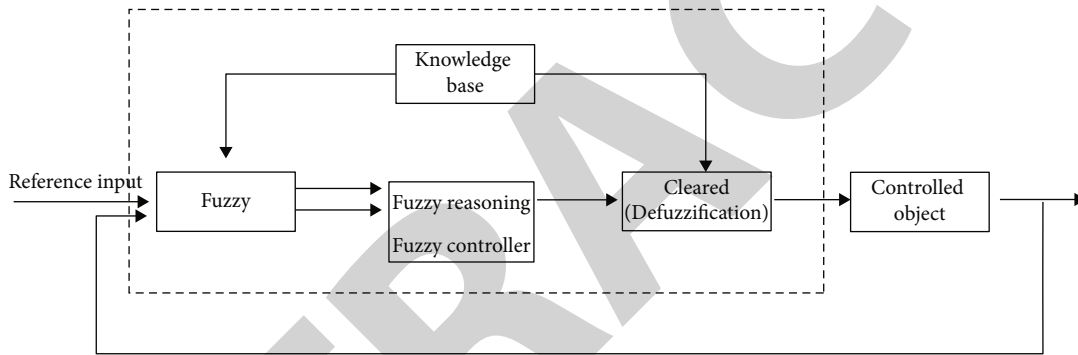


FIGURE 4: Schematic diagram of fuzzy controller.

### 3.3. Synthesis Operation.

$$z = (x \text{ and } y) \circ R, \quad (12)$$

where  $x$  and  $y$  represent the input fuzzy quantity,  $z$  represents the output fuzzy quantity, and represents the sentence connection operator, and “ $\circ$ ” represents the composition element operator.

**3.4. Clarity Calculation.** The calculation results obtained above are fuzzy quantities, which must be used in the actual operation and control, and finally need to carry out clarity calculation.

$$z_o = Df(z), \quad (13)$$

where  $z_o$  represents the clarity amount and  $Df$  is the clarity operator.

At present, the common network software platform architecture is generally divided into C/S and B/S. The previous building energy consumption management platform usually adopts the form of traditional C/S architecture, that is, client/server architecture. Its feature is that users connect to special servers through client software, and all operations are completed based on the client. Therefore, the operation

of C/S architecture needs to establish a special local server to complete various connections and information interaction, which is less flexible. At the same time, the client software is developed for special projects and servers, which is difficult to upgrade and maintain and has low universality. The B/S architecture, namely, browser/server, is an improvement based on the C/S architecture. In order to solve the problem of poor universality and flexibility of the original C/S architecture, the application of Internet and web side technology is added. Through the application of dynamic web page technology and cloud server technology, the B/S architecture can realize cross space and cross platform development and use. Users only need to visit the web page through the browser anytime and anywhere to realize the functions that need complex client software in C/S architecture, which greatly reduces the development cost and operation and maintenance cost of the platform.

The infrastructure of B/S architecture is divided into presentation layer, application layer, and data layer, as shown in Figure 5 [23, 24].

When using this mode, the operations of various functions are mainly concentrated on the web page, and the data interaction is realized through the connection between the web server and the database with the help of the browser software on the personal computer and mobile phone. Users



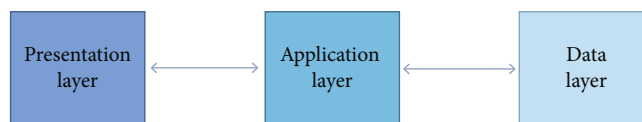


FIGURE 5: Basic B/S architecture.

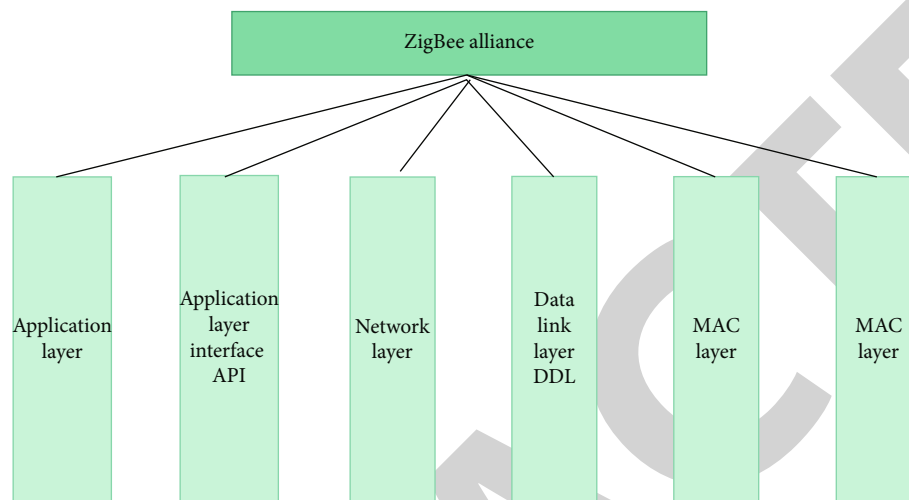


FIGURE 6: Z-stack protocol stack structure.

can use a variety of browsers, such as Internet Explorer, Google Chrome browser, and 360 browser to access the web interface. Only the commonly used browser can solve the functions that can be realized by the specific and professional application client required in the original traditional mode.

There are many contents of ZigBee protocol. CC2530 chip has provided ZigBee physical layer and MAC layer functions. ZigBee development is mainly for various specific applications. The upper layer protocol needs to use a mature ZigBee protocol stack, which is implemented by code. All devices in the same network must conform to a protocol stack specification. Z-stack is a protocol stack launched by TI company and ZigBee alliance. It is suitable for TI's CC2530 series chips. CC2530 chip is used in the hardware design of intelligent lighting system, so Z-stack protocol stack is used for development. Z-stack is constructed with the idea of the operating system and adopts the event round robin mechanism. After the initialization of each layer is completed, the system enters the low-power mode. When an event occurs, the system is awakened and enters the interrupt processing event. After the event is completed, it reenters the low-power mode. If several events occur at the same time, the system will judge the priority and process them one by one. This system can greatly reduce the power consumption of the system. The workflow of Z-stack mainly includes system startup, driver initialization, osal initialization and startup, and task polling of the operating system. The structure of Z-stack protocol stack is shown in Figure 6.

According to IEEE 802.15.4 and ZigBee standards, the Z-stack protocol stack implements API application function interface layer, Hal hardware abstraction layer, MAC media

access layer, NWK network layer, osal operating system abstraction layer, security layer, and ZDO device object layer [25].

In the protocol stack, the application layer has covered the APS sublayer and ZDO connected with the network layer. The network layer ensures the correct operation of the MAC layer and provides a suitable interface to connect the application layer, including two service entries: data service entry and management entry. The former realizes network level protocol data unit and protocol specific routing. The latter can configure a new device, start a network, join or leave the network, address allocation, etc. The security specification involves the security methods provided by ZigBee, including key establishment, key transmission, framework protection, and device management. The media access control layer follows the IEEE 802.15.4 protocol and is responsible for the establishment, maintenance, and termination of wireless data links between devices, data transmission and reception in confirmation mode, optional time slots, low delay transmission, and supports various network topologies. Each device in the network is addressed with a 16-bit address. The semiopen source code, media access layer, network layer, and application support layer of Z-stack protocol stack have not been modified, but the developers of Z-stack provide a fully functional API function set to modify and write to meet the needs of practical applications. The general steps for Z-stack protocol stack to realize wireless data communication are networking, calling the networking function of the protocol stack, and adding the network function to realize the establishment of the network and the addition of nodes. Sending: the sending node calls the wireless data sending function of the protocol stack to

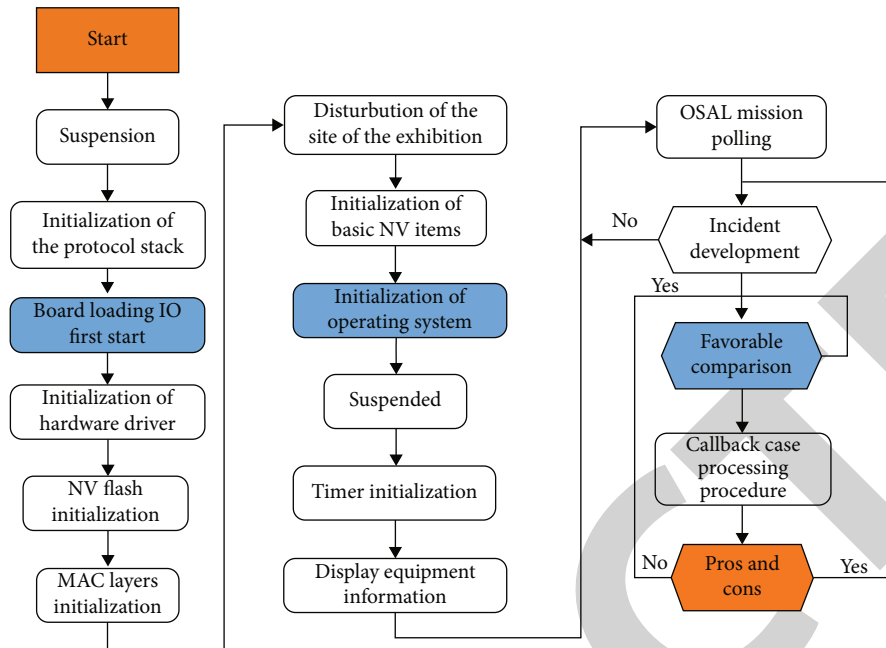


FIGURE 7: Z-stack workflow.

realize wireless data sending. Receiving: the receiving node calls the wireless data receiving function of the protocol stack to realize wireless data receiving. The main workflow chart of Z-stack is shown in Figure 7.

The intelligent lighting system is composed of PC host computer measurement and control center and wireless sensor control network. The PC host computer measurement and control center is the host computer human-computer interaction interface made by LabVIEW, and the wireless sensor control network is composed of ZigBee network. ZigBee network includes ZigBee coordinator, ZigBee LED dimming node, and ZigBee illumination intensity node. PC upper computer measurement and control center communicates with ZigBee coordinator through serial port; ZigBee coordinator communicates with light intensity node and dimming node through ZigBee wireless network; ZigBee LED dimming node is equipped with LED lamps, and the light intensity node is equipped with light intensity sensor. The overall framework of intelligent lighting system based on ZigBee technology is shown in Figure 8.

The main tasks of ZigBee coordinator in ZigBee wireless network include device discovery, device identification, and network establishment. ZigBee coordinator communicates with PC upper computer measurement and control center through serial port, obtains the control command sent by it, and uploads the light intensity detection data. Figure 9 is the workflow chart of ZigBee coordinator.

ZigBee's network establishment includes two processes: the coordinator initiates the network establishment and channel selection process. Routing node and terminal node join the network process. ZigBee sensor network is established by the network initiated by the coordinator. In the layered communication protocol, the upper and lower layers communicate through the service access point (SAP). The

new network starts with the request function NLME\_NETWORK\_FORMATION.request primitive and establishes the network by calling the network layer request function NLME\_networkformationrequest0. It is mainly divided into the following seven steps:

- (A) The application layer sends NLME\_networkformationrequest to the network layer
- (B) After receiving the request, the network layer sends the MAC\_MlmeScanReq request to the MAC layer
- (C) MAC layer starts channel energy detection and feeds back the MAC\_MLME\_SCAN\_CNF detection results to the network layer
- (D) The network layer selects the best channel group according to the result returned by the MAC\_MLME\_SCAN\_CNF and sends a request to the MAC layer using the MAC\_MlmeScanReq primitive
- (E) MAC layer scans the channel and reports the scanning information to the network layer
- (F) The network layer selects the channel and pan identifier according to the scanning results and then sets the 16-bit short address 0x0000 of the coordinator in the network
- (G) The network layer sends the MAC\_MlmeStartReq request primitive to the MAC layer. If the status information returned by the MAC layer function MAC\_MLME\_STAR\_CNF is success, the network is established successfully

The coordinator establishes ZigBee network through the above seven steps. After completing network establishment

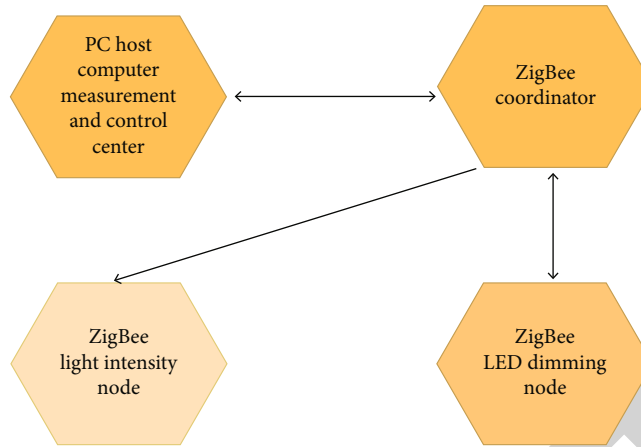


FIGURE 8: Overall framework of ZigBee-based intelligent lighting system.

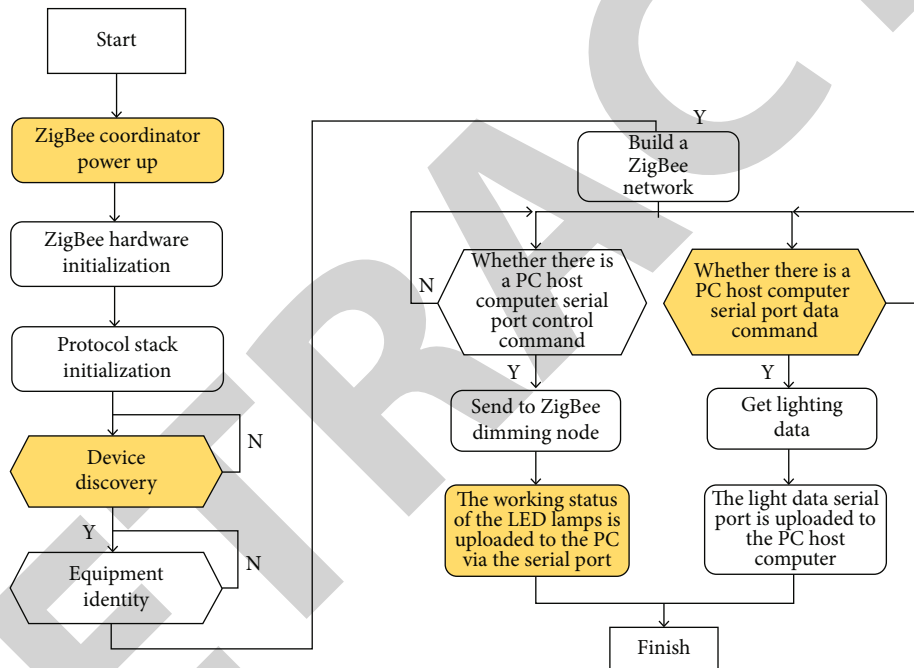


FIGURE 9: Workflow of ZigBee coordinator.

and channel selection, the coordinator is equivalent to a routing device in the network. The network establishment process is shown in Figure 10.

If each equipment wants to join the network established by the coordinator, it must join the network access process through a certain application. After the establishment of the network coordinator, the coordinator passively waits for the network device to apply to join the network. As long as the received MAC layer sends the MAC mlmessociatereq request primitive, it indicates that there is a node device applying to enter the network through the MAC layer, as shown in Figure 11, mainly through the following eight steps.

LabVIEW programming environment is the same as other visual development environments. The program interface and code are separated. The program interface is called

VI front panel, and the code is called VI program block diagram. The front panel is a graphical user interface with interactive input and output VI controls, which are called input control and display control, respectively. Input controls, including switches, buttons, and other types of input devices, can input the input control data and provide it to the program block diagram. The display control includes graphics (graph and chart), LED, and other display output objects. The data processed by the program block diagram is displayed through the display control. The front panel inputs and outputs data, and the data processing is realized by program code programming. The program programming in LabVIEW is built in the form of block diagram. The program block diagram is the graphical source code to realize the logic function of VI system. The programming elements in the block diagram include not only the connection

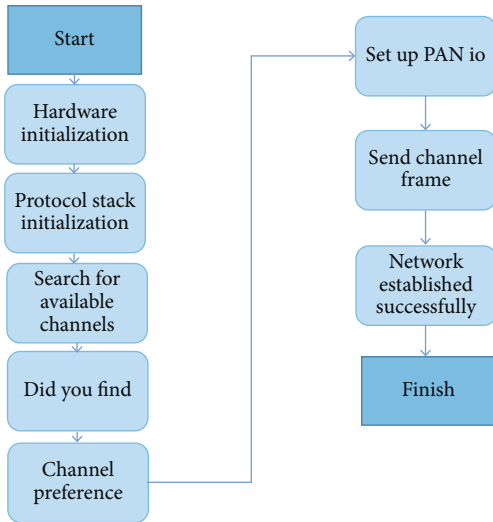


FIGURE 10: Flowchart of network establishment.

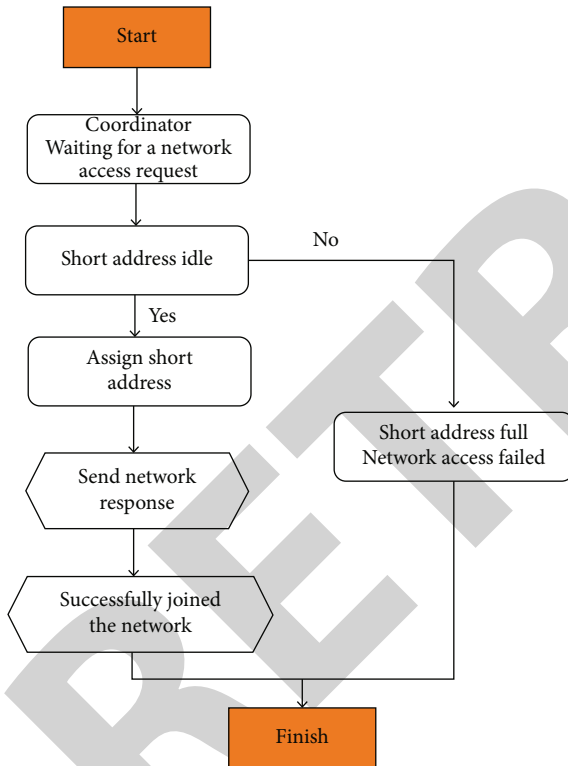


FIGURE 11: Flowchart of node network access.

terminals corresponding to the controls on the front panel. There are also functions, sub-VI, constants, structures, and connections. The node types and functions of the program block diagram are shown in Table 3.

Each object is wired to create a program block diagram. Connection connects the input control with the display control and function or sub control, from the data of the input control to the stream function and sub-VI, then from these functions and VI to other functions and sub-VI, and finally to the display control. The intelligent lighting system of

green building is mainly composed of ZigBee wireless sensor control network and PC host computer measurement and control center. The ZigBee coordinator in the wireless sensor control network is connected with the PC host computer measurement and control center through 230 to USB serial port. The communication connection between the two completely depends on serial communication, so the host computer needs to configure the driver and related programs of serial communication, that is to say, serial communication is the most critical step to be realized by LabVIEW. Ni company provides users with a variety of hardware devices in LabVIEW to meet different measurement and control requirements, including data acquisition hardware (DAQ), real-time measurement and control, GPIB, serial port and instrument control, and sound and vibration measurement and analysis; through rich drivers, LabVIEW can easily connect and communicate with any hardware device provided by Ni. Through general drivers or interfaces, such as visa, IVI, OPC, and ActiveX DLL, LabVIEW can communicate with almost any manufacturer or even self-made hardware. The connection between the upper computer of the intelligent lighting system and the wireless sensor control network can be realized by calling the visa serial port function through LabVIEW.

The above eight VI can be configured with serial communication function, and the specific functions are shown in Table 4.

Intelligent lighting system PC: the main functions of host computer measurement and control center are as follows: analyze the light intensity data uploaded by ZigBee coordinator through serial port; display the light intensity data after analysis; display the historical data drawing of light intensity data; save the historical data of light intensity; after analyzing the light intensity data, the brightness PWM value of the lamp is transmitted to the ZigBee coordinator through the serial port; users can turn on and off the lights manually; users can send instructions directly to ZigBee coordinator through serial port.

On the basis of hardware circuit design and system function design of intelligent lighting system, the overall scheme of intelligent lighting system and the overall framework of intelligent lighting system are designed. This paper introduces the software development environment of wireless sensor control network and PC host computer measurement and control center, designs the program of ZigBee coordinator, ZigBee light intensity node, and ZigBee LED dimming node of wireless sensor control network, and designs the LabVIEW program of green building intelligent lighting system of PC host computer measurement and control center.

#### 4. Experiment and Discussion

The fuzzy controller includes four parts: fuzzification, fuzzy reasoning, knowledge base, and clarity. The schematic diagram of the fuzzy controller is shown in Figure 12.

Each input of the fuzzy controller corresponds to a fuzzy language variable [26]. The value of fuzzy language variable is not an exact number, but a fuzzy set composed of some fuzzy languages. For example, if “the influence between

TABLE 3: Node types and functions.

Node type	Function
Function	The elements of a function in execution are equivalent to operators and functions
Sub-VI	Take the whole VI program Z as a part of another VI program, which is equivalent to a subroutine
Express	Sub-VI assisting in measurement tasks
Structure	Execute control elements, such as for loop, while loop, and conditional structure

TABLE 4: Serial port subplate selection node.

VI name	Function
Visa configuration serial port	Serial port initialization configuration
VISA write	Writes data from the buffer to the specified serial port
VISA read	Read the byte length of the specified length from the serial port to the buffer
Number of bytes of visa serial port	Returns the number of input buffer bytes of the specified serial port
Visa serial port interrupt	Send interrupt operation to the specified serial port
Visa set I/O buffer size	Sets the size of the serial port IO buffer
Visa off	Close the serial port
Visa empties the I/O buffer	Clear serial port I/O buffer

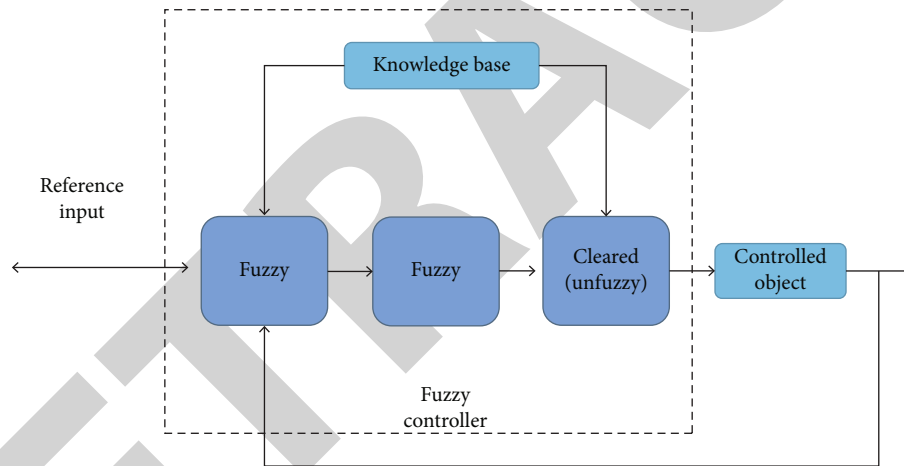


FIGURE 12: Schematic diagram of fuzzy controller.

two things” is taken as a fuzzy language variable, the value of fuzzy language variable is a fuzzy set composed of fuzzy languages such as “big” and “big.” Fuzzification is to transform the precise input into the membership degree of each language value of fuzzy language variable. The knowledge base consists of two parts: database and rule base. The database contains the parameters required for the scale transformation of input variables, the fuzzy segmentation of universe space, the selection of membership function, and so on. The rule base contains the rules of fuzzy reasoning, which is composed of a series of fuzzy language rules in the form of “If then.” Each fuzzy rule includes antecedent and consequent. The antecedent is composed of input and state, and the output variable is consequent. Fuzzy control rules are the basis of fuzzy control. Fuzzy rules can be obtained through expert experience, control engineering knowledge, operator experience, and so on. Fuzzy reasoning is to carry out fuzzy reasoning according to the rules in the rule base.

It is assumed that a fuzzy rule base is established for a two input one output fuzzy controller, as shown in

$$\begin{aligned}
 R_2 & \text{ if } x \text{ is } A_2 \text{ and } y \text{ is } B_2 \text{ then } Z \text{ is } C_2, \\
 R_N & \text{ if } x \text{ is } A_n \text{ and } y \text{ is } B_n \text{ then } Z \text{ is } C_n, \\
 R_1 & \text{ if } x \text{ is } A_1 \text{ and } y \text{ is } B_1 \text{ then } Z \text{ is } C_1.
 \end{aligned} \tag{14}$$

If the input  $x$  of the controller is  $A$  and  $y$  is  $B$ , the expression of the output fuzzy variable  $Z$  can be deduced according to the fuzzy rules in the rule base, as shown in

$$\begin{cases} c = (A \text{ and } B) \circ R, \\ R \equiv \bigcup_{j=1}^n R_n, \\ R_n = (A_n \text{ and } B_n) \circ c. \end{cases} \tag{15}$$

TABLE 5: Uniform quantization.

Quantization level	-5	-4	-3	-2	-1	0	1	2	3	4	5
Variation range	(-5.5, -4.5)	(-4.5, -3.5)	(-3.5, -2.5)	(-2.5, -1.5)	(-1.5, -0.5)	(-0.5, 0.5)	(0.5, 1.5)	(1.5, 2.5)	(2.5, 3.5)	(3.5, 4.5)	(4.5, 5.5)

TABLE 6: Nonuniform quantization.

Quantization level	-5	-4	-3	-2	-1	0	1	2	3	4	5
Variation range	(-3.2, -1.60)	(-1.6, -0.8)	(-0.8, -0.4)	(-0.4, -0.2)	(-0.2, -0.1)	(-0.1, 0.1)	(0.1, 0.2)	(0.2, 0.4)	(0.4, 0.8)	(0.8, 1.6)	(1.6, 3.2)

Among them, the “and” operation usually uses the method of taking the small or quadrature, and the “O” synthesis operation usually uses the method of maximum, minimum, or maximum product. Clarity is to solve the fuzzy. The output fuzzy quantity is obtained through fuzzy reasoning. For the actual control computer, only the accurate quantity can be recognized. Defuzzification is to accurately solve the output fuzzy quantity. The fuzzy quantity is transformed into the required accurate quantity. There are usually methods such as maximum center of gravity method and maximum center of gravity method.

As explained above, fuzzy control is a method of simulating human actual control. In the process of practical manipulation, the following kind of speech formula is usually used to express the actual control mode of experts. If (meet some conditions) then (draw some corresponding conclusions) this formula is full of fuzzy concepts. For example, “if the air humidity is low, wear more clothes” and other sentences, in which “low” and “more” are vague and unclear. Such if then formula is usually called fuzzy conditional statement. Therefore, fuzzy control principles belong to fuzzy statements. The premise is the assumption in the application of objective reality, and the conclusion is the solution to this assumption. For the fuzzy system of input or output, there are corresponding solutions such as multiple input and multiple output and multiple input and single output. For example, for the scheme of multiple input and single output, the expression of fuzzy control rules is shown in [27]

$$\begin{aligned}
 R_1 &: \text{if } x = A_1, y = B_1, \text{ then } z = c_1, \\
 R_2 &: \text{if } x = A_2, y = B_2, \text{ then } z = c_2, \\
 R_3 &: \text{if } x = A_3, y = B_3, \text{ then } z = c_3.
 \end{aligned} \tag{16}$$

The three letters belong to language variables, but  $x$  and  $y$  are conditional input variables, and  $Z$  belongs to control variation.  $A_i$ ,  $B_i$ , and  $C_i$  ( $=1, 2, \dots$ ), they are the amount of language change in their respective domains, and all these principles together form a rule database.

Fuzzy control has the following basic operations.

(1) Fuzzification operation

$$x = \text{Fz}(x_o). \tag{17}$$

(2) Sentence connection operation

$$R = \text{also}(R_1, R_2, \dots, R_N). \tag{18}$$

(3) Synthetic operation

$$z = (x \text{ and } y) \circ R. \tag{19}$$

(4) Clarity operation

The calculation results obtained above are fuzzy quantities, which must be used in the actual operation and control, and finally need to carry out clarity calculation.

$$z_o = \text{DF}(z), \tag{20}$$

where  $z_o$  represents the clarity amount and DF is the clarity operator.

The knowledge base of fuzzy controller consists of two parts. One part is the database used, and the other part is the collection of all fuzzy control rule bases. The database contains some parameter data related to data analysis, such as numerical conversion and spatial segmentation rules. Fuzzy control rules are the experience of system operators in years of hard work.

**4.1. Input Conversion.** For the processing of actual input variables, it is necessary to convert them to the required range in a linear or nonlinear way.

The universe is either continuous or discrete. Generally speaking, quantization can be uniform or nonuniform. Tables 5 and 6 show the case of uniform quantization and the case of nonuniformity, respectively.

*4.2. Fuzzy Segmentation of Input and Output Space.* Various hypothetical languages in the relevant provisions of fuzzy control form the fuzzy input space, and the language representing the corresponding solutions forms the fuzzy output space. The variable values of various hypothetical situations all belong to the fuzzy language pseudonym Lu, and all these language names together constitute the fuzzy set of various hypothetical languages. Each fuzzy language name will be associated with a fuzzy set, and how fine its fuzzy control can depend entirely on its order of magnitude. If negative  $B_i$  stands for negative large, it is called NB for short; negative medium stands for negative medium, referred to as NM for short; negative small stands for negative small, abbreviated as NS; zero stands for zero, abbreviated as ZE; positive small stands for positive small, abbreviated as PS; positive medium stands for center, referred to as PM for short; positive big stands for Zhengda, abbreviated as Pb. The number of fuzzy segmentation also gives the number of fuzzy rules in the optimal case. For example, for a two input single output fuzzy system, the fuzzy segmentation number is 3 and 7, and then, the rule of the optimal number of products is 21. Therefore, the more the number of fuzzy segmentation, the more the number of controllable criteria; the fuzzy segmentation cannot be too large; otherwise, more controllable rules are needed, which also makes things complicated. Similarly, if the number of fuzzy segmentation is small, the rules will be too general and it is difficult to adjust the relevant situations. Nowadays, there is still a lack of a guiding way and process that can give a good number of fuzzy segmentation, which still needs to seek experience and try.

According to the theory of fuzzy control and the composition principle of fuzzy controller, the intelligent lighting system adopts the error  $e = E_d - E_i$  and error change  $Se$  between indoor light intensity  $E_i$  and illuminance set value  $E_d$  as the input variables of fuzzy controller, and the output is the system control value PWM to form a two-dimensional fuzzy controller. In building characters, the standard of light intensity is generally more than 150 lx. It will not exceed 750 lx. According to the illuminance requirements of building lighting, the universe of light intensity is  $[0, 1000 \text{ lx}]$ , the set value of light intensity of building lighting is  $e_d = 500 \text{ lx}$ , the basic universe of light intensity error  $E$  is  $[-500, 500]$ , the basic universe of error change  $O_e$  is  $[-100, 100]$ , and the basic universe of system control value PWM output is  $[0, 100\%]$ . According to the basic rules of light intensity control, when the indoor light intensity is greater than the set value of light intensity, the LED lamp is turned off. Therefore, when  $e < 0$ , the LED lamp is turned off and the PWM output value is 0. Therefore, when designing the fuzzy controller of intelligent lighting system, the basic domain of illumination intensity error  $E$  is  $[0, 500]$ , excluding the case that the indoor illumination intensity is greater than the set value of illumination intensity, which verifies the effectiveness of the experiment.

## 5. Conclusion

Aiming at the problem of energy consumption in buildings, in response to the key energy-saving project “green lighting” of the 12th Five-Year Plan, a green building intelligent lighting system based on the Internet of things is designed. The specific work is mainly divided into four stages: intelligent lighting system design, system hardware design, system software design, and system fuzzy control algorithm design. Firstly, the task function of the intelligent lighting system of green building is analyzed as a whole. The main tasks of the intelligent lighting system are detecting the light intensity of indoor specified position, intelligent dimming of indoor specified position light source, uploading the indoor light intensity data, and light source working state data. The wireless sensor network and intelligent lighting control system are selected and analyzed, and then, the basic lighting sensor network and intelligent lighting control system are selected from the PC. After determining the functional requirements of the intelligent lighting system, the hardware circuit of the intelligent lighting system is designed. From ZigBee selection and light intensity sensor selection in wireless sensor control network to ZigBee wireless communication module circuit design, light intensity sensor circuit design and LED lamp driving circuit design. Finally, cc2530f256 of Company II is selected as the ZigBee chip of wireless sensor control network, and bh1750fvi digital light intensity sensor is selected as the sensor of system light intensity acquisition node. Based on the hardware circuit design and system function design of intelligent lighting system, the overall software scheme of intelligent lighting system is designed. The overall framework of intelligent lighting system is designed. This chapter introduces the software development environment of wireless sensor control network and PC upper computer measurement and control center, designs the program of ZigBee coordinator, ZigBee light intensity node, and ZigBee LED dimming node of wireless sensor control network, and designs the LabVIEW program of green building intelligent lighting system of PC upper computer measurement and control center. Finally, the design and research of intelligent lighting system control algorithm are introduced, and the fuzzy control algorithm is applied to intelligent lighting system. In this paper, the fuzzy control system is introduced, and the fuzzy controller of the intelligent lighting system is designed. The fuzzy control rule table and fuzzy control query table of the intelligent lighting system are obtained through the fuzzy control algorithm. The best adjustment value of the intelligent dimming can be obtained through the fuzzy control query table. The intelligent dimming control of intelligent lighting system can be realized by command. For the work done in this paper, the following aspects can be further studied in the future: for different types of building structures and facility types, further study the node layout strategy for energy consumption data collection and expand the collected data types so that the system can be universal in various types of buildings.

## Research Article

# GIS-Based Urban Agglomeration Landscape Dynamic Observation and Simulation Prediction Algorithm

**Meng Liu** 

*Academy of Fine Arts, XinXiang University, Xingxiang, Henan 453000, China*

Correspondence should be addressed to Meng Liu; [liumeng0317@xxu.edu.cn](mailto:liumeng0317@xxu.edu.cn)

Received 23 February 2022; Revised 25 March 2022; Accepted 2 April 2022; Published 23 April 2022

Academic Editor: Yanqiong Li

Copyright © 2022 Meng Liu. This is an open access article distributed under the Creative Commons Attribution License, which permits unrestricted use, distribution, and reproduction in any medium, provided the original work is properly cited.

In order to improve the intelligence level of urban agglomeration landscape, this paper conducts dynamic observation and simulation prediction of urban agglomeration landscape based on geographic information system. There are many characteristics of GIS technology itself that can be well matched with urban landscape research, so in the process of actually studying the green space landscape pattern, GIS technology has a very large space to play. The first is to use GIS technology to collect basic data of different types of scenic spots. Raster data and vector data are two important data in GIS technology. Among them, vector data with point, line, and surface morphology can relatively express the landscape ecology. Raster data is to determine the specific position of each pixel through the vertical and horizontal row and column relationship of the pixel, which is relatively simple in structure and easy to topology. According to the characteristics of the urban agglomeration landscape, the urban agglomeration landscape is reconstructed on the virtual simulation platform using GIS technology. It can meet the long-term sustainable development of the ecological environment of the scenic area. The research of this paper mainly belongs to the scope of practical research. Taking the existing research results as the first point of experimental research, combined with the relevant research results of design, the dynamic observation and simulation prediction algorithm of urban agglomeration landscape are constructed.

## 1. Introduction

In the process of urban environment planning in the past, it was often based on paper maps combined with corresponding historical data and information to integrate all the data through manual on-site surveys, so as to realize the planning of the urban environment. In this way, it not only consumes a lot of manpower, material resources, and financial resources but also because of the large amount of content designed in urban environmental planning; the workload is large, the process of manual data collection is slow, and there is a certain information gap, which leads to information collection [1]. Inaccurate and untimely phenomena occur. GIS technology, geographic information system, and RS technology, remote sensing technology, combined with advanced computer technology, can efficiently collect and store urban environmental spatial information and output the collected

information in the form of data, with extremely high information collection and transmission capabilities, so it also has higher application value. In urban environmental planning, RS and GIS technologies can efficiently collect urban population information, building structure, urban greening distribution, and other information and form a complete urban environmental information database, which is processed by advanced computer technology such as layer overlay and makes GIS used as a database in urban environmental planning [2–4].

With the continuous development of science and technology, in the process of urban environmental planning, the application of GIS technology has become more and more obvious, which can greatly improve the efficiency of urban environmental planning, increase the efficiency of staff, and thus promote urban development. However, in the actual application process, some cities still have certain



problems in the application of GIS technology in urban environmental planning, and the application level is low, which restricts the pace of urban environmental planning. The timely and accurate urban environmental information obtained by using GIS technology can greatly reduce the burden of manual surveys, thereby completing more planning tasks within a certain period of time [5–9]. However, in the actual application process, GIS technology is only used as information query, and simple icon drawing tools did not apply GIS technology in depth, which not only affected the urban environmental planning process but also caused a serious waste of available resources [10–11].

The geographic information system integrates relatively complete spatial information and geographic distribution data. GIS uses computer hardware and software as the technical carrier to realize the functions of geographic distribution data collection, storage, calculation, analysis, and display [12]. The application of GIS technology in landscape planning and analysis of landscape development trends is more common in foreign countries. With technical exchanges and cooperation, the frequency of using GIS in landscape planning in China has gradually increased. With the acceleration of the information age, the state has increased its efforts to build smart scenic areas, and the planning of vegetation landscape patterns has become an important part of smart scenic areas. In this study, GIS is used as a technology to support the dynamic observation and simulation prediction algorithm of the simulated urban agglomeration landscape. The specific realization ideas are as follows: ① using GIS technology to obtain basic data of the research area, including topographic point cloud data, surface orthophotos, vegetation distribution maps, and other information, and calculate and analyze the vegetation landscape pattern index of the area and analyze the vegetation distribution; ② plan the vegetation pattern of the scenic spot according to the advantages and disadvantages of vegetation distribution, and use basic data to build terrain, trees, and grassland models in the computer to present a virtual vegetation pattern simulation [13, 14]. As a result of planning, the use of simulation for vegetation planning in smart scenic areas is conducive to changing the landscape pattern index in real time, revising the vegetation layout, predicting the planning efficiency and scientificity of vegetation in scenic areas, and providing decision support for smart city cluster landscape planning and design.

## 2. GIS Technology-Based Urban Agglomeration Landscape Dynamic Observation and Simulation Prediction Algorithm

*2.1. Color Description of Urban Agglomeration Landscape Pictures Based on GIS Technology.* RGB color balance is a very typical color description method. The light matching to be measured satisfies Grassman's law. The specific  $R$ ,  $G$ , and  $B$  tristimulus values are shown in the following formula:

$$C[C] = R[R] + G[G] + B[B]. \quad (1)$$

In

$$\begin{cases} R = \int_{\lambda} k\varphi(\lambda)\bar{r}(\lambda)d\lambda, \\ G = \int_{\lambda} k\varphi(\lambda)\bar{g}(\lambda)d\lambda, \\ B = \int_{\lambda} k\varphi(\lambda)\bar{b}(\lambda)d\lambda, \end{cases} \quad (2)$$

where  $C$  represents the color to be measured,  $[M]$  represents three stimulus value units,  $\lambda$  represents the wavelength of the light to be measured,  $k$  represents the spectral distribution coefficient,  $\varphi(\lambda)$  represents the spectral distribution function, and  $\bar{r}$ ,  $\bar{g}$ , and  $\bar{b}$  represent the three stimulus values of the spectrum. The modeling process through the image map is shown in Figure 1.

*2.2. Urban Height Form.* The research on the height of the city should establish dimensions from the perspectives of managers and experiencers. From the perspective of city managers, continue the landscape pattern, shape the characteristic city image, and establish the city's morphological order from the overall level; from the perspective of city experiencers, outline a beautiful city outline at the human scale and experience the city space [15, 16]. Based on this goal, a three-dimensional interactive model is used as a tool to guide the shaping of the height of the city. Multifactor evaluation is to extract the important evaluation factors that are highly controlled by the city, assign weight values, and establish evaluation standards and systems to obtain a highly partitioned extended model. Using GIS as the platform, through the determination of the guidance range and systematic calculation, a three-dimensional guidance model is initially established. Based on the guiding objectives, two levels of "functionality + environmental," three types of elements, and six specific land use factors are selected for comprehensive evaluation. Functional factors mainly consider factors related to the potential of land use, including two types of factors, land value and land accessibility, and specifically cover four types of specific land use factors, planning location, benchmark land price, urban roads, and urban hub stations; environmental factors mainly from the perspective of human settlements, based on landscape elements, two types of specific land use factors in mountainous areas and waterfront areas are evaluated. (1) For land benchmark land price and location value, the land benchmark land price reflects the current value of the land parcel and reflects the overall level and changing trend of land prices in the land market. The value of land parcels sensitively reflects various land use conditions such as location, urban facilities, and environmental factors. These conditions spontaneously dominate the reasonable construction height of land use and potentially reflect the differences in land economic conditions and intensive use value. The planned location reflects the future value of the plot. The central area of the city plays a positive role in economic development and has comparative advantages over other areas [17]. For value assignment

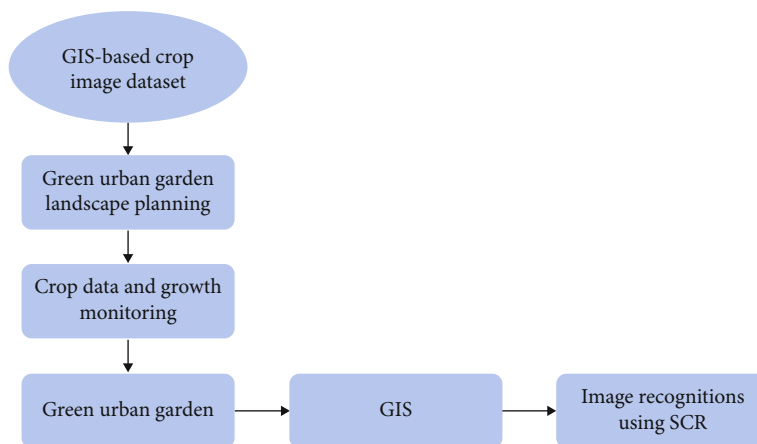


FIGURE 1: GIS city data processing.

method, judge the value of the plot based on the weight of the planned area. The higher the weight of the plot, the higher the value of the land. In the core area of the city, the weight of land parcels is the highest, followed by the weight of the city subcenter and core land parcels, and the weight of other parcels in the periphery is the lowest. Docking functional units with high-level partitions and establish a partitioned and hierarchical overall height control system. Delimit high priority development areas, high general development areas, and highly strictly controlled areas. High priority development areas are mainly landmark skyscrapers and super high-rise buildings to fully demonstrate the image of the city; high general development areas are mainly small high-rise and high-rise buildings to create a rich city skyline; highly strictly controlled areas are multistorey and low-rise buildings; the construction is mainly based on strict control of construction in accordance with rigid requirements, viewing corridors, wind corridors, landscape relations, and airports. At the same time, the corresponding partitions of the building height are divided into nine levels, which more clearly expresses the control of the base building height of the plot [18].

**2.3. Ecological Landscape Indicators.** Through the analysis method of landscape index and space, the relationship between topography and landscape structure characteristics can be quantitatively obtained, and the condition of landscape structure can be accurately evaluated, so as to better explain the relationship between landscape structure and function and finally adjust protection based on this ecological environment and economic structure. The ecological landscape pattern reflects the gathering and dispersion of landscape elements in the space. The elements are the location, size, type, direction, shape, and direction of the space. Quantitative analysis of landscape pattern is to construct the connection of landscape structure, phenomenon, and process, which can better explain and understand the function of landscape [19]. Landscape ecologists have proposed a variety of evaluation indicators for the spatial pattern of the landscape; various indicators rely on information as shown in Figure 2.

Calculates the mean of the vegetation landscape type dimension. The dimension value reflects the shape characteristics of the vegetation landscape and is an important indicator of the complexity of the shape of the landscape patch. The analysis of the spatial landscape pattern can be realized through the quantification of the dimensions [20]. The calculation method of the average value of the subdimensions of the landscape type is

$$Z = \frac{\sum_{j=1}^m \sum_{i=1}^n [2 \ln(0.25 Q_{i,j}) / \ln(\lambda_{ij})]}{H}, \quad (3)$$

where the patch area, number, and patch perimeter of the vegetation landscape are represented by  $\lambda_{ij}$ ,  $H$ , and  $Q$ , respectively; the proportion of vegetation patch  $i$  in the total vegetation is  $Q_i$ ; and  $m$  and  $n$  represent the total number of vegetation patch types and the number of patches covered by different types of vegetation patches.

- (1) *Diversity Index.* Set the number of a certain type of block type  $i$  as  $m$  and the area as  $a_{ij}$ ; then, the area formula of this type of block is [21]

$$A_i = \sum_{i,j=1}^m a_{ij}. \quad (4)$$

On this basis, use the spatial analysis of GIS to obtain the landscape element transfer matrix. The Shannon diversity index of the landscape is used to reflect the number of landscape elements and the changes in the proportions of all landscape elements. When the prime area of all landscapes is equal, the diversity of the landscape is the highest, which is expressed by  $H_{\max}$ .

$$H = - \sum_{i=1}^n p_i \log 2^{p_i}, \quad (5)$$

where  $p_i$  represents the ratio of the total area occupied by landscape type  $i$  and  $n$  represents the total number of types.

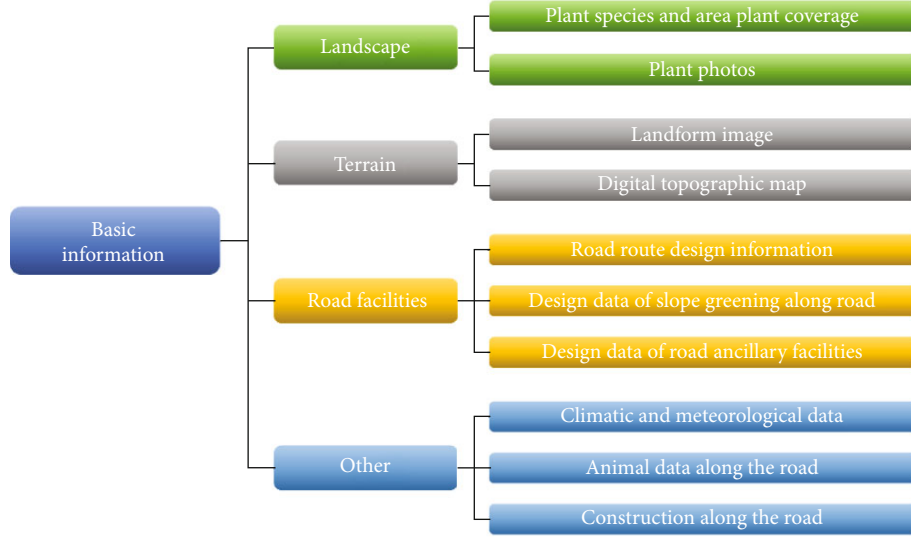


FIGURE 2: Basic information structure diagram.

The Shannon evenness index  $E$  of the landscape is used to describe the uniformity of the distribution of different landscape elements, and the formula is as follows:

$$E = \frac{H}{H_{\max}} * 100\%. \quad (6)$$

- (2) For the calculation of species diversity index, there are many calculation methods for diversity index. This study adopts Shannon diversity index [22]. The calculation of this index involves evenness index and species richness index. The calculation formula is

$$D = - \sum_{i=1}^F B_i \ln B_i, \quad (7)$$

where  $B_i$  represents the proportion of the important value of the  $i$ th species,  $F$  is the species richness index,  $D$  is the Shannon diversity index, and  $V$  is the Pielou evenness index. The upper limit of the species diversity index and the actual surveyed species diversity index are represented by  $D_{\max}$  and  $D$ , respectively, and the Pielou uniformity index is the ratio of  $D$  to  $D_{\max}$ .

- (3) *Dominance Degree*. The dominance degree is used to measure the degree of dominance of one or more landscape types within the structure of the landscape [23]. The specific calculation formula is

$$D = \log 2^n + \sum_{i=1}^m (p_i) \cdot \log 2^{p_i}. \quad (8)$$

In the formula,  $D$  represents the degree of dominance, and the meaning between  $p_i$  and  $m$  is the same as the above formula. The smaller the value of  $D$ , the closer the proportions of landscape types are; the larger the value of  $D$ , it means that the landscape is controlled by only one or a few types. However, it needs to be pointed out that when  $D = 0$ ; this type of index has no effect in a completely homogeneous landscape.

- (4) *Fragmentation Degree*. It reflects the degree of fragmentation of landscape patches by measuring the number of plates per unit area [24]. The specific calculation formula is

$$F = \frac{\sum_{i=1}^m n_i}{A}, \quad (9)$$

where  $F$  represents the fragmentation degree of the landscape,  $n_i$  represents the number of patches of the  $i$ th landscape type, and  $A$  represents the total area of the landscape. The larger the  $F$ , the more fragmented the patches of the landscape.

- (5) *Subdimension*. Previous studies have proved that, compared to the shape and structure of all other landscape types, mosaics in the landscape are the most typical fractal geometry. Fractal theory can be used to study quantification and then be measured by the shape of perimeter. The fractal dimension describes the characteristic parameters of the geometric shape. Because the shape of other graphs reflected as a function of perimeter changes with perimeter changes, it can also quantitatively test the fractal structure of landscape mosaics [25]. The formula of the fractal dimension value model of the landscape type is as follows:

$$\ln [A(r)] = \frac{2}{D_i} \ln [P(r)] + C, \quad (10)$$

where  $A(r)$  represents the area,  $P(r)$  represents the perimeter,  $r$  represents the measurement scale,  $D_i$  represents the fractal dimension in the two-dimensional Euclidean space, and  $C$  represents the constant. According to the perimeter and area data of all patches, by constructing a regression model with the shape of the above formula, the fractal dimension  $D_i$  of this landscape type can be obtained. The size of  $D_i$  represents the stability and complexity of the landscape type. The specific numerical theoretical range is between 1 and 2. The larger the value, the more complex the shape of the landscape;  $D_i = 1$  represents the shape of the landscape patch. It is a square;  $D_i = 2$  means that the shape of the landscape patch is the most complicated. In addition, the fractal dimension  $D_i$  can be used to compare the pattern characteristics of landscape elements to determine the impact of different ecological factors on the landscape pattern. If two landscape pattern elements have the same fractal dimension, it means that there is a certain pattern difference between the two.

(6) *Optimal Planning of Urban Ecological Landscape.*

The urban ecological landscape image texture is analyzed by analyzing the contrast, information entropy, correlation coefficient, and angular second-order four texture features, and the maximum likelihood method is used to classify its ecological landscape data to realize the optimal layout of the layout [26]. If  $n''$  represents the pixel value,  $p(i'', j'')$  represents the element in the  $i''$  row and  $j''$  column in the landscape image cooccurrence matrix;  $(i'', j'')$  represents the gray value of the cooccurrence matrix of the ecological image, using the above method to describe the vector of texture features that are widely used in practical applications and analyze the texture of the urban ecological landscape image, and the selected vectors of texture features are information entropy (ENT), angular second moment (ASM), contrast (CON), and correlation function (COR). The specific calculation formula is as follows:

$$\text{ENT} = \sum_{i''=1}^{n''} \sum_{j''=1}^{n''} p(i'', j'') \times \ln p(i'', j''), \quad (11)$$

$$\text{ASM} = \sum_{i''=1}^{n''} \sum_{j''=1}^{n''} p(i'', j'')^2, \quad (12)$$

$$\text{CON} = \sum_{i''=1}^{n''} \sum_{j''=1}^{n''} p(i'', j'') \times (i'' - j'')^2, \quad (13)$$

$$\text{COR} = \frac{[\sum_{i''=1}^{n''} \sum_{j''=1}^{n''} i'' * j'' p(i'', j'') - \mu_x \mu_y]}{(\sigma_x \sigma_y)}. \quad (14)$$

### 3. Result Analysis

Human modern life and urban construction continue to erode and invade urban green space, severely breaking the ecological stability and ecological functionality of the original landscape pattern and also destroying the biodiversity of the original habitat [27, 28]. The pace of urban green space construction cannot keep up with the wanton and disorderly urban expansion process, which has broken the green space matrix pattern in the natural state, causing it to be fragmented into a large number of highly fragmented patches of different sizes. The ecological function and ecology of the green space landscape benefits are greatly reduced. The construction of a reasonable ecological network can alleviate and suppress the high fragmentation of urban green landscapes and can effectively enhance the continuity of urban green landscapes [29]. Therefore, urban ecological corridors should be constructed rationally and used as links to connect discrete patches to form a scientific and rational ecological network and urban green space system. Through the three-dimensional analysis and research of the virtual urban landscape, planning managers can analyze and evaluate the color design, layout, spatial volume relationship, and the relationship between the building and the environment of the planning technical solutions of important areas in the city according to requirements, so as to develop and construct in the city. Pursue a corresponding balance in economic, social, and environmental benefits. At the same time, planning managers can also use the simulated three-dimensional landscape to track the construction and development of urban morphology, and according to the requirements of different stages of urban construction and development, timely adjust the corresponding regulatory detailed planning and urban design plan to better guide the urban landscape construction.

In order to verify the overall effectiveness of the method for optimizing garden landscape spatial pattern gradient under big data analysis, it is necessary to test the method of optimizing garden landscape spatial pattern gradient under big data analysis. In this test, plant diversity is important for evaluating garden landscape spatial pattern gradient [30]. Indicators, using the gradient optimization method of garden landscape spatial pattern under big data analysis (Method 1), the gradient optimization method of spatial landscape at all levels under the background of rapid urbanization (Method 2) and the gradient optimization method of landscape pattern based on land use (Method 3) perform tests to establish the spatial coordinate system of the garden landscape spatial gradient pattern and compare the plant species in the garden landscape spatial pattern gradient optimized by three different methods. The test results are shown in Figure 3. The different shapes in the figure represent different plant species. According to the test results of the gradient optimization method of garden landscape spatial pattern under big data analysis, it can be seen from the

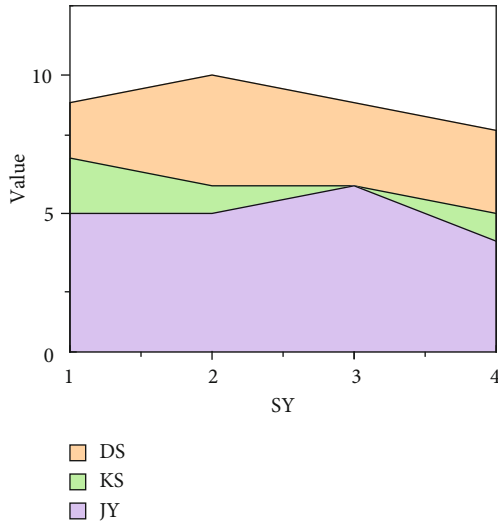


FIGURE 3: Comprehensive force measurement of three different methods.

analysis of Figure 3 that using the method of gradient optimization of garden landscape spatial pattern under big data analysis, there are many kinds of plants in the gradient pattern, and the distribution is even. The test results of the gradient optimization method of the spatial landscape at all levels under the background of rapid urbanization, the analysis shows that the gradient pattern obtained by the gradient optimization method of the spatial landscape at all levels under the background of rapid urbanization has fewer plant species and the gradient optimization method of the landscape pattern based on land use, like Figure 4. According to the analysis of the test results, the plant species in the gradient pattern obtained by using the land-use-based landscape pattern gradient optimization method are relatively single. Comparing the optimization results of the three different methods and Figure 5, it can be seen that there are more plant species in the gradient pattern optimized by the gradient optimization method of the garden landscape spatial pattern under the big data analysis.

#### 4. Effect Evaluation

Figure 6 shows the test results of the gradient optimization method of garden landscape spatial pattern under big data analysis. The gradient pattern optimized by the method of garden landscape spatial pattern gradient optimization under big data analysis has more plant species. Figure 6 represents the comprehensive measurement of the gradient of the garden landscape spatial pattern. The value is taken in the interval  $[-2, 2]$ . The closer the value of  $Q$  is to 0, the better the obtained optimization result of the spatial pattern gradient of the garden landscape. The gradient optimization method of garden landscape spatial pattern under big data analysis, the gradient optimization method of spatial landscape at all levels under the background of rapid urbanization, and the gradient optimization method of landscape pattern based on land use were tested [31].

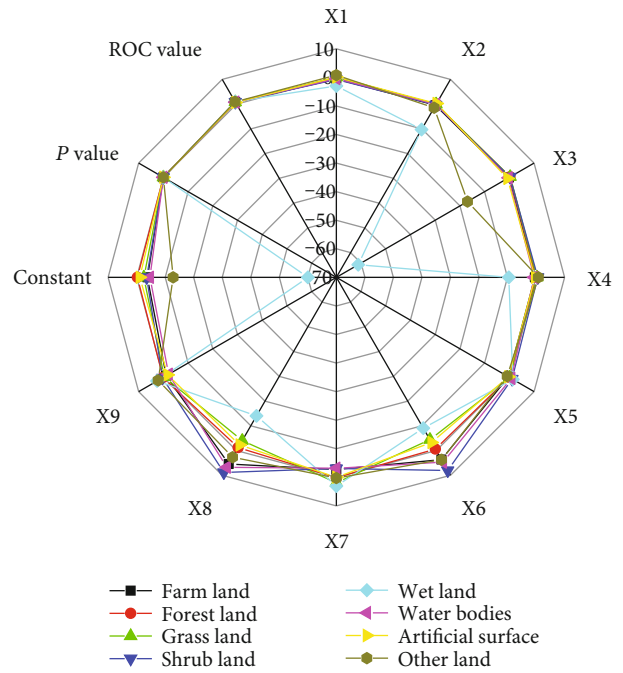


FIGURE 4: Driving forces of evolution of main landscape types.

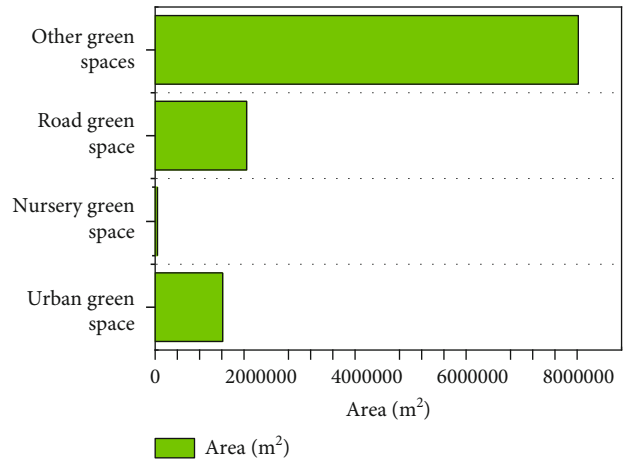


FIGURE 5: Green space occupancy ratio.

The degree of fragmentation of the landscape in the study area has been kept in a relatively high state as a whole, which is related to the fact that the terrain of the area is more mountainous and hillier. The degree of landscape fragmentation first increased due to the rise of scattered urban buildings and the impact of human deforestation and land reclamation activities, and then, the degree of fragmentation began to decline due to the closure of reclaimed areas and scattered buildings [32]. It reflects the characteristics of landscape ecology in the process of urban development. Socio-economic and policy planning factors play an important role in the change of urban landscape pattern, and good management and planning intervention have a positive impact on urban ecological construction, like Figure 7.

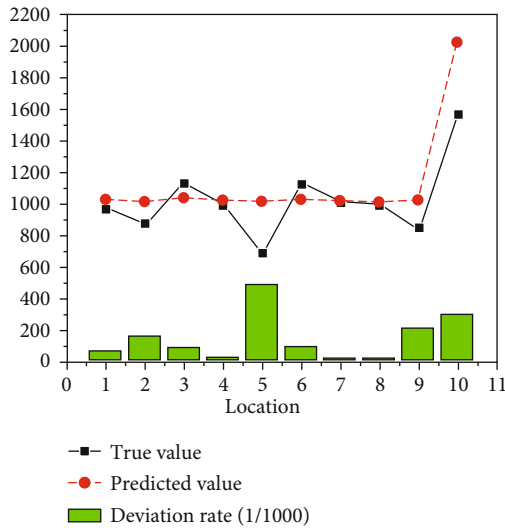


FIGURE 6: Experimental data monitoring bit rate comparison results.

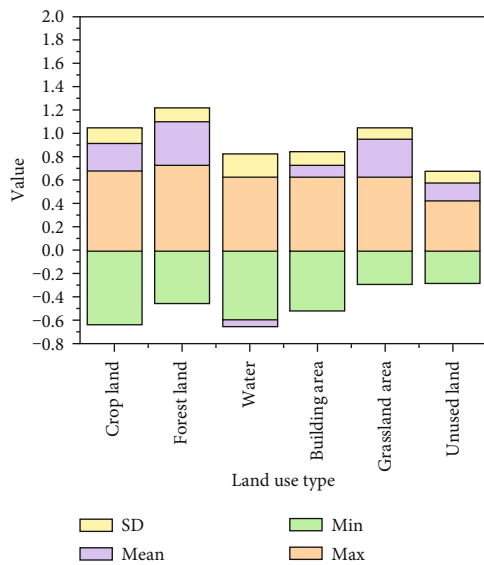


FIGURE 7: The relation NDVI based on different land use type.

After the method is applied, it has effectively improved the actual environmental problems of the city. Compared with the data from 2012 to 2018, the research method has significantly reduced the sulfur dioxide and smoke and dust content of the city, and the rainfall and green areas have increased. The research method fully takes into account the area and area and proportion of its ecological landscape, and the diversity of the planned ecological landscape allows the city's environmental problems to be effectively controlled during the test period. In order to further verify the effectiveness of the research method through simulation, on the basis of the above experiments, experiments are carried out on the accuracy of the optimal planning of the urban ecological landscape color balance layout with different methods. The higher the accuracy, the higher the preci-

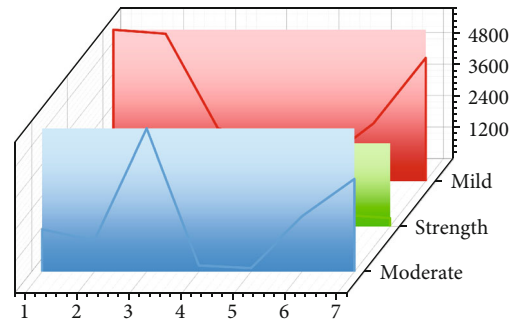


FIGURE 8: Area composition of soil erosion intensity in different types of areas.

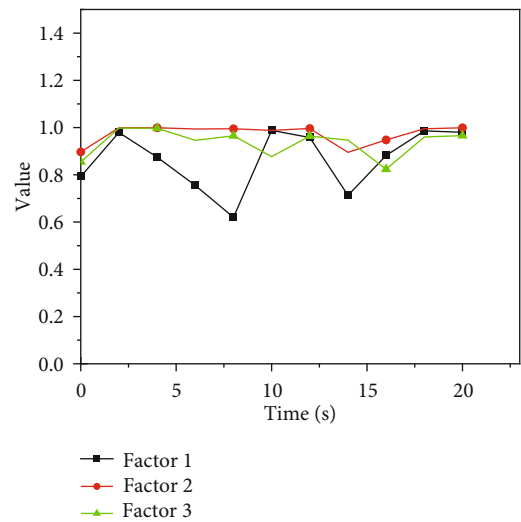


FIGURE 9: The R2 of each factor varies over time.

sion of the method application process planning. If the accuracy of the method is low, it will directly lead to a rough problem of the landscape planning effect, which cannot meet the current basic requirements in this field.

It can be seen from the experimental results in Figure 8 that the accuracy and adaptability of the two methods fluctuate during the landscape planning process, but the accuracy of the research method fluctuates less and has better adaptability. Within a reasonable length of landscape planning, the research method has a higher precision of landscape planning, indicating that the method proposed by the research is more precise in application. The above experiments prove that the research method has a good effect on the color balance planning of urban ecological landscape, like Figures 8 and 9.

## 5. Conclusions

Vegetation planning virtual simulation technology to study vegetation is the main coverage part of the smart scenic area. This article uses GIS technology to obtain the problems in the vegetation pattern of the scenic area and rationally plans the vegetation of the smart scenic area in the virtual simulation platform, which is the long-term sustainability of the

smart scenic area. Development provides a scientific reference basis to improve the intelligent level of vegetation planning in scenic spots.

In order to keep up with the process of urbanization, the gradient pattern of the garden landscape space needs to be optimized. When the current gradient optimization method is used to optimize the garden landscape spatial pattern gradient, the optimized gradient pattern has few plant species and uneven distribution, which cannot effectively optimize the garden landscape spatial pattern gradient. A big data analysis of the garden landscape is proposed. The spatial pattern gradient optimization method solves the shortcomings of the current method and optimizes and improves it, laying the foundation for the development of garden landscape. Provide technical support for ecological environment management and protection. However, limited by the depth and breadth of the research, this design did not accumulate data on the rich animal and plant resources of the wetland. This point will be the focus of the next stage of research, and special research work will be carried out. On the other hand, in-depth research on the optimal design of countermeasures for the dynamic evolution of wetland landscapes provides suggestions for improving the ecological restoration rate of wetland landscapes.

Secondly, the vegetation landscape planning method uses GIS technology as an auxiliary guidance technology, which is a quantitative reference tool for rational planning of vegetation patterns. In future research, the role of GIS in spatial pattern planning and design will be further exerted, and a complete spatial pattern planning system will be constructed by combining GIS technology and modern technical means, starting from digital image processing and imagery. Information feature extraction, digital technology to obtain multi-level ground data, in-depth exploration of the temporal and spatial variation factors and influencing mechanisms of vegetation coverage by means of a combination of maps and numbers, provide a scientific basis for in-depth optimization of vegetation coverage. ecosystem.

### Data Availability

The data used to support the findings of this study are available from the corresponding author upon request.

### Conflicts of Interest

The author declares that no known competing financial interests or personal relationships that could have appeared to influence the work reported in this paper.

### Acknowledgments

This work was supported by the Education Department of Henan Province and the 2019 Young Backbone Teachers' Project of Colleges and Universities in Henan Province (The Research and Teaching Exploration on Landscape Design of Central Plains' Urban Agglomerations from the Perspective of Narrative) (No. 2019GGJS250).

### References

- [1] N. Cui, N. Malleon, V. Houlden, and A. Comber, "Using VGI and social media data to understand urban green space: a narrative literature review," *ISPRS International Journal of Geo-Information*, vol. 10, no. 7, p. 425, 2021.
- [2] Y. Lap-fu, "Retracted article: Environmental planning and economic efficiency of green cities based on improved neural network and satellite remote sensing," *Arabian Journal of Geosciences*, vol. 14, no. 14, pp. 1–19, 2021.
- [3] P. Xie, D. Liu, Y. Liu, and Y. Liu, "A least cumulative ventilation cost method for urban ventilation environment analysis," *Complexity*, vol. 2020, 13 pages, 2020.
- [4] P. Nageler, G. Zahrer, R. Heimrath et al., "Novel validated method for GIS based automated dynamic urban building energy simulations," *Energy*, vol. 139, pp. 142–154, 2017.
- [5] J. Beal, K. Usbeck, J. Loyall, M. Rowe, and J. Metzler, "Adaptive opportunistic airborne sensor sharing," *ACM Transactions on Autonomous and Adaptive Systems (TAAS)*, vol. 13, no. 1, pp. 1–29, 2018.
- [6] B. Chen, B. Xu, and P. Gong, "Mapping essential urban land use categories (EULUC) using geospatial big data: progress, challenges, and opportunities," *Big Earth Data*, vol. 5, no. 3, pp. 410–441, 2021.
- [7] Y. Peng, S. W. Li, and Z. Z. Hu, "A self-learning dynamic path planning method for evacuation in large public buildings based on neural networks," *Neurocomputing*, vol. 365, pp. 71–85, 2019.
- [8] P. Siritiasatien, S. Chadsuthi, K. Jampachaisri, and K. Kesorn, "Dengue epidemics prediction: a survey of the state-of-the-art based on data science processes," *IEEE Access*, vol. 6, pp. 53757–53795, 2018.
- [9] C. Prener, "Digitizing and visualizing sketch map data: a semi-structured approach to qualitative GIS," *Cartographica: The International Journal for Geographic Information and Geovisualization*, vol. 56, no. 4, pp. 267–283, 2021.
- [10] D. Pan, Z. Xu, X. Lu, L. Zhou, and H. Li, "3D scene and geological modeling using integrated multi-source spatial data: methodology, challenges, and suggestions," *Tunnelling and Underground Space Technology*, vol. 100, article 103393, 2020.
- [11] Z. Lv, X. Li, W. Wang, B. Zhang, J. Hu, and S. Feng, "Government affairs service platform for smart city," *Future Generation Computer Systems*, vol. 81, pp. 443–451, 2018.
- [12] D. Yao, "Application of GIS remote sensing information integration in eco-environmental quality monitoring," *International Journal of Environmental Technology and Management*, vol. 24, no. 5/6, pp. 375–389, 2021.
- [13] C. Li, J. He, and X. Duan, "Modeling the collaborative evolution of urban land considering urban interactions under intermediate intervention, in the urban agglomeration in the middle reaches of the Yangtze River in China," *Land*, vol. 9, no. 6, p. 184, 2020.
- [14] Z. Zhang, B. Hu, W. Jiang, and H. Qiu, "Identification and scenario prediction of degree of wetland damage in Guangxi based on the CA-Markov model," *Ecological Indicators*, vol. 127, article 107764, 2021.
- [15] S. Wang and K. Gu, "Pingyao: the historic urban landscape and planning for heritage-led urban changes," *Cities*, vol. 97, article 102489, 2020.
- [16] A. S. Barau, R. Maconachie, A. N. M. Ludin, and A. Abdulhamid, "Urban morphology dynamics and environmental change in Kano, Nigeria," *Land Use Policy*, vol. 42, pp. 307–317, 2015.

- [17] C. Yin, M. Yuan, Y. Lu, Y. Huang, and Y. Liu, "Effects of urban form on the urban heat island effect based on spatial regression model," *Science of the Total Environment*, vol. 634, pp. 696–704, 2018.
- [18] D. Ugalde, P. F. Parra, and D. Lopez-Garcia, "Assessment of the seismic capacity of tall wall buildings using nonlinear finite element modeling," *Bulletin of Earthquake Engineering*, vol. 17, no. 12, pp. 6565–6589, 2019.
- [19] W. Kuang, Y. Liu, Y. Dou et al., "What are hot and what are not in an urban landscape: quantifying and explaining the land surface temperature pattern in Beijing, China," *Landscape Ecology*, vol. 30, no. 2, pp. 357–373, 2015.
- [20] J. P. Reis, E. A. Silva, and P. Pinho, "Spatial metrics to study urban patterns in growing and shrinking cities," *Urban Geography*, vol. 37, no. 2, pp. 246–271, 2016.
- [21] S. Das, B. Pradhan, P. K. Shit, and A. M. Alamri, "Assessment of wetland ecosystem health using the pressure–state–response (PSR) model: a case study of Mursidabad District of West Bengal (India)," *Sustainability*, vol. 12, no. 15, p. 5932, 2020.
- [22] D. Rocchini, M. Marcantonio, and C. Ricotta, "Measuring Rao's Q diversity index from remote sensing: an open source solution[J]," *Ecological Indicators*, vol. 72, pp. 234–238, 2017.
- [23] A. Lausch, T. Blaschke, D. Haase et al., "Understanding and quantifying landscape structure - a review on relevant process characteristics, data models and landscape metrics," *Ecological Modelling*, vol. 295, pp. 31–41, 2015.
- [24] P. Liu, Y. Hu, and W. Jia, "Land use optimization research based on FLUS model and ecosystem services- setting Jinan City as an example," *Urban Climate*, vol. 40, article 100984, 2021.
- [25] M. Carpineti, A. Rossoni, A. Senese, D. Maragno, G. A. Diolaiuti, and A. Vailati, "Multifractal analysis of glaciers in the Lombardy region of the Italian Alps," *Journal of Physics: Complexity*, vol. 2, no. 2, article 025003, 2021.
- [26] Z. Szantoi, F. J. Escobedo, A. Abd-Elrahman, L. Pearlstine, B. Dewitt, and S. Smith, "Classifying spatially heterogeneous wetland communities using machine learning algorithms and spectral and textural features," *Environmental Monitoring and Assessment*, vol. 187, no. 5, pp. 1–15, 2015.
- [27] J. Wu, Q. Zhu, N. Qiao et al., "Ecological risk assessment of coal mine area based on "source-sink" landscape theory - a case study of Pingshuo mining area," *Journal of Cleaner Production*, vol. 295, article 126371, 2021.
- [28] R. K. Upadhyay, "Markers for global climate change and its impact on social, biological and ecological systems: a review," *American Journal of Climate Change*, vol. 9, no. 3, pp. 159–203, 2020.
- [29] L. Sturiale and A. Scuderi, "The evaluation of green investments in urban areas: a proposal of an eco-social-green model of the city," *Sustainability*, vol. 10, no. 12, p. 4541, 2018.
- [30] H. Zhang, P. Y. Lai, and C. Y. Jim, "Species diversity and spatial pattern of old and precious trees in Macau," *Landscape and Urban Planning*, vol. 162, pp. 56–67, 2017.
- [31] S. Li, X. Zhao, J. Pu, P. Miao, Q. Wang, and K. Tan, "Optimize and control territorial spatial functional areas to improve the ecological stability and total environment in karst areas of Southwest China," *Land Use Policy*, vol. 100, article 104940, 2021.
- [32] T. Wu, P. Zha, M. Yu et al., "Landscape pattern evolution and its response to human disturbance in a newly metropolitan area: a case study in Jin-Yi metropolitan area," *Land*, vol. 10, no. 8, p. 767, 2021.



## Research Article

# Research on Garden Ecosystem Based on Monitoring Sensing Technology

**Lixia Qiang**  and **Jie Wang**

*School of Environmental Art, Hebei Academy of Fine Arts, Hebei, China 050700*

Correspondence should be addressed to Lixia Qiang; qlx@hbafa.edu.cn

Received 22 February 2022; Revised 14 March 2022; Accepted 29 March 2022; Published 23 April 2022

Academic Editor: Wen Zeng

Copyright © 2022 Lixia Qiang and Jie Wang. This is an open access article distributed under the Creative Commons Attribution License, which permits unrestricted use, distribution, and reproduction in any medium, provided the original work is properly cited.

Monitoring and evaluating the state variables of garden ecological processes on a long-term scale is one of the hot issues in current garden ecosystem observation research. In view of the problems of poor real-time transmission and storage of observation data in garden ecosystem observation stations, low data sharing, serious data fragmentation, weak construction of big data analysis platform, and lack of real-time prediction and early warning of garden fires, this paper combines remote sensing technology, vorticity correlation technology, and monitoring and sensing technologies such as quadratic survey technology and wireless sensor network, realizes long-term and continuous comprehensive observation of water, soil, air, and growth elements in garden ecosystems, provides the real-time automatic storage and display of carbon budget data, water flux data, flux of energy and meteorological data between garden ecosystems and the atmosphere, storage and display of garden ecosystem service functions, and quantity of value, realizes the monitoring of garden fires and the prediction and early warning of garden fire risks, and can also provide technical support and exploration for the long-term automated observation used for garden ecosystems.

## 1. Introduction

Long-term and continuous human disturbance seriously threatens the stability and species diversity of garden ecosystems. How to continuously and effectively realize the monitoring of the ecosystem is a key topic and direction worthy of research and has received great attention from experts within the industry in recent years [1, 2].

The experimental stations established for the observation of garden ecosystems continue to emerge, and the combination of remote sensing observation and ground point observation makes the observation scale change from the station scale to the regional scale [3, 4]. Typical comprehensive observations of garden ecosystems include the National Ecological Observation Network (NEOT), the International Long-term Ecological Observation and Research Network (ILTER), and the Global Carbon Flux Network (FLUXNET) [5, 6]. In China, some exploration and analysis have also been made in the monitoring of garden ecosystems, typically in terms of involvement and analysis of monitoring technology and mon-

itoring content [7, 8]. However, there are still problems such as poor real-time transmission and storage of observation data, low data sharing, serious data fragmentation, and weak construction of big data analysis platforms. Wireless sensor network (WSN) technology has the advantages of real-time monitoring and rapid response. Therefore, it has real-time transmission and storage of sensor data and saves it within a certain period of time, which lays the foundation for subsequent data analysis and mining while providing support.

Forest fires seriously affect the forest type, carbon reserve, and biodiversity of the garden ecosystem, leading to the risk of the decline of the function of the garden ecosystem, the transformation of the forest type, and even the disappearance of the garden [9, 10]. In recent years, climate warming and human activities have made the forest fire situation more severe. There are frequent sightseeing tours in the forest farm and frequent sacrificial activities of nearby residents, which brings challenges to garden fire prevention. Therefore, real-time monitoring of garden fires is crucial for maintaining the safety of garden ecosystems. The existing

garden ecosystem observation station focuses on the research on the impact of fire on the garden ecosystem, and there are few related reports on the real-time monitoring and forecasting and early warning of garden fires [11, 12]. However, it should be noted that due to the particularity of the composition of gardens, the ecosystem needs to be studied, especially in terms of an ecological environment that can provide a “beautiful landscape” for subsequent sustainable development [13, 14].

For the monitoring of garden ecological environment, it is often necessary to integrate sensor observation and software integration. By focusing on the analysis of garden ecosystem, water flux, energy change, spatiotemporal dynamic change, driving mechanism, etc., this provides corresponding support for the garden ecological environment relying on multiple technologies such as sensor network, telemetry, and flux observation. In view of these deficiencies and requirements, this paper realizes long-term and continuous observation of various related elements of the garden ecosystem (water, energy, soil, and air), etc. relying on monitoring and sensing technology, and realizes the especially early warning judgment and analysis of evolution trend and garden fire of the garden ecosystem through real-time storage and timely processing, to further protect the garden ecosystem and improve the protection efficiency and quality.

## 2. Monitoring Sensing Technology

For monitoring sensors, it mainly includes specific sensitive components and corresponding circuits. The monitoring sensors can be used to realize the conversion of measurement information into signals according to certain rules, realize the output of specific forms of information, and realize the information transmission, processing, and analysis of data.

For the intelligent monitoring architecture of the sensor network, by integrating the data of various sensing devices such as video and infrared, the characteristics of the relevant targets are obtained from multiple angles and aspects, forming a diverse feature space dimension, which is more conducive to the identification and extraction of targets [15, 16]. The specific fusion is shown in Figure 1. Through the fusion of images, videos, and other data, the characteristics of the target are associated and extracted into a vector file to identify the target characteristics.

The corresponding data collection, sorting, processing, analysis, and fusion of the data collected are performed by all sensing devices (such as remote sensing and telemetry sensing devices) in the sensor network. As far as the multimedia monitoring network is concerned, streaming media data processing has higher requirements on the accuracy of data collection and data processing capability. Currently, the main body is the data fusion of graphics and images, and other sensor networks involve data for comprehensive time fusion. In particular, the corresponding feature fusion recognition for the target is to perform the corresponding recognition processing based on the combined associated features after classification [17, 18].

The processing and analysis of target images mainly involve video data, audio data, and basic data. Among them, the basic data mainly includes infrared sensing equipment and traditional telemetry data. Usually, the basic data is characterized by a small data flow. Compared with basic data, audio and video data are relatively large and redundant. It needs to be collected, processed, organized, and analyzed with the help of means and hardware devices with strong computing power, so as to realize data compression and feature processing.

According to the corresponding displacement speed information, the change of the pose state is judged, so as to obtain its own motion trajectory and realize relative positioning. Then, the corresponding state and speed information are obtained and calculated by

$$\begin{cases} X_h(k) = X_h(k-1) + \begin{bmatrix} \cos(\alpha_h(k-1)) \\ \sin(\alpha_h(k-1)) \end{bmatrix} \cdot V(k) \cdot \Delta T, \\ \alpha_h(k) = \alpha_h(k-1) + \theta(k). \end{cases} \quad (1)$$

The comprehensive positioning technology needs to measure both the direction and the velocity of the mobile node. If the initial position and movement direction of the node are known, without the influence of other external factors, the positioning trajectory in the ideal state should be exactly the same as the actual movement trajectory [19, 20]. However, it cannot be ignored that errors are bound to exist, and the positioning accuracy will eventually be affected by the corresponding angle error, speed error, etc., resulting in a certain deviation in the positioning accuracy.

- (a) Original initialization: at this stage, set the corresponding initialization value, and meanwhile, set the initial state of relative positioning as shown in

$$\begin{cases} X_h(0) = [0 \ 0]^T, \\ \alpha_h(0) = 0 \end{cases} \quad (2)$$

It should be noted that the initialized position can also be set to other values, which is only a certain measurement reference and does not represent the actual meaning. MSNIMA only makes comprehensive use of relative positioning instead of absolute positioning.

- (b) Position evaluation: on the basis of initialization, the historical results of relative positioning are evaluated with an algorithm, to obtain the current position information, and the accuracy  $\bar{p}$  of radio frequency positioning is directly used for calculation
- (c) Determining the threshold value and setting the corresponding threshold value and the length of the history record

The specific process is as follows:

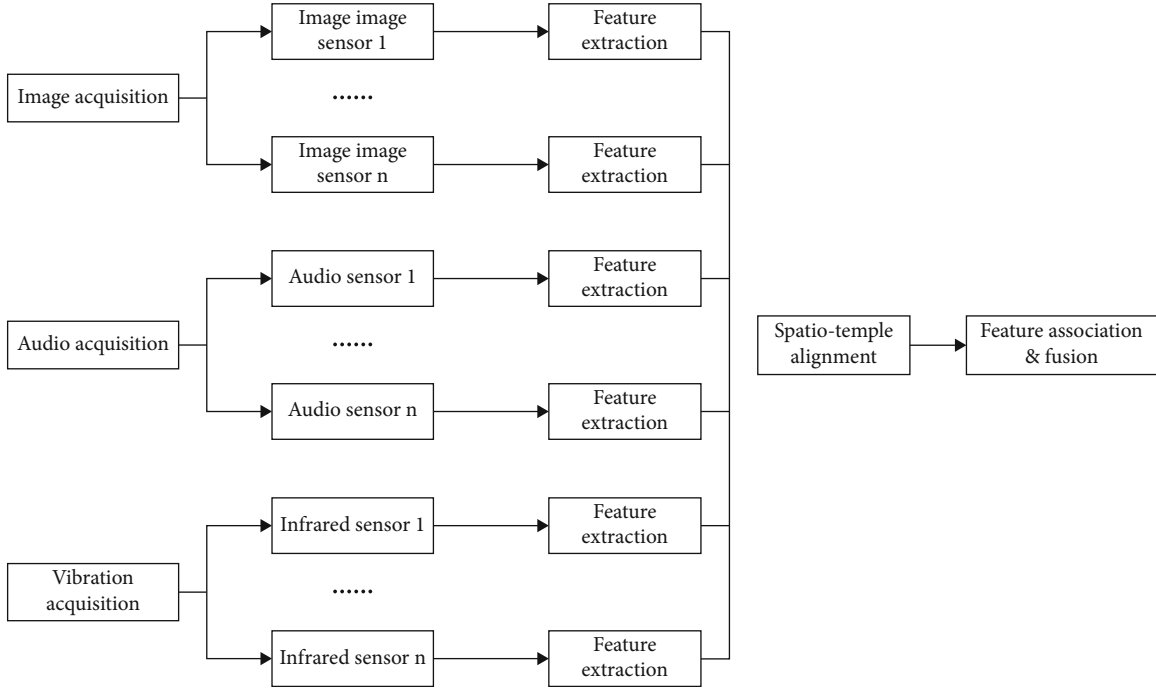


FIGURE 1: Heterogeneous sensing feature fusion process.

- (1) Express the most recent  $N$  times of effective RF positioning results with

$$Y_r^{kN} = [X_r(k-N), X_r(k-N+1), \dots, X_r(k-1)] \quad (3)$$

- (2) Translate the relative positioning result and the radio frequency positioning result so that the center of the two is the origin, and the translated coordinate matrix is expressed by

$$CY_r^{kN} = [CX_r(k-N)CX_r(k-N+1) \dots CX_r(k-1)] = [X_r(k-N) - C_r^{kN}(X_r(k-N+1) - C_r^{kN} \dots X_r(k-1) - C_r^{kN})], \quad (4)$$

$$CY_h^{kN} = [CX_h(k-N)CX_h(k-N+1) \dots CX_h(k-1)] = [X_h(k-N) - C_h^{kN}(X_h(k-N+1) - C_h^{kN} \dots X_h(k-1) - C_h^{kN})], \quad (5)$$

$$C_r^{kN} = \frac{1}{N} \cdot \sum_{i=0}^{N-1} X_r(k-N+i), \quad (6)$$

$$C_h^{kN} = \frac{1}{N} \cdot \sum_{i=0}^{N-1} X_h(k-N+i) \quad (7)$$

The height of the flux observation tower of the super observatory is 40 m. Meteorological sensors and infrared

thermal imagers are distributed on the tower, as shown in Figure 2. The  $30\text{ m} \times 30\text{ m}$  plots around the super observatory are also distributed with vegetation DBH sensors, litter sensors, soil temperature sensors, soil moisture sensors, and soil heat flux sensors.

**2.1. GetCapabilities Interface (Table 1).** GetCapabilities is used to obtain the information of the service itself, and the user will determine the functions provided by the service to the outside world according to the information of the service itself.

The response of the server after receiving the GetCapabilities request is CapabilitiesDocument, and the content contained in CapabilitiesDocument mainly includes ServiceIdentification: SPS service identity.

**2.2. DescribeTasking Interface (Table 2).** DescribeTasking mainly provides task planning for users who sends requests and is a very important operation of the SPS service.

The response of this interface is DescribeTaskingRequestResponse. The structure description is shown in Figure 3.

### 3. Construction of Field Observation Test Platform

The field observation experiment is composed of ground observation, Landsat TM/OLI sensor, and Terra MODIS sensor observation. The ground observation includes three scales: plot scale, vegetation transect scale, and regional scale. From the perspective of observation targets, the basic experiments are divided into five categories, namely, carbon budget observation, water flux observation, energy flux

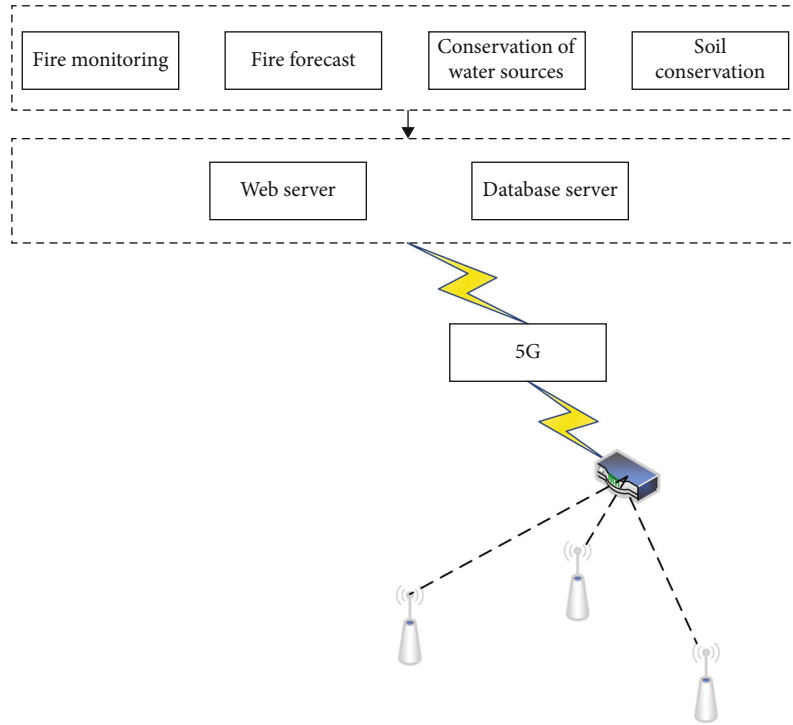


FIGURE 2: Overall framework of the platform.

TABLE 1: GetCapabilities parameter description.

Name	Whether mandatory	Client side	Server side
Service	Yes	User specified	Check the user's request parameters
Request	Yes	User specified	Request parameter value
Accept versions	No	Automatically added by the system	Check parameters
Sections	No	The system provides default values	Respond according to parameter value
updateSequence	No	The system provides default values	Respond according to parameter value
AcceptFormats	No	The system provides default values	Respond according to parameter value

TABLE 2: DescribeTasking parameter description.

Name	Actual meaning	Type	Whether mandatory
Service	Type of service	Character string	Yes
Request	Name of the operation	Character string	Yes
Version	Version	Character string	Yes
SensorID	Device ID of the sensor	Character string	Yes

observation, garden fire risk monitoring, and scale conversion experiments.

**3.1. Carbon Budget Observation.** In this experiment, according to the carbon cycle process of the garden ecosystem, three types of parameters related to carbon cycle were selected for observation, namely, carbon flux, vegetation biomass, and soil carbon transect reserve.

- (1) Observation of Carbon Flux. Eddy correlation systems are considered the best way to measure carbon dioxide

fluxes. In order to carry out the research on the vertical distribution of CO<sub>2</sub> concentration, the installation heights of the 7-layer closed-circuit CO<sub>2</sub>/H<sub>2</sub>O meter are 1 m, 7 m, 11 m, 15 m, 23 m, 31 m, and 38 m, respectively

- (2) Observation of Vegetation Biomass. Vegetation biomass is divided into belowground biomass and aboveground biomass. The underground biomass of four 15 m × 15 m plots was measured by root-drill sampling, weighing method after dried, and the forest age was observed in four plots of 15 m × 15 m
- (3) Observation of Soil Carbon Reserve. Vegetation soil samples were collected at sampling depths of 0-10 cm and 10-30 cm, respectively. The laboratory used potassium dichromate volumetric method which is used to measure soil organic matter content to estimate soil carbon storage

**3.2. Water Flux Observations.** Garden ecosystems play an important role in the terrestrial water cycle. After the

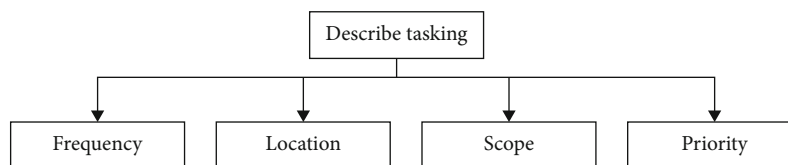


FIGURE 3: DescribeTaskingResponse structure.

precipitation is intercepted by the garden and falls to the ground, a certain amount of precipitation and runoff will be formed. Therefore, vegetation evapotranspiration and soil water conservation are the two most important links in the water cycle of garden ecosystems.

- (1) **Precipitation Observation.** The precipitation data of the  $30\text{ m} \times 30\text{ m}$  observation plot was measured by the automatic weather station tipping bucket rain gauge, and the precipitation data of the super observation station was measured by the rain sensor installed at a height of 23 m
- (2) **Observation of Vegetation Evapotranspiration.** At the super observatory, one set of open-circuit  $\text{CO}_2/\text{H}_2\text{O}$  meters and seven sets of closed-circuit  $\text{CO}_2/\text{H}_2\text{O}$  meters were used to observe  $\text{H}_2\text{O}$  concentration to obtain continuous time series observation data to estimate vegetation evapotranspiration in garden ecosystems
- (3) **Observation of Soil Moisture Content.** In order to verify the accuracy of the satellite remote sensing inversion of soil moisture and to study the law of surface heat and moisture transfer, the burial depth of the sensor is set to [5,100]

**3.3. Energy Flux Observation.** Solar short-wave radiation and atmospheric long-wave radiation are the energy sources of garden ecosystems. In the  $30\text{ m} \times 30\text{ m}$  observation plot, the automatic weather station measures the photosynthetically active radiation. The soil heat flux plates were buried at a depth of 3 cm and 5 cm, to measure the soil heat flux.

**3.4. Garden Fire Monitoring.** Meteorological factors (wind speed, wind direction, precipitation, air temperature, and relative air humidity), litter volume, and soil moisture are the input parameters of the garden risk forecast model, and the model outputs the garden fire risk level according to real-time data. At the super observatory, wind speed and direction are measured by three-dimensional ultrasonic anemometers and three-layer wind speed sensors (installation heights of 1 m, 7 m, and 11 m); air temperature and relative humidity are measured by three-layer atmospheric temperature and humidity sensors (installation heights of 1 m, 7 m, and 11 m). In the  $30\text{ m} \times 30\text{ m}$  observation plot, wind speed, wind direction, air temperature, and relative air humidity were measured by automatic weather stations.

In the super observatory, the infrared thermal imager installed at a height of 38 m has an effective monitoring

radius of 3 km, which realizes all-weather  $360^\circ$  panoramic monitoring of garden infrared thermal images.

**3.5. Scale Conversion Test.** Developing a scale conversion method between ground observation points and multisource and multiscale remote sensing pixels has always been one of the core issues faced by ecologists [21, 22]. The experiment integrates remote sensing technology, flux observation technology, quadratic survey method, etc., provides vegetation NPP, surface temperature, and soil water content observation data at three scales (sample plot scale, vegetation transect scale, and regional scale), and provides data support for the research on multiscale conversion methods of temperature and soil water content.

## 4. Simulation Experiment

The carbon budget data, water flux data, energy flux data and meteorological data automatically observed by the field observation and test platform are automatically transmitted to the database server in real time through the wireless sensor network, which provides data support for the construction of the data visualization platform.

**4.1. Ecological Wireless Sensor Network.** The wireless sensor network is a multihop self-organizing network formed by the ecological observation sensors deployed in the area and communicating with each other through the wireless network communication protocol, which realizes the real-time and automatic acquisition and storage of the measurement data. Landscape-scale observations based on wireless sensor networks fill the scale gap between ground point observations and remote sensing satellites and can provide pixel-scale observations for verification and scale conversion of remote sensing inversion results.

The user requirements for the wireless sensor network design of the entire observation system are as follows:

- (1) The exact location of the sensor nodes is determined by experts and mainly depends on the characteristics of forest type and site conditions. The network technology must be able to support the placement of sensor nodes in arbitrary locations. Furthermore, in order for the collected data to be representative of plant physiology and ecology, the sensor network must be able to cover  $1\text{--}1.5\text{ km}^2$  and consist of more than 70 sensor devices
- (2) The network must be able to operate on its own without any mandatory user intervention. They must be able to withstand temperature fluctuations, heal

themselves when the environment changes, and be able to operate for years without human intervention

- (3) Each node must be able to report sensor measurements every 30 min. The network must successfully and securely transmit sensor data to the gateway device, and it must provide users with remote monitoring capabilities, i.e., the ability to remotely assess the health of the network. Ecologists must be able to access the data collected by the sensors within minutes of the measurement

**4.2. Collection System Design.** The core of the entire garden ecological monitoring and sensing is to realize data collection, that is, to use the data collection module to realize the collection of various elements of the principle ecosystem, and to achieve specific display, storage, processing, and output through the data processing module. The particular acquisition system is shown in Figure 4.

From the data acquisition structure diagram in Figure 4, its main data acquisition part includes two major parts: data acquisition and data processing. The monitoring sensor is an important medium to realize data collection. The main function of the sensor is to use the specific object to be monitored to realize the transformation of the physical parameter signal and realize the output of the signal for data transmission. Therefore, the relative accuracy of data acquisition is largely subject to the inherent performance requirements of the sensor itself. In the specific design process, it may be necessary to analyze the data collection from hardware and software according to the corresponding garden ecological environment requirements.

From the perspective of the specific garden ecosystem, the data information of garden temperature and humidity can be collected through outdoor temperature and humidity sensors, and the corresponding technology can be used to collect data. The main function of the system is to use data collection, data processing, data analysis, and visualization. According to the specific needs and status quo of the garden ecosystem, it is set to 1 min, 5 min, etc. according to the specific time mode. After the data collection button is turned on, by selecting the corresponding interval, the system can automatically collect data, separate the data, save it as a text file, and judge whether the system is running normally through these data [23, 24].

**4.3. Design of Remote Monitoring System.** Relying on the analysis of the garden ecosystem based on monitoring and sensing, its monitoring mainly realizes the monitoring and analysis of the temperature, illumination, humidity, and rainfall within the garden and transmits the collected data to the actual client through 5G communication, so that the staff can use the Internet browser to browse and analyze the data information. The specific structural design of the remote monitoring system is shown in Figure 5.

The whole system of monitoring and sensing mainly includes four modules: monitoring sensor, data acquisition and analysis, system server, and remote client side. Among them, the role of the system server is to provide services. In a specific garden ecosystem, the main role of the server

side is to provide services for corresponding parameters and analyze specific sensor technologies.

The remote client side provides users with local basic programs and services and realizes the connection between the client side and the server based on the garden ecological server to ensure the normal operation of the program.

SmartMesh IP is a low-power wireless network product based on the IEEE802.15.4e TSCH standard developed by the Dust Networks Product Group of Linear Technology, which meets the above user requirements. SmartMesh IP consists of a single network manager (for monitoring and managing network performance and security and for receiving data to be uploaded to the data center) and up to 100 wireless nodes (for collecting and relaying data). The nodes form a redundant multihop and self-healing wireless mesh network around the manager (Figure 6). Currently, 76,000 SmartMesh networks have been deployed worldwide. The reliability of data transmission exceeds 99%, and the average current consumed on the routing node is less than  $50 \mu\text{A}$ , making the battery life more than 10 A.

Currently, 5 SmartMesh networks are deployed in this experiment. Among them, 4 SmartMesh networks are deployed in 4 observation plots of  $30 \text{ m} \times 30 \text{ m}$ ; each SmartMesh network consists of a manager, 14 sensor nodes, and multiple relay nodes, in case some sensor nodes are deployed too far from the rest of the network to connect. The SmartMesh network deployed at the super observatory consists of a manager, 29 sensor nodes, and multiple relay nodes. The network manager is installed 2 m above the ground and uploads sensor data and network statistics to the data center server via GSM/GPRS/4G.

The location of sensor nodes is selected according to characteristics such as forest type and site conditions. The sensor nodes cover an area between 1 and  $1.5 \text{ km}^2$ . Network managers are deployed in open areas with good cellular connectivity. Once the sensors and network manager are in place and the device is turned on, utilize the monitoring tools built into the manager to verify connectivity between the sensors. The relay nodes are placed iteratively and the updated connection information is verified. When verifying the connection information, the Dust Networks' rule is followed; that is, each node has at least 3 neighbors connected to it, and its received signal strength is higher than  $-85 \text{ dBm}$ .

#### 4.4. Function of the Platform

**4.4.1. Service Function Subsystem of Garden Ecosystem.** The service function of garden ecosystem refers to the natural environment conditions and utility that the garden ecosystem provides for human survival.

- (1) Observation and Evaluation of Carbon Fixation and Oxygen Release Function. Based on vegetation biomass data, carbon flux data, and satellite remote sensing data, the platform simulates the regional-scale net primary production (NPP) and further estimates the carbon fixation and oxygen release function of garden ecosystem. Specific functions include query and statistical analysis of  $\text{CO}_2$  concentration, vegetation DBH,

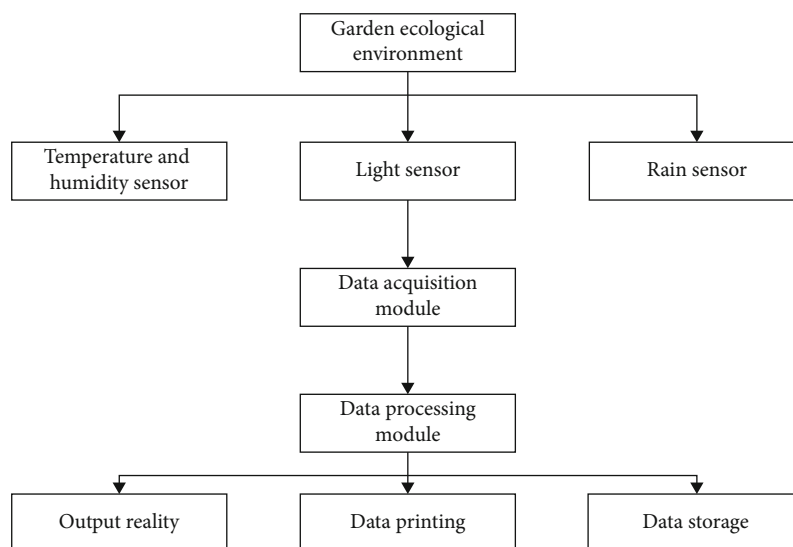


FIGURE 4: Structure diagram of data acquisition system.

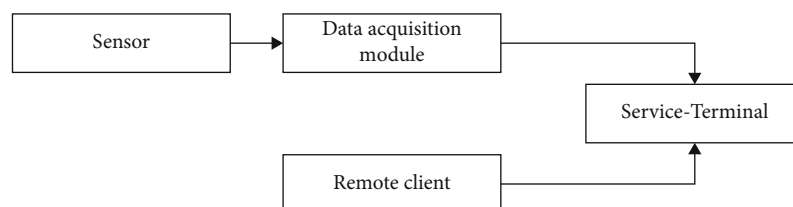


FIGURE 5: Structure diagram of remote monitoring system.

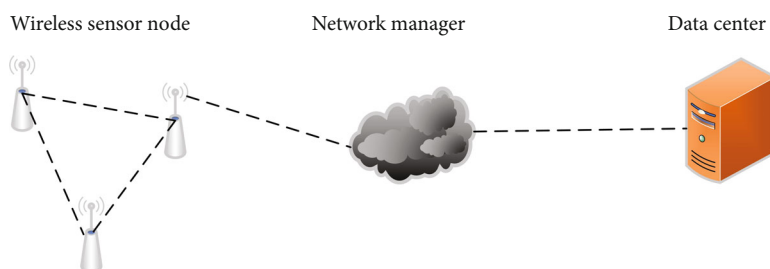


FIGURE 6: Observation system network topology.

and litter thickness; estimation, query, and statistical analysis of vegetation carbon storage and soil carbon storage; and estimation, query, and statistical analysis of forest carbon sequestration and oxygen release and its ecosystem service value [25, 26]

- (2) Observation and Evaluation of Water Conservation Function. The platform simulates regional-scale soil water content based on water vapor flux data, soil temperature and humidity data, atmospheric temperature and humidity data, and satellite remote sensing data and further estimates the water conservation function of garden ecosystems. Specific functions include query and statistical analysis of precipitation, H<sub>2</sub>O concentration, and soil water content; estimation, query, and statistical analysis

of evapotranspiration; and estimation, display, and statistical analysis of garden water conservation and its ecosystem service value

- (3) Observation and Evaluation of Conservation Soil Function. The platform simulates the regional-scale soil nitrogen, phosphorus and potassium content based on soil nitrogen, phosphorus and potassium content data, and satellite remote sensing data and further estimates the soil function of garden ecosystem conservation. Specific functions include query and statistical analysis of soil nitrogen content, soil phosphorus content, and soil potassium content and estimation, display, and statistical analysis of garden soil retention and fertilizer retention and its ecosystem service value

**4.4.2. Forest Fire Management Subsystem.** The forest fire management subsystem consists of two parts: the prediction and early warning of the garden fire danger level and the monitoring of the garden fire.

- (1) Prediction and Early Warning of Garden Fire Danger Level. Based on meteorological factors (wind speed, wind direction, precipitation, air temperature, and relative air humidity), litter volume, and soil moisture content, the platform establishes a garden fire risk forecast model to evaluate and warn the garden fire risk level. Specific functions include query and statistical analysis of meteorological factors, ground combustibles, and soil moisture content and real-time forecast, mid-term forecast, and historical data query of fire danger levels
- (2) Garden Fire Monitoring. The platform uses infrared thermal imagers to monitor garden fires in a 360° panorama around the clock. Once the image pixel value exceeds the threshold, a fire alarm will be triggered and a rescue plan will be generated. There are 4 specific functional modules: (1) fire monitoring module, which provides real-time video monitoring, fire alarm, and dynamic playback functions; (2) fire inspection module, which provides fire alarm, fire information query, patrol check-in, and sudden fire use approval, issuing notices, inspection and assessment, and fire filing functions; (3) firefighting module, which provides two-dimensional and three-dimensional electronic sand table, formulating and issuing firefighting plans, command, and dispatching functions; and (4) basic information module, which provides query and display of geomorphic information firefighting, road information, water source information, equipment information, population distribution, sensitive points, and biological isolation zones

**4.4.3. Scale Conversion Subsystem.** Based on the observation data of 30 m × 30 m observation plots and super observation stations and Landsat TM/OLI image data (spatial resolution of 30 m), the platform uses remote sensing data-driven model to realize the data of garden vegetation GPP, NPP and realize the conversion of garden vegetation GPP, NPP, and soil water content data from site scale to 30 m spatial resolution scale with remote sensing data-driven model. Based on the site observation data, Landsat TM/OLI image data, and Terra MODIS sensor image data (with a spatial resolution of 500 m), the model was used to realize the conversion of garden vegetation GPP, NPP, and soil water content data from site scale to 30 m spatial resolution scale and 500 m spatial resolution. The platform provides query and display of garden vegetation GPP, NPP, and soil moisture data at four scales: site scale, 30 m, 500 m spatial resolution scale, and regional scale.

#### 4.5. System Design

**4.5.1. Overall Design.** In order to facilitate development and maintenance of good scalability, this paper divides the SPS

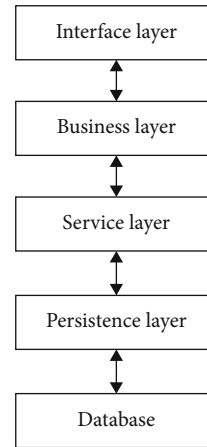


FIGURE 7: SPS service architecture.

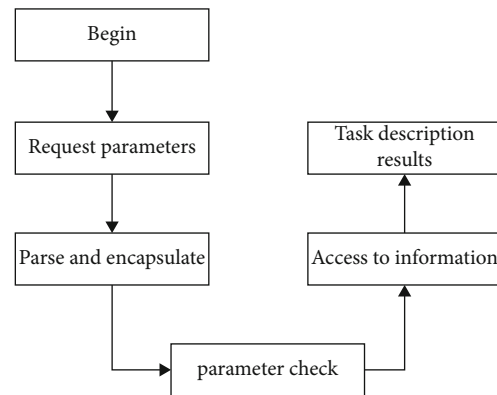


FIGURE 8: DescribeTasking logic flow.

service into four layers, and its architecture diagram is shown in Figure 7.

**4.5.2. Processing Flow.** According to the above overall design, when processing user requests, the core interface operations and extended interface operations of SPS will complete a series of operations according to a consistent processing flow.

Through the request of the 3 versions and parameter verification, it will be called by the service layer interface. The BasicSensorPlannerOperator service first checks whether the request has additional requirements. Currently, the request is not allowed to have additional requests by default. The task ID is obtained from the procedure parameter of the request and then reads the corresponding information from the database. The successfully obtained task description information will also be returned to the user in xml format, as shown in Figure 8.

#### 4.6. Application Implementation

**4.6.1. Development Environment.** The ultimate purpose of studying SPS service specification in this paper is to integrate it into the ecological environment monitoring system. Due to the advantages of java language cross-platform, once



compiled, and executed everywhere, this system will be implemented mainly by using java language.

**4.6.2. Application Demonstration and Testing.** Since the SPS service studied in this paper is a part of the ecological environment monitoring system, in order to facilitate the testing of the service, the front-end test page is designed while the server-side development of the SPS service is completed.

After testing, the submit interface and the other six interfaces can achieve the corresponding functions according to the expected design, and the SPS service can run normally. It can be seen that the SPS service can complete various functions of the sensing resource task planning stage. Simulation experiments show that monitoring and sensing technology can effectively support the research of garden ecosystem.

## 5. Conclusions

In order to practice “lucid waters and lush mountains are invaluable assets,” it is necessary to pay more attention to the protection of garden ecosystems along with economic development. However, due to the vast territory of China, it is difficult to achieve full coverage by relying solely on human resources for traditional monitoring and analysis. In response to these requirements and deficiencies, this paper attempts to introduce monitoring and sensing technology, through long-term and continuous comprehensive observation of water, soil, air, and biological elements in the garden ecosystem, to try to explore the coupling between the atmosphere, biosphere, and geosphere. It provides important data support for the contribution of the garden ecosystem in the regional carbon cycle, realizes the monitoring, prediction, and early warning of garden fires, and enhances the comprehensive application of wireless sensor network technology, remote sensing technology, flux observation technology, and methods, and finally, it provides an important basis for garden protection. The simulation experiment results show that the monitoring sensor technology can effectively realize the support of garden ecosystem research.

## Data Availability

The data used to support the findings of this study are available from the corresponding author upon request.

## Conflicts of Interest

The authors declare no conflicts of interest.

## References

- [1] F. Laender, J. R. Rohr, and R. Ashauer, “Reintroducing environmental change drivers in biodiversity-ecosystem functioning research,” *Trends in Ecology & Evolution*, vol. 31, no. 12, pp. 905–915, 2016.
- [2] D. Bilder and K. D. Irvine, “Taking stock of the *Drosophila* research ecosystem,” *Genetics*, vol. 206, no. 3, pp. 1227–1236, 2017.
- [3] C. C. Wall, C. Anderson, J. M. Jech, S. M. van Parijs, L. Hatch, and J. Gedamke, “Leveraging big data: how acoustic archives facilitate ecosystem research,” *Journal of the Acoustical Society of America*, vol. 141, no. 5, pp. 3940–3950, 2017.
- [4] M. Rebetz, G. V. Arx, and A. Gessler, “Meteorological data series from Swiss long-term forest ecosystem research plots since 1997,” *Annals of Forest Science*, vol. 75, no. 2, pp. 41–50, 2018.
- [5] S. Janne, B. Pia, and H. Jani, “Toward more integrated ecosystem research in aquatic and terrestrial environments,” *Bioscience*, vol. 65, no. 2, pp. 174–182, 2015.
- [6] H. Cai, X. Di, and S. X. Chang, “Carbon storage, net primary production, and net ecosystem production in four major temperate forest types in northeastern China,” *Canadian Journal of Forest Research*, vol. 46, no. 2, pp. 143–151, 2016.
- [7] A. Aoki-Yoshida, R. Aoki, N. Moriya et al., “Omics studies of the murine intestinal ecosystem exposed to subchronic and mild social defeat stress,” *Journal of Proteome Research*, vol. 15, no. 9, pp. 3126–3138, 2016.
- [8] M. Musche, M. Adamescu, P. Angelstam et al., “Research questions to facilitate the future development of European long-term ecosystem research infrastructures: a horizon scanning exercise,” *Journal of Environmental Management*, vol. 250, no. 2, p. 109479, 2019.
- [9] B. Jha, C. Ae, and D. Adbac, “Mapping change in biodiversity and ecosystem function research: food webs foster integration of experiments and science policy,” *Advances in Ecological Research*, vol. 61, no. 3, pp. 297–322, 2019.
- [10] X. Chen, S. de Vries, T. Assmuth et al., “Research challenges for cultural ecosystem services and public health in (peri-) urban environments,” *Science of the Total Environment*, vol. 651, no. 3, pp. 2118–2129, 2019.
- [11] R. Danilo, B. Luciano, and A. Leonardo, “Novel perspectives on bat insectivory highlight the value of this ecosystem service in farmland: research frontiers and management implications,” *Agriculture Ecosystems & Environment*, vol. 266, no. 2, pp. 31–38, 2018.
- [12] J. S. Kominoski, E. E. Gaiser, and S. G. Baer, “Advancing theories of ecosystem development through long-term ecological research,” *Bioscience*, vol. 68, no. 8, pp. 554–562, 2018.
- [13] J. M. Jech, J. K. Horne, D. Chu et al., “Comparisons among ten models of acoustic backscattering used in aquatic ecosystem research,” *Journal of the Acoustical Society of America*, vol. 138, no. 6, pp. 3742–3764, 2015.
- [14] S. Arabi and A. Nahman, “Impacts of marine plastic on ecosystem services and economy: State of South African research,” *South African Journal of Science*, vol. 116, no. 5/6, 2020.
- [15] W. Mengist, T. Soromessa, and G. Legese, “Ecosystem services research in mountainous regions: a systematic literature review on current knowledge and research gaps,” *Science of the Total Environment*, vol. 702, 2020.
- [16] B. Martin-Lopez, M. R. Felipe-Lucia, and E. M. Bennett, “A novel telecoupling framework to assess social relations across spatial scales for ecosystem services research,” *Journal of Environmental Management*, vol. 241, no. 1, pp. 251–263, 2019.
- [17] T. H. Oliver, M. S. Heard, N. Isaac et al., “A synthesis is emerging between biodiversity-ecosystem function and ecological resilience research: reply to Mori,” *Trends in Ecology & Evolution*, vol. 31, no. 2, pp. 89–92, 2016.
- [18] D. D. Engel, M. A. Evans, B. S. Low, and J. Schaeffer, “Understanding ecosystem services adoption by natural resource

- managers and research ecologists,” *Journal of Great Lakes Research*, vol. 43, no. 3, pp. 169–179, 2017.
- [19] T. M. Wittman and D. E. Bennett, “A synthesis of research on the human dimensions of sagebrush ecosystem management,” *Rangeland Ecology & Management*, vol. 78, no. 3, pp. 155–164, 2021.
- [20] R. K. Gould, L. L. Bremer, and P. Pua’Ala, “Frontiers in cultural ecosystem services: toward greater equity and justice in ecosystem services research and practice,” *Bioscience*, vol. 2, no. 12, pp. 12–20, 2020.
- [21] M. A. Daam, H. Teixeira, and A. I. Lillebo, “Establishing causal links between aquatic biodiversity and ecosystem functioning: status and research needs,” *Science of the Total Environment*, vol. 656, no. 15, pp. 1145–1156, 2019.
- [22] T. R. Angradi, J. J. Launspach, D. W. Bolgrien et al., “Mapping ecosystem service indicators in a Great Lakes estuarine area of concern,” *Journal of Great Lakes Research*, vol. 42, no. 3, pp. 717–727, 2016.
- [23] L. Uusitalo, S. Korpinen, J. H. Andersen et al., “Exploring methods for predicting multiple pressures on ecosystem recovery: a case study on marine eutrophication and fisheries,” *Continental Shelf Research*, vol. 121, no. 2, pp. 48–60, 2015.
- [24] J. E. Hobbie, G. R. Shaver, E. B. Rastetter et al., “Ecosystem responses to climate change at a Low Arctic and a High Arctic long-term research site,” *Ambio*, vol. 46, no. 1, pp. 160–173, 2017.
- [25] L. Musinguzi, V. Natugonza, and R. Ogutu-Ohwayo, “Paradigm shifts required to promote ecosystem modeling for ecosystem-based fishery management for African inland lakes,” *Journal of Great Lakes Research*, vol. 43, no. 1, pp. 1–8, 2017.
- [26] A. E. Arbi, A. Rochex, and G. Chataigne, “The Tunisian oasis ecosystem is a source of antagonistic *Bacillus* spp. producing diverse antifungal lipopeptides,” *Research in Microbiology*, vol. 167, no. 1, pp. 46–57, 2016.

## Research Article

# Exploration on Elderly Accessible Information Interaction Design Using Fuzzy Control

Hui Peng 

*School of Art and Design, Zhengzhou University of Light Industry, Zhengzhou, Henan 450000, China*

Correspondence should be addressed to Hui Peng; 2020007@zzuli.edu.cn

Received 13 January 2022; Revised 8 February 2022; Accepted 21 February 2022; Published 23 April 2022

Academic Editor: Wen Zeng

Copyright © 2022 Hui Peng. This is an open access article distributed under the Creative Commons Attribution License, which permits unrestricted use, distribution, and reproduction in any medium, provided the original work is properly cited.

With the increasing elderly population, the information intellectualization demand also rises substantially. At the same time, intelligent information interaction system- (IIS-) controlled wheelchair's automatic obstacle avoidance techniques have become extremely important in an intelligent social context. Therefore, this paper proposes an IIS to help disabled groups and some older people enjoy the barrier-free information design and improve product information manipulation experience. Firstly, the functional requirements of the IIS are analyzed, and the overall scheme of the IIS is designed. Then, the control mode of IIS is determined. Secondly, following research on the obstacle avoidance algorithm (OAA) based on fuzzy control, the obstacle avoidance control strategy is formulated for the elderly accessible wheelchair IIS. Finally, experiments are designed to verify the control performance and simulate the automatic OAA of the designed IIS. The experimental results indicate that the touch screen control system (TSCS) of mobile phone (MPHN) is more sensitive for the elderly accessible wheelchair control information system. By comparison, the joystick control system (JCS) is more straightforward to manipulate than the touch screen. The practicability of these two control methods is very strong. These two independent control methods meet the control performance requirements and improve the automatic obstacle avoidance performance of IIS. The proposed IIS based on TSCS and JCS can respond to input commands in real time, help the IIS avoid obstacles, and acquire images, among other functions. Therefore, the proposed intelligent wheelchair design improves the interactive performance of the intelligent operating system, facilitates the travel of the elderly and the disabled, and has good practical value.

## 1. Introduction

Today, the overall world population is aging. For the first time in history, older people might outnumber children in years to come. Like many developed countries, China has also entered an aging society. Nevertheless, Chinese society has some unique characteristics. For example, as the Chinese tradition extends, respect and care for the elderly are deemed a virtue, and people pay more attention to the life of the elderly. Meanwhile, with the rapid social development and family planning policies, most Chinese families have undergone substantial structural changes. As a result, many elderlies are left unattended or forced to live alone, aggravated by rapid urbanization that has attracted most young people out of their hometowns. Not to mention the many disabled who still demand further social attention to lead a better life. These social matters have become a concern for

both the state and society. Thus, more attention is being paid to improving the life quality of the elderly and the disabled. Notably, the present work holds that barrier-free information communication is the most important for these particular groups. It has high practical significance under science and technological development and the intelligent era [1].

Information interaction design is an interdisciplinary subject of information design, interaction design, and sensory design. Information design deals with the organization and representation of data: transforming data into valuable and meaningful information. Interaction design is carried out according to the sensory needs of different users to improve information efficiency. In this paper, the interaction design based on fuzzy control theory is carried out for the elderly accessible wheelchair operating system. It was aimed at improving the user experience of elderly wheelchair users. At present, wheelchairs have become a scientific and reliable

resort for many people with physical impairment, including some elderly and physically disabled groups. Mainly, wheelchairs can either be controlled manually or electronically (automatically). Apparently, the manual operation requires family or professional nurses' assistance, sometimes not feasible for low-income or solidary groups. On the other hand, the automatic wheelchair control system performs poorly in obstacle avoidance, especially in multiobstacle environments. The handling of information interaction systems needs to be improved. In a nutshell, these wheelchairs are far from intelligent [2, 3]. For example, most available wheelchairs are not equipped with an antilock braking system (ABS) to avoid skidding [4]. Accordingly, Wu et al. [5] introduced a wheelchair-intelligent ABS structure to improve user safety, including the adaptive neural fuzzy inference system (ANFIS) and friction coefficient estimation system. The friction coefficient estimation system used a particle filter (PF) to quickly adapt to nonlinear states and unknown environments. The system provided accurate ABS braking control according to the road's friction coefficient range. The ABS used a gyroscope to detect wheelchair acceleration and angle and then calculated the parameters. The user could click the on-chair stop button to activate the ABS. The results implied that the proposed ABS could effectively shorten the braking time and distance and improve wheelchair riding safety. Luo et al. [6] designed a toilet-assisted wheelchair system to solve the problems of difficulty getting up and unsanitary toilet treatment for the disabled, the elderly, and other wheelchair users. The designed wheelchair system adopted a single-chip microcomputer (SCM) for intelligent information control. It had two main functions: assisting wheelchair users in getting into the wheelchair and collecting the pollutants discharged. Experiments showed that the toilet-assisted wheelchair was more ergonomic in helping users get up and more convenient and hygienic in treating toilet waste than similar products.

With the rapid development of mobile terminal platform technology and the increasing popularity of the smartphone (SPHN), more and more services have been offloaded to terminals. Android operating system has been widely used as the mainstream mobile operating system because of its free features and powerful functions. Employing the Android platform to realize more daily applications, especially mobile portable medical devices, has become an important research field. Arguably, with the growing trend of worldwide population aging, the intelligent wheelchair will get a higher market share shortly. Meanwhile, all nations invest more resources into intelligent and more user-friendly wheelchair Research and Development (R&D). Moreover, designers need to fully consider the actual scenarios and users' practical needs during the marketization of intelligent wheelchairs. For example, there is an increasing number of solitary elderly wheelchair users. Monitoring functions and more accessible human-computer interaction (HCI) design might be of great importance for these groups. Based on the above analysis, the present work designs a wheelchair intelligent information interaction system (IIIS) based on obstacle avoidance algorithm (OAA). Then, the wheelchair IIIS's obstacle avoidance function is improved using fuzzy control theory. The obstacle

avoidance performance is verified through experimental design. Therefore, the proposed wheelchair IIIS can improve the convenience of system operation, facilitate the elderly and the disabled to move more conveniently and quickly, and has certain practical value

## 2. Materials and Methods

### 2.1. IIIS Information Scheme Design of Wheelchair Operating System

*2.1.1. Information Function Requirements of Wheelchair Operating System.* A wheelchair IIIS is designed to facilitate the movement of the elderly and some particular groups. Safety is the top priority. Meanwhile, the wheelchair should be designed with easy-to-accessible and detailed information operating systems. Overall, the design should adhere to safety, reliability, and accessibility principles [7, 8]. The functions of the wheelchair IIIS read as follows:

- (1) The intelligent wheelchair can turn around, change direction, and emergency brake during driving. These systems should be made simple and with remote monitoring functions
- (2) Upon encountering obstacles, the intelligent wheelchair should avoid obstacles automatically
- (3) To enable users to control better, the intelligent wheelchair should be able to monitor the surrounding environment in real time
- (4) On irregular road sections, the wheelchair should not fall, and it can automatically alarm against an emergency

*2.1.2. Overall IIIS Scheme Design.* Generally, the intelligent wheelchair comprises a mechanical structure and operating system. The operating system is similar to human organs and is the core part of the entire intelligent wheelchair, whereas the mechanical structure is identical to the human body, carrying the hardware circuit of the operating system [9, 10]. There are two most common wheelchairs: traditional wheelchairs and simple electric wheelchairs. Traditional wheelchairs generally need extra assistance to manipulate and, thus, increase the labor cost. The electric wheelchair controls the movement through the joystick, with certain potential safety concerns in use [11, 12]. Against these problems, this section designs a wheelchair IIIS with a personnel monitoring function and automatically obstacle avoidance function.

The intelligent wheelchair mounts a chassis driven by a four-wheel robot. The seat is installed on the moving mechanism. Three ultrasonic sensors are installed in the forward direction of the wheelchair. The control joystick and control button are installed on the right armrest of the wheelchair, which can control the moving direction and accelerate and decelerate, brake, and whistle. The wheelchair IIIS equips with both the touch screen control system (TSCS) and joystick control system (JCS). Additionally, a camera is set above the wheelchair to collect the environmental information.

Then, the wireless communication module transmits the camera images to the SPHN so that the user can understand the surroundings in real time, to better control the wheelchair. Figure 1 presents the overall framework of the designed wheelchair IIIS.

Figure 1 reveals that the microcontroller (MC) is the core part of the wheelchair IIIS, responsible for controlling the wheelchair operating system. The motor drive module controls the forward and the reverse rotations, acceleration, and deceleration. Meanwhile, the motor drive module detects obstacles and transmits the information to the MC to avoid the obstacles automatically. Wireless fidelity (Wi-Fi) module is connected with the MC through the serial port to realize the remote control. The angle sensor module measures the inclination angle of the wheelchair during movement to judge the wheelchair's real-time states. In front of the steps, the wheelchair IIIS can timely brake to prevent the wheelchair from falling. Even if the wheelchair falls accidentally, the monitoring alarm module will send an alarm signal in time to the guardians of the user in the form of short messages. Simultaneously, the wheelchair IIIS can alarm to remind the surrounding people to help the vulnerable users. The camera module collects the environmental images around the wheelchair. It transmits them to the SPHN for users to observe the situation behind the wheelchair and operate safely.

*2.1.3. Design of Intelligent Wheelchair Control Mode.* Most wheelchair users are either the elderly or with impaired legs and feet. Therefore, the advantages and disadvantages of control methods for different groups differ significantly, which should be a top concern in wheelchair IIIS design. So far, two control methods prevail in the market: TSCS and JCS. Figure 2 illustrates the existing form of HCI mode.

(1) *Voice Control System.* The user sends instructions to the operating system in the form of speech. Upon receiving user instructions, information identification and response are activated. Thanks to the fast-growing speech recognition technology in recent years, voice control is seeing broader applications in intelligent terminals. However, voice control has some defects. For instance, unclear voice commands can hardly be correctly recognized. Thus, the current voice control technology heavily depends on users' voice clarity. The interactive effect of voice information needs to be improved.

(2) *TSCS.* Users can simply slide their fingers on the SPHN screen to send commands to the operating system. It is widely used because TSCS is easy to learn, convenient, and simple to operate. Besides, it can also be remotely operated through SPHN.

(3) *Visual Control System.* This control method collects the user's gestures and other limb movements through the visual sensor. The advantages are easy to operate and highly reliable. The disadvantages are high requirements for hardware equipment, complex control algorithm, cross-disciplinary methodology, high price, and some technical problems.

Therefore, the visual control mode will not be considered in the proposed wheelchair IIIS.

(4) *JCS.* Mainly, the JCS sees applications in electric wheelchairs. It is relatively straightforward and flexible, so it is widely used.

Therefore, the proposed wheelchair IIIS combines the TSCS with JCS to simultaneously realize traditional control and remote control based on the analysis above.

*2.1.4. Design of Obstacle Avoidance Mode of the Wheelchair IIIS.* Wheelchair IIIS uses sensors to collect environmental information to avoid obstacles automatically. In recent years, there have been many kinds of sensors. Still, only three types are often used in robot obstacle avoidance, namely, ultrasonic measurement, infrared measurement, and image acquisition [13].

(1) *Ultrasonic Measurement.* The so-called ultrasonic sensor detects objects through ultrasonic waves, as shown in Figure 3. The ultrasonic sensor module sends out the short wavelength sound signals to detect direction. The sound wave will be reflected from the object along the way, and the MC will pinpoint the object according to the calculated reflection time. Such a detection method is relatively simple and is more robust against environmental influences.

(2) *Infrared Measurement.* Like ultrasonic measurement, the wave (light) is reflected once it reaches an object. The reflection time is used for measurement. Nevertheless, unlike ultrasonic measurement, it is highly sensitive to environmental impact.

To sum up, the ultrasonic measurement is relatively simple and more robust to environmental factors. Thus, the proposed wheelchair IIIS employs ultrasonic sensors.

*2.2. Elderly Accessible Wheelchair IIIS Design Based on Fuzzy Control.* Obstacle avoidance system (OAS) is the crucial link of wheelchair IIIS, so there are high requirements for its reliability. Specifically, it should mainly concern two functional requirements: the sensor control module and OOA. Because of the complexity of the wheelchair environment, there are many uncertainties, such as motor effects, which might affect the performance of wheelchair IIIS [14]. To this end, this section applies the fuzzy control algorithm in the OAS of wheelchair IIIS.

*2.2.1. Fuzzy Control.* The idea of fuzzy control is to control objects with computers over people. Essentially, it is a computer simulation of people's ideas of control [15]. Artificial control experiences will be coded into fuzzy rules. Thus, fuzzy control is an intelligent control approach, as demonstrated in Figure 4.

Figure 4 indicates that the fuzzy controller contains the fuzzy interface, inference engine, defuzzification interface, and knowledge base. The fuzzy interface maps the accurate input variable into the corresponding fuzzy quantity to

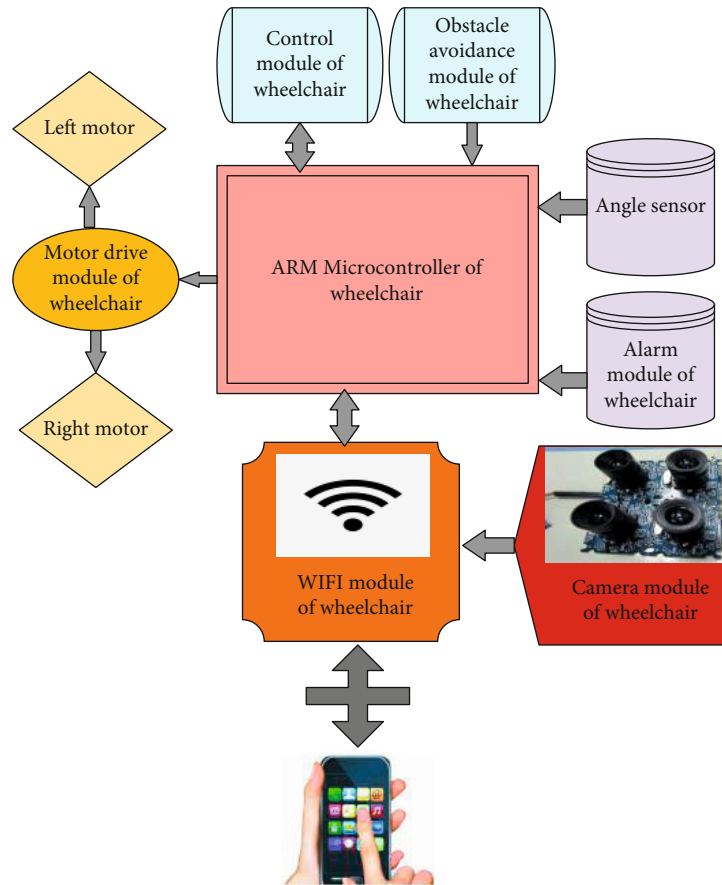


FIGURE 1: Overall diagram of wheelchair IIIS.

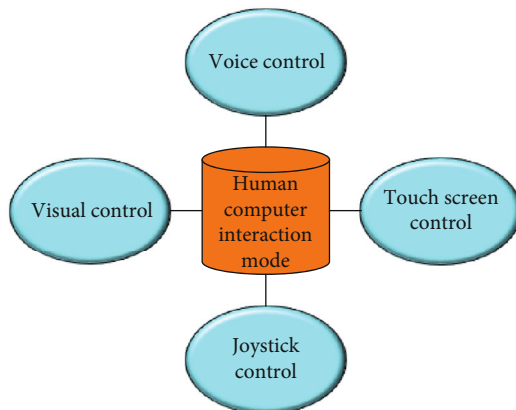


FIGURE 2: Main forms of HCI

promote the controller to identify the output quantity. The inference engine can change fuzzy input into fuzzy output. The defuzzification interface is responsible for transforming the unrecognizable fuzzy quantities into recognizable quantities. Lastly, the knowledge base includes a database and rule base. The database can save the data in the controller. At the same time, the rule base is a fuzzy rule collection written in fuzzy language simulating human thought [16, 17]. Fuzzy controllers work like this: firstly, it fuzzifies the output

and then turns it into the fuzzy quantity the fuzzy system recognizes. Secondly, it infers the input based on fuzzy control rules through an inference engine to obtain the output of the fuzzy system. Thirdly, it transforms the output into identifiable quantities and transmits them to the controlled objects. Finally, it completes an entire control process. Further, the fuzzy controllers compare the input and output and calculate the deviation, and a new round of the fuzzy control process begins to obtain a new control quantity. Overall, the fuzzy control is an iteration process based on one such circle [18, 19].

Advantages of fuzzy control are as follows: (1) fuzzy control is a rule-based control, which directly adopts language control rules. The starting point is the control experience of field operators or the knowledge of relevant experts. It does not build an accurate mathematical model of the controlled object, so the control mechanism and strategy are easy to accept and understand. The design is simple and easy to apply. (2) It is easier to establish language control rules from the qualitative understanding of industrial processes. Thus, fuzzy control is very suitable for those objects whose mathematical model is difficult to obtain, dynamic characteristics are challenging to grasp, or changes are very significant. (3) The model-based control algorithm and system design method easily lead to significant differences due to different starting points and performance indexes. Nevertheless, a

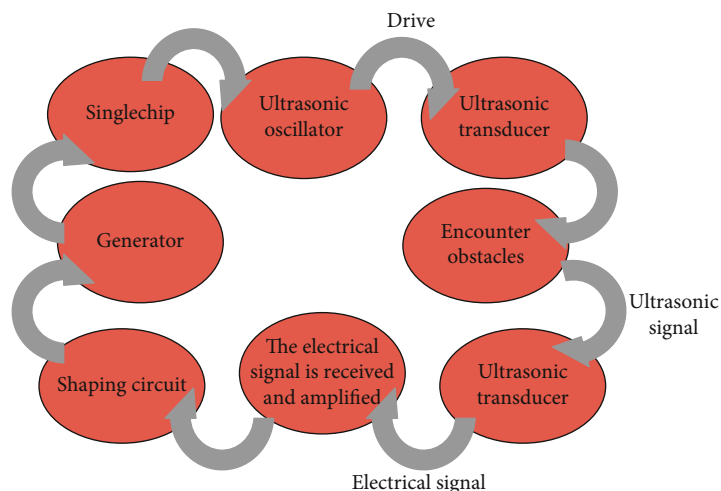


FIGURE 3: Ultrasonic sensor obstacle detection.

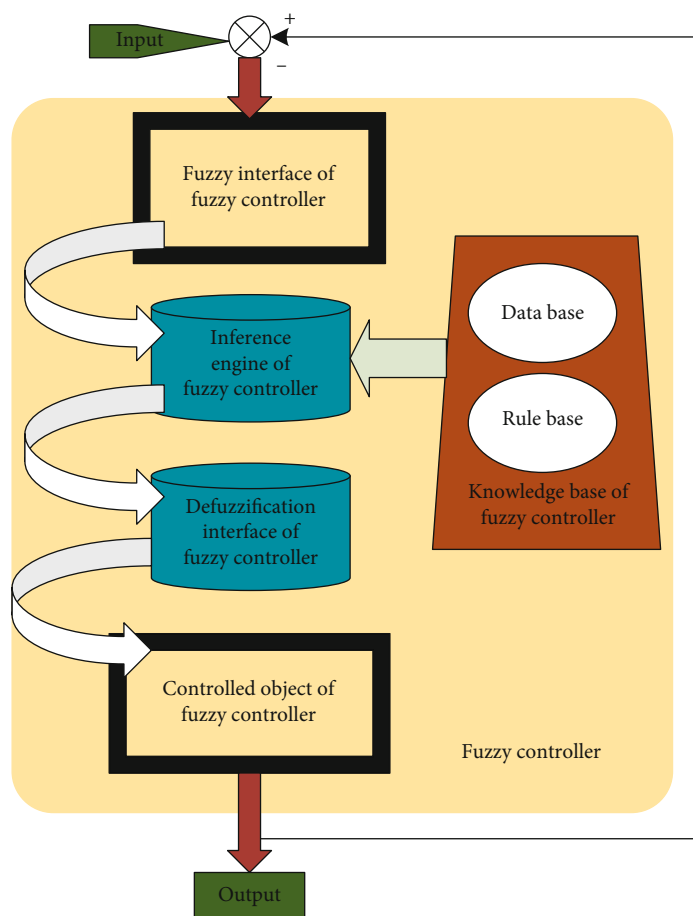


FIGURE 4: Schematic diagram of fuzzy control.

system language control rule has relative independence. The fuzzy connection between these control rules makes it easy to find a compromise choice, so the control effect is better than that of the conventional controller. (4) Fuzzy control is designed based on heuristic knowledge and language deci-

sion rules, which is conducive to simulating the process and method of manual control, enhancing the control system's adaptability, and making with a certain level of intelligence. (5) The fuzzy control system has strong robustness and has significantly weakened the influence of disturbance and

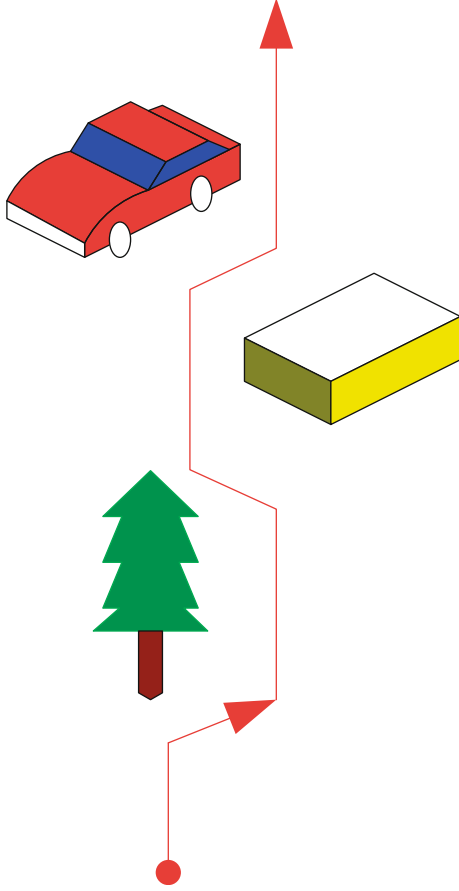


FIGURE 5: Wheelchair OAS path selection.

parameter change on the control effect. Hence, it is especially suitable for controlling nonlinear, time-varying, and pure delay systems.

A fuzzy controller can be one-dimensional (1D), two-dimensional (2D), or even three-dimensional (3D). The 1D fuzzy controller contains only one input, the deviation between system output and expected value. Equation (1) expresses its fuzzy relationship:

$$R_{(x,y)} = \bigcup_i^n A_i \times B_i. \quad (1)$$

In Equation (1),  $A_i$  represents the input subset, and  $B_i$  denotes the output subset.

The 2D fuzzy controller has two inputs: deviation and the deviation derivative to time. At present, the 2D fuzzy controller is most widely used. Equation (2) calculates its fuzzy relationship:

$$R_{(x,y)} = \bigcup_{i=1}^n (A_{1i} \times A_{2i}) \times B_i. \quad (2)$$

In Equation (2),  $A_{1i}$  and  $A_{2i}$  represent the input subset, and  $B_i$  indicates the output subset.

The 3D fuzzy controller has three inputs: deviation, the first derivative of deviation to time, and the second derivative of deviation to time. Because the 3D fuzzy con-

troller has many input variables, multiple control rules are required, increasing system calculation and the control time while reducing system response. Therefore, 3D fuzzy controllers are hardly seen in practical applications.

### 2.2.2. Design Method of Fuzzy Controller

(1) *Fuzzification.* The fuzzification process collects sensor information and converts them into language quantity. Then, it establishes membership function (MF) for different language quantities and finally expresses it through a fuzzy set [20]. In general, the method of changing digital variables into fuzzy linguistic quantities reads as follows:

- (1) Single point set method: it fuzzifies the input data  $x$ 's exact value and then turns it into two separate fuzzy sets. The fuzzy set is marked as  $A$ , and the single point set is as follows:

$$\mu_A = \begin{cases} 1 & (x = x_0) \\ 0 & (x \neq x_0) \end{cases} \quad (3)$$

Importantly, the single point set method only transforms the digital quantity into fuzzy quantity on the surface, but it does not transform the digital quantity into fuzzy quantity in essence.

- (2) Triangular fuzzy set method: the noisy fuzzy input is a fuzzy random variable. Such MF is regarded as an isosceles triangle. In fuzzy triangular sets, the vertices are the average of random numbers, and the length of the bottom edge is  $2\sigma$  ( $\sigma$  is the standard deviation (SD) of a random number)
- (3) Normal distribution function method: it is the most commonly used MF among fuzzy variables, as expressed by

$$\mu_A(x) = e^{-(x-x_0)^2/2\sigma^2} \quad (4)$$

In Equation (4),  $x_0$  refers to the expected value, and  $\sigma$  represents the SD.

(2) *Knowledge Base.* The knowledge base is at the core of the fuzzy controller and is a set of expert-generated rule bases [21]. Fuzzy rules can be established through parameter settings, such as state, output, and control variables. Meanwhile, the knowledge base should consider the compatibility and integrity between control rules. Usually, the description accuracy depends on the input of fuzzy variables. Precisely, more input leads to higher accuracy and more complex rules until the control rules become too complex to maintain proper efficiency and control effect. Therefore, the fuzzy variables should be set according to the specific situation. Each fuzzy rule determines a fuzzy  $R_i$  relationship. Then, iteratively, the fuzzy relationship  $R$  of the whole system



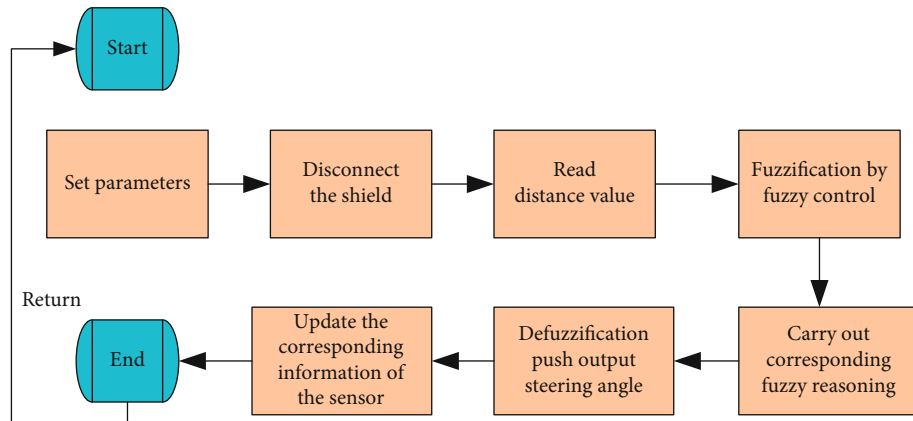


FIGURE 6: Flow of fuzzy control program.

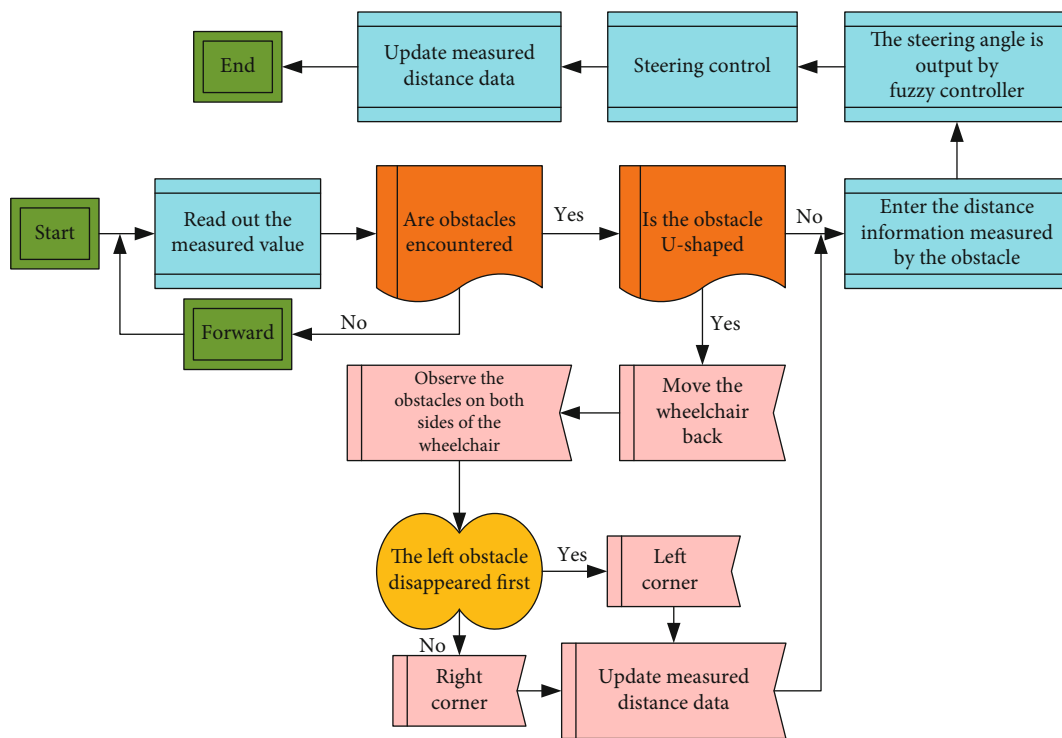


FIGURE 7: Flow of the proposed fuzzy automatic obstacle avoidance control strategy.

can be obtained through the logical relationship between fuzzy statements, as shown below:

$$R = R_1 \cup R_2 \cup \dots \cup R_m = \bigcup_{i=1}^m R_i. \quad (5)$$

(3) *Fuzzy Reasoning.* Simply put, fuzzy reasoning compares the fuzzy input with the fuzzy rule base and then outputs the reasoning results according to the reasoning method. It often uses the likelihood inference method and the min-max method.

(4) *Defuzzification.* Generally, the control signal is an exact quantity, but fuzzy reasoning generates a fuzzy quantity, so it is necessary to fuzzify the output [22]. Barycenter,

weighted average, and maximum membership methods are often used in practical applications.

2.3. *Fuzzy Obstacle Avoidance Information Interactive Control Strategy for Wheelchair IIS Operating System.* The right priority selection strategy is adopted to improve the efficiency and accuracy of wheelchair OAS. In simple terms, the wheelchair will prefer to move towards the right when it gets too close to an object. Nevertheless, if the obstacle is happened to be on the right, the wheelchair will choose to move to the left. Since obstacles' relative positions to the wheelchair are random, the wheelchair OAS might choose different paths every time. Figure 5 manifests the wheelchair OAS flow.

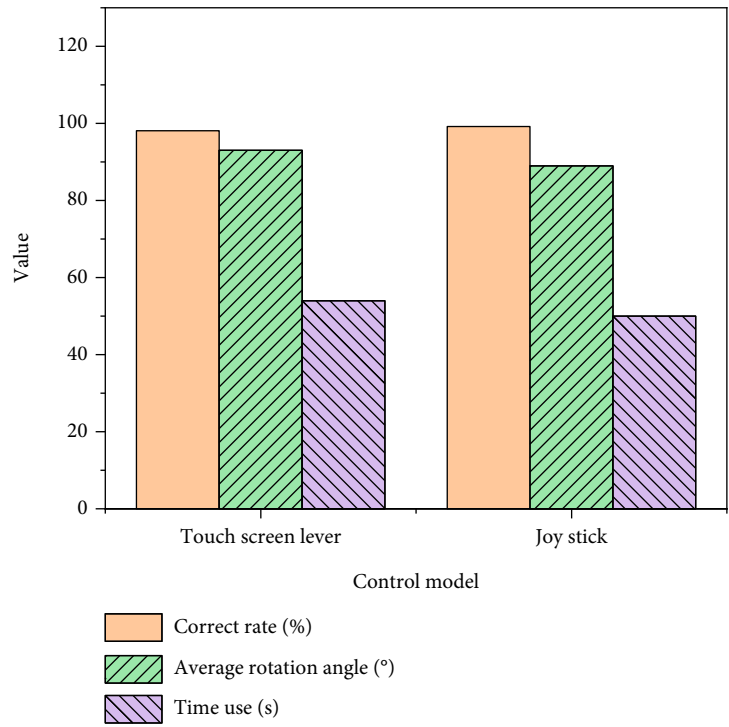


FIGURE 8: Experimental comparison of different control modes.

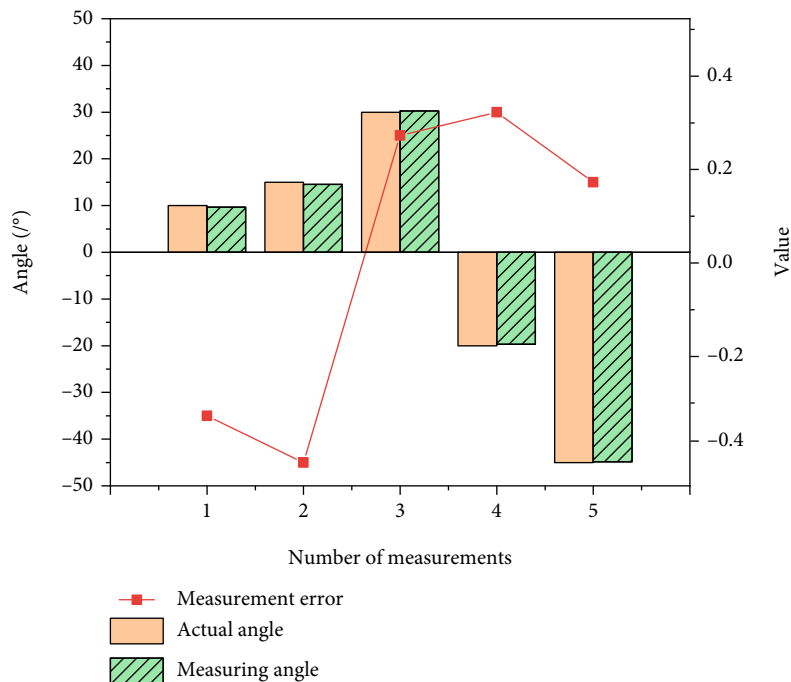


FIGURE 9: Angle measurement results.

Further, practical applications have to consider dead corners in wheelchair operations. In that case, the wheelchair will be surrounded by obstacles from three directions. Therefore, a reverse path selection design must be included in wheelchair OAS. Specifically, against multiple obstacles, the wheelchair OAS first selects a path, remembers it, and

then selects the new path based on historical memories if the path is still obstructed. The operation will repeat itself until all obstacles are avoided.

2.4. *Software Implementation of OAA.* Subsequently, OAS inputs the obstacle distance information and the direction

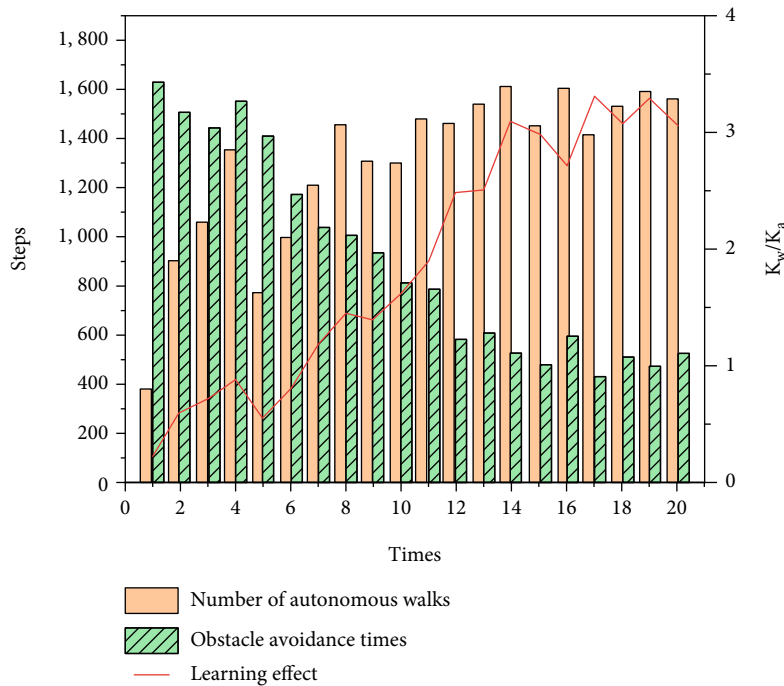


FIGURE 10: Simulation effect and learning effect.

angle between the wheelchair and the target and outputs the wheelchair steering angle. Here, the OAA of the wheelchair IIS is coded by C programming language. Figure 6 demonstrates the core part of the fuzzy control-based wheelchair OAA.

This section proposes to combine the wheelchair OAS operating system with a fuzzy control-based active user control strategy. Doing so improves the information collection rate, the information interaction effect, and the obstacle avoidance performance of the wheelchair. Specifically, the wheelchair motion control is realized by the user. The proposed automatic obstacle avoidance control strategy will guide the wheelchair to avoid obstacles successfully. Figure 7 displays the procedure flow of the proposed fuzzy automatic obstacle avoidance control strategy.

Based on Figure 7, the programming software codes the wheelchair OAA. Then, the OAA will be further tested through practical obstacle avoidance experiments.

### 3. Results

**3.1. Information Interactive Performance Test of Wheelchair IIS Operating System's Directional Control.** The experimental steps of the control and operation performance test of the wheelchair IIS are as follows. First, the TSCS experiment is designed for the intelligent wheelchair IIS. Then, the JCS experiment is carried out. The proposed wheelchair IIS controls the front, rear, left, and right acceleration and deceleration of the wheelchair, respectively. SPHN TSCS interface is more suitable for elderly information acquisition. Specifically, it marks the four virtual buttons with prominent direction symbols. Then, it develops the acceleration, deceleration, emergency stop, braking, and whistle buttons. As

such, it substantially improves the controllable interactive performance of the interface. Now that everything is ready, the TSCS and JCS control the wheelchair to accelerate, decelerate, and brake in the front, rear, left, and right directions, respectively. Figure 8 specifies the results.

Figure 8 indicates that the accuracy of SPHN TSCS is 98.1%, the average angle is  $93^\circ$ , and the total time cost is 54 seconds. The accuracy of the JCS is 99.2%, the average angle is  $89^\circ$ , and the total time cost is 50 seconds. Hence, the sensitivity of SPHN TSCS is higher than JCS; the joystick is more convenient to manipulate than the SPHN touch screen. The practicability of these two control methods is both very strong. Therefore, the proposed two independent control methods meet control performance requirements.

**3.2. Angle Acquisition and Measurement.** Mpu-6050 triple-axis gyroscope module is used to collect the inclination angle of the wheelchair. The theoretical measurement range is  $-180^\circ \sim 180^\circ$ , and the accuracy is  $0.01^\circ$ . Here, the accuracy of angle acquisition and measurement is measured by absolute error (AERR). AERR is the difference between the analysis result and the actual value. The accuracy is usually expressed through error. The smaller the error is, the higher the accuracy of the analysis result is. Figure 9 displays the actual measurement results.

Figure 9 signifies that the maximum measurement error of the module is  $0.3^\circ$  and the minimum is  $-0.45^\circ$ . Thus, the measurement accuracy is very high, and the functional performance is stable and reliable, meeting the design requirements. The obstacle avoidance control realized by the ultrasonic module can achieve a good obstacle avoidance effect in single and multiple obstacle environments. Ultrasonic obstacle avoidance has a larger obstacle avoidance

angle and is safer than infrared obstacle avoidance. Therefore, the proposed fuzzy obstacle avoidance control strategy is feasible and meets the design requirements.

**3.3. Simulation Analysis of OAA.** The learning conditions in the obstacle avoidance simulation experiment are set as follows: the total number of moves per time is 1,000 steps, and the number of learning times is 20. Figure 10 illuminates the specific simulation effect and learning effect.

Figure 10 corroborates that during the learning process of automatic obstacle avoidance, the number of steps of autonomous walking of the intelligent wheelchair fluctuates significantly at the beginning and gradually decreases at the end. The steps of the obstacle avoidance movement also change greatly at the beginning and then slowly stabilize a little later. The learning effect is the ratio of the number of steps of autonomous walking to the number of steps of obstacle avoidance movement. The learning effect is significantly improved with the increase of learning times, so the obstacle avoidance performance of the proposed wheelchair IIS has been improved.

## 4. Conclusion

Nowadays, there has been a rising voice for improving the quality of life of the elderly and the disabled. The present work holds that the elderly's convenience to move is of utmost importance and practical significance. To this end, this paper designs a wheelchair IIS based on fuzzy control theory and OAA. At the same time, a fuzzy obstacle avoidance control strategy is proposed for the wheelchair IIS. Then, practical experiments are designed to test the performance of the proposed OAA of wheelchair IIS. The experimental outcomes are as follows. (I) The accuracy is 98.1%, the average rotation angle is  $93^\circ$ , and the total time cost is 54 seconds for the TSCS. (II) For JCS, the accuracy is 99.2%, the average angle is  $89^\circ$ , and the total time cost is 50 seconds. Hence, the SPHN TSCS is more sensitive than the JCS, and the control joystick is more convenient to manipulate than the touch screen in the SPHN for the elderly. The two independent control modes meet the control performance requirements, which improves the automatic obstacle avoidance performance of the wheelchair IIS and has certain practical value. Based on their sensory functions, elderly users can obtain new experiences through different control methods. Also, they can enjoy barrier-free interaction between people and information equipment. The research deficiency is that the OAS experiment only involves static objects and lacks a dynamic performance test. Therefore, there is a need to continue to expand the use scene of the wheelchair IIS in future research.

## Data Availability

The labeled dataset used to support the findings of this study are available from the corresponding author upon request.

## Conflicts of Interest

The author declares no competing interests.

## Acknowledgments

This research supported by the 2018 National Social Science Foundation Art Project No. 18BG128 and 2021 Humanities and Social Science Research Project of Henan Provincial Education Department: "Research on User-Oriented Interface Information Visualization for the Aging", Project No. 2021-ZZJH-452.



## References

- [1] L. F. Sang, J. Z. Fu, Z. X. Gan, H. B. Wang, and Y. Tian, "Design and analysis of folding mechanism for intelligent wheelchair-stretcher robot," *Journal of Zhejiang University (Engineering Science)*, vol. 53, no. 4, pp. 613–620, 2019.
- [2] M. Z. Mistarihi, R. A. Okour, and A. A. Mumani, "An integration of a QFD model with Fuzzy-ANP approach for determining the importance weights for engineering characteristics of the proposed wheelchair design," *Applied Soft Computing*, vol. 90, article 106136, 2020.
- [3] M. F. R. Al-Okby, S. Neubert, N. Stoll, and K. Thurow, "Development and testing of intelligent wheelchair controller for quadriplegic Patients," *Advances in Science, Technology and Engineering Systems Journal*, vol. 3, no. 5, pp. 220–225, 2018.
- [4] X. Teng, L. Cong, J. Qiu, and A. Zhang, "Control design of an intelligent wheelchair based on a single-chip microcomputer," *Nanjing Xinxing Gongcheng Daxue Xuebao*, vol. 11, no. 4, pp. 495–498, 2019.
- [5] B. F. Wu, P. J. Chang, Y. S. Chen, and C. W. Huang, "An intelligent wheelchair anti-lock braking system design with friction coefficient estimation," *IEEE Access*, vol. 6, pp. 73686–73701, 2018.
- [6] M. Luo, D. Zhang, Q. Hu, X. Li, and Y. Qing, "Innovative design of an intelligent wheelchair," in *In 2020 2nd International Conference on Artificial Intelligence and Advanced Manufacturing (AIAM)*, pp. 69–74, Manchester, United Kingdom, 2020.
- [7] T. Y. Kim, D. W. Seo, and S. H. Bae, "Design of case-based intelligent wheelchair monitoring system," *Journal of the Chosun Natural Science*, vol. 10, no. 3, pp. 162–170, 2017.
- [8] B. Zhang, H. Eberle, C. Holloway, and T. Carlson, "Design requirements and challenges for intelligent power wheelchair use in crowds: learning from expert wheelchair users," *Age*, vol. 46, no. 12, p. 2, 2021.
- [9] D. Kumar, R. Malhotra, and S. Sharma, "Design and construction of a smart wheelchair," *Procedia Computer Science*, vol. 172, pp. 302–307, 2020.
- [10] X. Shi, H. Lu, and Z. Chen, "Design and analysis of an intelligent toilet wheelchair based on planar 2DOF parallel mechanism with coupling branch Chains," *Sensors*, vol. 21, no. 8, p. 2677, 2021.
- [11] K. Rahimunnisa, M. Atchaya, B. Arunachalam, and V. Divyaa, "AI-based smart and intelligent wheelchair," *Journal of applied research and technology*, vol. 18, no. 6, pp. 362–367, 2020.
- [12] S. R. Avutu, S. Paul, and D. Bhatia, "Design and feasibility test of an indigenous motorized wheel for manual wheelchair,"

- International Journal of Manufacturing, Materials, and Mechanical Engineering (IJMMME)*, vol. 9, no. 3, pp. 42–55, 2019.
- [13] Y. Rabhi, M. Mrabet, F. Fnaiech, P. Gorce, I. Miri, and C. Dziri, “Intelligent touchscreen joystick for controlling electric wheelchair,” *Irbm*, vol. 39, no. 3, pp. 180–193, 2018.
- [14] J. Woo, K. Yamaguchi, Y. Ohyama, and Department of Mechanical Engineering, School of Engineering, Tokyo University of Technology 1404-1 Katakura, Hachioji, Tokyo 192-0982, Japan, “Development of a control system and Interface design based on an electric wheelchair,” *Journal of Advanced Computational Intelligence and Intelligent Informatics*, vol. 25, no. 5, pp. 655–663, 2021.
- [15] W. Li, J. Zhang, T. Zhao, and J. Ren, “Experimental study of an indoor temperature fuzzy control method for thermal comfort and energy saving using wristband device,” *Building and Environment*, vol. 187, article 107432, 2021.
- [16] H. Benyazza, M. Bouhedda, and S. Rebouh, “Zoning irrigation smart system based on fuzzy control technology and IoT for water and energy saving,” *Journal of Cleaner Production*, vol. 302, article 127001, 2021.
- [17] C. Aguiar, D. Leite, D. Pereira, G. Andonovski, and I. Škrjanc, “Nonlinear modeling and robust LMI fuzzy control of overhead crane systems,” *Journal of the Franklin Institute*, vol. 358, no. 2, pp. 1376–1402, 2021.
- [18] T. Zhou, C. Liu, X. Liu, H. Wang, and Y. Zhou, “Finite-time prescribed performance adaptive fuzzy control for unknown nonlinear systems,” *Fuzzy Sets and Systems*, vol. 402, pp. 16–34, 2021.
- [19] M. A. Balootaki, H. Rahmani, H. Moeinkhah, and A. Mohammadzadeh, “Non-singleton fuzzy control for multi-synchronization of chaotic systems,” *Applied Soft Computing*, vol. 99, article 106924, 2021.
- [20] D. Li, H. Cao, and X. Chen, “Fuzzy control of milling chatter with piezoelectric actuators embedded to the tool holder,” *Mechanical Systems and Signal Processing*, vol. 148, article 107190, 2021.
- [21] C. C. Ku, W. J. Chang, M. H. Tsai, and Y. C. Lee, “Observer-based proportional derivative fuzzy control for singular Takagi- Sugeno fuzzy systems,” *Information Sciences*, vol. 570, pp. 815–830, 2021.
- [22] L. Xu, Z. Wang, Y. Liu, and L. Xing, “Energy allocation strategy based on fuzzy control considering optimal decision boundaries of standalone hybrid energy systems,” *Journal of Cleaner Production*, vol. 279, article 123810, 2021.

## Research Article

# Scenario Analysis of Water-Saving Potential in Yeast Manufacturing Industry under the Guidance of Water Intake Quota

Yubo Zhang <sup>1,2</sup> and Xue Bai <sup>1,2</sup>

<sup>1</sup>China National Institute of Standardization, Beijing 100191, China

<sup>2</sup>Key Laboratory of Energy Efficiency, Water Efficiency and Greenization for State Market Regulation, Beijing 102299, China

Correspondence should be addressed to Xue Bai; [baixue@cnis.ac.cn](mailto:baixue@cnis.ac.cn)

Received 3 March 2022; Revised 23 March 2022; Accepted 2 April 2022; Published 23 April 2022

Academic Editor: Yanqiong Li

Copyright © 2022 Yubo Zhang and Xue Bai. This is an open access article distributed under the Creative Commons Attribution License, which permits unrestricted use, distribution, and reproduction in any medium, provided the original work is properly cited.

While yeast manufacturing consumes a large amount of water per unit of product, water use efficiency varies widely within the industry due to disparity in water-saving technologies. By stipulating water intake per unit of product, the *Norm of Water Intake--Part 41: Yeast Production* (GB/T 18916.41-2019) will standardize production water use and improve the water-saving level of the yeast manufacturing industry. This paper estimates the industry's production capacity from 2020 to 2024 through regression analysis. It examines the distribution of water use efficiency under different policy scenarios based on the standard for water intake, including the business-as-usual scenario, the bottom-line scenario, the ideal scenario, and the expected scenario. Then, the water use of the yeast manufacturing industry under different scenarios is calculated, and the water-saving potential is analyzed by comparing it with the business-as-usual scenario. The results indicate that depending on the intensity of policy implementation, the average annual water savings will range from  $2.5 \times 10^6 \text{ m}^3$  to  $14 \times 10^6 \text{ m}^3$ . The cumulative water savings will add up to  $16 \times 10^6 \text{ m}^3$  to  $51 \times 10^6 \text{ m}^3$  in the next five years, which is very large.

## 1. Introduction

Common challenges regarding water resources in the world include rising demands for water resources due to population growth, difficulty in balancing agriculture and urban development, and various consequences of changing climate. The water-saving potential is an essential indicator to measure and guide water resource allocation and planning. As a part of the fermentation industry, the yeast manufacturing industry mainly produces yeast and yeast derivatives. While yeast manufacturing consumes a large amount of water per product, water use efficiency varies widely due to disparity in water-saving technologies. At present, water intake per product unit stands at about  $70\sim 100 \text{ m}^3/\text{t}$  for yeast and  $95\sim 120 \text{ m}^3/\text{t}$  for yeast derivatives. There is considerable room for water saving in the industry as a whole. The *Norm of Water Intake--Part 41: Yeast Production* (GB/T 18916.41-2019) [1], one of China's national

standards for water use, specifies water intake per unit of yeast and yeast derivatives. Under this norm, water authorities carry out planned water management and water licensing, and yeast manufacturers control water saving. The standard reflects the current level of water use in the yeast manufacturing industry and will steer the drive towards a higher level of water saving.

Many studies on potential energy savings and emission reductions regarding energy and resource conservation can be found. Typical models include the Market Allocation of Technologies Model (MARKAL) [2, 3], the Asian-Pacific Integrated Model (AIM) [4], the Long-range Energy Alternatives Planning System (LEAP) [5, 6], the Computational General Equilibrium Model (CGE) [7], and cluster analysis [8]. Regarding water-saving areas, research mainly focuses on agricultural irrigation [9], residential water use, and total water consumption in regions or cities. The Alliance for Water Efficiency [10] evaluated water-saving potential for

single-family households in Detroit via inefficient toilet replacement and estimated a saving value of 9,721 gallons per year. The average potential for potable water savings by using rainwater and greywater ranges from 39.2% to 42.7% among the sample blocks in southern Brazil [11]. Analysis for the water-saving potential in California shows that water savings would be 0.74 million to 1.6 million acre-feet per year in the commercial, institutional, and industrial sectors, and 2.2 million to 3.6 million acre-feet water per year would be reduced at home due to the considerable progress in improving water use efficiency [12]. Qin et al. [13] calculated the water-saving potential of the Beijing-Tianjin-Hebei area in the dimensions of water saving and resource saving by analyzing the process and influencing factors of water use in various industries in the region. Zhu [14] compared the industrial water use efficiency of different areas in China and estimated the water-saving potential of other provinces with the water use efficiency of Shandong Province as a reference. Song and Gao [15] identified the advanced level of urban water use based on the normal distribution and comprehensively proposed a coefficient to assess urban water-saving potential. Zhao et al. [16] examined the water consumption of thermal power generation and evaluated its water-saving potential by comparing it with the indicators in the relevant national standards. Zhao Z et al. [17] evaluated the water resource utilization efficiency and water-saving potential development landscape and path of different scenarios in 2035 in comparison to Shenzhen. Recently, study on the coal-to-synthetic natural gas process showed that by taking water-saving gasification technology, zero liquid discharge, integrating the water networks, and improving other units, water consumption can be lower than 3.50 t/kNm<sup>3</sup> water saved [18].

The existing studies on water-saving potential are mainly conducted about water appliances and unconventional water use at a regional scale, with few studies specific to industries. Water quota is also rarely considered. Without adequate decision-making support for quotas and policy targets, the norm fails to produce the desired effect. The scenario analysis is commonly used in forecasting and assessing the water availability and consumption [19, 20], simulation and impact of technological introduction, and governance regimes about water [21–24].

In this work, we used a combination of regression analysis and scenario analysis to explore the changes in the corresponding industry scale and water intake after the implementation of the water intake quota standard, establish a water-saving forecast model, and explore its water-saving potential.

## 2. Method

Based on stipulated water use level, combined with survey data, industry size in five years (2019–2024) after the *Norm of Water Intake--Part 41: Yeast Production* (GB/T 18916.41–2019) enters into force is identified through regression analysis. Taking into account the distribution of water use levels in the industry when the standard was

released (2019), three policy scenarios of water use are designed, in contrast to the business-as-usual (BAU) scenario where the norm is absent, to analyze the possible impact of the standard on water use efficiency. Water savings under these scenarios are estimated, that is, the water-saving potential brought by the standard under different scenarios.

## 3. Production Capacity Forecast

Yeast and yeast derivatives are the main products of the yeast manufacturing industry, approximately representing 70% and 30% of the industrial production capacity, respectively. Yeast, characterized by complete yeast cells, includes highly active dry yeast, fresh yeast, nutritional yeast, and inactive yeast. Yeast derivatives encompass yeast extract, autolysed yeast, yeast protein, polypeptide, yeast cell wall, and yeast zymosan. According to the *China Yeast Industry Analysis Report, 2020–2026: Development Model and Planning*, China's yeast production grew year by year from 2012 to 2018 as the specific numbers are 280,000 tons, 294,000 tons, 308,000 tons, 318,000 tons, 330,000 tons, 350,000 tons, 373,000 tons, and 394,000 tons (Figure 1).

Based on the 2012–2018 data of yeast production, the linear regression equation for annual yeast production is created in Excel, as shown below:

$$y = 1.5845x + 25.957. \quad (1)$$

The results show that the correlation coefficient ( $r$ ) of variables in the linear regression equation is 0.9798. In other words, yeast production is positively and increasingly correlated with the year.

According to the equation, it is inferred that, after implementing the norm mentioned above, the annual yeast production will be 402,000 tons, 420,000 tons, 438,000 tons, 457,000 tons, and 474,000 tons from 2020 to 2024, respectively. Since yeast and yeast derivatives account for 70% and 30% of the total production capacity according to industry research, it is estimated that the annual output of yeast derivatives during this period will reach 172,000 tons, 180,000 tons, 188,000 tons, 196,000 tons, and 203,000 tons, respectively.

## 4. Scenario Analysis of Water Use in the Yeast Manufacturing Industry

The structure of production capacity with different water use efficiency before the *Norm of Water Intake--Part 41: Yeast Production* (GB/T 18916.41–2019) takes effect (2019) is regarded as the BAU scenario (scenario 0). Based on the standard for water intake specified in the norm (Table 1), three states of water use efficiency distribution after the entry into force of the norm are drawn, i.e., the bottom-line scenario (scenario 1), the ideal scenario (scenario 2), and the expected scenario (scenario 3), to represent different water-saving management levels and policy implementation intensity. Table 2 shows the specific scenario setting method and the policy implication.

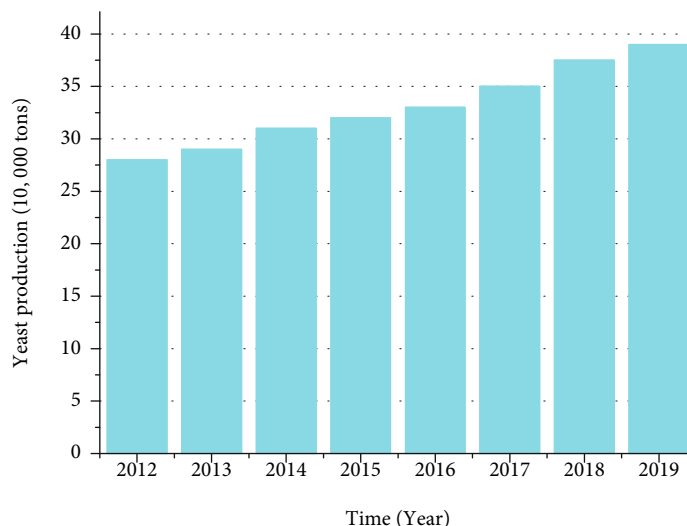


FIGURE 1: Yeast production capacity, 2012–2019.

TABLE 1: The quota for water intake specified in the norm GB/T 18916.41-2019 (in cubic meters per ton).

	Yeast	Yeast derivatives
Existing enterprises	85	115
Newly built (renovated, expanded) enterprises	70	100
Advanced enterprises	65	90

According to the survey of yeast factories, yeast output totals 202,000 tons. Among them, about 32,000 tons, that is, 16% of the surveyed production capacity, used  $85 \text{ m}^3/\text{t}$  of water per unit of product in 2016. In addition, 60% met the standard ( $70 \text{ m}^3/\text{t}$ ) for water use efficiency of newly built (renovated and expanded) enterprises, while 24% reached the advanced level ( $65 \text{ m}^3/\text{t}$ ).

Enterprises covered by the survey are generally large and technologically advanced in China. Those not included in the study may be small and relatively backward, with a weak capacity to promote cleaner production and advanced technology. Hence, their water use efficiency is very likely to exceed  $85 \text{ m}^3/\text{t}$ . Taking into account the water use efficiency and production capacity of such enterprises, more than 30% of the yeast production capacity in China has water use efficiency higher than  $85 \text{ m}^3/\text{t}$ ; about 55% has water use efficiency up to the minimum standard, but still below the standard for newly built (renovated and expanded) enterprises ( $70\sim 85 \text{ m}^3/\text{t}$ ); about 10% reaches the standard for newly built (renovated and expanded) enterprises, but not the advanced level ( $65\sim 70 \text{ m}^3/\text{t}$ ); and around 5% achieved the advanced level ( $65 \text{ m}^3/\text{t}$ ).

Suppose the norm of water intake is not adopted. In that case, under the BAU scenario, the water efficiency is slowly improving from 30%, 55%, 10%, and 5% of 2019 to 10%,

60%, 20%, and 10% of 2024 for the production capacity of more than  $85 \text{ m}^3/\text{t}$ , in the range of  $70\sim 85 \text{ m}^3/\text{t}$ , in the field of  $65\sim 70 \text{ m}^3/\text{t}$ , and less than  $65 \text{ m}^3/\text{t}$ , respectively, as in Figure 2.

In the bottom-line scenario, with the norm's implementation, the backward production capacity meets the standard, and five years after the norm takes effect, the main production capacity (60%) reaches the bars for newly built enterprises, and the production capacity that only passes the bars for existing enterprises and reaches the advanced ones, respectively, accounts for 20%. More specifically, the production capacity of water use efficiency in the range of  $70\sim 85 \text{ m}^3/\text{t}$ , in the field of  $65\sim 70 \text{ m}^3/\text{t}$ , and less than  $65 \text{ m}^3/\text{t}$  slowly changed from 70%, 20%, and 10% to 20%, 60%, and 20%, respectively, as shown in Figure 3. The production capacity below the minimum standard is eliminated in the ideal scenario. All the production capacity reaches the advanced level five years after the norm enters into force (2024), as shown in Figure 4. The production capacity below the minimum standard is eliminated in the expected scenario. 70% of the production capacity in the industry gradually reaches the standard for newly built (renovated and expanded) enterprises, and 30% reaches the advanced level five years after the norm enters into force (2024), as shown in Figure 5.

## 5. Analysis of Water-Saving Potential

Water savings from yeast and yeast derivative production are estimated by calculating water use under different scenarios and comparing it with the BAU scenario.

*5.1. Calculation of Water Use under the BAU Scenario.* The BAU scenario (scenario 0) assumes that the industry water efficiency is slowly increasing, including the backward capacity that does not meet existing enterprises' standards. In the BAU scenario, water efficiency remains the same after



TABLE 2: Scenario design for water-saving potential calculation.

No.	Parameter setting method	Policy implication
Scenario 0: BAU scenario	Industry water efficiency is slowly increasing, including the backward capacity that does not meet the standard for existing enterprises (Figure 2).	The norm is not implemented, a benchmark scenario compared to other scenarios.
Scenario 1: bottom-line scenario	The backward production capacity meets the standard. Five years after the norm takes effect, the main production capacity (60%) reaches the bars for newly built enterprises. The production capacity that only passes the bars for existing enterprises and reaches the advanced ones, respectively, accounts for 20% (Figure 3).	Policy implementation is weak. Only the minimum requirements are met, representing the bottom line of water savings.
Scenario 2: ideal scenario	The backward production capacity meets the standard. Five years after the norm takes effect, all the production capacity is advanced (Figure 4).	The norm plays a significant role in significantly improving the water efficiency of the yeast manufacturing industry. The estimates represent the ideal amount of water savings.
Scenario 3: expected scenario	The backward production capacity meets the standard. Five years after the norm takes effect, with the replacement of production capacity, 70% of the production capacity in the industry reaches the bars for newly built enterprises, and 30% reaches the advanced level (Figure 5).	The norm plays a role in improving the water efficiency of the yeast manufacturing industry. The estimates represent the expected amount of water savings.

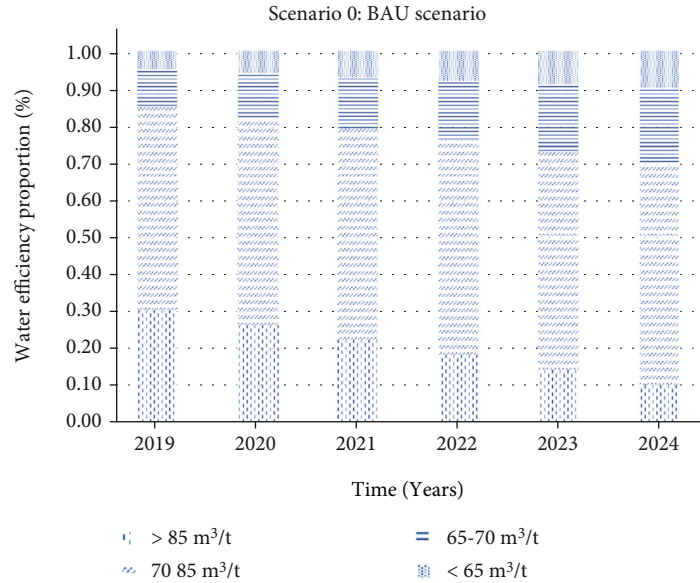


FIGURE 2: Water efficiency distributions in scenario 0.

2019 as in 2018. In other words, 30%, 55%, 10%, and 5% of the production capacity have water use per unit of product larger than  $85 \text{ m}^3/\text{t}$ , in the range of  $70\sim 85 \text{ m}^3/\text{t}$ , in the field of  $65\sim 70 \text{ m}^3/\text{t}$ , and less than  $65 \text{ m}^3/\text{t}$ , respectively. With the advancement of technology, the water efficiency of the industry is slowly improving. By 2024, the excellent production capacities that achieve the above water efficiency will be 10%, 60%, 20%, and 0%. From 2019 to 2024, the water used for yeast production is calculated to be  $31.27 \times 10^6 \text{ m}^3$ ,  $31.56 \times 10^6 \text{ m}^3$ ,  $32.60 \times 10^6 \text{ m}^3$ ,  $33.62 \times 10^6 \text{ m}^3$ ,  $34.68 \times 10^6 \text{ m}^3$ , and  $35.55 \times 10^6 \text{ m}^3$ , respectively. The water used to produce yeast derivatives is estimated to be  $18.40 \times 10^6 \text{ m}^3$ ,

$18.56 \times 10^6 \text{ m}^3$ ,  $19.25 \times 10^6 \text{ m}^3$ ,  $19.92 \times 10^6 \text{ m}^3$ ,  $20.58 \times 10^6 \text{ m}^3$ , and  $21.11 \times 10^6 \text{ m}^3$ , respectively. Thus, the water consumption of the yeast manufacturing industry as a whole in the next five years will reach  $49.67 \times 10^6 \text{ m}^3$ ,  $50.12 \times 10^6 \text{ m}^3$ ,  $51.85 \times 10^6 \text{ m}^3$ ,  $53.54 \times 10^6 \text{ m}^3$ ,  $55.25 \times 10^6 \text{ m}^3$ , and  $56.66 \times 10^6 \text{ m}^3$ , respectively. Table 3 shows the output and water use of different products and the total water use under the BAU scenario in the next five years.

5.2. *Water-Saving Potential in the Bottom-Line Scenario.* The bottom-line scenario (scenario 1) assumes that the backward production capacity meets the standard, and five years after

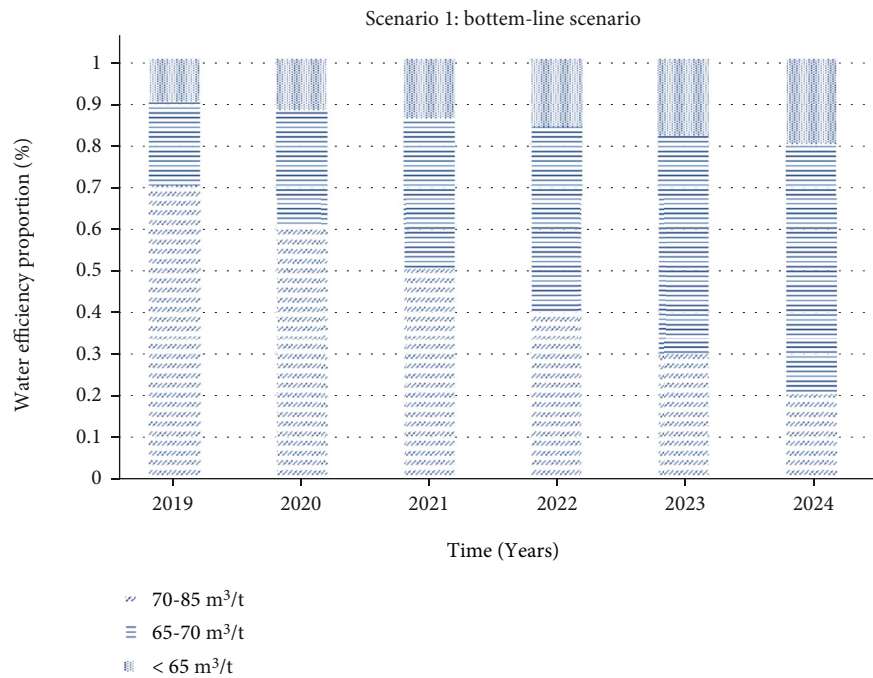


FIGURE 3: Water efficiency distributions in scenario 1.

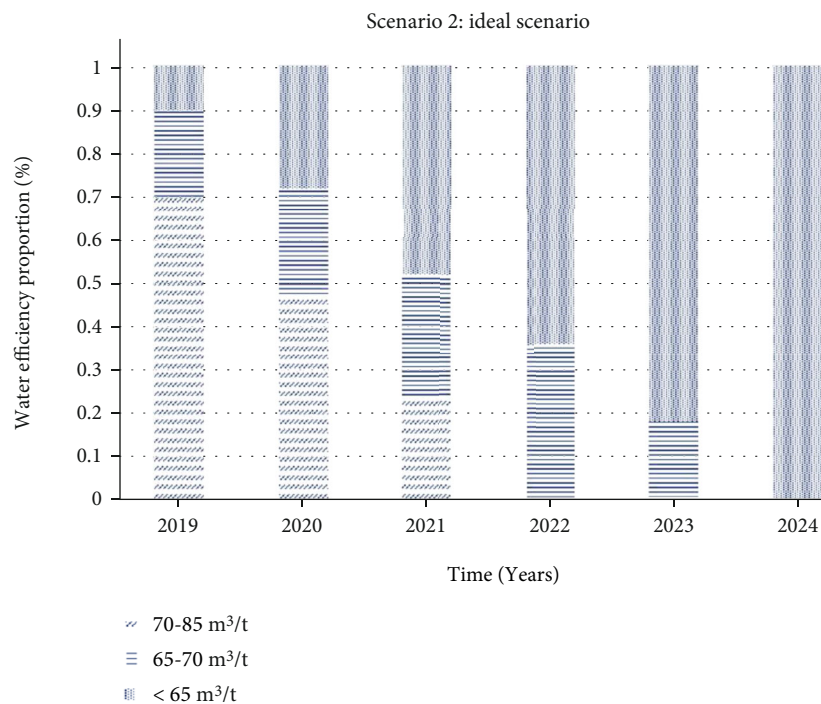


FIGURE 4: Water efficiency distributions in scenario 2.

the norm takes effect, the main production capacity (60%) reaches the bars for newly built enterprises, and the production capacity that only passes the bars for existing enterprises and reaches the advanced ones, respectively, accounts for 20%. That is to say, in the bottom-line scenario, the production capacity of water use efficiency in the range of 70~85 m<sup>3</sup>/t, in the field of 65~70 m<sup>3</sup>/t, and less than

65 m<sup>3</sup>/t slowly changed from 70%, 20%, and 10% to 20%, 60%, and 20%, respectively. From 2019 to 2024, the water used for yeast production is calculated to be 29.06 × 10<sup>6</sup> m<sup>3</sup>, 29.19 × 10<sup>6</sup> m<sup>3</sup>, 30.01 × 10<sup>6</sup> m<sup>3</sup>, 30.79 × 10<sup>6</sup> m<sup>3</sup>, 31.60 × 10<sup>6</sup> m<sup>3</sup>, and 32.23 × 10<sup>6</sup> m<sup>3</sup>, respectively. The water used for the production of yeast derivatives is estimated to be 17.37 × 10<sup>6</sup> m<sup>3</sup>, 17.42 × 10<sup>6</sup> m<sup>3</sup>, 17.97 × 10<sup>6</sup> m<sup>3</sup>, 18.50 ×

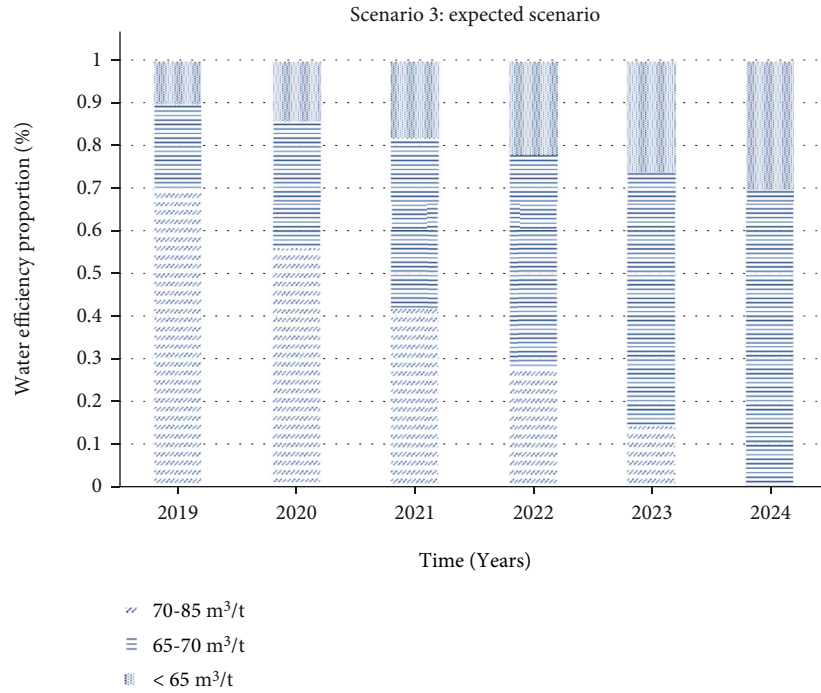


FIGURE 5: Water efficiency distributions in scenario 3.

TABLE 3: Water use calculation of the yeast manufacturing industry in the BAU scenario, 2019–2024.

Year		2019	2020	2021	2022	2023	2024	
Yeast	Output ( $\times 103 \text{ m}^3$ )	394	402	420	438	457	474	
	Water efficiency distribution (%)	<65 $\text{m}^3/\text{t}$	5	6	7	8	9	10
		65-70 $\text{m}^3/\text{t}$	10	12	14	16	18	2
		70-85 $\text{m}^3/\text{t}$	55	56	57	58	59	6
		>85 $\text{m}^3/\text{t}$	30	26	22	18	14	1
Water intake ( $\times 106 \text{ m}^3$ )	31.27	31.56	32.60	33.62	34.68	35.55		
Yeast derivatives	Output ( $\times 103 \text{ m}^3$ )	169	172	180	188	196	203	
	Water efficiency distribution (%)	<90 $\text{m}^3/\text{t}$	5	6	7	8	9	10
		90~100 $\text{m}^3/\text{t}$	10	12	14	16	18	2
		100~115 $\text{m}^3/\text{t}$	55	56	57	58	59	6
	>115 $\text{m}^3/\text{t}$	30	26	22	18	14	1	
Water intake ( $\times 106 \text{ m}^3$ )	18.40	18.56	19.25	19.92	20.58	21.11		
Total water intake ( $\times 106 \text{ m}^3$ )		49.67	50.12	51.85	53.54	55.25	56.66	

106  $\text{m}^3$ ,  $19.00 \times 106 \text{ m}^3$ , and  $19.39 \times 106 \text{ m}^3$ , respectively. Therefore, the water consumption of the yeast manufacturing industry as a whole in the next five years will be  $46.42 \times 106 \text{ m}^3$ ,  $46.61 \times 106 \text{ m}^3$ ,  $47.98 \times 106 \text{ m}^3$ ,  $49.29 \times 106 \text{ m}^3$ ,  $50.60 \times 106 \text{ m}^3$ , and  $51.62 \times 106 \text{ m}^3$ , respectively. Compared with the BAU scenario, water savings in the bottom-line scenario are expected to reach  $3 \sim 5 \times 106 \text{ m}^3$  per year and  $24 \times 106 \text{ m}^3$  in total by 2024, the water efficiency increased by 8.9%. Table 4 shows the output and water use of different products and the total water use in the next five years in the bottom-line scenario and water savings compared with the BAU scenario.

5.3. *Water-Saving Potential in the Ideal Scenario.* The ideal scenario (scenario 2) assumes that the backward production capacity meets the standard, and five years after the norm takes effect, all the production capacity is advanced. In other words, under the ideal scenario, 100% of the production capacity uses less than  $65 \text{ m}^3/\text{t}$  of water per unit of product. In the early implementation of the norm, the water use of the whole industry will shrink due to water use efficiency improvement of inefficient production capacity. Still, later, it will tend to rise, driven by a substantial increase in production. From 2019 to 2024, the water used for yeast production is calculated to be  $29.06 \times 106 \text{ m}^3$ ,  $28.18 \times 106 \text{ m}^3$ ,

TABLE 4: Water use calculation of the yeast manufacturing industry in the bottom-line scenario, 2019–2024.

Year		2019	2020	2021	2022	2023	2024	
Yeast	Output ( $\times 103 \text{ m}^3$ )	394	402	420	438	457	474	
	Water efficiency distribution (%)	$<65 \text{ m}^3/\text{t}$	10	12	14	16	18	20
		$65\text{-}70 \text{ m}^3/\text{t}$	20	28	36	44	52	60
		$70\text{-}85 \text{ m}^3/\text{t}$	70	60	50	40	30	20
	Water use ( $\times 106 \text{ m}^3$ )	29.06	29.19	30.01	30.79	31.60	32.23	
Yeast derivatives	Output ( $\times 103 \text{ m}^3$ )	169	172	180	188	196	203	
	Water efficiency distribution (%)	$<90 \text{ m}^3/\text{t}$	10	12	14	16	18	20
		$90\text{-}100 \text{ m}^3/\text{t}$	20	28	36	44	52	60
		$100\text{-}115 \text{ m}^3/\text{t}$	70	60	50	40	30	20
	Water intake ( $\times 106 \text{ m}^3$ )	17.37	17.42	17.97	18.50	19.00	19.39	
Total water intake ( $\times 106 \text{ m}^3$ )	46.42	46.61	47.98	49.29	50.60	51.62		
Annual water savings ( $\times 106 \text{ m}^3$ )	3.25	3.51	3.87	4.24	4.65	5.04		
Total water savings ( $\times 106 \text{ m}^3$ )	3.25	6.76	10.63	14.87	19.52	24.56		
Water efficiency increased (%)	6.5	7.0	7.5	7.9	8.4	8.9		

TABLE 5: Water use calculation of the yeast manufacturing industry under the ideal scenario, 2019–2024.

Year		2019	2020	2021	2022	2023	2024	
Yeast	Output ( $\times 103 \text{ m}^3$ )	394	402	420	438	457	474	
	Water efficiency distribution (%)	$<65 \text{ m}^3/\text{t}$	10	28	48	64	82	1
		$65\text{-}70 \text{ m}^3/\text{t}$	20	25	28	36	18	0
		$70\text{-}85 \text{ m}^3/\text{t}$	70	47	24	0	0	0
	Water intake ( $\times 106 \text{ m}^3$ )	29.06	28.18	27.85	27.46	28.04	28.44	
Yeast derivatives	Output ( $\times 103 \text{ m}^3$ )	169	172	180	188	196	203	
	Water efficiency distribution (%)	$<90 \text{ m}^3/\text{t}$	10	28	48	64	82	1
		$90\text{-}100 \text{ m}^3/\text{t}$	20	25	28	36	18	0
		$100\text{-}115 \text{ m}^3/\text{t}$	70	47	24	0	0	0
	Water intake ( $\times 106 \text{ m}^3$ )	17.37	16.87	16.78	16.66	17.01	17.26	
Total water intake ( $\times 106 \text{ m}^3$ )	46.42	45.05	44.62	44.12	45.05	45.70		
Annual water savings ( $\times 106 \text{ m}^3$ )	3.25	5.07	7.23	9.42	10.20	10.97		
Total water savings ( $\times 106 \text{ m}^3$ )	3.25	8.32	15.55	24.96	35.16	46.13		
Water efficiency increased (%)	6.5	10.1	13.9	17.6	18.5	19.4		

$27.84 \times 106 \text{ m}^3$ ,  $27.46 \times 106 \text{ m}^3$ ,  $28.04 \times 106 \text{ m}^3$ , and  $28.44 \times 106 \text{ m}^3$ , respectively. The water used for the production of yeast derivatives is estimated to be  $17.37 \times 106 \text{ m}^3$ ,  $16.87 \times 106 \text{ m}^3$ ,  $16.78 \times 106 \text{ m}^3$ ,  $16.66 \times 106 \text{ m}^3$ ,  $17.01 \times 106 \text{ m}^3$  and  $17.26 \times 106 \text{ m}^3$ , respectively. Hence, the water consumption of the yeast manufacturing industry as a whole in the next five years will stand at  $46.42 \times 106 \text{ m}^3$ ,  $45.05 \times 106 \text{ m}^3$ ,  $44.62 \times 106 \text{ m}^3$ ,  $44.12 \times 106 \text{ m}^3$ ,  $45.05 \times 106 \text{ m}^3$ , and  $45.70 \times 106 \text{ m}^3$ , respectively. Compared with the BAU scenario, annual water savings under the ideal scenario are expected to reach  $3 \sim 11 \times 106 \text{ m}^3$ , making a total of  $46 \times 106 \text{ m}^3$  by 2024. Table 5 shows the output and water use of different products and the total water use in the next five years under the bottom-line scenario and water savings are shown in Table 5.

**5.4. Water-Saving Potential in Expected Scenarios.** The expected scenario (scenario 3) assumes that the backward production capacity meets the standard, and five years after

the norm takes effect, 70% of the production capacity reaches the bars for newly built enterprises, and 30% reaches the advanced level. In other words, in the expected scenario, 70% and 30% of the production capacity reduce water use to  $65\text{-}70 \text{ m}^3/\text{t}$  and less than  $65 \text{ m}^3/\text{t}$ , respectively. In the early implementation of the norm, the water use of the whole industry will decline due to water use efficiency improvement of inefficient production capacity. Still, it will increase later as production expands significantly. From 2019 to 2024, the water used for yeast production is calculated to be  $29.06 \times 106 \text{ m}^3$ ,  $28.96 \times 106 \text{ m}^3$ ,  $29.55 \times 106 \text{ m}^3$ ,  $30.07 \times 106 \text{ m}^3$ ,  $30.60 \times 106 \text{ m}^3$ , and  $30. \times 106 \text{ m}^3$ , respectively. The water used to produce yeast derivatives is estimated to be  $17.37 \times 106 \text{ m}^3$ ,  $17.30 \times 106 \text{ m}^3$ ,  $17.72 \times 106 \text{ m}^3$ ,  $18.10 \times 106 \text{ m}^3$ ,  $18.45 \times 106 \text{ m}^3$ , and  $18.68 \times 106 \text{ m}^3$ , respectively. Hence, the water consumption of the yeast manufacturing industry as a whole in the next five years will amount to  $46.42 \times 106 \text{ m}^3$ ,  $46.26 \times 106 \text{ m}^3$ ,  $47.27 \times 106 \text{ m}^3$ ,  $48.17 \times$

TABLE 6: Water use calculation of the yeast manufacturing industry in the expected scenario, 2019–2024.

Year			2019	2020	2021	2022	2023	2024
Yeast	Output ( $\times 10^3 \text{ m}^3$ )		394	402	420	438	457	474
	Water efficiency distribution (%)	$<65 \text{ m}^3/\text{t}$	10	14	18	22	26	30
		$65\text{--}70 \text{ m}^3/\text{t}$	20	30	40	50	60	70
		$70\text{--}85 \text{ m}^3/\text{t}$	70	56	42	28	14	0
	Water intake ( $\times 10^6 \text{ m}^3$ )		29.06	28.96	29.55	30.07	30.60	30.93
Yeast derivatives	Output ( $\times 10^3 \text{ m}^3$ )		169	172	180	188	196	203
	Water efficiency distribution (%)	$<90 \text{ m}^3/\text{t}$	10	14	18	22	26	30
		$90\text{--}100 \text{ m}^3/\text{t}$	20	30	40	50	60	70
		$100\text{--}115 \text{ m}^3/\text{t}$	70	56	42	28	14	0
	Water intake ( $\times 10^6 \text{ m}^3$ )		17.37	17.30	17.72	18.10	18.45	18.68
Total water intake ( $\times 10^6 \text{ m}^3$ )			46.42	46.27	47.27	48.17	49.05	49.61
Annual water savings ( $\times 10^6 \text{ m}^3$ )			3.25	3.85	4.58	5.36	6.20	7.06
Total water savings ( $\times 10^6 \text{ m}^3$ )			3.25	7.10	11.68	17.04	23.24	30.30
Water efficiency increased (%)			6.5	7.7	8.8	10.0	11.2	12.5

$106 \text{ m}^3$ ,  $49.05 \times 10^6 \text{ m}^3$ , and  $49.61 \times 10^6 \text{ m}^3$ , respectively. Compared with the BAU scenario,  $3 \sim 7 \times 10^6 \text{ m}^3$  of water can be saved annually under the expected scenario, making  $30 \times 10^6 \text{ m}^3$ . By 2024, the water efficiency will increase by 12.5%. Table 6 shows the output and water use of different products and the total water use in the next five years under the expected scenario and water savings compared with the BAU scenario.

## 6. Conclusion

This study uses a combination of regression analysis and scenario analysis to explore the changes in the corresponding industry scale and water intake after the implementation of the water intake quota standard, establish a water-saving forecast model, and explore its water-saving potential. The results show that under the guidance of different implementation efforts and policies, the predicted average annual water saving within five years after implementing the standard is  $5 \sim 9 \times 10^6 \text{ m}^3$ . The accumulated water saving will be about  $24\text{--}46$  million  $\text{m}^3$ , and the water efficiency will be increased by  $8.9\text{--}19.4\%$ . Due to the high concentration of yeast manufacturing industry, the likely expected scenario is that all production capacity will meet the new (reconstruction and expansion) index requirements stipulated in the water intake quota standard, and 30% of them will reach the advanced value after five years. Compared with the BAU scenario, the annual water saving after implementing the standard will get more than  $7 \times 10^6 \text{ m}^3$ . The total water savings will exceed  $30 \times 10^6 \text{ m}^3$  by 2024 in total. The water efficiency will increase by about 12.5% in the typical situation. Therefore, the water intake norm will help create huge water-saving potential in the yeast manufacturing industry.

## Data Availability

All data can be obtained through the manuscript or by contacting the authors.

## Conflicts of Interest

The authors declare that they have no conflicts of interest.

## References

- [1] J. Wang, H. Chen, J. Li et al., *Norm of Water Intake — Part 41: Yeast Production*, Standards Press of China, Beijing, China, 2019.
- [2] R. O. Mendelsohn, A. Dinar, and L. Williams, “The distributional impact of climate change on rich and poor countries,” *Environment & Development Economics*, vol. 11, no. 2, pp. 159–178, 2006.
- [3] M. A. Trail, A. P. Tsimpidi, L. Peng et al., “Impacts of potential  $\text{CO}_2$ -reduction policies on air quality in the United States,” *Environmental Science & Technology*, vol. 49, no. 8, pp. 5133–5141, 2015.
- [4] Z. Wen, F. Meng, and M. Chen, “Estimates of the potential for energy conservation and  $\text{CO}_2$  emissions mitigation based on Asian-Pacific integrated model (AIM): the case of the iron and steel industry in China,” *Journal of Cleaner Production*, vol. 65, no. 4, pp. 120–130, 2014.
- [5] A. Smith, F. Kern, R. Raven, and B. Verhees, “Spaces for sustainable innovation: solar photovoltaic electricity in the UK,” *Technological Forecasting and Social Change*, vol. 81, pp. 115–130, 2014.
- [6] R. K. Bose, “Energy demand and environmental implications in urban transport—case of Delhi,” *Atmospheric Environment*, vol. 30, no. 3, pp. 403–412, 1996.
- [7] A. Schaefer and H. D. Jacoby, “Technology detail in a multisector CGE model: transport under climate policy,” *Energy Economics*, vol. 27, pp. 1–24, 2005.
- [8] S. Petcharat, S. Chungpaibulpatana, and P. Rakkwamsuk, “Assessment of potential energy saving using cluster analysis: a case study of lighting systems in buildings,” *Energy & Buildings*, vol. 52, pp. 145–152, 2012.
- [9] D. Wu, Y. Cui, and Y. Luo, “Irrigation efficiency and water-saving potential considering reuse of return flow,” *Agricultural Water Management*, vol. 221, pp. 519–527, 2019.

- [10] Alliance for Water Efficiency, M. A. Dickinson, B. Christiansen, and L. Smith, *An Assessment of Water Affordability and Conservation Potential in Detroit, Michigan*, KOHLER press, Chicago, 2020.
- [11] E. Ghisi and D. F. Ferreira, "Potential for potable water savings by using rainwater and greywater in a multi-storey residential building in southern Brazil," *Building & Environment*, vol. 42, no. 7, pp. 2512–2522, 2007.
- [12] N. R. D. Council and P. Institute, *Urban Water Conservation and Efficiency Potential in California*, Pacific Institute and the Natural Resources Defense Council, New York Oakland, 2014.
- [13] C. Qin, Y. Zhao, H. Li, and J. Qu, "Assessment of regional water-saving potential," *South-to-North Water Transfers and Water Science & Technology*, vol. 19, no. 1, pp. 36–42, 2021.
- [14] Q. Zhu, "Empirical study on China's industrial water use efficiency and water-saving potential," *Journal of Industrial Technological Economics*, vol. 9, pp. 48–51, 2007.
- [15] G. Song and W. Gao, "Evaluation of China's urban water-saving potential," *Journal of Arid Land Resources and Environment*, vol. 31, no. 12, pp. 1–7, 2017.
- [16] J. Zhao, D. Wu, X. Hui, Y. Han, and T. Wang, "Analysis for water use-consumption and water-saving potential of the thermal power industry in China," *Journal of North China University of Water Resources and Electric Power (Natural Science Edition)*, vol. 42, no. 2, pp. 95–103, 2021.
- [17] Z. Zhao, L. Zhao, Y. Wang, and T. Yuan, "Analysis of water resources utilization efficiency and water saving potential in Xiong'an new area under different scenarios," *Journal of Natural Resources*, vol. 34, no. 12, pp. 2629–2642, 2019.
- [18] C. Wang, S. He, S. Li, and L. Gao, "Water saving potential of coal-to-synthetic natural gas," *Journal of Cleaner Production*, vol. 280, article 124326, 2021.
- [19] J. Okungu, J. Adeyemo, and F. Otieno, "Scenario analysis of water supply and demand using WEAP model: a case of Yala catchment, Kenya," *American Journal of Water Resources*, vol. 5, no. 4, pp. 125–131, 2017.
- [20] S. Giertz, B. Diekkrüger, A. Jaeger, and M. Schopp, "An interdisciplinary scenario analysis to assess the water availability and water consumption in the Upper Ouémé catchment in Benin," *Advances in Geosciences*, vol. 9, pp. 3–13, 2006.
- [21] S. Eisaku, M. Yoshiyuki, Y. Ikuo, K. Tomijiro, H. Koji, and H. Tadayoshi, "Scenario analysis for reduction of pollutant load discharged from a watershed by recycling of treated water for irrigation," *Journal of Environmental Sciences*, vol. 22, no. 6, pp. 878–884, 2010.
- [22] L. W. Keeler, A. Wiek, D. D. White, and D. A. Sampson, "Linking stakeholder survey, scenario analysis, and simulation modeling to explore the long-term impacts of regional water governance regimes," *Environmental Science & Policy*, vol. 48, pp. 237–249, 2015.
- [23] M. Ghiyasi and A. Dehnokhalaji, "A scenario-based model for resource allocation with price information," *Foundations of Computing and Decision Sciences*, vol. 46, no. 4, pp. 339–360, 2021.
- [24] V. Sivagurunathan, S. Elsawah, and S. J. Khan, "Scenarios for urban water management futures: a systematic review," *Water Research*, vol. 211, article 118079, 2022.

## Research Article

# Analysis of Water Supply-Demand Based on Socioeconomic Efficiency

Wenyang Ren <sup>1</sup>, Xue Bai <sup>2,3</sup>, Yuetian Wang <sup>1</sup>, Chaoming Liang <sup>1</sup>, Siyan Huang <sup>1</sup>,  
Zhiying Wang <sup>1</sup> and Liu Yang <sup>1</sup>

<sup>1</sup>College of Geoscience and Surveying Engineering, China University of Mining and Technology (Beijing), Beijing 100083, China

<sup>2</sup>China National Institute of Standardization, Beijing 100191, China

<sup>3</sup>Key Laboratory of Energy Efficiency, China National Institute of Standardization, Beijing 102299, China

Correspondence should be addressed to Liu Yang; yang\_l@126.com

Received 7 March 2022; Revised 22 March 2022; Accepted 29 March 2022; Published 20 April 2022

Academic Editor: Wen Zeng

Copyright © 2022 Wenyang Ren et al. This is an open access article distributed under the Creative Commons Attribution License, which permits unrestricted use, distribution, and reproduction in any medium, provided the original work is properly cited.

Water resource is an important factor restricting social-economic development. Hebei Province is one of the regions suffering from severe water shortage in China. Based on the Water Resources Assessment and Planning model, population growth, economic growth, water-saving, and integrated scenarios were established. The water demand and supply in Hebei Province in 2025 and 2035 were forecasted in this study. The research results show that agriculture is the main unmet water demand sector. In the absence of large-scale population inflows, the local population growth has little impact on the changes in water supply-demand. Economic development is one of the main factors affecting water balance. The water-saving scenario has the greatest impact on water supply-demand. Compared to population and economic growth scenarios, the simulation results of water demand and unmet water demand were the smallest. Under an integrated scenario, the current situation of water shortage in Hebei has been greatly improved, but there is still a demand shortage of  $44.12 \times 10^8 \text{ m}^3$  in 2030. It is necessary to take measures to improve the carrying capacity of water resources in various regions of Hebei Province and narrow the regional gap. This study provided a reference for the rational utilization of water resources.

## 1. Introduction

Water is the source of all life. With the development of social economy, the available water resources are gradually decreasing globally [1–3]. Water scarcity has been listed as a major crisis of the 21st century [4, 5]. Globally, approximately 71% of the population suffers from moderate to severe water stress for at least 1 month per year [6]. By 2025, two-thirds of countries will face water scarcity [7]. The per capita water resources in China are only 1/4 of the world's per capita availability [8]. At present, water resources have become a restrictive factor affecting sustainable economic and social development. Hebei, as one of the “capital circle” regions, is an important part of the national regional development [9]. However, the per capita water resources in Hebei Province are only 1/7 of the national average, which is a serious water shortage area.

The shortage of water resources and the imbalance of supply-demand restrict the economic and social development seriously, and it is imminent to allocate and utilize water resources rationally [10, 11].

Water supply-demand balance analysis refers to the analysis of the structural relationship between water supply and water demand in a certain region [12, 13]. Many scholars have studied the water supply-demand and its influencing factors. The prediction of impact factors mainly focuses on population, economy, land use area, and water quota. Fullerton and Cardenas [14] applied a linear transfer function (LTF) for short-term forecasting of water demand for residential and nonresidential customers in Phoenix. Sun [15] used the logistic model and the grey prediction model to predict the population and agricultural irrigation area, respectively. The domestic and agricultural water demand was calculated. Socioeconomic, environmental,

and landscape pattern indicators were selected to predict urban water demand by employing a weighted model [16]. The dynamic change of water resources is affected by multiple factors. The study of a single factor is slightly insufficient for simulating water resource demand. As a new generation of water resource management software, the WEAP model can simulate the interaction between various factors [17]. The assessment of specific water resource issues can be placed within a comprehensive framework that better simulates changes in the water system. The WEAP model has been widely used in the balance of water supply-demand due to its comprehensiveness, intuition, and ease of operation. The Water Resources Assessment and Planning (WEAP) and Modular Three-dimensional Finite-difference Ground-water Flow (MODFLOW) models were used to evaluate the water balance in seven water basins of Syria [18]. Zerkaoui et al. [19] analyzed the demand for water resources under the changes of individual factors such as population growth, climate change, and agricultural land use changes and explored the possibility of water resource allocation in Mabtough watershed. Abdi and Ayenew [20] evaluated the application of the WEAP model in the Ketar subwatershed and used the WEAP model to simulate the hydrological process of the subwatershed. Yang et al. [21] used the WEAP model to evaluate the water shortage in the Beijing catchment area at the watershed scale and discussed the application advantages of the WEAP model in water resource management. Liu et al. [22] established a water energy model by coupling the WEAP and Low Emissions Analysis Platform (LEAP) models and discussed the energy-saving and water-saving effects of different policies in Beijing. The balance of water supply and demand is inseparable from the local social and economic development. It is important to the choice of scale for the study of urban water balance. However, according to the current research, most of the research focuses on the basin scale, and the related research on the administrative area scale is seriously insufficient.

The reasonable prediction of future changes in water resources is of great value to water resource utilization. Scenario analysis has become the main method for studying the response of water resources to changing environmental conditions. Under the assumption that a phenomenon or trend will continue into the future, scenario analysis makes predictions about the possible situations or consequences of a predicted object [23, 24]. Milano et al. [25] analyzed the hydrological-climatic characteristics of water crisis in the SPM basin based on historical monitoring data and proposed the implementation of effective water-saving policies. Wang et al. [26] explored the response of river water quantity and water quality to environmental changes by establishing a combined model of water quantity and water quality in the Luanhe River Basin. Freund et al. [27] used the Soil and Water Assessment Tool (SWAT) and Regional Climate (HIRHAM) models to carry out a scenario analysis of the impact of global change on the water volume of the Black Sea Basin. At present, there are many researches on the response mechanism of natural conditions when setting the scenario of water supply and demand balance. Further,

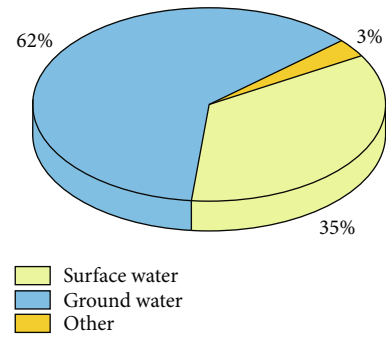


FIGURE 1: Water supply structure in Hebei Province.

the research of one or several scenarios was focused, but the simulation analysis of comprehensive scenario was limited.

Owing to uneven spatiotemporal distribution of water resources in Hebei, the utilization of water resources varies with cities, and the problem of water supply and demand has become increasingly prominent. Given to the uncertainty of national social and economic development, the establishment of multifactor and all-round scenarios can better provide scientific advice and reference for dealing with future water resource crises. In this paper, the population growth, economic growth, water-saving, and integrated scenarios were established at the administrative district scale. The water resources in Hebei Province were predicted under different scenarios. This study closely combined the balance of water supply-demand with socioeconomic development, which can identify the intraregional differences in water supply-demand, providing theoretical support for water management and sustainable development in Hebei Province. Hebei Province is located in the southeastern part of North China ( $36^{\circ} 03' \sim 42^{\circ} 40' N$ ,  $113^{\circ} 27' \sim 119^{\circ} 50' E$ ), with Beijing and Tianjin in the inner ring and Bohai Sea in the east, which is an important province in North China. Hebei Province has a land area of  $188,800 \text{ km}^2$  with high terrain in the northwest and low terrain in the southeast. It is the only province in China with plateaus, mountains, hills, plains, lakes, and seashores. The plain area in Hebei Province accounts for 43.3%, about  $81,459 \text{ km}^2$ ; the mountainous area is  $90,280 \text{ km}^2$ , accounting for 48.1% of the total area.

The average surface water resources in Hebei Province for many years are  $120.17 \times 10^8 \text{ m}^3$ , and the distribution of surface water resources is uneven. According to the 2020 Hebei Water Resources Bulletin, Chengde has the most abundant surface water resources, and Hengshui has the least. Moreover, Hebei Province has the most serious over-exploitation and the largest funnel area in China, accounting for 1/3 of the total overexploitation area. The groundwater overexploitation plain area in Hebei Province is  $67,000 \text{ km}^2$ , accounting for 90% of plain area [28].

The average water supply in Hebei Province from 2010 to 2020 was  $185.2 \times 10^8 \text{ m}^3$ . As shown in Figure 1, groundwater supply accounts for 62% of the total water supply, which is the main water source; surface water and other account for 35% and 3%, respectively. Hebei Province



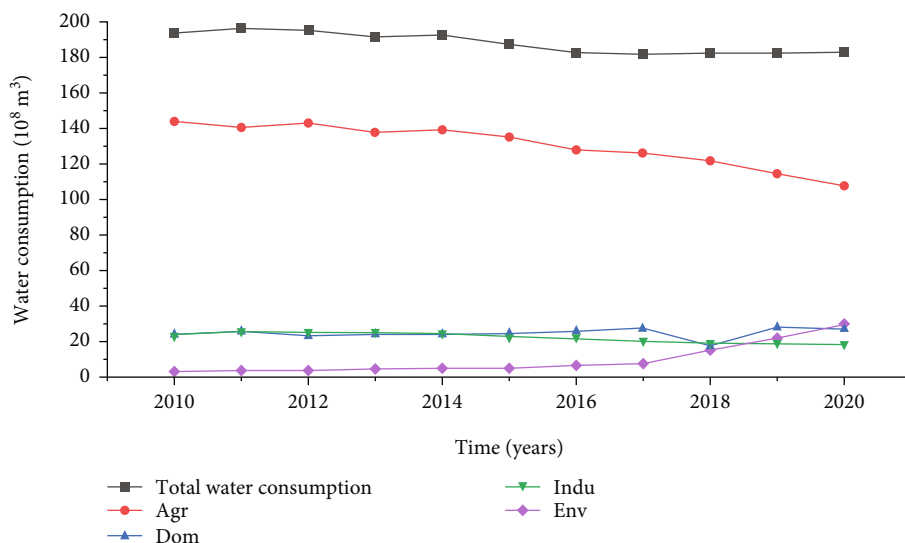


FIGURE 2: The water consumption structure of Hebei Province from 2010 to 2020.

TABLE 1: Data sources of the study area.

Data types	Scale	Description	Data sources
Vector data	Geographic	Boundaries, reservoirs, DEM	Geospatial Data Cloud ( <a href="http://www.gscloud.cn/search">http://www.gscloud.cn/search</a> )
Water supply	Meteorology	Precipitation, temperature, evaporation	China Meteorological Science Data Sharing Network; European Centre for Medium-Range Weather Forecasts
	Runoff	Streamflow	European Centre for Medium-Range Weather Forecasts
	Reservoir	Initial storage, volume	Hebei Provincial Department of Water Resources, Annual Report on national water situation
	Groundwater	Groundwater initial storage, maximum withdrawal	Hebei Water Resources Bulletin
	Water supply network	Leakage rate of water supply network	Hebei Water Resources Bulletin, China Urban Statistical Yearbook
Water demand	Domestic water		
	Industrial water	Annual water use rate, consumption, reuse rate	Hebei Statistical Yearbook, Hebei Water Resources Bulletin, Water Resources Bulletin and statistical yearbook of each city, literature
	Agricultural water		
	Environmental water		
Social and economic	Population	Resident population, birth rate, mortality rate, natural growth rate	Hebei Statistical Yearbook, Hebei Water Resources Bulletin
	GDP	Industrial added value, water consumption per 1570 dollars of industrial added value	
	Land use	Irrigation area, glassland	Hebei Rural Statistical Yearbook, China Environmental Statistical Yearbook

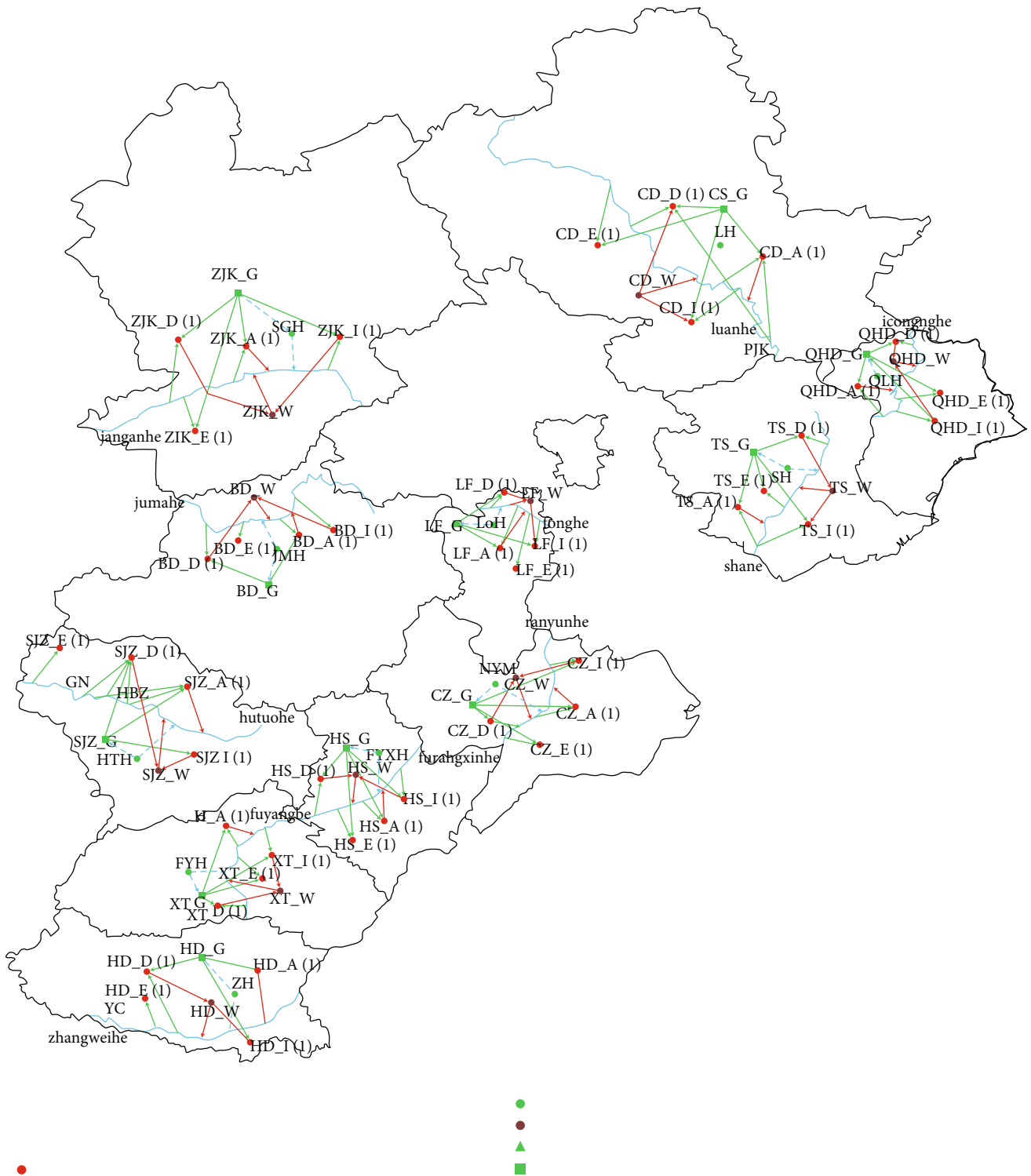


FIGURE 3: The schematic model of the Hebei WEAP.

TABLE 2: Key assumptions of the population growth scenarios.

Population change ( $P$ )	High-speed growth (P1)	Medium-speed growth (P2)	Low-speed growth (P3)
Natural population growth rates (%)	4	2	0.5

TABLE 3: Key assumptions of the economic growth scenarios.

Economic development (E)	High-speed growth (E1)	Medium-speed growth (E2)	Low-speed growth (E3)
Growth rate of industrial added value (%)	10	6	4.6

TABLE 4: Key assumptions of the water-saving scenarios.

Water-saving (W)	High efficiency (W1)	Medium efficiency (W2)	Low efficiency (W3)
Residential water consumption quota (L/(person-d))	60	80	110
Water consumption per 1570 dollars of industrial added value (m <sup>3</sup> )	8	10	12
Effective utilization coefficient of farmland irrigation	0.747	0.714	0.68
Reuse rate of industrial water (%)	98	95	93
Leakage rate of water supply network (%)	8	10	12
Glassland water consumption quota (m <sup>3</sup> /m <sup>2</sup> ·a)	0.5	0.6	0.7

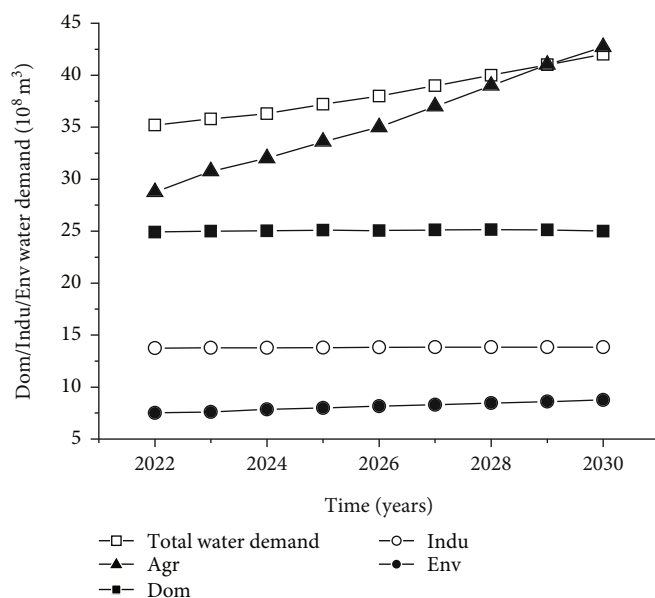


FIGURE 4: Water demand of different sectors in Hebei Province from 2022 to 2030 under reference scenario.

mainly includes four water use sectors: as shown in Figure 2, total water consumption decreased from  $193.68 \times 10^8 \text{ m}^3$  to  $182.77 \times 10^8 \text{ m}^3$ . The agricultural sector is the main source of water consumption in Hebei Province. Due to the implementation of agricultural water-saving policies, agricultural water consumption has been declining in recent years.

In this work, we proposal a WEAP model to analysis the water resources in China. Reference scenario, population growth scenario, economic growth scenario, water-saving scenario, and 27 integrated scenarios were set up. This study provided a reference for the rational utilization of water resources.

## 2. Materials and Methods

**2.1. Data Collection and Analysis.** The spatial vector data used in this study was obtained from the Geospatial Data Cloud (<http://www.gscloud.cn/search>). The meteorological

data was collected from China Meteorological Science Data Sharing Network (<http://data.cma.cn/>) and European Centre for Medium-Range Weather Forecasts (ECMWF) (<https://cds.climate.copernicus.eu/>).

In this paper, water supply data mainly includes river runoff, groundwater resources, and reservoir water storage. The water consumption data was divided into four categories: agricultural water, industrial water, domestic water, and environmental water. The socioeconomic data used in this study mainly include the resident population of each city, population birth rate, population mortality rate, natural population growth rate, irrigation area, effective utilization coefficient of farmland irrigation, industrial added value, water consumption per 1570 dollars of industrial added value, leakage rate of water supply network, and reuse rate of industrial water. The data sources include “Hebei Water Resources Bulletin,” “Hebei Statistical Yearbook,” “Hebei National Economic and Social Development Statistical

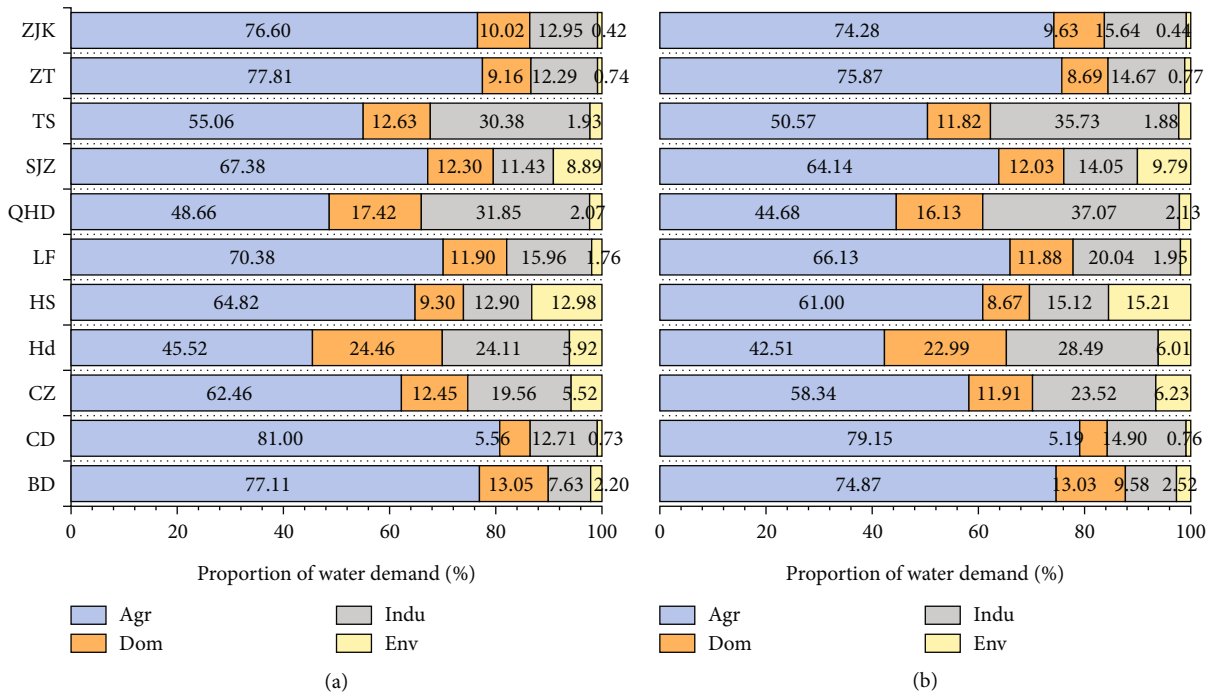


FIGURE 5: Proportion of water demand of cities in Hebei Province under reference scenario: (a) 2025; (b) 2030

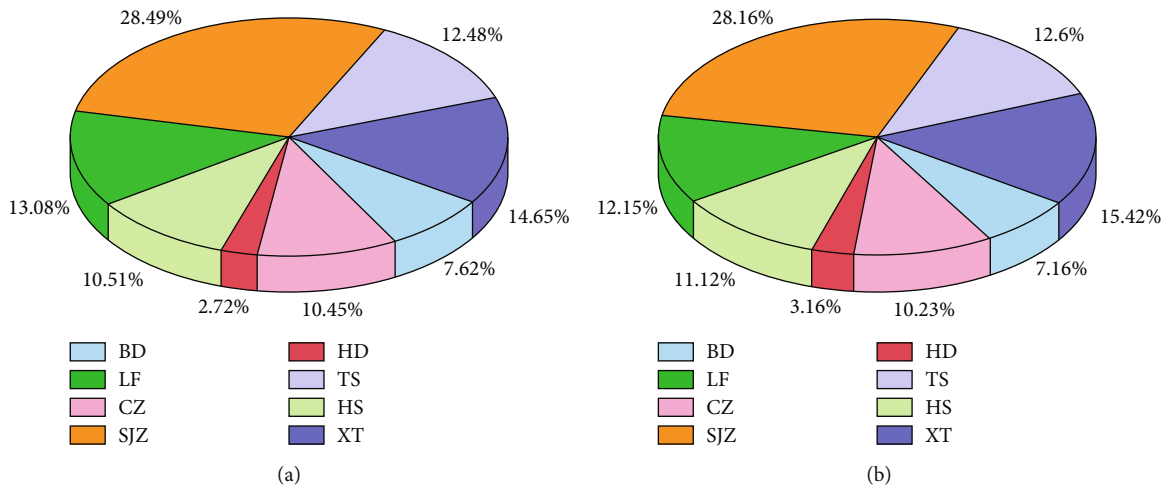


FIGURE 6: Proportion of unmet water demand of cities in Hebei Province under reference scenario: (a) 2025; (b) 2030.

Bulletin,” “Hebei Rural Statistical Yearbook,” “China Environmental Statistical Yearbook,” “China Urban Statistical Yearbook,” Water Resources Bulletin and statistical yearbook of each city, and literature. The main data sources are shown in Table 1.

2.2. WEAP Model Description. By generalizing the water resource system, the WEAP model could realize the simulation, prediction, and management of water resources. Generally, the water resource system is generalized into the following elements: demand sites, rivers, catchment basins, reservoirs, groundwater, transmission links, return flows, wastewater treatment, etc. [29]. The WEAP model is a new

generation of water resource planning software developed by the Stockholm Environment Institute. It is a comprehensive model that considers water resource development in the context of water supply, water quality, and ecosystems. WEAP software studies a city, a single subcatchment, or a complex river system [17, 30].

2.3. Model Generalization. According to the completeness of data collection, 2011 was used as the current base year in this study, and the water supply-demand from 2022 to 2030 was forecasted. In this paper, month was selected as the time step, and January was taken as the starting year of hydrology. The study area was divided into Baoding (BD),

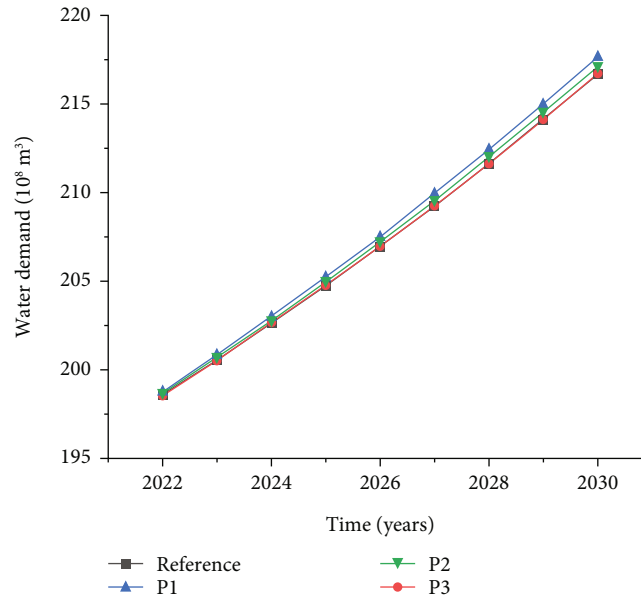


FIGURE 7: Water demand in different population growth scenarios from 2022 to 2030.

TABLE 5: Water demand of different population growth scenarios in 2025 and 2030 (unit:  $10^8 \text{ m}^3$ ).

Year	Reference	High-speed growth (P1)	Medium-speed growth (P2)	Low-speed growth (P3)
2025	204.72	205.22	204.97	204.78
2030	216.64	217.67	217.15	216.77

Chengde (LH), Cangzhou (CZ), Handan (HD), Hengshui (HS), Langfang (LF), Qinhuangdao (QHD), Shijiazhuang (SJZ), Tangshan (TS), Xingtai (XT), and Zhang jiakou (ZJK) (all these cities are located in China). Combined with the characteristics of water consumption in Hebei Province, the water resources system was generalized into a network consisting of rivers, reservoirs, and groundwater as water supply sites and domestic, agricultural, industrial, and ecological water consumption as demand sites. The final generalization of Hebei Province is 44 demand sites, 11 catchment basins, 11 rivers, 11 groundwater nodes, 11 wastewater treatment plant nodes, 22 runoff/infiltration links, 85 transmission links, and 44 return flow links. The generalized diagram of the Hebei WEAP model is shown in Figure 3.

**2.4. Model Calibration.** To ensure the reliability of the data, the model accuracy needs to be verified. According to the Water Resources Bulletin and the statistics of water consumption data, the water shortage in Hebei Province in 2011 was  $68.41 \times 10^8 \text{ m}^3$ . The simulation result of unmet water demand in 2011 is  $66.65 \times 10^8 \text{ m}^3$ , which was close to actual result. Therefore, in this paper, the Hebei WEAP model established could meet the accuracy requirements of the balance analysis of water resource supply-demand.

**2.5. Model Scenario Design.** Based on the current account year parameters, the reference scenario simulates future

changes without the intervention of any external factors, such as new policies and technologies. In the reference scenario, the factors affecting water supply and demand were estimated based on historical years.

**Population growth scenarios.** Combined with the current socioeconomic development and fertility policies, low-speed growth, medium-speed growth, and high-speed growth scenarios have been set. According to the “Hebei Province Urban System Plan (2016-2030),” the total population will be controlled at about 84 million by 2030. Refer to the “Hebei Province Population Development Plan (2018-2035)” and “National Population Development Plan (2016-2030),” considering the current population changes in Hebei Province; the natural population growth rates of the different scenarios are shown in Table 2.

According to the development goals of the 14th Five-Year Plan of Hebei Province, with reference to the regional GDP of Beijing-Tianjin-Hebei in recent years and the current economic situation, the economic high-speed, medium-speed, and low-speed development scenarios have been established (Table 3).

Based on the “14th Five-Year Plan for Urban and Municipal Infrastructure Construction in Hebei Province,” “Hebei Province Water-Saving Action Implementation Plan,” “Hebei Province Agricultural Sustainable Development Plan (2016-2030),” “National Water-Saving Action Plan,” “Beijing-Tianjin-Hebei Coordinated Development Outline,” and “Hebei Water Consumption Quota,” water-saving scenarios were set. The main indicators are shown in Table 4.

### 3. Scenario Analysis

**3.1. Reference Scenario Analysis.** Based on reference scenario, water demand of different sectors is shown in Figure 4. With the development of social economy and population growth,

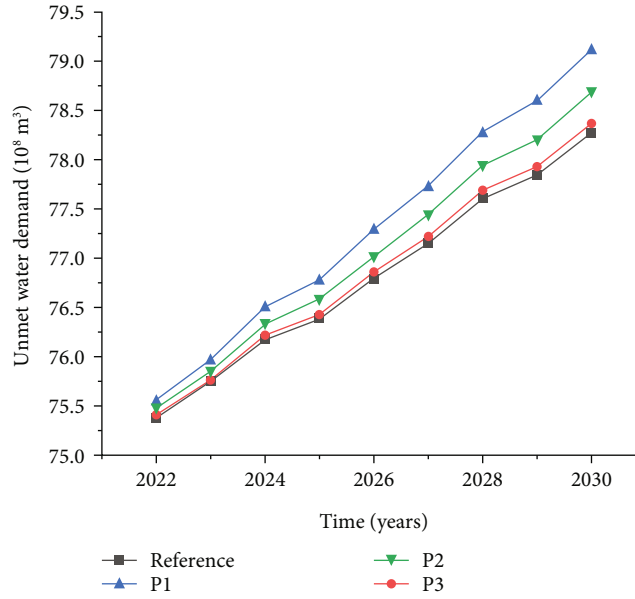


FIGURE 8: Unmet water demand in different population growth scenarios from 2022 to 2030.

TABLE 6: Unmet water demand of different population growth scenarios in 2025 and 2030 (unit:  $10^8 \text{ m}^3$ ).

Year	Reference	High-speed growth (P1)	Medium-speed growth (P2)	Low-speed growth (P3)
2025	76.38	76.78	76.58	76.42
2030	78.27	79.12	78.70	78.37

the total water demand has an increasing trend. The total water demand will increase from  $194.15 \times 10^8 \text{ m}^3$  in 2011 to  $204.71 \times 10^8 \text{ m}^3$  in 2025 and will reach  $216.64 \times 10^8 \text{ m}^3$  by 2030. Agricultural, domestic, industrial, and environmental water demand will increase to  $138.13 \times 10^8 \text{ m}^3$ ,  $24.93 \times 10^8 \text{ m}^3$ ,  $33.60 \times 10^8 \text{ m}^3$ , and  $8.05 \times 10^8 \text{ m}^3$  in 2025. By 2030, four categories of water demand will reach  $140 \times 10^8 \text{ m}^3$ ,  $25.31 \times 10^8 \text{ m}^3$ ,  $42.89 \times 10^8 \text{ m}^3$ , and  $9.36 \times 10^8 \text{ m}^3$ , respectively. The agricultural sector is the main water-requiring project in Hebei province. In 2025, the agricultural water demand will account for 67.74% of the total water demand, and the industrial, domestic, and environmental water demand will account for 16.41%, 12.18%, and 3.93%, respectively. Compared with 2025, the proportion of industrial water demand will increase, accounting for 19.8% of the total water demand in 2030.

The water demand structure of cities in Hebei Province is shown in Figure 5. In 2025, the agricultural water demand in Chengde and Xingtai will account for a larger proportion of total water demand, 81% and 77.81% in 2025, while Handan and Qinhuangdao account for only 45.52% and 48.66%, but the proportion of domestic water demand is the largest. Qinhuangdao, Tangshan, and Handan will account for the largest proportion of industrial water demand, accounting for 31.85%, 30.38%, and 24.11%, respectively. Hengshui and Shijiazhuang will have a larger proportion of environmental water demand, accounting for 12.98% and 8.89% of

the total water demand. By 2030, to a certain extent, the proportion of industrial water demand will increase in all cities. In the future, the industrial development of Hebei Province and the high-tech transformation of traditional industries will become important factors for water demand [31].

The simulation results showed that unmet water demand was derived from agricultural irrigation. In 2025 and 2030, the unmet water demand of agricultural sector will reach  $63.39 \times 10^8 \text{ m}^3$  and  $63.92 \times 10^8 \text{ m}^3$ , accounting for 83% and 81.67% of the total, respectively. According to the future development trend and simulation results, the proportion of environmental and domestic water unmet demand will increase, and the industrial water unmet demand will be less. As shown in Figure 6, the unmet water demand in Shijiazhuang will be the most serious. However, the proportion of water shortage in all cities will decrease by 2030, while the proportion of water shortage in Tangshan, Hengshui, and Xingtai will increase year by year.

**3.2. Population Growth Scenario Analysis.** Over time and population, the simulation results show a gradual upward trend between population growth scenarios. There is a certain difference in the range of changes between different scenarios. Compared with reference scenario, the P1, P2, and P3 scenarios will increase the water demand by  $0.5 \times 10^8 \text{ m}^3$ ,  $0.25 \times 10^8 \text{ m}^3$ , and  $0.06 \times 10^8 \text{ m}^3$  in 2025. By 2030, water demand will increase by  $1.03 \times 10^8 \text{ m}^3$ ,  $0.51 \times 10^8 \text{ m}^3$ , and  $0.13 \times 10^8 \text{ m}^3$ , respectively (Figure 7 and Table 5). Figure 8 and Table 6 show the changes in unmet water demand under population growth scenarios. Under P1, P2, and P3 scenarios, the water shortage in 2025 will increase by  $0.4 \times 10^8 \text{ m}^3$ ,  $0.2 \times 10^8 \text{ m}^3$ , and  $0.04 \times 10^8 \text{ m}^3$ , respectively. Compared with reference scenario, while in 2030, it will increase by  $0.85 \times 10^8 \text{ m}^3$ ,  $0.43 \times 10^8 \text{ m}^3$ , and  $0.1 \times 10^8 \text{ m}^3$ .

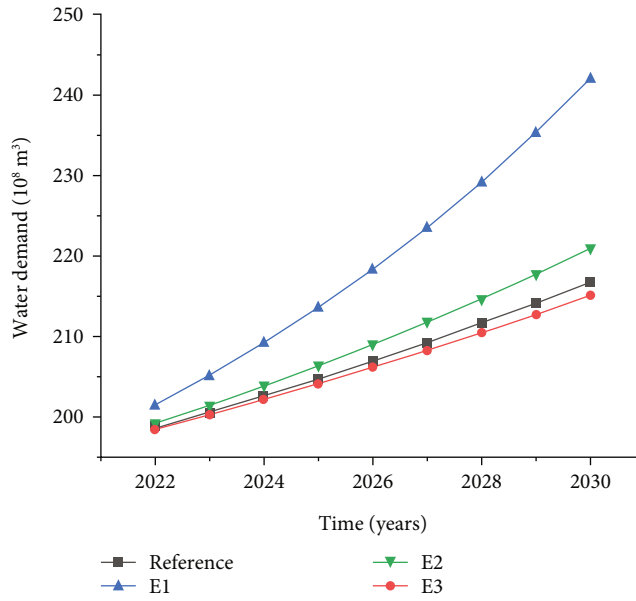


FIGURE 9: Water demand in different economic growth scenarios from 2022 to 2030.

TABLE 7: Water demand of different economic growth scenarios in 2025 and 2030 (unit:  $10^8 \text{ m}^3$ ).

Year	Reference	High-speed growth (E1)	Medium-speed growth (E2)	Low-speed growth (E3)
2025	204.72	213.52	206.35	204.08
2030	216.64	242.05	220.91	215.04

TABLE 8: Unmet water demand of different economic growth scenarios in 2025 and 2030 (unit:  $10^8 \text{ m}^3$ ).

Year	Reference	High-speed growth (E1)	Medium-speed growth (E2)	Low-speed growth (E3)
2025	76.38	76.94	76.48	76.34
2030	78.27	80.22	78.56	78.16

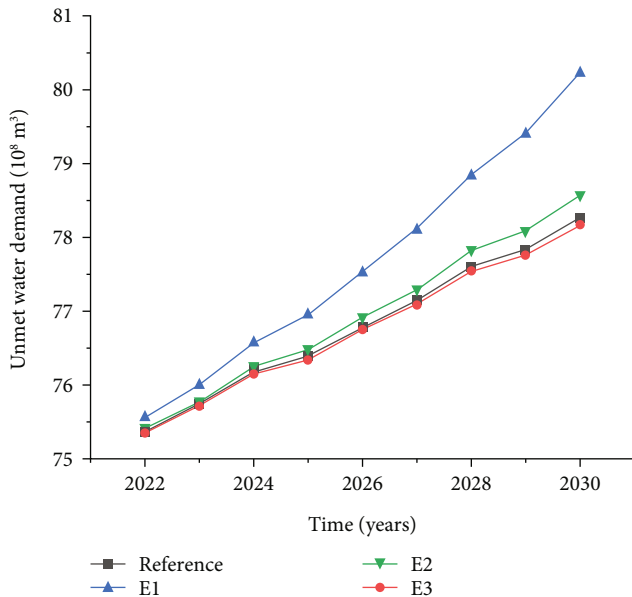


FIGURE 10: Unmet water demand in different economic growth scenarios from 2022 to 2030.

Due to the large population of Hebei Province, the differences in the simulation results between the population growth scenarios are limited. Additionally, because of the

economic and cultural development gap between Hebei and Beijing-Tianjin, the population of Hebei Province has mainly moved out to Beijing and Tianjin for many years [32, 33]. In the absence of large-scale population inflows in Hebei, the local population growth alone has little impact on the carrying capacity of water resources. However, it is necessary to improve the leakage rate and water supply capacity of the water supply pipe network in time.

3.3. *Economic Growth Scenario Analysis.* The results show that water requirement and water demand will increase exponentially under economic growth scenarios as a whole. The change rate of industrial added value under the low-speed economic growth scenario is smaller than that of reference scenario, and the unmet water demand is slightly smaller than the simulation results of reference scenario. As shown in Figure 9 and Table 7, compared with E1 and E2 scenarios, the water demand in 2025 will be reduced by  $2.27 \times 10^8 \text{ m}^3$  and  $9.44 \times 10^8 \text{ m}^3$  under E3 scenario; by 2030, the water demand will be reduced by  $4.27 \times 10^8 \text{ m}^3$  and  $25.41 \times 10^8 \text{ m}^3$ . Under E1 scenario, the water demand in 2025 and 2030 will increase by  $8.8 \times 10^8 \text{ m}^3$  and  $26.41 \times 10^8 \text{ m}^3$  compared with reference scenario. Under E1, E2, and E3 scenarios, the water demand in 2030 will be 1.25, 1.14, and 1.11 times that of 2011, respectively. As can be seen from Figure 10 and Table 8, compared with reference scenario, the change in unmet water demand is smaller under E2 and E3 scenarios, but larger in the E1 scenario.

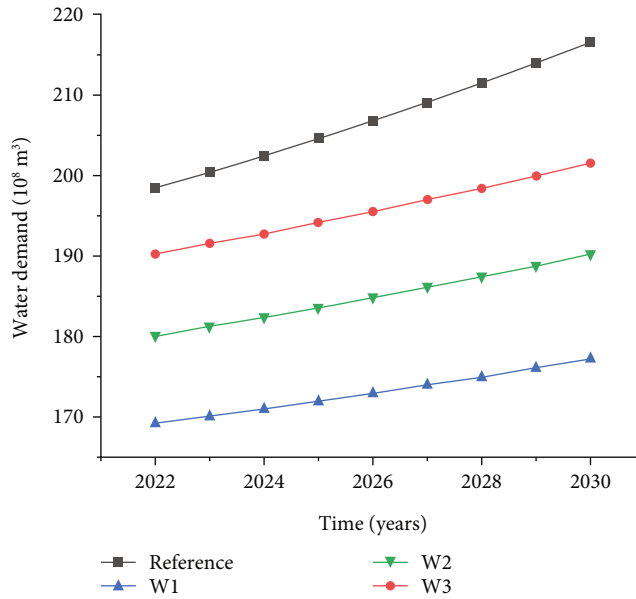


FIGURE 11: Water demand in different water-saving scenarios from 2022 to 2030.

TABLE 9: Water demand of different water-saving scenarios in 2025 and 2030 (unit:  $10^8 \text{ m}^3$ ).

Year	Reference	High efficiency (W1)	Medium efficiency (W2)	Low efficiency (W3)
2025	204.72	172.02	183.67	194.21
2030	216.64	177.28	190.28	201.65

From the above analysis results, it can be seen that compared with the current year, the economic growth scenarios will increase the pressure on the water supply-demand in Hebei Province in the future. In particular, under the conditions of rapid economic growth, the contradiction between supply and demand of water resources is more prominent. Economic development will have a significant impact on the balance of water supply and demand, which is one of the main factors affecting the water balance.

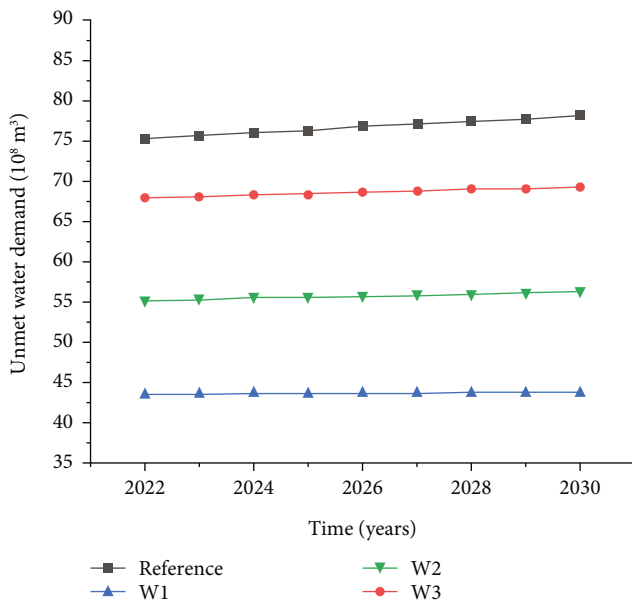


FIGURE 12: Unmet water demand in different water-saving scenarios from 2022 to 2030.

3.4. Water-Saving Scenario Analysis. For the water demand in Hebei Province, the role of water-saving measures is more obvious. Compared with the reference scenario, under high-efficiency water-saving measures (W1), the water demand in 2025 and 2030 will be reduced by  $32.7 \times 10^8 \text{ m}^3$  and  $39.36 \times 10^8 \text{ m}^3$ , respectively; under the low-efficiency water-saving scenario (W3), the water demand will be reduced by  $10.51 \times 10^8 \text{ m}^3$  and  $14.99 \times 10^8 \text{ m}^3$  (Figure 11, Table 9). From Figure 12 and Table 10, it can be seen that under the water-saving scenarios, the unmet water demand does not change significantly with time, but the unmet water demand varies greatly under different scenarios. Compared with the reference scenario, the W1, W2, and W3 scenarios will reduce unmet water demand by  $8.95 \times 10^8 \text{ m}^3$ ,  $22 \times 10^8 \text{ m}^3$ , and  $34.5 \times 10^8 \text{ m}^3$  in 2030, respectively.

Liu [34] established a water-saving development scenario for Beijing-Tianjin-Hebei and concluded that water demand and unmet water demand in Hebei will be  $186.61 \times 10^8 \text{ m}^3$  and  $52.69 \times 10^8 \text{ m}^3$  in 2030. The calculation results are within the simulation results of the three water-saving scenarios established in this paper, which is relatively close to the medium-efficiency water-saving scenario. The water-saving scenarios could reduce the amount of water resources used by changing the water consumption of different sectors, improving the utilization efficiency, and reducing water loss.



TABLE 10: Unmet water demand of different water-saving scenarios in 2025 and 2030 (unit:  $10^8 \text{ m}^3$ ).

Year	Reference	High efficiency (W1)	Medium efficiency (W2)	Low efficiency (W3)
2025	76.38	43.56	55.59	68.44
2030	78.27	43.77	56.27	69.32

TABLE 11: The supply and demand of water resources in Hebei Province under S6 scenario.

Year	Water demand ( $10^8 \text{ m}^3$ )		Unmet water demand ( $10^8 \text{ m}^3$ )	
	2025	2030	2025	2030
Reference	204.71	216.64	76.38	78.27
S6	172.94	179.50	43.73	44.12

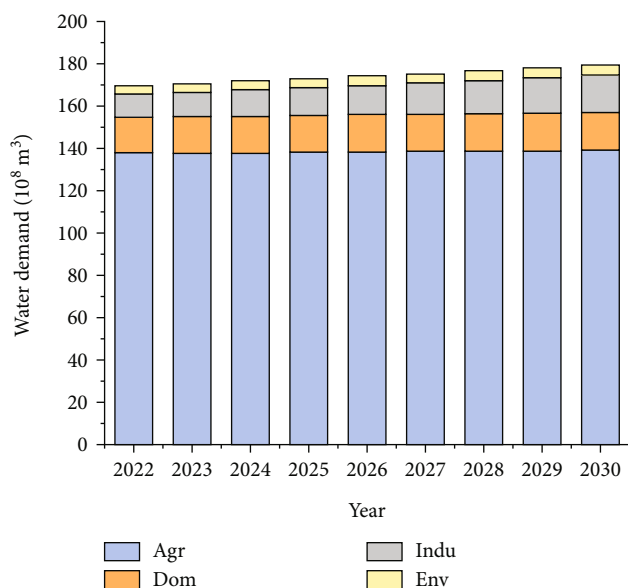


FIGURE 13: Water demand in different sectors of Hebei Province from 2022 to 2030 under S6 scenario.

Compared with the population growth scenario and the economic growth scenario, the water-saving scenario has the greatest impact on water supply-demand. Therefore, under the premise of ensuring normal economic and social development, it is necessary to develop water-saving measures to improve the sustainable utilization and development of water resources.

**3.5. Integrated Scenario Analysis.** Simulation results of water resources in different scenarios in 2025 and 2030 in Hebei Province are shown in Table S1. Combining with population, economy, and water-saving factors, 27 kinds of scenarios were established to study the impact on water supply-demand under the combined action of three scenarios.

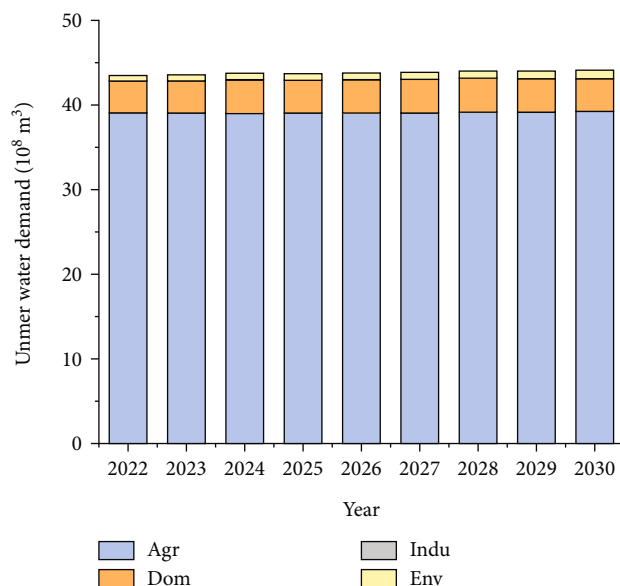


FIGURE 14: Unmet water demand in different sectors from 2022 to 2030 under S6 scenario.

TABLE 12: Water demand of each city under S6 scenario (unit:  $10^8 \text{ m}^3$ ).

Scenario	Reference		S6	
	2025	2030	2025	2030
BD	29.72	30.23	26.97	27.15
CD	18.97	20.64	17.05	18.27
CZ	14.92	15.84	12.78	13.32
HD	13.08	14.13	10.13	10.81
HS	11.24	12.24	9.05	9.49
LF	14.72	14.96	12.80	12.78
QHD	7.58	8.31	5.30	5.57
SJZ	34.06	35.36	28.17	28.74
TS	28.99	31.46	22.02	23.32
XT	20.31	21.72	18.51	19.50
ZJK	11.12	11.75	10.16	10.56

Due to the limitation of space, this paper discussed the balance of water supply-demand by taking “high-speed population growth, medium-speed economic growth, high-efficiency water-saving” (S6) as an example. Under S6 scenario, due to the change of per capita water consumption quota and the improvement of water resource utilization efficiency, the water demand and unmet water demand showed a gradual decreasing trend compared with reference scenario (Table 11).

As shown in Figures 13 and 14, the water demand of industrial sector in Hebei Province will grow faster from 2022 to 2030, but the unmet water demand will be less. The main reason is that water-saving measures have reduced the water consumption of 1570 dollars of industrial added value and improved the reuse rate of industrial water greatly.

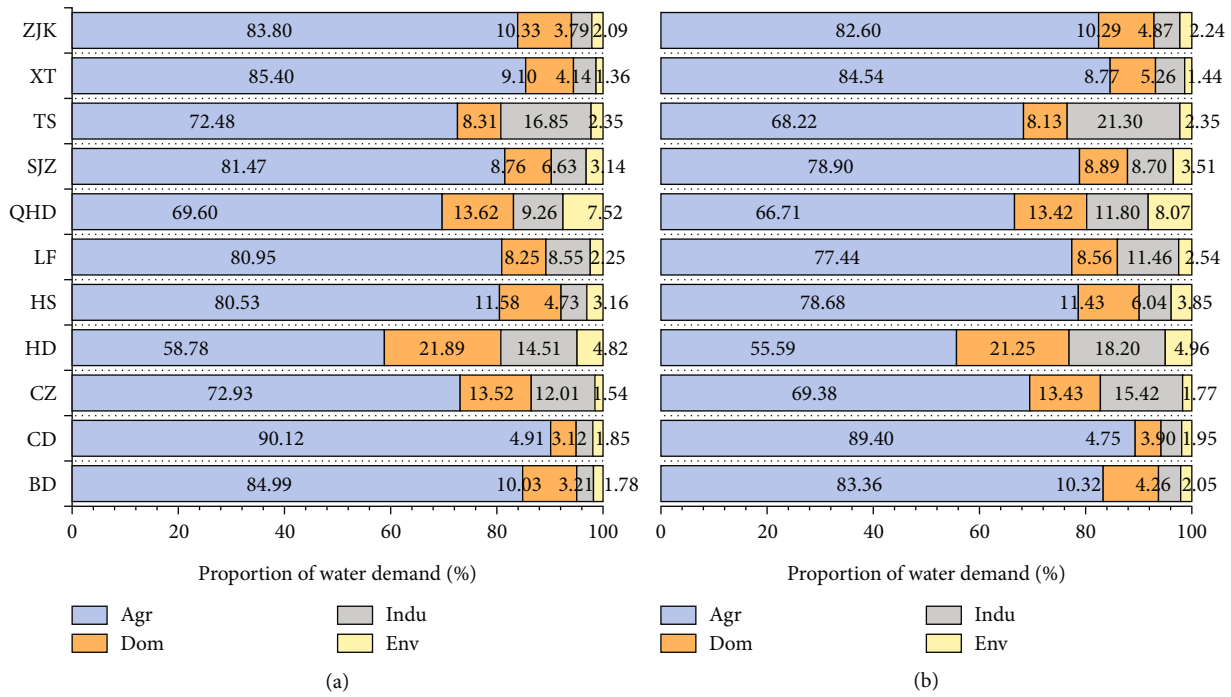


FIGURE 15: Proportion of water demand of different sectors in cities of Hebei Province under S6 scenario: (a) 2025; (b) 2030.

TABLE 13: Unmet water demand of each city under S6 scenario (unit:  $10^8 \text{ m}^3$ ).

Scenario Year	Reference		S6	
	2025	2030	2025	2030
BD	5.82	5.61	1.23	1.06
CD	0.00	0.00	0.00	0.00
CZ	7.99	8.01	5.70	5.69
HD	2.08	2.47	0.00	0.00
HS	8.03	8.71	5.34	5.70
LF	9.99	9.51	7.58	7.08
QHD	0.00	0.00	0.00	0.00
SJZ	21.76	22.04	11.89	11.76
TS	9.53	9.86	3.61	3.64
XT	11.19	12.07	8.38	9.19
ZJK	0.00	0.00	0.00	0.00

The results showed that agricultural water consumption will have a downward trend but will account for the vast majority. In the next decade, the water demand and unmet water demand will still be dominated by agricultural water.

Compared with reference scenario, the water demand of each city will decrease (Table 12). Therefore, under the constraints of water-saving measures, despite rapid population growth and moderate economic growth, the contradiction between water supply and demand cannot be exacerbated. Figure 15 showed the proportion of water demand by different sectors in each city in 2025 and 2030. For example, in 2025, the proportion of domestic and industrial water demand in Cangzhou will be 13.53% and 12.01%, respectively, while industrial water demand will exceed the propor-

tion of domestic water demand in 2030. For Tangshan City, the proportion of industrial water demand, domestic water demand, and agricultural water demand will reach 16.85%, 8.31%, and 72.48% in 2025, respectively; in 2030, agricultural water demand will drop to 68.22% and industrial water demand will increase to 21.30%. With the strengthening of ecological protection in recent years, the ecological water demand in various cities is also steadily improving. It can be seen that with the changes of economic society or human activities, the structure of water demand in Hebei Province will also change.

Under S6 scenario, there will be significant changes in unmet water demand. For example, the unmet water demand in Handan City in 2025 and 2030 will be  $2.08 \times 10^8 \text{ m}^3$  and  $2.47 \times 10^8 \text{ m}^3$ , respectively. However, there will be no unmet water demand in Handan under S6 scenario. In addition, the unmet water demand in other cities will also be significantly improved. The contradiction between supply and demand will be greatly alleviated (Table 13 and Figure 16). In 2025 and 2030, the agricultural unmet water demand in all cities will be more than 80%, followed by domestic sector. Due to the improvement of the environment, environmental water demand and unmet water demand are also increasing. It is necessary to further rationally allocate water for the ecological environment.

#### 4. Discussion

4.1. Analysis of Results and Suggestion. Under the coordinated development of Beijing-Tianjin-Hebei, Beijing-Tianjin industries are gradually transferring to Hebei Province. In addition, Hebei Province needs to ensure the safety of water supply and ecological security in Beijing-Tianjin,

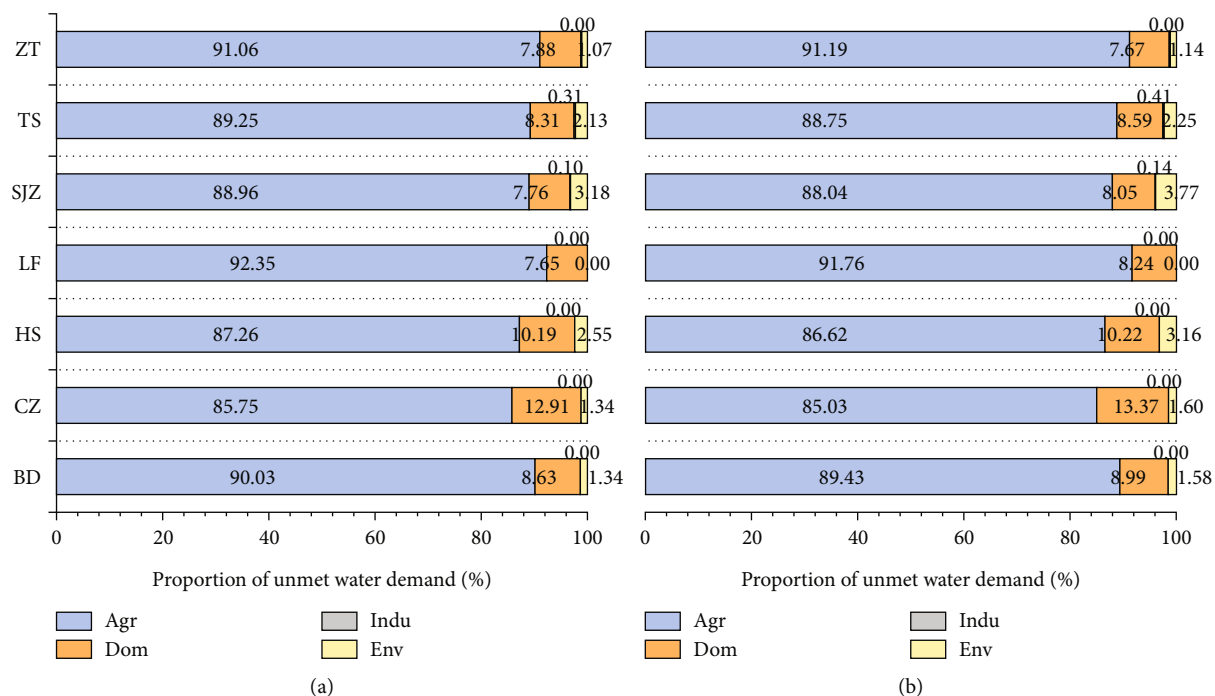


FIGURE 16: Proportion of unmet water demand of different sectors in cities of Hebei Province under S6 scenario: (a) 2025; (b) 2030.

so that the tension of water supply will further increase. At present, most scholars have evaluated the supply and demand of water resources in Beijing-Tianjin-Hebei [35–38]. However, due to the economic differences in Beijing-Tianjin-Hebei, the development and utilization of water resources are different [38].

From the perspective of each city, there will be no unmet water demand in Handan under S6 scenario. Zhangjiakou, Chengde, and Qinhuangdao still have better utilization of water resources, and there is no water shortage. The research results by Yu et al. [9] and others show that Zhangjiakou and Chengde have better ecological environment and higher water carrying capacity, which are important water conservation areas. However, Shijiazhuang, Cangzhou, Xingtai, Langfang, and Hengshui have a heavy industrial structure and low water resource utilization efficiency, which is consistent with the results of this study [9]. Due to natural conditions and policy factors, the water carrying capacity in central Hebei is higher than that in northern and southern Hebei [39]. The water resources in the central and southern regions of Hebei are generally poor, and the unmet water demand level is relatively high [40]. Zhang et al. [41] analyzed cities in Hebei Province from four dimensions: water ecology, water environment, water quantity, and water use. The study found that the water ecology was suboptimal in Zhangjiakou, Chengde, Tangshan, and Qinhuangdao; Baoding, Cangzhou, Xingtai, and other places had poor water environment; Chengde, Qinhuangdao, and Zhangjiakou had better water quantity; Handan City has a good degree of water use. The water resources are sufficient to support local residents' water use in Handan. Overall, the simulation results in this paper are similar to the previous results. Dur-

ing the “14th Five-Year Plan” period, Hebei Province should take measures to narrow the regional gap [39].

The research in this paper showed that agriculture will be the main water consumption sector in Hebei Province, and industrial water will be relatively less, which indicates that the overall level of economic and industrial development is relatively limited. In terms of water consumption structure, it can be found that the proportion of agricultural and domestic water consumption will gradually decrease, while industrial and environmental water consumption will increase by 2030. Due to the transfer of industries in Beijing-Tianjin, industrial water demand in Hebei Province will increase. At the same time, it can be found that there is almost no industrial unmet water demand in each city, indicating that the improvement of industrial water consumption efficiency can solve the problem of unmet water demand. Because of the enhancement of environmental awareness, the urban greenland has expanded, resulting in an increase in ecological water consumption. For Beijing-Tianjin-Hebei region, Liu et al. showed that the proportion of agricultural and industrial water consumption will continue to decline by 2030, while the proportion of domestic and environmental water consumption will increase to varying degrees, which is different from the analysis results in this study [42].

From population growth, economic growth, and water-saving scenarios, it can be seen that implementation of water-saving measures is the most effective way to alleviate water shortage. The inefficient use of water resources in Hebei Province shows the low level of industrialization especially in the agricultural sector. By analyzing panel data, Lin et al. [43] believed that economic development was related to

regional water use structure and water use efficiency. Population and economic development are closely related to water-saving technologies. Li et al. [44] showed that population carrying capacity and economic development are the main factors affecting the utilization of water resources in Hebei Province. It is necessary to improve water-saving technologies, develop industries with low water consumption, and apply other water supplies on a large scale.

Agriculture and industry are key sectors in policy-making for water resource management in Hebei Province [45]. The research in this paper showed that improving water-saving technology can effectively alleviate the contradiction between water supply-demand. However, the simulation results showed that only using groundwater and surface water resources cannot meet water supply-demand. Due to the uneven distribution of water resources, it is necessary to build interbasin water transfer facilities [46]. The water supply from the South-to-North Water Diversion has a significant effect on alleviating the severe water shortage in Hebei Province [47]. Moreover, it is necessary to rationally plan the water resource utilization model and adjust the industrial structure. The overexploitation of groundwater in Hebei Province is a serious problem. The water-saving irrigation was considered an important way to reduce groundwater depletion [48]. In the agricultural sector, a complete farmland irrigation system should be established, and agricultural planting methods should be adjusted to reduce the proportion of agricultural water use and overall scale. The economic growth is closely related to industrial and agricultural water consumption [28]. To reduce water consumption and the connection between industry and agriculture, it is necessary to develop high value-added industries and high-end service industries and transfer high water-consuming industries. In addition, the government should strengthen the treatment of wastewater, improve the utilization rate of reclaimed water, and encourage the development of environment-friendly fields.

**4.2. Shortage of Research.** Due to lack of data, agricultural water consumption was entered based on an annual scale in this study. In fact, due to the influence of cultivation time, the agricultural water consumption data in different months are different. A total of 27 kinds of comprehensive scenarios are set up in this paper, but affected by space constraints, only one kind of scenario results was selected for analysis in detail. In this study, only the impact of policy constraints on water resources was considered, and the impact of natural factors was not considered. The impact of natural factors such as climate change on water resources in Hebei Province will be further studied in another manuscript.

## 5. Conclusions

The WEAP model was established in this paper. Reference scenario, population growth scenario, economic growth scenario, water-saving scenario, and 27 integrated scenarios were set up. The results showed that the local population growth has little impact on the changes in water supply and demand in the absence of large-scale population inflows.

Economic development will have a significant impact on the balance of water supply-demand. Under the low-efficiency, medium-efficiency, and high-efficiency water-saving scenarios, compared with reference scenario, the unmet water demand in different water-saving scenarios in 2030 was reduced by  $8.95 \times 10^8 \text{ m}^3$ ,  $22 \times 10^8 \text{ m}^3$ , and  $34.5 \times 10^8 \text{ m}^3$ , respectively.

The simulation results showed that the situation of unmet water demand in Hebei Province will be greatly improved by 2030. However, there will still be unmet water demand of  $44.12 \times 10^8 \text{ m}^3$ , mainly due to the unmet water demand of agricultural sector. Further, it is essential to strengthen wastewater treatment and improve the utilization rate of reclaimed water for the supply and demand of water resources.

## Data Availability

All data in the current work can be obtained from the manuscript and through contact with the corresponding author.

## Conflicts of Interest

The authors declare that they have no conflicts of interest.

## Acknowledgments

The work was supported by the National Key Research and Development Program of China (Grant No. 2017YFF0206701) and Fundamental Research Funds for the Central Universities (Grant No. 2021YJSDC10).

## Supplementary Materials

Table S1: simulation results of water resources in different scenarios in 2025 and 2030 in Hebei Province (*Supplementary Materials*)

## References

- [1] T. Endo, K. Kakinuma, S. Yoshikawa, and S. Kanae, "Are water markets globally applicable?," *Environmental Research Letters*, vol. 13, no. 3, article 034032, 2018.
- [2] I. H. Goender, U. Sahlin, and G. C. O'Brien, "Bayesian network applications for sustainable holistic water resources management: modeling opportunities for South Africa," *Risk Analysis*, vol. 10, no. 8, article 13798, 2021.
- [3] J. Wilcox, F. Nasiri, S. Bell, and M. S. Rahaman, "Urban water reuse: a triple bottom line assessment framework and review," *Sustainable cities and society*, vol. 27, pp. 448–456, 2016.
- [4] V. Srinivasan, E. F. Lambin, S. M. Gorelick, B. H. Thompson, and S. Rozelle, "The nature and causes of the global water crisis: syndromes from a meta-analysis of coupled human-water studies," *Water Resources Research*, vol. 48, no. 10, p. W10516, 2012.
- [5] F. Khosravi, *The Potential for Environmental Impact Assessment (EIA) in Iran's Water Management*, University of Liverpool, 2019.

- [6] M. M. Mekonnen and A. Y. Hoekstra, "Four billion people facing severe water scarcity," *Science Advances*, vol. 2, no. 2, pp. e1500323–e1500323, 2016.
- [7] A. Asghar, J. Iqbal, A. Amin, and L. Ribbe, "Integrated hydrological modeling for assessment of water demand and supply under socio-economic and IPCC climate change scenarios using WEAP in Central Indus Basin," *Journal of Water Supply: Research and Technology - AQUA*, vol. 68, no. 2, pp. 136–148, 2019.
- [8] F. Huang, T. S. Du, S. F. Wang et al., "Current situation and future security of agricultural water resources in North China," *Strategic Study of CAE*, vol. 21, no. 5, pp. 28–37, 2019.
- [9] H. Z. Yu, L. J. Li, and J. Y. Li, "Evaluation of water resources carrying capacity in the Beijing-Tianjin-Hebei Region based on quantity-quality-water bodies-flow," *Resources Science*, vol. 42, no. 2, pp. 358–371, 2020.
- [10] A. Karimi and R. Ardakanian, "Development of a dynamic long-term water allocation model for agriculture and industry water demands," *Water Resources Management*, vol. 24, no. 9, pp. 1717–1746, 2010.
- [11] C. X. Deng, D. M. Zhu, X. D. Nie et al., "Precipitation and urban expansion caused jointly the spatiotemporal dislocation between supply and demand of water provision service," *Journal of Environmental Management*, vol. 299, no. 4, article 113660, 2021.
- [12] O. K. M. Ouda, "Water demand versus supply in Saudi Arabia: current and future challenges," *International Journal of Water Resources Development*, vol. 30, no. 2, pp. 335–344, 2014.
- [13] A. Saleem, I. Mahmood, H. Sarjoughian, H. A. Nasir, and A. W. Malik, "A water evaluation and planning-based framework for the long-term prediction of urban water demand and supply," *SIMULATION*, vol. 97, no. 5, pp. 323–345, 2021.
- [14] T. M. Fullerton and J. P. Cardenas, "Forecasting water demand in Phoenix, Ariz," *Journal American Water Works Association*, vol. 108, no. 10, pp. E533–E545, 2016.
- [15] X. B. Sun, *Urban Water Supply and Demand Balance Analysis Based on SWAT and WEAP Models*, Beijing University of Civil Engineering and Architecture Beijing, China, 2020.
- [16] G. M. Sanchez, A. Terando, J. W. Smith, A. M. Garcia, C. R. Wagner, and R. K. Meentemeyer, "Forecasting water demand across a rapidly urbanizing region," *Science of the Total Environment*, vol. 730, article 139050, 2020.
- [17] D. Yates, J. Sieber, D. Purkey, and A. Huber-Lee, "WEAP21—a demand-, priority-, and preference-driven water planning model," *Water International*, vol. 30, no. 4, pp. 487–500, 2005.
- [18] K. A. Mourad and O. Alshihabi, "Assessment of future Syrian water resources supply and demand by the WEAP model," *Hydrological Sciences Journal*, vol. 61, no. 2, pp. 393–401, 2016.
- [19] L. Zerkaoui, M. Benslimane, and A. Hamimed, "Planning and systematic management of water resources by the WEAP model, case of the Mabtouh watershed (northwestern Algeria)," *Arabian Journal of Geosciences*, vol. 11, no. 24, p. 779, 2018.
- [20] D. A. Abdi and T. Ayenew, "Evaluation of the WEAP model in simulating subbasin hydrology in the Central Rift Valley basin, Ethiopia," *Ecological Processes*, vol. 10, no. 1, p. 41, 2021.
- [21] L. Yang, X. Bai, N. Z. Khanna et al., "Water evaluation and planning (WEAP) model application for exploring the water deficit at catchment level in Beijing," *Desalination and Water Treatment*, vol. 118, pp. 12–25, 2018.
- [22] G. Y. Liu, J. M. Hu, C. C. Chen et al., "LEAP-WEAP analysis of urban energy-water dynamic nexus in Beijing (China)," *Renewable and Sustainable Energy Reviews*, vol. 136, article 110369, 2021.
- [23] N. S. Arunraj, S. Mandal, and J. Maiti, "Modeling uncertainty in risk assessment: an integrated approach with fuzzy set theory and Monte Carlo simulation," *Accident Analysis and Prevention*, vol. 55, pp. 242–255, 2013.
- [24] C. L. Dong, G. Schoups, and N. Giesen, "Scenario development for water resource planning and management: a review," *Technological Forecasting and Social Change*, vol. 80, no. 4, pp. 749–761, 2013.
- [25] M. Milano, E. Reynard, M. G. Muniz, and J. Guerrin, "Water supply basins of São Paulo metropolitan region: hydro-climatic characteristics of the 2013–2015 water crisis," *Water*, vol. 10, no. 11, p. 1517, 2018.
- [26] J. H. Wang, W. H. Xiao, H. Wang, Z. K. Chai, C. W. Niu, and W. Li, "Integrated simulation and assessment of water quantity and quality for a river under changing environmental conditions," *Chinese Science Bulletin*, vol. 58, no. 27, pp. 3340–3347, 2013.
- [27] E. R. Freund, K. C. Abbaspour, and A. A. Lehmann, "Water resources of the Black Sea Catchment under future climate and landuse change projections," *Water*, vol. 9, no. 8, p. 598, 2017.
- [28] L. L. Yu, M. H. Ling, F. Chen, Y. Y. Ding, and C. M. Lv, "Practices of groundwater over-exploitation control in Hebei Province," *Water Policy*, vol. 22, no. 4, pp. 591–601, 2020.
- [29] M. D. Fard and H. S. Sarjoughian, "A RESTful framework design for componentizing the water evaluation and planning (WEAP) system," *Simulation Modelling Practice and Theory*, vol. 106, article 102199, 2021.
- [30] M. Karamouz, H. Barkhordari, and E. E. Sarindizaj, "Dynamics of water allocation: tradeoffs between allocator's and farmers' benefits of irrigation practices," *Journal of Irrigation and Drainage Engineering*, vol. 147, no. 6, 2021.
- [31] Z. C. Xu, H. Y. Sun, F. T. Wang, and S. Y. Ma, "The present and future of sustainable utilization of water resources in Hebei Province," *South-to-North Water Transfers and Water Science and Technology*, vol. 31, no. 6, pp. 74–77, 2007.
- [32] S. Y. Wang, *Research on Forecast of Labor Supply and Demand in Hebei Province from 2020 to 2050*, Hebei Normal University, Hebei, China, 2020.
- [33] Y. Q. Chen, Z. Y. Sun, and L. W. Cai, "Population flow mechanism study of Beijing-Tianjin-Hebei urban agglomeration from industrial space supply perspective," *Sustainability*, vol. 13, no. 17, p. 9949, 2021.
- [34] H. L. Liu, *Water Resources Sustainable Use Evaluation and Water Resources Allocation in Beijing-Tianjin-Hebei Region*, North China Electric Power University, Beijing, China, 2020.
- [35] L. F. Wu, X. R. Guo, and T. Chen, "Grey relational entropy calculation and fractional prediction of water and economy in the Beijing-Tianjin-Hebei Region," *Journal of Mathematics*, vol. 2021, Article ID 4418260, 16 pages, 2021.
- [36] X. T. Zeng, Z. J. Hu, J. Zhang et al., "Toward a sustainable water resources management in Beijing-Tianjin-Hebei urban agglomeration: a scenario analysis of combined strategy regulation with Green Z-score criterion," *Urban Water Journal*, vol. 16, no. 8, pp. 1–17, 2019.
- [37] L. Sun, B. L. Pan, A. Gu, H. Lu, and W. Wang, "Energy-water nexus analysis in the Beijing-Tianjin-Hebei region: case of

- electricity sector,” *Renewable & Sustainable Energy Reviews*, vol. 93, pp. 27–34, 2018.
- [38] Y. J. Li, Z. Y. Zhang, and M. J. Shi, “Restrictive effects of water scarcity on urban economic development in the Beijing-Tianjin-Hebei City Region,” *Sustainability*, vol. 11, no. 8, p. 2452, 2019.
- [39] Y. X. Wang, S. J. Zhang, Q. H. Xu, Y. W. Zhang, and X. D. Chen, “Assessment of water crisis in South Central Hebei,” *Information Technology and Industrial Engineering*, vol. 1, pp. 965–972, 2014.
- [40] H. D. Wang, Y. H. Xu, R. S. Sulong, H. L. Ma, and L. F. Wu, “Comprehensive evaluation of water carrying capacity in Hebei Province, China on principal component analysis,” *Frontiers in Environmental Science*, vol. 9, article 761058, 2021.
- [41] S. H. Zhang, M. S. Xiang, J. S. Yang, W. W. Fan, and Y. J. Yi, “Distributed hierarchical evaluation and carrying capacity models for water resources based on optimal water cycle theory,” *Ecological Indicators*, vol. 101, no. 6, pp. 432–443, 2019.
- [42] Q. Liu, S. C. Dong, F. J. Li, H. Cheng, Y. Yang, and B. Xia, “Research on supply and demand balance of water resources in Beijing-Tianjin-Hebei Region,” *IOP Conference Series: Earth and Environmental Science*, vol. 381, no. 1, article 012057, 2019.
- [43] X. X. Lin, J. H. Sha, and J. J. Yan, “Impacts of water resources on economic development in Beijing-Tianjin-Hebei Region,” in *In Proceedings of the 2015 International Conference of Environment, Manufacturing Industry and Economic Development*, pp. 311–317, Lisbon, Portugal, 2015.
- [44] X. Li, D. Q. Yin, X. J. Zhang et al., “Mapping the distribution of water resource security in the Beijing-Tianjin-Hebei Region at the county level under a changing context,” *Sustainability*, vol. 11, no. 22, p. 6463, 2019.
- [45] M. F. Colosimo and H. Kim, “Incorporating innovative water management science and technology into water management policy,” *Energy, Ecology&Environment*, vol. 1, no. 1, pp. 45–53, 2016.
- [46] S. J. Liu, W. H. Zhang, J. W. Yun, Q. Q. Kou, L. L. Bao, and J. J. Liu, “Study on the ecological compensation sharing in the central line of the south-to-north water diversion project,” *Applied Applied Ecology and Environmental Research*, vol. 17, no. 4, pp. 9937–9946, 2019.
- [47] Y. X. Wang, L. Cheng, H. L. Tian, and X. H. Liu, “Water supply eco-economic benefit evaluation of middle route of south-to-north water diversion project in Hebei water-recipient area,” *IOP Conference Series: Earth and Environmental Science*, vol. 191, article 012064, 2018.
- [48] H. B. Zhang, V. P. Singh, D. Y. Sun, Q. J. Yu, and W. Cao, “Has water-saving irrigation recovered groundwater in the Hebei Province plains of China?,” *International Journal of Water Resources Development*, vol. 33, no. 4, pp. 534–552, 2017.

## Research Article

# Application Research of Deep Learning Technology in Natural Landscape Animation Design

Lili Xu  and Lilei Wen

*School of design art, Xijing University, Xi'an, Shaanxi Province, China 710123*

Correspondence should be addressed to Lili Xu; 20130104@xijing.edu.cn

Received 12 January 2022; Revised 13 February 2022; Accepted 19 February 2022; Published 19 April 2022

Academic Editor: Wen Zeng

Copyright © 2022 Lili Xu and Lilei Wen. This is an open access article distributed under the Creative Commons Attribution License, which permits unrestricted use, distribution, and reproduction in any medium, provided the original work is properly cited.

Due to the limitation of technology and cost, the animation design of natural landscape in the past was often dealt with relative simplicity. With the increasing level of audience appreciation and the continuous development of animation technology, new requirements are put forward for the design of natural landscape animation. In order to make the animation design effect of natural landscape more real, the synthetic aperture radar image is firstly analyzed to obtain the location of mountains, farmland, rivers, villages, roads, and buildings. Considering the superiority of U-Net network in image semantic segmentation, this paper constructs a semantic segmentation model based on U-Net structure. In this model, dense connection module is introduced in downsampling, and spatial void pyramid structure is introduced in upsampling to retain more image features, to achieve accurate segmentation of satellite images. Experimental results show that the proposed algorithm has higher segmentation accuracy than other algorithms. After accurate classification of natural scene images, it can provide a guarantee for designing more real natural landscape animation design effects.

## 1. Introduction

Most of the landforms in animated films about natural landscapes are fond of mixing mountains, hills, forests, and rivers. On the one hand, it makes artists develop their imagination better, and on the other hand, it also enriches the visual experience of the audience. However, plain terrain is not much. When the art design is carried out to the production level, the actual terrain proportion in the natural environment should be considered first. At the same time, paying attention to the proportion of plants to characters and scenes, each plant has its own volume. We should not only consider the beauty of individual plants but also focus on the unity and harmony of the group effect. Too characteristic monomer design put together may not be able to achieve beautiful group effect. In the production of the environment, the vegetation is programmed to be copied and arranged in the scene. Dense plants are more likely to produce visual repetition [1]. If the vegetation in the animated film is too inconsistent with real life, it will produce a “sense of repulsion” in the vision and reduce the beauty of the pic-

ture. Therefore, how to carry out animation design according to the proportion of real terrain environment has important research significance.

The elements of landscape environment design mainly include the following five parts. The first is the terrain. According to the terrain scale, it can be divided into large terrain, small terrain, and micro terrain. Among them, plains, hills, mountains, and other terrain with a larger area of land are the large terrain. Landforms with small geographical areas such as ramps, tablelands, and flat lands are small landforms. The terrain with small fluctuation, such as grassland and sand dune, belongs to microtopography. Water body is one of the important elements in landscape design. According to its morphology, it can be divided into moving water and still water. Rivers, waterfalls, and streams are moving water, while pools are still water. The change of moving water and standing water in form makes the design of landscape environment also have infinite change. The third is plants; plants are full of vitality, which has a high ornamental value. Plant morphology can change with climate and environment. By making full use of plants, the

design effect of landscape environment can be greatly enhanced. The fourth is the sky scene, that is, the atmospheric environment. Atmospheric environment is changeable; day and night changes and seasonal changes belong to the sky scene. The sky scene endows the landscape environment with the beauty of time and space interaction. The fifth is the landscape facilities; the artificial facilities that people need in the process of leisure, life, and entertainment are all landscape facilities [2]. Landscape facilities can effectively meet people's needs, more importantly through the design of the landscape.

In the real world, the main factors affecting vegetation are the geographical location and climate of growth. Vegetation design should be created on the premise of respecting the objective reality. Common plants include trees, shrubs, ferns, grasses, weeds, and mosses. The more detailed the plant species are planned, the richer and more vivid the natural environment of the art design will be. There are too many plants in nature. As an important part of the rich picture, the stone and earth blocks of different shapes and sizes, broken branches, and fallen leaves are indispensable. They will be scattered randomly on the ground to make the environment more vivid. If artists can classify common and representative plant events according to botanical theory, it would be very worthwhile to use it as a reference for art design. In order to carry out animation design according to the proportion of real terrain, the natural environment can be classified according to image classification and image segmentation technology and then according to the classified data, to make animation design and to achieve high-quality animation design effect.

In recent years, deep learning has made great achievements in computer vision, image classification, and image segmentation. The special network structure of deep learning can transfer extracted feature values through neurons, and each layer can extract and learn the features transferred from the previous layer to continue transmission, to extract the optimal feature values [3]. Methods in the field of image semantic segmentation include AlexNet, FCN, U-Net, SegNet, and ResNet. AlexNet has achieved successful application of ReLU, Dropout, and local response normalization (LRN) in convolutional neural networks, etc. [4]. FCN changed AlexNet and VGG full connection layer to convolution layer [5]. FCN downsampling carries out feature extraction for the image and deconvolution for upsampling. This ensures that the output image is the same size as the input image. Based on FCN network architecture, literature [6] proposed to learn a multilayer deconvolution network to replace simple bilinear interpolation. Literature [7] proposed that SegNet is based on encoder-decoder architecture. The convolution layer and pooling layer constitute the encoder, while the convolution layer and upsampling layer constitute the decoder. The function of the encoder is to extract the feature image, and the function of the decoder is to return the feature image to the same size as the input image.

The similarity between SegNet and deconvolution network is that the network structure is similar. The difference is that SegNet removes the two fully connected layers in the middle of the network and uses the batch normalization

method and Softmax classifier. The advantages of SegNet are high efficiency and low memory consumption, while the disadvantages are low accuracy. Pooling layer is introduced in FCN and SegNet networks. The advantage of this method is that the image size is reduced while the receptive field is increased, but the disadvantage is that part of the position information is lost. Literature [8] designs a network dedicated to image pixel prediction. The network does not contain pooling layer, and the convolution layer adopts extended convolution. The advantage of this network is that the extended convolution increases the receptive field of the convolution kernel. It can fuse the multiscale context information of captured image and improve the accuracy of pixel prediction.

The advantage of ResNet residual block model is to reduce the gradient disappearance problem caused by the increase of neural network depth. It uses the cascade operation between encoder and decoder to fuse the high-level information with the shallow level information. Its advantage is to avoid the loss of high-level semantic information and preserve image features as much as possible. Deep learning can realize object segmentation and extraction by computer. It learns features of lower and higher levels through special network models and has higher learning efficiency [9]. Deep learning segmentation of image feature elements can achieve better experimental results through many data experiments. Therefore, deep learning algorithm can be used to segment and extract feature images from satellite images.

Aiming at the problems of confusion and unclear recognition in segmentation, this paper proposes an image segmentation algorithm based on deep learning based on U-Net. The innovations and contributions of this paper are listed below. (1) In order to improve the accuracy of image segmentation, the specific part of image is input by attentional supervision mechanism during the fusion of image feature information. (2) After accurate classification of natural scene images, it can provide a guarantee for designing more real natural landscape animation design effects.

The structure of this paper is listed as follows. The related theories are described in the next section. The proposed method is expressed in Section 3. Section 4 focuses on the experiment and analysis. Section 5 is the conclusion.

## 2. Related Theories

*2.1. Early Remote Sensing Image Scene Classification Method.* Before the rise of deep learning, scene classification of high-resolution remote sensing images was based on manual features. Among them, there are color histogram, scale-invariant feature transformation, universal search tree, and other classic manual features. However, manual feature design needs a lot of prior knowledge and is time-consuming and laborious, and the effect is poor. In order to obtain a higher accuracy of scene classification, manual coding features appear later. The main idea of this method is to further abstract the image based on manual features. The most typical feature of manual coding is the visual word bag model [10]. Although hand-coded features can improve classification accuracy, it is limited by the upper limit of



underlying features. Therefore, there are obvious shortcomings of weak generalization ability and low classification accuracy when only using low-level features in scene classification tasks of high-resolution remote sensing images.

**2.2. Deep Neural Network.** The concept of neural networks was inspired by the 1943 model of artificial neurons. Then, the perceptron algorithm is proposed and the MCP model is used to successfully classify multidimensional data. However, subsequent experiments show that this model can only deal with linear classification problems. Until 1986, Hinton, the father of neural network, invented back propagation (BP) algorithm. It uses Sigmoid to carry out nonlinear mapping, so the nonlinear classification problem is solved. However, the neural network is still faced with problems such as gradient disappearance, time-consuming training network, and difficulty in local optimization.

A solution to the problem of gradient disappearance is proposed in deep network training. First, the unsupervised method is used to pretrain the network, so that the network weight has a good initial value. Then, the network is optimized in a more detailed and supervised way to further improve the network performance. Subsequently, ReLU activation function, AlexNet [11], and a series of new technologies and network architectures were proposed. It makes deep neural network really receive wide attention.

Deep neural networks can be roughly divided into two categories: one is deep neural network (DNN) with one-dimensional vector input; the other is the input of two-dimensional image or three-channel color image DNN. The former is represented by deep belief network (DBN), while the latter is represented by convolutional neural network (CNN).

**2.3. Research Status of Deep Learning in Remote Sensing Image Classification.** The scene classification methods of high-resolution remote sensing images based on deep learning can be divided into three categories according to the supervision methods: full supervision method, semisupervision method, and weak supervision method.

**2.3.1. Fully Supervised Classification Methods.** Fully supervised learning, also known as supervised learning, is a method of learning data and its corresponding labels and then used for network training. At present, most of the high-resolution remote sensing scene classification methods based on deep learning can be classified as full supervision. Subject-based model is an effective method. Literature [12] proposed an adaptive deep sparse semantic model. It makes full use of the multilevel semantics of remote sensing image scenes. At the semantic level, sparse thematic features and deep features are effectively integrated, which effectively improves the ability of feature representation and thus achieves a higher level of classification.

It is also a common method to improve the scene classification accuracy of remote sensing images by fusing multilayer deep features. Literature [13] realized that most existing CNN methods only use feature vectors of the last fully connected layer for scene classification, which ignores

local information of images. Although some images have similar global characteristics, they belong to different categories. The reason is that the category of the image may be highly correlated with local features rather than global features. Therefore, the features of the last convolutional layer and the last fully connected layer of the deep neural network are firstly extracted as local features and global features, respectively. Then, the clustering method is used to cluster the global features into multiple sets. Then, the local features are rearranged according to the similarity between the local features and the cluster center. Finally, the global and local remote sensing image features can be obtained through the fusion of the two.

**2.3.2. Semisupervised Classification Method.** Semisupervised learning can make use of many unlabelled samples, so the need for label samples is reduced, which to some extent solves the problem of insufficient label samples in the field of deep learning. From the perspective of enlarging tag sample size, literature [14] proposed a generation framework based on semisupervised deep learning features. The framework can be trained to automatically expand the number of label samples. Firstly, the tagged samples were used to fine-tune the pretrained CNN, and then, the deep features extracted from the fine-tuned CNN were used to train the support vector machine (SVM). At the same time, the method combines multiple support vector machines to identify easily confused category samples, which effectively improves the labelling accuracy and the number of label samples. Therefore, it can effectively improve the generalization ability and classification accuracy of the network.

**2.3.3. Weakly Supervised Classification Methods.** A combination of weak supervision and deep learning is also widely used. In literature [15], features extracted from labelled images are taken as the source domain, while features extracted from unlabelled images are taken as the target domain. Then, it is used for network training and optimization of specified loss functions to classify labelled and unlabelled data.

**2.3.4. Qualitative Comparison of Supervision Methods.** The classification method based on total supervision has remarkable effect and high accuracy. However, all the above monitoring methods require many labelled samples to train the classification network, and labelled samples are often difficult to obtain. It takes a lot of time and energy to label unlabelled images, which limits the further development of full supervision methods. The semisupervised classification method can train the network with many unlabelled samples so that the network can obtain more “extra” information, thus improving the robustness of the network. However, only unlabelled samples can be used to refine the feature space constructed by labelled samples, without significantly increasing the discriminant information, thus limiting the classification accuracy.

### **3. Image Segmentation Algorithm Based on U-Net Structure**

Considering the superiority of U-Net network in image semantic segmentation and dense connection network, this

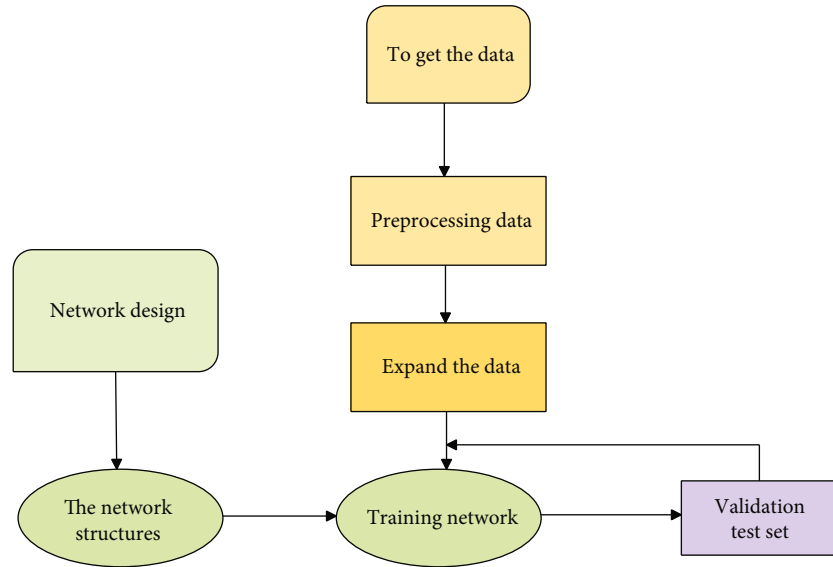


FIGURE 1: Flow of the proposed algorithm.

paper constructs a semantic segmentation model based on U-Net structure. Its network structure consists of encoder, decoder, dense connection module, ASPP, and CBAM.

- (1) Encoder includes dense connection module and maximum pooling layer. The dense connection module extracts the semantic features of the image through the convolution layer, and the maximum pooling layer performs downsampling operation on the feature information of the image
- (2) Dense connection module reuses the image features of the previous layer. ASPP is introduced to increase the receptive field of image feature information and improve the robustness of image feature. Introducing CBAM to conduct attention supervision when learning deep feature information can effectively extract feature information of elements
- (3) Decoder part includes dense connection module and deconvolution layer. The deconvolution layer upsamples the image feature information so that the size of the input image and the output image remain unchanged

**3.1. Algorithm Flow.** The algorithm implementation process includes network design, network construction, data acquisition, data preprocessing, and data expansion. The algorithm flow is shown in Figure 1.

**3.2. Network Structure.** Based on the original U-Net network, the dense connection module, ASPP, and CBAM modules are introduced in this paper. Its network structure is shown in Figure 2.

The input image size is  $480 \times 480$ . The dense connection module includes two convolution and two feature fusion, and the image size does not change to  $480 \times 480$ . After the maximum pooling layer, the image size is 1/2 of the original,

that is,  $240 \times 240$ . Record the dense connection module and the maximum pooling operation as one operation unit. Then, the image size becomes a feature map of  $30 \times 30$  after three times of operation. ASPP and CBAM are introduced before deconvolution (upsampling) of feature images. ASPP can fuse deeper image details. CBAM does not affect the size of the feature graph. Network learning integrates the feature graph and weight graph of channel and spatial attention model by dot product and then inputs the fused result graph into the deconvolution layer (upsampling). Deconvolution is performed during upsampling, and the image size is doubled, i.e.,  $60 \times 60$ . After intensive connection module, the image size is still  $60 \times 60$ . Finally, the image size was restored to  $480 \times 480$  after three operations.

**3.2.1. Dense Connection.** In deep learning networks, the problem of gradient disappearance becomes more and more obvious with the deepening of network depth. In this paper, the dense connection module is introduced by referring to the concept of dense connection in DenseNet. All layers of the network are connected while ensuring maximum information transmission between layers. In order to ensure the feedforward characteristics, each layer splices the input of all previous layers and then transmits the output feature graph to all subsequent layers.

The operation process is as follows. The input image size is  $480 \times 480$ . The dense connection module includes two convolution and two feature fusion. The convolution kernel is 3 by 3. The step size is 2. The number of convolution kernels is 64. After four intensive connection modules and pooling operations, a feature map with a size of  $30 \times 30$  was obtained.

Batch normalization (BN) layer is added between each convolutional layer and activation function, which normalizes data from each batch during each random gradient decline. As a result, the mean value and variance of data from each channel in the output feature graph are 0 and 1,

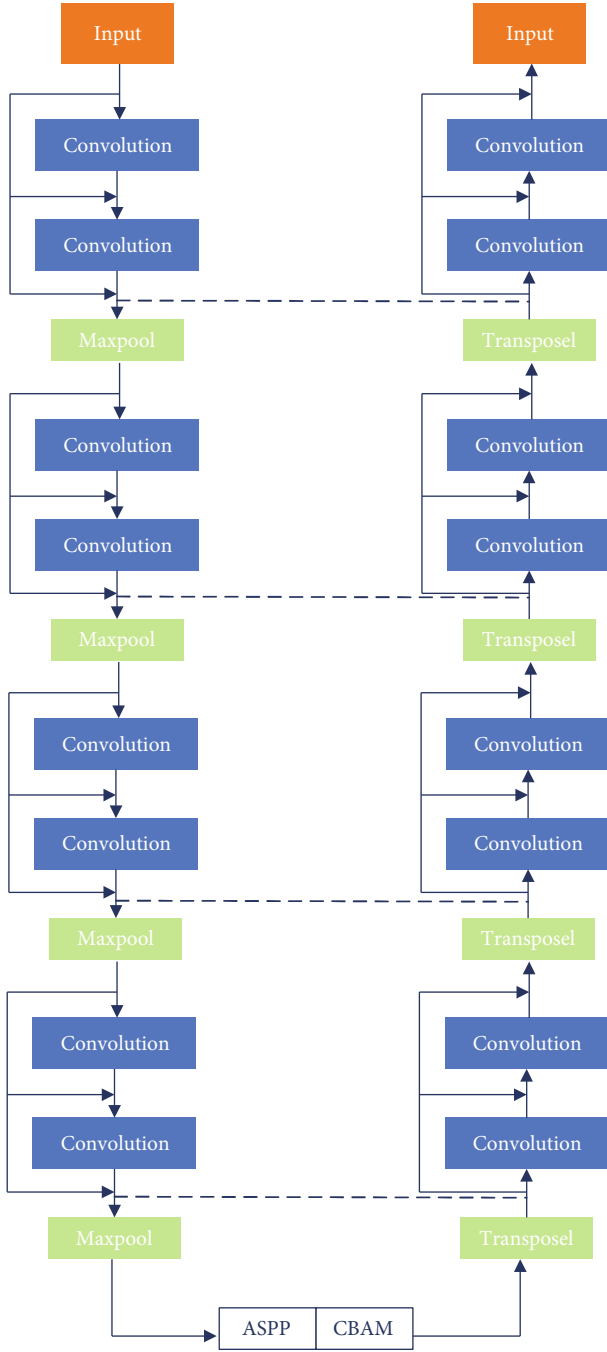


FIGURE 2: The network structure of the proposed model.

which reduces the gradient disappearance during network learning. ReLU activation layer is introduced to activate features.

**3.2.2. Pyramid Structure of Void Space.** The structure of aorous spatial pyramid pooling (ASPP) is introduced before upsampling. The basic element of the pyramid structure of void space is the convolution of void with different expansion rates. The advantages of empty convolution are as follows: (1) Without increasing parameters, the receptive field of convolution kernel is increased. (2) Under the condition

of no loss of information in downsampling, the convolution output range of spatial information is larger, so that the network retains more image features. The convolution kernel of the empty convolution in this paper is  $3 \times 3$ . The empty convolution with expansion rates of 2, 4, 8, and 16 replaces the original ordinary convolution. This makes the model segmentation image clearer, as shown in Figure 3.

ASPP performs six convolution operations on the input feature graph. Convolution kernel size of the first convolution is  $1 \times 1$ , and that of the second to the fifth is  $3 \times 3$ . The empty convolution with expansion rates of 2, 4, 8, and 16 replaced the original ordinary convolution to obtain multiscale characteristic information. The average pooling method is introduced into the model. After global mean pooling of the input feature graph, the feature graph is fed into the convolution kernel with a size of  $1 \times 1$ . Use BN operation and upsample to image original size. Then, the feature images fused with six multiscales are sent into the convolution layer with a size of  $1 \times 1$ . Finally, the output feature map is fed into the attentional mechanism model.

**3.2.3. Attention Mechanism Module.** CBAM is introduced after ASPP and before upsampling. CBAM module (including channel attention and spatial attention two submodules) is shown in Figure 4.

After the input feature image passes through the channel attention submodule and the spatial attention submodule, the feature image multiplied by the output results of the two submodules is sent to the coding stage for upsampling. CBAM can effectively extract feature information of elements by attentional supervision when learning deeper feature information through space and channel. The realization process is as follows.

$$F' = W_c(F)F \otimes F'' = W_s(F')F', \quad (1)$$

where the characteristic graph of  $F$ , after being operated by channel attention module and spatial attention module, is  $F'$  and  $F''$ , respectively.  $\otimes$  means multiply elements by elements.

The realization process of channel attention module is as follows. Global average pooling (AvgPool) and global maximum pooling (MaxPool) were performed on input feature graph  $F$ , and the results were  $A_1$  and  $B_1$ , respectively. Then, feature elements  $g$  and  $h$  were obtained by adding  $g_1$  and  $h_1$  through multilayer perceptron (MLP) to obtain  $C_1$ . The feature of channel attention is the result of fusion of  $C_1$  and  $F$ . The operation process is as follows.

$$W_c(F') = (\text{MLP}(\text{AvgPool}(F) + \text{MLP}(\text{MaxPool}))), \quad (2)$$

$$W_c(F') = (M_1(M_0(g_1)) + M_1(M_0(h_1)))W_c(F') = (G + H), \quad (3)$$

$$W_c(F') = (C_1), \quad (4)$$

where  $M_0$  and  $M_1$  are the two-layer parameters of MLP.

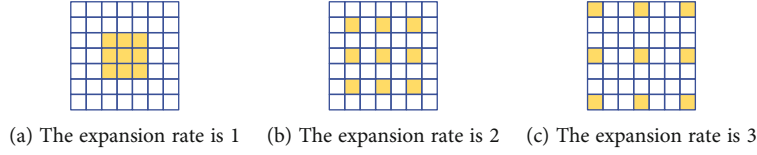


FIGURE 3: The structure of ASPP.

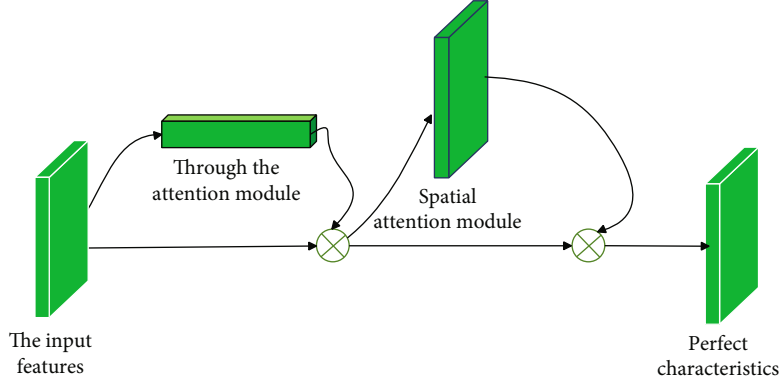


FIGURE 4: Overall structure of attention model.

Sigma is the sigmod activation function.  $M_0$  needs to be activated using the ReLU function.

The realization process of spatial attention module is as follows: the results of average pooling and maximum pooling of input feature maps are  $g_2$  and  $h_2$ . Then,  $g_2$  and  $h_2$  are fused for  $3 \times 3$  convolution operation to obtain feature graph  $C_2$ . The spatial attention feature is the result of  $C_2$  and  $F$  fusion. The operation is as follows.

$$W_s(F) = (f([\text{AvgPool}(F) ; \text{MaxPool}(F)])), \quad (5)$$

$$W_s(F) = (f(g_2 ; h_2)), \quad (6)$$

$$W_s(F) = (C_2), \quad (7)$$

where  $F$  represents the  $3 \times 3$  convolution operation.

**3.3. Coordinate Point Data.** In this paper, the obtained satellite image information is optimized and the images without elements are eliminated. First, OpenStreetMap captures coordinates of the image based on latitude and longitude. Then, the corresponding position in Mapbox is located according to the endpoint coordinate data, and Labelme is used to annotate the data. In order to solve the problems of different image sizes, unclear image content, large amount of data, and slow training speed, the captured image was preprocessed to adjust the size to  $480 \times 480$  to improve the training speed of the model. In this paper, random flipping, image noise, image brightness, and other methods are used to enhance the data, to avoid the overfitting phenomenon of the network, and to achieve better training of the network model.

## 4. Experimental Results and Analysis

**4.1. Experimental Data.** Two real polarimetric SAR data are used to verify the algorithm. The first data is the data image

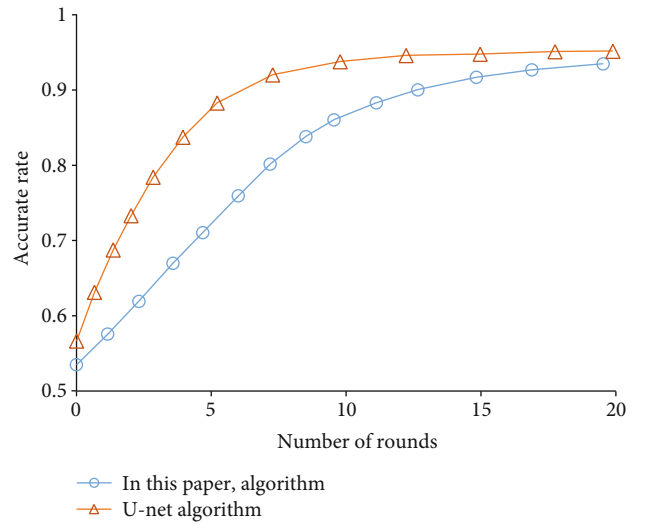


FIGURE 5: The change of accuracy rate in network training stage.

obtained by RADARSAT-2. The second data is a NASA/JPLAIRSAR image of the San Francisco area. The image contains five types of ground objects, namely, mountains, farmland, rivers, villages, roads, and buildings.

**4.2. Performance Specifications.** Accuracy, recall, and precision were used to evaluate the segmentation effect of the proposed algorithm.

$$\text{Accuracy} = \frac{\text{TP} + \text{TN}}{\text{TP} + \text{TN} + \text{FP} + \text{FN}}, \quad (8)$$

$$\text{Recall} = \frac{\text{TP}}{\text{TP} + \text{FN}}, \quad (9)$$

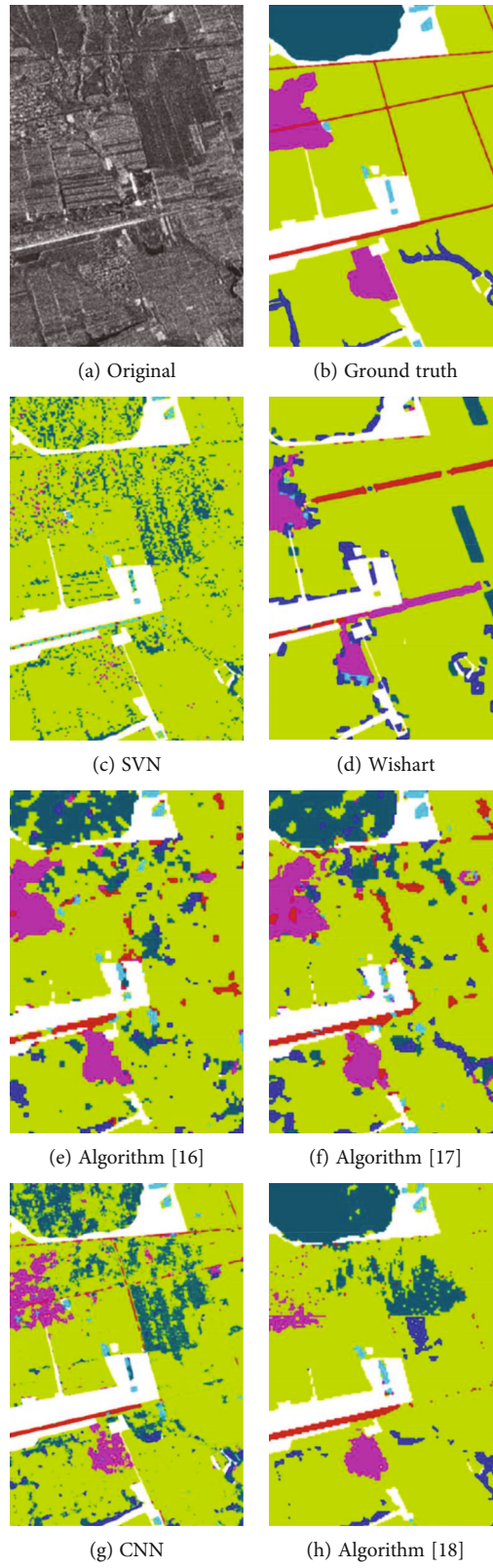


FIGURE 6: Continued.



(i) Proposed

FIGURE 6: The classification results.

TABLE 1: Classification accuracy on RADARSAT-2 image.

Algorithm	Mountain	Farmland	River	Village	Road	Building
SVM	97.71	97.06	78.83	63.44	90.8	93.71
Wishart	51.64	95.15	96.17	94.97	95.02	87.8
Algorithm [16]	99.6	98.05	96.35	91.19	94.33	89.6
Algorithm [17]	99.79	99.38	98.57	96.6	98.03	96.34
CNN	98.77	96.79	88.78	92.47	89.63	93.84
Algorithm [18]	92.52	96.12	92.9	94.03	94.06	86.33
Proposed	99.89	99.57	99.01	98.96	99.65	98.7

$$\text{Precision} = \frac{\text{TP}}{\text{TP} + \text{FP}}, \quad (10)$$

where TP is a true case, TN is a true negative case, FP is a false positive case, and FN is a false negative case.

The accuracy analysis results of U-Net and the algorithm presented in this paper in the training process are shown in Figure 5.

As can be seen from Figure 5, after 20 iterations in the training process, the accuracy of the algorithm in this paper is always higher than that of U-Net. This proves the feasibility of the proposed algorithm for image segmentation.

#### 4.3. Comparison and Analysis of Algorithms

**4.3.1. Experimental Results of RADARSAT-2 Data.** The proposed algorithm was compared with other 6 typical algorithms, including SVM algorithm, Wishart algorithm, algorithm [16], algorithm [17], CNN, and algorithm [18]. Figure 6 and Table 1 are the classification results and classification accuracy values.

As can be seen from Figure 6(c), SVM algorithm has serious misclassification, especially in the upper and left part of the image. Figure 6(d) is the classification result of the Wishart algorithm, in which bare land and water are seriously confused. In addition, the classification confusion of farmland and river also exists. Figures 6(e) and 6(f) are the classification results of literature [16] and literature [17] algorithms. There are many misclassified pixels in both class

plots. At the same time, there is the problem of internal pixel discontinuity in the image.

Figure 6(g) shows the classification results of CNN algorithm. The results are clearer than those of the previous algorithms. However, the category of farmland excessively affects the classification of the whole image, and many pixels that do not belong to the category of farmland are classified as the category of farmland. Figure 6(h) shows the classification results of literature [18] algorithm, and the classification confusion of village and road categories is serious. Figure 6(i) shows the classification results of the proposed algorithm, and its classification performance is greatly improved compared with other algorithms. The classification image of the proposed algorithm is cleaner and has better spatial connectivity.

As shown in Table 1, the overall classification accuracy of the proposed algorithm is higher than that of other algorithms. The classification accuracy of the Wishart algorithm is 1.25% lower than that of the algorithm in this paper. However, it should be noted that the algorithm uses 5% of real marker pixels as training samples, while the algorithm in this paper only uses 1% of real marker pixels.

#### 4.3.2. Experimental Results of San Francisco Area Data.

Table 2 shows the classification results and classification accuracy values of data in San Francisco area by SVM algorithm, Wishart algorithm, this paper algorithm, and CNN algorithm, respectively. Table 2 shows that the overall

TABLE 2: Classification accuracy on San Francisco image.

Algorithm	Mountain	Farmland	River	Village	Road	Building
SVM	85.63	57.56	24.5	59.33	12.56	49.97
Wishart	93.83	88.11	45.17	39	59.11	66.32
CNN	97.1	83.56	78.11	82.33	87.67	89.45
Proposed	98.89	91.2	95.58	98.11	96.56	96.76

classification accuracy of the proposed algorithm is higher than that of other algorithms.

## 5. Conclusion

Powered by the continuous development of human civilization, landscape design has become an important issue for more and more professionals. Animation technology also plays an increasingly important role in landscape design. In order to realize that the animation design effect of natural landscape is close to the real effect, the synthetic aperture radar image is firstly analyzed to obtain the location of mountains, farmland, rivers, villages, roads, and buildings. In this paper, we design an improved U-Net network structure, which can induce dense connection modules in downsampling. Before upsampling, ASPP and CBAM are introduced to segment satellite image road elements accurately. Experimental results show that the segmentation accuracy of the proposed algorithm is higher than that of other comparison algorithms. The feasibility of the proposed algorithm in landscape design is verified. Although through the algorithm in this paper, the location of mountains, farmland, rivers, villages, roads, and buildings in natural scenes can be obtained. However, the actual scene environment will be more complex, and how to achieve high-precision image classification in a more complex environment is the follow-up research.

## Data Availability

The labelled datasets used to support the findings of this study are available from the corresponding author upon request.

## Conflicts of Interest

The authors declare that they have no competing interests.

## Acknowledgments

This work is supported by the Xijing University.

## References

- [1] A. Chirico, F. Ferrise, L. Cordella, and A. Gaggioli, "Designing awe in virtual reality: an experimental study," *Frontiers in Psychology*, vol. 8, p. 2351, 2018.
- [2] X. Ziya, G. Xiaru, L. Haohao, L. Naixin, and F. Yanhua, "Landscape environment design of long shadow historical section," *Chinese & Overseas Architecture*, vol. 7, 2018.
- [3] X. Li, W. Zhang, and Q. Ding, "Deep learning-based remaining useful life estimation of bearings using multi-scale feature extraction," *Reliability Engineering & System Safety*, vol. 182, pp. 208–218, 2019.
- [4] K. Lee, S. H. Sung, D.-h. Kim, and S.-h. Park, "Verification of normalization effects through comparison of CNN models," in *2019 International Conference on Multimedia Analysis and Pattern Recognition (MAPR)*, pp. 1–5, Ho Chi Minh City, Vietnam, 2019.
- [5] J. Zhang, X. Hu, Z. Ning et al., "Energy-latency tradeoff for energy-aware offloading in mobile edge computing networks," *IEEE Internet of Things Journal*, vol. 5, no. 4, pp. 2633–2645, 2018.
- [6] S. Zhao, M. Hu, Z. Cai, Z. Zhang, T. Zhou, and F. Liu, "Enhancing Chinese character representation with lattice-aligned attention," *IEEE Transactions on Neural Networks and Learning Systems*, pp. 1–10, 2021.
- [7] A. Mittal, R. Hooda, and S. Sofat, "LF-SegNet: a fully convolutional encoder–decoder network for segmenting lung fields from chest radiographs," *Wireless Personal Communications*, vol. 101, no. 1, pp. 511–529, 2018.
- [8] Y. Zhang and A. Jatowt, *Image Tweet Popularity Prediction with Convolutional Neural Network*, Springer, Cham, 2019.
- [9] Q. Zhang, Z. Cui, X. Niu, S. Geng, and Y. Qiao, *Image Segmentation with Pyramid Dilated Convolution Based on ResNet and U-Net*, Springer, Cham, 2017.
- [10] X. Liu, S. Zhang, T. Huang, and Q. Tian, "E<sup>2</sup>BoWs: an end-to-end bag-of-words model via deep convolutional neural network for image retrieval," *Neurocomputing*, vol. 395, pp. 188–198, 2020.
- [11] S. Sengan, L. Arokia Jesu Prabhu, V. Ramachandran, V. Priya, L. Ravi, and V. Subramaniaswamy, "Images super-resolution by optimal deep AlexNet architecture for medical application: a novel DOCALN1," *Journal of Intelligent & Fuzzy Systems*, vol. 39, no. 6, pp. 8259–8272, 2020.
- [12] Q. Zhu, Y. Zhong, L. Zhang, and D. Li, "Adaptive deep sparse semantic modeling framework for high spatial resolution image scene classification," *IEEE Transactions on Geoscience and Remote Sensing*, vol. 56, no. 10, pp. 1–16, 2018.
- [13] Y. Yuan, J. Fang, X. Lu, and Y. Feng, "Remote sensing image scene classification using rearranged local features," *IEEE Transactions on Geoscience and Remote Sensing*, vol. 57, no. 3, pp. 1779–1792, 2019.
- [14] Z. Ning, X. Hu, Z. Chen et al., "A cooperative quality-aware service access system for social Internet of vehicles," *IEEE Internet of Things Journal*, vol. 5, no. 4, pp. 2506–2517, 2017.
- [15] S. Zhao, M. Hu, Z. Cai, and Z F Liu, "Dynamic modeling cross-modal interactions in two-phase prediction for entity-relation extraction," *IEEE Transactions on Neural Networks and Learning Systems*, 2021.

- [16] X. Huang, C. Liao, M. Xing et al., "A multi-temporal binary-tree classification using polarimetric RADARSAT-2 imagery," *Remote Sensing of Environment*, vol. 235, article 111478, 2019.
- [17] Q. Xie, J. Wang, C. Liao et al., "On the use of Neumann decomposition for crop classification using multi-temporal RADARSAT-2 polarimetric SAR data," *Remote Sensing*, vol. 11, no. 7, p. 776, 2019.
- [18] H. Xiping, J. Cheng, M. Zhou et al., "Emotion-aware cognitive system in multi-channel cognitive radio ad hoc networks," *IEEE Communications Magazine*, vol. 56, no. 4, pp. 180–187, 2018.



## Research Article

# Construction of Evaluation Model of Tennis Skills and Tactic Level and Application of Grey Relational Algorithm

Ling Wang 

*School of Physical Education and Health, Heze University, Heze, Shandong 274000, China*

Correspondence should be addressed to Ling Wang; wangling@hezeu.edu.cn

Received 14 February 2022; Revised 1 March 2022; Accepted 10 March 2022; Published 13 April 2022

Academic Editor: Wen Zeng

Copyright © 2022 Ling Wang. This is an open access article distributed under the Creative Commons Attribution License, which permits unrestricted use, distribution, and reproduction in any medium, provided the original work is properly cited.

Based on the application characteristics of the world's elite tennis players' skills and tactics, this paper establishes the evaluation model of skill and tactic level. According to the principle of normal distribution, taking the overall average as the reference value and the overall standard deviation as the discrete distance, the deviation method commonly used in sports statistics is adopted to formulate the grade evaluation standard. The standard is divided into five evaluation grades: excellent, good, passing, poor, and extremely poor. The equivalent evaluation scale of diagnostic indexes of tennis skill and tactic level is established. It also discusses many factors that characterize the skills and tactics of tennis singles. At the same time, it introduces the grey relational algorithm, constructs the evaluation model of skills and tactic level, and makes an example application. Through experimental analysis, it is concluded that this model can be applied not only to the diagnosis of individual athletes but also to the evaluation of a sports team. This article is aimed at further enriching the analysis system of tennis skills and tactics.

## 1. Introduction

With the continuous development of tennis and the increasing influence, tennis is becoming more and more popular with the public [1]. Most people have participated in the tennis competition, which has set off a wave of tennis in China's social development [2]. Tennis has high technical requirements. Among all sports, the rules and requirements of tennis for athletes' behaviors on the court are more detailed and strict. Under the background of actual economic globalization and material and cultural diversification, how to improve the competition skills of Chinese tennis players and promote the development of tennis in China has become an important direction for the development and reform of tennis in China [3]. Game technical and tactical statistics is a cognitive activity that uses concrete data to reflect the quantitative relationship and characteristics between each link of the game technical and tactical and each component of the system [4]. It is characterized by using a large number of specific data to reflect the present situation, changes, and rules of technical and tactical activities in the competition. The purpose is to grasp the overall

quantitative characteristics of technical and tactical activities in the competition, so as to realize the essence of technical and tactical activities in the competition. Tennis skills and tactics are complex and changeable, and it is often difficult to make accurate and scientific decisions on such problems [5]. With the development of information technology, decision-making can be carried out with more information, which greatly increases the complexity of decision-making, and restricts the right decision-making based on personal knowledge and experience. Most of the traditional game analysis is based on the general mathematical statistics. By looking up the literature, we make a primary analysis of the statistical data [6]. The statistical index is too simple, and the information of competitive state of diagnosis feedback is small. Although some methods of multivariate analysis have been used for diagnosis and evaluation and some progress has been made, these methods often fail to find the crux of the problems in the training process and the competition process.

Whether the players successfully use the skills and tactics in the competition often becomes the decisive factor of the competition [7]. The diagnosis and analysis of tennis skills

and tactics are mostly based on the comparative analysis of various technical statistical indicators of athletes in the competition, in order to provide reference for training and formulating competition strategies and tactics. The competitive state of athletes is a complex system, and many contradictions in the system cannot be solved only by dealing with the quantity relationship [8]. Therefore, we cannot just stay in the study of quantitative relationship, but we must study things, characteristics, and values, and we must study the relationship and changes of these three, in order to get a solution to the contradictions [9]. At present, most of the researches are based on the technical and tactical characteristics of the first few athletes in the whole competition or a certain competition. However, the performance of sports competition is restricted by athletes' competitive state during the competition period, environmental factors in the competition, and accidental factors in the competition, and competitive sports itself has the characteristics of unpredictability and contingency of the competition results, so it is difficult for other players to refer to and evaluate the winning rules of tennis skills and tactics [10]. From the literature reports, the technical and tactical research of sports competition has been a very important research topic in sports research for a long time. This paper reviews the current research methods of sports techniques and tactics, aiming at reflecting the current research level and current situation of sports techniques and tactics from the perspective of methodology.

In the process of the continuous development of ball games, the rules of the game are also evolving. Different stages of development have different characteristics, so it is very important to accurately understand and grasp the development trend and objective laws of tennis [11]. In the previous comparative analysis of athletes' skills and tactics, the technical and tactical data of each competition were only isolated individuals, and there were no systematic comparison and evaluation of the quality differences between each competition. The lack of longitudinal analysis cannot directly reflect the ups and downs of athletes' staged competitive state and the fluctuation of various technical and tactical application effects [12]. The technical and tactical analysis of tennis matches cannot be separated from the understanding of the objective laws of this event. Only by starting from the basic theory of special training, following the winning rule and grasping the competitive elements, can the evaluation model be constructed properly and accurately reflect the situation of tennis players' skills and tactics [13]. The results can be helpful to the diagnosis and analysis of coaches and the arrangement of the next training plan, so that the evaluation model can stand the test of practice. The evaluation model of sports skill and tactic level designed in this paper is based on the basic principle of grey relational algorithm, and the evaluation model of sports skill and tactic level based on grey relational algorithm is constructed [14]. A tennis match is described with an introduction matrix of game state transition. On this basis, the winning probability of the match is calculated by Markov chain and the competitive efficiency values of various game states are further determined. Compared with the traditional evaluation and

analysis method of tennis match, this method can not only make descriptive statistical analysis of techniques and tactics through the transition probability of various match states but also determine the influence of various match states on the winning probability of the whole match.

## 2. Related Work

Literature [15], by using the fast video analysis system of tennis match and the data collection and intelligent analysis system of tennis skills and tactics, makes a simple statistical analysis of the technical and tactical characteristics of Chinese women tennis team by video statistics and points out some problems existing in the economic indicators of Chinese women tennis players. In literature [16] by using the methods of literature, mathematical statistics, and comparison, the technical and tactical indexes of tennis women's singles players in the competition were statistically analyzed. Literature [17] points out that there is a significant gap between Chinese tennis women's singles players and world-class tennis women's singles players in terms of technical and tactical indicators such as the scoring rate of the first serve, the scoring rate of the second serve, the scoring rate of receiving the serve, the success rate of breaking, and nondestructive mistakes. Literature [18] and Literature [19], respectively, studied the diagnosis and evaluation of tennis attack tactic level in the research of "Diagnosis and evaluation of tennis attack tactics level" and "Application of multivariate analysis in tennis evaluation." Literature [20] pointed out that it is also a requirement of technical and tactical decision to simulate and predict the influence of various technical and tactical indicators on the results of the competition through technical and tactical modeling research. Literature [21] describes the theory and method of mathematical simulation competitive diagnosis of ball games in the research of "Theory and practice of mathematical simulation competitive diagnosis of ball games." It was successfully deduced with an example of mathematical simulation of tennis match. Literature [22] introduces matter-element analysis into the diagnosis method by using the basic idea of technical and tactical characteristic model. Using extension set and correlation function, the characteristic model of tennis women's doubles skills and tactics is divided into three dimensions. They are basic skills, basic tactics, and the substructure of sending and gaining and losing. Literature [23] uses a mathematical simulation diagnosis method to diagnose and evaluate competitive state. It opens up a new way to study the competitive state. He can not only make general descriptive statistics on the competition state but also determine the influence of various competition states on the winning probability of the whole competition through mathematical calculation. Literature [24] studies the theory and methods of data mining and discusses the application of data mining based on association analysis and data mining based on rough set in the field of tennis technical and tactical decision-making and makes a concrete application case analysis.

Based on the research of related literatures, this paper finds that due to the different items and requirements, there

are various theories and methods used in technical and tactical research, each of which has its own characteristics. Based on the analysis and research of the advantages and disadvantages of these methods, this paper puts forward a new evaluation model construction method of tennis skills and tactics. Based on the theory of grey correlation algorithm, this paper uses a grey correlation method to construct the diagnosis and evaluation system of tennis skill and tactic level. By using the methods of literature review, questionnaire survey, and video statistics, the evaluation indexes of tennis skills and tactics were established. The indicators that are highly representative and can objectively reflect the actual situation are selected. It has solved the technical and tactical landing decision-making problems such as the analysis of the association rules of the last two beats, the association rules of the first three beats of the serving wheel, and the association analysis of the first two beats of the receiving service. Experiments show that the comprehensive evaluation model of tennis skills and tactics based on the grey relational algorithm is practical and feasible. Provide objective and scientific decision support for the evaluation of tennis skills and tactics.

### 3. Methodology

*3.1. Concept and Significance of Tennis Skill and Tactic Level Evaluation.* Technology and tactics are two frequently used terms in sports, and they are two necessary links to improve the competitive level. Technology is the way to complete actions; tactics are the strategies and actions taken to defeat opponents. Technology is interpreted as the experience and knowledge accumulated by human beings in the process of utilizing and transforming nature and embodied in productive labor and also refers to other operational skills [25]. Continue to narrow the scope to tennis, and technology is one of the performance characteristics of tennis. It mainly includes serving, receiving, forehand shooting down the earth, backhand shooting down the earth, interception, high-pressure ball, lob, and small ball. According to the theory of sports training, sports technology refers to the method of completing sports movements, which is an important determinant of athletes' competitive ability.

Sports tactics refer to all kinds of strategies and actions taken to defeat opponents or achieve ideal results according to the competition rules of special sports. Here, strategy refers to premeditation and on-the-spot strategy before the game. Action refers to the behavior mode of carrying out pregame planning and on-the-spot strategy. Tactics consist of tactical concepts, tactical guiding ideology, tactical principles, tactical awareness, tactical knowledge, tactical forms, and tactical actions [26]. There are technical and tactical behaviors in any sports competition, but different sports require different levels of skills and tactics. The quantitative diagnosis of technical and tactical level is to use scientific detection methods to obtain information related to athletes' technical and tactical level. Then analyze the information, so as to evaluate the technical and tactical level of athletes, find out the shortcomings, and provide the basis for improving the technical and tactical training quality. We diagnose the cause of failure and its degree according to certain procedures or rules. The specific steps are shown in Figure 1.

Tactical ability refers to the ability of athletes to master and use tactics, which is the main component of the overall competitive ability of athletes. Good tactics, if the athletes cannot perform effectively in the competition, or if the athletes do not follow the original tactical plan according to the changes of the competition situation, they are likely to fall into a passive position and fail to achieve the expected competition results [27]. Therefore, it puts forward high requirements for athletes' tactical ability. In the ball game, the complexity and flexibility of techniques and tactics and their flexible application in the game make the ball game performance and sports quality show a nonlinear relationship, and it is difficult to predict the athletes' performance according to sports quality, while techniques and tactics play an extremely important role in the outcome of the game.

Technology and tactics are dialectically interrelated, interdependent, and mutually restricted. It is the material basis of technology and tactics. In the competition, technology is always reflected in tactical coordination and action, and it can be fully played and played a good role in time. Advanced tactics can in turn actively promote the improvement and development of technology. Scientific and systematic diagnosis and analysis of players' technical and tactical ability are one of the core contents to improve the scientific training and participation of tennis events.

The strength of athletes' tactical ability is reflected in the advanced tactical concept, the strength of individual tactical awareness and cooperation awareness, the amount of tactical theoretical knowledge, the quality and quantity of mastered tactical actions, the immediacy and effectiveness of tactics, etc. In sports, the degree of dependence of competition results on skills and tactics is quite different among different sports groups. The technical and tactical requirements of various events are divided into three levels: basic role, important role, and decisive role. For sports with high technical and tactical requirements, the successful application of athletes' technical and tactical skills in the competition often determines the outcome of the competition, which is a very important factor.

The technical and tactical characteristic model refers to the sum of the technical and tactical characteristics that athletes need to have when they take up the role of a special task in competitive sports. The establishment of the technical and tactical characteristic model is the logical starting point for the practical research of athletes' training and training, and it is also an important foundation for a series of athletes' team management and development techniques. The statistical analysis of sports skills and tactics is mainly that the technical and tactical information indicators in sports competitions are listed into tables in advance, and then the technical and tactical indicators are recorded and counted by on-the-spot observation or watching the video of the competition, so as to obtain the technical and tactical counting data of athletes in the competition, and then further statistical analysis and collation of these technical and tactical data are carried out, and the technical and tactical rules reflecting the athletes' competition performance are obtained. The frame structure of the comprehensive evaluation system of technology and tactics in this paper is shown in Figure 2.

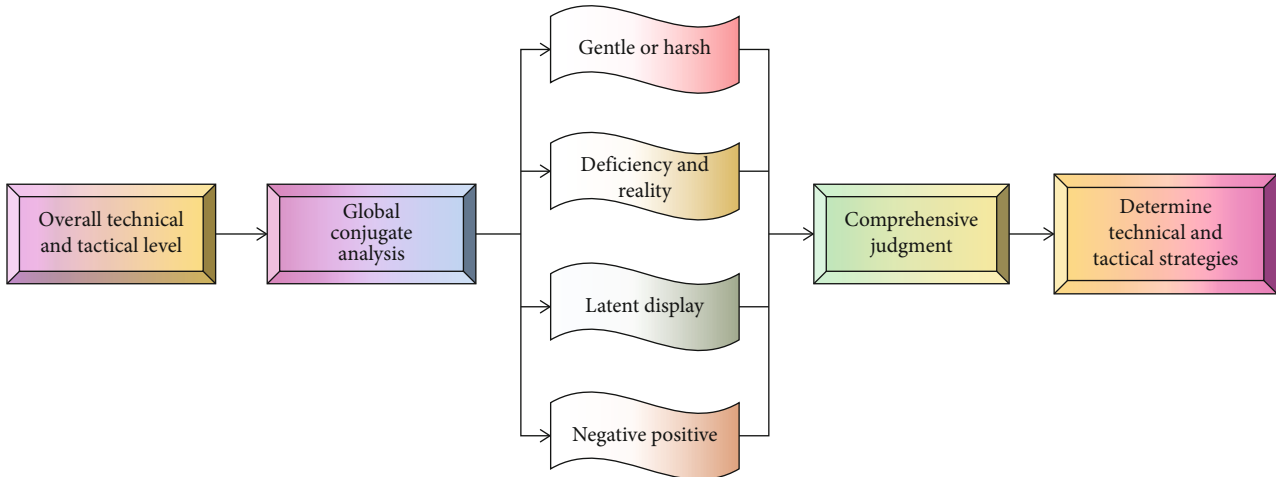


FIGURE 1: Quantitative diagnosis process of athletes' technical and tactical level.

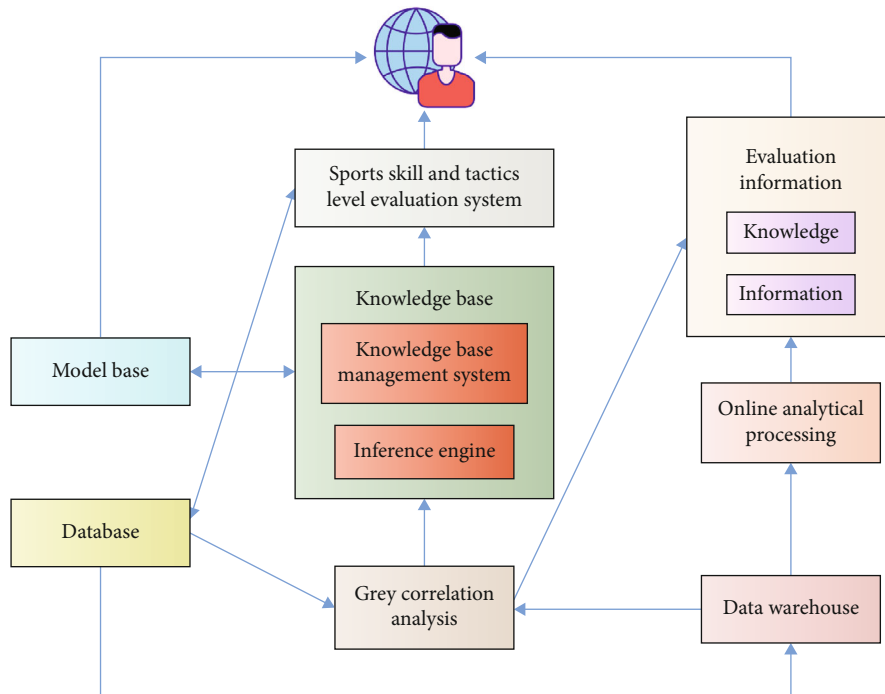


FIGURE 2: Framework of comprehensive evaluation system of tactics and techniques.

Evaluation usually means to determine the meaning, value, or state of an object through detailed and careful research and evaluation. Modeling technical and tactical behavior is also a way to study the performance of competitive sports. Sports model is an analytical technology that provides practical information, because it directs the modeler's attention to key features of data, which can successfully describe athletes' performance in competition, and the model can reliably predict future competitions according to the deep-seated features of sports performance.

3.2. Evaluation Model of Tennis Skill and Tactic Level Based on Grey Relational Algorithm. Grey system correlation analysis is not only an important part of grey system theory but

also the cornerstone of grey system analysis, modeling, prediction, and decision-making. Research in recent years shows that grey relational theory is undoubtedly the most widely used and dynamic part of grey system theory. Association analysis can find interesting relationships between things hidden in large databases. These connections can be given in the form of association rules and frequent item sets. Association analysis can be applied to business management, medical diagnosis, scientific data analysis, and other fields. The existing grey relational analysis is based on the following idea: according to the similarity of geometric shapes of series curves, it is judged whether the relationship is close. The closer the curves are, the greater the correlation between the corresponding series, and vice versa. Association analysis

can find interesting relationships between things hidden in large databases. These rules or relationships can be found by using an algorithm of association rules.

At present, the construction of grey relational grade algorithm model is mainly from two angles. On the one hand, the correlation degree is constructed by reflecting the similarity of development process or magnitude between two sequences. On the other hand, it is constructed by reflecting the similarity of the development trend or curve shape of the two series, that is, the closeness of the relative change trend between the main engraved series curves. In practical applications such as grey clustering and grey decision-making, the correlation analysis of the closeness between each known pattern and the ideal pattern is often used. The closer the known pattern and the ideal pattern are, the higher the closeness and the larger the value of the closeness. That is to say, this correlation analysis is a kind of proximity analysis, not similarity analysis.

Grey comprehensive evaluation is mainly based on the following models:

$$R = E \times W. \quad (1)$$

In the formula,  $R = [r_1, r_2, \dots, r_m]^T$  is the comprehensive evaluation result vector of  $m$  evaluated objects.  $W = [w_1, w_2, \dots, w_n]^T$  assigns  $n$  vectors to the weights of  $n$  evaluation indicators, where

$$\sum_{j=1}^n w_j = 1. \quad (2)$$

$E$  is the evaluation matrix of each index:

$$E = \begin{bmatrix} \xi_1(1) & \xi_1(2) & \dots & \xi_1(n) \\ \xi_2(1) & \xi_2(2) & \dots & \xi_2(n) \\ \dots & \dots & \dots & \dots \\ \xi_m(1) & \xi_m(2) & \dots & \xi_m(n) \end{bmatrix}. \quad (3)$$

In the formula,  $\xi_i(k)$  is the correlation coefficient between the  $k$ -th index of the  $i$ -th scheme and the  $k$ -th optimal index. The value of  $R$  is obtained, and the techniques and tactics of the evaluation objects are sorted. Determine the optimal set of metrics ( $F^*$ ). Assume

$$F^* = [j_1^*, j_2^*, \dots, j_n^*]. \quad (4)$$

In the formula,  $j_k^*(k = 1, 2, \dots, n)$  is the optimal value of the  $k$ -th index. If it is a high-quality index, the optimal value is the maximum value among the schemes; if it is a low-quality index, the optimal value is the lowest value among the schemes. After selecting the optimal index set, the matrix  $D$  can be constructed:

$$D = \begin{bmatrix} j_1^* & j_2^* & \dots & j_n^* \\ j_1^1 & j_2^1 & \dots & j_n^1 \\ \dots & \dots & \dots & \dots \\ j_1^m & j_2^m & \dots & j_n^m \end{bmatrix}. \quad (5)$$

The evaluation index system of tennis technical and tactical effectiveness is the main basis for judges to score the skills and tactics used by tennis players in tennis matches. The establishment of tennis technical and tactical efficiency evaluation system needs to be based on the basic unit skill process and divide the whole tennis game into several basic unit competition modules. According to the athletes' "score and loss of beat number" in the basic compound competition process, this paper analyzes and judges the base station performance and economic characteristics of tennis players. The basic unit competitive process refers to the process of offensive and defensive confrontation between players in the competition for every point, which is the most basic unit of the tennis competition process. The "winning and losing scores" produced by each basic unit competitive process is not only the expression form of athletes' technical and tactical application but also the stage characteristics of the basic unit competitive process of tennis competition. Scoring rate and utilization rate are the most basic evaluation parameters for the technical and tactical analysis of the holding-racquet-net-against-net event.

Sports competition behavior and its results are influenced by many factors. The complexity and difficulty of explaining these factors make some scholars begin to study sports competition from a systematic point of view. Although it is still inconclusive whether the technical and tactical behavior of sports competition is a self-organizing system or a complex system, it is based on the systematic view to study sports competition. In the course of the competition, in order to give full play to the technology, reasonable tactical choice is also necessary. In the process of sports training, tactical awareness must be used to guide technical training. Only in this way can we train the most useful skills in the competition. On the other hand, it is necessary to choose a tactical system suitable for athletes from their technical characteristics.

The first step of technical and tactical statistical analysis is to collect data according to statistical indicators. According to the different collection time, it can be divided into two categories: on-the-spot collection and postmatch collection. On-the-spot collection means real-time collection of skills and tactics during athletes' competitions. On-the-spot data collection has few indicators and reflects little information, but the collection time is short, which is conducive to rapid information feedback, and is mainly used for technical and tactical statistics of sports teams during competitions. Postmatch collection refers to technical and tactical collection by watching video data after the game. Because this kind of collection is not limited by time, it can observe and record as many technical and tactical indicators as possible, which is conducive to more detailed and in-depth technical and tactical research of the game. For discrete data series, the

so-called closeness of two curves refers to the closeness of curve slopes of two time series in each corresponding time period. If the curve slopes of two curves are equal or have little difference in each time period, the correlation coefficient between them will be larger; otherwise, it will be smaller.

The physical characteristic displacement difference  $d_{ij}^{(0)}(t)$  describing similarity and the physical characteristic velocity difference  $d_{ij}^{(1)}(t)$  and acceleration difference  $d_{ij}^{(2)}(t)$  describing similarity are used to reflect the degree of correlation between sequences. Order

$$\begin{aligned} d_{ij}^{(0)}(t) &= \sum_{k=1}^n |x_i(k) - x_0(k)|, \\ d_{ij}^{(1)}(t) &= \sum_{k=1}^{n-1} |x_i(k+1) - x_0(k+1) - x_i(k) + x_0(k)|, \\ d_{ij}^{(2)}(t) &= \sum_{k=2}^{n-1} |[x_i(k+1) - x_0(k+1)] - 2[x_i(k) + x_0(k)] \\ &\quad + [x_i(k-1) - x_0(k-1)]|. \end{aligned} \quad (6)$$

Then, the formula for calculating the B-type correlation degree is:

$$r(X_0, X_1) = \frac{1}{1 + (1/n)d_{ij}^{(1)}(t) + (1/(n-1))d_{ij}^{(0)}(t) + (1/(n-2))d_{ij}^{(2)}(t)}. \quad (7)$$

As a net-separated confrontation event, the competition for each ball in the competition is a unit competition process. Therefore, the analysis of the structure of gains and losses is an important part of the whole competition and the whole competitive process. The structure of winning and losing points in tennis has many characteristics: due to the fierce confrontation in tennis competition, the scores in the competition include both active offensive scores and the mistakes of opponents. When watching the game, we often see the unforced errors of athletes. Because of the different times when athletes' best state appears in the course of competition, the proportion of athletes' gains and losses is different in different stages of competition. The success or failure of high-level competitions often takes the gain or loss of one or two key balls as the inflection point, showing a clear trend. The final result of a tennis match is calculated by scores, so scoring and losing points are the starting points to guide training and competition.

In the process of establishing the technical and tactical characteristic model, we discuss it from three aspects: basic technology, basic tactics, and the structure of gains and losses. Technology is the foundation of tactics and the necessary condition for tactics to be realized. The basic skills of tennis singles include serving, receiving, forehand, backhand, chopping, volley ball, high-pressure ball, putting small ball, and picking high ball. On the structure of score and

loss, it is discussed from two aspects: the means and timing of score. In terms of means of gain and loss, we use active scoring as the index, and in terms of scoring opportunity, we use the first four beat scoring and stalemate scoring stages to describe.

#### 4. Result Analysis and Discussion

Only analyzing the single technical and tactical indicators of tennis players can not reflect the problems existing in the whole competition process, and the results are rather one-sided. Therefore, it is necessary to comprehensively evaluate the effectiveness of each technical and tactical indicator from a comprehensive perspective and obtain the comprehensive evaluation results, so as to reflect the quality of the whole competition. Among the various techniques of tennis, serving is the only one that is not restricted by opponents. A good serve can not only score directly but also mobilize the opponent into his own tactical design. A good serve is not only a sharp weapon to score directly but also an important means to take the initiative and create a winning chance. As the most efficient scoring method, the technique before the net is often ignored by the bottom-line players, but under the trend of comprehensive technology, the technique before the net gradually shows its importance.

During the whole game, because there are not too many differences in serving speed, serving strength, and other aspects between players of both sides of the game, this research activity will analyze the importance of serving and receiving in the whole tennis game from the third row of the game to the whole game with the aid of this stage of attack and defense stalemate. Statistical analysis of a certain technical and tactical index of athletes can evaluate the local situation of athletes' technical and tactical application in the competition. If we want to evaluate the technical and tactical performance of the whole competition, we need to "integrate" the application of each tactical index in the competition. Figure 3 is a schematic diagram of the average utilization rate and average scoring rate of each beat technique and tactics used in the basic unit competition of the world's elite tennis players in hard court competition.

The differences in the average utilization rate and average scoring rate of each beat technique and tactics in the basic unit competitive process show the differences in the characteristics of technique and tactic application and scoring effect in the three stages.

Considering the characteristics of association rule algorithm, that is, it produces frequent itemsets in combination. However, the decision-making requirement of the hitting point of tennis ball is in order, and it is related to the hitting effect. Therefore, the grey relational algorithm is used to mine the characteristics of hitting point of tennis technique and tactics. It can excavate and analyze the relationship between the hitting point and the winning and losing points of the first two strokes of the serving wheel and the receiving wheel and can also analyze the correlation between the hitting point and the winning and losing points of the last two strokes of each score. The evaluation index mainly involves three aspects, namely, benefit index, cost index,

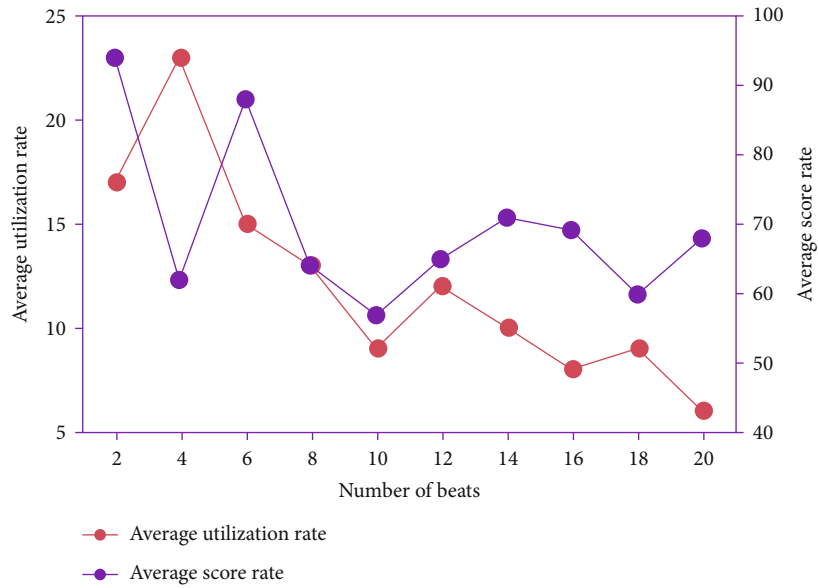


FIGURE 3: Average utilization rate and average score rate of each beat in hard court competition.

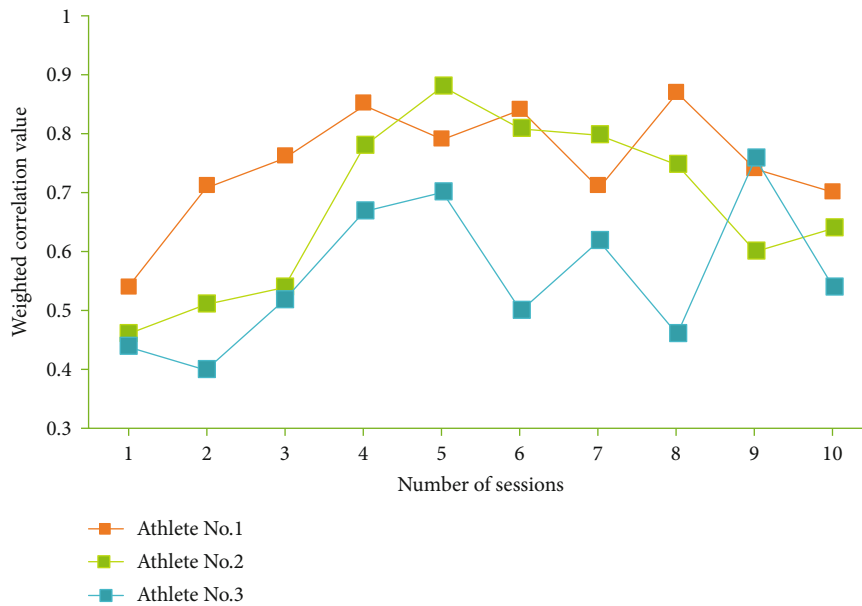


FIGURE 4: Trend chart of comprehensive evaluation of athletes' skills and tactics.

and moderate index. The larger the benefit index, the better the effect. The smaller the cost index, the better the effect. Moderate index indicates that the better the effect. Because the benefit index, cost index, and moderate index belong to three different categories and have different properties, they should be dimensionless. Select the data of the technical and tactical effects used in 10 games of Athlete No.1, Athlete No.2, and Athlete No.3, and get the comprehensive evaluation of the competition technical and tactical as shown in Figure 4.

Through further observation of the contents in the picture, it is found that the comprehensive technical and tactical value of Athlete No.3 in the competition is good, the competitive state is relatively stable, and the competitive performance conforms to the law of sports training, which

reflects the scientificity and effectiveness of Athlete No.3's usual training.

The "three-stage index evaluation method" is characterized by the division of "stages" according to the law of hitting order in tennis matches, so that the strength of the same player in different periods or among different players in the same period can be compared. It is a macroscopic evaluation of an athlete's ability to play on the spot in the competition. Its advantages are easy to understand and easy to operate. In order to verify the accuracy and feasibility of this algorithm, this paper compares the accuracy and recall of different algorithms. The obtained accuracy is shown in Figure 5, and the comparison of recall rate is shown in Figure 6.

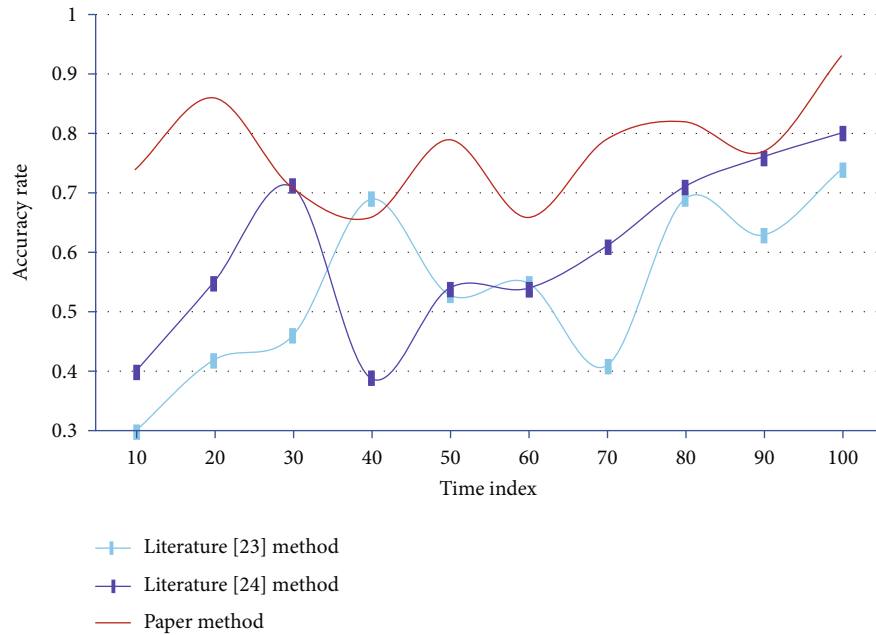


FIGURE 5: Comparison of accuracy of different algorithms.

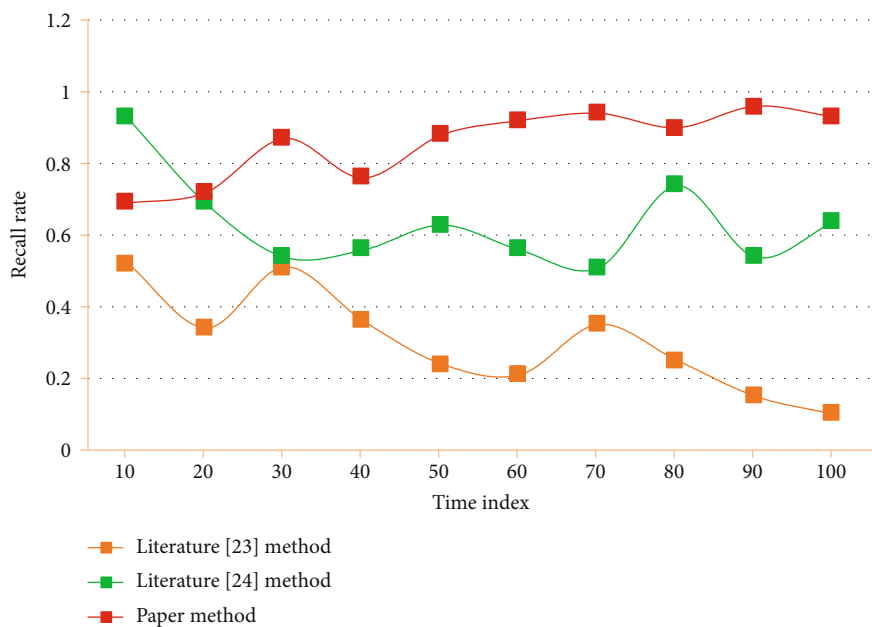


FIGURE 6: Comparison of recall rates of different algorithms.

By analyzing Figure 5, we can see that the accuracy rate of this algorithm is higher than that of literature [23] and literature [24], and it is concluded that this algorithm has the highest accuracy rate. In the comparison of the recall rate of the three algorithms, the recall rate of this algorithm is the best, which is higher than those of the other two algorithms. This further demonstrates the accuracy and superiority of this algorithm.

The “stalemate stage” is an important stage to evaluate the skill level of tennis players in the whole game. At this

stage, the two sides of the competition are in a state of close competition for a long time, and there is not much difference in the strength relationship between them, so it is impossible to win or lose in a short time. If you want to beat your opponent in tennis, you must break your opponent’s serve, or your opponent’s serve point. Therefore, receiving and serving technology is an important technology in parallel with serving technology. With the development of baseline technology, service receiving technology has become more and more aggressive, and the traditional passive return has been



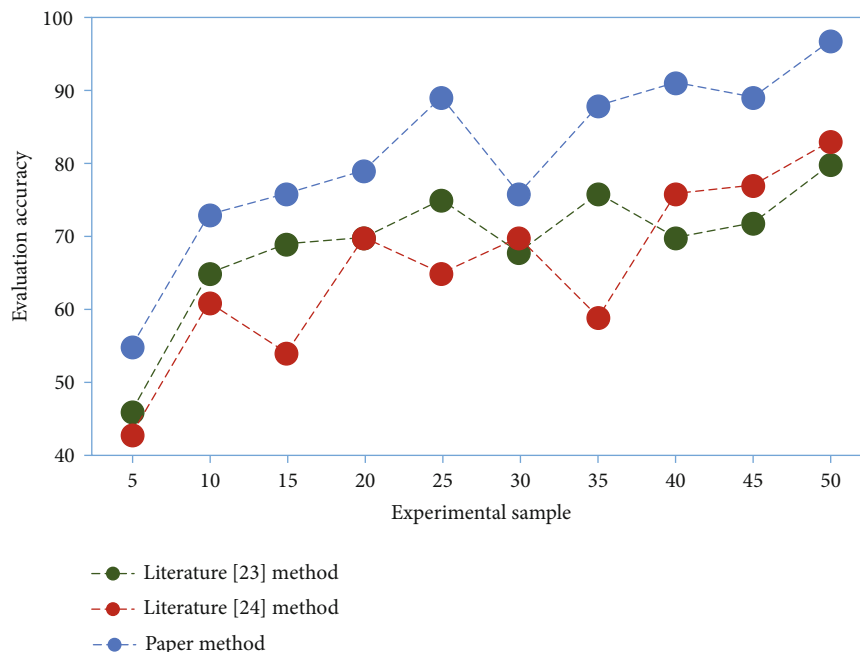


FIGURE 7: Accuracy of different models in evaluating technical and tactical level.

replaced by active service receiving and attacking. Practical experiments are carried out on the model established in this paper. By comparing the models in literature [23] and literature [24], the accuracy of three different models in evaluating tennis skills and tactics is obtained. The results are shown in Figure 7.

Through analysis, it can be concluded that the accuracy of the models in literature [23] and literature [24] in evaluating the technical and tactical level is comparable. Among them, the model in this paper has the highest accuracy in evaluating the technical and tactical level. Further confirmed the practicability and feasibility of this model.

Different indexes can reflect different contents and have different comparability. We should use standardized processing methods to process the original data, reduce the influence of dimensions, and ensure that different indexes can carry out quantitative calculation. From the gray absolute correlation degree, it shows that there is a certain correlation between the two sequences. However, from the perspective of grey proximity correlation degree and grey similarity correlation degree, it shows that the two sequences are neither close nor similar. Therefore, in the actual cluster analysis and decision analysis, we should choose a unified correlation degree according to the actual target to be analyzed, and some cannot choose grey absolute correlation degree; some can choose grey proximity correlation.

There are many indexes for evaluating the technical and tactical effectiveness of tennis events. Only by selecting the indexes that are highly representative and can objectively reflect the actual situation can we comprehensively reflect the level of competition quality. The evaluation model of tennis technical and tactical level based on grey relational algorithm can quantitatively reflect the advantages and disadvantages of athletes' technical and tactical efficiency in dif-

ferent periods, and it has certain practical value in tennis technical and tactical efficiency evaluation.

## 5. Conclusions

In competitive tennis, technique and tactics are one of the main factors that affect the competition results, and whether it is successfully used or not often becomes the decisive factor for the outcome of the competition. Therefore, it is an important topic in the research field of sports technology and tactics to study the technical and tactical rules of tennis competitive competition and improve the scientific level of technical and tactical decision-making. In this paper, based on the basic principle of grey relational algorithm, starting from grey relational algorithm, the evaluation model of sports skill and tactic level based on grey relational algorithm is constructed. Through the analysis of the overall technical and tactical level and conjugation, it is known that there is a great gap between China's elite players and the world's elite players in basic technology. However, the technique of baseline pumping is comparable to that of the world's best players. There is a gap in the basic skills and tactics and the use of play, but there is little difference in the structure of gains and losses. The ability to score in the first four beats is weak, and the ability to win quickly needs to be improved.

In this study, the evaluation index system of tennis skills and tactics is selected, and the comprehensive evaluation of tennis skills and tactics is carried out by using the grey relational algorithm. Experiments show that the method based on grey correlation can comprehensively evaluate tennis skills and tactics. The evaluation method is scientific and effective. To some extent, it can predict the competitive state of athletes in a certain period of time, and it can also provide

data support for empirical facts, so as to provide reference for coaches' decision-making and athletes' training adjustment. It has certain practical value in the evaluation of tennis skills and tactics. The purpose of this evaluation model is to provide objective and accurate data for coaches and athletes in the future training competition, to guide the development of scientific training, and to provide some overall ideas and suggestions for the development of tennis skills and tactics. The research on sports skills and tactics has always been a hot issue in the field of sports competition. Due to the limited research energy and ability of the author, as far as the current research results of this study are concerned, some work needs further in-depth study in the future.

### Data Availability

The labeled dataset used to support the findings of this study is available from the corresponding author upon request.

### Conflicts of Interest

The author declares no competing interests.

### References

- [1] J. Carboch, T. Kocib, M. Cabela, and J. Kresta, "Tactics in tennis doubles: analysis of the formations used by the serving and receiving teams," *International Journal of Physical Education, Fitness and Sports*, vol. 9, no. 2, pp. 45–50, 2020.
- [2] H. Zhe and H. Yujiao, "Research on table tennis tactics based on artificial intelligence," *Agro Food Industry Hi-Tech*, vol. 28, no. 1, pp. 624–627, 2017.
- [3] X. Ma, D. Zeng, R. Wang, J. Gao, and B. Qin, "An intelligent price-appraisal algorithm based on grey correlation and fuzzy mathematics," *Journal of Intelligent and Fuzzy Systems*, vol. 35, no. 3, pp. 2943–2950, 2018.
- [4] J. Margarito, R. Helaoui, A. M. Bianchi, F. Sartor, and A. G. Bonomi, "User-independent recognition of sports activities from a single wrist-worn accelerometer: a template-matching-based approach," *IEEE Transactions on Biomedical Engineering*, vol. 63, no. 4, pp. 788–796, 2016.
- [5] D. Lipshutz, Y. Bahroun, S. Golkar, A. M. Sengupta, and D. B. Chklovskii, "A biologically plausible neural network for multi-channel canonical correlation analysis," *Neural Computation*, vol. 33, no. 9, pp. 2309–2352, 2021.
- [6] D. T. Gescheit, R. Duffield, M. Skein, N. Brydon, S. J. Cormack, and M. Reid, "Effects of consecutive days of match play on technical performance in tennis," *Journal of Sports Sciences*, pp. 1988–1994, 2017.
- [7] B. Changstrom and N. Jayanthi, "Clinical evaluation of the adult recreational tennis player," *Current Sports Medicine Reports*, vol. 15, no. 6, pp. 437–445, 2016.
- [8] M. King, A. Hau, and G. Blenkinsop, "The effect of ball impact location on racket and forearm joint angle changes for one-handed tennis backhand groundstrokes," *Journal of Sports Sciences*, vol. 35, no. 13, pp. 1231–1238, 2016.
- [9] S. Mecheri, G. Laffaye, C. Triolet et al., "Relationship between split-step timing and leg stiffness in world-class tennis players when returning fast serves," *Journal of Sports Sciences*, vol. 37, no. 17, pp. 1962–1971, 2019.
- [10] B. M. Pluim, F. Loeffen, B. Clarsen, R. Bahr, and E. A. L. M. Verhagen, "A one-season prospective study of injuries and illness in elite junior tennis," *Scandinavian Journal of Medicine & Science in Sports*, vol. 26, no. 5, pp. 564–571, 2016.
- [11] F. Tubez, B. Forthomme, J. L. Croisier et al., "Inter-session reliability of the tennis serve and influence of the laboratory context," *Journal of Human Kinetics*, vol. 66, no. 1, pp. 57–67, 2019.
- [12] V. Roy, L. Lee, M. Uihlein, I. Roy, and K. Lee, "Ultrasonographic comparison of the lateral epicondyle in wheelchair-user (and able-bodied) tennis players: a pilot study," *Journal of Spinal Cord Medicine*, vol. 44, pp. 29–36, 2021.
- [13] M. Smith, M. Ellmore, G. Middleton, P. Murgatroyd, and T. Gee, "Effects of resistance band exercise on vascular activity and fitness in older adults," *International Journal of Sports Medicine*, vol. 38, no. 3, pp. 184–192, 2017.
- [14] Z. Bańkosz and T. Stefaniak, "Elbow joint position and hand pressure force sense under conditions of quick reaction in table tennis players," *Kinesiology*, vol. 53, no. 1, pp. 95–103, 2021.
- [15] V. Seetharamaiah, A. Gantaguru, and S. Basavarajanna, "A comparative study to evaluate the efficacy of platelet-rich plasma and triamcinolone to treat tennis elbow," *Indian Journal of Orthopaedics*, vol. 51, no. 3, pp. 304–311, 2017.
- [16] S. Zhang and H. Mao, "Optimization analysis of tennis players' physical fitness index based on data mining and mobile computing," *Wireless Communications and Mobile Computing*, vol. 2021, Article ID 9838477, 11 pages, 2021.
- [17] V. Nista-Piccolo, J. R. Z. Júnior, M. C. Nascimento, M. Sartori, and K. De Angelis, "Heart rate variability in tennis players," *Revista Brasileira de Medicina do Esporte*, vol. 25, no. 3, pp. 202–206, 2019.
- [18] T. Ishihara, S. Sugawara, Y. Matsuda, and M. Mizuno, "The beneficial effects of game-based exercise using age-appropriate tennis lessons on the executive functions of 6–12-year-old children," *Neuroence Letters*, vol. 642, pp. 97–101, 2017.
- [19] C. Sáenz-Moncaleano, I. Basevitch, and G. Tenenbaum, "Gaze behaviors during serve returns in tennis: a comparison between intermediate- and high-skill players," *Journal of Sport & Exercise Psychology*, vol. 40, no. 2, pp. 49–59, 2018.
- [20] A. Yz, C. Ctc, and D. Ngma, "The effects of visual training on sports skill in volleyball players," *Progress in Brain Research*, vol. 253, pp. 201–227, 2020.
- [21] B. Duran and S. Sadry, "The effect of physical activity on the skeletal maturity of the wrist bone and cervical vertebra of children," *Progress in Nutrition*, vol. 22, no. 4, pp. 2–9, 2020.
- [22] P. J. O'Halloran, M. Amoo, D. Johnson et al., "Sports & exercise related traumatic brain injury in the Republic of Ireland—the neurosurgical perspective," *Journal of Clinical Neuroscience*, vol. 81, pp. 416–420, 2020.
- [23] N. Malliaropoulos, J. F. Kaux, S. L. Garrec, and H. Lohrer, "Sports and exercise medicine coming together," *British Journal of Sports Medicine*, vol. 53, no. 24, pp. 1505–1506, 2019.
- [24] L. Zhang, M. Wang, Z. Yang, Y. Jiang, and Y. Cui, "Machine learning for Internet congestion control: techniques and challenges," *IEEE Internet Computing*, vol. 23, no. 5, pp. 59–64, 2019.
- [25] H. Ahmed and A. K. Nandi, "Three-stage hybrid fault diagnosis for rolling bearings with compressively sampled data and subspace learning techniques," *IEEE Transactions on Industrial Electronics*, vol. 66, no. 7, pp. 5516–5524, 2019.

- [26] F. A. Moura, R. E. A. van Emmerik, J. E. Santana, L. E. B. Martins, R. M. L. de Barros, and S. A. Cunha, "Coordination analysis of players' distribution in football using cross-correlation and vector coding techniques," *Journal of Sports Sciences*, vol. 34, no. 24, pp. 2224–2232, 2016.
- [27] T. Kempton, N. Kennedy, and A. J. Coutts, "The expected value of possession in professional rugby league match-play," *Journal of Sports Sciences*, vol. 34, no. 7, pp. 645–650, 2016.

## Research Article

# Clothing Modular Design Based on Virtual 3D Technology

Jiao Wang<sup>1</sup> and Yijun Zhong<sup>2</sup> 

<sup>1</sup>*Institute of Art & Design, Changsha University of Science & Technology, Changsha, 410114 Hunan, China*

<sup>2</sup>*Art Design Institute, Hunan Women's University, Changsha, 410004 Hunan, China*

Correspondence should be addressed to Yijun Zhong; 202014340603@stu.csust.edu.cn

Received 20 February 2022; Revised 10 March 2022; Accepted 21 March 2022; Published 13 April 2022

Academic Editor: Yanqiong Li

Copyright © 2022 Jiao Wang and Yijun Zhong. This is an open access article distributed under the Creative Commons Attribution License, which permits unrestricted use, distribution, and reproduction in any medium, provided the original work is properly cited.

In order to improve the effect of online clothing modular design, this paper adopts the improved linear skinning technology. Moreover, without changing the original input value, this paper uses the QLERP interpolation method to interpolate the rotations of multiple joints into one and determines the rotation angle through the calculation of the rotation center point, so as to subtly solve the problem of skin depression and distortion, and greatly improving the authenticity of the experiment. In addition, this paper combines the virtual 3D technology to build a clothing modular design system to improve the effect of online clothing design. The simulation test results show that the clothing modular design system based on virtual 3D technology proposed in this paper basically meets the current online clothing modular design requirements.

## 1. Introduction

Informatization is one of the important themes of contemporary society, and various embedded information systems are constantly integrated into people's lives, becoming an important force for improving the quality of life. With the rapid development of microelectronic technology and material technology, various microprocessing devices are emerging, which provides a solid technical foundation for the integration of electronic equipment and clothing [1]. The digital clothing system improves the ability of users to obtain and process information anytime and anywhere by integrating data collection, wireless transmission, positioning and navigation, video collection, and other information processing functions in clothing. The combination of digital clothing and job requirements is of great significance to improve the efficiency of workers in different industries in dealing with problems [2]. The embedded computer system for clothing is centered on the wearer. Due to the limitations of people's physical ability, feeling, and cognition, strict requirements are put forward for the function, performance, structural layout, and other aspects of the computer system [3]. The combination between soft clothing and hard computer modules, especially how to improve the practical per-

formance of the system under special use environments and operating conditions through the integration of clothing and computer systems has become the key to the realization of the system.

The garment CAD system is involved in all aspects of garment production, including the creation of fashion designers, the drawing of clothing renderings, the drawing of clothing samples, the confirmation and modification of industrial patterns, and industrialized process processing, such as push plates and layouts. The garment CAD system can generally be divided into the garment design system and style design system. The garment piece design system includes three functional modules: template design, grading, and layout. The hardware devices required for the garment piece design system include a host computer, a digitizer, and a plotter. The advantage of CAD technology is in grading and nesting, especially the grading has been fully automated. The grading of garment pieces is a repetitive and tedious task. It takes a lot of time and energy to use manual methods. Due to the low efficiency of traditional grading, the size and specifications of garments are often incomplete.

Using CAD technology, you only need to input the corresponding specifications in the size table, and within a few minutes to ten minutes, the complete set of specifications

can be quickly provided, and the accuracy is very high. However, manual grading will affect its accuracy because each person's grading method is different. Using computer grading can also provide nonstandard body-shaped clothing pieces, which can meet market demand in time and improve product competitiveness. On the layout module, there are two methods of automatic layout and man-machine interactive layout in domestic and foreign systems. Compared with traditional methods, the advantages of CAD technology are obvious. The module itself has functions such as selection, translation, flipping, rotation, cutting, and automatic tightening. With the improvement of the requirements for the fit and comfort of clothing and the acceleration of clothing style changes, the establishment of 3D human models and the study of 3D clothing CAD technology have become the most important research direction and research focus of clothing CAD technology.

This paper combines the virtual 3D technology to construct a clothing modular design system, improves the effect of online clothing design, and provides a reference for the subsequent online clothing design.

## 2. Related Work

Literature [4] summarizes the necessity of combining the Internet and personalized clothing customization by analyzing the life cycle of clothing commodities, the situation of unsalable products, and the development status of Internet technology. Literature [5] analyzes the difference between the network and the traditional sales model, points out that the network personalized clothing is a new trend of clothing marketing strategy, and, on this basis, summarizes the effective measures to combine clothing personalized customization and network retail mode. Literature [6] starts from the concept of clothing personalized design and customization and studies and predicts the development direction of clothing style customization from a perceptual perspective. Literature [7] adopts the combination of questionnaire survey and expert interviews, uses SPSS software to scientifically analyze the survey data, summarizes the factors that affect consumers' choice of online custom clothing, and provides effective suggestions for the clothing online customization industry. Literature [8], through the investigation and analysis of the homogenization phenomenon of the clothing market, concluded that the traditional single consumption can no longer meet the needs of consumers and other problems, and the clothing market needs personalized customization to obtain and protect the interests of enterprises and consumers. Literature [9] established a digital and intelligent MTM customization system on the basis of personalized customization process, pattern generation technology, and three-dimensional measurement technology to meet the individual needs of consumers and improve the level of digital and intelligent manufacturing of enterprises. On the basis of the existing research, in order to better meet the personalized customization needs of consumers, the clothing module is used as the customization unit, and the cheongsam style is coded based on the coding principle, and the module coding database is established to create a customized

cheongsam. The basic principle of the module configuration of the process; based on this principle, the efficiency of the process design is verified through practical application to ensure the scientificity and rationality of the design results [10].

Reference [11] divides the design elements into three levels and makes a detailed study of the design elements. The first-level element refers to the shape of the element, such as circle, square, pocket, collar, T-shaped, and X-shaped. The secondary element refers to the quality of the element, such as color number, roughness, smooth wrinkle, tightness, bump, and soft and hard. The tertiary element refers to the quantitative state of the element, such as size, number, number, length, area, and quantity. Literature [12] analyzed several important characteristics in clothing design, including body shape change, clothing modeling, comfort function embodiment, clothing material selection, and decorative pattern design. Literature [13] focused on analyzing the interest of clothing in terms of outer contour, internal structure line, pattern, color, processing technology, etc., such as fabric splicing, color splicing, text pattern design, and internal structure line design; the interesting design is integrated into the interesting design of clothing. Xie Xiu-hong analyzed the main points of clothing design and came to the conclusion: Only by grasping the brand positioning, developing the trend, and integrating the color and regional environment can the clothing products meet the new demands of the clothing market. Reference [14] analyzes the design and development process of clothing from the perspective of creating user experience value. In the experience economy, experience becomes an independent economic provision carried by products and services. The experience itself contains value at the same time, and the user experience value is a new user value, which comes from the user's overall perception and evaluation of the experience provided by the enterprise. Through the user's involvement in the development of clothing products, on the one hand, it can promote two-way communication, establish an effective feedback system, and make the product truly meet the needs of users; on the other hand, users become the cooperative developers of enterprise products, and the participation process also creates experience value [15]. Reference [16] starts from the perspective of bionic design of clothing, studies the method of bionic design of clothing, and discusses the laws of bionic design of clothing. Literature [17] pointed out that clothing bionic design has both entertainment function and obvious educational function. From the research of experts and scholars, in addition to ensuring the practicality of clothing, they should also pay attention to the safety of clothing. On this basis, they must add a certain interest to meet the needs of the market. From the perspective of the details of clothing, the elements of clothing design include silhouette, collar, sleeve, color, pattern, and fabric. The requirements for clothing should start from these design elements and use different combinations to achieve the ideal design

The perceptual engineering system based on information technology is a system that uses an expert system to convert consumers' sensory images into detailed elements of design.

It mainly includes a perceptual database, an image database, a knowledge database, and a design and color database. The methods used include brain waves, eye tracking, expressions, behaviors, and questionnaires [18]. Experts and scholars have conducted extensive research on Kansei Engineering and its applications and have had preliminary applications in many industries. Reference [19] conducted a systematic study on the perceptual design method according to the perceptual characteristics of clothing. It summarizes and analyzes the elements of clothing design, the perceptual characteristics of clothing, the relationship between the two, and the rules of clothing design and builds a knowledge platform for clothing perceptual design. Literature [20] proposed a complete study of expert knowledge acquisition and formal representation, clothing interaction design based on knowledge platform, and the realization of the unification of expert cognition and customer cognition in the process of recommendation interaction. Reference [21] studied the application of Kansei Engineering in clothing. They captured the user's feelings about clothing according to the evaluation of ergonomics and psychology and then defined the design features of clothing through user sensibility and finally combined the consumer's image with the clothing. Feeling translation becomes a design element and is used in clothing design.

### 3. Improvement of Bone Skinning and Optimization of Depth Information

The human body consists of two parts: skin and bones. Polygon static meshes constitute human skin and joint chains with topology structure constitute bones. When the bone node moves, its transformation matrix is mapped onto the skin static mesh, causing the skin to distort. In response to the above phenomenon, scientists have proposed a variety of solutions, the more typical ones are the multielement skinning algorithm and the linear skinning algorithm. Through the pair analysis of the two algorithms, this paper proposes an improved linear skinning algorithm based on it, which uses the QLERP interpolation algorithm to transform the skeleton matrix information. In this paper, the weight value of each vertex is allocated reasonably, and the purpose is to optimize the model. Moreover, this paper smoothes the joints of the limbs to solve the problem of skin depression and make up for the obvious seam phenomenon at the joints of limbs.

First, the barycentric coordinates are briefly introduced. Since the three-dimensional human body and cloth model meshes used in the virtual fitting system are all triangular meshes, and the triangle itself is a two-dimensional object, it is necessary to use the method of barycentric coordinates to convert the two-dimensional coordinates into coordinates associated with the triangular surface but not associated with its 3D coordinate space. The barycentric coordinates here are generalized coordinates, and the purpose is to rearrange and define the vertices of each local model in a linear combination. The barycentric coordinates must satisfy two properties. First, the defined value will not change when imitation transformation occurs. In addition, as long as there is a point

in the defined space that satisfies the functional requirements of linear reconstruction, it is the barycentric coordinates.

At present, great progress has been made in the calculation of the barycentric coordinates by the finite element method and the definition of the barycentric coordinates of any point of the polyhedron by the mean value theorem. The stoke calculation method is shown in

$$x = \int_t \frac{v(t)}{|v(t) - x|} d_{s_x} / \int_t \frac{v(t)}{|v(t) - x|} d_{s_x}. \quad (1)$$

In the formula,  $S_x$  represents a sphere centered on  $x$ , the unit is 1,  $v(t)$  and  $x$  are vectors in any direction, and  $(v(t) - x)/|v(t) - x|$  is the normal vector on  $S_x$ .

$v(t)$  is parameterized, and the formula is shown in

$$v_t = \sum_i \phi_i(t) v_i. \quad (2)$$

In the formula,  $\phi_i(t)$  represents the barycentric coordinates obtained by the original method. The next step is to discretize  $x$ , as shown in

$$w(x, v(t)) = \frac{1}{|v(t) - x|}, \quad (3)$$

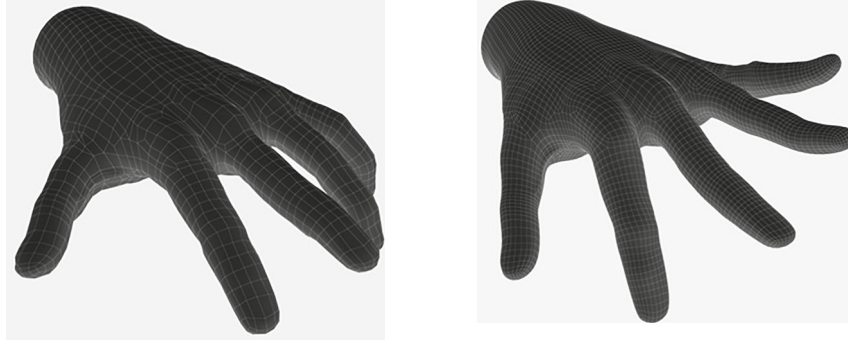
$$w_i = \int_t \frac{\phi_i(t)}{|v(t) - x|} d_t, \quad (4)$$

$$\frac{\int_t w(x, v(t)) v(t) d_T}{\int_t w(x, v(t)) d_T} = \frac{\sum_t w_t v_t}{\sum_t w_t}. \quad (5)$$

In the formula, the distances calculated by  $x$  and  $v(t)$  in the mean calculation are both Euler distances, and Euler distances do not include internal distances. When a concave polygon is encountered, errors will occur, and through the mean calculation, there may be negative coordinates, which is not in line with reality. In this case, it is only necessary to omit the value expressed as a negative coordinate.

The MVC barycentric coordinate method completes the transformation of coordinates from three-dimensional to four-dimensional, making the operation process simpler.

Single joint-driven or mesh-driven motion can make the model appear bulky and inflexible. The skeletal skinning technology combines the two, making the movement of the characters more flexible and realistic. The skinned mesh is used to render the character, and each bone that drives the movement of the human body will affect a part of its corresponding mesh. In particular, the node bones will share the same vertex and weight value. However, due to the hierarchical division of the human body structure, each bone needs to establish a separate mesh, and the skin is used as a mesh on top of the bone. When the bones move, the vertices of the skin mesh will also change accordingly. At this time, there will be obvious cracks at the joints of the limbs, and the skin mesh will appear obvious depression and distortion.



(a) The effect diagram of skin deformation (b) The effect diagram after using the method in this paper

FIGURE 1: Comparison of the effect before and after using the improved linear skinning algorithm.

The three-dimensional space is extended to a four-dimensional space, which is used to deal with the mesh deformation problem in the skinning method. The calculation principle of the double quaternary method is as follows.

$T$  is the translation transformation matrix, where  $i$ ,  $j$ , and  $k$  are the imaginary parts in the four-element vector; then, the calculation process of  $T$  is as follows:

$$T = 1 + \frac{\varepsilon}{2}(t_0i + t_1j + t_2k), \quad (6)$$

where  $r$  is the rigid transformation matrix, where  $a$  is the unit vector and  $\theta$  is the rotation angle, and the formula is shown in

$$R = \cos \frac{\theta}{2} + \sin \left( \frac{\theta}{2} \right) a. \quad (7)$$

The transformation matrix  $Q$  can be obtained by matrix multiplication of formulas (6) and (7). The formula is shown in

$$Q = T \times R. \quad (8)$$

The algorithm selects any point on the model for double quaternary transformation, the original point coordinate is  $P(t_x, t_y, t_z)$ , and the transformed point is set as  $P$ ; then, the formula is shown in

$$P = Q \left[ 1 + \frac{\varepsilon}{2}(t_xi + t_yj + t_zk) \right] \overline{Q^*}. \quad (9)$$

In the formula,  $\overline{Q^*}$  is the conjugate complex of  $Q^*$  and  $Q^*$  is the adjoint matrix of  $Q$ .

The algorithm uses the double quaternary algorithm to successfully convert the points in the three-dimensional space into the points in the four-dimensional space, which makes the vector expression more accurate, effectively solves the problems of skin depression, and runs very fast.

The linear skinning algorithm linearly combines the parameters of each vertex bone in the mesh that affects the motion and sets different weights according to the degree of control. The transformation weights of all joint points

are summed to obtain the motion-deformed position of each skin mesh node. The calculation formula is shown in

$$v' = \sum_{j=1}^n w_j F'(j) F(j)^{-1} v. \quad (10)$$

In the formula,  $v$  represents the coordinates of the skin node under  $T$ -pose in world coordinates, the transformed coordinate value,  $W_j$  represents the weight value of the  $j$ th bone, and  $n$  represents the number of bound bone joints. For bones that are not related to motion, the weight is recorded as 0, and the bone weights of all control nodes satisfy the sum = 1.

The linear skinning algorithm is simple, but due to the low degree of freedom of this method, the constraints of the rotation matrix are ignored in the interpolation calculation. At this point, the model will suffer from dents and volume loss problems due to excessive motion. To solve this problem, this paper proposes an improved linear skinning algorithm. Without changing the linear skin data input, the QLERP interpolation method is used to interpolate multiple joint rotations into one, and the rotation angle is determined by the calculation of the rotation center point. The QLERP rotation interpolation formula is shown in

$$\text{qlerp} = \frac{(1-w)p + wq}{\|(1-w)p + wq\|} \quad (11)$$

In the formula,  $PQ$  represents the quaternion of the connected joints, respectively,  $w$ , and  $(1-w)$  represent the weights corresponding to the joints  $p$ ,  $q$ , respectively.

The comparison of the effect before and after skinning using the method in this paper is shown in Figure 1.

After experimental verification, the method uses the original data to make changes, avoids the reinput of data, greatly improves the running speed, and effectively avoids the skin distortion and sunken problems caused by overfitting.

The commonly used method is the interframe difference method, which performs subtraction between adjacent frames on consecutively sorted images, cuts off the static background, and leaves the moving target. However, traditional area detection methods must use special marking

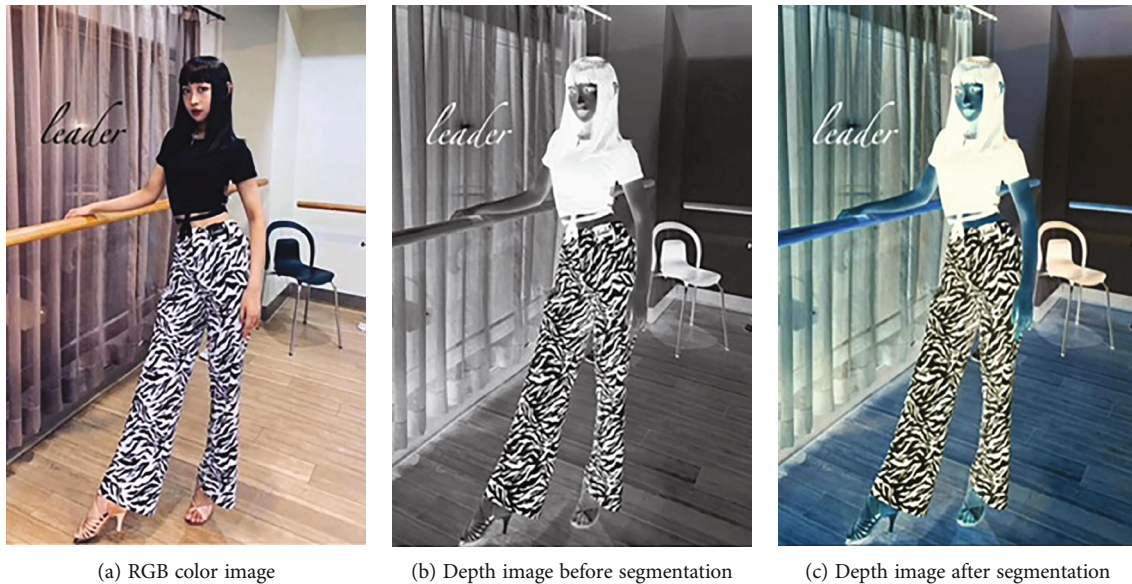


FIGURE 2: Comparison of the effect before and after using the domain segmentation  $R$  value to process the depth information.

methods to capture motion and can only extract a single target, which cannot meet the complexity characteristics of virtual fitting, as shown in

$$\text{body}(x, y) = \begin{cases} 0, & \text{depth}(x, y) \leq bc.z - T, \\ 0, & \text{depth}(x, y) \geq bc.z - T, \\ 255, & \text{otherwise.} \end{cases} \quad (12)$$

The distance between the depth camera and the target object is limited to an integer set range, where the maximum distance is 255 and the minimum is 0, beyond which depth images cannot be recorded. When the value is larger, the distance between the object and the camera is farther, and the smaller the value is, the closer the distance between the object and the camera is. After obtaining the depth image, it firstly divides the obtained  $640 * 480$  depth image into nine equal parts based on the kinect coordinate system. The central area is the target area, and similar pixels are found in the eight neighborhoods of each point to form the human body area pixel set  $R$ . Then, the threshold value  $T$  is set in the  $z$ -axis direction, and the points within the range of the central region  $R$  are binarized to obtain a segmented depth image. The comparison before and after using the domain segmentation  $R$  value to process the depth information is shown in Figure 2:

In this paper, the idea of domain segmentation is used, and a threshold value  $T$  is used to filter the input information according to the depth value. Moreover, the values of pixels in the neighborhood around each point are weighted to obtain pixels, which are combined into a human body region pixel combination  $R$ , and a complexity calculation is performed on them, thereby obtaining a pure target human body.

When using the Kinect device, the depth images acquired with the Kinect will appear noise and black holes due to uneven reflection values at the edges of the model

and occluded areas. If it is directly applied to the virtual fitting system, it will reduce the quality of the depth image and affect the experimental effect. Then, how to reduce these noises outside the background and retain the edge of the target human silhouette is a problem that needs to be solved. This section introduces a variety of filtering methods, and carefully analyzes and compares them. Finally, a high-efficiency bilateral filtering method is selected to remove noise, which ensures the authenticity and real-time performance of virtual fitting.

In order to remove noise, in addition to avoiding the interference of human factors to the greatest extent, scientists have proposed a variety of filtering methods, most of which are improvements on the basic filtering formula. The basic filtering formula is shown in

$$I(x, y) = \frac{1}{w_p} \sum_{i,j \in \Omega} w_{i,j} * n(i, j). \quad (13)$$

In the formula, the set of points contained in the noise image to be processed is represented by  $n(i, j)$ , and the weight value of a point in the pixel space is represented by  $w(i, j)$ . The standard comparison value of all point weight values is denoted by  $w_p$ , and the field set of pixel points is denoted by  $\Omega$ . After formula operation, the most filtered image set  $I(x, y)$  is obtained.

The Gaussian filter method is a linear processor. It processes each pixel point according to the weighted average process and pays attention to eliminating the spatial distance of the pixel point. It is mainly used to remove Gaussian noise. The calculation formula is shown in

$$W_{(i,j)} = \exp\left(-\frac{(i-x)^2 + (j-y)^2}{2\sigma_r^2}\right). \quad (14)$$



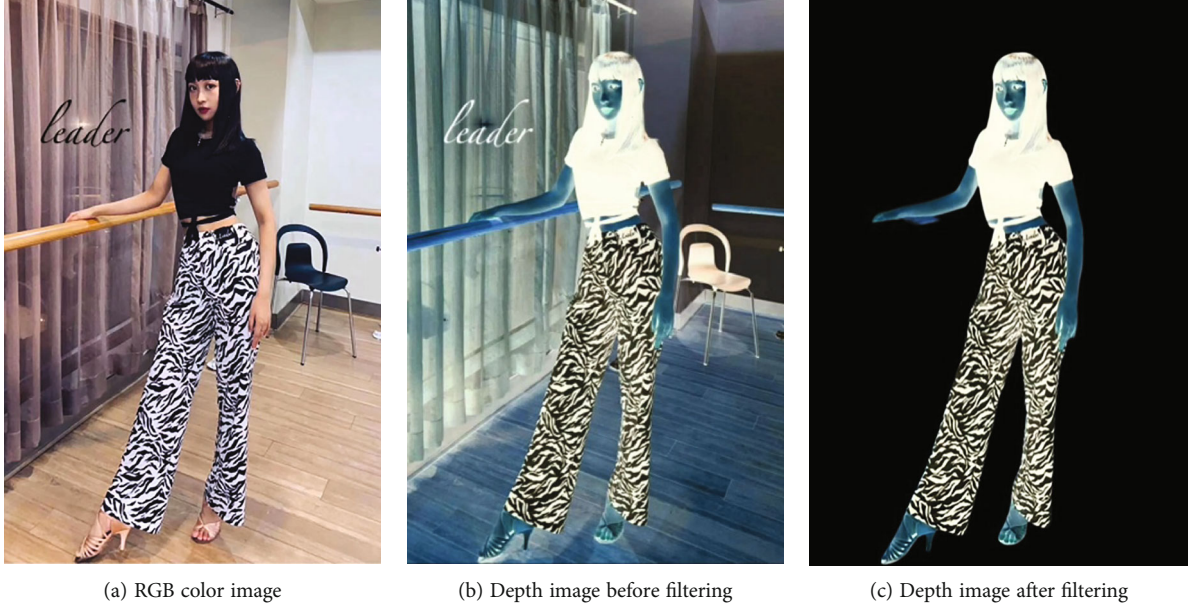


FIGURE 3: Comparison of the effect before and after using bilateral filtering.

In the formula, the standard deviation of the Gaussian function is represented by  $\partial_r$ , which can determine the filtering performance. The weight value of the pixel  $(i, j)$  in the filter is denoted by  $W_{(i,j)}$ . When the weight value is larger, it means that the distance between the pixel points is farther and farther, and the correlation is smaller, and vice versa, the correlation is larger.

The advantage of the Gaussian filtering method is that it can be efficiently calculated by Fourier transform, and the calculation is simple, and the simple foreground and background can be effectively segmented, so as to obtain a relatively complete target human body. The disadvantage is that the edge processing is not smooth, the filtering effect is not obvious, and when changing a viewing angle, the image jumps to a large extent.

Moreover, this paper proposes a bilateral filtering method with two functions, and the so-called bilateral filtering means to ensure the similarity of pixels in the two domains of space and amplitude. In this paper, this method is used to denoise the depth image, and the edge of the image is preserved while filtering. The specific methods are shown in

$$W_r = \exp\left(-\frac{(i-x)^2 + (j-y)^2}{2\partial_r^2}\right), \quad (15)$$

$$W_t = \exp\left(-\frac{|I(i,j) - I(x,y)|}{2\partial_t^2}\right), \quad (16)$$

$$W = W_r \times W_t. \quad (17)$$

In the formula,  $W_r$ ,  $W_t$  represents the spatial domain weight and image gray domain weight, respectively, and  $\partial_r$ ,  $\partial_t$  represents the standard deviation of the amplitude range and the standard deviation of the spatial range, respectively.

The closer  $(x, y)$  and  $(r, t)$  are, the closer the weight  $w$  is to the standard value.

Since bilateral filtering has dual function characteristics, its filtering effect is jointly controlled by two parameters. Since the two parameters are finally multiplied, when the value of a quantity in  $\partial_r, \partial_t$  tends to the minimum value of 0, the phenomenon of edge blurring will occur. Therefore, it is necessary to ensure that the two parameters are greater than 0 at the same time. Since the effect caused by the amplitude change is more obvious than the spatial change, it is best to set  $\partial_r \leq \partial_t$ , that is, the change value  $\partial_t$  of the amplitude is smaller than the change value  $\partial_r$  of the spatial range. The main function of  $\partial_t$  is to increase the constant in the image coverage interval, so as to make the obtained image smoother, and the main function is to preserve the edge information of the image. Therefore, multiplying the two parameters will increase the performance of the two parameters, effectively remove noise, smooth the picture, and protect the edge of the contour. In the experiment of this paper,  $\partial_r = 4$  and  $\partial_t = 4$  are the parameters with the best effect of bilateral filtering. The before and after effect comparison chart is shown in Figure 3.

Using bilateral filtering method to effectively remove noise not only solves the problem that Gaussian filtering cannot preserve image edge information but also ensures the smoothness of the image, greatly improves the recognition rate of depth information, and has strong real-time performance.

#### 4. Clothing Modular Design Based on Virtual 3D Technology

The database can display the types and information of stored fabrics, accessories, etc. for users. Users can choose their favorite fabrics and accessories according to the clothing styles they have determined and use the system's image processing function to display the final clothing effect of

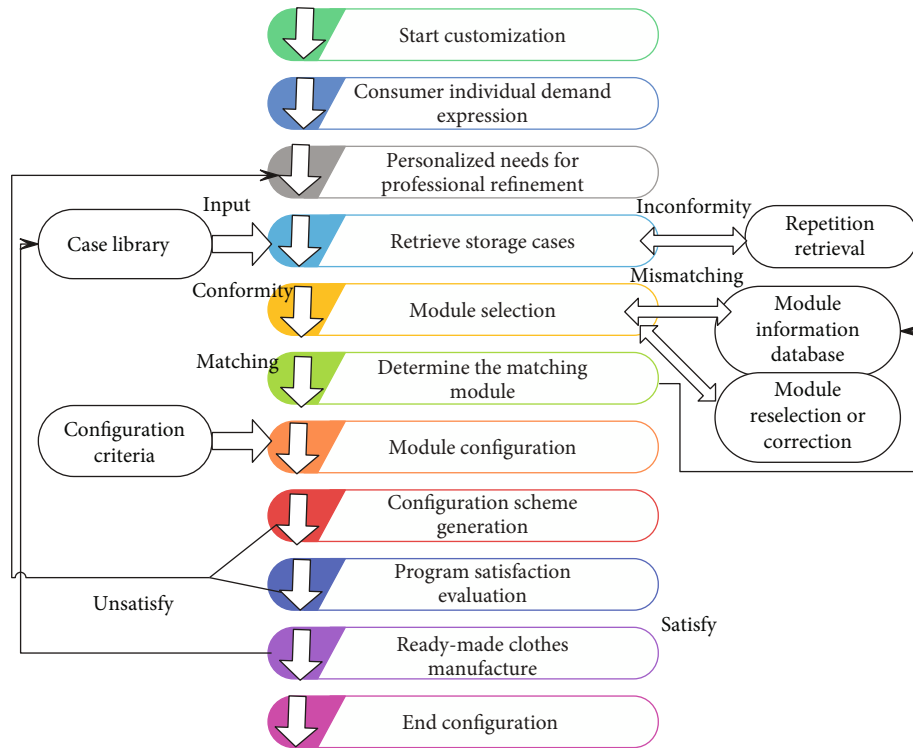


FIGURE 4: Modular customization process.

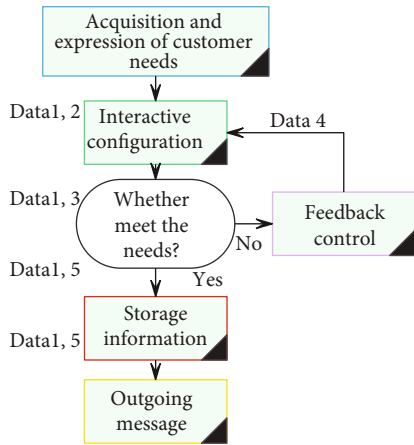


FIGURE 5: Personalized clothing design process.

personalized customized clothing to users in real time. The specific modular customization process is shown in Figure 4.

The personalized clothing design process is shown in Figure 5. The process contains 5 basic data information; data 1 and data 2 constitute the customer’s demand information. Among them, data 1 represents anthropometric data, which provides basic size information for clothing design. The accuracy of anthropometric data determines whether the clothing fits. Data 2 represents the customer’s perceptual demand data, which determines the personalized style of clothing products. Data 3 represents clothing design information, which is interactively transformed from data 2, including clothing styles. However, the design information at this time is still a preliminary result and needs to be fed

TABLE 1: Statistical data of experimental verification of clothing modular design system based on virtual 3D technology.

Number	Fitting effect	Design effect	Number	Fitting effect	Design effect
1	93.32	89.28	24	87.47	86.00
2	87.12	87.42	25	93.34	87.66
3	87.17	88.91	26	89.56	85.20
4	93.48	90.79	27	87.87	89.32
5	88.51	83.47	28	89.43	89.42
6	88.63	88.68	29	92.03	85.58
7	88.43	83.28	30	88.74	85.03
8	87.92	83.45	31	92.10	89.55
9	93.29	91.86	32	89.06	85.51
10	93.94	87.70	33	88.62	91.25
11	91.87	85.88	34	92.79	87.95
12	87.63	91.07	35	90.84	85.87
13	88.82	84.50	36	92.58	90.95
14	88.18	86.00	37	88.98	85.99
15	90.09	89.89	38	92.96	86.16
16	93.77	88.20	39	93.37	84.90
17	91.07	84.00	40	87.62	90.04
18	93.70	88.95	41	91.34	89.91
19	88.79	84.59	42	89.92	88.20
20	91.95	84.77	43	87.07	89.61
21	90.14	88.56	44	87.06	86.63
22	87.52	91.70	45	88.90	86.69
23	89.69	88.15			

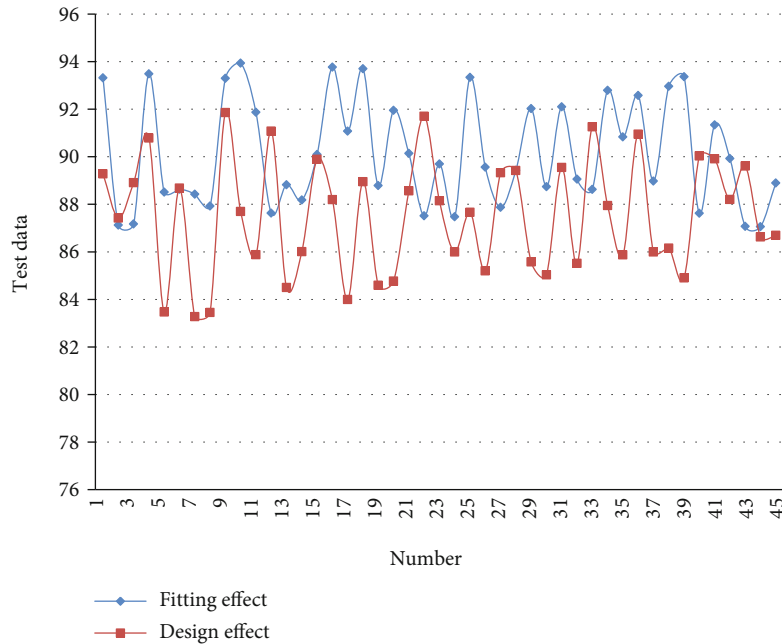


FIGURE 6: Parameter statistics of clothing modular design system based on virtual 3D technology.

back to obtain feedback information, that is, data 4. Data 4 enters the interactive selection stage and interacts again, and this cycle is repeated until a satisfactory configuration of clothing design information is obtained, and these clothing design information forms data 5. Data 5 is used as storage information and output with data 1 to provide data support for the next interaction.

On the basis of the above research, the effect of the clothing modular design system based on virtual 3D technology proposed in this paper is verified, and the online clothing fitting effect and clothing design effect of the system in this paper are counted, and the results shown in Table 1 and Figure 6 are obtained.

From the above research, it can be seen that the clothing modular design system based on virtual 3D technology proposed in this paper basically meets the current online clothing modular design requirements.

## 5. Conclusion

CAD technology leads garment enterprises to develop new products quickly and efficiently. It has the characteristics of sophisticated design, labor saving, time saving and material saving, high efficiency, and low consumption. Garment enterprises need to adapt to the fast-paced and multivariety needs of the international market under the new situation and provide high-quality products to the market at the lowest cost and in the shortest time. The use of advanced computer technology has become the first choice, which can transform and enhance the production structure and productivity of the traditional clothing industry. Nowadays, more and more garment enterprises realize the superiority and importance of using CAD system and gradually use CAD technology as a modern and effective means to replace

traditional design work. This paper combines the virtual 3D technology to construct a clothing modular design system, improves the effect of online clothing design, and provides a reference for the subsequent online clothing design. The simulation test results show that the clothing modular design system based on virtual 3D technology proposed in this paper basically meets the current online clothing modular design requirements.

## Data Availability

The labeled dataset used to support the findings of this study is available from the corresponding author upon request.

## Conflicts of Interest

The authors declare no competing interests.

## Acknowledgments

This work was funded by the Hunan Provincial Social Science Achievement Review Committee Project (XSP21YBC019).

## References

- [1] L. Chen and Y. Lin, "Research on the application of digital printing pattern in custom clothing design," *International Journal of Social Science and Education Research*, vol. 4, no. 6, pp. 144–149, 2021.
- [2] X. J. Zhu, H. Lu, and M. Rättsch, "An interactive clothing design and personalized virtual display system," *Multimedia Tools and Applications*, vol. 77, no. 20, pp. 27163–27179, 2018.
- [3] S. Bogović, Z. Stjepanović, A. Cupar, S. Jevšnik, B. Rogina-Car, and A. Rudolf, "The use of new technologies for the development of protective clothing: comparative analysis of body

- dimensions of static and dynamic postures and its application,” *Autex Research Journal*, vol. 19, no. 4, pp. 301–311, 2019.
- [4] T. J. Tselepis, “When clothing designers become business people: a design centred training methodology for empowerment incubation,” *International Journal of Fashion Design, Technology and Education*, vol. 11, no. 3, pp. 299–309, 2018.
- [5] R. M. Abdullajonovna, S. F. A. Kizi, and M. G. Khayitovna, “Expert analysis of the quality of materials for special clothing,” *JournalNX*, vol. 7, no. 3, pp. 399–402, 2020.
- [6] B. E. Jin and D. C. Shin, “The power of 4th industrial revolution in the fashion industry: what, why, and how has the industry changed?,” *Fashion and Textiles*, vol. 8, no. 1, pp. 1–25, 2021.
- [7] S. Starkey, S. Alotaibi, H. Striebel, J. Tejada, K. Francisco, and N. Rudolph, “Fashion inspiration and technology: virtual reality in an experimental apparel design classroom,” *International Journal of Fashion Design, Technology and Education*, vol. 14, no. 1, pp. 12–20, 2021.
- [8] I. Jasiuk, D. W. Abueidda, C. Kozuch, S. Pang, F. Y. Su, and J. McKittrick, “An overview on additive manufacturing of polymers,” *JOM*, vol. 70, no. 3, pp. 275–283, 2018.
- [9] A. Mackey, R. Wakkary, S. Wensveen, and O. Tomico, “Can I wear this? Blending clothing and digital expression by wearing dynamic fabric,” *International Journal of Design*, vol. 11, no. 3, pp. 51–65, 2017.
- [10] C. Black, C. Freeman, and A. Rawlings, “Problem-based learning: design development of female chef’s jackets,” *International Journal of Fashion Design, Technology and Education*, vol. 11, no. 1, pp. 123–128, 2018.
- [11] Y. Zhao, “Manufacturing personalization models based on industrial big data,” *Journal of Discrete Mathematical Sciences and Cryptography*, vol. 21, no. 6, pp. 1287–1292, 2018.
- [12] S. Gill and C. J. Parker, “Scan posture definition and hip girth measurement: the impact on clothing design and body scanning,” *Ergonomics*, vol. 60, no. 8, pp. 1123–1136, 2017.
- [13] J. Park, K. Park, B. Lee, H. You, and C. Yang, “Classification of upper body shapes among Korean male wheelchair users to improve clothing fit,” *Assistive Technology*, vol. 31, no. 1, pp. 34–43, 2019.
- [14] S. Miell, S. Gill, and D. Vazquez, “Enabling the digital fashion consumer through fit and sizing technology,” *Journal of Global Fashion Marketing*, vol. 9, no. 1, pp. 9–23, 2018.
- [15] S. Y. Kim and J. Ha-Brookshire, “Evolution of the Korean marketplace from 1896 to 1938: a historical investigation of Western clothing stores’ retail and competition strategies,” *Clothing and Textiles Research Journal*, vol. 37, no. 3, pp. 155–170, 2019.
- [16] P. Milošević and S. Bogović, “3D technologies in individualized chest protector modelling,” *Textile & Leather Review*, vol. 1, no. 2, pp. 46–55, 2018.
- [17] T. Maxmudjon, “The figurative expression of the composition of costume,” *Innovative Technologica: Methodical Research Journal*, vol. 2, no. 10, pp. 38–42, 2021.
- [18] J. Louis-Rosenberg and J. Rosenkrantz, “Anti-entrepreneurs using computation to unscale production,” *Architectural Design*, vol. 90, no. 2, pp. 112–119, 2020.
- [19] S. K. Seo and C. Lang, “Psychogenic antecedents and apparel customization: moderating effects of gender,” *Fashion and Textiles*, vol. 6, no. 1, pp. 1–19, 2019.
- [20] Y. M. Kwon, Y. A. Lee, and S. J. Kim, “Case study on 3D printing education in fashion design coursework,” *Fashion and Textiles*, vol. 4, no. 1, pp. 1–20, 2017.
- [21] A. Ihsan, N. Fadillah, and C. Gunawan, “Acehnese traditional clothing recognition based on augmented reality using hybrid tracking method,” *Indonesian Journal of Electrical Engineering and Computer Science*, vol. 20, no. 2, pp. 1030–1036, 2020.

## Research Article

# Big Data Analysis of Water Saving Standard Based on Bibliometrics

Xue Bai <sup>1,2</sup>, Meng Hao <sup>3</sup>, Mengting Hu <sup>1,2</sup> and Liu Yang <sup>3</sup>

<sup>1</sup>China National Institute of Standardization, Beijing 100191, China

<sup>2</sup>Key Laboratory of Energy Efficiency, Water Efficiency and Greenization for State Market Regulation, Beijing 102299, China

<sup>3</sup>College of Geoscience and Surveying Engineering, China University of Mining and Technology (Beijing), Beijing 100083, China

Correspondence should be addressed to Liu Yang; yang\_l@126.com

Received 10 March 2022; Revised 21 March 2022; Accepted 25 March 2022; Published 11 April 2022

Academic Editor: Yanqiong Li

Copyright © 2022 Xue Bai et al. This is an open access article distributed under the Creative Commons Attribution License, which permits unrestricted use, distribution, and reproduction in any medium, provided the original work is properly cited.

At present, water-saving standard is an important technical means to implement national water-saving actions and the strictest water resources management system. In order to analyze the development process and research fields of water-saving standards in China, this paper makes quantitative statistics and qualitative analysis on seven aspects of water-saving standards, such as annual publication, drafting unit, research fields, and progress. The results show that the annual release of water-saving standards generally showed a trend of first rising and then declining, and the release reached its peak in 2017. The contribution of China National Institute of Standardization to the development of water-saving standards is dominant. From the point of view of water department, the water-saving standards in the industrial field are comprehensive. Our finding are helpful to better understand the development process of water-saving standards and provide reference for further improving the water-saving standard system and building a water-saving society.

## 1. Introduction

More people and less water, uneven distribution of water resources in time and space, and prominent contradiction between supply and demand are the basic water conditions in China [1, 2]. Problems such as weak awareness of water conservation, extensive water use, water pollution, and large gap between the utilization efficiency of water resources in China and the international advanced level have aggravated the status quo of water resources shortage [3–5], which has become the bottleneck of ecological civilization construction and sustainable economic and social development.

Water conservation is the fundamental way to solve the problem of water shortage in China [6]. We should realize the importance of water saving from the strategic height of realizing the sustainable development of the Chinese nation and accelerating the construction of ecological civilization; vigorously promote water conservation in agriculture, indus-

try, towns, and other fields; promote water saving in water-deficient areas. The CPC Central Committee and the State Council attached great importance to water conservation and issued a series of laws, regulations, and policy documents on water conservation management. In 2002, the Water Law of the People's Republic of China clearly stipulated "The state shall strictly save water, vigorously promote water conservation measures, popularize new technologies and processes for water conservation, develop water-saving industries, agriculture and services, and establish a water-saving society." This provides legal guarantee for the all-round construction of water-saving society. And a series of water-saving policies, such as "red line of water efficiency control," "combination of total amount control and quota management," and "ten actions of water saving for all the people" were launched. In the "National Water Saving Action Plan," the short-term and long-term goals of improving water use efficiency and controlling water consumption [7] are put forward.

With the proposal of water-saving policy, a number of water-saving standards covering many fields were drafted and released, so as to change the extensive use of water resources, curb unreasonable water demand, greatly improve the efficiency and benefit of water resources utilization, and strongly support the high-quality development of economy and society.

Although the water-saving standards are gradually increasing, few scholars discuss the development process of water-saving standards in China at present. The research mainly focuses on the single water-saving field of industry or irrigation, and there is little application of integration with high-end information technologies such as big data, so the traditional analysis method is not enough to intuitively reflect its evolution process [8]. Therefore, this paper takes the national water-saving standards as an example, adopts the bibliometric methods commonly used in big data analysis at present [9–12], makes visual research on water-saving standards from different angles with the help of CiteSpace software, identifies the emerging hot spots and frontiers in the field of water-saving more scientifically and accurately, summarizes the main subject categories, and makes qualitative and quantitative analysis, so as to better assist researchers to determine the future research direction.

## 2. Research Methods and Data Sources

**2.1. Data Sources.** In this paper, the National Standard Information Network and China National Knowledge Internet (CNKI) are selected as data sources, and the relevant water-saving standards in China are statistically analyzed. When searching in China Academic Journals and Magazines Publishing General Database (CNKI included), words such as “water saving, irrigation, sewage reuse, water fetching” are used as the keywords, and the searching time span is 2002–2021. In order to ensure that the original data is comprehensive, accurate, and highly credible, the database search results are processed by eliminating duplicates and abolishing standard deletion. Finally, 289 existing water-saving-related standards are obtained, and the standard level is the national standard.

**2.2. Research Methods.** This paper mainly uses bibliometric analysis to analyze water-saving standards, so as to describe, evaluate, and predict the development trends of water-saving standards [13, 14]. Common bibliometric analysis software includes CiteSpace, VOSviewer, Bibexcel, and NetDraw (all software is open source and can be used for free). In contrast, CiteSpace integrates the methods of cluster analysis, cooperative network analysis, multidimensional scale analysis, etc., and focuses on detecting and analyzing the development trend of research frontiers, the relationship between research frontiers and their knowledge bases, and the internal relations among different studies [15–17]. Therefore, with the help of CiteSpace 5.8.R2 bibliometrics visual analysis software, this paper makes statistical and visual analysis of water-saving standards from 2002 to 2021, draws a knowledge map [18], and shows the development law of the standard-making field through elements such as node size, network connection, and keywords.

## 3. Status Quo of Water-Saving Standardization

**3.1. Time Series Analysis of the Annual Release of Water-Saving Standards.** Since 2000, in order to adapt to the new situation of water resources and water pollution in China, the state has strengthened the work of water-saving standardization. After more than 20 years of efforts, the formulation of water-saving standards has made great progress.

According to the distribution of the annual publication quantity of water-saving standards by 2021, it can be seen that the annual publication quantity of standards generally showed a trend of first rising and then declining, and the annual release quantity reached its peak in 2017, accounting for 16% of the total release quantity (Figure 1). The concentrated release in 2017 is closely related to the *13th Five-Year Plan for the Construction of Water-saving Society* in which “improving the water-saving standard system” is clearly put forward. We should improve the water quota standards of agriculture, industry, service industry, and urban living industry in each provincial administrative region, speed up the formulation and revision of national water quota standards for industries and services with high water consumption, and implement mandatory water quota standards. Regularly organize and carry out water quota assessment and guide and promote all localities to revise the industry water quota in time; pay close attention to the formulation of water-saving basic management, water-saving evaluation, and other national standards; and improve the water-saving standard system. The standards released in 2017 cover water intake quota, water efficiency of products, water-saving enterprises, reverse osmosis water treatment equipment, sewage treatment, seawater cooling water treatment chemicals, and many other aspects.

### 3.2. Analysis of Water-Saving Standard Drafting Unit

**3.2.1. Cooperation of Water-Saving Standard R&D (Research and Development) Units.** Through the cooccurrence analysis of water-saving standard R&D units, we can identify the core units in this field and the cooperative relationship among them. CiteSpace is used to build the cooperation network of water-saving standard R&D units (Figure 2). The size of nodes in the figure represents the frequency of cooccurrence of core units. The larger the nodes, the more frequently the unit cooperate with other units. The number and thickness of lines represent the intensity and closeness of cooperation between units. The more and thicker of the connections, lead to the stronger the connection between units. It can be seen from the figure that there are 393 nodes and 1411 link lines, with a network density of 0.0183. The number of nodes and link lines is relatively large, and the density is relatively high. Therefore, it can be seen that there are many links between units, and the structure of cooperative networks among units is relatively tight, which indicates that the drafting of each standard needs the cooperation of multiple units. For example, the water intake quota of wool textile products was jointly drafted by China Textile Economic Research Center, Shandong Jining Ruyi Wool Textile Co., Ltd., China National Institute of Standardization, Zhejiang Jiaying Xinlong Dyeing and Finishing Co., Ltd., China Wool Textile Association and

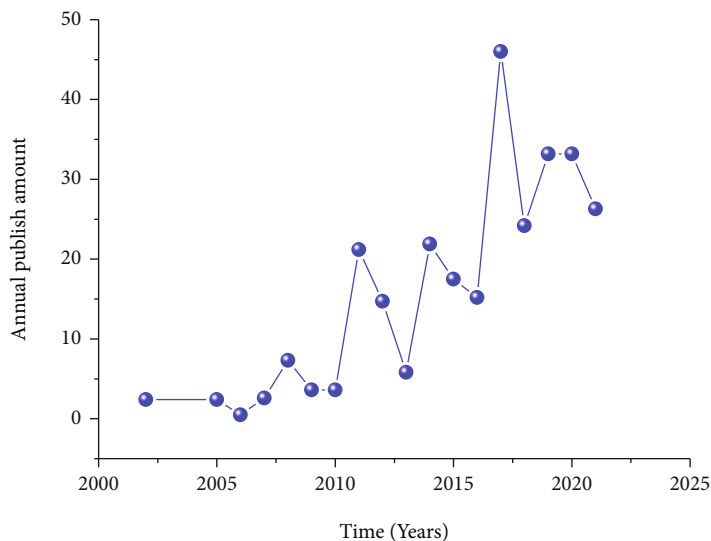


FIGURE 1: Release trend statistics of national water-saving standards (2002-2021).

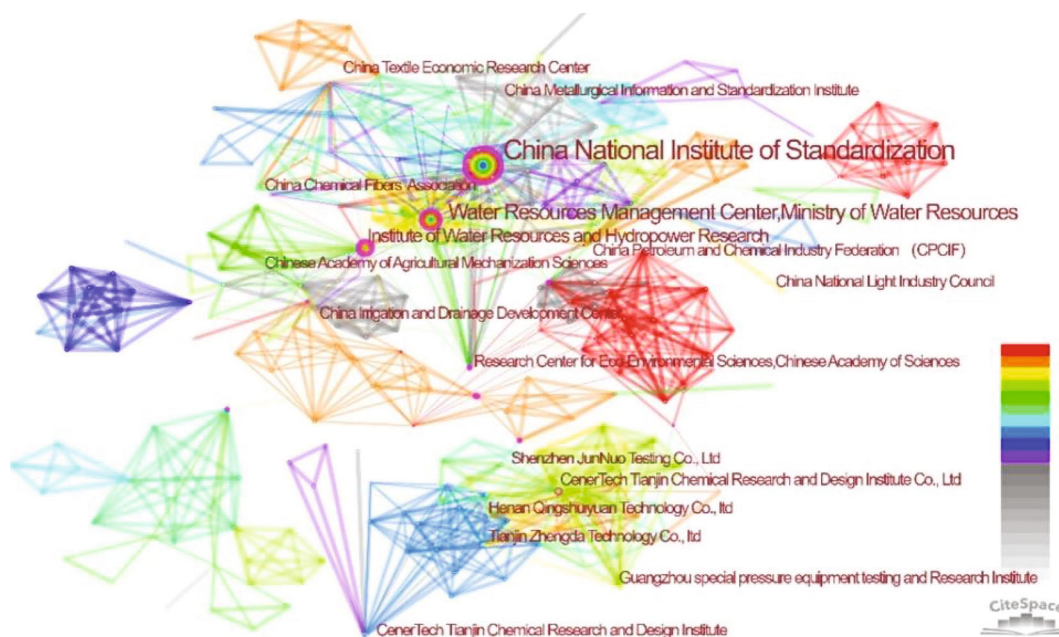


FIGURE 2: Cooperation diagram of national water-saving standard R&D unit.

Water Resources Management Center of Ministry of Water Resources.

In order to show the importance of each R&D unit in the field of water saving more intuitively, the statistics of the units with high frequency of occurrence and large intermediary centrality value (Table 1) show that the cooccurrence frequency ranking of R&D units is not completely consistent with the centrality ranking, mainly because of the different emphasis of cooccurrence frequency and centrality, with cooccurrence frequency focusing on the frequency of occurrence of R&D units and centrality focusing on the “importance” and “core position” of R&D units in the cooccurrence network. Among

them, China National Institute of Standardization has the highest cooccurrence frequency (93) and centrality (0.62), which indicates that it plays a leading role in the development of water-saving standards. The water resources management center of the Ministry of Water Resources (49) ranks second in cooccurrence frequency and only ranks fifth in centrality (0.25). China National Institute of Standardization has the closest cooperation with China Petroleum and Chemical Industry Federation and Water Resources Management Center of Ministry of Water Resources, and most of the standards of water intake quota were drafted jointly with the above two units, respectively.

TABLE 1: Contribution frequency and centrality of water-saving standard R&amp;D unit.

No.	Keyword	Frequency	Centrality
1	China National Institute of Standardization	93	0.50
2	China Institute of Water Resources and Hydropower Research	29	0.41
3	Research Center for Eco-Environmental Sciences, CAS	6	0.31
4	MCC Capital Engineering & Research Incorporation Limited	4	0.28
5	Water Resources Management Center of Ministry of Water Resources	49	0.25
6	Beijing University of Civil Engineering and Architecture	3	0.23
7	Shanghai Light Industry Research Institute Co., Ltd.	3	0.20
8	North China Municipal Engineering Design & Research Institute Co., Ltd.	3	0.20

3.2.2. *Water-Saving Standard R&D Contribution Index.* In order to quantify the contribution degree of the drafting unit in developing a standard, first, according to the ranking of the drafting unit of the standard, it is qualitatively divided into leading (ranking no. 1 in the drafting unit of the standard), presiding (ranking no. 2 and no. 3 in the drafting unit of the standard) and participating (ranking no. 4 and later in the drafting unit of the standard). Then, according to the degree of contribution, the top five in the drafting unit are assigned, respectively, and those ranked no. 6 and later are classified into one category for weight assignment (Table 2).

The contribution index of each drafting unit in the development of water-saving standards can be calculated according to the number of participants in different orders and the corresponding index weights. The formula is as follows:

$$CI = \sum_{t=1}^k \lambda_t N_t \quad (t = 1, 2, 3 \dots, 6), \quad (1)$$

where CI represents the contribution index of each drafting unit,  $t$  represents the ranking of drafting units,  $\lambda_t$  is the index weight, and  $N_t$  represents the number of drafting standards.

The top 15 contributing units are listed in the following table (Table 3), and these units have made important contributions to the formulation of water-saving standards. China National Institute of Standardization ranked first with a contribution index of 84.4, with a total of 134 national standards developed, including 30 leading researches, 60 presiding researches, and 44 participating researches. The contribution index was much higher than that of the second-ranked Water Resources Management Center of the Ministry of Water Resources (19.9).

3.3. *Research Field and Progress Analysis of Water-Saving Standards.* Keywords of water-saving standard are the main induction and generalization of standard content. By clustering and cooccurrence analysis of keywords, we can understand the focus of standard development, so as to better analyze the research field and development trend of water-saving standard.

3.3.1. *Research Field of Water-Saving Standards.* The keywords of 289 water-saving standards are visually analyzed, and the keywords cluster map is obtained. As can be seen from Figure 3, water-saving standards are mainly divided into six cat-

TABLE 2: Ranking weight value of drafting unit.

Unit ranking	1	2	3	4	5	6
Weight	1	0.8	0.6	0.4	0.2	0.1

egories: water intake quota, water treatment agent, urban area, reclaimed water, limited value, and cooling water, which reflects the research field of water-saving standards in China. Among them, the overlapping patches are reclaimed water and urban areas, which indicates that reclaimed water is mainly used in cities. The largest patch is the water intake quota, which indicates that the water-saving standard of water intake quota series accounts for a large proportion, so this paper takes the related research of water intake quota as an example to analyze.

With the vigorous development of China's various construction undertakings and the increasing improvement of people's living standards, the exploitation and utilization of water resources in China have increased rapidly, and the problems of lack of water resources and water environmental pollution have become increasingly prominent [19]. The status quo of low efficiency, high growth, and heavy pollution of industrial water use in China is extremely incompatible with China's water resources conditions. Strengthening industrial water conservation and changing the backward situation of China's industrial water management is a very important and extremely urgent task, and it is also an objective requirement for China's deep-rooted reform of water-saving management under the conditions of market economy. In this context, the formulation of water intake quota standards for industrial enterprises has been carried out.

The number of water intake quota standards released was 61, accounting for 21.11% of the total number of standards, including a *General Principle for the Preparation of Water Intake Quotas for Industrial Enterprises* (hereinafter referred to as the "General Rules for Water Intake Quotas") and 60 water intake quota standards. The water intake quota for industrial enterprise products is the basic standard in China's industrial water use and water-saving standard system, one of the main indicators of the national assessment of the utilization efficiency of water resources in regions, industries and enterprises and the evaluation of water-saving levels, the control indicators for the purchase, management and distribution of national water resources supply and enterprise water resources



TABLE 3: Contribution index of water-saving standard R&amp;D.

Ranking	Unit name	Contribution index
1	China National Institute of Standardization	84.4
2	Water Resources Management Center, Ministry of Water Resources	19.9
3	China Petroleum and Chemical Industry Federation	15.5
4	China Institute of Water Resources and Hydropower Research	15
5	Cener Tech Tianjin Chemical Research & Design Institute	11.3
6	China Irrigation and Drainage Development Center	10
7	He'nan Qingshuiyuan Technology Co., Ltd.	9.2
8	Guangzhou Special Pressure Equipment testing and Research Institute	7.4
9	Center Tech Tianjin Chemical Research and Design Institute Co, Ltd.	6.6
10	Institute of Seawater Desalination and Multipurpose Utilization, SOA (Tianjin)	6.6
11	Nanjing University	6.1
12	Institute of Environmental Protection of Light Industry	6
13	China Metallurgical Information and Standardization Institute	6
14	The Institute of Seawater Desalination and Multipurpose Utilization, MNR (Tianjin)	6
15	Jomoo Kitchen & Bathroom Co., Ltd	5.2

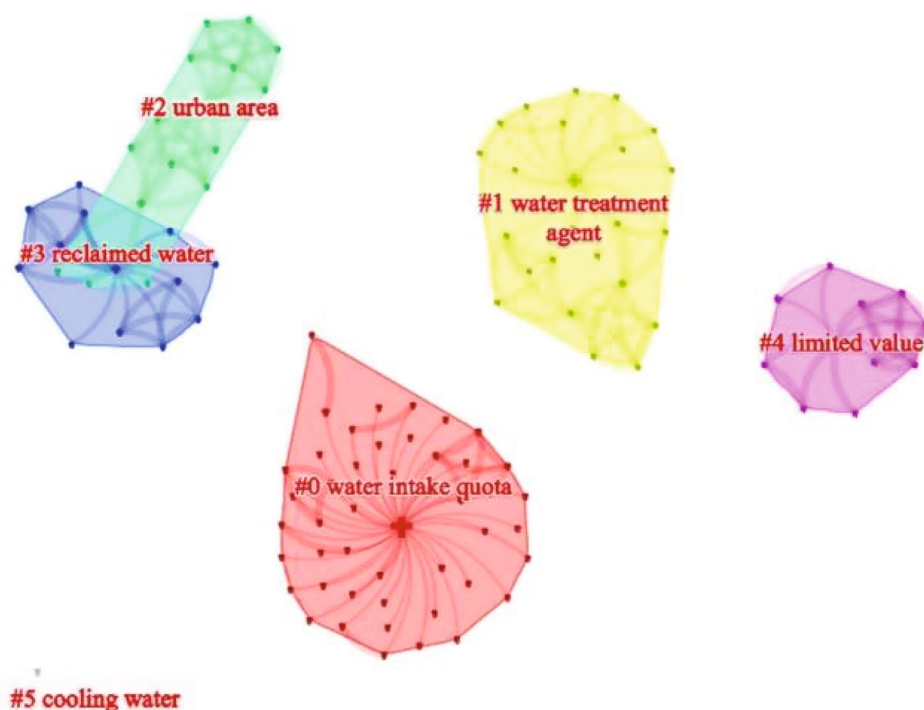


FIGURE 3: Main research field of water-saving standards.

plans, the indicators for evaluating the rational use of water and water conservation technologies of enterprises, and the basis for industrial enterprises to formulate production plans and water supply plans. The formulation of this standard will guide and standardize the revision of industrial water intake quotas, which is conducive to the formulation of a series of national standards for water intake quotas in related industrial industries and is conducive to strengthening the management of industrial water conservation. It was first released on August

29, 2002, implemented on January 1, 2003, and revised to be released again on June 16, 2011. The 60 national water intake quota standards are mainly formulated for high water use industries such as electric power, iron and steel, textile, paper, petroleum and chemical industry, food fermentation, nonferrous metals, coal, and medicine (Figure 4), which have played an important role in the country's water resources demonstration, planned water use and water withdrawal permit system, and achieved huge water-saving benefits.

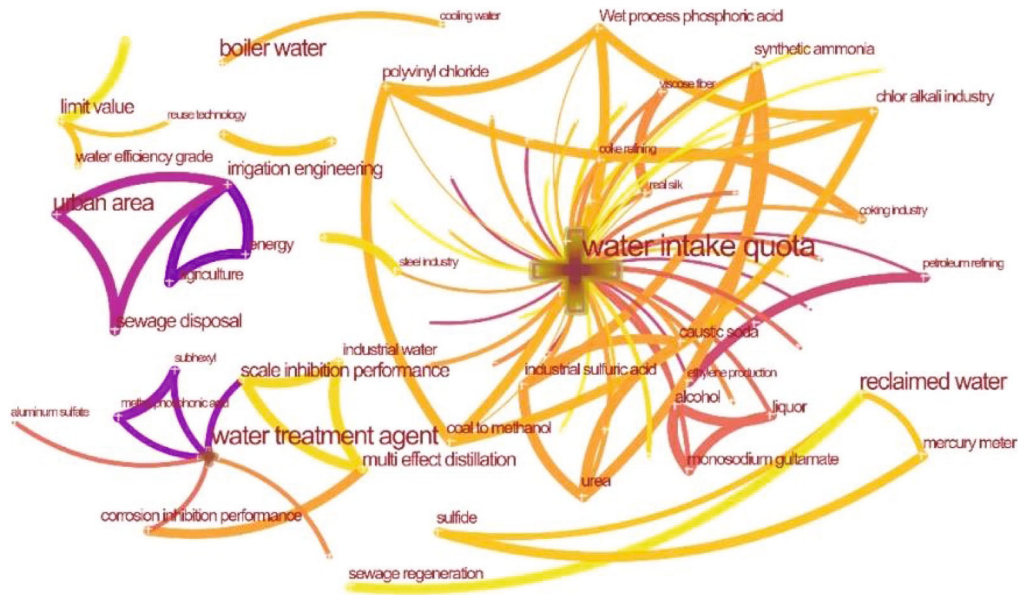


FIGURE 4: Relationship diagram of water conservation standard.

Top 20 keywords with the strongest citation bursts

Keywords	Year	Strength	Begin	End	2002-2021
City	2002	0.69	2002	2002	-----
Irrigation project	2002	1.33	2007	2012	-----
Agriculture	2002	0.88	2007	2012	-----
Water resources	2002	0.88	2007	2012	-----
Treatment agent	2002	1.33	2008	2008	-----
Sewage disposal	2002	1.1	2010	2011	-----
Iron and steel enterprises	2002	1.25	2011	2011	-----
Water intake quota	2002	1.77	2012	2012	-----
Technical guideline	2002	0.75	2012	2012	-----
Water treatment agent	2002	3.09	2014	2016	-----
Sea water desalination	2002	1.13	2014	2016	-----
Drip irrigation pipe	2002	1.15	2017	2017	-----
Steel industry	2002	0.91	2017	2017	-----
Reporting guide	2002	0.79	2017	2019	-----
Boiler water	2002	1.27	2018	2018	-----
Regenerated water	2002	1.88	2019	2021	-----
Management norm	2002	1.17	2019	2021	-----
Reuse technology	2002	1.05	2019	2019	-----
limit vaue	2002	0.82	2019	2019	-----
Scale inhibition performance	2002	0.78	2019	2021	-----

FIGURE 5: Water-saving standard keyword burst diagram.

3.3.2. *Research Progress on Water-Saving Standards.* The emergence of water-saving standard keywords indicates that the frequency of use of keywords in a short period of time has increased significantly, and the frontier of the research field can be judged according to the word frequency change

of the emerging words. Through the sudden detection of keywords from 2002 to 2021, obtained a year ranking graph containing 20 keywords with strong bursts, in order to further understand the standard setting fields in different periods, according to the keyword start and end time shown

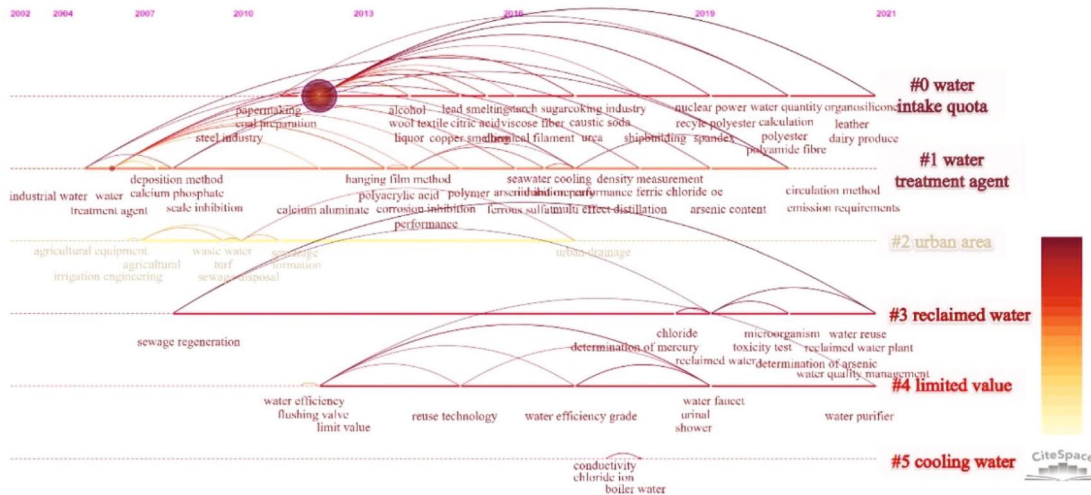


FIGURE 6: Timeline diagram of the water-saving standard research.

in Figure 5 and the relationship between each other, the frontier research progress of water-saving standard formulation can be divided into four stages. The first phase of the burst time is 2002, the prominence is “city,” indicating that water-saving measures were first implemented in the city, and the second phase is 2007-2012, mainly for the development of water-saving standards for industry and agriculture, of which “agriculture” and “irrigation project” have the longest emergence time, and water conservation of agricultural irrigation has been committed to from 2007 to 2012 [20–22]. In addition, there is the release of technical guidelines, which mainly include terms, definitions, and technical basis, which provide reference for the drafting and compilation of relevant series of water-saving standards. The third phase is 2014-2019, in which the research on desalination was joined [23]. The fourth phase is 2019-2021, which focused on water conservation control from the aspects of water recycling and the use of reclaimed water [24, 25].

The timeline chart of water-saving standard keywords (Figure 6) can reflect the evolution of water-saving standard research over time, and the future development trend can be seen from the content of standard development in the past two years. For example, most of the standards in 2019 are focused on product water efficiency, including urinals and dishwashers, and this series of standards provides a standard basis for the establishment and implementation of water efficiency labeling of water products in China.

### 3.4. Analysis of the Attribution of Water-Saving Standards

**3.4.1. Field of Attribution of Water-Saving Standards.** In the national water-saving standards released in 2002-2021, there were a total of 119 water-saving standards in the industrial field, accounting for 41.18%, ranked first in various fields, and the standards for industrial water-saving have been relatively comprehensive, respectively, the national standards for water intake quotas in 60 high-water-using industries such as thermal power generation, steel joint enterprises, petroleum refining, textiles, papermaking, nonferrous metals, and food

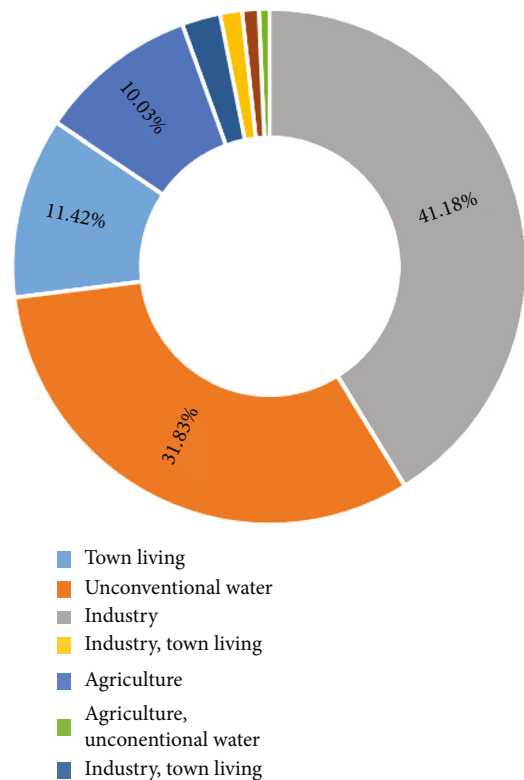


FIGURE 7: Distribution map of water-saving standards by fields.

fermented paper have been formulated; the number of unconventional water-related water-saving standards is 92, accounting for 31.83%, ranking second in various fields; the water-saving standards in the field of urban life is 33, accounting for 11.42%, ranking third in all fields. The specific situation is as shown in Figure 7. The category of water-saving standards is a more intuitive display of the research areas of water-saving standards.

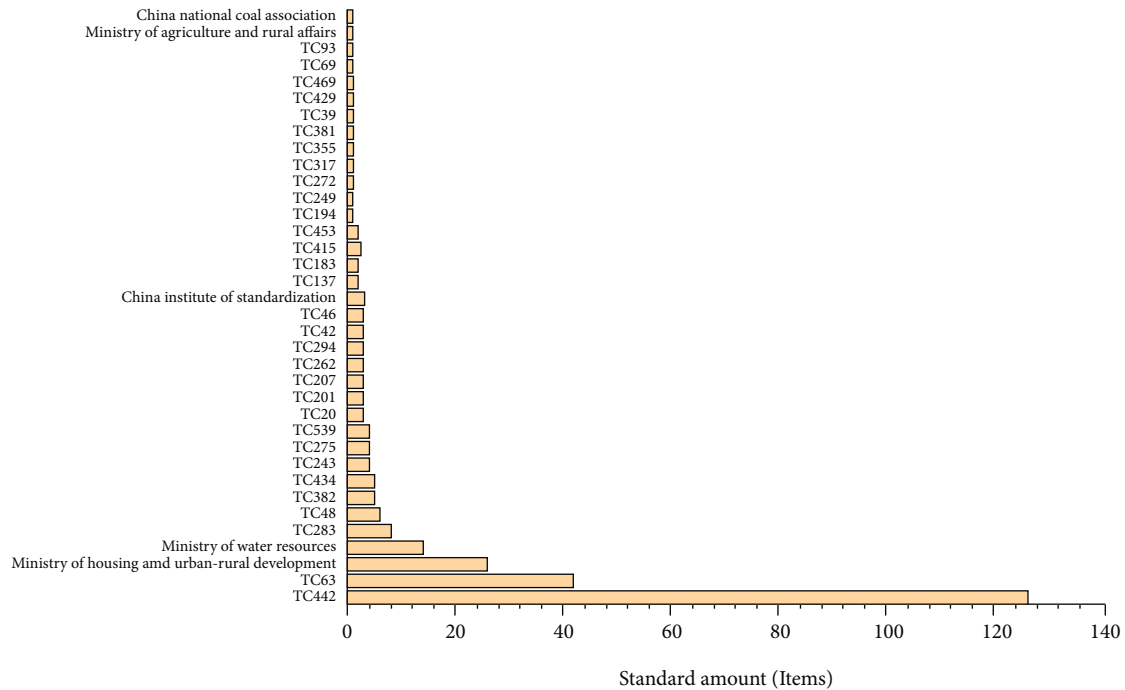


FIGURE 8: Distribution map of water-saving standard focal units.

**3.4.2. Water-Saving Standard Focal Units.** The largest number of focal units is the National Water-saving Standardization Technical Committee (SAT/TC 442), which proposes a series of standards such as water intake quotas and water efficiency evaluation of water-using units, which provides a technical basis for the formulation and implementation of policies such as water efficiency of water-saving enterprises and key industrial enterprises; followed by the National Chemical Standardization Technical Committee (SAC/TC63), which is responsible for the formulation of a series of standards for water treatment agents and reclaimed water quality measurement, a total of 31 items, accounting for about 74% of the total, which are applied in the field of unconventional water; The Ministry of Housing and Urban-Rural Development proposed standards about the main urban sewage recycling and building reclaimed water design, the latter clearly stipulates that when all kinds of buildings and residential buildings are constructed, their overall planning should include the comprehensive utilization of sewage, wastewater, rainwater resources, and the construction of reclaimed water facilities; the Ministry of Water Resources ranks fourth, and the scope of the standards proposed by it is mainly water-saving equipment, water-saving technology, evaluation, water quota, and basic common standards, although the number is relatively small, but it plays an important role. For example, the basic common standard is widely used in the preparation and revision of water-saving standards and water-saving work, which is the basis for other water-saving standards (Figure 8).

## 4. Conclusions

Through the analysis of the water-saving standard development units in the past 20 years, it is found that the relevant water-saving standards are mainly formulated by the China

Institute of Standardization, and its development standards mainly include basic common standards such as industrial water-saving terminology, water-use statistics, water balance testing, and general rules for the compilation of water intake quotas, as well as specific standards such as water intake quotas and water-saving enterprises in various industries. The overall trend of first rising and then falling shows that with the gradual improvement of water-saving awareness, the gap in China's water-saving standards has been significantly improved. The formulation of water-saving standards has a great impact on China's industrial, agricultural, and domestic water sectors, in order to adapt to the development of China's modernization, we should improve the water-saving standard system as soon as possible.

## Data Availability

All data can be obtained in current manuscript through contact corresponding authors Liu Yang.

## Conflicts of Interest

The authors declare that they have no conflicts of interest.

## Authors' Contributions

Xue Bai and Meng Hao contributed equally to this work.

## References

- [1] H. Mengting, B. Xue, and C. Rong, "Status quo of standardization of water saving in China, problems and suggestions," *Standards Science*, vol. 1, pp. 6–9, 2020.
- [2] Z. Liping, X. Jun, and H. Zhifang, "Analysis on water resources status and water resources security in China," *Resources and*

- Environment in the Yangtze River Basin*, vol. 18, no. 2, pp. 116–120, 2009.
- [3] M. Jing, C. Tao, S. Bifeng, and W. Dangxian, “Comparison of water resources utilization at home and abroad and its development trend,” *Advances in Water Resources and Hydropower Science and Technology*, vol. 27, no. 1, 2007.
- [4] H. Cheng, Y. Hu, and J. Zhao, “Meeting China’s water shortage crisis: current practices and challenges,” *Environmental Science & Technology*, vol. 43, no. 2, pp. 240–244, 2009.
- [5] X. Chen, F. Li, X. Li, Y. Hu, and P. Hu, “Evaluating and mapping water supply and demand for sustainable urban ecosystem management in Shenzhen, China,” *Journal of Cleaner Production*, vol. 251, article 119754, 2019.
- [6] T. Haiou, L. Hongxiao, and L. Huamin, “Principles of urban water-saving planning and evaluation method of water-saving effect,” *Journal of Shandong Agricultural University: Natural Science Edition*, vol. 33, no. 3, pp. 356–359, 2002.
- [7] M. Pingsen, L. Yanjiao, M. Changshu, G. Shixiang, and Y. Shude, “Allocation of water resources in Yunnan province based on total water consumption and efficiency control,” *Advances in Water Resources and Hydropower Science and Technology*, vol. 1, 2015.
- [8] X. Haozhen, W. Lei, H. Weihua, L. Qunying, and H. Tianming, “Evolution path and development frontier analysis of ecological and environmental problems of cite space-based hydropower station,” *Hydropower and Energy Science*, vol. 39, no. 8, pp. 71–75, 2021.
- [9] X. Li, E. Ma, and H. Qu, “Knowledge mapping of hospitality research – a visual analysis using CiteSpace,” *International Journal of Hospitality Management*, vol. 60, pp. 77–93, 2017.
- [10] C. Chaomei, H. Zhigang, L. Shengbo, and H. Tseng, “Emerging trends in regenerative medicine: a scientometric analysis in CiteSpace,” *Expert Opinion on Biological Therapy*, vol. 12, no. 5, pp. 593–608, 2012.
- [11] X. Li and H. Li, “A visual analysis of research on information security risk by using CiteSpace,” *IEEE Access*, vol. 6, pp. 63243–63257, 2018.
- [12] S. Liu, Y. P. Sun, X. L. Gao, and Y. Sui, “Knowledge domain and emerging trends in Alzheimer’s disease: a scientometric review based on cite space analysis,” *Neural Regeneration Research*, vol. 14, no. 9, pp. 1643–1650, 2019.
- [13] I. Zupic and T. Cater, “Bibliometric methods in management and organization,” *Organizational Research Methods*, vol. 18, no. 3, pp. 429–472, 2015.
- [14] L. Yang, Q. Wang, X. Bai, J. Deng, and Y. Hu, “Mapping of trace elements in coal and ash research based on a bibliometric analysis method spanning 1971–2017,” *Minerals*, vol. 8, no. 3, p. 89, 2018.
- [15] C. Chen, “CiteSpace II: detecting and visualizing emerging trends and transient patterns in scientific literature,” *Journal of the American Society for Information Science and Technology*, vol. 57, no. 3, pp. 359–377, 2006.
- [16] Q. Xiaonan, L. Xiaoli, and W. Chunyou, “Knowledge graph of domestic ecological security research—econometric analysis based on Citespace,” *Chinese Journal of Ecology*, vol. 34, no. 13, pp. 3693–3703, 2014.
- [17] X. Ding and Z. Yang, “Knowledge mapping of platform research: a visual analysis using VOSviewer and CiteSpace,” *Electronic Commerce Research*, vol. 4, 2020.
- [18] C. Yue, L. Zeyuan, C. Jin, and H. Jianhua, “Development process of scientific knowledge graph,” *Studies in Science of Science*, vol. 26, no. 3, pp. 449–460, 2008.
- [19] L. Keling and Y. Liu, “Characteristics of ecological footprint change of water resources based on energy theory: a case study of Beijing,” *Soil and Water Conservation Research*, vol. 28, no. 3, pp. 406–414, 2021.
- [20] B. Xue, Z. Chunyan, L. Yongpan, and S. Jing, “Status quo and suggestions of industrial water-saving standardization in China,” *China Standardization*, vol. 10, pp. 75–79, 2012.
- [21] X. P. Deng, S. Lun, H. Zhang, and N. C. Turner, “Improving agricultural water use efficiency in arid and semiarid areas of China,” *Agricultural Water Management*, vol. 80, no. 1–3, pp. 23–40, 2006.
- [22] L. Bo, Y. Liu, and X. Di, “Theory and method of estimating the water-saving potential of agricultural irrigation in irrigation area,” *Transactions of the Chinese Society of Agricultural Engineering*, vol. 27, no. 1, pp. 10–14, 2011.
- [23] S. Yongchao, X. Lixin, G. Tingting, and Z. Xiaokai, “Reverse osmosis seawater desalination pretreatment process,” *Chemical Industry and Engineering Progress*, vol. 35, no. 11, pp. 3658–3662, 2016.
- [24] H. Yaqi and W. Wenyong, “Review and development strategy of irrigation with unconventional water resources in China,” *Engineering Science*, vol. 20, no. 5, pp. 69–76, 2018.
- [25] C. Bingjian, G. Feng, H. Chao, L. Zhongyang, F. Xiangyang, and C. Erping, “Status quo and research progress of agricultural utilization of unconventional water resources,” *Journal of Irrigation and Drainage*, vol. 38, no. 7, pp. 60–68, 2019.

## Research Article

# Indoor Smart Design Algorithm Based on Smart Home Sensor

Ruili Zheng 

*School of Art & Design Pingdingshan University, Pingdingshan, Henan 467000, China*

Correspondence should be addressed to Ruili Zheng; 3138@pdsu.edu.cn

Received 18 January 2022; Revised 24 February 2022; Accepted 3 March 2022; Published 11 April 2022

Academic Editor: Wen Zeng

Copyright © 2022 Ruili Zheng. This is an open access article distributed under the Creative Commons Attribution License, which permits unrestricted use, distribution, and reproduction in any medium, provided the original work is properly cited.

Modern home furnishings have solved the most basic housing problems, but how to make homes more informatized and modern has become the focus of people's growing concern. With the rapid development of information technology, improving the intelligent level of family life and modern lifestyle is bound to be the trend of future development. This paper studies a smart home control system based on wireless sensor network positioning, which can perceive the home environment through the sensor module, and the control module can automatically control common electrical appliances to achieve real-time data monitoring and alarm functions. Specifically, it includes a positioning module, a communication module, and a server: the positioning module is connected to the server through the communication module, and the positioning module is used to obtain user location information in real time and report user location information to the server at intervals. The server receives the user reported at intervals through the communication module. Location information and remotely control smart home devices based on user location information. The research results show that the method proposed in this paper can separately monitor each part of the home and send it to the home appliance control module through the server to control the home appliance, optimize the living environment, and realize the remote control and monitoring of the smart home.

## 1. Introduction

In related technologies, the startup or shutdown of smart home devices requires the user to actively operate on the mobile phone. No matter this operation is to open and close the smart home device in real time or at a fixed time, the mobile phone will send a command to the server through the network after it is triggered. And then, the smart home device can be turned on or off remotely by the server through the network. This control method that completely relies on the user's active operation to remotely control smart home devices is too rigid and inflexible. Once the user forgets to operate and triggers the mobile phone, it will bring a lot of inconveniences, the experience of smart home devices [1–8].

The design of smart home (as shown in Figure 1) should be implemented in accordance with the following principles: first, convenience and practicality. The purpose of designing smart homes is to provide people with a more comfortable and safe working and living environment. The key to analyzing smart home products is to take practical applications as

the core, abandon the design that only has display functions, and integrate humanity at the same time. The second is the principle of reliability. The intelligent building includes various intelligent subsystems in the architecture. To realize 7 × 24 uninterrupted operation of these subsystems, attention must be paid to their safety, reliability, and fault tolerance. For each subsystem, use power system backup and other means to ensure the normal operation of the system in order to cope with a variety of complex environmental changes. The third is standardization. The design of traditional smart home solutions should be implemented in accordance with national and regional standards to ensure the scalability and redundancy of system applications. The fourth is convenience. The simplicity of the wiring installation will affect the installation cost. The design of a more convenient installation system can better reduce the installation and maintenance costs. You can choose to arrange it during the broadband wiring process. Smart homes can control various devices with the help of Internet of Things technology. As a brand-new industry, it is still in the groping and development stage and has not yet formed a market consumption

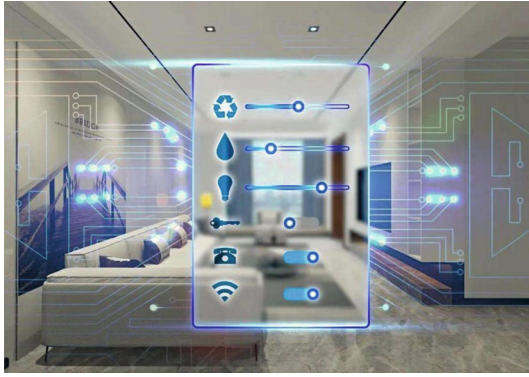


FIGURE 1: Smart home.

concept. However, with the gradual popularization of the smart home market, it will be more difficult to recultivation of consumer habits. The safety precaution system in the smart home is to be fully prepared to prevent dangerous situations and keep family members in a safe state where there is no infringement and no accidents [9–14].

As early as January 1984, technology companies applied integrated and informatized equipment buildings to an old 38-story financial building in the United States at the time and systematically systemized the elevators, lighting, and air conditioning equipment in the building, detection and control, and use voice communication in information provision. This is the first “intelligent building” recognized in the world. In the early 1980s, with the introduction of a large number of household appliances using emerging electronic technologies, the concept of home electronics (HE) began to appear. Bill Gates’ Microsoft has spent a huge amount of money to build a technologically advanced mansion. The electrical equipment in the house is connected through the network, and there is a dedicated server in the control background, and the home system is controlled and managed by the computer. In May 1998, Singapore launched an intelligent home system. Nearly 30 residential communities have adopted the system. Residents have also installed the system in the United States. The system mainly includes security alarms, monitoring functions, electrical control functions, and message functions. In 2016, Google released a smart home device called GoogleHome [15–23]. To this end, many modern technologies have been concentrated, such as, sensor technology, computer technology, and electronic communication technology.

In August 2014, Samsung acquired SmartThings, an open platform for smart homes, and focused on promoting its plans for the “Internet of Things.” SmartThings technology allows users of hardware devices such as Samsung smart phones and smart watches to easily control smart home devices by manipulating these daily devices. Therefore, SmartThings has been regarded as the top priority of Samsung’s smart home and “Internet of Things” plans. Samsung is also constantly expanding the company’s other equipment to adapt, so that more mobile terminals can be connected to this platform and actively cooperate with third-party manufacturers to make this platform cover household energy,

safety management, medical care, health, and other fields. In terms of function, the smart home forms the only management center, and the control center can be mobile phones of various brands or smart bracelets [24–27].

Apple held the Worldwide Developers Conference (WWDC) in 2014, where Homekit was grandly released. Apple said that the platform is a joint Siri function and allows users to control their homes through devices such as Apple phones and tablets. Apple is preparing to carry out Apple (MFi) certification for third-party products to improve the portability and versatility of the products. On June 3, 2015, Apple’s first public release of Homekit smart home products came from 5 manufacturers. These products can control lights, temperature, air conditioning, TVs, and other household appliances through iPhone, iPad, or iPod-Touch. As a very practical smart home platform, Homekit smart home platform is loved by many consumers and brings users a very good smart home control experience. On June 13, 2016, the Apple Developer Conference was held in San Francisco. The meeting announced that builders began to support Homekit. The Homekit platform will allow users to control all mobile terminals through OS devices and can convert iPhones or iPads into command systems for thermostats, lights, garage doors or door locks, and many other smart home devices.

In 2009, Haier cooperated with China Telecom to launch U.S. home, the future development direction of home furnishing is considered to be the convenient, innovative, comfortable, and high-quality living environment and lifestyle advocated by Haier Group. It is not only a global R&D base for manufacturing intelligent products but also the world’s leading smart home appliances and household products are also developed and manufactured by them, and it is also a supplier and developer that provides a full set of intelligent solutions and products. Let the world and home become the life concept of human beings simultaneously, and allow people to experience and enjoy the high-quality life around the world and give users more opportunities to use personalized Haier products. Haier Group has won many patents and its own proprietary science and technology thanks to Haier Group’s own U.S. company, home development team, and the world’s top laboratories, among which U. The home development team is composed of a number of highly qualified and capable Ph.Ds and professional intelligent developers and has proposed solutions for smart homes and smart supermarkets. Haier’s high-quality and innovative smart lifestyle is the trend of the future family. Haier Group has a legal SP service qualification and a full line of smart appliances and positions the SMS service as a basic platform, providing a series of guarantees for SMS notification and remote control measure [28, 29].

Due to the vigorous development of the home furnishing market, many companies in the industry have emerged. The products they produce provide some functional devices that are scattered and cannot be concentrated for users to experience. This violates the smart home’s outstanding features of intelligence and convenience. The main work that Huawei has done is to develop from the general direction and integrate the interconnection issues of various devices in the

home. Focus on research to solve the problem of how to connect and communicate between mobile and cloud devices. Hilink was created to enable the terminal nodes of various home furnishing platforms to communicate and connect with each other to create a good experience to serve consumers and feel the real home experience. Node devices with Hilink can be connected together in its area, without us having to retype the password again; completely eliminating this link can not only save the user's precious time but also enjoy the convenience brought by the device and a quick experience. Terminals that support the Hilink open protocol allow us to use APP or cloud technology to remotely control device nodes that support the protocol. It can connect quickly, shorten the process, have high security, support multiple protocols, and support SDK opening.

In addition, the home functions designed by Xiaomi are mainly operated and used by mobile phones, and as far as the equipment is concerned, they are also developed and designed by themselves. In order to make users feel better, Xiaomi has launched a router of its own brand that is the entire data and control core. And Xiaomi's products are not priced high, the main consumer group is young people, because young people are more receptive to new things plus they have a relatively good appearance and low prices. Since 2015, its products have ranked first in terms of router sales and mobile phone software downloads. In addition to most of the common functions, the home furnishings designed by it not only have rich functions but also have the design of air purification and personalized scenes.

## 2. System Algorithm

A smart home control system based on wireless sensor network positioning proposed in this paper is shown in Figure 2. It includes a positioning module 1 and a communication module and a server; the positioning module is connected to the server through the communication module. The positioning module is used to obtain user position information in real time and report the user position information to the server at intervals. The user location information reported at intervals is received through the communication module, and the smart home equipment is remotely controlled according to the user location information.

The remote control of the smart home device according to the user's location information shown in the figure includes the following: the server compares the received user location and the location of the smart home device each time with the map and judges that the user is close to the smart home device's home trend or stays away from the smart home device trend and calculates the road distance between the two, when the user is away from the home trend and the road distance is greater than the user set threshold, it will issue an instruction to turn off the smart home device. When the road distance is less than the threshold set by the user, an instruction to start the smart home device is issued. The server shown in the figure includes a user location information receiving module connected in sequence, a distance calculation processing module, and an instruction sending

module. The positioning module outputs and connects to the user location information receiving module.

The solution proposed in this paper can make intelligent judgment and analysis by collecting user location information. Server remotely activates or closes group smart home equipment, which is flexible and reliable in use and significantly enhances the user's experience. The positioning module includes a target node worn on a user and a beacon node for assisting in the setting. The beacon node is a target node with known position coordinates, and the target node is based on an improved artificial bee colony algorithm positioning, specifically:

- (1) Initialize the population size; generate  $M$  initial nectar sources (i.e.,  $M$  initial coordinates) of the target node and the maximum number of cycles
- (2) Picking bees to search for new nectar sources. For the bee picking in step  $L$ , set the total number of bees to  $N$ , the size of the bee group to  $M$ , and the spatial dimension of the bees to search for new nectar sources as  $D$ , and search in the neighborhood of the current nectar source. The new nectar source includes:
  - (a) The space of the current nectar source's dimension is divided into intervals according to the following formula:

$$Y_{i,j}^h = X_i^j + \frac{2h-H}{H} (X_i^j - X_k^j), h \in [0, H], \quad (1)$$

where  $Y$  represents the  $h$ th interval point obtained by the division.  $x$  represents the  $i$ th current honey source generated in the  $j$ th dimension space, and  $x$  represents the  $k$ th current honey source generated in the  $j$ th dimension space,  $i = 1, 2, \dots, j = 1, 2, D, k = 1, 2, \dots, M$ , and  $k \neq i$

- (b) For each interval  $Y$ , divide the interval into  $Z$  subintervals according to the following formula:

$$Y_{i,j}^{h,z} = Y_{i,j}^h + \sin \left( \frac{z - \text{rand}(0, 1)}{2Z} \pi \right) (Y_{i,j}^h - Y_{i,j}^{h+1}), \quad z \in [1, Z]. \quad (2)$$

In the formula,  $Y$  represents the  $z$ th subinterval point obtained by dividing the interval  $Y$  wrongly,  $\text{rand}(0, 1)$  represents a uniformly distributed random value between 0 and 1, and  $Y + 1$  represents the  $h + 1$ th interval point obtained by the division

- (c) Calculate the fitness function value of each subinterval point, select the subinterval point with the largest fitness value as the representative nectar source of the corresponding interval



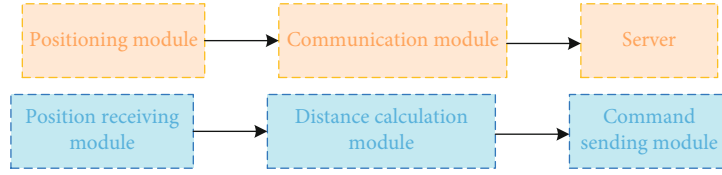


FIGURE 2: Smart home control system.

- (d) Calculate the difference between the fitness value of each representative nectar source and  $X$ :

$$W_i^j = \min \left\{ f(U_{i,j}^h) - f(X_i^j) \right\}, \quad f(U_{i,j}^h) - f(X_i^j) > 0, h \in [1, H]. \quad (3)$$

In the formula,  $W_i$  represents the smallest difference between the fitness value of each representative nectar source and  $X$ ,  $f(U)$  represents the fitness value of the representative nectar source in the interval  $Y$ ,  $f(x)$  represents the fitness value of  $X$

- (e) Select  $W_i$  correspondingly represents the source of nectar, as the new source of nectar found
- (3) Calculate the fitness value of the new nectar source and the current nectar source, compare the fitness value of the new nectar source and the current nectar source, and eliminate the nectar source with a smaller fitness value
  - (4) Follow the bees to select the pickers according to the selection probability, update their own nectar sources according to the nectar sources corresponding to the selected pickers, and search for new nectar sources in the neighborhood near the current nectar source
  - (5) Repeat the operations of (2) and (3), record the nectar source with the largest fitness value, and add 1 to the current number of cycles
  - (6) After reaching the maximum number of cycles, take the nectar source coordinates with the maximum fitness as the optimal coordinates of the target node

When the traditional artificial bee colony algorithm searches for a new nectar source in the neighborhood of the current nectar source, the search has a large randomness, and the update is unstable. The space is divided into multiple intervals for searching, which improves the efficiency of search and the stability of nectar update, which can achieve more efficient target node positioning and ensure the real-time and accuracy of user positioning in the smart home control system. The  $M$  initial nectar sources that generate the target node specifically include:

- (1) Use the following formula to randomly generate an initial nectar source:

$$X_i^{j0} = X_{\min}^{j0} + \text{rand}(0, 1) \left( X_{\max}^{j0} - X_{\min}^{j0} \right). \quad (4)$$

In the formula,  $x_i$  represents the  $i$ th initial honey source generated in the  $j$ th dimension space, and  $x_{\min}$  represents the minimum value of the  $i$ th initial honey source generated in the  $j$ th longitude space.  $x_{\max}$  represents the  $i$ th initial honey source generated in the  $j$ th dimension space. The maximum value in the original,  $\text{rand}(0, 1)$ , represents a uniformly distributed random value between 0 and 1

- (2) Calculate the corresponding reverse honey source for each initial honey source:

$$X_i^{j0'} = \text{rand}(0, 1) \left( X_{\max}^{j0} + X_{\min}^{j0} \right) - X_i^{j0}. \quad (5)$$

In the formula,  $x_i$  represents the reverse honey source of the  $i$ th initial honey source generated in the  $j$ th dimension space;

- (3) Calculate the fitness values of all initial nectar sources and reverse nectar sources, and sort all the initial nectar sources and reverse nectar sources generated in descending order of fitness value to form a nectar source set and the fitness in the nectar source set. The first  $M$  nectar sources with better values are screened out and used as the  $M$  initial nectar sources of the target node

Compared with the traditional artificial bee colony algorithm that directly randomly generates the initial nectar source at the beginning stage, the method of generating the initial nectar source described in this article can improve the quality of the initial nectar source and the efficiency of solving, so that the initial nectar source is distributed as evenly as possible, thereby improving the overall. The stability and speed of target node positioning ensure that the target node can obtain its own location attribute information quickly and well, laying a good foundation for the smart home control system to remotely control smart home equipment in real time and accurately. Suppose the position coordinates of the nectar

source  $X$  are  $(a, b)$  to define the calculation formula of the fitness value as:

$$f(X) = \min \left( \left| \sqrt{(a-x_i)^2 + (b-y_i)^2} - \bar{D}\lambda_{xi} \right|, i = 1, \dots, \Phi \right), \quad (6)$$

where  $f(X)$  represents the fitness value of nectar  $X$  ( $x_{ii}$ ) represents the position of the  $i$ th beacon node,  $D$  represents the average hop distance sent by the first beacon node received by nectar  $X$ , and  $x_i$  represents the number of hops between the honey source  $X$  and the  $i$ th beacon node;  $\Phi$  is the set number of beacon nodes.

This article defines the calculation formula of the fitness value and participates in the target node positioning based on the improved artificial bee colony algorithm according to the above formula, which can better improve the positioning accuracy of the target node, reduce the positioning error, and balance the communication task of the sensor node. The speed of locating the target node is improved, which is beneficial to realize the effective remote control and monitoring of the accurate angle of the smart home.

Assuming that the coordinates of the three base stations A1, A2, and A3 in Figure 3 are  $(x_1, y_1)$ ,  $(x_2, y_2)$ , and  $(x_3, y_3)$ , and the mobile node  $M(x, y)$  is the three circles of intersection. The distances from the mobile node  $M$  to the base stations A1, A2, and A3 are  $d_1$ ,  $d_2$ , and  $d_3$ , respectively. Then, the following formula can be obtained:

$$\begin{cases} (x-x_1)^2 + (y-y_1)^2 = d_1^2, \\ (x-x_2)^2 + (y-y_2)^2 = d_2^2, \\ (x-x_3)^2 + (y-y_3)^2 = d_3^2. \end{cases} \quad (7)$$

Subtracting the first two formulas from the third formula in the above formula, we get:

$$\begin{cases} 2(x_1-x_3)x + 2(y_1-y_3)y = x_1^2 - x_3^2 + y_1^2 - y_3^2 + d_3^2 - d_1^2, \\ 2(x_2-x_3)x + 2(y_2-y_3)y = x_2^2 - x_3^2 + y_2^2 - y_3^2 + d_3^2 - d_2^2. \end{cases} \quad (8)$$

From this, the position coordinates of the mobile node  $M$  can be obtained as shown in the following formula:

$$\begin{bmatrix} x \\ y \end{bmatrix} = \frac{1}{2} \begin{bmatrix} x_1 - x_3 y_1 - y_3 \\ x_2 - x_3 y_2 - y_3 \end{bmatrix}^{-1} \begin{bmatrix} x_1^2 - x_3^2 + y_1^2 - y_3^2 + d_3^2 - d_1^2 \\ x_2^2 - x_3^2 + y_2^2 - y_3^2 + d_3^2 - d_2^2 \end{bmatrix}. \quad (9)$$

The hyperbolic positioning method is shown in the following formula, assuming that we can use a certain measurement method to calculate the distance between the moving node  $M$  and the base stations  $S_1$  and  $S_2$ , where  $dl, 2 = d_1.d$  2. The mathematical equation of the hyperbola is shown in the following formula:

$$|MF_1 - MF_2| = 2a. \quad (10)$$

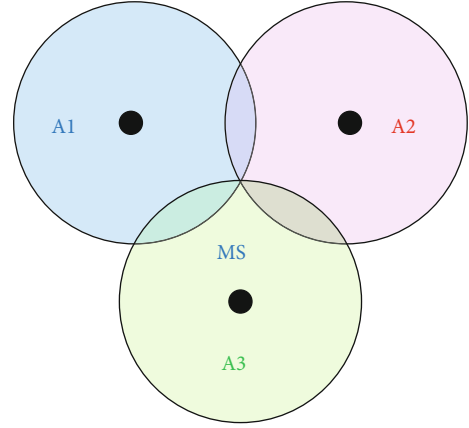


FIGURE 3: Triangulation method.

$M$  is a point on the curve,  $2a$  is the distance between the two focal points  $F_1$  and  $F_2$  on the two curves, and we can conclude from the above formula that the position of node  $M$  is at the focal point where  $S_1$  and  $S_2$  are located, sum on the hyperbola with two focal differences of  $dl, 2$ . Suppose that the coordinates of  $S_1, S_2$ , and  $S_3$  are  $(0, 0)$ ,  $(0, y_2)$ , and  $(X_3, y_3)$ , and the coordinates of the mobile node  $M$  are  $(X, y)$ . inferred:

$$\begin{cases} d_{1,2} = d_2 - d_1 = \sqrt{x^2 + (y-y_2)^2} - \sqrt{x^2 + y^2}, \\ d_{1,3} = d_3 - d_1 = \sqrt{(x-x_3)^2 + (y-y_3)^2} - \sqrt{x^2 + y^2}, \\ d_{2,3} = d_3 - d_2 = \sqrt{(x-x_3)^2 + (y-y_3)^2} - \sqrt{x^2 + (y-y_2)^2}. \end{cases} \quad (11)$$

After simplifying the above formula, we can get:

$$\begin{aligned} & [4d_{1,2}^2(b^2 + 1) - 4y_2^2]y^2 + [8abd_{1,2}^2 + 4(y_2^2 - d_{1,2}^2y_2)]y \\ & + [4a^2d_{1,2}^2 - (y_2^2 - d_{1,2}^2)^2] = 0. \end{aligned} \quad (12)$$

From the above, two answers can be drawn, one is the interference position and the other is the position of  $M$ . If you want to accurately estimate the position of the  $M$  node, you can use some auxiliary conditions such as the azimuth angle of incidence to eliminate the interference node. The method obtains the approximate location of the mobile node  $M$ . The positioning algorithm experiment result graph is shown in Figure 4. Correspondingly, the data vs. distance is shown in Figure 5.

### 3. Smart Home System Design Based on Sensor Technology

For people, the home environment is not just a living space. From its warmth and beauty to the present, people care about its comfort, controllability, convenience, safety, and the ability to intelligently control home appliances and other equipment. With the advancing of the times, it is an

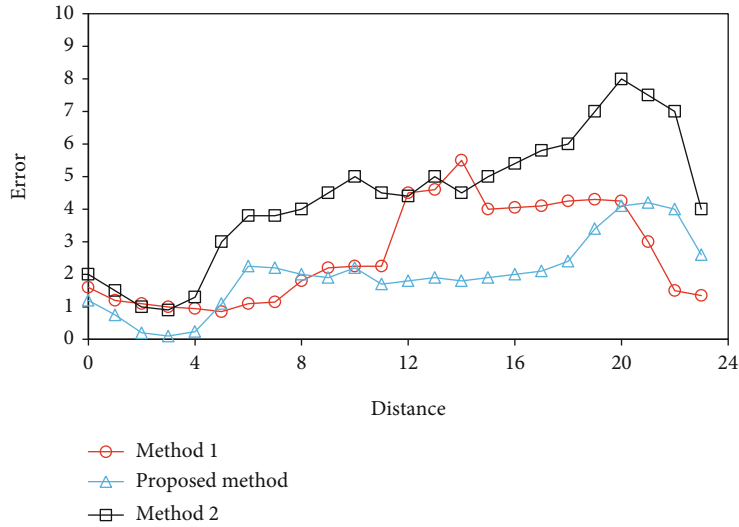


FIGURE 4: Positioning algorithm experiment result graph.

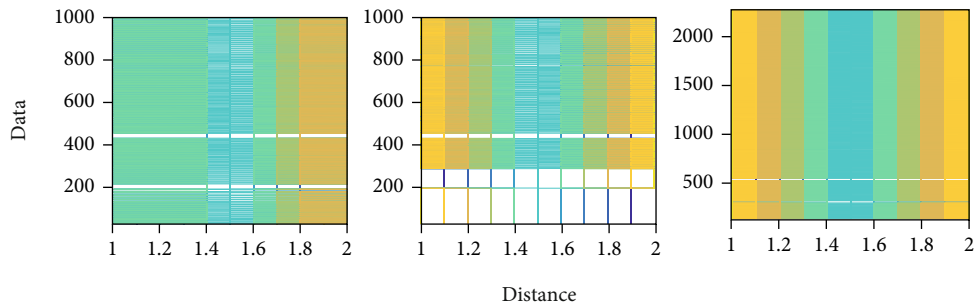


FIGURE 5: Data vs. distance.

inevitable trend to realize the networking and intelligence of the home. Based on the use characteristics of home intelligence, the design of the smart home software system needs to meet the goals of convenience and easy operation. In addition, the existing smart homes are expensive, with high installation costs, and difficult to maintain in the later stage, so that smart homes cannot be popularized in ordinary households on a large scale. Through analysis, it can be seen that the key points that the existing smart home system needs to be improved include the security and timeliness of network formation and the unity of the agreement. According to the current development of smart homes, the specific requirements will be described from economics and functionality, mainly as follows: (1) economics: considering that smart homes can be universally distributed to households of all classes, first, consider product design low. The system should not be too complicated, as long as it meets the main needs of life. (2) Functionality: the design of the home system can best be manipulated through the mobile phone, which is convenient for users to check at any time. Also, pay attention to environmental protection; hardware can run with low energy consumption. Strengthen safety monitoring to detect the danger of gas leakage and home invasion in time. Real-time response speed must be fast, power supply must be long-lasting, etc. Through the

analysis of the user's economic and functional requirements, the smart home system designed in this paper is mainly composed of three major blocks. They are the ZigBee network, server, and mobile terminal remote control APP in the home. There are mainly terminal devices (temperature and humidity sensors, light sensors, gas sensors, human infrared sensors, switch control modules) and gateways inside the home. The gateway device is composed of CC2530 module and ARM processor (detailed introduction will be given later). The ZigBee wireless technology is used for the communication between the terminal device and the gateway. Add the IP address in the gateway to the router, and join the Internet in this way. The gateway and the server use socket technology for communication, and the mobile APP and the server also use socket technology for mutual data access. Finally, the user can use the mobile phone client to control the terminal device. At the same time, the user can also use the voice keyword dialogue to switch and control the household appliances in the family to enhance the user's sense of experience. The convergence is shown in Figure 6.

The whole system uses STM32RCT6 single-chip micro-computer as the control core, integrates a variety of sensors, and uses WiFi technology to upload sensor data to the cloud in real time to complete the data interaction between the system and the cloud. Users can login to the cloud through

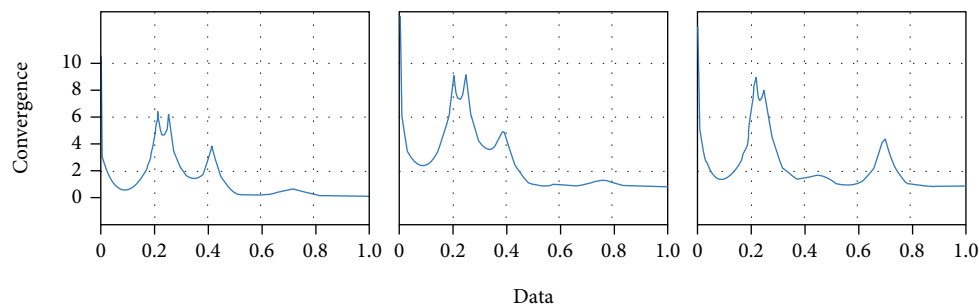


FIGURE 6: Convergence.

WeChat, mobile APP, and computer web pages to remotely monitor the peripheral sensor data of the system in real time. When the system detects an abnormal home environment, it will send an alarm email via the cloud to the mailbox designated by the user and at the same time automatically control the corresponding electrical appliances to reduce its harm. In addition, the system has a home appliance control module, which is composed of a relay and an infrared remote control circuit. Relays are used to control low-power appliances in the home, and infrared remote controls are used to control high-power air conditioners. The system perceives the home environment through the sensor module, the control module can automatically control common electrical appliances, and the communication module can realize real-time data monitoring and alarm functions.

The hardware design part of this system mainly includes sensor module, WiFi module, control module, and power circuit design.

Sensors play a vital role in the system. All the perception of the external environment is detected by sensors, and a variety of sensors with different functions are applied according to design requirements.

**3.1. Smoke and Gas Sensors.** The MQ sensor series includes smoke, liquefied gas, natural gas, coal gas, carbon monoxide, alcohol and air quality detection, and other rich smoke and gas sensors, and all support digital and analog output methods. When the digital output mode is selected, the threshold of the sensor can be adjusted by an external hardware potentiometer. The hardware interfaces of different types of sensors in the MQ series are completely the same. In the system design process, the MQ-2 smoke sensor is selected. In order to be compatible with a variety of smoke and gas sensors, the module reserves multiple digital output sensor interfaces, which can detect multiple air quality safety parameters at the same time, and there is no need to modify the software during use.

When there is a detected gas in the air, the conductivity of the MQ-2 smoke sensor will increase, and the weak signal output by the sensor will be amplified, filtered, and level adjusted through the front circuit in the conversion circuit to change the conductivity. The change corresponds to the output signal of gas concentration. If you need to accurately monitor the detected gas, you can choose the analog signal output. Its analog voltage output is proportional to the concentration of the ambient gas to be detected, which can be

measured by using the system main control chip STM32RCT6 with its own ADC peripheral. The sensor has high sensitivity and good stability and can detect fire smoke and combustible gas leakage in the home. The data is compared in Figure 7.

**3.2. Photosensitive Sensor.** The photosensitive sensor is a sensitive element that uses a photosensitive element to convert a light signal into an electrical signal. It is mainly composed of a photosensitive resistor and an LM393 voltage comparator. The working principle is based on the internal photoelectric effect. The sensor voltage comparison threshold is adjusted by the potentiometer hardware. When the ambient light changes, the voltage at both ends of the photoresistor changes accordingly. The voltage comparator can be compared with the threshold voltage to make the system know the current brightness of the environment.

**3.3. Other Sensor Temperature and Humidity Sensor.** In addition to the above-mentioned sensors, the sensor module also includes a temperature and humidity sensor and a human body infrared pyrosensor. This system uses DHT11 temperature and humidity sensor to sense the temperature and humidity parameters of the home environment. It is a temperature and humidity composite sensor with a calibrated digital signal output. The accuracy humidity is  $\pm 5\%RH$ , the temperature is  $\pm 2^\circ C$ , and the range humidity is 20% to 90%. RH: temperature is 0~50°C. Using single-bus communication, only one wire can be used to communicate with the main control chip, which has the characteristics of convenient use, small size, and low power consumption. The pyroelectric sensor uses the temperature change feature to detect the infrared radiation of the human body. The human body has a constant body temperature, generally at 37°C, which emits infrared rays with a wavelength of about 10  $\mu m$ . Passive infrared probes work by detecting infrared rays of about 10  $\mu m$  emitted by the human body. The infrared light of about 10  $\mu m$  emitted by the human body is enhanced by the Feiner filter in the sensor and then collected on the infrared sensor source. The infrared sensor source loses the charge balance when the temperature of the infrared radiation of the human body changes and discharges the charge outward. The subsequent circuit will detect the presence of the human body after the detection process. The power comparison is shown in Figure 8.

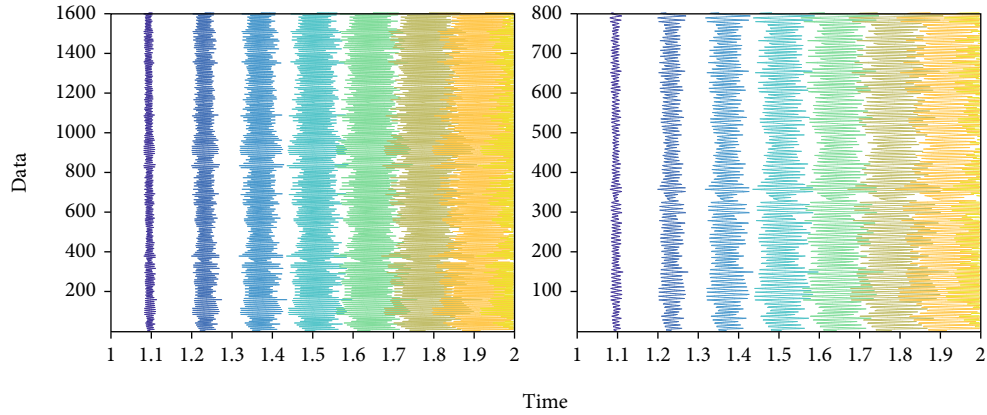


FIGURE 7: Data comparison.

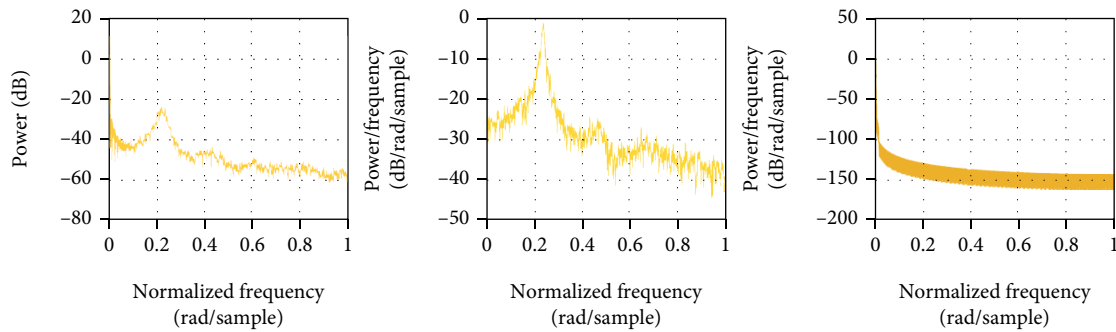


FIGURE 8: Power comparison.

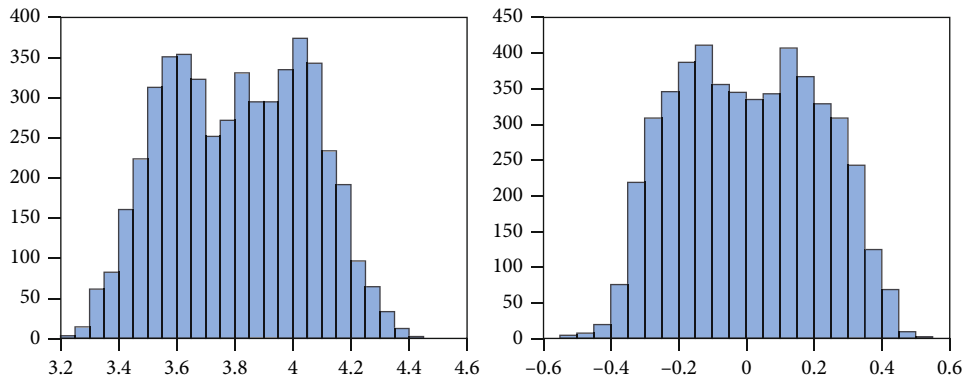


FIGURE 9: Fourier analysis.

As an IoT device, the quality of system communication affects the stability of the entire system. The communication module of this system adopts the industrial grade WiFi module ESP8266. The main control chip communicates with the WiFi module through the serial port, and the WiFi module is connected to the Internet through the TCP/IP protocol, thereby connecting the system to the Internet in real time, achieving the purpose of remote control of smart homes and environmental data monitoring.

For the control part, this system not only uses a common relay module to control low-power electrical appliances but also adds an infrared remote control circuit to control

high-power air conditioners. Relay is a commonly used device for weak current control and strong current. It is used in the system to control the main automation equipment, but has limited capacity for high-power air-conditioning. Therefore, an infrared remote control module is added to the system to simulate infrared codes through the main control chip, which can be flexibly used for switching and temperature control of high-power air conditioners, and has the advantages of low power consumption and stable performance.

This system needs to use 3.3 V and 5 V dual power supply. The power module is powered by 5 V DC, which can be directly supplied to the 5 V module circuit, and then through

the 3.3 V voltage regulator module to generate 3.3 V voltage for use by other modules. The Fourier analysis is shown in Figure 9.

#### 4. Conclusion

A set of smart home system is designed, which can sense the home environment through the sensor module, and the control module automatically controls the common electrical appliances to realize real-time data monitoring and alarm functions. This system combines sensor technology and smart home system design, which has important practical significance for the application of smart sensors in smart home in the future.

Due to the limitation of my own ability and experimental resources, the realization of the functions of the smart home system is not perfect. The distance threshold in the node localization algorithm is only obtained by RSSI measurement and calculation in the laboratory environment. The actual home environment is more complicated. Therefore, the next step needs to consider the selection of the lower threshold that affects the complex home environment. This is also an issue that needs to be further optimized in the future.

#### Data Availability

The data used to support the findings of this study are available from the corresponding author upon request.

#### Conflicts of Interest

The author declares that there is no known competing financial interest or personal relationship that could have appeared to influence the work reported in this paper.

#### References

- [1] C. Wang, L. Qiongyang, X. Liudong, G. Quanlong, C. Yang, and Y. Min, "Reliability analysis of smart home sensor systems subject to competing failures," *Reliability Engineering & System Safety*, vol. 221, p. 108327, 2022.
- [2] C. Dhanusha and A. V. Senthil Kumar, "Deep recurrent Q reinforcement learning model to predict the Alzheimer disease using smart home sensor data," *IOP Conference Series: Materials Science and Engineering*, vol. 1074, no. 1, article 012014, 2021.
- [3] P. Gupta, R. McClatchey, and P. Caleb-Solly, "Tracking changes in user activity from unlabelled smart home sensor data using unsupervised learning methods," *Neural Computing and Applications*, vol. 32, no. 16, pp. 12351–12362, 2020.
- [4] S. Pattamaset and J. S. Choi, "Irrelevant data elimination based on a k-means clustering algorithm for efficient data aggregation and human activity classification in smart home sensor networks," *International Journal of Distributed Sensor Networks*, vol. 16, no. 6, 155014772092989 pages, 2020.
- [5] S. Fong, J. Li, W. Song, Y. Tian, R. K. Wong, and N. Dey, "Predicting unusual energy consumption events from smart home sensor network by data stream mining with misclassified recall," *Journal of Ambient Intelligence and Humanized Computing*, vol. 9, no. 4, pp. 1197–1221, 2018.
- [6] M. Lussier, A. M. Sdicu, and H. Bussey, "Memory, executive functions, and naturalistic assessment of activities of daily living in mild cognitive impairment using smart home sensors," *Gerontechnology*, vol. 17, no. s, p. 15, 2018.
- [7] S. Zhang, P. McCullagh, H. Zheng, and C. Nugent, "Situation awareness inferred from posture transition and location: derived from smartphone and smart home sensors," *IEEE Transactions on Human-Machine Systems*, vol. 47, no. 6, pp. 814–821, 2017.
- [8] L. Huang, J. Li, and Q. Shi, "Approximation algorithms for the connected sensor cover problem," *Theoretical Computer Science*, vol. 809, no. C, pp. 563–574, 2020.
- [9] C. Gurcan and C. Mecit, "Queue length estimation from connected vehicles with range measurement sensors at traffic signals," *Applied Mathematical Modelling*, vol. 99, pp. 418–434, 2021.
- [10] M. Saoudi, F. Lalem, A. Bounceur et al., "D-LPCN: a distributed least polar-angle connected node algorithm for finding the boundary of a wireless sensor network," *Ad Hoc Networks*, vol. 56, pp. 56–71, 2017.
- [11] A. Abu-Affash, P. Carmi, and M. J. Katz, "Minimizing total interference in asymmetric sensor networks," *Theoretical Computer Science*, vol. 889, pp. 171–181, 2021.
- [12] J. A. Brander and E. J. Egan, "The winner's curse in acquisitions of privately-held firms," *Review of Economics & Finance*, vol. 65, pp. 249–262, 2017.
- [13] C. Victor and M. Craig, "An industrial IoT sensor system for high-temperature measurement," *Computers and Electrical Engineering*, vol. 95, p. 107439, 2021.
- [14] H. Jeong, T. H. Kim, and A. R. Han, "P. 171 effects of Korean dementia simulation program for caregivers of the elderly with dementia pilot study," *European Neuropsychopharmacology*, vol. 29, no. Supl.6, pp. S131–S132, 2019.
- [15] X.-B. Jin, C. Dou, T.-l. Su, X.-f. Lian, and Y. Shi, "Parallel irregular fusion estimation based on nonlinear filter for indoor RFID tracking system," *International Journal of Distributed Sensor Networks*, vol. 12, no. 5, 1472930 pages, 2016.
- [16] P. Klibano, M. Marinacci, and S. Mukerji, "A smooth model of decision making under ambiguity," *Econometrica*, vol. 73, no. 6, pp. 1849–1892, 2005.
- [17] T. Peleh, X. Bai, M. J. H. Kas, and B. Hengerer, "RFID-supported video tracking for automated analysis of social behaviour in groups of mice," *Journal of Neuroscience Methods*, vol. 325, p. 108323, 2019.
- [18] M. Simão, P. Neto, and O. Gibaru, "EMG-based online classification of gestures with recurrent neural networks," *Pattern Recognition Letters*, vol. 128, no. C, pp. 45–51, 2019.
- [19] Y. Pan, Y. Wu, and Y. Xin, "Development trend of smart home industry a case study of Haier Smart Home," in *Proceedings of 3rd International Conference on Innovations in Economic Management and Social Science (IEMSS 2021)*, pp. 195–208, Seoul, South Korea, 2021.
- [20] M. Wendy, M. Jenny, and L. Katarzyna, "The effectiveness of smart home technologies to support the health outcomes of community-dwelling older adults living with dementia: a scoping review," *International Journal of Medical Informatics*, vol. 153, p. 104513, 2021.
- [21] S. Peng, L. Baobao, and S. Tao, "Injury status and strategies of female 7-a-side rugby players in Anhui Province," *Sports Boutique*, vol. 38, no. 3, pp. 72–74, 2019.

- [22] P. Guild, M. R. Lininger, and M. Warren, "The association between the single leg hop test and lower-extremity injuries in female athletes: a critically appraised topic," *Journal of Sport Rehabilitation*, vol. 30, no. 2, pp. 1–7, 2020.
- [23] B. K. Sovacool and D. F. Del Rio Dylan, "Corrigendum to "Smart home technologies in Europe: a critical review of concepts, benefits, risks and policies" [Renew Sustain Energy Rev 120 (2020) 109663]," *Renewable and Sustainable Energy Reviews*, vol. 148, p. 111277, 2021.
- [24] L. Xuejia, "Research on design strategy of computer user interface based on smart home for the elderly," *Journal of Physics: Conference Series*, vol. 2021, no. 2, pp. 465–486, 1915.
- [25] X. Gengyi, "Machine learning in smart home energy monitoring system," *IOP Conference Series: Earth and Environmental Science*, vol. 769, no. 4, pp. 343–354, 2021.
- [26] C. Zhou, T. Huang, and S. Liang, "Smart home R&D system based on virtual reality," *Journal of Intelligent & Fuzzy Systems*, vol. 40, no. 2, pp. 3045–3054, 2021.
- [27] P. Norbert, "Chancen und Risiken von smart home," *Datenschutz und Datensicherheit-DuD*, vol. 45, no. 2, pp. 95–101, 2021.
- [28] N. Neda, "Architecture of a smart home for aging in place," *Innovation in Aging*, vol. 4, Supplement 1, p. 39, 2020.
- [29] G. G. Wang, A. H. Gandomi, A. H. Alavi, and D. Gong, "A comprehensive review of krill herd algorithm: variants, hybrids and applications," *Artificial Intelligence Review*, vol. 51, no. 1, pp. 119–148, 2019.

## Research Article

# Application of Adaptive PID Temperature Control Algorithm under Spatial Thermal Model of ALD Reaction Chamber

Zhenqiang Liu,<sup>1</sup> Jinhui Lei<sup>1</sup> ,<sup>1</sup> Yan Chen,<sup>1</sup> Yang Xia,<sup>2</sup> Jiaheng Feng,<sup>2</sup> Shuaiqiang Ming,<sup>2</sup> and Wa Mao<sup>1</sup>

<sup>1</sup>School of Information Engineering and Automation, Kunming University of Science and Technology, Kunming, Yunnan 650500, China

<sup>2</sup>Kemin Electronic Equipment Technology co., LTD, Jiaxing, Zhejiang 314000, China

Correspondence should be addressed to Jinhui Lei; [ljh13700650851@163.com](mailto:ljh13700650851@163.com)

Received 10 February 2022; Revised 28 February 2022; Accepted 16 March 2022; Published 11 April 2022

Academic Editor: Wen Zeng

Copyright © 2022 Zhenqiang Liu et al. This is an open access article distributed under the Creative Commons Attribution License, which permits unrestricted use, distribution, and reproduction in any medium, provided the original work is properly cited.

The study aims to expand the application of the proportion integral derivative (PID) algorithm and improve the practical application of the PID algorithm to the atomic layer deposition (ALD) process. First, the ALD process is analyzed, and the application method of the PID algorithm is determined. Second, the research conditions of the PID algorithm based on the ALD process are designed. Finally, the temperature control operation of the PID algorithm in the ALD reaction chamber is modeled and experimentally studied under different research conditions. The results show that temperature significantly impacts the reaction chambers of stainless steel and aluminum. When the heating temperature increases, the temperature of the stainless steel chamber will also change, and the maximum difference between the chamber and the heating temperature is about 33°C. In contrast, the temperature of the aluminum chamber varies little with the heating temperature. The maximum difference between the chamber temperature and heating temperature is about 350°C, which shows that the temperature of the stainless steel chamber is better controlled and is more practical under the same temperature conditions. The pressure change has little effect on the temperature change of the reaction chamber of the two materials. The temperature curves of the two chambers show that the PID temperature control system can be used normally and has strong practicability. The study provides technical support for improving the PID temperature control system and the rational use of the PID temperature control algorithm in the ALD process.

## 1. Introduction

In recent years, atomic layer deposition (ALD) technology has attracted extensive attention because of its accurate material synthesis and modification characteristics (precise to nuclear scale). In particular, ALD is excellent in researching and developing new nanocatalytic materials [1]. Moreover, the PID (proportional, integral, and differential) temperature control algorithm to the ALD process can effectively control the temperature of the ALD reaction chamber, provide a suitable reaction environment for the ALD process, and improve the production speed [2]. Although the application of the PID temperature control algorithm to

the ALD process is not perfect, many studies provide technical support for the application of the PID temperature control algorithm.

Gilbert and Leeuwen (2020) pointed out that ALD is a thin film growth technology with surface self-limiting reaction, and it can accurately control the growth of thin films. There is no ALD alumina reaction group on the surface of polyolefin membrane, resulting in the slow growth and nucleation of ALD alumina and the low reaction efficiency in the early stage. The final development of alumina primarily forms clusters rather than intact and covered films [3]. Tomer et al. (2019) argued that temperature uniformity in the reaction chamber could be well solved by using the



partition heating method, the PID controller with anti-integral saturation method, and the feed forward compensation PID control algorithm [4]. Huang et al. (2018) pointed out that temperature control is a concern of most industrial enterprises. The temperature control quality directly affects the quality of products and the efficiency of enterprises. However, temperature control accuracy is low due to temperature-controlled components' different characteristics, and the adjustment time is long in actual production [5]. Li et al. (2020) pointed out that the PID algorithm can automatically identify different parameters according to the actual situation, which significantly simplifies the debugging process and saves time. The response and accuracy of temperature control are improved, which has a tremendous practical effect on enhancing efficiency [6].

Grillo et al. (2018) argued that the temperature control system is designed, including hardware and software design. Finally, the response ability and stability of the steep curve of the PID algorithm are tested by a simulation experiment. The results show that the system has a fast response ability and strong strength, which improves temperature control accuracy [7]. Mu et al. (2019) uttered that ALD is a nanofilm preparation technology. The controllable thickness and uniform film could be obtained by self-restrictive precursor alternating saturation reaction. It could be used as a water-insulating and oxygen-insulating layer in electronic devices, a transistor gate dielectric layer, and a surface passivation layer of solar cells. Therefore, ALD is widely used in microelectronics, solar cells, flexible electronics, and other fields. Temperature is one of the most critical factors affecting the quality and efficiency of thin films. However, the existing conventional control methods have poor temperature stability, long stability adjustment time, and significant temperature fluctuation under the condition of external interference, which directly affects the microsurface morphology of the deposited thin film. The PID temperature control algorithm can improve the transient performance of the system through rolling optimization and output correction under external interference. It has the characteristics of processing time delay, constraint ability, and low requirement for mathematical model. It has been successfully applied in the field of automatic control and temperature control [8].

In summary, applying the PID temperature control algorithm to the ALD process is not perfect. ALD and the PID temperature control algorithm are introduced and analyzed in this case. Then, the research method of PID temperature control algorithm under different temperature and pressure conditions is designed according to the characteristics of ALD and PID. On this basis, the research model is implemented. Finally, the PID temperature control algorithm in the ALD reaction chamber is comprehensively analyzed through experiments. This research provides new ideas for using the PID temperature control algorithm to control the temperature in the ALD reaction chamber. The utilization rate of the PID temperature control algorithm in the ALD production process is improved, and the production quality and efficiency of ALD are enhanced.

## 2. Research Methods

*2.1. Methodology and Theory.* ALD is used to manufacture nanodevices, and it is a chemical vapor deposition technology [9]. It is a film growth technology with a surface self-limiting reaction, which can accurately control the growth of films. ALD coats the polyolefin membrane to produce a composite membrane of nanoalumina polyolefin. There is no ALD alumina reaction group on the surface of the polyolefin membrane, which results in slow growth and nucleation of ALD alumina and low reaction efficiency, making most of the final grown alumina forms clusters rather than completely covered films. The system of ALD is very complex. The whole system mainly includes a gas pipeline, precursor container, control system, reaction chamber, and vacuum pump. The reaction chamber comprises a wafer, vacuum chamber, and surrounding resistance wire [10]. The internal temperature control of the ALD vacuum reaction chamber is nonlinear, hysteretic, and time-varying. The materials inside the vacuum chamber should be stainless steel, aluminum, quartz, and graphite, which can meet all the above requirements [11]. The basic working process of ALD is that the bottom of the chamber is connected with the vacuum pump to pump air inside the chamber. Then, the precursor enters the vacuum chamber through the electromagnetic switch. Finally, the liquid in the precursor enters the reaction chamber through the gas pipeline to complete the reaction [12]. The reaction process of ALD is shown in Figure 1.

Figure 1 shows that the ALD reaction system includes a gas pipeline, a precursor container, a control system, a reaction chamber, and a vacuum pump. The combination of the control system and the vacuum pump provides power for the whole system. The reaction completes if the liquid in the precursor gasifies and enters the vacuum reaction chamber [13]. After each ALD reaction, the chemicals generated are rinsed with N<sub>2</sub> to remove the determinations, and finally, a complete deposited film is formed [14]. Figure 2 shows the circulation flow of ALD.

Figure 2 shows that the flow of the ALD process is controlled by programmers ( $t_1$ ,  $\Delta t_1$ ,  $t_2$ ,  $\Delta t_2$ ,  $t_3$ ,  $\Delta t_3$ ) to generate 2D materials. A digital control system carries out the ALD process. In the production process of the ALD process, if you need to improve the quality and efficiency of process production, you can improve the cycle times of the ALD process and keep the temperature appropriate in the cycle process. Figure 3 shows the basic software configuration in the ALD control system.

Figure 3 shows that each link of the ALD process can be managed separately in the control software. The PID adaptive temperature control system in the ALD reaction chamber can control the temperature of ALD in real time and ensure that the liquid in the precursor can be gasified normally and enter the reaction chamber smoothly, promoting the complete reaction in the reaction chamber [15]. And the temperature in the ALD reaction chamber can keep high through PID temperature control technology to increase the number of ALD cycles and improve production efficiency. The PID temperature control algorithm calculates and

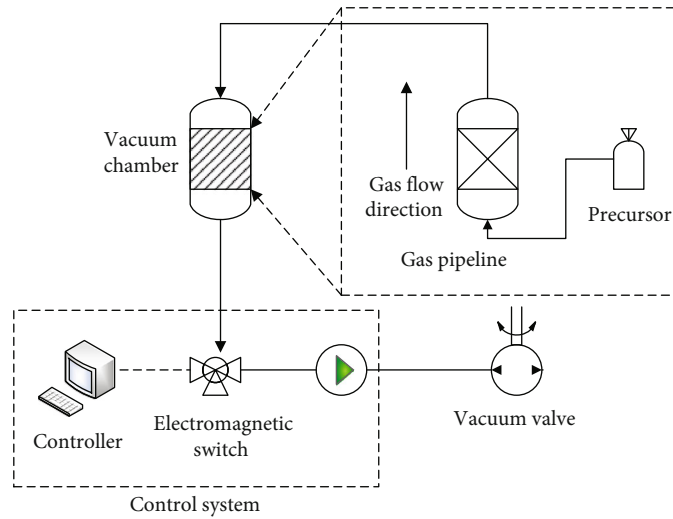


FIGURE 1: ALD reaction system.

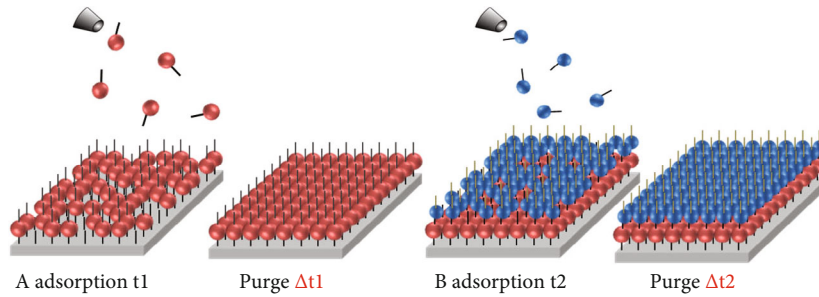


FIGURE 2: Flow of the ALD process.

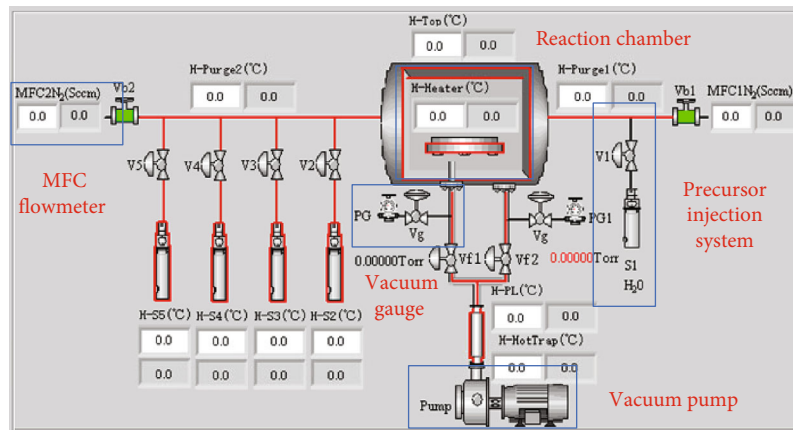


FIGURE 3: Basic configuration of the software in the ALD control system.

controls the system temperature through *P* (proportion), *I* (integral), and *D* (differential) parameters. The PID temperature control system can only predict and adjust the system temperature by adjusting *P*, *I*, and *D* parameters in real time [16]. Figure 4 shows the basic principle of the PID temperature control system.

Figure 4 shows that when the predetermined temperature is set, the PID temperature control algorithm will adjust

the temperature through *P*, *I*, and *D*, making the temperature of the controlled element reach the predetermined value. Real-time feedback will output through the feedback system [17].

2.2. Temperature Control System and ALD Control System. The improved ALD control system can realize the substantial increase of the total output and the

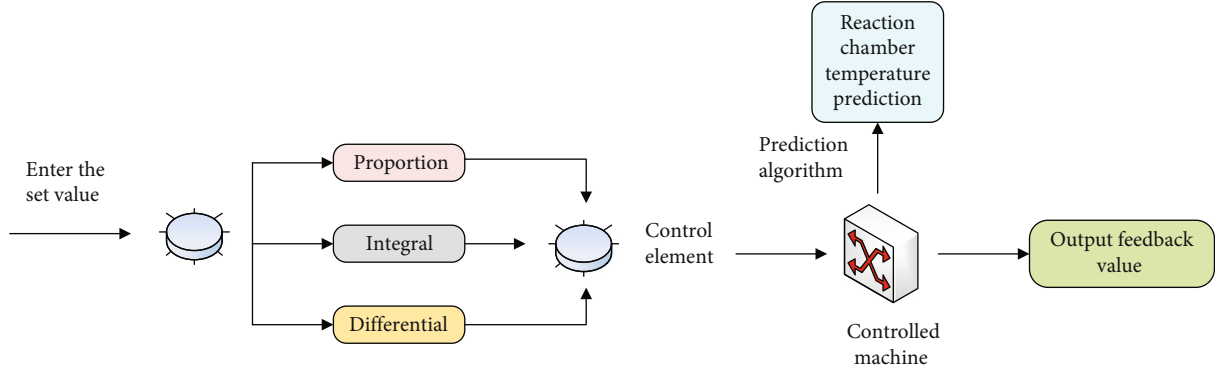


FIGURE 4: Basic principle of the PID temperature control algorithm.

intellectualization of the control system [18]. Usually, an ALD control system consists of an upper computer human-computer interaction system and a lower computer, a vacuum chamber, a temperature control system, and other modules. The upper computer can obtain and interact with data through human operation. When the data are input, the basic parameters of each overall control point are also included [19]. The model of the upper computer is the InTouch configuration software of WonderWare Company. The essential control of the lower computer is realized through the InTouch configuration software. Table 1 shows the basic parameters of the upper computer.

Table 1 shows an advanced host computer operating system, which requires comprehensive upgrading of CPU, a memory card, a hard disk, a graphics card, a system, a program, and a server to obtain more accurate data. In the ALD process, the parameters of all control components are set through the upper computer calculated. The airflow in the vacuum pump is calculated as [20]

$$L_{HFC} = \frac{(KV\rho_{x_2})}{T}, \quad (1)$$

where  $V$  represents the electrical frequency signal,  $\rho_{x_2}$  represents vacuum density,  $T$  represents time,  $L_{HFC}$  represents the gas flow, and  $K$  represents the vacuum parameter in the ALD process reaction chamber. The dynamic pressure inside the vacuum chamber is calculated as

$$\begin{aligned} PV &= \frac{m}{M}RT, \\ P_0 - P &= \frac{RT}{VM} \int_0^t (L_{MFC} - L_{pump}) dt, \\ P &= P_0 - \frac{RT}{VM} \int_0^t (\Delta L) dt, \end{aligned} \quad (2)$$

where  $t$  is the time,  $V$  is the volume inside the chamber,  $P$  is the air pressure inside the chamber,  $M$  is the molar mass of

the gas,  $R$  is the molar constant of the gas,  $T$  is the temperature in the reaction chamber, and  $\Delta L$  represents the gas flow difference in the reaction chamber [21]. The calculation equation of temperature control voltage is

$$U_d = \left(\frac{t}{T}\right)^* U_{AN}, \quad (3)$$

where  $t$  is the time,  $T$  is the cycle time of the voltage pulse, and  $U_{AN}$  represents the average voltage of the pulse. For the temperature test inside the reaction chamber, the temperature of the reaction chamber wafer needs to be measured, and the calculation method adopts the least square method [22]. The calculation equations are as follows:

$$\|\delta\|_2^2 = \sum_{i=0}^m \omega(X_i) [S(X_i) - f(X_i)]^2, \quad (4)$$

$$f(x) = \{(x_i), (y_i), i = 0, 1, \dots, m\}, \quad (5)$$

$$\delta_i = S\left(x_i\right) - y_i, \quad (6)$$

$$\delta_i = S(x_i) - y_i, S(x) = a_0\varphi_0(x) + a_1\varphi_1(x) + \dots + a_n\varphi_n(x), \quad (7)$$

where  $f(x)$  represents the data set and  $S(x)$  represents the fitting curve.  $x_i$  and  $y_i$  represent the dataset of two sets of data, respectively. If the linear independent group of the space where  $s(x)$  is located is  $\varphi_0(x), \varphi_1(x), \dots, \varphi_n(x)$ , the calculation equation of the least square method is

$$\|\delta\|_2^2 = I(a_0, a_1, \dots, a_n) = \sum_{i=0}^m \omega(x_i) \left[ \sum_{j=0}^n a_j \varphi_j(x_i) - f(x_i) \right]^2, \quad (8)$$

$$\frac{\partial I}{\partial a_k} = 2 \sum_{i=0}^m \omega(x_i) \left[ \sum_{j=0}^n a_j \varphi_j(x_i) - f(x_i) \right] \varphi_k(x_i) = 0. \quad (9)$$

TABLE 1: Basic parameters of the upper computer.

Components	Parameters
CPU	Morethanthe3G
Main memory	Morethanthe2G
Hard disk	Morethanthe100G
Graphics card	2GDiscretegraphicscard
System	WindowsXPSP3
Program	Intouch9.6
Server	OPCLink8.0

Equation (9) is used to calculate the minimum value, which is recorded as

$$(\varphi_j, \varphi_k) = \sum_{i=0}^m \omega(X_i) \varphi_j(X_i) \varphi_k(X_i), \quad (10)$$

$$(f, \varphi_k) = \sum_{i=0}^m \omega(X_i) f(X_i) \varphi_k(X_i) = d_k, \quad (11)$$

$$G = \sum_{j=0}^n (\varphi_k, \varphi_j), \quad (12)$$

where  $G\vec{a} = \vec{d}$ . If orthogonal polynomials are used for least-squares fitting,  $G$  is a nonsingular matrix and satisfies the following equations:

$$(\varphi_j, \varphi_k) = \sum_{i=0}^m \omega(x_i) \varphi_j(x_i) \varphi_k(x_i) = \begin{cases} 0, & j \neq k \\ A_k > 0, & j = k \end{cases}, \quad (13)$$

$$a_k^* = \frac{(f, \varphi_k)}{(\varphi_k, \varphi_k)}, \quad (14)$$

where  $a_k^*$  represents the final calculation result. The PID temperature control algorithm controls the temperature of the ALD reaction chamber by changing the initial temperatures, the pressure, and the time gradients. And it is comprehensively studied by comparison [23]. Table 2 shows the conditions for temperature measurement of the ALD reaction chamber.

Table 2 shows that the temperature of the ALD reaction chamber is measured under different initial chamber temperatures and different channels. The time change is as follows: change the initial temperature, last for one hour and record the information; change the initial pressure, last for 15 min; and record the relevant information. And the commonly used stainless steel and aluminum reaction chambers are analyzed in six channels of the ALD reaction chamber. The two reaction chamber materials are compared to determine what materials fit the PID temperature control system. The PID temperature control system is adjusted to make it suitable for more materials and promote its application

TABLE 2: Temperature measurement conditions of the ALD reaction chamber.

Number	Heater	Pumpline	Purge1	Purge2	Hottrap
1	50	150	100	100	400
2	70	150	100	100	400
3	100	150	100	100	400
4	150	150	100	100	400
5	200	150	100	100	400
6	250	150	100	100	400
7	300	150	100	100	400
8	350	150	100	100	400
9	400	150	100	100	400
10	450	150	100	100	400
11	500	150	100	100	400
12	550	150	100	100	400

and development. The comparison between PID and other temperature control algorithms is shown in Table 3.

Table 3 shows that the PID temperature control algorithm is more suitable because of its flexibility, convenient debugging, and high control accuracy.

**2.3. PID Temperature Control Algorithm.** The PID control algorithm comprises a PID regulator, an actuator, and a controlled object [24]. The general calculation equation is as follows:

$$v(t) = Kp \left[ e(t) + \frac{1}{T_j} \int e(t) dt + T_D \frac{de(t)}{dt} \right], \quad (15)$$

where  $v(t)$  represents the output value of the controller,  $e(t)$  represents the error of the control system,  $Kp$  represents the proportional coefficient,  $T_j$  is the integral constant, and  $T_D$  is a constant. When the PID control algorithm is operated by a computer [25], the calculation equation is as follows:

$$v(kT) = K_p \left\{ e(kT) + \frac{T}{T} \sum_{i=0}^k e(iT) + \frac{Td}{T} [e(kT) - e(kT - T)] \right\}, \quad (16)$$

where  $v(kT)$  represents the output value when the system is controlled by a computer, and other parameters have the same meaning in Equation (15). The results can also be calculated by an integral coefficient and differential coefficient [26]. The calculation equations are as follows:

$$K_I = \frac{K_p T}{T_I}, \quad (17)$$

$$K_D = \frac{K_p T_D}{T}, \quad (18)$$

$$u(k) = K_p e(k) + K_j \sum_{j=0}^k e(j) + K_D [e(k) - e(k-1)]. \quad (19)$$

TABLE 3: Advantages of the PID temperature control algorithm.

Temperature control algorithm	Advantages	Shortcomings
PID	Easy to debug, high control precision, strong anti-interference ability, high stability ability	Coordination is not good enough
Fuzzy control	Strong robustness and fast response	The parameters are complex and expensive
Neural network control	The algorithm is simple and easy to implement in hardware and software	The system is complex and requires more human coordination

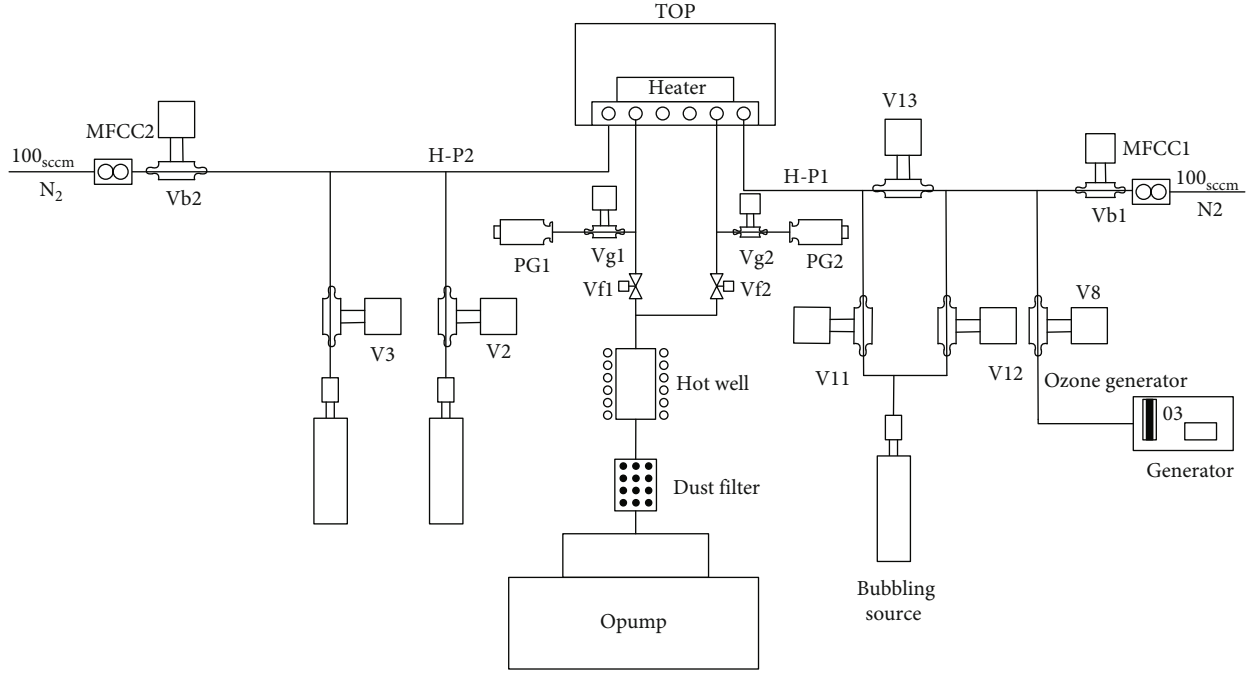


FIGURE 5: Basic framework of the dual-cavity ALD system.

In Equations (17), (18) and (19), (16), and (17) are the calculation equations of integral coefficient and differential coefficient, respectively. And the three equations are used for calculating discrete positions. After a simple calculation is performed, the following equation is obtained [27]:

$$u(k-1) = K_p \left\{ e(k-1) + \frac{T}{T_i} \sum_{j=0}^{k-1} e(j) + \frac{T_D}{T} [e(k-1) - e(k-2)] \right\}, \quad (20)$$

where  $(k-1)$  is the same as the parameter in the above equation, and it is the sampling times in the test process. The following equation is obtained by sorting out Equations (19) and (20) [28]:

$$\begin{aligned} u(k) - u(k-1) &= K_p \left\{ e(k) - e(k-1) + \frac{T}{T_i} e(k) + \frac{T_D}{T} [e(k) - 2e(k-1) + e(k-2)] \right\}. \end{aligned} \quad (21)$$

The final calculation equation can be obtained, and it is as follows:

$$\begin{aligned} u(k) = u(k-1) + K_p \left\{ [e(k) - e(k-1)] + \frac{T}{T_i} e(k) \right. \\ \left. + \frac{T_D}{T} [e(k) - 2e(k-1) + e(k-2)] \right\}. \end{aligned} \quad (22)$$

After Equation (22) is simplified, this can be obtained as

$$u(k) = u(k-1) + a_0 e(k) - a_1 e(k-1) + a_2 e(k-2). \quad (23)$$

The position calculation equation of PID in the computer control system is obtained, and the final result needs to be fuzzified. If the input value is defined between  $[-x, x]$  and the fuzzy value is a value in  $\{-m, -m+1, \dots, 0, \dots, m-1, m\}$ , the quantization factor of the fuzzy value can be calculated [29]. The calculation equation is

$$t = \frac{m}{x}, \quad (24)$$

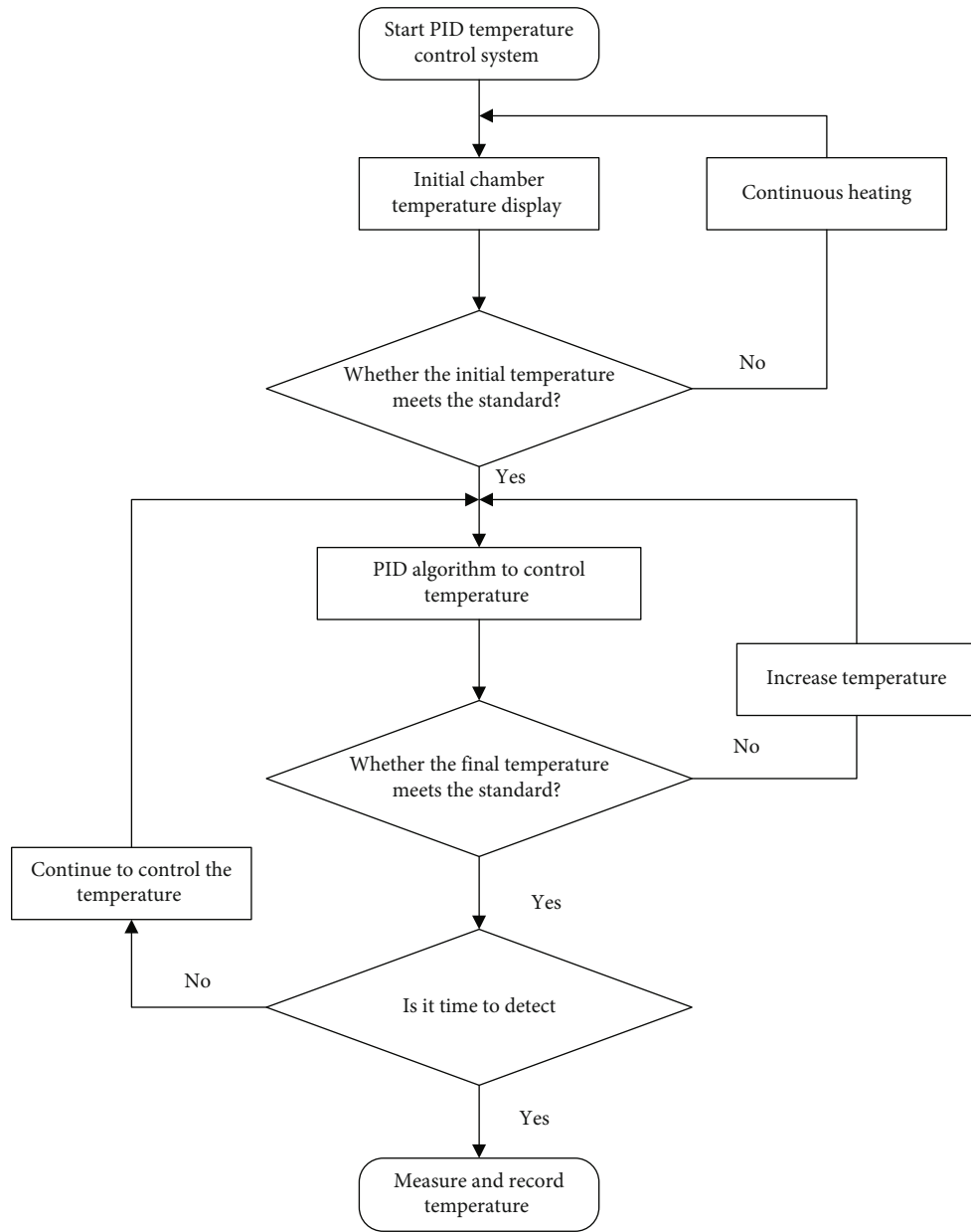


FIGURE 6: Basic flow of temperature control using the PID temperature control algorithm.

where  $t$  represents the quantization factor of the fuzzy value. The amount of fuzzy control can also be calculated [30]. The calculation equation is as follows:

$$V = (R \times RB) \bullet T, \quad (25)$$

where  $V$  represents the amount of control fuzzy,  $R$  represents the fuzzy number of input values,  $T$  is the fuzzy coefficient,  $\times$  represents the direct operation of fuzzy values, and  $\bullet$  the synthesis operation of fuzzy values [31]. The discrete domain calculation equation of the fuzzy value is

$$v_o = \frac{\sum_{i=1}^n v_i \mu(v_i)}{\sum_{i=1}^n \mu(v_i)}, \quad (26)$$

where  $v_o$  is the accuracy of the output value and  $v_i$  represents the variable of the output value. In addition, the calculation equations of three control parameters  $P$ ,  $I$ , and  $D$  are [32]

$$K_P = K_{P0} + \{Ei, ECi\}_P, \quad (27)$$

$$K_I = K_{I0} + \{Ei, ECi\}_I, \quad (28)$$

$$K_D = K_{D0} + \{Ei + ECi\}_D, \quad (29)$$

where  $K_{P0}$ ,  $K_{I0}$ , and  $K_{D0}$  represent the initial values of the three control parameters  $P$ ,  $I$ , and  $D$ , respectively. Through the adjustment of the PID temperature control algorithm, the results of the final three parameters can be calculated as  $K_P$ ,  $K_I$ , and  $K_D$  [33].

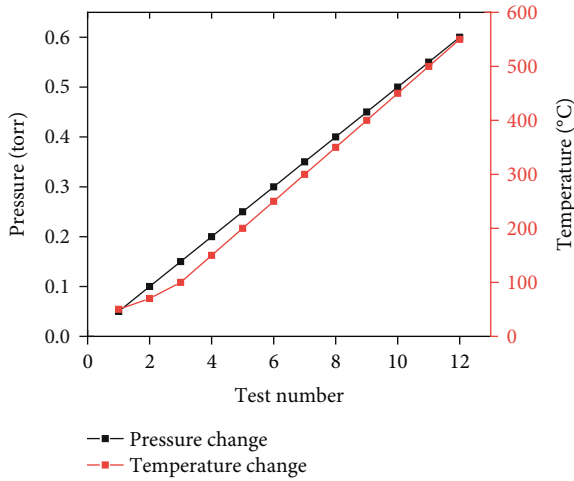


FIGURE 7: Relevant variables.

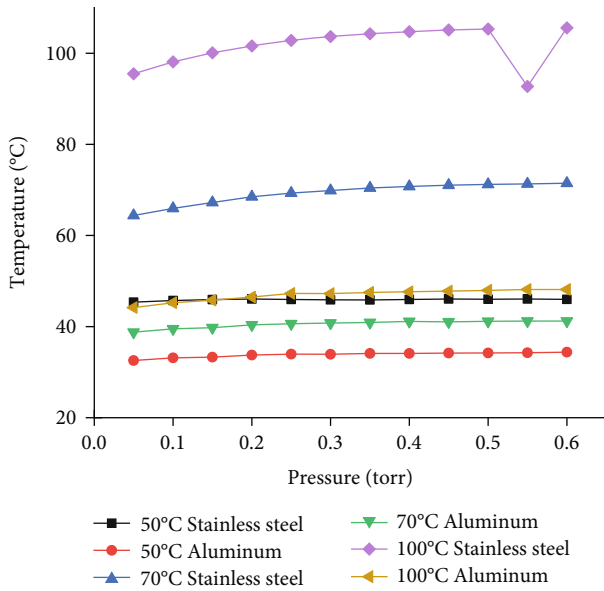


FIGURE 8: Record results of the PID temperature control algorithm at 50°C, 70°C, and 100°C.

2.4. Modeling of PID Based on ALD Reaction Chamber. The PID temperature control algorithm based on the ALD reaction chamber is studied, and the specific equipment used is the dual cavity ALD system. Figure 5 shows the basic structural framework of the dual cavity ALD system.

Figure 5 shows that the PID temperature control algorithm can be compared with different materials with strong responses in the dual cavity ALD system. After that, the PID temperature control algorithm can automatically select ALD chamber materials and improve its performance through the feedback of different materials [34]. The PID temperature control algorithm is studied by recording and analyzing the reaction chamber temperature in the ALD process system [35]. Figure 6 shows the basic process of using the PID temperature control system to control the reaction chamber temperature in the ALD process system.

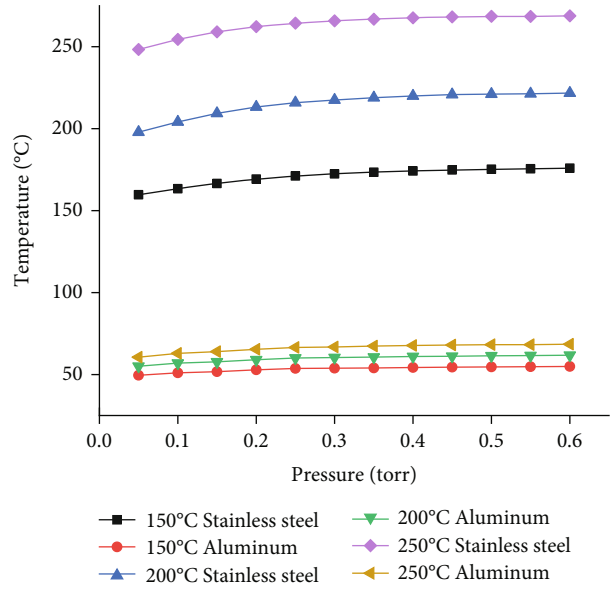


FIGURE 9: Record results of the PID temperature control algorithm at 150°C, 200°C, and 250°C.

Figure 6 shows that at the beginning, the reaction chamber of the ALD process needs to be heated, and the temperature should reach the initial temperature required by the experiment. Then, the initial temperature of the chamber is detected to judge whether the temperature meets the standard. If the temperature does not meet the standard, the reaction chamber needs to be heated again. If the temperature meets the standard, the next step is continued. The PID temperature control algorithm is used to control the temperature in the reaction chamber. During the control process, it is necessary to change the chamber temperature regularly and then detect whether the temperature meets the standard. If it does not meet the standard, it needs to be reheated. If it meets the standard, go to the next step to judge whether it is time to record. If the temperature cannot be recorded, continue maintaining the temperature by PID. If it is recorded, the temperature is recorded and adjusted in real time, and the research results are analyzed according to the recorded data.

### 3. Research Results

3.1. ALD Reaction Chamber. According to the above research methods, the PID temperature control algorithm is studied based on different materials of the ALD reaction chamber. Figure 7 shows the research conditions of other chamber materials.

Figure 7 shows that the chambers of the two materials are experimentally studied under the same conditions, in which the pressure changes are 0.05, 0.1, 0.15, 0.2, 0.25, 0.3, 0.35, 0.4, 0.45, 0.5, 0.55, and 0.6, respectively, and the temperature changes are 50, 70, 100, 150, 200, 250, 300, 350, 400, 450, 500, and 550°C, respectively. The research under different pressures and temperatures can reflect the temperature tolerance of the two materials and test the

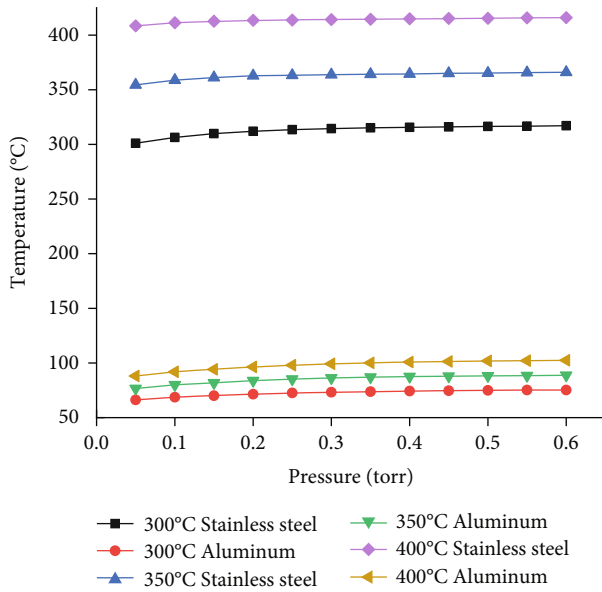


FIGURE 10: Record results of the PID temperature control algorithm at 300°C, 350°C, and 400°C.

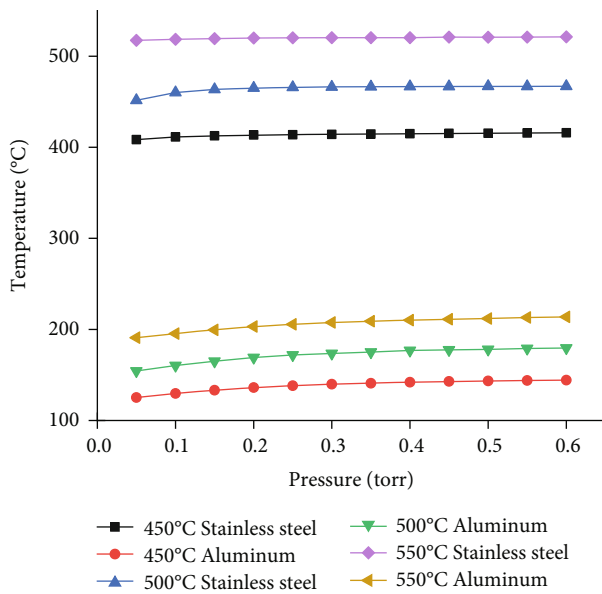


FIGURE 11: Record results of the PID temperature control algorithm at 450°C, 500°C, and 550°C.

influence of the two materials on the temperature tolerance under different pressure conditions

**3.2. PID Research and Analysis Based on ALD.** Through the research on the PID temperature control test for reaction chambers of different materials under different conditions, the heat resistance and pressure resistance of other materials are analyzed, which can reveal the service status of the PID temperature control algorithm. This verifies the performance of the PID temperature control algorithm through different materials and improves the authenticity and feasi-

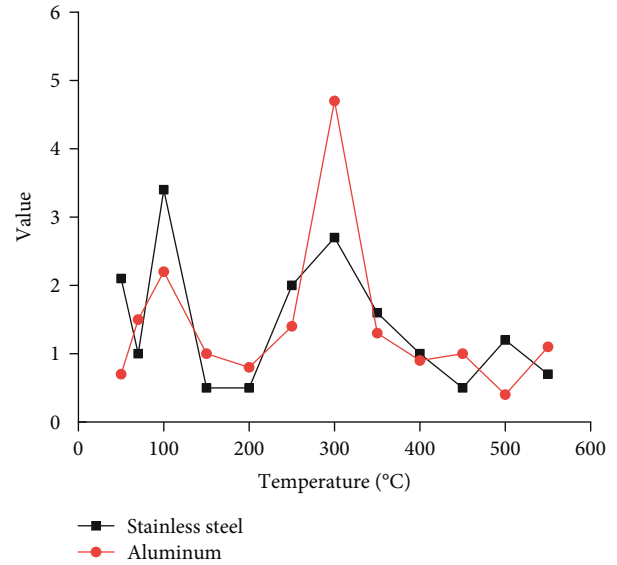


FIGURE 12: Comparison of the errors of temperature control systems.

bility of the research. Figure 8 shows the temperature recording results.

Figure 8 shows that when the results of the PID temperature control records are 50°C, 70°C, and 100°C, the temperature of the stainless steel chamber is at 100°C with an error of about  $\pm 5^\circ\text{C}$ . The temperature of the aluminum chamber is at 50°C, which is maintained at about 30°C, and the error is about  $\pm 3^\circ\text{C}$ .

Figure 9 shows that when the results of the PID temperature control algorithm are 150°C, 200°C, and 250°C, the temperature of the stainless steel chamber is at 250°C with an error of about  $\pm 2^\circ\text{C}$ . The temperature of the aluminum chamber is at 150°C with an error of about  $\pm 1^\circ\text{C}$ .

Figure 10 shows that when the results of the PID temperature control algorithm are 300°C, 350°C, and 400°C, the temperature of the stainless steel chamber is at 400°C with an error of about  $\pm 1^\circ\text{C}$ . The temperature of the aluminum chamber is at 300°C with an error of about  $\pm 3^\circ\text{C}$ .

Figure 11 shows that when the results of the PID temperature control algorithm are 450°C, 500°C, and 550°C, the temperature of the stainless steel chamber is at 550°C with an error of about  $\pm 3^\circ\text{C}$ . The temperature of the aluminum chamber is at 450°C with an error of about  $\pm 5^\circ\text{C}$ . Figure 12 shows the difference between the predicted error and the actual error of the two materials.

Figure 12 shows that the maximum difference between the prediction error of the cavity temperature of stainless steel and its actual error is about  $3^\circ\text{C}$ . In contrast, the maximum difference between the prediction error of the cavity temperature of aluminum and the actual error is about  $5^\circ\text{C}$ . Therefore, the PID temperature control system is reasonable for error control.

Figures 8–11 show that the temperature changes of the two materials are not significant by applying the PID temperature control algorithm to the reaction chambers of the two materials under different conditions. It is concluded that



the pressure has little effect on the temperature resistance of the ALD reaction chamber. Still, the temperature of the reaction chamber varies significantly at different initial temperatures. When the initial temperature is 50°C, the temperature difference between the two materials is not significant, maintaining at about 20°C. Therefore, the reaction chambers of these two materials are suitable for temperature regulation with a temperature control system above 50°C. With the initial temperature increase, the temperature difference between different materials begins to increase gradually under the PID temperature control algorithm. The temperature difference has risen to about 50°C under the condition of 70°C. At 550°C, the reaction chamber gap of the two materials reached the maximum, maintaining at about 320°C. However, when the change of the reaction chamber of the two materials under the PID temperature control algorithm is analyzed, it is found that the temperature change of stainless steel is more significant than that of the aluminum chamber. The temperature tolerance of the reaction chamber made of stainless steel is sensitive. When the heating temperature increases, the temperature of the stainless steel reaction chamber increases rapidly, while the temperature of the aluminum reaction chamber decreases. This proves that the temperature tolerance of the aluminum reaction chamber is high. Still, the overall temperature of the reaction chamber made of different materials does not change much under the PID temperature control algorithm, and the performance of the PID temperature control system is also stable under different pressures. The curve remains stable and in an ideal state. This shows that the PID temperature control algorithm can be used under different temperatures and pressures.

#### 4. Conclusion

The PID temperature control algorithm is used to analyze its application to the ALD reaction chamber. The test is taken in the reaction chamber with different materials, different reaction temperatures, and different pressure changes. The simulation experiment found that the reaction chambers with different materials have different tolerance sensitivity to different temperature changes. Among them, the temperature sensitivity of stainless steel is more significant than aluminum, and the difference between the two is very large. Then, the temperature changes of the two materials under different pressure conditions are compared. The results show that the pressure changes have little effect on the temperature changes of the reaction chamber of different materials. Finally, it is concluded that different temperature changes and different pressure changes have little influence on the PID temperature control algorithm. This proves that the PID temperature control algorithm can be used normally in reaction chambers with different materials, temperatures, and pressures. The optimization of the traditional PID algorithm found that the error of the optimization algorithm is fewer in the temperature control process, and the maximum difference between the prediction error and the actual error is 3°C and 5°C. The optimization results of the PID temperature control algorithm are ideal. Although this study pro-

vides a lot of research data, the sample size used in the comparison is still small. The size will be expanded in the future, and the practical application of the PID temperature control algorithm will be strengthened.

#### Data Availability

The labeled dataset used to support the findings of this study are available from the corresponding author upon request.

#### Conflicts of Interest

The author declares no competing interests.

#### References

- [1] H. B. Zhang, S. Christopher, and L. Marshall, "ALD: new catalyst synthesis and modification process (English)," *Chinese Journal of Catalysis*, vol. 40, no. 9, pp. 91–103, 2019.
- [2] R. Li, F. Wu, P. Hou, and H. Zou, "Performance assessment of FO-PID temperature control system using a fractional order LQG benchmark [J]," *IEEE Access*, vol. 8, no. 99, pp. 116653–116662, 2020.
- [3] N. Gilbert and F. V. Leeuwen, "Chromatin modified in a molecular reaction chamber," *Nature*, vol. 579, no. 7800, pp. 503–504, 2020.
- [4] S. Tomer, A. Vandana, J. Panigrahi, R. Srivastava, and C. M. S. Rauthan, "Importance of precursor delivery mechanism for Tetra-kis-ethylmethylaminohafnium/water atomic layer deposition process," *Thin Solid Films*, vol. 692, p. 137629, 2019.
- [5] H. Huang, S. Zhang, Z. Yang et al., "Modified Smith fuzzy PID temperature control in an oil-replenishing device for deep-sea hydraulic system," *Ocean Engineering*, vol. 149, no. 1, pp. 14–22, 2018.
- [6] M. Li, W. Wu, and X. Yang, "Research on fuzzy fractional order PID control of liquid temperature in displacement digester [J]," *Palpu Chongi Gisul/Journal of Korea Technical Association of the Pulp and Paper Industry*, vol. 52, no. 5, pp. 15–30, 2020.
- [7] F. Grillo, V. B. Hao, D. L. Zara, and A. A. I. Aranink, "From single atoms to nanoparticles: autocatalysis and metal aggregation in atomic layer deposition of Pt on TiO<sub>2</sub> nanopowder," *Small*, vol. 14, no. 23, pp. 45–46, 2018.
- [8] Y. Mu, T. L. Hu, C. Chen, H. Gong, and S. J. Li, "Development of temperature control system of DFB laser using analog PID control [J]," *Infrared and Laser Engineering*, vol. 48, no. 4, p. 405001, 2019.
- [9] D. M. Fryauf, A. C. Phillips, M. J. Bolte, A. Feldman, G. S. Tompa, and N. P. Kobayashi, "Scaling atomic layer deposition to astronomical optic sizes: low-temperature aluminum oxide in a meter-sized chamber [J]," *ACS Applied Materials & Interfaces*, vol. 10, no. 48, pp. 41678–41689, 2018.
- [10] E. R. Borujeny, O. Sendetskyi, and M. D. Fleischaer, "Low thermal budget heteroepitaxial gallium oxide thin films enabled by atomic layer deposition [J]," *ACS Applied Materials and Interfaces*, vol. 12, no. 39, pp. 44225–44237, 2020.
- [11] Y. Wu, M. H. Raza, Y. C. Chen, P. Amsalem, and N. Pinna, "A self-limited atomic layer deposition of WS<sub>2</sub> based on the chemisorption and reduction of Bis(t-

- butylimino)bis(dimethylamino) complexes [J],” *Chemistry of Materials*, vol. 31, no. 6, pp. 1881–1890, 2019.
- [12] A. Alnuaimi, I. Almansouri, I. Saadat, and A. Nayfeh, “High performance graphene-silicon Schottky junction solar cells with  $\text{HfO}_2$  interfacial layer grown by atomic layer deposition,” *Solar Energy*, vol. 164, pp. 174–179, 2018.
- [13] M. Snure, S. R. Vangala, T. Prusnick, G. Grzybowski, and K. D. Leedy, “Two-dimensional BN buffer for plasma enhanced atomic layer deposition of  $\text{Al}_2\text{O}_3$  gate dielectrics on graphene field effect transistors,” *Scientific Reports*, vol. 10, no. 1, p. 14699, 2020.
- [14] Z. Zhu, S. Merdes, and O. Ylivaara, “ $\text{Al}_2\text{O}_3$  thin films prepared by a combined thermal-plasma atomic layer deposition process at low temperature for encapsulation applications,” *Physica Status Solidi (a)*, vol. 217, no. 8, 2020.
- [15] J. Q. Li, J. P. Li, J. Z. Wang, and J. M. Sun, “Structure and dielectric property of high-k  $\text{ZrO}_2$  films grown by atomic layer deposition using tetrakis(dimethylamido)zirconium and ozone,” *Nanoscale Research Letters*, vol. 14, no. 1, p. 154, 2020.
- [16] S. Kui, W. Ming, Y. Guo, and X. Feng, “Improving the performance of thermoelectric materials by atomic layer deposition-based grain boundary engineering,” *Structural Chemistry*, vol. 39, no. 5, p. 7, 2020.
- [17] J. Zhang, H. Sun, Y. Qi, and S. Deng, “Temperature control strategy of incubator based on RBF neural network PID,” *World Scientific Research Journal*, vol. 6, no. 1, pp. 7–15, 2020.
- [18] Z. A. Zhe, K. A. Ye, and L. A. Chang, “Atomic layer deposition-induced integration of N-doped carbon particles on carbon foam for flexible supercapacitor,” *Journal of Inorganic Materials (English)*, vol. 6, no. 1, pp. 209–215, 2020.
- [19] D. Gaboriau, M. Boniface, A. Valero et al., “Atomic layer deposition alumina-passivated silicon nanowires: probing the transition from electrochemical double-layer capacitor to electrolytic capacitor[J],” *ACS Applied Materials & Interfaces*, vol. 9, no. 15, p. 13761, 2017.
- [20] S. Zhang, E. Yu, S. Gates et al., “Helium interactions with alumina formed by atomic layer deposition show potential for mitigating problems with excess helium in spent nuclear fuel,” *Journal of Nuclear Materials*, vol. 499, pp. 301–311, 2018.
- [21] Y. Yang, L. Na, and J. Sun, “Intense electroluminescence from  $\text{Al}_2\text{O}_3/\text{Tb}_2\text{O}_3$  nanolaminate films fabricated by atomic layer deposition on silicon,” *Optics Express*, vol. 26, no. 7, pp. 9344–9352, 2018.
- [22] X. Shen, C. Li, C. Shi et al., “Core-shell structured ceramic non-woven separators by atomic layer deposition for safe lithium-ion batteries,” *Applied Surface Science*, vol. 441, no. 31, pp. 165–173, 2018.
- [23] Z. Ou, Y. Yang, and J. Sun, “Electroluminescent  $\text{Yb}_2\text{O}_3:\text{Er}$  and  $\text{Yb}_2\text{Si}_2\text{O}_7:\text{Er}$  nanolaminate films fabricated by atomic layer deposition on silicon,” *Optical Materials*, vol. 80, pp. 209–215, 2018.
- [24] X. U. Zhi, X. U. Ming, W. Cheng, H. Peng, and Y. Ding, “High-precision, temperature control based on grading-structure and PID-feedback strategies,” *Transactions of the Japan Society for Aeronautical and Space Sciences*, vol. 61, no. 2, pp. 51–59, 2018.
- [25] M. M. Gani, M. S. Islam, and M. A. Ullah, “Optimal PID tuning for controlling the temperature of electric furnace by genetic algorithm [J],” *SN Applied ences*, vol. 1, no. 8, p. 880, 2019.
- [26] A. Magalhes, J. D. Backer, and G. Bolmsj, “Thermal dissipation effect on temperature-controlled friction stir welding [J],” *Soldagem & Inspeção*, vol. 24, no. 3, pp. 24–32, 2019.
- [27] H. W. Yin, Y. J. Zhao, and X. G. Nie, “Design of temperature control and bipolar PID control algorithm for heating room based on ARM,” *Journal of Pingdingshan University*, vol. 34, pp. 35–40, 2019.
- [28] J. Możaryn, J. Petryszyn, and S. Ozana, “PLC based fractional-order PID temperature control in pipeline: design procedure and experimental evaluation [J],” *Meccanica*, vol. 56, no. 4, pp. 855–871, 2021.
- [29] Y. Cheng, “Research on intelligent control of an agricultural greenhouse based on fuzzy PID control [J],” *Journal of Environmental Engineering and Science*, vol. 15, no. 3, pp. 113–118, 2020.
- [30] M. F. Al Andzar and R. D. Puriyanto, “PID control for temperature and motor speed based on PLC [J],” *Signal and Image Processing Letters*, vol. 1, no. 1, pp. 7–13, 2019.
- [31] A. Shikano, L. Tonthat, and S. Yabukami, “A simple and high-accuracy PID-based temperature control system for magnetic hyperthermia using fiber optic thermometer,” *IEEE Transactions on Electrical and Electronic Engineering*, vol. 16, no. 5, pp. 807–809, 2021.
- [32] S. J. Hammoodi, K. S. Flayyih, and A. R. Hamad, “Design and implementation speed control system of DC motor based on PID control and matlab simulink [J],” *International Journal of Power Electronics and Drive Systems*, vol. 11, no. 1, p. 127, 2020.
- [33] Q. Cheng and K. Zhang, “Design of temperature intelligent PID control system based on genetic algorithm,” *Journal of Shenyang University of Technology*, vol. 40, no. 4, pp. 459–463, 2018.
- [34] L. Hua, C. T. Zhang, W. Q. Lu, and J. Wang, “Stove temperature control application simulation based on fuzzy self-adaptive PID,” *Journal of Guangxi University of Technology*, vol. 29, pp. 37–42, 2018.
- [35] H. Liang, Z. K. Sang, Y. Z. Wu, Y. H. Zhang, and R. Zhao, “High precision temperature control performance of a PID neural network- controlled heater under complex outdoor conditions,” *Applied Thermal Engineering*, vol. 195, no. 1, p. 117234, 2021.

## Research Article

# Analysis of an Enterprise Human Resource Management Performance Evaluation Model Based on the DEA Method

Bing Gao <sup>1</sup> and XiMeng Zhang<sup>2</sup>

<sup>1</sup>*School of Management, Henan University of Science and Technology, Luoyang 471000, China*

<sup>2</sup>*International Education College, Henan University of Science and Technology, Luoyang 471000, China*

Correspondence should be addressed to Bing Gao; 9905553@haust.edu.cn

Received 19 January 2022; Revised 24 February 2022; Accepted 9 March 2022; Published 8 April 2022

Academic Editor: Wen Zeng

Copyright © 2022 Bing Gao and Xi Meng Zhang. This is an open access article distributed under the Creative Commons Attribution License, which permits unrestricted use, distribution, and reproduction in any medium, provided the original work is properly cited.

Performance evaluation is an important and central part of the human resource management system and the process of assessing performance and documenting performance with uniform criteria. Based on the hypothesis of high-performance work systems and HRM effectiveness, this paper proposes a DEA model for evaluating the performance of HRM in enterprises through case studies, field interviews, and questionnaires and tests the validity of the model, by establishing an evaluation index system with HRM in large enterprises as the core, orders and customers as output indicators, and the number of personnel and total costs as input indicators and using the AHP method to optimise the DEA model applied to specific cases for testing. At the same time, the degree of variation between technical level, professional level, and strategic HRM gradually narrows as the HRM performance of the enterprise increases. Finally, targeted solution suggestions are given in relation to the actual situation.

## 1. Introduction

As we all know, the human resources system in China was established relatively late, and the overall performance of human resource management in enterprises is relatively lagging behind, but the performance itself is a very important part of the process of human resources development in enterprises. For the purpose of further improving the overall economic efficiency of enterprises, scientific research must be conducted on the performance evaluation system, in addition to this, the objective requirements of the times should be fully integrated with theory and practice, and the relevant research content should be put into practice from the practical point of view, in order to achieve the premise of further improving the overall economic efficiency of enterprises and to realise the system performance and human resource management-related theory. This is also vital for the long-term development of the enterprise.

Performance evaluation plays a very important role in the development of human resources. There is a strong link between work, pay, training, and performance, and the per-

formance system is also the type of system that has a direct link with the employees of the company [1]. It is also a fundamental type of system that is directly linked to the employees. The performance system determines to a large extent the effectiveness of the company's own operations. Firstly, the determination of remuneration must be based on performance assessment. The basic principle of distribution according to work in China must be based on performance appraisal, which is also the basis for the reasonable distribution of the remuneration package of the enterprise's employees, or the most important basis for determining the wages of the enterprise's employees, especially the floating wages [2, 3]. Through the application of the performance evaluation system, it not only is possible to improve the basic state of the employees' work to a large extent but also has a very important role in cultivating the overall enthusiasm and initiative of the employees. Secondly, the placement and promotion of staff are based on performance appraisal. The placement of staff should be adjusted on the basis of the performance appraisal of the staff concerned. In addition, in the actual job transition process, the staff's own

TABLE 1: Main items and contents of performance appraisal.

Tier 1 indicators	Tier 2 indicators	Tier 3 indicators
Product indicators	Number of orders	Number of standing orders Number of random orders
	Number of clients	Long-term clients Random clients
Input indicators	Costs	Advertising costs Other costs
	Personnel	Company staff Other staff

TABLE 2: Quarterly performance indicators.

Decision-making units	Input indicators		Output indicators	
	Number of employees	Total costs	Number of orders	Number of customers
DMU (1)	32	50	72	40
DMU (2)	24	64	6	8
DMU (3)	60	24	46	40
DMU (4)	56	50	16	20
DMU (5)	18	30	44	16
DMU (6)	76	56	20	40

working ability must be determined by means of performance appraisal, so that the deployment of staff can be completed better [4]. Thirdly, the planning of employees' future careers must be based on performance appraisals. Performance appraisals can provide a more accurate understanding of the employee's own abilities, so as to plan the future career direction for the employee, and it is also vital to maximise the effect of future training for the employee [5]. Fourthly, the motivation of the employees themselves must be mobilised through performance appraisal. By linking the performance appraisal system to rewards and introducing a system of rewards and penalties [6, 7], it is also important for employees to be motivated to excel in the future.

Gronroos [8] proposed the concept of customer-perceived service quality (CPQ) or service performance as a tool to measure the extent to which the service level of an enterprise can meet customer expectations. Parasuraman et al. [9–11] viewed service performance as the difference between the level of service performance perceived by customers and the level of service performance expected and proposed the SERVQUAL model to evaluate service performance. Subsequently, the SERVQUAL scale has been widely used in service industries such as retail, catering, IT services, banking, insurance, transport, and libraries [12–15]. In addition to performance management methods for tangible products and services, internal corporate management has also applied performance management theories and methods such as internal customer service performance and satisfaction to improve effectiveness or efficiency, and service processes and standards have been developed in the professional fields of accounting, auditing, training, and IT services. For example, in the 1980s, the UK National Com-

puter and Telecommunications Agency (CCTA) proposed a set of IT service management standards library—the IT Infrastructure Library (ITIL) [16]. The library of standards was applied and recognised in UK businesses and became a common international standard in the field of IT services. In the three major international performance awards such as the Malcolm Baldrige National Performance Award in 1987, the European Performance Award in 1992, and the Deming Award in Japan in 1951, human resource management constitutes a performance indicator for evaluation [17]. In August 2004, the Chinese National Standard GB/T19580-2004 also contains performance indicators for human resource management. This set of standards has gradually been applied and promoted in enterprises such as Haier.

In the existing quality award evaluation guidelines, the quality standards of HRM focus on process records, control standards, and documentary evidence in HRM processes, such as training time and operational documentation records. There is a lack of quality theories and methods for corporate HRM and a lack of frameworks and standards for judging the quality of corporate HRM. At the same time, the human resource management (HRM) theory and practice have long focused on the enhancement of job performance by individual factors. Researchers in the fields of selection, performance, and compensation management have based their management decisions primarily on the assessment of individual differences, and an underlying logical assumption of these studies is that individual characteristics can determine changes in job performance. However, researchers who view HRM as a system have proposed concepts and theories such as high-performance work systems [18], HRM best practices [19], and HRM control systems [20], which suggest that there are several best HR practices or work systems that will have a direct impact on organisational performance to such an extent that they can affect organisational performance regardless of changes in organisational conditions or circumstances that can affect organisational performance [21, 22]. Among these, Waldman [23] argues that systemic factors can have an impact on job performance, whereas previously systemic factors were treated as uncontrollable factors.

In recent years, human resource management theory and many enterprises are studying the methods and implementation of performance appraisal, and the performance appraisal of enterprise marketing personnel is particularly

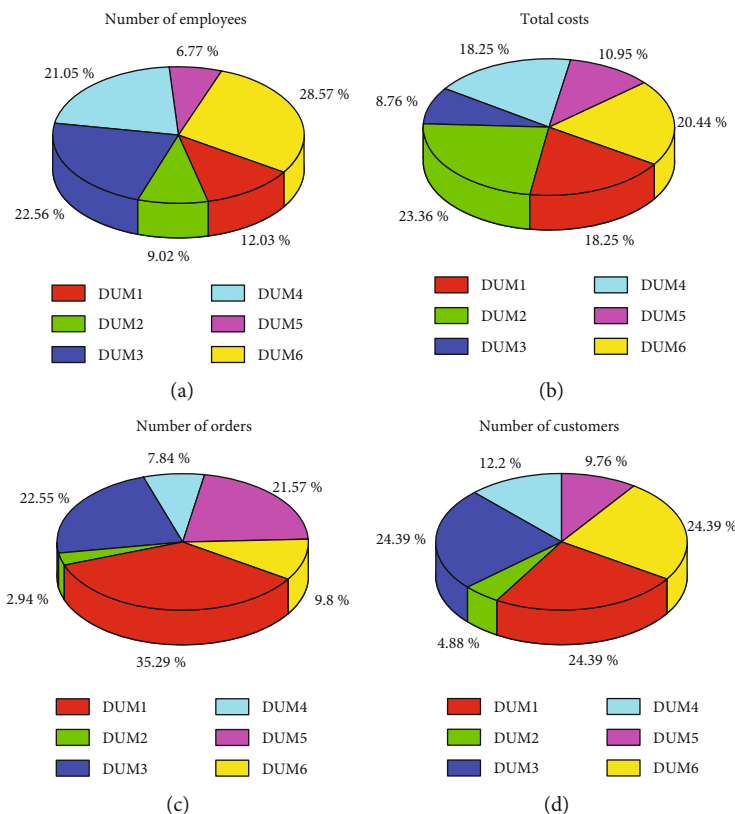


FIGURE 1: Comparison of pie charts of performance input and output parameters across the six divisions. (a) Number of employees. (b) Total costs. (c) Number of orders. (d) Number of customers.

TABLE 3: Selected Input index.

DMU ( <i>i</i> )	Input1/10 thousand	Input2/person
DMU (1)	8.36	8
DMU (2)	10.64	11
DMU (3)	8.15	5
DMU (4)	6.68	4
DMU (5)	18.26	9
DMU (6)	15.70	12

important. However, there are currently some problems in the performance appraisal of marketing personnel in enterprises, such as the lack of performance appraisal indicators and standards and neglect of the performance appraisal of the team. In practical application, there are many methods of performance evaluation concerning human resource management. For example, Argenti (1976), kravarthy (1986) established a multifactor evaluation model, but because the weight of the evaluation model is difficult to determine, it is more difficult to operate in the practical application; the same traditional AHP method is also due to the determination of the weight, so that the model and method increase the subjectivity of people leading to inaccurate assessment results; from 1978, the DEA method is used in domestic and foreign decision-making. Since 1978, the DEA method has been widely used in the field of decision-making at home and abroad, but as it tends to lose potential optimal combinations when used alone, on this basis, many

scholars have proposed improved algorithms for DEA, and thus, the DEA/AHP model was created.

## 2. The Complexity of Enterprise HRM Performance Evaluation and the Issues It Should Address

Performance evaluation is a very important part of an enterprise's human resource management system and is one of the most critical indicators for managers to evaluate performance. However, at present, the construction of performance evaluation systems in domestic HRM systems is still in its infancy, with many companies relying on performance evaluation for systematic alignment and overall evaluation. However, as the most important application of performance evaluation is to analyse the relevant data in the evaluation system, which is done within a specific time frame, a complete evaluation system has not yet been formed from the perspective of the long-term application, and the most important reason for the above problems is that many enterprises in China currently have a large lack of knowledge about the performance evaluation system; the importance attached to the evaluation system is also the most important reason for the above problems that many enterprises in China are not aware of the performance appraisal system, and the degree of importance they attach to it is also clearly insufficient.

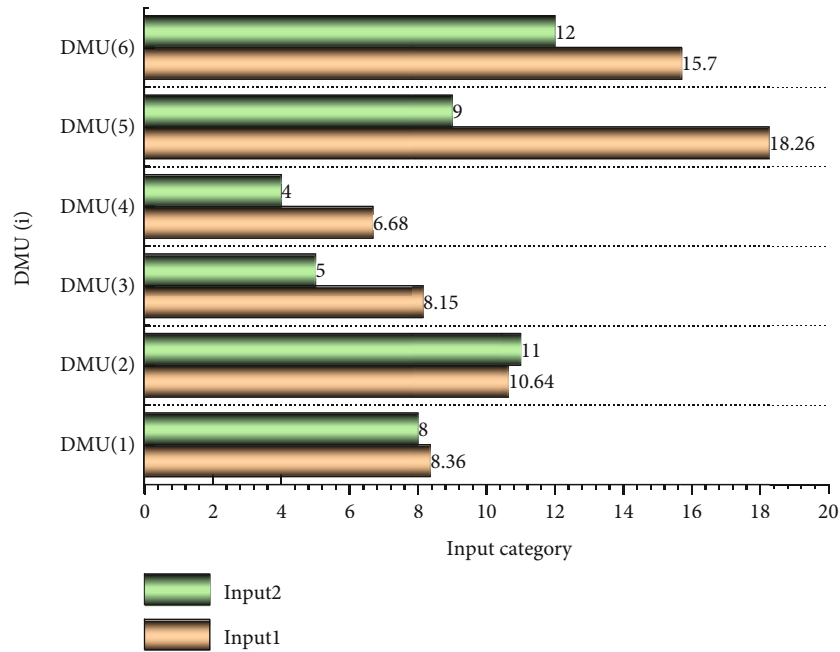


FIGURE 2: Comparison of the two input value tables.

TABLE 4: Output statistic data.

DMU (i)	Business ratio	Operating cost	Quality of work life	Satisfaction	Cycle efficiency	Utilisation	Organisational efficiency	Equipment	Efficiency
DMU (1)	78.00	0.51	0.68	0.78	17.14	0.75	0.82	0.73	0.86
DMU (2)	68.82	0.42	0.75	0.85	20.80	0.83	0.86	0.70	0.83
DMU (3)	76.67	0.64	0.70	0.75	17.70	0.78	0.79	0.78	0.87
DMU (4)	72.50	0.77	0.73	0.71	14.30	0.85	0.90	0.86	0.93
DMU (5)	86.25	0.81	0.82	0.84	12.50	0.89	0.85	0.83	0.92
DMU (6)	84.00	0.47	0.66	0.70	15.98	0.73	0.72	0.72	0.79

Performance evaluation is one of the most crucial components in the development of human resources in enterprises, but it has been a relatively short period of time since the performance evaluation system was adopted as a management system in China, and therefore, there is relatively little research on it [24]. Based on this, the problems related to the performance evaluation of human resource management systems in domestic enterprises are addressed, and the performance evaluation of enterprise human resource management is targeted to achieve the purpose of better human resource management.

The evaluation process of HRM performance should pay attention to the following issues: (1) The implementation of HRM will have an impact on all aspects of enterprise operations, and the evaluation of HRM performance cannot only evaluate the performance of the business process itself [25]. (2) The HRM proposed in the paper is on the basis of a sys-

tem, which is an input-output system, so the performance evaluation has multiple input and output evaluation issues. It shows that HRM performance has measurability, and the most accurate evaluation of HRM implementation can be achieved by integrating all input and output indicators and establishing a complete indicator system. (3) HRM is a long-cycle process, and the evaluation indicators that enterprises pay attention to at different stages of HRM implementation are also different.

*2.1. Determination of an Enterprise HRM Performance Evaluation Index System.* HRM has an important relationship with the internal support system, the capability support system, and the resource input support system, and each support system has an independent contribution to HRM performance. Among them, each variable in resource input can be regarded as HRM input, and all of them can be used

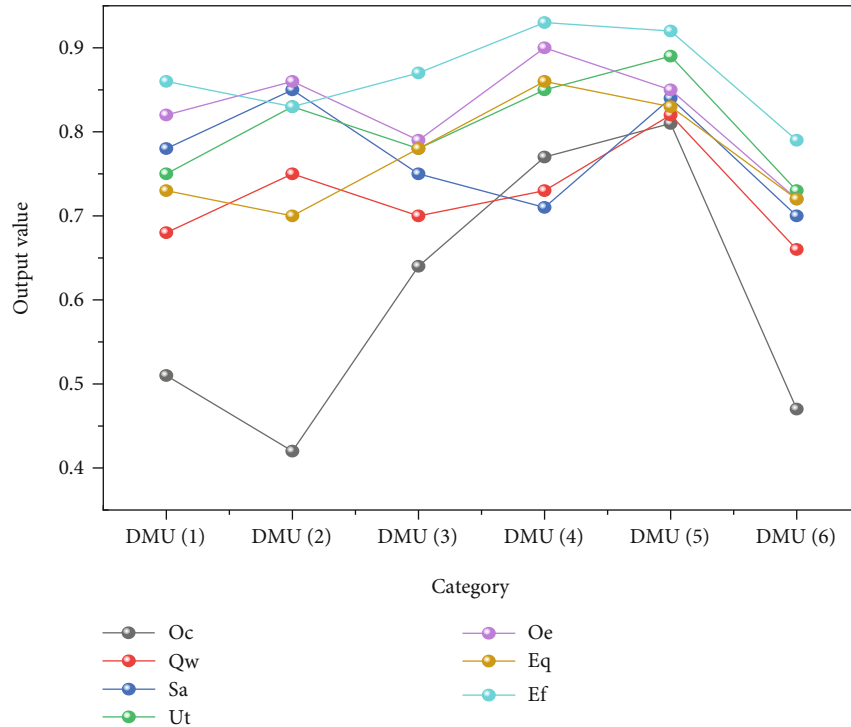


FIGURE 3: Comparison of output data for the two output indicators.

TABLE 5: Valid values for the 6 decision units.

DMU ( <i>i</i> )	1	2	3	4	5	6
DMU (1)	0.2145	0.3210	0.2070	0.2461	0.1949	0.1772
DMU (2)	0.0579	0.0872	0.1035	0.1146	0.0740	0.1497
DMU (3)	0.2145	0.1743	0.2071	0.2282	0.1950	0.1995
DMU (4)	0.1073	0.0937	0.1117	0.1232	0.1461	0.1578
DMU (5)	0.1908	0.0918	0.1636	0.1233	0.1949	0.1577
DMU (6)	0.2146	0.2295	0.2070	0.1642	0.1949	0.1577

as input indicators for HRM performance evaluation, while the indicators of HRM implementation effect can be used as output indicators [26]. The input-output indicator system of HRM performance evaluation is established by considering the input of enterprises to the implementation of HRM and the complexity of HRM performance evaluation. In order to improve the overall competitiveness of the company, the business processes of the company are redesigned in order to obtain an improvement in performance in terms of costs, etc. This improvement is mainly reflected in the economic benefits achieved by the company and the increase in organisational efficiency. In this paper, we use effectiveness and efficiency to measure the economic and organisational value of HRM. The performance appraisal of HRM must be carried out in order to achieve the enterprise’s goals, so the development of its appraisal index system also needs to reflect the long-term and short-term goals of the enterprise, so the performance appraisal index can be determined to objectively reflect both the short-term and long-term benefits of the enterprise. The indicators for performance appraisal are shown in Table 1.

### 3. Construction of the DEA/AHP Model

3.1. *Introduction to the DEA Model.* The method and model were developed by the famous American operations researchers W. W. Cooper, A. Charnier, and others as a way to evaluate efficiency [27]; it is a useful method to study the relative effectiveness between decision units with the same type of decision; here, the C2R model is introduced, and the model is as follows.

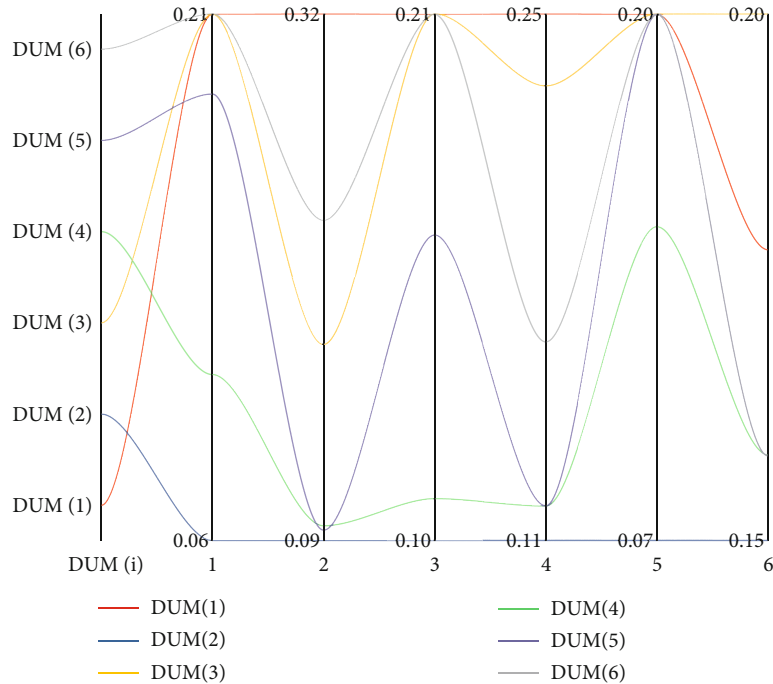
Suppose there are  $n$  DMUs, each using  $m$  inputs  $x_i$  ( $i = 1, 2 \dots \dots, m$ ) to produce  $s$  output  $y_r$  ( $r = 1, 2, \dots, s$ ). represents the potential amount by which  $DMU_k$  all input terms can be scaled down in equal proportions; the weights  $\lambda = (\lambda_1, \lambda_2 \dots \dots, \lambda_n)$  represent a polyhedral vector linking all information, and the  $C^2R$  model can then be expressed as

$$\begin{aligned} & \max [\theta - \varepsilon(\hat{e}^T s^- + e^T s^+)] \\ & \text{s.t. } \sum_{j=1}^n x_j \lambda_j + s^- = \theta x_{j0} \quad \sum_{j=1}^n y_j \lambda_j - s^+ = y_{j0} \end{aligned} \quad (1)$$

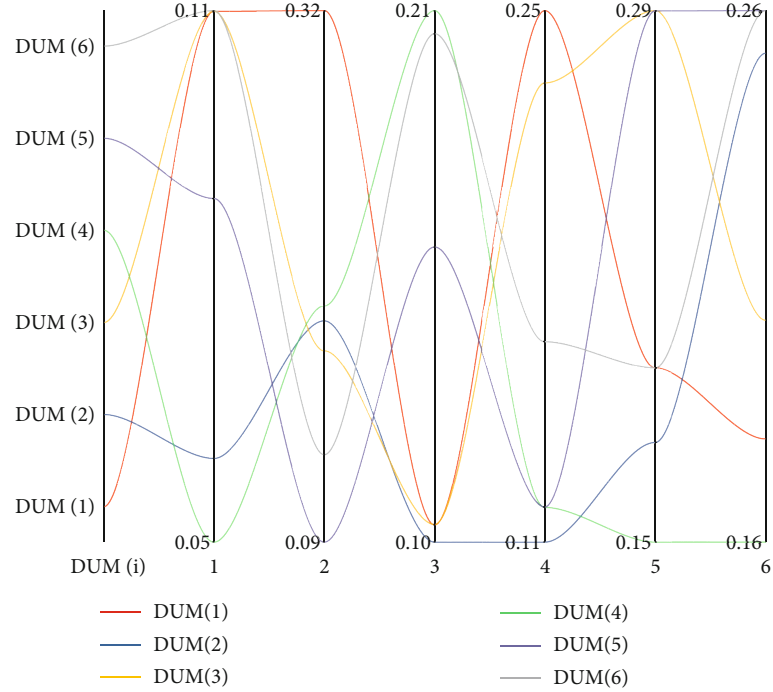
$\lambda_j \geq 0; j = 1, 2, \dots, n$ ,  $s^-$  is the slack variable, and  $s^+$  is the residual variable.

$\hat{e}$  and  $e$  are  $m$ -dimensional and  $s$ -dimensional column vectors with component 1, respectively;  $\varepsilon$  is a non-Archimedean infinitesimal quantity (a quantity smaller than any quantity greater than zero).

3.2. *Optimising DEA Models Using AHP.* In this paper, a modified DEA/AHP method is used to divide all the decision-making units (DMUs) into two groups and compare them with each other using the traditional DEA



(a)



(b)

FIGURE 4: Comparison of the effective values of the 6 decision units (a) Output1. (b) Output2.

method. As the AHP here has only one level, the size of the eigenvector at position  $i$  here reflects the priority of the  $i$ th decision unit.

3.3. *Constructing Judgement Matrices Using the DEA Method.* If there are a total of  $n$  decision units, each with a total of  $m$  input indicators and  $s$  output indicators, any

two decision units are divided into a group, assumed to be 1 and 2, and their RMS values are calculated separately. Since even decision units with a relative validity value of 1 are not necessarily all good in overall performance, in order to be able to distinguish whether a decision unit is better overall, we use cross-efficiency to evaluate it, a way of providing the cross-efficiency of a decision unit under the most



TABLE 6: Ranking of weight values for the six divisions.

DMU ( <i>i</i> )	DEA/AHP calculated value (weight)	Rank
DMU (1)	0.2364	1
DMU (2)	0.1018	6
DMU (3)	0.1710	3
DMU (4)	0.1283	5
DMU (5)	0.2026	2
DMU (6)	0.1599	4

favourable weighting of the other decision units. The specific model is as follows.

$$\begin{aligned}
 \max &= h_{11} = \sum_{r=1}^s U_r y_{r1} \\
 \text{s.t.} & \sum_{r=1}^m U_r y_{rj} - \sum_{i=1}^m V_i x_{ij} \leq 0 \quad j = 1, 2, \\
 & \sum_{i=1}^m V_i x_{i1} = 1 \\
 & U_r \geq \varepsilon > 0, \quad r = 1, 2, \dots, s, \\
 & V_i \geq \varepsilon > 0 \quad i = 1, 2, \dots, m,
 \end{aligned} \quad (2)$$

$$\begin{aligned}
 \max &= h_{21} = \sum_{r=1}^s U_r y_{r2} \\
 \text{s.t.} & \sum_{r=1}^m U_r y_{r1} - \sum_{i=1}^m V_i x_{i1} = 0 \quad j = 1, 2, \\
 & \sum_{i=1}^m V_i x_{i2} = 1 \\
 & \sum_{r=1}^s U_r y_{r2} \leq 1 \\
 & U_r \geq \varepsilon > 0, \quad r = 1, 2, \dots, s,
 \end{aligned} \quad (3)$$

where  $m$  is the number of input indicators,  $s$  is the number of output indicators,  $n$  is the number of decision units, and  $v_i$  is the weight of input indicator  $i$ .  $u_r$  is the weight of output indicator  $r$ .  $X_{ij}$  is the value of input indicator  $i$  for the  $j$ th decision unit.  $y_{rj}$  is the value of output indicator  $r$  for the  $j$ th decision unit. And so on,  $h_{ab}$  and  $h_{bb}$  can be derived.

The ratio of the efficiency of decision unit 1 to decision unit 2 is

$$a_{12} = (h_{11} + h_{12}) / (h_{22} + h_{21}). \quad (4)$$

In general, for  $n$  decision units, their two-by-two efficiency ratio is

$$\begin{aligned}
 a_{ij} &= (h_{ij} + h_{ji}) / (h_{ji} + h_{jj}), \\
 a_{ji} &= 1/a_{ij}, \\
 a_{ii} &= 1.
 \end{aligned} \quad (5)$$

Using the DEA method above, a judgement matrix can be constructed. Moreover, the matrix constructed by this method does not contain subjectivity and does not require a consistency test.

**3.4. Sorting by the AHP Method.** Using the judgement matrix derived from the DEA method above, the AHP method is applied to solve for the maximum eigenvalue of the judgement matrix and its eigenvector [28]. Since the AHP in the above algorithm has only one level, the eigenvector ranked in the  $j$ th position is also the priority of the  $j$ th decision unit.

## 4. Empirical Analysis

**4.1. Example.** A large enterprise completes its sales tasks for the year and has an existing department divided into six divisions (DMU1-DMU6). The quarterly performance of its six teams is evaluated, and the evaluation indicators are divided into the number of employees, total costs, number of orders, and number of customers according to the nature of the inputs and outputs, as shown in Table 2.

A pie chart of the input and output indicators is given in Figure 1.

### 4.2. Calculation of Input Indicators

- (1) Capital input indicator: HRM consulting cost is borne by these 6 DMUs on average; the labour cost of personnel is calculated by multiplying the number of personnel directly involved in HRM in each department by the average labour cost; the training cost is calculated by multiplying the number of personnel involved in relevant training in each department by the average training cost per person; the equipment cost is calculated by combining the costs of relevant equipment purchased for each department. In other words, capital investment = HRM consulting fee + labour cost of personnel + training cost + equipment cost
- (2) The input of the number of personnel is determined by the sum of the number of employees and leaders of the department who directly participate in HRM
- (3) The input of staff participation and support is calculated by summing fuzzy mathematical methods
- (4) The time commitment indicator is the sum of the time spent on training by each subdepartment

The sum of the time spent on the implementation of the HRM project is calculated. The data for the input indicators are shown in Table 3.

A visual comparison histogram of the two input indicators is given in Figure 2.

**4.3. Calculation of Output Indicators.** The evaluation indicators of both effectiveness and organisational efficiency are multi-indicator comprehensive evaluation problems, and the nature of each subindicator varies greatly, so the efficacy coefficient method is used in this paper to process these 2

TABLE 7: Synthetic efficacy coefficients of benefit and organisational efficiency.

Serial number	Comprehensive efficacy coefficient								
	DMU (1)	DMU (2)	DMU (3)	DMU (4)	DMU (5)	DMU (6)	DMU (7)	DMU (8)	DMU (9)
Output1	70.00	68.56	71.59	73.56	79.25	69.89	76.52	78.36	72.33
Output2	72.06	75.63	73.45	75.98	73.42	67.84	79.65	76.32	72.16

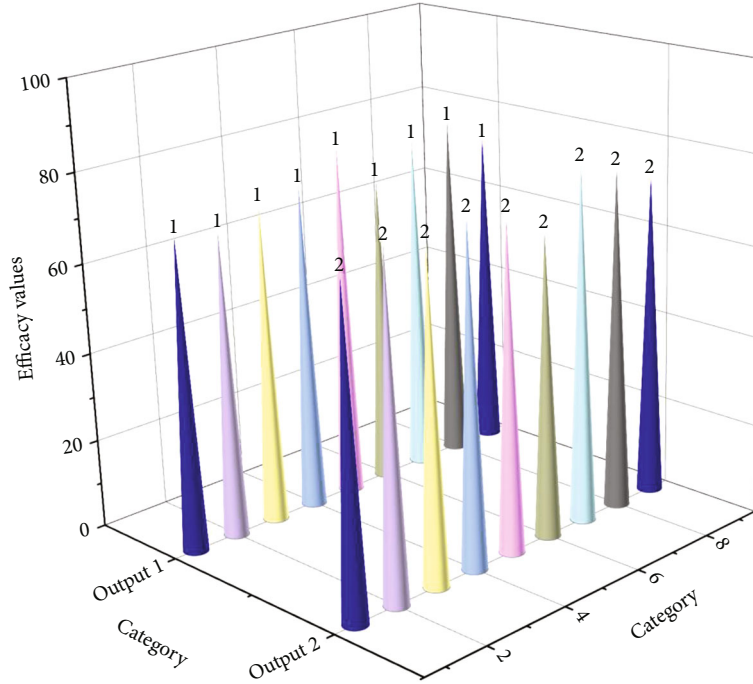


FIGURE 5: Comparison of data by division for the two outputs.

output indicators [29]. Table 4 shows the output indicator data.

In Figure 3, a visual comparison of the output data obtained by processing the two output indicators is presented.

4.4. *Finding the Valid Values of the Decision Cells.* Using Equations (2) and (3), the valid values of each decision cell in each group were solved using the operations research software QM, and the valid values were obtained as in Table 5.

A comparison of the decision values for the six cells of the two outputs is shown in Figure 4.

Some of the indicators are given in Table 6 in order to compare values for each component of the data using the fuzzy integrated judgement method. The utilisation rate of human resources is the ratio of the number of personnel used to the total number of employees on the rolls. Cost ratio of business process value-added activities and process activity cycle efficiency were calculated by the job cost method in the literature [30]. The paper’s algorithm assigns a weight of 3 to the more important indicators, followed by a value of 2. The others are sufficient to distinguish the relative quantitative degree of each evaluation indicator, and the efficacy coefficients are shown in Table 7.

A comparison of the two outputs is shown in Figure 5.

4.5. *The Final Judgement Matrix A of the DEA Model Is Obtained by a Two-by-Two Comparison.*

$$A = \begin{bmatrix} 1 & 3.704 & 1 & 2 & 1 & 1.124 \\ 0.2698 & 1 & 0.498 & 0.930 & 0.380 & 0.950 \\ 1 & 2 & 1 & 0.852 & 1 & 1.266 \\ 0.5 & 1.075 & 0.540 & 1 & 0.749 & 1 \\ 1 & 2.632 & 1 & 1.333 & 1 & 1 \\ 0.889 & 1.053 & 0.791 & 1 & 1 & 1 \end{bmatrix} \quad (6)$$

4.6. *AHP Ranking.* The decision unit weights were derived using the known AHP method of ranking, which resulted in the performance of the six divisions of 0.2364, 0.1018, 0.1710, 0.1283, 0.2026, and 0.1599. The ranking of the weight values is as follows.

The ranking using the AHP method yields the weight pairs of decision units as shown in Figure 6.

As can be seen from Table 6, the AHP optimization DEA method has been used to rank the performance of each department using a complementary approach and to further differentiate the process decision units with a valid value of 1

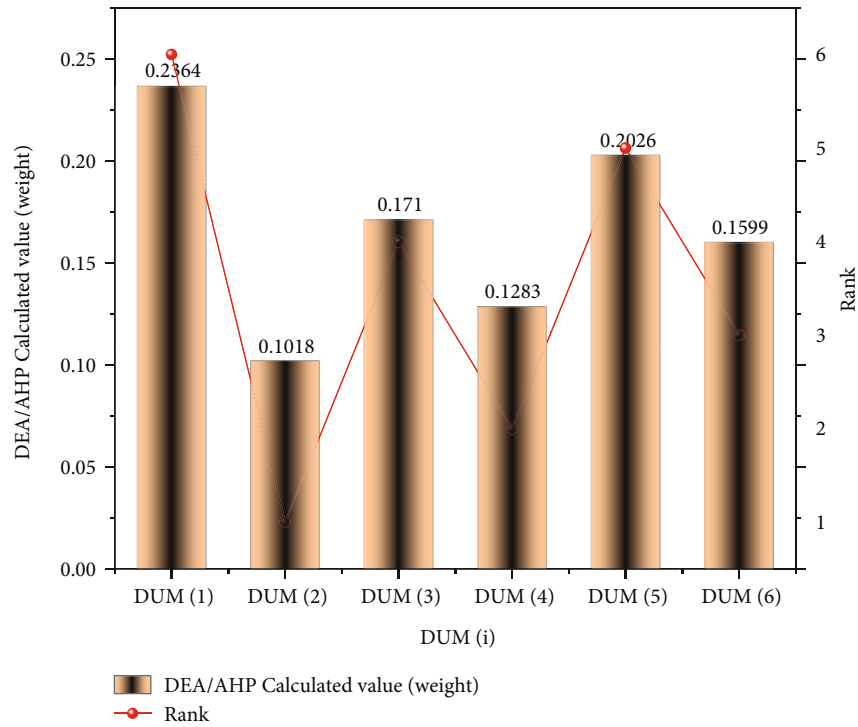


FIGURE 6: Comparison of the weights of the decision units from ranking using the AHP method.

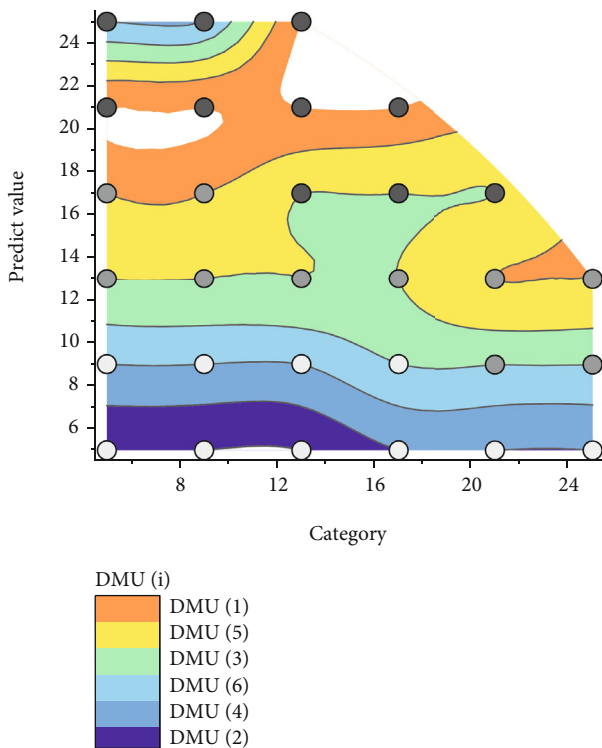


FIGURE 7: Results of the six divisional forecasts.

results of HRM performance evaluation according to each stage. After refinement, the company then selects HRM performance evaluation indicators that meet the objectives of the next phase and uses the abovementioned method to evaluate HRM performance and identify weaknesses and opportunities for improvement, forming a cycle of continuous improvement so that corporate strategy can be achieved through HRM.

Finally, the kernel was used to make predictions about the future development of the six divisions, the results of which are shown in Figure 7.

### 5. Conclusion

The role played by a scientific human resource management performance evaluation system is crucial to the overall development of domestic enterprises, and by building a high-quality, systematic corporate HR performance evaluation system, it is equally crucial to the better future development of domestic enterprises. The use of the AHP-optimised DEA model to evaluate the performance of corporate HRM in the article is reflected in the following three main aspects. On the one hand, the new method realises the problem that the original DEA method cannot be fully ranked and further distinguishes the decision units with an effective value of 1 in DEA. On the other hand, the new method still retains the characteristics of the original DEA, i.e., the analysis of the economic significance of some indicators when evaluating the performance of decision units with multiple inputs and outputs. Finally, the new method compensates for the shortcomings of the traditional AHP method, which is too

in the DEA. The objective judgement matrix used in the AHP method reduces the difficulty of making judgements on process performance.

The company uses the proposed superefficient DEA model to evaluate the performance of HRM and refine the

subjective and dependent, by using data to analyse the validity of the proposed model.

## Data Availability

The data used to support the findings of this study are available from the corresponding author upon request.

## Conflicts of Interest

The authors declare that they have no known competing financial interests or personal relationships that could have appeared to influence the work reported in this paper.

## References

- [1] G. Tasseron and K. Martens, "Urban parking space reservation through bottom-up information provision: an agent-based analysis," *Computers, Environment and Urban Systems*, vol. 64, pp. 30–41, 2017.
- [2] N. K. Avkiran, "Association of DEA super-efficiency estimates with financial ratios: investigating the case for Chinese banks," *Omega*, vol. 39, no. 3, pp. 323–334, 2011.
- [3] L. Wang, "Traffic reservation policy and practice in Shenzhen," *Traffic & Transportation*, vol. 32, Supplement 1, pp. 97–107, 2019.
- [4] G. Xu, H. Yang, W. Liu, and F. Shi, "Itinerary choice and advance ticket booking for high-speed-railway network services," *Transportation Research Part C: Emerging Technologies*, vol. 95, pp. 82–104, 2018.
- [5] J. Li and H. Gao, "Global tourism from the perspective of informatization," *Tourism Tribune*, vol. 31, no. 9, pp. 24–26, 2016.
- [6] M. E. Kuwaiti and J. M. Kay, "The role of performance measurement in business process re-engineering," *International Journal of Operations & Production Management*, vol. 20, no. 11/12, pp. 1411–1426, 2000.
- [7] R. H. Green, J. R. Doyle, and W. D. Cook, "Preference voting and project ranking using DEA and cross-evaluation - Science-Direct," *European Journal of Operational Research*, vol. 90, no. 3, pp. 461–472, 2016.
- [8] Z. Sinuany-Stern, A. Mehrez, and Y. Hadad, "An AHP/DEA methodology for ranking decision making units," *International Transactions in Operational Research*, vol. 7, no. 2, pp. 109–124, 2000.
- [9] K. Zhong, P. Wang, J. Pei, J. Xu, Z. Han, and J. Xu, "Multiobjective optimization regarding vehicles and power grids," *Wireless Communications and Mobile Computing*, vol. 2021, Article ID 5552626, 6 pages, 2021.
- [10] J. R. Doyle and R. H. Green, "Efficiency and cross-efficiency in DEA: derivations, meanings and uses," *Journal of Operational Research*, vol. 45, no. 5, pp. 567–578, 2018.
- [11] Q. Lin, *Research on Parking Problem of Social Vehicles in Baiyun Airport Arrival Curbside Based on Reservation Mechanism*, [MA. Thesis], Institutes of Technology of South China, China, 2017.
- [12] H. D. Sherman and J. Zhu, "Benchmarking with quality-adjusted DEA (Q-DEA) to seek lower-cost high-quality service: evidence from a US bank application," *Annals of Operations Research*, vol. 145, pp. 11–19, 2006.
- [13] H. P. Maria, P. Artur, and M. Luiz, "Motivations, emotions and satisfaction: the keys to a tourism destination choice," *Journal of Destination Marketing & Management*, vol. 16, article 100332, 2019.
- [14] M. Sathye, "Technical efficiency of large bank production in Asia and the Pacific," *Multinational Finance Journal*, vol. 9, no. 1/2, pp. 1–22, 2005.
- [15] Y. Shimizu and Y. Sahara, "A supporting system for evaluation and review of business process through activity-based approach," *Computers & Chemical Engineering*, vol. 24, no. 2-7, pp. 997–1003, 2000.
- [16] R. Dayal, V. Vijayakumar, R. C. Kushwaha et al., "A cognitive model for adopting ITIL framework to improve IT services in Indian IT industries," *Journal of Intelligent & Fuzzy Systems*, vol. 39, no. 6, pp. 26–35, 2020.
- [17] M. Chen, S. Yi, and X. Yang, "A study of application of ABC method in BPR," in *International Conference on Agile Manufacturing, ICAM*, pp. 605–610, Beijing: ICAM, 2019.
- [18] J. Yuan, L. Li, E. Wang, and M. J. Skibniewski, "Examining sustainability indicators of space management in elderly facilities—a case study in China," *Journal of Cleaner Production*, vol. 208, pp. 144–159, 2019.
- [19] J. Feinglass, G. Norman, R. L. Golden, N. Muramatsu, M. Gelder, and T. Cornwell, "Integrating social services and home-based primary care for high-risk patients," *Population Health Management*, vol. 21, no. 2, pp. 96–101, 2018.
- [20] J. Wang and B. Wu, "Domestic helpers as frontline workers in China's home-based elder care: a systematic review," *Journal of Women & Aging*, vol. 29, no. 4, pp. 294–305, 2017.
- [21] J. Shen, S. Tang, and C. Xu, "Analysis and research on home-based care for the aged based on insurance policy under government leading," *AMSE Journals-AMSE IIETA-Series: Advances A*, vol. 54, no. 1, pp. 106–126, 2017.
- [22] L. Egholm, L. Heyse, and D. Mourey, "Civil society organizations: the site of legitimizing the common good—a literature review," *VOLUNTAS: International Journal of Voluntary and Nonprofit Organizations*, vol. 31, no. 1, pp. 1–18, 2020.
- [23] S. P. Osborne, Z. Radnor, and K. Strokosch, "Co-production and the co-creation of value in public services: a suitable case for treatment?," *Public Management Review*, vol. 18, no. 5, pp. 639–653, 2016.
- [24] M. A. Lamboy-Ruiz, J. N. Cannon, and O. V. Watanabe, "Does state community benefits regulation influence charity care and operational efficiency in U.S. non-profit hospitals?," *Journal of Business Ethics*, vol. 158, no. 2, pp. 441–465, 2019.
- [25] G. Zabolotnaya and A. Larionov, "Arrangements for the transfer of social-services delivery to non-governmental providers (regional practices, Russia)," *Nispacee Journal of Public Administration and Policy*, vol. 12, no. 2, pp. 251–274, 2019.
- [26] A. Pawlak, "The quality of care provided in nursing homes for the elderly," *Family Medicine and Primary Care Review*, vol. 3, no. 3, pp. 197–201, 2015.
- [27] C. Y. Chao, P. Y. Ku, Y. T. Wang, and Y. H. Lin, "The effects of job satisfaction and ethical climate on service quality in elderly care: the case of Taiwan," *Total Quality Management & Business Excellence*, vol. 27, no. 3–4, pp. 339–352, 2016.
- [28] P. Leibkuechler, "Trust in the digital age—the case of the Chinese social credit system," in *Redesigning Organizations*, pp. 279–289, Springer, Cham, 2020.

- [29] J. W. Mack, J. Jacobson, D. Frank et al., "Evaluation of patient and family outpatient complaints as a strategy to prioritize efforts to improve cancer care delivery," *The Joint Commission Journal on Quality and Patient Safety*, vol. 43, no. 10, pp. 498–507, 2017.
- [30] H. B. Kwon, J. Lee, and J. J. Roh, "Best performance modeling using complementary DEA-ANN approach," *Benchmarking*, vol. 23, no. 3, pp. 704–721, 2016.

## Research Article

# Research on Furniture Design Integrating Ming-Style Furniture Modeling Elements and Image Sensor Data: Taking Suitable Old Furniture as an Example

Wei Chen <sup>1,2</sup>

<sup>1</sup>Academy of Art & Design, Nanchang Institute of Technology, Nanchang, Jiangxi 330044, China

<sup>2</sup>The Graduate School of Dong-A University, Busan, Republic of Korea 49315

Correspondence should be addressed to Wei Chen; [chenwei@nut.edu.cn](mailto:chenwei@nut.edu.cn)

Received 27 January 2022; Revised 14 March 2022; Accepted 15 March 2022; Published 6 April 2022

Academic Editor: Zhongchang Wang

Copyright © 2022 Wei Chen. This is an open access article distributed under the Creative Commons Attribution License, which permits unrestricted use, distribution, and reproduction in any medium, provided the original work is properly cited.

Ming-style furniture, adhering to the excellent traditional Chinese history and culture, is the pinnacle of traditional Chinese-style furniture, which vividly embodies the cultural essence of Chinese-style furniture. However, with the current popularity of smart home products, there are many obstacles for elderly users to use smart home products. Voice interaction is one of the main interaction methods of smart home products. The design strategy of voice user interface for aging smart home products is studied to improve the experience of elderly users in operating smart home products. Based on image sensing technology, combining Ming-style furniture modeling elements, and based on context theory research, this paper proposes four types of smart home contexts for elderly users, including user context, task context, time context, and environmental context, so as to propose a specific smart home product voice user interface design strategy. According to the user's situational characteristics, a multichannel interaction design of voice user interface is proposed, an emotional and personalized voice user interface is constructed, and a design strategy of context memory assisting the dialogue process is constructed. According to the task, time, and environmental situation of elderly users, it proposes design strategies such as active interactive voice user interface design and provides continuous behavioral service experience. *Conclusion.* The research results provide a method and strategy reference for the design and development of the voice user interface of smart home products and provide a more natural and comfortable experience of using smart home products for elderly users.

## 1. Introduction

Ming-style furniture is a manifestation of social stability and a developed agricultural handicraft industry in the Ming dynasty, and it is also a manifestation of rapid economic development. Carpenters and craftsmen gained more space, especially in the middle and late Ming dynasty, where the economy and commodities were abundant, foreign trade was opened, and the urban economy developed rapidly, especially in Jiangnan and Hainan, which made the various cultural customs and economics of the Ming dynasty exceed the previous generation. In the mid-Ming dynasty, the construction of residential buildings and private gardens entered a prosperous period, and a large number of buildings and gardens needed high-end furniture to furnish them. This

created a large demand for Ming-style furniture. It also promoted the development of furniture manufacturing. A large amount of high-grade wood such as rosewood and red sandalwood were shipped back from Nanyang, which is rich in high-grade wood. The research of furniture craftsmanship and aesthetic exploration by a group of workers and cultural people in the Ming dynasty played a certain role in promoting the maturity of Ming furniture style. Ming-style furniture in China is the pinnacle and treasure in the history of Chinese furniture [1–5].

At present, most scholars and interior designers in China are very interested in understanding and researching the unique Ming furniture in China, especially scholars in universities. There are many articles and materials for learning in books, professional forums, academic journals, and

reports. Although there are many materials, the ones that are truly valuable are rare. Some of the current works did not fully display the cultural essence contained in Ming-style furniture, especially the understanding of the concept of Chinese elements, but this is also an opportunity for us to further improve [6, 7]. The requirements of the aging population for furniture functions must meet the requirements of both ergonomics and physiological functions.

On the other hand, the development of the Internet, Internet of Things, big data, and artificial intelligence technology has made smart home products widely used, providing users with intelligent and convenient services. With the increasingly serious problem of population aging, more and more elderly people come into contact with and use smart home products. Due to their physical, psychological, and behavioral particularities, there are more obstacles in the use of smart home products [8–11]. A good voice user interface design for smart home products plays an important role in improving the experience of elderly users. Due to the natural nature of the interaction method, voice user interfaces have good application prospects in aging smart home products, as shown in Figure 1.

With the support of increasingly mature voice interaction technology, voice interaction has become one of the interactive methods of smart home products. Some scholars have conducted research on the voice user interface of smart home products. Through emotional interaction experimental research, questionnaire analysis, and comprehensive data analysis, Liao and others have concluded that the degree of emotional interaction between users and smart home products determines the degree of personification of smart home assistants, and the degree of personification of smart home products voice assistants and user satisfaction is proportional. Zhou analyzed the characteristics of communication and dialogue between people and proposed a method of intelligent voice emotional interaction design. One is to perceive the user's emotional state, and the other is to automatically substitute the device into the corresponding situation and give the corresponding response. The above method is used to give the user provide matching services and content to meet the individual needs of users and enhance user experience [12–16]. Based on the physiological and psychological changes of the aging population, "furniture suitable for the elderly" should take safety and rationality as the primary principle; from an environmental point of view, the value of body changes, positioning, and activity routes should be considered, taking into account the use function and mental function and making the best possible. It may provide a safe, comfortable, and convenient life experience for the elderly.

Some scholars have also conducted research on the feedback time of the voice user interface. Li et al. obtained the speech rate information during the user's voice interaction process through experimental tests. They found that the control of the voice user interface feedback time can guide the user's interaction experience and emotional changes during the voice interaction process and proposed a speech rate detection module. It is added to the design of the voice user interface so that the user has a good sense of time in the interface experience. Chen and others conducted experi-

ments on the feedback time of the voice wakeup link and voice dialogue link in the voice user interface of smart products. The study found that users have different needs for feedback time in different links of voice interaction, and different wakeup methods have their own. In a specific time frame, optimizing the feedback duration of the voice user interface is conducive to improving user experience and satisfaction [17–20].

Wu Yu made some design suggestions for the voice user interface in the smart home scene: one is to set the character model; the other is to incorporate a multichannel interaction mode, combining visual and voice channels to enhance the voice interaction experience; the third is to make mistakes for users prevent and correct, guide users to complete the correct input process. There are few researches on the voice user interface of smart home products for elderly users, and a small number of scholars have paid attention to this issue. Based on the status quo of aging, Jia Guozhong studied the possible problems of voice interaction for elderly users using smart home products. Through experiments, he found that the wakeup word design should be concise and choose a name that is easy for the elderly to remember. To wake up the system, in terms of voice task setting, elderly users prefer a warm and quiet female role; the content and logic of the dialogue should be concise and easy to understand. Wang Pankai takes the elderly companion robot as the research object, studies the voice interaction experience design method of the elderly companion robot, and builds the elderly voice interaction framework on the basis of analyzing the cognitive characteristics of the elderly and summing up the theoretical research on voice interaction. In the voice interaction design of the elderly companion robot, design strategies and methods such as self-explanatory voice interaction, custom wakeup words, automatic volume adjustment, and the addition of special language for the elderly are used [21–24].

In recent years, with the development of context-aware technology, adaptive user interfaces based on context-awareness are the main development trend in the future. Analyzing the smart home situation of elderly users and studying specific smart home product voice user interface design strategies are the basis for the design and development of smart home product adaptive voice user interfaces. However, there is a lack of research and exploration in this area in existing research. This is the research of this article, which provided an opportunity.

Driven by the country's favorable policy environment and industrial technological innovation in recent years, the Internet of Things has shown a strong momentum of development in various emerging areas of its industry.

After the 25th Five-Year Development Plan, the country has issued a number of policies that have a profound impact on the development of the Internet of Things industry. With the accelerated integration of mobile Internet and Internet of Things and the strong support of national policies, smart homes have become the layout and competition in the Internet of Things field [25–28].

Internet companies such as Google, Apple, Samsung, and Xiaomi have greatly promoted the layout of smart

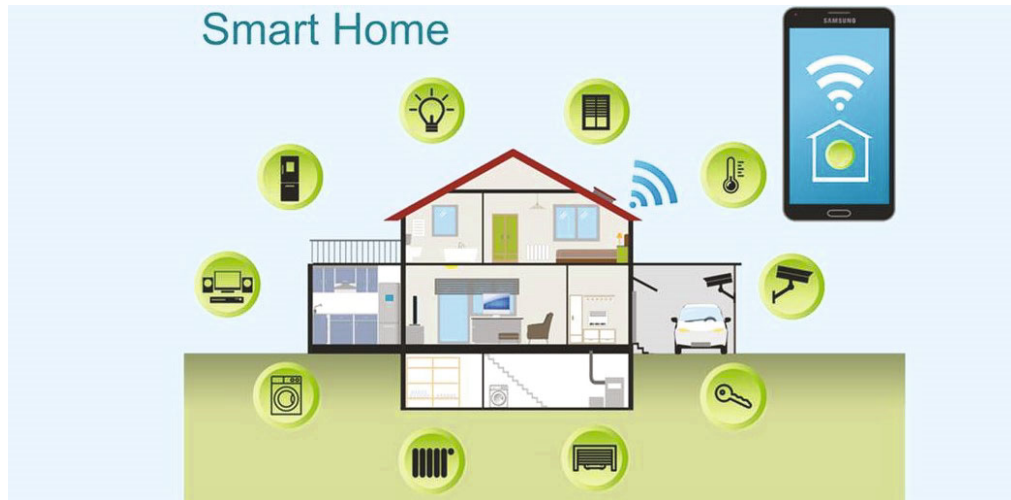


FIGURE 1: Smart home.

homes. At present, they have formed a series of innovative products such as smart home appliances and smart homes. These smart terminal products are combined with mobile applications to better serve users. Services are thereby attracting more and more users to deploy the smart ecosystem. China currently has 688 million Internet users, the largest number of Internet users in the world. Among them, the number of mobile phone users is unsurpassed by other countries. The 620 million mobile phone users give China a unique foundation in the “Internet+” industry. “Human and smart home” are fully connected to realize smart life.

- (1) In terms of policy: driven by the favorable national policy environment and industrial technology innovation in recent years, the Internet of Things has shown a strong momentum of development in various emerging fields of its industry, and the development of Internet of Things technology has also been included in the national major science and technology projects. Following the formulation of the “Twelfth Five-Year” development plan for the Internet of Things, a number of national policies have had a profound impact on the development of the Internet of Things industry. Smart home, as the hottest field in the Internet of Things, has unlimited prospects. The national policy puts forward the two double + concepts of smart networking + smart “product + service”, clearly pointing out and vigorously supporting the development direction of smart home
- (2) Economic aspect: my country’s smart homes are in the development stage. Although the market prospects are good, the current consumer awareness of smart homes is still lacking. Smart homes have a low level of education in the consumer market. Experience is also a factor that mainly affects consumers’ purchase of smart home products. Second, the high prices of existing smart home products limit the level of consumer groups, and only higher-income groups will seek more convenience in life

- (3) Social aspect: my country’s smart home; the scale of the market has been expanding year by year, and the continuous rise of my country’s national economy has also promoted the scale development of high-income groups, and the disposable income of residents across the country has increased year by year
- (4) Technical aspects: the technological development of big data, Internet of Things, and cloud computing effectively promotes and integrates the overall development of smart homes. Although my country’s technical fields are in the budding stage of the international level, the current government and various enterprises’ judging from the support and experience of technology R&D investment, these technologies will continue to innovate in the future, and smart homes will also continue to develop. The development of China’s smart home is in the growth stage as a whole, and the improvement of the overall technology will help drive consumers’ interest in smart homes [29–32]

At this stage, the smart home market has been very hot, whether it is a variety of smart small hardware or the overall smart home wiring system, they have been made to look good. The vigorous development of the Internet industry has brought the world into the era of mobile Internet connectivity. With the continuous innovation of smart hardware, control methods other than mobile phones have gradually emerged. But at present, most of the smart home products are connected to mobile phones, and smart devices are controlled and monitored through mobile applications. Mobile phones have become the best control terminal for smart home products.

## 2. Analysis of User Needs of Suitable Old Furniture

Scholars have carried out research on the definition and types of situations. Bill Schilit and others put forward that



the situation contains three important aspects, including “where are you,” “who are you with,” and “resources near you”. Dey defines context as any information that can be used to describe the status of an entity. An entity is considered to be a person, place, or object related to the interaction between the user and the application (including the user and the application itself). Chen believes that in the context of smart space, the concept of context provides a method for computer systems to automatically reason about the user’s situation. Therefore, it allows the system to predict user needs and take actions on behalf of the user and proposes that in the smart space system, the user positioning, user identity, and user intent are commonly used contextual information in research. The color, material, and shape of furniture are the breakthrough points of emotional design. Combined with storage, limb assist function design, video communication, etc., we can coordinate to create an environment suitable for the life of the elderly and meet the needs of emotional interaction.

Dey enumerates the main context types describing the situation of a specific entity as location, identity, activity, and time. These context types not only answer the question of who, what, when, and where but also serve as an index to other contextual information sources. Ryan et al. divide the type of situation into place, environment, identity, and time. Dou Jinhua and Qin Jingyan proposed four types of situations: user, environment, task, and device. User context includes individual and social context. Environmental context refers to the physical environment. Task context includes user tasks and related events or behaviors. Device context includes device attributes and related events and other equipment attributes.

In family life, home furnishing products have a particularly close relationship with people, and home also integrates most of the contents of people’s lives. Each family has different family members. There are free people living alone, a newly married couple, a sweet family of H, a happy family of three generations, and a rare family of four generations. Due to the characteristics of different families, the user differences faced by household products are very large, and there are also differences in abilities between each family member. This requires smart home products to take into account the versatility of the product at the beginning of the design. Usually, I have to conduct man-machine analysis before designing products, but I often ignore the needs of disadvantaged groups and only consider the standard of “healthy people.” For the elderly, children, pregnant women, and disabled people in the family, household products are used much more frequently than barrier-free facilities in the public environment. In the process of designing products, safety and convenience should be considered. The user’s ability and the size of the man-machine enhance the humanization of the product.

Based on previous research on the situational theory, the smart home situation of elderly users is divided into four types, namely, user situation, task situation, time situation, and environmental situation. The user situation includes the sensory, cognitive, and emotional characteristics of elderly users. The task context includes the purpose context

and behavior context of the elderly users. The time context includes the time of daily events and the time of special events. The combination of structure and function of furniture should be simple and intuitive, the design should not be too obscure and complicated, and a certain guiding performance should be given to make it easy for the elderly to operate and save labor and convenience. The environmental context mainly includes physical environmental factors, as shown in Figure 2.

For the elderly and disadvantaged groups, smart home appliances are mainly used in the home, so the principle of universal design should be considered when designing. The user context of the elderly includes four aspects: sensory characteristics, cognitive characteristics, emotional characteristics, and personality characteristics of elderly users. With the increase of age, the sensory function of the elderly declines, and the sensory function of vision and hearing is the most common manifestation. The cognitive changes of the elderly refer to the obvious changes in the brain’s ability to receive, extract, and judge information and cannot distinguish things smoothly and complete the task process. Cognitive changes are mainly manifested in attention, memory, perception, and thinking. In other aspects, cognitive ability will also change in strength and weakness with increasing age. Along with the physical decline of the elderly, their psychological status has also quietly changed, which affects the emotional state of the elderly in their daily lives. Personality is the essential psychological feature of an individual when facing himself or the outside world. The classic Big Five personality theory proposes five personality dimensions—extroversion, easygoing, conscientiousness, neuroticism, and openness. The personality of the elderly is affected by the synergistic effect of multiple factors such as increasing age, acquired life experience, and environment and also presents differentiated personality characteristics. The sensory characteristics, cognitive characteristics, emotional characteristics, and personality characteristics of the elderly are different. Universal design has seven principles: fair use, flexible use, simple and intuitive, perceptible information, fault tolerance, minimize physical effort, and provide enough space and size for users to be close to use. These principles provide a framework for the design practice of smart home products, but not only applicability must be considered in the design practice process but also other factors such as economy, culture, environment, and craftsmanship and other factors must be integrated into the product design. For example, the design of the handle avoids sharp shapes and is installed in a visually striking place, suitable for holding and exerting force, and has a damping device for easy opening and closing.

Purpose guides users to generate behavioral actions to complete the set tasks, and demand is the motivation for generating behavioral goals. Through literature research, observation, interviews, and other methods, analyze and extract the needs of the elderly in home life, including physiological needs, health needs, safety needs, social or emotional needs, information needs, entertainment needs, respect for needs, and needs for realization of self-worth. The predicted error is plotted in Figure 3.

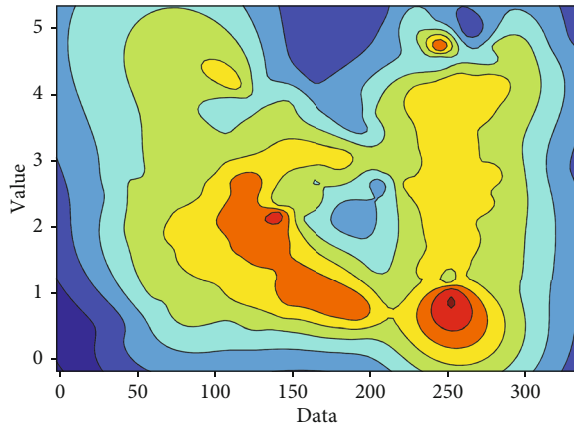


FIGURE 2: Data.

Leisure and social behaviors refer to behavioral activities that meet the spiritual and emotional needs of the elderly, including social interaction behaviors, cultural and entertainment behaviors, shopping behaviors, family interaction behaviors, and outing behaviors. The behavior types of elderly users are shown in Figure 4.

The home space is the main living environment for the elderly, and the physical environment is the main component of the home environment, including indoor temperature, humidity, light, and air quality. The outdoor physical environment includes temperature, humidity, ultraviolet index, and wind, which have a certain impact on the travel of the elderly. These factors are all environmental situations closely related to the elderly. Among indoor and outdoor environmental factors, quiet and noisy environments will have an impact on the experience of elderly users using the voice user interface, and the noise level is an important factor that needs to be considered in the design of an aging voice interactive interface. Universal design has seven principles: fair use, flexible use, simple and intuitive, perceptible information, fault tolerance, minimize physical effort, and provide enough space and size for users to be close to use.

Many mathematical models, such as activation functions, are required for the recognition technology of human action expressions. Generally speaking, the number output of the activation function is bounded and can be used as the input of the lower neuron. For example, the sigmoid function:

$$f(z) = \frac{1}{1 + e^{-z}}. \quad (1)$$

tanh function:

$$\tanh(x) = \frac{e^x - e^{-x}}{e^x + e^{-x}}, \quad (2)$$

where  $x$  means the variable.

Relu function:

$$\max(0, x). \quad (3)$$

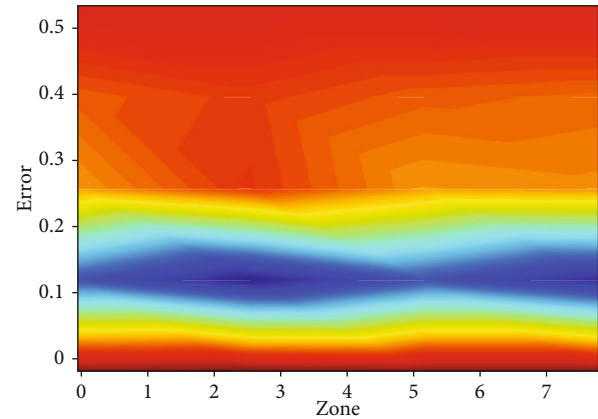


FIGURE 3: Error.

In addition, the loss function is also used, which is also called the cost function. Random events or variables related to random events in the loss function represent possible damage or risk factors. The loss function is often used as the learning principle associated with optimization problems, that is, to minimize the loss function as an evaluation system. Usually, a machine uses many algorithms when learning. These algorithms correspond to fixed objective functions. When performing classification operations or regression operations, these objective functions can be improved. These objective functions are often loss functions. Time context includes daily event time and special event time. Most elderly people have regular daily life events, and the daily fixed event time is similar. Emotional interaction is an important component to draw closer to the elderly and smart homes. “Furniture for the elderly” can try to take advantage of this opportunity to combine emotional interaction with artificial intelligence technology to consider different types of elderly in detail.

The loss function is usually a nonnegative value function, used to evaluate the error between the predicted value and the true value  $Y$  corresponding to the system.

$$\hat{Y} = f(X). \quad (4)$$

The loss function can generally be expressed as

$$L(Y, f(x)). \quad (5)$$

There is usually a positive correlation between the value of the loss function and the performance of the model.

Suppose the sample set is

$$(X, Y) = (x_i, y_i), \quad y_i, i \in [1, N]. \quad (6)$$

There are  $N$  samples in total, among which the true value of sample  $i$  is

$$y_i, i \in [1, N]. \quad (7)$$

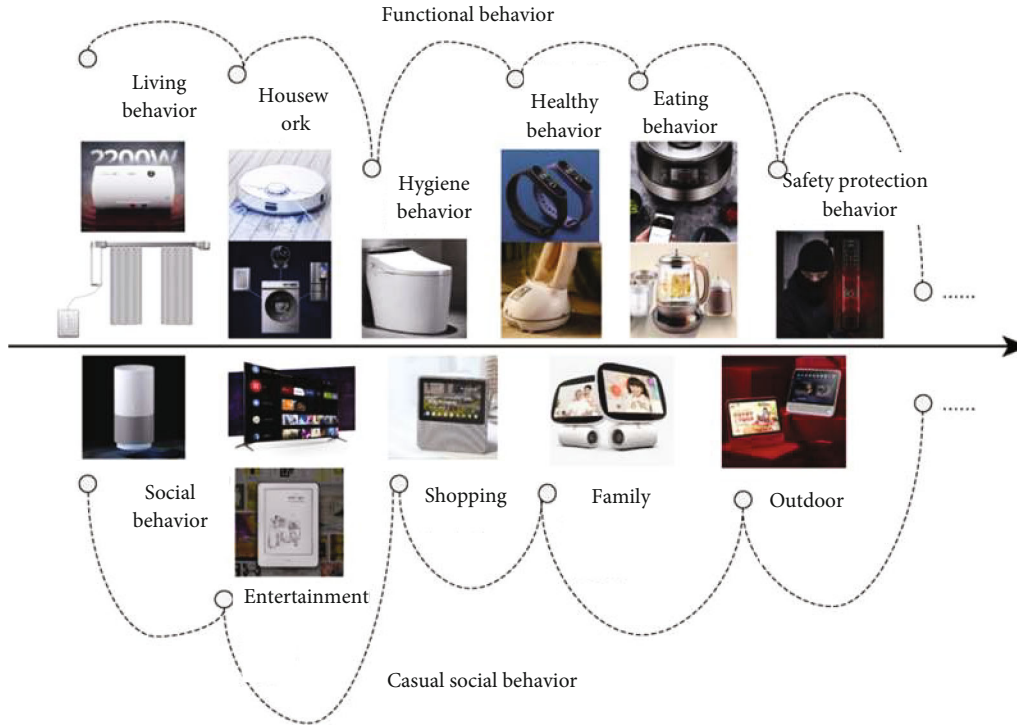


FIGURE 4: Social behavior.

The predicted value of sample  $i$  is

$$\hat{y}_i = f(x_i), \quad i \in [1, N]. \quad (8)$$

$f$  represents its classification or regression function. Then, the total loss function is

$$L = \sum_{i=1}^N l(y_i, \hat{y}_i). \quad (9)$$

The commonly used loss functions in regression problems are average absolute error- $L1$  loss function.

The average absolute error (MAE) represents the sum of the absolute value of the difference between the estimated value and the target value. It is also a commonly used regression loss function, which reflects the average degree of error of the estimated value, and there is no need to explore the positive and negative of the error. The minimum average absolute error value is 0 and the maximum is  $\infty$ . The formula is shown in

$$L_{MAE} = \frac{\sum_{i=1}^N |y_i - f(x_i)|}{n}. \quad (10)$$

Mean square error- $L2$  loss function: the mean square error (MSE) is the constant value of the error in the regression loss function, which is mainly used to represent the difference between the predicted value and the target value in the regression function value. In the process of use, it is gen-

erally squared. The function of this constant is expressed as follows:

$$L_{MSE} = \frac{\sum_{i=1}^n |y_i - f(x_i)|^2}{n}. \quad (11)$$

The difference from the  $L1$  loss function is that there is an additional step of square calculation.

The classification problem is more specific than the regression problem. The target quantity only exists in a limited set and is discrete. Classification problems are often one more step than regression problems and are used to judge categories. The loss function of the regression problem is the performance measurement function, and the loss function of the classification problem cannot be directly used for performance measurement. The final evaluation criterion is not the distance from the target, but the accuracy of the category judgment. In order to maximize the accuracy of category judgment, I need to define different loss functions for classification problems. These principles provide a framework for the design practice of smart home products, but not only applicability must be considered in the design practice process but also other factors such as economy, culture, environment, and craftsmanship and other factors must be integrated into the product design. Through reasonable function classification, augmented reality technology assistance, and improved system security, the necessary auxiliary functions are selected, and the configuration is optimized according to the specific characteristics of the

elderly, so as to improve the function integration of the smart home system for “suitable furniture for the elderly”.

0-1 loss function: here, I take the problem of two classification as an example to explain the error rate = 1-the correct rate. At this time, the 0-1 loss function is defined as follows:

$$L = \frac{\sum_{i=1}^n I(f(x_i) \neq y_i)}{n}. \quad (12)$$

Cross entropy loss function (logistic regression): logistic regression is mainly used to solve two classification problems and can be further divided into loss function and activation function. The former is also called cross entropy function and the latter is called sigmoid function. The final target subformula is as follows:

$$L(\theta) = y \log(h_{\theta}(x)) + (1 - y) \log(1 - h_{\theta}(x)). \quad (13)$$

In this article, categorical\_crossentropy is the main categorical cross entropy function. Compared with other functions of the same class, this function is more suitable for multiclass scenarios, and softmax is also used as the activation function of the output layer in the research process. For example, the time of getting up and going to sleep is relatively fixed every day, and the meal time in the morning, midnight, and evening is relatively fixed, and weekly exercise leisure time is also regular. The time of daily events has individual differences, and the regular schedule of the elderly in each family is different. In daily life, the elderly also has special arrangements for activities, such as shopping in shopping malls and other special events. These are some activities arranged by the elderly according to the special needs of their lives, which are uncertain and irregular. The full range of functional services in the context of networking provides a guarantee for the seamless connection between furniture design products and the behavioral characteristics of the elderly.

### 3. User Interface Design of Shilao Furniture

With the increase of age, the hearing and memory functions of elderly users decline, and single-channel voice interaction is likely to increase the cognitive load of elderly users. The voice user interface of aging smart home products uses voice as the main information interaction method and assists in visualizing visual information to enhance the voice user interface interaction experience and promote the multichannel perception of the voice interaction system by elderly users. Specifically, visual design is incorporated into the interactive process of voice wakeup, command input, information transmission, confirmation feedback, and other links. For example, in the voice wakeup link, the voice user interface responds with voice and is accompanied by a short light for visual response and combined with text, images, and other graphical user interface elements; in the instruction input link, supplemented by the graphical user interface to display the text information “in process,” visually reminding elderly users that the voice input link is in progress; in

the information in the communication link, the voice is the main way to interact with the elderly users, supplemented by text messages and light flashing effects to remind the elderly users that the information has been communicated; if there is an interruption in the voice interaction process, the voice prompts the elderly users whether they need to continue the conversation. In the feedback link, in the multi-round dialogue mode, the voice is the mainstay and the graphical user interface assists in confirming the information. In the single-round dialogue mode, the dialogue is ended with a specific sound effect after the voice feedback. The value with different zone is shown in Figure 5.

In the process of voice user interface dialogue, understanding the pronouns used by elderly users is an important part of the continuous voice communication process. The cognitive characteristics of elderly users lead to pronoun ambiguity, unclear pronunciation, and dialogue content in the process of voice dialogue. For phenomena such as memory ambiguity, the voice dialogue must continue to track the context to achieve multiple rounds of dialogue and continuous interaction and promote the matching of high and low contexts in the voice interaction process. The context memory function of the voice interaction system needs to record the content information of multiple rounds of dialogue. In the process of continuous dialogue with elderly users, the voice user interface can prompt the elderly users to forget the information content according to the context information of the voice dialogue and continue the dialogue. Complete the voice service process.

The emotional needs of elderly users are an important factor considered in the design of the voice user interface of smart home products. The emotional voice interaction design analyzes the tone, volume, speaking speed, and other information in the voice stream of elderly users to perceive the emotional state of elderly users in the current situation. And adjust the tone, volume, speaking rate, and other states of the voice feedback in real time, and conduct appropriate emotional interactions with elderly users. For example, when the voice interaction system recognizes that an elderly user has sadness, depression, and other emotions, the system uses a gentle voice to talk to the elderly user and actively prompts the elderly user to use a certain system function through voice commands, such as video or voice with their children talking and listening to music or opera, as shown in Figure 6.

At the same time, in order to bring a more comfortable voice service experience to the elderly users, do not blame the elderly users when there are communication barriers at any stage of the voice interaction, so as not to bring frustration and failure to the elderly users and affect their response. The voice user interface should enhance error prompts based on contextual information, actively adopt a friendly dialogue mode, and understand and guide elderly users to smoothly conduct voice dialogues so that elderly users can maintain a positive and optimistic emotional state during the interaction process and improve the satisfaction of elderly users.

Design voice user interface assistants suitable for aging smart home products. Through the design of age, gender, appearance, speech speed and tone, dialogue content, etc.,

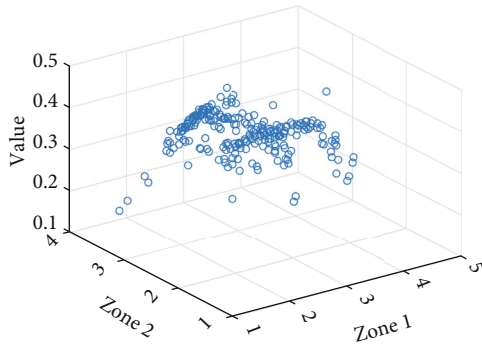


FIGURE 5: Value with different zone.

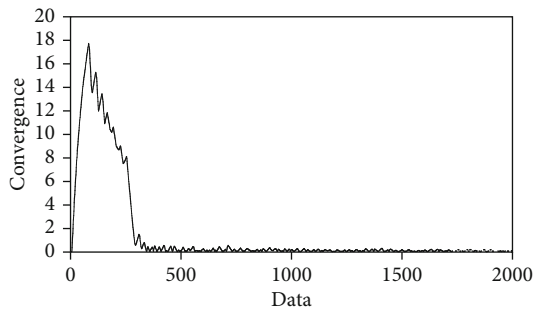


FIGURE 6: Convergence.

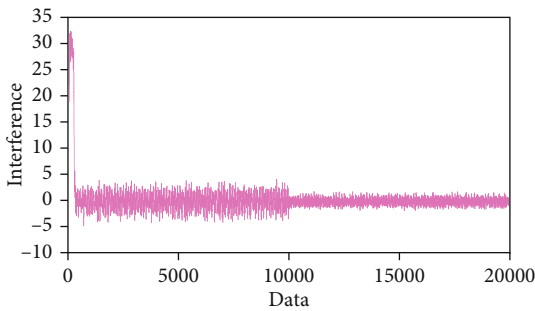


FIGURE 7: Interference.

voice assistants are given personality characteristics. The personalization design of voice assistants can easily make elderly users feel dependent. Sense of trust is to establish the trust relationship between elderly users in smart home products. By analyzing the personality characteristics of elderly users, smart home products can provide voice assistants that match the personality characteristics of elderly users. Take the elderly users with extroverted personality characteristics as an example. They are enthusiastic, active, self-confident, and talkative and like to interact with others. Aiming at elderly users with extroverted personality, the voice assistant is designed to be younger, confident and lively voice image, and dialogue tone. Too high, the conversation speed is fast, the frequency of active dialogue is high, and the colloquial language is added to the content of the dialogue to be closer to the personality characteristics of the elderly users. Take the Microsoft Personalized Dialogue System as an example. Microsoft Xiaoice is a personalized

dialogue system entity, defining her personality to cover basic attributes and interest attributes, including the ability to interact with dialogue, sound, and vision, and the content of the dialogue reflects the set personality.

After many times of use, the voice interaction system records and analyzes the fluency of the communication process and common problems when the elderly users use smart home products to conduct conversations and actively provides voice assistance to guide the elderly users to learn and use the voice user interface of smart home products. Actively remind the elderly users of the operation methods and the functions supported by the equipment, and use video tutorials to assist the elderly users in memory and improve the self-efficacy of the elderly users in using smart home products. The interference of the proposed method based on MATLAB is shown in Figure 7.

The behaviors of elderly users are mainly divided into functional behaviors and casual social behaviors. From the perspective of task context, the voice user interface of smart home products should provide voice services that conform to the behavior context according to the behavior patterns of elderly users. Aiming at the functional behavior of elderly users, short command and question-and-answer dialogue are adopted to ensure the accuracy of speech recognition and improve the efficiency of task completion. For the casual social behavior of elderly users, it is necessary to ensure the comfort of natural voice communication and enhance the emotional experience of elderly users. The voice user interface of smart home products participates in the entire process from the generation of behavior to the end of the task, and the dialogue mode is automatically switched according to the type of behavior of the elderly users to ensure the continuity of the completion of the tasks in the smart home environment of the elderly users.

The time context of elderly users is divided into daily event time context and special event time context. Aiming at the time situation of daily events, the design of the adaptive voice user interface is designed according to the time and events on the timeline, and the characteristics of voice intonation, speaking rate, timbre, and volume are adjusted to adapt to changes in the status of elderly users. For example, in the morning, the elderly users are given a relaxed and pleasant atmosphere with a lively voice, and music services are recommended; while reading a book and the newspaper, a peaceful atmosphere is created with an elegant and soft voice, and question and answer services are recommended. The voice of the old users gives the elderly users a quiet and relaxing atmosphere and recommends storytelling services. For special event time scenarios, since the individual voice needs of elderly users are dynamically changing, the design of the voice interactive interface dialogue mechanism needs to take the initiative to respond to the voice needs of elderly users randomly. For example, elderly users tend to forget the time of special events. The voice user interface of smart home products provides the elderly users with the appointment function. By waking up the voice assistant, the voice assistant will be notified of the event and reminder time of the appointment. When the appointment time comes, the voice assistant will switch to lively. The voice



FIGURE 8: Smart home products for elderly users.

mode actively prompts elderly users to avoid the inferiority complex of elderly users with weakened memory. Figure 8 shows the voice user interface design strategy of smart home products in the time context of elderly users.

It provides environmental analysis reports and provides specific home and out-of-home recommendations to elderly users through a voice user interface. The feedback mode of the voice user interface of smart home products should be adaptively adjusted according to the environmental situation and the location and status of elderly users. When the elderly user is in a noisy environment, the voice user interface automatically improves the voice feedback of the voice interaction. When the elderly user is in a quiet environment, the voice user interface reduces the voice feedback of the voice interaction and performs voice interaction in a gentle way. The distance between elderly users and smart home products is dynamically changing, adjust the sound feedback according to the distance, so as to avoid the phenomenon that the distance is far away or the sound is too loud, which will cause discomfort to the elderly users. At the same time, the design of the voice user interface also needs to consider the static state or motion state of the elderly users themselves and adaptively adjust the volume and pitch.

#### 4. Conclusions

The research of this paper includes the design of active interactive voice user interface and the construction of continuous behavioral service experience; for the time context, it proposes a design strategy for the daily event time context and the special event time context; for the environmental context, it proposes matching appropriate content services, adaptive adjustment design strategies for voice interactive feedback. The research results can provide designers and developers with a reference for aging-appropriate voice user interface design methods and strategies and provide elderly users with a more comfortable interactive experience of smart home products.

#### Data Availability

The data used to support the findings of this study are available from the corresponding author upon request.

#### Conflicts of Interest

The author declares that there are no known competing financial interests or personal relationships that could have appeared to influence the work reported in this paper.

#### Acknowledgments

This article is the research result of the Humanities and Social Science Research Project in Jiangxi Province, “Research on the Risk of Excessive Use of Materials in Modern Home Decoration and Its Prevention and Control” (Project Number: YS20224).

#### References

- [1] Y. Yu, C. Yang, Q. Deng, T. Nyima, S. Liang, and C. Zhou, “Memristive network-based genetic algorithm and its application to image edge detection,” *Journal of Systems Engineering and Electronics*, vol. 32, no. 5, pp. 1–9, 2021.
- [2] Y. Ishida and S. Hashimoto, “Asymmetric characterization of diversity in symmetric stable marriage problems: an example of agent evacuation,” *Procedia Computer Science*, vol. 60, no. 1, pp. 1472–1481, 2015.
- [3] P. Zoha and R. Kaushik, “Image edge detection based on swarm intelligence using memristive networks,” *IEEE Transactions on Computer-Aided Design of Integrated Circuits and Systems*, vol. 37, no. 9, pp. 1774–1787, 2018.
- [4] J. Pais, “Random matching in the college admissions problem,” *Economic Theory*, vol. 35, no. 1, pp. 99–116, 2008.
- [5] J. J. Jung and G. S. Jo, “Brokerage between buyer and seller agents using constraint satisfaction problem models,” *Decision Support Systems*, vol. 28, no. 4, pp. 291–384, 2020.
- [6] Y. Liu and K. W. Li, “A two-sided matching decision method for supply and demand of technological knowledge,” *Journal of Knowledge Management*, vol. 21, no. 3, pp. 592–606, 2017.
- [7] J. Byun and S. Jang, “Effective destination advertising: matching effect between advertising language and destination type,” *Tourism Management*, vol. 50, no. 10, pp. 31–40, 2015.
- [8] A. Nagamani, S. Anuktha, N. Nanditha, and V. Agrawal, “A genetic algorithm-based heuristic method for test set generation in reversible circuits,” *IEEE Transactions on Computer-Aided Design of Integrated Circuits and Systems*, vol. 37, no. 2, pp. 324–336, 2018.
- [9] C. Koch and S. P. Penczynski, “The winner’s curse: conditional reasoning and belief formation,” *Journal of Economic Theory*, vol. 174, pp. 57–102, 2018.

- [10] C. K. Karl, "Investigating the winner's curse based on decision making in an auction environment," *Simulation and Gaming*, vol. 47, no. 3, pp. 324–345, 2016.
- [11] D. Ettinger and F. Michelucci, "Creating a winner's curse via jump bids," *Review of Economic Design*, vol. 20, no. 3, pp. 173–186, 2016.
- [12] J. A. Brander and E. J. Egan, "The winner's curse in acquisitions of privately-held firms," *Review of Economics & Finance*, vol. 65, pp. 249–262, 2017.
- [13] Z. Palmowski, "A note on var for the winner's curse," *Economics/Ekonomia*, vol. 3, no. 15, pp. 124–134, 2017.
- [14] B. R. Routledge and S. E. Zin, "Model uncertainty and liquidity," *Review of Economic Dynamics*, vol. 12, no. 4, pp. 543–566, 2009.
- [15] D. Easley and M. O'Hara, "Ambiguity and nonparticipation: the role of regulation," *The Review of Financial Studies*, vol. 22, no. 5, pp. 1817–1843, 2009.
- [16] P. Klibano, M. Marinacci, and S. Mukerji, "A smooth model of decision making under ambiguity," *Econometrica*, vol. 73, no. 6, pp. 1849–1892, 2005.
- [17] Y. Halevy, "Ellsberg revisited: an experimental study," *Econometrica*, vol. 75, no. 2, pp. 503–536, 2007.
- [18] D. Ahn, S. Choi, D. Gale, and S. Kariv, "Estimating ambiguity aversion in a portfolio choice experiment," *Working Paper*, vol. 5, no. 2, pp. 195–223, 2019.
- [19] T. Hayashi and R. Wada, "Choice with imprecise information: an experimental approach," *Theory and Decision*, vol. 69, no. 3, pp. 355–373, 2010.
- [20] K. Zima, E. Plebankiewicz, and D. Wiczorek, "A SWOT analysis of the use of BIM technology in the Polish construction industry," *Buildings*, vol. 10, no. 1, p. 16, 2020.
- [21] S. Peng, L. Baobao, and S. Tao, "Injury status and strategies of female 7-a-side rugby players in Anhui Province," *Sports Bou-tique*, vol. 38, no. 3, pp. 72–74, 2019.
- [22] P. Guild, M. R. Lininger, and M. Warren, "The association between the single leg hop test and lower-extremity injuries in female athletes: a critically appraised topic," *Journal of Sport Rehabilitation*, vol. 30, no. 2, pp. 1–7, 2020.
- [23] U. G. Inyang, E. E. Akpan, and O. C. Akinyokun, "A hybrid machine learning approach for flood risk assessment and classification," *International Journal of Computational Intelligence and Applications*, vol. 19, no. 2, p. 2050012, 2020.
- [24] Q. Liu, S. Du, B. Wyk, and Y. Sun, "Double-layer-clustering differential evolution multimodal optimization by speciation and self-adaptive strategies," *Information Sciences*, vol. 545, no. 1, pp. 465–486, 2021.
- [25] H. R. Medeiros, F. D. Oliveira, H. F. Bassani, and A. Araujo, "Dynamic topology and relevance learning SOM-based algorithm for image clustering tasks," *Computer Vision and Image Understanding*, vol. 179, pp. 19–30, 2019.
- [26] Y. Deng, D. Huang, S. Du, G. Li, and J. Lv, "A double-layer attention based adversarial network for partial transfer learning in machinery fault diagnosis," *Computers in Industry*, vol. 127, p. 103399, 2021.
- [27] J. J. Chan, K. K. Chen, S. Sarker et al., "Epidemiology of Achilles tendon injuries in collegiate level athletes in the United States," *International Orthopaedics*, vol. 44, no. 3, pp. 585–594, 2020.
- [28] W. Li, G. G. Wang, and A. H. Gandomi, "A survey of learning-based intelligent optimization algorithms," *Archives of Computational Methods in Engineering*, vol. 28, no. 5, pp. 3781–3799, 2021.
- [29] G. G. Wang, A. H. Gandomi, A. H. Alavi, and D. Gong, "A comprehensive review of krill herd algorithm: variants, hybrids and applications," *Artificial Intelligence Review*, vol. 51, no. 1, pp. 119–148, 2019.
- [30] Y. Liu, A. Pei, F. Wang et al., "An attention-based category-aware GRU model for the next POI recommendation," *International Journal of Intelligent Systems*, vol. 36, no. 7, pp. 3174–3189, 2021.
- [31] Y. Liu, Z. Song, X. Xu et al., "Bidirectional GRU networks-based next POI category prediction for healthcare," *International Journal of Intelligent Systems*, vol. 10, no. 1, pp. 1–9, 2021.
- [32] L. Qi, C. Hu, X. Zhang et al., "Privacy-aware data fusion and prediction with spatial-temporal context for smart city industrial environment," *IEEE Transactions on Industrial Informatics*, vol. 17, no. 6, pp. 4159–4167, 2021.

## Research Article

# English Pronunciation Calibration Model Based on Multimodal Acoustic Sensor

Yurui Zhou<sup>1</sup> and Guolong Zhao <sup>2</sup>

<sup>1</sup>School of Foreign Languages, Xinyang University, Xinyang 464000, China

<sup>2</sup>College of Teacher Education, Xinyang Normal University, Xinyang 464000, China

Correspondence should be addressed to Guolong Zhao; [zgl5127@xynu.edu.cn](mailto:zgl5127@xynu.edu.cn)

Received 18 January 2022; Revised 26 February 2022; Accepted 4 March 2022; Published 5 April 2022

Academic Editor: Wen Zeng

Copyright © 2022 Yurui Zhou and Guolong Zhao. This is an open access article distributed under the Creative Commons Attribution License, which permits unrestricted use, distribution, and reproduction in any medium, provided the original work is properly cited.

In recent years, with the increasing frequency of international exchanges, people have gradually realized that language is a tool of communication and communication, and language learning should attach importance to oral teaching. However, in traditional classrooms, one of the problems faced by oral teaching is the mismatch of the teacher-student ratio: a teacher has to deal with dozens of students, one-on-one oral teaching and pronunciation guidance is impossible, and it is also affected by the teachers and the environment constraints. Therefore, the research on how to efficiently automate pronunciation training is becoming more and more popular. Many phonemes in English have different facial visual features, especially vowels. Almost all of them can be distinguished by the roundness and tightness of the lips in appearance. In order to give full play to the role of lip features in oral pronunciation error detection, this paper proposes a multimodal feature fusion model based on lip angle features. The model interpolates the lip features constructed based on the opening and closing angles and combines audio and video in time series. Feature alignment and fusion and feature learning and classification are realized through the two-way LSTM SOFTMAX layer, and finally, end-to-end pronunciation error detection is realized through CTC. It is verified on the GRID audio and video corpus after phoneme conversion and the self-built multimodal test set. The experimental results show that the model has a higher false pronunciation recognition rate than the traditional single-modal acoustic error detection model. The increase in error detection rate is more obvious. Verification by the audio and video corpus with white noise was added, and the proposed model has better noise immunity than the traditional acoustic model.

## 1. Introduction

The ultimate goal of English learning is communication. The method of communication is mainly spoken language, and spoken language is realized through voice. As one of the three major elements of language, speech, is the foundation and necessity of learners and it plays a vital role in second language acquisition. Therefore, English teaching should also be based on English phonetics teaching. However, in most colleges and universities, the English phonetics course is only a “semi-independent” course. In addition, traditional English phonetics teaching is based on the monomodal teaching of students’ hearing, which makes students lose their interest in phonetic learning. Secondly, restricted by the Chinese exami-

nation system, most students tend to “dumb English”, because of emotional attitude, learning motivation, individual differences, and other factors, and most people speak a strong Chinese English. With the development of advanced science and technology, English phonetic teaching is no longer “speaking and ear learning” or traditional single-modal teaching, but gradually becoming a multimodal teaching combining multimedia technology and visual speech software. Teachers can use multimodality. The synergistic effect of attitude enables students to understand the characteristics of English pronunciation from hearing, vision, and touch and improve English pronunciation. Figure 1 shows the multimodal [1–10].

In traditional English learning, teachers pay more attention to writing and grammar teaching, and oral training has



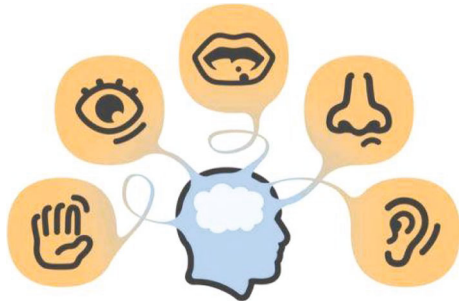


FIGURE 1: Multimodal model.

always been neglected. Therefore, some people ridicule that the students taught by Chinese English teaching are “dumb English,” that is, most Chinese students can proficiently master English written test skills in test-oriented education, but few students are proficient in daily oral communication in English. In recent years, with the increasing frequency of international exchanges, people have gradually realized that language is a tool of communication, and language learning should pay attention to oral teaching. However, in traditional classrooms, one of the problems faced by oral teaching is the mismatch of the teacher-student ratio: a teacher has to deal with dozens of students, one-on-one oral teaching and pronunciation guidance is impossible, and it is also affected by the teachers and the environment constraints. Therefore, the research on how to efficiently automate pronunciation training is becoming more and more popular. Since the second half of the 20th century, educational technology has been one of the fastest growing fields. The use of computers as a communication medium and the emergence of the Internet have reshaped the role of computers in language learning. The computer is no longer just a tool for information processing and display, it has been given the function of communication. As a result, the Computer Assisted Language Learning (CALL) system came into being. Qian et al. divides the development of CALL into three stages, namely, active, interactive, and comprehensive [11–16].

In college oral English teaching, educators generally believe that the main task of oral teaching is to help students convey existing ideas in new languages and more refined and authentic expressions. Therefore, teachers place great emphasis on language imitation and neglect content creation when arranging oral teaching tasks, which causes language learning to break away from nonlinguistic factors, such as thought, culture, and context on which language depends, and even lack the endogenous expressive power of language learning. Although there are more and more researches on oral English in the domestic and foreign language circles, how to improve the oral level of the larger group of non-English majors and how to improve the efficiency of output training in oral English classes, so as to counteract the initiative of students in oral learning, there is too little research on independence and creativity [17–21]. Therefore, how to make full use of the limited class time to improve the status quo of college students’ English pronunciation is a question worthy of consideration by college teachers.

Multimodal research emerged in the West in the 1990s. The New London Group put forward “multiple literacy,” which was the first to apply multimodality to language teaching. Representatives of Western studies of multimodality teaching include Stein and Royce. In China, foreign language teaching based on multimodality has also made some progress. Multimodal theory is based on Halliday’s system functional linguistic theory. It encourages teachers to include two or more modal symbols in their instructional design and appropriately uses images, sounds, text, and other interactive methods to stimulate students’ learning in language. Multiple sensory experience is a teaching mode that mainly includes the training of multimodal teaching design (instructional design) and multiple reading and writing (multiliteracy), which can simulate the real context to the greatest extent and enrich the communication occasions, and it can also allow students to imitate language and create to the greatest extent and express the content so as to meet the requirements of oral teaching. Since the rise of this theory in the 1990s, although there have been a few case studies suggesting that it can effectively improve the teaching efficiency of oral English classrooms, it has been seldom used in oral English teaching, and there is still a lack of scientifically designed empirical research. In addition, with the development of information technology, more and more speech analysis software has emerged, and multimodal teaching research based on speech technology is imperative. This article is mainly based on phonetic technology, combined with linguistics, phonetics, and acoustics and explores the advantages of multimodal English phonetic teaching through the visualization of English phonetic characteristics [22–25]. In view of this, this paper proposes a multimodal end-to-end English pronunciation error detection and correction model based on audio and video. It does not require forced phoneme alignment of the pronunciation video signal to be processed and uses rich audio and video features for pronunciation error detection.

## 2. Multimodal Theory

Modality is a form of information transmission and communication. Regardless of spoken language mode or written language mode, it needs to rely on the language medium of sound signs or written signs or nonverbal media such as images, actions, and technical equipment. There is an interactive relationship of complement, reinforcement, synergy, and overlap between them. Multimodality refers to the inclusion of different symbolic modalities in a communication product or communication activity. It also refers to various ways of mobilizing different symbolic resources in a specific text to construct meaning. Multimodal discourse, as a communicative phenomenon, is mainly based on Halliday’s system-functional linguistic theory. It is believed that other sign systems outside language, such as images and sounds, are also sources of meaning and have conceptual, interpersonal, and language functions. Article function, in the teaching design, the teacher integrates the modal symbols of two or more symbols into the teaching design and presents the teaching content of the teaching mode, which

is multimodal teaching. In the field of multimodal teaching research, the New London Group has pioneered the application of multimodality to language teaching. They believe that cultivating students' multiple literacy and multimodal meanings is the main task of language teaching. Stein clearly proposed the multimodal teaching method (multimodal pedagogies), pointing out that the multimodal teaching method highlights the indivisibility of the body and the brain to participate in communication through multimodal and multisensory collaboration. Therefore, teachers should design multimodal teaching tasks. Students should also use multiple modalities to complete tasks. The most fruitful research on multimodal discourse analysis is by Kress and van Leuwen, who proposed a design plan and application principles for the cultivation of multiple literacy skills in a multimodal environment. Royce then analyzes the complementary relationship between images and text in multimodal texts and the coordination relationship between multiple symbolic modalities in language teaching, provides an understanding of how teachers should use the visual and auditory modalities presented on the computer in the classroom, to help students develop a multimodal discourse communicative competence for research, and specifically pointed out that the reading and writing activities integrated into multimodal teaching methods can also be introduced into listening and speaking classes to cultivate students' listening and speaking skills. With the rise of multimedia teaching, Jewitt explored the relationship between teaching and modern media technology by observing the resource allocation of rhythm, multimodality, and interactivity when teachers use new technologies, it is done by multiple modalities, and points out that students should transform multiple modal signals in the learning process and practice teaching design together with teachers [26–30]. To a large extent, the accuracy of error detection is improved, especially in a noisy environment. Aiming at the shortcomings that the current lip feature extraction algorithm is too complicated, and the characterization ability is insufficient; a feature extraction scheme based on the opening and closing angle of the lips is proposed.

It can be seen that relevant researches at home and abroad agree with this multimodal collaborative and multimedia teaching model, which also laid a solid theoretical foundation for the application of multimodality in oral teaching. However, the current domestic and foreign researches generally have the following two problems: (1) most of the researches are based on case studies, and there is a lack of rigorous randomized controlled empirical research, so the credibility of the results needs to be improved; and (2) the current multimodal research are mostly concentrated in the areas of listening, reading, and writing and less involved in oral teaching.

The characteristics of English pronunciation include two aspects: segment and super segment. Segments mainly refer to vowels and consonants; super segments include intonation, stress, and rhythm. Therefore, the focus of English phonetic multimodal teaching is how to enable students to accurately grasp the characteristics of pronunciation through multimodal sensory stimulation. As far as English speech segment teaching is concerned, three-dimensional animation

can be used to intuitively and vividly present the dynamic process of tongue position and lip shape in the pronunciation process, coupled with sensory stimulation such as hearing and touch and corresponding text modalities, and students can master the essentials of pronunciation quickly and comprehensively and get twice the result with half the effort. Take a program based on the English course of the University of Iowa in the United States to help Chinese English learners learn American pronunciation as an example. For example, the monophonic image shows the dynamic process of the pronunciation organs (tongue-jaw-lips-vocal cords) during the pronunciation of the vowel. In addition, the real-life three-dimensional animation can also truly present the mouth shape during pronunciation (see Figure 2(a)). A little fingertip can be placed between the upper and lower teeth when the sound is pronounced, which is convenient for students to feel the sense of touch. For English diphthongs, it is also possible to combine real-person facial profiles to enable students to master the essentials of pronunciation through video teaching. For example, diphthongs are a process of sliding from to, when pronounced, the lips are rounded to the corners of the mouth and the corners of the mouth are slightly grinning backwards, and the tongue is raised from the back of the tongue to the front of the tongue and approaching the upper palate forward, with the tip of the tongue touching the gums (see Figure 2(b)). Therefore, this research adopts a rigorous scientific research design and observes the application effect of multimodal theory in college oral English teaching through randomized controlled research, in order to provide new ideas for college oral English teaching practice.

### 3. Working Principle of Multimodal Pronunciation Calibration

Many students will have the problem of substandard pronunciation in the process of learning English, but it is very difficult to solve the problem of misreading only by themselves. Therefore, the research of automatic pronunciation error detection has practical significance. Most spoken pronunciation errors can be divided into four types: phoneme mispronunciation, missed pronunciation, pronouncing more pronouncing, and pronouncing time error. Phoneme is the smallest unit in the audio field. Any English word or sentence can be composed of phoneme.

When the vowel sounds are pronounced, the lips continue to remain open, and the various organs in the oral cavity are not in direct contact and will not hinder the passage of the pronunciation airflow. For vowels, the appearance can be distinguished by the roundness of the lips, the position of the tongue, and the tightness of the lips. In the frequency domain, the angle can be distinguished by the formant. The formant is the frequency band where the sound energy is concentrated. In fact, there are many correlations between the formant and the position of the tongue. There are three formants (F1, F2, and F3) for each vowel. Generally, F1 and F2 can be used to distinguish vowels. In the corresponding relationship between American vowels and formants, the horizontal line represents F2 and the

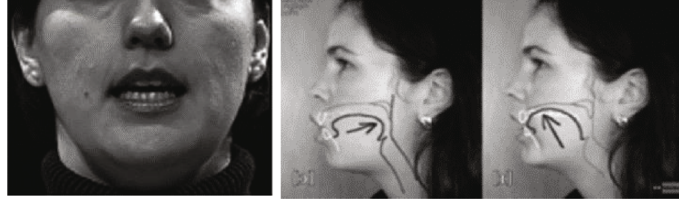


FIGURE 2: Mouth shape during pronunciation.

vertical line represents F1. Therefore, the pronunciation accuracy of each phoneme is the key information to measure the correctness of pronunciation.

In the field of acoustics, F1 relates to the height of the tongue, and F2 relates to the front and back of the tongue. For example, in the two phonemes of /I/ and /a:/, /I/ has a lower F1 and a higher F2, and /a:/ has a higher F1 and a lower F2. As can be seen, /I/ in front has a higher tongue position than /a:/. Therefore, the tongue position information during pronunciation can be judged based on the difference of formants, and corrective opinions are given for this information. It can help students learn English pronunciation better.

**3.1. Visual Field.** In the visual field, the roundness of the lips can be used to judge the pronunciation of different vowels: (1) the lips are obviously opened and rounded when pronounced, and the lips are obviously not as round when pronounced and (2) the roundness of the lips is closely related to the pronunciation of vowels, and suggestions for correcting errors can be given based on the roundness of the lips. The pronunciation of consonants is different from vowels. There is a blockage of sound airflow in the oral cavity. There is little difference in the appearance of the lips, so it is difficult to judge them with the visual information of the lips, which is mainly judged by the acoustic characteristics. The pronunciation of consonants can be judged from the pronunciation position and the way of pronunciation, according to the position of the consonant when it is pronounced. /p/, /b/, and /m/ use the lips to pronounce. /s/, /z/, /ts/, and /dz/ use the tongue and front jaw to pronounce. According to the way of pronunciation, /p/, /b/, /t/, /d/ first block the airflow during the pronunciation and then release it. There are also other consonant pronunciation positions and ways in the picture. In the audio field, the main difference between unvoiced and voiced sounds is whether the vocal cords vibrate or not. Vibration affects the frequency spectrum of the sound. This feature can be used to distinguish consonants. When the detection model detects the wrong pronunciation of consonants, it can give learners suggestions for correcting errors according to the way of pronunciation and the position of pronunciation. Pronunciation error detection is to detect the phoneme sequence of the pronunciation sentence to find the wrong part and error type of the phoneme pronunciation. This section will analyze the pronunciation principle of spoken language.

Audio feature extraction is an important step in improving the accuracy of detection in oral pronunciation detection. The obtained audio features are more suitable for

deep learning models than the original audio. Common feature extraction methods in the field of speech detection include Linear Prediction Coefficient (LPC), FBank (Filter Bank), and Mel-Frequency Cepstral Coefficient (MFCC).

**3.2. Preemphasis.** The sound propagation is essentially the propagation of energy. The energy loss of high-frequency sound is more serious than that of lower-frequency sound. The domain is more stable, and the spectrum can be obtained with the same signal-to-noise ratio over the entire frequency band. The preemphasis is calculated as follows:

$$s'_m = s_m - 0.95s_{m-1}, \quad (1)$$

where  $s_m$  represents the sampling point of the sound.

**3.3. Framing.** Sound framing is a fixed-duration segmentation process for sound in the time domain. In essence, a fixed number of sampling points are integrated into a unit, and the sampling value is generally 512. Another important aspect is to remove the effect between the vocal cords and the lips during vocalization. This can make the high-frequency formant more obvious. After framing, the audio signal is characterized by frame unit.

**3.4. Windowing.** After framing, the signal becomes smoother through Hamming window processing, reducing the size of sidelobes after fast Fourier transform processing and solving the problem of spectrum leakage. Compared with the ordinary rectangular window function, the Hamming window can obtain a higher quality spectrum. As shown in the following formula:

$$s''_n = \left\{ 0.54 - 0.46 \cos \left( \frac{2\pi(n-1)}{N-1} \right) \right\} s_n, \quad (2)$$

where " $s_n$ " is the  $n$ th sampling point of preemphasis in a single frame.

**3.5. Fast Fourier Transform.** Compared with the time domain, it can reflect the characteristics of the sound signal in the frequency domain, so the sound signal is changed into the frequency domain. The energy distribution can be analyzed more intuitively, and the difference in energy distribution shows the difference in sound characteristics. Therefore, the energy distribution on the spectrum can be obtained through windowing and fast Fourier transform. The square of the spectrum can be calculated by the square of the modulus and the average spectrum of the output signal, as shown in the following formula:

$$S_k(i) = \sum_{n=1}^N s_n''(i) \cos\left(\frac{2\pi kn}{N}\right) - j \sum_{n=1}^N s_n''(i) \sin\left(\frac{2\pi kn}{N}\right), 1 \leq k \leq K,$$

$$P_k(i) = \frac{1}{N} |S_k(i)|^2. \quad (3)$$

Among them,  $K$  is the Fourier transform length, where  $i$  represents the number of frames,  $n$  represents the number of sampling points, and  $s_n''(i)$  represents the value of the  $n$  sample point after windowing the  $i$  frame;  $S_k(i)$  is the  $k$ th value of the frame information spectrum.  $P_k(i)$  represents the  $k$ th value of the power spectrum of the  $i$  frame.

**3.6. Mel Filter Bank.** After obtaining the frequency spectrum and power spectrum, there is still a lot of useless information in the frequency domain signal. Therefore, the amplitude of the frequency domain needs to be filtered through the Mel filter bank, and each single value represents a frequency band. Finally, the 26-dimensional Mel filter value is obtained:

$$M = 1125 \log\left(1 + \frac{x}{700}\right),$$

$$f_n = \frac{sf_n}{K},$$

$$mfb_{nf} = 700\left(e^{f_{nf}/1125} - 1\right),$$

$$Rf_{nf} = \sum_{k=1}^{K/2} P_k \left[ (f_k - mfb_{nf}) / (mfb_{nf+1} - mfb_{nf}) \right], f_{nf}$$

$$\leq Mf_k \leq f_{nf+1},$$

$$Rf_{nf} = \sum_{k=1}^{K/2} P_k \left[ (mfb_{nf+2} - f_k) / (mfb_{nf+2} - mfb_{nf+1}) \right], f_{nf+1}$$

$$\leq Mf_k \leq f_{nf+2}. \quad (4)$$

**3.7. Logarithm.** The human ears perception of sound signals is a nonlinear process, so nonlinear processing is required before cepstrum analysis can be performed. Nonlinear processing is the logarithmic operation of the value obtained by Mel filtering, as shown in the following formula. The prediction is shown in Figure 3.

$$LRf_{nf} = \log\left(Rf_{nf}\right). \quad (5)$$

**3.8. Discrete Cosine Transform.** In fact, each filter is partially repetitive in the filtering frequency band, so the energy value obtained also has a certain relevance. Discrete cosine transform can perform dimensionality reduction, compression, and abstract processing of data. After processing, the characteristic parameters have no imaginary part, which is more convenient in calculation. The discrete cosine transform dimension is 13, and the value of  $nc$  is between 1 and 13. The calculation is shown below.

$$D_{nc} = \sqrt{\frac{2}{NF}} \sum_{nf=0}^{NF-1} LRf_{nf} \cos\left(\frac{\pi nc}{NF}(nf + 0.5)\right) a_{nf}. \quad (6)$$

**3.9. Dynamic Characteristics.** Sound is a continuous signal in the time domain. The continuous signal is a dynamic process, but a single frame only reflects the characteristics of a single moment and cannot reflect the continuity of the signal. Therefore, the feature dimension is increased, and the dimension of the frame before and after it is added, which is the common first-order difference and second-order difference. The first-order difference calculation is as follows:

$$d_t = \frac{\sum_{st=1}^{ST} st(c_{t+st} - c_{t-st})}{2\sum_{st=1}^{ST} st^2}, \quad (7)$$

where the  $d_t$  indicates that the first-order difference is added to the data with the number of frames  $t$ , and  $ct + s$   $t$  is the feature of  $t + st$  frame. In calculating the second-order difference,  $ct + st$  indicates the first-order difference result of the corresponding frame, and  $d_t$  corresponds to the second-order difference value. The predicted value is shown in Figure 4.

Multimodal features can fuse and combine the feature information of multiple modals to provide more comprehensive information for the spoken pronunciation detection model. Multimodal fusion can be divided into feature-level fusion, decision-level fusion, and hybrid fusion based on the fusion relationship. Feature-level fusion feature fusion is also called front-end fusion. This method refers to the fusion of the input data that enters the model before the model learning, that is, the feature of each mode is fused through a certain method before entering the training model. We can understand this process as the process by which humans recognize the surrounding things. People recognize an object not only by its shape but also by combining its taste, touch, and other aspects to make judgments. These features are combined and transmitted to the brain for judgment. In practical applications, feature fusion needs to cascade the features of multiple modes after time synchronization and then uses a classifier to model this fusion feature. The current feature fusion methods mainly include feature direct connection, feature weighting, feature projection and mapping, and auditory feature enhancement. Decision fusion is also called back-end fusion, which uses the prediction results obtained after different modal information is trained separately for further fusion. This fusion method does not require the feature alignment of the two modalities in the previous period, and separate training of different modalities to avoid a huge impact on the results when a certain modal information is missing or an error occurs. Common decision fusion methods include maximum fusion, average fusion, Bayesian rule fusion, and ensemble learning. In order to balance the advantages of feature-level fusion and decision-level fusion in different aspects, some researchers have proposed a hybrid fusion model.

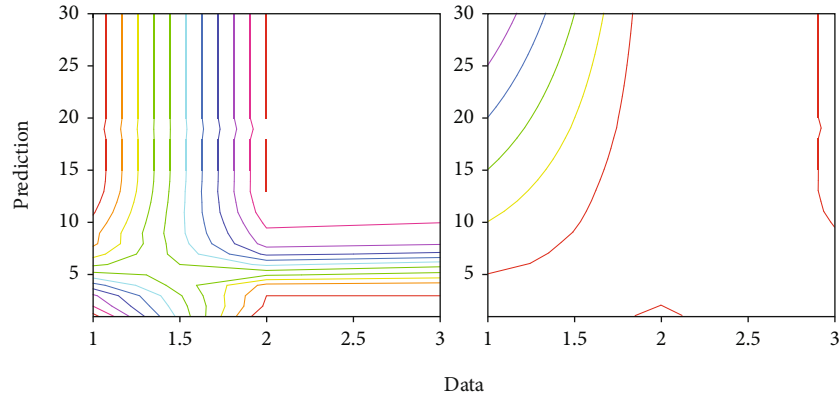


FIGURE 3: The prediction.

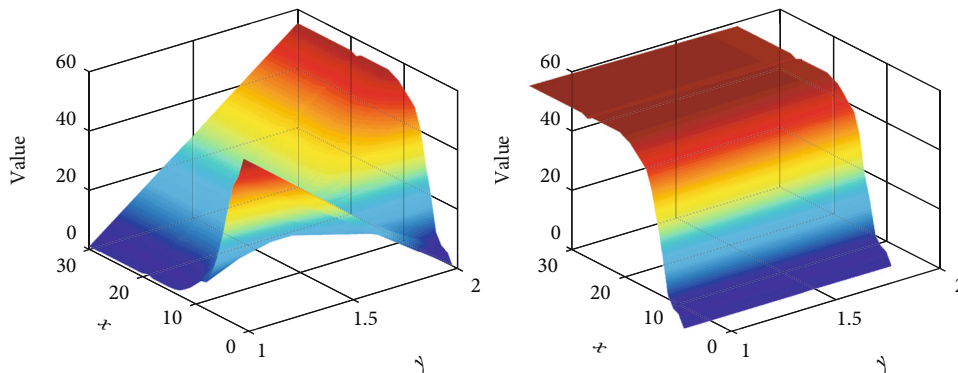


FIGURE 4: Predicted value.

#### 4. System Construction

This section introduces the design process of an end-to-end multimodal pronunciation detection system, including corpus construction, audio and video data preprocessing, audio and video feature extraction, audio and video information fusion, and end-to-end pronunciation detection model construction. The most important thing in the framework is the fusion of audio and video information and the construction of end-to-end pronunciation detection models. The overall framework design of the system has five parts. The first part establishes an audio and video corpus, obtains audio and video files and annotation files suitable for multimodal detection, and records a multimodal pronunciation test set. The second part preprocesses audio information and video information separately. The third part extracts feature of audio information and video information, respectively. The fourth part establishes a pronunciation detection model based on audio and video feature level fusion, and the fifth part realizes pronunciation detection and error correction. The specific framework is shown in Figure 5. Compared with monomodal acoustic corpus, audio and video corpora are more scarce, and most audio and video corpora are not open to the outside world. GRID corpus is a sentence-level audio and video corpus that is rarely public at present, and it is widely used in the field of lip recognition.

To achieve a good recognition effect for a multimodal pronunciation detection model, a suitable audio and video data set must be selected. The quality of the audio and video data set has a decisive effect on the recognition accuracy. Common audio and video data sets include the AVLetters data set based on letter words, the BANCA data set based on number sequences, the GRID data set based on phrases, and the OuluVS data set based on everyday sentences.

The system architecture of the multimodal BiLSTM-CTC acoustic model based on audio and video fusion is mainly composed of the following parts. The first part preprocesses the audio to extract the acoustic features and preprocesses the video to get the key points of the lips. Information, normalization, and feature enhancement are performed to obtain video features. The second part interpolates the video information to ensure that the audio and video information rate is the same, and the audio and video are aligned and cascaded to obtain the audio and video fusion characteristics. The third part is the BiLSTM network, which uses the LSTM network to learn timing features, and through the Softmax classification layer, the probability of the output sequence is obtained. The fourth part is the CTC output layer, which is used to generate prediction output sequences. The error variation is shown in Figure 6. This model performs feature fusion on modalities with data synchronization and low correlation and performs decision

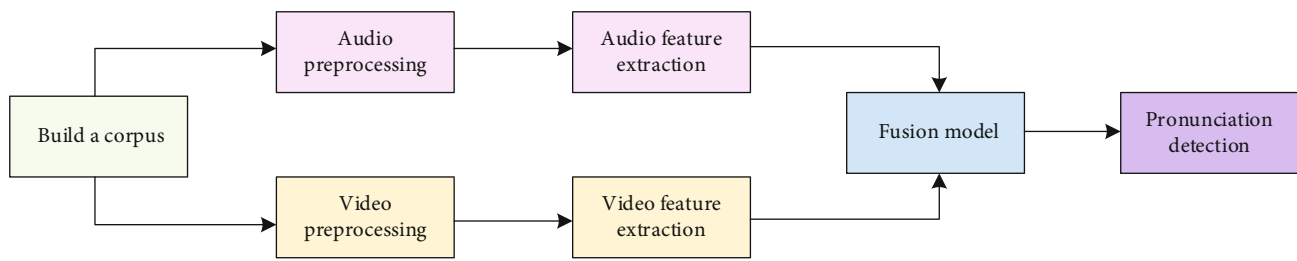


FIGURE 5: The specific framework.

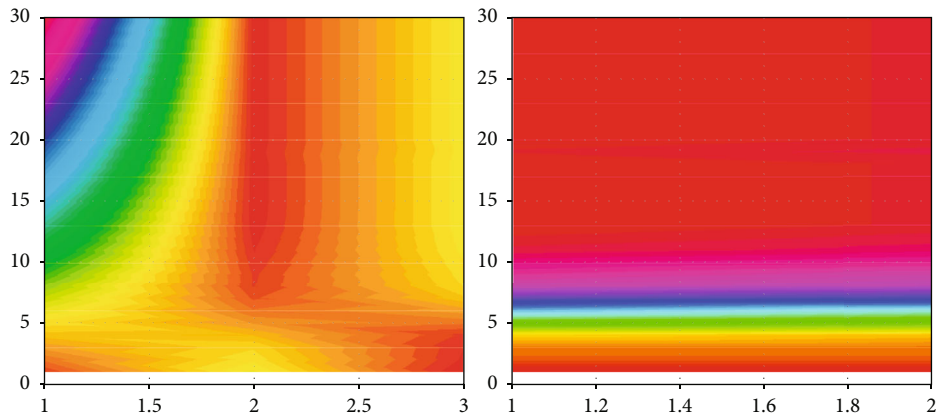


FIGURE 6: Error variation.

fusion on modalities with different data and updates and strong correlation.

The experimental data set in this chapter comes from the GRID phoneme annotation corpus constructed in previous content and the self-constructed multimodal pronunciation test set. The GRID corpus contains 34 speakers (18 males and 16 females), each with 1,000 spoken pronunciation videos and audio, the sampling rate of audio is 50 kHz, and the resolution of video is 720×576 dpi. The original GRID data set annotation file has annotated the words in the sentence. In Section 3, all the word annotations have been converted into phoneme annotations with reference to the cmudict dictionary to make it consistent with the usage of the model. The video data set of 1 out of 34 people does not exist, so the audio and video set of 33 people is selected, and each person selects the audio data set of 200 sentences, totaling 6600 video files. One-tenth of the audio and video files are selected as the model test set, and the remaining files are the training set. The self-built multimodal pronunciation test set is also used as the test set. In order to better reflect the robustness of the model, white noise is added to the original audio data set. The noise comes from the NoiseX-92 noise library. The audio data set after the noise is added and the audio stream of the original data set still need to be consistent. If this change will cause the audio information and the video information to be inconsistent in timing, it will affect the accuracy of multimodal detection. The signal-to-noise ratio of the added white noise is 10 dB audio signal, as shown in Figure 7(a). Compared with Figure 7(b), the audio after adding noise

still maintains the synchronization relationship at the same sampling point. In actual engineering applications, there is a chance that it will have a better effect than pure feature fusion or decision fusion.

In the experiment, the feature fusion of audio and video information is carried out first, and the fusion feature is input into the long and short-term memory network. In the experiment, the structure of the bidirectional long and short-term memory network with 3 hidden layers is selected. The lip key point position information dimension is 40 dimensions, and the angle information dimension is 6 dimensions. The MFCC coefficient of the audio input is 39 dimensions. After feature fusion, the key point position fusion feature is 79 dimensions, and the angle fusion human feature is 45 dimensions. The number of iterations is set to 300, and the training batch size is set to 64. The experiment is based on the Windows 10 64-bit operating system and the Urbanu 18.4 operating system, the CPU is Intel I7, and the GPU is NVIDIA gtx1080.

Under the condition of no noise, the speech recognition training process of speech modal, multimodal based on key point position fusion, and multimodal based on angle feature fusion are shown in Figure 8. It can be seen from the above three figures that as the number of model iterations increases, the loss of the training set is continuously reduced, and the training accuracy is also continuously improved. Besides, the two subfigures are similar since variation is also similar. Among the three schemes, the angle feature fusion and the speech monomodal speech recognition converge faster and basically converge around the 150th round. The

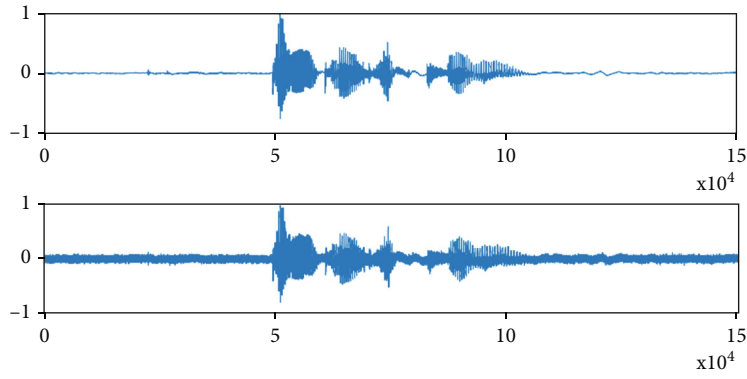


FIGURE 7: Audio signal with/without noise.

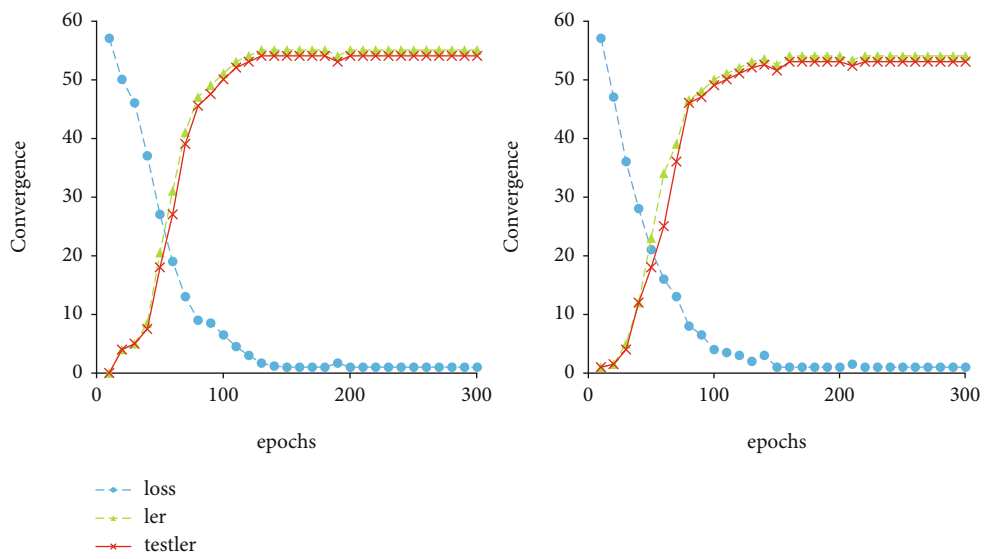


FIGURE 8: Training of the model.

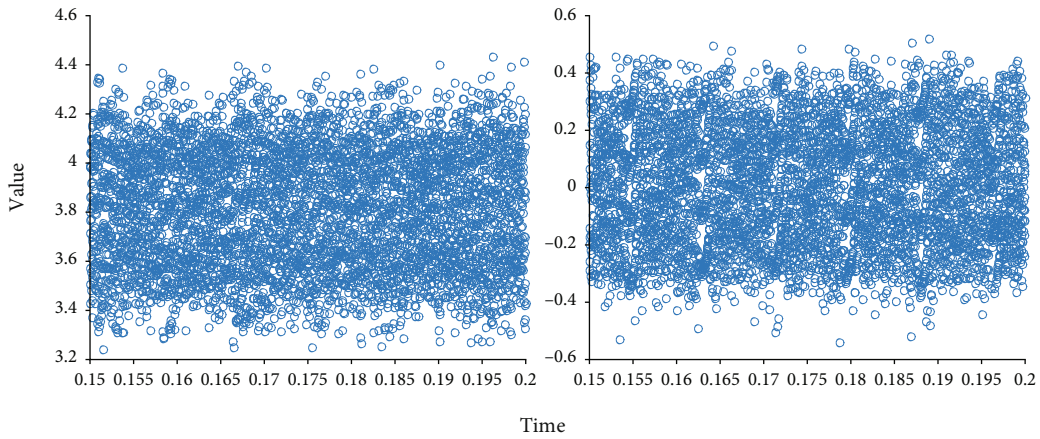


FIGURE 9: Predicted value vs time.

multimodal fusion based on key point features converges slowly, and it gradually converges in the 250th round. The predicted value vs time is compared in Figure 9. It can be

seen from the figure that the value varies all the time. Though the waveform in these subfigures are similar, the average value is completely different.

## 5. Conclusion

From the perspective of multimodal discourse analysis, guided by the theory of systemic functional linguistics, combined with the characteristics of the oral English classroom, this study proposes a new mode of college English oral teaching based on the multimodal theory and conducts a randomized controlled demonstration research. The research found that compared with the traditional oral English teaching mode, the multimodal collaborative and student-centered multimodal output design in the multimodal oral English teaching can effectively improve the students' oral English level and also provide a good foundation for the college oral English classroom teaching.

## Data Availability

The data used to support the findings of this study are available from the corresponding author upon request.

## Consent

The patient picture information involved in the manuscript has obtained my consent, and there is no violation of privacy and illegal use.

## Conflicts of Interest

The authors declare that they have no known competing financial interests or personal relationships that could have appeared to influence the work reported in this paper.

## Acknowledgments

This work was supported by the Xinyang University.

## References

- [1] L. Wang and W. Gou, "Influence of Negative Transfer of Dialects on English Pronunciation and Teaching Strategies," in *Proceedings of 4th International Workshop on Education Reform and Social Sciences (ERSS 2021)*, pp. 2–7, Chengdu, China, 2021.
- [2] X. Wenqi and P. Moonyoung, "Using automatic speech recognition to facilitate English pronunciation assessment and learning in an EFL Context," *International Journal of Computer-Assisted Language Learning and Teaching*, vol. 11, no. 3, pp. 74–91, 2021.
- [3] G. Zhang, P. Anand, K. S. Cheung Simon, H. C. Ching, and D. Sadia, "Quality evaluation of English pronunciation based on artificial emotion recognition and Gaussian mixture model," *Journal of Intelligent & Fuzzy Systems*, vol. 40, no. 4, pp. 7085–7095, 2021.
- [4] H. Jia, "Analysis on the path of English pronunciation teaching in colleges and universities," *Advances in Higher Education*, vol. 5, no. 1, pp. 1–9, 2021.
- [5] H. Chao, Z. Feng, F. K. Soong, M. Chu, and R. Wang, "Automatic mispronunciation detection for Mandarin," in *IEEE International Conference on Acoustics*, pp. 5077–5080, Las Vegas, NV, USA, 2018.
- [6] I. Rehman, A. Silpachai, J. Levis, G. Zhao, and R. Gutierrez-Osuna, "The English pronunciation of Arabic speakers: a data-driven approach to segmental error identification," *Language Teaching Research*, vol. 1, no. 2, 2020.
- [7] P. A. Dixon, "Book review: English pronunciation teaching and research: contemporary perspectives," *RELC Journal*, vol. 52, no. 1, 2021.
- [8] G. Min, "Factors affecting Yi ethnic minority EFL learners' English pronunciation learning in Leshan Normal University, Sichuan, China," *English Language Teaching*, vol. 13, no. 6, pp. 104–118, 2020.
- [9] H. C. Chen and J. X. Tian, "Developing and evaluating a flipped corpus-aided English pronunciation teaching approach for pre-service teachers in Hong Kong," *Interactive Learning Environments*, vol. 1, pp. 1–14, 2020.
- [10] V. Aulia, "English pronunciation practices: from tongue twisters to YouTube Channel," *Script Journal Journal of Linguistic and English Teaching*, vol. 5, no. 1, pp. 44–54, 2020.
- [11] X. Qian, H. Meng, and F. Soong, "The use of DBNHMMs for mispronunciation detection and diagnosis in L2 English to support computer-aided pronunciation training," in *Thirteenth Annual Conference of the International Speech Communication Association*, shanghai ,china, 2021.
- [12] K. Li, X. Qian, and H. Meng, "Mispronunciation detection and diagnosis in L2 English speech using multidistribution deep neural networks," *IEEE ACM Transactions on Audio, Speech, and Language Processing*, vol. 25, 2017.
- [13] R. I. Gusdian and R. Lestiono, "Incorporating Hijaiyah sounds in English pronunciation class: students' perception," *Journal of English Educators Society*, vol. 5, no. 1, pp. 83–88, 2020.
- [14] A. P. Gilakjani and R. Rahimy, "Using computer-assisted pronunciation teaching (CAPT) in English pronunciation instruction: a study on the impact and the teacher's role," *Education and Information Technologies*, vol. 25, no. 2, pp. 1129–1159, 2020.
- [15] K. N. Anastazija, M. C. Pennington, and P. Rogerson-Revell, "Martha C. Pennington and Pamela Rogerson-Revell. English pronunciation teaching and research: contemporary perspectives," *Journal of Second Language Pronunciation*, vol. 6, no. 2, pp. 265–269, 2020.
- [16] K. Yeni, R. Amin, and C. Raqib, "Designing phonetic alphabets for Bahasa Indonesia (PABI) for the teaching of intelligible English pronunciation in Indonesia," *Indonesian Journal of Applied Linguistics*, vol. 9, no. 3, pp. 726–734, 2020.
- [17] Y. Liu and K. W. Li, "A two-sided matching decision method for supply and demand of technological knowledge," *Journal of Knowledge Management*, vol. 21, no. 3, pp. 592–606, 2017.
- [18] J. Byun and S. Jang, "Effective destination advertising: matching effect between advertising language and destination type," *Tourism Management*, vol. 50, no. 10, pp. 31–40, 2015.
- [19] T. Aki and M. D. Kim, "Exploring Japanese EFL learners' attitudes toward English pronunciation and its relationship to perceived accentedness," *Language and Speech*, vol. 1, 2021.
- [20] K. Igarashi, I. Wilson, and I. Wilson, "Improving Japanese English pronunciation with speech recognition and feedback system," *SHS Web of Conferences*, vol. 77, article 02003, 2020.
- [21] Z. Qian, L. Yonghong, and L. Guo, "The facilitation of modern technics for English pronunciation class in foreign language learning in China," *Journal of Physics: Conference Series*, vol. 1437, no. 1, pp. 012027–012027, 2020.



- [22] G. Celia, "Teaching L2 English pronunciation: research and course Design," *Studies*, vol. 41, no. 2, pp. 215–224, 2019.
- [23] J. A. Brander and E. J. Egan, "The winner's curse in acquisitions of privately-held firms," *Review of Economics & Finance*, vol. 65, pp. 249–262, 2017.
- [24] Z. Palmowski, "A note on var for the winner's curse," *Economics/Ekonomia.*, vol. 15, no. 3, pp. 124–134, 2017.
- [25] I. Y. Pavlovskaya and L. Hao, "The influence of breathing function in speech on mastering English pronunciation by Chinese students," in *Proceedings of the 3rd International Conference on Social Sciences, Public Health and Education*, pp. 43–50, Huhhot, China, 2019.
- [26] B. M. Celeste and C. C. Patricia, "The voice of novices on the teaching of English pronunciation," *Praxis Educativa*, vol. 23, no. 3, pp. 1–9, 2019.
- [27] G. F. Smith and British Broadcasting Corporation, "Learning English: pronunciation," *Journal of Second Language Pronunciation*, vol. 5, no. 2, pp. 333–338, 2019.
- [28] C. JYH, "The choice of English pronunciation goals: different views, experiences and concerns of students, teachers and professionals," *Asian Englishes*, vol. 21, no. 3, pp. 264–284, 2019.
- [29] D. Ahn, S. Choi, D. Gale, and S. Kariv, "Estimating ambiguity aversion in a portfolio choice experiment," *Quantitative Economics*, vol. 5, no. 2, pp. 195–223, 2019.
- [30] T. Hayashi and R. Wada, "Choice with imprecise information: an experimental approach," *Theory & Decision*, vol. 69, no. 3, pp. 355–373, 2010.

## Research Article

# Streaming Media Music Classroom Teaching Mode and Effect Analysis Based on Audio Band Analysis Technology

Huizhong Wang <sup>1,2</sup>

<sup>1</sup>Faculty of Education, Nanyang Institute of Technology, Nanyang, Henan 473004, China

<sup>2</sup>College of Culture and Art, Hoseo University, Yashan City, Zhongqing South Road 31499, Republic of Korea

Correspondence should be addressed to Huizhong Wang; wanghuizhong@nyist.edu.cn

Received 20 January 2022; Revised 24 February 2022; Accepted 4 March 2022; Published 31 March 2022

Academic Editor: Wen Zeng

Copyright © 2022 Huizhong Wang. This is an open access article distributed under the Creative Commons Attribution License, which permits unrestricted use, distribution, and reproduction in any medium, provided the original work is properly cited.

Music teaching mode refers to the basic structure or framework of various types of music teaching activities under the guidance of certain music teaching ideas and music teaching theories. The process of music teaching needs to reflect the procedural coping strategies. With the continuous deepening of quality education reform, higher vocational colleges pay more attention to cultivating students' professional skills and vocational abilities. Therefore, many schools need to change the current situation of music teaching in higher vocational colleges and explore new music teaching models. School teaching expects to further stimulate students' interest in music learning and give full play to the aesthetic education function of music teaching. This article focuses on the research and evaluation of the music teaching model around the audio recognition technology and organically combines the music education theory with the music teaching practice. Research through the construction of a new mode of music teaching in higher vocational colleges, enrich the music teaching methods of music courses, and improve the effect of music teaching. The research has realized the aesthetic education function that music teaching should have in quality education. At the same time, the research results also provide a reference for music teaching in similar higher vocational colleges.

## 1. Introduction

Music education is an important carrier of humanistic quality education in higher vocational colleges. Music education has become an important way for higher vocational colleges to cultivate students' aesthetic ability, cultivate students' moral sentiment and promote students' all-round development. Music teaching mode is an important aspect of music teaching, and it also an important content of music educators' research. At present, academic circles at home and abroad have conducted researches on music teaching models from multiple angles, and many research results have obtained. However, there is still a lack of research on the music teaching mode of higher vocational colleges. In addition, there are relatively many researches on music teaching mode in domestic and foreign academic circles. There are differences in the form of music teaching in many links. At present, music teaching has also achieved good research results. However, the existing research content related to music teaching in higher vocational education is still rela-

tively lacking. The current teaching environment, teaching objects, and teaching process analysis are relatively insufficient. This article analyzes the current situation of music teaching in higher vocational colleges from the aspects of teaching object, teaching situation, and teaching effect. Research discovers that there are diversified problems, analyzes the causes, and refines relevant teaching concepts. The research then took Hubei Transportation Vocational and Technical College as an example to build an analysis framework and analyze the music teaching model. Researching and constructing a music teaching model that truly suits the characteristics of higher vocational colleges have strong theoretical significance for the study of music teaching models in higher vocational colleges [1–3].

Currently, most of the music teachers in higher vocational colleges graduated from relevant music colleges. In daily music teaching, there have been studies that have borrowed more from the teaching mode of music majors in ordinary colleges and universities to organize teaching. At present, there is a relatively lack of teaching experience and

practical cases in higher vocational colleges that can be used for reference. On the one hand, the existing research lacks practical research on music teaching mode in higher vocational colleges. The teaching mode is single, and the teaching structure is relatively loose [4–6]. On the other hand, the musical foundation of the teaching objects is weak, and the learning goals are not clear. Therefore, the teaching effect of music education in higher vocational colleges is not ideal. Music teaching not only did not bring students emotional pleasure but also brought depression of interest. Classrooms have only become a channel for obtaining credits [7–9].

The article uses literature research method, investigation research method, system analysis method, process analysis method, and other research methods to carry out research. The article focuses on the current research situation at home and abroad, the actual situation of music education in higher vocational colleges, the analysis framework of music teaching models, the construction of new music teaching models, and the implementation of path operations. Through literature research, it found that strengthening the practical links of music education has become the consensus of current music education research. Research on the scientific application of psychological principles has also become a common feature of contemporary music education and educational research at home and abroad. It can be seen that the current strengthening of music education practice has become the consensus of current music education research. Psychological research on scientific application has also become a common feature of music education and educational research at the current stage. Through investigation and research, it is found that higher vocational music education has not yet formed a mature music teaching model. Through investigation and research, it found that there is no mature music teaching model for music education in higher vocational colleges. The current music teaching structure is relatively loose, the curriculum setting is relatively random, and there is no fixed and unified teaching material [10–13]. The music quality of music teaching objects is generally low, and the effect of classroom music teaching is generally poor. Investigating the reasons found that it manifested in the problems of music education in higher vocational colleges. In addition, strengthening the research of music teaching in higher vocational colleges and reforming the mode of music teaching are important means to improve the level of music education in higher vocational colleges. Music teaching mode specifically refers to the completion of specific music teaching goals based on specific music teaching theories. This mode is relatively stable and maneuverable. This mode is also an integral part of the music teaching framework and its program system [14–16].

The school also pays attention to the education and cultivation of students' values, morals and ethics, aesthetic sentiments, and innovative consciousness. Music education is an important part of humanistic quality education in higher vocational colleges. Music teaching has offered as a public elective course in many higher vocational colleges. At present, music education in higher vocational colleges has problems in varying degrees, such as single music teaching mode and loose music teaching structure. In addition, the musical

foundation of music teaching objects is weak, and the learning goals are not clear. At present, there is a relatively simplistic trend in the mode of higher vocational music teaching. The structure of music teaching is relatively loose. In addition, the basis of music teaching objects is relatively weak. The learning objectives of music teaching are not clear enough. The effect of music teaching is not ideal for the previous music training. Music education in many higher vocational colleges is a mere formality, and the effect of music teaching is not ideal. In some colleges, music classes have only become a channel for obtaining credits [17–19]. The aesthetic education function of music teaching is difficult to realize. The article focuses on the characteristics of the times, vocational education, and students' personalities of music teaching activities. The article emphasizes the application of the laws of educational psychology and summarizes and puts forward the idea of "internal drive guidance." The article is innovative in the concept of music teaching reform and creatively summarizes and puts forward the "drive-guidance" model. The article has designed three presentation methods, which have greater practical significance in practice and have achieved good research results [20–23]. The research logical structure of this paper is shown in Figure 1.

## 2. Existing Research Results and Literature Review

This article collects more than 200 books, papers, and other documents through the library, CNKI, and <http://Weipu.com>. This article focuses on the literature review of music teaching, teaching mode, and music teaching mode. This article focuses on the study of music teaching mode in higher vocational colleges. This article's research on the music teaching mode in the field of vocational colleges found that most of the existing studies belong to journal papers. There are relatively few doctoral and master's theses. The article further reviews the classification of teaching modes under the guidance of different teaching theories in the main literature.

*2.1. Research Status of Music Teaching Mode.* In accordance with the idea of "internal drive guidance," this article uses systematic methods and process methods to establish an analysis framework for music teaching models. The text analyzes the elements of the music teaching model. The essentials put forward in this article include music teaching philosophy, music teaching goals, music teaching theory, activity framework, implementation conditions, operating procedures, and effect evaluation. The main teaching content proposed in this paper involves many aspects. Emphasis includes music teaching philosophy and goals, including the theoretical carding and implementation conditions of music teaching, including music teaching evaluation and other content. This paper focuses on the main body of teachers and students and further researches on music teaching. A related theoretical framework model is constructed. The article further analyzes the content of the framework of music teaching activities around elements such as teachers, students, lesson content, and music teaching methods. On

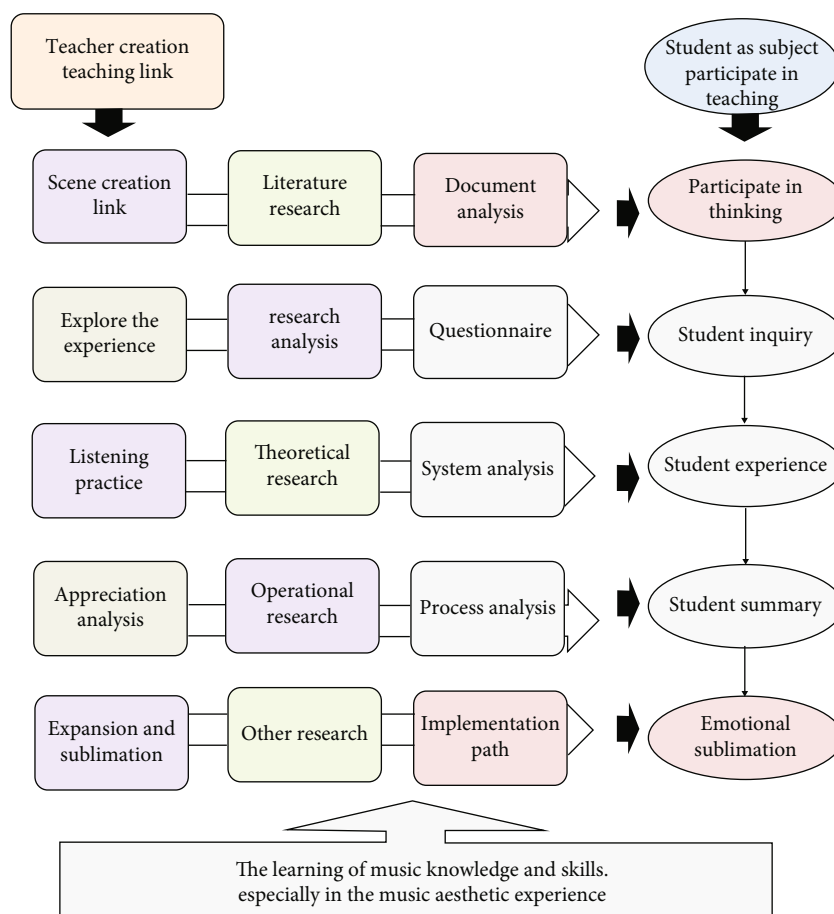


FIGURE 1: The research logical structure of this paper.

this basis, the article combines the characteristics of music education in higher vocational colleges to construct a “drive-guide” model. The article designs and proposes three presentation methods, namely, training-inquiry presentation based on professional needs, self-guided learning presentation method based on network resources, and experience-practical presentation based on the popularization of music. The article optimizes the curriculum system, curriculum music syllabus, and basic music teaching resources for higher vocational talent training. The article focuses on classroom music teaching design, network classroom construction, practice position construction, teacher team construction, music teaching object analysis, etc., and puts forward coping strategies and implementation suggestions [24–26].

There is a big difference between foreign vocational education and domestic vocational education, and related research is very different. Foreign vocational education research is relatively mature, and its theories are more. Specifically, these online resources are helpful for music learning. Contribute to the enrichment of music learning. The article also puts forward some opinions on the performance requirements of music popularization. The article further clarifies the key content of music classroom design. According to these literature research findings, the most important feature of this article is the in-depth application of psycho-

logical principles. We were influenced by these theories in the process of reviewing the literature. At the same time, as far as the literature we have contacted with, the foreign researches are more of the macroscopic results of pedagogy and educational psychology [27–30]. At the micro-specific level, there are few studies specifically targeting the “music education model.” The main reason is that the information collection channels are relatively limited. In addition, the differences between Chinese and foreign music education itself also were taken into consideration. Model analysis results are shown in Figure 2.

**2.2. Research Progress of Multimedia Music Teaching.** Each teaching mode was verified under the guidance of a certain teaching theory. According to different teaching objects, a complete set of procedural strategies was constructed according to specific teaching goals. In the book “Constructivism in Education,” American Stiffer et al. expounded the rich new ideas of constructivism. The core point of the research is constructivism. Specifically, it should be student-centered, emphasizing students’ active exploration of knowledge, active discovery, and active construction of the meaning of the knowledge learned. The teaching theory of constructivism provides a scientific theoretical basis for the construction of the music teaching mode of this thesis. In addition, music classroom teaching focuses on practicality.

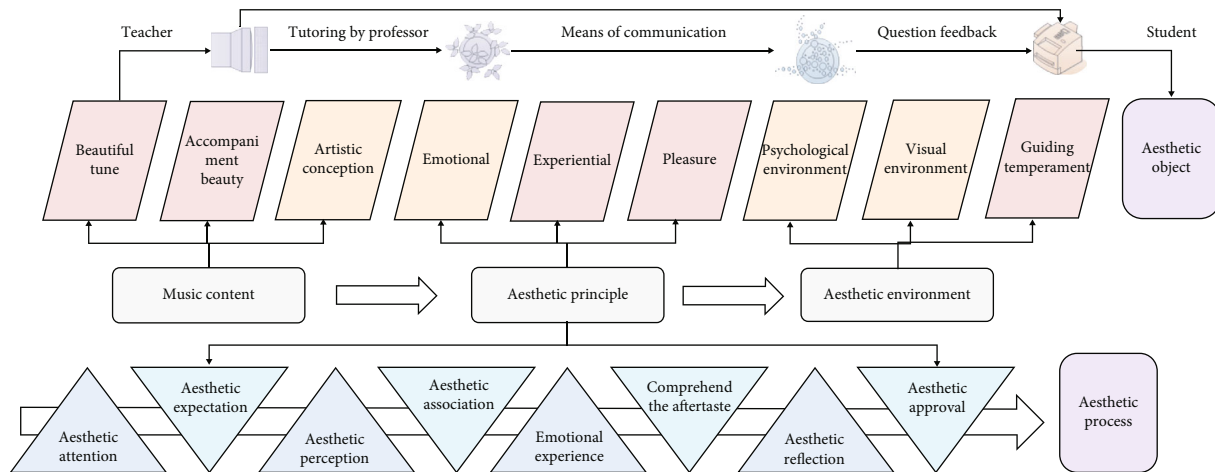


FIGURE 2: The theoretical model of the influence of background music aesthetics on college students.

This paper focuses on optimizing the teaching methods of higher vocational music in the classroom. The course teaching system has been improved, the music course training syllabus has been constructed, and the educational resources of the music classroom have been enriched. Furthermore, according to the many demands of music classroom teaching, corresponding teaching strategy and facility suggestions are put forward. The above two theories belong to the theory of constructivism. Compared with behaviorism, it is a kind of progress. Student initiative is valued, and research emphasizes student-centeredness. Following such a process, later teaching models tend to use multiple teaching theories. Research is moving towards a more complete and diversified era. It is difficult to put forward specific opinions in this field in this article [31–33].

The music curriculum reform started in September 2011, and it has been nearly ten years. The high school music curriculum reform is an integral part of the basic education curriculum reform. The reform of high school music curriculum involves curriculum nature, value, philosophy, goals, content, teaching, evaluation, management, and other content. The research fully reflects the new teaching method guided by the new curriculum concept. The music curriculum has brought a fundamental change in the roles of teachers and students. Great changes have taken place in the way students learn. The education reform of music curriculum has entered its tenth year today, and the reform of high school music curriculum involves the basic curriculum reform content. High school music courses focus on the intrinsic value, ideas, goals, and teaching evaluation of the curriculum. The research in this paper fully analyzes the new course teaching concepts and methods and truly makes the teaching activities full of interactivity. Change the existing methods of teaching and learning. The existing model reform has gradually replaced the traditional “lesson preparation.” Along with the curriculum reform, the teaching design of high school music has continuously optimized. In terms of teaching content, teaching process, and methods, the research all reflects the way of curriculum reform with students as the main body and aesthetics as the core. The

specific content includes music teaching design, standard, scientific, and artistic teaching under the curriculum concept. Curriculum reform enables the implementation of music teaching design. The design of high school music teaching is the foothold for deepening the concept of curriculum reform [34–37].

**2.3. Summary of the Research on Music Teaching Evaluation.** The theoretical viewpoints of constructivism include constructivist view of knowledge, view of students, view of learning, and view of teachers. Constructivist view of teaching: as an important part of the philosophy of learning, constructivism is a further development after the development of behaviorism to cognitivism. Many views and propositions of this theory are reasonable. The theory has certain reference significance to the education reform practice. Constructivism emphasizes that students are the main body of information processing and the active constructor of meaning. Students are not passive receivers and objects of knowledge. At present, constructivist theory has formed some specific teaching techniques in actual education that can promote the psychological development of students. This method has increasingly widely used. At present, the main meaning of interactive teaching refers to the interaction between students and teachers. Students are not simply passive recipients and objects of knowledge in the traditional sense. At the same time, interactive constructivism has also developed some practical teaching skills to promote the development of students’ mental health in real life. Such methods are more widely used, including relatively mature inquiry-based learning techniques, incremental learning techniques, and learning techniques in the form of random access. Among them, relatively mature technologies mainly include inquiry learning, scaffolding teaching, and random access teaching. The main influence of constructivism on instructional design is mainly used in the cultivation of students’ perception. Research focuses on the differences in learners’ personality. Research focuses on the creation of a teaching atmosphere. Pay attention to the cultivation of students’ inquiry and creativity. Constructivist learning theory

is a major breakthrough in traditional learning theory. This theory puts forward a series of new theoretical viewpoints on learning and teaching, emphasizing the important role of “context” and “collaboration” in the construction of meaning. In turn, instructional design pays attention to the design of the learning environment at the beginning. Research focuses on the integration of learning theory with education and teaching practice and promotes the in-depth progress of education reform.

Studying the curriculum design in related teaching activities is a systematic and scientific plan set in advance for the final teaching practice. The key content of constructivism teaching is to cultivate students’ self-perception ability and to carry out adaptive education according to the individual differences of participants. This kind of theoretical learning is also a great breakthrough and innovation for the traditional teaching mode. It breaks through the simple static mode of teaching and learning and builds a new teaching environment of collaborative context. The teaching design at the macro level will eventually be perfected in practice. Instructional design can be carried out on different levels. The classification and levels of instructional design focus on different types and levels of needs. The specific operations can be targeted. First, proceed from the classification, including three aspects. The first category is instructional design at a macro level. The second category is teaching design at the meso level. The third category is microlevel instructional design. Macro teaching design belongs to “education system design.” It starts with reforming the relationship between education, society, and human development. This research focuses on the reform of the teaching system for the cultivation of new century and new talents.

*2.4. Research on the Evaluation Model of Music Teaching.* The famous German educator Herbart divides teaching into four stages in the book “General Pedagogy.” The four stages include “understanding, association, system, and method.” The research reveals the regularity of classroom teaching. The research explains the characteristics of students’ psychological activities in these four stages and the teaching methods that teachers should adopt, that is, the famous “quadrants” teaching model. Later, through his student practice and development, a “traditional teaching mode” has gradually formed. The research results have become the dominant teaching model in the 20th century. Herbart’s teaching model emphasizes teacher-centered and teacher-led teaching. This paper also focuses on exploring the characteristics of these activities from the four psychological stages of students. Emphasis is placed on analyzing teachers’ teaching methods. Classroom instruction is conducted by subdividing into four instructional quadrants. This teaching practice mode has been gradually developed, and a new teaching system has gradually formed, which has become the mainstream teaching mode in the current social environment. This model takes the teacher as the teaching center and pays attention to the absorption and exploration of knowledge by students. It is also an active teaching method. Pay attention to students’ mastery of knowledge. However, this method ignores the subjectivity of students. Students are in a passive

learning state. From the perspective of learning psychology, this is a behaviorist theory. In terms of constructivism, American Bruce and Joyce and Marshall will put forward the concept of teaching mode in the book “Teaching Mode.” The research believes that the teaching model has a landmark and important significance in theory. The contemporary teaching models at home and abroad are based on the teaching models of two scholars. Existing research also provides important reference value for the music teaching mode of higher vocational colleges. The two scholars divided the teaching mode into four main types, namely, social teaching mode, information processing teaching mode, personal teaching mode, and behavioral system teaching mode. Moreover, they extended 23 kinds of presentation methods. The interrelationships between model elements are shown in Figure 3.

### **3. The Changes and Influencing Factors of Multimedia Music Teaching Design**

Music instructional design is a subdiscipline constructed in instructional design. The teaching design link is the first link in the teaching of music teachers. The formulation of music teaching design was built on the characteristics of music discipline. Existing research defines the design of teachers and courses. The research emphasizes the task design of music teaching design and then systematically and comprehensively establishes the role of educators, participants, and teaching links in teaching design activities.

*3.1. The Systematic Analysis of Teaching Activities.* The discipline of instructional design emerged after the 1960s. With the design of the teaching system, a specialized research field has gradually formed. First, starting from the history and current situation in the field of international instructional design research, almost all first-class instructional design experts have a profound educational psychology background. This article conducts interdisciplinary research as a researcher. The current discipline has a long history of research on teaching mode. The continuous improvement of the teaching system has gradually built a relatively complete research system. Generally speaking, almost all current teaching institutions and education experts need to cultivate relatively deep psychological knowledge. In particular, interdisciplinary experts have a better understanding of how to disassemble professional knowledge and pass it on to student groups. The designer of the teaching and the object he faces, under the premise of respect, understanding, and cooperation, completes the activities of teaching and learning. Second is the theory of constructivism. The emergence of this theory hailed as a revolution in contemporary educational psychology. Constructivism can be traced back to Piaget and Vygotsky’s early research theories. It can gradually become popular since the 1990s. Contemporary Western irrational philosophical trends are gradually emerging. Network communication technology and multimedia technology continue to advance. Model analysis results are shown in Figure 4.

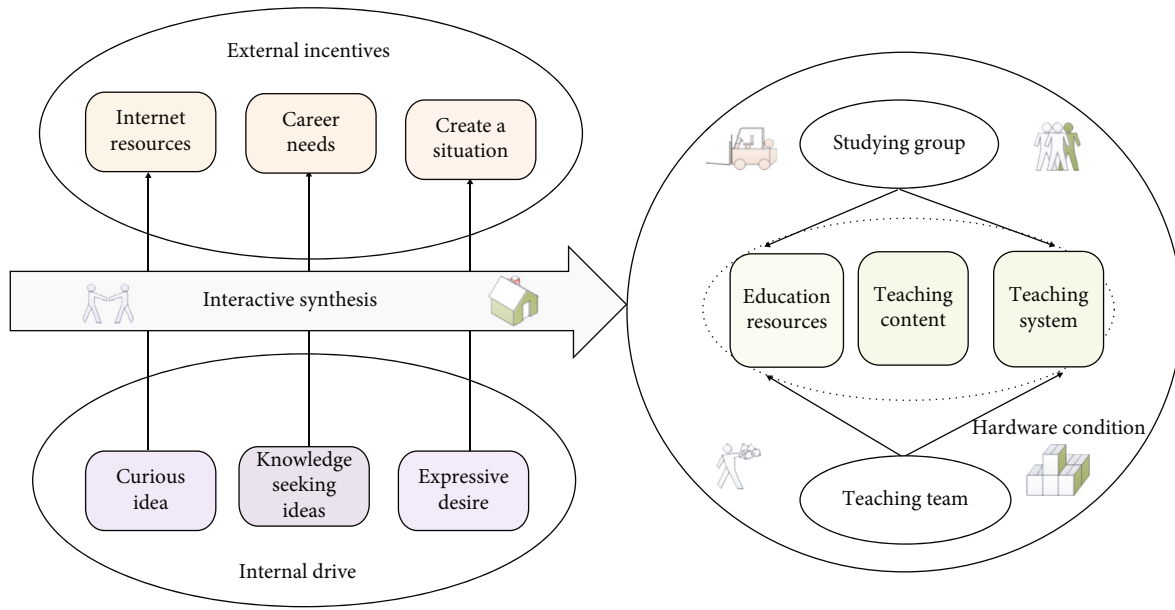


FIGURE 3: Diagram of the main factor system of teaching mode.

The curriculum reform cycle in countries all over the world is ten years. Microteaching design mainly faces the development of a certain course. The Madhyamika teaching design is mainly carried out in specific subject areas or in a number of interrelated teaching units. This method is called “discipline instructional design.” The role is equivalent to curriculum design and the units and modules in the subject. In general, countries around the world have relatively consistent timings for curriculum reform, generally set in ten years as a cycle. Microclassrooms are designed from the outset to focus on individual teaching units in specific subject areas. Through the design of teaching fragments, students can be familiar with and master the main content of the course teaching as soon as possible. This method is relatively more mature in application and more systematic in teaching design. The design of the course needs to consider the interaction of many factors and then meet the specific teaching objectives. The content can also include the design of teaching fragments. The application of this method is also the most common, so that the teaching design is really applied. Secondly, according to the scope and size of the problems in teaching, teaching design can be divided into three levels. One is classroom-centered. The second is “system”-centered. The third is product-centered. Class-centered mainly reflected in education and teaching ideas. The content of the school is based on the syllabus or curriculum standards, as well as the general teaching plan requirements. The curriculum was designed for the content, objects, and environmental conditions of the teaching. The curriculum usually is completed by the teacher. The specific “system” is the center, and the teacher, subject experts, and administrators work together to complete. There are also courses that are product-centric, and the content of the course is designed with media materials and teaching aids needed in teaching as products. Courses often need to determine which products have a broad market and can meet specific teaching

goals and demand. Model analysis results are shown in Figure 5.

In addition, the setting of music teaching curriculum also includes many aspects such as moral education and aesthetic education. Curriculum reform puts more emphasis on aesthetic education as the core and is aimed at teaching and educating people. At the current stage, my country has already started the reform of curriculum teaching in an all-round way, and teaching design must also give corresponding higher-level requirements. In the design of the whole teaching system, the artistic characteristics of music course teaching are more obvious and prominent. The curriculum reform puts more emphasis on the concept of taking aesthetics as the core and educating people as the goal. Under the background of fully implementing subject teaching, teaching design must put forward higher requirements. In the implementation of teaching design activities, the music subject is particularly prominent in terms of artistic characteristics. Consider that music itself is an important part of human art. The teaching design of music can improved through the creativity of teachers. The full implementation of the new educational concept can enhance the advantages of the discipline. At the same time, music discipline is one of the basic disciplines of school education. The subject can implement aesthetic education for students. In addition, music teaching is an important part of our country’s basic education. Music education assumes different responsibilities. On the one hand, it is an important way to implement aesthetic education for students. On the other hand, music education can improve teaching design and research effects and strengthen the logical teaching system design of subject teaching. In the study of music design, follow the systematic methods and rules of design. The school develops training courses that can enhance students’ high-level spiritual pursuits. The curriculum can provide effective guidance for students’ personality development, ability generation, values,

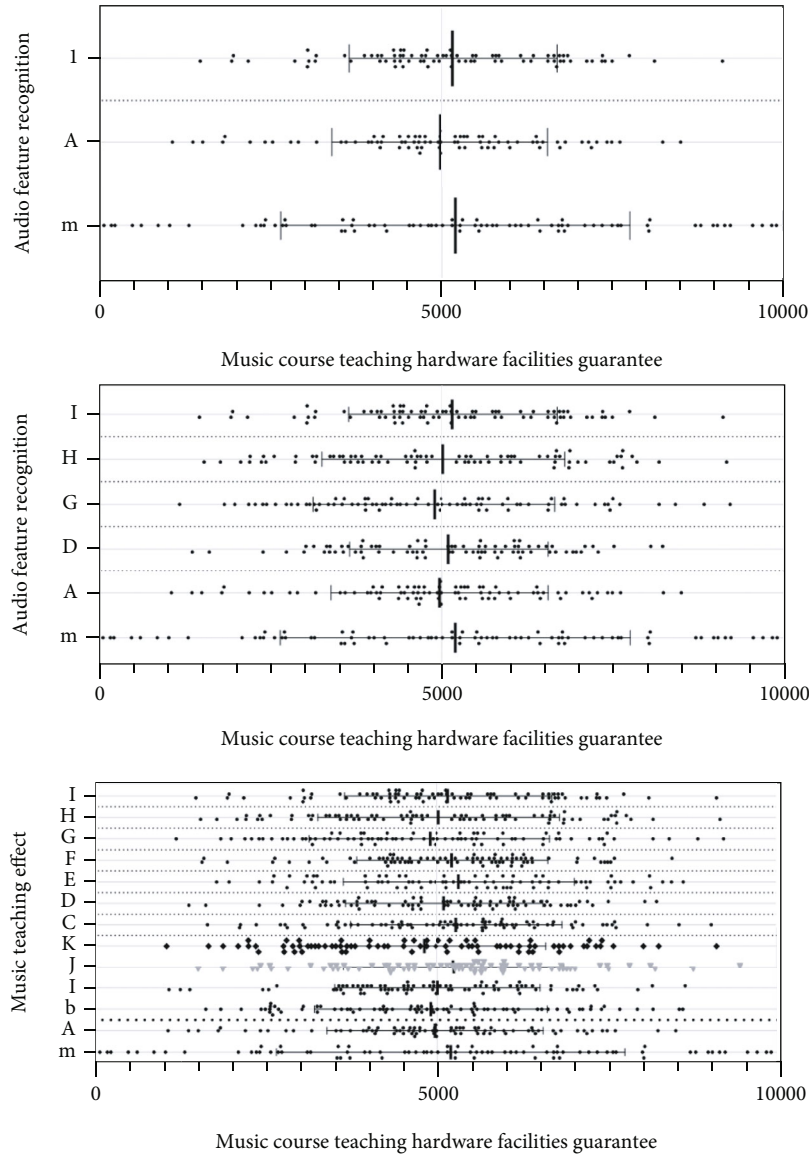


FIGURE 4: Analytical results of the research model of music teaching evaluation.

and outlook in life, specifically, starting from the students' high-efficiency learning needs and selecting limited class hours and textbook capacity. Explore and research more scientific teaching process and teaching mode. It has been common for schools to ignore music teaching for a long time. Especially in our country's curriculum reform, the implementation of the high school music curriculum of aesthetic education has experienced a difficult development process. Model analysis results are shown in Figure 6.

**3.2. The Method of Combing the Elements of Teaching Mode.** Specifically, teaching activities have two main bodies, namely, teachers and students. These two types of subjects were interactively linked by means of communication. Teachers are mainly responsible for teaching tutoring, while students are responsible for asking questions and feedback. Teachers belong to a certain teaching team. Students belong to a certain study group. The object of teaching activities is

teaching content. It should note that the teaching content is set around the purpose of teaching. Teaching content generally includes knowledge, thoughts, and feelings. The purpose of teaching is affected by factors such as students' cognition, how to say the quality, and the strength of learning ability. Compared with the related teaching content, the goals of the whole course or music teaching are different. The content is attached to the material carrier and presents various existence. Some forms are text, some are pictures, some are sounds, and some are videos.

The function of forgetting gate is to determine the part discarded from the input information  $h_{t-1}$  and  $x_t$  and output a value between 0-1. The larger the value, the more information is retained. The output of forgetting gate is calculated as follows:

$$f_t = \sigma(W_f \cdot [h_{t-1}, x_t] + b_f), \tag{1}$$



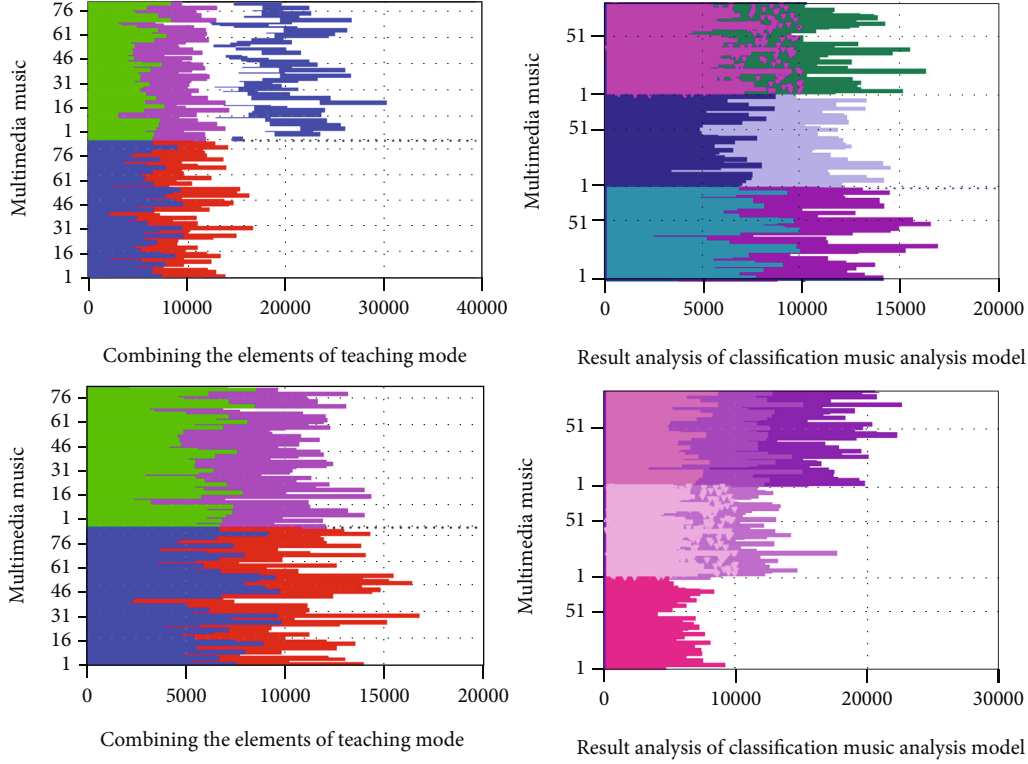


FIGURE 5: Result analysis of categorized music subject analysis model.

$$\dot{i}_t = \sigma(W_i \cdot [h_{t-1}, x_t] + b_i), \quad (2)$$

$$C'_t = \tanh(W_C \cdot [h_{t-1}, x_t] + b_C). \quad (3)$$

Suppose that index evaluation set is represented by  $A$ ,  $r_j$  is represented the membership degree vector, and the data set is represented as follows:

$$r_j = (r_{j1}, r_{j2}, r_{j3}, r_{j4}, r_{j5}). \quad (4)$$

In the formula,  $r_j$  represents the membership degree vector corresponding to the index evaluation set  $A$ . Assumptions are as follows:

$$B = (B_1, B_2, B_3, B_4, B_5). \quad (5)$$

Self-organizing process adaptively forms the first-level intermediate model:

$$z_k = f_k(v_i, v_j), i, j = 1, 2, \dots, 6. \quad (6)$$

And in the training set  $A$ , the parameter prediction method is used to predict the coefficient of  $z_k$ . In the test set  $B$ , the competition model  $\{z_k\}$  is filtered through external specifications, and the middle candidate injury model  $w_k = (z_k)$  is collected and used as the input of the second layer of the network.

In addition, teaching content has multiple carrier forms at the same time. When constructing teaching mode or designing teaching in this article, we can choose suitable carrier form according to the needs of teaching form. For exam-

ple, if you feel that the text is boring, you can express the text as subtitles. Then, mark the text in the video, and the effect will be much better. At the same time, the means of dissemination has changed from distributing paper materials to watching videos. The constituent elements of teaching activities are the basic framework system for building teaching models. Different teaching modes have different feedback forms for each element. For example, some models focus on the role of teachers. Some models favor the active participation of students. Some models rely on the transformation of teaching content. Some models focus on the reform of teaching methods. Therefore, when constructing the teaching model in this article, it will be designed in accordance with the requirements of the teaching philosophy and the actual conditions of each element. Model analysis results are shown in Figure 7.

The teaching mode is a set of structured and systematic framework built based on teaching theories under the guidance of teaching concepts. Considering that music teaching is an important part of human art teaching, the improvement of music teaching design still mainly depends on teachers' teaching. In the process of implementing the new teaching concept, the advantages of music discipline can be continuously carried forward. In addition, music education cannot only learn the relevant knowledge of music theory; in addition, it can also cultivate students' appreciation ability and improve students' aesthetic education. The composition of the teaching model includes teaching concepts, teaching goals, and teaching theories. The specific content also includes content such as activity framework, implementation conditions, operating procedures, and effect evaluation.

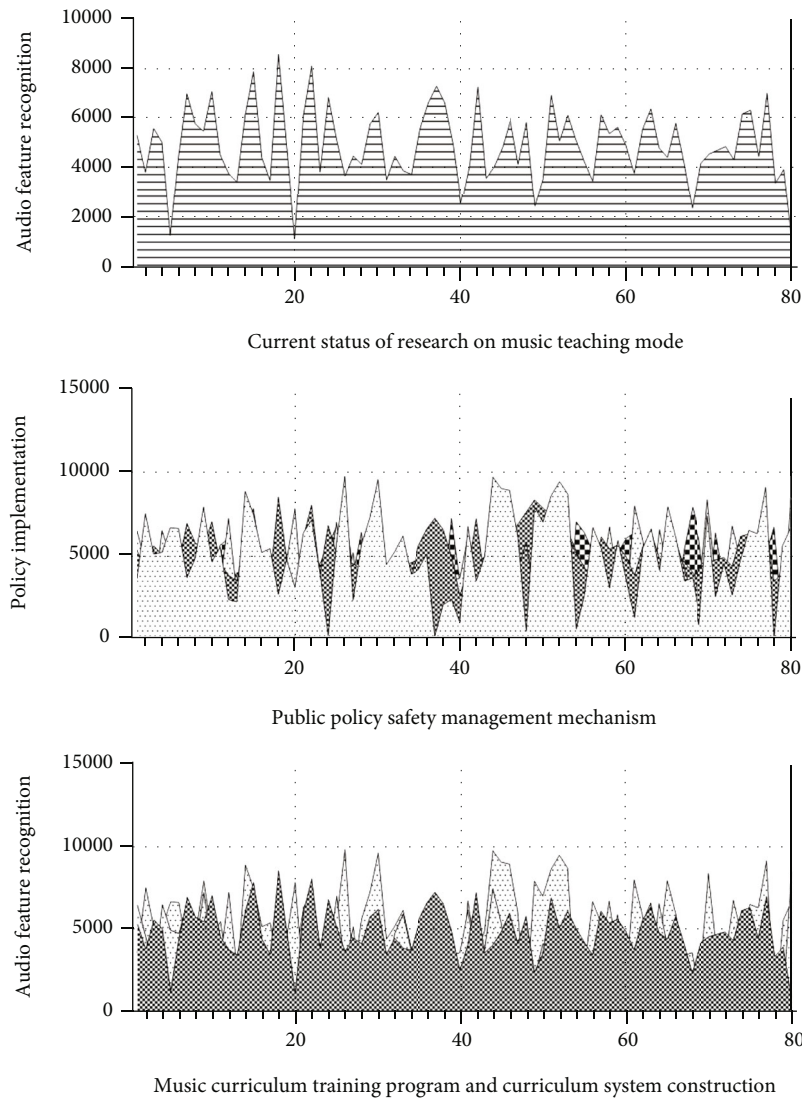


FIGURE 6: Music curriculum training program and curriculum system construction.

Among them, the teaching concept is a kind of guiding tendency with purpose. This concept focuses on the direction and uniqueness of the teaching model. This mode is also the essence and soul of the teaching mode. The teaching philosophy is often based on a certain theory, combined with the actual situation of teaching to get a guiding point of view. The teaching goal is the inclination requirement in the process of talent training. This view is different from the micro-teaching purpose of the previous article.

Shape the general functional relationship between the output  $y$  of the injury model and the input  $x_1, x_2, \dots, x_n$ . The Kolmogorov-Gabor polynomial is as follows:

$$y = f(x_1, x_2) = a_0 + a_1x_1 + a_2x_2 + a_3x_1^2 + a_4x_2^2 + a_5x_1x_2. \quad (7)$$

We treat each of the monomials as  $m$  input models in the original structure of the modeling network:

$$v_1 = a_0, \quad v_2 = a_1x_1, \quad v_3 = a_2x_2, \quad \dots, \quad v_6 = a_5x_1x_2. \quad (8)$$

The final information  $i_t \times C_t'$  is expressed as the value that can be obtained  $C_t$  from the output information of the joint forgetting gate:

$$C_t = f_t * C_{t-1} + i_t * C_t'. \quad (9)$$

The calculation method is as follows:

$$O_t = \sigma(W_o \cdot [h_{t-1}, x_t] + b_o), \quad (10)$$

$$h_t = o_t * \tanh(C_C). \quad (11)$$

Coverage index calculates the ratio of predicted items to all unscored items, so as to measure the comprehensiveness of prediction. Assuming that  $h$  items are predicted, the calculation method of coverage is as follows:

$$\text{Cov} = \frac{h}{n}. \quad (12)$$

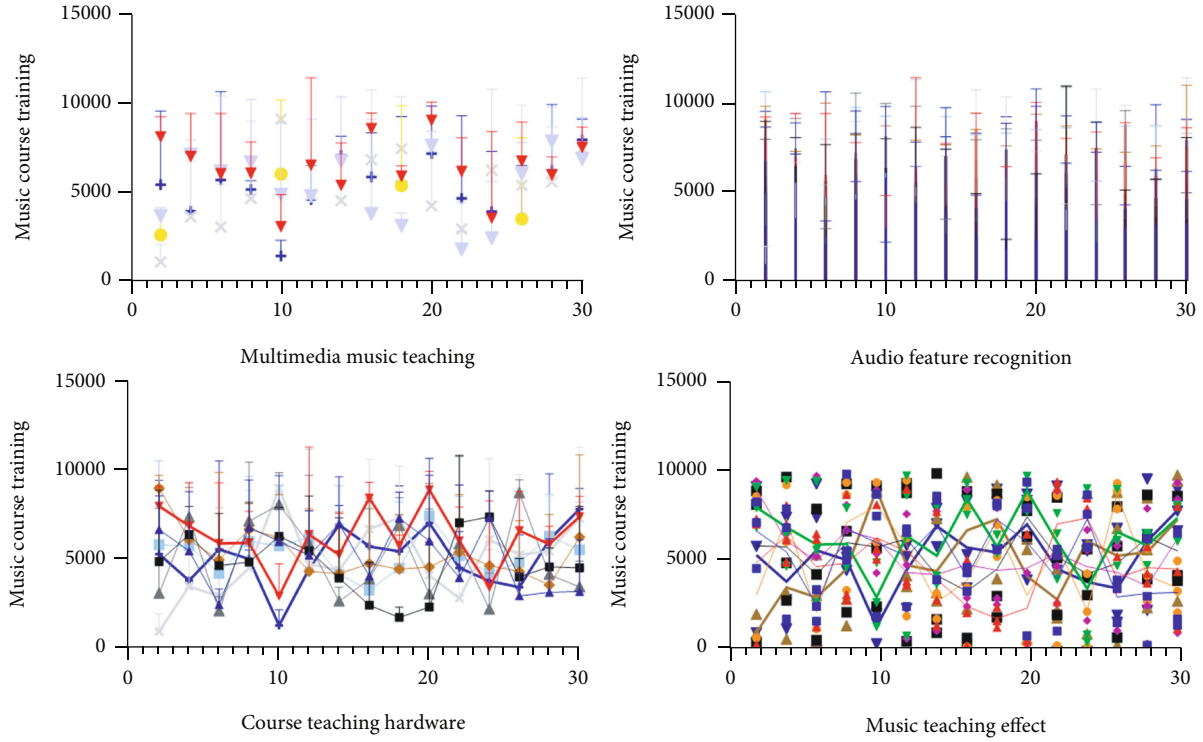


FIGURE 7: Music curriculum syllabus and condensed teaching content.

Recall index is also used to evaluate the system effect in the field of information retrieval. The larger the recall value is, the better the recommendation quality of the algorithm is.

$$\text{recall} = \frac{\text{Hits}}{|\text{test}|} = \frac{|\text{test} \cap \text{Top} - N|}{|\text{test}|}. \quad (13)$$

In order to verify the clustering effect of user attributes, the contour coefficient  $S$  is used to evaluate the clustering result, and the specific expression is as follows:

$$S(i) = \frac{b(i) - a(i)}{\max\{a(i), b(i)\}}. \quad (14)$$

The goal is the core element of the teaching model. According to the requirements of the concept and the actual situation, the research formulates the correct teaching goals. This has also become the key to constructing a teaching model. The different teaching goals determine the different teaching modes. Teaching objectives determine the setting of courses in teaching activities. The teaching process is the arrangement of teaching content and the design of teaching strategies. At the same time, teaching goals are also a measure of teaching evaluation. Teaching evaluation must be developed around teaching goals. Teaching theory is a systematic method system that serves the model. Teaching content is the concrete expression of teaching philosophy. The study of teaching mode is the specific content based on philosophy, psychology, and pedagogy. The teaching mode was

completed under the guidance of a certain teaching theory. Model analysis results are shown in Figure 8.

The activity framework is the basic framework established based on the teaching activity system. This is the main content of the teaching model. The essence of the teaching activity framework lies in the setting of teaching goals. Under the guidance of certain teaching theory, reasonably plan and arrange each teaching element in the teaching implementation process, to achieve the optimization of the teaching process. The teaching activity framework includes the determination of the teaching subject and setting of teaching content. Many elements in the process of teaching implementation, such as the design of teaching methods, should be optimized. The core content of the teaching activity framework is teaching communication activities. The main difference between different teaching modes lies in the different teaching activities process. Model analysis results are shown in Figure 9.

3.3. *Suggestions on the Implementation of New Music Teaching Mode and Teaching Improvement.* Implementation conditions, operating procedures, teaching evaluation, etc., are auxiliary contents that serve the main contents. Once a stable teaching activity framework is formed, the model builds the main skeleton of the teaching model. Implementation conditions refer to the guarantees of various conditions that play a role in the specific implementation of the teaching model. The main content is music teaching. The implementation of teaching content requires the support of various teaching software and hardware. Among them, the hardware content includes multimedia classrooms necessary

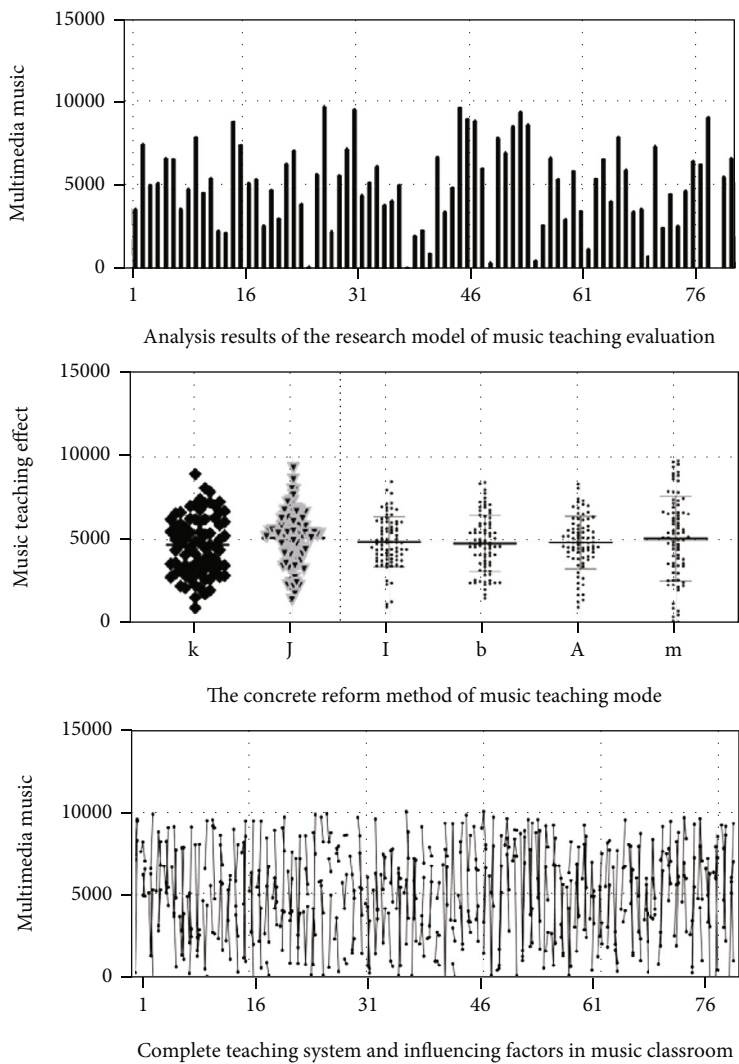


FIGURE 8: The construction of teaching staff in music courses.

Differentiated selection mode of music course training program

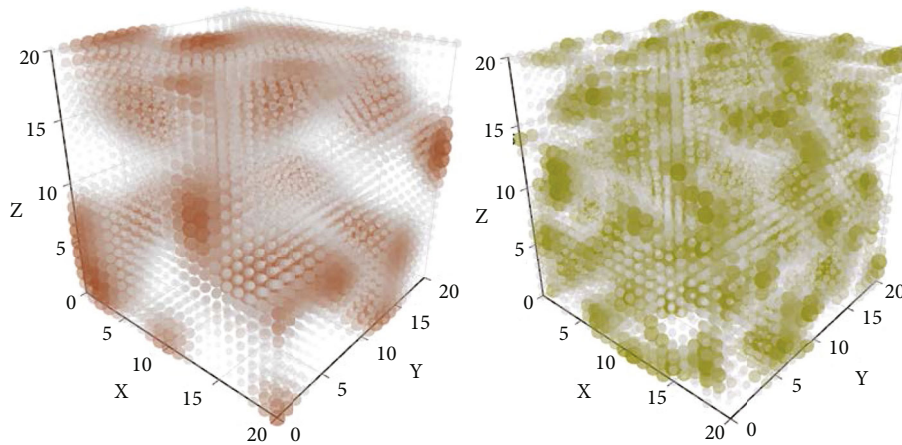


FIGURE 9: Guarantee of teaching hardware facilities for music courses.

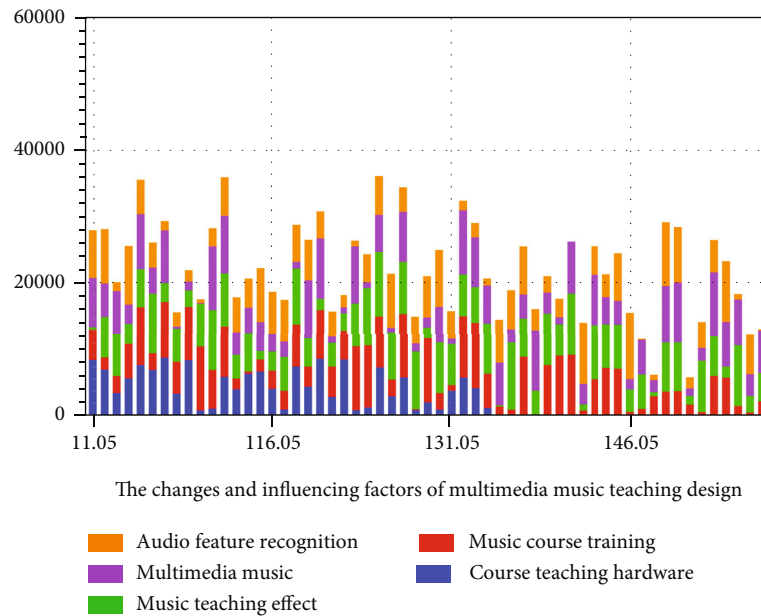


FIGURE 10: Differential selection mode of the music course training program.

for music teaching, including audio equipment and other teaching facilities. Software support mainly includes factors such as teacher-student relationship and teaching environment. Operating procedures are specific instructions for the implementation of the teaching mode. The content serves as a scientific arrangement to support the operation of the teaching mode. Teaching activity as an interactive activity is complicated to operate and requires many skills. Therefore, the model needs a good set of operating procedures. Teaching evaluation is a judgment on the teaching process and teaching results according to specific teaching goals. Teaching evaluation is a method to test whether the teacher has completed the teaching task. The content includes the verification of teaching links and teaching design.

At the same time, teaching evaluation is also an effective means to test the teaching model. In summary, as a framework system and strategy system, the teaching mode covers almost the entire teaching process. This is the main content of the teaching mode. Under the guidance of a certain teaching theory, rationally plan and arrange each teaching element in the teaching implementation process. The essence of the teaching activity framework lies in the setting of teaching objectives. The activity frame is the basic frame established based on the teaching activity system. The optimization of the teaching process is also critical. The framework of teaching activities mainly involves the setting of teaching subject and teaching content. Many elements of the teaching implementation process also need to be optimized. The model rationally regulates the internal relations between the elements in the teaching activities. After the model analysis, the optimal result of the teaching process was realized. The study of music teaching mode in higher vocational colleges provides an operation mode that can directly be imitated for music teaching. The research results provide music teachers with theoretical examples of teaching models. This article studies the improvement of students'

cognition of teaching theory. Unify teaching ideas and teaching-related theories. The soul of the teaching model is the ideological tool to carry out teaching reform. The advancement and effectiveness of teaching reform measures are largely related to their guiding theories. Teaching concepts and theories put forward at different times. Different methods have specific applicable conditions and scope. Therefore, combined with the current status quo, the research suggests that schools should carry out reforms of good teaching models. The study believes that the school should strengthen the research and study system methods and process methods to reform the teaching mode. Model analysis results are shown in Figure 10.

First, the communication process model in communication theory explains the elements involved in the teaching communication process. The model reveals the dynamic interrelationships among various elements in the teaching process. The model believes that the teaching process is a complex and dynamic communication process. Second, the communication theory points out the two-way nature of the teaching process. The design of the teaching process must pay attention to the analysis and arrangement of both teaching and learning. The teaching model makes full use of feedback information to adjust and control the feedback link at any time. The expected teaching effect was achieved after model analysis. Finally, the study of communication process can provide basis and reference for teaching design, for example, content analysis, audience analysis, media analysis, and effect analysis. These contents can provide learning content analysis, learner analysis, and selection of teaching media for teaching design. The framework system of communication theory is consistent with the content of teaching activities. Teaching activity is a kind of communication activity. Therefore, many principles and methods of communication are very useful for teaching activities. According to system theory, process theory, and communication

Complete teaching system and influencing factors in music classroom

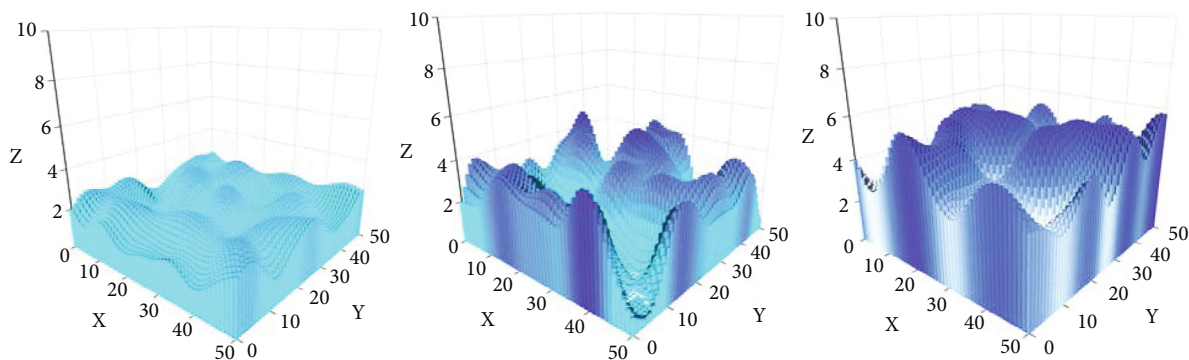


FIGURE 11: Analysis on the effect of the implementation of new music teaching mode.

theory, the model can establish the main factor system diagram of teaching mode. According to system theory, the relationship between various factors can be analyzed. According to the process theory, the order of setting up these factors can be determined. According to the theory of communication, the operation process of the teaching system can be analyzed. Model analysis results are shown in Figure 11.

**3.4. Research on the Concrete Reform of Music Teaching Mode.** Special attention is paid to the communication theory developed on the basis of the two theories. This theory is closer to the implementation of teaching activities and requires in-depth study and mastery. The systematic approach requires that teaching activities be regarded as a complex system with various factors closely linked together. Students need to consider the problem comprehensively and systematically. Process theory believes that everything appears as a process form. The processes can be transformed into each other under certain conditions, and the transformation of the process is not a simple repetition. Each transformation of the process can enter a higher stage. The research regards the music teaching process as a combination of multiple subprocesses. Through overall coordination and mutual support, the optimization of efficiency can be achieved. The communication method is to simplify the communication process into several components. The model continues to analyze the status and role of these elements in the communication process. There are interactions and connections between these elements. Teaching activities are the process of delivering corresponding content to teaching objects through teaching media in accordance with established teaching goals.

#### 4. Conclusion

From a practical business perspective, the research suggests strengthening the research on various teaching modes, curriculum forms, teaching content, and teaching methods. Research should accurately grasp various teaching models, curriculum forms, and teaching methods. The research suggests that students are proficient in using various teaching

methods. At the same time, it recommended actively carrying out teaching and research activities. The research has mastered the questionnaire survey and teaching resources. Lay the foundation for the follow-up reform of teaching mode.

First, strengthen research on teaching reform itself. Teaching reform itself is also a subject, which requires continuous learning and practice, to promote the teaching reform. For the reform of higher vocational music education, it is necessary to provide corresponding experience reference. Therefore, teachers and teams are required to learn and research various teaching modes according to actual needs. Research the curriculum format and teaching methods, and understand their advantages and disadvantages. Students must have proficiency in creating and using various teaching methods and means. At the same time, do a good job of investigation and research around specific teaching reforms. Accurately grasp the characteristics of music education in higher vocational colleges today.

Second, the teaching content must be updated in time. The purpose of music education is to enable students to acquire knowledge and abilities related to music. After the discipline has specified these goals, they constitute the teaching content. For example, after the knowledge of music was concretized, it involves many contents such as musical instruments, music theory, genres, characters, and works. The teaching content is complex and constantly enriched and developed. Therefore, we must select and update the teaching content according to the teaching requirements and the characteristics of the times. The research centers on educational purposes and disseminates content that students love to hear.

Third, we must continuously improve teaching methods. To achieve the teaching goal, we must rely on a certain dissemination carrier. With the advancement of science and technology and the development of the times, various modes of communication continue to emerge. The mode of communication greatly changes the way people behave. These communication methods provide a reference for teaching methods in terms of convenience, vividness, and interactivity. Therefore, music education in higher vocational colleges must also keep up with the times and continue to absorb

new elements. For example, based on online interactive platforms and microlectures, strengthen students' learning and research in this area. Focus on the characteristics of the era, school characteristics, and student personality. The research and development of teaching form is the key and difficult point of this article. Only by continuously carrying out teaching research and reforms and accumulating experience and resources can we gradually achieve better reform results.

## Data Availability

The data used to support the findings of this study are available from the corresponding author upon request.

## Conflicts of Interest

The author declares no known competing financial interests or personal relationships that could have appeared to influence the work reported in this paper.

## References

- [1] S. K. Mydhili, S. Periyanyagi, S. Baskar, P. M. Shakeel, and P. R. Hariharan, "Machine learning based multi scale parallel K-means++ clustering for cloud assisted Internet of Things," *Peer-to-Peer Networking and Applications*, vol. 13, no. 6, pp. 2023–2035, 2020.
- [2] N. Pourdamghani and K. Knight, "Neighbors helping the poor: improving low-resource machine translation using related languages," *Machine Translation*, vol. 33, no. 3, pp. 239–258, 2019.
- [3] J. E. Varajao, "A new process for success management-bringing order to a typically ad-hoc area," *The Journal of Modern Project Management*, vol. 5, no. 3, pp. 94–99, 2018.
- [4] H. Aguinis, Y. H. Ji, and H. Joo, "Gender productivity gap among star performers in stem and other scientific fields," *Journal of Applied Psychology*, vol. 103, no. 12, pp. 1283–1306, 2018.
- [5] S. Banerjee and S. Venaik, "The effect of corporate political activity on MNC subsidiary legitimacy: an institutional perspective," *Management International Review*, vol. 58, no. 5, pp. 813–844, 2018.
- [6] X. Wang and P. Lei, "Does strict environmental regulation lead to incentive contradiction? – evidence from China," *Journal of Environmental Management*, vol. 269, article 110632, 2020.
- [7] S. Yue, R. Lu, H. Chen, and J. Yuan, "Does financial development promote the win-win balance between environmental protection and economic growth?," *Environmental Science and Pollution Research*, vol. 25, no. 36, pp. 36438–36448, 2018.
- [8] S. Nakayama and J. Takayama, "Traffic network equilibrium model for uncertain demands," *Proceedings of the 82nd Transportation Research Board Annual Meeting*, vol. 2, 2021.
- [9] M. J. Mokarram, T. Niknam, J. Aghaei, M. Shafie-khah, and J. P. S. Catalao, "Hybrid optimization algorithm to solve the nonconvex multiarea economic dispatch problem," *IEEE Systems Journal*, vol. 13, no. 3, pp. 3400–3409, 2019.
- [10] Q. Guo, Z. Zhu, L. Qiang, D. Zhang, and W. Wenqing, "A dynamic emotional session generation model based on Seq2-Seq and a dictionary-based attention mechanism," *Applied Sciences*, vol. 10, no. 6, pp. 1910–1967, 2020.
- [11] H. Ren, X. Mao, W. Ma, J. Wang, and L. Wang, "An English-Chinese machine translation and evaluation method for geographical names," *ISPRS International Journal of Geo-Information*, vol. 9, no. 3, pp. 139–201, 2020.
- [12] J. Arús-Pous, T. Blaschke, S. Ulander, J.-L. Reymond, H. Chen, and O. Engkvist, "Exploring the GDB-13 chemical space using deep generative models," *Journal of Cheminformatics*, vol. 11, no. 1, pp. 20–29, 2019.
- [13] T. Moon, T. I. Ahn, and J. E. Son, "Long short-term memory for a model-free estimation of macronutrient ion concentrations of root-zone in closed-loop soilless cultures," *Plant Methods*, vol. 15, no. 1, pp. 1–12, 2019.
- [14] A. Velloso, A. Street, D. Pozo, J. M. Arroyo, and N. G. Cobos, "Two-stage robust unit commitment for co-optimized electricity markets: an adaptive data-driven approach for scenario-based uncertainty sets," *IEEE Transactions on Sustainable Energy*, vol. 11, no. 2, pp. 958–969, 2020.
- [15] S. K. Dwivedi, R. Amin, S. Vollala, and R. Chaudhry, "Blockchain-based secured event-information sharing protocol in internet of vehicles for smart cities," *Computers and Electrical Engineering*, vol. 86, no. 1, pp. 1–9, 2020.
- [16] Z. Khan and S. Amin, "Bottleneck model with heterogeneous information," *Transportation Research Part B Methodological*, vol. 112, no. 1, pp. 157–190, 2018.
- [17] J. M. Cairney, K. Rajan, D. Haley et al., "Mining information from atom probe data," *Ultramicroscopy*, vol. 159, no. 1, pp. 324–337, 2020.
- [18] Z. Yang and L. S. C. Pun-Cheng, "Vehicle detection in intelligent transportation systems and its applications under varying environments: a review," *Image and Vision Computing*, vol. 69, pp. 143–154, 2018.
- [19] M. Guo and N. Arunkumar, "Construction of employee training program evaluation system of three exponential forecast based on sliding window," *Cluster Computing*, vol. 22, no. 3, pp. 6865–6870, 2019.
- [20] F. Sadile, A. Bernasconi, F. Carbone, F. Lintz, and G. Mansueto, "Histological fibrosis may predict the failure of core decompression in the treatment of osteonecrosis of the femoral head," *International Journal of Surgery*, vol. 44, pp. 303–308, 2017.
- [21] C. M. Kang, S. H. Lee, and C. C. Chung, "Multirate lane-keeping system with kinematic vehicle model," *IEEE Transactions on Vehicular Technology*, vol. 67, no. 10, pp. 9211–9222, 2018.
- [22] K. P. Wijayarathna, V. V. Dixit, L. Denant-Boemont, and S. T. Waller, "An experimental study of the Online Information Paradox: does en-route information improve road network performance?," *PLoS One*, vol. 12, no. 9, pp. 184–191, 2017.
- [23] A. Edrees, H. Abdelhamed, and M. L. Lawrence, "Construction and evaluation of type III secretion system mutants of the catfish pathogen *Edwardsiella piscicida*," *Journal of Fish Diseases*, vol. 41, no. 5, pp. 805–816, 2018.
- [24] K. Alexiou and J. Wiggins, "Measuring individual legitimacy perceptions: scale development and validation," *Strategic Organization*, vol. 17, no. 4, pp. 470–496, 2019.
- [25] J. M. Cairney, K. Rajan, D. Haley et al., "Mining information from atom probe data," *Ultramicroscopy*, vol. 159, no. 1, pp. 324–337, 2020.
- [26] T. Fischer and C. Krauss, "Deep learning with long short-term memory networks for financial market predictions," *European Journal of Operational Research*, vol. 270, no. 2, pp. 654–669, 2018.

- [27] S. K. Dwivedi, R. Amin, S. Vollala, and R. Chaudhry, "Block-chain-based secured event-information sharing protocol in internet of vehicles for smart cities," *Computers and Electrical Engineering*, vol. 86, no. 1, pp. 1–9, 2020.
- [28] A. Chen, J. Kim, S. Lee, and Y. Kim, "Stochastic multi-objective models for network design problem," *Expert Systems with Applications*, vol. 37, no. 2, pp. 1608–1619, 2010.
- [29] S. M. Hosseiniinasab, S. N. Shetab-Boushehri, S. R. Hejazi, and H. Karimi, "A multi-objective integrated model for selecting, scheduling, and budgeting road construction projects," *European Journal of Operational Research*, vol. 271, no. 1, pp. 262–277, 2018.
- [30] K. Alexiou and J. Wiggins, "Measuring individual legitimacy perceptions: scale development and validation," *Strategic Organization*, vol. 17, no. 4, pp. 470–496, 2019.
- [31] J. Barrera-Martinez, M. Lopez-Fernandez, and Romero-Fernandez, "The link between socially responsible human resource management and intellectual capital," *Corporate Social Responsibility and Environmental Management*, vol. 26, no. 1, pp. 71–81, 2019.
- [32] S. Schnelle, J. M. Wang, R. Jagacinski, and H. J. Su, "A feedforward and feedback integrated lateral and longitudinal driver model for personalized advanced driver assistance systems," *Mechatronics*, vol. 50, pp. 177–188, 2018.
- [33] E. M. A. Ahmed, "A hydrologic-economic-agronomic model with regard to salinity for an over-exploited coastal aquifer," *Journal of Geosciences*, vol. 12, no. 12, pp. 1–12, 2019.
- [34] L. Ye and T. Yamamoto, "Modeling connected and autonomous vehicles in heterogeneous traffic flow," *Physica A: Statistical Mechanics and its Applications*, vol. 490, no. 40, pp. 269–277, 2018.
- [35] S. K. Dwivedi, R. Amin, S. Vollala, and R. Chaudhry, "Block-chain-based secured event-information sharing protocol in internet of vehicles for smart cities," *Computers and Electrical Engineering*, vol. 86, no. 1, pp. 1–9, 2020.
- [36] P. Alessio, C. Peter, and H. Robert, "Prolonging the lifetime of old steel and steel-concrete bridges: assessment procedures and retrofitting interventions," *Structural Engineering International*, vol. 29, no. 4, pp. 507–518, 2019.
- [37] Z. Khan and S. Amin, "Bottleneck model with heterogeneous information," *Transportation Research Part B: Methodological*, vol. 112, no. 1, pp. 157–190, 2018.



## Research Article

# Athletes' State Monitoring under Data Mining and Random Forest

**Xiaolei Li** 

*Physical Education Department of Public Basic Education Department, Henan Vocational University of Science and Technology, Zhoukou, Henan 466000, China*

Correspondence should be addressed to Xiaolei Li; [guijihkzd123456@163.com](mailto:guijihkzd123456@163.com)

Received 14 January 2022; Revised 16 February 2022; Accepted 22 February 2022; Published 25 March 2022

Academic Editor: Wen Zeng

Copyright © 2022 Xiaolei Li. This is an open access article distributed under the Creative Commons Attribution License, which permits unrestricted use, distribution, and reproduction in any medium, provided the original work is properly cited.

The study aims to train athletes to be in top form and at their best in the competition. Based on the relevant theoretical research, archers are taken as the research subjects, the characteristics of archery are analyzed, and the electroencephalogram (EEG) features of the athletes in different stages of precompetition training are monitored. And the athletes' competitive state monitoring model based on random forest (RF) is implemented and tested. The experimental results show that the athletes' dominant frequency of brain band  $\alpha$ , EEG entropy, central fatigue index, excitation inhibition index, and cerebral state index in precompetition training is significantly different from those in training ( $P < 0.05$ ). The monitoring model implemented classifies athletes' competitive states. Compared with the support vector machine (SVM) classification model, its classification accuracy is higher than 90%. The overall classification accuracy is 89.74%, more significant than SVM. The research provides a reference for monitoring athletes' competitive states and helps them regulate their states in real time.

## 1. Introduction

Archery is popular among people in China and symbolizes China's traditional culture. It is listed as one of the events in second Olympic Games in 1900 [1]. As a traditional sport, it attracts more and more attention due to the excellent performance of Chinese archers in various world events in recent years. Monitoring electroencephalogram (EEG) is a method of recording brain activities using electrophysiological indexes. In the early 1950s, scientists in the former Soviet Union studied the application of EEG to sports training [2]. Schchumiller studied athletes' EEG and obtained their states at different stages in acquiring the relevant skills. Majiev et al. discussed the EEG features of athletes when they are feeling fatigued. And the related research becomes more and more extensive with the development of science and technology.

EEG is used for concussion injury and recovery. Wilde et al. (2020) combined EEG and neurocognitive data. They

proposed the indexes to enhance brain function, which can significantly change the diffusion of athletes suffering from concussion and have clinical application value for a concussion [3]. Zhao et al. (2021) used the deep learning method to analyze the EEG signals of athletes and designed a channel attention module connected to the input layer of convolutional neural networks (CNN) to reduce the risk of suffering from concussion again after recovery training [4]. Besides, EEG can evaluate athletes' competitive state and guide athletes' training. Duru and Assem (2018) used the psychological subtraction method to discuss the effectiveness of nerves and utilized EEG to measure the cognitive dynamics of karate athletes during the break time and in doing sports [5]. Sultanov and İsmailova (2019) explored the relationship between EEG rhythm oscillation and competitive anxiety when opening and closing eyes. They also took young football players as the experimental subject to test their sports competition anxiety, recorded their prefrontal EEG with a single channel mobile EEG system, and analyzed the EEG

rhythm as a predictor of stress with a regression model. This study provides a method for predicting athletes' emotional states [6]. Bailey et al. (2019) used portable EEG equipment to track the psychological state of climbers during the climbing activity. The results show that climbers are more relaxed (at the critical moment) and ( $\alpha$  activity) have introverted attention ( $\theta$  activities) when challenging more difficult routes [7]. Tharawadeepimuk and Wongsawat (2021) used the brain topographic map (absolute force) and brain connectivity (coherence and amplitude asymmetry) to analyze the psychological factors when doing sports. They evaluated athletes' performance in competition through noninvasive quantitative EEG [8]. Bieru et al. (2021) used EEG to record the brain activity of 12 judo athletes and 11 volleyball athletes during hand flexor contraction and relaxation, which helps coaches evaluate the training effect of athletes [9]. Zhu (2021) assessed the impact of EEG information and central nervous transmission on athletes' regulation and training, providing a basis for improving the level of archery training [10].

In short, the above studies are mainly on athletes' concussion injury and evaluate their psychological state via EEG. Still, there are few on the application of EEG to monitoring athletes' competitive states. Therefore, archers are taken as the research subject to explore the characteristics of archery and test the EEG of the national team under different training states. An athletes' competitive state monitoring model is implemented based on the random forest (RF) and used to test the EEG of athletes in the precompetition training stage. The EEG characteristics of archers under different training states are analyzed. The evaluation criteria of test indexes are constructed, and the model's performance is tested. The innovation is to classify the competitive state of athletes based on RF, so that coaches can intuitively and conveniently know the states of athletes. The study provides a fundamental tool for coaches to monitor and control athletes' competitive states, which has practical significance.

## 2. Research Methods

**2.1. EEG.** Classifying the competitive states of athletes can better detect and adjust the states of athletes. The commonly used classifiers include the nearest neighbor algorithm, naive Bayesian classifier, radial basis function neural networks, and RF. The nearest neighbor algorithm is simple and easy to implement, but it performs poorly when the samples are imbalanced. Naive Bayesian works well on small-scale data and can complete multiple classification tasks, but it needs a priori probability before use. The structure of radial basis function neural networks is simple, but it cannot display the reasoning process. RF can highly parallelize the training. It can randomly select the node division features of a decision tree (DT) and mark the importance of each feature in the output results. The data trained after random sampling has small variance and strong generalization ability. Therefore, RF is selected as the classifier to test athletes' competitive states.

EEG is obtained by recording brain activities using electrophysiological indexes. EEG presents neural electrical

activities by following a specific law. Specifically, the frequency of the activities is 1-30 Hz and can be divided into six bands, namely,  $\delta$ ,  $\theta$ ,  $\alpha_1$ ,  $\alpha_2$ ,  $\beta_1$ , and  $\beta_2$  [11]. The frequency of  $\delta$  is 1~3 Hz, and its amplitude is 20~200  $\mu V$ . This waveform can be measured in infancy or immature intellectual development and when people are exhausted, sleepy, or under anesthesia [12]. The frequency of  $\theta$  is 4~7 Hz, and its amplitude is 5~20  $\mu V$ . This waveform is more common among adults with frustrated will, depression, or psychosis. The wave frequency of  $\alpha$  is 8~13 Hz (the average is 10 Hz), and its amplitude is 20~100  $\mu V$ , the most common waveform in human brain waves. When people are quiet and close their eyes, this waveform appears frequently, but when people open their eyes or receive other stimuli, this waveform will disappear immediately [13].  $\alpha_1$  represents the regulation factor, and the performance of the human brain in the state is concentrated and inspired [14].  $\alpha_2$  is a state in which the brain is highly awake, focused, and detached [15]. The frequency of  $\beta$  is 14~30 Hz, and its amplitude is 100~150  $\mu V$ . This waveform will appear when people are nervous and impassioned. The original slow wave will immediately become a single fast waveform [16].  $\beta$  can help athletes reduce tension and pressure and improve their ability to respond and deal with emergencies.  $\beta_1$  wave shows that the human brain is in a thinking state [17].  $\beta_2$  shows that the brain is alert and excited [18]. If the athlete's  $\beta$  waveform fluctuates significantly, the excitability of the athlete's central nervous system gets stronger, his speed and intensity of nerve are strengthened, and his stress ability is improved, forming an excellent state to win in the competition.

**2.2. RF Model.** RF is one of the tools for data mining. As its name implies, RF uses a random method to build a DT in a forest. In RF, there are no relations between any DTs. Therefore, DT should be discussed first in the study of RF [19].

DT is a commonly used classification method. Its generation falls into two steps. One is the splitting of nodes. When the attribute represented by a node cannot make judgments, this node should be divided into two subnodes (if it is not a binary tree, it will be divided into  $n$  subnodes). This node is called an internal node, and the node that can judge the attribute is called a leaf node, forming a tree structure. The other is the determining of the threshold. An appropriate threshold should be selected to minimize the classification error rate. Figure 1 shows the schematic diagram of DT.

The DTs are commonly used by iterative dichotomizer 3 (ID3), C4.5, and classification and regression tree (CART). Among the above, the classification effect of CART is better than others. It selects the optimal feature through the *GINI* coefficient minimization criterion, determines the optimal binary segmentation point of the feature, and generates a binary tree. If there are  $K$  categories in CART, the probability that the sample points belong to class  $k$  is  $p_k$ , and the *GINI* index of the probability distribution is calculated by

$$\text{GINI} = \sum_{k=1}^K p_k(1-p_k). \quad (1)$$

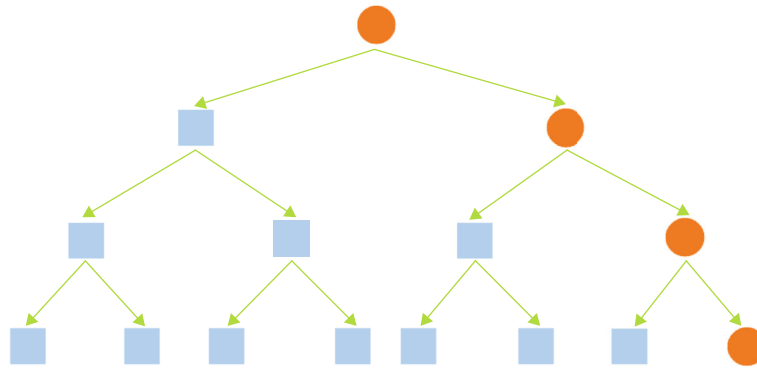


FIGURE 1: Schematic diagram of DT (represents internal nodes and represents leaf nodes).

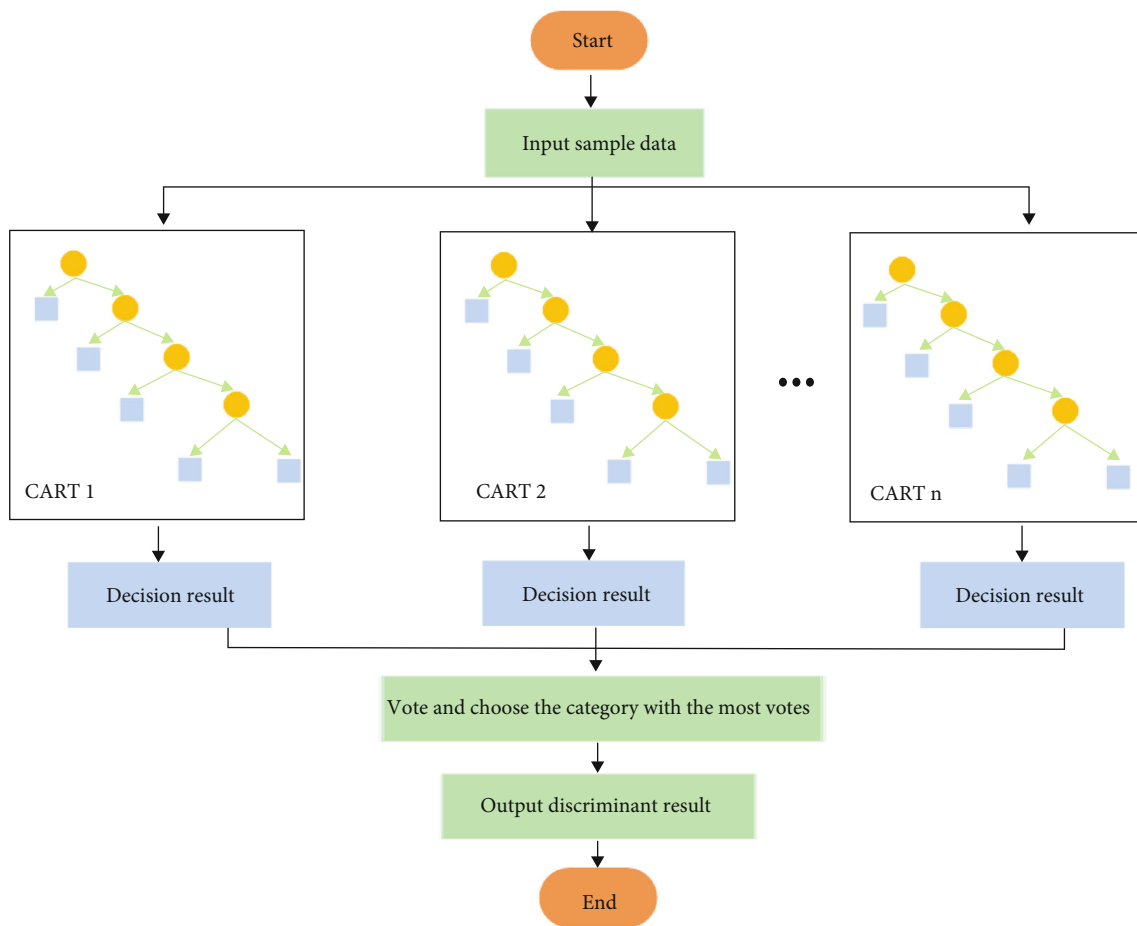


FIGURE 2: RF model.

For the second classification problem, if the probability of the sample point as the first class is  $p$ , the *GINI* index of the probability distribution is calculated by

$$GINI(p) = 2p(1 - p). \tag{2}$$

If the training sample set  $D = [(x_1, y_1), (x_2, y_2), \dots, (x_n, y_n)]$ ,  $x$  is the eigenvector,  $y$  is the sample type, and its *GINI*

index is calculated by

$$GINI(D) = 1 - \sum_{k=1}^K \left( \frac{|C_k|}{|D|} \right)^2. \tag{3}$$

In equation (3),  $|C_k|$  is the number of  $K$ -type sample points in  $D$ .

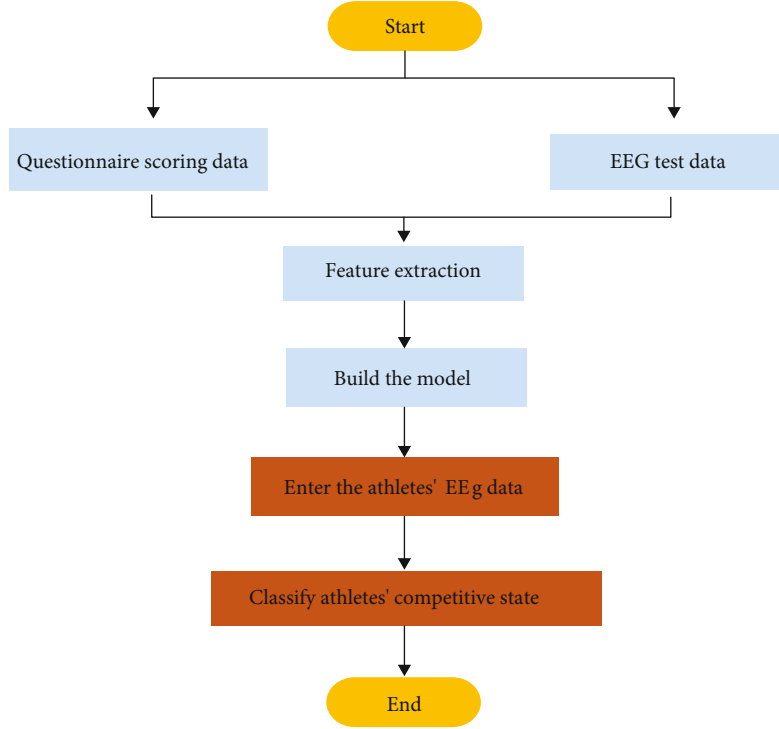


FIGURE 3: Athletes' competitive state monitoring model.

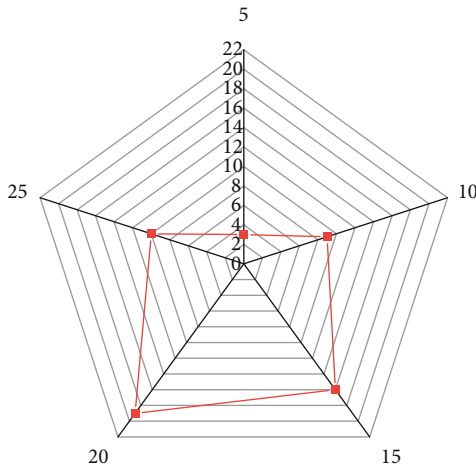


FIGURE 4: Athletes' questionnaire survey results.

$D$  is divided into  $D_1$  and  $D_2$  according to whether feature  $A$  takes its possible value  $a$ , and then

$$D_1 = \{(x, y) \mid A(x) = a\}, \quad (4)$$

$$D_2 = \{(x, y) \mid A(x) \neq a\}. \quad (5)$$

In equations (4) and (5), if  $D = D_1 + D_2$ , then the GINI index of  $D$  under the condition of  $A = a$  is calculated by

$$\text{GINI}(D, A_a) = \frac{|D_1|}{|D|} \text{GINI}(D_1) + \frac{|D_2|}{|D|} \text{GINI}(D_2). \quad (6)$$

RF is composed of multiple DTs. Each DT decides the final classification result of the test sample by voting. The model is shown in Figure 2.

**2.3. Theoretical Research on Competitive States.** Competitive states are the spiritual activities in competitive sports events and training. Stone et al. believes that competitive states are the best preparation for sports performance obtained by athletes through corresponding training [20]. They are the best short-term states of psychology and physics. Some Chinese scholars define competitive states as instant states when athletes compete. These states change dynamically, and athletes' best performance in psychology and physics is called "the best competitive state." Bompá, a Romanian Canadian Sports Training scholar, uttered that the competitive state could be measured and evaluated, and he classified the competitive states. If he achieved more than 98% of the best results last year, the athletes have the best competitive state. If he completed 96.5%~98%, the athlete's state is normal; if he achieved 95%~96.5% best results, the athlete's state is poor; if the best results are less than 95%, the athlete's state is worst. Here, the view of Chinese scholars is that the competitive state is an instant state when athletes participate in the competition.

**2.4. Characteristics of Archery.** Archery is an ancient sport. Athletes complete bow pulling and archery action by standing still and coordinating force. The characteristics of archery show the role of muscle in antifatigue ability during long-time training [21]. The basic requirements of archery are fast, accurate, and stable. "Fast" means that athletes'

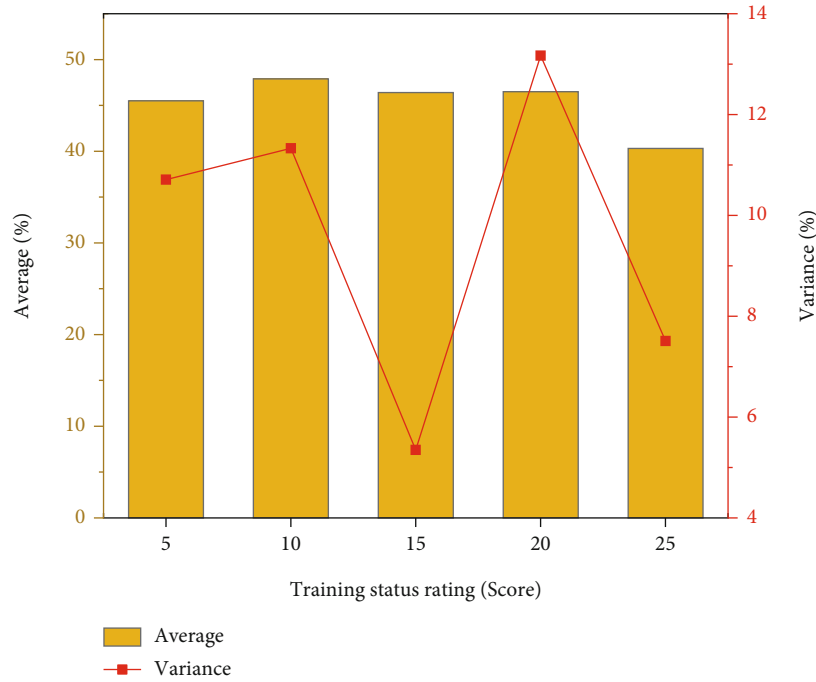


FIGURE 5: Dominant frequency of the athletes' brain band  $\alpha$  under different training states.

TABLE 1: The scoring criteria of the dominant frequency of brain band  $\alpha$  in different training states.

Scores of the dominant frequency of brain band $\alpha$	Information dispersion	Scattered information	Evenly distribution	Concentrated information	Highly concentrated information
5	<30.7	30.7-40.5	40.6-47.8	47.9-60.8	>60.8
10	<27.8	27.8-43.9	44.0-51.7	51.7-64.5	>64.5
15	<24.6	24.6-41.7	41.8-48.4	48.5-63.3	>63.3
20	<27.1	27.1-44.2	44.3-50.7	50.8-62.7	>62.7
25	<27.5	27.5-38.7	38.8-45.1	45.2-56.3	>56.3

technical actions should be clear and fast. In the face of changes in the external environment, athletes should respond quickly and adjust themselves quickly. "Stability" means that athletes need to overcome external and internal interference and give stable play to their technical level and control their emotions. "Accurate" means that athletes can play their technical actions and hit the target accurately in the competition.

Compared with other sports, archery athletes are greatly affected by their psychological load. No matter in training and conditions, athletes have tremendous psychological pressure. The training activities require concentration, sensitive and accurate proprioception, precise nerve control, fast response, good information processing ability, decisive decision-making, and regular exertion of ability under huge stress, all of which depend on the quality of athletes' brain function. The adaptation level of archers to the psychological load will be directly reflected in the central nervous system changes. Because it is simple, noninvasive, and repeatable, EEG is one of the important means of clinical medicine and brain cognitive science. The research athletes' EEG features can help athletes regulate their brain mechanism in

daily training and competition, enabling them to participate in the competition in the best form and achieve the best results.

Some scholars found that athletes' EEG features could reflect their tension and competitive states before the competition. Some scholars analyzed the EEG of swimmers the day before the match and found that there are special spatial configurations of serotonin, acetylcholine, and dopamine in their brain center. This demonstrates those athletes' psychological state changes before the competition, and their psychological loads before the competition can be monitored by their EEG.

*2.5. Athletes' Competitive State Monitoring Based on RF.* The training state and brain features of athletes are tested through experiments. According to the scores, the EEG features of athletes with different scores are extracted, respectively, the test indexes that can reflect athletes' training state are selected, and the scoring standards of each index are established. Then, the athletes' competitive state monitoring model is implemented based on the model. According to the results, the real-time detection of athletes' competitive

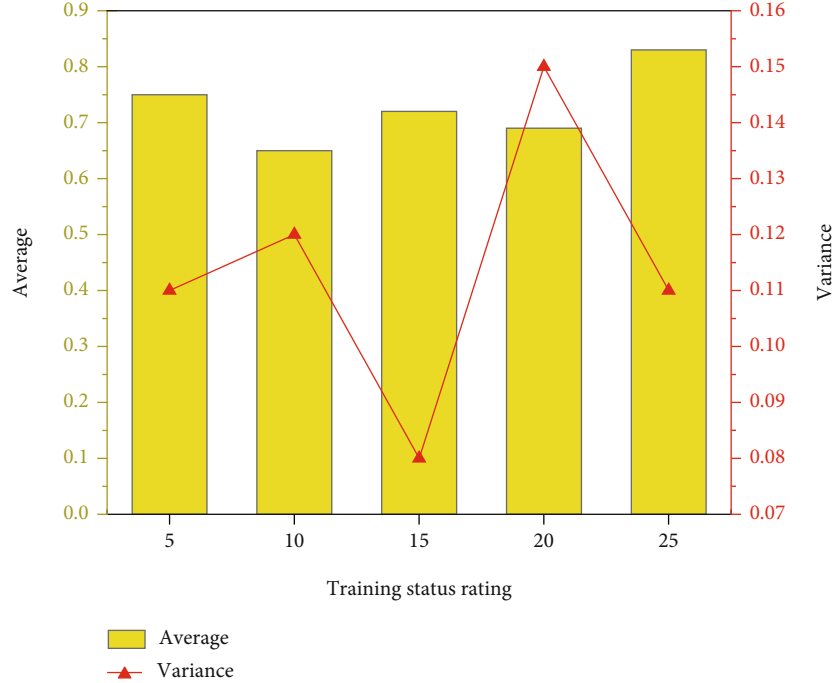


FIGURE 6: Athletes' EEG entropy test results in different training states.

TABLE 2: Scoring standard of the athletes' EEG entropy test in different training states.

Values of EEG entropy	Better	Good	Normal	Poor	Worse
5	<0.43	0.43-0.52	0.53-0.68	0.69-0.85	>0.85
10	<0.47	0.47-0.57	0.58-0.71	0.72-0.80	>0.80
15	<0.53	0.53-0.65	0.66-0.74	0.75-0.88	>0.88
20	<0.50	0.50-0.64	0.64-0.72	0.73-0.87	>0.87
25	<0.57	0.57-0.74	0.75-0.85	0.85-0.90	>0.90

states is realized, and the coaches can help regulate athletes' competitive states according to the results. The implementation process of athletes' competitive state monitoring model is shown in Figure 3.

The classification accuracy of RF is essential to measure the classification results of the RF model, which indicates the proportion of correct classification datasets to the length of all datasets. Its calculation equation is

$$\text{Accuracy} = \frac{T_{\text{correct}}}{T_{\text{all}}}. \quad (7)$$

In equation (7),  $T_{\text{correct}}$  is the number of correct data for RF classification in the test set, and  $T_{\text{all}}$  is the data length of all test sets.

**2.6. Experimental Methods.** Selection of subjects is as follows: the sample set of the experiment is the archers of the national training team, and the total number of subjects is 57.

Test steps are as follows: use EEG to test the athletes, respectively, and fill in the athlete's psychological fatigue questionnaire and automatic force rating table.

Test indexes are as follows: dominant frequency of  $\alpha$  brainwave, EEG entropy, central fatigue index, excitation inhibition index, and brain functional state index.

The dominant frequency of brain band  $\alpha$  [22] is as follows: it is the probability of each waveform. When the probability of the dominant frequency is the maximum, other frequencies will decrease. And the information in the brain will be more concentrated. On the contrary, when the probability of the dominant frequency in the brain decreases, the brain's concentration will decrease, reflecting the concentration of athletes' attention to a specific event.

EEG entropy [23] is as follows: it shows the uncertainty of brain band  $\alpha$  and the order of dominant frequency. It also reflects the response of athletes to external interference. The entropy value of EEG is between 0 and 1. The smaller the entropy value is, the less the brain band  $\alpha$  is. The better the order of the dominant frequency is, the smaller the influence of external interference on athletes is. It shows that the information in the athletes' brains is messy, and the impact of external interference is great.

Major neurotransmitter levels include  $\gamma$ -gamma-aminobutyric acid (GABA), glutamic acid (Glu), acetylcholine receptor (AChR), acetylcholine (ACh), 5-hydroxytryptamine (5-HT), noradrenaline (NE), and dopamine (DA). Among them, GABA is an inhibitory neurotransmitter, and it affects

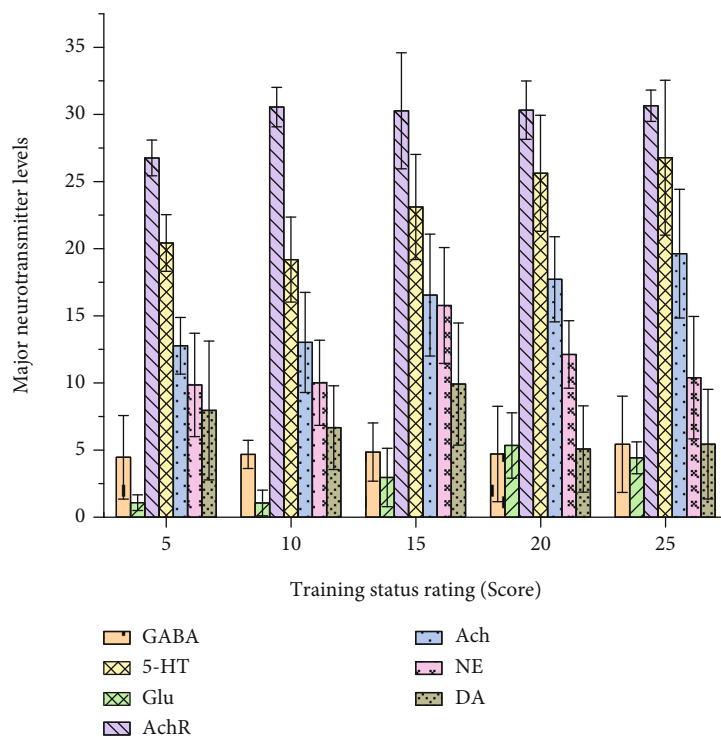


FIGURE 7: Test results of primary neurotransmitter levels of athletes in different training states.

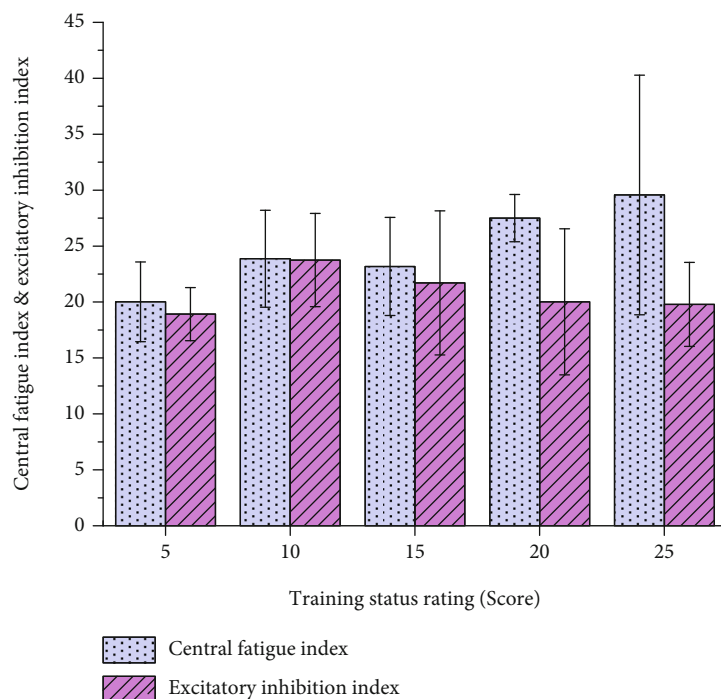


FIGURE 8: Test results of central fatigue index and excitation inhibition index of athletes in different training states.

the excitability of neurons greatly. Glu is an excitatory neurotransmitter. AchR includes muscarinic receptors and nicotinic receptors. The former produces a parasympathetic excitatory effect, and the latter can excite postganglionic neurons in an autonomic ganglion. Ach makes the human

brain stay conscious. 5-HT is a messenger and can produce pleasant emotions. It has an important impact on regulating brain activities such as emotion and energy. NE has both inhibitory and excitatory effects. DA is related to human lust and feelings and conveys excitement and happiness.

TABLE 3: Scoring criteria of central fatigue index of athletes in different training states.

Central fatigue indexes	Very relaxed	Relaxed	No fatigue	Mildly fatigued	Very fatigued
5	<12.7	12.7-16.9	17.0-22.5	22.6-27.7	>27.7
10	<15.2	15.2-19.7	19.8-27.4	27.5-33.1	>33.1
15	<13.6	13.6-19.3	19.4-26.1	26.2-33.5	>33.5
20	<20.6	20.6-25.3	25.4-32.7	32.8-39.1	>39.1
25	<20.7	20.7-27.3	27.4-32.9	33.0-39.7	>39.7

TABLE 4: Scoring criteria of excitation inhibition index of athletes in different training states.

Excitatory inhibitory indexes	Very depressed	Depressed	Normal	Excited	Very excited
5	<10.0	10.0-15.5	16.0-21.5	21.5-27.5	>27.5
10	<13.5	13.5-21.5	22-27.5	28.0-32.5	>32.5
15	<12.5	12.5-18.0	18.5-25.0	25.5-31.5	>31.5
20	<11.0	11.0-16.5	17.0-22.5	23.0-28.0	>28.0
25	<10.0	10.0-16.5	17.0-23.0	23.5-27.5	>27.5

Central fatigue index [24] is as follows: a value used to show the degree of fatigue.

Excitation inhibition index [25] is as follows: a value used to reflect whether the brain is excited.

Brain function state index [26] is as follows: a value used to reflect brain synergy.

Data processing is as follows: it is used to score the athletes according to the questionnaire, and then the training status of the athletes is evaluated (the scores of the two questionnaires account for 50%, respectively). Athletes' psychological fatigue questionnaire is developed by Raedke and Smith in 2001. In the questionnaire, athletes' psychological states fall into three dimensions: emotional/physical exhaustion, reduced sense of achievements, and negative evaluation of sports, including 15 questions. The survey results of athletes' psychological fatigue questionnaire are divided into five grades: "Never," "rarely," "sometimes," "often," and "always," with scores of 5 points, 10 points, 15 points, 20 points, and 25 points, respectively. The automatic force rating table is also divided into five levels, namely "very relaxed", "relaxed", "slightly laborious", "laborious" and "very laborious" and the corresponding scores are 5 points, 10 points, 15 points, 20 points, and 25 points, respectively.

When the athlete's final score is 5 points, 10 points, 15 points, and 20 points, it indicates that the athlete is not tired. When his score is 25 points, the athlete is in a state of fatigue.

In the questionnaire surveys, 57 athletes' psychological fatigue questionnaires are distributed, and 57 are recovered, with a recovery rate of 100%. The number of effective questionnaires is 57, and the questionnaire efficiency is 100%. 57 automatic force rating questionnaires are distributed, and 57 are recovered, with a recovery rate of 100%. The number of effective questionnaires is 57, and the questionnaire efficiency is 100%.

### 3. Results

3.1. Brain Function Feature Data of Different Competitive States. The questionnaire survey results on 57 athletes of the national training team are shown in Figure 4.

Figure 4 shows that the size of athletes with 5 points is small, and 3 athletes' psychological states are "relaxed." The numbers of athletes with 15 points and 20 points are more significant, and they are 16 and 19, respectively, indicating that the overall competitive state of the athletes is poor.

The dominant frequency of the athletes' brain band  $\alpha$  in different competitive states is tested, and the average variance under different training degrees is calculated. The results are shown in Figure 5.

Figure 5 shows that when the scores of training states are 5 points, 10 points, 15 points, and 20 points, the values of athlete's brain band  $\alpha$  are approximate, and the difference is not statistically significant. When the athlete's training score is 25 points, the values of their dominant frequency of brain band  $\alpha$  are lower than that of other states. Compared with the nonfatigue state of 5 points, 10 points, 15 points, and 20 points,  $P > 0.05$  and the difference are statistically significant.

The values of athletes' dominant frequency of brain band  $\alpha$  in different training states are analyzed, and the corresponding scoring criteria are shown in Table 1.

The EEG entropy of athletes under different training states is tested, and the test results are shown in Figure 6.

Figure 6 shows that when the score of the training state is 25, their average score of the EEG entropy test is higher than that of others, which has a significant difference compared with other training states ( $P < 0.05$ ), which is statistically significant. The EEG entropy of athletes at other scores is not statistically significant.

The scoring standard of the athletes' EEG entropy test in different training states is established, as shown in Table 2.

The primary neurotransmitter levels of athletes under different training states are tested, and the test results are shown in Figure 7.

Figure 7 shows that with the increase of training state scores, 5-HT and Ach in the main neurotransmitter levels of athletes are growing, while DA shows a change of low-high-low. As athletes continue to exercise, their dopamine level gradually rises. When the athletes feel fatigued, their states become worse, the pivot fatigue gradually appears,



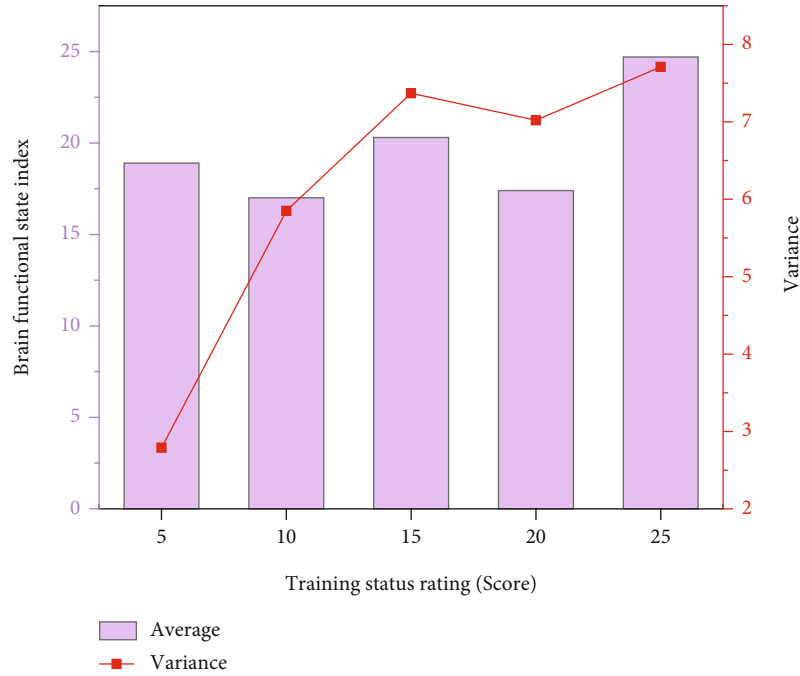


FIGURE 9: Test results of brain state indexes of athletes in different training states.

TABLE 5: Evaluation criteria of brain state indexes of athletes in different training states.

Brain state indexes	Excellent coordination	Good synergy	General synergy	Poor synergy	Very poor synergy
5	<9.3	9.3-14.6	14.7-21.9	22.0-28.6	>28.6
10	<10.7	10.7-15.3	15.4-26.1	26.2-28.7	>28.7
15	<7.8	7.8-16.5	16.6-22.7	22.8-24.3	>24.3
20	<4.6	4.6-13.1	13.2-21.1	21.2-23.6	>23.6
25	<16.3	16.3-20.6	20.7-27.5	27.6-34.7	>34.7

and their excitement decreases, which makes their dopamine level decrease accordingly. However, with the loss of athletes' training state, pivot fatigue gradually increases, and athletes' 5-HT and Ach also increase.

The central fatigue index and excitation inhibition index of athletes in different training states are tested, and the results are shown in Figure 8.

Figure 8 shows that the central fatigue index is also rising with the continuous rise of athletes' training state scores. This indicates that the worse the athletes' states are, the more exhausted the athletes feel. And there is a significant difference between athletes' central fatigue index and their dominant frequency of 20 and 25 points and between their central fatigue index and their dominant frequency of

5, 15, and 20 points ( $P < 0.05$ ), which is statistically significant.

Under different training states, athletes' 5-HT, Ach, and central fatigue indexes change regularly. Their levels of 5-HT and Ach will increase when the central nervous system is anoxic and glucose-deficient. Based on the above, the evaluation standard of the central fatigue indexes to evaluate athletes' fatigue states is only discussed. The scoring standards of central fatigue index and excitation inhibition index of athletes in different training states are shown in Tables 3 and 4.

The brain state indexes of athletes in different training states are tested, and the test results are shown in Figure 9.

Figure 9 shows that when the training state score of athletes is 25 points, the brain state index of athletes is the highest, which is significantly different from that of athletes at 5 points, 10 points, 15 points, and 20 points ( $P < 0.05$ ). There is no significant difference in athletes' brain function state index at other points.

The evaluation criteria of brain state indexes of athletes in different training states are established, as shown in Table 5.

**3.2. Model Performance Test.** According to the evaluation criteria, the competitive states of athletes are divided into five levels: excellent, good, general, poor, and very poor. The monitoring model and the classification model based on SVM monitor the competitive states of athletes, respectively, and the test results of classification accuracy are shown in Figure 10.

Figure 10 shows that when the RF model classifies the competitive state of athletes, the classification accuracy is greater than that of SVM models. When the competitive

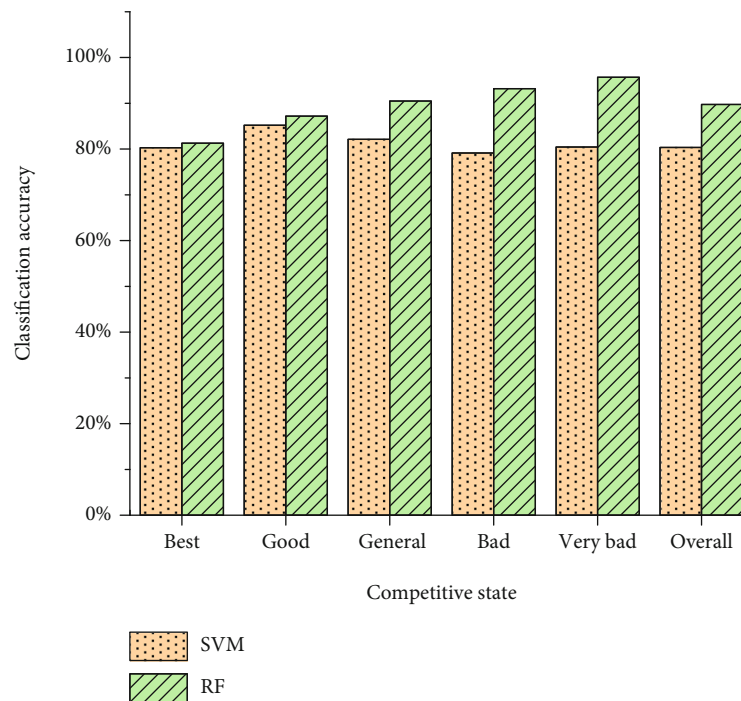


FIGURE 10: Classification accuracy of athletes' competitive states based on the RF model and SVM model.

state of athletes is in the better and good states, the classification accuracy gap between the RF model and SVM model is small. Still, the competitive states of athletes are general and poor. When their states are very poor, the classification accuracy of the RF model is more than 90%, and it is much higher than that of SVM models. The overall classification accuracy of the RF model is 89.74%, which is much higher than 80.35% of SVM models. This proves that the RF model is better in detecting athletes' competitive states.

#### 4. Conclusion

The competitive ability of athletes is affected by their competitive states. In the training stage, coaches usually regulate the competitive state of athletes employing training rhythm control and psychological counseling, so that athletes can participate in the competition in the best form and play their best in the match. The characteristics of archery are analyzed, and athletes' competitive states are monitored through their EEG features. The athletes' training state is evaluated using the questionnaires survey, the EEG feature data under different training states are collected, and the EEG characteristic evaluation criteria are established. The criteria provide a basis for constructing the classification standard of athletes' competitive states. An athlete's competitive state monitoring model is implemented based on RF and tested. The experimental results show that when the athlete's training state is 25 points, his dominant frequency, EEG entropy, central fatigue index, excitation inhibition index, and brain state index are significantly different from those of the other athletes ( $P < 0.05$ ). The athletes' competitive states are classified using the monitoring model, and the classification accuracy of each index is greater than that of the SVM model. The

overall classification accuracy is 89.74%, higher than that of the SVM model. The research helps coaches regulate athletes' competitive state in training, but there are still some shortcomings. For example, the size of the samples is too small, and the model implemented still has much room for improvement, which will be the focus of the follow-up research.

#### Data Availability

The labeled dataset used to support the findings of this study are available from the corresponding author upon request.

#### Conflicts of Interest

The author declares no competing interests.

#### References

- [1] Y. H. Tsai, S. Y. Wu, W. L. Hu et al., "Immediate effect of non-invasive auricular acupoint stimulation on the performance and meridian activities of archery athletes," *Medicine*, vol. 100, no. 8, article e24753, 2021.
- [2] M. Fink, "Random controlled trial of sham electroconvulsive therapy and other novel therapies," *The Journal of ECT*, vol. 37, no. 3, pp. 150-151, 2021.
- [3] E. A. Wilde, N. J. Goodrich-Hunsaker, A. L. Ware et al., "Diffusion tensor imaging indicators of white matter injury are correlated with a multimodal electroencephalography-based biomarker in slow recovering, concussed collegiate athletes," *Journal of Neurotrauma*, vol. 37, no. 19, pp. 2093-2101, 2020.
- [4] T. Zhao, J. Zhang, Z. Wang, and R. Alturki, "An improved deep learning mechanism for EEG recognition in sports health

- informatics,” *Neural Computing and Applications*, vol. 33, pp. 1–13, 2021.
- [5] A. D. Duru and M. Assem, “Investigating neural efficiency of elite karate athletes during a mental arithmetic task using EEG,” *Cognitive Neurodynamics*, vol. 12, no. 1, pp. 95–102, 2018.
- [6] M. Sultanov and K. İsmailova, “EEG rhythms in prefrontal cortex as predictors of anxiety among youth soccer players,” *Translational Sports Medicine*, vol. 2, no. 4, pp. 203–208, 2019.
- [7] A. Bailey, A. Hughes, K. Bullock, and G. Hill, “A climber’s mentality: EEG analysis of climbers in action,” *Journal of Outdoor Recreation, Education, and Leadership*, vol. 11, no. 1, pp. 53–69, 2019.
- [8] K. Tharawadeepimuk and Y. Wongsawat, “Quantitative EEG in sports: performance level estimation of professional female soccer players,” *Health Information Science and Systems*, vol. 9, no. 1, pp. 1–15, 2021.
- [9] D. E. Bieru, M. R. Rusu, M. L. Calina, M. I. Marin, N. Ç. Korkmaz, and R. U. S. U. Ligia, “Identifying the muscle contraction activity at athletes using brain mapping,” *BRAIN. Broad Research in Artificial Intelligence and Neuroscience*, vol. 11, no. 4Sup1, pp. 81–100, 2020.
- [10] C. Zhu, “EEG and central nervous system transmitter on athletes training,” *Revista Brasileira de Medicina do Esporte*, vol. 27, no. 7, pp. 703–705, 2021.
- [11] A. Lin, K. K. L. Liu, R. P. Bartsch, and P. C. Ivanov, “Dynamic network interactions among distinct brain rhythms as a hallmark of physiologic state and function,” *Communications Biology*, vol. 3, no. 1, pp. 1–11, 2020.
- [12] Z. Tian, B. Y. Kim, and M. J. Bae, “Study on acoustic analysis of Cleveland dam waterfull sound,” *International Journal of Engineering Research and Technology*, vol. 13, no. 6, pp. 1159–1164, 2020.
- [13] R. A. Martin, A. Cukiert, and H. Blumenfeld, “Short-term changes in cortical physiological arousal measured by electroencephalography during thalamic centromedian deep brain stimulation,” *Epilepsia*, vol. 62, no. 11, pp. 2604–2614, 2021.
- [14] H. Zhu, F. Yang, Z. Bao, and X. Nan, “A study on the impact of Visible Green Index and vegetation structures on brain wave change in residential landscape,” *Urban Forestry & Urban Greening*, vol. 64, article 127299, 2021.
- [15] Y. I. Sysoev, V. A. Prikhodko, R. T. Chernyakov, R. D. Idiyatullin, P. E. Musienko, and S. V. Okovityi, “Effects of alpha-2 adrenergic agonist mafedine on brain electrical activity in rats after traumatic brain injury,” *Brain Sciences*, vol. 11, no. 8, p. 981, 2021.
- [16] S. S. Abed and Z. F. Abed, “User authentication system based specified brain waves,” *Journal of Discrete Mathematical Sciences and Cryptography*, vol. 23, no. 5, pp. 1021–1024, 2020.
- [17] A. A. Jamebozorgy, Z. Bolghanabadi, A. Mahdizadeh, and A. Irani, “Effect of neurofeedback on postural balance and attention of women with knee osteoarthritis after bilateral total knee replacement,” *Archives of Rehabilitation*, vol. 21, no. 1, pp. 40–53, 2020.
- [18] D. Wilfried, C. D. G. Nina, and B. Silvia, “Effectiveness of Menosan®\_Salvia officinalis\_ in the treatment of a wide spectrum of menopausal complaints. A double-blind, randomized, placebo- controlled, clinical trial,” *Heliyon*, vol. 7, no. 2, article e05910, 2021.
- [19] E. Alcobaca, S. M. Mastelini, T. Botari et al., “Explainable machine learning algorithms for predicting glass transition temperatures,” *Acta Materialia*, vol. 188, pp. 92–100, 2020.
- [20] M. H. Stone, W. G. Hornsby, G. G. Haff et al., “Periodization and block periodization in sports: emphasis on strength-power training—a provocative and challenging narrative,” *The Journal of Strength & Conditioning Research*, vol. 35, no. 8, pp. 2351–2371, 2021.
- [21] K. J. Sarro, T. D. C. Viana, and R. M. L. De Barros, “Relationship between bow stability and postural control in recurve archery,” *European Journal of Sport Science*, vol. 21, no. 4, pp. 515–520, 2021.
- [22] I. S. Ramsay, P. Lynn, B. Schermitzler, and S. R. Sponheim, “Individual alpha peak frequency is slower in schizophrenia and related to deficits in visual perception and cognition,” *Scientific Reports*, vol. 11, no. 1, pp. 1–9, 2021.
- [23] B. García-Martínez, A. Fernández-Caballero, L. Zunino, and A. Martínez-Rodrigo, “Recognition of emotional states from EEG signals with nonlinear regularity- and predictability-based entropy metrics,” *Cognitive Computation*, vol. 13, no. 2, pp. 403–417, 2021.
- [24] S. Deepa, A. Kumaresan, P. Suganthirababu, R. Vijayaraghavan, and J. Alagesan, “Analyzing the casual relationship between physiological biomarkers and scales in assessing Parkinson’s disease-related-fatigue: an attempt to optimize the exercise strategy,” *Annals of the Romanian Society for Cell Biology*, vol. 25, no. 6, pp. 988–993, 2021.
- [25] H. Bruining, R. Hardstone, E. L. Juarez-Martinez et al., “Measurement of excitation-inhibition ratio in autism spectrum disorder using critical brain dynamics,” *Scientific Reports*, vol. 10, no. 1, pp. 1–15, 2020.
- [26] B. G. Fahy and D. F. Chau, “The technology of processed electroencephalogram monitoring devices for assessment of depth of anesthesia,” *Anesthesia & Analgesia*, vol. 126, no. 1, pp. 111–117, 2018.

## Research Article

# Intelligent Design Model of Urban Landscape Space Based on Optimized BP Neural Network

Guoping Wu,<sup>1</sup> Yihua Miao,<sup>1,2</sup> and Fang Wang<sup>3</sup> 

<sup>1</sup>Department of Architecture, Shijiazhuang Institute of Railway Technology, Shijiazhuang 050041, China

<sup>2</sup>Hebei Jinshi Architectural Design Co., Ltd., Shijiazhuang 050000, China

<sup>3</sup>School of Architecture and Art, Hebei University of Engineering, Handan, Hebei 056038, China

Correspondence should be addressed to Fang Wang; wangfang@hebeu.edu.cn

Received 11 January 2022; Revised 23 February 2022; Accepted 28 February 2022; Published 25 March 2022

Academic Editor: Wen Zeng

Copyright © 2022 Guoping Wu et al. This is an open access article distributed under the Creative Commons Attribution License, which permits unrestricted use, distribution, and reproduction in any medium, provided the original work is properly cited.

Urban landscape space planning is an important application field of landscape ecology. With the continuous development of the field of architectural optimization, more and more optimization methods have sprung up, including various intelligent optimization algorithms. Such intelligent optimization algorithms usually rely on traditional building performance simulation methods to obtain building performance indicators for optimization in the optimization process. However, intelligent optimization algorithms generally require large-scale calculations. At the same time, the time required for building performance simulation is often limited by the complexity of the building model and the configuration of the computer, which leads to too long performance optimization time for designers in the project. With efficient and accurate feedback, building performance optimization methods based on intelligent optimization algorithms are mainly used in scientific research and are difficult to invest in actual projects. Because the traditional BP neural network has its own limitations and its insufficient sample size and weak generalization ability in complex prediction problems, this paper uses the learning algorithm of optimizing the BP neural network to propose an urban landscape space intelligent design model. This article introduces the artificial neural network, a new application technology with the assistance of a geographic information system, and establishes a BP neural network model for urban landscape ecological planning. Seven elements of distance and number of residential points are used as input variables, patch density, fractal dimension, the Shannon diversity index, and aggregation degree are selected as output changes, and 20 samples are carefully collected to train the network. The results show that the network convergence effect is ideal and the generalization ability is strong, which provides a new simulation analysis method for landscape ecological planning.

## 1. Introduction

Landscape ecological planning is a practical activity that uses the principles of landscape ecology to solve ecological problems at the landscape level. It embodies the application value of landscape ecology. It is particularly important to apply it to urban fringe areas with fragile ecology and complex landscape pattern changes. Landscape ecological planning can be understood as follows: based on regional, natural, social, economic, and other aspects of information, dynamic planning of the regional landscape pattern from a macro-, overall, and comprehensive perspective was developed, in order to optimize the structure, protect the ecological bal-

ance, and promote the sustainable development the goal of the region. The landscape pattern can be reflected by a set of landscape indices, so the landscape ecological planning process is essentially a nonlinear mapping process, that is, the nonlinear mapping relationship between various terrain factors and various interference effects (especially man-made effects) and a set of landscape indices. In recent years, the artificial neural network methods that have emerged at home and abroad can extract regular knowledge from the most primitive or statistical data, which is very suitable for quantitative landscape ecological planning. With the development of artificial neural network technology, researchers have designed a variety of neural network models, which

describe and simulate the biological nervous system at different levels from different angles, and are used in various fields, of which 80%~90% of the artificial neural network models use BP network or its variation reflects the most elite part of the artificial neural network [1–9].

From the application level, the time required for urban landscape performance optimization will directly determine the availability of optimization algorithms. Algorithm-based urban landscape performance optimization is mainly divided into two parts: urban landscape performance simulation and urban landscape performance optimization. The traditional urban landscape performance simulation process is usually completed by various simulation software such as EnergyPlus. The urban landscape performance optimization process is usually completed by intelligent algorithms such as a genetic algorithm through large-scale cluster search and other methods. Therefore, the calculation time of the entire urban landscape performance optimization process consists of two parts, which will directly determine the optimization efficiency. AgdasD. et al. believe that the computing time of the integrated feedback system EnergyPlus is several times that of other urban landscape energy consumption estimation methods, and the computing time of the energy consumption simulation algorithm is an important part of the overall computing time. Si B. et al. compared seven performances of three intelligent optimization algorithms, including optimization efficiency, and the results showed the optimization efficiency of the three algorithms. Although they are not all the same, there is no big difference, and the optimization efficiency is not high. Therefore, when designers use algorithms to optimize urban landscape performance, they often consider simplifying urban landscape models to save optimization time, especially thermal physical models. Therefore, it is a very important and urgent problem to take into account the complex urban landscape performance simulation and efficient urban landscape performance optimization. This is one of the reasons why this paper uses the optimized BP neural network algorithm to replace the dynamic simulation method of EnergyPlus [10–14].

Because the BP (backpropagation) neural network has the characteristics of self-learning, self-adaptation, distributed storage, etc., it is widely used in nonlinear prediction. Some literature uses momentum gradient descent BP neural network algorithm to predict the settlement of deep foundation pits. However, the momentum gradient algorithm also has its own shortcomings, such as slow convergence and easy to fall into local minimums. Therefore, traditional BP algorithms also have certain limitations. Genetic algorithm (GA) has a strong global optimization capability, which is globally optimized through selection, crossover, and mutation operations. Therefore, the use of a genetic algorithm to optimize a BP neural network can effectively make up for the shortcomings of the traditional BP neural network [15–22].

Since the relationship between building performance indicators and variables is mostly black box models (such as the EnergyPlus simulation software) rather than direct mathematical expressions, building performance optimization usually

cannot use traditional optimization methods based on functional expressions and tends to choose smart algorithms. In view of the high robustness of intelligent algorithms to optimization problems, there is no lack of research on using intelligent algorithms to optimize building performance at home and abroad.

Echenagucia et al. achieved the optimization of energy consumption including heating, cooling, and lighting based on the positional relationship of open spaces in the office building and the parameters of the transparent envelope structure in the initial stage of building design. The corresponding optimization suggestions are given in the form of the solution. Chen Tianchi uses Rhinoceros&Grasshopper as the platform, Octopus as the multiobjective optimization platform, and Ladybug+Honeybee as the simulation software platform. The multiobjective optimization is carried out with the sunlight index and natural ventilation index as the objective function, so as to integrate energy-saving optimization and other technologies into the early stage of building design. The final optimization results are presented with the Pareto boundary values. Chen Hang is based on the parameterized platform Rhinoceros&Grasshopper. The objective function selects the total energy consumption of the building throughout the year (optimization target is the smallest), daylight uniformity (optimization target is the largest), and glare occurrence probability (optimization target is the smallest), three optimization variables. It is the window parameter of the building's transparent envelope structure; the standard model used for optimization is the standard model of the interior corridor slab space building in the office building in cold areas, and the extracted standard model is the final research object. Finally, a multiangle analysis is carried out on the optimized optimal solution set to provide a theoretical basis for the architectural window design in the early stage of architectural design. Ma Chong takes the exterior windows of office buildings in Guangzhou as the optimization object, takes low energy consumption and high comfort as the optimization goals, establishes a multiobjective optimization problem, and uses EnergyPlus and GenOpt to analyze and solve them in parallel. The author first compares the advantages and disadvantages of traditional algorithms and genetic algorithms, then determines the optimization decision variables as multiple shading forms, and sorts and screens them for their energy-saving potential; finally, the author chooses the total energy consumption of the room and the dissatisfaction PDD. In order to optimize the goal, multiobjective optimization is carried out, the optimization result is finally analyzed, and the most suitable sunshade form for office buildings in the Guangzhou area is given [23–28]. The combination of the artificial neural network and other traditional methods will promote the continuous development of artificial intelligence and information processing technology.

Since this method contains many nonlinear elements (such as activation functions), its application scenarios have been greatly expanded, which can be summarized as the following three points: (1) regression problem: use BP neural network to establish the mapping relationship between the independent variable and the objective function; (2)

classification problem: put the independent variable in a certain way; and (3) data compression: reduce data dimensions during data transmission or storage.

## 2. Optimize the BP Neural Network Model

In recent years, artificial neural networks are developing more deeply on the road of simulating human cognition. The artificial neural network is a new type of algorithm formed by simulating the biological organization of the human brain. In the initial stage of development, artificial neural networks were called perceptrons, and there was only one level. The unique nonlinear adaptive information processing capability of the artificial neural network overcomes the shortcomings of traditional artificial intelligence methods for intuition, such as pattern, speech recognition, and unstructured information processing, making it useful in neural expert systems, pattern recognition, intelligent control, combinatorial optimization, forecasting, and other fields that have been successfully applied. This perceptron model has many advantages, such as a simple model and low computational complexity. It can fit the internal relationship between the decision variable and the objective function by learning various training sets to solve the problem of the limited ability of explicit function fitting. However, since this model cannot fit nonlinear problems, its applicable scenarios are greatly restricted. Therefore, the artificial neural network based on the BP algorithm (BP neural network for short) came into being. This method introduces the backward propagation of errors into the learning process, so that the algorithm corrects the errors by itself to meet certain error requirements. Therefore, this paper uses the global search capabilities of genetic algorithms to optimize the BP neural network structure to obtain optimized initial weights and thresholds, so that the search space of the solution can be located near the global optimal solution, and then uses the BP neural network algorithm to find the global optimal solution, so that it finally converges to the global optimal solution.

The BP algorithm is used in a multilayer feedforward network with a nonlinear transfer function, and it can theoretically approximate any nonlinear mapping relationship. This extraordinary advantage makes the multilayer feedforward network more and more widely used. The basic principle of the traditional BP algorithm is to use the gradient descent method to make the change of the connection weight and bias always move in the direction of error reduction and finally achieve the minimum error. The BP algorithm has the characteristics of simple structure, a small amount of calculation, strong parallelism, and high robustness. It is currently one of the most mature training algorithms used in neural network training. However, it also has many inherent flaws:

- (1) Local convergence: from the principle point of view, the optimization purpose of the BP neural network is to find the minimum value of the error loss function. Due to the complex structure of the multilayer BP neural network, the optimal solution of its loss

function is actually a nonlinear model optimization process. First of all, each update of the connection weight and bias of the neural network is updated by the gradient descent direction of some samples, which will make the algorithm very easy to fall into the local optimum. Furthermore, since the initial parameters (including connection weights and bias) of the neural network are initialized randomly each time, and the neural network can fit a multidimensional complex nonlinear model, the optimal value of each local convergence will have a certain difference

- (2) Sample forgetting and slow convergence: because the traditional BP algorithm uses a sample-by-sample training algorithm, when the number of samples is large, the overall error of the neural network will be biased toward the gradient and error of the samples that are sorted later, which makes the neural network produce forgetting before. The trend of the sample will also cause the convergence speed to slow down or even fail to converge, which greatly limits the application of neural networks to multivariate complex problems

The activation function in the neural network is one of the key factors that determine the performance of the neural network, and it is an important part of the nonlinear transformation of the neural network model. Since the mathematical models of many engineering problems are nonlinear, and linear models have many defects, it is extremely important to introduce activation functions (especially nonlinear activation functions). There are many types of activation functions in traditional BP neural networks, and the more widely used Sigmoid function (Figure 1) expression is:

$$f(x) = \frac{1}{1 + e^{-x}}. \quad (1)$$

It can be seen from the function expression that this function is a nonlinear function with a value range of (0, 1). With the increase of the independent variable  $x$ , the derivative of the function first increases and then decreases. Only when the value of  $x$  is near 0, the derivative value is the largest. Due to its nonlinearity and global derivability, the Sigmoid function is extended in the traditional BP neural network. However, as the application of the BP neural network has become more extensive, the actual problems have become more complicated, and the model complexity of the BP neural network has become higher and higher. This exposes the defects of the Sigmoid function, mainly for the following two points: (1) the problem of gradient disappearance: it can be seen from the function expression that when the input value is too small, the gradient almost approaches 0. This will make the update gradient too small and cause training stagnation and gradient disappearance. (2) Although the function is centrally symmetrical, the symmetrical point is not the origin, which will make the input

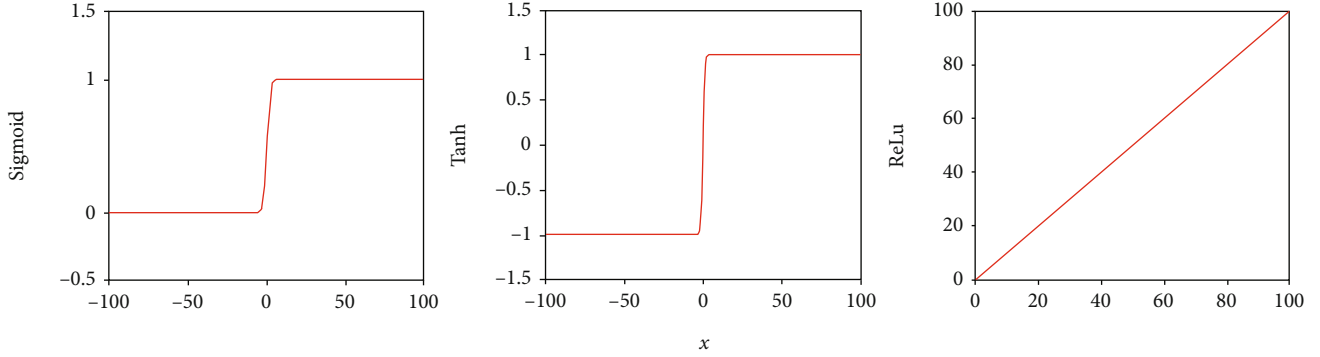


FIGURE 1: Different functions.

variables of the hidden layer not centrally symmetrical at the origin, which will affect the gradient descent method.

In response to these problems, in the development process of the activation function, many improved functions were used to replace the Sigmoid function, including the  $\tanh$  function. The expression of this function (Figure 1) is

$$f(x) = \frac{1 - e^{-2x}}{1 + e^{-2x}}. \quad (2)$$

However, when the value of  $x$  is too large or too small, there will still be the problem of gradient disappearance, which essentially does not solve the defects left by the Sigmoid function.

The emergence of the ReLU function has accelerated the final breakthrough in the direct supervision of deep network training. Its use effect in the network is significantly better than the previous Sigmoid and  $\tanh$  functions, and it is the most widely used activation function. The ReLU activation function has the following advantages: it solves the problem of gradient disappearance and improves the training speed of the network. Its function expression is

$$\text{ReLU}(x) = \begin{cases} x, & x > 0 \\ 0, & x \leq 0 \end{cases}. \quad (3)$$

The function image is shown in Figure 1. The ReLU function can effectively solve the problem of gradient disappearance, and because the function is simple in operation and will not activate all neurons at the same time, the application effect of the ReLU function in the BP neural network is better than other functions.

BP neural network includes two processes of signal forward propagation and error backpropagation and consists of an input layer, a hidden layer, and an output layer. When the actual output and expected output of the signal passing forward exceed the set threshold, it will enter the backpropagation phase. Due to the characteristic of gradient descent of the error function, the connection weight of the hidden layer can be continuously adjusted to optimize the learning network structure. BP neural network is suitable for nonlinear prediction due to its self-learning and self-adaptive characteristics, and it is widely used in the field of data prediction.

Due to the large numerical difference between each input index and output index, the original data needs to be standardized before entering the system. The standardized expression is

$$x_{ij}' = \frac{x_{ij} - \bar{x}_j}{S_j}, \quad (4)$$

$$S_j = \sqrt{\frac{1}{m_{i=1}} \sum_{i=1}^m (x'_{ij} - x_j)^2},$$

$$\bar{x}_j = \frac{1}{m} \sum_{i=1}^m x_{ij},$$

where  $x$  is the index and  $S$  is the standard deviation.

Genetic algorithm is inspired by natural selection and genetic theories. It finds the global optimal solution through three genetic operators of selection, crossover, and mutation and has strong global optimization capabilities. It mainly includes the processes of genetic coding, fitness function design, selection, crossover, and mutation.

- (1) Genetic coding: convert the solution space of the problem to a search space that can be processed by the genetic algorithm. It mainly includes real number encoding and binary encoding. This article encodes based on the characteristic of real number encoding that it is not easy to fall into the local extremum
- (2) Fitness function design: the fitness function is the basis for selecting outstanding individuals based on the objective function and should be nonnegative and as simple as possible. This article uses the reciprocal of the sum of squares of errors, as shown in the following formula

$$f = \frac{1}{\sum_{i=1}^N (Y_i - T_i)^2}, \quad (5)$$

where  $N$  is the total number of input samples,  $Y_i$  is the actual output of the  $i$ -th sample, and  $T_i$  is the expected output of the  $i$ -th sample

- (3) Selection operation: according to the “survival of the fittest” mechanism, individuals with greater fitness are selected to form a new population. The greater the fitness value of the individual, the greater the probability of being selected into the new population. The selection operation mainly includes the roulette method and tournament method. This article chooses the roulette method. Thus, it becomes

$$p_k = \frac{F_k}{\sum_{i=1}^N F_i}, \quad (6)$$

where  $F_k$  is the fitness value of the individual

- (4) Crossover operation: the chromosomes of two individuals in the population are crossed and exchanged, and the excellent characteristics are inherited to the new individual. Since this article is a real number encoding method, it becomes

$$\begin{aligned} a_{kj} &= a_{kj}(1-b) + a_{ij}b, \\ a_{ij} &= a_{ij}(1-b) + a_{kj}b, \end{aligned} \quad (7)$$

where  $b$  is a random number between 0 and 1

- (5) Mutation operation: its codes string to other alleles to produce excellent individuals. The individual gene mutation operation is shown in the following formula:

$$a_{ij} = \begin{cases} a_{ij} + (a_{ij} - a_{\max}) \times f(g), & r > 0.5 \\ a_{ij} + (a_{\min} - a_{ij}) \times f(g), & r \leq 0.5 \end{cases}. \quad (8)$$

In the formula:  $a_{\max}$  and  $a_{\min}$  are the upper and lower bounds of gene  $a_{ij}$ , respectively.

$$f(g) = r_2 \left( 1 - \frac{g}{G_{\max}} \right)^2, \quad (9)$$

where  $r_2$  is a random number,  $g$  is the current iteration number,  $G_{\max}$  is the maximum evolution number, and  $r$  is a random number between 0 and 1. BP neural network has strong local searchability and is very effective in data fitting, but it is very sensitive to the initial weight and threshold of the network. The slow convergence speed and the defects of easy to fall into the local minimum will lead to poor prediction results. However, genetic algorithms have strong global search capabilities due to their selection, crossover, and mutation operations. Combining the advantages of genetic algorithm and BP neural network, a high-precision prediction model is constructed, as shown in Figure 2.

### 3. Design Model Analysis

Combining with fuzzy systems, genetic algorithms, and evolutionary mechanisms to form computational intelligence, it has become an important direction of artificial intelligence and will be developed in practical applications. The hidden layer neuron combination method and the learning rate are combined for training, and the mean square error of the training set and the mean square error of the test set are averaged to obtain the mean square error of the training set (MSE) average value and test set mean square error (MSE) average value, as shown in Table 1. Figure 3 shows the training set MSE average value, the test set MSE average value, and the trend of training times at convergence with the learning rate picture. It can be found that the average mean square error of the training set first rapidly decreases with the increase of the learning rate and then slowly increases; while the test set is slightly different, the average mean square error of the training set first decreases rapidly with the increase of the learning rate and then increases rapidly; training Algebra increases first and then decreases as the learning rate increases. Among them, when the learning rate is 0.001, the training algebra is the least, the convergence speed is the fastest, but the mean square error average of the training set, and the test set is the largest, that is, the model falls into the local optimum. When the learning rate is 0.007, the average mean square error of the training set and the mean square error of the test set both reach the lowest value. When the learning rate increases to 0.013, the average values are higher, the number of training is less, and the situation of nonconvergence or local optimality begins to appear. In order to ensure that the model fully converges while preventing the occurrence of overfitting, this model chooses 0.007 as the optimal learning rate.

Based on the optimal learning rate of 0.007, the first set of training is performed on the hidden layer combination, each combination is calculated five times, and the mean square error of the training set and the mean square error of the test set are calculated. The results are shown in Table 1. In order to observe the impact of these 64 combinations on the performance of the neural network more intuitively, the data in the table will be presented in the three-dimensional scatter plots (Figure 3). As shown in this figure, the blue cross is the mean square error of the training set, and the orange circle is the mean square error of the test set. Among them, the size of the cross and the circle represents the relative size of the mean square error, and the larger the shape, the larger the value. It can be seen that when the number of neurons in hidden layer 1 and hidden layer 2 is both at a small level, the average mean square error of the training set and the average mean square error of the test set are both at a higher level. The data set has almost no fitting and generalization capabilities. As the number increases, the mean square error of the training set and the mean square error of the test set rapidly decrease, and the fitting effect begins to increase. Figure 3 is a partial three-dimensional scatter plot after filtering out part of the excessively high mean square error, in order to more clearly



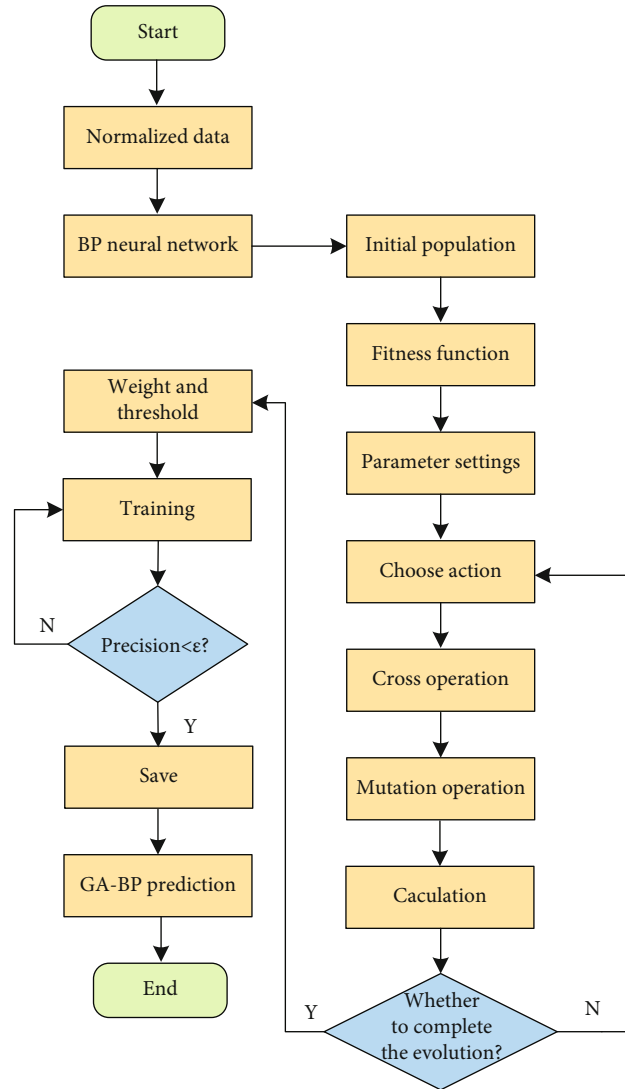


FIGURE 2: GA-BP neural network model prediction flow chart.

TABLE 1: Neural network performance indicators vs. different learning rates.

Learning rate	0.001	0.003	0.005	0.007	0.009	0.011	0.013
Train MSE	0.3646	0.1298	0.09251	0.08215	0.1806	0.1925	0.1845
Test MSE	0.7623	0.4177	0.1876	0.1396	0.5894	0.6963	0.5397
Number of iterations	60558	94401	129025	126755	126850	93139	101829

observe the mean square error at the optimal solution. The mean square error of the training set and the mean square error of the test set also decrease until the maximum number of neurons is reached. A [45,45] combination scheme was used.

Therefore, based on the combination scheme of [45,45], a second set of hidden layer combination schemes is set for training. The combination scheme and training results are shown in Figure 4. Each group of schemes is calculated five times, and the average square error of the training set and the average square error of the test set are averaged. The

average square error of the training set and the average square error of the test set are calculated. The data in the table is the same. It is presented in a three-dimensional scatter chart, as shown in Figure 4.

From Figure 4, it can be found that as the number of hidden layer 1 and hidden layer 2 neurons increases, the average mean square error of the training set generally shows a trend of decreasing, while the average mean square error of the test set tends to decrease first and then increase. Obviously, at a certain combination of neurons, the neural network has reached the maximum generalization ability. Before that,

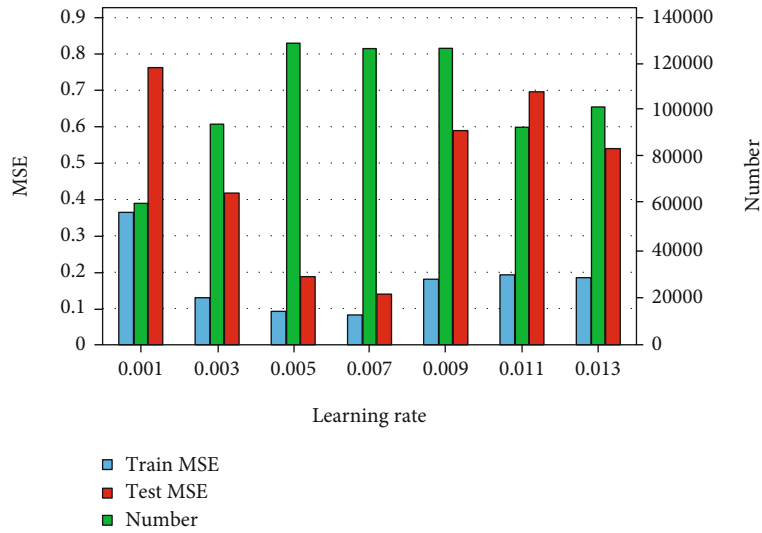


FIGURE 3: The trend of neural network performance indicators changing with learning rate.

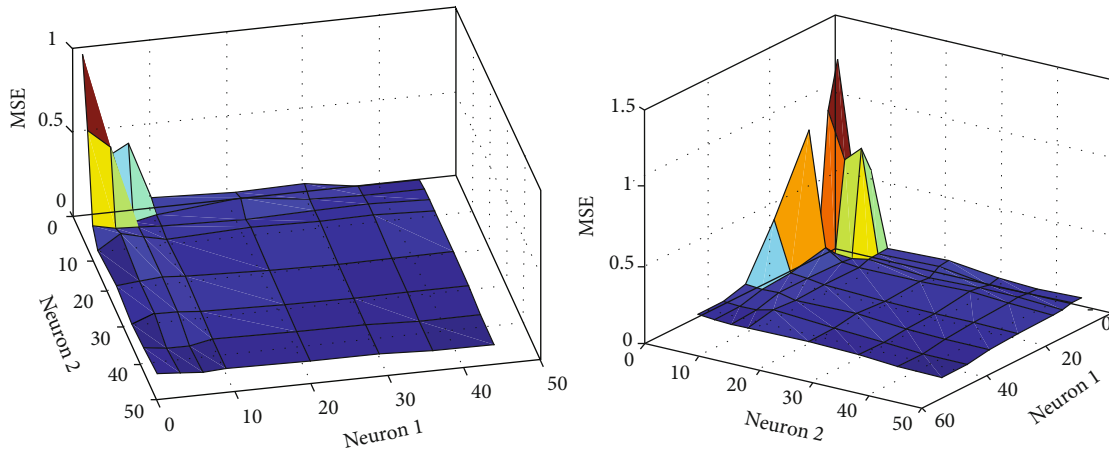


FIGURE 4: 3D data.

the neural network fitting ability and generalization ability continued to increase. After that, the neural network fitting ability continued to increase, but the generalization ability began to decrease, and the model began to appear overfitting.

Combining Figure 5, it can be found that when the structure of the hidden layer is [54,54], the average mean square error of the training set of the neural network is the lowest among all neuron combination schemes, which is 0.001461, but the corresponding the average mean square error of the test set is as high as 0.008668. This shows that the BP neural network under this combination has a strong fitting ability, but with low generalization ability, serious overfitting phenomenon, and poor predictive ability for the objective function of the unknown scheme. When the structure of the hidden layer is [45,43], the average mean square error of the training set is 0.003414, and the fitting ability ranks 9th among all combinations, but the average mean

square error of the test set is 0.003809, and the generalization ability is the most strong, that is, the model has good generalization ability while fully converging and belongs to the most superior model in all groups.

For the final selected BP neural network model, the group with the strongest generalization ability among the five training results is selected as the optimal model, and its accuracy and stability are analyzed in detail. Figure 6 is the distribution diagram of the true value (or actual value) obtained by simulation in the training set. The abscissa is the number of sample sequences. Figure 6 is a comparison diagram of the true value obtained by the simulation in the test set and the predicted value of the optimal neural network model. The abscissa is the number of sample sequences, a total of 997 groups, and the ordinate is also -0.4-0.4. The average daily cooling energy consumption in summer during the four days can be seen qualitatively from Figure 6 in which the predicted value of the

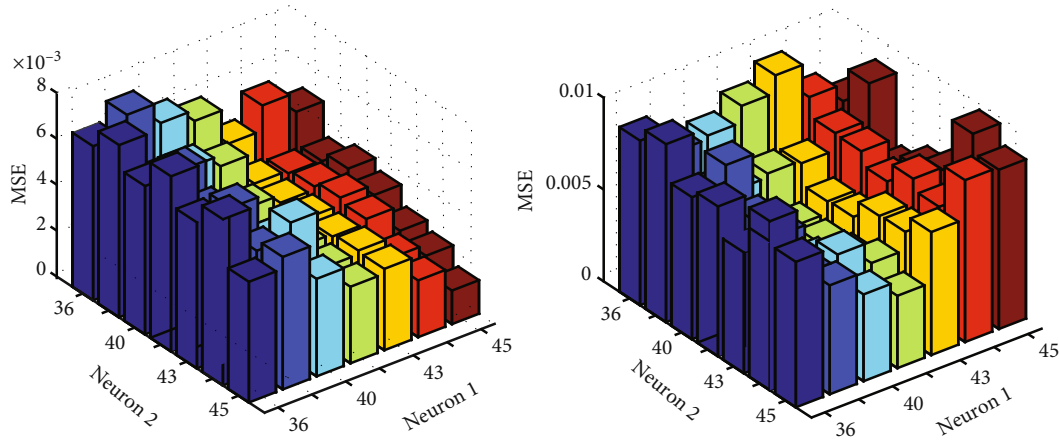


FIGURE 5: Mean square error.

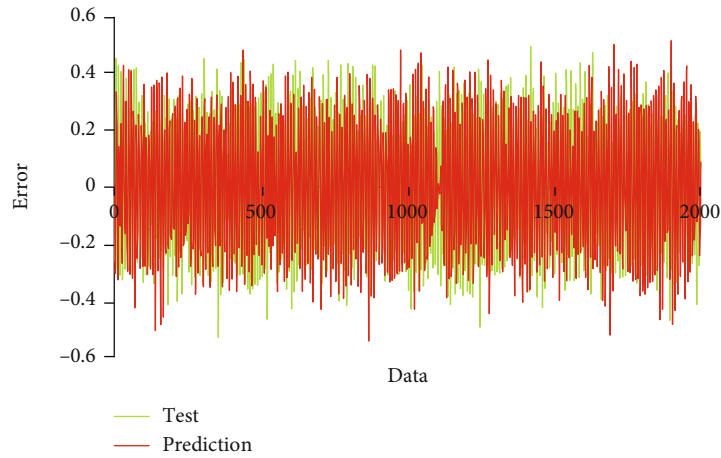


FIGURE 6: Comparison of test and prediction.

average daily cooling energy consumption in summer is in good agreement with the true value, and the prediction model has a strong ability to fit and generalize.

In fact, the convergence process of the solution set in the evolutionary algorithm consists of two parts: one is the closeness between the Pareto optimal solution set and the full solution set, and the other is the closeness between the Pareto optimal solution set and the real Pareto optimal solution set. It can reflect the convergence process from the local optimal solution to the global optimal solution. But the Pareto frontier in actual engineering is often unpredictable (this is the core problem that the optimization method needs to solve), so the second part of the convergence process often cannot give a quantitative or qualitative judgment. Therefore, this section mainly focuses on the analysis of the convergence process mentioned in the first part and analyzes the convergence process with the changing trend of the maximum and minimum values of the two solutions.

As shown in Figure 7. The Pareto optimal solution and the minimum value of the full solution set in the two objective function dimensions have little change. This is mainly

because the optimization objective of this paper is the minimum value of the function. The maximum changes in the two dimensions are more obvious, and the maximum value of the Pareto optimal solution is often smaller than the full solution set. As the evolution progresses, the maximum values of the two gradually approach and eventually tend to coincide. This is mainly because, first, the proportion of the Pareto optimal solution set in the full solution set has increased and the distance between the second optimal solution and the dominant solution is getting closer. It can also be seen in the figure that the maximum values of energy consumption and thermal comfort both increase with the growth of evolutionary algebra and eventually stabilize, while the minimum values remain basically unchanged. This shows that the two objective functions seek to find the minimum value of the understanding set and remain stable in the early stage of evolution, while the maximum value develops toward the direction of increasing the universality of the solution set. It should be noted that the maximum value of APMV's total solution set and the Pareto solution set has a slight upward trend in the 55th generation, which means that the solution set is still evolving in the direction

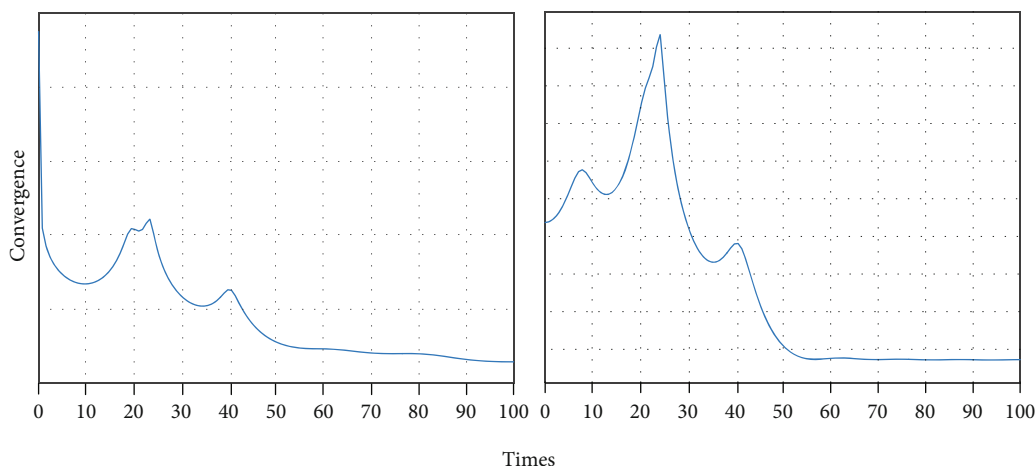


FIGURE 7: Convergence.

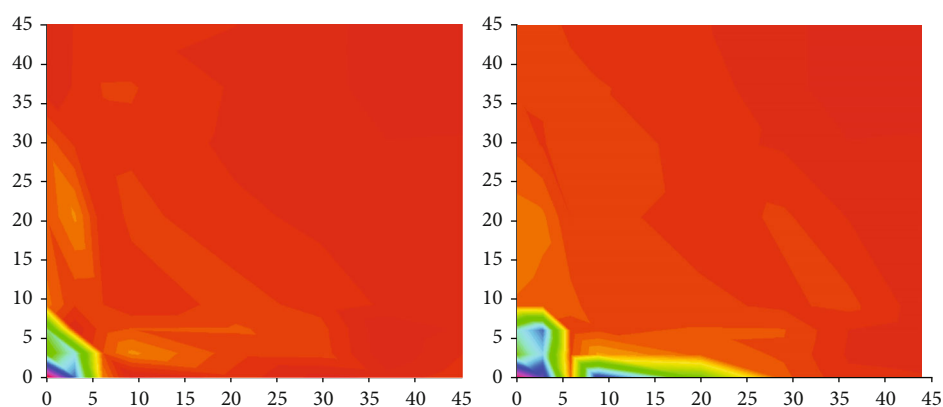


FIGURE 8: MSE variation.

of increasing generality, rather than not converging. The MSE variation is shown in Figure 8.

It can also be known from the figure that the fluctuation range of the maximum value is relatively large; especially, the energy consumption is more obvious. There may be two reasons for this phenomenon. One is that most of the decision variables in this case are discrete variables, and the other is that the previous multigeneration solutions hover in multiple local optimal points, and finally, they are near the stable place due to variation. This phenomenon can be explained by the outliers in the box chart. This is very normal, and it is also the meaning of the mutation rate setting in the algorithm.

#### 4. Conclusion

The research in this article still has some shortcomings. As far as the scope of application is concerned, although the two algorithms used in this article are theoretically suitable for most building performance prediction and optimization problems, the building performance prediction and optimization platform built in this article are only suitable for spa-

tial parameter optimization of small- and medium-sized urban landscapes in cold regions. On the one hand, the spatial generation method in this paper is derived from the architectural features of small- and medium-sized urban landscapes; on the other hand, the data set used for algorithm model training in this paper is also derived from the performance simulation results of small- and medium-sized urban landscapes in cold areas. In terms of algorithm theory, with the continuous development of deep learning and intelligent algorithms, many new algorithms continue to emerge, and it is very likely that there will be algorithms with better performance than the algorithms in this article in the future. Therefore, how to build a building performance prediction and optimization platform with wider applicability and better algorithm performance requires further research.

#### Data Availability

The data used to support the findings of this study are available from the corresponding author upon request.

## Conflicts of Interest

The authors declare that they have no known competing financial interests or personal relationships that could have appeared to influence the work reported in this paper.

## References

- [1] Z. Li and X. Zhao, "BP artificial neural network based wave front correction for sensor-less free space optics communication," *Optics Communications*, vol. 385, pp. 219–228, 2017.
- [2] X. Xiao-wei, "Study on the intelligent system of sports culture centers by combining machine learning with big data," *Personal and Ubiquitous Computing*, vol. 24, no. 1, pp. 151–163, 2020.
- [3] T. Zhang, S. Liu, W. Xiang, L. Xu, K. Qin, and X. Yan, "A real-time channel prediction model based on neural networks for dedicated short-range communications," *Sensors*, vol. 19, no. 16, pp. 3541–3541, 2019.
- [4] G. Jingjing, Z. Dong, C. Zhang, X. Du, and M. Guizani, "Dynamic stress measurement with sensor data compensation," *Electronics*, vol. 8, no. 8, pp. 859–859, 2019.
- [5] J. J. Jung and G. S. Jo, "Brokerage between buyer and seller agents using constraint satisfaction problem models," *Decision Support Systems*, vol. 28, no. 4, pp. 291–384, 2020.
- [6] C. Mingan, J. Xianqing, L. Shangbing, and Z. Xu, "Compensation of turbulence-induced wavefront aberration with convolutional neural networks for FSO systems," *Chinese Optics Letters*, vol. 19, no. 11, pp. 110601–110626, 2021.
- [7] J. Byun and S. Jang, "Effective destination advertising: matching effect between advertising language and destination type," *Tourism Management*, vol. 50, no. 10, pp. 31–40, 2015.
- [8] F. Qian and L. Yang, "The green building environment of the gymnasium," *Applied Mechanics and Materials*, vol. 878, pp. 202–209, 2018.
- [9] C. Blackburn, A. Harding, and J. Moreno-Cruz, "Toward deep-decarbonization: an energy-service system framework," *Current Sustainable Renewable Energy Reports*, vol. 4, no. 4, pp. 181–190, 2017.
- [10] H. Wu, Y. Yu, H. Fu, and L. Zhang, "On the prediction of chemical exergy of organic substances using least square support vector machine," *Energy Sources Part A Recovery Utilization and Environmental Effects*, vol. 39, no. 24, pp. 2210–2215, 2017.
- [11] D. Ettinger and F. Michelucci, "Creating a winner's curse via jump bids," *Review of Economic Design*, vol. 20, no. 3, pp. 173–186, 2016.
- [12] J. A. Brander and E. J. Egan, "The winner's curse in acquisitions of privately-held firms," *Review of Economics Finance*, vol. 65, pp. 249–262, 2017.
- [13] R. M. A. van der Slikke, M. A. M. Berger, D. J. J. Bregman, and H. E. J. Veeger, "From big data to rich data: the key features of athlete wheelchair mobility performance," *Journal of Biomechanics*, vol. 49, no. 14, pp. 3340–3346, 2016.
- [14] M. Pascal and P. Pierre, "Spatial segregation and urban structure," *Journal of Regional Science*, vol. 59, no. 3, pp. 480–507, 2019.
- [15] P. Klibano, M. Marinacci, and S. Mukerji, "A smooth model of decision making under ambiguity," *Econometrica*, vol. 73, no. 6, pp. 1849–1892, 2005.
- [16] Y. Halevy, "Ellsberg revisited: an experimental study," *Econometrica*, vol. 75, no. 2, pp. 503–536, 2007.
- [17] T. F. Stepinski and A. Dmowska, "Complexity in patterns of racial segregation," *Chaos Solitons and Fractals the interdisciplinary journal of Nonlinear Science and Nonequilibrium and Complex Phenomena*, vol. 140, pp. 110207–110214, 2020.
- [18] T. Gergő, J. Wachs, R. Di Clemente et al., "Inequality is rising where social network segregation interacts with urban topology," *Nature Communications*, vol. 12, no. 1, pp. 1143–1143, 2021.
- [19] J. Jiayi, C. Ming, and Z. Junhua, "How does residential segregation affect the spatiotemporal behavior of residents? Evidence from Shanghai," *Sustainable Cities and Society*, vol. 69, p. 102834, 2021.
- [20] N. Ta, M. P. Kwan, S. Lin, and Q. Zhu, "The activity space-based segregation of migrants in suburban Shanghai," *Applied Geography*, vol. 133, p. 102499, 2021.
- [21] S. Park, T. M. Oshan, A. El Ali, and A. Finamore, "Are we breaking bubbles as we move? Using a large sample to explore the relationship between urban mobility and segregation," *Computers, Environment and Urban Systems*, p. 86, 2021.
- [22] K. Urbanowicz and L. Nyka, "Interactive and media architecture - from social encounters to city planning strategies," *Procedia Engineering*, vol. 161, no. C, pp. 1330–1337, 2016.
- [23] S. T. Moghadam and P. Lombardi, "An interactive multi-criteria spatial decision support system for energy retrofitting of building stocks using CommuntiyVIZ to support urban energy planning," *Building and Environment*, vol. 163, no. C, pp. 106233–106233, 2019.
- [24] M. Sanchez-Sepulveda, D. Fonseca, J. Franquesa, and E. Redondo, "Virtual interactive innovations applied for digital urban transformations. Mixed approach," *Future Generation Computer Systems*, vol. 91, pp. 371–381, 2019.
- [25] Y. Deng, D. Huang, S. Du, G. Li, and J. Lv, "A double-layer attention based adversarial network for partial transfer learning in machinery fault diagnosis," *Computers in Industry*, vol. 127, article 103399, 2021.
- [26] Q. Zuo, W. Leonard, and E. E. MaloneBeach, "Integrating performance-based design in beginning interior design education: an interactive dialog between the built environment and its context," *Design Studies*, vol. 31, no. 3, pp. 268–287, 2010.
- [27] W. Li, G. G. Wang, and A. H. Gandomi, "A survey of learning-based intelligent optimization algorithms," *Archives of Computational Methods in Engineering*, vol. 28, pp. 3781–3799, 2021.
- [28] G. G. Wang, A. H. Gandomi, A. H. Alavi, and D. Gong, "A comprehensive review of krill herd algorithm: variants, hybrids and applications," *Artificial Intelligence Review*, vol. 51, no. 1, pp. 119–148, 2019.

## Research Article

# Analysis of Ecological Environment Evaluation and Coupled and Coordinated Development of Smart Cities Based on Multisource Data

Qianwei Ma <sup>1</sup> and Yanxia Yang<sup>2</sup>

<sup>1</sup>Information Center, Dongying Housing and Urban Rural Construction Development Service Center, Dongying, Shandong 257001, China

<sup>2</sup>Department of Information Engineering, Dongying Technician College, Dongying, Shandong 257001, China

Correspondence should be addressed to Qianwei Ma; [mqwqwm@163.com](mailto:mqwqwm@163.com)

Received 12 January 2022; Revised 8 February 2022; Accepted 18 February 2022; Published 24 March 2022

Academic Editor: Wen Zeng

Copyright © 2022 Qianwei Ma and Yanxia Yang. This is an open access article distributed under the Creative Commons Attribution License, which permits unrestricted use, distribution, and reproduction in any medium, provided the original work is properly cited.

In order to further enhance the ecological environment construction of smart cities and promote its deep integration with advanced technologies, such as the new generation of artificial intelligence and big data, this study constructs a data fusion framework for the ecological environment of smart cities driven by multisource data and constructs an ecological environment evaluation index system of smart cities in Guangzhou from 2010 to 2018. The ecological environment status of smart cities in Guangzhou is analyzed by principal component analysis, and finally the correlation influence degree of each principal component content on the ecological environment index of smart cities is analyzed. The results show that environmental excellence ( $K_1$ ), environmental restoration response ( $K_2$ ), and environmental pollution pressure ( $K_3$ ) are the main components of the ecological environment in Guangzhou smart city. The environmental excellence and environmental restoration response level are relatively high, and the environmental pressure system is relatively low, in which the greenland coverage rate increases from 41.3% to 44.0%, and the urban sewage treatment rate and the decontamination rate of urban refuse increase year by year, from 73.1% to 94.6% and from 72.1% to 99.9%, respectively. The results of principal component correlation analysis show that there are interactive influences among environmental excellence ( $K_1$ ), environmental restoration response ( $K_2$ ), and environmental pollution pressure ( $K_3$ ). The ecological environment index of smart cities increases with the improvement of environmental excellence and environmental restoration response capacity, but gradually decreases with the increase of environmental pollution pressure. Generally speaking, improving environmental excellence and environmental restoration response will be the key to improve the ecological environment construction capacity of smart cities in the future.

## 1. Introduction

Nology to all walks of life in the city, so as to realize the deep integration of urban informatization, industrialization, ecologicalization, and urbanization, improves the quality of urbanization, realizes fine and dynamic management, and improves the effectiveness of urban management and the quality of life of citizens [1, 2]. Up to now, smart city is no longer an independent informatization and digitization but the embodiment of a series of integrated services and operation capabilities of finance, science and technology, data,

ecological environment, and other applications [3, 4]. The 2018 China Network Security and informatization Work Conference pointed out that it is necessary to vigorously promote the in-depth integration of artificial intelligence, big data, digitization, informatization, and urban development to provide a strong technical guarantee for the construction of smart cities. Taking the “1 + N + 1” comprehensive solutions of smart city as an example, 1 represents the smart city cloud, which is the digital base of the city; N represents the smart city cloud as the support, through the cross-border and fusion application of cloud

data, to create solutions for N industries, including urban greening, environmental pollution control, transportation, medical health, AI education, and other different scenarios, and finally forms a smart city brain by integration [5].

The construction of ecological civilization is an essential link in the development process of smart city [6, 7]. In recent years, the contradiction between the rapid economic development and the construction of ecological environment has become increasingly obvious. As a densely populated area, the city is facing the problems of weakening environmental greening, ecological environment pollution, and scarcity of natural resources in the development process [8, 9]. The 19th National Congress of China clearly pointed out in the construction of smart cities and ecological civilization that in the future, the integration of ecological environment and smart city should be accelerated based on the concepts of green, low-carbon, convenient, efficient, and rapid response; under the support of new generation of information technology, the green smart city should be built to play the basic role of environmental informatization in China's environmental management innovation [10, 11]. Therefore, improving the ecological environment construction of smart city and promoting its deep integration with the new generation of artificial intelligence, big data, and other advanced technologies will be the development trend of smart and ecological city in the future [12]. Guangzhou, as a national pilot smart city, is also the core of Guangdong's smart city cluster, and its construction and development model can be used as a construction sample for Guangdong and even the whole country. However, the existing studies still focus on the evaluation of information technology and technological innovation, while ignoring the importance of ecological environment construction.

Based on this, this study takes the first batch of smart cities, Guangzhou as the research object, according to the opinions and suggestions on the development of "smart city" and "ecological civilization" in the new urbanization construction, constructs a data fusion framework for the ecological environment of smart cities driven by multisource data, constructs the Guangzhou smart city ecological environment evaluation index system from 2010 to 2018, and uses the principal component analysis method to analyze the ecological environment status of smart cities in Guangzhou. Finally, by constructing response surface model, this paper analyzes the correlation influence degree of each principal component content on the ecological environment index of smart cities, thus revealing the current development trend of ecological environment construction of smart cities in Guangzhou.

## 2. Materials and Methods

**2.1. Construction of Environment Evaluation Index System.** The ecological environment evaluation system of smart city is a systematic analysis of comprehensive factors such as natural ecological environment, environmental governance, and environmental carrying capacity. Based on this, this paper focuses on the ecological environment evaluation of smart cities and focuses on the evaluation of the ecological

environment of smart cities, with emphasis on the three main factors of environmental state, environmental response, and environmental pressure corresponding to the ecological environment construction, while following the principles of systematic, complete, quantifiable, and traceable data to determine the ecological environment evaluation indicators. This study selects nine indexes, such as greenland coverage rate, forest coverage rate, water supply popularizing rate, decontamination rate of urban refuse, urban sewage treatment rate, comprehensive utilization rate of industrial solid waste, industrial waste gas discharge, industrial wastewater discharge, and industrial solid waste discharge to construct an ecological environment evaluation index system of smart city, as shown in Table 1.

**2.2. Selection of Evaluation Methods and Data Sources.** This study uses the principal component analysis to carry out statistical analysis. Under the condition of minimum loss of information, multiple indexes are transformed into fewer comprehensive evaluation indexes (i.e., principal components), in which each principal component is a linear combination of the original index variables, and the correlation between the principal components is unknown [13, 14]. Based on this, this study selects Guangzhou City in the Pearl River Delta region as the research object and uses the principal component analysis method to evaluate the environmental index system.

**2.2.1. Selection of Dimensionless Method.** Due to the great differences in the value range, measurement unit, and data nature of the selected indexes, in order to get more objective weight, this study adopts entropy method to standardize the data, and the calculation formula is as follows:

$$P_{ij} = \frac{(Q_{ij} - \bar{Q}_{ij})}{S_j}, \quad (1)$$

$$S_j = \sqrt{\frac{1}{n} \sum_{i=1}^n (Q_{ij} - \bar{Q}_{ij})^2}. \quad (2)$$

Among them,  $P_{ij}$  is the data result after standardization processing;  $Q_{ij}$  is the original data of the calendar year in the  $j$ th index research period, and  $\bar{Q}_{ij}$  is the average data in the  $j$ th index research period; and  $S_j$  is the standard deviation of the  $j$ th index.

**2.2.2. Construction of Principal Component Factor Score Function.** The standardized coefficient matrix of evaluation index system can be obtained after data standardization processing, and then, principal component factor analysis is carried out by SPSS software, so as to obtain variance contribution rate, component matrix, and component score coefficient matrix of each component.  $M$  principal components with accumulated variance contribution rate greater than 90% are selected as principal components, and the principal component factor score function  $K_m$  is constructed by combining the component matrix, and its calculation

TABLE 1: Construction of ecological environment evaluation index system of smart city.

System layer	Index layer	Unit	Index code
Environment evaluation index system of smart city	Decontamination rate of urban refuse	%	$X_1$
	Forest coverage rate	%	$X_2$
	Greenland coverage rate	%	$X_1$
	Water supply popularizing rate	%	$X_4$
	Urban sewage treatment rate	%	$X_5$
	Industrial waste gas discharge	100 million cu.m	$X_6$
	Utilization rate of industrial solid waste	%	$X_7$
	Industrial wastewater discharge	100 million tons	$X_8$
	Industrial solid waste discharge	10000 tons	$X_9$

formula is as follows:

$$K_m = A_{m1}P_1 + A_{m2}P_2 + \dots + A_{mn}P_n. \quad (3)$$

Among them,  $K_m$  is the score function of principal component factor;  $P_1, P_2 \dots P_n$  are the standardized evaluation indexes of ecological environment; and  $A_{m1}, A_{m2} \dots A_{mn}$  are the factor coefficients of the  $m$ th principal component.

**2.2.3. Determination of Comprehensive Evaluation Index.** With the variance contribution rate of each component and the factor score function of each main component are combined, the comprehensive evaluation index  $K_i$  of ecological environment in smart city is finally obtained, and its calculation formula is as follows [15, 16].

$$K_i = \sum_{m=1}^t F_m K_{im}. \quad (4)$$

Among them,  $K_i$  is the comprehensive evaluation index of the  $i$ th ecological environment evaluation index in smart city,  $F_m$  is the variance contribution rate of the  $m$ th principal component, and  $K_{im}$  is the score function of the  $m$ th principal component factor in the  $i$ th year.

**2.2.4. Data Sources and Analysis.** The index data of this study are all from the *Guangdong Statistical Yearbook* from 2010 to 2018, and the principal component analysis method of SPSS20.0 is used for data processing and analysis.

**2.3. Correlation Analysis of Environment Evaluation Indexes.** In order to further consider the correlation effect of the principal components of ecological environment in Guangzhou smart city, this study uses the principal components as response variables, and the ecological environment index of smart city as dependent variable to build a response surface model, using Deign Expert 10.0 Software to design Box-Beheken response surface test and analyze the results. The results of variance analysis obtained are shown in the following Table 2. The binary multiple regression equation for the Smart City Ecosystem Index is as follows:  $R = 78.06 + 7.28A + 6.34B - 2.24C - 1.11AB - 0.61AC - 2.23BC - 0.79A^2 + 1.05B^2 - 0.48C^2$ ,  $F = 8.95$ , which shows that the response surface model constructed in this study has  $P <$

0.01, indicating that the model has significant differences and can be used for the correlation analysis on influencing factors of ecological environment index of smart cities in Guangzhou.

### 3. Results and Discussion

#### 3.1. Empirical Analysis on the Principal Components of Ecological Environment Construction in Guangzhou Smart City

**3.1.1. Extraction and Structural Analysis of Principal Components.** SPSS20.0 is used to conduct factor analysis on the standardized coefficient matrix, and three principal components which can fully reflect the ecological environment of Guangzhou City are selected under the condition of eigenvalue  $> 1$ . The cumulative variance rates are 63.53%, 78.33%, and 91.02%, respectively. Further analysis is carried out on the structure of each principal component. Table 3 shows the analysis results of the ecological environment component matrix and principal component scores in Guangzhou. It can be seen that among the components of the first principal component, forest coverage ( $X_2$ ), water supply popularizing rate ( $X_3$ ), and greenland coverage rate in built-up area ( $X_4$ ) account for the largest proportion. Therefore, the first principal component of Guangzhou ecological environment is set as variable  $K_1$ , representing environmental excellence. Similarly, the second and third principal components of Guangzhou's ecological environment are set as variables  $K_2$  and  $K_3$ , respectively. Among the elements of  $K_2$ , the proportion of decontamination rate of urban refuse ( $X_1$ ), urban sewage treatment rate ( $X_5$ ), and comprehensive utilization rate of industrial waste ( $X_7$ ) is the largest, so the proposed variable  $K_2$  is the environmental restoration response; among the elements of  $K_3$ , the proportion of industrial waste gas discharge ( $X_6$ ), industrial wastewater discharge ( $X_8$ ), and industrial solid waste discharge ( $X_9$ ) is the largest, so the proposed variable  $K_3$  is environmental pollution pressure. To sum up, the principal components of Guangzhou's ecological environment are environmental excellence ( $K_1$ ), environmental restoration response ( $K_2$ ), and environmental pollution pressure ( $K_3$ ).



TABLE 2: Variance analysis results of response surface test design of ecological environment index in smart city.

Source	Sum of squares	df	Mean square	F value	P value
Model	819.66	9	91.07	8.95	0.0043
A-environmental excellence rate	424.28	1	424.28	41.68	0.0003
B-environmental remediation capability	321.31	1	321.31	31.57	0.0008
C-environmental pollution pressure	39.96	1	39.96	3.93	0.088
AB	4.91	1	4.91	0.48	0.5099
AC	1.5	1	1.5	0.15	0.7124
BC	19.85	1	19.85	1.95	0.2053
A <sup>2</sup>	2.61	1	2.61	0.26	0.628
B <sup>2</sup>	4.66	1	4.66	0.46	0.5203
C <sup>2</sup>	0.98	1	0.98	0.096	0.7652
Residual	71.25	7	10.18		
Lack of fit	70.37	3	23.46	107.42	0.0003
Pure error	0.87	4	0.22		
Cor total	890.91	16			

Note: \* indicates significant difference,  $P < 0.05$ ; \*\* indicates extremely significant.

TABLE 3: Component matrix of ecological environment in Guangzhou.

Index	Component		
	1	2	3
$X_1$	-0.945	0.561	-0.084
$X_2$	0.933	0.165	-0.182
$X_3$	0.928	0.277	-0.218
$X_4$	0.799	-0.296	0.212
$X_5$	0.462	0.856	0.200
$X_6$	-0.327	-0.846	0.495
$X_7$	0.528	0.731	0.341
$X_8$	-0.051	-0.702	0.589
$X_9$	-0.099	-0.091	0.957

3.1.2. *Dynamic Measurement of Principal Component and Comprehensive Evaluation Index.* According to the results of principal component structure analysis, the comprehensive evaluation index in each principal component of ecological environment in Guangzhou is calculated by using formula (2) and formula (3). The dynamic changes of index parameters of each principal component with the study year are shown in Figures 1–3, respectively. As a first-tier city in China, Guangzhou was selected into the first batch of smart cities in 2014. In the development of smart city construction, the ecological construction of Guangzhou presents a steady rising trend and is superior to the level of smart city construction in five years. In general, the response level of environmental excellence and environmental restoration is relatively high, and the environmental pressure system is relatively poor. In recent years, Guangzhou has always followed the development concept of “low carbon economy, smart city, happy life” as an ecological smart city and vigorously promoted the organic integration of economic construction and ecological construction [17]. Figure 1 shows the dynamic change law of each index parameter under the con-

dition of environmental excellence ( $K_1$ ). It can be seen from Figure 1 that the excellent environment rate, as the first principal component, is the main factor affecting the ecological environment of smart cities in Guangzhou. During 2010–2018, the greenland coverage rate and forest coverage rate of built-up area showed an overall growth trend, in which the greenland coverage rate of built-up area increases from 57.0% to 58.98% and then slightly decreased to 58.59%, with the overall greening rate improving to a certain extent. As a supplementary factor for the environmental excellence, the water supply popularizing rate showed a dynamic and balanced development trend, and the overall water supply rate reached 98%, which was in the forefront of the country.

Figure 2 shows the dynamic change law of each index parameter of environmental restoration response ( $K_2$ ). It can be seen from Figure 2 that the urban sewage treatment rate, decontamination rate of urban refuse, and comprehensive utilization rate of industrial solid waste are the three major indexes that feed back the ecological environment restoration response ability of smart city. Generally speaking, the urban sewage treatment rate and decontamination rate of urban refuse in Guangzhou are increasing year by year, from 73.1% to 94.6% and 72.1% to 99.9%, respectively. The improvement of environmental protection technology of wastewater and solid waste effectively promotes the environmental restoration response capacity in Guangzhou. On the other hand, the comprehensive utilization rate of industrial solid waste has always been in a state of dynamic fluctuation, ranging from 83.76% to 90.77%. Since 2014, Guangzhou has attached great importance to the construction of “smart Guangzhou” ecological environment, put forward the development concept of “low-carbon economy, smart city, happy life,” and issued the “1 + 15” policy document system to promote the development of ecological smart city, calling on local universities, such as Sun Yat-sen University and South China Agricultural University, to jointly develop green treatment technology of waste gas, waste liquid, and solid waste,

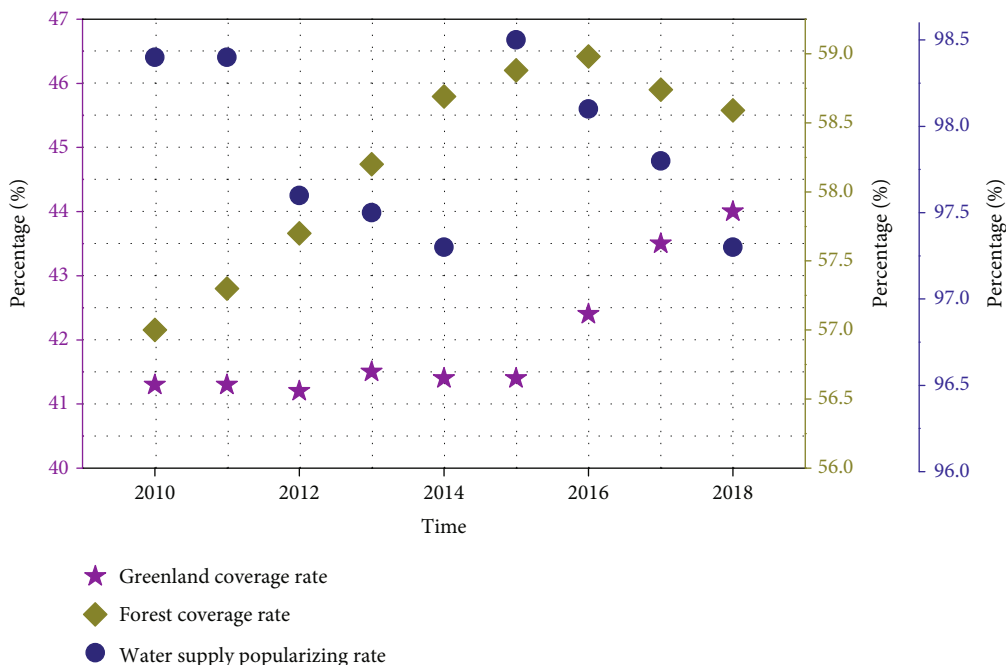


FIGURE 1: Dynamic change law of each index parameter of environmental excellence ( $K_1$ ).

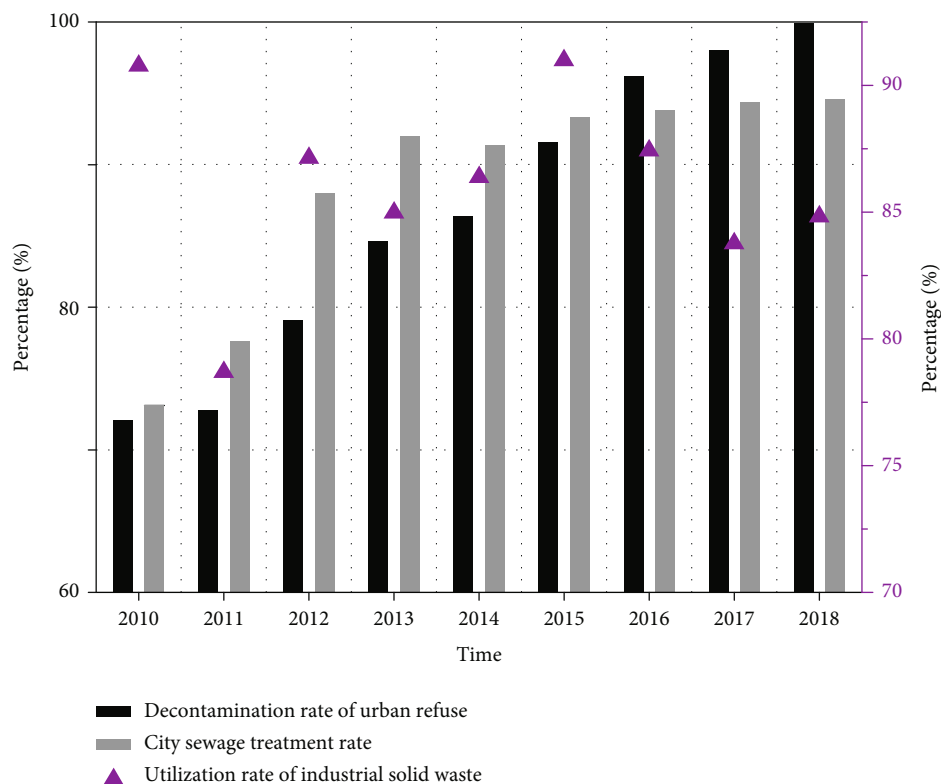


FIGURE 2: Dynamic change law of each index parameter of environmental restoration response ( $K_2$ ).

comprehensively improve the restoration and response capabilities of ecological environment [18].

Although the restoration and response capabilities of ecological environment in Guangzhou smart city is

improving year by year, it is also facing the environmental pollution pressure caused by the discharge of waste gas, waste liquid, and solid waste. Figure 3 shows the dynamic change law of various index parameter of environmental

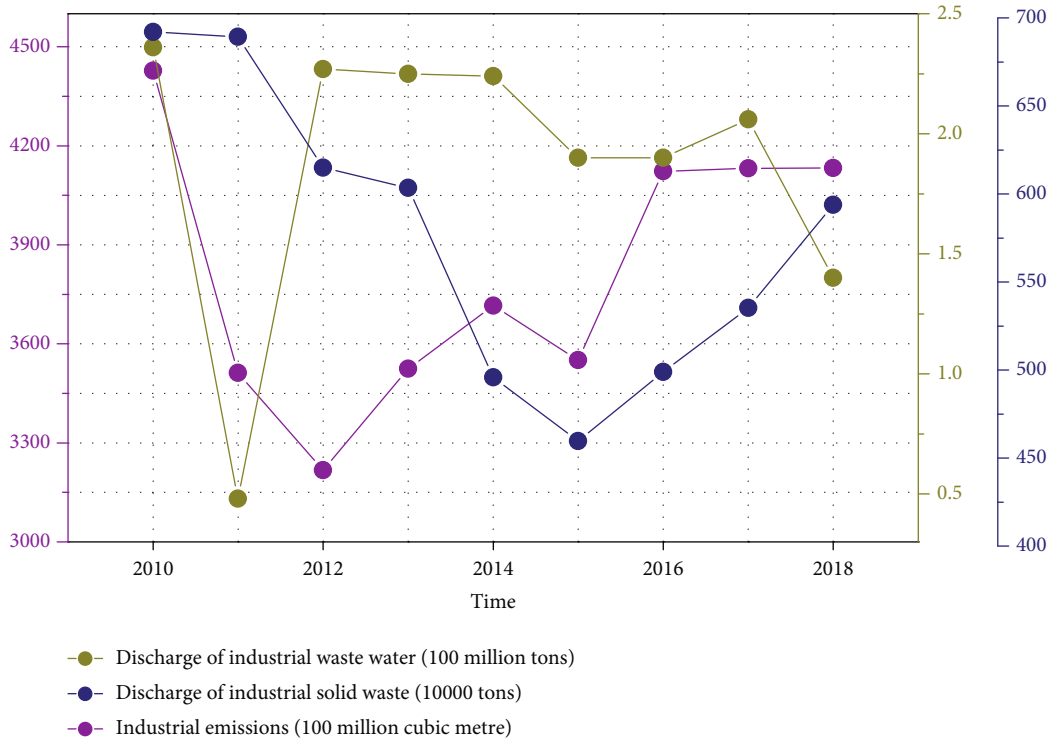
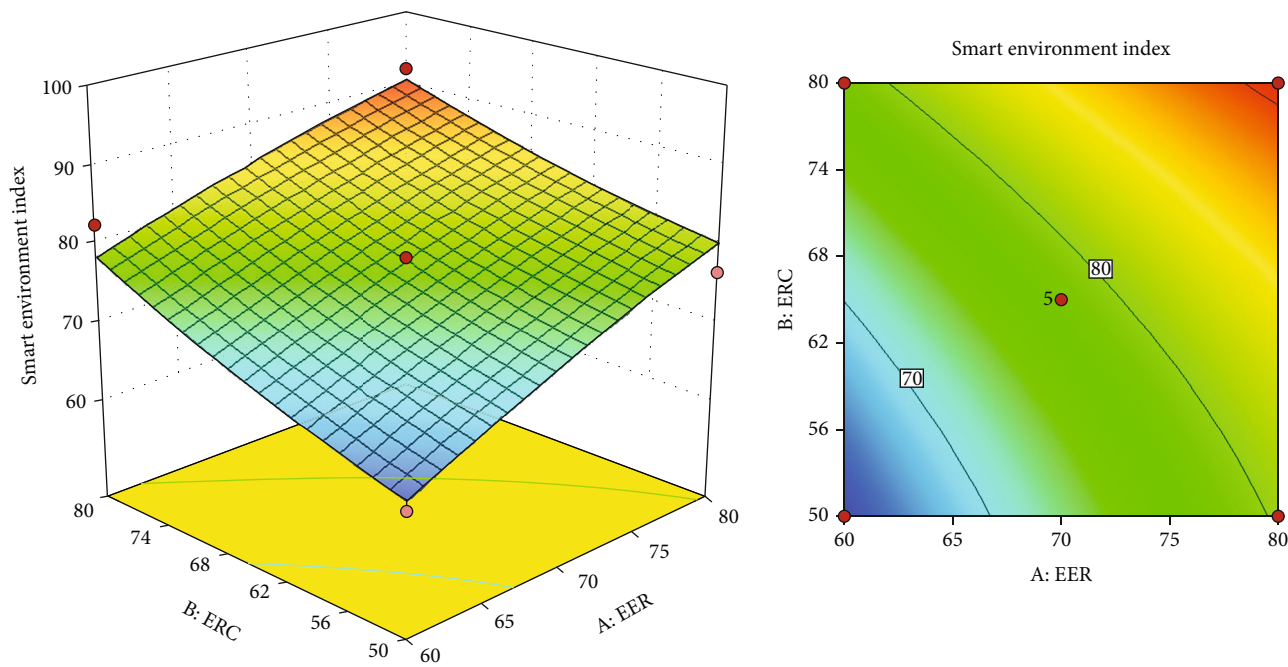


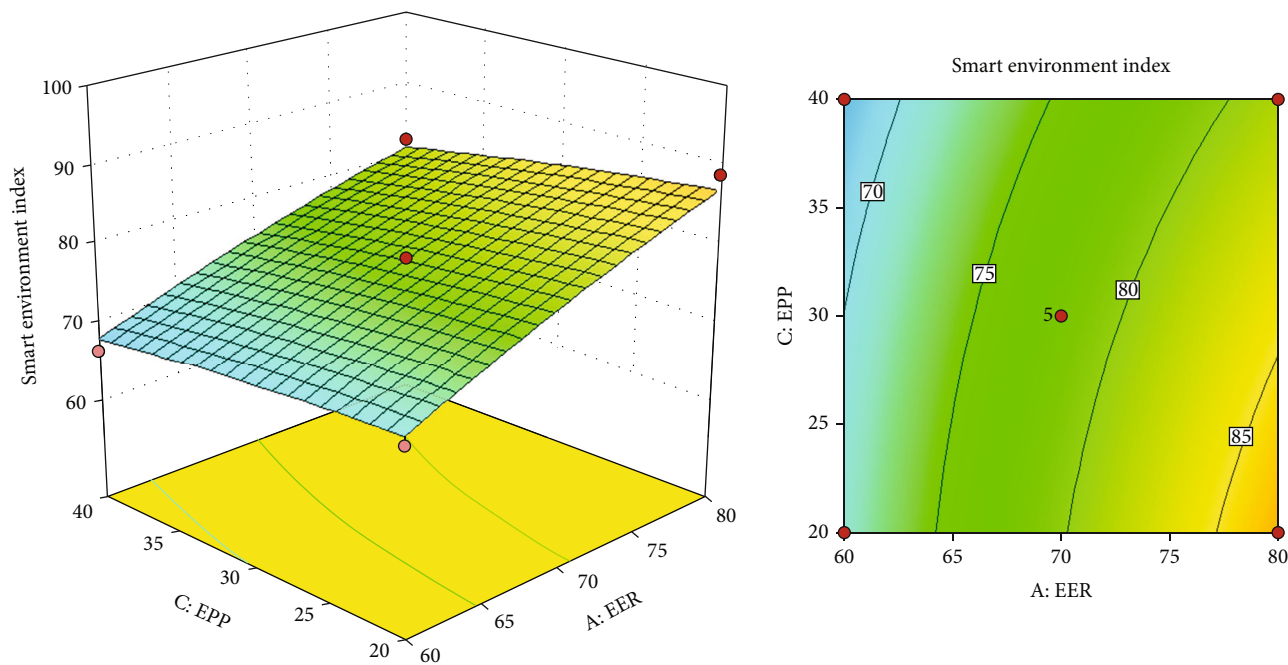
FIGURE 3: Dynamic change law of each index parameter of environmental pollution pressure ( $K_3$ ).

pollution pressure ( $K_3$ ). It can be seen from Figure 3 that the discharge of waste gas, waste liquid, and solid waste generally shows a trend of first decreasing and then increasing, among which the discharge of industrial wastewater rebounded sharply to 2.27 after reaching the lowest value of 48 million tons in 2011, and then maintained a relatively stable state. The discharge of solid waste first decreased from 6.921 million tons in 2010 to 4.596 million tons in 2015, and then gradually increased to 5.9377 million tons. The discharge of industrial waste gas decreased from 442.737 billion cubic meters in 2010 to 321.75 billion cubic meters in 2012, and then increased to 413.217 billion cubic meters year by year. It can be seen that despite the great pressure, Guangzhou has taken corresponding improvement measures in various aspects to effectively alleviate the pressure of environmental pollution. For example, in terms of air environment improvement, deepen the source analysis of nitrogen oxides and volatile organic compounds by implementing PM2.5 and ozone coordinated control; strengthen the control of mobile source pollution, promote the early elimination of old cars, and increase the prevention and control of pollution such as diesel trucks, ships, and construction machinery. In the aspect of water environment improvement, by strengthening the water environment management of the main stream of the Dongjiang River North, the back channel of the Pearl River, the Baini River, and the front channel of the Pearl River, to ensure the rectification of block and the central environmental protection inspectors and to ensure that the water quality meets the requirements [19].

3.2. Correlation Analysis on Principal Components of Ecological Environment Construction in Guangzhou Smart City. The contour of the response surface model is the projection of the response surface 3D model in the horizontal direction, which reflects the degree of interaction between two interactive factors. The more the contour tends to be elliptical, the more significant the interaction between the two factors is. The more the contour tends to be circular, the less significant the interaction is [20, 21]. Figure 4 shows the correlation between each principal component of ecological environment evaluation system in Guangzhou smart city. By analyzing and comparing the contour map of two principal components, it can be seen that the steepness of contour line of environmental pollution pressure ( $K_3$ ) is more gentle than that of environmental excellence ( $K_1$ ) and environmental restoration response ( $K_2$ ), which indicates that the significance of environmental excellence ( $K_1$ ) and environmental restoration response ( $K_2$ ) is greater than that of environmental pollution pressure ( $K_3$ ). By further comparing the contour map of the environmental excellence ( $K_1$ ) and the environmental restoration response ( $K_2$ ), the steepness of the environmental restoration response ( $K_2$ ) is greater, which indicates that the influence of the environmental restoration response ( $K_2$ ) on the ecological environment index of smart cities is more obvious [22]. On the other hand, by analyzing and comparing the pairwise principal component 3D interaction model, it can be seen that when  $K_1$  and  $K_2$  interact, the ecological environment index of smart city increases with the improvement of environmental excellence and environmental restoration

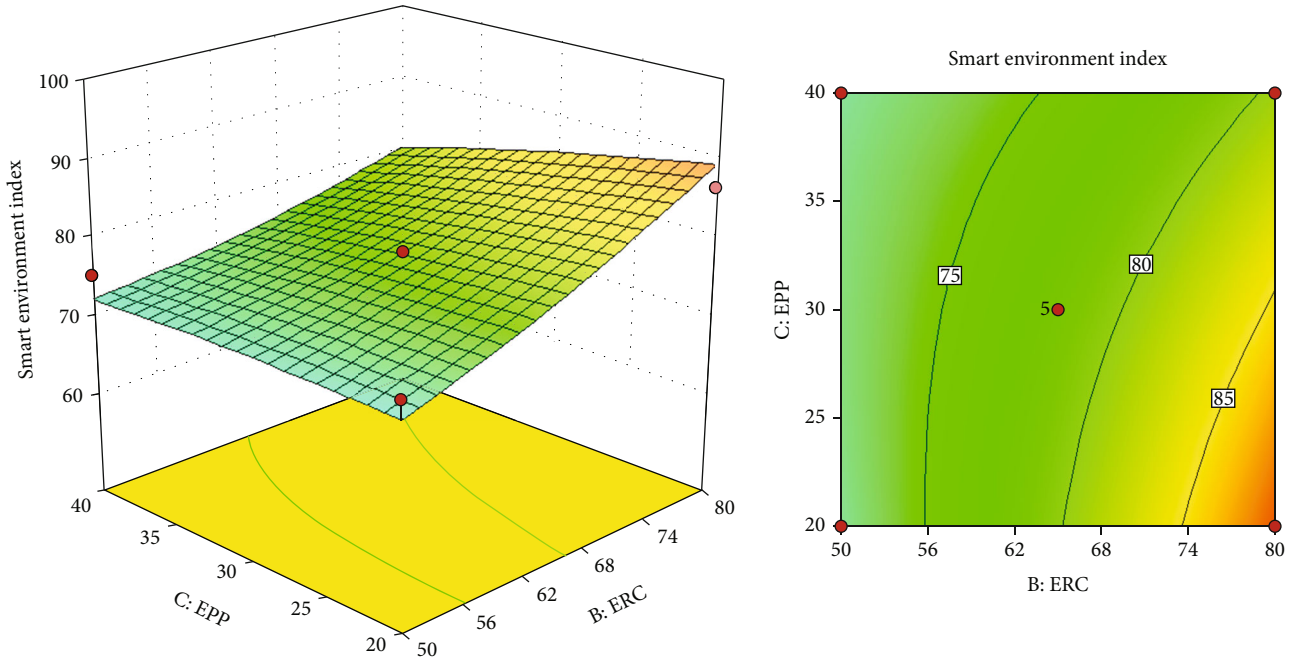


(a) Correlation analysis between environmental excellence ( $K_1$ ) and environmental restoration response ( $K_2$ )



(b) Correlation analysis between environmental excellence ( $K_1$ ) and environmental pollution pressure ( $K_3$ )

FIGURE 4: Continued.



(c) Correlation analysis between environmental restoration response ( $K_2$ ) and environmental pollution pressure ( $K_3$ )

FIGURE 4: Correlation and influence of principal components in ecological environment evaluation system of smart cities in Guangzhou.

response; when  $K_1$  and  $K_3$  interact, the ecological environment index of smart city increases with the increase of environmental excellence ( $K_1$ ), showing a linear growth trend, while gradually decreases with the increase of environmental pollution pressure ( $K_3$ ). The optimization analysis shows that when the state of environmental excellence tends to the maximum ( $K_1 = 80$ ), the environmental restoration effect tends to the maximum ( $K_2 = 80$ ) and the environmental pollution pressure tends to the minimum ( $K_3 = 20$ ), at this time, the ecological environment index of the smart city can reach the maximum value of <http://95.43>. To sum up, although the pressure of environmental pollution will have a certain degree of negative impact on the ecological environment of smart city, the key to improve the ecological environment construction of smart city is to improve the environmental excellence and the environmental restoration response.

#### 4. Conclusion

- (1) By integrating the natural ecological environment, environmental governance, environmental carrying capacity, and other comprehensive elements, a data fusion framework for the ecological environment of smart cities driven by multisource is constructed, and an ecological environment evaluation index system of smart city in Guangzhou from 2010 to 2018 is constructed
- (2) The results of empirical analysis on principal component show that environmental excellence ( $K_1$ ), environmental restoration response ( $K_2$ ), and envi-

ronmental pollution pressure ( $K_3$ ) are the main components of the ecological environment of smart city in Guangzhou. The environmental excellence and environmental restoration response level are relatively high, and the environmental pressure system is relatively low, among which the greenland coverage rate increases from 41.3% to 44.0%, and the urban sewage treatment rate and the decontamination rate of urban refuse increase year by year, from 73.1% to 94.6% and from 72.1% to 99.9%, respectively

- (3) The results of principal component correlation and influence analysis on ecological environment construction of smart city in Guangzhou show that there are interactions among environmental excellence ( $K_1$ ), environmental restoration response ( $K_2$ ), and environmental pollution pressure ( $K_3$ ). The ecological environment index of smart cities increases with the improvement of environmental excellence and environmental restoration response, but decreases gradually with the increase of environmental pollution pressure. Generally speaking, improving environmental excellence and environmental restoration response is the key to enhance the ecological environment construction of smart cities

#### Data Availability

The labeled dataset used to support the findings of this study is available from the corresponding author upon request.

## Conflicts of Interest

The authors declare no competing interests.

## References

- [1] L. Qi, C. Hu, X. Zhang, M. R. Khosravi, and T. Wang, "Privacy-aware data fusion and prediction with spatial-temporal context for smart city industrial environment," *IEEE Transactions on Industrial Informatics*, vol. 17, 2021.
- [2] K. Chaturvedi, A. Matheus, S. H. Nguyen, and T. H. Kolbe, "Securing spatial data infrastructures for distributed smart city applications and services," *Future Generation Computer Systems*, vol. 101, no. 12, pp. 723–736, 2019.
- [3] H. R. Chi and A. Radwan, "Multi-objective optimization of green small cell allocation for iot applications in smart city," *IEEE Access*, vol. 8, pp. 101903–101914, 2020.
- [4] L. Xiong, S. Xue, S. Yang, and C. Han, "Multi-source macro data process based on the idea of sample=overall in big data: an applicability study on influence factors to smart city," in *2015 International Conference on Logistics, Informatics and Service Sciences (LISS)*, pp. 1–6, Barcelona, 2015.
- [5] A. R. Honarvar and A. Sami, "Multi-source dataset for urban computing in a smart city," *Data in Brief*, vol. 22, no. 2, pp. 222–226, 2019.
- [6] K. Lundberg, B. Balfors, and L. Folkesson, "Framework for environmental performance measurement in a Swedish public sector organization," *Journal of Cleaner Production*, vol. 17, no. 11, pp. 1017–1024, 2009.
- [7] S. Sakakibara, S. Saiki, M. Nakamura, and S. Matsumoto, "Indoor environment sensing service in smart city using autonomous sensor box," in *2016 IEEE/ACIS 15th International Conference on Computer and Information Science (ICIS)*, pp. 1–6, Okayama, Japan, 2016.
- [8] M. M. Hassan, H. S. Albakr, and H. Al-Dossari, "A cloud-assisted internet of things framework for pervasive healthcare in smart city environment," *Proceedings of the 1st International Workshop on Emerging Multimedia Applications and Services for Smart Cities - EMASC 14*, 2014, pp. 9–13, Orlando, Florida, USA, 2014.
- [9] J. M. Batalla, P. Krawiec, C. X. Mavromoustakis et al., "Efficient media streaming with collaborative terminals for the smart city environment," *IEEE Communications Magazine: Articles, News, and Events of Interest to Communications Engineers*, vol. 55, no. 1, pp. 98–104, 2017.
- [10] I. Nina, G. Olga, and V. Murgul, "The methodological aspect of the landscape and ecological forming of a comfortable environment for the smart city," *MATEC Web of Conferences*, vol. 106, no. 4, 2017.
- [11] A. Luvisi and G. Lorenzini, "Rfid-plants in the smart city: applications and outlook for urban green management," *Urban Forestry Urban Greening*, vol. 13, no. 4, pp. 630–637, 2014.
- [12] M. Jedliński, "The position of green logistics in sustainable development of a smart green city," *Procedia-Social and Behavioral Sciences*, vol. 151, no. 10, pp. 102–111, 2014.
- [13] S. Salvatore, J. G. Bramness, and J. RIslien, "Exploring functional data analysis and wavelet principal component analysis on ecstasy (mdma) wastewater data," *BMC Medical Research Methodology*, vol. 16, no. 1, pp. 81–93, 2016.
- [14] H. He, C. Tian, G. Jin, and K. Han, "Principal component analysis and fisher discriminant analysis of environmental and ecological quality, and the impacts of coal mining in an environmentally sensitive area," *Environmental Monitoring and Assessment*, vol. 192, no. 4, pp. 207–218, 2020.
- [15] Y. Dong-Mei, Z. Xing-Guo, W. Yun, and C. Dang-Qun, "Principal component analysis and comprehensive evaluation on quality traits of peanut parents," *Journal of Plant Genetic Resources*, vol. 12, no. 4, pp. 507–512, 2011.
- [16] L. Zhu and M. Li, "The application of principal component analysis in comprehensive evaluation of liaohe river water quality," *Advanced Materials Research*, vol. 779-780, no. 9, pp. 1596–1599, 2013.
- [17] W. Chen, "Environmental externalities of urban river pollution and restoration: a hedonic analysis in Guangzhou (China)," *Landscape Urban Planning*, vol. 157, no. 6, pp. 170–179, 2017.
- [18] X. Yang, S. Huang, W. U. Qunhe, R. Zhang, and G. Liu, "Diversity and vertical distributions of sediment bacteria in an urban river contaminated by nutrients and heavy metals," *Frontiers of Environmental Science Engineering*, vol. 7, no. 6, pp. 851–859, 2013.
- [19] B. Y. Yang, Z. Qianmin, S. W. Howard, M. G. Vaughn, S. J. Fan, and K. K. Liu, "Global association between ambient air pollution and blood pressure: a systematic review and meta-analysis," *Environmental Pollution*, vol. 235, no. 4, pp. 576–588, 2018.
- [20] A. Dev, C. Maheswaran, and S. Shanmugam, "Failure-mode analysis of macro-synthetic and hybrid fibre-reinforced concrete beams with GFRP bars using acoustic emission technique," *Construction and Building Materials*, vol. 249, no. 21, 2020.
- [21] U. Bektimirova, E. Sharafutdinov, A. Tleuken, C. S. Shon, D. C. Zhang, and J. Kim, "Optimization of compressive strength of reactive powder concrete for an energy storage pile application using response surface method," *Materials Science Forum*, vol. 950, no. 2, pp. 117–122, 2019.

## Research Article

# Research on the Current Situation and Countermeasures of English Listening Teaching Based on Multimedia Intelligent-Embedded Processor

Huanping Guo 

Foreign Language Department, Lüliang University, Lüliang 033000, China

Correspondence should be addressed to Huanping Guo; 20111042@llu.edu.cn

Received 8 January 2022; Revised 14 February 2022; Accepted 19 February 2022; Published 21 March 2022

Academic Editor: Wen Zeng

Copyright © 2022 Huanping Guo. This is an open access article distributed under the Creative Commons Attribution License, which permits unrestricted use, distribution, and reproduction in any medium, provided the original work is properly cited.

In order to improve the effect of English listening teaching, this paper combines the interactive needs of English listening teaching to analyze the current problems in English listening teaching. Moreover, according to the actual needs of the intelligent English teaching system, this paper conducts research on the high-order cumulant signal-to-noise ratio estimation method and combines data analysis to improve the algorithm to obtain an intelligent algorithm suitable for English listening teaching. In addition, this paper combines the algorithm to construct an English listening teaching system based on a multimedia intelligent-embedded processor and applies the embedded processor to intelligent English listening teaching. Finally, this paper builds an intelligent system to solve the current problems in English listening teaching and improve the effect of English teaching.

## 1. Introduction

At present, there are still major problems in English listening teaching in some colleges and universities, but this teaching link is the key to improving students' English ability. Therefore, in the future development process, colleges and universities need to continuously improve and innovate teaching models and teaching ideas based on current problems and use advanced teaching methods to improve students' English skills. From the perspective of teachers, English teachers in colleges and universities do not pay enough attention to the teaching of English listening, and the formalization is obvious, and the recording of English texts is mainly played in the class, and the mode is relatively simple. Some teachers think that the English listening link is a waste of most of the class time, so they often omit this link in class, resulting in lower listening proficiency of students [1]. From the perspective of students, there are two main factors that affect the improvement of their English listening level: knowledge barriers and noninformation barriers. The so-called intellectual barriers are problems in cultural background knowledge and language knowledge, including grammatical knowledge, vocabulary knowledge, and phonetic knowledge. Having

good speech skills is the prerequisite and foundation of listening. Individual learners have been practicing English for many years, and their reading and writing skills have reached a certain level, but their listening skills are relatively low. The main reason is the lack of phonetic knowledge [2]. In recent years, the scale of enrollment of colleges and universities has been expanding, and the entrance threshold has been gradually reduced. Due to the poor English foundation of students, their pronunciation skills are even worse. Nonintellectual barriers refer to barriers in listening methods, skills, and psychology. College students have poor learning foundations and skills, so they will inevitably have emotions such as fear and anxiety during the learning process, which directly leads to a decrease in their interest in English learning. In addition, methods and skills are also key factors that affect the improvement of English listening ability, so they need to be paid attention to. From the perspective of college English courses, although this subject is a basic course, there is still a problem of a small amount of courses. However, the emergence of this problem will directly cause students to ignore this course and attach importance to other "professional" courses that involve more. In addition, even if the amount of courses is up to

the standard, some colleges and universities still involve less listening courses and cannot provide students with comprehensive listening training [3]. The emotional factors that affect college students' English listening learning include motivation, attitude, personality, belief, and self-confidence. The learning motivation is the inner force that promotes students to carry out learning activities and directly affects the learning effect. It mainly includes result motivation, integration motivation, and instrumental motivation. Self-confidence is the judgment and evaluation of students on their own learning process, which can guide students to actively participate in learning activities. All in all, emotion is the filter of knowledge learning, and the knowledge input to the brain can only be fully absorbed by students after being filtered. Interaction design has developed rapidly in recent years, and along with the cross-development of other professions and technologies, it has produced many amazing results, changing and subverting people's lifestyles, the behavioral relationship between "people and things," and "people and things." The group relationship of "people" and the cultural relationship of "people and society" have been redefined under the impetus of new technology. The revolution of information technology has brought tremendous changes to the development of human society and directly promoted the overall innovation of production methods, communication channels, and business models related to the design discipline. From the perspective of disciplinary development, we need to review interaction design from the perspective of evaluation and then reverse the evaluation method of interaction design. This paper combines the multimedia intelligent-embedded processor to analyze English listening teaching and builds an intelligent English listening model to improve the effect of English listening teaching.

## 2. Related Work

In the embedded field, embedded processors play an important role and are leading the development of the entire embedded field. Many domestic and foreign companies have participated in the development boom of embedded processors and developed various products. The development version of the commercial embedded processor has further promoted the research and application of embedded processors [4]. At present, the embedded processor system is widely used, and the smart terminal field is widely optimistic. Many domestic and foreign developers are increasing investment and developing new products. The embedded processor will be their preferred operating system. As an excellent representative of free software, Linux has developed rapidly in less than ten years due to its unique characteristics of high efficiency, safety, and dynamic loading [5]. At present, the scope of application of embedded systems at home and abroad mainly includes aerospace, NASA's Mars Climate Orbiter, "Polar Lander," and "Deep Space Two," and other Mars probes use embedded systems. In the VxWorks system, information appliances include digital set-top boxes, digital TVs, video phones, home networks, and mobile PDAs; the industrial market has control equip-

ment, industrial control boards, instruments, etc. [6]; in addition to advanced medical diagnostic equipment, smart houses, smart office, etc. are indispensable for the core technology of embedded systems [7]. Due to the rapid development of technology, the diversification of user needs, and the continuous advancement of differentiation, the development of embedded intelligent terminal systems has become an emerging scientific research field and industry. According to the definition of the British Institute of Electrical Engineers, an embedded system is a device that controls and monitors auxiliary equipment, machinery, or even factory operations [8]. Embedded systems mainly include hardware and software. With the increase in system complexity and the development of hardware integration technology, a higher-performance microprocessor has become the core hardware component of the embedded system; the software has only the program block with a single control function which has developed into a software system with layers and embedded operating systems [9]. With the deepening of the information age, the development of digitization has become an inevitable trend, and one of the core technologies of digitization is digital signal processing [10]. Digital signal processing is the use of computers or special processing equipment to collect, transform, filter, estimate, enhance, compress, and identify signals in digital form to obtain a signal form that meets people's needs. Digital signal processing (DSP) is an emerging discipline that involves many disciplines and is widely used in many fields at the same time [11]. For example, in the field of mathematics, calculus, probability and statistics, stochastic processes, and numerical analysis are all basic tools for digital signal processing and are closely related to network theory, signal and system, cybernetics, communication theory, and fault diagnosis. In recent years, some emerging disciplines, such as artificial intelligence, pattern recognition, and neural networks, are inseparable from digital signal processing [12]. It can be said that digital signal processing takes many classic theoretical systems as its theoretical basis and at the same time makes itself the theoretical basis of a series of emerging disciplines. With the rapid development of computer and information technology, digital signal processing technology emerged and developed rapidly. Especially in the application of embedded computers, DSP technology has become one of the mainstream directions of computer technology development today, mainly in the field of measurement and control. The purpose of the embedded system is to provide a complex digital system with multitasking and networking as the core which is easy to develop. From the perspective of digital technology and information technology, embedded systems have become the basic technology of modern information network technology applications and have become the basic technology in the field of modern industrial control [13]. Although the theory of digital signal processing has developed rapidly, it is no exaggeration to say that the birth and development of DSP chips have played a very important role in the technical development of communications, computers, and control in the past 20 years [14]. The task of digital signal processing needs to be completed by DSP devices to a large extent. DSP technology has become a cutting-edge



technology that people are paying more and more attention to and getting rapid development. DSP is a device that processes a large amount of information with digital signals. The new DSP not only has data processing capabilities but also integrates more and more other components inside, which can form a new DSP-embedded application system, which not only has other microprocessing. The advantages of the embedded system of the processor and the single-chip microcomputer have a unique high-speed digital signal processing capability [15].

### 3. High-Order Cumulant Signal-to-Noise Ratio Estimation Method

The main step of the high-order cumulant method is to calculate the result of the conversion of high-order quantities into signal moments. According to the connection of signal moment, noise power, and signal power, the estimated value of signal and noise power is calculated, respectively, and then, the corresponding signal-to-noise ratio is obtained. For a zero-mean  $k$ -order random process  $x(n)$ , the values of  $l$  have different time nodes: the higher-order moments and higher-order cumulants of  $x(n), x(n-k_1), \dots, x(n-k_{l-1})$  are defined as equations (1) and (2):

$$m_l(k_1, k_2, \dots, k_{l-1}) = \text{mom}\{x(n), x(n-k_1), \dots, x(n-k_{l-1})\}, \quad (1)$$

$$c_l(k_1, k_2, \dots, k_{l-1}) = \text{com}\{x(n), x(n-k_1), \dots, x(n-k_{l-1})\}. \quad (2)$$

We assume that  $X = (x_1, \dots, x_l)$  is a vector and  $I = (1, 2, \dots, l)$  is the indicator set of vector  $X$ . If  $I \subseteq I_x$ , then  $X_I$  represents each component of  $IX$  vectors. Suppose the vector  $X_I = (\chi_1, \dots, \chi_n)$ , and if  $\chi_i = 1$ , then  $i \in I$ , and if  $\chi_i = 0$ , then  $i \notin I$ . These vectors have a one-to-one correspondence with the set  $I \subseteq I_x$ . Therefore, you can get [16]

$$\begin{aligned} m_x(I) &= m_x^{(X(I))}, \\ c_x(I) &= c_x^{(X(I))}. \end{aligned} \quad (3)$$

In other words,  $m_x(I)$  and  $c_x(I)$  are the moments and cumulants of the subvector  $X$  of  $X_I$ . According to the above formula, we get [17]

$$c_x(I) = \sum_{U_p I_p = I} (-1)^{q-1} (q-1)! \prod_{p=1}^q m_x(I_p). \quad (4)$$

Among them,  $C_x(I)$  represents the sum in all divisions of  $I$   $1 \leq q \leq N(I)$ .

For formula (4),  $l=1$ ,  $l=2$ , and  $l=3$  are as follows:

$$l=1 : c_1(x_1) = E\{x_1\}, \quad (5)$$

$$l=2 : c_2(x_1, x_2) = E\{x_1 x_2\} - E\{x_1\}E\{x_2\}, \quad (6)$$

$$\begin{aligned} l=3 : c_3(x_1, x_2, x_3) &= E\{x_1 x_2 x_3\} - E\{x_1\}E\{x_2 x_3\} \\ &\quad - E\{x_2\}E\{x_1 x_3\} - E\{x_3\}E\{x_1 x_2\} + 2E\{x_1\}E\{x_2\}E\{x_3\}. \end{aligned} \quad (7)$$

Based on the previous derivation of the formula and their respective connections, for a complex random variable with zero mean, the moment is defined as [18]

$$M_{p+q,p} = E[x^p (x^*)^q]. \quad (8)$$

We define its cumulative amount as

$$C_{p+q,p} = \text{cum}[x, \dots, x, x^*, \dots, x^*]. \quad (9)$$

Among them,  $x$  is the  $p$  item, and  $x^*$  is the  $q$  item.

For a complex random process  $x$  with zero mean, we have

$$\begin{aligned} \text{cum}_4^1(l_1, l_2, l_3) &= \text{cum}_4[X^*(k), X(k+l_1), X(k+l_2), X^*(k+l_3)] \\ &= E[X^*(k)X(k+l_1)X(k+l_2)X^*(k+l_3)] \\ &\quad - E[X^*(k)X(k+l_1)] \cdot E[X(k+l_2)X^*(k+l_3)] \\ &\quad - E[X^*(k)X(k+l_2)] \cdot E[X(k+l_1)X^*(k+l_3)] \\ &\quad - E[X^*(k)X(k+l_3)] \cdot E[X(k+l_1)X^*(k+l_2)], \end{aligned} \quad (10)$$

$$\begin{aligned} \text{cum}_4^2(l_1, l_2, l_3) &= \text{cum}_4[X(k), X(k+l_1), X(k+l_2), X(k+l_3)] \\ &= E[X(k)X(k+l_1)X(k+l_2)X(k+l_3)] \\ &\quad - E[X(k)X(k+l_1)] \cdot E[X(k+l_2)X(k+l_3)] \\ &\quad - E[X(k)X(k+l_2)] \cdot E[X(k+l_1)X(k+l_3)] \\ &\quad - E[X(k)X(k+l_3)] \cdot E[X(k+l_1)X(k+l_2)], \end{aligned} \quad (11)$$

$$\begin{aligned} \text{cum}_4^3(l_1, l_2, l_3) &= \text{cum}_4[X(k), X(k+l_1), X(k+l_2), X^*(k+l_3)] \\ &= E[X(k)X(k+l_1)X(k+l_2)X^*(k+l_3)] \\ &\quad - E[X(k)X(k+l_1)] \cdot E[X(k+l_2)X^*(k+l_3)] \\ &\quad - E[X(k)X(k+l_2)] \cdot E[X(k+l_1)X^*(k+l_3)] \\ &\quad - E[X(k)X^*(k+l_3)] \cdot E[X(k+l_1)X(k+l_2)]. \end{aligned} \quad (12)$$

According to the formula of the above algorithm, the MPSK signal is simulated below, assuming that the complex digital sequence of the MPSK signal is

$$r_k = \sqrt{E}a_k + n_k = x_k + n_k \quad k = 1, 2, \dots, N. \quad (13)$$

In the formula, the noise of the mean value is zero, the variance is the complex Gaussian random variable with the variance  $N_0$ ,  $E$  is the energy of the transmitted symbol, and  $a_k \in \{\exp(j2\pi(m-1)/M), m = 1, \dots, M\}$ ,  $M$  is the signal modulation order.

It is defined that the signal  $x_k = \sqrt{E}a_k$  and the noise  $n_k = n_{1k} + jn_{2k}$  are not related to each other. According to the previous definition, we can get complex Gaussian random

variables with  $n_{lk}$  and  $n_{Qk}$  mean zero and variance  $N_0/2$ , and they are not related to each other.  $\text{SNR} = E/N_0$  is the signal-to-noise ratio.

For MPSK signals with  $\{A \exp(j2\pi(m-1)/M), m = 1, \dots, M\}, A = \sqrt{E}$ . Normally, to define that the transmitted signals are not related to each other, it is only necessary to calculate the value of the cumulant function when  $l_1 = l_2 = l_3 = 0$ .

$$\begin{aligned} E[X(k)X(k)X(k)X(k)] &= \frac{1}{M} \sum_{m=1}^M A^4 \exp\left(\frac{4 \cdot j2\pi(m-1)}{M}\right) = \begin{cases} A^4 & M = 2, 4, \\ 0 & M = 8, 16, 32 \dots \end{cases} \\ E[X(k)X(k)X(k)X^*(k)] &= \frac{1}{M} \sum_{m=1}^M A^4 \exp\left(\frac{2 \cdot j2\pi(m-1)}{M}\right) = \begin{cases} A^4 & M = 2, \\ 0 & M = 4, 8 \dots \end{cases} \\ E[X^*(k)X(k)X(k)X^*(k)] &= \frac{1}{M} \sum_{m=1}^M A^4 \exp\left(\frac{0 \cdot j2\pi(m-1)}{M}\right) = A^2 \quad M = 2, 4, 8 \dots, \\ E[X^*(k)X(k)] &= E[|X(k)|^2] = \frac{1}{M} \sum_{m=1}^M A^4 \exp\left(\frac{0 \cdot j2\pi(m-1)}{M}\right) = A^2 \quad M = 2, 4, 8 \dots, \\ E[X(k)X(k)] &= E[X^2(k)] = \frac{1}{M} \sum_{m=1}^M A^4 \exp\left(\frac{2 \cdot j2\pi(m-1)}{M}\right) = \begin{cases} A^2 & M = 2, \\ 0 & M = 4, 8 \dots \end{cases} \end{aligned} \quad (14)$$

It can be obtained by formulas ((3)-(4)), ((3)-(5)), ((3)-(6)), ((3)-(7)), ((3)-(8)), ((3)-(9)), and ((3)-(10)).

$$\begin{aligned} C_{20} &= E[X^2], \\ C_{21} &= E[|X|^2], \end{aligned} \quad (15)$$

$$\begin{aligned} C_{41} &= \text{cum}(X^*, X, X, X) = E[X^*XXX] - 3E[X^2] \cdot E[|X|^2] \\ &= E[X^*XXX] - 3C_{20}C_{21}, \end{aligned} \quad (16)$$

$$\begin{aligned} C_{42} &= \text{cum}(|X|^*, |X, X, X|) = E[|X|^*|XXX|] - 2(E[|X|^2])^2 \\ &\quad \cdot E[X^2] \cdot E[|X|^2] = E[|X^*|XXX|] - 2C_{21}^2 - |C_{20}|^2. \end{aligned} \quad (17)$$

Because the fourth-order cumulant is zero, noise and signal are not related to each other. According to the previous formula and properties, we can get the following:

$$C_{r,21} = C_x, \quad \frac{1}{21} C_n \quad (18)$$

$$C_{r,41} = C_x, \quad (19)$$

$$C_{r,42} = C_{x,42}, \quad (20)$$

$\sigma_r^2$ ,  $\sigma_x^2$ , and  $\sigma_n^2$  represent the variances of received signal, sent signal, and noise, respectively. When  $M = 2$ , that is, BPSK signal, there are

$$C_{x,21} = \sigma_x^2 = E, \quad C_{x,42} = -2E^2, \quad C_{x,41} = -2E^2. \quad (21)$$

When  $M \geq 4$ , which is a high-order MPSK signal, there are

$$C_{x,21} = \sigma_x^2 = E, \quad C_{x,42} = E^2, \quad C_{x,41} = 0. \quad (22)$$

From the above, we can get the relationship between the cumulant of MPSK signal and its symbol energy, as shown below:

$$E = \sigma_x^2 = \begin{cases} \sqrt{C_{x,42}/2}, & M = 2, \\ \sqrt{|C_{x,42}|}, & M \geq 4. \end{cases} \quad (23)$$

From formula (20),  $C_{r,42} = C_{x,42}$ , and formula (23) can be written as follows:

$$E = \sigma_x^2 = \begin{cases} \sqrt{C_{r,42}/2}, & M = 2, \\ \sqrt{|C_{r,42}|}, & M \geq 4. \end{cases} \quad (24)$$

From formula (18), we can get the following:

$$\sigma_r^2 = \sigma_x^2 + \sigma. \quad (25)$$

In summary, we can give the steps of signal-to-noise ratio estimation as follows:

- (1) The algorithm obtains the cumulant estimated value  $C_{r,42}$  and the variance estimated value  $C_{r,21}$  according to the collected signal  $r_k, k = 1, 2 \dots, N$
- (2) The algorithm calculates the noise variance estimate  $\sigma_n^2 = \sigma_r^2 - \sigma_x^2$
- (3) The algorithm calculates the energy  $E$  of the signal

The following algorithm calculates the estimated signal-to-noise ratio.

$$\text{SNR} \frac{E}{N} = \frac{S_x^2}{S_n^2} = \frac{S_x^2}{S_r^2 - S_x^2} = \begin{cases} \frac{\sqrt{C_{r,42}/2}}{C_{r,21} - \sqrt{|C_{r,42}|/2}} & \text{BPSKsignal} \\ \frac{\sqrt{|C_{r,42}|}}{C_{r,21} - \sqrt{|C_{r,42}|}} & \text{MPSKsignal} \end{cases} \quad (26)$$

When the modulation order is unknown, certain calculations are required. The algorithm first performs a simple analysis of the order and uses the analysis results to make the following assumptions:

$$\Delta = \frac{|C_{r,41}|}{|C_{r,42}|} = \frac{|C_{x,41}|}{|C_{x,42}|} \begin{cases} > 0.5 \text{ The received sequence is BPSK signal,} \\ < 0.5 \text{ The received sequence is a non-BPSK signal.} \end{cases} \quad (27)$$

Theoretically, the results obtained by formula (26) and the second-order fourth-order estimation method ((3)-(28)) are the same.

$$\widehat{\text{SNR}}_{\text{complex}} = \frac{\sqrt{|2M_2^2 - M_4|}}{M_2 - \sqrt{|2M_2^2 - M_4|}}, \quad (28)$$

$$\text{SNR}_{\text{real}} = \frac{(1/2)\sqrt{6M_2^2 - 2M_4}}{(M_2 - (1/2))\sqrt{6M_2^2 - 2M_4}} = \frac{\sqrt{|M_4 - 3M_2|/2}}{M_2 - \sqrt{|M_4 - 3M_2|/2}}. \quad (29)$$

In the above formula,  $M_2$  and  $M_4$  are the second-order and fourth-order quantities of the received sequence  $r(n)$ . The following formulas  $M_2$  and  $M_4$  are related to the power of the collected signal.

$$M_2 = \frac{1}{N} \sum_{n=0}^{N-1} |y_n|^2, \quad (30)$$

$$M_4 = \frac{1}{N} \sum_{n=0}^{N-1} |y_n|^4.$$

For the above formula, there is such a relationship between the moment and the cumulant, as shown below:

$$M_2 = E[|X|^2] = C_{21}, \quad (31)$$

$$M_4 = E[|X|^4] = E[X^*XXX^*].$$

When  $M \geq 4$ ,  $C_{20} = 0$ ,  $C_{r,42} = M_4 - 2M_2^2$ . When  $\nu$ , since the constellation diagram of the BPSK signal is one-dimensional, so  $C_{20} = C_{21}$ , then  $C_{r,42} = M_4 - 3M_2^2$  at this time. Figure 1 shows the root-mean-square error of the signal-to-noise ratio estimation by the higher-order cumulative estimation method.

In actual situations, generally speaking, when perceiving the spectrum, the prior information of authorized users will not be obtained. Therefore, there are certain limitations to the estimation of the signal-to-noise ratio. In order to improve the accuracy of spectrum sensing, appropriate channel quality metrics and related reliable estimation algorithms are required. The following will expand the range of modulation methods to estimate the unified signal-to-noise ratio.

$$Y_i = X_i + W_i. \quad (32)$$

In the formula,  $Y_i$  is the received signal,  $X_i$  is the transmitter signal, and  $W_i$  is the channel noise.

The other  $\nu$  represents the second moment of the received signal  $Y_i$ .

$$M_2 = E[|Y_i|^2] = E[|X_i|^2] + 2 \text{Re} \{E[|X_i|W_i^*]\} + E[|W_i|^2]. \quad (33)$$

$E[\ ]$  is the statistical mean value formula. The fourth moment of the received signal  $Y_i$  can be expressed as follows:

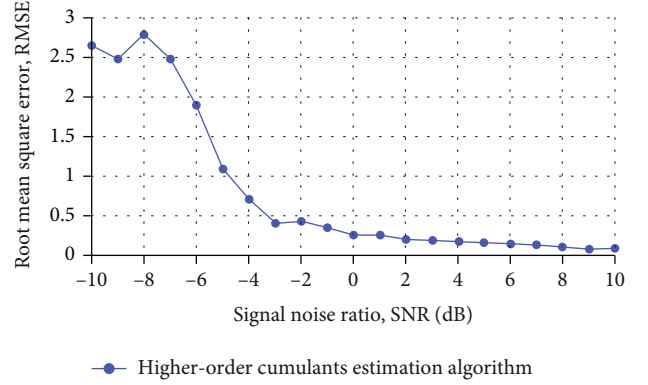


FIGURE 1: The root mean square error of the signal-to-noise ratio estimation method of the order cumulant estimation method.

$$\begin{aligned} M_4 &= E\left[|Y_i|^4\right] = E[|X_i|^4] + 4 \text{Re} \{E[|X_i|^2 X_i W_i^*]\} \\ &\quad + 2 \text{Re} \left\{E\left[(X_i W_i^*)^2\right] + 4E[|X_i|^2 |W_i|^2]\right\} \\ &\quad + 4 \text{Re} \{E[X_i |W_i|^2 W_i^*]\} + E[|W_i|^4]. \end{aligned} \quad (34)$$

We assume that the signal  $X_i$  and the noise  $W_i$  are independent zero-mean random processes, and  $W_i$  is a complex Gaussian; the kurtosis of  $Y_i$  is defined as follows:

$$C_Y = \frac{M_4}{M_2^2} = \frac{E[|Y_i|^4]}{E[|Y_i|^2]^2}. \quad (35)$$

Similarly, the kurtosis of  $X_i$  is represented by  $C_X$ . Through some algorithm operations, the estimated value  $\hat{\gamma}$  of the average signal-to-noise ratio can be derived from (32)–(35).

$$\begin{aligned} \hat{\gamma} &= \frac{E[|X_i|^2]}{E[|W_i|^2]} = \frac{(C_Y - 2)}{(C_X - C_Y)} \\ &\quad + \frac{4.3 \sqrt{(4 - 2C_Y)^2 - (C_X - C_Y)(2 - C_Y)}}{2(C_X - C_Y)}. \end{aligned} \quad (36)$$

The derivation of the above formula not only satisfies the low-order statistics BPSK and MPSK but is also suitable for 16QAM and 64QAM. This expands the range of modulation methods. Figure 2 shows that the improved SNR estimation algorithm can satisfy 16QAM SNR estimation. Figure 3 shows that the improved SNR estimation algorithm can satisfy 64QAM SNR estimation.

The above simulation results show that the improved SNR estimation algorithm can more accurately estimate the SNR for 16QAM and 64QAM modulated signals.

Figures 4 and 5 show the simulation results of BPSK and MPSK signals by the improved SNR estimation algorithm under the same conditions as the classical high-order cumulants.

Derived by the above formula, the simulation results obtained are shown in Figures 4 and 5. For BPSK and QPSK

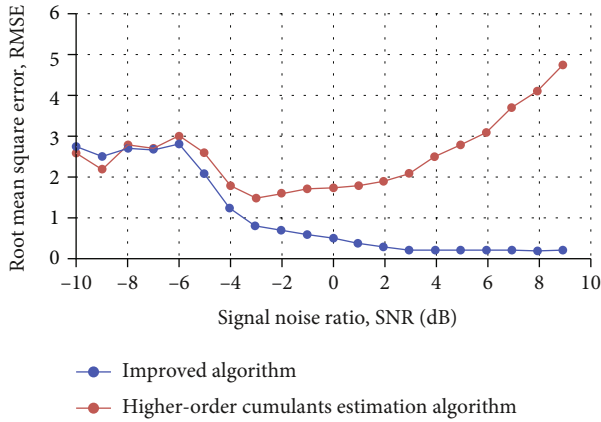


FIGURE 2: Comparison of improved 16QAM SNR estimation algorithm and high-order cumulant estimation.

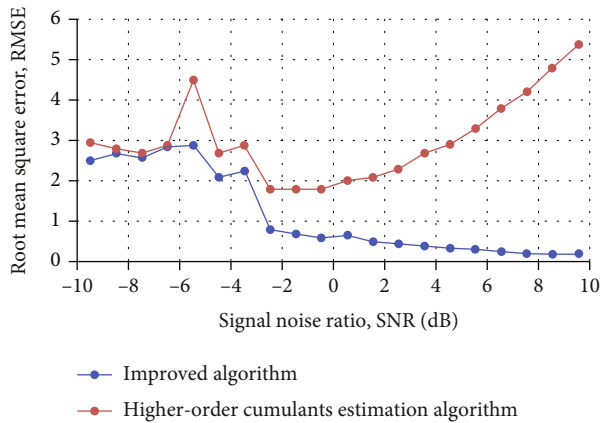


FIGURE 3: Comparison of improved 64QAM SNR estimation algorithm and high-order cumulant estimation.

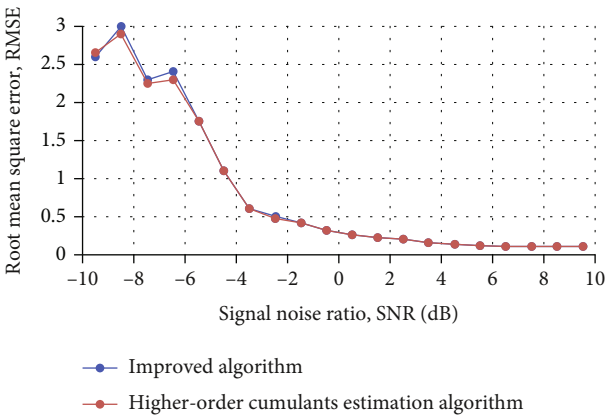


FIGURE 4: Comparison of improved BPSK signal-to-noise ratio estimation algorithm and high-order cumulant estimation.

signals, the improved SNR estimation algorithm is not only equivalent to the high-order cumulant, but the improved algorithm can estimate the SNR of 16QAM and 64QAM more accurately.

Through the above research, the embedded processor signal-to-noise ratio processing method of this paper is con-

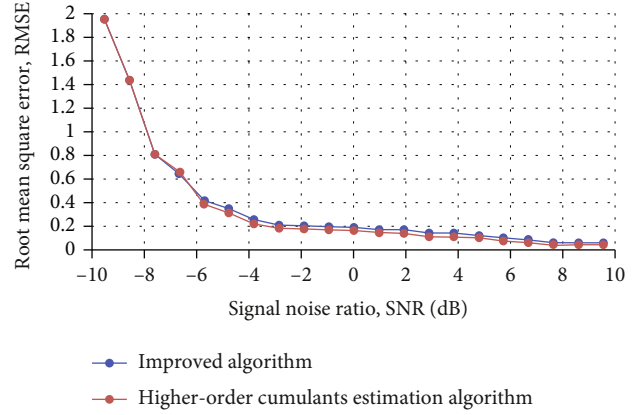


FIGURE 5: Comparison of improved QPSK signal-to-noise ratio estimation algorithm and high-order cumulant estimation.

structed. This method is applied to English listening teaching, and then the embedded system of English listening teaching can be constructed.

#### 4. English Listening Teaching System Based on Multimedia Intelligent-Embedded Processor

As a basic compulsory course for college students, college English listening and speaking is essential to improve students' comprehensive ability and employability. In recent years, many scholars have conducted research on multimedia teaching and the newly emerged "hybrid" teaching, "flipped classroom" and "MOOC," and other computer-assisted teaching methods, but their focus and classification methods are not the same. The article regards "hybrid" teaching, "flipped classroom," "MOOC," and "online live broadcast" commonly adopted by Chinese universities and primary and secondary schools during the epidemic as "new multimedia teaching." However, the current English listening teaching in colleges and universities in my country has not fully utilized the advantages of the "new multimedia," which has caused a waste of valuable resources such as new multimedia resources and teacher and student time. Teachers combine their own years of teaching experience and summarized the questions collected in the form of tests, interviews, and questionnaires from the three aspects of students, teachers, and schools. According to previous researches, college students generally have problems in the cognitive and technical aspects of the multimedia teaching style of college English listening courses. First of all, at the cognitive level, the vast majority of students are basically ignorant of "new multimedia teaching." According to previous investigations, students are already familiar with multimedia teaching synonymous with PPT. However, the "new multimedia teaching" form synonymous with "hybrid" teaching, "flipped classroom," "MOOC," and "online live broadcast" has only begun to appear and mature in recent years. Even in colleges and universities with relatively better teaching conditions, it is still not popularized, especially in primary and secondary schools. Therefore, most college students have never heard of new multimedia forms such as "hybrid" teaching, "flipped classroom," and "MOOC" before

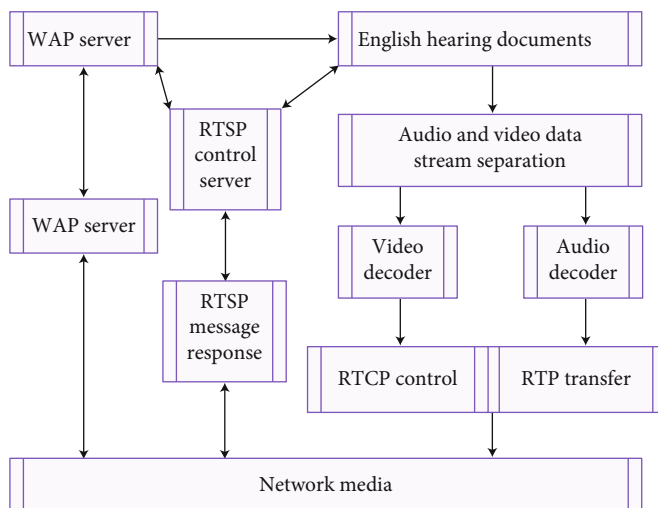


FIGURE 6: Framework structure of mobile streaming media service.

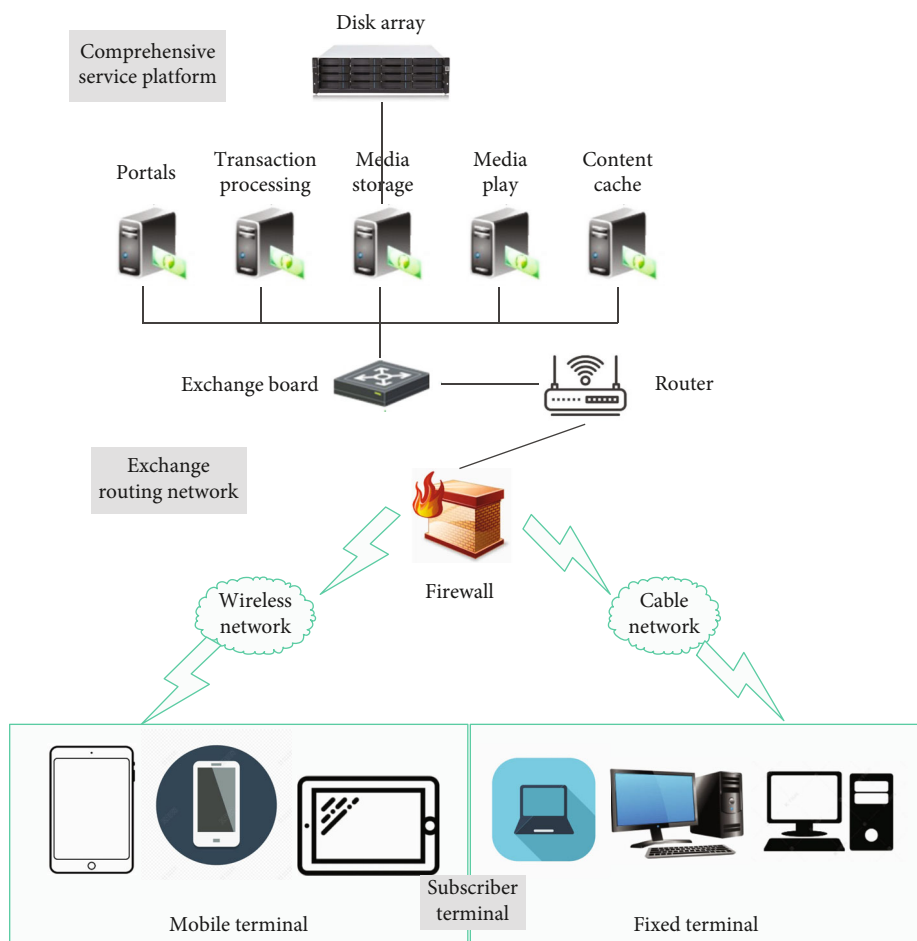


FIGURE 7: The structure of English listening streaming media on-demand system.

entering the school. The lack of understanding of new multimedia teaching methods will create obstacles for them to quickly adapt to college listening courses. Secondly, at the technical level, students have insufficient grasp of the technology and operation methods required by the new multi-

media. Although the current college students are called the “indigenous people” of the Internet age, there are still some students with poor family conditions who are unfamiliar with the operation of computers and mobile phones. In addition, even students who are proficient in the operation

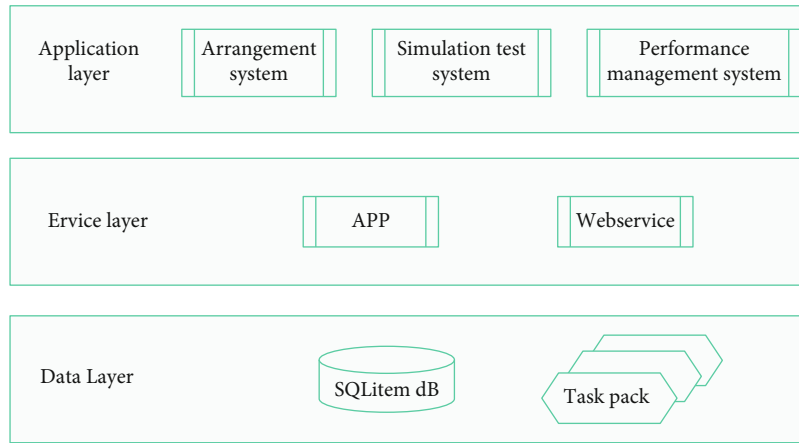


FIGURE 8: System overall architecture diagram.

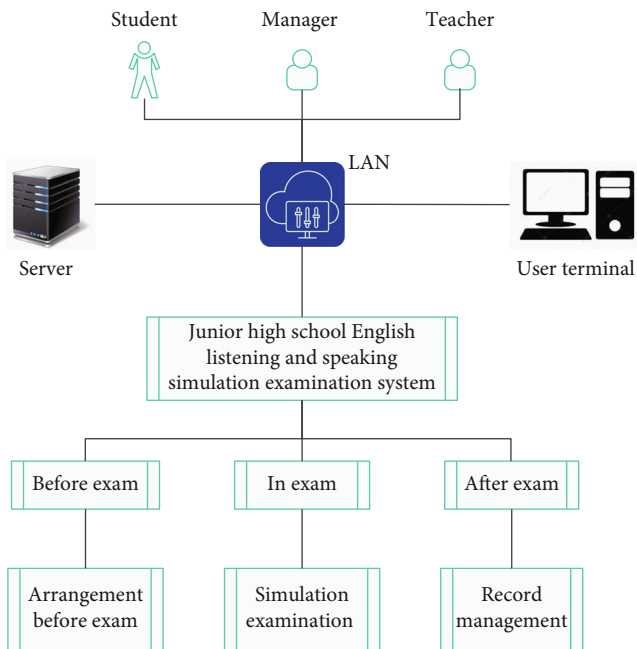


FIGURE 9: The functional overview of the English listening test system.

of computers and mobile devices are basically only familiar with a few instant messaging, social software, shopping, and film and television software. For a new client developed for learning purposes, students may not be able to operate it at all. In the new multimedia environment, few students have any knowledge of the audio clips, video clips, and subtitle addition technologies and corresponding software often assigned by listening teachers. Therefore, students currently lack the skills needed to complete multimedia assignments and activities.

The “new multimedia teaching” model represented by “mixed” teaching, “flipped classroom,” and “MOOC” has appeared for many years and has become the development trend of college English listening teaching in the future. Some problems in the school may cause the development of “new multimedia teaching” to fail to achieve the expected

TABLE 1: The effect of high-order cumulant signal-to-noise ratio estimation method in English listening speech processing.

Number	Noise removal evaluation	Number	Noise removal evaluation
1	96.575	21	93.920
2	95.868	22	95.849
3	95.864	23	94.595
4	94.477	24	94.248
5	97.208	25	96.740
6	95.225	26	95.717
7	93.223	27	93.508
8	94.886	28	93.193
9	94.097	29	94.106
10	96.675	30	93.495
11	94.100	31	97.959
12	96.788	32	93.903
13	97.437	33	97.317
14	95.712	34	94.710
15	97.076	35	97.268
16	94.022	36	95.471
17	93.720	37	93.140
18	95.436	38	94.428
19	93.175	39	93.752
20	96.474	40	95.167

results after years of development. First, the top-level design is not in place. The top-level design is one of the most critical influencing factors for the failure of universities to efficiently and smoothly carry out the new multimedia teaching reform. School management must fully realize the necessity, system, and complexity of “hybrid” teaching reform. According to the research team’s understanding, some colleges and universities have carried out “mixed” teaching reforms for many years, but they are still limited to a few classes of a certain profession led by a certain teacher in the initial experiment, and the reform effect has been minimal. The main reason is that the management only regards

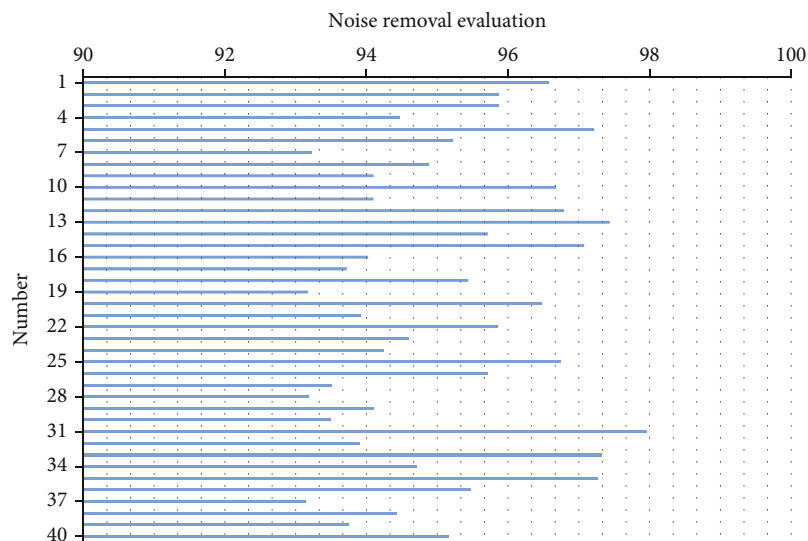


FIGURE 10: Statistical diagram of the effect of the high-order cumulant SNR estimation method.

blended teaching as an attempt and has not seen that “blended” teaching is the inevitable direction of teaching reform in colleges and universities. Second, the hardware and technical guarantees are insufficient. Compared with traditional classrooms, new multimedia teaching is highly dependent on the overall construction of “network+computer/mobile terminal.” At present, college students have basically realized that each person has a smart phone. Even if they do not have a computer, they can use the smart phone client for online learning. However, because ordinary mobile data access is often expensive, students using the mobile network to study are equivalent to increasing the financial burden of students. In addition, the implementation of new multimedia teaching puts forward higher technical requirements for teachers, especially older teachers with high professional titles and teaching management departments, and it undoubtedly increases the workload of teachers and administrators.

Based on the above analysis, this paper combines multimedia technology and applies embedded processors to intelligent English listening teaching to build an intelligent system to solve the current problems in English listening teaching and improve the effect of English teaching.

The frame structure of the mobile streaming media server is shown in Figure 6. The working process is briefly described as follows: The system separates the audio and video data streams of English listening. The audio encoder and the video encoder are used to encode, respectively, and the streaming media data is transmitted one-to-one or one-to-many by RTP. Real-time Transmission Control Protocol (RTCP) provides a reliable transmission mechanism for sequentially transmitting data packets and provides flow control or congestion control. The Wireless Application Communication Protocol (WAP) technology is a standard for mobile terminals to access wireless information services. The user obtains the audio file list, audio file introduction, and audio file data by communicating with the WAP server. Moreover, it responds to the WAP server through the Hypertext Transfer Protocol (HTTP).

TABLE 2: English listening teaching effect of multimedia intelligent-embedded processor.

Number	Teaching evaluation	Number	Teaching evaluation
1	89.730	21	83.676
2	87.008	22	89.250
3	88.109	23	89.125
4	86.330	24	89.903
5	89.669	25	84.251
6	91.903	26	89.314
7	90.358	27	83.889
8	90.043	28	90.088
9	85.478	29	85.581
10	87.510	30	92.598
11	91.046	31	85.521
12	88.561	32	87.329
13	89.814	33	84.669
14	85.498	34	87.509
15	83.896	35	83.304
16	90.657	36	91.257
17	89.571	37	92.427
18	90.425	38	82.733
19	84.397	39	89.935
20	88.743	40	89.445

On the basis of absorbing the advanced technology of other audio and video on-demand systems, this paper combines many years of English listening teaching experience and the characteristics of English listening learning to construct an English listening on-demand system based on streaming media technology to provide comprehensive solutions and technical support for software development. The English listening streaming media on-demand system is mainly composed of three parts: a comprehensive service

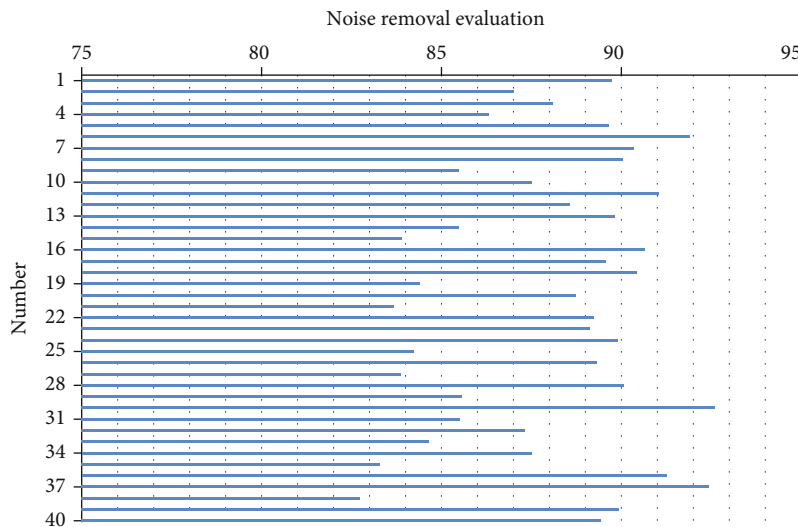


FIGURE 11: Statistical diagram of English listening teaching effect of multimedia intelligent-embedded processor.

platform, a switching routing network, and a user terminal. The system structure is shown in Figure 7.

The overall system architecture is shown in Figure 8. The front UI interface is displayed as three module entrances, which is a WPF design method. The realization of UI operation needs the support of BLL (business logic layer). DAL (data access layer) is the operating layer of the database, providing data for the business logic layer or presentation layer.

The function summary of the English listening test system is shown in Figure 9:

The system constructed above can effectively improve the current problems in English listening teaching and can test the teaching effect through the simulated listening test function. Next, the effect of the department of this paper will be evaluated through experimental research.

This paper evaluates the effect of the signal-to-noise ratio algorithm constructed in this paper in the processing of English listening sound waves through simulation experiments. The statistical results are shown in Table 1 and Figure 10.

The above experiments verify that the high-order cumulant signal-to-noise ratio estimation method is very effective in English listening speech processing. After that, the teaching effect of the English listening teaching system based on the multimedia intelligent-embedded processor constructed in this paper is evaluated, and the results shown in Table 2 and Figure 11 are obtained.

Through the above experimental analysis, it can be seen that the multimedia intelligent-embedded processor English listening teaching system constructed in this paper can play an important role in listening teaching and effectively improve the existing problems in listening teaching.

## 5. Conclusion

Listening teaching is a long-term comprehensive skill training process with strong continuous inertia. Relying on short-term intensive listening training cannot improve listening level in any way. Because of the different grades in middle

school and university, foreign language teaching is basically test-oriented education, focusing on the dissemination of foreign language knowledge, neglecting the cultivation of foreign language ability, and reading and listening and speaking. This has caused the students to have defects in listening. One of the most important manifestations is that there are very few listening classes at each stage, and at the internship stage, English learning has been completely put aside. Because there is no regular learning and training, it is impossible to improve listening skills in any way. This paper combines the multimedia intelligent-embedded processor to analyze English listening teaching and constructs an intelligent English listening model to improve the effect of English listening teaching. The experimental analysis shows that the multimedia intelligent-embedded processor English listening teaching system constructed in this paper can play an important role in listening teaching and effectively improve the existing problems in listening teaching.

## Data Availability

The labeled dataset used to support the findings of this study are available from the corresponding author upon request.

## Conflicts of Interest

The author declares no competing interests.

## Acknowledgments

This study is sponsored by the Research Fund for Shared High-quality School Courses of Lüliang University “Viewing, Listening, and Speaking” (XJKC202137) and the Special Project of Foreign Language Teaching and Research in Colleges and Universities of Shanxi Province in 2021 “Research on Metonymy Mechanism in Classical Narrative Literature” (SXSXL2021SX0084).



## References

- [1] P. H. Kumar and M. N. Mohanty, "Efficient feature extraction for fear state analysis from human voice," *Indian Journal of Science & Technology*, vol. 9, no. 38, pp. 1–11, 2016.
- [2] R. Rhodes, "Aging effects on voice features used in forensic speaker comparison," *International Journal of Speech Language & the Law*, vol. 24, no. 2, pp. 177–199, 2017.
- [3] A. K. Hill, R. A. Cárdenas, J. R. Wheatley et al., "Are there vocal cues to human developmental stability? Relationships between facial fluctuating asymmetry and voice attractiveness," *Evolution and Human Behavior*, vol. 38, no. 2, pp. 249–258, 2017.
- [4] M. Woźniak and D. Połap, "Voice recognition through the use of Gabor transform and heuristic algorithm," *Nephron Clinical Practice*, vol. 63, no. 2, pp. 159–164, 2017.
- [5] T. Haderlein, M. Döllinger, V. Matoušek, and E. Nöth, "Objective voice and speech analysis of persons with chronic hoarseness by prosodic analysis of speech samples," *Logopedics Phoniatics Vocology*, vol. 41, no. 3, pp. 106–116, 2016.
- [6] S. S. Nidhyananthan, K. Muthugeetha, and V. Vallimayil, "Human recognition using voice print in LabVIEW," *International Journal of Applied Engineering Research*, vol. 13, no. 10, pp. 8126–8130, 2018.
- [7] F. L. Malallah, K. N. Y. M. Saeed, S. D. Abdulameer, and A. W. Altuhafi, "Vision-based control By hand-directional gestures converting To voice," *International Journal of Scientific & Technology Research*, vol. 7, no. 7, pp. 185–190, 2018.
- [8] M. Sleeper, "Contact effects on voice-onset time in Patagonian Welsh," *Acoustical Society of America Journal*, vol. 140, no. 4, pp. 3111–3111, 2016.
- [9] T. G. Kang and N. S. Kim, "DNN-based voice activity detection with multi-task learning," *IEICE Transactions on Information and Systems*, vol. 99, no. 2, pp. 550–553, 2016.
- [10] H. N. Choi, S. W. Byun, and S. P. Lee, "Discriminative feature vector selection for emotion classification based on speech," *Transactions of the Korean Institute of Electrical Engineers*, vol. 64, no. 9, pp. 1363–1368, 2015.
- [11] C. T. Herbst, S. Hertegard, D. Zangger-Borch, and P. Å. Lindstedt, "Freddie Mercury-acoustic analysis of speaking fundamental frequency, vibrato, and subharmonics," *Logopedics Phoniatics Vocology*, vol. 42, no. 1, pp. 1–10, 2017.
- [12] J. Al-Tamimi, "Revisiting acoustic correlates of pharyngealization in Jordanian and Moroccan Arabic: implications for formal representations," *Laboratory Phonology*, vol. 8, no. 1, pp. 28–40, 2017.
- [13] C. Kim and R. M. Stern, "Power-normalized cepstral coefficients (PNCC) for robust speech recognition," *IEEE/ACM Transactions on audio, speech, and language processing*, vol. 24, no. 7, pp. 1315–1329, 2016.
- [14] K. Noda, Y. Yamaguchi, K. Nakadai, H. G. Okuno, and T. Ogata, "Audio-visual speech recognition using deep learning," *Applied Intelligence*, vol. 42, no. 4, pp. 722–737, 2015.
- [15] Y. Qian, M. Bi, T. Tan, and K. Yu, "Very deep convolutional neural networks for noise robust speech recognition," *IEEE/ACM Transactions on Audio, Speech, and Language Processing*, vol. 24, no. 12, pp. 2263–2276, 2016.
- [16] J. Li, L. Deng, Y. Gong, and R. Haeb-Umbach, "An overview of noise-robust automatic speech recognition," *IEEE/ACM Transactions on Audio, Speech, and Language Processing*, vol. 22, no. 4, pp. 745–777, 2014.
- [17] S. Watanabe, T. Hori, S. Kim, J. R. Hershey, and T. Hayashi, "Hybrid CTC/attention architecture for end-to-end speech recognition," *IEEE Journal of Selected Topics in Signal Processing*, vol. 11, no. 8, pp. 1240–1253, 2017.
- [18] E. Vincent, S. Watanabe, A. A. Nugraha, J. Barker, and R. Marxer, "An analysis of environment, microphone and data simulation mismatches in robust speech recognition," *Computer Speech & Language*, vol. 46, no. 3, pp. 535–557, 2017.

## Research Article

# Music Trend Prediction Based on Improved LSTM and Random Forest Algorithm

Xiangli Liu 

*College of Continuing Education, Zibo Vocational Institute, Zibo, Shandong 255000, China*

Correspondence should be addressed to Xiangli Liu; 10943@zbbc.edu.cn

Received 10 January 2022; Revised 30 January 2022; Accepted 11 February 2022; Published 22 March 2022

Academic Editor: Wen Zeng

Copyright © 2022 Xiangli Liu. This is an open access article distributed under the Creative Commons Attribution License, which permits unrestricted use, distribution, and reproduction in any medium, provided the original work is properly cited.

As one of the entertainment consumption products, pop music attracts more and more people's attention. In the context of big data, many pop music listeners can determine the development trend of pop music to a large extent. In order to predict the trend of pop music, we can dig and analyze the audience's preferences and preferences deeply based on massive user data. This paper proposes a music trend prediction method based on improved LSTM and random forest algorithm. The algorithm first performs abnormal data processing and normalization processing on the test data set. Then the important features are selected by the random forest algorithm and corrected by the rough set compensation system. Finally, the prediction is made by improving LSTM. In the experiment, RMSE and MAER are used as the performance evaluation indexes of the algorithm, and the results show that the proposed algorithm can better predict the music popularity trend. At the same time, the root means square error and mean absolute error index are improved obviously.

## 1. Introduction

With the continuous improvement of people's living standards in our country, more and more people like to listen to music, and the demand for online music is also growing [1]. As growing number of people enjoy electronic music, various electronic music platforms have emerged. These music platforms provide customers with various personalized services, such as music recommendations and social networking [2]. These music platforms allow online artists to share their original music on the platform, providing an easy way for online artists to become online celebrities [3]. Nowadays, more and more original artists are willing to share their original music on electronic music platforms, with tens of thousands of new original songs appearing on music platforms each month. At the same time, many users enjoy music on the electronic music platform every day, resulting in millions of user records of listening, downloading, and collecting music [4]. Such massive data resources have a vital role in guiding the grasp of music trends.

With the rapid development of the Internet, "Internet plus" products have emerged in the music field, including

online music platforms with increasing number of users [5]. The standardization of music copyright has affected the distribution of user groups. Retaining old users and attracting new users has become the focus of our work [6]. The app users will choose is influenced by many factors and whether a music platform is liked by songs users is important [7]. Through the user base, we can talk about the problem of a diversified profit model. From the user perspective, the most popular songs are most likely to be clicked on, regardless of personal preferences [8]. However, from the perspective of history and the current situation, the popularity of music is mainly judged by managers' intuition, which is lacking scientific and practical basis, and the results are not satisfactory. Therefore, accurately predicting the popular trend of songs has become the top priority to attract users [9].

Only scientific predictions can make the correct decision. So far, there have been many methods to predict data, but the nature of prediction can be divided into quantitative and qualitative [10]. Qualitative analysis is generally analyzed by induction, deduction, analysis, synthesis, abstraction, and generalization. Quantitative analysis usually

includes two aspects: causality study and statistical analysis. Regardless of which method is used, prediction accuracy is crucial [11]. In order to improve the accuracy of prediction, it is usually necessary to compare various prediction methods and either choose the best method or combine various prediction methods for prediction [12]. The commonly used statistical analysis models mainly include the exponential smoothing method, trend extrapolation method, and moving average method. The standard causality research mainly includes the linear regression causality model [13].

The music trend prediction can be realized by time series regression and other prediction models. The regressive integrated moving average model (ARIMA) was proposed in the literature [14]. Although it can predict well based on dynamic data and its characteristics, the selection of different times and parameters in ARIMA is not universal; so, it is necessary to preprocess and classify the data of each artist and then adjust the parameters one by one. A three-order exponential smoothing model was proposed in the literature [15]. It can predict the time series with both trend and seasonality, but it is sensitive to selecting data sets and periods. In addition, for curves higher than second-order fitting, uncontrollable divergence will occur. The model of STL decomposition (seasonal and trend decomposition using loess) is proposed in the literature [16]. Although universal and robust, it is only suitable for additive models and cannot be automatically processed adjusting sudden data changes. RNN (recurrent neural network) proposed in the literature [17]. However, the feedback can be given according to the previous data and the nonlinear dynamic system. Nevertheless, the convergence is poor, even if the corresponding features are added, and the prediction effect is not ideal.

Various research methods have been used to predict the trend of pop music. Collect and integrate the massive music library resources and user behaviors of various platforms, thus forming the big data set of pop music. Accurate analysis of specific attributes of this data set can finally accurately control the trend of pop music. This paper proposes pop music trend prediction based on improved LSTM and random forest algorithm. Firstly, the LSTM network is optimized to increase the attention layer. Then, the stochastic forest regression prediction model is constructed. In the experimental part, the collected data sets are analyzed and processed firstly, the important features of the data are extracted by the random forest model, and then the improved LSTM is used for prediction.

## 2. The Algorithm Is Proposed in This Paper

### 2.1. Improved LSTM Algorithm

**2.1.1. LSTM Network.** Long-short-term memory (LSTM) is a recurrent neural network (RNN) [18], solving time series problems. The problems of gradient explosion and gradient disappearance in RNN are also solved effectively. The contents of cell state  $c_n$  in LSTM are controlled by two gates. One is the forgetting gate, which determines how much of the unit state  $c_{n-1}$  from the last moment remains at the current moment  $c_n$ . The other is the input gate, which

determines how much of the network's input  $i_n$  is saved to cell state  $c_n$  at the current moment. The current output value  $b_n$  of LSTM is determined by the output gate and cell state  $c_n$ . The structural principle of LSTM is shown in Figure 1 [18].

LSTM is divided into encoder and decoder. The encoder realizes the isometric learning of the input feature data, and the decoder calculates the reconstruction error. Let the input sample  $I_1, I_2 \dots, I_T$  be defined as  $\{I_x\}_{x=1}^t$ , and the observation window size is represented by  $t$ . If researchers' type  $I_x = \{i_{x1}, i_{x2}, \dots, i_{xt}\}$  is in any of these, they will have  $I_x = \{i_{x1}, i_{x2}, \dots, i_{xt}\}$ . The encoder implied state vector corresponding to the  $x$  column of any sequence  $I_x$  in time  $n \in \{1, 2, \dots, t\}$  is shown in Formula (1):

$$b_E^{nx} = z \left( M i_{nx} + R b_{(n-1)x} \right), \quad (1)$$

where  $b_{(n-1)x} \in R^w$  is the output state vector of the  $x$  coding unit at the moment  $n - 1$ . Input vector  $i_{nx} \in R^w$ ,  $M, R$  is the coefficient weight matrix of order  $w \times d$  and  $w \times w$ . Function  $z(\cdot)$  is usually the activation function "tanh." Taking each column vector in  $I_x$  as input to the encoder results in the following.

$$b_{nx} = z_t^{\text{etc}} \left( i_{nx}, b_{(n-1)x} \right), \quad (2)$$

where  $b_{nx}$  refers to the output of the  $x$  coding unit at moment  $n$ .  $t$  is the parameter set of the encoding part.  $z_t^{\text{etc}}(\cdot)$  is usually set to the tanh activation function. After the whole sequence is input to the encoder, the output sequence set  $\{b_{nx}\}_{x=1}^{tx}$  can be obtained. Then, the pooling step is performed as follows.

$$b_x = \frac{\sum_{y=1}^{tx} b_{xy}}{t_x}, \quad (3)$$

$$b_x = b_{n,tx}, \quad (4)$$

$$b_x = \max_y \{b_{nx}\}_{x=1}^{tx}, \quad (5)$$

where  $y$  is the number of rows of  $b_{nx}$ . After the pooling step,  $b_x$  enters the decoder. The inputs can be refactored into formulas (6) and (7).

$$\tilde{b}_{nx} = z_\alpha^{\text{dec}} \left( b_x, b_{(n-1)x} \right), \quad (6)$$

$$\tilde{i}_{n_x} = \rho \left( \tilde{b}_{n_x} \right), \quad (7)$$

where  $\tilde{i}_{n_x}$  refers to the reconstructed data.  $\tilde{b}_{n_x}$  refers to the decoder implicit state vector.  $z_\alpha^{\text{dec}}(\cdot)$  and  $\rho(\cdot)$  are usually set to the activation function "tanh." The LSTM model is finally obtained by minimizing the function  $\sum_{x=1}^t i_{n_x} - \tilde{i}_{n_x}^2$ . The LSTM network structure is shown in Figure 2.

**2.1.2. Attention Mechanism.** After the attention mechanism was proposed, it was applied in visual images for the first time [18]. The subsequent rapid application has influenced the development of many artificial intelligence fields based

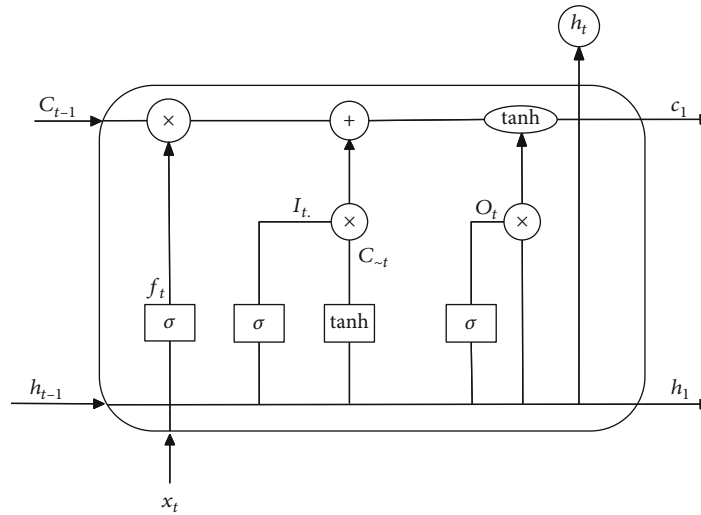


FIGURE 1: Structure of LSTM network.

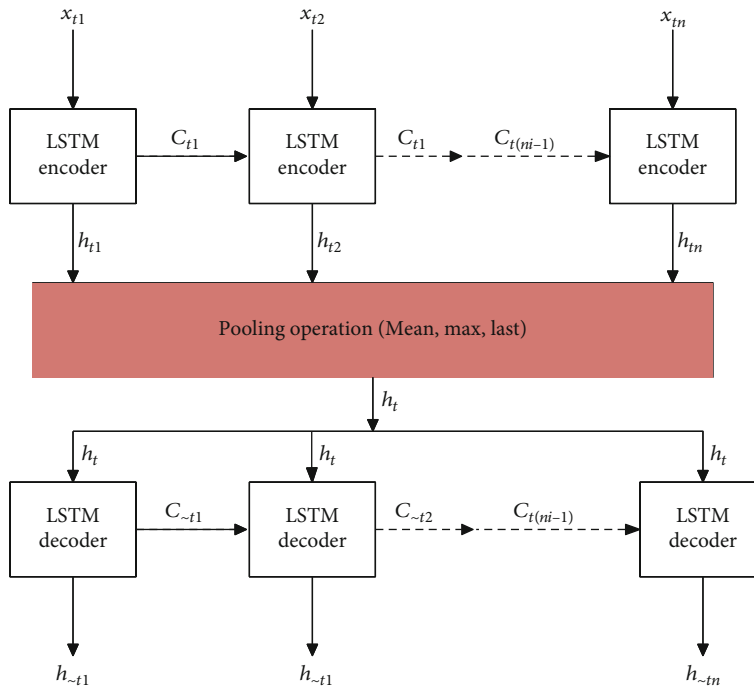


FIGURE 2: Structure of LSTM.

on depth algorithms. At present, attention mechanism has been successfully applied to image processing, natural language processing, and data prediction. Meanwhile, an attention mechanism has been applied to neural network machine translation and achieved fruitful results. Taking Ali music platform as an example, the output information is obtained through the LSTM network. Then, the output information is computed. Finally, the attentional probability distribution of feature information is obtained. In this way, we can master the output state of LSTM unit at each moment and provide an important basis for predicting music popularity trend.

*2.1.3. Improve the LSTM Model.* The improved LSTM model adds an attention layer after the LSTM structure. The LSTM and attention mechanism model has been applied to relational classification and achieved good results. The application of the combined model to the prediction of time series data, especially public data, is still in the stage of continuous improvement. In this paper, the mechanism combining LSTM and attention mechanism are used to predict the corresponding singers and songs on the Ali Cloud music platform. Based on the past historical data, two dimensions of “daily broadcast volume” and “average broadcast volume of consecutive three days” were selected to predict the song

broadcast volume of singers in the next 60 days. The overall model construction adopted is shown in Figure 3.

## 2.2. Prediction Model Based on Random Forest

### 2.2.1. Similar Day Data Sets Were Obtained by Fuzzy Clustering

(1) *Fuzzy Clustering Principle of C-Means*. For a given data set  $I = \{i_1, i_2, \dots, i_t\}$ , the C-mean fuzzy clustering is determined. Researchers must enter the number of categories  $C$ , each cluster's center  $w_y (y = 1, 2, \dots, c)$ . For each sample  $i_z$ , there is a corresponding membership function  $\mu_{xz} = \mu_{I_x}(i_z)$ , that is, the membership degree of the  $z$  sample to class  $I_x$ . The clustering loss index function based on membership function can be expressed as Equation (8):

$$Y = \sum_{y=1}^z \sum_{x=1}^t \left[ \mu_y(i_x) \right]^h i_x - w_y^2, \quad (8)$$

where  $h$  represents the weighted index, also known as the smoothing factor, and the sharing degree of sample among fuzzy classes. There are still controversies about the optimal value of  $h$  in the academic circle. Considering the amount of calculation and the calculation accuracy, the weighted index is usually 2.

If the partial derivative of  $Y$  concerning  $w_y$  and  $\mu_y(i_x)$  is 0, the necessary conditions for  $Y$  to obtain the minimum value can be obtained by formulae (9) and (10):

$$w_y = \frac{\sum_{x=1}^t \left[ \mu_y(i_x) \right]^h i_x}{\sum_{x=1}^t \left[ \mu_y(i_x) \right]^h}, \quad (9)$$

$$\mu_y(i_x) = \frac{i_x - w_y^{2/h-1}}{\sum_{s=1}^z i_x - w_s^{-2/h-1}}. \quad (10)$$

Therefore, generating  $c$ -mean fuzzy clustering is the number of input categories  $c$ . Initialize the center  $w_y (y = 1, 2, \dots, c)$  of each cluster. For sample  $i_z$ , the corresponding membership function is  $\mu_{xz} = \mu_{I_x}(i_z)$  and then repeatedly uses formula (9) and formula (10) to calculate  $w_y (y = 1, 2, \dots, c)$  and  $\mu_{xz} = \mu_{I_x}(i_z)$ . The clustering centre and membership function can be determined until the accuracy requirement is satisfied.

(2) *Determination of the Optimal Cluster Number*. When  $c$ -means fuzzy clustering is used for cluster analysis, the number of categories  $c$  must be set in advance [19]. The value of  $c$  has a profound influence on clustering. If the number of clustering is too large, the samples of the same kind will be divided into different classes. If the number of clustering is too tiny, data of different classes may be grouped into the same class. The setting of the wrong clustering number will lead to the wrong clustering result and even make the itera-

tion unable to converge. Therefore, it is necessary to calculate the number of clustering by setting optimization criteria.

The basic idea for calculating the number of clusters is to introduce outcome evaluation indicators. By increasing the number of clusters and judging the change of evaluation indexes, the optimal number of clusters can be calculated from the results of the optimal indexes. As for the result evaluation index, the evaluation of clustering results is mainly carried out from two aspects: similarity of the same class and difference of different classes. Therefore, the evaluation indexes can be determined as intraclass similarity  $X_g$  and interclass similarity  $X_r$  [20]:

$$X_{gx} = \frac{1}{t_x} \sum_{i \in I_x} i - c_x, \quad (11)$$

where  $t_x$  is the amount of data in the class.  $i$  is the sample object.  $c_x$  is the center of class  $I_x$ . The smaller the value of  $X_{gx}$  is, the more concentrated the data points are in the center of the class and the more similar the data samples are:

$$X_{rxy} = m(c_x - c_y), x \neq y, \quad (12)$$

where  $c_x$  is the center of class  $I_x$ .  $c_y$  is the center of class  $I_y$ . The larger the  $X_{rxy}$  value is, the farther the center distance between adjacent classes is, and the smaller the similarity between classes is.

Therefore, comprehensive evaluation indicators can be obtained.

$$Y_X = \sum_{x=1}^c \frac{t}{t_x} X_{gx} + \sum_{x=1}^c \sum_{y=x+1}^c \frac{1}{X_{rxy}}. \quad (13)$$

Therefore, the calculation and determination process of the optimal cluster number is as follows:

- (1) Determine the range of classification numbers. Generally, the classification number  $c$  is set to  $c \in [2, \sqrt{t}]$ , where  $t$  represents the number of all sample data
- (2) Perform a clustering operation for each  $c$  value
- (3) Analyze the data obtained from each cluster based on the result evaluation index. The optimal clustering number can be determined by finding the inflection point and different minimum point in the evaluation index to obtain the relation between data

2.2.2. *Establishment of the Stochastic Forest Regression Prediction Model*. The prediction result of random forest is composed of the prediction result of each decision tree [21]. Therefore, the critical step of random forest prediction is decision tree and forest formation, as shown in Figure 4.

This paper uses the bootstrap algorithm to extract the training set and its features for music trend prediction. Then, select the CART algorithm as the regression decision tree generation algorithm. Therefore, the splitting of nodes

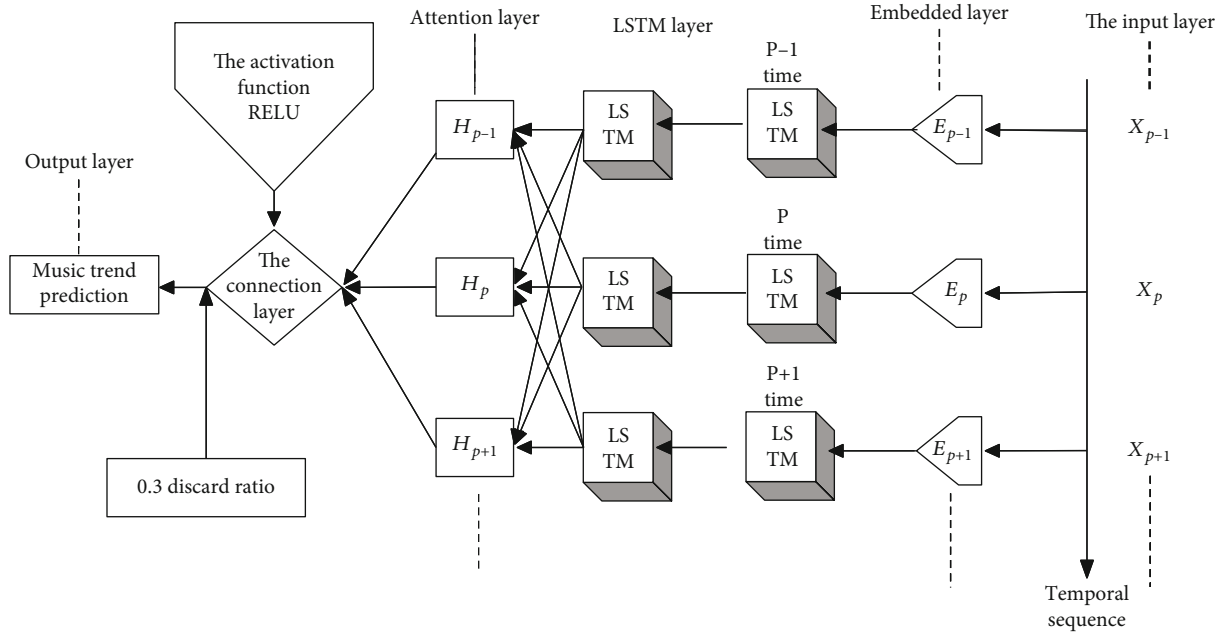


FIGURE 3: The LSTM model structure is adopted.

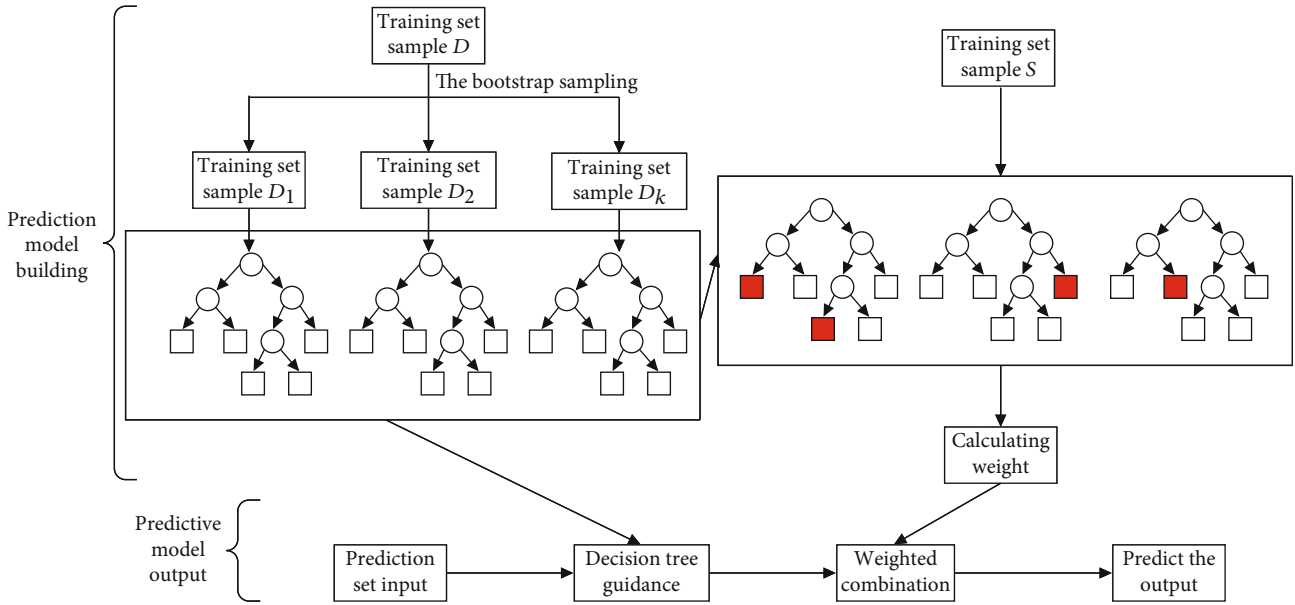


FIGURE 4: Random forest prediction flowchart.

is based on the minimum mean square error, and its calculation method is shown in Equation (14).

$$w = \min_{G,s} \left[ \min_{c_1} \sum_{i_x \in D_1(G,s)} (j_x - c_1)^2 + \min_{c_2} \sum_{i_x \in D_2(G,s)} (j_x - c_2)^2 \right], \quad (14)$$

where  $s$  represents all training sets of the current node.  $G$  represents the feature set extracted from the current node. Training set  $s$  is divided into subsets  $D_1$  and  $D_2$  according to feature  $G$ . By traversing the values of  $G$ , the sum of the minimum mean square deviation of the output values  $j_x$  of subset  $D_1$  and  $D_2$  can be calculated. Finally, all attributes are traversed to obtain the value  $w$  of the minimum mean square deviation, the value of the corresponding attribute, and corresponding attribute, and the growth information

of the node is obtained. The process is repeated for each generated child node until the termination condition is reached. The termination conditions are set as follows:

- (1) Reach the set tree depth  $d$
- (2) The samples on the node are less than the minimum number of samples  $s$
- (3) The minimum mean square error reaches the salt value  $w_0$

After the decision tree is generated, a similar method is used to train all the training sets obtained by sampling to form a random forest.

The steps of building the stochastic forest prediction model are as follows:

- (1) First, the  $c$ -mean fuzzy clustering method processes the original data. After obtaining similar daily data, it was divided into two parts: training set  $D$  and test set  $S$ . Let the sample size of  $D$  be  $T$  and let the attribute size of the sample in  $D$  is  $W$
- (2) Sample size was extracted from training set  $D$  by bootstrap resampling. Can also the training set of  $T$ , repeated  $Z$  times,  $Z$  training sets  $\theta_1, \theta_2, \dots, \theta_Z$ , be obtained? Each training set can generate a corresponding decision tree  $\{N_1(\theta_1), N_2(\theta_2), \dots, N_Z(\theta_Z)\}$ . Therefore,  $Z$  is the number of decision trees in the random forest
- (3) Use training set  $\theta_1, \theta_2, \dots, \theta_Z$  to generate the corresponding CART decision tree. In decision tree generation,  $c$  dimension attribute features are extracted from  $M$  dimension attribute features for each split node without putting back. These attributes and their corresponding values were traversed, and the minimum mean square value was calculated to obtain the optimal segmentation criterion
- (4) Train each decision tree until the termination condition is reached

The established random forest model is used to substitute the test set data.

- (1) After normalized processing, the input data is matched with similar daily data. Substitute in the random forest prediction model  $\{N_1(\theta_1), N_2(\theta_2), \dots, N_Z(\theta_Z)\}$  formed by the corresponding similar days
- (2) It was substituted into each decision tree of the growth model, and the splitting criterion of the culture process was like that of the model. Until the end. Then, the weight of each nonzero leaf node is calculated, and the weight calculation formula is shown in Formula (15)

$$m_x = \frac{t(x \in l(\theta))}{T\{x \in S\}}. \quad (15)$$

- (3) After obtaining the weight of the leaf node, the weight of the decision tree can be calculated according to Equation (16)

$$m_n = \frac{\sum m_l J_{nx}}{\sum J_x}. \quad (16)$$

- (4) After the decision tree's root, node, weight, and other information are saved, the random forest prediction model is established

After establishing the random forest prediction model, the steps for prediction are as follows.

- (1) After normalized processing, the input data is matched with similar daily data. Substitute in the model  $\{N_1(\theta_1), N_2(\theta_2), \dots, N_Z(\theta_Z)\}$  of random forest prediction formed by the corresponding similar days
- (2) Each decision tree is cultivated, and the splitting criterion in the cultivation process is like the model. After the prediction results of each tree are obtained, the weight data generated by the test set is utilized. A weighted average is used to get the final prediction

$$j = \sum_{n=1}^Z m_n J_n. \quad (17)$$

### 2.2.3. Prediction Result Evaluation and Rough Set Correction

(1) *Evaluation Criteria for Prediction Results.* This paper uses the random forest regression model to predict the results. Then, the average absolute error, average relative error, and  $R^2$  ( $R^2$  is used here to measure the fitting degree of the prediction result and the actual curve, namely, the correlation coefficient) qualified rate are used to judge the prediction result.

(2) *Rough Set Theory.* When using random forest or other regression algorithms for regression prediction, the prediction results tend to be conservative and smooth due to the specificity of regression theory. When the predicted curve has multiple peak values or the difference square changes significantly, the prediction results will have a conspicuous error near the peak value. The rough set can overcome this shortcoming. It is a mathematical tool to deal with fuzzy and uncertain problems in big data [22]. At the same time, it can effectively analyze and process incorrect and incomplete information, requires error compensation, is inconsistent, and has data loss. The hidden knowledge is mined, and the underlying laws in the original data are revealed.

(3) *Construction of the Rough Set Compensation System.* The prediction model of music popularity trend can be expressed by Formula (18).

$$\begin{cases} j'_{n+1} = j_{n+1} + s|z_{n+1} - z_n|, \\ z_{n+1} = j_{n+2} - j_{n+1}, \\ z_n = j_{n+1} - j_n, \end{cases} \quad (18)$$

where  $j'_{n+1}$  represents the data after compensation at time  $n + 1$ . Before time  $n + 1$ , this value represents the popularity of music.  $j_{n+1}$  represents the result of random forest prediction at time  $n + 1$ .  $z_{n+1}$ , and  $z_n$  represents the difference between the two sides of the prediction function at time  $n + 1$ .  $s$  is the scale factor, which is the key to music prediction and correction. It will be calculated by the rough set theory below in order to use rough set theory to calculate scale factor  $s$ .

According to the rough set theory requirements, an information system should be constructed first. Here, it is assumed that the information system based on rough set theory is  $Z = (P, G)$ , and set  $P$  is the set of predicted values output by random forest prediction.  $P = C \cup S$  is the attribute set. The conditional attribute  $C$  represents the consistent rule, and the data feature is extracted from the set of predicted values.  $S = \{s\}$  represents the decision attribute; that is, the scale factor to be obtained. Each attribute in  $C$  can be represented by the information contained in  $P$ . Finally, after rule deletion, we try to obtain the representation of attribute  $S$ .

As for the conditional attribute represented by  $C = \{g, h, c\}$ , based on previous research results, the conditional attribute  $D$  is defined here, where

$$g = \frac{|z_{n+1} - z_n|}{j_n}, \quad (19)$$

$$h = \text{sgn}(z_{n+1} - z_n), \quad (20)$$

$$c = \left| \frac{j_n}{m(j_n)} \right|, \quad (21)$$

for the decision attribute represented by  $D$ . The attributes before  $n$  can be calculated according to Equation (22). The values after  $n + 1$  are the decision targets to be determined.

$$s_n = \frac{j'_n - j_n}{|z_n - z_{n-1}|}. \quad (22)$$

### 3. Experimental Results and Analysis

#### 3.1. Description of Sample Data

*3.1.1. Source of Sample Data.* The data set used in this paper comes from Ali Cloud music platform. Ali Cloud Music is a large music platform under Alibaba, which has accumulated many users and music library resources after years of development. In terms of the number of artists and the variety of songs, the platform is the best of its kind. More importantly,

there is a wealth of user activity off the platform: uploading songs and downloading albums. Both the rich resources and the active degree of users play a significant role in guiding the trend of music.

Given the data information under the music platform, the sample data provided by the platform are two tables. One is the user behavior table (time span 2020.03.01-2020.08.31) p2\_mars\_tianchi\_users\_action. The function of this table is to represent the behavior of users on Ali music platform. The other is p2\_Mars\_tianchi\_songs. The information expressed in this table includes information about the singer and the corresponding song, such as the album, initial popularity.

The data sets p2\_mars\_tianchi\_user\_actions.csv and p2\_Mars\_tianchi\_songs.csv used in the paper are covered by (2020.03.01-2020.08.31). There are a total of 6 months of user behavior information and song information. According to the data set statistics, the total initial play popularity (historical play) of the songs included in the data set was 261.07 million. Users recorded 4.78 million playback behaviors.

*3.1.2. Data Preanalysis and Pretreatment.* The goal of this paper is to predict the number of songs played by the corresponding singers. Therefore, in processing the data set, we should locate the number of songs played by singers. According to the 6-month data from 2020.03.01 to 2020.08.30 given in the data set, the trend chart of songs played by singers was made. Select the combined daily broadcast volume and the mean value of consecutive three days as the sample value at a particular time point. The training set of the neural network is constructed by "sliding," and its model parameters are set as follows:

- (1) Number of input nodes = 2
- (2) Number of output nodes = 1
- (3) Propagation step = 64
- (4) Number of nodes of hidden layer = 128
- (5) Activation function = REL
- (6) Regular optimization (dropout discard ratio) = 0.3
- (7) Learning rate = 0.001

*3.2. Experimental Results.* Figure 5 shows the average number of streams, downloads, and favorites for any artist in each region over the past six months. As can be seen from the chart, the number of plays, collections, and downloads of an artist's songs is the best predictor of whether an artist will be famous in a certain period.

For the song playback data of all singers, demean, variance normalization, and scaling were carried out  $[-1,1]$ , and the length of the mean filter was set as  $\text{ave filter} = 4$ . The prediction curve shown in Figure 6 can be obtained using the original broadcast volume for prediction. As can be seen from Figure 6, there are deviations in the prediction results of some singers based on the original data.

Figure 7 shows the experimental results of predicting the number of songs played in the next 60 days by using the



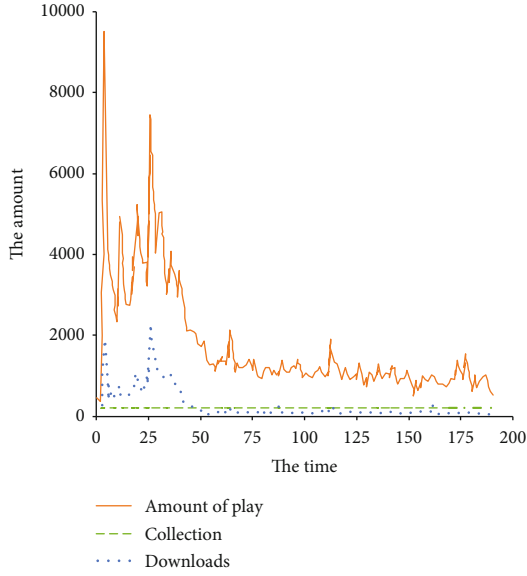


FIGURE 5: The average number of songs played, downloaded, and saved.

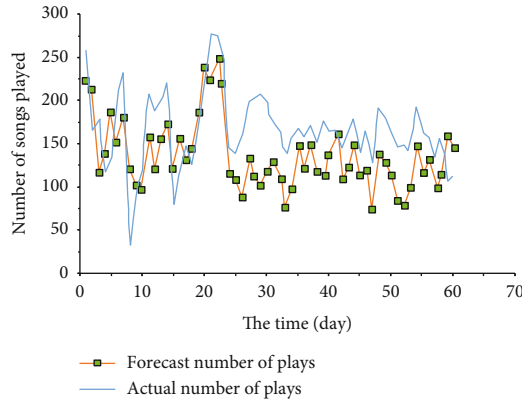


FIGURE 6: Compare the predicted play of the song with the actual play.

average number of songs played by singers (after scaling). As can be seen from Figure 7, the prediction result using the average number of songs played is better than that using the original number of songs played. The prediction matches the number of songs played by artists over the next 60 days.

RMSE and MAE are used to compare other forecasting methods. RMSE and MAE are the most used measures of variable accuracy. It is also an important yardstick of the evaluation model. RMSE measures the average size of the error, and MAE is the average error of the general form. The specific calculation method is as follows:

$$RMSE = \sqrt{\frac{1}{t} \sum_{x=1}^t [j - \hat{j}]^2}, \quad (23)$$

$$MAE = \frac{1}{t} \sum_{x=1}^t |j - \hat{j}|, \quad (24)$$

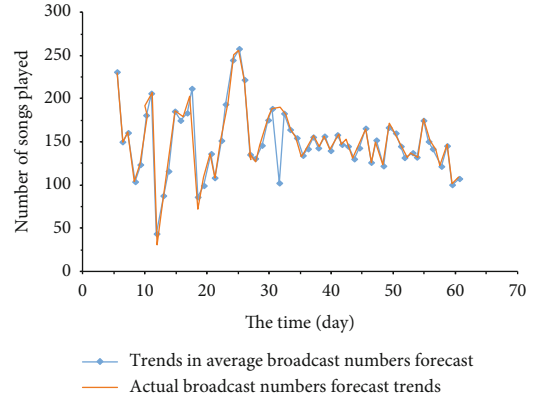


FIGURE 7: Using average play data to predict the number of songs being played compared to the number of actual plays.

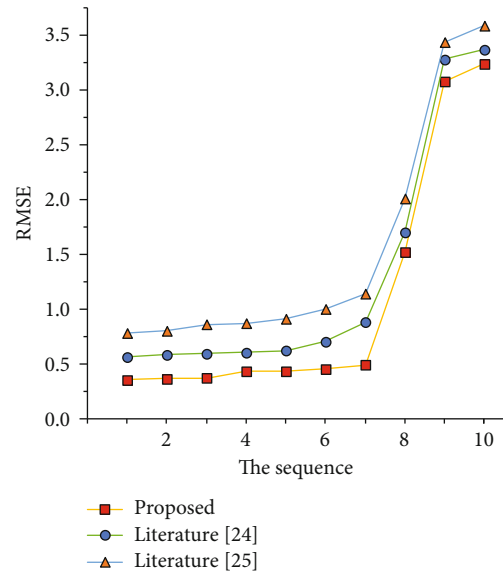


FIGURE 8: Comparison of RMSE index among three models.

where  $j$  is the observed value,  $\hat{j}$  is the original value, and  $t$  is the number of observations. The experiment in this paper randomly selects ten artists in the data set. It predicts the number of songs played by artists from August 1 to August 31, 2020, by using SVM, LSTM, and the improved LSTM algorithm used in this paper. The predicted results, root mean square error and mean absolute error, are shown in Figures 8 and 9.

As can be seen from Figures 8 and 9, the prediction model proposed in this paper has a better prediction effect (RMSE and MAE indicators) in predicting the number of songs played by ten artists. Compared with the traditional method, LSTM and SVM are reduced from the original 0.08 and 0.067 to 0.048 and 0.035, respectively, and the error rates are reduced by 36.7% and 28.5%, respectively. It is proved that the model proposed in this paper is more suitable for predicting the trend of music popularity. Figure 10 shows the influence degree of RMSE and MAE of different model parameters. It is not difficult to find that both

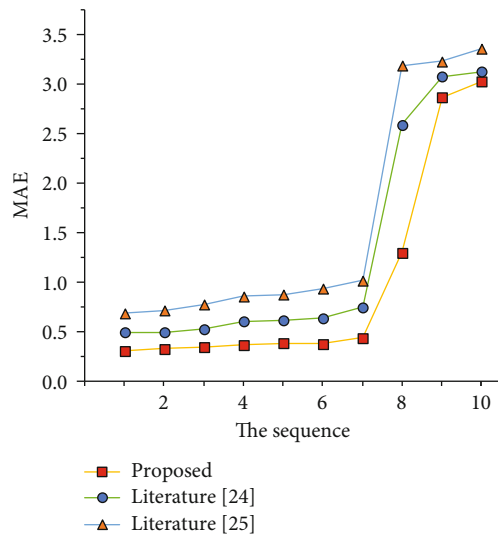


FIGURE 9: Comparison of MAE index among three models.

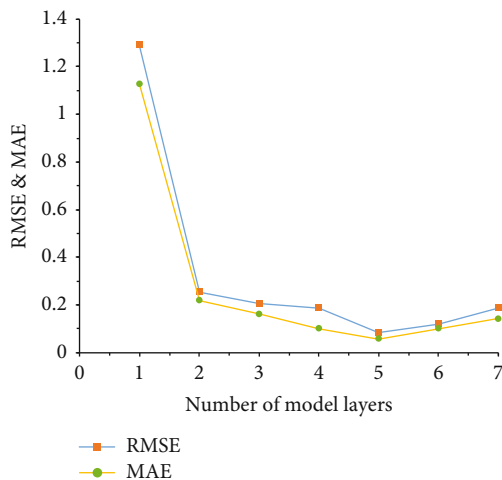


FIGURE 10: The influence of different prediction model layers on RMSE and MAE.

indicators are declining with model layers in a particular range. However, after exceeding a specific range, it shows an upward trend. The number of layers used in this model is 6.

#### 4. Conclusion

The data in this paper is from Ali music platform, and the popular trend of music is predicted in big data. Based on the historical playback data of one user, this paper achieves accurate control of music trends in a period by predicting the playback amount of artists' songs in the target time. This paper proposes a music trend prediction method based on improved LSTM and random forest algorithm. The algorithm predicts whether a singer's songs will be popular in the future based on the average number of songs played in the past period. The experimental results show that the predicted results of the proposed algorithm are consistent with

the actual songs played by singers in the next 60 days. At the same time, RMSE and MAE were significantly improved. Experimental results show that the proposed algorithm is more stable, accurate, and suitable for music trend prediction under big data background. In the future, the following types of work can try to combine the prediction model to improve the prediction effect. In this paper, the factors affecting the number of songs played are not considered comprehensively when selecting corresponding features. The effect of prediction needs to be further improved. Therefore, other comprehensive characteristics affecting song playback volume can be further explored in the later stage.

#### Data Availability

The labeled dataset used to support the findings of this study are available from the corresponding author upon request.

#### Conflicts of Interest

The author declares no competing interests.

#### References

- [1] S. C. Brown and D. Knox, "Why go to pop concerts? The motivations behind live music attendance," *Musicae Scientiae*, vol. 21, no. 3, pp. 233–249, 2017.
- [2] S. Song and M. Yoo, "The role of social media during the pre-purchasing stage," *Journal of Hospitality and Tourism Technology*, vol. 7, no. 1, pp. 84–99, 2016.
- [3] J. W. Morris, "Music platforms and the optimization of culture," *Social Media Society*, vol. 6, no. 3, 2020.
- [4] J. P. Simon, "New players in the music industry: lifeboats or killer whales? The role of streaming platforms," *Digital Policy, Regulation and Governance*, vol. 21, no. 6, pp. 525–549, 2019.
- [5] X. Xie, X. Xie, and C. Martínez-Climent, "Identifying the factors determining the entrepreneurial ecosystem of internet cultural industries in emerging economies," *International Entrepreneurship and Management Journal*, vol. 15, no. 2, pp. 503–522, 2019.
- [6] C. H. Hsiao, J. J. Chang, and K. Y. Tang, "Exploring the influential factors in continuance usage of mobile social Apps: satisfaction, habit, and customer value perspectives," *Telematics and Informatics*, vol. 33, no. 2, pp. 342–355, 2016.
- [7] I. Kamehkhosh, G. Bonnin, and D. Jannach, "Effects of recommendations on the playlist creation behavior of users," *User Modeling and User-Adapted Interaction*, vol. 30, no. 2, pp. 285–322, 2020.
- [8] N. Askin and M. Mauskapf, "What makes popular culture popular? Product features and optimal differentiation in music," *American Sociological Review*, vol. 82, no. 5, pp. 910–944, 2017.
- [9] K. Volchek, A. Liu, H. Song, and D. Buhalis, "Forecasting tourist arrivals at attractions: search engine empowered methodologies," *Tourism Economics*, vol. 25, no. 3, pp. 425–447, 2019.
- [10] R. Villegas, J. Yang, and Y. Zou, "Learning to generate long-term future via hierarchical prediction," in *international conference on machine learning*, pp. 3560–3569, PMLR, 2017.
- [11] L. Yan, H. T. Zhang, J. Goncalves et al., "An interpretable mortality prediction model for COVID-19 patients," *Nature machine intelligence*, vol. 2, no. 5, pp. 283–288, 2020.

- [12] Z. Wang and R. S. Srinivasan, "A review of artificial intelligence based building energy use prediction: contrasting the capabilities of single and ensemble prediction models," *Renewable and Sustainable Energy Reviews*, vol. 75, pp. 796–808, 2017.
- [13] K. C. Green and J. S. Armstrong, "Simple versus complex forecasting: the evidence," *Journal of Business Research*, vol. 68, no. 8, pp. 1678–1685, 2015.
- [14] N. S. Arunraj and D. Ahrens, "A hybrid seasonal autoregressive integrated moving average and quantile regression for daily food sales forecasting," *International Journal of Production Economics*, vol. 170, pp. 321–335, 2015.
- [15] S. Smyl, "A hybrid method of exponential smoothing and recurrent neural networks for time series forecasting," *International Journal of Forecasting*, vol. 36, no. 1, pp. 75–85, 2020.
- [16] Q. Wen, J. Gao, X. Song, L. Sun, H. Xu, and S. Zhu, "RobustSTL: a robust seasonal-trend decomposition algorithm for long time series," *Proceedings of the AAAI Conference on Artificial Intelligence*, vol. 33, pp. 5409–5416, 2019.
- [17] X. Y. Zhang, F. Yin, Y. M. Zhang, C. L. Liu, and Y. Bengio, "Drawing and recognizing chinese characters with recurrent neural network," *IEEE Transactions on Pattern Analysis and Machine Intelligence*, vol. 40, no. 4, pp. 849–862, 2018.
- [18] Z. Huang, W. Xu, and K. Yu, "Bidirectional LSTM-CRF models for sequence tagging," 2015, arXiv preprint arXiv: 1508.01991.
- [19] M. Ren, P. Liu, Z. Wang, and J. Yi, "A self-adaptive fuzzy c-means algorithm for determining the optimal number of clusters," *Computational Intelligence and Neuroscience*, vol. 2016, 12 pages, 2016.
- [20] H. Verma, R. K. Agrawal, and A. Sharan, "An improved intuitionistic fuzzy c-means clustering algorithm incorporating local information for brain image segmentation," *Applied Soft Computing*, vol. 46, pp. 543–557, 2016.
- [21] T. Shaikhina, D. Lowe, S. Daga, D. Briggs, R. Higgins, and N. Khovanova, "Decision tree and random forest models for outcome prediction in antibody incompatible kidney transplantation," *Biomedical Signal Processing and Control*, vol. 52, pp. 456–462, 2019.
- [22] R. H. Hariri, E. M. Fredericks, and K. M. Bowers, "Uncertainty in big data analytics: survey, opportunities, and challenges," *Journal of Big Data*, vol. 6, no. 1, 2019.

## Retraction

# Retracted: Analysis of Learning Ability of Ideological and Political Course Based on BP Neural Network and Improved $k$ -Means Cluster Algorithm

### Journal of Sensors

Received 8 August 2023; Accepted 8 August 2023; Published 9 August 2023

Copyright © 2023 Journal of Sensors. This is an open access article distributed under the Creative Commons Attribution License, which permits unrestricted use, distribution, and reproduction in any medium, provided the original work is properly cited.

This article has been retracted by Hindawi following an investigation undertaken by the publisher [1]. This investigation has uncovered evidence of one or more of the following indicators of systematic manipulation of the publication process:

- (1) Discrepancies in scope
- (2) Discrepancies in the description of the research reported
- (3) Discrepancies between the availability of data and the research described
- (4) Inappropriate citations
- (5) Incoherent, meaningless and/or irrelevant content included in the article
- (6) Peer-review manipulation

The presence of these indicators undermines our confidence in the integrity of the article's content and we cannot, therefore, vouch for its reliability. Please note that this notice is intended solely to alert readers that the content of this article is unreliable. We have not investigated whether authors were aware of or involved in the systematic manipulation of the publication process.

Wiley and Hindawi regrets that the usual quality checks did not identify these issues before publication and have since put additional measures in place to safeguard research integrity.

We wish to credit our own Research Integrity and Research Publishing teams and anonymous and named external researchers and research integrity experts for contributing to this investigation.

The corresponding author, as the representative of all authors, has been given the opportunity to register their agreement or disagreement to this retraction. We have kept a record of any response received.

### References

- [1] G. Zeng, "Analysis of Learning Ability of Ideological and Political Course Based on BP Neural Network and Improved  $k$ -Means Cluster Algorithm," *Journal of Sensors*, vol. 2022, Article ID 4397555, 11 pages, 2022.

## Research Article

# Analysis of Learning Ability of Ideological and Political Course Based on BP Neural Network and Improved $k$ -Means Cluster Algorithm

Guidong Zeng 

Xingjian College, Xijing University, Xi'an, Shaanxi 710123, China

Correspondence should be addressed to Guidong Zeng; [zengguidong3@xijing.edu.cn](mailto:zengguidong3@xijing.edu.cn)

Received 4 January 2022; Revised 24 January 2022; Accepted 9 February 2022; Published 21 March 2022

Academic Editor: Yanqiong Li

Copyright © 2022 Guidong Zeng. This is an open access article distributed under the Creative Commons Attribution License, which permits unrestricted use, distribution, and reproduction in any medium, provided the original work is properly cited.

With the rapid development of technologies such as big data analysis, machine learning, and cloud computing, artificial intelligence has made breakthrough progress in many fields. Artificial intelligence technology has also brought profound changes to higher education. Therefore, the ideological and political course in colleges and universities should integrate artificial intelligence technology into the teaching of ideological and political education and create an “intelligent ideological and political learning” to adapt to the goal of educational reform in the new era. This paper presents a research method of innovation ability of ideological and political course based on BP neural network and improved  $k$ -means clustering algorithm. Firstly, this method obtains the objective index that can comprehensively measure the learning ability through BP neural network and acquires the evaluation score of learning ability. Then, SPSS software is utilized to test the correlation between the influencing factors and the index, harvesting the factors that significantly affect graduate students' ideological and political learning ability. Finally, an improved  $k$ -means clustering algorithm is designed, which clusters the graduate students according to the different characteristics of the survey objects and gives targeted suggestions for each class of individuals to improve their ideological and political learning ability. The experimental results indicate that the proposed method is feasible and effective. The research method of ideological and political course ability proposed in this paper is of great significance to the promotion of ideological and political education in the era of big data.

## 1. Introduction

Artificial intelligence technology, as an important driving force of future educational reform, not only profoundly affects the traditional teaching mode of ideological and political education in colleges and universities but also poses a severe challenge to the orientation of the roles of teachers and students in the process of ideological and political education [1]. Based on the advantages of human-computer cooperation, cross-border integration, cocreation, and sharing brought by artificial intelligence technology, the personalized education model advocated by modern educational ideas has a practical basis.

Throughout the practice of educational informatization at home and abroad, the practical conditions for applying artificial intelligence technology to the field of education

have matured, and related theoretical research and practical exploration are being carried out simultaneously [2]. Du et al. [3] proposed an English network teaching method based on artificial intelligence technology and WBIETS system, improving the deep learning network and taking it as the core algorithm of WBIETS system. Sun et al. [4] put forward the decision tree algorithm and the implementation model of English teaching evaluation based on neural network, which could help teachers improve their education level and students' English scores. The collaborative recommendation algorithm obtains a good accuracy in the course recommendation task according to the history of students' course selection records [5, 6]. In the big data environment, machine learning is used to predict learning results in online courses [7].

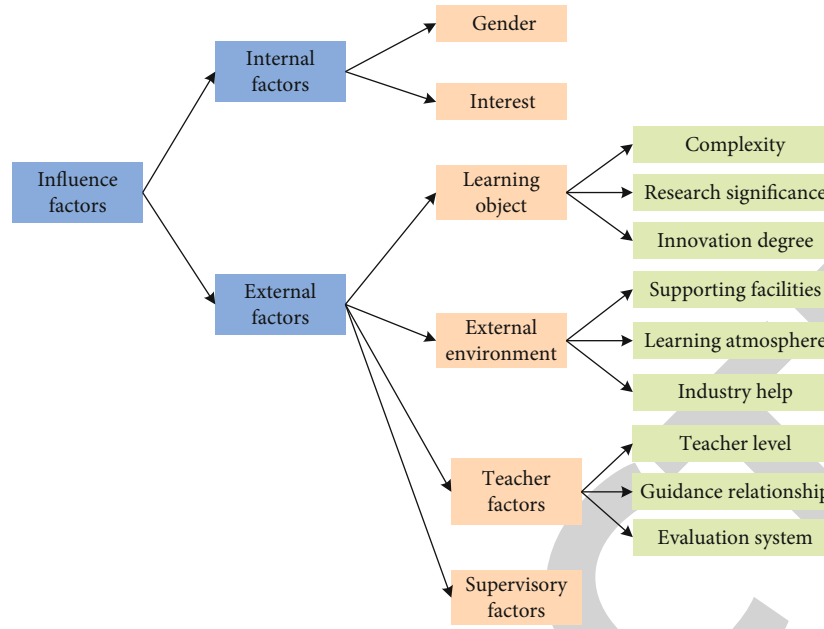


FIGURE 1: Related factors of graduate students’ ideological and political learning ability.

TABLE 1: Statistical table of sample distribution ( $n = 1200$ ).

Category	Project	Quantity	Percentage	Category	Project	Quantity	Percentage
Gender	Man	569	45.50%	Learning atmosphere	Good	527	42.40%
	Woman	681	54.50%		Common	723	57.80%
Interest	High	551	44.10%		Enormous	310	24.80%
	Low	699	55.90%	More	321	25.70%	
Degree of difficulty	Difficult	669	53.50%	Industry help	Common	359	28.70%
	Easy	581	46.50%		Less	210	16.80%
Research significance	Great	434	34.70%		Minimum	50	4.00%
	Common	816	65.30%	Teacher level	Higher	916	73.30%
Degree of innovation	High	681	54.50%		Common	334	26.70%
	Supporting facilities	Low	569	45.50%	Learning relationship	Very harmonious	235
Perfect		1166	85.30%	Fairly harmonious		644	51.50%
Imperfect		184	14.70%	Common		297	23.80%
Supervisor	Timely and accurate	956	76.50%	Evaluation system	Extremely discordant	74	5.90%
	Need to be improved	294	23.50%		Perfect	1195	81.20%
				Imperfect	235	18.80%	

The ideological and political theory course in colleges is the main channel to strengthen and improve the ideological and political education of students and postgraduates. In China, the demand and trend of the integration and innovation of artificial intelligence technology and ideological and political education are becoming more and more obvious, while there are still some bottlenecks in the integration process. Therefore, educational practitioners should reflect from the perspective of the gap between traditional teaching mode and modern technology, providing a three-dimensional thinking for the practice of “intelligent thinking and politics” in colleges and universities in China.

Educational data mining and learning analysis are new research fields. It is worth studying if various statistical and

machine learning methods are applied to enhance ideological and political classroom education. Neural network and clustering algorithm are commonly used data mining methods. Neural network is widely used in pattern recognition, analysis, control, and prediction. Literature [8] proposes research on the optimization of scientific research performance management based on BP (back propagation) neural network. This algorithm uses neural network to construct the performance evaluation model of social science research in colleges and universities. The experimental results demonstrate that the model is an efficient evaluation method. BP neural network extracts six paper features, two journal features, nine author features, eight reference

TABLE 2: Evaluation score of graduate students' ideological and political learning ability.

Evaluation score of ideological and political learning ability			Theoretical achievement		
			Be poor	Common	Good
Participation in ideological and political ability competition	Participated in	Win a prize	3	6	9
		Unawarded	2	5	8
	Did not attend	1	4	7	

TABLE 3: Statistical table of correlation and difference between postgraduate's learning ability and its internal factors.

Project	Relevance $P$	Difference $S_{ig}$
Gender	0.283	0.161
Interest	0.007	0.003

features, and five early citation features to predict the citation times of a single paper [9].

In the era of big data, clustering analysis of massive data is an important research direction. Clustering algorithm has been widely used in education, e-commerce, transportation, and other fields [10].  $k$ -means is widely used because of its high efficiency and easy understanding. However, the initial clustering center of traditional  $k$ -means algorithm is randomly selected, which easily leads to the clustering result falling into local optimum [11]. Meanwhile, the random method will also lead to the instability of the initial clustering center selection, which makes the clustering result unstable. Many scholars have done a great number of researches on the initial clustering center selection of  $k$ -means algorithm. For example, adaptive cuckoo and gravity search algorithm are used to optimize the initial cluster center by introducing swarm intelligence algorithm. However, the algorithm has not been applied because of its complexity [12]. Some scholars optimize the initial clustering center from the perspective of sample data density and distance. For example, Kalevala et al. [13] considered local distance to optimize the algorithm. Tang et al. [14] consider density and distance step by step, but calculating the data weight increases the time consumption. Yu et al. [15] proposed LOF algorithm to build a potential background dictionary from the perspective of local density and effectively excluded abnormal objects by calculating local density and abnormal values, yet there was a problem of inaccurate selection of cluster centers.

Domestic colleges and universities are also paying more and more attention to the cultivation of ideological and political classroom thinking ability and innovation ability of college students. Nevertheless, the effect is not obvious. This paper studies how to improve the ideological and political learning ability of postgraduates. Firstly, the influencing factors of learning ability are preliminarily determined through data collection and screening of effective information. Then, a specific standard to measure the abstract term learning ability is formulated according to BP neural net-

work. Thus, the correlation between learning ability and influencing factors is analyzed to screen out the influencing factors with significant correlation. Finally, these factors will be used as variables to improve  $k$ -means clustering, and specific suggestions will be put forward for each type of individuals.

## 2. Algorithm Model in This Paper

*2.1. Collect Data to Preliminarily Determine the Influencing Factors.* This paper investigates the factors that affect students' learning ability in ideological and political class. Data were collected by literature survey, questionnaire survey, and focus interview. The interview outline is listed on the basis of literature survey. Graduate students and graduate tutors from different majors were invited in the form of interview groups to deeply explore the internal and external factors related to learning ability. The internal factors affecting learning ability include gender and interest, as shown in Figure 1.

External factors include learning objects, external environment, teacher factors, and supervision factors. The learning object is subdivided into the difficulty, innovation, and research significance of the subject. The external learning environment is subdivided into teaching facilities, learning atmosphere, and ideological and political help to the industry. Teachers' factors are subdivided into teachers' level, guiding-learning relationship, and evaluation system. Based on this, a questionnaire was compiled. In this study, 1230 formal questionnaires were distributed, and 1200 were effectively recovered. The effective questionnaire recovery rate was 97.56%, which was statistically significant. Sample distribution is shown in Table 1.

### 2.2. Evaluation Model of Students' Learning Ability Based on BP Neural Network

*2.2.1. BP Network Design.* The design of BP network includes the input layer, the output layer, the number of nodes in the hidden layer, and the transfer function between layers.

(1) *Enter the Number of Layer Nodes.* The number of input layer nodes corresponds to the number of evaluation indexes. Based on many research findings, the evaluation indexes are test scores, creative ability, scientific research ability, paper writing ability, and competition level. According to the analysis, the evaluation indexes of graduate students' ideological and political learning ability are as

TABLE 4: Statistical table of correlation and difference between postgraduates' learning ability and external factors.

Project		Relevance $P$	Difference $S_{ig}$
Learning object	Difficulty degree of subject	0.01	0.015
	Research significance	0.131	0.253
	Degree of innovation	0.009	0.02
External environment	Learning atmosphere	0.003	0.084
	Teaching facilities	0.878	0.68
	Industry help	0	0.005
Teacher factor	Teacher level	0.01	0.014
	Learning relationship	0.009	0.012
Supervision factor	Evaluation system	0.007	0.013
	Supervising work	0.005	0.006

follows:  $5(x_1 - x_5)$ , so these five evaluation indexes are taken as input nodes  $n = 5$ .

(2) *Number of Output Layer Nodes.* This paper takes the final evaluation result as the output of the network. Number of output nodes  $m = 1$ .

(3) *Number of Hidden Layer Nodes.* Based on the Kolmogorov theorem proved by Hecht-Nielsen, three-layer BP neural network can approximate any continuous function under reasonable structure and proper weight conditions. Therefore, the three-layer BP network is selected in order to simplify the calculation.

There is no optimal theoretical method to determine the number of hidden layer nodes, which is a more complicated problem. Too few nodes will lead to poor fault tolerance. Too much network training time will be increased and generalization ability will be reduced. Therefore, the designer's experience and many experiments are usually used to determine the optimal number of hidden nodes. This paper chooses the number of implicit nodes  $s = 3$  after empirical analysis.

### 2.2.2. BP Network Learning Algorithm

- (1) Input: dataset  $D$ . Learning rate  $\alpha$ :  $\alpha \in [0, 1]$ . Stop condition: the error rate specifies the threshold  $\theta$ . The maximum number of iterations is  $T$ .
- (2) Initial link weight:  $T = 0$ ,  $g_{pq}^{(T)}$ ,  $s_q^{(T)}$ ,  $\omega_{qk}^{(T)}$ ,  $b_k^{(T)}$
- (3) Input samples  $(u_h, x_h)$  in turn, and calculate the expected predicted value  $x_k$
- (4) Update the link weight:

$$\begin{aligned}
 g_{pq}^{(T+1)} &= g_{pq}^{(T)} + \Delta g_{pq}^{(T)}, \\
 s_q^{(T+1)} &= s_q^{(T)} + \Delta s_q^{(T)}, \\
 \omega_{qk}^{(T+1)} &= \omega_{qk}^{(T)} + \Delta \omega_{qk}^{(T)}, \\
 b_k^{(T+1)} &= b_k^{(T)} + \Delta b_k^{(T)},
 \end{aligned} \tag{1}$$

where  $g_{pq}^{(T)}$ ,  $\omega_{qk}^{(T)}$  represents the forward propagation connection weight.  $s_q^{(T)}$ ,  $b_k^{(T)}$  represents the back propagation connection weight

- (5)  $T = T + 1$ , judge whether the stopping condition is met. If the model error is less than the specified threshold or the maximum iteration times are greater than the threshold, stop the iteration. Otherwise, return to Step 3
- (6) Output:  $g_{pq}^{(T)}$ ,  $s_q^{(T)}$ ,  $\omega_{qk}^{(T)}$ ,  $b_k^{(T)}$ . The output value of the  $k$ th neuron in the output layer is

$$\hat{x}_k = f \left( \sum_{q=1}^d \omega_{qk} z_q + b_k \right), \tag{2}$$

where  $z_q$  indicates hidden input

*2.2.3. Application of BP Network Model.* Based on the above analysis, this paper uses Python to build a three-layer BP neural network with 5 input neurons, 3 hidden layer neurons, and 1 output neuron. When the five evaluation indexes: examination score, creation ability, scientific research ability, thesis writing ability, and competition level, are used as inputs, the input data (training samples) need to be normalized. The linear function is used as the transfer function because the input layer only transmits data. The neurons in the hidden layer adopt S-type function (Sigmoid function). At the same time, the learning rate is 0.6, and the convergence error threshold is 0.001. Finally, the evaluation results were reverse-normalized and the evaluation scores were obtained as shown in Table 2.

The number of training samples selected is 200, which can satisfy the fitting. 100 people are employed to predict the test model. The prediction results are compared with the expert evaluation results, and the prediction accuracy is observed. Finally, it demonstrates that the evaluation model of graduate students' ideological and political learning ability based on BP neural network is reasonable and effective.



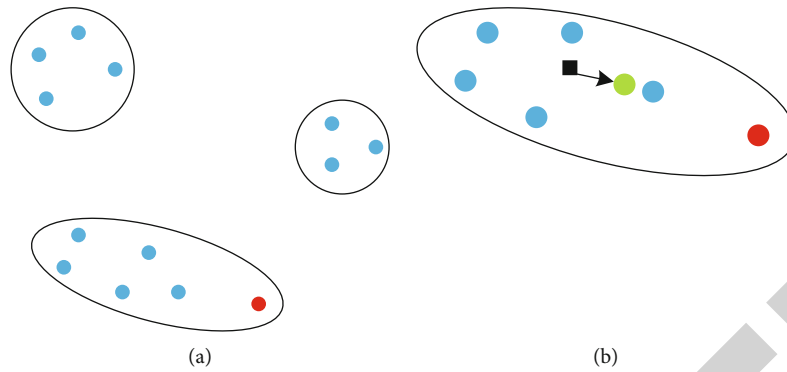


FIGURE 2: Replacement of outliers and pseudocenters.

2.3. *Screening the Significant Influencing Factors of Ideological and Political Learning Ability.* The influencing factors of graduate students' ideological and political learning ability collected by qualitative investigation methods such as focus interview and expert discussion are subjective and can only be defined as a preliminary scope. This paper studies the correlation degree between these factors and ideological and political learning ability in quantitative form after determining the measurement standard according to BP neural network. In this way, the factors with significant correlation can be screened out, and the weak correlation factors can be filtered out, ensuring the accuracy of the research. Based on the evaluation score of ideological and political learning ability obtained by the BP neural network mentioned above, the correlation degree between the internal and external influencing factors such as ideological and political learning ability and interest, learning atmosphere, evaluation system, teacher's teaching, and ideological and political learning ability is studied. In this study, SPSS 22.0 was used for Spearman correlation analysis.

The Spearman correlation coefficient between two random variables  $u$  and  $x$  is recorded as  $r$  [16], and its formula is

$$r = 1 - \frac{(6 \sum_{p=1}^n D_p^2)}{[n(n^2 - 1)]}, \quad (3)$$

where

$$\sum_{i=1}^n D_p^2 = \sum_{p=1}^n (U_p - V_p)^2, \quad (4)$$

where  $u$  represents the evaluation score of learning ability.  $x$  represents 9 significant influencing factors.  $U_p$  and  $V_p$  represent the rank after sorting variables  $u$  and  $x$ , respectively.  $n$  represents the sample size.

2.3.1. *Research on Internal Influencing Factors.* Table 3 is a statistical table of the correlation and difference between postgraduate's learning ability and internal influencing factors. According to the correlation test, gender and interest are significantly related to learning ability ( $P < 0.01$ ).

According to the difference test, there are significant differences between the two variables and learning ability ( $P < 0.05$ ).

There is no significant correlation between gender and learning ability ( $P > 0.01$ ), and there is no significant difference between gender and learning ability ( $P > 0.05$ ).

Interest and ideological and political learning ability have a very significant correlation ( $P < 0.01$ ), and the difference between interest and learning ability is extremely significant ( $P < 0.05$ ). Among them, the more interest in learning, the stronger the learning ability, indicating a positive correlation trend. This phenomenon also accords with people's consistent thinking. The more interested you are, the more time and energy you put into it, and the stronger your ideological and political thinking ability.

2.3.2. *Research on External Influencing Factors.* Table 4 is a statistical table of the correlation and difference between graduate students' ideological and political learning ability and external influencing factors. The correlation test indicates that the difficulty and innovation degree of the subject in the learning object, the learning atmosphere and industry help in the external environment, all variables in the teacher factors and supervision work have significant correlation with the ideological and political learning ability ( $P < 0.01$ ) and significant difference ( $P < 0.05$ ). The correlation and difference of other variables are not significant.

Learning object: the difficulty and innovation degree of the subject in the learning object have a very significant correlation with the learning ability ( $P < 0.01$ ), and the difference in the influence on the ideological and political learning ability is extremely significant ( $P < 0.05$ ). However, the relevance and difference of research significance are not notable. Among them, the higher the learning ability, the higher the difficulty and innovation degree of the subject. This just indicates that people with strong ideological and political learning ability have stronger ability to solve difficult problems, while the significance of research is the selectivity of topics, which has little to do with learning ability.

The external environment: the learning atmosphere and industry help in the external environment have a very significant correlation with the ideological and political learning ability ( $P < 0.01$ ), and the difference in their influence is extremely significant ( $P < 0.05$ ). However, the relevance

and difference of teaching facilities are not significant. Among them, the study of ideological and political courses has a great relationship with the learning atmosphere of the school. The stronger the learning atmosphere, the higher the enthusiasm for learning ideological and political affairs. If the future industry needs more ideological and political education, the demanders will study more enthusiastically.

All the variables in teachers' factors have a very significant correlation with the ability of ideological and political learning ( $P < 0.01$ ), and they have a significant influence on the ability of ideological and political learning.

The difference of influence is extremely enormous ( $P < 0.05$ ). Among them, the higher the level of teachers and the more concerned about students, the higher the students' learning enthusiasm. The stricter the evaluation system is, the harder students will study in order to pass the exam, which is positively related to their learning ability.

Factors of supervision: there is a very significant correlation between supervision and ideological and political learning ability ( $P < 0.01$ ), and the difference of influence on ideological and political learning ability is extremely remarkable ( $P < 0.05$ ). Among them, the timelier the teacher's supervision is done, the students will naturally keep up with the learning progress in time.

In this study, questionnaire survey and group discussion were used to explore the ideological and political learning ability and influencing factors of postgraduates, and the following conclusions were drawn. (1) Both internal and external factors of ideological and political learning ability had significant influence on it. Among them, the internal factors include interest, and the external factors include the difficulty and innovation of the subject in the learning object, the learning atmosphere, and industry help in the external environment, all variables in the teacher factors and supervision. (2) Interest and industry help have the greatest correlation with ideological and political study.

**2.4. Improve the Clustering of Significant Influencing Factors of  $k$ -Means Algorithm.** In order to improve the clustering accuracy of significant influencing factors of ideological and political ability, this paper proposes an improved  $k$ -means algorithm DC  $k$ -means (density parameter and center replacement  $k$ -means) based on density parameters and center replacement. The algorithm uses the density parameters of data objects to gradually determine the initial cluster center and uses the center replacement method to update the initial center that deviates from the actual position. Therefore, DC  $k$ -means is more accurate than the traditional clustering algorithm.

The DC  $k$ -means proposed in this paper firstly determines the initial cluster center by calculating the density parameters of each data object in the dataset, avoiding the unstable clustering result caused by randomly selecting the initial cluster center. Secondly, the biased cluster centers generated by the traditional  $k$ -means algorithm are replaced to avoid the influence of outliers on the clustering results.

**2.4.1. Selection of Initial Cluster Centers Based on Density Parameters.** DC  $k$ -means adopts the strategy of selecting

TABLE 5: Software and hardware configuration environment of the experiment.

CPU	Inter(R) Core (TM) i7-8565U CPU @ 1.80 GHz
RAM	LPDDR3 2133 MHz (8 GB)
Hard disk	NVMe PCIe high-speed solid-state drive
OS	Microsoft Windows 10 Enterprise (64 bit)

cluster center based on density parameter increment. This section and subsequent discussions assume that in Euclidean space  $R^m$ , dataset  $D = \{y_1, y_2, \dots, y_n\}$  contains  $n$  data objects. Every object  $y_i = \{y_{p1}, y_{p2}, \dots, y_{pm}\}$  has  $m$  attributes. Dataset  $D$  is divided into  $k$  clusters by a clustering algorithm  $C = \{C_1, C_2, \dots, C_K\}$ , where  $|C_K|$  is the number of data objects contained in the class cluster  $C_K$ . The corresponding center point of each cluster in cluster set  $C$  is  $V = \{V_1, V_2, \dots, V_K\}$ . Euclidean distance  $d(y_p, y_q)$  between any two data objects  $y_p$  and  $y_q$  in dataset  $D$  is defined as

$$d(y_p, y_q) = \sqrt{(y_{p1} - y_{q1})^2 + (y_{p2} - y_{q2})^2 + \dots + (y_{pm} - y_{qm})^2}. \quad (5)$$

Based on Euclidean distance, the maximum distance (LaDist) and minimum distance (SmDist) between all data objects are defined as follows:

$$\begin{aligned} \text{Laipst} &= \sum_{p=1}^{n-1} \max_{1 \leq p < q \leq n} d(y_p, y_q)^2, \\ \text{Smipst} &= \sum_{p=1}^{n-1} \min_{1 \leq p < q \leq n} d(y_p, y_q)^2. \end{aligned} \quad (6)$$

Although it is assumed above that the dataset  $D$  is divided into  $k$  clusters, the number of data objects in each cluster generated by different clustering algorithms may be different. As the number of data objects changes, the distance between each data object pair will also alter. Define the dynamic average distance (Divests) based on the maximum distance and minimum distance between all data objects:

$$\text{Divests} = \frac{(\text{LaDist} + \text{SmDist})}{(2 * K)}, \quad (7)$$

where  $k$  is the number of clusters into which dataset  $D$  is divided. According to the dynamic average distance, the density parameter can be defined as follows.

In dataset  $D$ , the number of data objects in the circular area with  $y_p$  as the center and Divests as the radius is called

TABLE 6: Description of 8 simulated datasets and 8 UCI real machine datasets.

Datasets	Points number	Cluster number	Dimension
Normal	200	5	2
D900	900	9	2
R15	600	15	2
N7	28000	7	2
K3	102000	3	2
Curve	180	3	2
Pathbased	300	3	2
Semicircle	300	3	2
Iris	150	3	4
Seeds	210	3	7
Haberman	306	2	3
Column	310	3	6
Hayes-Roth	132	3	5
Ionosphere	351	2	34
PageB locks	5473	5	10
Magic	19020	2	10

TABLE 7: Comparison of precision purity of different algorithms.

Datasets	$k$ -medoids	$k$ -means++	DC $k$ -means
Normal	68.52	82.57	99.5
D900	75.29	81.13	99.78
R15	73.22	92.24	99.67
N7	82.3	88.16	100
K3	86.9	86.9	100
Curve	67.5	89.91	99.22
Pathbased	61.42	75.27	75.25
Semicircle	88.05	100	100
Iris	77.09	83.22	92.67
Seeds	69.64	76.55	89.12
Haberman	72.92	73.31	86.97
Column	70.41	72.25	72.31
Hayes-Roth	43.37	47.99	47.99
Ionosphere	67.12	71.33	72.53
PageB locks	91.03	90.99	92.8
Magic	65.89	66.09	66.48

the density parameter of data object  $y_p$ , that is,

$$\rho(y_p, \text{DyAveDpst}) = \sum_{p=1, q \neq p}^n j(\text{DyAveDpst} - d(y_p, y_q)), \quad (8)$$

where  $j()$  is a jump function.  $j(y) = 1$  when  $y \geq 0$ ; otherwise,  $j(y) = 0$ .

In the process of finding the center of initial cluster, most density-based clustering algorithms are more dependent on external parameters in the choice of neighborhood radius.

Improper parameter selection will greatly affect the performance of the algorithm. To solve this problem, this paper first defines the dynamic average distance (Divests) based on the maximum distance and minimum distance between all data objects. The distance dynamically changes with each iteration, which can obtain the neighborhood radius of different division stages in time, to determine the density parameters more efficiently and stably and reduce the influence of external parameters on clustering results.

**2.4.2. Replacement of Cluster Center.** Another defect of traditional  $k$ -means algorithm is that it is very sensitive to outliers of dataset. In fact, some initial cluster centers generated by traditional  $k$ -means algorithm are not real cluster centers in the target dataset (this paper calls these points “pseudocenters”). In addition, the position of the generated cluster center will deviate from that of the actual cluster center due to the influence of outliers. This problem will seriously reduce the accuracy of traditional  $k$ -means algorithm.

The center generated by  $k$ -medoids clustering algorithm is always the real data point of the target dataset. Inspired by  $k$ -medoids algorithm, this paper proposes to update the pseudocenters generated by traditional  $k$ -means algorithm by using center replacement method. Once the  $k$ -means algorithm creates a pseudocenter for a class cluster, it will be replaced by the nearest point in the class cluster. At the same time, the neighboring point should be as far away from the outliers of this cluster as possible. In the process of clustering, the pseudocenter centers are updated in turn until all the real cluster centers are specified.

Figure 2 shows the replacement process of clusters containing outliers and their corresponding pseudocenters. In Figure 2, the blue dots represent normal data objects and the red dots represent outliers. Figure 2(a) shows a dataset composed of three clusters randomly generated by Python software. The cluster at the bottom left of Figure 2(a) contains an outlier represented by a red dot. Figure 2(b) shows the replacement process of the center point of this kind of cluster. Without outlier interference, the traditional  $k$ -means algorithm takes the object represented by the black rectangle as the cluster center. However, if the outliers in the cluster are considered, the obtained cluster center will deviate from the “actual” cluster center. As shown in Figure 2(b), along the arrow direction, the center of the cluster moves from the position of the black rectangle to the position of the green rectangle. This deviation will lead to the performance degradation of clustering algorithm. In fact, with the deviation of cluster center, many data objects that do not belong to this cluster will be included in the next iteration of clustering algorithm. In Figure 2(b), this paper uses an improved method to take the blue dot in the red rectangular box as the final cluster center. The center is the actual data object, which is closest to the black rectangle and as far away from the red outlier as possible.

**2.4.3. DC  $k$ -Means Process and Time Analysis.** The flow of DC  $k$ -means algorithm is shown in Algorithm 1. DC  $k$ -means algorithm can not only find the center of initial cluster stably but also can deal with outliers. In Algorithm 1: (1)

TABLE 8: Summary of correlation of influencing factors.

Project	Interest	Teacher level	Degree of innovation
<i>P</i> value	0.007	0.01	0.009
Project	Gender	Learning relationship	Evaluation system
<i>P</i> value	0.283	0.009	0.007
Project	Research significance	Teaching facilities	Learning atmosphere
<i>P</i> value	0.131	0.878	0.003
Project	Supervising work	Difficulty degree of subject	Industry help
<i>P</i> value	0.005	0.01	0

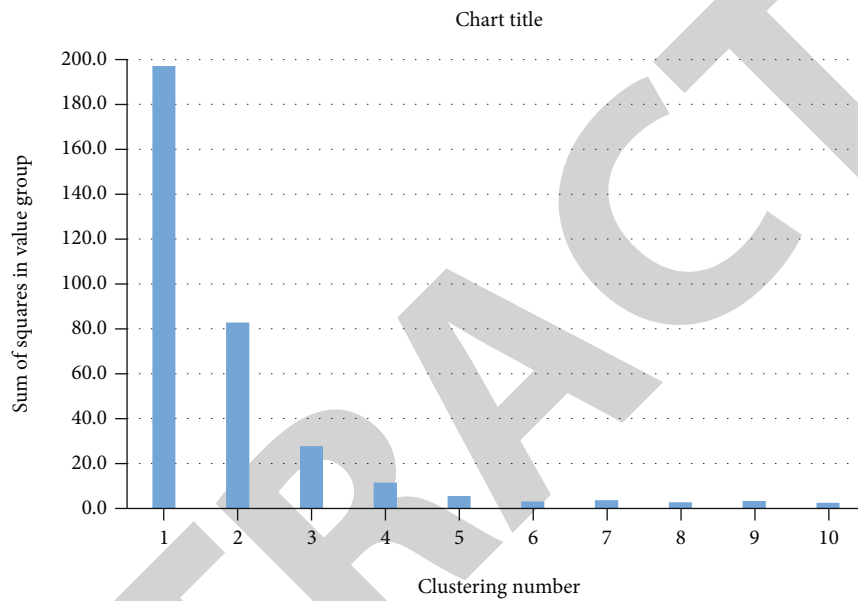


FIGURE 3: Sum of squares in value group under different clustering numbers.

TABLE 9: Final cluster center.

	Cluster				
	1	2	3	4	5
Learning ability evaluation score	7	8	1	4	1
Interest	High	High	Low	Low	Low
Learning relationship	Very harmonious	General harmony	Common	Common	General harmony
Industry help	Common	Enormous	Smaller	Larger	Enormous
Difficulty degree of subject	Easy	Difficult	Easy	Difficult	Difficult
Degree of innovation	Low	High	Low	Low	High
Supervision factor	Accurate and timely	Accurate and timely	Accurate and timely	Need to be improved	Need to be improved
Learning atmosphere	Good	Good	Common	Good	Common
Teacher level	Higher	Common	Higher	Higher	Higher
Evaluation system	Imperfection	Improve	Improve	Improve	Improve

calculate the dynamic average distance between all data objects in dataset  $D$ . (2) Calculate the density parameters of all data objects. (3) Find  $k$  initial cluster centers of dataset  $D$  and put them into set  $V$  according to the density parameter. Steps (4)–(8) realize the final division of dataset  $D$ . Specifically, step (5) initializes each cluster. (6) Put the data object into the corresponding class cluster. (7) Update the cluster center by using the center replacement method.

Input: dataset  $D = \{y_1, y_2, \dots, y_n\}$ , number of clusters  $K$ .

Output:  $C = \{C_1, C_2, \dots, C_K\}$  of dataset  $D$ .

Algorithm:

- (1) Calculate the dynamic average distance (Divests) between any pair of data objects  $(y_p, y_q)$  in dataset  $D$
- (2) For  $p = 1, 2, \dots, n$ , do calculate the density parameter  $\rho(y_p, \text{DyAveDpst})$  of the data object  $y_p$
- (3) For  $k = 1, 2, \dots, K$ , do//find  $k$  initial cluster centers and put them into the initial cluster center set  $V$ . Select the data object  $y$  with the highest density parameter from dataset  $D$ , and delete all data objects about  $y$  from dataset  $D$ . Set  $y$  as the center of the  $k$ th initial cluster and  $v_k$ .  $V \leftarrow v_k$ ;//put  $v_k$  into set  $V$  in the center of the initial cluster
- (4) Repeat
- (5) Let  $C_k = \emptyset (1 \leq k \leq K)$ //initialize each cluster  $C_k$
- (6) For  $p = 1, 2 \dots, n$  do//put each data object in  $D$  into the corresponding cluster. Calculate the distance between the centers of each cluster in data objects  $y_p$  and  $V$ . Put  $y_p$  into the corresponding class cluster according to the nearest principle
- (7) For  $k = 1, 2, \dots, K$ , do//update the center of each cluster. Calculate the distance between the center  $v_k$  of the cluster  $C_k$  and other data objects in the cluster; find the nearest data object  $(v_k')$  to  $v_k$ . At the same time,  $(v_k')$  should be as far away from the outliers in  $C_k$  as possible. If  $v_k \neq v_k'$   $v_k \leftarrow v_k'$ // $v_k'$  is updated as the new center of class  $C_k$
- (8) Until  $\sum_{i=1}^K \sum_{x \in C_i} d(v_i, x)^2$  converted//until the standard function  $\sum_{i=1}^K \sum_{x \in C_i} d(v_i, x)^2$  converges to a constant, at which point  $v_k$  is the new center of class  $C_k$

Assume that there are  $n$  data objects in dataset  $D = \{y_1, y_2, \dots, y_n\}$ . Every data object  $y_i = \{y_{i1}, y_{i2}, \dots, y_{im}\}$  is a dimension vector of  $m$ . The DC  $k$ -means algorithm will divide dataset  $D$  into  $k$  clusters  $C = \{C_1, C_2, \dots, C_K\}$  through  $h$  iterations.

According to the individual's theoretical and practical ability, BP neural network divides the learning ability of ideological and political education into nine levels. Subjective and abstract indicators are standardized, making individuals more different. It is found that the factors

significantly related to the evaluation scores of ideological and political learning abilities are interest, guidance and learning relationship, industry help, project difficulty, innovation degree, teachers' level, supervision factors, evaluation system, and learning atmosphere. Those factors that have significant correlation and difference with the ideological and political learning ability and the evaluation score of the ideological and political learning ability are selected as cluster variables so that there are significant differences among all kinds, and the significance of cluster analysis is clarified. In the experimental part, DC  $k$ -means cluster analysis will be used to classify different research individuals, and according to the characteristics of each category, targeted suggestions will be put forward for their graduate students to improve their ideological and political learning ability.

### 3. Experiment and Analysis

**3.1. Experimental Configuration and Indicators.** The experimental code is written by Python language, aiming to verify the actual effect of this algorithm in the analysis of learning ability of ideological and political courses in colleges and universities. The specific software and hardware configuration environment of the experiment is listed in Table 5.

The experimental dataset for verifying DC  $k$ -means clustering algorithm consists of 8 simulation datasets and 8 UCI real machine learning datasets, as shown in Table 6. The data used to verify the ideological and political ability analysis algorithm in this paper consists of real student data collected in Section 2.1.

**3.2. Performance Indicators.** The accuracy of clustering results can usually be measured by external evaluation indexes, such as  $F$ -measure, entropy, and purity. This paper uses purity index to evaluate the accuracy of clustering results, which is defined as

$$\left( \text{purity} = \sum_{p=1}^K \frac{|C_p|}{n} \max \left( \frac{m_{pq}}{|C_p|} \right) \right), \quad (9)$$

where  $|C_p|$  is the number of all data objects in the cluster  $C_p$ .  $m_{pq}$  is the number of members of class cluster  $C_p$  belonging to class cluster  $C_q$ .  $K$  is the number of clusters in the target dataset.  $n$  is the number of data objects contained in the target dataset. In this paper, the value of purity index is converted into percentage for comparison.

**3.3. Comparative Experiment.** In the experiment, the clustering results generated by different datasets are evaluated.

Table 7 lists the processing accuracy of  $k$ -medoids,  $k$ -means++, and DC  $k$ -means for the 16 datasets listed in Table 6. The DC  $k$ -means algorithm can keep the same result every time, so it only needs to be run once. On the contrary, the accuracy of the other two algorithms is the average of 10 repeated experiments. As can be seen from Table 6, since the center of the initial cluster is randomly selected, the accuracy of  $k$ -medoids algorithm is the worst

among the three algorithms. In  $k$ -means++ algorithm, except for the first initial cluster center, other cluster centers are no longer randomly selected. Therefore, the accuracy of  $k$ -means++ algorithm is better than that of  $k$ -medoids algorithm. DC  $k$ -means introduces the density parameter to select the initial cluster center and adopts the center replacement strategy in the update stage. Therefore, the clustering accuracy of DC  $k$ -means is the best among the three clustering algorithms, indicating the effectiveness of the improved  $k$ -means clustering algorithm designed in this paper.

**3.4. Feasibility Analysis.** According to the individual's theoretical and practical ability, the learning ability is divided into 9 levels by BP neural network, which standardizes subjective and abstract indicators, thus making individuals more different. Through correlation analysis, it is found that the factors significantly related to the evaluation score of ideological and political learning ability are interest, guidance and learning relationship, industry help, project difficulty, innovation degree, teachers' level, supervision factors, evaluation system, and learning atmosphere. These factors with significant correlation and difference with ideological and political learning ability and the evaluation score of ideological and political learning ability are selected as cluster variables to make significant differences between various types, so as to clarify the significance of cluster analysis. The following uses the improved cluster analysis method to classify different research individuals and puts forward targeted suggestions for their graduate students to improve their ideological and political learning ability according to the characteristics of each category.

According to Table 8, among the preliminarily determined influencing factors, only gender, research significance, and teaching facilities have little influence on ideological and political learning ability. Therefore, the remaining nine factors and dependent variables that are significantly related to the ideological and political learning ability are selected into the classification variables of cluster analysis.

The sum of squares within the group represents the sum of squares of errors of the sample data and their mean values of each level or group, which reflects the dispersion of the observed values of each sample, also known as the sum of squares of errors. In this study, the sum of squares within each group is obtained by using Python language.

$$S_E = \sum_{p=1}^r \sum_{q=1}^{n_p} (y_{pq} - \bar{y}_p)^2, \quad (10)$$

where  $y_{pq}$  is a random variable within the group.  $y_p$  is the sample mean, and  $n$  is the sample size.

Cluster the above selected 10 factors, and calculate the sum of squares within the group corresponding to different cluster numbers, as shown in Figure 3. When the cluster number is 5, the sum of squares within the group basically does not change, so the cluster number  $k$  in this study is 5.

After 50 iterations and reclassification, the final clustering results are as follows.

**3.5. Clustering Results and Related Suggestions.** In order to improve the learning ability of postgraduates, this paper classifies postgraduates into 5 categories by cluster analysis based on the evaluation scores of each postgraduates' influencing factors on learning ability. Finally, according to the characteristics of each category, it puts forward specific suggestions for postgraduates to improve their learning ability. The results are as follows.

The first category: the theoretical knowledge of general industries. For this type of talents, we should start to create opportunities for practical application and encourage them to apply the theoretical knowledge they have learned to practice.

The second category: all-round knowledge-based high-end industries. The industry in which this type of talents is located has the highest requirements for ideological and political learning ability, and the difficulty and innovation degree of the research topics are high. For this class, the most important thing is to equip a strong team of teachers to improve their mathematical research ability.

The third category: other knowledge types in the literary industry. These individuals are at the lowest level in theoretical achievement and practical ability. For this kind of talents, cultivating interest in ideological and political learning is the easiest way to achieve.

The fourth category: the theoretical knowledge of middle-end industries. For this type of graduate students, schools should carry out more activities in ideological and political practice and improve ideological and political literacy to cultivate interest in learning.

The fifth category: other knowledge-based industries in high-end industries. This type of industry has a high demand for ideological and political education. For this type of graduate students, schools should also carry out more practical activities and lectures on improving literacy to cultivate interest and improve the atmosphere of learning.

## 4. Conclusion

The ideological and political theory course in colleges and universities is the main channel to strengthen and improve the ideological and political education of college students. This paper proposes an analysis algorithm based on BP neural network and improved  $k$ -means clustering, aiming to realize the research of students' innovative ability in ideological and political course. The algorithm collects the influencing factors of ideological and political learning ability. And BP neural network is used to quantify the learning ability and solve the problem of index weight. In the meantime, it avoids artificial subjective factors and ensures the reliability of evaluation results. Then, the correlation analysis screens out the influence of ideological and political learning ability on privacy. Finally, an improved DC  $k$ -means clustering algorithm is designed, which is applied to cluster-related ideological and political research individuals. The experimental results demonstrate that the improved clustering algorithm designed in this paper has high clustering accuracy. This paper can effectively analyze the learning ability of ideological and political course based on BP neural

## Research Article

# Building a Performance Management System for Hospitals Based on Diagnosis-Related Group (DRG) Payment

Shaolin Zhao, Yingying Gu, and Zhenju Huang 

*Comprehensive Assessment and Management Department, Nantong First People's Hospital, Nantong, Jiangsu 226001, China*

Correspondence should be addressed to Zhenju Huang; [nthzj00228@163.com](mailto:nthzj00228@163.com)

Received 4 January 2022; Revised 24 January 2022; Accepted 5 February 2022; Published 19 March 2022

Academic Editor: Wen Zeng

Copyright © 2022 Shaolin Zhao et al. This is an open access article distributed under the Creative Commons Attribution License, which permits unrestricted use, distribution, and reproduction in any medium, provided the original work is properly cited.

With the deepening of the national medical and health system reform, various supporting reform measures are being promoted. The reform of medical insurance payment methods is an important part of the process, and payment through diagnosis-related groups (DRGs) will gradually become the main way for medical insurance to pay medical institutions. According to the analysis of the impact of DRG payment on hospital performance management, this research examines the construction and implementation of the internal performance management system (IPMS) based on DRG payment in hospitals. The IPMS based on DRG payment includes four elements: organizational management system, assessment system, communication and feedback system, and information support system. In addition, this study explores how IPMS can be implemented in hospitals, including the preparation before implementation, key points to be grasped during implementation, and considerations to be focused on.

## 1. Introduction

The payment system based on diagnosis-related groups (DRGs) is a popular tool for financing inpatient care. DRGs were born in the US in the late 1960s and have since been introduced in Europe, Australia, and some Asian countries, where they have been localized, resulting in several localized versions of DRGs [1–4]. This kind of system clusters similar patients based on the related data, and the hospital is responsible for paying a constant price for patients treated in the DRGs [5, 6]. The payment system based on DRGs separates the hospital's profits from its underlying cost base, thus moving a significant amount of financial risk from the system level to the hospital level; in other words, the hospitals have to deal with the uncertain financial results related to the provision of healthcare services [7].

Although there are many versions of DRGs, the principles are basically the same between different versions of DRGs and the differences are mainly in the details of case grouping and the coding system. Scholars in China have been interested in DRGs since the late 1980s, and the Beijing version of DRGs (BJ-DRGs), completed in 2008, was the first

complete localized version of DRGs in China. Jian et al. applied a total of 1.3 million inpatient records from 154 hospitals in Beijing in 2008 to explore the performance of DRG systems [8]. Qiao et al. analyzed the factors associated with the influence of DRG-based stroke patients on in-hospital costs in Jiaozuo, Henan province, and offered theoretical instructions for healthcare payment and healthcare resource allocation [9]. Wang et al. adopted multiple linear regression analysis to examine the correlation between the total medical costs of inpatients and the age, gender, length of stay, region, and economic level of the hospital, thus better researching DRG payment systems [10]. In recent years, China has continued to promote the implementation of DRG payment at the national level. In 2017, the government began to promote the piloting of DRG payment nationwide. In 2019, the National Health Insurance Administration (NHA) and others officially identified 30 cities as pilot cities for DRG payment and at the same time released the technical specifications for the national piloting of DRG payment and the grouping scheme; in 2020, NHA released the DRG payment piloting scheme (1.1). In 2020, NHA published the disease diagnosis-related grouping (CDS-DRG) subgrouping plan

(version 1.0), which provides for 376 DRGs. The CHS-DRG marked the completion of the top-level design of the national pilot of DRG payment in China and the beginning of the actual payment stage of DRG payment.

The differences in social and health systems in different countries have led to significant differences in the approaches to hospital performance management. The US has a highly market-based healthcare system with a complex and diverse structure, corresponding to a wide range of health insurance forms. Due to the constraints of the healthcare market and health insurance, hospital performance management is predominantly customer oriented. Also, the US healthcare system is considered to be the most expensive but least effective in the world compared to other countries and the main drivers of healthcare costs are institutionalized medical practices and reimbursement policies, technology-related costs, and consumer behavior [11]. The UK is a typical country with a National Health Service, with particular attention being paid to controlling provider-induced cost inflation. After all, healthcare and related policies are the government's duty in the UK [12]. As a result, performance evaluation of hospitals in the UK focuses on both quality and efficiency. Singapore has a typical dual health service system, meaning that both public and private providers play an important role. This has brought Singapore's healthcare system to the same level as other advanced countries [13]. Hospital performance is first and foremost concerned with how much patients benefit and is evaluated in terms of quality of service, consumption of care, the efficiency of service, and safety of care.

Various management tools and methods have been applied in the performance management of public hospitals, mainly including the balanced scorecard [14–16], key indicators [17, 18], management by objectives [19, 20], 360-degree appraisal [21], and the point counting method. However, they are often focused on the specific application of management methods, mainly on the assessment and evaluation of performance indicators. The results of these assessments are mainly used for the distribution of hospital bonuses, but no systematic research has been carried out on the internal performance management system of public hospitals, which has not played a significant role in promoting the overall development of hospitals. At the same time, as DRG payment is still in the process of being fully promoted in the country, research on the impact of DRG payment on the internal performance management system of public hospitals is not yet detailed and in depth.

## 2. Research Implications

The medical insurance DRG payment refers to the grouping of cases based on clinical diagnosis, treatment modalities, and individual characteristics of the cases. The medical insurance agency predetermines the payment criteria based on the case grouping, and the actual payment is settled according to the number of cases provided by the medical institution according to the criteria of the grouping. Commonly used indicators for evaluating the performance of healthcare services based on DRGs include three dimen-

sions: capacity, efficiency, and safety, of which three indicators, namely, the number of DRG groups, total weights, and hospital and department case mix index (CMI), can be used to evaluate the service capacity of healthcare institutions. The DRGs can be used to evaluate the efficiency of a health facility, and the safety of a health facility can be evaluated by the low-risk group mortality or low- and medium-risk group mortality. The ultimate goal of DRG payment is to achieve a win-win situation for health insurance, medical institutions, and patients, in which government health insurance funds are not overspent and are managed and operated more effectively; medical institutions are more rational in their treatment behavior, medical expenses are reasonably compensated, and medical technology is effectively improved; and patients are able to enjoy better medical services, further reducing the actual medical burden on patients, while the patient billing process will be more convenient and efficient.

DRGs have changed the patient payment model and will have a significant impact on the organization and management of hospital performance, the choice of evaluation indicators, costing methods, quality of care, communication and feedback, and the development of information technology. Hospitals must focus on improving their management and medical service capabilities, improving the quality of their medical services, further improving the level of hospital treatment and services, correcting irregular treatment behavior of medical staff, reducing unreasonable treatment and services, and improving their management and treatment service capabilities. As China's medical insurance system continues to be optimized and improved, medical insurance patients have become a major component of public hospital patients, so changes to the medical insurance payment method have also become an important factor affecting the internal operation and management of public hospitals. It is worthwhile to study how the internal performance management of hospitals can adapt to the impact of the health insurance payment reform on hospitals. This paper examines the construction and implementation of an internal performance management system in public hospitals in the context of DRG payment, with a view to improving the overall operational efficiency and management level of public hospitals, which has important theoretical and practical implications for internal hospital management.

## 3. Building the IPMS for Public Hospitals Based on DRG Payment

*3.1. Overview of IPMS.* IPMS is a set of concepts, principles, procedures, and methods to systematically manage the performance of a hospital at all levels in order to achieve its vision or mission, according to its stage of development, context, and environment, and guided by the overall strategic objectives of the hospital. As shown in Figure 1, IPMS can be divided into four components: organizational management, assessment, communication and feedback, and information support, while the process of performance management is a PDCA continuous improvement process



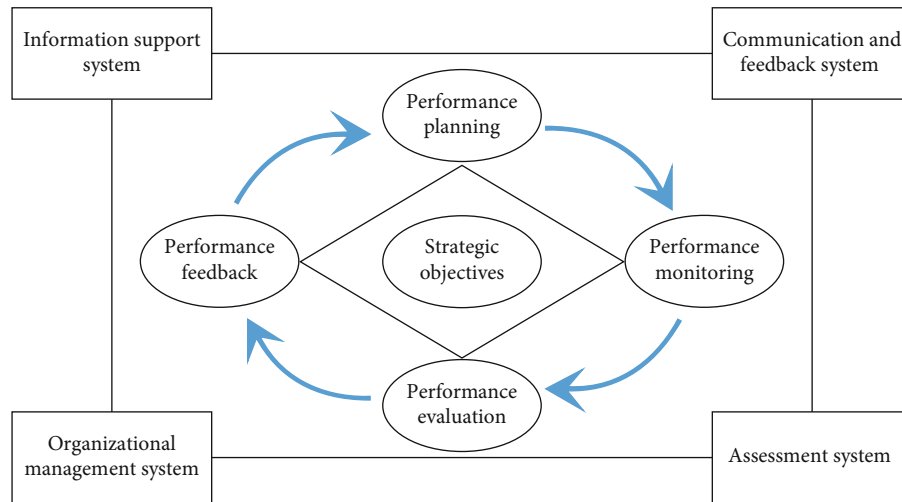


FIGURE 1: Framework of IPMS.

consisting of performance planning, performance monitoring, performance evaluation, and performance feedback.

**3.2. Constructing the Organizational Management System.** The multidisciplinary treatment model is a treatment model in which specialists from various fields in the hospital conduct a comprehensive consultation on a specific case, integrating their opinions and forming the best treatment plan. Performance management in hospitals is a systematic project that requires the participation of multiple departments throughout the hospital. As shown in Figure 2, this system consists of a performance management leadership team composed of personnel from various departments, including finance, personnel, medical, health insurance, information, medical records, and nursing, with a performance management office and, if required, an expert advisory group, which brings together the various management functions of the hospital and provides multidepartmental collaboration to solve problems in performance management.

### 3.3. Constructing the Assessment System

**3.3.1. Workload Assessment.** Departmental workload can be calculated based on DRG case weights, which can be shared between the physician and nursing groups. However, the input parameters in this study are not fixed [22]. The detailed calculation formula is shown as follows:

$$WA = \sum_{i=1}^n CW_i \times CN_i, \quad (1)$$

where WA refers to the workload assessment,  $CW_i$  refers to the  $i$ th DRG case weight, and  $CN_i$  refers to the number of the  $i$ th DRG case.

**3.3.2. Operational Assessment.** The DRG patient groups in the assessment department can be assessed separately for physician and nursing groups, with separate target values

for physician and nursing groups based on the controllability of costs for the physician and nursing groups.

The physician and nursing groups calculate the controllable costs of physicians and nursing care for each DRG group based on clinical pathways and historical data and set physician and nursing care cost targets for each DRG group in conjunction with health insurance payments.

$$OAS_i = \frac{CTV_i}{CC_i}, \quad (2)$$

where  $OAS_i$  refers to the operational assessment score for the  $i$ th DRG case,  $CTV_i$  refers to the cost target value for the  $i$ th DRG case, and  $CC_i$  refers to the current cost for the  $i$ th DRG case.

$$OAS = \sum_{i=1}^n \frac{OAS_i \times CN_i}{TN_i}, \quad (3)$$

where OAS refers to the operational assessment score and  $TN_i$  refers to the total number of DRG cases.

**3.3.3. KPI Assessment.** The KPI indicators are set based on the objectives of hospital performance management, taking into account the quality of medical services, safety of medical services, and operational efficiency and effectiveness. The physician and nursing groups are assessed separately. The detailed assessment indicators and weights are shown in Table 1. The selection of KPI indicators and the weighting of each indicator can be adjusted regularly according to the needs of hospital management and development.

**3.4. Constructing the Communication and Feedback System.** The targets of communication in performance management include both external and internal communication, with external communication mainly referring to hospital business-related authorities (e.g., health insurance and price departments) and internal communication referring to all departments and staff within the hospital. The medical

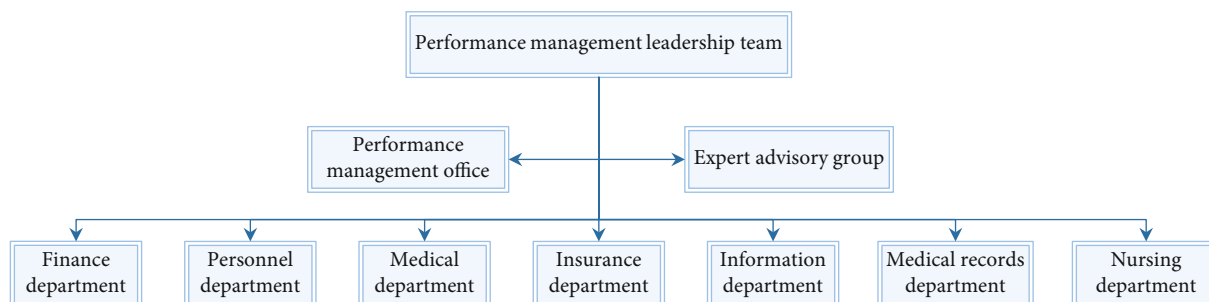


FIGURE 2: Organizational structure of IPMS.

TABLE 1: KPI indicators and weights.

Dimension	KPI indicators for physician groups	Weight	KPI indicators for nursing groups	Weight
Finance	Bed occupancy rate (10%)	20%	Bed occupancy rate (20%)	20%
	Cost consumption index (10%)			
Customer	Patient satisfaction (10%)	10%	Patient satisfaction (10%)	10%
Internal processes	Time consumption index (10%)	40%	Time consumption index (10%)	40%
	Mortality in the low and medium risk group (10%)		Mortality in the low and medium risk group (10%)	
	Incidence of hospital admissions (5%)		Incidence of hospital admissions (10%)	
	Case quality (5%)		Other quality of care and safety (10%)	
Quality and safety of other care (10%)				
Learn and growth	Number of DRG groups (5%)	30%	Number of DRG groups (10%)	40%
	CMI value (10%)		CMI value (10%)	
	Out-of-region patient rates (5%)		Chinese medicine nursing technology (10%)	
	Percentage of TCM medical services (5%)			
	Scientific research capacity (5%)			

insurance department is the policy maker for DRG payment. Hospitals need to keep the medical insurance department informed of the policies related to DRG payment and provide feedback on any problems in the implementation of DRG payment. Under the DRG payment model, hospitals also need to work with the pricing department to improve the reasonableness of their fees and charges.

Performance management is a continuous improvement process, and communication and feedback are very important throughout the whole process of performance management in hospitals. Before performance management is carried out, a series of presentations should be made within the hospital, such as the purpose and meaning of applying DGR-related indicators to performance management and the policies related to DRG payment. Performance targets should be set and refined through staff participation and communication, such as the weighting of DRG cases, DRG group costs, and the setting of KPI indicators. During the performance appraisal process, communication with hospital staff is required to identify any problems that may arise during the performance appraisal process, such as whether DRG cases are correctly grouped and coded and whether DRG case costs exceed the standard. Once the performance appraisal results are finalized, they should be analyzed and fed back to the

appraisee in a timely manner, so that further efforts and improvements can be made, for example, the number of DRG groups in the main hospital team, the total weight of cases, and the ranking of CMI values.

3.5. *Constructing the Information Support System.* The establishment and implementation of performance management systems in hospitals cannot be separated from the support of information technology, and by improving the level of information technology construction, the efficiency and effectiveness of hospital performance management can be improved. Only by establishing a comprehensive performance management information system based on DRG payment, meeting the needs of integrated management of performance management before, during, and after the event and achieving a high degree of integration of business and finance, can performance management objectives be achieved in a timely and efficient manner.

The IPMS based on DRG payment needs to be composed of several submodules to achieve its objectives. As shown in Figure 3, this system includes DRG management, health insurance monitoring, performance evaluation, cost accounting, bonus accounting, and intelligent analysis systems and the data between each submodule system should be able to share and interoperate.

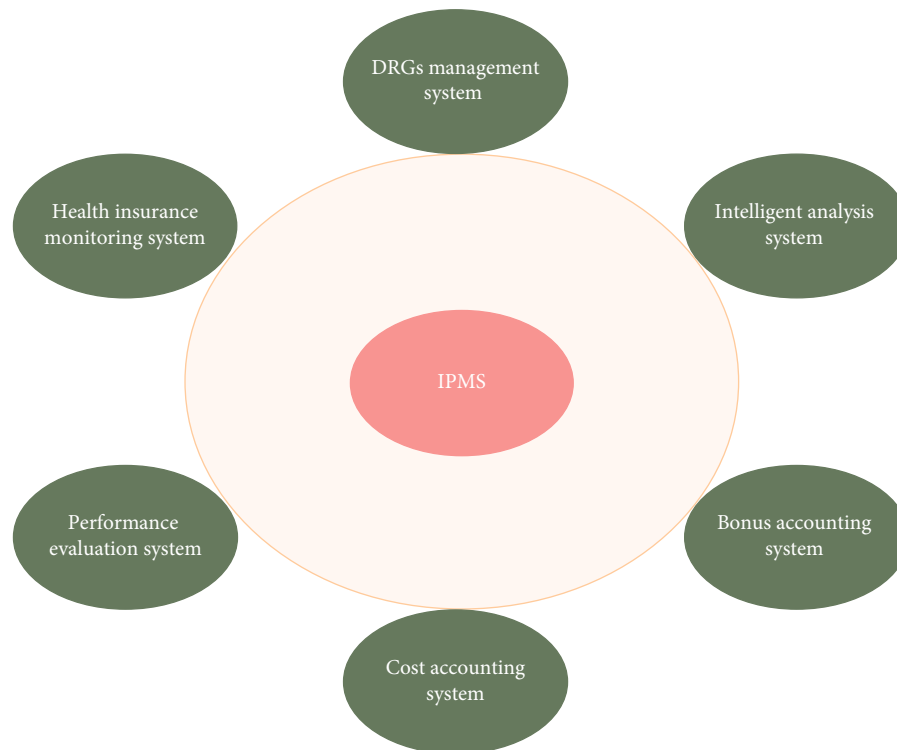


FIGURE 3: Submodule systems in IPMS.

## 4. Implementation of IPMS for Public Hospitals Based on DRG Payment

### 4.1. Preliminary Preparation for Implementation

**4.1.1. Strengthening the Management of the First Page of a Patient Case.** The core principle of DRGs is case grouping, and the first page of the hospital case is the key, which includes the primary diagnosis, surgery, operation, and secondary diagnosis. All of this data comes from the first page of the case, so whether the first page of the case is completed completely and accurately is directly related to whether the case can be entered into the grouping and whether the grouping is correct. Whether the relationship between the main diagnosis of the case and the chief complaint and medical history is reasonable, the relationship between the surgical operation and the main diagnosis, the logical relationship between the secondary diagnosis, the corresponding comorbidities and complications, etc., will all be the basis for whether the case is correctly grouped. Hospitals need to further strengthen the training related to the completion of the first page of the case, guide the medical staff of clinical departments to fill in the first page of the case correctly, and establish a corresponding management system and reward and punishment system.

**4.1.2. Strengthening Clinical Pathway Management.** Regardless of whether it is single-patient payment or DRG payment, clinical pathways are critical. Specifically, the final classification of DRG cases into which group is determined by the clinical medical behavior and the front page of the

case is only a reflection of the clinical medical behavior. Hospitals need to strengthen their understanding of the importance of clinical pathways by leveraging the restraining effect of DRG payment on medical behavior and thus strengthen the management of clinical pathways. At the same time, by strengthening the management of clinical pathways to regulate the treatment and service behaviors of hospital medical staff, it is a very effective means to control the unreasonable increase of medical costs and improve the quality and efficiency of hospital medical services.

**4.1.3. Strengthening Cost Management for Disease Types.** DRGs are a prepayment-based payment system, which is completely different from the item-based postpayment system. As it stands now, many of the items that can generate profits for hospitals will become costs that hospitals will have to bear. Under the DRG payment model, there is a need to shift from the existing departmental costing to more refined and accurate patient costing, as well as to strengthen the management of the departmental drug and consumable secondary pool and to establish target costs and fixed cost standards for each DRG group in the department.

### 4.2. Key Points for Implementation

#### 4.2.1. Enhancing the Integration of DRGs with Performance Management

**(1) Achieving Performance Management Goals.** The realization of the hospital's overall strategic goal is not only the main starting point of the hospital's IPMS but also the main target task that the hospital's IPMS needs to achieve.

Without the overall strategy of the hospital as a guide, the IMPS of the hospital will have no support and direction. Therefore, the combination of DRGs and IPMS is conducive to better realize the strategic goals and performance management goals of the hospital.

By incorporating DRG-related indicators into the hospital performance management system, the overall strength of the hospital and talents can be evaluated more objectively, saving daily operating costs and thus enhancing the hospital's ability to develop in a sustainable manner. For example, raising the DRG overall competency index will promote a balanced development of talents; raising the CMI value of each department will increase the influence of the hospital in the industry and at the same time promote the cultivation and growth of the talent team; assessing the weighting of DRG cases and the level of cost control of disease types will motivate hospital staff and save operational costs, etc.

*(2) Reinforcing Performance Organization Management.* Organizational management is the basis for achieving the hospital's performance management objectives. At present, however, hospital management is generally not sufficiently aware of the impact of DRG payments on the hospital, believing that DRG payments are a matter of the quality of the first page of the case and are only a matter for the case department. As a result, they only put the work related to DRGs in the case room and do not fully understand the impact of DRGs on the internal management of the hospital.

At the health insurance level, DRGs are just a payment method, but from the perspective of internal hospital operations, DRGs are more of a management tool. The core of DRGs is the change in pricing mechanism, which poses a new challenge to the internal operation and management of hospitals, and this is the key to the impact of DRGs on the internal operation and management of hospitals. This is the key to the impact of DRGs on internal operations management. Therefore, hospitals need to pay close attention to this and make full use of DRG-related management tools so that they can play a greater and more significant role in internal operations management, especially internal performance management.

*4.2.2. Using DRG Indicators for Performance Evaluation.* This section uses data from four surgical departments in a hospital: urology, gastroenterology, hepatobiliary, and cardiothoracic, as an example, to analyze how to evaluate departmental performance using DRG-related indicators, including departmental workload performance, operational performance, and KPI performance evaluation.

*(1) Workload Performance Evaluation.* The workload performance of the four surgical departments of urology, gastroenterology, hepatobiliary, and cardiothoracic was evaluated using two methods: medical service performance points, and DRG case weights, and compared.

TABLE 2: Performance points and case weights of surgical departments.

No.	Department	Performance point		DRG case weight	
		Total points	Rank	Total weight	Rank
1	Urology	1,394,255	3	1,428	3
2	Gastroenterology	1,928,976	1	1,145	4
3	Hepatobiliary	1,098,267	4	1,769	2
4	Cardiothoracic	1,562,787	2	1,974	1
Total		5,984,285		6,316	

According to the results shown in Table 2, the workload performance calculated by the two methods was compared and the ranking of all three departments changed, except for urology, where the ranking changed from 1st to 4th, cardiothoracic surgery from 2nd to 1st, and hepatobiliary surgery from 4th to 2nd.

As shown in Figure 4, the specific analysis of DRG-related indicators for the four surgical departments shows that the decrease in the ranking of the gastrointestinal surgery department is mainly due to the high-time consumption index and cost consumption index. When calculating the workload by item performance points, more items done by the patient result in higher workload points, but when calculating the workload by DRG case weights, more items become useless and the longer the patient stays, the more efficient the use of beds. Cardiothoracic surgery moved up in the rankings mainly due to a higher CMI, indicating that the original project performance points did not fully reflect the technical difficulty of the disease types admitted to the unit and the workload of the medical staff. The increase in ranking for hepatobiliary surgery is also due to a higher CMI and a lower time and cost consumption index.

*(2) Operational Performance Evaluation.* Based on the historical data for each DRG group, a target cost for each DRG group can be calculated. In order to better represent the change in cost for each DRG group, the average historical cost for each DRG group over the last 3 years can be taken and different weights can be assigned to each year, with more recent years being given a greater weight and more distant years being given a smaller weight.

As shown in Figure 5, there are five urology groups, and based on the results of the costing for each disease group, the historical costs for each group for the last three years from 2017–2019 can be calculated and different weights of 20%, 30%, and 50% can be assigned to each group when calculating the target cost.

After calculating the target cost for each DRG group in the department as described above, the target cost for each DRG group in the department was compared with the actual cost of the group in the current period to calculate an operational assessment score for each group. The total group score and the operational assessment score for the whole department can then be calculated based on the operational assessment score for each group and the number of cases, as shown in Table 3.

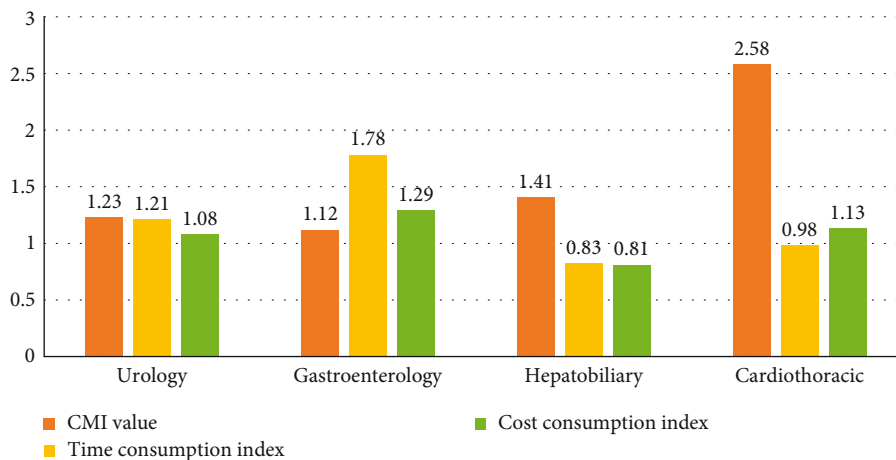


FIGURE 4: Departmental DRG-related indicator calculation results.

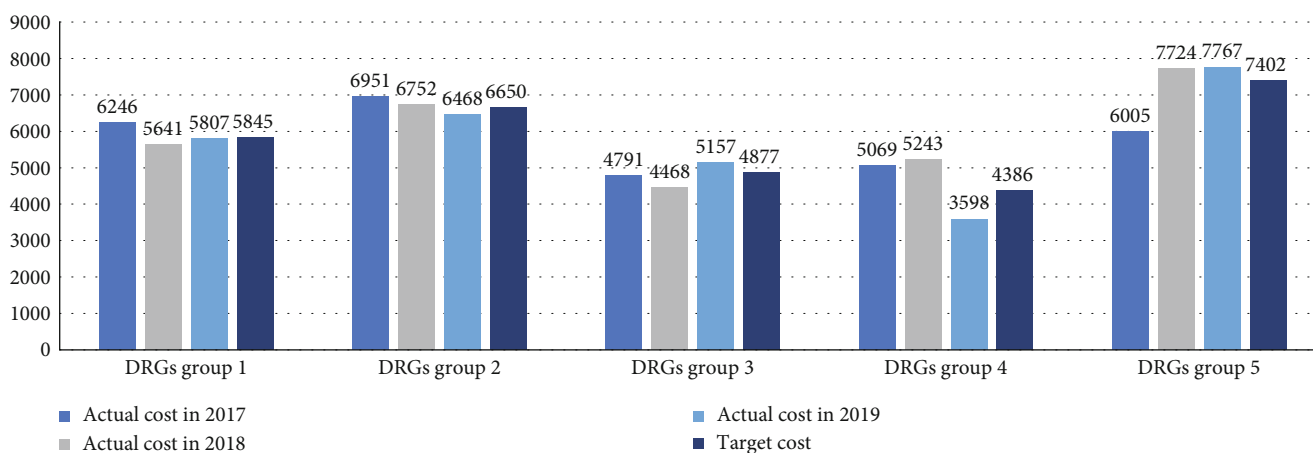


FIGURE 5: Target costs for each DRG patient group in urology (unit: Yuan).

TABLE 3: Urology operation performance assessment.

	Number of cases	Target cost (Yuan)	Actual cost (Yuan)	Appraisal score	Total score
DRG group 1	378	5,936	6,674	88.94	33,619.32
DRG group 2	336	6,745	5,324	126.69	42,567.84
DRG group 3	449	5,046	6,132	83.56	37,518.44
DRG group 4	259	4,581	5,356	82.29	21,313.11
DRG group 5	308	7,405	7,125	103.93	32,010.44
Total	1,730				167,029.15

Thus, the urology operation assessment score is  $167,029.15/1730 = 96.55$ . Using the same methodology as the above, the operational assessment scores for the three departments of gastroenterology, hepatobiliary surgery, and cardiothoracic surgery can be calculated as 92.76, 117.22, and 99.18, respectively.

(3) *KPI Performance Evaluation.* In the KPI appraisal system for doctors' groups constructed using the balanced scorecard (BSC) tool, the KPI appraisal scores of the doctors' groups can be calculated by assuming that all the KPI appraisal indicators of the doctors' groups except the DRG-related indicators are full scores and the DRG-related indicators are appraised according to the scoring criteria, as shown in Tables 4 and 5.

Due to the specialist nature of each department, the number of DRG groups and CMI values in the above KPI vary greatly between departments, so only the department itself can be compared before and after, mainly to assess the progress of the department. As the time consumption index and cost consumption index are industry comparable, they can

TABLE 4: Scoring criteria for DRG-related indicators.

Indicator	Scoring criteria
Number of DRG groups	The number of DRG groups in each assessment unit in the previous year as the base, plus (minus) one point for each additional (reduced) group in each assessment unit in the current assessment period, with a maximum of two points for each assessment unit in the current period
CMI value	The CMI value of each assessment unit in the previous year will be used as the base, and 1 point will be added (subtracted) for every 1% increase (decrease) in each assessment unit during the current assessment period, with a maximum of 2 points added to each assessment unit in the current period
Time consumption index	Each assessment unit will be based on 1, and 0.2 points will be deducted (added) for every 1% increase (decrease) in each assessment unit during this assessment period, with a maximum of 2 points added for each assessment unit in the current period
Cost consumption index	Each assessment unit will be based on 1, and 0.2 points will be deducted (added) for every 1% increase (decrease) in each assessment unit during this assessment period, with a maximum of 2 points added for each assessment unit in the current period
Mortality in low- and medium-risk groups	5 points deducted for each case during this assessment period

TABLE 5: KPI performance evaluation.

Dimension	KPI indicator	Urinary surgery	Gastrointestinal surgery	Hepatobiliary surgery	Cardiothoracic surgery
Finance (20%)	Bed occupancy rate (10%)	10.00	10.00	10.00	10.00
	Cost consumption index (10%)	9.40	5.20	11.20	7.70
Customer (10%)	Patient satisfaction (10%)	10.00	10.00	10.00	10.00
Internal processes (40%)	Time consumption index (10%)	6.80	6.10	10.30	9.20
	Mortality in the low- and medium-risk groups (10%)	10.00	10.00	10.00	10.00
	Incidence of hospital admissions (5%)	4.90	4.70	5.25	4.80
	Case quality (5%)	5.20	4.80	5.05	5.10
	Quality and safety of other care (10%)	10.00	10.00	10.00	10.00
Learn and growth (30%)	Number of DRG groups (5%)	6.20	5.70	5.00	4.10
	CMI value (10%)	11.80	8.20	9.90	5.60
	Out-of-region patient rates (5%)	5.00	4.48	5.00	4.80
	Percentage of TCM medical services (5%)	4.90	4.97	4.90	5.15
	Scientific research capacity (5%)	5.10	5.35	5.10	5.20
Total		99.30	89.50	101.70	84.65

be used directly to assess the department’s comparison with industry averages. Mortality in the low- and medium-risk groups is a medical safety indicator that needs to be closely controlled, so points are deducted more heavily if it occurs.

4.2.3. *Applying DRG Performance Evaluation Results.* The results of hospital performance evaluations can be used in a number of ways. This section describes how the results of DRGs can be used to calculate performance bonuses, evaluate specialty development, and control healthcare costs.

(1) *Calculating Performance Bonuses.* The workload performance bonus can be calculated by the following formula:

$$WPB = TW \times UP, \tag{4}$$

where WPB refers to the workload performance bonus, TW refers to the total weight of the DRG case, and UP refers to the unit price of the DRG case.

After obtaining the value of the workload performance bonus, the actual performance bonus issued can be calculated through the following formula:

$$APB = WPB + OARP \times KPIOARP, \tag{5}$$

where APB refers to the actual performance bonus issued, OARP refers to the operational assessment rewards and penalties, and KPIOARP refers to the KPI assessment rewards and penalties. The results are shown in Table 6.

TABLE 6: Actual performance bonus issued.

Department	Actual performance bonus issued
Urinary surgery	1,165,576.89
Gastrointestinal surgery	1,146,248.24
Hepatobiliary surgery	1,789,254.98
Cardiothoracic surgery	1,452,729.66

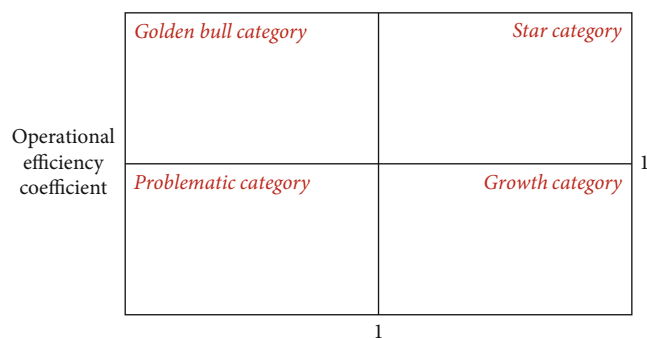


FIGURE 6: Department categories.

(2) *Evaluating Specialist Development.* Using the DRGs and other indicators such as operations, the development of each hospital specialty can be evaluated and more targeted development recommendations can be made for each specialty. As shown in Figure 6, departments can be classified into four categories: star, golden calf, problem, and growth, based on their technical difficulty and operational efficiency factors, with different development goals and directions.

The first quadrant is the star category: the CMI of the department is higher than the industry average (technical difficulty coefficient  $> 1$ ), and the department has a positive income and expenditure balance (operational efficiency coefficient  $> 1$ ). These departments are the leaders of the hospital's development and should be fostered and developed to become national key specialties and regional treatment centers.

The second quadrant is the Golden Bull category: the CMI of the department is lower than the industry average (technical difficulty coefficient less than 1), but the department has a positive income and expenditure balance (operational efficiency coefficient greater than 1). This type of department can bring economic benefits to the hospital but should be improved by optimizing the structure of the patient group and improving the technical level of the department.

The third quadrant is the problematic category: the CMI value is below the industry average (technical difficulty factor less than 1), and the department has a negative income and expenditure balance (operating efficiency factor less than 1). This is a serious problem, and the department must not only try to control its operating costs but also improve its medical skills.

The fourth quadrant is the growth category: the department has a CMI above the industry average (technical difficulty coefficient greater than 1), but a negative income and

expenditure balance (operating efficiency coefficient less than 1). These departments have a high level of medical technology and are influential in the industry but need to take steps to control operating costs.

## 5. Conclusion

In recent years, as the national health system reform has been increasing, so have the corresponding reform measures. In this context, this study constructs a performance management system within public hospitals based on DRG payment and explores the specific content of this system from four aspects: organizational management, assessment and evaluation, communication and feedback, and information support. In addition, the paper discusses how to implement an IPMS in hospitals, including the preparatory work before implementation and the key points to be grasped during the implementation process. In summary, this system will help to build a better internal performance management system in hospitals.

However, there are some limits of applying DRG performance evaluation results. For example, the scope of application is limited. To be specific, the objective of DRGs is to classify the output of healthcare services and only inpatient cases where the clinical diagnosis and treatment modality have a clear impact on the resource consumption and outcome of the patient are suitable. However, it cannot be applied to all patients in performance management, e.g., patients with the same diagnosis and treatment modalities but with very different resource consumption and treatment outcomes are not suitable for DRGs, so a combination of methods is needed for performance management within hospitals.

## Data Availability

The labeled dataset used to support the findings of this study are available from the corresponding author upon request.

## Conflicts of Interest

The authors declare no competing interests.

## Acknowledgments

This work is supported by the Nantong First People's Hospital.

## References

- [1] M. Cacace and A. Schmid, "The role of diagnosis related groups (DRGs) in healthcare system convergence," *BMC Health Services Research*, vol. 9, no. 1, pp. 1-2, 2009.
- [2] J. L. Freeman, "Refined DRGs: trials in Europe," *Health Policy*, vol. 17, no. 2, pp. 151-164, 1991.
- [3] Z. Gong, S. J. Duckett, D. G. Legge, and L. Pei, "Describing Chinese hospital activity with diagnosis related groups (DRGs): a case study in Chengdu," *Health Policy*, vol. 69, no. 1, pp. 93-100, 2004.

- [4] B. Reid, G. Palmer, and C. Aisbett, "The performance of Australian DRGs," *Australian Health Review*, vol. 23, no. 2, pp. 20–31, 2000.
- [5] R. B. Fetter, Y. Shin, J. L. Freeman, R. F. Averill, and J. D. Thompson, "Case mix definition by diagnosis-related groups," *Medical Care*, vol. 18, no. 2, pp. 1–53, 1980.
- [6] N. Goldfield, "The evolution of diagnosis-related groups (DRGs)," *Quality Management in Healthcare*, vol. 19, no. 1, pp. 3–16, 2010.
- [7] L. Kuntz, S. Scholtes, and A. Vera, "DRG cost weight volatility and hospital performance," *OR Spectrum*, vol. 30, no. 2, pp. 331–354, 2008.
- [8] W. Y. Jian, M. Lu, T. Cui, and M. Hu, "Evaluating performance of local case-mix system by international comparison: a case study in Beijing, China," *The International Journal of Health Planning and Management*, vol. 26, no. 4, pp. 471–481, 2011.
- [9] D. Qiao, Y. Zhang, and M. R. Khosravi, "Big data-enabled analysis of DRGs-based payment on stroke patients in Jiaozuo, China," *Journal of Healthcare Engineering*, vol. 2020, Article ID 6690019, 9 pages, 2020.
- [10] Z. Wang, R. Liu, P. Li, and C. Jiang, "Exploring the transition to DRGs in developing countries: a case study in Shanghai, China," *Pakistan Journal of Medical Sciences*, vol. 30, no. 2, pp. 250–255, 2014.
- [11] S. Kumar, N. S. Ghildayal, and R. N. Shah, "Examining quality and efficiency of the US healthcare system," *International Journal of Health Care Quality Assurance*, vol. 24, no. 5, pp. 366–388, 2011.
- [12] K. Grosios, P. B. Gahan, and J. Burbidge, "Overview of healthcare in the UK," *EPMA Journal*, vol. 1, no. 4, pp. 529–534, 2010.
- [13] C. H. How and K. M. Fock, "Healthcare in Singapore: the present and future," *Singapore Medical Journal*, vol. 55, no. 3, pp. 126–127, 2014.
- [14] X. Y. Chen, K. Yamauchi, K. Kato, A. Nishimura, and K. Ito, "Using the balanced scorecard to measure Chinese and Japanese hospital performance," *International Journal of Health Care Quality Assurance*, vol. 19, no. 4, pp. 339–350, 2006.
- [15] F. Rabbani, S. N. Lalji, F. Abbas et al., "Understanding the context of balanced scorecard implementation: a hospital-based case study in Pakistan," *Implementation Science*, vol. 6, no. 1, pp. 1–14, 2011.
- [16] K. B. Walker and L. M. Dunn, "Improving hospital performance and productivity with the balanced scorecard," *Academy of Health Care Management Journal*, vol. 2, 2006.
- [17] A. Nocera, "Performance-based hospital funding: a reform tool or an incentive for fraud?," *Medical Journal of Australia*, vol. 192, no. 4, pp. 222–224, 2010.
- [18] V. Sonmez and L. Pintelon, "A survey on performance management of operating rooms and a new KPI proposal," *Quality and Reliability Engineering International*, vol. 36, no. 8, pp. 2595–2609, 2020.
- [19] J. Braithwaite, J. I. Westbrook, and R. D. Lansbury, "Beyond management by objectives: the implementation of a goal-directed performance management system in an Australian teaching hospital," *Australian Health Review: A Publication of the Australian Hospital Association*, vol. 14, no. 2, pp. 110–126, 1991.
- [20] R. M. Spano and S. H. Lund, "Management by objectives in a hospital social service unit," *Social Work in Health Care*, vol. 1, no. 3, pp. 267–276, 1976.
- [21] X. Chen, J. Sheng, B. Tong, H. Qi, M. Zhu, and Z. Ye, "The development and application of a phased 360-degree performance appraisal feedback system for operating room nurses," *Chinese Journal of Nursing*, vol. 48, no. 12, pp. 1074–1076, 2013.
- [22] B. Cheng, K. Lu, J. Li, H. Chen, X. Luo, and M. Shafique, "Comprehensive assessment of embodied environmental impacts of buildings using normalized environmental impact factors," *Journal of Cleaner Production*, vol. 334, article 130083, 2021.



## Research Article

# Sports Training Intensity Information Fusion Method Based on Kinect Sensor

**Yan Huo** 

*Department of Physical Education, Anhui University of Finance & Economics, Bengbu 233030, China*

Correspondence should be addressed to Yan Huo; 120080917@aufe.edu.cn

Received 17 January 2022; Revised 9 February 2022; Accepted 21 February 2022; Published 16 March 2022

Academic Editor: Wen Zeng

Copyright © 2022 Yan Huo. This is an open access article distributed under the Creative Commons Attribution License, which permits unrestricted use, distribution, and reproduction in any medium, provided the original work is properly cited.

In order to improve the information fusion effect of sports training intensity, this paper analyzes the information fusion process of Kinect sensor. In order to prevent the simulation platform from exceeding its working space and ensure that the sports athletes obtain a more realistic sense of motion, the adaptive washout algorithm can change the adaptive parameters online in real time according to the input athlete's acceleration and angular velocity and the current motion state of the simulation platform. Moreover, this paper uses Kinect as the input device and combines the human node model to identify the features of training intensity information. After constructing an intelligent system, the performance of the system of this paper is verified. The research results show that the sports training intensity information fusion method based on the Kinect sensor proposed in this paper has a good effect in sports training intensity information fusion.

## 1. Introduction

Data fusion analysis technology [1] is an automated information processing technology that avoids the shortcomings of individual information, takes advantage of global information, and makes use of the complementarity between multisource heterogeneous data. It makes the mass information analysis result more reliable and accurate through the computer. Data fusion analysis technology is mainly to collect multisource heterogeneous data from multiple sensors and filter, analyze, synthesize, evaluate, and predict redundant or complementary information according to certain criteria. After that, the management personnel will take corresponding actions according to the processing results [2]. In academia, data fusion is defined as an information processing process that automatically analyzes information obtained by various sensors in chronological order according to certain criteria and performs systematic evaluation and prediction for a certain purpose. According to the definition, the key to data fusion is the method used and the process of research, and the sensor is the cornerstone of information collection [3].

The main goal of data fusion analysis technology is to analyze the obtained data and finally come to a decision, and the correctness and security of the decision are the standard of measurement. There are many usage scenarios of data fusion analysis methods, such as image processing, signal processing, and network security field. The main purpose is to achieve target state assessment, target attribute recognition, behavioral intention analysis, situation assessment, threat analysis, etc. The main theoretical knowledge is pattern recognition, uncertainty theory, artificial intelligence, neural network, and decision theory. Data fusion provides an efficient data processing technology foundation for information processing systems and domestic and foreign combat management. Filtering out some redundant data can improve the processing efficiency of the system, while complementary multisource heterogeneous data ensures the accuracy of system analysis. Data fusion technology expands the time and space dimensions of data, improves the reliability of the system, increases the credibility of target or event determination, and reduces the uncertainty of information. The connectivity and real-time communication between each unit and the central server in the data processing

system with multiple heterogeneous information sources, various processing platforms, and multiuser systems are verified. With the rapid development of network in the new century, the amount of data is huge, from TB level to PB level, which is called big data. Its data formats and types are diverse, such as web/database logs, images, voice and video, and coordinates, and data structures are also diverse, such as massive standardized, semistandardized, and non-standardized network or sensor data, and data fusion technology has entered the new journey.

This paper analyzes the information fusion process of the Kinect sensor, combines the training intensity analysis process to research, analyzes the sports training intensity information fusion process, and proposes an intelligent information fusion system to provide a theoretical reference for subsequent sports training intensity information fusion.

## 2. Related Work

Reference [4] invented a massive data access method in a cloud computing environment. Literature [5] clarifies a data processing method and system that combines fast data and big data. The big data and fast data are classified and transmitted, and the rapidly generated data uses the process of distributed structure to perform high-speed operations, while big data is used for high-speed computing. It is transmitted first and then statistical analysis. Reference [6] invented a fusion system to classify massive data streams according to requirements and proposed methods such as data concept drift and trigger classification, which enhanced the scalability and accuracy of the system. Literature [7] invented a big data segmentation method, which selects data according to data-related partitions, selects classification according to data-independent partitions, uses dynamic models to complete data-independent partitions, calculates the weights of different categories of data-independent partitions, and finally establishes a mathematical model. This method guarantees the speed and quality of data segmentation. Reference [8] proposed a method and system for network resource evaluation based on big data. A large amount of data is collected through stochastic models, then data mining technology is used to filter noise, and a part of simple data and its values are obtained through the K-means algorithm, so as to obtain relevant indicators and evaluate the resource quality of the analyzed system according to the obtained indicators. In Reference [9], aiming at the common limitations of existing wireless network mobile user positioning methods (including GPS, AOA, TSOA, and TOA), an improved fusion analysis method is used to enhance the accuracy of location assessment in wireless networks. Reference [10] gives a comprehensive and detailed introduction to the current state of multisensor data fusion and conducts an in-depth study of its concept, efficiency, challenges, and existing methods. Reference [11] proposed two Bayesian data analysis methods in different situations for the distributed target detection problem in sensor networks. The decision of local sensors was transmitted to the fusion center, and the optimal Bayesian theory was used for fusion analysis. Perform performance analysis experi-

ments on sensors with different numbers and locations. Reference [12] introduced the multisensor data analysis technology into the IDS, carried out the hierarchical analysis of data, information, and knowledge for the system, and finally regarded the fusion analysis as an important stage of the IDS. Reference [13] uses artificial intelligence technology to fuse information from different intrusion detection sensors to provide a decision engine for the Intelligent Intrusion Detection System (IIDS), which uses fuzzy cognitive graphs (FCMs) and fuzzy rule-based causal knowledge. The method was obtained and successfully introduced into IIDS of CCSR (the Center for Computer Security Research). Reference [14] introduced the MapReduce architecture under the Hadoop platform and introduced the MapReduce algorithm based on data mining, machine learning, and similarity join. In the context of big data, the literature [15] proposed an improved K-means algorithm suitable for different structured big data because the K-means clustering algorithm cannot effectively deal with the combination of structured and unstructured data. Reference [16] analyzes the web logs in the network, calculates the possibility and success of attack behaviors according to the existing vulnerability of the server, and finally evaluates the performance of each server according to the D-S evidence theory. Reference [17] designed a framework with a certain ability to process big data. The parallel Apriori algorithm based on MapReduce uses a large number of computers for data distribution and effectively handles large-scale data. Reference [18] proposed a regression algorithm based on parallel prediction of large datasets, which effectively reduces the time for predicting datasets while maintaining a high accuracy. Reference [19] proposed a MapReduce-based Apriori algorithm and FP-growth algorithm, but this method scans the database more frequently, and the number of candidate sets is relatively large in the process of the algorithm. In the process of massive data processing, in order to solve the problem of database access and storage, literature [20] proposed a horizontal storage model, and submitted the I/O performance during data processing

## 3. Sports Training Intensity Information Fusion Filter

The structure of the adaptive washout algorithm is roughly the same as the classic washout algorithm, and its structure is shown in the figure. The algorithm is based on the classic washout algorithm and uses model reference adaptive theory to improve it. In order to prevent the simulation platform from exceeding its working space and at the same time to ensure that the sports athletes obtain a more realistic sense of movement, the adaptive washout algorithm can change the adaptive parameters online in real time according to the input acceleration and angular velocity of the athletes and the current motion state of the simulation platform.

The adaptive washout algorithm is divided into frequency adaptive washout algorithm and gain adaptive washout algorithm according to the different adaptive parameters. Since the frequency self-adaptive washout algorithm has many self-adaptive parameters, a large amount of

calculation, and is not easy to program, while the gain self-adaptive washout algorithm has a simple form and few self-adaptive parameters, so this paper chooses the gain self-adaptive washout algorithm. In the gain adaptive algorithm, its adaptive filter can change the parameter gain of the filter in real time according to the current motion state of the athletes and the simulation platform, so as to prevent the simulation platform from exceeding the working space and enable the athletes to obtain a more realistic sense of movement.

The acceleration adaptive high-pass filter is composed of adaptive gain, linear high-pass filter and adaptive algorithm. Its principle structure is shown in Figure 1. The linear high-pass filter is a third-order high-pass filter. The transfer function of the acceleration adaptive high-pass filter is

$$\frac{a_h(s)}{a(s)} = \frac{ks^3}{(s^2 + 2\xi_h\omega_h s + \omega_h^2)(s + \omega_m)}. \quad (1)$$

In the formula,  $k$  is the adaptive gain.

The above formula is written as a differential equation in the form

$$a_h = ka - c_1 v_h - c_2 x_h - c_3 \int x_h dt. \quad (2)$$

In the formula,  $v_h$  is the speed signal output by the adaptive high-pass filter, and  $x_h$  is the displacement signal output by the filter,  $c_1 = 2\xi_h\omega_h + \omega_m$ ,  $c_2 = 2\xi_h\omega_h\omega_m + \omega_h^2$ ,  $c_3 = \omega_h^2\omega_m$ .

The value of adaptive gain  $k$  is between 0 and 1 and can be adjusted in real time according to the current input acceleration and the position of the platform. For example, when the input acceleration signal is small or the simulation platform is close to the neutral position, the gain  $k$  should be as close to 1 as possible. When the input acceleration signal is large or the analog platform is close to the limit position, in order to prevent it from exceeding the limit, it is necessary to reduce the adaptive gain to reduce its output. To this end, the construction cost function is [20]

$$J = \frac{1}{2} \left[ W_1(a_h - a)^2 + W_2 v_h^2 + W_3 x_h^2 + W_4 \left( \int x_h dt \right)^2 + W_5(k - k_0)^2 \right]. \quad (3)$$

In the formula,  $W_1$  is the weight coefficient of the acceleration fidelity term,  $W_2$  is the weight coefficient of the speed penalty term,  $W_3$  is the weight coefficient of the displacement penalty term,  $W_4$  is the weight coefficient of the displacement integral penalty term,  $W_5$  is the weight coefficient of the adaptive gain penalty term, and  $k_0$  is the initial value of the adaptive gain, which is generally 1.

In the cost function, the effect of the acceleration fidelity term is to improve the fidelity of the washout algorithm and ensure that the dynamic simulation is more realistic. The function of speed penalty, displacement penalty, and displacement integral penalty is to limit the speed and displacement of the simulation platform, prevent the platform from exceeding the limit, and make the simulation platform

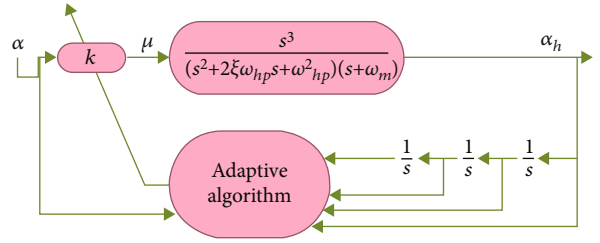


FIGURE 1: The structure of the acceleration adaptive high-pass filter.

return to the neutral position as soon as possible. In order to make the adaptive gain change around its initial value, an adaptive gain penalty term is added.

At present, there are many methods for solving the cost function, such as the gradient method, Newton-Raphson method, and conjugate gradient method. This paper chooses the gradient method to solve the cost function. The gradient method searches in the negative gradient direction on the surface formed by the cost function  $J$  until  $J$  reaches the minimum value.

According to the gradient method to calculate the minimum value of the cost function, the rate of change of the adaptive gain is [21]

$$\dot{k} = -G \frac{\partial J}{\partial k}. \quad (4)$$

In the formula,  $\dot{k}$  is the adaptive gain change rate, and  $G$  is the adaptive search step size.

By obtaining partial derivatives of  $k$  at both ends of formula (3), we can obtain

$$\begin{aligned} \frac{\partial J}{\partial k} = & W_1(a_h - a) \frac{\partial a_h}{\partial k} + W_2 v_h \frac{\partial v_h}{\partial k} + W_3 x_h \frac{\partial x_h}{\partial k} \\ & + W_4 \int x_h dt \frac{\partial \int x_h dt}{\partial k} + W_5(k - k_0). \end{aligned} \quad (5)$$

By substituting formula (5) into formula (4) and performing the pull transformation, the adaptive gain can be obtained as

$$\begin{aligned} k = \frac{G}{s + GW_5} \left[ -W_1(a_h - a) \frac{\partial a_h}{\partial k} - W_2 v_h \frac{\partial v_h}{\partial k} - W_3 x_h \frac{\partial x_h}{\partial k} \right. \\ \left. - W_4 \int x_h dt \frac{\partial \int x_h dt}{\partial k} + W_5 k_0 \right]. \end{aligned} \quad (6)$$

At the same time, taking the partial derivatives of  $k$  at both ends of formula (2), respectively, we can get [22]

$$\frac{\partial a_h}{\partial k} = a - c_1 \frac{\partial v_h}{\partial k} - c_2 \frac{\partial x_h}{\partial k} - c_3 \frac{\partial \int x_h dt}{\partial k}. \quad (7)$$

So far, the function of the acceleration adaptive high-pass filter can be realized by formula (2), formula (6), and formula (7). First, the acceleration  $a$  of the filter input is

multiplied by the initial value of the adaptive gain and input to the linear high-pass filter. Through formula (2), the response of each movement amount such as output acceleration, velocity, and displacement can be obtained, and the response of each partial derivative term can be obtained by formula (7). After getting the response of the above variables, the adaptive gain  $k$  can be obtained by combining formula (6). In this way, the input of the linear high-pass filter in the next cycle of filtering can be calculated, and by repeating the above steps, the adaptive high-pass filtering function of the acceleration signal can be realized.

The angular velocity adaptive high-pass filter is similar to the acceleration adaptive high-pass filter. It consists of three parts: adaptive gain, linear high-pass filter, and adaptive algorithm. Its structure is shown in Figure 2. Among them, the linear high-pass filter adopts a second-order high-pass filter. The transfer function is still formula (13). The transfer function of the adaptive high-pass acceleration filter is

$$\frac{\omega_h(s)}{\omega(s)} = \frac{ks^2}{s^2 + 2\xi_h\omega_h s + \omega_h^2}. \quad (8)$$

In the formula,  $k$  is the adaptive gain.

The above formula is written as a differential equation in the form

$$\dot{\omega}_h = k\omega - c_1\alpha_h - c_2 \int \alpha_h dt. \quad (9)$$

In the formula,  $\alpha_h$  is the angle signal output by the adaptive high-pass filter,  $c_1 = 2\xi_h\omega_h$ ,  $c_2 = \omega_h^2$ .

In the same way, the adaptive gain of the angular velocity adaptive high-pass filter can be continuously adjusted between 0 and 1 according to the current input angular velocity and the attitude of the platform to ensure a better dynamic simulation effect of the simulation platform. When the input angular velocity signal is too small or the attitude angle of the simulated platform is close to zero, the adaptive gain is as close to 1 as possible. When the input angular velocity signal is too large or the attitude angle of the simulation platform is too large, in order to prevent the platform from exceeding the limit, it is necessary to reduce the adaptive gain to reduce its output. To this end, the construction cost function is

$$J = \frac{1}{2} \left[ W_1(\omega_h - \omega)^2 + W_2\alpha_h^2 + W_3 \left( \int \alpha_h dt \right)^2 + W_4(k - k_0)^2 \right]. \quad (10)$$

In the formula,  $W_1$  is the weight coefficient of the angular velocity fidelity term,  $W_2$  is the weight coefficient of the angle penalty term,  $W_3$  is the weight coefficient of the angle integral penalty term,  $W_4$  is the weight coefficient of the adaptive gain penalty term, and  $k_0$  is the initial value of the adaptive gain, which is generally 1.

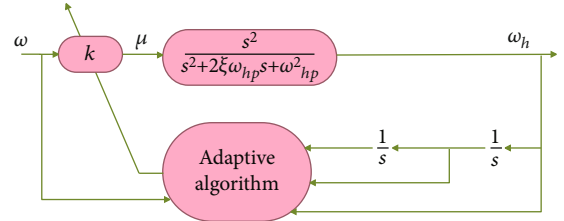


FIGURE 2: The structure of the angular velocity adaptive high-pass filter.

In the cost function, the effect of the angular velocity fidelity term is to improve the fidelity of the washout algorithm and ensure that the dynamic simulation is more realistic. The function of the angle penalty item is to limit the attitude angle of the simulation platform and prevent the platform movement from exceeding the limit. The function of the angle integral penalty is to make the simulation platform return to the neutral position as soon as possible. In order to make the adaptive gain change around its initial value  $k_0$ , an adaptive gain penalty term is added. Similarly, for solving the cost function of the angular velocity adaptive high-pass filter, the gradient method is still used. If the gradient method is used to solve the cost function, the rate of change of the adaptive gain is

$$\dot{k} = -G \frac{\partial J}{\partial k}. \quad (11)$$

In the formula,  $\dot{k}$  is the adaptive gain change rate, and  $G$  is the adaptive search step size.

$$\begin{aligned} \frac{\partial J}{\partial k} = & W_1(\omega_h - \omega) \frac{\partial \omega_h}{\partial k} + W_2\alpha_h \frac{\partial \alpha_h}{\partial k} \\ & + W_3 \int \alpha_h dt \frac{\partial \int \alpha_h dt}{\partial k} + W_4(k - k_0), \end{aligned} \quad (12)$$

$$\begin{aligned} k = & \frac{G}{s + GW_4} \left[ -W_1(\omega_h - \omega) \frac{\partial \omega_h}{\partial k} - W_2\alpha_h \frac{\partial \alpha_h}{\partial k} \right. \\ & \left. - W_3 \int \alpha_h dt \frac{\partial \int \alpha_h dt}{\partial k} + W_4 k_0 \right], \end{aligned} \quad (13)$$

$$\frac{\partial \omega_h}{\partial k} = \omega - c_1 \frac{\partial \alpha_h}{\partial k} - c_2 \frac{\partial \int \alpha_h dt}{\partial k}. \quad (14)$$

So far, the function of the angular velocity adaptive high-pass filter can be realized by formula (9), formula (13), and formula (14). First, the angular velocity  $\omega$  input by the filter is multiplied by the initial value of the adaptive gain and input to the linear high-pass filter. Through formula (9), the response of each movement amount such as output angular velocity and angle can be obtained, and the response of each partial derivative term can be obtained by formula (14). After obtaining the response of the above variables, the adaptive gain  $k$  can be obtained by combining formula (13), so that the input of the linear high-pass filter can be calculated for the next period of filtering. By repeating the

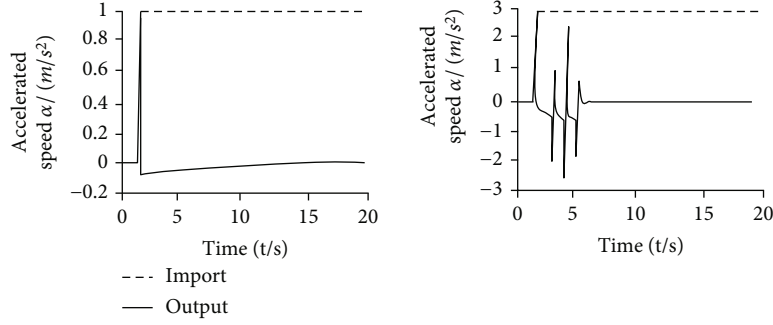


FIGURE 3: The response of the adaptive algorithm under different amplitude step inputs.

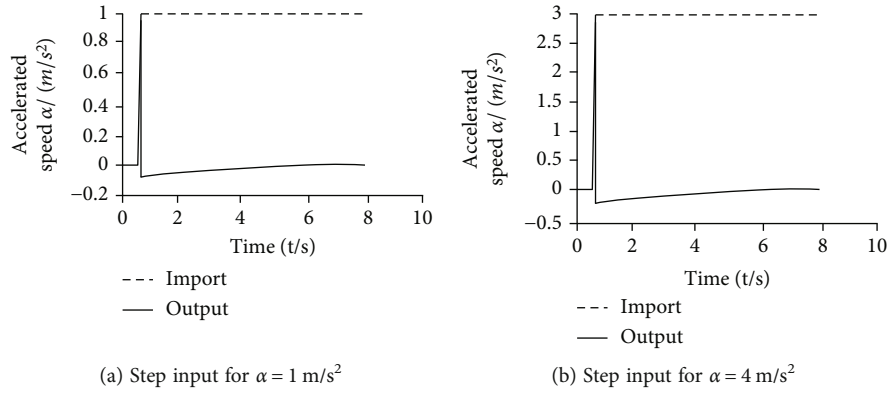


FIGURE 4: The response of the improved adaptive high-pass filter under different amplitude step inputs.

above steps, the adaptive high-pass filtering function of the angular velocity signal can be realized.

For an acceleration adaptive high-pass filter, a step signal is used as the input. When the input amplitude increases to a certain extent, the output of the filter will become oscillating and diverging. As shown in Figure 3, when the step signal is  $a = 1 \text{ m/s}^2$ , the output tends to be stable. When the step signal is  $a = 3 \text{ m/s}^2$ , the output appears as oscillation and divergence.

This paper first analyzes the stability of the adaptive high-pass filter using the Hurwitz stability criterion, which analyzes the stability of linear systems, and finds the reasons for the unstable output. After that, the algorithm is improved so that the adaptive gain has nothing to do with the input amplitude. Therefore, it is ensured that the output will not become divergent due to the increase of the input amplitude, false hints are reduced, and the authenticity and stability of the dynamic simulation are improved.

This paper takes the third-order adaptive high-pass filter of the high-pass acceleration channel as an example to analyze the adaptive washout algorithm. Since the filter is a non-linear time-varying system, it must be linearized first, and then, its stability can be judged by the Hurwitz stability criterion. If the adaptive high-pass filter is linearized, its form needs to be transformed. First, formula (13) is transformed into the following form:

$$k = \frac{G(W_5 k_0 - u)}{s + GW_5}. \quad (15)$$

In the formula,  $u = W_1(a_h - a)(\partial a_h / \partial k) + W_2 v_h (\partial v_h / \partial k) + W_3 x_h (\partial x_h / \partial k) + W_4 \int x_h dt (\partial \int x_h dt / \partial k)$ .

Substituting formula (15) into formula (1), the transfer function of the acceleration adaptive high-pass filter can be obtained as

$$\frac{a_h}{a} = \frac{G(W_5 k_0 - u)s^3}{(s^2 + 2\xi_h \omega_h s + \omega_h^2)(s + \omega_m)(s + GW_5)}. \quad (16)$$

Formula (16) is written as a differential equation in the form

$$\begin{aligned} G(W_5 k_0 - u)a &= \dot{a}_h + (2\xi_h \omega_h + \omega_m + GW_5)a_h \\ &+ (\omega_m GW_5 + 2\xi_h \omega_h GW_5 + 2\xi_h \omega_h \omega_m + \omega_h^2) \\ &\cdot \int a_h dt + (2\xi_h \omega_h \omega_m GW_5 + \omega_h^2 GW_5 + \omega_h^2 \omega_m) \\ &\cdot \iint a_h dt^2 + \omega_h^2 \omega_m GW_5 \iiint a_h dt^3. \end{aligned} \quad (17)$$

Formula (17) is organized into the following form:

$$\dot{a}_h + d_3(t)a_h + d_2(t) \int a_h dt + d_1(t) \iint a_h dt^2 + d_0(t) \iiint a_h dt^3 = d(t). \quad (18)$$

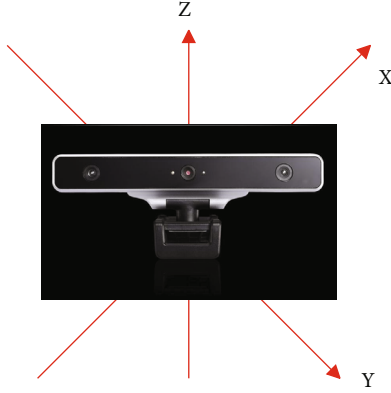


FIGURE 5: Coordinate system under Kinect.

In the formula,

$$\begin{aligned}
 d_0(t) &= \omega_h^2 \omega_m GW_5 + GW_4 \frac{\partial \int x_h dt}{\partial k} a; \\
 d_1(t) &= 2\xi_h \omega_h \omega_m GW_5 + \omega_h^2 GW_5 + \omega_h^2 \omega_m + GW_3 \frac{\partial x_h}{\partial k} a; \\
 d_2(t) &= \omega_m GW_5 + 2\xi_h \omega_h GW_5 + 2\xi_h \omega_h \omega_m + \omega_h^2 + GW_2 \frac{\partial v_h}{\partial k} a; \\
 d_3(t) &= 2\xi_h \omega_h + \omega_m + GW_5 + GW_1 \frac{\partial a_h}{\partial k} a; \\
 d(t) &= G \left( W_5 k_0 + W_1 \frac{\partial a_h}{\partial k} \right) a.
 \end{aligned} \tag{19}$$

Equation (18) is a time-varying linear differential equation, and its features are not easy to analyze. However, when the input signal is constant, that is, after a long enough time, the partial derivative terms in the coefficients of the differential equation and the constant terms tend to be constant, that is,

$$\begin{aligned}
 \lim_{t \rightarrow \infty} \frac{\partial a_h(t)}{\partial k} &= \lim_{s \rightarrow 0} s \frac{\partial a_h(s)}{\partial k} = \lim_{s \rightarrow 0} s \frac{s^3}{(s^2 + 2\xi_h \omega_h s + \omega_h^2)(s + \omega_m)} \frac{r}{s} = 0, \\
 \lim_{t \rightarrow \infty} \frac{\partial v_h(t)}{\partial k} &= \lim_{s \rightarrow 0} s \frac{\partial v_h(s)}{\partial k} = \lim_{s \rightarrow 0} s \frac{r^3}{(s^2 + 2\xi_h \omega_h s + \omega_h^2)(s + \omega_m)} \frac{r}{s} = 0, \\
 \lim_{t \rightarrow \infty} \frac{\partial x_h(t)}{\partial k} &= \lim_{s \rightarrow 0} s \frac{\partial x_h(s)}{\partial k} = \lim_{s \rightarrow 0} s \frac{r^3}{(s^2 + 2\xi_h \omega_h s + \omega_h^2)(s + \omega_m)} \frac{1}{s^2} = 0, \\
 \lim_{t \rightarrow \infty} \frac{\partial (\int x_h dt)(t)}{\partial k} &= \lim_{s \rightarrow 0} s \frac{\partial (\int x_h dt)(s)}{\partial k} \\
 &= \lim_{s \rightarrow 0} s \frac{s^3}{(s^2 + 2\xi_h \omega_h s + \omega_h^2)(s + \omega_m)} \frac{r}{s^3} = \frac{r}{\omega_h^2 \omega_m}.
 \end{aligned} \tag{20}$$

Therefore, the coefficients and constant terms of the differential equations will also tend to be constants. At this time, the system represented by formula (18) can be

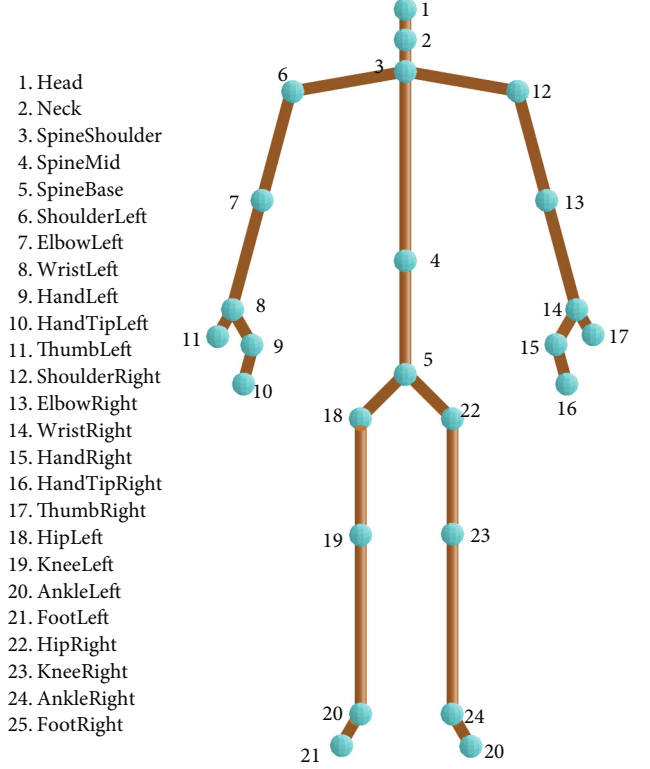


FIGURE 6: The names of the 25 joint points of the human body in the second generation of Kinect.

regarded as a linear time-invariant system:

$$\dot{a}_h + d_3 a_h + d_2 \int a_h dt + d_1 \iint a_h dt^2 + d_0 \iiint a_h dt^3 = d. \tag{21}$$

Then, the feature equation of this closed-loop system is

$$D(s) = s^4 + d_3 s^3 + d_2 s^2 + d_1 s + d_0 = 0. \tag{22}$$

According to the Hurwitz stability criterion, the necessary and sufficient conditions for the system to remain stable are as follows:

- (1) Each coefficient is positive
- (2) The main determinant composed of the coefficients of the feature equation of the system is

$$\Delta = \begin{vmatrix} d_3 & d_1 & 0 & 0 \\ 1 & d_2 & d_0 & 0 \\ 0 & d_3 & d_1 & 0 \\ 0 & 1 & d_2 & d_0 \end{vmatrix} \tag{23}$$

All subdeterminants on its main diagonal are positive.

Through the above analysis, it can be known that the stability of the acceleration adaptive high-pass filter is related to the input amplitude. An input with an excessively large

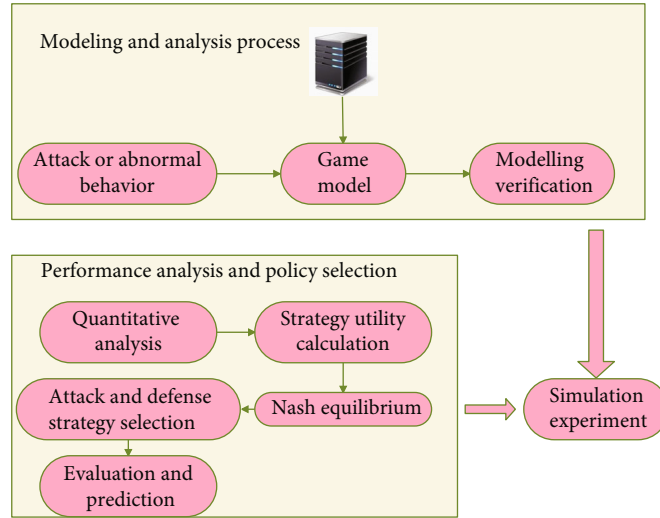


FIGURE 7: Decision-level fusion analysis method.

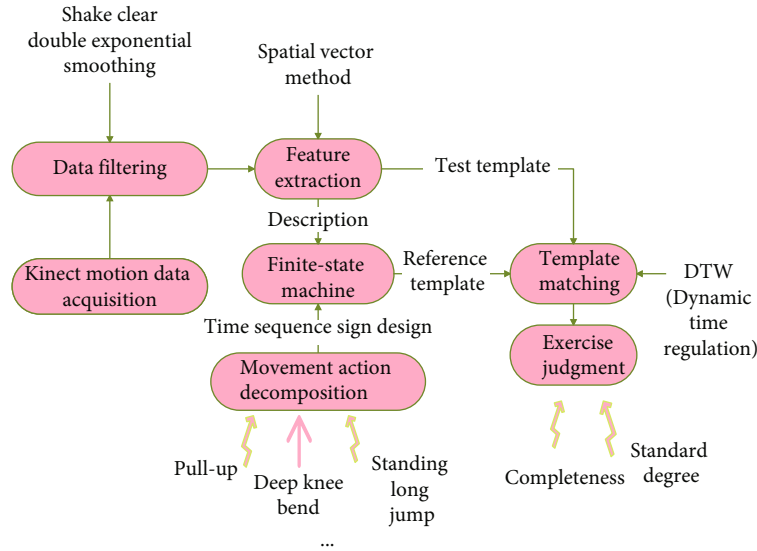


FIGURE 8: The framework of the motion recognition algorithm.

amplitude will make the system unable to meet the condition (2), which will cause the system to oscillate and diverge.

The analysis shows that for an adaptive high-pass filter, the adaptive gain is related to the amplitude of the input signal and affects the stability of the system, that is, the same adaptive high-pass filter. When the input signal amplitude is small, its output is stable. However, when the input amplitude increases to a certain extent, the output becomes oscillating and diverging.

In order to overcome this shortcoming of the traditional adaptive filter, it needs to be improved so that the amplitude of the input signal does not affect the adaptive gain. The improvement plan is to normalize and replace the adaptive law with the following formula:

$$\dot{k} = -G \sum_{i=1}^5 W_i \frac{e_i(\partial e_i / \partial k)}{\alpha + (\partial e_i / \partial k)^2}. \quad (24)$$

$\alpha > 0$  is introduced to avoid possible division by zero.  $e_i$  ( $i = 1, 2, \dots, 5$ ) can be obtained by writing Equation (3) as follows:

$$J = \frac{1}{2} \left[ W_1(a_h - a)^2 + W_2v_h^2 + W_3x_h^2 + W_4 \left( \int x_h dt \right)^2 + W_5(k - k_0)^2 \right] = \frac{1}{2} \sum_{i=1}^5 W_i e_i^2. \quad (25)$$

In order to limit the parameter adjustment rate within a certain range, the saturation feature is introduced, namely,

$$\dot{k} = -G \text{sat} \left( \sum_{i=1}^5 W_i \frac{e_i(\partial e_i / \partial k)}{\alpha + (\partial e_i / \partial k)^2}, \beta \right). \quad (26)$$

In the formula,  $\beta > 0$ , and

$$\text{sat}(x, \beta) = \begin{cases} -\beta, & x < -\beta, \\ x, & -\beta < x < \beta, \\ \beta, & x > \beta. \end{cases} \quad (27)$$

The improved adaptive washout algorithm is simulated, as shown in Figure 4.

It can be seen from Figure 4 that after the above correction, the gain of the adaptive washout algorithm has nothing to do with the input amplitude, so as to ensure that the output will not become divergent due to the increase of the input amplitude, which improves the stability of the washout algorithm. In addition, since the composition of the cost function is not changed, and the dimension of the gain itself is 1, this normalization process makes the gain more in line with its physical meaning.

#### 4. Sports Training Intensity Information Fusion Method Based on Kinect Sensor

After Kinect “sees” the three-dimensional world through the camera, it uses computer graphics vision technology to first separate the human body from the background image and identify various parts of the human body. Furthermore, it extracts human bone features and joint point data and generates three-dimensional (3D) spatial coordinate data containing 25 joint points of the human body. The Kinect coordinate system in this study is shown in Figure 5. The name of each joint point and its position in the human body are shown in Figure 6.

Decision-level fusion is the fusion and dissemination of the uncertainty of each partial fusion result. After analyzing the current situation of data fusion at home and abroad, the deficiencies of decision-level data fusion are summarized. (1) The core of the decision-level fusion system is to conduct a comprehensive analysis of the decision results of the multi-sensor system, and most of the local results are inaccurate and not detailed, and some are contradictory, which greatly increases the risk of the fusion system. This time, synthesizing the analysis results of local sensors in the case of a large amount of conflicting information has become a problem that the cloud monitoring information system must solve. (2) The amount of data collected by the cloud monitoring system is large, the data structure is complex, and there are many types of data. The existing decision-level fusion analysis methods all need to preprocess the original data, which is expensive. Therefore, fast and efficient fusion analysis for big data has become a “bottleneck” restricting decision-level fusion. The design of the analysis method proposed in this paper is shown in Figure 7.

In view of the analysis of the requirements for the use of this system, combined with the relevant research of previous scholars, this paper believes that the extraction of the temporal and spatial signs of the movement at different times during the movement process is the guarantee of the recognition accuracy. After that, this paper uses the template matching

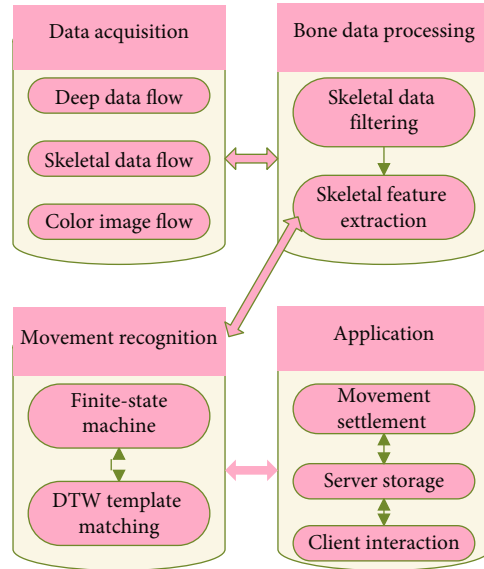


FIGURE 9: The flow of the motion recognition algorithm.

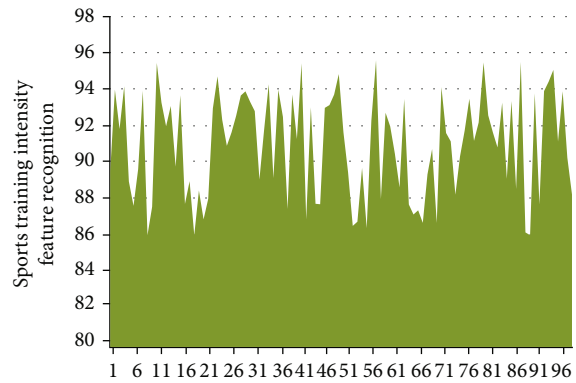


FIGURE 10: The effect of sports training intensity feature recognition.

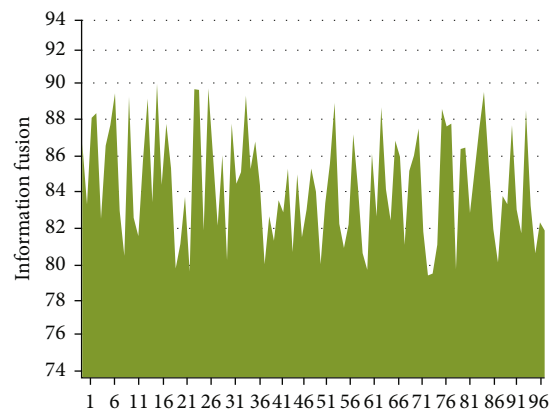


FIGURE 11: Information fusion effect of sports training intensity information fusion method based on Kinect sensor.

method of the sequential signs of movement and action connection as the motion recognition method of this system. The overall framework is shown in Figure 8.



The flow of the motion recognition algorithm is shown in Figure 9.

**Data collection:** the algorithm accepts the real-time data stream collected by Kinect, including depth data stream, bone data stream, color image stream, and bone data stream, which will be used in the subsequent motion recognition process. In addition, other data will be used for client interaction and storage at the application layer. **Bone data processing:** the algorithm first uses the combined filtering method of jitter removal and double exponential smoothing to filter the data from the bone data stream collected by the algorithm. The smooth bone data lays the foundation for the smooth output of bone features. Then, the space vector method is used to extract the joint angle features of the bone data. **Motion recognition:** after the bone data is processed, a motion finite state machine template based on joint angle features is established for different motions. The DTW template matching algorithm is matched with real-time motion data to perform the motion recognition of the formulated motion. **Application:** for the above motion recognition, it only recognizes a periodic action in the motion process. It is also necessary to continuously recognize and settle the movement process, and the client needs to do the main interactive feedback according to different finite state machine states. Finally, the data is stored on the server for use by other applications.

After constructing the above system, the system is tested and verified. This paper uses Kinect and performance sports training intensity identification, mainly through action analysis.

After constructing the above system, the system is tested and verified. In this paper, Kinect is used to identify the features of sports training intensity, which is mainly identified through action analysis. Firstly, the results of the identification of sports training intensity features are counted as shown in Figure 10. Secondly, the effect of fusion of Kinect sensor and exercise training intensity information is counted, as shown in Figure 11.

From the above research, it can be seen that the sports training intensity information fusion method based on the Kinect sensor proposed in this paper has a good effect in sports training intensity information fusion.

## 5. Conclusion

Data fusion is similar to the process of human self-energy analysis. The data collected by the sensor system is first obtained. This information is generally time-varying, uncertain, incomplete, redundant, complementary, and so on. Then, it preprocesses and comprehensively analyzes this information and rationally optimizes and combines all the collected data based on the redundancy and complementarity of multidimensional physical features such as space, time, pop, and frequency spectrum. As a result, it obtains more accurate information about the detected environment and targets, improves the recognition ability of the system, and ensures the correct and effective operation of the system. This paper analyzes the Kinect sensor's information fusion process, combined with the training intensity analysis pro-

cess to study, analyzes the sports training intensity information fusion process, and proposes an intelligent information fusion system to provide a theory for subsequent sports training intensity information fusion. Through research, it can be seen that the sports training intensity information fusion method based on the Kinect sensor proposed in this paper has a good effect in sports training intensity information fusion.

## Data Availability

The labeled dataset used to support the findings of this study is available from the corresponding author upon request.

## Conflicts of Interest

The author declares no competing interests.

## Acknowledgments

This study is sponsored by Anhui University of Finance and Economics.

## References

- [1] A. Y. Osipov, R. S. Nagovitsyn, F. H. Zekrin, D. A. Zubkov, and T. V. Zhavner, "Crossfit training impact on the level of special physical fitness of young athletes practicing judo," *Sport Mont*, vol. 17, no. 3, pp. 9–12, 2019.
- [2] D. Henriques-Neto, J. P. Magalhães, M. Hetherington-Rauth, D. A. Santos, F. Baptista, and L. B. Sardinha, "Physical fitness and bone health in young athletes and nonathletes," *Sports Health*, vol. 12, no. 5, pp. 441–448, 2020.
- [3] T. M. Kravchuk, N. M. Sanzharova, J. V. Golenkova, and I. B. Katrechko, "Influence of means of parterre gymnastics on physical fitness of young athletes in acrobatic rock and roll," *Health, Sport, Rehabilitation*, vol. 6, no. 3, pp. 19–25, 2020.
- [4] D. Okun and K. Mulyk, "Investigation of the relationship between the indicators of physical preparedness and the basic technique elements of young water-salomon athletes," *Slobzhanskyi Herald of Science and Sport*, vol. 5, no. 61, pp. 69–71, 2017.
- [5] O. Politko, "Model characteristics of physical development and special physical preparedness of swimmers 12–15 years old," *Slobzhanskyi Herald of Science and Sport*, vol. 64, no. 2, pp. 45–49, 2018.
- [6] G. Chang, "Retracted article: Urban air pollution diffusion status and sports training physical fitness measurement based on the internet of things system," *Arabian Journal of Geosciences*, vol. 14, no. 16, pp. 1–11, 2021.
- [7] B. Silva and F. M. Clemente, "Physical performance characteristics between male and female youth surfing athletes," *The Journal of Sports Medicine and Physical Fitness*, vol. 59, no. 2, pp. 171–178, 2019.
- [8] L. P. Ariani, "The effect of repetition sprint training method combined with the level of physical fitness toward the speed of 100 meter run," *International Journal of Engineering, Science and Information Technology*, vol. 1, no. 3, pp. 59–63, 2021.
- [9] A. V. Titova, O. G. Chorniy, A. A. Dolgov, and T. A. Gladyr, "Parameters of biochemical control as a criteria of adaptive

- changes in the organism of athletes with various fitness levels engaged in the conditions of power fitness,” *Ukrainian Journal of Medicine, Biology and Sports*, vol. 3, no. 2, pp. 278–283, 2018.
- [10] T. Chernykh, V. Mulik, and D. Okun, “Study of the level of physical fitness of young acrobat athletes at the initial stage of training,” *Slobozhanskyi Herald of Science and Sport*, vol. 7, no. 5(73), pp. 61–65, 2019.
- [11] P. Kostiantyn, G. Grygoriy, P. Vasyl et al., “Correlation analysis of readiness indicators of athletes and their competitive results in kettlebell sport,” *Journal of Physical Education and Sport*, vol. 17, no. 3, pp. 2123–2128, 2017.
- [12] L. A. Sarafyniuk, A. V. Syvak, Y. I. Yakusheva, and T. I. Bor-ejko, “Correlations of cardiointervalographic indicators with constitutional characteristics in athletes of mesomorphic somatotype,” *Biomedical and biosocial anthropology*, vol. 35, no. 35, pp. 17–22, 2019.
- [13] V. V. Artiuh, Z. L. Kozina, V. O. Koval, D. V. Safronov, S. V. Fomin, and Y. O. Novikov, “Influence of application of special means of development of equilibrium and precision-target movements on the level and structure of psychophysiological indicators, physical and technical readiness of archers,” *Health, Sport, Rehabilitation*, vol. 4, no. 4, pp. 7–16, 2019.
- [14] Y. Strykalenko, O. Shalar, V. Huzar, R. Andrieieva, I. Zhosan, and S. Bazylyev, “Influence of the maximum force indicators on the efficiency of passing the distance in academic rowing,” *Journal of Physical Education and Sport*, vol. 19, no. 3, pp. 1507–1512, 2019.
- [15] F. Fachrezzy, I. Hermawan, U. Maslikah, H. Nugroho, and E. Sudarmanto, “Profile physical fitness athlete of slalom number water ski,” *International Journal of Educational Research & Social Sciences*, vol. 2, no. 1, pp. 34–40, 2021.
- [16] R. L. Kons, E. Franchini, and D. Detanico, “Relationship between physical fitness, attacks and effectiveness in short-and long-duration judo matches,” *International Journal of Performance Analysis in Sport*, vol. 18, no. 6, pp. 1024–1036, 2018.
- [17] Z. Kozina, I. Sobko, L. Ulaeva et al., “The impact of fitness aerobics on the special performance and recovery processes of boys and girls 16-17 years old engaged in volleyball,” *International Journal of Applied Exercise Physiology*, vol. 8, no. 1, pp. 98–113, 2019.
- [18] V. I. I. Zalyapin, A. P. Isaev, A. S. Bakhareva, and A. S. Aminova, “Modelling the spectral characteristics of the circulatory system of athletes-skiers,” *Journal of Computational and Engineering Mathematics*, vol. 6, no. 4, pp. 57–68, 2019.
- [19] P. Kyzim and S. Humeniuk, “Characteristics of the leading factors of special physical preparedness of athletes from acrobatic rock and roll at the stage of preliminary basic training,” *Slobozhanskyi Herald of Science and Sport*, vol. 7, no. 3(71), pp. 48–53, 2019.
- [20] D. Detanico, R. L. Kons, D. H. Fukuda, and A. S. Teixeira, “Physical performance in young judo athletes: influence of somatic maturation, growth, and training experience,” *Research Quarterly for Exercise and Sport*, vol. 91, no. 3, pp. 425–432, 2020.
- [21] E. A. Bondareva, O. I. Parfenteva, A. V. Kozlov et al., “The Ala/Val polymorphism of the UCP2 gene is reciprocally associated with aerobic and anaerobic performance in athletes,” *Human Physiology*, vol. 44, no. 6, pp. 673–678, 2018.
- [22] R. L. Kons, D. Detanico, J. Ache-Dias, and J. Dal Pupo, “Relationship between physical fitness and match-derived performance in judo athletes according to weight category,” *Sport Sciences for Health*, vol. 15, no. 2, pp. 361–368, 2019.

## Research Article

# Predictive Analysis and Simulation of College Sports Performance Fused with Adaptive Federated Deep Learning Algorithm

**Wei Sun** 

*Sports and Military Education Department, Zhejiang University of Water Resources and Electric Power, Hangzhou 310018, China*

Correspondence should be addressed to Wei Sun; [sunwei@zjweu.edu.cn](mailto:sunwei@zjweu.edu.cn)

Received 22 January 2022; Revised 14 February 2022; Accepted 23 February 2022; Published 15 March 2022

Academic Editor: Yanqiong Li

Copyright © 2022 Wei Sun. This is an open access article distributed under the Creative Commons Attribution License, which permits unrestricted use, distribution, and reproduction in any medium, provided the original work is properly cited.

With the widespread use of intelligent teaching, data containing student performance information continues to emerge, and artificial intelligence technology based on big data has made a qualitative leap. At present, the prediction of college students' sports performance is only based on the past performance, and it does not reflect the student's training effect very well. In order to solve these problems, this paper puts forward the analysis and simulation of college sports performance fusion with adaptive federated deep learning algorithm, aiming to study the influencing factors of student sports performance and suggestions for improvement. This paper uses an adaptive federated learning method and a personalized federated learning algorithm based on deep learning and then proposes a student performance prediction method. These methods integrate the quantitative methods of motor skill assessment and establish standards for college students, which are good standards for evaluating college students' sports skills. This paper adopts the performance prediction framework and then establishes the sports performance prediction model. Through the analysis of sports performance analysis examples, it is concluded that the model proposed in this paper can accurately predict the student's sports performance, and the average accuracy rate of each sports item has reached 91.7%.

## 1. Introduction

*1.1. Background.* The contradiction between the demand for physical and mental health in today's society and the continuous decline in the physical and mental health of young people is attracting attention from all walks of life. Physical health is the basis for a person's all-round development, and physical fitness is an important part of health and an important content of quality education. Federated learning is essentially a distributed machine learning technology and a machine learning framework. The rapid development of university informatization and the continuous advancement of software engineering technology have promoted the process of education informatization in China. Teachers have accumulated a large amount of student learning data in the education process, but these data are currently only stored in the system's database and have no real effect. Through data mining technology, users can obtain useful knowledge and discover relevant laws from these data and information. These data can provide good decision-making

basis for optimizing all links of education and improving the quality of education.

*1.2. Significance.* The performance prediction warning is to predict the student's final grade through various data reflecting the student's learning situation during the learning process and to give early warning to those who may fail in their academic performance. Therefore, studying the prediction model of curriculum performance has important practical significance in improving the quality of education and reducing the dropout rate of students. Aiming at physical education in a Chinese university, this paper studies a performance prediction model based on adaptive correlation deep learning algorithm and uses this model to build a course performance early warning system. This article focuses on the issue of college sports, will strengthen the work of college sports, enhance the quality of students, promote the overall development of students, and further emphasize the value and importance of research, so as to better play the leading role of the evaluation mechanism.

This research establishes a scientific and reasonable student quality evaluation index system, which has specific theoretical and practical significance for effectively promoting the health of students.

**1.3. Related Work.** Federated learning and deep learning are currently hot research topics, and there are more and more application fields. Liu et al. introduced a privacy protection machine learning technology called federated learning and proposed a gated recurrent unit neural network algorithm based on federated learning for traffic prediction. The algorithm he proposed is different from the current centralized learning method. In the security parameter mechanism, data privacy can be effectively guaranteed [1]. Manias and Shami proposed federated learning and deployed a joint model on the transportation infrastructure through ITS case studies to improve the ability of automobiles to recover from failures using smart technology, while reducing recovery time and improving compatibility [2]. Ahmed et al. proposed an embedding model based on federated learning for transaction classification tasks, which can learn low-dimensional continuous vectors through high-frequency trading commodities. They conducted in-depth experimental analysis on the amount of high-dimensional transaction data to verify the performance of the development model based on the attention mechanism and federated learning [3]. Alguliyev et al. proposed a deep learning method for big data privacy protection analysis, which converts the sensitive part of personal information into nonsensitive data. In order to reduce the loss in data conversion, they added the sparsity parameter to the objective function of the autoencoder through the Kullback-Leibler divergence function [4]. Khan et al. proposed a two-stage calculation model based on deep neural networks, which uses standard learning methods to automatically extract information features from RNA sequences. The method they proposed does not require a lot of ergonomics and professional knowledge to design an accurate recognition model [5]. The deep learning model proposed by Farooq and Bazaz can intelligently adapt to the new ground reality in real time. Every time a new data set is received from evolving training data, there is no need to retrain the model from scratch. The model was validated with historical data, and a 30-day forecast of disease transmission was given in the five states most severely affected by the new coronavirus in India [6]. Voegelé et al. proposed a performance prediction method, which aims to automatically extract and convert workload specifications for load testing and model-based performance prediction of session-based application systems. This method (WESSBAS) includes three main components, hierarchical modeling of workload specifications that are not related to systems and tools and converting instances into executable workload specifications for load generation tools and model-based performance evaluation tools [7].

**1.4. Innovation.** The prediction model proposed in this paper has a certain impact on the cultivation of students' comprehensive physical quality and overall development. Experimental results show that a variety of strategy selection

methods based on deep learning algorithms can allow quantitative models to help schools formulate strategies. In this article, the author will train neural networks by creating samples to innovate performance prediction models.

## 2. Adaptive Federated Deep Learning Algorithm

**2.1. Adaptive Federated Learning Method.** Federated learning is a distributed machine learning method. The training data used for model learning is scattered on each mobile device, and all training of the model is realized through iterative global aggregation and update. Considering an actual distributed data training scenario, there are currently  $N$  scattered clients, and the whole composed of these clients is represented as a user set  $P$ , that is,  $|P| = N$ . Each client  $n$  has a local data set  $S_n$  that is kept and controlled by itself, and the amount of data contained in it is  $D_n$ , that is,  $|S_n| = D_n$ , the total amount of data in the client set  $P$  is denoted as  $D = \sum_{n=1}^N D_n$ . Assuming that these data are collected together in a centralized manner to train a neural network model, the weight parameter  $W$  of the model obeys an  $m$ -dimensional real number space. Then, the expression of the loss caused by the model fitting the  $i$ th sampled data point  $(x_i, y_i)$  is shown in

$$f_i(W) = l(x_i, y_i, W). \quad (1)$$

In the process of model learning, this paper continuously optimizes the loss function through optimization algorithms [8]. In order to find the optimal model parameters, the value of the loss function is minimized, and the training process of the neural network is regarded as an optimization problem. The definition of neural network optimization goal is shown in

$$\min_{W \in R^m} f(W) = \frac{1}{D \sum_{i=1}^D f_i(W)}. \quad (2)$$

Now, considering the scattered form of data, for each client  $n$ , all data on the device can be regarded as a partition of global data, and the loss caused by this data partition is shown in

$$F_N(W) = \frac{1}{D_N \sum_{i \in S_n} f_i(W)}. \quad (3)$$

Then, the global optimization goal defined in formula (2) can be rewritten into the form shown in

$$\min_{W \in R^m} f(W) = \sum_{n=1}^N \frac{D_n}{D} F_N(W). \quad (4)$$

If the data partition  $S_n$  is formed by uniformly randomly distributing the global training samples on the client set  $P$ , this means that all global samples obey an implicitly unknown distribution. The training data on the client is equivalent to being sampled independently from this

distribution, so the data of each client in the set  $P$  can be regarded as subject to independent and identical distribution (IID) [9]. In probability theory and statistics, IID data collection means that the random variable represented by each data has the same probability distribution as other variables, and all variables are independent of each other. In this case, the optimization training of the model conforms to the independent and identical distribution assumption of the traditional distributed optimization problem. Then, the value of the global loss function  $f(W)$  is equivalent to the expectation of the local loss function on each data partition  $S_n$ , that is, formula (5) holds. In contrast to this, if the data partitions  $S_n$  on the set  $P$  are not formed by the uniform random distribution of the global training samples, then the data of each client in the set  $P$  does not obey the independent and identical distribution (non-IID) [10].

$$f(W) = E_{S_n} \{F_N(W)\}. \quad (5)$$

In summary, for training data scattered on multiple clients, the global optimization problem in the learning process of the model can be transformed into the sum of multiple local problems and distributed to each client for joint solution. This is also the prototype of the idea of federated learning. The calculation process of federated learning can be described with reference to Figure 1. Assuming that a certain function as an optimization target is defined on a plane, and its graph has a bowl shape, the blue curve is a contour line, that is, this line represents a constant value of the function.

In order to optimize the communication cost of federated learning and improve its efficiency, it is necessary to analyze and elaborate its communication process in detail [11]. The network protocol of the federated learning architecture is shown in Figure 2. The participants of the protocol are client devices and servers, and the latter provides a cloud-based distributed service platform.

In the process of federated average Fed Avg, the algorithm adds a complete gradient descent step to each device to improve communication efficiency. The specific implementation is that in each round of global training, each client performs a complete gradient update calculation and then implements the gradient descent process, thereby calculating the local model parameter update  $W_t^n$ , as shown in

$$W_t^n = W_{t-1} - n \nabla F_n(W_{t-1}), \quad (6)$$

because the parameter update of the global model performed on the server can be expressed in the form shown in.

$$W_t = \sum_{n=1}^N \frac{D_n}{D} (W_{t-1} - n \nabla F_n(W_{t-1})). \quad (7)$$

Therefore, combining formulas (6) and (7), the parameters of the global model can be calculated by the method shown in

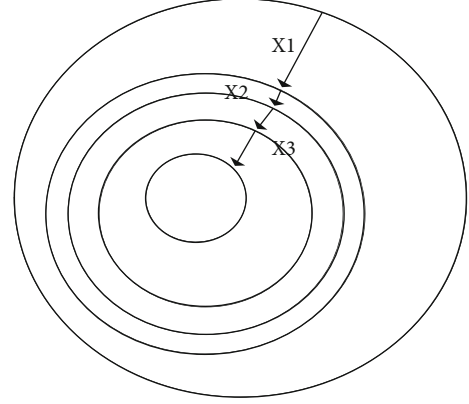


FIGURE 1: Principle of gradient descent.

$$W_t = \sum_{n=1}^N \frac{D_n}{D} W_t^n. \quad (8)$$

Therefore, after each client  $n$  calculates the parameter update  $W_t^n$  of its own local model, it uploads it to the server for global aggregation to obtain the parameter update of the global model. Then, the server starts the next round of iteration and distributes the model obtained from the previous round of training to the device to train the next round of updates.  $W_t^n$  through the implementation of a complete gradient descent and model update operations on the device. The Fed Avg algorithm provides better performance than Fed SGD and reduces communication overhead. Therefore, this algorithm is regarded as a standard algorithm for federated learning, has a high degree of recognition, and is widely used [12].

**2.2. Personalized Federated Learning Algorithm Based on Deep Learning.** In federated learning, it is assumed that there are  $N$  clients  $C_i, i = 1 \dots N$ , which jointly learn together under the scheduling of the central server. Define the data set on all clients as  $D = \{D_1, \dots, D_N\}, i = 1, \dots, N$  and the corresponding data set on each client as  $D_i$ . Assume that the data set on each client obeys a distribution  $P_i$ , and the size of each data set is  $|D_i|$ . For each data set, each item is  $(x, y)$ , where  $x \in R$  is the corresponding input feature. Define the loss function on each client as  $L_i(\hat{y}, y): R^t \rightarrow R$ . Assuming that  $w_i$  is a model parameter corresponding to each client, the model on each client can be expressed as  $\hat{y} = f(w_i, x)$ , and the optimization goal for each client is:

$$\arg \min L_i(w_i) = E_{D-P} [L_i(\hat{y}, y)]. \quad (9)$$

Putting  $\hat{y} = f(w_i, x)$  into the above formula, it can get the following expression:

$$\arg \min L_i(w_i) = E_{D-P} [L_i(\hat{y}, y)] = \frac{1}{|D_i|} \sum_j^{D_i} L_i(f(w_i, x_j), y_j). \quad (10)$$

The federated average algorithm is an algorithm under the classic federated framework. The algorithm obtains the

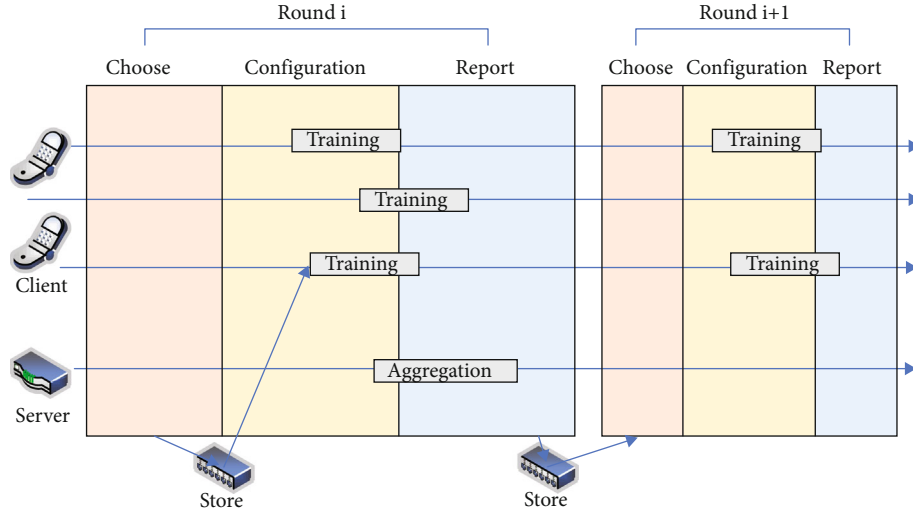


FIGURE 2: Network protocol for federated learning.

final model by optimizing the aggregate value of the loss function on the client side [13]. The federated average algorithm is a learning algorithm for the global model, so the model parameters on each client are the same, that is,  $w_0 = w_1 = \dots = w_i$ . The optimization goals of the federated average algorithm are:

$$\text{where } L(w) = \sum_i^N E_{D-P} [L_i(\hat{y}, y)] \approx \sum_i^N \frac{1}{|D_i|} \sum_j^{|D_i|} L_i(f(w, x_j), y_j), \quad (11)$$

where  $N$  represents the number of clients,  $B$  represents the size of the local training batch,  $E$  represents the local training round,  $T$  represents the entire representative round [14], and  $\beta$  represents the rate of learning. Figure 3 shows a schematic diagram of independent identically distributed and nonindependently identically distributed sampling when the number of clients is 4, the overall data category is 3, and the data category sampled on each client is 2.

After determining the setting of the calculation parameters, this article compares the parameter settings in Table 1.

The method used in the comparison operation is the federated average learning algorithm (FedAvg). The main purpose of computational exploration is to explore the influence of personalized federated data sets constructed by different data sets on the algorithm, explore the influence of different data distributions on the results of the algorithm, and explore the difference between the results of local independent calculation methods and the use of federated average calculation methods [15]. For any two clients  $C_i$  and  $C_j$ , suppose they receive the model parameter  $w$  at the same time. After the partial update procedure of the client, the updated parameters on the two clients are  $w_i$  and  $w_j$ . Then, the update of the corresponding gradient for each client is:

$$g_i = w_i - w, g_j = w_j - w. \quad (12)$$

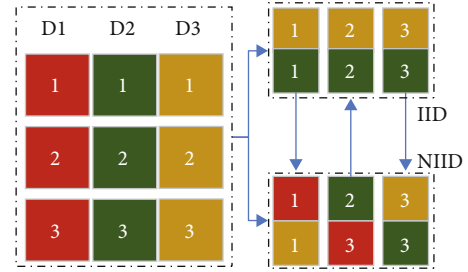


FIGURE 3: Nonindependent and identically distributed and independent and identically distributed data set construction.

The correlation between the two clients based on the model parameter  $w$  is defined by the cosine similarity of the gradients uploaded by two clients, as shown in the following formula:

$$\text{sim}(i, j) = \frac{g_i^T g_j}{|g_i| |g_j|}. \quad (13)$$

Specifically, the randomly initialized global model is sampled, and the number of samples in this paper is 100. The global initialization model for each sampling can calculate the similarity value  $\text{sim}(i, j)$  between any two clients. The mean value of the similarity of 100 samples is counted as  $E[\text{sim}(i, j)]$ . Through the analysis of these calculation results, some important factors related to personalization can be discovered. Table 2 shows the corresponding calculation results.

The analysis of the calculation results can be considered that if each client can obtain a positive gain in a nonindependent and identically distributed scenario, then personalized learning can be well realized [16].

Generally, assuming that the parameter of the model is  $w$ , define a model based on this parameter, denoted as  $f_w$ . When the initialization parameters are applied to a new task  $T_i$ , based on the stochastic gradient descent algorithm, the

TABLE 1: Federated averaging algorithm exploration operation parameters.

Numbering	Data set	Data distribution	Calculation	Total client	Number of categories	Number of training sets
3-1-1	MNIST	IID	Independent calculation	9	9	2600
3-1-2	MNIST	IID	Federated computing	9	9	2600
3-1-3	MNIST	NIID	Independent calculation	9	9	2600
3-1-4	MNIST	NIID	Federated computing	9	9	2600
3-1-5	EMNIST	IID	Independent calculation	9	18	3600
3-1-6	EMNIST	IID	Federated computing	9	18	3600
3-1-7	EMNIST	NIID	Independent calculation	9	18	3600
3-1-8	EMNIST	NIID	Federated computing	9	18	3600

TABLE 2: Federal average experimental results (%).

Numbering	c1	c2	c3	c4	Average
3-1-1	88	82.5	84.9	83.4	84.7
3-1-2	80.2	81.2	84.5	82	81.975
3-1-3	81.4	86.5	83.5	89.3	85.175
3-1-4	81.9	87.7	81.6	81.7	83.225
3-1-5	83.3	85	85.7	84.3	84.575
3-1-6	85.2	80.9	80.9	87.7	83.675
3-1-7	87.9	86.2	89.7	87.3	87.775
3-1-8	85.5	80.2	80.8	83.5	82.5

parameters of the model will change from  $w$  to  $w'_i$ , then the change of the parameters can be represented by formula (14), where  $L$  represents the loss function and  $\beta$  represents the learning rate on the task, which is a hyperparameter.

$$w'_i = w - \beta \nabla_w L_{T_i}(fw). \quad (14)$$

Through the federated average learning algorithm, the key factors related to personalization in federated learning are explored. This section proposes a personalized federated learning algorithm based on deep learning. The core is to model the correlation between clients [17]. The algorithm includes personalized algorithms for the client and server, and different weights are assigned to the client through correlation, and a personalized integration strategy is realized.

**2.3. Methods of Predicting Student Performance.** In the input layer, construct the grade matrix of  $T$  semester student-course data as  $G$ ,  $G^{(n)}$  is the row vector of the student's score for each course, and  $G_j$  is the column vector of each student's score in different courses. In the formula,  $(i, j) \in \Omega$ , this article uses  $G^{(n)}$  and  $G_j$  as the prediction model input [18].

This article maps and projects the rows and columns of the performance matrix and summarizes the hidden features of athletes and courses. Since the constructed score matrix is very sparse, embedding layer mapping can be used to reduce the dimensionality of the data and reduce the sparseness of the data. It uses formula (15) to perform nontraditional operations. For the hypothetical score formula  $G_{nj}$ , there are:

$$xs = \text{Tanh}(G^{(n)} \bullet W_s), xc = \text{Tanh}(G_j \bullet W_c). \quad (15)$$

Among them,  $xs, xc \in G^k$  are the potential special factors of the students and the potential special factors of the course, respectively.  $Ws \in G^{m \times k}$ ,  $Wc \in G^{k \times n}$  is the characteristic corresponding ratio matrix of athletes and sports items. The noncalculated result uses the commonly used activation function Tanh function. Different weight values are added to the student potential feature vector and the curriculum potential feature vector. Each student's performance and each sport's characteristics have different importance, which can be transformed according to the following formula:

$$xsa = \text{Softmax}(xs \bullet W_{sa}) \bullet xs, xca = \text{Softmax}(xc \bullet W_{ca}) \bullet xc. \quad (16)$$

Among them,  $W_{sa}$  and  $W_{ca}$  are proportional factors,  $xs$  and  $xc$  is divided into student potential feature vector and course potential feature vector [19]. Among them, multilayer perception is transformed according to formula (17). Its purpose is to simulate the special structure of the data and perform two-layer nonlinear mapping of the hidden personality of students and the hidden characteristics of sports items:

$$Hs = \text{sigmoid}(xsa \bullet W_s' + bs). \quad (17)$$

The result of the performance deduction in this article is expressed as the result of the product. This article uses bilinear pooling to obtain the predicted value of the performance. Its main function is to reduce the amount of calculation while reducing the dimensionality, prevent the model from overfitting, and improve the generalization ability of the model. The output value is converted in the bilinear pooling layer as follows:

$$g = K^T Q(p_s^T * q_c). \quad (18)$$

Among them,  $K$  is the proportional factor,  $*$  in the formula represents Hadamard, and  $Q$  is the activation formula. Simulate  $T$  academic year's sports performance, specifically expressed as:

$$L = \min_{Ws} \frac{1}{2} \sum_{i,j \in w} \left( G_{ij} - h^T Q(p_s^{(i)} * q_{cj}) \right)^2 + \partial |Ws|. \quad (19)$$

Among them,  $W$  is the set of unknown parameters in the model, and  $h^T Q(p_s^{(i)} * q_{cj})$  is the deduction result of the formula output by the nonlinear pooling layer [20]. Use  $ps$  ( $ps \in$

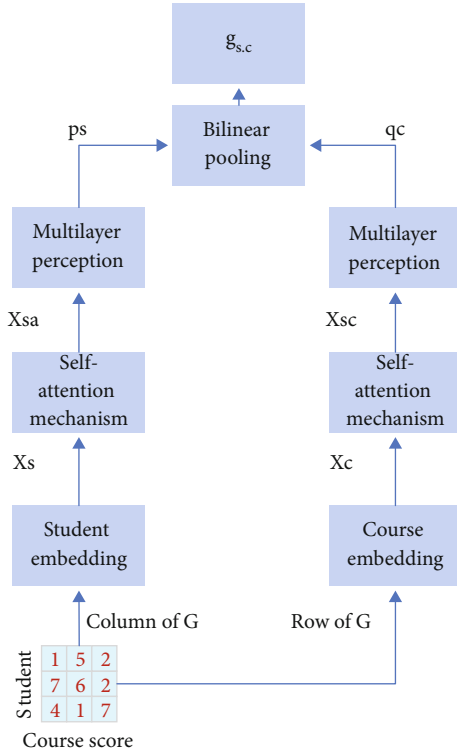


FIGURE 4: The frame structure of the depth matrix factorization model.

$G^k$ ),  $qc(qc \in G^k)$  to represent the potential  $k$  dimension characteristics of students  $s$  and courses  $c$ . The deduction performance of the athlete  $s$  in the sports project  $c$  can be calculated as:

$$\hat{g}_{s,c} = p_s^T qc. \quad (20)$$

This formula can predict students' grades in the  $T$  semester. The structure of student performance prediction method based on deep learning is shown in Figure 4.

### 3. Performance Prediction Model Experiment and Analysis

**3.1. Performance Prediction Framework.** In order to verify the accuracy of the performance prediction model proposed in this paper, this paper designs two experiments: (1) multi-source small sample, focusing on the fusion of multispatial data and the impact of multidimensional behavior on academic performance [21]; (2) single-source large sample, focusing model's prediction accuracy for large sample and the difference in behavior patterns of different groups of students in liberal arts and sciences. The research framework of this article is shown in Figure 5.

It can be seen from Figure 5 that this research framework is mainly composed of academic prediction and early warning feedback. The main data sources of this research include digital educational administration system, all-in-one card, and cloud classroom online learning data. In this article, the experiment attempts to build a multidimensional behav-

ioral quantitative calculation system to ensure the protection of secret data, encrypt key personal information, and divide the academic performance into various intervals based on the average score [22]. The early warning feedback part includes providing feedback and early warning to high-risk students based on the predicted results.

This article establishes a classification model based on machine learning algorithms to predict academic performance and builds classification models based on five machine learning algorithms: RF random forest, GBRT gradient boosting decision tree, KNN nearest neighbor, SVM support vector machine, and extreme gradient boosting XGBoost. Table 3 shows the experiments and experimental results to verify the prediction results.

RF (random forest), GBDTm and XGBoost all belong to the ensemble learning model. The purpose of ensemble learning is to improve the generalization ability and robustness of a single learner by combining the prediction results of multiple base learners. That is, there is a strong dependency between individual learners and a serialization method that must be generated serially, and there is no strong dependency between individual learners and a parallelization method that can be generated at the same time. The former is represented by boosting, and the latter is represented by bagging and "random forest."

Although the five machine learning algorithms have their own performance advantages, in general, the classification performance of the five machine learning algorithms has a small gap on this data set [23]. The experimental result is that more data sources can make the prediction results more accurate. In order to better illustrate this point, this study considered the performance prediction model based on SVM and also compared the performance of three different feature combinations, as shown in Figure 6.

As shown in Figure 6, from DI to D1+D2 and DI+D2 +D3, all five classification evaluation indicators increase significantly with the increase of data source types. This experiment proves that richer data sources help to explore the deep-level mechanism of student behavior. All five evaluation indicators of C-3 (accuracy, accuracy, recall,  $f$ , and AUC) are significantly higher than C-1 and C-2. This result shows that the multifeature combination (namely, C-3) proposed in this research can significantly improve the predictive ability of academic performance.

In addition, this article calculates and supplements six other indicators and also calculates the Pearson correlation  $r$  between these indicators and academic performance. The closer the absolute value of  $r$  is to 1 or -1, the stronger the correlation between the two, and the closer  $r$  is to 0, the weaker the correlation between the two. The index evaluation is shown in Figure 7.

In the smart campus environment, this study collected student behavior data noninvasively, established a high-precision sports performance prediction model, and provided a basis for decision-making for college administrators [24]. This research has obtained conclusions on the behavior patterns of students with different liberal arts backgrounds and their impact on academic performance, which will help managers to further guide and optimize students' daily behaviors.



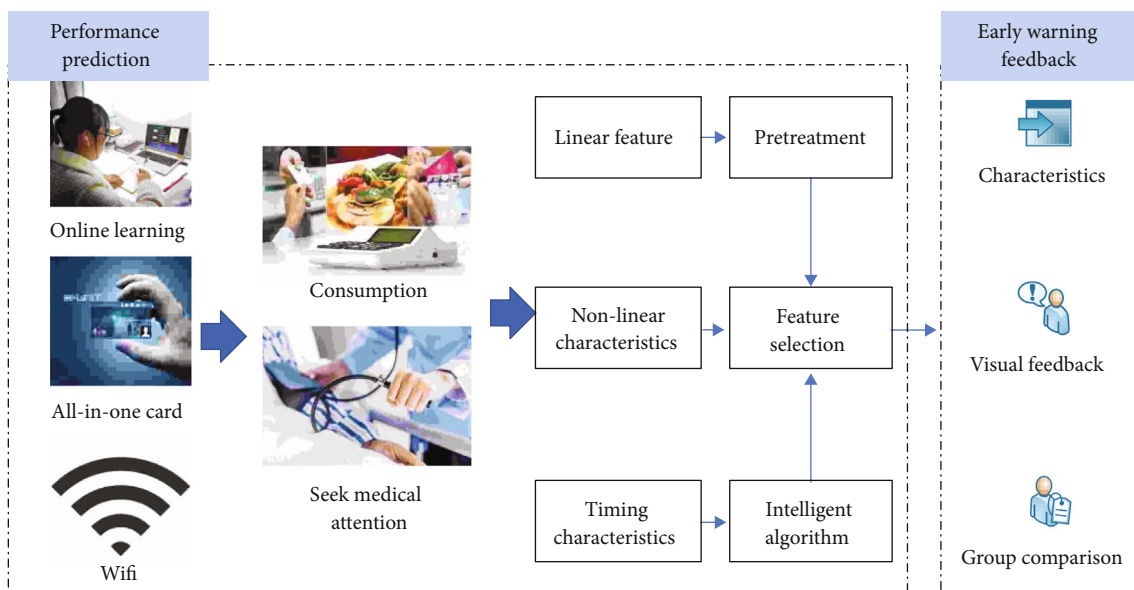


FIGURE 5: Data perception + behavior feature library → time series.

TABLE 3: Experimental classification results.

Data	Feature	Algorithm	Accuracy	Precision	Recall	AUC
D1 (SPOC)	C-1	RF	0.114	0.502	0.459	0.533
		GBRT	0.439	0.343	0.909	0.604
D2 (all-in-one card)	C-2	KNN	0.606	0.542	0.230	0.702
		SVM	0.018	0.534	0.615	0.527
D3 (WiFi)	C-3	XGBoost	0.723	0.906	0.128	0.181

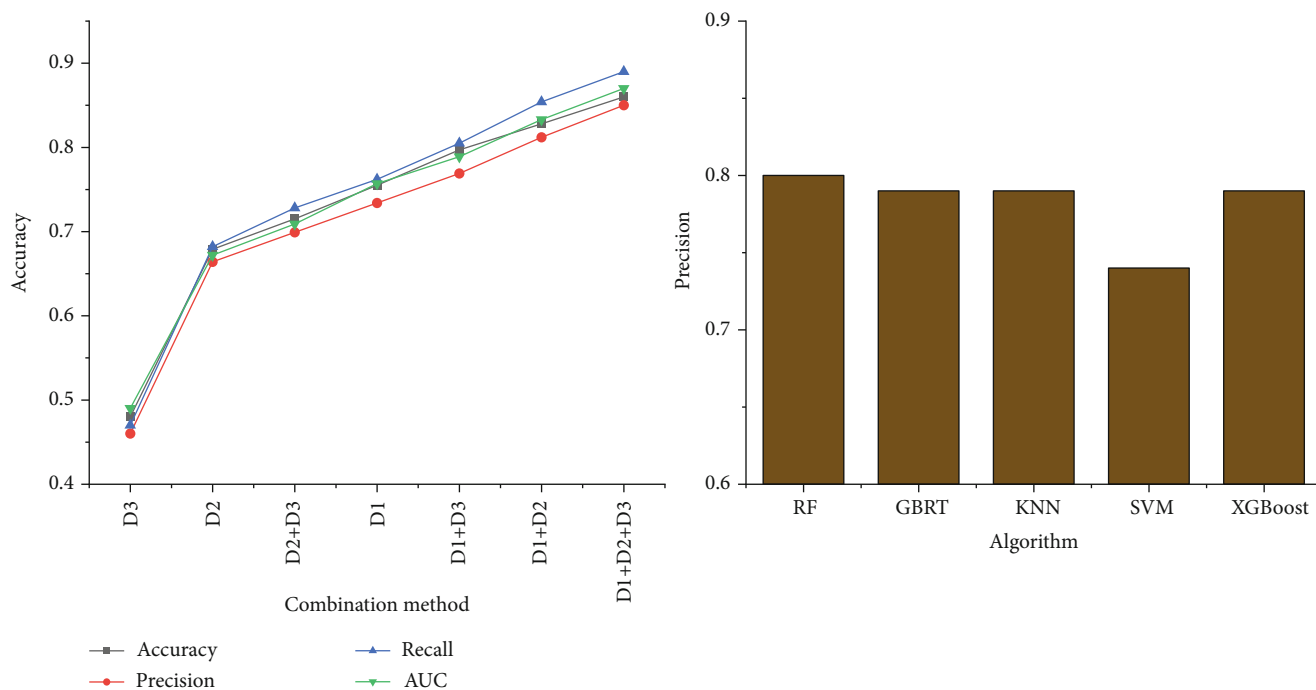


FIGURE 6: Comparison of accuracy values between three data set combinations and feature combinations.

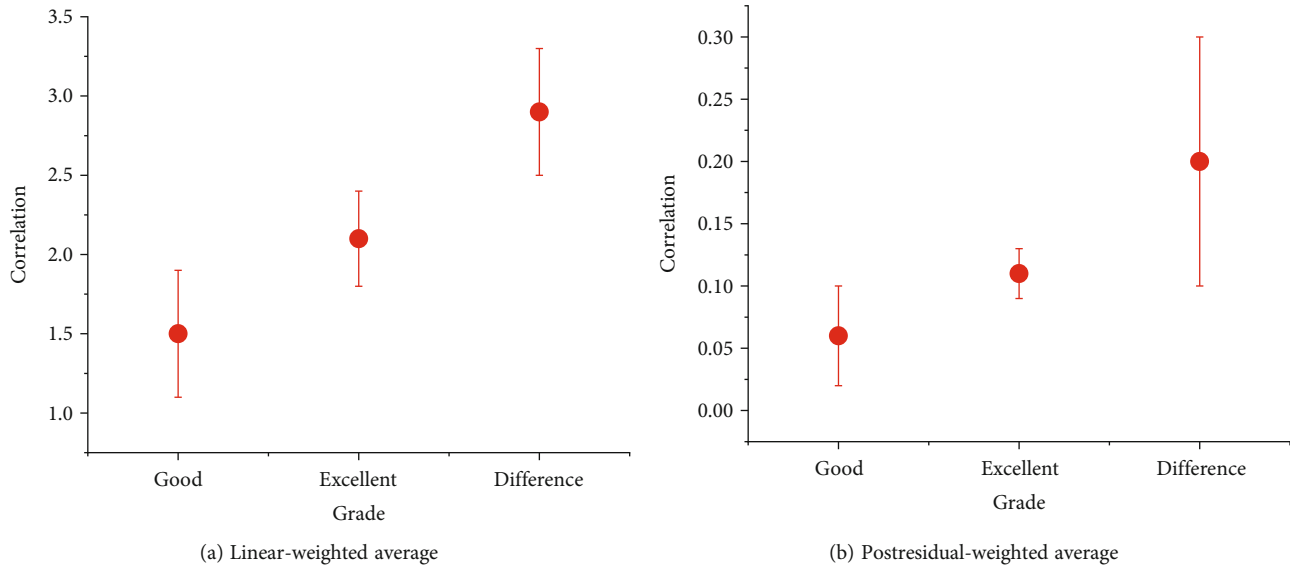


FIGURE 7: Example of feedback to high-risk students.

### 3.2. Establishment of Sports Performance Prediction Model.

The research of performance prediction model is to predict the specific aspects of specific students. Now, by predicting specific physical abilities and specific abilities, we can comprehensively improve sports performance and create more economic value. This article has achieved this goal. In the process of modern sports training, coaches conduct regular assessments and evaluations of students, estimate their specific performance based on the results of the assessment items, and adjust their regular training plans. These data need to provide a basis for students' training. Over the years, coaches and scholars have continued to study, provide scientific improvement programs for student training, clarify students' sports training goals, and cultivate many outstanding sports talents through the establishment of performance prediction models. Therefore, the research of sports performance prediction model is a highly scientific and practical research.

This article will survey 100 students aged 18 to 21 from a sports school in China. Scientific index selection is the prerequisite for establishing an evaluation model. Through a variety of mathematical statistical methods and scientific selection of parameter indicators, this article can provide a reliable basis for formulating students' training goals. Therefore, this article needs a mathematical analysis of whether the special performance and various special fitness indicators are normally distributed. After the scientific data test, the special performances and the special fitness indexes investigated are normal, which is enough to show that the method of screening indexes through factor analysis has scientific hypothesis for this topic. In order to clarify the degree of closeness between the variables, this article first conducts a correlation analysis and establishes a correlation coefficient matrix.

There are many physical factors that affect sports performance. Through research and statistics, this article classifies and sorts out the indicators that can accurately reflect the

physical fitness level and the typical indicators closely related to the development of specific performance and obtains the four-element regression equation of the student's specific physical fitness indicator system, that is, a special performance prediction model. Among them, the prediction model includes 30-meter running with a gun (continuous), 3-step approach and 5-step jump, and a ball with a weight of 300 grams on the shoulder during the full approach, dependent variable: specific performance.

The purpose of the evaluation system established is to enable students to obtain objective and quantitative evaluations of the training and development level of various indicators. According to the individual development characteristics of the students and the development requirements of special sports events, the main special physical fitness that affects the performance is grasped as a whole. Therefore, the establishment of an evaluation system is the basis and prerequisite for quantitative monitoring of model training and an important link in the implementation of system control. The system has a good reference for training planning and implementation, as well as the evaluation and feedback of training effects.

In order to explain the differences between the four special physical fitness sensitive indicators that influence youth sports performance extracted by factor analysis, this study adopted the standard percentage method to evaluate the individual indicators of the main influencing factors. According to the relevant statistical analysis described above, it is shown that the normal distribution of various indicators of specific performance and specific physical fitness is better, as shown in Figure 8.

Using factor analysis and other mathematical statistical methods to analyze, in order to make the special physical fitness training of these students truly scientific, optimize the special physical fitness training system and other factors that may affect the special performance. Physical education teachers can comprehensively consider factors such as

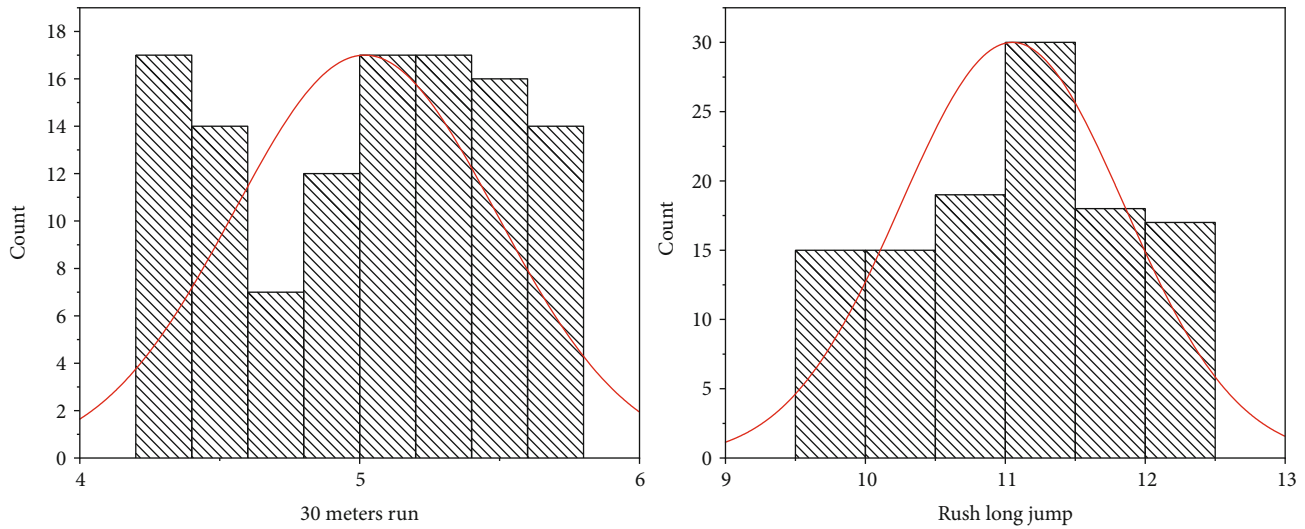


FIGURE 8: Normality test results of 2 indicators.

general abilities, special skills, and body shape in the process of adopting modular special physical fitness training to achieve the best results of scientific training.

**3.3. Examples of Sports Performance Analysis.** The basic process of establishing a special motor skill evaluation system in this paper is to screen out all the difficult movements that can reflect the level of motor skills, establish an effective technical level evaluation index system, and construct a scoring scale one by one. Sports index testing is actually testing and scoring students in accordance with the scoring standards, and the accuracy of the evaluation results is evaluated by a dedicated coach. Table 4 shows the test results of the subject’s body type and fitness index.

From the results of the cluster analysis, it can be seen that among the indicators selected for the second time, the 1-minute push-up and the right-angle support are classified into one category, indicating that there is a very high degree of correlation between these two indicators. For a sports student, if the performance of 1-minute push-ups is excellent, then his performance of right angle support must be excellent, and vice versa, so this article only needs to select representative indicators.

Existing predictive models for student specific performance generally use multiple regression methods and gray models. This paper establishes the functional relationship between specific performance and quality training level and then predicts performance through student performance recognition. These predictive models reflect the relationship between special performance and training indicators to a certain extent and provide corresponding guidance for trainees’ training. However, the decisions of these models are based on certain assumptions, so formulas for special performance prediction models must be set in advance. In fact, the functional relationship between special performance and various related factors is very complicated, and the presumed formula does not fit these relationships well.

After a lot of training and prediction tests, this article found that adding some test data will affect the convergence

TABLE 4: Test results of physical fitness indicators.

Index	Average	Standard deviation	Lowest value	Highest value
Height	172	3.6	154	186
Weight	60	2.7	41	76
Shoulder width	35	2.9	30	40
Chest circumference	84	2.5	79	89
Waistline	67	2.8	62	72
Hips	91	3.5	86	96
Upper limb length	71	4.7	66	76
Arm length	46	4.1	41	51
Tight upper arm circumference	29	2.8	24	34
Relax upper arm	30	2.5	25	35
Thigh circumference	54	3.3	49	59
Standing long jump	2.04	2.3	-2.96	7.04
Seated pregenus	29	4.9	24	34
Minute push-ups	87	2.2	82	92
Cross jump test	8	4.3	3	13
1 minute skipping rope	143	4.6	138	148
800 m run	193	5	188	198
30-meter run	5	2	4	6

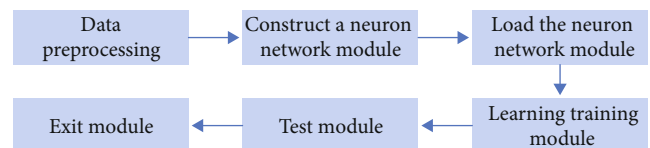


FIGURE 9: Block diagram of training prediction process.

speed and prediction accuracy of the model. For example, due to some special circumstances, the training time is not long enough, or there is a deviation in certain index tests.

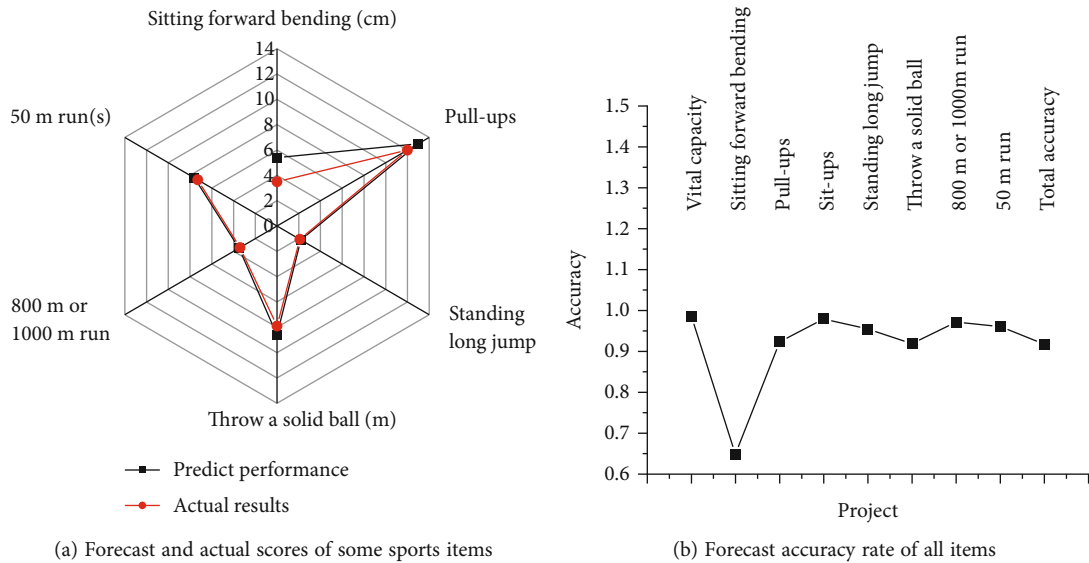


FIGURE 10: Accuracy of performance prediction.

Therefore, this kind of data was excluded in the test. Federated learning algorithms have high requirements for computer configuration, especially memory, due to the huge amount of calculation. The entire training prediction process consists of 6 modules, as shown in Figure 9.

This article uses body shape, physical function, physical strength, ontology knowledge, operational knowledge, basic skills, technical combination, sports learning experience, sports competition participation experience, etc. as secondary indicators, reflecting the diversification of sports quality evaluation. On this basis, this article subdivides 25 three-level indicators, which are easy to operate and quantify, and scientifically assign weights to the above indicators.

According to the prediction model proposed in this article, 100 students' 9 sports performances were predicted and compared with their actual scores. The comparison results are shown in Figure 10.

It can be seen from Figure 10 that there is not much difference between the predicted result and the actual score, and the overall accuracy rate has reached 91.7%. The experimental results show that the model can provide relatively accurate prediction results for teachers and students.

#### 4. Discussion

The above are the main research results of this article. Although the algorithm proposed in this paper can better improve the problems caused by the average aggregation method of the classic federated learning algorithm, there are still some problems that have not been considered. In terms of privacy protection, this article adopts a privacy protection method consistent with the classic Fed Avg, that is, to protect privacy by transferring model parameters while retaining the original data locally. However, this level of privacy protection cannot meet the requirements of higher levels. In the future, more secure privacy protection technologies can be explored to empower federated learning. This paper is based on the performance prediction model con-

structed by federated learning and deep learning algorithms, which can provide teachers and students with relatively accurate prediction results. However, the accuracy of the stage performance prediction model to predict the final score interval is not good, so the next work needs to optimize the construction of the stage performance prediction model.

#### 5. Conclusions

This paper studies a performance prediction model based on federated learning and deep learning algorithms and uses this model to implement a sports performance early warning system. In this article, the author will use a deep learning algorithm to predict the performance of 100 students based on a real-world application of improved algorithms, investigate the impact of physical learning on physical performance, and analyze the classification rules generated for students in various basic courses. This model can provide teachers with real-time understanding of the training situation of class students, the results of course performance prediction, and early warning to notify students in crisis, so that the quality of class teaching can be improved by guiding students in crisis in advance. It can provide students with real-time understanding of personal learning situation, sports performance prediction results, and viewing early warning reasons and learning suggestions, so that they can avoid missed courses through strengthened training.

#### Data Availability

The data used to support the findings of this study are available from the corresponding author upon request.

#### Conflicts of Interest

The author declares no conflicts of interest.

## References

- [1] Y. Liu, J. Yu, J. Kang, D. Niyato, and S. Zhang, "Privacy-preserving traffic flow prediction: a federated learning approach," *IEEE Internet of Things Journal*, vol. 7, no. 8, pp. 7751–7763, 2020.
- [2] D. M. Manias and A. Shami, "Making a case for federated learning in the internet of vehicles and intelligent transportation systems," *IEEE Network*, vol. 35, no. 3, pp. 88–94, 2021.
- [3] U. Ahmed, G. Srivastava, and C. W. Lin, "A federated learning approach to frequent itemset mining in cyber-physical systems," *Journal of Network and Systems Management*, vol. 29, no. 4, pp. 1–17, 2021.
- [4] R. M. Alguliyev, R. M. Aliguliyev, and F. J. Abdullayeva, "Privacy-preserving deep learning algorithm for big personal data analysis," *Journal of Industrial Information Integration*, vol. 15, pp. 1–14, 2019.
- [5] S. Khan, M. Khan, N. Iqbal, T. Hussain, S. A. Khan, and K. C. Chou, "A two-level computation model based on deep learning algorithm for identification of piRNA and their functions via Chou's 5-steps rule," *International Journal of Peptide Research and Therapeutics*, vol. 26, no. 2, pp. 795–809, 2020.
- [6] J. Farooq and M. A. Bazaz, "A deep learning algorithm for modeling and forecasting of COVID-19 in five worst affected states of India," *Alexandria Engineering Journal*, vol. 60, no. 1, pp. 587–596, 2021.
- [7] C. Voegelé, A. V. Hoorn, E. Schulz, W. Hasselbring, and H. Krcmar, "WESSBAS: extraction of probabilistic workload specifications for load testing and performance prediction—a model-driven approach for session-based application systems," *Software & Systems Modeling*, vol. 17, no. 2, pp. 443–477, 2018.
- [8] Y. Wang, Y. Tian, X. Yin, and X. Hei, "A trusted recommendation scheme for privacy protection based on federated learning," *CCF Transactions on Networking*, vol. 3, no. 3-4, pp. 218–228, 2020.
- [9] Y. Qi, M. S. Hossain, J. Nie, and X. Li, "Privacy-preserving blockchain-based federated learning for traffic flow prediction," *Future Generation Computer Systems*, vol. 117, no. 2946, pp. 328–337, 2021.
- [10] A. B. Giles, J. E. Davies, K. Ren, and B. Kelaher, "A deep learning algorithm to detect and classify sun glint from high-resolution aerial imagery over shallow marine environments," *ISPRS Journal of Photogrammetry and Remote Sensing*, vol. 181, no. 4, pp. 20–26, 2021.
- [11] F. Wang, L. Xing, H. P. Bagshaw, M. K. Buyyounouski, and B. Han, "Automated needle digitization in ultrasound-based prostate high dose-rate brachytherapy using a deep learning algorithm," *International Journal of Radiation Oncology • Biology • Physics*, vol. 108, no. 3, pp. S129–S130, 2020.
- [12] D. Sudha and J. Priyadarshini, "An intelligent multiple vehicle detection and tracking using modified vibe algorithm and deep learning algorithm," *Soft Computing*, vol. 24, no. 22, pp. 17417–17429, 2020.
- [13] C. Liu and X. Zheng, "Exploring resource management for innovation power network based on deep learning algorithm," *Neural Computing and Applications*, vol. 33, no. 9, pp. 4013–4025, 2021.
- [14] G. Agarwal and H. Om, "Performance of deer hunting optimization based deep learning algorithm for speech emotion recognition," *Multimedia Tools and Applications*, vol. 80, no. 7, pp. 9961–9992, 2021.
- [15] X. W. Jiang, T. H. Yan, J. J. Zhu et al., "Densely connected deep extreme learning machine algorithm," *Cognitive Computation*, vol. 12, no. 5, pp. 979–990, 2020.
- [16] M. R. Struyvenberg, J. D. Groof, J. Putten et al., "297 - deep learning algorithm for characterization of Barrett's neoplasia demonstrates high accuracy on Nbi-zoom images," *Gastroenterology*, vol. 156, no. 6, p. S-58, 2019.
- [17] S. Dong, Y. Zhang, Z. He, N. Deng, X. Yu, and S. Yao, "Investigation of support vector machine and back propagation artificial neural network for performance prediction of the organic Rankine cycle system," *Energy*, vol. 144, pp. 851–864, 2018.
- [18] C. Tirupathinaidu, N. Jain, T. Renganathan, and S. Pushpavanam, "Unified thermodynamic model for performance prediction of adiabatic feedstock gasifiers," *Industrial and Engineering Chemistry Research*, vol. 59, no. 44, pp. 19751–19769, 2020.
- [19] D. D. Dang, X. T. Pham, and C. C. Nguyen, "Thermal performance prediction in the air gap of a rotor-stator configuration: effects of numerical models," *Journal of Thermal Science*, vol. 29, no. 1, pp. 206–218, 2020.
- [20] D. J. Armaghani, R. S. Faradonbeh, E. Momeni, A. Fahimifar, and M. M. Tahir, "Performance prediction of tunnel boring machine through developing a gene expression programming equation," *Engineering with Computers*, vol. 34, no. 1, pp. 129–141, 2017.
- [21] Z. Zhao, Q. Quan, and K. Y. Cai, "A health performance prediction method of large-scale stochastic linear hybrid systems with small failure probability," *Reliability Engineering and System Safety*, vol. 165, pp. 74–88, 2017.
- [22] S. Woodman, H. Hiden, and P. Watson, "Applications of provenance in performance prediction and data storage optimisation," *Future Generation Computer Systems*, vol. 75, pp. 299–309, 2017.
- [23] D. López-Plaza, F. Alacid, J. M. Muyor, and P. Á. López-Miñarro, "Sprint kayaking and canoeing performance prediction based on the relationship between maturity status, anthropometry and physical fitness in young elite paddlers," *Journal of Sports Sciences*, vol. 35, no. 11, pp. 1083–1090, 2017.
- [24] A. M. Al-Faifi, B. Song, M. M. Hassan, A. Alamri, and A. Gumaei, "Performance prediction model for cloud service selection from smart data," *Future Generation Computer Systems*, vol. 85, pp. 97–106, 2018.

## Research Article

# Inverter Design and Droop Parallel Control Strategy Based on Virtual Impedance

Lu Wang 

*School of Mathematics and Information Engineering, Chongqing University of Education, Chongqing 400065, China*

Correspondence should be addressed to Lu Wang; wanglu@cque.edu.cn

Received 20 January 2022; Revised 16 February 2022; Accepted 21 February 2022; Published 11 March 2022

Academic Editor: Wen Zeng

Copyright © 2022 Lu Wang. This is an open access article distributed under the Creative Commons Attribution License, which permits unrestricted use, distribution, and reproduction in any medium, provided the original work is properly cited.

The present work is aimed at improving the performance of the multiobjective energy parallel step-by-step power generation system and enhancing the reliability and stability of the energy supply. Firstly, the difficulties of the ring current control method of the inverter power supply are summarized. Secondly, the causes of ring current in the circuit are analyzed. On this basis, the topology structure of the primary circuit of the inverter unit is designed, and the simulation model of the droop control is proposed for the inverter power supply. Finally, experiments are implemented to test the performance of the model. The results demonstrate that the waveform quality of the output voltage of the parallel system controlled by the virtual impedance technology is significantly improved. Specifically, the harmonic content near the fundamental wave significantly decreases compared with the original, from 6% to about 2%. Besides, the interference of the ring current to the parallel control inverter of the power supply system is weakened, and the output stability of the inverter power supply is improved. This study designs the structure of the inverter converter based on multiobjective decision-making and discusses the droop parallel control strategy. It provides a specific reference for controlling the circuit parallel system and has positive promotion significance for sustainable energy management and the rational utilization of electric energy.

## 1. Introduction

As the basis for the survival and development of human society, energy has always been the focus of research in related fields in various countries. With the rapid growth of the consumption of fossil fuels, such as oil and natural gas, all countries in the world are facing severe challenges in terms of energy consumption and environmental pollution [1, 2]. The widespread use of fossil fuels has caused severe damage to the ecological environment, indirectly affecting human development. At present, China's energy structure has many flaws. Coal energy consumption accounts for the most significant proportion of all primary energy resources, followed by oil, natural gas, hydropower, and nuclear power [3, 4]. It can be seen that China's energy consumption structure is very unreasonable, and the proportion of clean energy and the renewable energy consumption is much smaller than that of fossil energy [5]. Therefore, developing and improving the utilization efficiency of new energy and renewable energy is inevitable to solve the current global energy crisis. Electric-

ity is the most popular energy form at present, which is cleaner and more convenient, playing the role of the lifeline of human society.

Energy shortage and environmental degradation are major issues faced by all countries worldwide for social development [6, 7]. Improving energy efficiency, accelerating the development of environmentally friendly, clean, and renewable energy, and strengthening the use of renewable energy are important choices in the national energy strategy. The development and utilization of renewable energy are fundamental for implementing the scientific development concept, building a resource-saving society, and achieving sustainable development [8]. It is also an important measure to protect the environment and deal with climate change. Distributed power generation has the advantages of saving energy, environmental protection, high efficiency, and flexibility, becoming the focus of relevant research fields worldwide. The distributed generation system with multiple power sources in parallel plays a vital role in promoting the development and utilization of renewable energy, expanding the capacity

of the power supply system, and improving the reliability of the power supply [9, 10]. The distributed power system has the following characteristics. First, the power source can configure various power sources through the power conversion network. Second, all distributed power sources are connected to the alternating current (AC) grid bus and play a role together. Third, a parallel inverter power supply is usually employed for small distributed generation systems. Fourth, the parallel connection of the inverter power supply does not require connecting wires, which is especially suitable for the inverter power supply to be connected to the power grid. An ideal distributed generation system consists of the parallel inverter power module, output line impedance, AC bus, and loads connected to the AC bus. Notably, the inverter power supply is the heart of the distributed generation system [11, 12]. It converts distributed energy sources into electricity through inversion, current sharing, and other techniques that enable the system to operate parallel with the grid. In the distributed generation of renewable energy, the inverter parallel connection control is critical in the parallel inverter system. The research on inverter parallel technology started late in China, and the parallel control study is immature. Most parallel systems use distributed control. This method has the great advantage that when there is a failure in the parallel system, the system will be automatically exited, effectively improving the system reliability. Connecting each module in parallel is suitable for current sharing control, and the information exchange between the modules is carried out through interconnection. This control method improves the redundancy of the parallel system, thus significantly improving reliability. However, more parallel modules and the wiring distance will easily interfere with the interconnection signal. Removing the interconnection between inverters in a parallel system can eliminate the above defects and improve the system's reliability. However, this operation will cut off the information exchange between parallel modules, dramatically increasing the difficulty of control. At present, the realization and parallel control of inverter modules is a hotspot in microgrid research. Nowadays, growing power equipment has begun to use unique power supplies. Paralleling the power supplies of the inverter power system can effectively improve the quality and efficiency of the power supply and prevent grid pollution, which has far-reaching significance. Some achievements have been made in researching inverter paralleling technology, but there are still many problems. Related research in China is in its infancy. The research on parallel control technology enables inverters to operate stably in parallel, which is of great practical significance.

Therefore, the present work firstly analyzes the parallel ring current control method of the inverter power supply and clarifies the difficulties of ring current control. Secondly, the ring current causes are analyzed to propose a corresponding current sharing control scheme based on the parallel system. The system control ideas are described in detail and comprehensively from the perspectives of central circuit topology, output characteristics and power control, inverter voltage synthesis, and power system monitoring of wireless parallel inverters. In addition to the digital simulation of the parallel control strategy of the inverter power

supply, an experiment is designed to test its performance, hoping to achieve satisfying research results.

## 2. Literature Review

Lin et al. [13] designed an improved virtual impedance consisting of a resistor tuned by active deviation and a complex impedance component adjusted by a reactive variation to achieve accurate power distribution. They found that the droop control would cause system voltage amplitude and frequency deviations under steady-state conditions. The low-pass filter in the power calculation loop would reduce the system's dynamic performance. Peng et al. [14] combined the improved particle swarm optimization with virtual impedance. They used the algorithm to find the optimal parameters in the coupling compensation so that the system could guarantee a stable operating state. However, experimental results showed that introducing this algorithm would lead to poor dynamic performance. Chen et al. [15] proposed a two-level adaptive virtual impedance control scheme. The authors adjusted the active power through the maximum power bus in the first-level control to ensure the power-sharing of the system; they utilized the second-level control to eliminate the shared errors for active power, unbalanced power, and harmonic power. Zhang et al. [16] proposed an enhanced proportional power distribution strategy based on the adaptive virtual impedance to solve the power coupling in complex impedance environments. However, introducing a central controller resulted in time delay and signal error. Geng et al. [17] studied the resistive microgrid and adopted the method of virtual negative reactance control and adaptive virtual resistance. In this way, they eliminated the coupling between the active and reactive power of the inverter and realized distributed "plug and play" for power inverters. Liu et al. [18] introduced virtual impedance into the circuit to improve line impedance characteristics and solve the problem of system output power coupling. Still, they proved that virtual impedance would reduce the standard bus voltage.

Here, based on the parallel connection of two inverters, the equivalent output impedance of the parallel inverter system is shaped by introducing and designing the value of virtual complex impedance to realize power decoupling. In addition, an improved droop control method is proposed based on the original virtual impedance control. This scheme furnishes the parallel inverter system with a fast dynamic response speed, realizes good power sharing, and compensates for the voltage drop caused by the introduction of virtual impedance. Consequently, the system frequency deviation is within the controllable range, and the system frequency remains stable. Figure 1 displays the research framework.

## 3. Theory and Method

*3.1. Parallel Circulation Control Method for Inverter Power Supply.* The research on parallel inverter control technology began in the early 1980s. The rapid development of computer technology promotes the continuous innovation of power and electronic technologies, and research has also

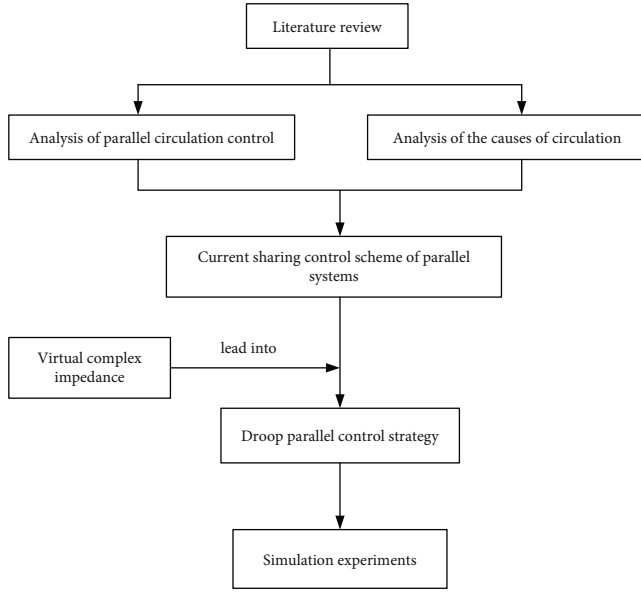


FIGURE 1: Research route.

made significant progress in inverter technology. In the field of inverter technology, parallel AC power supply has attracted increasing attention. The success of control schemes and concrete products has set a crucial benchmark for the high-performance development of parallel inverter power systems [19, 20]. Parallel inverter operation is deeply studied based on the successful experience of paralleling process. However, the inverter power supply outputs AC varying according to the sine wave law. Therefore, the parallel operation is more complicated than the parallel direct current (DC) power supply, primarily manifested in three aspects.

First, the inverter's voltage frequency and phase should be strictly synchronized, which is the premise to ensure that the inverter with the same capacity outputs the same active power when running in parallel [21, 22]. However, it is a great challenge to ensure voltage, frequency, and phase synchronization. Even if the voltage and frequency are consistent, a slight phase difference will cause serious balance problems for the output of active power of inverter voltage [23]. The smaller the output power, the greater the influence of phase difference on the inverter power supply. In more severe cases, rectification may even occur.

Second, the output voltage amplitude will be uneven after the phase and frequency are synchronized, generating many reactive circulating current components at the output current. The consistency will also increase the loss of the inverter and even lead to power overload burning the power supply [24].

Third, after the output voltage of each inverter in parallel operation reaches sinusoidal waveform, indicating that the frequency, phase, and amplitude are the same, the inverter output will also affect the difference of harmonic components of each output voltage and generate parallel units between harmonic circulation.

Therefore, to meet the operation requirements of the inverter, the frequency, phase, amplitude, and waveform

height of the output voltage of each parallel unit need to be consistent, and the load current should be reasonably distributed [25]; the former is aimed at solving the problem of voltage phase waveform synchronization.

There are two typical ring current suppression methods for parallel operation of inverters: the coupling inductance method and the isolation transformer method.

When the output voltages of the two inverters are inconsistent, the coupled inductance method will produce circulating current flowing between the two inverters without passing through the load  $\dot{I}_H$ . Assuming that the inductors  $L1$  and  $L2$  are completely coupled, the size of the ring current is

$$\dot{I}_H = \frac{\dot{I}_{o1} - \dot{I}_{o2}}{2} = \frac{\dot{U}_{o1} - \dot{U}_{o2}}{2R + 4jX}, \quad (1)$$

where  $R$  represents the line resistance from the output terminal of the inverter voltage to the load,  $\dot{U}_{o1}$  and  $\dot{U}_{o2}$  denote the output voltage of the two inverters and the voltage of the parallel bus bar,  $L$  stands for the coupling inductance, and  $jX$  refers to the inductive reactance. Since  $R$  is much smaller than  $L$ , Equation (1) can be simplified as

$$\dot{I}_H = \frac{\dot{I}_{o1} - \dot{I}_{o2}}{2} = \frac{\dot{U}_{o1} - \dot{U}_{o2}}{4jX}. \quad (2)$$

Equation (2) shows that the size of the ring current is inversely proportional to the inductance value of the coupled inductor, and the coupled inductor significantly reduces the ring current. Suppose that the number of turns of the inductors  $L1$  and  $L2$  is  $N1 = N2 = N$ ; the two inductors are wound on the same iron core and are tightly coupled. When there is no ring current between the inverters,  $\dot{I}_{o1} = \dot{I}_{o2}$ . The magnetic flux of the iron core can be expressed as

$$\phi = \frac{L1 * I_{o1}}{N1} - \frac{L2 * I_{o2}}{N2} = 0. \quad (3)$$

Equation (3) indicates that due to the coupling effect of the ring current suppression inductors, the magnetic fluxes of the two inductors cancel each other out, and the equivalent inductance value of the inductors is zero. Therefore, the inductors do not affect the voltage regulation accuracy. The advantage of coupled inductor method is that it has a good circulation suppression effect, can suppress active power, reactive power, and DC circulation, has small volume, and does not affect the voltage stabilizing accuracy of output voltage. However, it is challenging to wind the multimachine parallel-coupled inductor.

The principle of the isolation transformer method to suppress the ring current is relatively simple. In essence, it uses the isolation of transformers to disconnect the circulating current path. The isolation transformer method can eliminate the DC loop-current caused by the inconsistent DC components of the inverter output voltage. Meanwhile, the isolation transformer can electrically isolate the input DC voltage and output voltage of each inverter module,



improving the reliability of the parallel inverter system. The isolation transformer method has a good circulation suppression effect, can reduce active and reactive circulation, and eliminates DC circulation; besides, it is easy to connect in multimachine parallel. However, isolation transformers have bulky volumes and significantly affect the voltage stabilization accuracy of parallel circulation bars.

**3.2. Cause Analysis of Circulation.** The different output characteristics of inverter modules in distributed generation systems will generate a circulating current between inverters. The parallel system can operate normally only when the parallel inverter does not produce a circulating current and expected load current. The causes of circulating current are analyzed in this section to eliminate the ring current between inverters [26]. Figure 2 illustrates the equivalent circuit between the two inverters.

In Figure 2,  $R_3$  denotes the load impedance of the inverter power supply;  $R_1$  and  $R_2$  are the impedance of the inverter power supply line;  $A_1$  refers to the current test;  $I_1$ ,  $I_2$ , and  $I_3$  represent the current corresponding to the three resistances, respectively;  $\dot{I}_1$ ,  $\dot{I}_2$ , and  $\dot{I}_0$  are the annular current in the corresponding circuit. When the output voltage waveform is sinusoidal and there is no waveform distortion, the relationship among  $A_1$ ,  $A_2$ , and  $A_3$  and  $I_1$ ,  $I_2$ , and  $I_3$  is described as

$$\begin{aligned} \dot{I}_1 &= \frac{(A_1 - A_3)}{R_1}, \\ \dot{I}_2 &= \frac{(A_2 - A_3)}{R_2}, \\ \dot{I}_0 &= \dot{I}_1 + \dot{I}_2. \end{aligned} \quad (4)$$

Equation (5) defines the circulating current  $\dot{I}_h$ .

$$\dot{I}_h = \frac{\dot{I}_1 - \dot{I}_2}{2}. \quad (5)$$

Equations (6) and (7) are set up when the three resistance impedance values are equal.

$$\dot{I}_h = \frac{(A_1 - A_2)}{2R} = \frac{\Delta A}{2R}, \quad (6)$$

$$\begin{cases} \dot{I}_1 = \frac{\dot{I}_0}{2} + \dot{I}_h, \\ \dot{I}_2 = \frac{\dot{I}_0}{2} - \dot{I}_h. \end{cases} \quad (7)$$

Equations (6) and (7) show that when two inverters are connected in parallel, the output current of different equipment consists of two parts: the output current under load and the circulating current between two parallel power supplies [27, 28]. The load distribution of parallel equipment is uniform; the output current of parallel equipment is affected

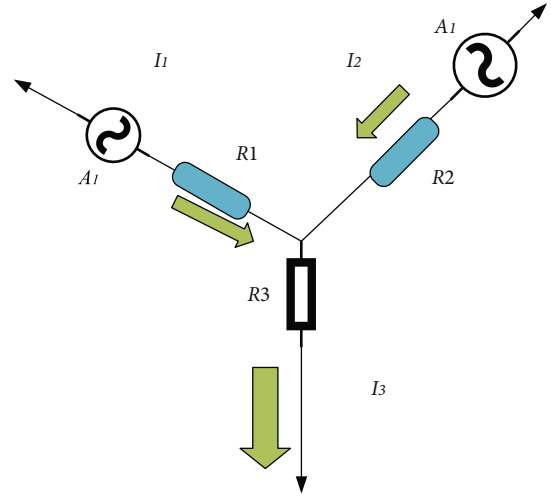


FIGURE 2: Equivalent parallel connection of two inverters.

by the circulating current. Suppose the output of each unit is different from a load of voltage circulating current. In that case, the output power of each division will change accordingly, resulting in a load imbalance on each power supply of the inverter. The impedance in the electronic circuit is minimal. Suppose the phase and amplitude of the output voltage vector of each parallel unit are inconsistent. In that case, even the most minor difference will produce magnetic flux far greater than the rated current of the system [29]. This current flows through the two inverters between the loads. If two inverters controlled by a closed voltage circuit are connected in parallel at this time, it will cause a pseudo short circuit of the system, which is extremely dangerous [30]. Therefore, it is necessary to equalize the current of the inverter power supply running in parallel to evenly distribute the current and thermal stress between the power supply units to prevent multiple power supplies from being in the current limiting mode.

**3.3. Current Sharing Control Schemes of Parallel System.** There are three common methods to balance the load current of inverter units in parallel systems: current sharing of series current limiting inductance, master-subsetting control, and maximum current automatic sharing. Figure 3 reveals the principle of current sharing of the series current limiting inductor method.

In the current sharing scheme of series current limiting inductors in Figure 3,  $U_a$  and  $U_b$  are the voltages across the inverter 1 and inverter 2, respectively;  $U_c$  is the voltage across the inductor;  $R_1$  and  $R_3$  are series resistance;  $R_c$  is the inductor resistance;  $L_1$  and  $L_2$  are the inductors;  $I_1$  and  $I_2$  are the currents in the series circuit. When there is no current flowing between the inverters, the output currents of the two inverters are balanced. Since the output current flows through the two coils in the direction shown in Figure 2, the magnetic fluxes generated by the two currents cancel each other out; in this way, the equivalent inductance value is close to zero, reducing the impact on the system voltage regulation accuracy [31, 32]. When the

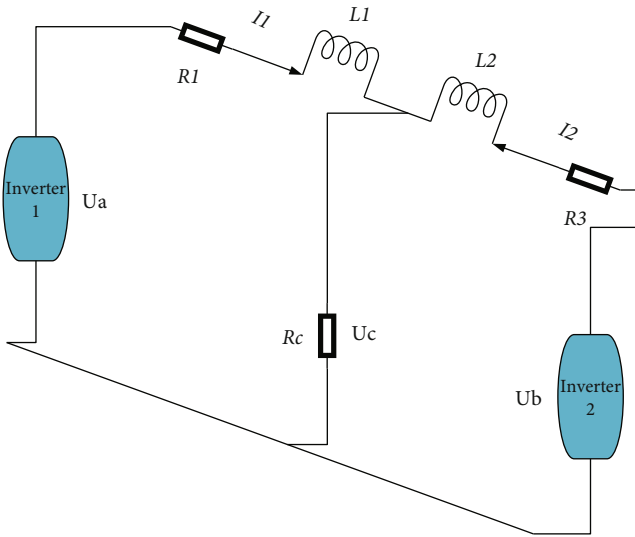


FIGURE 3: Current sharing of the series current limiting inductor.

current flows, the magnetic flux is caused by the increasing current, and the equivalent inductance value increases, effectively suppressing the ring current.

The master-subsetting control method is only applicable to parallel inverter systems with common current control types. Current control refers to the voltage-to-current dual control loop composed of the current loop as the inner loop and the voltage loop as the power module's outer loop [33, 34]. The parallel system adopts the master-subsetting to share the current, and the voltage-controlled inverting power supply and current-controlled inverting power supply are connected in parallel. In the parallel inverter, the "master module" is set to operate manually according to the voltage control law to control the output voltage of the parallel system to change sinusoidally [35, 36]. Other submodule devices run in the current control mode. Generate current in full accordance with the current command specified by the main module to eliminate the current flowing through the system effectively.

Figure 4 reveals the principle of automatic current sharing of maximum current.

In Figure 4,  $I_1$  and  $I_2$  are the output currents of the inverting power supply 1 and 2, respectively;  $D_1$  and  $D_3$  are the current controllers (current amplification) of the inverting power supply 1 and 2, respectively;  $D_2$  and  $D_4$  are voltage controllers (voltage amplification) of inverting power supply 1 and 2, respectively;  $c$  stands for the maximum current output by the inverting power supply. The diode is unidirectional. This feature can ensure that the inverter unit with the most extensive output current turns on the diode and continuously transmits the maximum current of the unit to the bus. However, in this process, diodes will lead to a voltage drop at both ends, resulting in the failure of current sharing of the main module and a particular error, and the submodule will have better current sharing. In fact, there are many ways to realize the current sharing regulation, such as designing a unique hardware system to complete the current sharing or designing a special software

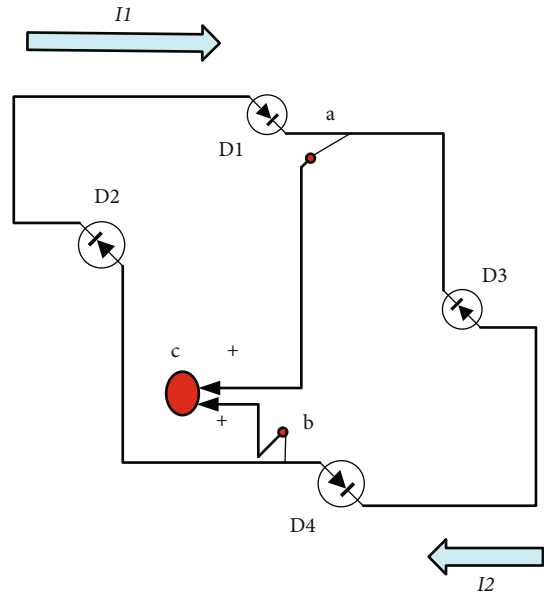


FIGURE 4: Automatic control principle of maximum current sharing.

to control the current sharing. Academic opinions are divided. Various current sharing methods will result in different stability and accuracy characteristics.

**3.4. Module Design of the Parallel System.** The parallel system of the inverter power supply is composed of multiple unit modules. The performance of different modules needs to be synchronized to ensure the effect and safety of use. Therefore, it is necessary to reasonably design the inverter structure and control strategy. Figure 5 shows the central circuit topology of the inverter unit designed here.

According to Figure 5, the topology of the primary circuit of the inverter unit is changed to integrate the parallel function of the inverter and the parallel system of the inverter power supply. The primary circuit of each parallel inverter unit adopts the main circuit of the full-bridge inverter. Without considering the equivalent series resistance of the filter capacitor, a filter is used to filter other bands in the bridge except for the higher harmonics of the output voltage.

In Figure 5,  $V_{dc}$  represents the DC input voltage of the system,  $T_1$ - $T_4$  denotes the power switch module,  $L$  and  $C$  stand for the output filter inductance and capacitance of the system,  $R_1$  refers to the equivalent series resistance of the filter inductance, and  $R_2$  signifies the system load. Equation (8) describes the frequency domain function between the voltage between points A and B and the output of the inverter unit.

$$G(s) = \frac{R_2}{RLC^2 + (L + R_1R_2C) + (R_2 + R_1)}. \quad (8)$$

**3.5. Droop Parallel Control Strategy of Inverter.** The parallel operation of the inverter power supply requires corresponding preconditions, and each parallel unit must be placed on

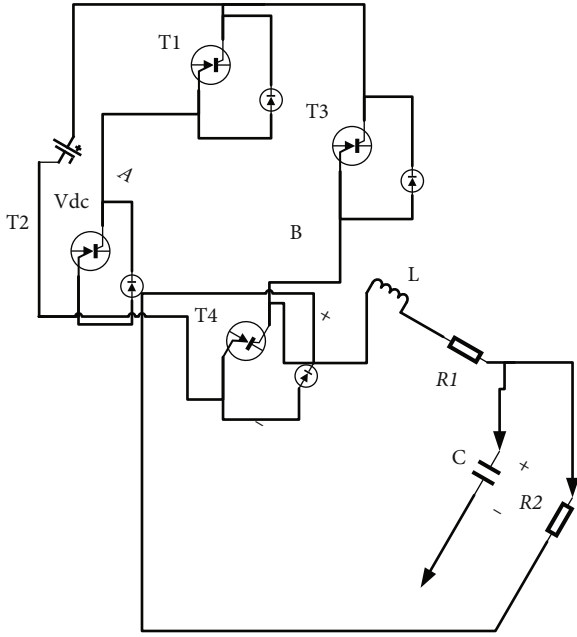


FIGURE 5: Main circuit topology of the inverter unit.

the AC bus network. At the beginning of the process, the frequency, phase, and amplitude of output voltage shall be consistent with that of the AC bus. Significant phase and amplitude differences will produce large active and reactive loop currents during operation. These currents may dramatically impact the stable operation of the AC bus and system and cause an overcurrent of the inverter power supply, ultimately damaging the inverter power supply. The inverter must be designed in the concrete plan to terminate the parallel operation automatically. During the operation of the inverter, there is a presynchronization process to ensure that the phase, frequency, and amplitude of the inverter power supply are consistent with the power grid. It also reduces the impact on the power supply of the microgrid and inverter itself. The phase-frequency tuning process of the inverter unit before the parallel operation is called parallel presynchronization of the inverter unit.

According to the power characteristics of the above parallel inverter system, some researchers have proposed a control technology that can wirelessly parallel inverter, namely, the voltage frequency droop method. The parallel inverter device can sense the output power of the power supply system, measure and adjust the output voltage, frequency, and amplitude control values through droop control, and obtain the system's active power and total reactive power. The output frequency and the active output power of the inverter with large output active power decrease due to the frequency drop characteristics. When the inverter outputs low active power, the output frequency increases due to the frequency reduction characteristics, increasing active power. The voltage amplitude of the inverter outputting ample reactive power decreases due to amplitude decrease, reducing the reactive power output. The voltage amplitude increases for the inverter with small reactive output power,

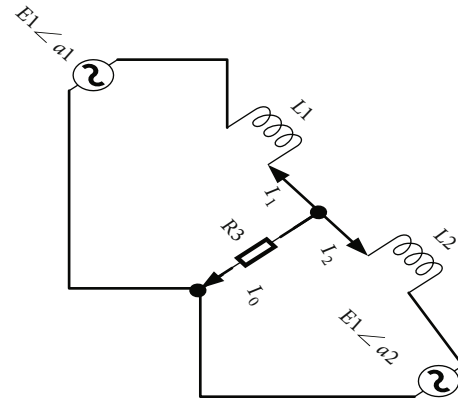


FIGURE 6: Equivalent circuit of the parallel system.

and the reactive output power decreases due to the amplitude decreasing characteristic. In other words, the equipment with low output power will increase the output according to the voltage frequency droop characteristics. In contrast, the relatively high output power equipment will reduce the output power. This self-regulation process is repeated in the parallel system until the minor loop point in the circuit is found.

The distributed generation system composed of parallel inverters has a complex structure. The AC voltage output by each inverter power supply is equivalent to a voltage source with mutually adjustable and controllable frequency, phase, and amplitude, and each unit shares the load current. In the distributed generation system, the line resistance is low, and the line impedance is inductive, which significantly simplifies the equivalent circuit of the parallel system, as shown in Figure 6.

Equation (9) signifies the negative power expression of the output power supply.

$$\begin{aligned} \bar{S}_i &= P_i + jQ_i = \vec{E} \vec{I}_i^* = E \left[ \frac{E_i \cos a_i + jE_i \sin a_i - E}{jX_i} \right]^* \\ &= \frac{E_1 E}{X_i} \sin a_i + j \left[ \frac{E_i E \cos a_i - E^2}{X_i} \right]. \end{aligned} \quad (9)$$

In Equation (9),  $\bar{S}_i$  represents the negative power of the output power supply;  $P_i$  and  $Q_i$  denote the active power and reactive power transmitted by the line, respectively;  $a$  refers to the angle between the output voltage vector of the inverting power supply  $E_i$  and the system output voltage vector  $E$ ;  $X_i$  indicates the output reactance of the inverting power supply.

Equation (10) reveals the output active power of each inverter in the equivalent circuit.

$$P_1 = \frac{E_1 E}{X_i} \sin \delta. \quad (10)$$

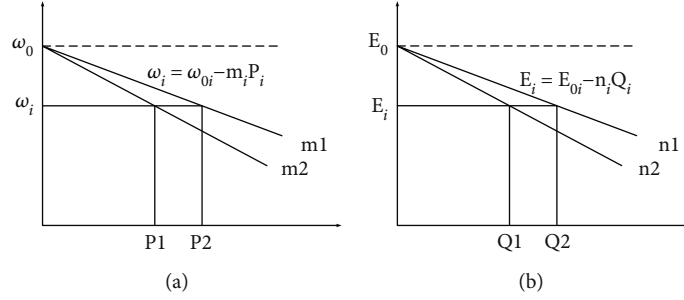


FIGURE 7: Droop inverter with different capacities: (a) active power; (b) reactive power.

In Equation (10),  $\delta$  represents the phase difference. Accordingly, Equation (11) demonstrates the output reactive power of each inverter in the equivalent circuit.

$$Q_i = \frac{E_i E \cos \delta_i - E^2}{X_i}. \quad (11)$$

Because the power output of parallel system  $E$  is strictly limited in practical application, it will not fluctuate wildly. Thus, the power output can be regarded as a constant approximately. Output impedance  $X_i$  is also a fixed value. Hence, Equations (10) and (11) can be simplified as

$$P_i = k \sin a, \quad (12)$$

$$Q_i = kE_i - b, \quad (13)$$

where  $k$  is the proportional coefficient and  $b$  is a constant. Equations (12) and (13) demonstrate that the active power depends on the value of the angle  $a$  between the inverter output voltage vector  $E_i$  and the system output voltage vector  $E$ . In contrast, the reactive power mainly depends on the value of the inverter output voltage vector  $E_i$ .

Because the internal resistance of the inverter is meager and the external output characteristics are complex, even a tiny difference in amplitude or phase will cause a large system cycle between the inverters. The present work uses the parallel voltage frequency droop method for control. The frequency and amplitude of the output voltage of each inverter power supply are adjusted according to Equations (14) and (15) based on the droop method to make the output characteristics smoother.

$$\omega_1 = \omega_{0i} - m_i P_i, \quad (14)$$

$$E_i = E_{0i} - n_i Q_i. \quad (15)$$

In Equations (14) and (15),  $P_i$  represents the active power,  $Q_i$  refers to the reactive power, and  $\omega_{0i}$  stands for the  $i$ th output angular frequency of inverter power supply under no load.  $E_{0i}$  indicates the output amplitude of the first inverter under no load.  $m_i$  denotes the droop coefficient of output angular frequency of the  $i$ th inverter power supply.  $n_i$  denotes the droop coefficient of the output voltage ampli-

tude of the  $i$ th inverter power supply. Figure 7 displays the scheme of droop inverter with different capacities.

Figure 7 presents the scheme of drooping characteristics when two inverters with different capacities are connected in parallel. Each inverter power supply in Figure 6 adjusts the frequency and amplitude of each output voltage back to a new and stable output operating point and distributes the output power reasonably. The same vertical slopes in the droop inverter characteristic diagram of the inverting power supply mean that each supply has stable performance and equal output power. If the droop slopes are different, the force is small when the slope is significant and vice versa.

In essence, the droop voltage frequency method takes the whole system with parallel inverters as the research object and detects the frequency and amplitude of output voltage. Then, it adjusts the active and reactive power by fine-tuning the frequency and amplitude to realize the reasonable distribution of power. Voltage frequency droop control reduces the active output by lowering or increasing the frequency to improve the active output. Reducing the voltage amplitude can reduce the reactive power; increasing the voltage can increase the reactive power. In short, this is a dynamic continuous self-adjustment according to voltage-frequency droop characteristics. In this way, the system can operate in a state where the circulation is the smallest.

Next, a virtual impedance is introduced into the circuit. In a low-voltage microgrid, the line impedance is primarily resistive. The system impedance is generally complex, and the resistance-inductance ratio in different systems is different, which is easy to cause power coupling. The method of introducing a virtual complex impedance can be adopted to solve the power coupling problem in the system. Besides, the value of the virtual complex impedance is designed according to the line impedance. The equivalent output impedance of the inverter is purely resistive or inductive, realizing the decoupled control of active power and reactive power. Figure 8 is a block diagram of the voltage and current double closed-loop control after introducing the virtual complex impedance.

In Figure 8, the virtual complex impedance  $Z_v(s)$  consists of a positive virtual resistance  $R_v$  and a negative virtual inductance  $L_v$ ;  $U^*(s)$  refers to the voltage command value generated by the droop control module;  $G_{PR}(s)$  and  $G_i(s)$  are the transfer functions of the regulators in the voltage outer loop and the current inner loop, respectively;  $K_{PWM}$

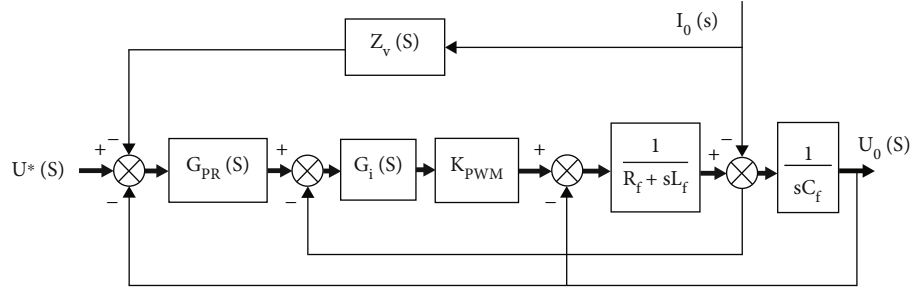


FIGURE 8: Block diagram of voltage and current double closed-loop control based on virtual complex impedance.

TABLE 1: System parameters.

Project	Numerical value
LC filter	$R_f = 0.0485 \Omega$ , $L_f = 20 \text{ mH}$ , $C_f = 20 \mu\text{F}$
Voltage control loop	$k_{vp} = 0.085$ , $k_{vi} = 10$ , $\omega_c = 10 \text{ rad/s}$
Current control loop	$k_{ip} = 4.35$

is the pulse width modulation (PWM) gain of the inverter;  $U_0(s)$  and  $I_0(s)$  are the actual value of the inverter output voltage and the reference value of the output current, respectively;  $R_f$ ,  $L_f$ , and  $C_f$  represent the filter resistor, filter inductor, and filter capacitor in the low-pass filter, respectively.

The transfer functions of the quasiproportional voltage and current regulators can be defined as

$$\begin{cases} G_{PR}(s) = k_{vp} + \frac{2k_{vi}\omega_c s}{s^2 + 2\omega_c s + \omega_0^2}, \\ G_i(s) = k_{ip}. \end{cases} \quad (16)$$

In Equation (16),  $k_{vp}$  and  $k_{vi}$  denote the voltage loop's proportional gain and resonance gain, respectively;  $k_{ip}$  represents the proportional gain of the current loop;  $\omega_c$  refers to the corner frequency of the cutoff frequency. The LC filtering and voltage and current double closed-loop control parameters are designed, respectively, to smoothly realize the droop control of the low-voltage inverter parallel system. The specific parameters are summarized in Table 1.

In this paper, after introducing the designed virtual complex impedance, the system impedance must be approximately resistive at the fundamental frequency to adapt to the traditional droop control. Besides, it needs to be resistive at the harmonic frequency to meet the requirements of power decoupling and suppress the interharmonic and higher-order harmonics of the output current of the converter. The virtual impedance value is designed according to the line impedance  $Z_n$  ( $n$  is 1 or 2) (assuming  $Z_n = 1 \Omega + 2 \text{ mH}$ ) parameters in Table 1 to select the value range and the optimal impedance value is determined according to the impedance angle change.

3.6. *Simulation and Experiment of Droop Parallel Control.* Figure 9 indicates the simulation model of the droop control inverter proposed here.

Figure 9 suggests that the primary circuit model of the inverter can be combined with the control strategy through the connection of controlled variables to establish the simulation model of the wireless parallel system of the inverter. Parallel inverter theory is developed with the following parallel control theory as the core. Therefore, the proper application of droop theory is the premise of the system's regular operation.

The parameter settings of the simulation model of the parallel inverter power system reported here are shown in Tables 2 and 3.

Due to the limited detection accuracy of voltage amplitude, voltage frequency, deflection coefficient, hardware circuit, and software control accuracy, it is difficult to match each inverter's actual values of controlled variables completely. When the parallel controlled variables do not check, it is critical to judge the stability of the performance of the connected system.

## 4. Results and Discussion

4.1. *Simulation Results of Droop Theory Application Experiment.* Figure 10 illustrates the simulation results of the parallel system when the parameters of the two inverters are the same.

In Figure 10, all parameters of the two inverters are assumed to be the same. The working state of the inverter parallel system under droop control is relatively stable. The output of active and reactive power is well separated and stably balanced. Each power supply provides half of the system's capacity, and the circulation defaults to zero. The results show that the droop theory can be applied to parallel inverter systems and achieve a good control effect under ideal conditions. The power loop theory believes that when the output impedance of the system accounts

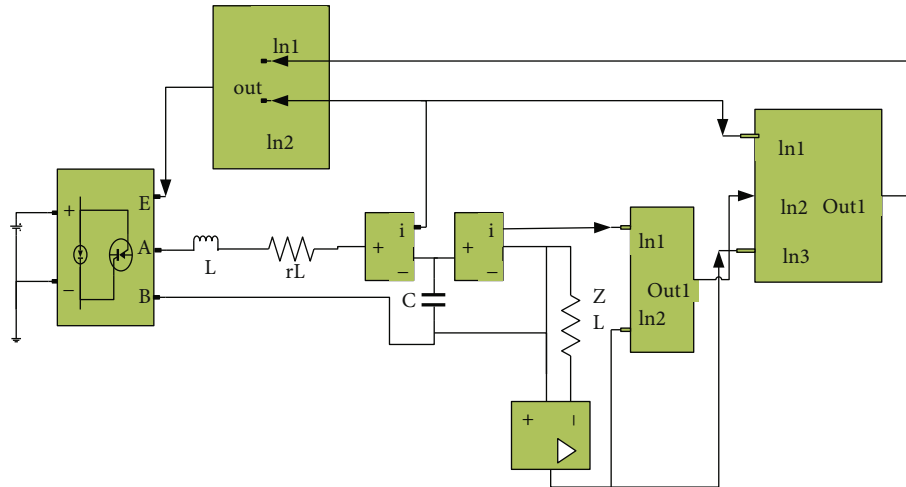


FIGURE 9: Simulation model of inverters controlled by the droop method.

TABLE 2: Parameters in the simulation system.

System parameters	$L$ (mH)	$r$ ( $\Omega$ )	$C$ ( $\mu\text{F}$ )	$E$ (V)
Numerical value	1	0.01	30	165

TABLE 3: System command parameters.

Instruction parameter	Voltage (V)	Voltage frequency (rad)	Sag coefficient $m$	Sag coefficient $n$
Numerical value	155	314	0.0001	0.0001

for a small proportion, the output impedance of the inverter is inductive in the entire frequency band. In other words, the output impedance of the system is not sensitive to the effect of the transition. The correct application of droop theory in the practical approach can be guaranteed to meet this point.

To further verify the inhibitory effect of circuit feedback on impedance  $R$ , set the impedance  $R$  of inverter 1 to  $0.01 \Omega$  and the impedance  $R$  of inverter 2 to  $0.1 \Omega$ . Figure 11 presents the simulation results of parallel operation with a  $6.0 \Omega$  impedance load under the condition of consistent other parameters.

According to Figure 11, when the impedances of the two inverters are different, the parallel system under droop control works stably, and the active power and reactive power are also stable and balanced. Through the feedback of induced current, they tend to zero. The results suggest that the circuit feedback of the inductor can reduce this effect. Therefore, when the two inverters work in parallel under different conditions, the droop control can continue to apply and obtain satisfying control efficiency.

**4.2. Analysis of System Performance.** Droop control plays a role in practical application, but it also has limitations. A parallel self-tuning virtual impedance strategy is proposed here. By improving the droop parallel control, the system can improve the dynamic tuning performance, steady-state

output frequency performance, and harmonic suppression to a certain extent. Figure 12 reveals the comparison of systematic dynamic adjustment characteristics before and after improvement.

As Figure 12 reveals, the parallel system of the inverting power supply is dynamically adjusted. The experimental conditions and parameters of the parallel system are the same as those of the simulation experiment, which means that the simulation system will produce periodic current waveforms. Figure 12 bespeaks that adding differential regulation to the power droop control of the system can significantly improve the dynamic regulation rate, speed up the power convergence, and improve the performance of the dynamic approach to a certain extent. Meanwhile, with the introduction of automatic control, even if the control voltage is different from the ring current of the original design, the ring current of the system is adequately controlled due to the compensation of the virtual impedance to the system. The command voltage of the whole system is significantly reduced only in the steady state, and the steady-state and dynamic performance is improved dramatically.

Figure 13 presents the active output frequency of the system.

Figure 13 signifies the comparison results of the active output frequency of the traditional droop parallel system and the droop automatic adjustment output frequency. It

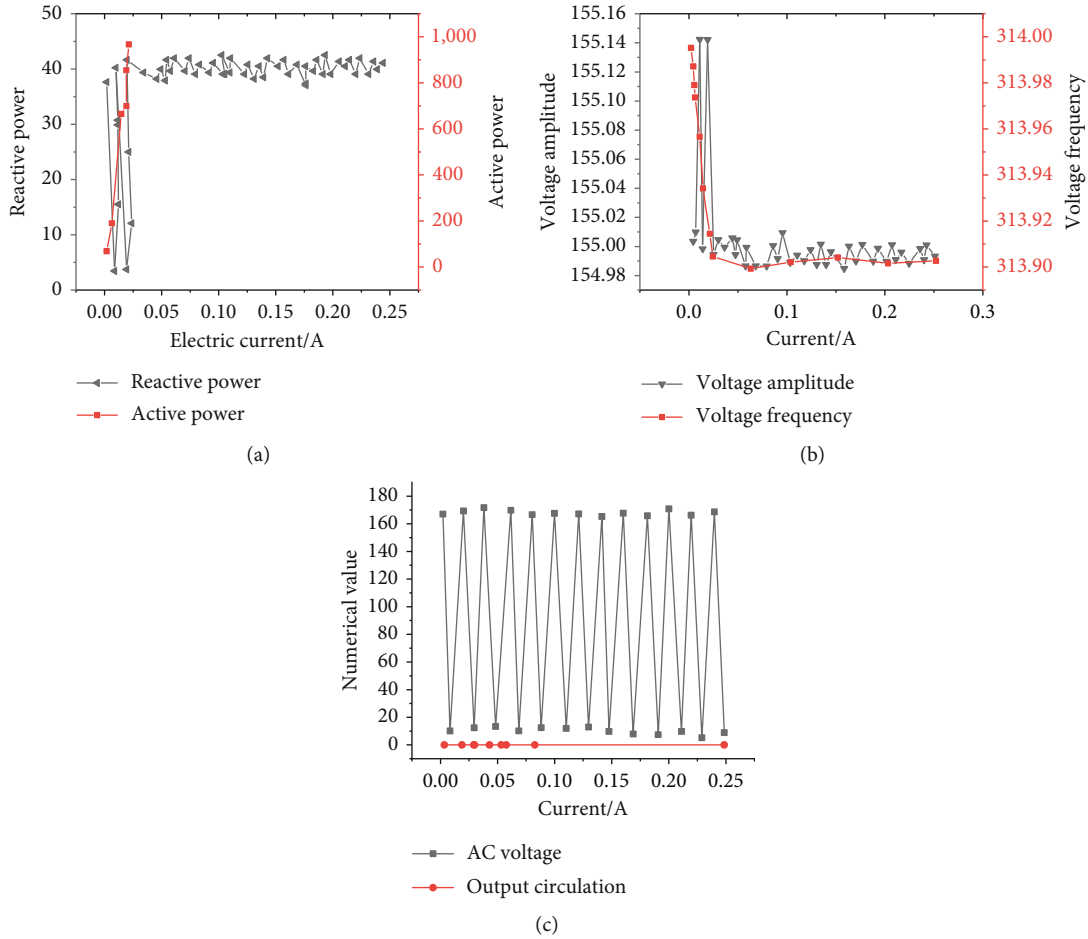


FIGURE 10: Simulation results of consistent inverter parameters: (a) power; (b) voltage; (c) frequency.

also implies that the conventional control method is adopted. The output frequency deviates from the control signal when the system reaches a stable state. When AC is connected to the grid, if the deviation is significant, it cannot meet the frequency requirements, which greatly limits the power range of the inverter. By dynamically adjusting the active power droop coefficient, the steady-state output frequency. Therefore, the system shows a small oscillation close to the driving frequency, which undoubtedly achieves the steady-state performance of the output frequency. Secondly, the dynamic response time of the system is hardly affected. The active power reduction factor can improve the steady-state index of the parallel system without affecting the dynamic performance of the system.

Figure 14 signifies the nonlinear load performance of the system.

Figure 14 reveals that both simulation systems are equipped with two bridge rectifier loads. It also implies that the waveform quality of the output voltage of the parallel system controlled by the virtual impedance technology has been significantly improved. Besides, the harmonic content near the fundamental wave is considerably lower than the original, from 6% to about 2%, declining four percentage

points. Therefore, virtual impedance technology can successfully apply droop theory to nonlinear loads and expand the scope of the parallel inverter system.

To sum up, two simulation tools are used to analyze the main circuit and control circuit of the unit module of the parallel system. Simultaneously, according to the specific requirements of the parallel function of the inverter, the output power measurement and unit calculation are carried out. Based on the function of parallel and control voltage synthesis, construction is implemented on a complete application simulation model of an inverter wireless parallel system. The dynamic and static simulation experiment of the fully connected droop control system fully reflects the accuracy and feasibility of the control theory. Moreover, the experimental comparison is made on the application simulation models of two groups of parallel systems with different control strategies. Compared with the conventional droop parallel control strategy, the control strategy in this study shows noticeable improvement in the dynamic performance and steady-state index of the system. The simulation model of a parallel wireless inverter system established here provides an experimental platform for future system theory research.

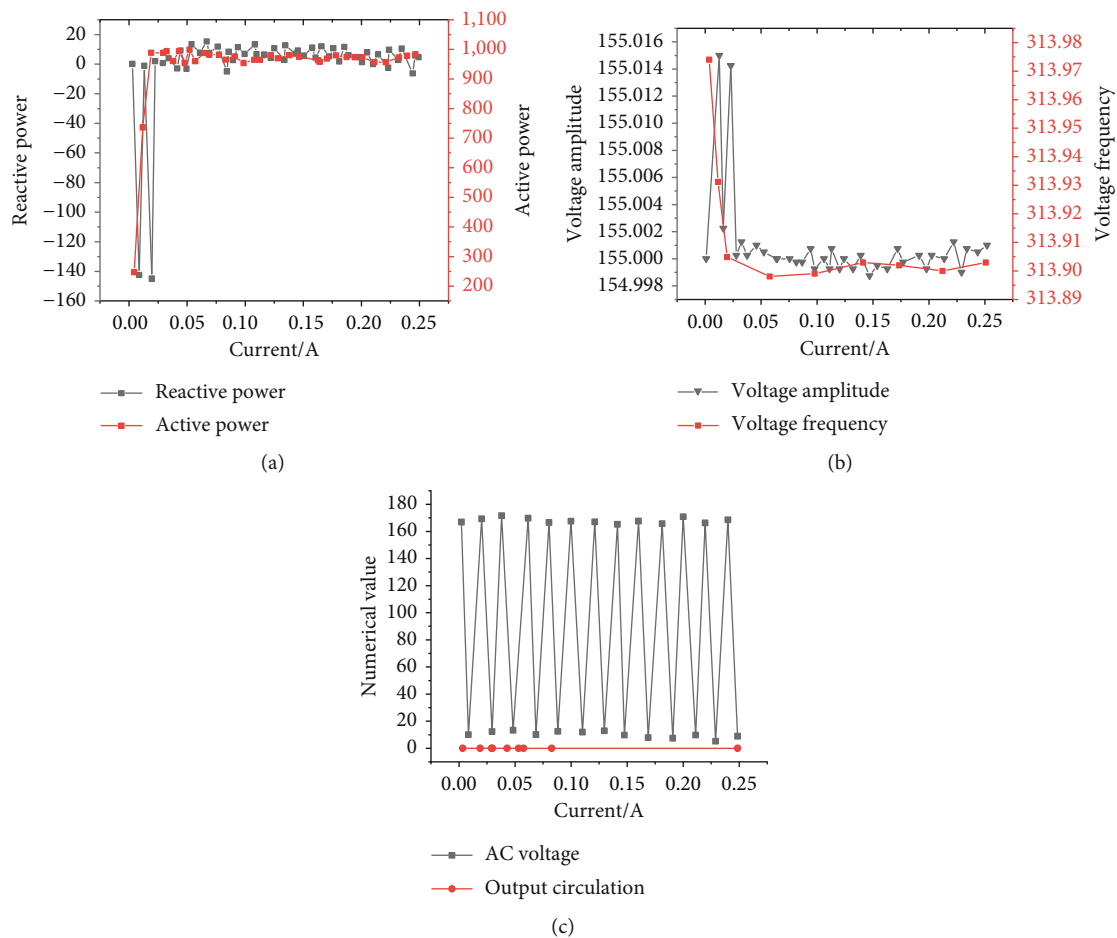


FIGURE 11: Simulation results of the parallel system with a different impedance of inverting power supply: (a) power; (b) voltage; (c) frequency.

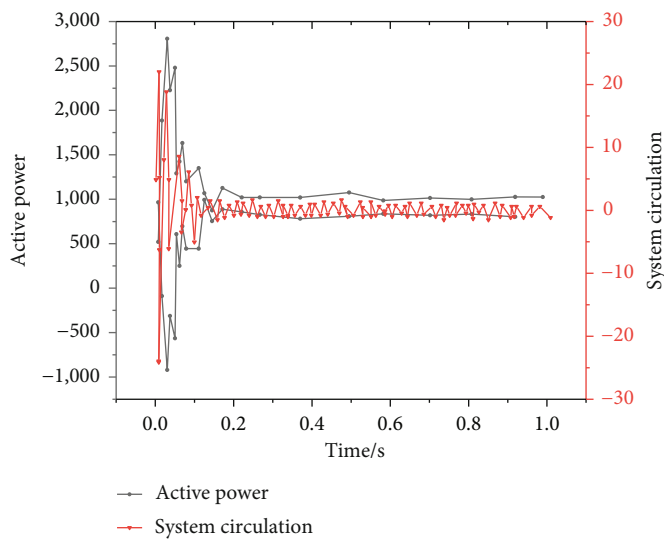


FIGURE 12: Comparison of systematic dynamic regulation characteristics.



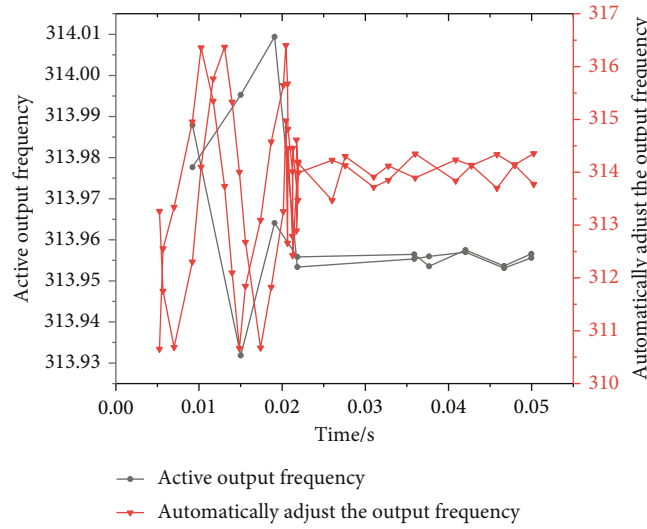


FIGURE 13: Active output frequency of simulation system.

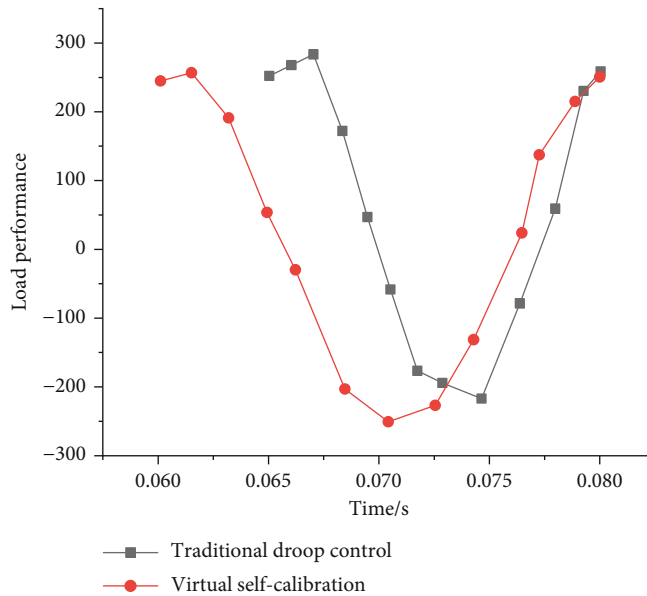


FIGURE 14: Comparison of system nonlinear load performance.

### 5. Conclusion

The rational utilization and sustainable development of energy are the hotspots of current research. This paper briefly introduces the current control method of the parallel loop of the inverter power supply. Then, three difficulties in the parallel operation of the inverter power supply are summed up, namely, the asynchronous voltage frequency and voltage phase of inverter power supply, the inconsistent amplitude of output voltage, and the influence of the difference of harmonic components in voltage. Besides, the present work discusses the current sharing control scheme of a traditional parallel system and proposes three current sharing control methods. The optimization methods of the main circuit topology, droop parallel control, and dynamic adjust-

ment of the unit inverter are designed based on the above analysis. Finally, simulation experiments are designed to verify its performance. The experimental results show that the control strategy proposed here has significantly improved the system's dynamic performance and steady-state index. The simulation model of the parallel wireless inverter system established here provides an experimental platform for future system theory research. There is still power coupling and unequal active power sharing due to inconsistent line impedance and mismatched inverter capacity in a low-voltage microgrid. Introducing the virtual impedance can realize the decoupling control of the power in the system; however, the increase of the equivalent output impedance of the system may reduce the system voltage. The improved droop control strategy proposed here can offset

the equivalent output impedance of the parallel inverter system by designing the value of virtual complex impedance to realize the purely resistive system impedance and the decoupling control of active power and reactive power.

Due to the limitation of the research capacity and research funds, the inverter design based on multiobjective decision-making reported here is not ideal. Moreover, in the open-circuit parallel system under droop control, the voltage and frequency change with the load, which affects the power supply quality. Dynamic compensation can eliminate some effects, but the effect cannot adapt to all practical applications. Follow-up research will improve these two points to enhance the value and reliability of the present work.

## Data Availability

The labeled dataset used to support the findings of this study are available from the corresponding author upon request.

## Conflicts of Interest

The author declares no competing interests.

## Acknowledgments

This research was supported by the project of Science and Technology Research Program of Chongqing Municipal Education Commission of China (Grant No. KJQN201901607), Chongqing Big Data Engineering Laboratory for Children, Chongqing Electronics Engineering Technology Research Center for Interactive Learning, Chongqing University Innovation Research Group, Chongqing Key Discipline of Electronic Information, Chongqing Natural Science Foundation Project (CSTC2021-msxm1993), and the Science and Technology Research Program of Chongqing Municipal Education Commission (Grant No. KJZD-M201801601).

## References

- [1] P. Herasymenko, "Mathematical analysis of dual-frequency load current of two-inverter power supply for induction heating systems," *Przełąd Elektrotechniczny*, vol. 1, no. 3, pp. 71–76, 2021.
- [2] D. Dietz, "Stochastic propagation delay through a CMOS inverter as a consequence of stochastic power supply voltage—part II: modeling examples," *IEEE Transactions on Electromagnetic Compatibility*, vol. 61, no. 1, pp. 233–241, 2019.
- [3] J. K. Sahani, A. Singh, and A. Agarwal, "A wide frequency range low jitter integer PLL with switch and inverter based CP in 0.18  $\mu\text{m}$  CMOS technology," *Journal of Circuits, Systems, and Computers*, vol. 29, no. 9, pp. 167–170, 2020.
- [4] S. Xu, B. Yang, and D. Li, "Analysis on the applicability of phase selection components of inverter power supply transmission line," *E3S Web of Conferences*, vol. 204, no. 13, 2020.
- [5] V. B. Ivanov, "Modeling of three-phase inverter power supply system in Simulink," *IOP Conference Series Materials Science and Engineering*, vol. 1032, no. 1, article 012054, 2021.
- [6] N. A. Windarko, A. Puryanto, R. P. Eviningsih, M. Z. Efendi, E. Prasetyono, and B. Sumantri, "Prototipe power supply gate driver untuk multilevel inverter dengan menggunakan flyback converter multi output," *Techné: Jurnal Ilmiah Elektroteknika*, vol. 19, no. 1, pp. 33–42, 2020.
- [7] C. Liu, S. H. Chang, Y. J. Chen et al., "A power supply consists of the DC-DC boost converter and a full-bridge inverter circuits for a PZT liquid pump," *International Journal of Information and Electronics Engineering*, vol. 9, no. 1, pp. 19–22, 2019.
- [8] G. Zhang, Z. Tian, P. Tricoli, S. Hillmansen, Y. Wang, and Z. Liu, "Inverter operating characteristics optimization for DC traction power supply systems," *IEEE Transactions on Vehicular Technology*, vol. 68, no. 4, pp. 3400–3410, 2019.
- [9] M. A. Hannan, Z. A. Ghani, M. M. Hoque, and M. S. Hossain Lipu, "A fuzzy-rule-based PV inverter controller to enhance the quality of solar power supply: experimental test and validation," *Electronics*, vol. 8, no. 11, 2019.
- [10] H. F. Baghtash, "Bias-stabilized inverter-amplifier: an inspiring solution for low-voltage and low-power applications," *Analog Integrated Circuits and Signal Processing*, vol. 105, no. 3, pp. 1–6, 2020.
- [11] S. Kundu, S. Banerjee, and S. Bhowmick, "Improved SHM-PAM-based five-level CHB inverter to fulfil NRS 048-2:2003 grid code and to apply as shunt active power filter with tuned proportional-resonant controller for improving power quality," *IET Power Electronics*, vol. 13, no. 11, pp. 2350–2360, 2020.
- [12] S. Somkun, "Unbalanced synchronous reference frame control of single-phase stand-alone inverter," *International Journal of Electrical Power & Energy Systems*, vol. 107, pp. 332–343, 2019.
- [13] L. Lin, G. Qian, H. Jian, and M. Hao, "An enhanced power sharing strategy for islanded microgrids using adaptive virtual impedances," in *IECON 2015-41st Annual Conference of the IEEE Industrial Electronics Society*, Yokohama, Japan, 2016.
- [14] Z. Peng, J. Wang, D. Bi et al., "Droop control strategy incorporating coupling compensation and virtual impedance for microgrid application," *IEEE Transactions on Energy Conversion*, vol. 34, no. 1, pp. 277–291, 2019.
- [15] Z. Chen, X. J. Pei, M. Yang, and L. Peng, "An adaptive virtual resistor (AVR) control strategy for low-voltage parallel inverters," *IEEE Transactions on Power Electronics*, vol. 34, no. 1, pp. 863–876, 2019.
- [16] J. Y. Zhang, J. Shu, J. Ning, L. Huang, and H. Wang, "Enhanced proportional power sharing strategy based on adaptive virtual impedance in low-voltage networked microgrid," *IET Generation Transmission & Distribution*, vol. 12, no. 11, pp. 2566–2576, 2018.
- [17] Y. M. Geng, M. Y. Hou, and G. F. Zhu, "Resistive droop control strategy of active power distribution for microgrid based on virtual impedance," *Electric Power Automation Equipment*, vol. 40, no. 10, pp. 132–138, 2020.
- [18] T. Liu, B. G. Guan, and Y. F. Liang, "Ring current suppression strategy between island microgrid parallel inverters based on virtual impedance," *Intelligent Computer and Application*, vol. 10, no. 1, pp. 160–164, 2020.
- [19] G. Gao, J. Zeng, J. Han, and X. Lei, "Design of backstepping controller for T-type network inverter," *IOP Conference Series Earth and Environmental Science*, vol. 467, no. 1, article 012030, 2020.
- [20] W. Lai, W. Chen, J. Li, X. Zhang, Z. Lin, and H. Li, "Nonlinear adaptive control of PV inverter for maximum solar energy harvesting using democratic joint," *IOP Conference Series: Earth and Environmental Science*, vol. 467, no. 1, article 012068, 2020.

- [21] G. Feng, P. Wang, H. X. Liang, K. Yu, and X. Zeng, "Arc suppression method for distribution network with new energy based on active inverter split-phase injection," *IOP Conference Series Earth and Environmental Science*, vol. 495, no. 1, article 012025, 2020.
- [22] D. Ma, K. Cheng, R. Wang, S. Lin, and X. Xie, "The decoupled active/reactive power predictive control of quasi-Z-source inverter for distributed generations," *International Journal of Control, Automation and Systems*, vol. 19, no. 2, pp. 810–822, 2021.
- [23] D. Ghaderi, S. Padmanaban, P. K. Maroti, B. Papari, and J. B. Holm-Nielsen, "Design and implementation of an improved sinusoidal controller for a two-phase enhanced impedance source boost inverter," *Computers & Electrical Engineering*, vol. 83, no. 2020, article 106575, 2020.
- [24] Q. Chen, J. Pan, S. Liu, G. Chen, and J. Xiong, "New type single-supply four-switch five-level inverter with frequency multiplication capability," *IEEE Access*, vol. 8, pp. 203347–203357, 2020.
- [25] F. Gonzalez-Hernando, J. San-Sebastian, A. Garcia-Bediaga, M. Arias, F. Iannuzzo, and F. Blaabjerg, "Wear-out condition monitoring of IGBT and mosfet power modules in inverter operation," *IEEE Transactions on Industry Applications*, vol. 55, no. 6, pp. 6184–6192, 2019.
- [26] J. Rąbkowski, H. Skoneczny, R. Kopacz, P. Trochimiuk, and G. Wrona, "A simple method to validate power loss in medium voltage SiC MOSFETs and Schottky diodes operating in a three-phase inverter," *Energies*, vol. 13, no. 18, 2020.
- [27] M. G. Varzaneh, A. Rajaei, A. Jolfaei, and M. R. Khosravi, "A high step-up dual-source three phase inverter topology with decoupled and reliable control algorithm," *IEEE Transactions on Industry Applications*, vol. 56, no. 4, pp. 4501–4509, 2020.
- [28] P. Mishra, A. K. Pradhan, and P. Bajpai, "Voltage control of PV inverter connected to unbalanced distribution system," *IET Renewable Power Generation*, vol. 13, no. 9, pp. 1587–1594, 2019.
- [29] Y. Li, Y. Wei, Q. Wang, Y. Huang, and J. Cheng, "Design method of high efficiency class-E inverter applied to magnetic coupled resonant wireless power transmission system," *Diangong Jishu Xuebao/Transactions of China Electrotechnical Society*, vol. 34, no. 2, pp. 219–225, 2019.
- [30] S. K. Kim, "Performance-recovery proportional-type output-voltage tracking algorithm of three-phase inverter for uninteruptible power supply applications," *IET Circuits, Devices & Systems*, vol. 13, no. 2, pp. 185–192, 2019.
- [31] T. Roy, N. Aarzo, P. K. Sadhu, and A. Dasgupta, "A novel three-phase multilevel inverter structure using switched capacitor basic unit for renewable energy conversion systems," *International Journal of Power Electronics*, vol. 10, no. 1/2, pp. 133–154, 2019.
- [32] D. T. Nugroho and T. Noguchi, "A different voltage-source power inverter with carrier based SPWM for open-end connection loads," *Energies*, vol. 12, no. 17, 2019.
- [33] D. Çelik, M. E. Meral, and M. Inci, "Virtual Park-based control strategy for grid-connected inverter interfaced renewable energy sources," *IET Renewable Power Generation*, vol. 13, no. 15, pp. 2840–2852, 2019.
- [34] J. Choi, A. Khalsa, D. A. Klapp, S. Baktiono, and M. S. Illindala, "Survivability of prime-mover powered inverter-based distributed energy resources during microgrid islanding," *IEEE Transactions on Industry Applications*, vol. 55, no. 2, pp. 1214–1224, 2019.
- [35] M. Parvez, M. F. M. Elias, N. A. Rahim, F. Blaabjerg, D. Abbott, and S. F. Al-Sarawi, "Comparative study of discrete PI and PR controls for single-phase UPS inverter," *IEEE Access*, vol. 8, pp. 45584–45595, 2020.
- [36] A. Ali, M. A. Sayed, and T. Takeshita, "Isolated single-phase single-stage DC-AC cascaded transformer-based multilevel inverter for stand-alone and grid-tied applications," *International Journal of Electrical Power & Energy Systems*, vol. 125, 2021.

## Research Article

# Design of Distributed Human Resource Management System of Spark Framework Based on Fuzzy Clustering

Qing Sun <sup>1</sup>, Tao Wu,<sup>1</sup> and Jia Hua<sup>2</sup>

<sup>1</sup>International Cooperation Department, Xuzhou University of Technology, Jiangsu Xuzhou 221018, China

<sup>2</sup>Human Resource Management Department, Xuzhou College of Industrial Technology, Jiangsu Xuzhou 221140, China

Correspondence should be addressed to Qing Sun; [sunq@xzit.edu.cn](mailto:sunq@xzit.edu.cn)

Received 5 January 2022; Accepted 26 January 2022; Published 11 March 2022

Academic Editor: Yanqiong Li

Copyright © 2022 Qing Sun et al. This is an open access article distributed under the Creative Commons Attribution License, which permits unrestricted use, distribution, and reproduction in any medium, provided the original work is properly cited.

The construction of human resource management system is a key part of enterprise management and control. A perfect human resource management system is conducive to the long-term development of enterprises. Aiming at improving the current situation of enterprise human resource management, a distributed human resource management system is proposed in this paper based on Spark framework. Aiming at the disadvantages of traditional  $k$ -means algorithm in processing massive data, such as low computational efficiency and high time complexity, an improved  $k$ -means algorithm based on Spark computing framework is proposed. Through the spatial location relationship with the cluster center, redundant calculation is reduced and the ability of processing massive data is improved for the system. Combined with the actual situation of the enterprise, the human resource management system architecture is designed by using Java EE human-computer interaction. The proposed system can achieve user management, employee information, attendance, evaluation, performance, salary, personnel change, and other business management. The experimental results demonstrate that the system can effectively reduce the time complexity of calculation and improve the system efficiency.

## 1. Introduction

With the continuous improvement of the level of social and economic development, many enterprises also began to expand their own team to achieve good development. At present, the rapid development of cloud computing and big data Internet technology also makes people gradually enter the intelligent information era. Many enterprises develop distributed systems to be applied to all kinds of business, such as collaborative office [1], document management [2], financial management [3], and other systems [4]. For the development of enterprises, talent is an important cornerstone for the development of enterprises. It is of great significance to develop and design a set of human resource management system to improve the working efficiency of talents in enterprises through reasonable human resource management [5]. In order to get rid of the obstacles caused by traditional human resource management to the development and expansion of enterprises and provide efficient enterprise human resource development platform, it is nec-

essary to design a perfect human resource management system [6]. In short, the construction of human resource management system is a key component for the development of enterprise management and control. It needs to be fully combined with other construction systems, and the starting point is based on the business form and long-term development strategy of the company [7]. At the same time, when designing the human resource management system, it is necessary to consider the full use of the existing human resources of enterprises. By analyzing the performance requirements of human resource management system design, the system needs to consider business process, data process, data dictionary, use case constraints, etc.

$k$ -means algorithm is an unsupervised learning algorithm and has become one of the most widely used clustering algorithms. With the rapid development of open-source distributed computing framework, clustering algorithm based on distributed computing platform can effectively solve the problem of memory overflow in single-machine mode [8, 9]. This direction has become a research

hotspot. At present, for the problem of parallelization of algorithms under large data sets, many scholars have optimized and realized the algorithm under the distributed framework of MapReduce [10, 11]. Moreover, the optimization method research under Spark framework is relatively few.

Aiming at the problem of high time complexity of  $k$ -means algorithm [12], literature [13] improved by introducing Canopy algorithm and maximum and minimum distance method on Spark platform. The convergence speed of the algorithm has been improved, but the problem of large amount of redundant computation has not been solved fundamentally. Literature [14] proposed a clustering algorithm based on distance triangle inequality in cloud computing framework. But the optimization strategy using triangle inequality principle needs to save the upper and lower bound information of each data. It is difficult to fully implement this in the Spark framework. Literature [15] compares the operating efficiency of  $k$ -means algorithm based on MapReduce and Spark. Its experimental results show that the Spark framework has a more efficient running speed for the algorithm that needs repeated iteration.

The innovations and contributions of this paper are listed below.

- (1) In order to solve the problem of large amount of redundant calculation of  $k$ -means algorithm, this paper introduces the spatial location relationship between grid cells and clustering centers
- (2) Because the triangle inequality optimization strategy is considered in this paper, the redundant distance calculation is greatly reduced
- (3) The improved algorithm is implemented in parallel under the Spark framework. It improves the processing power of large data sets. Finally, the effectiveness of the proposed algorithm is verified by experimental analysis

The structure of this paper is listed as follows. Distributed  $k$ -means optimization algorithm based on spark framework is described in the next section. The proposed system is expressed in Section 3. Section 4 focuses on the experiment and analysis. Section 5 is the conclusion.

## 2. Distributed $k$ -Means Optimization Algorithms Based on Spark Framework

**2.1. Spark Distributed Framework.** Spark is a commonly used distributed computing platform that can effectively process massive data analysis. It is a distributed computing framework based on Elastic Distributed Data Set (RDD) implementation initiated by AMPLab of UC Berkeley [16].

In the overall structure of Spark, each Spark application uses a driver program to initiate parallel operations on the cluster. The driver program can manage multiple actuator nodes simultaneously. In a distributed cluster environment, multiple working nodes can read data from the HDFS file system and convert it to RDD. An RDD is an immutable,

distributed collection of objects. Each RDD is divided into multiple partitions. These partitions run on different actuator nodes.

Compared with the disk-based MapReduce calculation mode, Spark does not need to save the intermediate results of iteration to disks. Thereupon, it has more efficient computing efficiency. The Spark-based algorithm has good scalability and can better adapt to large-scale data sets. In the clustering algorithm which needs many iterations, its advantage is more obvious.

**2.2.  $k$ -Means Algorithm.** The process of the traditional  $k$ -means algorithm [17] is as follows.

*Input:* number of clusters  $z$ , data set  $d$ .

*Output:*  $z$  class clusters.

The algorithm steps are as follows.

- (1) Select  $z$  points from data set  $d$  as the initial clustering centers
- (2) Allocate each data point in  $d$  to the nearest class cluster
- (3) Calculate the average value of vector coordinates of data points in each class cluster, and then, update the cluster center of this class cluster
- (4) Repeat steps (2) and (3) until the clustering center converges
- (5) The sum of squares of errors is used as a measure of clustering quality, and it is calculated by the following equation

$$S = \sum_{x=1}^z \sum_{d \in D_x} d - c_x^2, \quad (1)$$

where  $z$  is the number of class clusters and  $c_x$  is the cluster center of the  $x$ -th class cluster  $D_x$ .

The time complexity of  $k$ -means algorithm is  $\phi(tzw)$ , where  $t$  is the number of data points,  $z$  is the number of class clusters, and  $w$  is the number of iterations. The time complexity of the algorithm is relatively large, and affected by the number of class clusters, it increases with the increase of  $z$  value.

**2.3. Use  $k$ -Means Optimized by Spatial Information.** In every iterative calculation process of  $k$ -means algorithm, each data point needs to calculate the distance between it and  $k$  cluster centers. The redundancy of its calculation is great, especially when the value of  $k$  is large, which has a great influence on the time efficiency of the algorithm. To solve the problem of large redundancy of  $k$ -means algorithm, the more effective improvement strategy is triangle inequality method. Without changing the clustering results of  $k$ -means algorithm, it can greatly reduce the computational complexity. The redundancy of calculation can be greatly reduced by using the principle of triangle inequality. However, in a single iteration, for each data point, several distance calculations are still needed to find the nearest class cluster. In

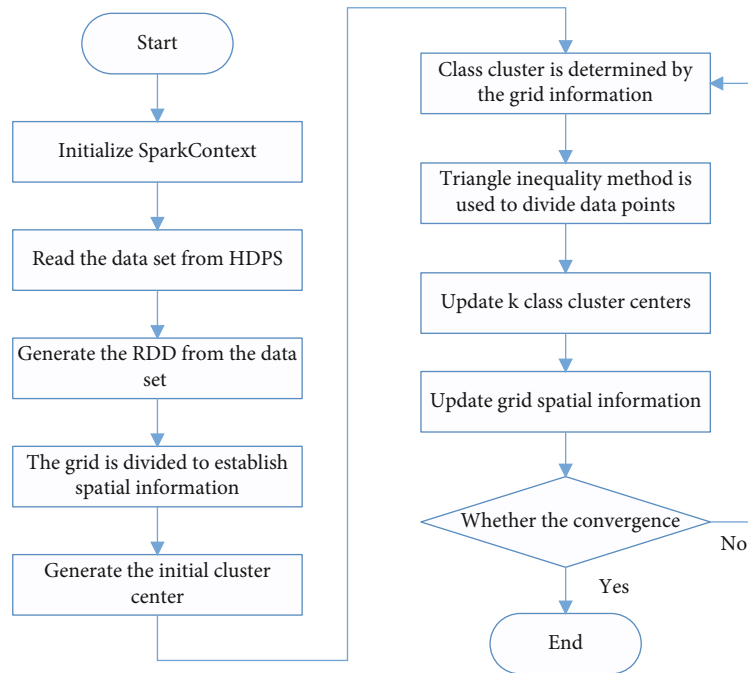


FIGURE 1:  $k$ -means optimization algorithm based on Spark framework.

fact, with the increase of  $k$  value, the number of calculations for a single data point will gradually increase, and the redundancy of calculation is positively correlated with  $k$  value. Aiming at the shortcomings of the triangle inequality optimization strategy, the spatial position information of data points is further considered to reduce the redundant computation.

**2.3.1. Spatial Position Relationship.** In order to further reduce the time complexity based on applying the triangle inequality strategy, the algorithm in this paper introduces the spatial position relationship between data points and clustering centers in  $k$ -means clustering. The basic idea can be described as follows. For any data point, if the spatial position relationship between it and  $k$  cluster centers can be known, then the closest cluster center to it can be accurately determined. Instead of doing  $k$  calculations, you just need to assign data points to the corresponding classes. Therefore, it is necessary to design a method that can efficiently save the spatial position relationship between all data points and  $k$  cluster centers. In view of the high efficiency of grid partitioning process, it is appropriate to use grid cells to store spatial location information of data points.

**2.3.2. Establish Spatial Location Information of Grid and Class Cluster.** First, the data set is meshed with a certain partition width in each dimension. Then, the position relationship between each grid containing data points and  $k$  cluster centers is judged.

Taking two-dimensional data as an example, for any grid  $C$ , the method to determine the spatial position relationship between grid  $C$  and  $k$  clustering centers is as follows.

- (1) First, find the class cluster closest to the center of grid  $C$  from  $z$  clustering centers and set it as  $A$ ,

whose distance is  $d_1$ . Let the concentric circle radius of the grid be  $r$ . Therefore, the maximum value of distance  $A$  for any point in grid  $C$  is  $d_1 + r$

- (2) Then, calculate the distance of other  $k - 1$  clustering centers in turn. Taking  $B$  as an example, let the distance between  $B$  and  $C$  be  $d_2$ . The minimum value of the distance  $B$  of any point in grid  $C$  is  $d_2 - r$ , if the following equation is satisfied

$$d_1 + r < d_2 - r. \quad (2)$$

That is, the closest distance between any point in grid  $C$  and  $B$  is still greater than the furthest distance between any point in grid  $C$  and  $A$ , so any point in grid  $C$  cannot belong to class cluster  $B$ . If the above equation is not satisfied, the score points inside grid  $C$  may belong to  $B$ . Grid  $C$  needs to record all possible belonging class clusters. In fact, when the number of meshes is large enough, the vast majority of meshes will have only one belonging class cluster. Only a small number of grids will belong to more than two class clusters. The average number of belonging class clusters per grid is slightly more than 1. By establishing the spatial location relationship between each grid and  $k$  cluster centers, the location relationship between all data points and  $k$  cluster centers is obtained.

**2.3.3. Clustering Using Spatial Location Information.** Take two-dimensional data as an example. Any data point is  $w(i, j)$ . Let the maximum value of dimension  $i$  be  $\max_i$  and the minimum value be  $\min_i$ . When meshing, the number of segments in one dimension is  $iNum$ . Let the dimension in which  $j$  resides be  $\max_j$  at its maximum and  $\min_j$  at its

minimum. In grid division, the number of segments in one dimension is  $jNum$ . According to the coordinates of data points, the grid position  $(i', j')$  of  $w$  can be quickly obtained by following the equation.

$$i' = \left( i - \min_i \right) \div \left( \max_i - \min_i + \delta \right) \times iNum, \quad (3)$$

$$j' = \left( j - \min_j \right) \div \left( \max_j - \min_j + \delta \right) \times jNum, \quad (4)$$

where  $\delta$  is a positive number less than 1.

The relationship between  $w$  and class cluster can be determined according to the relationship between the grid where data point  $w$  resides and  $k$  cluster centers. Namely, what cluster centers  $w$  may belong to. In this way, distance calculation between  $w$  and all cluster centers can be avoided.

**2.3.4. *k*-Means Optimization Algorithm in Spark Framework.** The algorithm flow of this paper is shown in Figure 1. The algorithm is implemented in parallel under the Spark framework. First, initialize Spark Context to determine the data set, number of cluster centers  $k$ , and maximum number of iterations. The data set is then read from the HDFS (Hadoop Distributed File System) file system and converted into an RDD collection. The Spark cluster partitions RDD sets based on the Spark Context information. It makes each partition run on each actuator node for grid partitioning and establishes the spatial information of grid and  $k$  cluster centers. Select the initial cluster center and start iterative calculation.

In each iteration calculation process, mapPartitions are processed for each RDD partition first. Cluster allocation is made to each data point. The corresponding grid is obtained by data point coordinates. Then, the relationship between grid and class cluster is utilized to determine the  $t (t \leq k)$  class clusters that data points may belong to. The triangle inequality method is utilized to find the nearest class from  $t$  cluster centers (instead of  $k$ ) to reduce the redundant distance calculation. After all data points were allocated, the class cluster centers of different actuator nodes were summarized by reduceByKey operations. New  $k$  clustering centers were obtained, and the spatial relationship between grid and class cluster was updated. Finally, the sum of squares of errors is calculated, and the next iteration is judged.

The key point of the optimization strategy is to use the grid structure to preserve the spatial relationship between all data points and  $k$  cluster centers and obtain the possible belonging class cluster of any data points according to this relationship. The effect of the proposed algorithm is similar to that of the triangle inequality, which does not change the final cluster center of  $k$ -means algorithm after clustering. This strategy can further reduce the amount of computation based on the application of triangle inequality.

**2.3.5. Time Complexity Analysis of the Algorithm.** The time complexity of the improved algorithm is effectively reduced. Reasonable selection of grid partition width can ensure that most grids have only one possible cluster. Only a small number of grids may belong to two or more class clusters. In this way, for most data points, only one distance calculation is

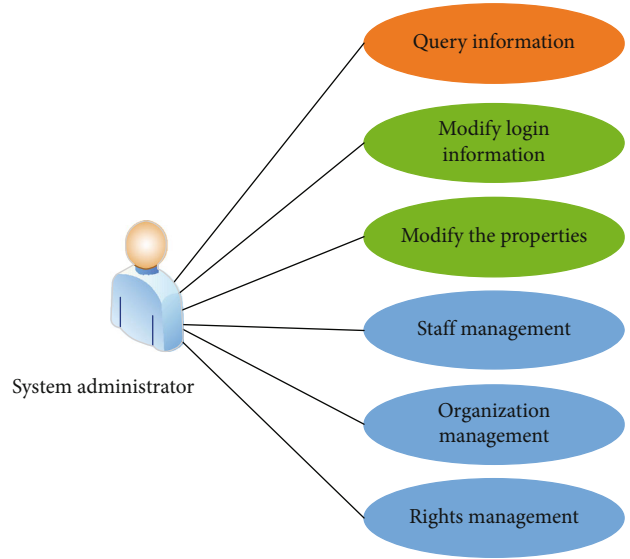


FIGURE 2: The system case for system administrator.

required, instead of  $k$  times. The time complexity of the improved algorithm is  $\phi(tw)$ , where  $t$  is the number of data points and  $w$  is the number of iterations.

Compared with the improved strategy of triangle inequality, the combination method using spatial position information has lower time complexity. Especially with the increase of  $k$  value, its advantage becomes more obvious.

Therefore, it can avoid a lot of redundant distance calculation process. For any data point, the advantage of using grid-based spatial location information is that most of the distance can be too far. It filters out the cluster center which obviously does not have the belonging relation, avoiding a lot of redundant distance calculation process.

### 3. The Design of Human Resource Management System

#### 3.1. Analysis of System Design Requirements

##### 3.1.1. Feasibility Analysis

- (1) Analyze the system from the perspective of technical feasibility. In order to be able to fully enhance the system application management decision-making level, many large and medium-sized enterprises are vigorously developing human resource management system. However, with the development and expansion of the enterprise team, the existing human resource management system cannot meet the needs of the enterprise. Enterprises began to increase the research and development of human resource management system, the formation of more and more mature human resource management technology. Therefore, Java EE-based human resource management system has technical feasibility
- (2) Analyze the system from the perspective of operational feasibility. Design based on Java EE technology human resource management system, which

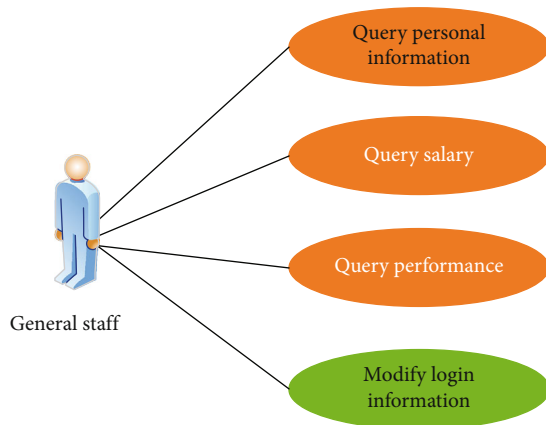


FIGURE 3: The system case for general staff.

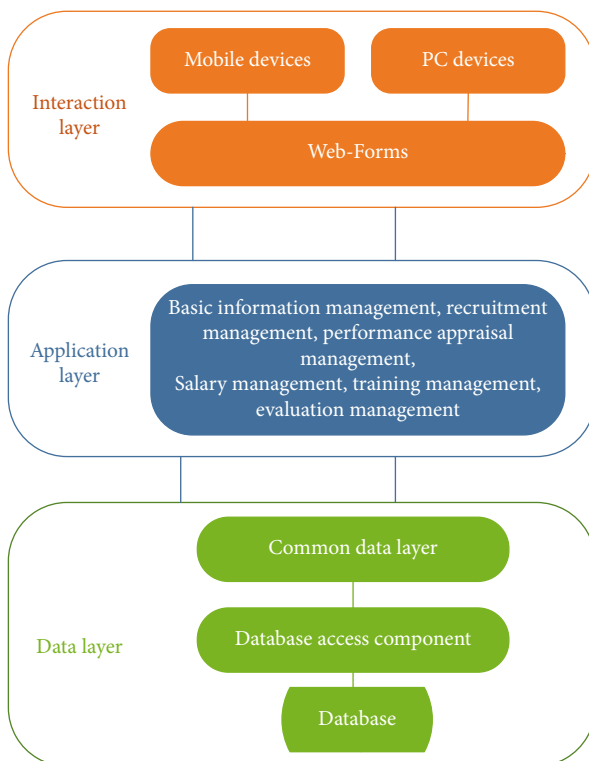


FIGURE 4: The human resource system business operation architecture diagram.

can facilitate the use of every common employee system. It realizes good man-machine interaction and ensures the feasibility of system development and operation

- (3) Analyze the system from the perspective of economic feasibility. The fundamental pursuit of enterprises is social and economic benefits, so how to maximize the benefits of enterprises is very important. And the enterprise's ability to bear the new technology also determines whether the enterprise can ensure the maximum benefit. The design of

human resource management system based on Java EE technology can effectively simplify the workflow of human resource management. It can make scientific and reasonable decision in real time and ensure the economic feasibility of the system

**3.1.2. Functional Requirement Analysis.** In the design of human resource management system based on Java EE, it is necessary to ensure that the system operation is efficient, simple, direct, powerful, and real-time. The general goal of system development is to complete the systematic, standardized, and automatic processing of all kinds of information. Based on the general task of system development, complete the function of human resource management system. It mainly includes organization management, recruitment management, employee information, training, attendance, performance, salary and welfare, enterprise culture, and other management modules. The system example for system administrators is shown in Figure 2, and the system example for common employees is shown in Figure 3.

**3.1.3. Analysis of Nonfunctional Requirements.** In the design of the human resource management system, nonfunctional requirement design includes the following two points.

- (1) Performance requirements of system operation speed, response efficiency, result accuracy, and other aspects
- (2) Reliability of users in terms of software failure frequency, easy recovery, severity, and predictability and security requirements to ensure that users use system identity, authorization, and privacy. Ensure safe and reliable operating environment of software system. Ensure that the operating interface of the system is aesthetically available. Ensure that the user's software is scalable, configurable, portable, and maintainable

**3.2. Overall Architecture of System Design.** Based on MVC three-tier architecture development platform, the system in this paper is divided into three levels, namely, interaction layer, application layer, and data layer. In the three-tier architecture design, the client can only provide better device application services. It has better system development architecture security than other development methods. Users can also access the data layer through the application layer, which effectively improves the overall data security. The architecture diagram of the system is shown in Figure 4.

**3.2.1. Interaction Layer.** When designing the interactive layer of the human resource management system in this paper, the C# language program is used to design the interactive interface, and the HTML5 technology is used to make forms. It can ensure the human resource management system to provide adaptive functions, combined with differentiated screen size, screen width, and height adjustment. It can also adjust the operation position of the system interface according to the user's requirements.



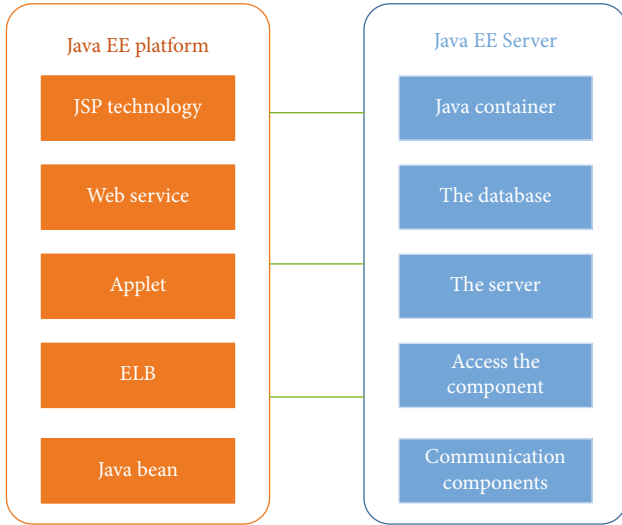


FIGURE 5: Composition of Java EE technology services.

TABLE 1: The results of running time.

Data size	$k$ value	$k$ -means	Literature [18]	Proposed	$\partial_1$	$\partial_2$
$3 \times 10^7$	20	532 s	263 s	257 s	0.538	0.035
	50	1275s	437 s	308 s	0.776	0.314
	100	2886 s	664 s	346 s	0.894	0.498
$5 \times 10^7$	20	815 s	379 s	328 s	0.616	0.149
	50	2032s	670 s	441 s	0.798	0.358
	100	4610 s	883 s	522 s	0.9	0.424

TABLE 2: The results of the sum of squares of errors with different algorithms.

Data size	$k$ value	$k$ -means	Literature [18]	Proposed
$3 \times 10^7$	20	$2.487 \times 10^{15}$	$2.534 \times 10^{15}$	$2.315 \times 10^{15}$
	50	$1.018 \times 10^{15}$	$1.015 \times 10^{15}$	$1.012 \times 10^{15}$
	100	$5.126 \times 10^{14}$	$5.111 \times 10^{14}$	$5.044 \times 10^{14}$
$5 \times 10^7$	20	$6.578 \times 10^{15}$	$6.603 \times 10^{15}$	$6.534 \times 10^{15}$
	50	$2.751 \times 10^{15}$	$2.762 \times 10^{15}$	$2.741 \times 10^{15}$
	100	$1.397 \times 10^{15}$	$1.396 \times 10^{15}$	$1.388 \times 10^{15}$

**3.2.2. The Application Layer.** As a large-scale software framework, human resource management system realizes the integration of multiple systems and improves the overall technical compatibility of the system. View the application layer as a development factory pattern, compatible with all subsystem functions. At the same time, the Web server can be utilized to parse the request of the business system, and the corresponding business program can be provided and operated.

**3.2.3. The Data Layer.** Introduce SQL advanced database technology into the data layer. The establishment of SQL database can realize the effective connection of various func-

tional components and ensure the processing performance of the database and data communication effectiveness. At the same time, it can be processed offline. The data layer wants to encapsulate data by transforming the data business into managed storage statements. Add information processing, expansion, separation, independence, and other functions to ensure that the operation portability of the system is fully improved. This makes it easier for more users to successfully connect to the system.

**3.3. Key Service Functions of the System.** Considering the actual human resource management needs, the Java EE framework is adopted in the process of human resource management system. It includes user management, employee information, organization, attendance, salary and welfare, performance, recruitment, training, and other different management modules, respectively. The user operation rights of each module are different.

### 3.3.1. Main Functional Modules

- (1) In the login management function module, the user enters the corresponding user name and password after successfully entering the login interface. If the match is successful, you can enter the system. If the match fails, the system displays a message indicating that the user name or password is incorrect and refreshes the login page again
- (2) In the attendance management function module, you can log in the attendance-related information of all employees of the enterprise. In this module to achieve the search, add, modify, delete, and other functions
- (3) In the enterprise internal transfer management module, you can choose the object of personnel transfer. It can submit the transfer process and complete all levels of approval. It can coordinate with the salary management module to complete the corresponding salary adjustment
- (4) In the performance management module, make equations of the corresponding performance appraisal plan. It can set clear assessment object and target, and choose appropriate assessment method and content. In the process of assessment, factors such as assessment principles, standards, methods, candidates, and data collection should be considered comprehensively
- (5) In the functional module of salary management, it can be adjusted appropriately according to the changing situation. You can also click Delete to complete the deletion
- (6) In the recruitment management function module, fill in the corresponding job information through recruitment. After completing the registration form, you can upload it to the system successfully

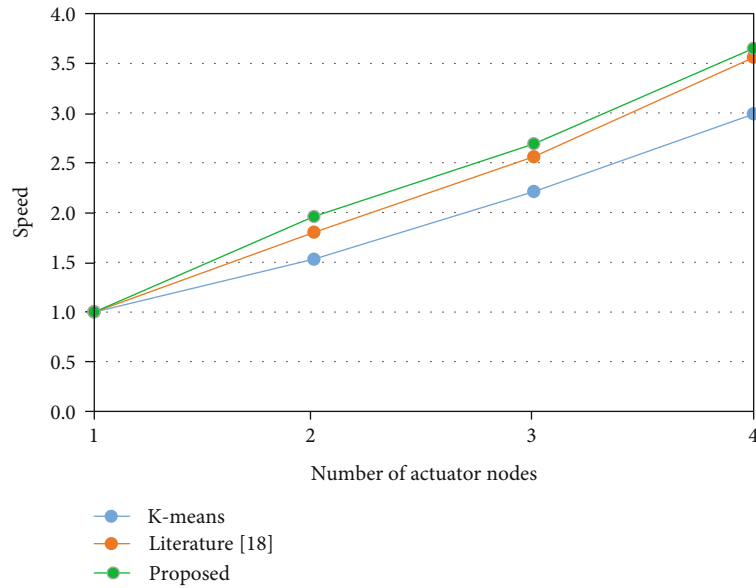


FIGURE 6: Comparison of parallelization time ( $k = 100$ ).

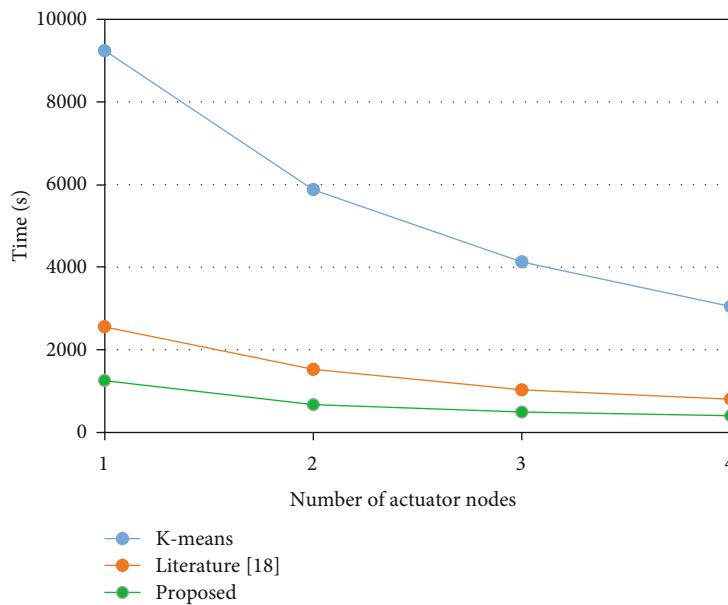


FIGURE 7: Comparison of algorithm acceleration ratio ( $k = 100$ ).

**3.3.2. Database Design.** The system is designed to establish SQL database, which can be optimized by SQL statement format. Get uniform specification code according to the object name of the database. It follows the debugging code specification, ensures the good design of database, and comprehensively improves the overall programming calculation efficiency. It can reduce unnecessary data redundancy to some extent and improve the database running efficiency of the system.

In order to realize the data function dynamically, it is necessary to establish the effective connection between the foreground and background of the system, as well as the effective connection between the database and the system

code. Establish Java database connection by using Java EE technology. It can provide standard database interface, and the system database connection steps are as follows.

- (1) Load the Java EE driver
- (2) Provide the main URL according to Java EE
- (3) Create a database connection
- (4) Create a statement
- (5) Execute database SQL statements
- (6) Obtain specific processing results

(7) Close the Java EE object

Figure 5 designs Java EE technology service composition for the database of the system.

## 4. Experiment and Analysis

The data set used in the test is the human resource data set of an enterprise. The writing language used in this experiment is Scala. To verify the effectiveness of the proposed algorithm, traditional  $k$ -means algorithm and reference [18] based on Spark framework are selected as the comparison algorithm. The algorithm in reference [18] adopts MLlib L.6.2. The initial cluster center was selected by random selection. All experiments were run for 20 times and averaged.

**4.1. Experimental Environment.** Spark distributed cluster is adopted in the experiment. Hadoop and Spark are installed on five VMS. Among them, one is responsible for the operation and management of driver programs, and the other four serve as actuator nodes.

*Software configuration:* Hadoop 2.6.0, JDK 1.7, Spark 1.6.0, MLlib 1.6.2, Scala 2.10.5.

*Hardware configuration:* 16 G memory, 1024 G hard disk.

### 4.2. Analysis of Experimental Results

**4.2.1. Comparison of Algorithm Performance.** Table 1 lists the comparison of the running time of the algorithm in this paper with traditional  $k$ -means and reference [18]. Table 2 lists the sum of squares of errors comparisons of the algorithms. Among them, the speed increase  $\partial_1$  and  $\partial_2$  are calculated as follows.

$$\partial_1 = \left(1 - \frac{n_2}{n_0}\right) \times 100\%, \quad (5)$$

$$\partial_2 = \left(1 - \frac{n_2}{n_1}\right) \times 100\%. \quad (6)$$

$n_0$  is the running time of  $k$ -means algorithm.  $n_1$  is the running time of the algorithm in reference [18].  $n_2$  is the running time of the algorithm in this paper.

As can be seen from the experimental results, the operating efficiency of the algorithm in this paper is significantly improved compared with the traditional  $k$ -means and literature [18] algorithm. When  $k$  value is small, the speed improvement is relatively insignificant because the improvement strategy in literature [18] has been able to avoid most redundant calculations. However, with the increase of  $k$  value, the improvement effect of the algorithm in this paper becomes more obvious.

By comparing the sum of squares of errors, the algorithm in this paper and the algorithm in literature [18] have no negative impact on the clustering quality of the original algorithm.

**4.2.2. Scalability Comparison.**  $4 \times 10^7$  data samples were utilized to test the scalability of the algorithm. Figure 6 shows

the comparison of parallelization time between traditional  $k$ -means, literature [18], and the algorithm in this paper. The algorithm in this paper has a more efficient clustering speed. The running time of the proposed algorithm decreases with the increase of actuator nodes. Meanwhile, due to the time cost of the Spark cluster, the running time of the algorithm does not decrease linearly with the increase of nodes.

Figure 7 shows the acceleration ratio comparison of the algorithms. The proposed algorithm has good scalability. With the expansion of cluster size, the acceleration ratio of the algorithm is basically consistent with that of literature [18].

## 5. Conclusion

In order to improve the current situation of human resource management, this paper puts forward a design method of human resource management system. Aiming at solving the problem of high computational complexity of traditional  $k$ -means algorithm, considering the spatial location relationship between data points and clustering centres and the advantages of grid division, this paper designs a clustering optimization algorithm to save the spatial location information of data points. The comparison results of parallel experiments based on Spark platform show that the computational efficiency of the proposed algorithm is significantly improved, and it has better scalability. On the premise of ensuring the system performance, how to further improve the scalability of the system is the next research direction.

## Data Availability

The labeled data set used to support the findings of this study is available from the corresponding author upon request.

## Conflicts of Interest

The authors declare no competing interests.

## References

- [1] S. Inoue and S. Fujita, "Collaborative illustrator with android tablets," in *2019 seventh international symposium on computing and networking workshops (CANDARW)*, pp. 208–214, Nagasaki, Japan, 2019.
- [2] V. L. Orlov and E. A. Kurako, "Electronic document management systems and distributed large-scale systems," in *2017 tenth international conference Management of Large-Scale System Development (MLSD)*, Moscow, Russia, 2017.
- [3] X. Mai, "Distributed accounting and blockchain technology in financial accounting," *Journal of Physics: Conference Series*, vol. 1881, no. 2, article 022078, 2021.
- [4] E. Doychev, P. Malinov, N. Velcheva, and Z. Duchevev, "A Genbank architecture: a distributed system for management of plant genetic resources," in *2020 IEEE 10th international conference on intelligent systems (IS)*, pp. 580–583, Varna, Bulgaria, 2020.

- [5] I. Makarova, K. Shubenkova, and A. Pashkevich, "Development of an intelligent human resource management system in the era of digitalization and talentism," in *2018 18th international conference on mechatronics-Mechatronika (ME)*, pp. 1–6, Brno, Czech Republic, 2018.
- [6] A. Y. Anisimov, A. S. Obukhova, Y. V. Aleksakhina, A. V. Zhaglovskaya, and A. A. Kudra, "Strategic approach to forming a human resource management system in the organization," *International Journal of Economic Perspectives*, vol. 11, no. 2, 2017.
- [7] I. Odun-Ayo, S. Misra, N. A. Omoregbe, E. Onibere, Y. Bulama, and R. Damasevicius, "Cloud-based security driven human resource management system," in *ICADIWT*, pp. 96–106, IOS Press, 2017.
- [8] C. Chen, K. Li, A. Ouyang, and K. Li, "Flinkcl: an OpenCL-based in-memory computing architecture on heterogeneous CPU-GPU clusters for big data," *IEEE Transactions on Computers*, vol. 67, no. 12, pp. 1765–1779, 2018.
- [9] D. Yu, Y. Ying, L. Zhang, C. Liu, and H. Zheng, "Balanced scheduling of distributed workflow tasks based on clustering," *Knowledge-Based Systems*, vol. 199, p. 105930, 2020.
- [10] M. Alkathiri, A. Jhummarwala, and M. B. Potdar, "Multi-dimensional geospatial data mining in a distributed environment using Map Reduce," *Journal of Big Data*, vol. 6, no. 1, pp. 1–34, 2019.
- [11] T. H. Sardar and Z. Ansari, "Partition based clustering of large datasets using Map Reduce framework: an analysis of recent themes and directions," *Future Computing and Informatics Journal*, vol. 3, no. 2, pp. 247–261, 2018.
- [12] M. M. Fard, T. Thonet, and E. Gaussier, "Deep k-means: jointly clustering with k-means and learning representations," *Pattern Recognition Letters*, vol. 138, pp. 185–192, 2020.
- [13] Z. Wang, A. Xu, Z. Zhang, C. Wang, A. Liu, and X. Hu, "The parallelization and optimization of K-means algorithm based on Spark," in *2020 15th International Conference on Computer Science & Education (ICCSE)*, pp. 457–462, IEEE, Delft, Netherlands, 2020, August.
- [14] A. S. Chitrakar and S. Petrovic, "Analyzing digital evidence using parallel k-means with triangle inequality on Spark," in *2018 IEEE international conference on big data (big data)*, pp. 3049–3058, IEEE, Seattle, WA, USA, 2018.
- [15] M. Saouabi and A. Ezzati, "A comparative between Hadoop MapReduce and Apache Spark on HDFS," in *Proceedings of the 1st International Conference on Internet of Things and Machine Learning*, pp. 1–4, New York, 2017.
- [16] T. Liu, "Personnel matching model of K-means clustering algorithm based on Spark platform," in *Proceedings of the 2020 Conference on Artificial Intelligence and Healthcare*, pp. 143–148, New York, 2020.
- [17] K. P. Sinaga and M. S. Yang, "Unsupervised K-means clustering algorithm," *IEEE Access*, vol. 8, pp. 80716–80727, 2020.
- [18] G. Zhang, C. Zhang, and H. Zhang, "Improved K-means algorithm based on density canopy," *Knowledge-Based Systems*, vol. 145, pp. 289–297, 2018.

## Research Article

# Evaluation and Promotion of a Multidimensional Information Intelligent Speech System in Dialect Teaching

Ya Pang 

School of Foreign Languages, Hainan Normal University, Haikou 571158, China

Correspondence should be addressed to Ya Pang; 030102@hainnu.edu.cn

Received 5 January 2022; Revised 23 January 2022; Accepted 17 February 2022; Published 8 March 2022

Academic Editor: Yanqiong Li

Copyright © 2022 Ya Pang. This is an open access article distributed under the Creative Commons Attribution License, which permits unrestricted use, distribution, and reproduction in any medium, provided the original work is properly cited.

Due to the wide scale of learners, large individual differences and scattered distribution, dialect teaching is difficult to carry out effectively by traditional school education. In order to improve the teaching level of dialect, taking Cantonese as an example, this paper constructs a teaching evaluation system based on multidimensional information. Through the questionnaire and investigation of large Cantonese training institutions in Guangdong Province, the data set is formed, the CMA-ES algorithm with efficient optimization ability is selected to optimize the SVM, and the model is compared with ACO and SVM without optimization algorithm. Experimental results show that the average accuracy of CMA-ES algorithm is 95.85% and the average running time is 21.0 ms on 8 data sets, which has obvious advantages relatively. Based on the evaluation model, the basis for teaching optimization is found through sensitivity analysis, and *student's language expression* is the most important index. And with the help of the intelligent voice system, the improvement measures for Cantonese teaching are proposed from the aspects of scene, oral, and scoring.

## 1. Introduction

UNESCO pointed out that among the more than 6000 Chinese languages in the world, about 96% of the language users' account for less than 3% of the total human population. On average, two languages disappear every month. As one of the countries with the richest language resources in the world today, our country's language resources are facing two basic facts: one is that there are many kinds of minority languages and Chinese dialects, and the language and culture is very rich. The other is that due to the rapid progress of urbanization and modernization with the continuous construction of China and the migration and exchanges between regions, minority languages and Chinese dialects are on the verge of disappearing. The protection of language resources, especially dialect resources, should not be limited to academic activities. The public should be involved in the protection of language resources. Evaluation is an important means to promote education reform, and teaching evaluation has become a hot issue in the field of education at home and abroad. Teaching evaluation is divided into formative evaluation and process evaluation. The former pays more

attention to students' academic performance, while the latter pays more attention to the status of students in the learning process. With the continuous advancement of education reform, process evaluation is more and more widely used in teaching evaluation. Process evaluation is carried out through the conditions of teachers and students in the classroom, which can reflect the scientific nature of the teaching process, and at the same time, judge the relationship between the teaching process and the teaching results based on the students' academic performance. The most important thing in dialect teaching is language cognition, reading, and comprehension. Bloom [1] thought that summative evaluation is designed to judge the achievements that students have achieved at the end of the course, and formative evaluation is intended to provide feedback and corrections at each stage of teaching and learning. Grant and Jay (2003) [2] put forward the concept of "reverse instructional design", and from the perspective of curriculum design dedicated to promoting students' understanding, six dimensions of understanding are proposed: explanation, paraphrase, application, insight, empathy, and self-awareness. The famous contemporary curriculum theory and education research expert, Anderson

(2008) [3]. The research team composed of nearly 10 experts further revised the idea of taxonomy of educational objectives initiated by Bloom et al. The original single-dimensional cognitive domain was changed to a two-dimensional division, namely, “Knowledge dimension” and “cognitive dimension,” the knowledge dimension includes four specific classification levels, namely, factual knowledge, conceptual knowledge, procedural knowledge, and reflection cognitive knowledge. The cognitive process follows cognitive complexity is ranked from low to high, including six categories: memory, comprehension, application, analysis, evaluation, and innovation, a total of 19 specific cognitive processes.

In terms of teaching optimization, with the support of intelligent technology, the classroom management system has developed rapidly. Considering that the classroom management system that provides classroom teaching evaluation must have the basic functions of real-time analysis, evaluation of the learning process, providing teachers with feedback information, etc. Lynnette is an intelligent guidance system that teaches students to solve linear equations [4]; Lumilo is a smart glass that can visualize information and perform certain virtual interactions [5]. Both can help teachers perceive students’ information in real time through a certain mechanism. FACT system is an intelligent classroom management system that can support students to solve mathematical problems collaboratively, and at the same time enhance teachers’ perception and control ability [6]. Spinoza provides guidance and assistance to students and teachers by analyzing the real-time codes and operating behaviors of students in the process of programming (Nisenbaum et al., 2019) [7]. MT-Classroom [8] is also a smart classroom, which enables students to learn on a touch-screen desktop. The built-in software analyzes the students’ learning in real time and sends them to the teacher. The teacher uses the tablet computer’s dashboard program to view student status and control the activity process in real time. In the behavioral evaluation model of teaching and learning, it mainly includes individual abnormal state, individual cognitive state, individual noncognitive state, group problem solving progress, group writing learning state, and teaching intervention. Common abnormal states of individual students include offline, silence, and abusive prompts, among which, abusive prompts are students’ “crafty” behaviors [9]. In the evaluation process of individual cognitive state, simple numerical evaluation is usually used, such as the number of correct answers, the number of attempts, and the number of help requests, which is a coarse-grained evaluation [10]. Individual noncognitive states mainly include concentration, emotion, and stress. Studies have shown that immersed in learning, physiologically manifested as happy and pleasant emotions, and have high concentration [11]. Group problem solving progress requires teachers to understand the learning situation and progress of the study group to help students solve problems [7]. Chi et al. [12] believe that monitoring the status of group collaborative learning is equally important. The higher the student’s participation in learning, the better the learning effect. In group collaborative learning, a member does not express opinions, but passively expresses opinions is passive learning [10]. Finally, it is teacher inter-

vention, which can be divided into cognitive intervention and noncognitive intervention according to the different status of students. Cognitive interventions include direct answers, hints, and prompts [10]. Noncognitive interventions are noncognitive feedback to students, including praise, reward, and criticism [13–15]. In the choice of evaluation method, Mullen et al. [16] first analyze the syntax between texts, and then further analyze the sentiment of the text based on the SVM algorithm. Moraes et al. [17] integrated machine learning algorithm and deep learning into teaching evaluation, compared the classification effect of support vector machine algorithm and artificial neural network algorithm, and proved the classification effect of ANN and support vector machine. In addition, fuzzy mathematics theory, analytic hierarchy process, and BP neural network are also often used in language teaching evaluation. Bamakan [18] and Gao [19] respectively, proposed the use of particle swarms, artificial fish swarms, and genetic algorithms for optimization. Although these methods have improved the blindness of support vector machine parameter selection to a certain extent, they all have varying degrees of premature problems, so that the predictive model is not the optimal model. In terms of the application of intelligent speech systems, the Bayesian network-based intelligent teaching system student model established by LAN [20] can not only objectively evaluate students’ cognitive abilities but also infer the student’s next learning behavior. Myers [21] uses an intelligent teaching system to automatically detect the emotional state of students and guide them into an active learning state. Based on previous research, this article found that mathematical algorithms are widely used in process teaching evaluation, but most of them use analytic hierarchy process, expert scoring, and other evaluation methods that are greatly affected by subjective factors, and algorithm optimization needs to be further improved. In this paper, SVM algorithm is used as the evaluation method of Cantonese teaching, and CMA-ES is used to optimize the SVM algorithm. This article constructs an evaluation index system from three perspectives of teaching language, teaching behavior, and teaching emotion, and fully considers the characteristics of procedural evaluation. Compare to SVM, ant colony algorithm optimized SVM and CMA-ES optimized SVM algorithm, select the algorithm with the highest accuracy rate as the evaluation method in this article, and apply the selected evaluation method to practice to obtain the most important influencing factors. The introduction of the intelligent voice system proposes measures for Cantonese teaching, fully considering the influence of the language environment and living environment on the teaching effect, and taking into account the practicality and innovation. In the evaluation process of this article, the effect of Cantonese teaching is divided into four levels: excellent, good, passing, and failing, and the optimized algorithm is used for empirical research. This paper takes a large Cantonese teaching institution as an example, selects the best plan through the comparison of three evaluation methods, evaluates the teaching effect of the institution, and introduces an intelligent voice system to propose an optimization strategy for Cantonese teaching.

## 2. Evaluation Index System of Cantonese Teaching

The Cantonese teaching evaluation system is an intuitive manifestation of multidimensional information processing, and requires a very deep understanding and research on the teaching system [22, 23]. Teaching evaluation is based on teaching activities and learning activities. The evaluation process focuses on improving ability of teachers and classroom teaching quality, and then evaluating classroom teaching design, process, and results. The current traditional teaching evaluation is manifested as a combination of internal and external multiple evaluations, process and performance evaluation judgments, on-site observation, and appraisal and screening by experts and peers. With the continuous development of information technology, teaching evaluation has undergone changes in terms of subject, content, methods, and results.

In terms of evaluation subjects, it is mainly divided into two aspects: internal subjects and external subjects. The internal subjects refer to the subjects that participate in the teaching activities, namely, students and teachers. External subjects refer to evaluators outside of teaching activities, including experts and colleagues. In terms of evaluation content, with the continuous advancement of education reform, education pays more attention to the change of emotional information, and the organic combination of emotional satisfaction and knowledge acquisition can more comprehensively evaluate the teaching effect. With the support of artificial intelligence technology, teachers and students' voices, facial expressions, and body postures can be collected through professional equipment to carry out teaching emotion recognition, and dynamic emotional changes can be obtained. In terms of evaluation methods, evaluation is the "baton" of teaching and provides decision-making materials for education optimization. Peer evaluation methods are widely used in teaching evaluation. The clarity of teacher teaching, the sufficient degree of content setting, and the sufficient degree of teacher-student interaction are often used. Used as an evaluation indicator, with the empowerment of artificial intelligence, cameras can be installed in the classroom to collect teacher and student voice, facial and posture information, carry out topic language analysis, topic behavior analysis, and topic emotion analysis to obtain students' attention, knowledge mastery, and interaction. Analyze the teaching effect based on the situation, emotional state, and other learning situations.

In terms of evaluation results, teaching evaluation can provide decision-making materials for improving education by judging and discovering value, and ultimately achieve value enhancement. Through the feedback of the evaluation results, it points to the multifaceted development of teachers and students, and exerts the function of their development value. Process evaluation aims to identify the teaching style by grasping the characteristics of the teacher's language structure, identify the classroom teaching structure through the teacher-student language interaction, and identify the classroom state through the voice intonation. From the perspective of students, it is possible to build a multidimen-

sional and multilevel teaching evaluation system by recording the number of times students have raised their hands to speak, their head-up rate, and their participation in discussions.

Based on the above analysis, it can be obtained that the classification of Cantonese teaching evaluation indicators is based on the two evaluation objects of teachers and students, and the evaluation indicators are divided into language, behavior, and emotion. In terms of language analysis, the indicators include the teacher's pronunciation standards, the teacher's intonation, the teacher's classroom organization structure, the teaching clarity, and the students' language expression. In terms of behavior analysis, the indicators include the teacher's body posture, student's head-up rate, classroom interaction, and participation in discussions. The indicators of sentiment analysis include teacher's emotional state, student's emotional state, student's attention, and satisfaction of students. The evaluation index system is shown in Figure 1 and the interpretation and definition of indicators are shown in Table 1.

The developed evaluation index system in Figure 1 can more comprehensively summarize the actual situation of Cantonese teaching. Using Cantonese teaching effect evaluation index data as the input sample of the evaluation model can realize the evaluation of Cantonese teaching effect.

## 3. The Method of Cantonese Teaching Evaluation

As one of the most difficult dialects in China, Cantonese has a complex composition and a variety of factors affecting Cantonese teaching, which belongs to the category of multidimensional information. As a common model for nonlinear relationship processing, SVM is consistent with the evaluation object of this paper. In order to make up for its inherent shortcomings, CMA-ES is also selected as the optimization algorithm.

*3.1. Evaluation Principle of SVM.* Support vector machines (SVM), as the latest content of statistical learning theory, was first proposed for pattern recognition problems, and it has shown its outstanding advantages over traditional methods such as neural networks in solving problems with limited samples, nonlinearity, and high-dimensional pattern recognition. With only a kernel function satisfying the Mercer condition, SVM can realize the problem solving by linear methods in high-dimensional space, which does not increase the computational complexity compared with the general linear model in low-dimensional space. It can be seen that the proposed kernel, like Radial basis kernel function, B-spline kernel function, and multilayer perceptron function, allows SVM to solve the up-dimensional disaster effectively. There are some problems in the running speed and parameter selection of SVM algorithm yet. The existing optimization methods such as artificial fish swarm and genetic algorithm improve the blindness of parameter selection of SVM to a certain extent, but they have different degrees of precocity simultaneously. In order to solve the problem of prediction accuracy, this

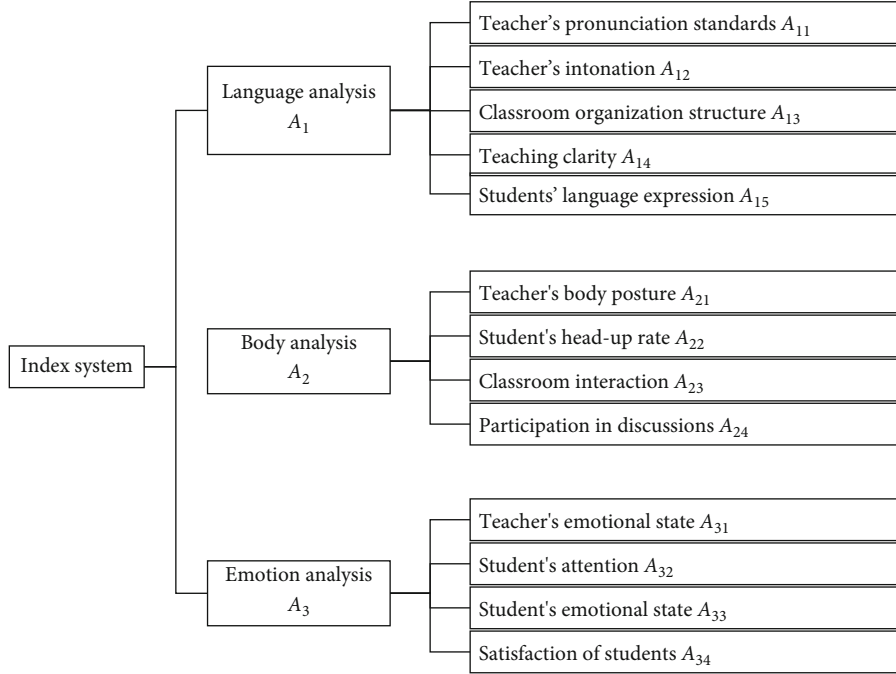


FIGURE 1: Evaluation index system of Cantonese teaching.

TABLE 1: Explanation of Cantonese teaching evaluation index.

Index		Explanation
$A_{11}$	Teacher's pronunciation standards	The teacher's pronunciation conforms to the pure Cantonese six tones
$A_{12}$	Teacher's intonation	How well the teacher's tone is accepted by the students
$A_{13}$	Classroom organization structure	The organization and hierarchy of lectures
$A_{14}$	Teaching clarity	Clarity of teaching content
$A_{15}$	Students' language expression	Student's language ability
$A_{21}$	Teacher's body posture	The teacher's physical movements in the teaching process
$A_{22}$	Student's head-up rate	The number of times the student raised his head to attend the class
$A_{23}$	Classroom interaction	The frequency of teacher-student interaction in the classroom
$A_{24}$	Participation in discussions	Enthusiasm of student for participating in discussions
$A_{31}$	Teacher's emotional state	Teachers' emotional state before, during, and after class
$A_{32}$	Student's attention	Student's attention during class
$A_{33}$	Student's emotional state	Students' emotional state before, during, and after class
$A_{34}$	Satisfaction of students	The degree of satisfaction of the students with the teacher's teaching methods and content

paper proposes a dialect teaching evaluation model based on covariance matrix adaptive evolutionary strategy (CMA-ES) to optimize SVM, which ensures the accuracy and running speed of the model. The basic idea of SVM is to map the data of sample space to a higher dimension or even infinite dimension feature space through a nonlinear mapping  $\varphi$  based on Mercer kernel expansion theorem, so that the highly nonlinear problems can be solved in feature space, as shown in Equation (1).

$$f(x) = \omega \bullet \varphi(x) + b, \quad (1)$$

where  $\omega$  is the weight vector,  $\omega \in R^n$ , and  $b$  is the offset,  $b \in R$ . It is assumed that all training data  $(x_i, y_i)$  can be fitted with  $f(x)$  within the accuracy  $\varepsilon$ .  $\varepsilon$  is the design parameter of the model, and  $\varepsilon > 0$ . Then the insensitive loss function is defined as Equation (2).

$$|y - f(x)|_\varepsilon = \begin{cases} 0; & |y - f(x)| \leq \varepsilon \\ |y - f(x)| - \varepsilon; & |y - f(x)| > \varepsilon \end{cases} \quad (2)$$

In consideration of the allowable fitting error, when the constraint conditions cannot be fully met, the loose other



variable  $\xi_i$  and  $\xi_i^*$  are introduced, and the optimization problem is like Equation (3).

$$\min = \frac{1}{2} \|\omega\|^2 + \gamma \sum_{i=1}^N (\xi_i + \xi_i^*), \quad (3)$$

where  $\gamma$  is the penalty coefficient, which is another important coefficient of the model, indicating the penalty degree for the training sample data exceeding the loss function.

**3.2. Performance Optimization of SVM.** Because the generalization ability of SVM is limited by the selection of penalty parameter  $c$ , RBF kernel function width  $\delta$  and insensitive loss function parameters  $\varepsilon$ , the optimization of SVM prediction performance is actually to solve the optimal parameter combination problem ( $\gamma$ ,  $\delta$ ,  $\varepsilon$ ). We use the mean square error ( $\Delta MSE$ ) of the trained model for prediction as an individual evaluation metric (i.e., fitness function), and the smaller the value of the metric, the higher the accuracy of the prediction.

CMA-ES shows good performance in solving global optimization problems, so it is used for adaptive parameter optimization selection of SVM parameters. The algorithm mainly consists of sampling and updating.

**3.2.1. Sampling.** CMA-ES uses Gaussian distribution  $N(m, \sigma^2 C)$ , and samples are collected in the solution space of the optimization problem to generate a population distribution composed of  $\alpha$  individuals  $z = (\gamma, \delta, \varepsilon)$ , which corresponds to the population in the optimization algorithm, as shown in Equation (4).

$$z_j^{(h+1)} = m^{(h)} + \sigma^{(h)} N_j \left( 0, C^{(h)} \right) j = (1, 2, \dots, \alpha), \quad (4)$$

where  $z_j^{(h+1)}$  is the  $j$ -th individual generation population  $h + 1$  and  $m^{(h)}$  is the mean value of population distribution of generation  $h$ , and  $\sigma^{(h)}$  is the global step size of generation  $h$ , and  $C^{(h)}$  is the covariance matrix of the population distribution of generation  $h$ , and the relationship of each parameter is shown in Equation (5).

$$C^{(h)} = B^{(h)} \left( D^{(h)} \right)^2 \left( B^{(h)} \right)^T, \quad (5)$$

where  $B^{(h)}$  is the orthogonal matrix and its column vector is the orthogonal basis of the eigenvector of  $C^{(h)}$ , which is used for the rotation of the hyper-ellipsoid, and  $D^{(h)}$  is the diagonal matrix, and the diagonal element is the square root of the characteristic of  $C^{(h)}$ , corresponding to each column vector of  $B^{(h)}$ , which is used for scaling the hyper-ellipsoid of population distribution.

**3.2.2. Updating.** The update operation is mainly for parameters  $m$ ,  $C$  and  $\sigma$ , as shown in Equations (6)–(8).

$$m^{(h+1)} = \sum_{i=1}^{\beta} \omega_i z_{1:\alpha}^{h+1}; \quad \sum_{i=1}^{\beta} \omega_i = 1 \quad (\omega_1 \geq \omega_2 \geq \dots \geq \omega_{\beta} \geq 0), \quad (6)$$

where  $\omega_i$  is the set weight and  $z_{1:\alpha}^{h+1}$  is the  $i$ -th optimal individual in the  $h + 1$  generation.

$$C^{(h+1)} = (1 - c_1 - c_{\beta}) C^{(h)} + c_1 \left[ p_{\gamma}^{(h+1)} \left( p_{\gamma}^{(h+1)} \right)^T + \delta \left( k_{\sigma}^{h+1} \right) C^{(h)} \right] + c_{\beta} \sum_{i=1}^{\beta} \omega_i y_{1:\alpha}^{h+1} \left( y_{1:\alpha}^{h+1} \right)^T, \quad (7)$$

where  $p_{\gamma}^{(h+1)} = (1 - c_{\gamma}) p_{\gamma}^{(h)} + k_{\sigma}^{(h+1)} \sqrt{c_{\gamma} \beta (2 - c_{\gamma})} (m^{(h+1)} - m^{(h)} / \sigma^{(h)})$  and  $c_{\gamma}$  is the update learning rate of  $p_{\gamma}$ .

$$\sigma^{(h+1)} = \sigma^{(h)} \exp \left( \frac{c_{\sigma}}{d_{\sigma}} \left( \frac{\|p_{\sigma}^{(h+1)}\|}{E(\|N(0, I)\|)} - 1 \right) \right). \quad (8)$$

To sum up, the SVM parameter optimization algorithm based on CMA-ES is as follows.

- (1) Input training set data samples  $S = \{(x_1, y_1), \dots, (x_l, y_l)\} \in R^m \times R$
- (2) Select appropriate parameters  $(\gamma, \delta, \varepsilon)$ .
- (3) Set parameters and initialization. The number of parent and child individuals in the population are  $\mu$  and  $\lambda$ , respectively, and  $\mu < \lambda$ . The maximum number of iterations is  $H$
- (4) Construct the training and test data set required for the experiment
- (5) Sample the population
- (6) Calculate the fitness of individual population
- (7) Update parameters
- (8) If the stop condition is reached, the optimization process stops, and the optimal individual  $(\gamma^*, \delta^*, \varepsilon^*)$  within its optimal fitness value are output. Otherwise, returns (5).
- (9) The working process of the evaluation system is shown in Figure 2

## 4. Experimental Results and Analysis

As a dialect, Cantonese is difficult to learn and start for people whose mother tongue is not it. In order to ensure the scientific and reliable data, we investigated large Cantonese teaching institutions in Guangdong, China. Sample data were collected according to the evaluation index

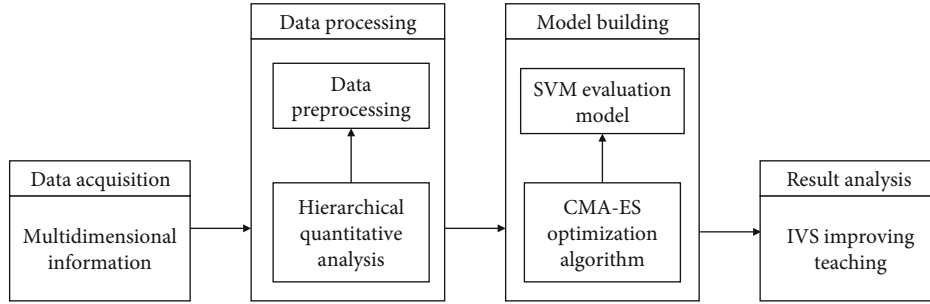


FIGURE 2: System working process block diagram.

TABLE 2: Accuracy comparison.

Data set	CMA-ES (%)	ACO (%)	SVM (%)
1	95.49	87.68	84.72
2	94.32	89.67	85.24
3	96.38	88.52	83.95
4	97.15	89.94	81.89
5	95.82	85.51	79.87
6	96.84	86.08	84.65
7	95.08	85.79	79.68
8	95.7	88.24	82.43

system of Cantonese teaching, and the quality level of large Cantonese teaching institutions and 160 data samples could be obtained for testing by evaluating the actual situation of Cantonese teaching and experts' evaluation of the effectiveness of Cantonese teaching. The 160 data samples are divided into 8 data sets, and each data set contained 20 samples. The training data of each group are input into SVM regressor for learning, and CMA-ES is used to optimize the punished parameter  $\gamma$  and the width of RBF kernel function  $\delta$ . The initial mean (population center)  $m^{(0)} = (\gamma, \delta, \epsilon)^{(0)}$ ,  $\gamma$  and  $\delta$  are set to  $[0.01, 100]$ , the maximum number of evolutionary generations is 100 and the termination threshold is set to 1. Meanwhile, the SVM hyperparameters  $(\gamma, \delta, \epsilon)$  are optimized using the CMA-ES algorithm, and the evaluation model is built with the final output optimal solution  $(\gamma^*, \delta^*, \epsilon^*)$ . After repeated experiments, the optimal solution on all data sets is  $\gamma^* = 129.92$ ,  $\delta^* = 11.63$ ,  $\epsilon^* = 0.003$ . In order to verify the optimization effectiveness of CMA-ES method in Cantonese teaching evaluation model, we also use ant colony optimization (ACO) and SVM model without optimization algorithm for comparative test. The accuracy results of the three schemes are presented in Table 2 and Figure 3. It can be seen that both ACO and CMA-ES have an optimization effect on SVM, but the optimization effect of ant colony algorithm is not obvious, and the accuracy of evaluation model only using SVM is not enough. The average accuracy of the model using CMA-ES method is 95.85%, which has high reliability. Relatively speaking, the accuracy of the three methods in dataset 5 is poor, which may be due to the low discrimination of its data sources.

In addition to accuracy, another important evaluation basis of SVM optimization algorithm is running time. Only

the optimization algorithm that meets both high accuracy and running time is the most cost-effective and most worthy method. Figure 4 shows that although the advantage of CMA-ES for ACO is not obvious in running time, it has a very significant optimization for SVM. It also indicates that CMA-ES has stronger performance when the amount of data is larger.

## 5. Teaching Improvement Measures

The main purpose of constructing a high-precision and efficient teaching evaluation model in this paper is to find the evaluation index that has the greatest impact on the evaluation results. Therefore, we can effectively improve Cantonese learning effect of students who are interested in Cantonese with the help of IVS. According to our data analysis results, we conduct further research in order to find more sensitive evaluation indicators. Our findings show that *teacher's pronunciation standard* ( $A_{11}$ ), *students' language expression* ( $A_{15}$ ), *classroom interaction* ( $A_{23}$ ), and *students' attention* ( $A_{32}$ ) have the higher impact on Cantonese teaching. It is obvious that these four indicators have a positive impact on the final teaching effect, so only their positive changes are considered in this paper when doing sensitivity analysis. Then we increase each index by 5%, 10%, and 15%, respectively, on the original basis, and the impact on the final evaluation results is shown in Figure 5.

Figure 4 clearly shows that  $A_{15}$  has the greatest impact on Cantonese teaching. For a language teaching dominated by interest, the quality of students' expression is the most intuitive embodiment of teaching effect. Teacher's pronunciation also has a great impact on teaching results, and with the increase of indicators, the improvement effect on teaching is more and more significant, indicating that the more standard teacher's pronunciation is, the better students' learning effect is. As for classroom interaction, a small increase has an obvious impact on the results, illustrating that teachers need to control the proportion of classroom interaction.

Cantonese has rich tones and syllables. Modern Putonghua has only four tones, while Cantonese dialect has nine tones and two inflections, and the difference between these nine tones is not obvious, so traditional teaching methods are not very effective in Cantonese teaching. Thus, IVS is more powerful in improving these two important indicators

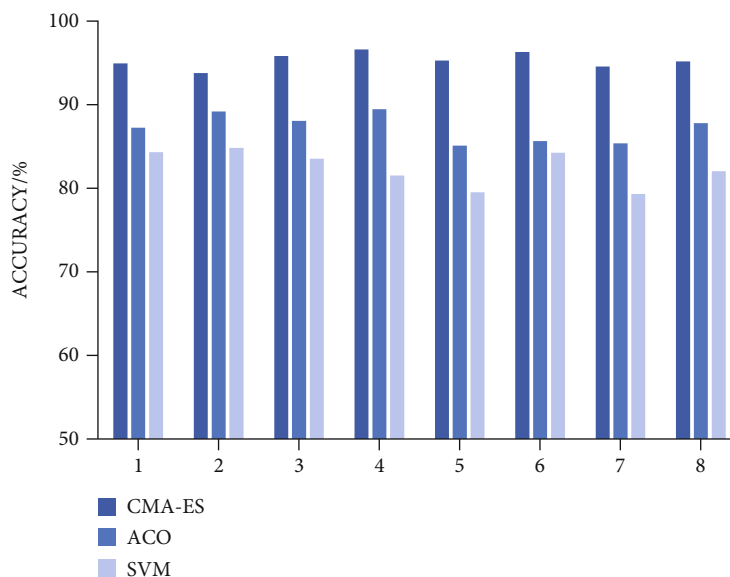


FIGURE 3: Accuracy comparison.

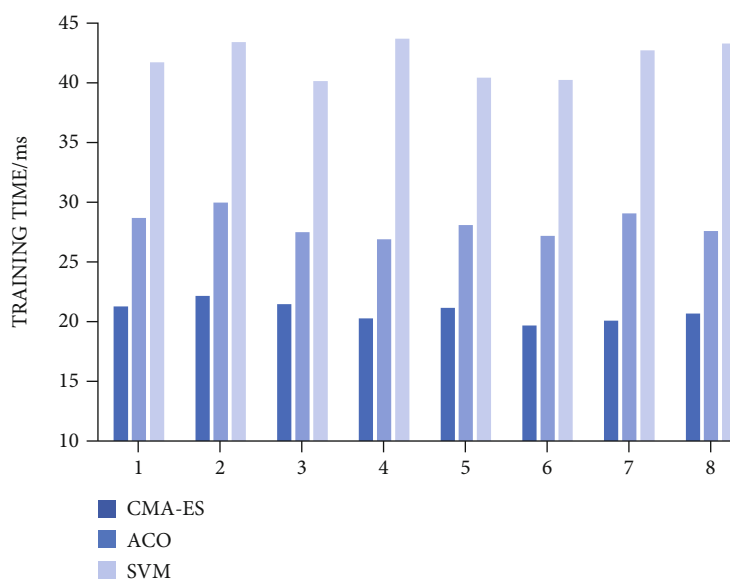


FIGURE 4: Training time comparison.

( $A_{11}, A_{15}$ ). With the support of speech recognition technology and speech synthesis technology, IVS realizes human-computer interaction (HCI) has two technical aspects: input and output. The input of HCI is based on the language information received by the computer, which is recognized and understood by speech recognition technology and then converted into text information. The output of HCI is based on the input text information, which is converted into easily understandable and applicable language information by speech synthesis technology. From the technical aspect, intelligent speech system has the functions of standard reading, speech synthesis, speech evaluation, and audio teaching courseware production. The hardware facilities of IVS support various audio teaching resources. Students can hear

the reading of pronunciation standards with a simple click, so as to lead students to perceive and remember standard and authentic Cantonese. In the environment where modern information technology is widely used in social life, Cantonese teaching must keep pace with the times, combine the content of English teaching, students' age and psychological characteristics, and take advantage of the rich learning resources and vivid knowledge presentation of the intelligent speech system to make students gain aural and visual freshness and endogenize the initiative of Cantonese learning.

*5.1. Optimize Situational Teaching.* Language learning is for communicative purposes, and dialects are more life-like, so only by learning language and using it in a communicative

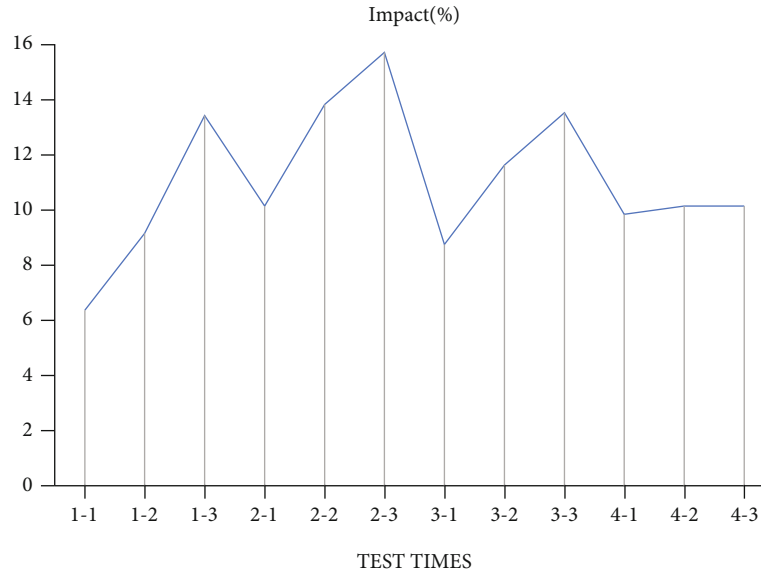


FIGURE 5: Sensitivity analysis results.

context can we have a true understanding of the words, sentences, and texts we learn and clarify the linguistic function in the complete internalization of knowledge. Through IVS, teachers can generate life scenes such as “buying vegetables,” “renting a house,” “traveling,” and “drinking morning tea” according to teaching needs, so that students can deepen their language learning in the context of Cantonese life. Therefore, the teaching can not only provide students with fresh audio-visual perception and sensory experience, mobilize students’ learning initiative, but also enable students to acquire knowledge and improve their ability in communication and interaction. For example, in the characteristic morning tea culture in Guangdong, the teacher first outlines the top view of the tea restaurant on the electronic blackboard. Under the guidance of the waiter, the students divide themselves into groups and complete the learning tasks in the process of “ordering” and “dining.”

**5.2. Optimize Oral Teaching.** Oral communication in Cantonese is far greater than written communication. Most people who are interested in learning Cantonese and can pay the corresponding tuition fees are adults with leisure time. Compared with step-by-step, they prefer to be rapidly improved, which has stronger requirements for teacher’s language level and teaching quality. Cantonese teachers should use IVS to construct and render real situations of oral communication, create more opportunities for students to use spoken language, lead them to be in oral communication situations, and let them start oral communication by role-playing and intelligent imitation with the advantages of technology such as dot reading, following, listening, and discriminating included in IVS. For example, teacher can create multiangle oral Q&A around simple sentence patterns, let students make corresponding answers according to the questions played by IVS, gradually shorten the reserved time for answers, and improve students’ oral response speed.

**5.3. Optimize Teaching Scoring.** IVS not only has a “mouth” that can speak standard Cantonese but also has “ears” that can carefully distinguish whether Cantonese pronunciation is standard. Speech recognition technology endows IVS with the function of automatic evaluation of English pronunciation through auditory processing, information conversion, and output, so as to timely and accurately help teachers and students compare standard pronunciation and correct pronunciation deviation in the form of quantitative score. Students can understand the problems existing in their pronunciation, conduct pronunciation correction exercises through the pronunciation comparison control button, and improve the pronunciation standard in repeated follow-up and evaluation with standard pronunciation. Through the all-round improvement of students’ “listening, speaking, reading, and writing” abilities, they can effectively integrate Cantonese learning into students’ daily lives and feel the charm of depalletizations. Give full play to the functions of the intelligent voice system, and then feedback to the classroom teaching, and conduct a second evaluation of Cantonese teaching, to achieve the PDCA cycle of evaluation.

## 6. Conclusion

The index factors affecting Cantonese teaching come from a wide range of sources, belong to multidimensional information, and there is a complex nonlinear functional relationship between the evaluation results and the evaluation indexes. For the objective science of teaching evaluation, this paper uses the commonly used nonlinear problem processing model SVM to solve it. However, SVM itself has some limitations. In order to improve the applicability of the model, this paper uses CMA-ES algorithm to optimize it. Experimental results show that, in terms of model accuracy, this method is 8% and 13% higher than ACO and SVM, respectively. In terms of running time, it is 7 ms and 21 ms,

respectively. It can be seen that the evaluation method in this article is highly scientific and reasonable. Therefore, relying on the evaluation model constructed in this paper and with the help of IVS, we can put forward targeted optimization measures for Cantonese teaching, which is of great significance to improve the Cantonese level of students with poor foundation. Due to conditions and time constraints, this paper has some deficiencies in data sources and evaluation methods. The evaluation data of this paper adopts the traditional questionnaire survey method. With the strengthening of the function of IVS, it can be combined with computational vision technology to judge the emotional attitude and interactive atmosphere in the classroom through expression and voice intonation recognition, and master the teachers' classroom control ability and emergency handling ability through expression recognition. We hope to provide personalized and targeted methods for the teaching evaluation and improvement of other dialects in future research.

### Data Availability

The labeled dataset used to support the findings of this study are available from the corresponding author upon request.

### Conflicts of Interest

The author declares no competing interests.

### Acknowledgments

This work was supported in part by the "An Acoustic Study of Syllables of Ha Dialect in Li language from the Perspective of Ecological Linguistics", a philosophy and social science planning project in Hainan province in China, 2018. (Grant No. HNSK.QN 18-29).

### References

- [1] B. S. Bloom, "Some theoretical issues relating to educational evaluation," in *Educational Evaluation: New Roles, New Means. The 63rd Yearbook of the National Society for the Study of Education, Part 2*, pp. 26–50, University of Chicago Press, Chicago, IL, 1969.
- [2] W. Grant and M. Jay, *Understanding by design*, vol. 13, Association for Supervisors, 2006.
- [3] L. W. Anderson, "Taxonomy for learning, teaching, and assessing," *European Legacy*, vol. 114, no. 458, pp. 1013–1014, 2001.
- [4] Y. Long and V. Alevan, "Supporting students' self-regulated learning with an open learner model in a linear equation tutor," in *Artificial Intelligence in Education*, pp. 219–228, Springer, Berlin, Heidelberg, 2013.
- [5] K. Holstein, B. McLaren, V. M. Alevan, and V. Alevan, "Co-designing a real-time classroom orchestration tool to support teacher-AI complementarity," *Journal of Learning Analytics*, vol. 6, no. 2, pp. 27–52, 2019.
- [6] K. VanLehn, H. Burkhardt, S. Cheema et al., "Can an orchestration system increase collaborative, productive struggle in teaching-by-eliciting classrooms," *Interactive Learning Environments*, vol. 2, pp. 1–19, 2019.
- [7] M. Tissenbaum, M. Lui, and J. D. Slotta, "Co-designing collaborative smart classroom curriculum for secondary school science," *Journal of Universal Computer Science*, vol. 18, no. 3, pp. 327–352, 2012.
- [8] R. Martinez-Maldonado, A. Clayphan, K. Yacef, and J. Kay, "MTFeedback: providing notifications to enhance teacher awareness of small group work in the classroom," *IEEE Transactions on Learning Technologies*, vol. 8, no. 2, pp. 187–200, 2014.
- [9] V. Alevan, I. Roll, B. M. McLaren, and K. R. Koedinger, "Help helps, but only so much: research on help seeking with intelligent tutoring Systems," *International Journal of Artificial Intelligence in Education*, vol. 26, no. 1, pp. 205–223, 2016.
- [10] K. Vanlehn, "The behavior of tutoring systems," *International Journal of Artificial Intelligence in Education*, vol. 16, no. 3, pp. 227–265, 2006.
- [11] M. Csikszentmihalyi, *Flow: The Psychology of Optimal Experience[M]*, Harper & Row, New York, 1990.
- [12] M. T. Chi and R. Wylie, "The ICAP framework: linking cognitive engagement to active learning Outcomes," *Educational Psychologist*, vol. 49, no. 4, pp. 219–243, 2014.
- [13] A. D. Tillery, K. Varjas, J. Meyers, and A. S. Collins, "General education teachers' perceptions of behavior management and intervention Strategies," *Journal of Positive Behavior Interventions*, vol. 12, no. 2, pp. 86–102, 2010.
- [14] S. Shen and M. Chi, "Reinforcement learning: the sooner the better, or the later the better?," in *Proceedings of the 2016 Conference on user modeling adaptation and personalization (UMAP'16)*, pp. 37–44, Association for Computing Machinery, New York, NY, USA, 2016.
- [15] M. S. Ausin, H. Azizoltani, T. Barnes, and M. Chi, "Leveraging deep reinforcement learning for pedagogical policy induction in an intelligent tutoring system," in *Proceedings of the 12th International Conference on Educational Data Mining (EDM 2019)*, pp. 168–177, Montreal, Canada, 2019.
- [16] T. Mullen and N. Collier, "Sentiment analysis using support vector machines with Di-verse information sources," in *Proceedings of the 2004 Conference on Empirical Methods in Natural Language Processing*, pp. 23–35, Barcelona, Spain, 2004.
- [17] R. Moraes, J. F. Valiati, and W. P. G. Neto, "Document-level sentiment classification: An empirical comparison between SVM and ANN," *Expert Systems with Applications*, vol. 40, no. 2, pp. 621–633, 2013.
- [18] S. M. H. Bamakan, H. Wang, T. Yingjie, and Y. Shi, "An effective intrusion detection framework based on MCLP/SVM optimized by time-varying chaos particle swarm optimization," *Neurocomputing*, vol. 199, pp. 90–102, 2016.
- [19] Y. Gao, Y. Shen, G. Zhang, and S. Zheng, "Information security risk assessment model based on optimized support vector machine with artificial fish swarm algorithm," in *Proc of Software Engineering and Service Science*, pp. 599–602, New York, 2015.
- [20] L. Wu, "Student model construction of intelligent teaching system based on Bayesian network," *Personal and Ubiquitous Computing*, vol. 24, no. 3, pp. 419–428, 2020.
- [21] M. H. Myers, "Automatic detection of a student's affective states for intelligent teaching systems," *Brain Sciences*, vol. 11, no. 3, p. 331, 2021.

- [22] B. Q. Cheng, K. Lu, J. Li, H. Chen, X. Luo, and M. Shafique, "Comprehensive assessment of embodied environmental impacts of buildings using normalized environmental impact factors," *Journal of Cleaner Production*, vol. 334, article 130083, 2021.
- [23] L. Lu, Z. Gu, D. Huang, Z. Liu, and J. Chen, "An evaluation framework for the public information guidance system," *KSCE Journal of Civil Engineering*, vol. 21, no. 5, pp. 1919–1928, 2017.

## Research Article

# Analysis of the Application of Virtual Reality Technology in Football Training

Kun Zhao<sup>1</sup> and Xueying Guo<sup>2</sup> 

<sup>1</sup>Physical Education Department, Civil Aviation University of China, Tianjin 300300, China

<sup>2</sup>Computer Science and Technology College, Civil Aviation University of China, Tianjin 300300, China

Correspondence should be addressed to Xueying Guo; [xyguo@cauc.edu.cn](mailto:xyguo@cauc.edu.cn)

Received 4 January 2022; Revised 24 January 2022; Accepted 9 February 2022; Published 7 March 2022

Academic Editor: Yanqiong Li

Copyright © 2022 Kun Zhao and Xueying Guo. This is an open access article distributed under the Creative Commons Attribution License, which permits unrestricted use, distribution, and reproduction in any medium, provided the original work is properly cited.

As computer science and information technology develop rapidly, virtual reality (VR) technology has evolved from theory to application. As a key technology in modern society, VR technology is increasingly influencing more and more aspects of people's daily lives, including sports training. VR technology can be seen as an assistive technology that provides specific support for athletes' sports training through various means such as simulating training scenarios and conducting data analysis. This paper focuses on exploring the application of VR technology in football training and the combination of sports training and VR technology. In addition, a feasibility analysis of the application of VR technology in football is carried out, and software such as Poser 8.0, 3ds MAX, and EON Studio in the virtual football training system are introduced. The aim is to further provide theoretical support for the development and research of virtual football sports system software and to study virtual systems that are not disturbed by external natural conditions. It will break through the limitations of sports training due to factors such as weather, player injuries, lack of training space, and funding. This is conducive to improving teaching and training methods, promoting the mastery of technical movement essentials and the improvement of football skills.

## 1. Introduction

As technology continues to develop and advance, virtual reality (VR), sometimes called virtual environments (VE), has become a trendy topic in recent years. The core concept of VR technology has been around dating back to 1965 [1]. However, the expensive cost of the device is a hurdle to its widespread deployment [2]. Also, due to the overhype and hype surrounding VR for a long time, the adoption of VR technology had hit a low point [3]. Thus, many experts had not been optimistic that VR technology would be widely used in the world. Nevertheless, VR technology has become increasingly popular with the advent of inexpensive consumer-grade VR headsets for gaming and entertainment in recent years [4]. Nowadays, it can be seen that VR has been extensively applied in a great variety of fields such as game [5–7], sport [8–10], film [11, 12], education [13], and construction [14] and brings great commercial value to soci-

ety. Therefore, research into the application of VR technology is very promising in the future.

VR is an advanced, human-computer interface that simulates a realistic environment where participants can move around in a virtual world, and they can see it from different perspectives and make the computer do things [15]. This emerging technology includes a wide range of fields such as computer science, engineering, and the social sciences [16]. Specifically, VR combines the contradictory aspects of the virtual and the real to create an immersive experience through the use of computer technology to create realistic three-dimensional animations. Then it is combined with sensor technology to give a realistic experience in terms of sight, sound, touch, and even smell, creating a simulated space like the real world. In other words, VR is a technology that normally provides interaction and immerses the senses of the users [17]. Hence, through the computer-generated images or animated characters and avatars, the users can

move around the virtual world and pick up and interact with virtual objects as they do so [18].

Interactivity is the essential part in VR technology because the users play a role in the media, and their actions can influence the experience or scenario unfolding in real time [19]. In this process, the users can better interact with the VR devices with the aid of computers and the corresponding devices. The other key element of VR technology is its immersion. In the environment of immersive VR, the users are perceptually encircled by the virtual environment, and their consciousness of the real world is minimised [20]. Therefore, since the sensory feeling from the real world is blocked, this could create the impression that a person has actually entered the virtual environment and construct an illusion of participation in the artificial world [21].

The fundamental purpose of VR technology is to ensure that participants can interact naturally with the virtual environment and achieve a realistic experience. Immersive VR systems allow users to be fully immersed in a computer-generated environment to create an immersive effect, but the hardware required is demanding and expensive, and not conducive to commercial development. The desktop VR systems use a computer screen or projection screen as the viewing window for the virtual environment and require the use of a handheld input device or position tracker to manipulate objects in the virtual environment, such as a “physical game console,” which is low cost and simple to use.

With the rapid development of technology, the market for VR technology has been growing, and sport is one of the areas where VR is developing rapidly. As the world of sport continues to grow and improve, countries around the world are investing more in sport, and virtual reality is becoming more prominent in sports teaching, simulation training, stadium construction, and event broadcasting. The recent Olympic Games, for example, are the clearest example of the use of VR technology to enhance sports technology. The modern competitive sport is rapidly developing to a high level of difficulty, standard, and precision, and the use of modern technology to assist physical education and training has become a favourable tool for improving the standard of competitive sport. The unpredictable and unexpected events in sports training, the disproportionate investment and output of training funds, and the unreasonable structure of investment all have an impact on the level of competition. There has been a lot of research into the use of VR technology in sports. Becker and Pentland built a Tai Chi trainer within a modified version of the Alive system [22]. Yang and Kim designed an immersive virtual training system based on VR technology known as “ghosts” [23]. Baek et al. designed a movement system that adjusts a given reference for the trainee, providing an analysis of the effect of the trainee’s movement following the reference [24]. Meng examined how VR technology can be used to build virtual physical education environments [25]. Tsai et al. proposed a VR-based basketball training system that can be used to help the athletes to get better tactics [26]. In China, VR technology is widely used in the fields of football, bed-vaulting, gymnastics, diving, and sailing. This suggests that VR technology, with its low cost and zero risk advantages,

has a wide range of application prospects in various fields. The combination of VR technology and sports can not only improve the training level of athletes and promote their athletic performance but also facilitate the development of national fitness sports with its low investment cost, small floor space, and ease of operation.

Football is one of the most popular sports in the world and attracts millions of spectators. However, the intense physical confrontation, the difficult manoeuvres, and the risky tackling of the ball in football can cause various degrees of physical injury. Therefore, it is essential to develop a training environment that is free from outside interference, avoids sports injuries, and gives the athletes a sense of immersion. The interactive, immersive, and imaginative nature of VR technology in sport means that VR has an important role to play in facilitating football training. Nowadays, in the globalised contemporary society, technology drives the progress of the society, and this is also reflected in professional football [27, 28]. The competitive environment of football has built a marketplace for technology-based innovation for coaches who are seeking to create a sustainable competitive advantage [29]. As VR technology can assist players to better train in football without the constraints of time and space, it has a broad application prospect in football training. After all, VR technology can be valuable enough to accurately measure the body movements with athletes during sports and subsequently for coaches and players to be able to perform data analysis.

In order to better explore the application of VR technology in football training, this paper focuses on researching various applications of VR technology in football training and analyzing the essential technologies that should be adopted in the VR training system. Also, this study suggests some positive effects of the VR training system.

## 2. Analysis of the Application of VR Technology in Football Training

VR technology in football training offers significant training efficiency and low training risk. At the same time, VR technology can reduce the distraction of the real environment for the players. As a result, VR technology is being widely used in football training.

Figure 1 shows an example of football training through VR devices. It can be seen that the athlete can train on the simulated real court with the headgear and wearables. The advantages of training football using VR technology are that it is convenient and can be done anywhere and that the computer can analyse data about the players, thus supporting them in getting better training.

*2.1. Basic Functions of Virtual Football Training System.* In order to meet the requirements of football training, there are several basic functions that the virtual football training system should meet with.

*2.1.1. A Football Training Ground with a Realistic Feel.* A virtual football training ground with a realistic feel needs





FIGURE 1: VR football training.

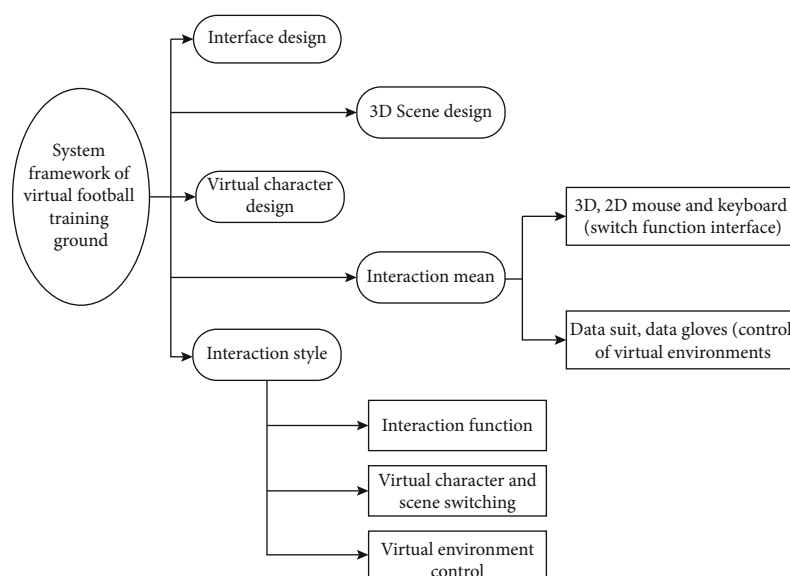


FIGURE 2: System framework of virtual football training ground.

to be created, so models of the goal, the football, the grass, and the surrounding trees and sky need to produce a vivid and realistic virtual training scene.

**2.1.2. Collect Athlete Physiological Data.** Athlete physiological and psychological health data is an important reference for evaluating the effectiveness of athletic training, and athletes' physiological data is mainly obtained through heart rate, electrocardiogram, and blood pressure.

**2.1.3. Movement Reenactment and Demonstration.** The virtual system should be able to record and represent the user's (athlete's or coach's) technical movements and clearly indicate the deficiencies between the two movements, which facilitates the correction of errors and the demonstration of technical skills.

**2.1.4. Graphical Analysis of Training Results.** The graphical display of the athletes' training effects and the results of

the error analysis can visually reflect the athletes' training effects and the degree of standardization of their movements, aiding teaching and training.

**2.2. Virtual Simulated Training Ground.** VR technology can be used to build a simulated training ground with the help of a three-dimensional image library to build a realistic training environment for football trainers and increase the realism of the clinical game. The virtual environment includes the background of the football field, the configuration of the field, the football game scenario, and the modelling of the virtual players. The virtual football training ground is created using multiple images, data, and pictures to create a three-dimensional environment almost similar to the real training ground. The trainer can experience many game situations and contingencies in advance in this environment, thus reducing the probability of friction and injury in the real game. The main system framework of the virtual football training ground is shown in Figure 2.

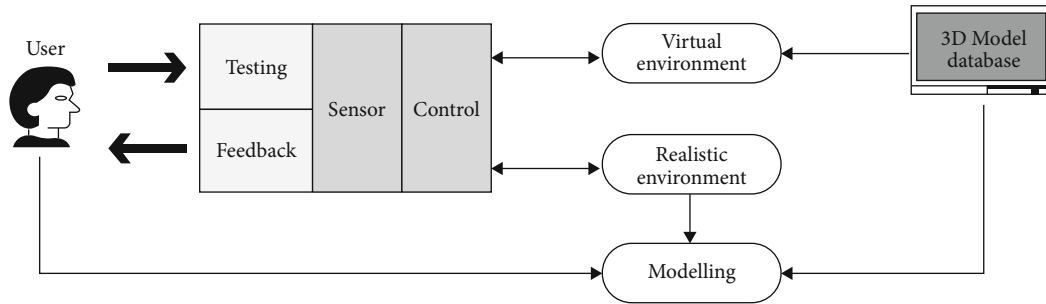


FIGURE 3: Basic framework of the VR system.

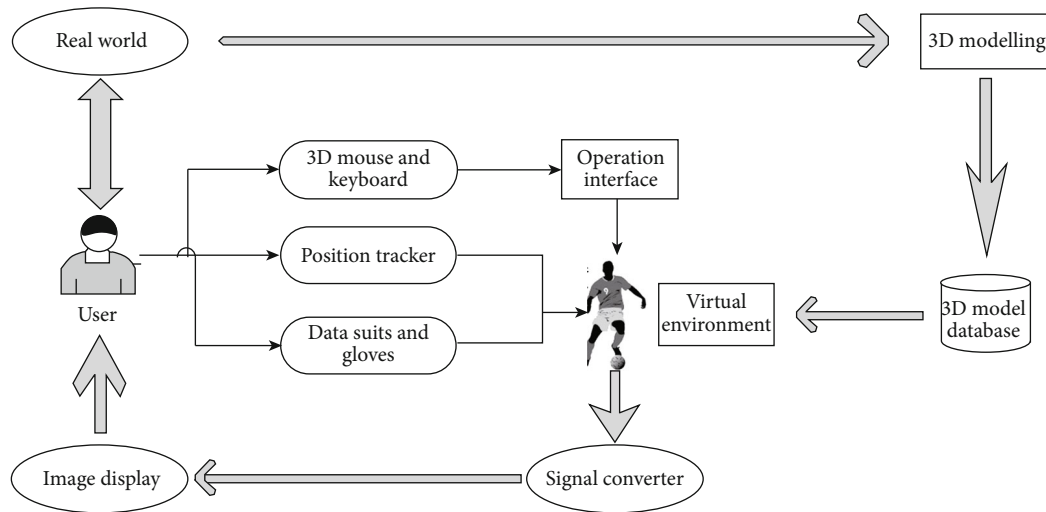


FIGURE 4: Principle of desktop virtual football training system.

From Figure 1, it can be seen that the system framework of the virtual football training ground mainly includes interface design, 3D scene design, virtual character design, interaction mean, and interaction style. The interface design is the home page of the system that the user sees when opening the system. The 3D scene design and virtual character design are the core parts of the whole system, and they are also the most complex technology in the system design, mainly including scene modelling technology, virtual human modelling technology, and collision detection technology. The virtual environment is controlled by the user, and the sensing device acquires the motion data through data suits, data gloves, position trackers, and other devices to control the virtual environment. In the interaction means, there are two different aspects. The first one is a 3D and 2D mouse and keyboard, which are used to switch function interfaces. The other one is a data suit and gloves which can be applied to control the virtual environments. These two means are quite essential to this whole framework because they can be regarded as the core parts of VR technology. In addition, there are three different interaction styles, that is, the interaction function, the virtual character and scene switching, and the virtual environment control. These functions can help the whole training system to achieve the interaction between users and computers. By these means, the athletes can better train in the virtual environment instead of the

true environment. Thus, through building a virtual simulated training ground, the football athletes can obtain better training without going to the true ground.

**2.3. Desktop Virtual Football Training System.** The basic framework of the VR system is shown in Figure 3. The system is based on the real world as the ontology, which is built into a 3D model and transformed into a virtual world. The virtual world forms a closed feedback control loop with the internal system through displays, sensors, etc., to achieve interaction between the virtual environment and the real world under the control of the user. It should be noticed that the 3D model database can store the 3D models and use them in various scenarios in order to meet the requirements of different true cases.

Based on the basic framework of the VR system, the principle of the desktop virtual football training system can be designed according to Figure 4.

The virtual environment is formed by first acquiring 3D data from the real world, creating a 3D model, and then integrating the individual 3D models to form the same virtual environment as the real world. The computer acquires the user's movement information through hardware devices such as data gloves, data suits, and position trackers and inputs the acquired movement information into the computer's virtual environment through 3D sensors. At the same

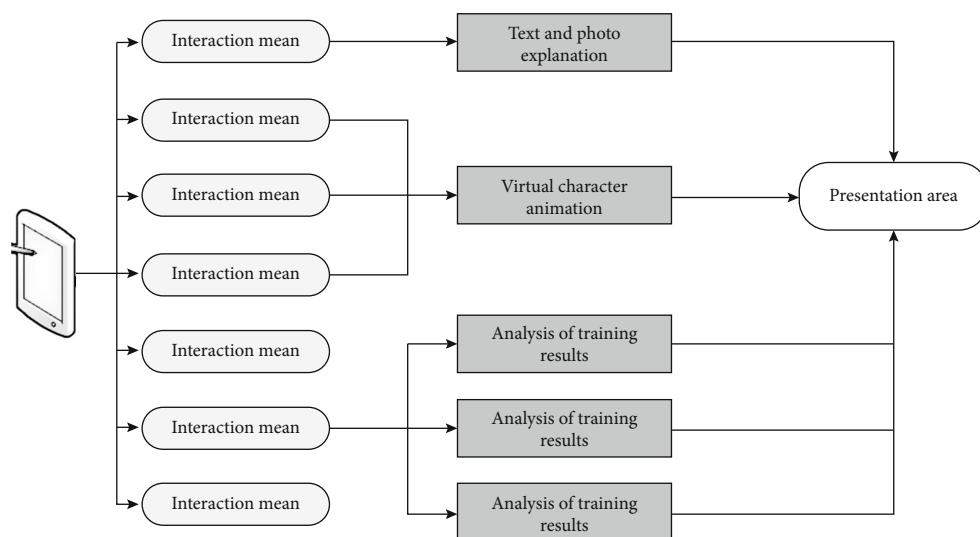


FIGURE 5: Function of interaction.

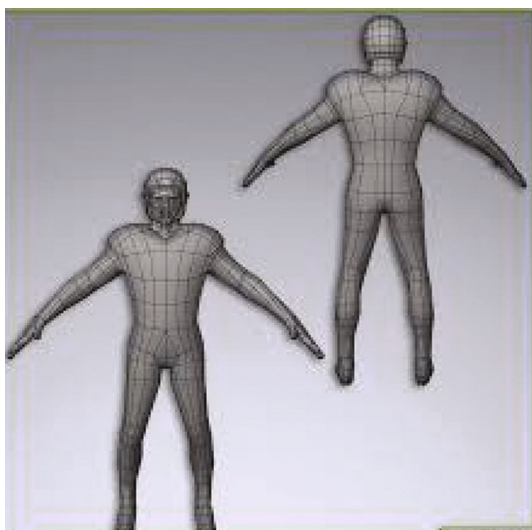


FIGURE 6: Virtual human modelling.

time, auxiliary tools such as the mouse and keyboard can help the user to switch and control the interface and interactive functions.

**2.4. Design of Interaction Function.** The football training system should also have certain interactive functions in its application as shown in Figure 5. Integrating football theory with technical and tactical teaching, together with virtual human animation demonstrations, is both convenient for teaching and conducive to the mastery of technical essentials and the improvement of the sport. At the same time, during the interaction between the computer and the athlete, data analysis can provide analytical support to the athlete in order to help them identify their strengths and weaknesses in training. Actually, data analytics are quite essential for both athletes and coaches. For athletes, they can clearly know their status during their training. For coaches, they can conduct greater strategies according to the data analysis function for the athletes.

VR technology makes use of many leading high technologies in the interaction process. Examples of such technologies are 3D image visualization generation systems, graphics workstations, 3D interactive compositors, headset displays, and many more. The 3D image visualization system is able to synthesize the natural environment such as wind direction, wind strength, temperature, and humidity to create a highly simulated virtual training environment. In the training of athletes, it can help to detect and analyse the reality of the athletes during solo training. For example, the system's sensors for physiological and biochemical testing allow for the analysis of physical injuries during exercise and the analysis and advice of athletes who are overloaded. In addition, the basic conditions of individually trained football players are tested in a timely manner, and the training content and duration are arranged according to their physical condition.

### 3. Key Technology in VR Football Training System

**3.1. Virtual Human Modelling.** Human modelling (e.g., Figure 6) is at the heart of virtual human motion simulation and uses a hierarchical modelling approach where movement of higher-level components changes the spatial position of lower-level components. For example, the movement of the knee joint changes the position of the lower leg and foot, and movement of the shoulder joint affects the position of the large and small arm. The muscle layer can be used to change the shape and posture of the body as required; the skin layer includes the texture and color of the skin, which gives the virtual character a vivid and realistic appearance.

There are many tools commonly used for modelling the human body, such as Maya, 3ds MAX, Make Human, and Poser 8.0. Poser 8.0 is a professional software for 3D design from Metacreations. It is simple to use, has a simple interface, and is flexible compared to similar 3D production

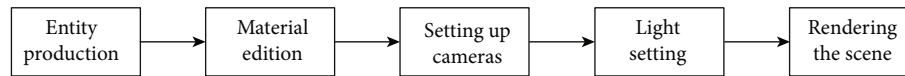


FIGURE 7: Process of modelling in football scenes.

software. Poser 8.0 allows for easy and intuitive skeletal construction of human models.

**3.2. Motion Data Information Capture.** Traditional methods of acquiring sports data are mainly based on the “active tracking method.” This technique requires the application of marker points to key areas of the subject’s body, but the requirements of athletes’ clothing in formal athletic competition limit the use of this technique. A common method of motion tracking without contact with the human body is “contactless tracking,” which involves setting up multiple sets of video capture devices at the site of a training or competition to capture the whole process of the athlete’s movement from all angles, using the main joints of the human body as nodes, and after postprocessing with specialized software to obtain 3D joint rotations in different postures. The main joints of the human body are used as nodes, which are then processed by specialized software to obtain 3D coordinate data of joint rotation in different postures.

**3.3. Virtual Football Ground Design.** There are many software tools used for virtual reality modelling, CAD is mostly used in mechanical engineering and manufacturing, and its graphics are highly accurate, but its lighting and animation functions are weak, and there is a gap with 3ds MAX. 3ds MAX is the tool of choice for modelling 3D scenes because of its powerful modelling capabilities and easy and fast production process. The application of 3ds MAX software for the modelling of football scenes and the animation of football movements mainly includes several processes as shown in Figure 7. Through these processes, the virtual football ground in the VR football training system can be designed for use.

**3.4. Virtual Football Training System Interaction Based on EON Studio.** EON Studio is a full-featured development tool designed for the integrated production of 3D/VR content and the development of interactive 3D applications. EON Studio can be easily combined with other 3D software to turn them into virtual reality objects and scenes without remodelling. First, select a frame function node in the EON simulation tree window and import it into the virtual scene and avatar file, convert it into the internal database, create the EON simulation tree structure in the database, form a tree hierarchy of frame function nodes, then drag the nodes set in the simulation tree window to the logic window, and set the logical relationship path between the nodes by connecting them. The model animation is set up and interacted with in the virtual environment.

## 4. Effects of VR Football Training System

**4.1. Improve Teamwork.** The effective playing formations can help teams to be comfortable in the game and help

to improve the coordination between players. The VR system is unique in its ability to organize formations in advance of a football match by organizing the formation to be used and the stage of the match at which it will be played. By inputting data on the various formations used in a football match, the system allows for the organization of special training sessions for a variety of formations designed to suit the opponent of the match. What is more, this system also allows for the design of multiple formations to enhance the coordination of training between players, maximising the coordination of training habits and individual levels. After all, this system can use emerging technologies such as big data analytics to analyse the motion data of athletes in order to improve the training results of the team. The VR football training system is therefore essential for improving the team’s coordination skills.

**4.2. Inspire Athletes’ Potential.** VR technology can not only reduce the risk to the athletes when training but also enable the design of a training programme that is tailored to the trainee’s training and stimulates the potential of the trainee. The technology can be used to test and analyse the abilities of coaches and trainees. Based on the data provided by the VR system, the user can identify their own strengths and weaknesses, thus targeting their weaknesses for improvement. At the same time, the VR system can accurately test the athletes’ skeletal growth and development and monitor, analyse, and regulate them continuously, thus helping them to adjust their game form and posture in time to achieve good results. Therefore, the VR training system allows for the full range of athlete training to be monitored and scientifically analysed from the preparation to the conduct of the competition. It is of great importance to the athletes and allows them to develop their potential to a great extent.

**4.3. Strengthen Core Athletes.** Although football is a collective game played by a team, each footballer plays a different role and is in a different position during the game. An excellent football team must have core players to perform difficult tackles, passes, etc. VR technology is different from the actual training of core players, mainly using stereoscopic glasses and data gloves to confront the opponent and find the right tactics. The simulation is not fundamentally different from a real football match because the atmosphere of the game and the audio-visual effects of the players are based on the actual game. The core athletes are able not only to train realistically but also to use the system to adapt their tactics and find the best way to train.

## 5. Conclusion

This paper provides a brief introduction to VR technology and an in-depth analysis of its use in football training.

Firstly, it analyses the basic functions that a virtual football training system needs to have. Based on these functions, it then introduces the virtual simulated training ground, the desktop virtual football training system, and the design of the interaction function. After that, this paper states some key technologies in the VR football training system, such as virtual human modelling, motion data information capture, virtual football ground design, and virtual football training system interaction based on EON Studio. All of these technologies are quite important to the VR training system because they can provide a solid foundation for football training. Through the VR training system, the athletes can get better training effects. For example, they can improve teamwork, inspire their potential, and strengthen the core athletes. Overall, VR technology has made a breakthrough in football training by virtue of its superiority and a high degree of simulation, and the VR system has been a key guide to the physical and tactical training of the players, greatly improving their psychological and teamwork during matches. Also, VR technology has an essential influence on both athletes and coaches. In this paper, the analyses suggest that VR technology will become a trend in the development of sports and provide solid technical support to enhance sports technology.

In order to promote better development of VR technology, this paper gives the following suggestions. Firstly, there is a need to strengthen the application of VR technology in sport, to promote cross-fertilization of disciplines and to use VR technology to solve the problems of poor teaching conditions, inadequate teacher reserves, and limited coaches. Through the advantages of VR technology, the athletes and coaches should get better training to improve their abilities. In addition, the relationship between virtual reality and football teaching and training needs to be properly addressed. The environment on the field is highly variable, and good results require not only skill and stamina but also the ability to quickly adjust to the player's competitive state, which cannot be simulated by many unexpected events in a virtual training system. Last but not least, it is necessary to encourage interdisciplinary research among PE teachers or students to improve the quality of their research and to develop excellent research talent.

## Data Availability

The labeled dataset used to support the findings of this study are available from the corresponding author upon request.

## Conflicts of Interest

The author declares no competing interests.

## Acknowledgments

This work is supported by the Civil Aviation University of China.

## References

- [1] I. E. Sutherland, "The ultimate display," in *In Proceedings of the International Federation for Information Processing Congress*, pp. 506–508, New York, 1965.
- [2] L. Valmaggia, "The use of virtual reality in psychosis research and treatment," *World Psychiatry*, vol. 16, no. 3, pp. 246–247, 2017.
- [3] K. R. Walsh and S. D. Pawlowski, "Virtual reality: a technology in need of IS research," *Communications of the Association for Information Systems*, vol. 8, no. 20, pp. 297–313, 2002.
- [4] I. Wohlgenannt, A. Simons, and S. Stieglitz, "Virtual reality," *Business & Information Systems Engineering*, vol. 62, no. 5, pp. 455–461, 2020.
- [5] E. C. Park, S. G. Kim, and C. W. Lee, "The effects of virtual reality game exercise on balance and gait of the elderly," *Journal of Physical Therapy Science*, vol. 27, no. 4, pp. 1157–1159, 2015.
- [6] R. J. Segura, F. J. del Pino, C. J. Ogáyar, and A. J. Rueda, "VR-OCKS: a virtual reality game for learning the basic concepts of programming," *Computer Applications in Engineering Education*, vol. 28, no. 1, pp. 31–41, 2020.
- [7] J. Blaha and M. Gupta, "Diplopia: a virtual reality game designed to help amblyopsics," in *In IEEE Virtual Reality (VR)*, pp. 163–164, Minneapolis, MN, USA, 2014.
- [8] L. Katz, J. Parker, H. Tyreman, G. Kopp, R. Levy, and E. Chang, "Virtual reality in sport and wellness: promise and reality," *International Journal of Computer Science in Sport*, vol. 4, no. 1, pp. 4–16, 2006.
- [9] R. Kulpa, F. Multon, and F. Argelaguet, "Virtual reality & sport," in *In ISBS-Conference Proceedings Archive*, New York California Newport Beach, 2015.
- [10] S. Jones and S. Dawkins, "The sensorama revisited: evaluating the application of multi-sensory input on the sense of presence in 360-degree immersive film in virtual reality," in *In Augmented reality and virtual reality*, pp. 183–197, Springer, Cham, 2018.
- [11] D. L. Neumann, R. L. Moffitt, P. R. Thomas et al., "A systematic review of the application of interactive virtual reality to sport," *Virtual Reality*, vol. 22, no. 3, pp. 183–198, 2018.
- [12] M. C. Reyes and S. Zampolli, "Screenwriting framework for an interactive virtual reality film," in *In 3rd Immersive Research Network Conference*, Coimbra, Portugal, 2017.
- [13] C. D. Wickens, "Virtual reality and education," in *In IEEE International Conference on Systems, Man, and Cybernetics*, pp. 842–847, Chicago, IL, USA, 1992.
- [14] T. Hilfert and M. König, "Low-cost virtual reality environment for engineering and construction," *Visualization in Engineering*, vol. 4, no. 1, pp. 1–18, 2016.
- [15] J. M. Zheng, K. W. Chan, and I. Gibson, "Virtual reality," in *IEEE Potentials*, vol. 17, no. 2, pp. 20–23, 1998.
- [16] L. Freina and M. Ott, "A literature review on immersive virtual reality in education: state of the art and perspectives," in *In Proceedings of the 11th International Scientific Conference Elearning and Software for Education*, pp. 133–141, Bucharest, 2015.
- [17] M. J. Schuemie, P. Van Der Straaten, M. Krijn, and C. A. Van Der Mast, "Research on presence in virtual reality: a survey," *Cyberpsychology & Behavior*, vol. 4, no. 2, pp. 183–201, 2001.
- [18] J. L. van Gelder, M. Otte, and E. C. Luciano, "Using virtual reality in criminological research," *Crime Science*, vol. 3, no. 1, 2014.

- [19] J. Fox, D. Arena, and J. N. Bailenson, "Virtual reality," *Journal of Media Psychology*, vol. 21, no. 3, pp. 95–113, 2009.
- [20] J. M. Loomis, J. J. Blascovich, and A. C. Beall, "Immersive virtual environment technology as a basic research tool in psychology," *Behavior Research Methods, Instruments, & Computers*, vol. 31, no. 4, pp. 557–564, 1999.
- [21] B. G. Witmer and M. J. Singer, "Measuring presence in virtual environments: a presence questionnaire," *Presence*, vol. 7, no. 3, pp. 225–240, 1998.
- [22] D. Becker and A. Pentland, "Using a virtual environment to teach cancer patients to Tai Chi," in *In Proceedings of International Conference on Automatic Face and Gesture Recognition*, pp. 157–162, Killington, Vermont, 1996.
- [23] U. Y. Yang and G. J. Kim, "Implementation and evaluation of "just follow me": an immersive, VR-based, motion-training system," *Presence: Teleoperators and Virtual Environments*, vol. 11, no. 3, pp. 304–323, 2002.
- [24] S. Baek, S. Lee, and G. J. Kim, "Motion evaluation for VR-based motion training," *EUROGRAPHICS*, vol. 20, no. 3, pp. 1–10, 2001.
- [25] J. N. Meng, "College physical education teaching aided by virtual reality technology," *Mobile Information Systems*, vol. 2021, 11 pages, 2021.
- [26] W. L. Tsai, T. Y. Pan, and M. C. Hu, "Feasibility study on virtual reality based basketball tactic training," in *IEEE Transactions on Visualization and Computer Graphics*, 2020.
- [27] S. LaValle, E. Lesser, R. Shockley, M. S. Hopkins, and N. Kruschwitz, "Big data, analytics and the path from insights to value," *MIT Sloan Management Review*, vol. 52, no. 2, 2011.
- [28] A. McAfee, E. Brynjolfsson, T. H. Davenport, D. J. Patil, and D. Barton, "Big data: the management revolution," *Harvard Business Review*, vol. 90, no. 10, pp. 60–68, 2012.
- [29] N. Piercy, B. Nicoulaud, J. M. Rudd, and G. J. Hooley, *Marketing Strategy & Competitive Positioning*, Harlow: Pearson, 6th edition, 2017.

## Research Article

# Design of Knitted Garment Design Model Based on Mathematical Image Theory

**Bojia Lu** 

*Northeast Electric Power University, Jilin, China 132011*

Correspondence should be addressed to Bojia Lu; [luboija@neepu.edu.cn](mailto:luboija@neepu.edu.cn)

Received 8 January 2022; Revised 28 January 2022; Accepted 9 February 2022; Published 1 March 2022

Academic Editor: Wen Zeng

Copyright © 2022 Bojia Lu. This is an open access article distributed under the Creative Commons Attribution License, which permits unrestricted use, distribution, and reproduction in any medium, provided the original work is properly cited.

Iconology is an approach used by Western art theorists and art history researchers to explain plastic art and even relative to other various plastic art activities. This article is aimed at researching and discussing the design of knitted garment design model based on mathematical image theory. This article first discusses the application of digital image processing in the field of knitted clothing; digital image processing technology has a wide range of applications in the field of knitted clothing, including four aspects of fiber, yarn, fabric, and clothing, and proposes digital image filtering technology and digital image fuzzy filtering algorithm and then researches and analyzes the drape performance of knitted fabrics. Fabric drape is an important performance that reflects the beauty of the appearance of the fabric. The design of knitted garments is discussed based on mathematical imagery, and finally, the pressure performance of knitted garments is tested and analyzed. The experimental results in this paper show that the data correlation of the clothing pressure measured in different situations of the upper body is 0.87328, 0.779832, and 0.780213, respectively, under the plain weave, rib, and mesh fabric clothing fabrics. It shows that under the pressure of this degree of knitted clothing, it is in line with the needs of human healthy growth, because a certain degree of clothing pressure can maintain human physical and mental health and improve the quality of life.

## 1. Introduction

With the continuous development and growth of the economic level, as the top “clothing” of clothing, food, housing, and transportation, people not only wear clothing for shame but also choose clothing for the needs of beauty. People continue to advocate leisure, comfort, and sports in people’s lives. The knitwear industry has developed rapidly and has become a clothing category that has received much attention and welcome nowadays, and it is gradually developing in the direction of fashion and outerwear. At the same time, we apply new technologies, new processes and new materials to the design of knitted clothing to make it more comfortable and better performance. In modern daily life, knitted clothing has always been in a very important position and has become an indispensable clothing category in people’s lives. In order to better adapt to the development status of the domestic market, many knitwear brands have begun to reduce the rate of basic knitwear leaving the factory, and more of them are shifting their attention to the design concept with a sense of design. Nowa-

days in the knitwear industry, many companies pay much attention to the promotion of corporate culture in the process of sales planning, instead of starting from the starting point of innovative design and using the most primitive methods to achieve the most ideal goals. Nowadays, influential materials such as painting and computer production are increasing rapidly in society. This is the reason why popular visual culture such as iconography has replaced classical text culture as the dominant cultural trend. The innovative design of knitted garments can completely find their own inspiration in iconography and present the latest concepts and methods of the knitted garment industry with various innovative methods.

The principle of mathematical iconography is intuitive and visual. At present, the application of mathematical iconography in knitted garment design is still only in the extraction and application of the image pattern itself, and there is no related principle combined with knitted garment design. Most designers in the knitwear industry only use suitable image styles to directly apply images to the design of knitwear and even copy them in the selection of images, without designing

and deforming the image itself. It does not start from the brand culture of knitwear design and the design connotation of the design works and does not carry out comprehensive design nor does it carry out the deformation design of the image from the perspective of form, style, and meaning. Therefore, it does not fully reflect the true value of images in knitwear design works. Therefore, how to use the principles of mathematical iconography to design knitted garments and how to decompose, reorganize, and extract connotations of images are particularly important for knitted garment brands.

According to the research progress at home and abroad, different scholars also have a certain degree of cooperative research on mathematical image theory and knitted garment design model: Kunihiko et al. proved that self-perspiration used in evaporative cooling (SPEC) clothing can effectively reduce skin temperature without increasing the humidity in the clothing. However, the cooling effect will be delayed until a sufficient amount of water permeates and evaporates. In this study, Kunihiko et al. hypothesized that wearer-controlled vaporization can improve the cooling effect. This study shows that SPEC-W can effectively reduce skin temperature without increasing the humidity in clothing [1]. The purpose of Ramzan et al. is to study the influence of stitching parameters and washing type on the dimensional characteristics of knitwear. Different stitching parameters are used, including stitch density, stitch type, stitch thread, and washing type. The key measurement values of the selected garment are used as output variables, namely, body width, sleeve length, body length, and shoulder width. The shrinkage rate was calculated by using the measurement results before and after washing. Studies have shown that stitching parameters have a significant impact on the shrinkage of knitted fabrics. Therefore, when developing patterns for fabric cutting, the expected shrinkage rate, that is, the residual shrinkage rate, must be considered to avoid accidental changes in the shape of the garment [2]. Tsypliashchuk et al. evaluated the effectiveness and safety of the 2 types of compressed knitwear VENOTEKS TREND and used it for conservative and injection venous sclerosis treatments for patients with clinical C1-C3 chronic venous diseases of the lower extremities. The study included a total of 30 patients, with a compliance rate of 92%. The results show that the 2 types of compressed knitwear, VENOTEKS TREND, statistically significantly reduced the degree of subjective symptoms, and it is effective and safe to treat edema syndrome after conservative treatment and sclerotherapy [3]. With the help of newer technology and combined with the main characteristics of clothing design, Tang discussed the related history, appearance, and corresponding connotation of clothing design, conducted in-depth and scientific research and discussion, and provided a new idea [4]. Itoh et al. evaluated the effectiveness of dimensionality reduction method in calculating similarity in image pattern recognition through mathematical experiments. Image pattern recognition is used to identify instances of specific objects and distinguish differences between images. This recognition uses pattern recognition technology to classify images [5]. Barbeiro and Lobo studied the optimized partial differential equation (PDE) model for image filtering. The gray image is represented by the vector field of two real-valued functions, and the image restoration problem is modeled through the evolution process, so

that the restored image meets the cross initial boundary value problem at any time [6]. The purpose of Rajalakshmi and Prince's research is to develop a mathematical model of the retinal layer with a complex neural structure that can detect incoming signals and convert the signals into an equivalent peak sequence. The proposed retinal layer model includes a photoreceptor, an outer plexiform structure (OPL), an internal plexiform structure (IPL), and a ganglion cell layer. They exhibit the characteristics of compression, brightness, and spatial-temporal filtering in visual information processing [7]. However, these scholars did not conduct research and discussion on the design of knitted garment design models based on mathematical iconology, but only discussed its significance unilaterally.

The innovations of this article are mainly reflected in the following: (1) Firstly, the application of digital image processing in the field of knitted clothing is discussed, and digital image filtering technology and digital image fuzzy filtering algorithm are proposed. (2) Then, the drape performance of knitted fabric garments was researched and analyzed, and the drape performance of the fabric is an important performance reflecting the beauty of the appearance of the fabric. (3) The design of knitted garments is discussed based on mathematical image science, and finally, the pressure performance of knitted garments is tested and analyzed.

## 2. Design Research Method of Knitted Garment Design Model Based on Mathematical Image Theory

*2.1. The Application of Digital Image Processing in the Textile and Apparel Field.* The development of digital image processing is closely related to the development of digital computers [8], as shown in Figure 1, for digital image processing technology. In recent years, with the development of computer science, digital image processing science and technology has also made rapid progress, and its field has gradually expanded, and considerable progress has been made in theoretical research and practical engineering applications [9]. Digital image processing is a general technology, combined with specific disciplines which can get a variety of effective application results [10].

Since the 1970s, image processing technology has been applied to textile defect detection research work [11]. In the 1980s, foreign scholars began to use image processing methods to identify structural parameters such as the weave of woven fabrics. Digital image processing technology is widely used in the field of textiles and clothing, which can include four aspects: fiber, yarn, fabric, and clothing:

- (1) The application in fiber is mainly reflected in the surface characteristic test of the fiber, such as the appearance and shape of the fiber, the fiber fineness, the measurement of the balance of the cotton web, and the measurement of the fiber profile rate [12]
- (2) The main application focus in yarn testing is yarn mixing state, yarn blending ratio test, and yarn appearance quality test



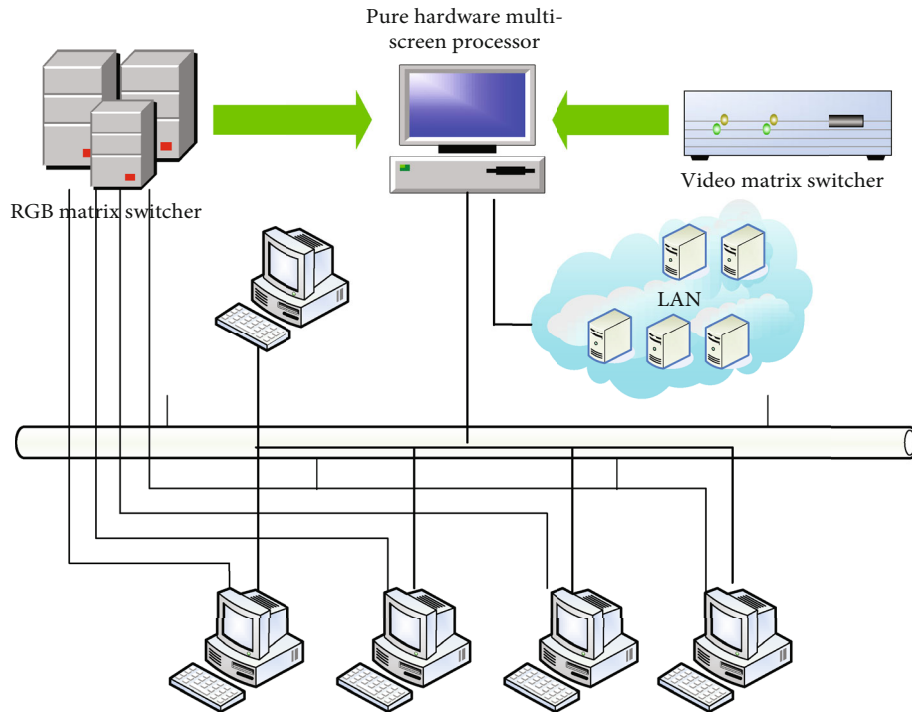


FIGURE 1: Digital image processing technology.

- (3) There are many applications in fabrics, including the surface quality of fabrics, such as fabric defect inspection, pilling analysis, fabric flatness evaluation, fabric wrinkle analysis, and other applications. The monitoring of fabric specifications mainly includes automatic monitoring of fabric warp and weft density and automatic identification of fabric structure and fabric performance detection such as automatic detection of fabric moisture permeability and objective evaluation of fabric drape performance [13]
- (4) The applications in clothing mainly include automatic measurement of control data of various parts of the three-dimensional human body, evaluation of clothing folds, and evaluation of clothing modeling [14]. Figure 2 shows the application of digital image processing technology in the textile and apparel field

In short, the combination of digital image processing technology and the textile and apparel field has greatly promoted the development of the textile industry, improved the traditional manual operation process in textile inspection, and promoted the automated process of textile inspection. It greatly improves work efficiency and solves many problems in textile testing technology from a novel perspective. It is a major change in the textile and apparel field.

**2.2. Digital Image Filtering Technology.** The processing of digital images usually starts with picture preprocessing. Filtering and restoring images is also a main content in the field of image preprocessing. Because image filtering is the most basic and critical research content in computer vision, it is the core technology for successfully realizing boundary

extraction, image classification, image understanding, and image description. Therefore, the quality of image filtering will directly affect the postprocessing [15]. In simple terms, image filtering technology is a technology that sets an appropriate filter algorithm for image information contaminated by noise, so that the image information output by the filter can finally be close to the original image information. Image filtering is to filter out the image noise while preserving the details of the image as much as possible. However, there are great similarities between the noise and the details of the image. These similarities make filtering noise and preserving details form an inherent conflict. Traditional image filtering algorithms are difficult to resolve such an inherent conflict [16]. At present, the mean filtering algorithm and the median filtering algorithm are the two most common filtering algorithms in the image filtering field, and they can have various filtering characteristics for various types of noise. The image is always contaminated by noise, and noise can appear in the process of acquiring the image, even in the propagation stage of the image, or in the reproduction stage of the image [17]. In image processing, eliminating noise in the image is the most critical task [18]. It can be understood as “a variety of reasons that prevent the human visual physiology organs or system sensors from understanding or studying the information of the image source they are touching” and usually refers to unpredictable random signals. Therefore, the way of expressing noise can completely rely on the expression of stochastic process, such as the way of calculating with probability method [19].

- (1) Impulse noise model's mathematical description is as follows:

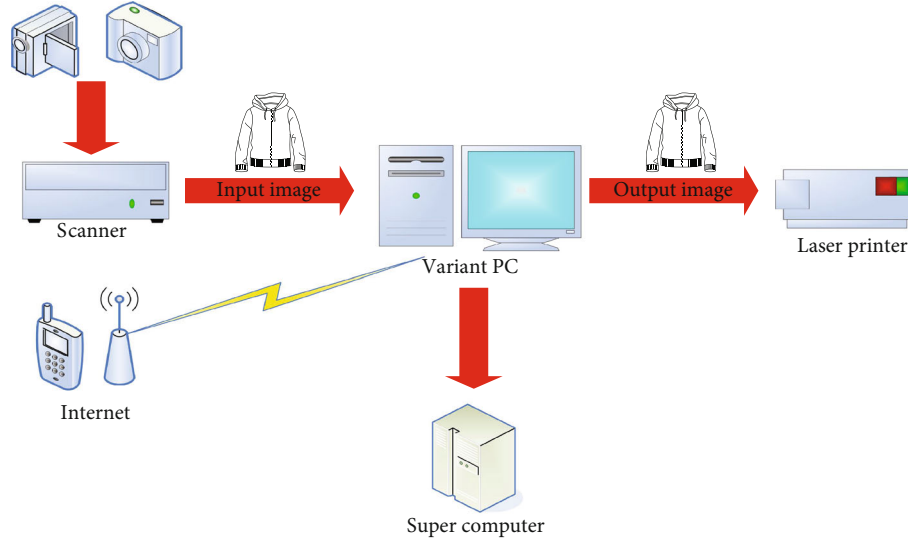


FIGURE 2: Application of digital image processing technology in the field of textile and clothing.

$$m(a, b) = \begin{cases} n(a, b); 1 - l_d, \\ \varphi(a, b); l_d. \end{cases} \quad (1)$$

Among them,  $n(a, b)$  and  $m(a, b)$ , respectively, represent the pixel gray scale value at  $(a, b)$  in the original image and the noise image,  $\varphi(a, b)$  represents the distribution of the signal-to-noise ratio, and  $l_d$  represents the distribution density of the original noise.

The density function of impulse noise can be given by the following:

$$l(k) = \begin{cases} l_u, & k = u, \\ l_v, & k = v, \\ 0, & \text{others.} \end{cases} \quad (2)$$

(2) Gaussian noise model's mathematical description is as follows:

$j(m, n) = s(m, n) + t(m, n)$ , where  $j(m, n)$  means that the original image function  $s(m, n)$  adds the effect of Gaussian noise  $t(m, n)$  pollution, as shown in Figure 3.

The probability density function of Gaussian noise can be given by the following:

$$l(k) = \frac{1}{\sqrt{2\pi}\delta} e^{-\frac{(k-u)^2}{2\delta^2}}. \quad (3)$$

There are generally two types of characteristic evaluations of image quality and image filtering effects: one is subjective evaluation method and the other is object evaluation method. The subjective evaluation method is largely affected by the observer's mentality and the external environment, so it is difficult to implement [20]. The objective evaluation

method is generally a method of evaluating the effect of image processing by using some statistically measured indicators and describing the curve that can reflect the characteristics of image processing itself. It can generally reflect the grayscale difference between the original image processing and the restored image. The most important features are the peak signal-to-noise ratio, mean square error, relative average absolute error, and normalized mean square error contribution rate. The main evaluation criteria of the objective evaluation method include the following:

(1) Peak signal-to-noise ratio is mathematically described as follows:

$$P = 10 \lg_{10} \frac{255^2}{\sum_{a=1}^{R_1} \sum_{a=1}^{R_2} [n(a, b) - m(a, b)]^2 / R_1 * R_2}. \quad (4)$$

(2) Mean square error's mathematical description is as follows:

$$M = \frac{\sum_{a=1}^{R_1} \sum_{a=1}^{R_2} [n(a, b) - m(a, b)]^2}{R_1 * R_2}. \quad (5)$$

(3) The relative average absolute error is described mathematically as follows:

$$A = \frac{\sum_{a=1}^{R_1} \sum_{a=1}^{R_2} |n(a, b) - m(a, b)|}{\sum_{a=1}^{R_1} \sum_{a=1}^{R_2} m(a, b)}. \quad (6)$$

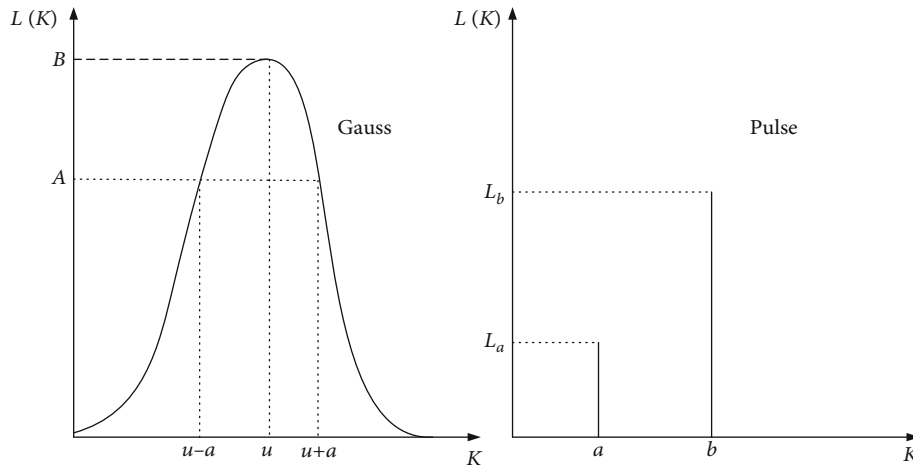


FIGURE 3: Gaussian pulse image.

(4) Normalized mean square error's mathematical description is as follows:

$$N = \frac{\sum_{a=1}^{R_1} \sum_{a=1}^{R_2} [n(a, b) - m(a, b)]^2}{\sum_{a=1}^{R_1} \sum_{a=1}^{R_2} m(a, b)^2}, \quad (7)$$

where  $n(a, b)$  and  $m(a, b)$ , respectively, represent the gray value of the filtered image and the gray value of the original image, and the image size is  $R_1 * R_2$ .

Usually in image processing, the peak signal-to-noise ratio and the average variance are used as the main indicators for the objective evaluation of the image.

**2.3. Digital Image Fuzzy Filtering Algorithm.** In the process of digital image processing, the earliest important data processing technique is the traditional filter processing algorithm such as linear filtering algorithm, because it can better deal with Gaussian noise. But once there is an additional noise in the signal processing, the data processing results become more common. Later, some nonlinear filtering algorithms were produced, which organically integrated statistical theory and made great progress. They can control impulse noise more effectively, but the effect of eliminating Gaussian noise is not outstanding. Later, due to the development of fuzzy technology and the deepening of scientific research, many researchers tried to merge the related theories of fuzzy mathematics with conventional filtering algorithms, resulting in several new filtering algorithms.

Due to the introduction of fuzzy technology in the image filter, many researchers have merged the traditional median filter algorithm with the fuzzy technology, resulting in a variety of dim median filter algorithms. Among them, this algorithm does not use the same method for all images. First, the fuzzy method is used to determine the degree of noise pollution of each pixel in the image, and then, the median filter calculation is changed according to the obtained value. The basic idea is as follows:

If an image is determined to be uncontaminated, the output image value is less than the input image value. If an image is judged to be a contaminated image, the image is replaced by the weighted sum of the input image value and

the output value calculated by traditional median filtering. Assuming that the greater the degree to which the pixel belongs to the noise, the greater the weighting coefficient of the traditional median filter calculation. The output pixel value of this calculation can be described as follows:

$$M(a, b) = (1 - s(a, b))k(a, b) + s(a, b)m(a, b), \quad (8)$$

$$E = \sum_T y(a, b).$$

Among them,  $m(a, b)$  represents the gray value of the pixel where the noise image  $(a, b)$  is located,  $M(a, b)$  represents the gray value of the output image,  $k(a, b)$  is the standard output of the traditional median filter algorithm, and  $s(a, b)$  represents the severity of the noise in the image. If  $s(a, b) = 1$ , it means that the image is completely uncontaminated. If  $s(a, b) = 0$ , it means that the image is completely noisy.

If the value of  $s(a, b)$  is between 0 and 1, it can be obtained by the following fuzzy rules:

- (i) If  $s(a, b)$  is small and  $t(a, b)$  is small, then  $s(a, b)$  is large
- (ii) If  $s(a, b)$  is small and  $t(a, b)$  is large, then  $s(a, b)$  is small
- (iii) If  $s(a, b)$  is large and  $t(a, b)$  is small, then  $s(a, b)$  is small
- (iv) If  $s(a, b)$  is large and  $t(a, b)$  is large, then  $s(a, b)$  is very large

Among them,

$$s(a, b) = |m(a, b) - k(a, b)|,$$

$$t(a, b) = \frac{|D(a, b) - w_1| + |D(a, b) - w_2|}{2}, \quad (9)$$

where  $w_1$  and  $w_2$ , respectively, represent the pixels closest to  $m(a, b)$  in the filter window. Small, large, and very large can

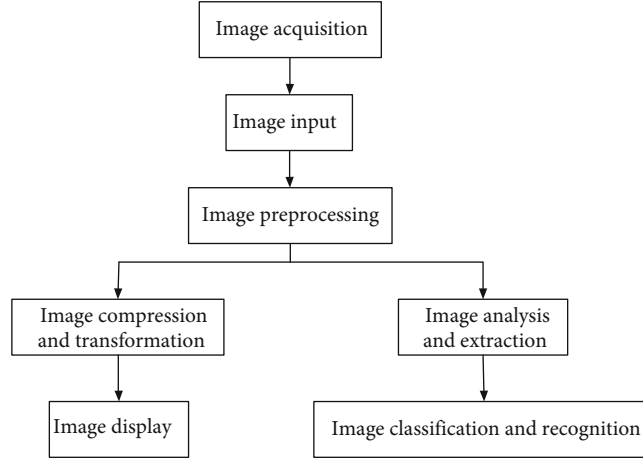


FIGURE 4: Research content of image processing technology.

TABLE 1: Fabric drape test results 1.

Serial number	Static drape coefficient (%)	Wavenumber (N)	Peak amplitude uniformity (%)	Uniformity of included angle of wave crest (%)	Dynamic drape coefficient ratio	Maximum peak amplitude (mm)	Minimum peak amplitude (mm)
Number 1	45.02	5	3.01	12.98	1.31	47.11	37.09
Number 2	49.79	7	2.98	19.79	1.29	47.03	38.02
Number 3	57.89	6	1.97	17.11	1.21	48.69	39.98
Number 4	52.01	6	2.78	14.03	1.09	46.98	40.12
Number 5	50.99	5	2.19	14.79	1.32	48.96	42.03
Number 6	52.05	6	6.02	19.89	1.19	49.02	30.18

be used to represent the fuzzy ensemble of all input variables, and an appropriate membership function method can also be selected to represent it.

The noise membership degree  $m(a, b)$  of the pixel can be determined by the following formula:

$$s_{x,y} = \frac{\sum_{(a,b) \in R_{x,y}} |m(a, b) - k(a, b)| * |c(a, b) - k(a, b)|}{\sum_{(a,b) \in R_{x,y}} |m(a, b) - k(a, b)|^2},$$

$$d = - \sum_{n=0}^H q(x_n) \log_2 q(x_n),$$
(10)

where  $c$  represents the desired output image and  $m$  represents the training image.

In addition, the basic idea of a fuzzy median filter algorithm is to project the image from the spatial domain to the fuzzy domain, define a local contrast operator in the fuzzy domain, filter in the fuzzy area, and then perform the inverse transformation. The specific ideas are as follows:

- (1) First calculate the fuzzy contrast of pixel  $m(a, b)$ :

$$G = \frac{|s_{a,b} - \bar{s}_{a,b}|}{\bar{s}_{a,b}},$$

$$T = \sum_{n=0}^H q^2(x_n),$$

(11)

where  $s_{a,b}$  represents the attribution degree of pixel  $m(a, b)$ ,  $\bar{s}_{a,b}$  represents the average attribution degree of its neighborhood, and  $G$  represents the corresponding blur contrast after normalization.

- (2) Selecting the linear membership function for  $s_{a,b}$  calculation in the above formula:

$$s_{a,b} = \gamma(m_{a,b}) = \frac{m_{a,b} - m_{\min}}{m_{\max} - m_{\min}},$$
(12)

TABLE 2: Fabric drape test results 2.

Serial number	Static drape coefficient (%)	Wavenumber (N)	Peak amplitude uniformity (%)	Uniformity of included angle of wave crest (%)	Dynamic drape coefficient ratio	Maximum peak amplitude (mm)	Minimum peak amplitude (mm)
Number 7	51.21	6	2.71	16.19	1.24	46.99	38.79
Number 8	44.01	6	2.59	16.49	1.41	44.02	36.02
Number 9	50.03	6	2.68	17.61	1.31	47.03	39.23
Number 10	49.12	6	2.72	19.02	1.34	47.69	40.41
Number 11	41.05	6	2.49	8.98	1.39	43.98	37.02
Number 12	51.08	6	3.31	14.59	1.23	47.95	38.21

where  $m_{\max}$  and  $m_{\min}$  represent the maximum gray scale and minimum gray scale of the image.

(3) Nonlinear transformation of  $G$ :

$$G^i = \psi(G). \quad (13)$$

Among them, the exponential function is selected:

$$\psi(m) = \frac{1 - c^{-lm}}{1 - c^{-l}}. \quad (14)$$

(4) Perform median filtering on the ambiguity  $G^i$  after convex transformation to obtain the filtered ambiguity  $G^j$ , and then calculate the adjusted pixel membership  $\hat{s}_{a,b}^i$  through  $G^j$ :

$$\hat{s}_{a,b}^i = \begin{cases} \frac{\bar{s}_{a,b}(1 - G^j)}{1 + G^j}, & s_{a,b} \leq \bar{s}_{a,b}, \\ 1 - \frac{(1 - \bar{s}_{a,b})(1 - G^j)}{1 + G^j}, & s_{a,b} > \bar{s}_{a,b}. \end{cases} \quad (15)$$

(5) Finally, calculating its corresponding gray value  $m_{a,b}^i$

$$m_{a,b}^i = \hat{s}_{a,b}^i(m_{\max} - m_{\min}) + m_{\min}. \quad (16)$$

For the actual image processing process, since the image is usually affected by the two kinds of noises, the denoising efficiency cannot be optimized simply by using any filter. If we can find a way to distinguish the images contaminated by impulse noise and Gaussian noise, then choose completely different filtering methods for the images con-

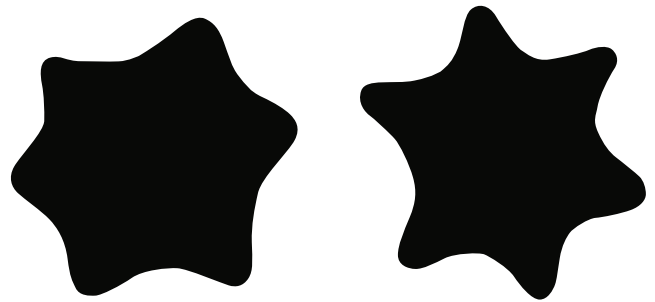


FIGURE 5: Comparison of the drape morphology of fabric no. 3 and fabric no. 11.

taminated by various noise environments. In theory, a better filtering effect will be obtained. Therefore, how to design a filtering algorithm to reduce the impact of mixed noise environmental pollution in practice has more practical values. The image processing process is shown in Figure 4

### 3. Experimental Results of Design Research on Knitted Garment Design Model Based on Mathematical Image Theory

3.1. *Drape Performance of Knitted Fabric Garments.* The drape of the fabric is an important performance reflecting the beauty of the appearance of the fabric and an important feature of the visual style of the fabric. It is particularly important for skirts. It is an important indicator for evaluating the aesthetics and comfort of the shape and directly affects the appearance of the skirt. The fabric sags due to its own weight in the natural drape state, which can form a soft, smooth, and uniform curvature surface, which is called the drape performance of the fabric. The static drape coefficient is the most common index to express the drape characteristics of the fabric. The smaller the static drape coefficient, the better the drape characteristics of the fabric, and vice versa. However, the static drape coefficient does not fully represent the drape form of the fabric, and most of the clothing worn on the human body are in a state of motion. In

TABLE 3: Uniformity indicator extraction results.

Serial number	Standard deviation of crest radius	Standard deviation of trough radius	Standard deviation of crest angle	Standard deviation of valley angle
Number 1	1.59	1.98	12.09	12.61
Number 2	1.58	1.58	5.82	8.31
Number 3	0.98	1.69	9.76	9.89
Number 4	1.79	2.08	8.21	10.43
Number 5	1.78	2.18	9.81	13.89
Number 6	1.19	1.87	10.02	11.78
Number 7	1.23	1.68	13.01	12.98
Number 8	1.51	1.82	11.39	12.69
Number 9	1.82	1.92	11.98	12.79
Number 10	1.64	1.68	10.02	16.02
Number 11	1.38	1.79	9.42	10.89
Number 12	1.73	1.58	8.02	11.99

TABLE 4: Nine experimental measuring points.

Numbering	Human body position	Numbering	Human body position	Numbering	Human body position
1	Front center of the waist	4	Center of the anterior abdominal wall	7	Mid-chest position
2	Left side of the waist	5	Left position of the anterior abdominal wall	8	Left side of the chest
3	Right side of the waist	6	Right position of the anterior abdominal wall	9	Right side of the chest

recent years, with the deepening of research, more and more attention has been paid to the beauty of the dynamic dress form of clothing, and this problem is more prominent for light and thin fabrics. Considering that the drape form of the fabric is of great significance, the XDP-1 fabric drape performance testing machine can be used to test the dynamic and static drape characteristics of the fabric.

The XDP-1 fabric drape characteristics' tester is a new type of test instrument designed by Shanghai Xinxian Instrument Equipment Co., Ltd. according to the FZ/T01045-1996 test specification. It uses image processing technology to measure the static and dynamic drape characteristics of the fabric. The structure is precise, and the operation is simple. It only needs to place the sample and use the mouse to control the "up," "down," and "test" buttons, and then, the computer can output and print the test results. Applied to the drape performance test of different fabrics, a number of performance indicators can be detected, mainly including the drape basic technical indicators and the drape auxiliary technical indicators. The basic indicators are divided into drape coefficient, wavenumber, average degree of peak amplitude, crest angle balance, and dynamic and static drape coefficient percentages. The auxiliary index is divided into the highest peak amplitude and the least peak amplitude. Among them, the measurement error of the drape coefficient is  $\leq \pm 1\%$ , which can more comprehensively reflect the drape characteristics of the fabric and help to make an objective evaluation of the wearability of the fabric. Among them, Table 1 and Table 2 are the test results of fabric drape.

It can be concluded from the statistical principle of static drape coefficient that the smaller the static drape coefficient,

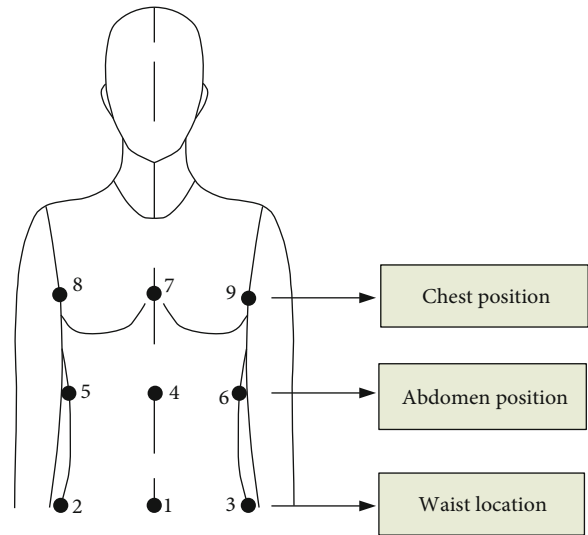


FIGURE 6: Distribution of pressure measurement points.

the better the drape characteristics of the fabric, and vice versa. According to the fabric drape test results in Table 1 and Table 2, it can be known that the static drape coefficient of fabric no. 3 is the highest, but the drape is poor, and the fabric is relatively stiff, which is not consistent with the drape projection shape. The static drape coefficient of no. 11 fabric is very small, the drape performance is good, the fabric is delicate, and the drape projection shape is uniform and natural. The comparison diagram of the two drape shapes is shown in Figure 5. The wave function reflects the number of bending of the fabric in the free drape state and

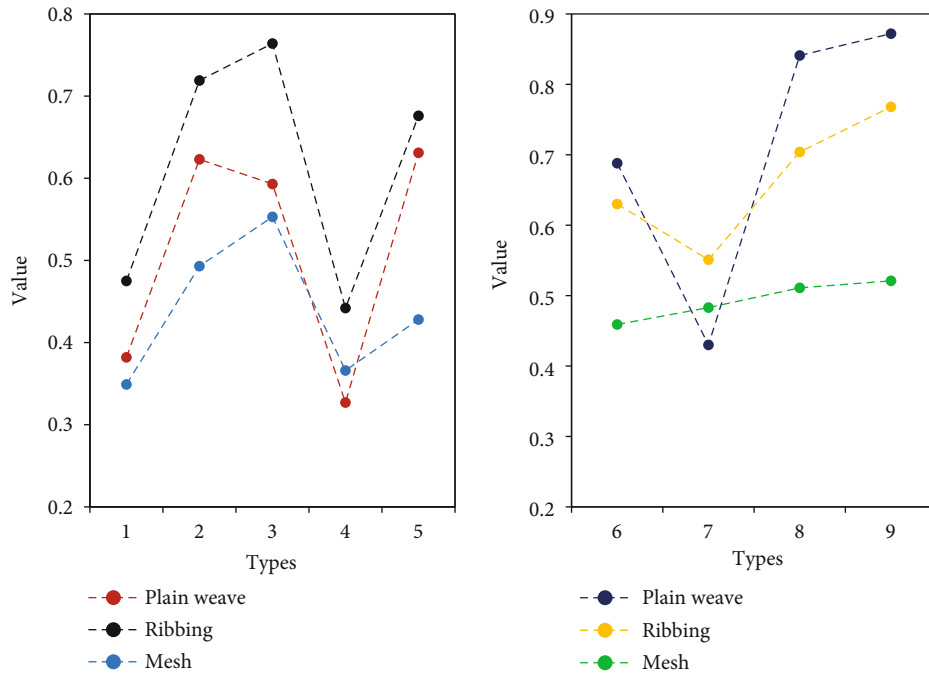


FIGURE 7: Clothing pressure value at each point (unit: kPa).

is one of the key parameters of the drape shape. Since the selected fabrics are light and thin woolen fabrics, there is a little difference in fabric characteristics. Knowing from the above discussion, the pendant wavenumber range of the selected sample is about 5-7. Among them, fabric no. 1 has the least number of dangling waves, which is five, while fabric no. 2 has the most dangling waves, which is seven. Technical indicators such as uniformity of wave crest amplitude and uniformity of included angle of wave crests show the drape form of the fabric in different viewing angles.

**3.2. Design of Knitted Garments Based on Mathematical Iconography.** The progress of computer and graphic information technology has laid a good foundation for obtaining objective measurement indicators of modern clothing modeling and created many effective methods, such as 3D scanning technology, computer simulation technology, and image processing technology. Clothing modeling includes external contour modeling and internal shape. We focus on the classification of the external contour shape of miniskirts. The objective shape evaluation index of clothing is refined through image processing technology, so first of all, it is necessary to expand the picture collection of the outer shape of the miniskirt.

Image acquisition technology is a key issue in image processing. The quality of image acquisition technology directly determines the quality of image levels and variable characteristic values. This article mainly uses photography to collect pictures on the outer shape of the miniskirt and requires that photography should be started when the indoor and outdoor natural light conditions are sufficient and the temperature is relatively stable; before each shooting, put the miniskirt on the human platform. After positioning the human platform, it rotates three times in the

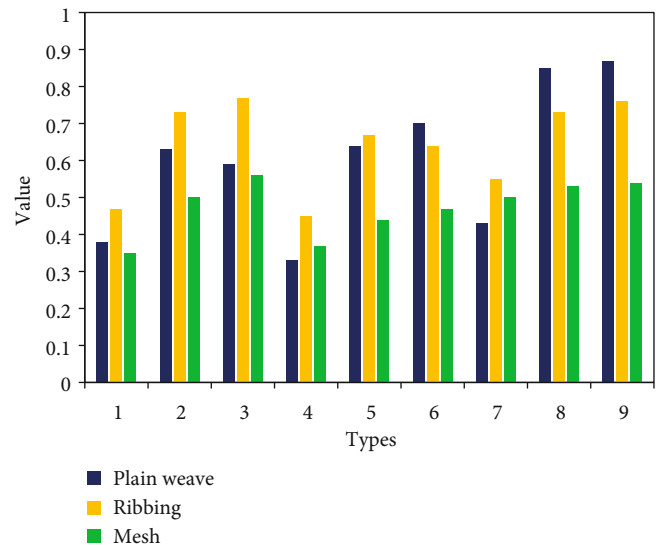


FIGURE 8: Clothing pressure values of different fabrics at different positions.

clockwise and counterclockwise directions of the hands, and after standing for about 3-5 minutes, all the skirts are attached to the human platform under the condition of automatic hanging and no dead ends, and the distance between the camera and the human platform is kept constant. The control parameters of the camera are kept unchanged at a fixed time parameter value, so as to avoid the deviation of the image collection of the appearance shape of the skirt caused by human factors and avoid the negative impact on the objective evaluation of the miniskirt. The shooting angle mainly includes the front, side, and bottom of the skirt. When shooting the bottom, the platform should

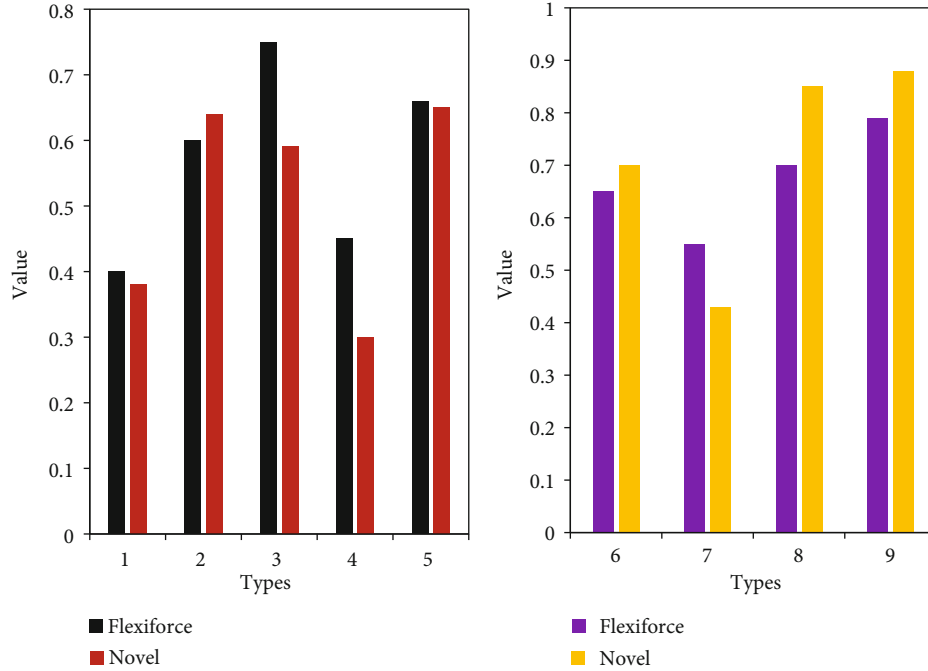


FIGURE 9: Comparison of the strength of the plain weave at various positions.

be placed vertically and hung together, and the photo should be taken from directly below the platform.

The standard deviation of crest radius, the standard deviation of trough radius, the standard deviation of crest included angle, and the standard deviation of trough angle selected in this article all consider the uniformity of related indexes from a mathematical point of view. The smaller the value of the standard deviation, the less obvious the change of its related index, which can indicate that the amplitude of the wave crest or trough radius and the wave crest or trough angle is smaller. This means that the more uniform the wave shape of the miniskirt is, the more beautiful the outer shape of the skirt. On the contrary, the more uneven the wave shape, the less beautiful the outer shape of the skirt. The test method is the formula calculation method that comes with the Excel spreadsheet, and the calculation results are shown in Table 3.

**3.3. Knitwear Pressure Performance Test Analysis.** With the continuous deepening of clothing pressure research, the research results related to the current stage of clothing pressure not only involve professional research results related to clothing fabrics but also involve other professional research content such as medical and health, sports science, and psychology. In the process of product design and manufacturing of clothing, not only the influence of wearing pressure is fully considered but also certain medical and health care wearing pressure functions and sports comfort are considered. And according to the most comfortable value of wearing pressure in various parts of the body, making the most optimal wearing pressure setting will greatly improve the wearing performance of the clothing, thereby enhancing the overall competitiveness of the apparel industry. On the

TABLE 5: Correlation analysis of the measured data of the two systems in the case of plain weave fabrics.

	Position (1-9)	FlexiForce	Novel
Position (1-9)	1	—	—
FlexiForce	0.55783	1	—
Novel	0.62987	0.87328	1

basis of the stress test system, we conducted an in-depth study on the clothing pressure changes of traditional knitted apparel and proposed the law of the air pressure distribution change of the upper body of the male human body under specific conditions. The novel pliance-x-32 clothing pressure measurement system is used to achieve clothing pressure measurement, which can grasp the objective measurement method of clothing pressure, the distribution of clothing pressure on parts of the human body, and the comfort characteristics of clothing pressure on the human body. At the same time, the novel pliance-x-32 pressure measurement system is used for objective clothing pressure measurement of the human body. The measurement preparation requirements are consistent with those of the FlexiForce sensor pressure measurement system. It is compared with the average value of the clothing air pressure of different parts of the upper body of the male human body obtained by the two pressure measurement systems, and the law of the distribution of the air pressure of the upper body of the male human body under certain conditions is obtained.

The clothing used in the measurement in this paper is mainly knitted seamless underwear, which is more in the market. The clothing fabric is mainly composed of cotton and ammonia, and certain physical properties of the clothing fabric have been tested. The fabric organization of the



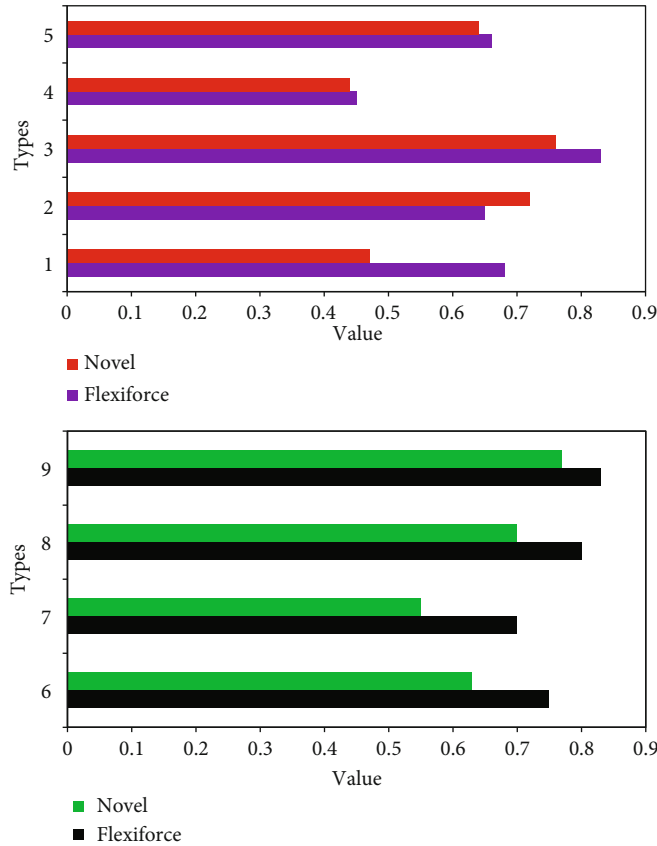


FIGURE 10: Comparison of the strength of rib tissue at various positions.

clothing mainly uses plain weave, rib weave, and mesh organization, and the fabric composition is 92% cotton and 8% spandex. The measurement position of clothing pressure mainly chooses the upper body of male human body, mainly chooses the position with relatively large pressure value, and selects 9 test positions for clothing pressure as shown in Table 4. The measurement positions are indicated by 1, 2, 3, 4, 5, 6, 7, 8, and 9, respectively.

Of the 9 selected points, points 1, 2, and 3 are on the waist and are on the same horizontal line; points 4, 5, and 6 are on the abdomen, and the three points are on the same horizontal line; points 7, 8, and 9 are on the same horizontal plane of the chest, and the distribution is shown in Figure 6.

Novel pliance-x-32 test system records clothing pressure data every 0.1 s during the measurement process, and the data of each part is measured for 30 s, and the measurement is kept standing, and the measurement results are saved in word form. The saved result has a total of 60 sets of data, except the highest value and the lowest value, and the average remaining pressure value is the measured value. The clothing pressure value of each measurement point is the average value of 5 testers at the test point, and the measurement result is shown in Figure 7. The measurement locations are represented by locations 1, 2, 3, 4, 5, 6, 7, 8, and 9.

The average pressure value measured at each location is shown in Figure 8. Although the clothing pressure value tested by the novel pliance-x-32 test system is different at each location, the pressure distribution law is basically the

TABLE 6: Correlation analysis of the data measured by the two systems under ribbed fabrics.

	Position (1-9)	FlexiForce	Novel
Position (1-9)	1	—	—
FlexiForce	0.379821	1	—
Novel	0.3298453	0.779832	1

same as the law obtained above. It can be seen from Figure 8 that, in general, the compression value of the clothes in the middle of the human body is generally smaller than that of the clothes on both sides. However, the compression value of the clothes formed by the rib weave on all parts of the human body exceeds the compression value of the clothes formed by the plain weave fabric. In the areas on both sides of the human chest, the clothes formed by the plain weave fabric are most stressed, and the clothes formed by the mesh tissue are usually relatively small.

Comparing the measurement data of the above two clothing pressure measurement systems can be obtained:

- (1) The pressure comparison of the test system under plain weave fabrics is shown in Figure 9

Through the correlation analysis of the two sets of data, the correlation of the measured data of the two systems as shown in Table 5 can be obtained.

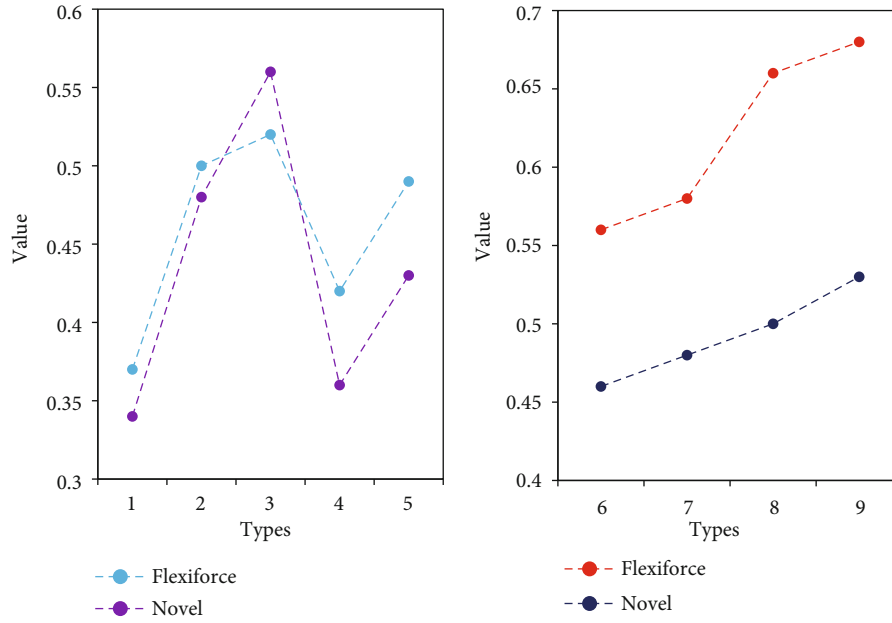


FIGURE 11: Comparison of the strength and small pressure of the mesh tissue at various positions.

It can be obtained from Table 5 that in the garment pressure measurement process of plain weave fabric, the correlation of the data measured by the two pressure measurement systems is 0.87328.

- (2) The pressure comparison of the test system under the rib weave garment fabric is shown in Figure 10.

Through the correlation analysis of the two sets of data, the correlation of the measured data of the two systems as shown in Table 6 can be obtained.

It can be obtained from Table 6 that in the garment pressure measurement process of the rib fabric, the correlation of the data measured by the two pressure measurement systems is 0.779832.

- (3) The pressure comparison of the test system under mesh fabrics is shown in Figure 11.

Through the correlation analysis of the two sets of data, the correlation of the measured data of the two systems as shown in Table 7 can be obtained.

It can be obtained from Table 7 that in the clothing pressure measurement process of the mesh fabric, the correlation of the data measured by the two pressure measurement systems is 0.780213.

#### 4. Discussion

Reasonable clothing pressure will also have a positive effect on human physiological health care. Therefore, the study of clothing pressure has increasingly become a major issue in the clothing industry. Under the influence of a certain degree of clothing pressure, it is an important reason for maintaining human physical and mental health and improv-

TABLE 7: Correlation analysis of the data measured by the two systems under the mesh fabric.

	Position (1-9)	FlexiForce	Novel
Position (1-9)	1	—	—
FlexiForce	0.893216	1	—
Novel	0.449762	0.780213	1

ing the quality of life. The fast and accurate objective measurement of clothing pressure is of great significance to the scientific research of clothing pressure, and it is also a key subject of the current scientific research of clothing pressure. In the analysis of the pressure performance measurement system for knitted garments, under the plain weave fabric, in the novel pliance-x-32 pressure measuring system and the FlexiForce pressure measuring system, the data correlation of the clothing pressure measured on different conditions of the upper body is 0.87328. Under the rib-woven garment fabric, the novel pliance-x-32 air pressure measurement system and the FlexiForce air pressure measurement system are on different parts of the upper body, and the data correlation of the measured clothing pressure is 0.779832. Under mesh fabrics, the novel pliance-x-32 air pressure measurement system and FlexiForce air pressure measurement system are on different parts of the upper body, and the data correlation of the measured clothing pressure is 0.780213. The results show that under the pressure of this degree of knitted garments, it is in line with people's healthy growth needs.

#### 5. Conclusions

Taking into account the drape characteristics of the fabric as the main aspect that affects the beauty of the fabric, it also

has a very important impact on the outer shape of the miniskirt. Therefore, this paper selects XDP-1 fabric that can express the drape characteristics of the fabric from a variety of perspectives, and the dynamic and static drape characteristics' tester detects the drape characteristics of the sample. The main measurement indicators are divided into dynamic and static drape coefficient, wavenumber, peak amplitude balance, peak angle balance, dynamic and static drape coefficient ratio, highest peak amplitude, and minimum peak amplitude, and the test results are recorded in a standardized manner. Using the camera method to collect pictures of the appearance of the miniskirt, the appearance of the miniskirt is converted into a digital image value and then use the comparative research data analysis results of the literature and select the corresponding objective evaluation index of the styling characteristics on the front, side, middle, and bottom of the miniskirt in turn. From a mathematical point of view, the calculation formulas of each index are determined, and these indexes are digitally extracted using image processing. With the improvement of people's living standards, people are paying more and more attention to the personalized and fashionable dress. The application of unconventional pleats, drape, exaggeration, and other design techniques has increased the fun and fashion of clothing modeling; at the same time, complex and simple styles of clothing coexist with diversification. Therefore, the use of modern technology such as digital image processing to study the relationship between the mechanical properties of fabrics and unconventional clothing styles and diversified styles can also be used as a future research direction.

### Data Availability

The data used to support the findings of this study are available from the corresponding author upon request.

### Conflicts of Interest

The author declares no conflicts of interest.

### Acknowledgments

This research study is sponsored by "Textile light" research project on higher education teaching reform of China Textile Industry Federation. The name of the project is Research on the Construction of Fashion Design Courses in the Context of "New Liberal Arts." The project number is 2021BKJGLX471. Thanks are due to the project for supporting this article!

### References

- [1] T. Kuniyoshi, N. Daiki, O. Kosuke, and K. Nakamura, "Cooling effects of wearer-controlled vaporization for extravehicular activity," *Aerospace Medicine and Human Performance*, 2017.
- [2] M. B. Ramzan, A. Rasheed, Z. Ali, S. Ahmad, M. S. Naeem, and A. Afzal, "Impact of wash types and stitching parameters on shrinkage of knitwear made from pique fabric," *International Journal of Clothing Science & Technology*, vol. 31, no. 2, pp. 232–242, 2019.
- [3] A. V. Tsypliyshchuk, I. M. Stoko, S. E. Kharitonova, E. S. Vunder, and D. M. Mamadaliev, "Compression knitwear VENOTEKS TREND in treatment of patients with chronic venous diseases of the lower limbs," *Angiologija i Sosudistaiia Khirurgija= Angiology and Vascular Surgery*, vol. 23, no. 3, pp. 167–171, 2017.
- [4] J. Tang, "A retracted article: agricultural climate change based on remote sensing images and fashion design innovation," *Arabian Journal of Geosciences*, vol. 14, no. 11, pp. 1–16, 2021.
- [5] H. Itoh, A. Imiya, and T. Sakai, "Dimension reduction and construction of feature space for image pattern recognition," *Journal of Mathematical Imaging and Vision*, vol. 56, no. 1, pp. 1–31, 2016.
- [6] S. Barbeiro and D. Lobo, "Learning stable nonlinear cross-diffusion models for image restoration," *Journal of Mathematical Imaging and Vision*, vol. 62, no. 2, pp. 223–237, 2020.
- [7] T. Rajalakshmi and S. Prince, "Study of a retinal layer model to generate a spike waveform for a color deficient and strabismus individual," *Biomedizinische Technik*, vol. 64, no. 3, pp. 285–295, 2019.
- [8] O. Y. Gorokhova, "Design principles for knitted items with bicomponent cloths," *Fibre Chemistry*, vol. 48, no. 4, pp. 339–341, 2016.
- [9] A. Soroudi, N. Hernández, J. Wipenmyr, and V. Nierstrasz, "Surface modification of textile electrodes to improve electrocardiography signals in wearable smart garment," *Journal of Materials Science: Materials in Electronics*, vol. 30, no. 17, pp. 16666–16675, 2019.
- [10] A. R. Gover, E. Latini, and A. Waldron, "Metric projective geometry, BGG detour complexes and partially massless gauge theories," *Communications in Mathematical Physics*, vol. 341, no. 2, pp. 667–697, 2016.
- [11] K. C. Ciesielski, G. T. Herman, and T. Y. Kong, "General theory of fuzzy connectedness segmentations," *Journal of Mathematical Imaging and Vision*, vol. 55, no. 3, pp. 304–342, 2016.
- [12] K. Nuthall, "EU knitwear sector faces risk of steep US tariffs," *Knitting International*, vol. 125, no. 3, pp. 28–29, 2019.
- [13] F. Lazina, "Far East Knitting, a name to reckon in knitwear industry," *The Textile Magazine*, vol. 60, no. 6, pp. 86–86, 2019.
- [14] P. Rodrigo, "Sri Lankan knitwear sector to overcome political crisis," *Knitting International*, vol. 125, no. 1, pp. 10–11, 2019.
- [15] H. Y. Yen and C. I. Hsu, "College student perceptions about the incorporation of cultural elements in fashion design," *Fashion and Textiles*, vol. 4, no. 1, pp. 1–16, 2017.
- [16] J. Shin and S. Kim, "A study on fashion design for female political leaders during foreign diplomatic tours, based on the Liaohu river civilization of the Neolithic era," *Archives of Design Research*, vol. 31, no. 1, pp. 189–209, 2018.
- [17] G. Appel, B. Libai, and E. Muller, "On the monetary impact of fashion design piracy," *International Journal of Research in Marketing*, vol. 35, no. 4, pp. 591–610, 2018.
- [18] W. Dilys, "Fashion design as a means to recognize and build communities-in-place," *She Ji the Journal of Design Economics & Innovation*, vol. 4, no. 1, pp. 75–90, 2018.
- [19] M. A. Isabel, C. Nogueira, J. Pereira, and R. Fonseca-Pinto, "On the geometric modulation of skin lesion growth: a mathematical model for melanoma," *Research on Biomedical Engineering*, vol. 32, no. 1, pp. 44–54, 2016.
- [20] N. M. Pahlevan, D. G. Rinderknecht, P. Tavallali et al., "Non-invasive iPhone measurement of left ventricular ejection fraction using intrinsic frequency methodology," *Critical Care Medicine*, vol. 45, no. 7, pp. 1115–1120, 2017.

## Research Article

# A Real-Time Biometric Encryption Scheme Based on Fuzzy Logic for IoT

Masoud Moradi,<sup>1</sup> Masoud Moradkhani ,<sup>2</sup> and Mohammad Bagher Tavakoli<sup>1</sup>

<sup>1</sup>Department of Electrical Engineering, Ilam Branch, Islamic Azad University, Ilam, Iran

<sup>2</sup>Department of Electrical Engineering, Arak Branch, Islamic Azad University, Arak, Iran

Correspondence should be addressed to Masoud Moradkhani; moradkhani.m@gmail.com

Received 6 November 2021; Revised 12 January 2022; Accepted 18 January 2022; Published 26 February 2022

Academic Editor: Yanqiong Li

Copyright © 2022 Masoud Moradi et al. This is an open access article distributed under the Creative Commons Attribution License, which permits unrestricted use, distribution, and reproduction in any medium, provided the original work is properly cited.

When millions of smart devices are connected to the Internet using the Internet of Things (IoT), robust security methods are required to deliver current information to the objects. Using IoT, the user can be accessed via smart device applications at any time and any place, which challenges IoT security and privacy. From security point of view, users and smart devices should have secure communication channel and digital ID. Authentication is the first step towards any security action. Biometric-based authentication can ensure higher security for developing secure access. In this paper, fingerprint is used as the biometric factor. After scanning the fingerprint using the cellphone's camera, the image is transmitted to the authentication system. Since the comparison time increases after increasing the database volume, instead of storing the scanned fingerprint image, some key features of the scanned fingerprint are extracted and transmitted to the learning system of the convolutional neural network for detection and authentication and stored in the database. In the user authentication phase, the authentication keys are identified and the passcodes for the user of interest are extracted, and zero code is sent to the forged people; finally, the passcode is examined to check if the user is legal or illegal. In this step, the legal codes for fuzzy encoding of the image and text information are activated, and encryption is carried out in multiple steps depending on the number of members. The final code is compressed using Huffman coding and used for transmission to the network or storage. The proposed method is tested in MATLAB, and the results show that an excellent security is achieved using this cascade encryption method. Conclusively, the proposed hybrid coding technique reduces the information volume by 15.9%.

## 1. Introduction

Internet of Things (IoT) is a keyword in which all digital devices are connected to exchange information with each other. These devices have captured our daily life, including home appliances, offices, and healthcare. Security is the major concern for IoT. IoT technology can be applied in healthcare services, home monitoring, smart home/cities (for security and monitoring purposes), and oil platform as a control platform. With IoT deployment on the cloud (as Cloud of Things) and the society becoming digital, the volume, diversity, and validity of data (for example, big data) are increasing considerably. Authentication is required whenever the devices are connected to ensure secure connection. Therefore, gateway authentication is secure for a

communication system. The existing vulnerabilities in IoT devices make them prone to collusion and forgery. The device authentication problem, or the question that if the device's ID is the same as what is being claimed, is a major problem. Therefore, biometric methods are used for authentication. A comprehensive architecture for biometric IoT and big data requires three challenges: (1) IoT devices have hardware and cannot process the encryption protocols that require resources. (2) The biometric devices introduce the data content of multimedia due to various biometric traits. (3) Fast growth of biometric-based devices and IoT contents generates a large volume of data for computational processing [1].

Biometric system is a set of technologies that extract data from biological or behavioral patterns of an individual (or other biological organisms) to identify it. The biometric systems rely

on specific biological patterns. Data is executed through algorithms to achieve a specific result, which is associated with positive identification of another user or individual.

Compared to passwords, biometric is a biological measurement technology that employs the unique nature of some physical or behavioral traits of the humans for verification/identification. Unlike conventional authentication methods like passwords and tokens, biometric technology uses physical devices for authentication [2]. The fact that the biometric traits cannot be forgotten or lost and are difficult to forge makes them more secure than conventional authentication. Many biometric traits can be defined from the human body. Examples of biometric traits include fingerprint, face, iris, and voice. In general, they can be classified into two classes of physiological and behavioral traits, as shown in Figure 1. The above classes have their own pros and cons and play a unique role in specific applications [3, 4].

Among all biometric identification systems, fingerprint identification systems have more applications. Patterns of ridges and valleys on the surface of the fingertip are determined in the first few months; even identical twins have different fingerprints [2]. The detection performance of fingerprint detection systems, measured with equal error rate (EER) [6], has been reported to be excellent [6].

Mobile devices like smart phones are not just to make phone calls or send short messages, they have become very strong, and more people, especially adults, tend to have a smart phone, like iPhone, and use it almost all throughout the day. With the development of wireless network technology to 4G and LTE, faster data transmission and network stability can be provided. Consumers can purchase their required items with a tap on their mobile device. Also, various applications can be installed on mobile phones, making its applications wider. In this context, an application captures fingerprint images, enabling the user to transmit biometric information of the fingerprint to different systems at any time. Accordingly, this paper presents a biometric encryption technique using fingerprint that creates new and different information codes of the original information through cascade fuzzy encoding and uses Huffman coding to compress the new information and send it to the Internet for storage or transmission.

This paper is focused on designing a fingerprint-based encrypted biometric system used for various smart applications. The proposed biometric system considers security of private data and smart information compression. Also, the proposed scheme balances security and performance.

In the security dimension, in the proposed method, a cascaded fuzzy encryption is used, which, while changing the information for each text, has created a unique code for compression and spreading information. In the compression dimension, the proposed method with two steps of compression during encryption is reduced to more information for storing or sending. Therefore, in this paper, we have been able to achieve good results for different text and image information with the help of a new biometric cryptographic approach with fingerprint. A significant point in this work is the real-time authentication with the help of fingerprints for transferring and storing confidential information as soon as possible. In these circumstances, each person by registering fingerprint

image at any moment is able to store and send their private information.

The rest of this paper is organized as follows. Section 2 reviews previous studies in the context of biometric encryption and compares them. Section 3 presents the biometric encryption system based on cascade fuzzy logic capable of information compression. Section 4 provides the empirical results and security analysis results. Finally, the paper is concluded and future suggestions are given in Section 5.

## 2. Related Work

Ensuring security through biometric authentication is a major challenge for network designers. The biometric information is very valuable and should be protected against fraud, especially during remote authentication and data exchange in wireless mesh networks like IoT. In [7], a secure biometric encryption has been presented for IoT based on fuzzy commitment that is suitable due to its ability to process and protect data against devices connected to the network. This paper, which is based on fingerprint methods, can be divided into two sections. First, on the transmitter side, a biometric trait vector is extracted using DWT, and then, data is encrypted to be transferred via the Internet. Second, on the receiver side, an authentication protocol is used to authenticate and decrypt the received data.

The authors have proposed a framework for ASIoT using biometric as an application [1]. The proposed biometric IoT includes seven layers to handle challenges of biometric applications and decision-making. In the rest of the paper, the design of the biometric IoT has been discussed from 4 points of view: (1) calculating parallel division and capture, (2) computational complexity, (3) device security, and (4) effectiveness of the algorithms. The empirical results have been presented to validate the effectiveness of the D&C method.

The IoT measurement abilities are now accessible as a public service. This new model that is called sensing as a service (S2aaS) allows the owners to sell/exchange data with the consumers interested in large markets. However, the service industry being open makes the S2aaS model subject to destructive attacks. In [8], a simple, efficient, and secure consensus scheme has been presented for the IoT-based S2aaS model. The users of the proposed system can access public services via a simple website, not a smart card, fast and securely. The fuzzy extraction algorithms, Diffie-Hellman elliptic curve, symmetric encryption, and hash functions have been used to develop a secure key consensus and data exchange session. Heavy processes are avoided in the critical and repeated intervals.

The authors of [9] have studied device fingerprinting (DFP) using interarrival time (IAT). IAT is the interval between two packets received subsequently. It has been observed that IAT is unique for a device because of the employed hardware and software. The works existing in the context of DFP employ statistical techniques to analyze IAT and generate more information using unique devices. This study presents a new idea of DFP by plotting IAT curves for the packets, 100 IATs in each diagram, and processing the resultant diagrams for device identification. This approach increases device DFP identification due to accessing deep learning libraries in image processing. In this study, two

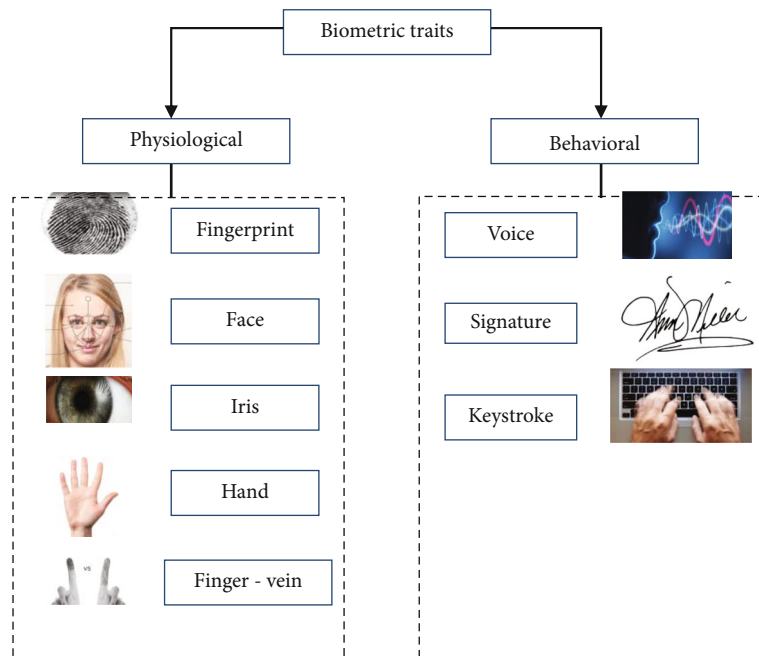


FIGURE 1: Classification of biometric traits (adapted from [5]).

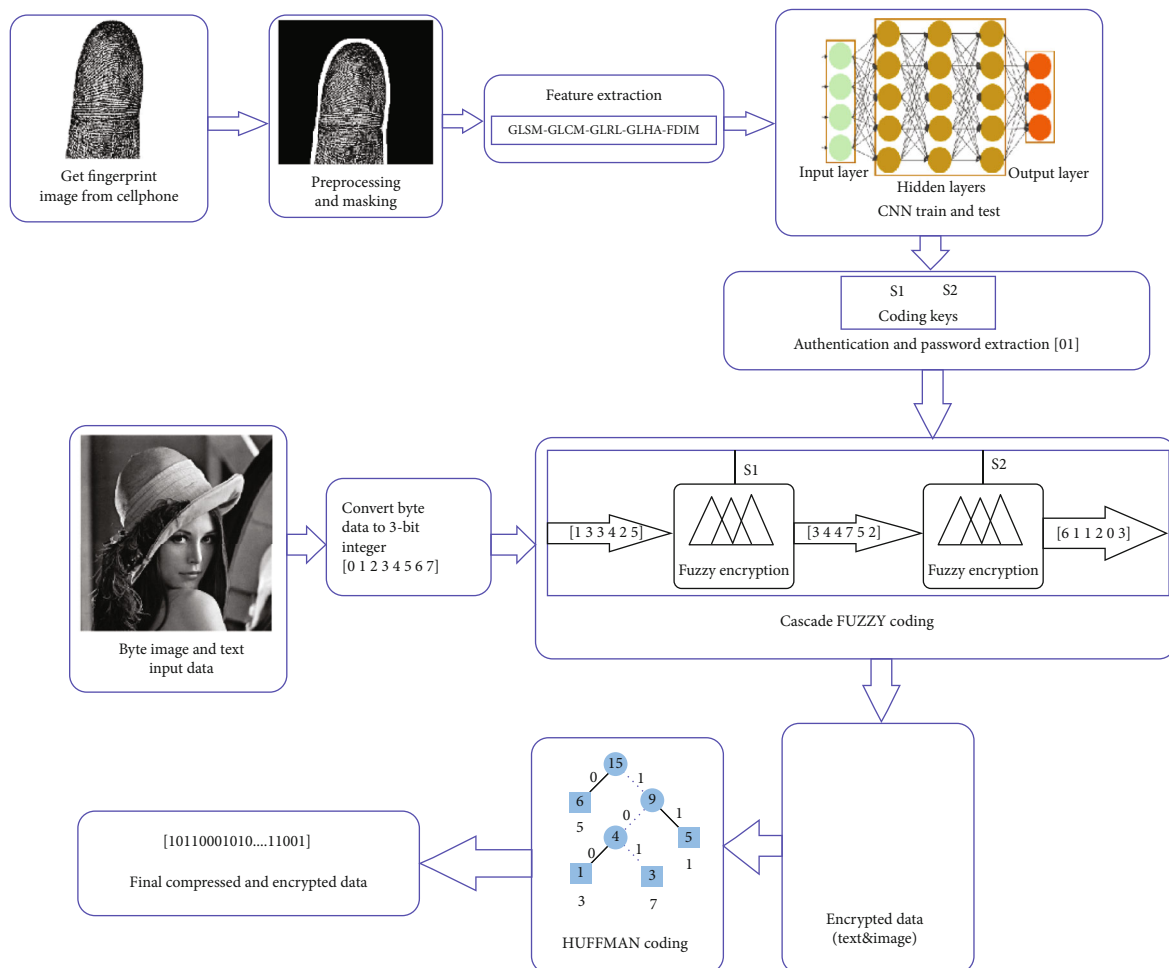


FIGURE 2: Flowchart of the proposed biometric encryption algorithm.



FIGURE 3: (a) Main fingerprint images. (b) Preprocessing and masking fingerprint images.

devices including iPad4 and iPhone 7 plus are connected to a router and the IAT diagrams are plotted; CNN is used to identify the devices, and an accuracy of 86.7% has been obtained.

Authentication with text passwords is still used widely, but it is insecure. Therefore, it is a major concern that is investigated using biometric authentication. In [10], the concept of securing the IoT network using biometric authentication through iris identification has been presented. In [11], the existing approaches for behavioral fingerprinting have been discussed generally, and their application on IoT devices has been evaluated.

In [12], a new software based on Java GUI has been presented for comparative fingerprint and iris biometric analysis. The first part is implemented using Java programming language in the GUI framework, called swing, while the rest of the paper discusses the advantages and disadvantages of both biometric methods and presents scientific data about the time of using fingerprint and iris detection for creating high-level security.

A new scheme, called human to object (H2O) has been presented for problem of sharing data and services in IoT [13]. The proposed approach is capable of continuous authentication of an entity in the network and presents the reliability assessment mechanism based on behavioral fingerprint. Accurate security analysis evaluates robustness of the proposed protocol.

In the context of essential urban infrastructures, trusting IoT data is of great importance, while most technology stacks provide a tool for authentication and encoding the device to cloud traffic. Currently, there is no mechanism to reject physical manipulation in IoT device sensors. To fill this gap, the authors of [14] have introduced a new method for hardware fingerprint extraction of an IoT sensor that can be used for identity authentication without being hidden. The proposed approach is detected by the behavior of analog circuits that apply an AC current with fixed frequency to the sensor while recording its output voltage.

In [15], a novel algorithm has been proposed for detecting people identity based on the image of the handwritten signatures. The proposed work combines textural and statistical

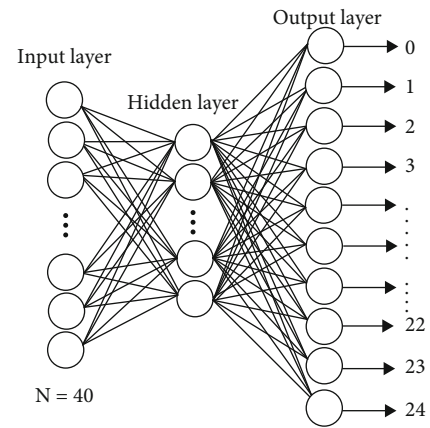


FIGURE 4: Structure of the studied CNN.

features extracted from the images of the signature. Local binary platform (LBP) and histogram of oriented gradient (HOG) features represent texture. The authors are classified regarding gender using machine learning techniques. The proposed technique is evaluated based on a dataset of 4790 signatures, and an incentive accuracy of 96.17, 98.72, and 100% is obtained for k-nearest-neighbor (kNN), decision tree, and support vector machine (SVM) classifiers.

In [16], a multilayer biometric identification system has been presented with a small computational complexity, which is proper for IoT devices. Also, due to hardware and software cooperation in realizing this system in a chain structure, locating and providing alternative paths for the system flow in case of attack is easier. To analyze security of this system, one of the elements of this system called advanced encryption system (AES) has been contaminated by four hardware Trojans that target different parts of this module. The target of these Trojans is to destroy the biometric data being processed by the biometric identification system. All hardware and software of this system are implemented using MATLAB and Verilog HDL.

In [17], a new identity authentication method for IoT based on electromagnetic noise has been presented. The main advantage of electromagnetic noise is that each electronic

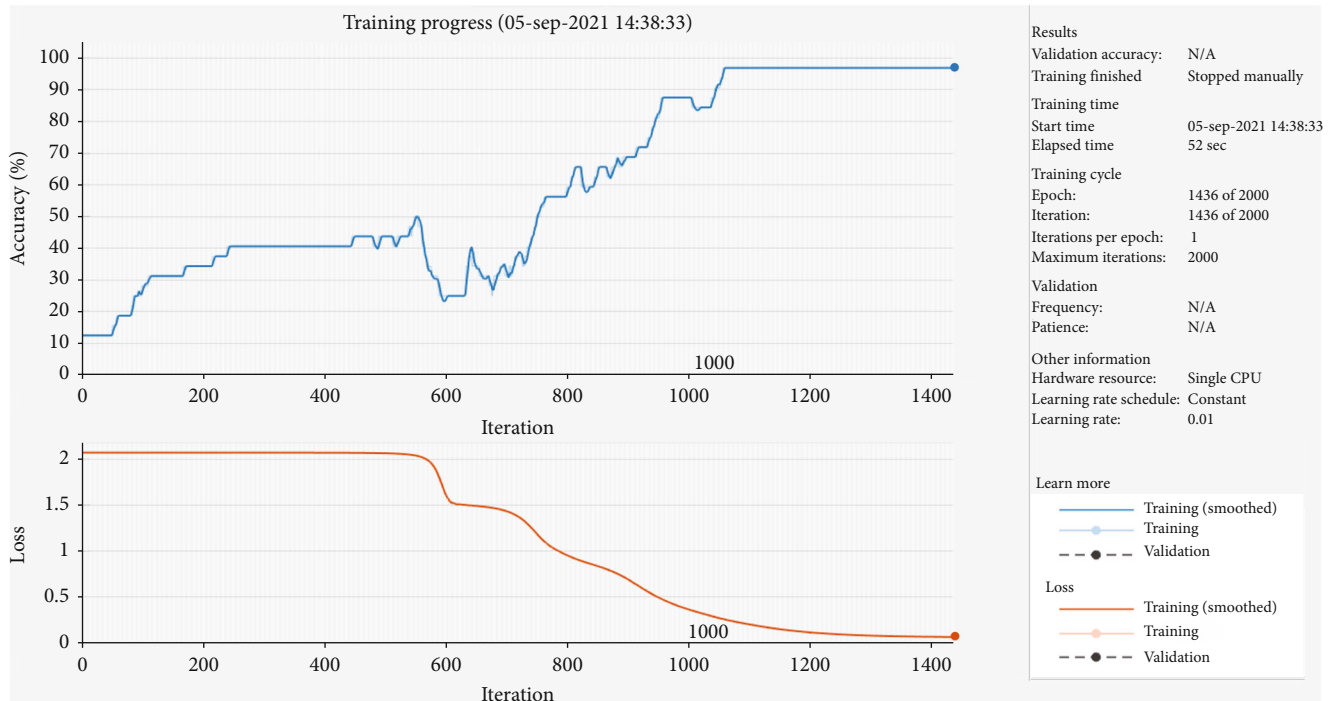


FIGURE 5: Block diagram of object classification.

device generates electromagnetic noise during normal operation. Some features of the electromagnetic propagation and machine learning algorithms are extracted for identifying devices based on these features. The proposed method achieves an accuracy of 77% while identifying the devices among a set of seven devices.

In [18], constraints of the IoT-based authentication scheme that has been introduced recently have been discussed for cloud computing. Also, an advanced three-step identity authentication scheme using chaos map has been presented. The cipher key is developed based on Diffie-Hellman key exchange based on Chebyshev chaos. Also, the cipher key is a long-term pass. It is ensured that the proposed scheme is secure against all attacks that might target the cipher key. Also, the proposed scheme can update the user’s cipher key locally. The proof of Burrows-Abadi-Needham verifies that the proposed method presents mutual authentication and cipher key agreement. In [19], a light encryption system that can be implemented on limited IoT devices has been presented. This algorithm is mainly based on the advanced encryption standard (AES) and a new chaotic S-box.

In [20], a tested and reliable scheme that provides AE through reinforcing mapping of a plain text to elliptic curve cryptography (ECC) has been presented. It withstands multiple cryptographic attacks like chosen plaintext attack (CPA) and chosen ciphertext attack (CCA). In [21], a novel approach using Huffman coding and wavelet decomposition for multispectral fingerprint biometric system has been presented. The technique promises to template the database as well as compressed templates. The compressed templates

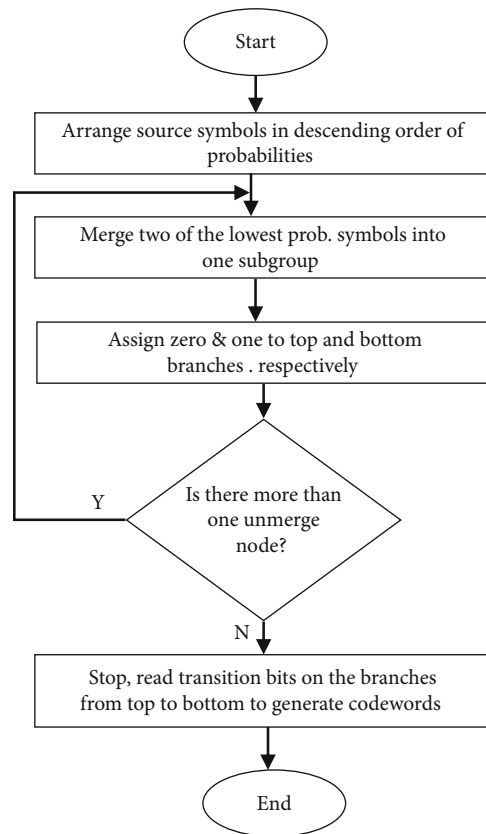


FIGURE 6: The flowchart of Huffman algorithm [28].



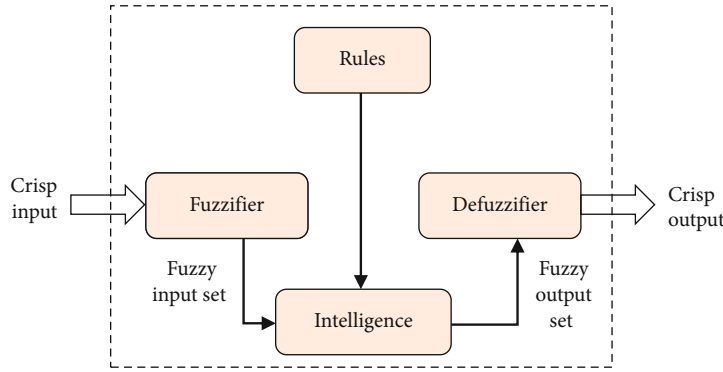


FIGURE 7: Block diagram of the fuzzy logic [25].

TABLE 1: Fuzzy rules of mapping.

Input (W)	0	1	2	3	4	5	6	7
Low	7	6	5	4	3	2	1	0
Mid	3	2	1	0	7	6	5	4
High	7	3	1	5	4	2	0	6

result in faster matching during authentication phase of the fingerprint biometric system. Moreover, the presented technique results in low revocability but high security to mitigate the effect of masquerade attacks.

Fuzzy fingerprint biometric-based key security (FFBKS) scheme is introduced by utilizing feature extraction, in [22]. Extracted feature vectors securely produce private key for user. This key is sent to every sensor node, and then, private key among sensor nodes is produced by pseudorandom number and user key. Then, adaptive possibilistic C-means clustering (APCMC) is initiated for nodes grouping based on distance and identifier among nodes. Here, group key is produced based on fuzzy membership function from prime numbers, and it is utilized for estimation of security. After grouping is formed, data transmission is carried out among group key by fuzzy membership, and sensor nodes are carried out by biometric-based private key. Cluster group keys are diverse from one cluster to another. Also in [23], an optical selective encryption scheme for the medical image based on the fast and robust fuzzy C-means clustering (FRFCM) algorithm and face biometric has been proposed.

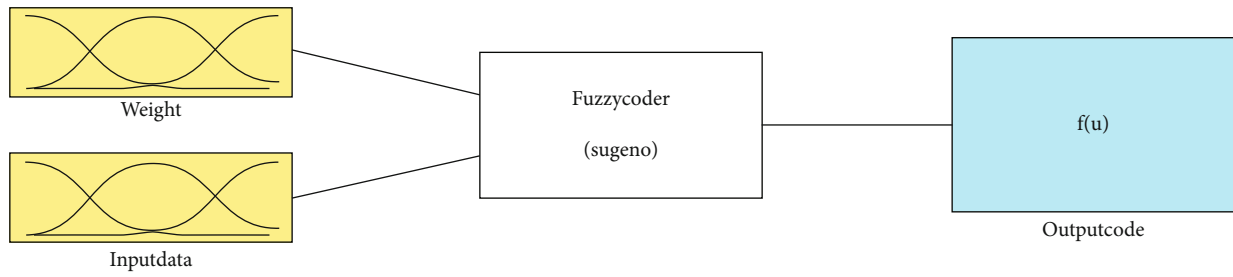
In [24], a new chaff generation algorithm for encryption which is computationally fast and viable for hardware acceleration by employing simple arithmetic operations has been proposed. Complexity study shows that the algorithm has a complexity of  $O(n^2)$ , which is a significant improvement over the existing method that exhibits  $O(n^3)$  complexity. With the new chaff generation algorithm, it becomes much more amenable to implement the fuzzy vault scheme in the resource-constrained environment of system-on-chip.

The literature review reveals that biometric encryption is one of the essential issues for IoT security. Among various biometric structures, fingerprint has more applications in encryption due to easier access and possibility of scanning

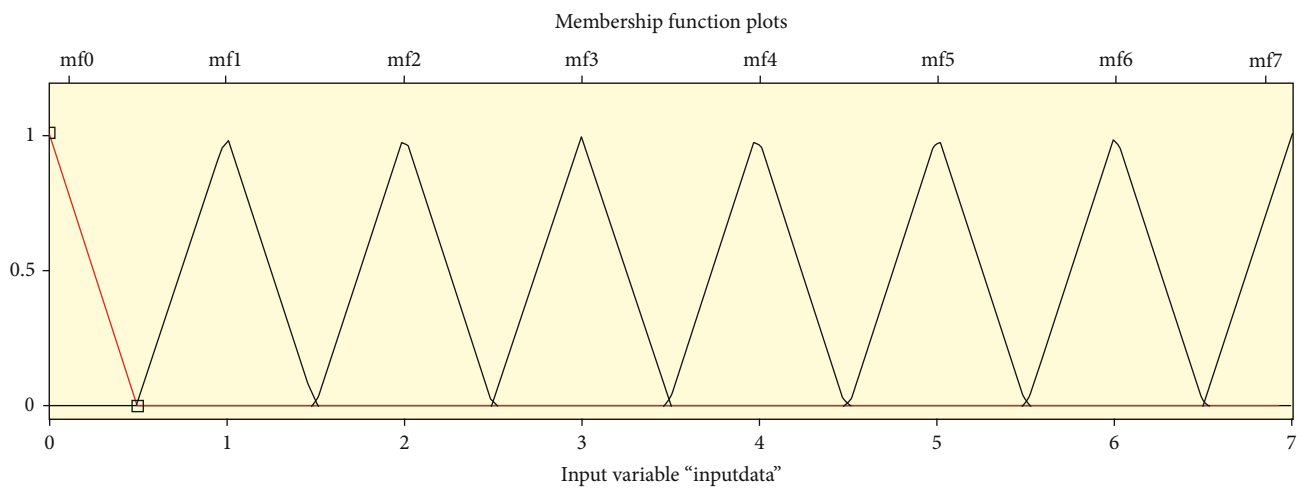
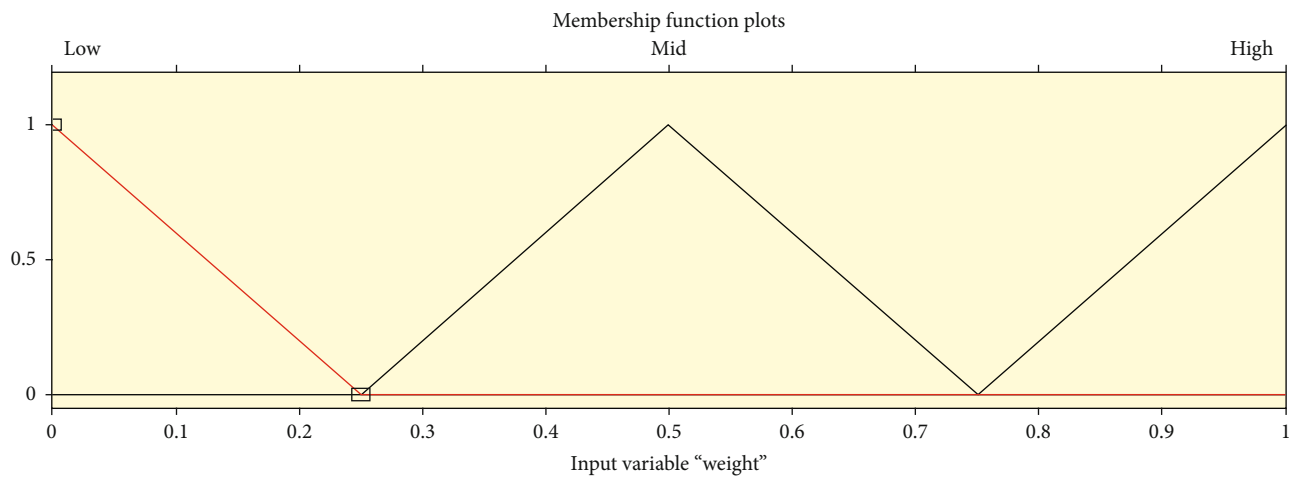
using smart phones. In this paper, this method is used along with authentication using a CNN to present a smart encryption based on cascade fuzzy logic and develop a secure encryption. To this end, Huffman coding is used for compression to achieve a lossless and asymmetric encryption. According to this structure, a private key is generated for each individual using the features extracted from the fingerprint image. The length of the passkey increases considering the number of subscriptions for the cascade fuzzy encoding structure and increasing number of cascade stages. This work is superior because the cipher keys are selected for each individual through selecting a set of analog keys for each stage. Also, the security of the proposed encryption is higher because the cipher keys depend on authenticating identities using fingerprint.

### 3. The Proposed Method

Fingerprint is unique for each individual and can be used as the signature of each individual to authenticate its identity. Most well-known apps of this type are used in criminology. However, today, demand for automatic fingerprint comparison is increasing. Among applications of this system, the followings can be mentioned: physical location access control, computer, network, resources, and bank accounts. There are ridges in the fingerprint images that are different from one individual to another. In this paper, a set of features is extracted for fingerprint images. These features represent the characteristics and position of the fingerprint ridges. First, the primary processes are applied to the images to show off the original fingerprint images along with the ridges, and then, various conventional features on the masked fingerprint image, including geometrical and statistical features, GLSM, GLCM, GLRL, GLHA, and FDIM, are extracted. These features are extracted and stored as the fingerprint information of the individuals instead of the original fingerprint image. In the next step, this information is transmitted to different individuals for authentication. In this work, the fingerprint information that is defined for 25 different individuals using phones is given to CNN for training. Figure 2 shows a schematic of the proposed approach for biometric encryption based on fuzzy cascade encryption. After authentication, the analog passcodes S1 and S2 that are initialized in the range of zero

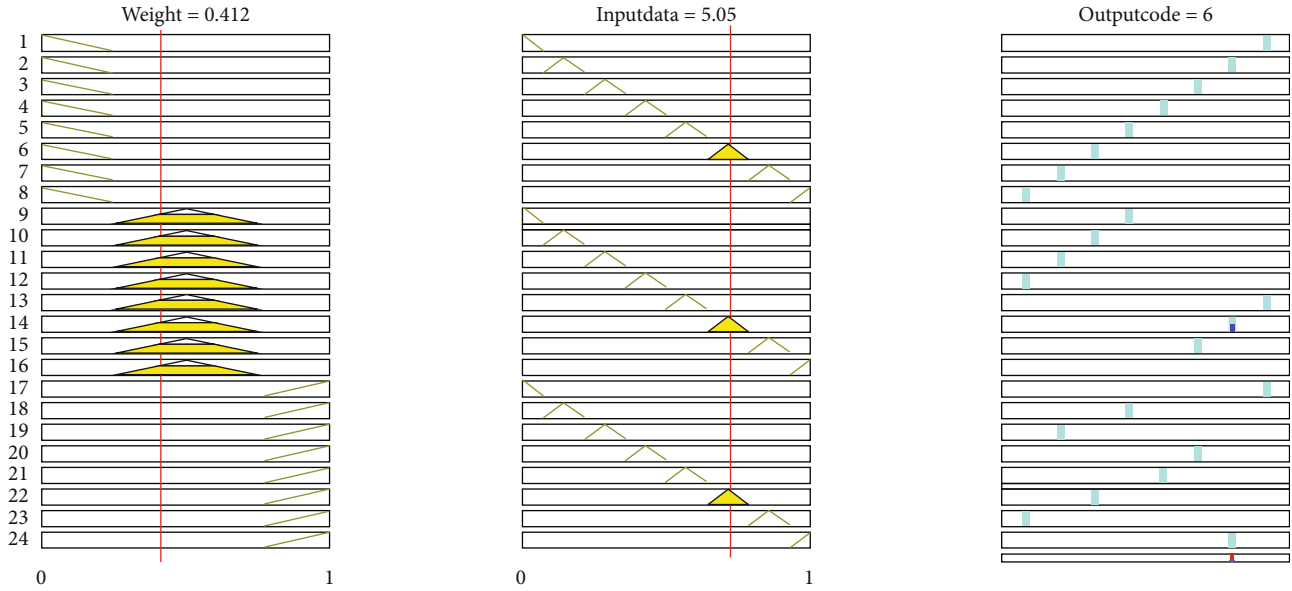


(a) Takagi-Sugeno

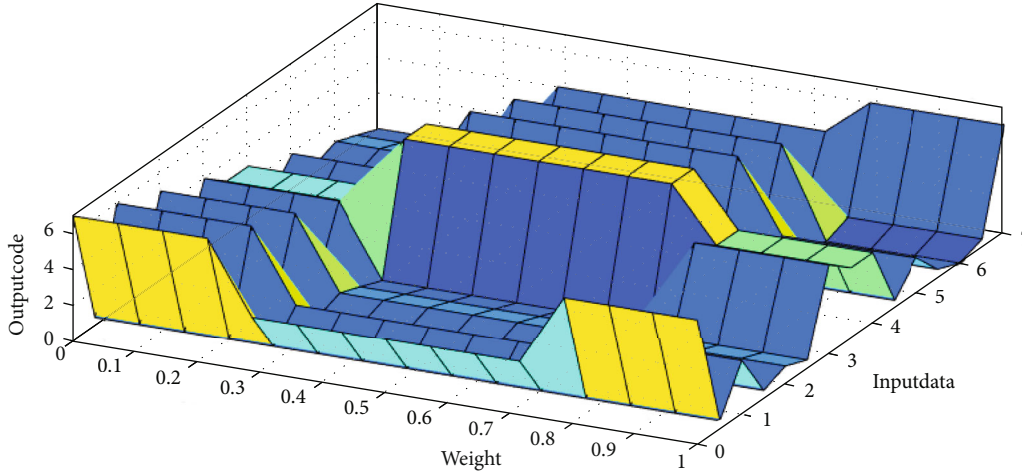


(b) Input membership functions

FIGURE 8: Continued.



(c) Fuzzy rules



(d) Input-output characteristics

FIGURE 8: Fuzzy logic block of the fuzzy encoder for determining different maps based on the private key.

and one are bicoated, and the information of the image or text of interest is encrypted in two fuzzy coding steps as shown in Figure 2. In the final step, the encrypted codes for 0, 1, 2, 3, 4, 5, 6, and 7 are compressed using the Huffman coding method so that the main code is not accessed easily. Now, the extracted binary codes are transmitted to the network to be stored or transmitted.

When decrypting the information of the stored or received data, fingerprint is used to restore the cipher keys. Then, the compressed information is retrieved for Huffman expansion, and the main information is retrieved for cascade fuzzy encoding using S1 and S2 keys. In the following, the proposed scheme, Huffman theory, and the proposed fuzzy logic are described.

**3.1. Receiving the Input Information.** First, the fingerprint image is received via a smart phone for identity authentication and identification. In this paper, the fingerprint images

of 25 individuals taken from the left index finger in 4 steps are used to encrypt a set of information, including image or text. Three fingerprint images are selected to train the CNN, and one image is used for the test.

**3.2. Preprocessing and Feature Extraction.** First, the fingerprint image of the individual is transmitted in accordance with Figure 3(a). After receiving the input frames, the Gaussian noise removal algorithm is applied to each fingerprint image to increase accuracy (in Figure 3(b)). After applying this filter, a polished image is obtained; thus, it is expected that feature points are extracted satisfactorily. In this step, a masking operation is applied to highlight the fingerprint image and its ridges to obtain more accurate information of the fingerprint image.

After masking, 40 different features, including geometrical and unique features, are introduced for object detection (GLSM, GLCM, GLRL, GLHA, and FDIM).

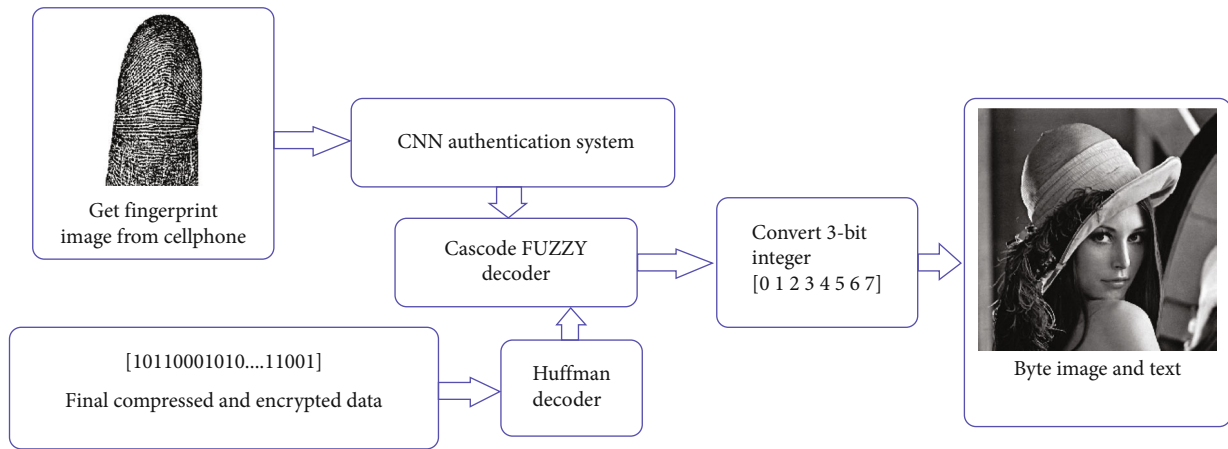
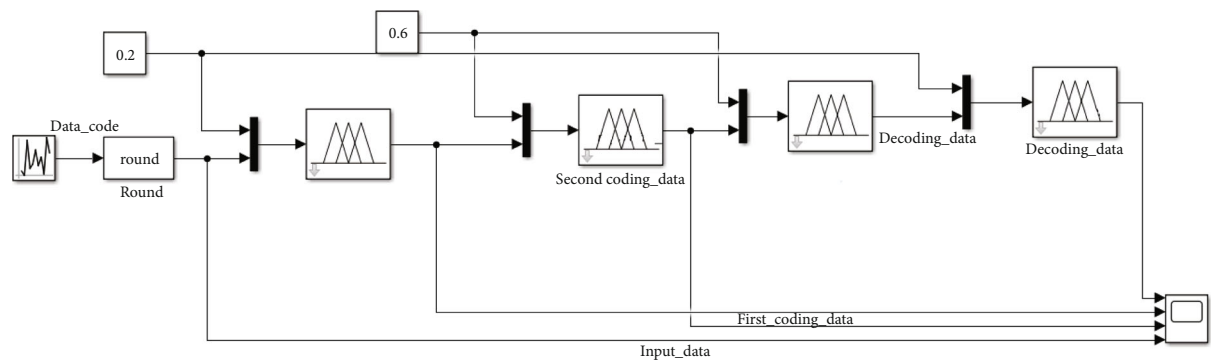
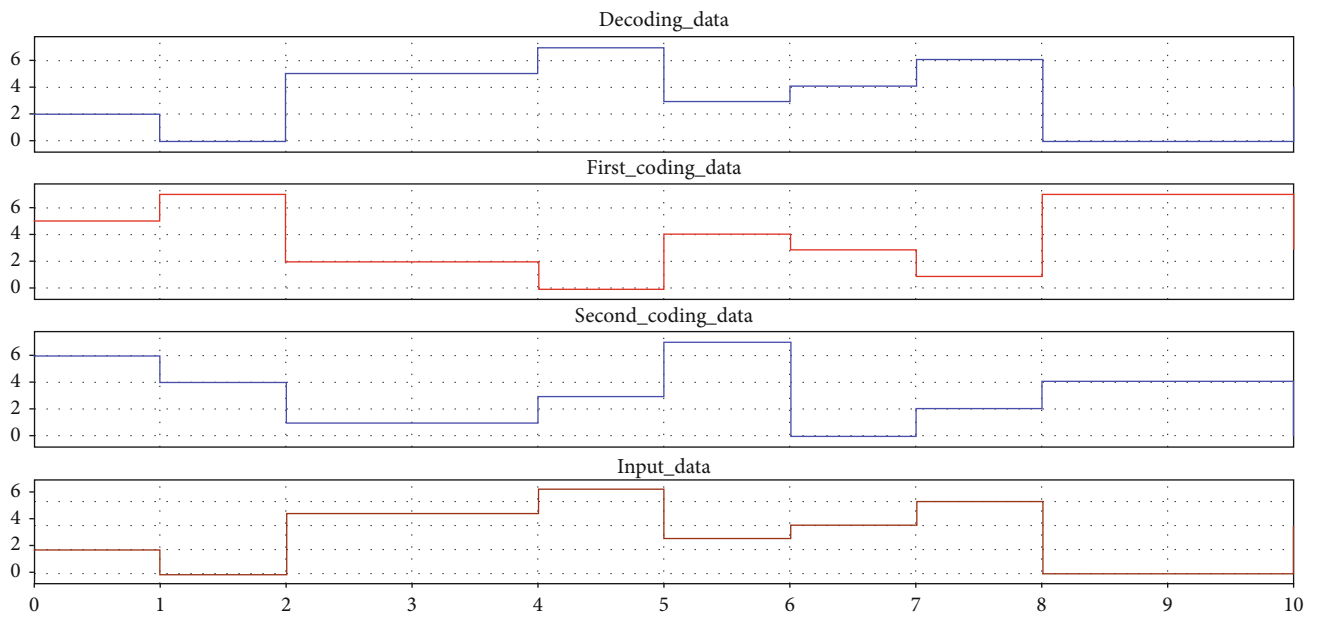


FIGURE 9: Block diagram of the proposed biometric encryption.



(a) Simulink representation



(b) Decoding and decryption for  $w = 0.2$  and  $0.6$

FIGURE 10: Output of the cascade encoder and decoder.

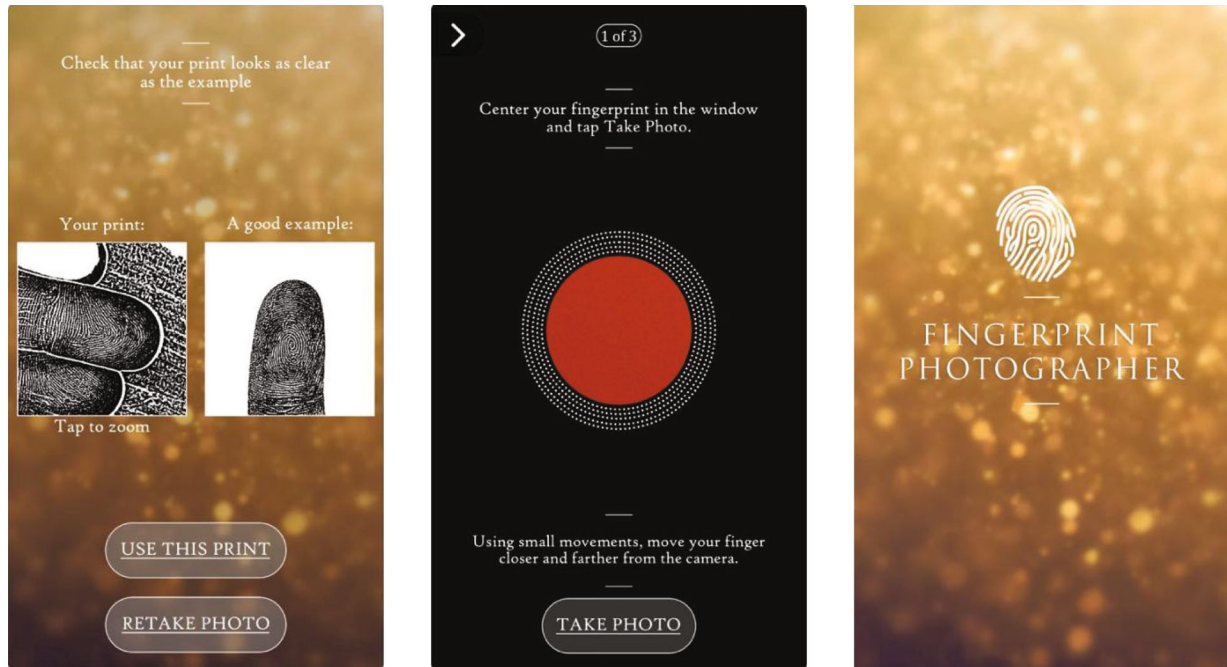


FIGURE 11: The software used for fingerprint images.

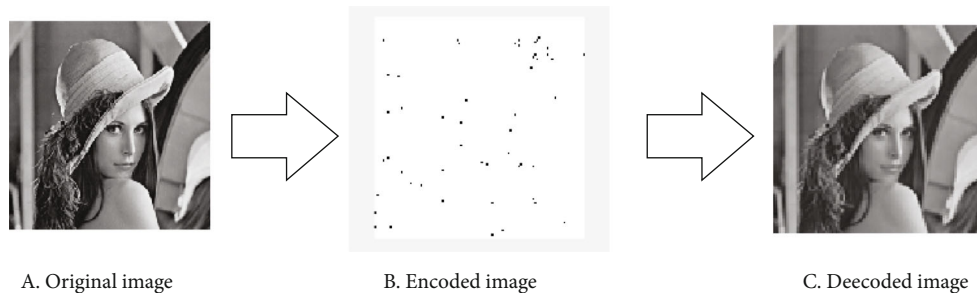


FIGURE 12: Performance of the proposed biometric encryption scheme.

**3.3. CNN Classification.** The input layer of the network contains neurons that code the values of the input features. Our training data includes  $32 \times 32$  pixel images of the fingerprint image dataset; thus, the input layer includes 40 neurons equivalent to various features.

The second layer is a hidden layer. The number of neurons in this layer is represented by  $n$ , and different values are tested for  $n$ . The given example represents a small hidden layer including  $n = 158$  neurons.

The output layer includes 25 neurons, representing 25 types of image labels. The output neurons are numbered from 0 to 24, and the neuron with maximum activation value is selected as the prediction result. Figure 4 shows the general structure of the CNN. Figure 5 shows the results of one test and training round. In general, the accuracy means that the model predicts the output correctly. In this work, the accuracy size is determined by dividing the number of correct authenti-

cation specimens from fingerprint to total image samples. According to this result, accuracy is 96.87%.

**3.3.1. Huffman Coding Theory.** Huffman programming in computer science and information theory that was developed by David Huffman in 1952 [25] is a technique to compress lossless data [26] based on coding of variable length source code proportional with the possibility of emergence, or in other words, it is expressed in image processing for image compression—with the possibility of repeating the color degree in the image array.

The Huffman coding theory depends on the two following laws [27]:

- (A) The symbols that occur frequently are represented with shorter code words compared to the symbols that occur rarely

TABLE 2: Display coding results in different stages.

Main data code.												
	6	2	6	5	7	3	7	6	7	5	5	6
	7	3	6	7	7	7	7	7	7	7	7	7
	7	7	7	7	0	4	1	0	0	0	0	0
	0	3	4	2	4	4	4	2	0	0	4	5
7	7	2	2	0	6	0	0	5	3	1	1	0
	0	0	1	3	7	0	2	1	7	1	7	7
	4	0	1	6	7	2	5	0	2	0	0	1
	6	2	0	5	0	4	5	2	1	0	1	2
	2	2	6	5	6	2	5	0	1	5	4	6
	7	1	2									
First data encrypted code.												
	1	5	1	2	0	4	0	1	0	2	2	1
	0	4	1	0	0	0	0	0	0	0	0	0
	0	0	0	0	7	3	6	7	7	7	7	7
	7	4	3	5	3	3	3	5	7	7	3	2
0	0	5	5	7	1	7	7	2	4	6	6	7
	7	7	6	4	0	7	5	6	0	6	0	0
	3	7	6	1	0	5	2	7	5	7	7	6
	1	5	7	2	7	3	2	5	6	7	6	5
	5	5	1	2	1	5	2	7	6	2	3	1
	0	6	5									
Second data encrypted code.												
	2	6	2	1	3	7	3	2	3	1	1	2
	3	7	2	3	3	3	3	3	3	3	3	3
	3	3	3	3	4	0	5	4	4	4	4	4
	4	7	0	6	0	0	0	6	4	4	0	1
3	3	6	6	4	2	4	4	1	7	5	5	4
	4	4	5	7	3	4	6	5	3	5	3	3
	0	4	5	2	3	6	1	4	6	4	4	5
	2	6	4	1	4	0	1	6	5	4	5	6
	6	6	2	1	2	6	1	4	5	1	0	2
	3	5	6									
Huffman Binary code (323 bit).												
	0	0	0	0	0	0	0	1	0	0	0	0
	0	0	0	1	1	0	0	1	0	1	1	0
	0	0	0	0	1	0	0	0	0	1	0	0
	0	1	0	0	0	0	1	0	0	1	0	1
	0	0	0	0	1	0	1	0	1	0	1	0
	1	0	1	0	1	0	1	0	1	0	1	0
1	1	0	1	0	1	0	1	1	0	1	0	0
	0	1	1	1	1	1	1	1	1	1	1	1
	1	1	1	0	1	0	1	0	1	0	0	0
	0	1	0	1	0	0	0	1	0	0	0	1
	0	0	0	0	1	1	1	1	1	0	1	0
	0	0	0	0	1	1	0	0	0	1	0	0
	1	1	1	0	0	0	0	1	1	1	1	0
	0	0	1	0	1	0	1	0	1	1	0	1

TABLE 2: Continued.

1	1	1	1	1	1	1	0	1	1	0	1
0	1	1	0	1	1	0	0	1	0	1	1
1	0	0	1	1	1	0	1	0	0	1	0
0	1	1	0	1	1	0	0	0	0	1	0
0	0	1	0	0	0	1	1	1	0	0	1
1	1	1	1	0	1	1	0	0	0	0	0
0	1	1	1	0	0	0	1	1	1	0	1
0	0	0	0	0	1	0	0	1	0	1	1
1	1	0	1	1	0	0	1	0	0	1	0
0	1	0	0	0	0	0	0	0	1	0	0
0	0	0	0	1	0	0	0	1	1	1	0
1	1	0	0	0	1	0	1	0	0	0	0
0	0	1	0	0	1	1	0	0	1	1	0

(B) Code words of the two symbols that are less frequent are the same

3.3.2. *Huffman Algorithm.* Implementation of the Huffman coding algorithm can be represented by the following steps:

- (i) Step 1. Sort the pixel values based on their probability values
- (ii) Step 2. Merge the two values with minimum probability; label one of them with zero and the other one with one
- (iii) Step 3. Add their probabilities
- (iv) Step 4. Specify two subsequent sets of the current set of singular values or pair of values
- (v) Step 5. Go to step 2 and continue until another root is obtained

3.3.3. *Huffman Flowchart.* The Huffman coding algorithm can be described using the flowchart shown in Figure 6:

3.3.4. *Classification and Labeling Items Based on Fuzzy Logic*

(1) *Fuzzy Logic Theory.* Fuzzy logic theory is widely used to model the concepts of human thinking and refers to unreliability of the existing information for decision-making based on various measures. Substitution competency is described against measures, and their significant weight associated with the mentioned linguistic values is broadcast in numbers. In the fuzzy set, the linguistic variables are used to describe the fuzzy conditions and convert the linguistic variables to numerical variables, and the real logical values with unit distances are substituted in the decision-making process [29]. Therefore, mathematically, a set is defined as a limited, unlimited, or countable unlimited set of elements. In each case, each element is either a member of the set or not. However, in fuzzy systems, the element might be a part of the set or outside the set. Therefore, the answer to the question X “member of a set A” has no certain correct or incorrect answer. Figure 7 shows block diagram of the fuzzy logic.

(1)1. *Fuzzy Set.* A fuzzy set A is defined in the global discourse that is specified by a membership function:  $\mu_A : U \rightarrow [0, 1]$  which is given in Eq. (1).

$$A = \left\{ (x, \mu_A(x)) \mid x \in U \wedge \mu_A(x) \in [0, 1] \right\} \quad (1)$$

For each  $x$  member of set A,  $\mu_A(x)$  represents the relationship degree of  $x$  in A.

$$x \in (A, \mu) \Leftrightarrow x \in A \wedge \mu(x) \neq 0 \quad (2)$$

In addition, using the membership function, each element  $x$ , which is a member of  $U$  describes a degree of relationship in each set A, expressing how much the element  $x$  belongs to the set A. Thus, an element with a relationship degree of zero indicates that this element is not included in the set, while an element with a relationship degree of one is completely included in the set.

(1)2. *Fuzzification.* Considering the application domain of the current study, the triangular membership function is used. A triangular fuzzy number A can be adjusted using three numbers ( $a$ ,  $b$ , and  $c$ ) with an adaptive function as in Eq. (3).

$$\mu_A(x) = \begin{cases} 0, & \text{se } x < a; \\ (x - a)/(b - a), & \text{se } a \leq x \leq b; \\ (c - x)/(c - b) & \text{se } b \leq x \leq c; \\ 0, & \text{se } c < x. \end{cases} \quad (3)$$

(1)3. *Fuzzy Inference.* Defuzzification is a process that generates the quantitative value and magnitude in the fuzzy logic; that is, the fuzzy numbers are converted to a unit number based on different methods, which describes the average maximum weight as in Eq. (4).

TABLE 3: Comparison of the proposed method to some state-of-the-art methods using biometric encryption.

Reference	Key point	Accuracy
[30]	It extracted 57 geometric features from hand (lengths, areas, angles, and ratios) and used Euclidean distance for classification.	93%
[31]	It used morphological operations (e.g., thinning) in order to create the line edge map and implement the Hausdorff distance for classification. Research was performed on the own database.	95%
[32]	It implemented various features extractors (e.g., CompCode, OLOF, and RLOC) and various matching methods (e.g., SVM and kNN). Research was performed on 5 different mobile devices.	56% -81%
[33]	Lightweight verification schema based on fusion of the features presented in this work.	91%
[7]	Characteristic vectors have to be extracted from the gray scale image using filtering or transformation techniques such as oriented field flow curves (OFFC), Gabor filter, discrete wavelet transform (DWT), fast Fourier transform (FFT), discrete cosine transform (DCT), and principal component analysis (PCA).	90%
[21]	Wavelet feature extracted.	98.9%
This work	40 different features, including geometrical and unique features, are introduced for object detection (GLSM, GLCM, GLRL, GLHA, and FDIM).	99.1%

$$Z_0 = \frac{\sum \mu(x)_i \times w_i}{\sum \mu(x)_i}. \quad (4)$$

According to Eq. (4),  $Z_0$  is the output of the defuzzifier,  $\mu(x)_i$  is the relationship degree with the fuzzy set, and  $w_i$  is the output fuzzy weight.

**3.4. Encryption under Fuzzy Mapping.** After determining a weight for elements 0 to 7 for compression, it is time to present a method to encrypt information based on a complex encryption. Therefore, in this section, a mapping is introduced that changes the octal codes with their real value. In this section, two numerical keys are defined as the private keys, which are developed using the authentication codes in the previous steps. In this case, the fuzzy coding system is defined that introduces unidentifiable maps in the range of [0,1] for this system. Table 1 represents the governing equations of this structure. Figure 8 shows the fuzzy structure of the fuzzy encoder for Takagi-Sugeno type and the input membership functions.

The important point in the proposed encryption method is changing the private key for private key characteristics of S1 and S2, such that the transmitter generates the private keys using fingerprint. In this paper, three ranges are selected for the private key value; by increasing the number of ranges, the number of maps can be increased to increase the security level. The important point in this study is that selecting the number change mapping or number mapping is arbitrary and provided by a nonlinear and unpredictable model, where the number of nonlinear mappings can be increased by increasing the private key range.

In this section, with the development of maps, the encryption complexity is further increased and smaller processes are required. After this step, the coded data is transmitted to the destination based on the defined path, and the received code is decrypted according to Figure 9. As can be seen in this figure, the inverse procedure of the encryption process is carried out to obtain the information packet. Therefore, in this structure, the received data along with the information of weights and cipher key are proc-

essed according to the steps shown in the above figure to obtain the code of the original data. In this set, to obtain the main key, the authentication condition and fingerprint are used. In these blocks in the fuzzy and Huffman sections, decoding and decryption are used. As examples of correcting the data encryption and decryption, as shown in Figure 10, different private key weights are examined and simulated for different inputs. After decryption, the code is obtained in the octal basis; in the last section, conversion block is used to convert it to the binary basis to calculate different values. The output code is the binary code of the original data, which is finally converted to the original data values, including image or text, using inverse conversion. In this paper, two cascade stages are used for fuzzy encoding and decryption to the number of authenticated individuals.

## 4. Experimental Results and Analysis

For this experiment, we used a database including 25 individuals, with four different fingerprints for each individual. The fingerprint images are taken using mobile phones using fingerprint photographer and transmitted to the proposed identifier system as shown Figure 11. Each individual has four fingerprints (samples), 3 cases are used for training, and 1 case is used for test; it can be said the 75% of data is for training and 25% is for test.

This system is implemented using Apple iPhone SE. The program is deployed on a router with IOS as Wi-Fi connection point connected to the LAN of a wired network that executes Ethernet services, and the images are transmitted to the authentication system using MATLAB2017b. After authentication, in case of identification, the code of the authenticated individual is extracted and the results are transmitted to the fuzzy encoder. Due to the limited number of subjects, two fuzzy stages are used for encoding and decoding; but as the number of cascade stages increases, more individuals can be covered. Finally, the encrypted code is compressed for 0-7 samples with a good compression coefficient for storage or transmission to the network under Huffman coding. The images are considered vertically for the left index finger.



After sending the fingerprint image to the authentication system, if the individual is identified, the private keys are transmitted to the output, and if the information is fake, the cipher key returns zero. Next, the extracted key is tested for two types of text and image data, where the results are described in the following.

**4.1. Text Data.** Here, the selected text includes the following sentence:

“hello, I am a good student. This new EEG DATA.”

In the first phase, the octal number codes of the text data are as follows, and the encoding results are as follows after two cascade fuzzy encoding steps with private keys of  $S1 = 0.2$  and  $S2 = 0.6$ . In this study, the text includes 48 characters that occupy 384 bits of the memory by assigning 8 bits of memory to each character. For the final code, the volume of the encoded file using cascade fuzzy encoding is 323 bits. Therefore, compression with a coefficient of 0.841 decreases to total volume of the text. Table 2 shows these steps.

**4.2. Image Data.** Here, an image, shown in Figure 12, is used as the personal information. The results after encryption and decryption are shown in Figures 12(b) and 12(c). As can be seen for a  $103 \times 103$  image, despite reducing volume from 84872 bits to 79136 bits and compressing the image with a coefficient of 93.2%, the image in Figure 12(b) is an obscure image of the original image being encrypted.

**4.3. Comparison.** In this section, we compare articles in the field of biometrics and information security with the help of hands, irises, and fingerprints. Table 3 shows the important points and the accuracy of each and is finally compared with our proposed technique. As can be seen, due to the uncertain complexity defined in the proposed encryption, we have been able to improve information security well. The compression provided along with the proposed encryption also helps to store information, which can increase the importance of this encryption.

## 5. Conclusion

In this study, we presented a reliable encryption scheme for the IoT that considers security requirements and material constraints of the connected objects. The purpose of this encryption scheme is to protect the authentication information (biometric of the user and object identities) and data exchange (approved after one session). The basis is the biometric fuzzy commitment and illustrating the security requirements at each step. Selection, encoding, features vector, quantitative code, and compression code techniques based on the Huffman coding are all without security threat. For encryption, the fuzzy encoding technique is used due to its low computational complexity. To extract the features vector, an analog code technique was used for the private cipher key, which increased the complexity of selecting the cipher key for fuzzy encoding, and the fuzzy stages generate a heterogeneous and unpredictable value for each numerical value of the cipher key. In the proposed cryptographic method, nested semantic cryptographic structure is introduced by determining the fingerprint-based key code, which is decoded and decrypted according to the fuzzy key

processes of confidential information. In addition to increasing security for encryption, this leads to an increase in compression and is an important benefit of the proposed method compared to biometric-based cryptographic methods. In the proposed method, we encounter the complexity of the Huffman coding method that in the future we plan to expand its method for other codes. According to the classification results, an EER of 3.12% is obtained for fingerprint images of different individuals.

## Data Availability

The data will be shared only at the request of the esteemed editor for review by the Reviewers.

## Conflicts of Interest

The authors declare that they have no conflicts of interest.

## References

- [1] K. L. Ang and K. P. Seng, “Biometrics-based Internet of Things and Big data design framework,” *Mathematical Biosciences and Engineering*, vol. 18, no. 4, pp. 4461–4476, 2021.
- [2] A. K. Jain, P. Flynn, and A. A. Ross, *Handbook of Biometrics*, Springer-Verlag New York, Inc, USA, 2008.
- [3] W. Ahmed, A. Rasool, J. Nebhen et al., *Security in Next Generation Mobile Payment Systems: A Comprehensive Survey*, 2021, <https://arxiv.org/abs/2105.12097>.
- [4] W. Yang, J. Hu, C. Fernandes, V. Sivaraman, and Q. Wu, “Vulnerability analysis of iPhone 6,” in *2016 14th Annual Conference on Privacy, Security and Trust (PST)*, pp. 457–463, Auckland, New Zealand, 2016.
- [5] W. Yang, S. Wang, N. M. Sahri, N. M. Karie, M. Ahmed, and C. Valli, “Biometrics for Internet-of-Things security: a review,” *Sensors*, vol. 21, no. 18, p. 6163, 2021.
- [6] G. Borghi, E. Pancisi, M. Ferrara, and D. Maltoni, “A double Siamese framework for differential morphing attack detection,” *Sensors*, vol. 21, no. 10, p. 3466, 2021.
- [7] A. Bentahar, A. Meraoumia, H. Bendjenna, S. Chitroub, and A. Zeroual, “Biometric cryptosystem scheme for Internet of Things using fuzzy commitment principle,” in *2018 International Conference on Signal, Image, Vision and their Applications (SIVA)*, pp. 1–6, Guelma, Algeria, 2018.
- [8] A. Bentahar, A. Meraoumia, L. Bradji, and H. Bendjenna, “Sensing as a service in Internet of Things: efficient authentication and key agreement scheme,” *Journal of King Saud University-Computer and Information Sciences*, vol. 17, 2021.
- [9] S. Aneja, N. Aneja, and M. S. Islam, “IoT device fingerprint using deep learning,” in *2018 IEEE International Conference on Internet of Things and Intelligence System (IOTAIS)*, pp. 174–179, Bali, Indonesia, 2018.
- [10] G. Meena and S. Choudhary, “Biometric authentication in internet of things: a conceptual view,” *Journal of Statistics and Management Systems*, vol. 22, no. 4, pp. 643–652, 2019.
- [11] B. Bezawada, I. Ray, and I. Ray, “Behavioral fingerprinting of Internet-of-Things devices,” *Wiley Interdisciplinary Reviews: Data Mining and Knowledge Discovery*, vol. 11, no. 1, article e1337, 2021.
- [12] K. G. Lalović and M. Z. Bogdanoski, “Java GUI application for comparing the levels of biometric security: Fingerprint vs. iris,”

- Vojnotehnički glasnik/Military Technical Courier*, vol. 69, no. 3, pp. 676–686, 2021.
- [13] M. Ferretti, S. Nicolazzo, and A. Nocera, “H2O: secure interactions in IoT via behavioral fingerprinting,” *Future Internet*, vol. 13, no. 5, p. 117, 2021.
- [14] F. Lorenz, L. Thamsen, A. Wilke et al., “Fingerprinting analog IoT sensors for secret-free authentication,” in *2020 29th International Conference on Computer Communications and Networks (ICCCN)*, pp. 1–6, Honolulu, HI, USA, 2020.
- [15] S. S. Gornale, S. Kumar, A. Patil, and P. S. Hiremath, “Behavioral biometric data analysis for gender classification using feature fusion and machine learning,” *Frontiers in Robotics and AI*, vol. 8, 2021.
- [16] S. Taheri and J.-S. Yuan, “A cross-layer biometric recognition system for mobile IoT devices,” *Electronics*, vol. 7, no. 2, p. 26, 2018.
- [17] A. Souza, I. Carlson, H. S. Ramos, A. A. Loureiro, and L. B. Oliveira, “Internet of Things device authentication via electromagnetic fingerprints,” *Engineering Reports*, vol. 2, no. 8, article e12226, 2020.
- [18] F. Wang, G. Xu, G. Xu, Y. Wang, and J. Peng, “A robust IoT-based three-factor authentication scheme for cloud computing resistant to session key exposure,” *Wireless Communications and Mobile Computing*, vol. 2020, Article ID 3805058, 15 pages, 2020.
- [19] B. M. Alshammari, R. Guesmi, T. Guesmi, H. Alsaif, and A. Alzamil, “Implementing a symmetric lightweight cryptosystem in highly constrained IoT devices by using a chaotic S-box,” *Symmetry*, vol. 13, no. 1, p. 129, 2021.
- [20] H. AlMajed and A. AlMogren, “A secure and efficient ECC-based scheme for edge computing and internet of things,” *Sensors*, vol. 20, no. 21, p. 6158, 2020.
- [21] A. Sharma, S. Arya, and P. Chaturvedi, “A novel image compression based method for multispectral fingerprint biometric system,” *Procedia Computer Science*, vol. 171, pp. 1698–1707, 2020.
- [22] B. Nivedetha and I. Vennila, “FFBKS: fuzzy fingerprint biometric key based security schema for wireless sensor networks,” *Computer Communications*, vol. 150, pp. 94–102, 2020.
- [23] Y. Shen, C. Tang, M. Xu, and Z. Lei, “Optical selective encryption based on the FRFCM algorithm and face biometric for the medical image,” *Optics & Laser Technology*, vol. 138, p. 106911, 2021.
- [24] M. Khalil-Hani, M. N. Marsono, and R. Bakhteri, “Biometric encryption based on a fuzzy vault scheme with a fast chaff generation algorithm,” *Future Generation Computer Systems*, vol. 29, no. 3, pp. 800–810, 2013.
- [25] D. Huffman, “A method for the construction of minimum-redundancy codes,” *Proceedings of the IRE*, vol. 40, no. 9, pp. 1098–1101, 1952.
- [26] B. O’Hanen and M. Wisan, *JPEG Compression*, 2005.
- [27] P. Kaur, *Compression using fractional Fourier transform, a thesis submitted in the partial fulfillment of requirement for the award of the degree of master of engineering in electronics and communication* Deemed University.
- [28] A. Odat, M. Otair, and M. Al-Khalayleh, “Comparative study between LM-DH technique and Huffman coding,” *International Journal of Applied Engineering Research*, vol. 10, no. 15, pp. 36004–36011, 2015.
- [29] H. M. Alabool and A. K. Mahmood, “Trust-based service selection in public cloud computing using fuzzy modified VIKOR method,” *Australian Journal of Basic and Applied Sciences*, vol. 7, no. 9, pp. 211–220, 2013.
- [30] S. Barra, M. De Marsico, M. Nappi, F. Narducci, and D. Riccio, “A hand-based biometric system in visible light for mobile environments,” *Information Sciences*, vol. 479, pp. 472–485, 2019.
- [31] M. Trik, S. Pour Mozaffari, and A. M. Bidgoli, “Providing an Adaptive Routing along with a Hybrid Selection Strategy to Increase Efficiency in NoC-Based Neuromorphic Systems,” *Computational Intelligence and Neuroscience*, 2021.
- [32] A. S. Ungureanu, S. Thavalengal, T. E. Cognard, C. Costache, and P. Corcoran, “Unconstrained palmprint as a smartphone biometric,” *IEEE Transactions on Consumer Electronics*, vol. 63, no. 3, pp. 334–342, 2017.
- [33] A. Gielczyk, M. Choraś, and R. Kozik, “Lightweight verification schema for image-based palmprint biometric systems,” *Hindawi, Mobile Information Systems*, vol. 2019, article 2325891, 2019.

## Research Article

# Application of Cellular Automata with Improved Dynamic Analysis in Evacuation Management of Sports Events

Jingyi Xie  and Li Zhang 

*Department of Physical Education, China University of Mining and Technology (Beijing), Beijing 100083, China*

Correspondence should be addressed to Jingyi Xie; [zqt2010701009p@student.cumtb.edu.cn](mailto:zqt2010701009p@student.cumtb.edu.cn)  
and Li Zhang; [zhanglicumtb@126.com](mailto:zhanglicumtb@126.com)

Received 5 January 2022; Revised 24 January 2022; Accepted 5 February 2022; Published 23 February 2022

Academic Editor: Wen Zeng

Copyright © 2022 Jingyi Xie and Li Zhang. This is an open access article distributed under the Creative Commons Attribution License, which permits unrestricted use, distribution, and reproduction in any medium, provided the original work is properly cited.

In this paper, the cellular automaton simulation technology is applied to the evacuation management of sports events, combined with the dynamic analysis method to analyze the collision of people in the evacuation process. At the same time, the cellular automaton model is used to refine the evacuation space to simplify environmental modeling, and the network model is used to determine the individual evacuation path from a macroperspective, simplify modeling, and improve simulation efficiency. In addition, this article simulates the evacuation process of the cellular automaton according to the actual evacuation situation of sports events and constructs the evacuation management system of sports events. Finally, this article evaluates the effect of the model in conjunction with experiments. The experimental results show that the role of the evacuation management system for sports events based on cellular automata proposed in this paper is obvious.

## 1. Introduction

The number of stadiums and sports venues with complex structures and diverse functions is rapidly increasing, and sports events of various levels are being held all over the world. In addition, due to the periodicity and intermittent nature of sports events, as well as the increasing use of postmatch use methods such as cultural performances, exhibitions, and food and entertainment [1], stadiums have become venues for large-scale cultural and entertainment activities. Therefore, stadiums have become one of the main gathering places for a large number of people in daily life. The magnificent buildings, complex structures, dense crowds, and numerous equipment have become the characteristics of stadiums. There is a major problem hidden behind these features, that is, security risks. The huge building and complex structure can easily cause the collapse of the stadium and make the safety exit not clear for evacuation [2]. Moreover, crowded people can easily lead to crowds, which can lead to stampede incidents. In addition, when there is many equipment, a little careless management can cause fire and explosion.

At the same time, dense crowds and large-scale venues often become targets of international terrorist attacks. Once these emergencies happen, it will inevitably cause casualties and property losses [3].

Today's stadium is a multipurpose venue mainly for holding sports events and carrying out a variety of activities. At the same time, stadiums have become densely populated places, full of major safety hazards. Therefore, relevant departments and related personnel are urgently required to take effective and feasible measures to minimize the occurrence of incidents and personal and property losses. At the same time, this also requires researchers and scholars to pay great attention to the evacuation of stadiums and gymnasiums. Due to the causes of casualties, there are not only the building structure of the venue itself but also the crowd and external human factors in the venue.

Cellular automata were originally used to simulate the self-replication function of living systems. Its core idea is to discretize the research object into cells with a finite number of states in space and then follow a certain random motion rule in the discretized time. This idea and method were adopted by evacuation researchers and established a

cellular automaton model in the field of evacuation research. The core of the cellular automaton model is the discretization of space and time. It divides the evacuation simulation environment into grids of equal size, and each grid is a cell. Usually, a cell can have three states, namely, occupied by evacuated individuals, occupied by obstacles, and idle; the state of each cell at a time can only be one of the three states, other cells adjacent to a certain cell. It is called the neighbor of this cell; the entire evacuation time is divided into small time slices; these time slices are called time steps; in each time step, the evacuated individual moves from the cell where it is currently located to according to the set movement rule. The neighbors may stay where they are. Therefore, the content of the model mainly includes spatial division method, neighbor type, and time-step update method.

This paper applies dynamic analysis to the evacuation management process of sports events and simulates the evacuation process of sports events through cellular automata to improve the evacuation management effect of sports events.

## 2. Related Work

Literature [4] studied the time required for evacuation and obtained the corresponding mathematical formula. Researchers on evacuation began to rise. Literature [5] investigates the behaviors of survivors in fires and uses them for statistical analysis. Literature [6] gives the relationship curve between crowd density and average crowd speed and applies computational simulation research methods to the evacuation of fire personnel. During this period, the evacuation of people was studied mainly through observation, investigation, statistics, and mathematical simulation.

There are many simulation models for evacuation, but researchers usually divide them into micromodels, macromodels, and mesoscopic models. The micromodel treats each person in the evacuation crowd as an independent individual for evacuation research. This type of model can show the individual's evacuation behavior more finely, but the amount of calculation is often large; the macromodel studies the evacuated crowd as a whole, and the evacuation crowd is regarded as a flowing fluid. An evacuated person is a particle in the fluid. This model mainly studies the characteristics of the evacuated crowd as a whole and cannot well represent the characteristics of the evacuated individuals; the mesoscopic model combines the microscopic model and the macroscopic model for evacuation of researchers. This model can not only study the individual behavior of evacuees but also study the overall characteristics of evacuees [6].

Models based on physical forces are also often regarded as continuous microscopic models. The model is continuous in time and space and simulates individual evacuation by calculating the force generated by itself and the environment on the individual. Its representative models are the magnetic field force model and the social force model. The magnetic field force model is a gravita-

tional model of pedestrian motion established by the literature [7] based on the principle of magnetic force. In the model, the target is regarded as the negative pole of the magnetic field, and the obstacle and the person are regarded as the positive pole. In this way, a gravitational force is formed between the person and the target and between the obstacle and the obstacle. Repulsion is formed, and people are evacuated under the action of gravity and repulsion. The social force model is proposed in the literature [8]. This model describes the interaction between people and the environment and goals as repulsive force, gravitational force, and self-driving force and establishes a dynamic differential equation system to describe the movement of people according to Newton's second law. The relationship between speed and position over time. Based on the agent theory in artificial intelligence based on the agent model, the literature [9] defines the evacuated individuals in the model as agent individuals with different characteristics to represent the differences between people in reality. This type of model is divided into single-agent model and multiagent model. The modeling ideas of the two are the same, but the multiagent model emphasizes the interaction between agents. The cellular automaton model is based on the cellular automaton idea proposed by Von Neumann. This model divides the evacuation space into discrete cell spaces with a finite number of states [10], so that the evacuees move in the cell space according to a certain rule to achieve the effect of evacuation simulation. Based on this model are the queuing model, route selection model, and random model. The difference between them is only the rules of individual movement on the cell. The queuing model emphasizes that people move in a certain queue order, the path selection model emphasizes to move according to the path search, and the random model emphasizes to move in the order of random selection. Based on agent and cellular automaton model [11], combine the agent model and cellular automaton model in evacuation modeling, use agent to describe individuals, and use cellular automata to divide the evacuation environment space, so that all the established model can better reflect the scalability of the environment and the intelligence of personnel.

For the study of crowd evacuation time, the literature [12] uses the Legion simulation system to simulate and calculate the three algorithms for evacuation time commonly used in domestic and foreign projects and analyzes and compares the results obtained. It is recommended to use the itinerary method as engineering calculation method for evacuation time of stadiums. For the research on how the structural characteristics of stadiums and stadiums affect the characteristics of evacuated individuals, the literature [13] studied the influence of the width of the safety exits of stadiums on crowding during evacuation and the influence of crowd panic on evacuation.

Literature [14] developed a simulation system for fire evacuation demonstration based on the Superscape system, which can be used for simulation training of evacuation in fire. Literature [15] developed a virtual exercise system named interFIRE VR, which is mainly used to

train personnel how to evacuate in a fire situation. Literature [16] developed a virtual exercise program to train relevant personnel on how to find a safe evacuation exit in a fire building and successfully evacuate. Literature [17] developed a building fire simulation prototype system FVR based on virtual reality and data simulation, which can be used for evacuation drills and fire rescue training in fire situations. Literature [18] proposed a simulation technology DIS and developed a fire remediation simulation drill DIS system. Its application can replace the existing actual field simulation training. Literature [19] uses game engine technology to develop a three-dimensional virtual exercise system to simulate the process of evacuation of personnel to a safe area in an organized and orderly manner according to the unified dispatch and command on the spot after an incident occurs. It can be seen from the above that the virtual exercise technology has been successfully applied by researchers in the simulation research of personnel evacuation, which makes the visual effect of simulation stronger, and the interaction between people and the system makes the individual evacuation in the system more reflected. The characteristics of people in reality can greatly promote the research of personnel evacuation simulation.

### 3. Application of Cellular Automata Based on Dynamic Model in Evacuation Management of Sports Events

The initial self-driving force of the pedestrian is represented by  $F_0$ , which includes two parts: one is the direction of the force, and the other is the magnitude of the force. First of

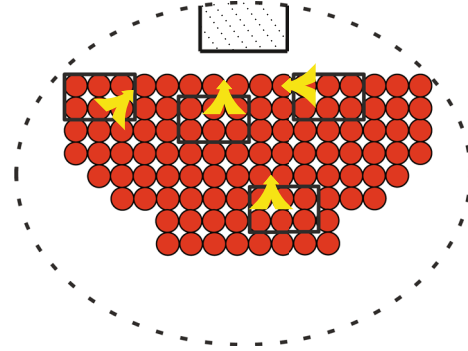


FIGURE 1: The direction of the initial self-driving force.

all, there are differences between different individuals. Therefore, we assume that the range of the initial self-driving force of pedestrians is  $0 \sim F_{\max}$ , where  $F_{\max}$  is the maximum value of self-driving force. Then, the initial self-driving force of pedestrians in the system is

$$|F_0| = F_{\max} \times \text{RAND}. \quad (1)$$

Secondly, taking into account the pedestrian's tendency to leave the dispersal space, it is assumed that the direction of the pedestrian's initial self-driving force  $F_0$  points to the cell around the pedestrian that is closest to the safety exit, as shown in Figure 1. When there are multiple locations around the pedestrian with the same distance to the safety exit, one of them is randomly selected as the direction of the initial self-driving force  $F_0$ , and the distance from a certain cell  $(x_i, y_i)$  around the pedestrian to the safety exit is

$$S_{ij} = \begin{cases} \min_j \left( \sqrt{(x_i - x_j)^2 + (y_i - y_j)^2} \right) & (x_i, y_i) \text{ pedestrian movement position,} \\ M & (x_i, y_i) \text{ is the wall of evacuation space.} \end{cases} \quad (2)$$

Among them,  $S_{ij}$  is the shortest distance between a cell  $(x_i, y_i)$  around the pedestrian and a cell  $(x_j, y_j)$  belonging to the safety exit. When  $(x_i, y_i)$  is a wall, the pedestrian will not choose this position, and  $M$  is a large constant, which means that the pedestrian's initial self-driving force  $F_0$  will not point to the wall.

When the direction of the pedestrian crowding force is closer to the direction from the pedestrian to a nearby pedestrian, the component force of the crowding force in that direction is greater. Therefore, the pedestrian's congestion force is decomposed into the two cells that deviate from its direction closest. With reference to the axioms of statics, the force decomposition must conform to the parallelogram law of force, and the crowding force  $F_0$  is decomposed into two decomposition forces  $F_1$  and  $F_2$ , as shown in Figure 2. Among them, the resolution is

as follows:

$$|F_m| = |F_0|(\cos \theta_m - \sin \theta_m), \quad m = 1, 2. \quad (3)$$

Among them,  $|F_m|$  is the force component of  $F_0$  in the  $\theta_m$  direction, and  $\theta_m$  is the angle between  $F_0$  and the pedestrian to the adjacent cell.

In addition, when there is a space in the two cell directions of the crowding force  $F_0$  decomposition, that is, when there is no pedestrian at that position, the component force in this direction remains on the pedestrian itself. Among them, pedestrians have a crowding force  $F_{0i}$  for pedestrians. However, the cell without pedestrians does not produce the crowding force but keeps this  $F_{0j}$  in the pedestrian itself, acts on the pedestrian itself, and exists as the pedestrian's self-driving force, as shown in

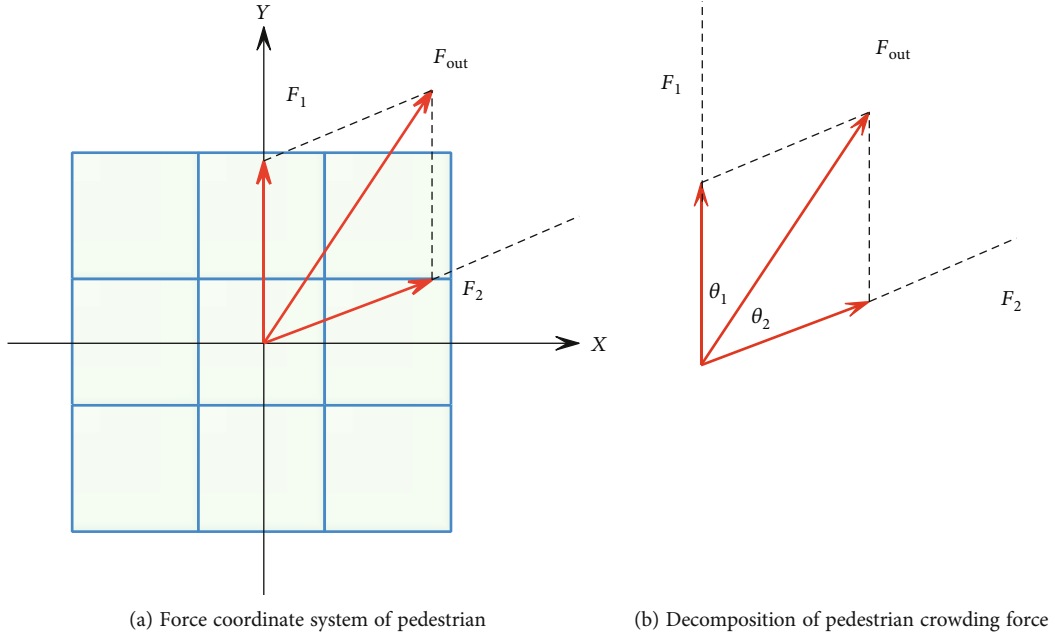


FIGURE 2: Pedestrian crowding force decomposition.

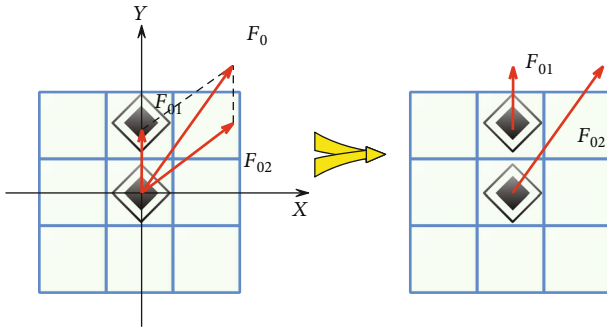


FIGURE 3: Decomposition of crowding force when there are space cells. (a) Pedestrian of crowding force. (b) Effect of crowding force.

Figure 3. That is, at this time, pedestrians are driven by their own driving force  $F_{0j}$ , which points to the space cell. Similarly, when the two directions are spaces, pedestrians are, respectively, driven by the driving forces  $F_{0i}$  and  $F_{0j}$  pointing to the two space cells, which may drive the pedestrian to move to these two positions.

Since the transmission of force requires a medium, when pedestrians are not in direct contact, the congestion force cannot be transmitted. Therefore, it is assumed that the pedestrian is only subjected to the crowding force of the eight pedestrians around the pedestrian, as shown in Figure 4. Combining the above-mentioned process of decomposing the crowding force, the crowding force of each pedestrian is decomposed to the corresponding pedestrian. This article counts the component forces of other pedestrians around the pedestrian in the direction of the pedestrian,  $F_1$  represents the combined force of the pedestrian crowding force, and  $F_{close}$  represents the

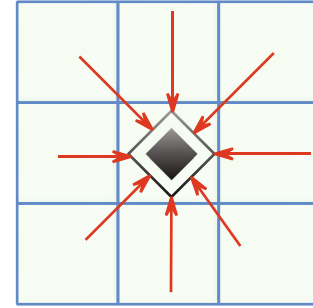


FIGURE 4: The crowding force of surrounding pedestrians on middle pedestrians.

scalar sum of the crowding force received by the pedestrian, as shown below:

$$F_1 = \sum_{i=1}^8 F_{i \rightarrow 1}, \quad (4)$$

$$F_{close} = \sum_{i=1}^8 |F_{i \rightarrow 1}|.$$

Among them,  $F_{i \rightarrow 1}$  is the component of the crowding force of the  $i$ th pedestrian around the pedestrian to the pedestrian.

The absorption and retransmission of the crowding force are carried out simultaneously. If pedestrians cannot absorb the congestion force, they will continue to transmit the congestion force to other people around. Therefore, it is necessary to consider that pedestrians may be subjected to the crowding force  $F_{out}$  that other pedestrians around cannot absorb. However, the congestion force component

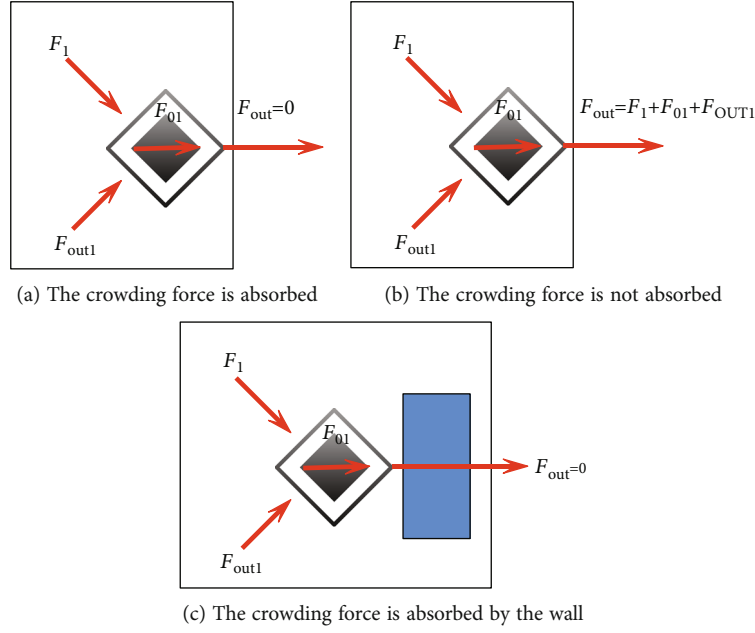


FIGURE 5: The process of absorption and retransmission of crowding force.

transmitted to the pedestrian is  $F_{out1}$ , and the pedestrian's congestion force absorption and retransmission process is shown in Figure 5. The transfer rule of crowding force is:

$$F_{out} = \begin{cases} 0 & |F_1 + F_{01} + F_{out}| \leq \alpha, \\ F_1 + F_{01} + F_{out} & |F_1 + F_{01} + F_{out}| > \alpha. \end{cases} \quad (5)$$

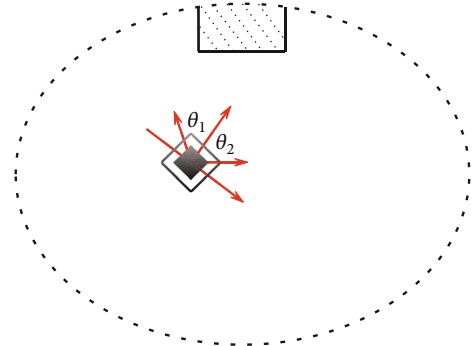
Among them,  $F_1$  is the combined force of the crowding force received by the pedestrian,  $F_{01}$  is the driving force transmitted by the pedestrian itself,  $F_{out}$  is the component of the crowding force that other pedestrians around cannot absorb the crowding force transmitted to the pedestrian,  $\alpha$  is the absorption coefficient, and  $F_{out}$  is the crowding force transmitted by pedestrians. The process of its decomposition and transmission refers to the above-mentioned decomposition and transmission process.

When pedestrians are crowded by surrounding pedestrians, the degree of panic among pedestrians is greater. Therefore, it is necessary to determine the pedestrian's panic coefficient  $p$ , and the pedestrian's panic coefficient  $P$  is determined by the scalar sum of the crowding force received by the pedestrian. Through the analysis of the above decomposition, transmission, absorption, and retransmission process, the crowding force received by pedestrians is divided into three parts.

- (1) The self-driving force of pedestrians interacts with other pedestrians. With reference to Newton's third law, the action of force is mutual, and pedestrians will receive a reaction force of the same magnitude and opposite direction as this driving force. Therefore, the pedestrian will receive the reaction force of the self-driving force, and the magnitude of this force is denoted as  $f_0$

TABLE 1: Relationship between panic coefficient and push force effect.

$f$	$p$
$\leq 100$	0.00
$\leq 200$	0.10
$\leq 300$	0.20
$\leq 400$	0.30
$\leq 500$	0.40
$\leq 600$	0.50
$\leq 700$	0.60
$\leq 800$	0.70
$\leq 900$	0.80
$\leq 1000$	0.90
$\geq 1000$	1.00

FIGURE 6: The distribution of self-driving force direction, where  $\theta_1 = \theta_2 = (1 - p) \times 90^\circ$ .

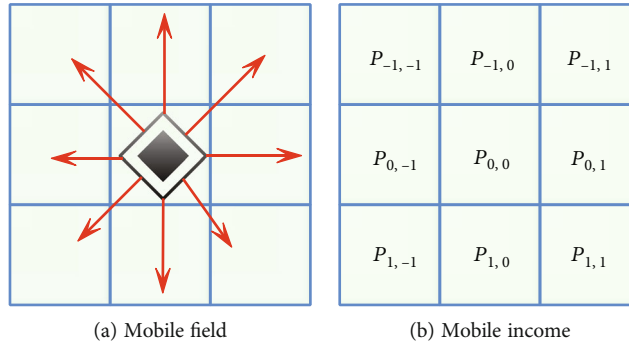


FIGURE 7: Pedestrians' mobility field and mobility revenue.

- (2) When the pedestrian's self-driving force acts on the surrounding pedestrians, each pedestrian may be subjected to the crowding force of eight other pedestrians around him, and the scalar and accumulation of each crowding force need to be recorded as  $f_1$
- (3) When pedestrians judge the absorption and retransmission of the congestion force, there are situations in which the congestion force cannot be absorbed and transferred. Pedestrians will be affected by the crowding force transmitted to the pedestrian that the surrounding pedestrians cannot absorb the crowding force and the reaction force generated by the pedestrians themselves being unable to absorb the crowding force and crowding other pedestrians. The scalar and accumulation of this part of the crowding force are denoted as  $f_2$

The congestion force of the above three parts is superimposed; that is, all the congestion force effects that pedestrians may receive in a time step are

$$f = f_0 + f_1 + f_2. \quad (6)$$

Through the analysis of simulation data and reference to related documents, the panic coefficient of pedestrians is calibrated. The relationship between the panic coefficient  $P$  and the crowding force effect is shown in Table 1.

The higher the pedestrian panic, the more the pedestrian expects to leave the evacuation space. Therefore, when the panic coefficient  $P$  is greater, the pedestrian's self-driving force is also greater, and its direction is closer to the safety exit. The self-driving force of pedestrians consists of two parts: the self-driving force new  $F_0$  that is expected to leave the safety exit generated by the panic coefficient  $P$  and the congestion force  $F_2$  that has not been transmitted at this time step.

The self-driving force new  $F_0$  must determine the magnitude and direction. First of all, the magnitude of this force consists of two parts, one part is the different crowding force caused by the different panic levels of pedestrians, and this part of the force is proportional to the panic coefficient  $p$ . The other part is the random self-driving force generated by pedestrians' own psychology toward safe exits, which is relatively random due to individual differences. Therefore,

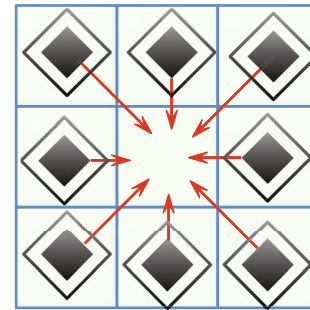


FIGURE 8: The moving field of the space cell.

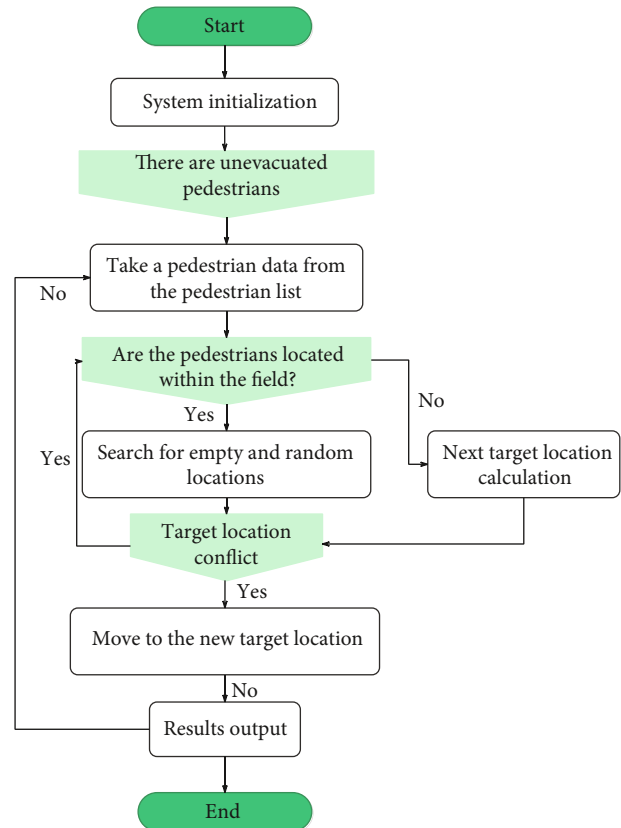


FIGURE 9: Personnel movement process.



the size of the pedestrian's self-driving force new  $F_0$  is

$$|\text{new}F_0| = p \times F_{\max} + A \times \text{RAND}. \quad (7)$$

Among them,  $|\text{new}F_0|$  is the magnitude of the pedestrian's self-driving force,  $p$  is the pedestrian's panic coefficient,  $F_{\max}$  is the maximum self-driving force, and  $A \times \text{RAND}$  is the random self-driving force generated by different pedestrians.

Secondly, the direction of the self-driving force new  $F_0$  is also determined by the panic coefficient  $p$ . When the pedestrian is in the most panic state, that is, when  $p = 1$ , the pedestrian expects to leave the evacuation space very much, so the direction of the self-driving force points to the nearest safety exit. When the pedestrian's fear coefficient is small, the pedestrian's psychological state is relatively stable. However, since the ultimate goal of the pedestrian is still to leave the evacuation space, the direction of its self-driving force should deviate at a certain angle along the exit direction. As  $p$  decreases, the deviation range increases. Therefore, taking the direction of pedestrians to the nearest safety exit as the normal direction, this paper believes that the direction of self-driving force is randomly distributed within the range of  $(1 - p) * 90^\circ$  on both sides of the normal, as shown in Figure 6.

In addition, the crowding force of pedestrians cannot be passed on in a time step. Therefore, in the process of judging that the congestion force absorption will be transmitted again, some pedestrians still have untransmitted congestion force  $F_2$  themselves, rather than being in a balanced state. However, force cannot disappear out of thin air. Therefore, this part of the force  $F_2$  is combined with the self-driving force new  $F_0$  generated by pedestrians and updated as the self-driving force for the next time step.

Therefore, the pedestrian self-driving force at the next time step is updated as

$$F_0 = \text{new}F_0 + F_2. \quad (8)$$

Among them,  $F_0$  is the initial self-driving force of the pedestrian at the next time step, new  $F$  is the self-driving force generated by the pedestrian itself, and  $F_2$  is the congestion force that has not yet been transmitted.

In the dynamic parameter model, all the positions that can be moved within a time step of the pedestrian are defined as the pedestrian's moving area. In the cellular automaton simulation, the pedestrian's moving area is a  $3 \times 3$  cellular area. Pedestrians occupy the center of the mobile field. Pedestrians can choose to wait or move to the other eight cells within a time step. Mobile revenue is the evaluation of pedestrians on all locations in the mobile field, as shown in Figure 7.

Because in the process of pedestrian evacuation, the main consideration is the pedestrian direction parameter and space parameter, therefore, these two parameters are used in the simulation of crowded evacuation to describe the movement benefits of pedestrians.

In the process of pedestrian movement, the pedestrian's movement income must first be calculated. Pedestrian's movement income consists of two parts: the direction parameter  $D_{ij}$  and the space parameter  $E_{ij}$ <sup>[19]</sup>.  $P_{ij}$  represents the mobile income of pedestrians; then, there is

$$P_{ij} = D_{ij} + E_{ij}. \quad (9)$$

During the evacuation of pedestrians, the purpose of pedestrians is to leave the evacuation space. Therefore, pedestrians always move in the direction of the safety exit; that is, pedestrians will choose the position closest to the safety exit in the moving area as their target location. The direction parameter  $D_{ij}$  refers to the reduced value of the distance for the pedestrian to reach the safety exit when the pedestrian moves from the initial position to the target position within a unit step.

When calculating this parameter, this thesis uses static domain parameters to express the attractiveness of different locations to pedestrians. When the target location is closer to the safety exit, pedestrians are more likely to choose the location, and the location is more attractive to pedestrians. In different models, due to different simulation rules, the static domain parameter calculation methods used are also different. In this paper, the static field parameter values based on Euclidean distance are used, and the calculation is as follows:

$$S_{xy} = \begin{cases} \min_n \left( \min_m \left( \sqrt{(x - x_n^m)^2 + (y - y_n^m)^2} \right) \right) & \text{cells}(x, y) \text{ are not walls or obstacles,} \\ M & \text{cells}(x, y) \text{ are walls or obstacles.} \end{cases} \quad (10)$$

Among them,  $(x, Y)$  is the coordinate of a cell in the system,  $S_{xy}$  is the static field parameter value of the cell  $(x, Y)$ ,  $x_n^m, y_n^m$  are the  $m$ th cell in the  $n$ th gate, and  $M$  is a large positive number, which means that pedestrians cannot move to this location.

Pedestrians have 9 optional positions in their moving fields, and each position has a static field parameter value. When the pedestrian stays still, the pedestrian's moving

income is 0. When a pedestrian moves horizontally or vertically, the pedestrian's step length is 1, and the movement gain is the difference between the pedestrian's current position and the static field parameter of the target position. When a pedestrian moves obliquely, that is, the pedestrian's step length is  $\sqrt{2}$ , and the movement benefit is the difference between the pedestrian's current position and the static field

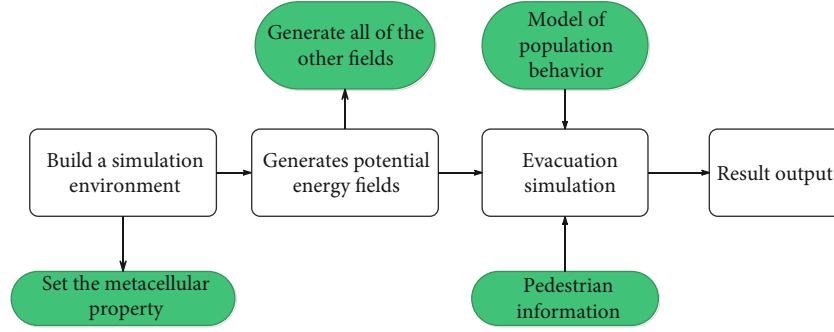


FIGURE 10: Simulation system structure.

parameter of the target position divided by  $\sqrt{2}$ . With pedestrians as the center, the direction parameter in the moving field is  $D_{ij}$ :

$$D_{ij} = \begin{cases} \frac{S_{oo} - S_{ij}}{1} & \text{when pedestrians wait or move horizontally or vertically,} \\ \frac{S_{oo} - S_{ij}}{\sqrt{2}} & \text{when pedestrians move obliquely.} \end{cases} \quad (11)$$

Among them,  $S_{oo}$  is the static field parameter value of the center position of the pedestrian moving field, and  $S_{xy}$  is the static field parameter value of the moving position that the pedestrian can choose.

When  $D_{ij} = 0$ , it means that when pedestrians choose this location, the distance to the safety exit will neither increase nor decrease. When  $D_{ij} > 0$ , it means that pedestrians choosing this location will reduce the distance to the safety exit; that is, pedestrians are more inclined to choose this location. When  $D_{ij} < 0$ , it means that pedestrians choosing this location will increase the distance to the safety exit. Therefore, pedestrians will reduce the possibility of choosing the location.

During the evacuation of pedestrians, the cell position in the moving area may be occupied, repelling pedestrians from entering this position. However, if there are space cells in the moving area, it will have the greatest attraction to pedestrians. Therefore, the value of the space parameter  $E_{ij}$  is given by

$$E_{ij} = \begin{cases} 1 & \text{cell position is empty,} \\ 0 & \text{central cell location,} \\ -1 & \text{cell position occupied.} \end{cases} \quad (12)$$

In addition, because the pedestrian direction parameters  $D_{ij}$  and  $E_{ij}$  space parameters are of different magnitudes, they cannot be added directly. Considering that when a position in the moving area is empty and the direction parameter of the position is the largest, the position of the pedestrian's maximum moving income is that position. When there is a moving position, the pedestrian's moving income is positive, but the position is occupied by other

pedestrians; the pedestrian will hardly choose this position. Therefore,  $\max(D)$  is taken as a constant parameter and multiplied by the space parameter  $E_{ij}$  to make it have the same magnitude as the space parameter  $E_{ij}$  and the direction parameter  $D_{ij}$ . Therefore, the pedestrian's mobile income  $P_{ij}$  is

$$P_{ij} = D_{ij} + E_{ij} \times \max(D). \quad (13)$$

Among them,  $P_{ij}$  is the pedestrian's movement income,  $D_{ij}$  is the pedestrian's direction parameter,  $E_{ij}$  is the pedestrian's space parameter, and  $\max(D)$  is the maximum value of the direction parameter's profit in the pedestrian movement field.

Similar to the moving area of pedestrians, the moving area of the space cell refers to the space cell as the center, and pedestrians in the eight positions around it may move to the space position, as shown in Figure 8. When formulating an appropriate probability model, the movement probability of the surrounding pedestrians is determined by the crowding force received and the initial target position, and the movement probability determines the moving pedestrian.

The final crowding force  $E$  of the eight pedestrians around the space cell is decomposed in the direction of the space cell, and the force component of the pedestrian in the direction of the cell is

$$|F_{ij \rightarrow \infty}| = \begin{cases} |F_{ij \rightarrow \infty}| & F_{ij \rightarrow \infty} > 0, \\ 0 & F_{ij \rightarrow \infty} \leq 0. \end{cases} \quad (14)$$

Among them,  $|F_{ij \rightarrow oo}|$  is the force component of the pedestrian  $(i, j)$  in the direction of the space cell in the moving field, and  $F_{ij \rightarrow \infty}$  is the force component of the pedestrian  $(i, j)$  in the direction of the space cell.

Therefore, the probability that pedestrians in the moving area of the space cell choose the cell due to the crowding force is

$$m_{ij} = \frac{|F_{ij \rightarrow \infty}|}{\sum(|F_{ij \rightarrow \infty}|)}. \quad (15)$$

TABLE 2: Effect evaluation of the dynamic analysis model.

Number	Dynamic simulation
1	87.9
2	88.9
3	94.6
4	92.9
5	87.0
6	92.2
7	94.0
8	86.8
9	89.6
10	89.2
11	86.4
12	91.2
13	87.0
14	93.2
15	92.6
16	86.4
17	94.0
18	89.7
19	93.3
20	90.1
21	89.7
22	86.1
23	92.3
24	90.1
25	95.0
26	90.8
27	94.9
28	91.4
29	93.1
30	89.5
31	94.6
32	92.6
33	93.7
34	90.0
35	91.1
36	92.0
37	90.2
38	93.4
39	90.3
40	91.7
41	90.7
42	88.1
43	87.9
44	88.7
45	92.6
46	93.8
47	87.5
48	86.3

TABLE 2: Continued.

Number	Dynamic simulation
49	91.4
50	94.2
51	93.0
52	94.6
53	88.1
54	89.4
55	89.9
56	91.7
57	94.7
58	93.6
59	91.7
60	93.0

Among them,  $m_{ij}$  is the probability of pedestrians  $(i, j)$  in the mobile field choosing space cells due to crowding forces.

The greater the crowding force component of the pedestrian in the direction of the space cell, the greater the probability that the pedestrian will choose the location, which is consistent with the fact that pedestrians are crowded to other locations due to the crowding force in the actual movement.

Secondly, it is also necessary to consider the pedestrian's own initial target location selection. After calculating the pedestrian income, the target positions of all pedestrians are obtained. Through the judgment of the congestion state, the situation where multiple pedestrians may choose a location is processed.  $q_{ij}$  indicates whether the pedestrian  $(i, j)$  in the mobile field chooses the location; then, there are

$$q_{ij} = \begin{cases} 1 & \text{pedestrians select this location,} \\ 0 & \text{pedestrians do not choose.} \end{cases} \quad (16)$$

Therefore, the probability that the pedestrian  $(i, j)$  in the moving field of the space cell selects the space cell due to its initial target position is

$$n_{ij} = \frac{q_{ij}}{\sum q_{ij}}. \quad (17)$$

Among them,  $n_{ij}$  is the probability that pedestrians  $(i, j)$  choose the space cell due to their own initial position selection. Finally, the probability of the pedestrian  $(i, j)$  in the space cell moving field moving to the space cell is

$$P_{ij} = \begin{cases} \beta * m_{ij} + (1 - \beta) * n_{ij} & \sum m_{ij} = 1 \text{ CO } \sum n_{ij} = 1, \\ m_{ij} & \sum m_{ij} = 1 \text{ CO } \sum n_{ij} = 0, \\ n_{ij} & \sum m_{ij} = 0 \text{ CO } \sum n_{ij} = 1, \\ 0 & \sum m_{ij} = 0 \text{ CO } \sum n_{ij} = 0. \end{cases} \quad (18)$$

TABLE 3: Effect evaluation of the evacuation management system for sports events based on the cellular automata.

Number	Evacuation effect
1	72.3
2	72.1
3	80.3
4	70.4
5	81.7
6	71.3
7	83.3
8	82.4
9	79.3
10	80.8
11	72.2
12	71.0
13	72.5
14	86.2
15	84.6
16	74.1
17	79.5
18	77.2
19	81.4
20	81.7
21	77.4
22	85.2
23	75.5
24	69.1
25	69.3
26	82.2
27	81.0
28	78.6
29	86.7
30	86.5
31	72.4
32	69.9
33	70.5
34	77.9
35	69.2
36	82.5
37	70.0
38	75.9
39	78.5
40	83.2
41	80.1
42	69.5
43	83.7
44	80.6
45	83.8
46	81.4
47	80.8
48	75.7

TABLE 3: Continued.

Number	Evacuation effect
49	84.2
50	74.3
51	70.3
52	76.2
53	77.1
54	84.0
55	85.3
56	76.8
57	85.1
58	86.1
59	74.1
60	72.7

Among them,  $m_{ij}$  is the probability of pedestrians  $(i, j)$  choosing the space cell due to crowding force,  $n_{ij}$  is the probability of pedestrians  $(i, j)$  choosing the space cell due to their own initial target position selection, and  $\beta$  is the adjustment parameter. When  $\beta$  is close to 1, the influence of pedestrian crowding force is relatively large. When  $\beta$  is close to 0, the influence of pedestrian's initial target position selection is relatively large. In this paper, 0.5 is considered to be equivalent. When  $\sum m_{ij} = 0$  and  $\sum n_{ij} = 0$ , it means that no pedestrian in the moving area has selected the space cell.

#### 4. Model Effect Analysis

The third part builds an intelligent evacuation model and evaluates the evacuation management effect of sports events on this basis. Generally speaking, whether a person can reach a goal grid is affected by knowledge, reason, physical strength, and other comprehensive forces. The method of movement is as follows in Figure 9.

According to cellular automata, this system includes scene editing, potential energy field calculation, crowd behavior model, and evacuation simulation. The structure is as follows in Figure 10.

The dynamic analysis model of this paper is studied through experimental research, and the performance effect of the cellular automata in the dynamic analysis model is statistically evaluated by the expert evaluation method, and the results shown in Table 2 below are obtained.

It can be seen from Table 2 that the cellular automata perform very well in the dynamic analysis model. On the basis of the above research, the evacuation management system of sports events based on the cellular automata constructed in this paper is evaluated, and the evaluation results are shown in Table 3 below.

From the experimental analysis, it can be seen that the evacuation management system for sports events based on the cellular automata proposed in this paper can play an important role in the evacuation of sports events.

## 5. Conclusion

In the study of evacuation of stadium personnel, it is necessary to study the evacuation characteristics of stadiums as well as the characteristics of individual personnel in evacuation situations. The research on the virtual exercise of stadium personnel evacuation includes the above two research aspects, which can provide an effective research approach for the evacuation of stadium personnel and even other venues. Therefore, the research on the virtual exercise system for evacuation of stadiums can not only provide a basis for determining the rationality of stadium construction but also provide a basis for the formulation of evacuation plans. This paper applies dynamic analysis to the evacuation management process of sports events and simulates the evacuation process of sports events through cellular automata to improve the evacuation management effect of sports events. The experimental research results show that the evacuation management system for sports events based on cellular automata proposed in this paper can play an important role in the evacuation of sports events.

## Data Availability

The data used to support the findings of this study are available from the corresponding author upon request.

## Conflicts of Interest

The authors declare that they have no known competing financial interests or personal relationships that could have appeared to influence the work reported in this paper.

## Acknowledgments

This work was supported by the project of Basic scientific research operation fees of central universities (2020SKTY01).

## References

- [1] Y. Cao, Z. Ding, F. Ren, and L. Guo, "Efficient multi-vehicle navigation based on trajectory vector features considering non-uniform destination distribution for emergency evacuation," *International Journal of Wireless and Mobile Computing*, vol. 16, no. 3, pp. 195–203, 2019.
- [2] Z. Cai, F. Ren, Y. Chi, X. Jia, L. Duan, and Z. Ding, "Multi-vehicles dynamic navigating method for large-scale event crowd evacuations," *Geo Informatica*, vol. 22, no. 2, pp. 435–462, 2018.
- [3] H. Dong, M. Zhou, Q. Wang, X. Yang, and F. Y. Wang, "State-of-the-art pedestrian and evacuation dynamics," *IEEE Transactions on Intelligent Transportation Systems*, vol. 21, no. 5, pp. 1849–1866, 2020.
- [4] M. W. Aziz, F. Naeem, M. H. Alizai, and K. B. Khan, "Automated solutions for crowd size estimation," *Social Science Computer Review*, vol. 36, no. 5, pp. 610–631, 2018.
- [5] S. Mustapha, A. Kassir, K. Hassoun, B. A. A. Modad, H. Abi-Rached, and Z. Dawy, "Joint crowd management and structural health monitoring using fiber optic and wearable sensing," *IEEE Communications Magazine*, vol. 57, no. 4, pp. 62–67, 2019.
- [6] M. M. de Almeida and J. von Schreeb, "Human stampedes: an updated review of current literature," *Prehospital and Disaster Medicine*, vol. 34, no. 1, pp. 82–88, 2019.
- [7] N. Dai and Y. Zhang, "RETRACTED ARTICLE: Rainfall-type landslide warning and sports public service performance evaluation based on data anomaly detection," *Arabian Journal of Geosciences*, vol. 14, no. 17, pp. 1–14, 2021.
- [8] U. Singh, J. F. Determe, F. Horlin, and P. De Doncker, "Crowd forecasting based on WiFi sensors and LSTM neural networks," *IEEE Transactions on Instrumentation and Measurement*, vol. 69, no. 9, pp. 6121–6131, 2020.
- [9] X. Xiao-wei, "Study on the intelligent system of sports culture centers by combining machine learning with big data," *Personal and Ubiquitous Computing*, vol. 24, no. 1, pp. 151–163, 2020.
- [10] J. Yu, C. Zhang, J. Wen, W. Li, R. Liu, and H. Xu, "Integrating multi-agent evacuation simulation and multi-criteria evaluation for spatial allocation of urban emergency shelters," *International Journal of Geographical Information Science*, vol. 32, no. 9, pp. 1884–1910, 2018.
- [11] X. Jian, H. Wang, and X. Zhang, "Optimal exit layout strategy for crowd safety evacuation in a ramp domain," *Journal of Management Science and Engineering*, vol. 2, no. 3, pp. 209–226, 2017.
- [12] Z. Shahhoseini and M. Sarvi, "Traffic flow of merging pedestrian crowds: how architectural design affects collective movement efficiency," *Transportation Research Record*, vol. 2672, no. 20, pp. 121–132, 2018.
- [13] X. Liu, S. Cao, L. Zheng, F. Gong, X. Wang, and J. Zhou, "POCA4SD: a public opinion cellular automata for situation deduction," *IEEE Transactions on Computational Social Systems*, vol. 8, no. 1, pp. 201–213, 2021.
- [14] B. L. Bennett, T. Hew-Butler, M. H. Rosner, T. Myers, and G. S. Lipman, "Wilderness Medical Society clinical practice guidelines for the management of exercise-associated hyponatremia: 2019 update," *Wilderness & Environmental Medicine*, vol. 31, no. 1, pp. 50–62, 2020.
- [15] S. Deng, C. Zhang, C. Li, J. Yin, S. Dustdar, and A. Y. Zomaya, "Burst load evacuation based on dispatching and scheduling in distributed edge networks," *IEEE Transactions on Parallel and Distributed Systems*, vol. 32, no. 8, pp. 1918–1932, 2021.
- [16] H. M. Al-Ahmadi, I. Reza, A. Jamal, W. S. Alhalabi, and K. J. Assi, "Preparedness for mass gatherings: a simulation-based framework for flow control and management using crowd monitoring data," *Arabian Journal for Science and Engineering*, vol. 46, no. 5, pp. 4985–4997, 2021.
- [17] J. M. Gurney, P. E. Loos, M. Prins, D. W. Van Wyck, R. R. McCafferty, and D. W. Marion, "The prehospital evaluation and care of moderate/severe TBI in the austere environment," *Military Medicine*, vol. 185, Supplement\_1, pp. 148–153, 2020.
- [18] A. Halder, K. Kuklane, M. Miller, A. Nordin, J. Unge, and C. Gao, "Physiological capacity during simulated stair climbing evacuation at maximum speed until exhaustion," *Fire Technology*, vol. 57, no. 2, pp. 767–790, 2021.
- [19] D. Sharma, A. P. Bhonekar, A. K. Shukla, and C. Ghanshyam, "A review on technological advancements in crowd management," *Journal of Ambient Intelligence and Humanized Computing*, vol. 9, no. 3, pp. 485–495, 2018.

## Research Article

# Emotional Calculation Method of Rural Tourist Based on Improved SPCA-LSTM Algorithm

Xi Chen <sup>1,2,3</sup>

<sup>1</sup>College of Geography and Tourism, Harbin University, Heilongjiang, Harbin 150086, China

<sup>2</sup>Heilongjiang Province Key Laboratory of Cold Region Wetland Ecology and Environment Research, Heilongjiang, Harbin 150086, China

<sup>3</sup>Harbin Institution of Wetland Research, Heilongjiang, Harbin 150086, China

Correspondence should be addressed to Xi Chen; chenxi005253@126.com

Received 4 January 2022; Revised 24 January 2022; Accepted 5 February 2022; Published 23 February 2022

Academic Editor: Wen Zeng

Copyright © 2022 Xi Chen. This is an open access article distributed under the Creative Commons Attribution License, which permits unrestricted use, distribution, and reproduction in any medium, provided the original work is properly cited.

New technologies such as big data and cloud computing provide new means and tools for rural development. The big rural tourism, with its convenience, quickness, and low threshold, presents great convenience for tourists' emotional calculation and has become one of the main sources of tourism big data. Under the guidance of big data theory and emotion theory, this paper proposes an emotional calculation method of rural tourists based on improved SPCA-LSTM algorithm, taking big text data as data source. Firstly, the improved TF-IDF algorithm is designed to highlight the importance of feature items, and the word vector trained by word2vec model is applied to represent the rural tourism data text. Then, a weighted sparse PCA (RSPCA) is constructed to reduce the dimension of massive word vector features. RSPCA introduces the weighted  $l_1$  optimization framework and LASSO regression model into the mathematical model of PCA algorithm and establishes a new data dimension reduction model. Thereupon, the long-term and short-term memory convolution network with attention mechanism is employed to extract text features. Finally, the feature vector is utilized to calculate the rural tourist's emotion by softmax function. The experimental results indicate that the improved SPCA-LSTM algorithm, whose performance index is better than other existing algorithms, is effective in calculating tourists' emotions. Also, it is more suitable for the research of tourist sentiment calculation in the era of big data.

## 1. Introduction

Rural revitalization is an important part of urban economic development and a beneficial assist for urban-rural integration. Rural tourism is a relatively efficient way that China has explored during poverty alleviation for more than 30 years, and a further way to overcome the problem of rural revitalization during the "14th five-year plan" [1]. New technologies, such as artificial intelligence, 5G, and big data, bring infinite possibilities to China's economic and social development, provide new means and tools for rural development, and are powerful support for rural revitalization in the new era. Not only does digital technology empowering rural revitalization change the traditional production mode and lifestyle, but also subtly changes farmers' practice and thinking mode.

Promoting rural revitalization and industrial prosperity is the endogenous power support. Rural characteristics and the law of information development should be respected. For villages with rich local characteristic resources and relatively complete information facilities, they can rely on "Internet +" to dig local characteristic cultural resources and do a good job of digital "cultural tourism" and "agricultural tourism" combined with articles to build Internet characteristic tourism villages [2].

With the rise of new media and social networks and the advent of the era of big data, various platforms have generated hundreds of millions of rural tourism-related data. The past data showcase that since 2009, the amount of data related to rural tourism has increased geometrically year by year. Due to the convenience of social transportation and the development of social networks, the data with "rural

tourism” as the key word is widely spread in rural areas. People’s demand for “rural tourism” is increasing day by day. The data of “rural tourism” can be analyzed and mined through various information release platforms [3, 4].

Rural tourism reception will increase steadily. Data show that from January to August 2020, the number of leisure agriculture and rural tourism in China decreased by 60.9% to 1.207 billion. The epidemic situation in COVID-19 has pushed the “pause button” for leisure agriculture and rural tourism. However, after the domestic epidemic was cleared, all localities restarted the rural leisure tourism market in an orderly manner. People’s enthusiasm for rural scenery and fresh air is high. With the gradual restoration of production and living order, the suppressed demand of urban and rural residents will continue to be released. The countryside with beautiful scenery and beautiful ecology is more attractive than ever before [5].

The rapid development of information technology provides an efficient and rapid way for rural tourist information acquisition [6]. The main reason for the popularity of rural tourism is that it provides tourists with multilevel experiences, and this information can be obtained through the classification of rural tourism big data driven by the rural revitalization strategy. The trend of rural tourism can be analyzed according to different types, different times, different spaces, and different groups. On various data platforms, search and collect data for specific keywords, and deeply analyze these data to get the corresponding results. The long-term data are verified and used as prediction support. Data mining on the future rural tourism market can make suggestions for future rural tourism [7].

Rural tourism is an activity of interpersonal communication and emotional exchange, and emotion runs through the whole process of tourism activities. “Emotion is a person’s attitude experience about whether objective things can meet his own needs.” Tourist emotion refers to the pleasure, excitement, sadness, anger, regret, and other emotional experiences generated by tourists in tourism activities due to the influence of personal factors or external environment on whether tourism activities meet individual basic needs and social needs and presents diversity and variability with the progress of tourism [8]. These emotions not only constitute an important tourist experience but also exert an important influence on tourist motivation, satisfaction, behavioral intention, and interpersonal interaction. In tourism, tourists get information and share their travel experiences through online platforms and social media. The text, image, audio, and video released by it become the main data source of tourism big data [9]. Among them, the texts content with its convenient, simple, intuitive, fast, and low threshold for tourists to express emotions and information exchange to provide convenience; in the tourism, big data occupies an increasingly important position. The mining of text data can provide decision support for tourism planning and marketing, making sentiment analysis in tourism big data a hot issue in tourism research [10].

With the deepening of research, emotion analysis, which is to effectively analyze and mine information and identify emotional tendencies, becomes more sophisticated. Also,

there are researches on emotion calculator, emotion summary, product attribute mining, and so on. In recent years, with the development of big data, there are many emotion analysis models and software at home and abroad, which provide strong support for emotion research. There are three methods of text sentiment analysis: dictionary-based method, machine learning method, and deep learning method [11]. The dictionary-based approach is mainly through the development of a set of emotional dictionaries and rules. Then, sentiment value is calculated by sentence breaking, analysis, and dictionary matching. Finally, the emotional value is used as the basis to judge the emotional tendency of the text. Although the method based on emotion dictionary has high accuracy, it has low recall rate. Another problem of the dictionary-based approach is the relatively high cost of dictionary construction [12]. The machine learning-based approach transforms the problem of text sentiment analysis into a supervised classification problem. Annotate the training text. Supervised machine learning is then carried out [13]. Finally, the test data is used to predict the results through the model. The method based on machine learning generally includes two steps: text preprocessing and the selection of classification algorithm. Methods based on deep learning use different artificial neural network models to map text big data into vector space to obtain numerical representation of words. The numerical expressions are then used as input to the deep learning model. The optimal model is obtained through training and parameter optimization. The process is much the same as that of emotion computing based on machine learning. However, the selection of feature extraction and classification model for text vectorization is different from machine learning [14, 15].

This paper proposes a rural tourist emotional calculation method based on the improved SPCA-LSTM algorithm according to the above research. The algorithm improves the traditional TF-IDF algorithm by considering the distribution and location information of feature items within and between classes and combines it with Word2vec word vector to express the text. Then, reweighted SPCA algorithm is used to reduce the dimensionality of the text word vector, so that the original data features of the sample can be retained as much as possible while reducing the dimensionality. Finally, long-short-term memory (LSTM) and attention mechanism network are used to realize the emotional computing of rural tourists.

## 2. Tourist Emotion Calculation Method in This Paper

*2.1. Text Representation and Feature Selection (Word Vector Representation).* In view of the shortcomings of traditional TF-IDF in the field of text classification, this paper improves the traditional TF-IDF algorithm to better reflect the importance of feature items in the text.

- (1) Introducing intraclass factors to describe the distribution relationship of feature items

The intraclass factor  $inter C_i$  is introduced to judge the uniformity of the distribution of feature words in the

intra-class documents, that the intra-class factor value is small means that the feature items are unevenly distributed in the class and may be distributed only in a few documents in the class, with weak classification ability. On the contrary, the feature item has strong classification ability. The calculation formula of in-class factor of characteristic term is shown in

$$\text{inter } C_i = \frac{1}{S_{ij}}, \quad (1)$$

where  $j$  represents the category.  $S_{ij}$  represents the standard deviation of feature item  $i$  in category  $j$ , which reflects whether feature items are evenly distributed in the category. The smaller the standard deviation, the more uniform the distribution, the stronger the classification ability of this feature word. The calculation of  $S_{ij}$  is shown in formula (2).

$$S_{ij} = \sqrt{\frac{\sum_{p=1}^K (tf_{ip} - \bar{t}f_{ij})^2}{K}}, \quad (2)$$

where  $K$  is the total number of documents in category  $j$ .  $tf_{ip}$  indicates the number of times that document  $p$  contains feature  $i$ .  $\bar{t}f_{ij}$  represents the mean number of times of all documents of feature word  $i$  in category  $j$ .  $\bar{t}f_{ij} = 1/K \sum_{k=1}^K tf_{ik}$ .

### (2) Improve the discrimination between classes

In order to improve the weight of feature items with high classification,  $m/m_i$  is used to express the importance of feature item  $i$  in category.  $N/n_i$  indicates the importance of feature items in all documents, where  $N$  represents the total number of documents in the corpus.  $n_i$  indicates the number of documents in which the feature word  $i$  appears in the corpus.  $m$  represents the total number of categories.  $m_i$  indicates the number of categories containing feature items. If the  $m/m_i$  value is larger, it indicates that feature items are distributed in fewer categories and have strong classification ability. If the value is small, the feature item is not representative. The specific calculation definition is shown in

$$TF_{ij} = \bar{t}f_{ij}, \quad (3)$$

$$IDF_i = \log \left( \frac{N}{n_i} \times \frac{m}{m_i} \right). \quad (4)$$

$TF_{ij}$  represents the word frequency of feature  $i$  relative to category  $j$ . The higher the value of  $TF_{ij}$ , the better the feature  $i$  can represent this category.  $IDF_i$  represents the distribution ratio of feature  $i$  among categories. The higher the  $IDF_i$  value, the stronger the category discrimination ability of characteristic  $i$ .

### (3) Word distance factor

The word distance indicates the difference between the last appearance position and the first appearance position

of the feature item in the document, reflecting the range of the feature item in the text. The larger the range of feature items in this document, that is, the larger the word distance, the better it can reflect the category of the document. On the contrary, if the feature items are only distributed in a small range and the word distance is small, the category of the document cannot be well represented. If this feature item appears frequently locally in a document, the TF value will be increased, affecting the final algorithm result. Therefore, this paper introduces the word distance factor to avoid this problem. The formula for calculating the word distance factor is shown in

$$WDF_{ip} = \frac{\text{last}(g_{ip}) - \text{first}(g_{ip}) + 1}{\text{fea}(p)}, \quad (5)$$

where  $\text{last}(g_{ip})$  represents the position number of the last appearance of feature item  $i$  in document  $p$ .  $\text{first}(g_{ip})$  represents the position number of the first appearance of feature item  $i$  in document  $p$ .  $\text{fea}(p)$  represents the total number of feature items in document  $p$ .

Considering the intra-class, interclass, and position factors of feature items, a feature item weight calculation method TF-IDF-ICP (interior factor, category factors, and position) for text classification is proposed, which is defined as

$$TF-IDF-ICP_{ip} = TF_i * IDF_i * \text{inter } C_i * WDF_{ip}, \quad (6)$$

where  $TF_i$  represents the word frequency of feature  $i$  relative to categories.  $IDF_i$  represents the distribution ratio of feature  $i$  among categories.  $\text{inter } C_i$  represents the intra-class factor.  $WDF_{ip}$  represents the word distance factor. Artificial neural network can only accept numerical input, not a word as a string. In order to enable the deep learning model to process text data, first of all, it is necessary to express natural language as a numerical vector that the model can recognize. Word2vec is based on the simple shallow artificial neural network, according to the given large corpus, through training and optimization model to get the training result—word vector. This word vector can quickly and effectively express a word as a numerical vector, and can measure the similarity between words well, so as to represent the different attributes of the word.

In text classification, it is necessary to convert the phrases in the text into low-dimensional word vectors. First, the text  $d$  is segmented by jieba. Text  $d$  after segmentation is  $D_i = [w_1, w_2, \dots, w_i, \dots, w_n]$ .  $w_i$  stands for the  $i$ th word in the document.  $n$  represents the total number of words in the document. Word2vec is then used to vectorize the text.  $w_i$  is expressed as  $[v_1, \dots, v_i, \dots, v_l]$ .  $l$  is the dimension of word vector, that is, each word is represented by  $l$  dimension. Word vectors trained by Word2vec retain the relevance of words in the original corpus, but ignore the importance of different words in the text. Therefore, this paper uses the improved TF-IDF algorithm TF-IDF-ICP to calculate the weight of each word and combine it with Word2vec word vector. The specific text representation is shown in



$$\text{vec}(d) = D * \text{TF-IDF-ICP}. \quad (7)$$

$D$  stands for Word2vec word vector.

The specific steps of weighting Word2vec are shown in Figure 1.

**2.2. Dimension Reduction of Word Vector.** It is a burden for the training and prediction of machine learning model to spend the conference. In this paper, the improved SPCA is designed to reduce the dimension of word vector to reduce the dimension of dataset. Then, the basic features are selected to minimize the information loss while compressing the data.

### (1) Reweighted $\ell_1$ optimization framework

$\ell_1$  optimization problem originates from  $\ell_0$  optimization problem.  $\ell_0$  optimization problem can be expressed as follows: given an  $m \times n$  matrix  $A$  and a nonzero vector  $b$ , where  $m \leq n$ . The sparse solution of  $Ay = b$  is solved. The mathematical form is as follows:

$$\begin{aligned} \min_{y \in \mathbb{R}^n} \|y\|_0, \\ \text{s.t. } Ay = b, \end{aligned} \quad (8)$$

where  $\|y\|_0$  represents the number of nonzero solutions of  $y$ . Since Equation (8) is a nonconvex optimization and NP difficult optimization problem, there is no effective solution at present, so only its approximate solution can be considered. Jojic et al. proved that the convex hull of  $\|y\|_0$  is completely  $\ell_1$  norm. Through convex analysis, it is reasonable to use  $\|y\|_1$  to replace  $\|y\|_0$  for optimization operation, thus leading to  $\ell_1$  optimization problem. The mathematical model for the optimization problem is shown as follows:

$$\begin{aligned} \min_{y \in \mathbb{R}^n} \|y\|_1, \\ \text{s.t. } Ay = b. \end{aligned} \quad (9)$$

$\|y\|_1 = \sum_{i=1}^n |y_i|$ , that is, the sum of absolute values of each element in the solution vector.  $\ell_1$  optimization problem is a convex optimization problem that can be efficiently solved by using a convex programming tool. Through numerous experiments, it is shown for  $\ell_1$  that by reasonably weighting their  $\ell_1$  norm and iteratively updating the weights, the performance of their  $\ell_1$  optimization framework is greatly enhanced. In the case of their  $\ell_1$  norm, the larger one is punished more than the  $\ell_0$  norm, according to the definitions for  $\ell_1$  and  $\ell_0$ , while their  $\ell_0$  norm treats both equally. Thus, if they add a weight matrix to the  $\ell_1$  optimization problem, their coefficients of different sizes are punished equally. Then, their  $\ell_1$  optimization problem will be infinitely close to their  $\ell_0$  optimization problem, resulting in a sparser solution. This is the advantage for a weighted  $\ell_1$  optimization framework. The optimization problem for a weighted  $\ell_1$  can be expressed as follows:

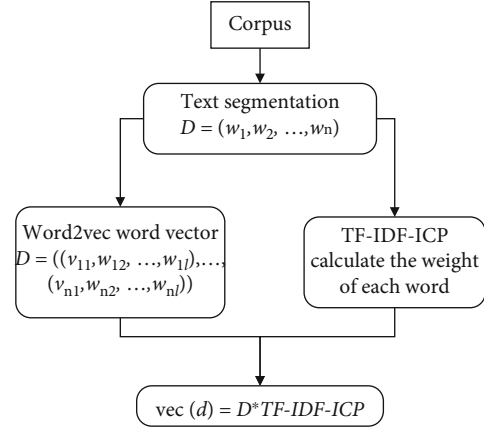


FIGURE 1: Flow chart of weighted Word2vec.

$$\min_{y \in \mathbb{R}^n} \|Wy\|_1. \quad (10)$$

By selecting an appropriate weighted matrix  $W$ , the reweighted  $\ell_1$  optimization problem obtains a sparser solution for  $\ell_1$  than the traditional  $\ell_1$  optimization problem, thus making the result more like the  $\ell_0$  optimization problem. The problem then turns to how to select a weighted matrix  $W$  so that the optimization problem for a reweighted  $\ell_1$  can obtain a rarer solution while ensuring that the result is correct. According to the correlation proof, the absolute value of the weight should be inversely proportional to the value of the corresponding element in the final solution. However, if the specific value of the final solution is not known, the appropriate weighting matrix cannot be selected. At the same time, if the appropriate weighting matrix cannot be selected, the correct final solution cannot be obtained. A reasonable choice to solve this problem is to use an iterative approach, that is, by setting the weighted matrix as the identity matrix at the beginning, they can obtain an approximate solution of the reweighted  $\ell_1$  optimization problem. In the second iteration, the weighted matrix can be updated according to the approximate solution obtained, and then, the process is repeated until the termination condition is satisfied.

### (2) Weighted sparse principal component analysis algorithm

Compared with the traditional  $\ell_1$  optimization framework, the reweighted  $\ell_1$  optimization framework can obtain sparser solutions. Therefore, in this paper, a new mathematical model is presented by introducing the reweighted  $\ell_1$  optimization framework and LASSO regression model into the principal component analysis algorithm. This is the reweighted sparse principal component analysis algorithm which aims to obtain more sparse solutions.

Weighted sparse principal component analysis algorithm is an optimization model based on principal component analysis algorithm, upon which an optimization framework and LASSO regression model are added to generate sparse solutions. The mathematical model of the principal component analysis algorithm is shown in formula:

$$\arg \min_{\mathbf{V} \in \mathbb{R}^{n \times g}} \mathbf{Y} - \mathbf{Y}\mathbf{V}\mathbf{V}^T \quad (11)$$

where the matrix  $\mathbf{Y}$  is an  $n \times c$  order matrix formed by the original data. The matrix  $\mathbf{V}$  is a set of orthogonal bases.  $\mathbf{V}^T$  represents the transpose matrix of the matrix  $\mathbf{V}$ . The principal component analysis algorithm reduces the dimension of the original data by using the base transformation method. The weighted sparse principal component analysis algorithm proposed in this paper adds an optimization frame and LASSO regression model to the principal component analysis algorithm. The mathematical model is as follows:

$$\arg \min_{\mathbf{G}, \mathbf{H}} \sum_{i=1}^n \mathbf{Y} - \mathbf{Y}\mathbf{H}\mathbf{G}^T + \lambda \|\mathbf{H}\|_F^2 + \|\mathbf{W} \cdot \mathbf{H}\|_1, \quad (12)$$

s.t.  $\mathbf{G}^T \mathbf{G} = \mathbf{I}, \mathbf{H}^T \mathbf{H} = \mathbf{I}$ ,

in which  $\mathbf{Y}$  is an  $n \times c$  matrix.  $\mathbf{G}$  and  $\mathbf{H}$  are orthogonal matrices of order  $c \times d$ . The matrix  $\mathbf{G}^T$  represents the transposition of the matrix  $\mathbf{G}$  in which  $\mathbf{G}_{c \times d} = [\mathbf{g}_1, \mathbf{g}_2, \dots, \mathbf{g}_d]$ .  $\mathbf{H}_{c \times d} = [\mathbf{h}_1, \mathbf{h}_2, \dots, \mathbf{h}_d]$ .  $\mathbf{W}$  is a weighted matrix of order  $c \times c$ , and the matrix  $\mathbf{W}$  is a diagonal matrix.  $\lambda$  is the regularization coefficient. After expanding the norm in formula (12), formula (13) can be get:

$$\arg \min_{\mathbf{G}, \mathbf{H}} \sum_{i=1}^n y_i - \mathbf{H}\mathbf{G}^T \mathbf{y}_i^2 + \lambda \sum_{j=1}^d \mathbf{h}_j^2 + \sum_{j=1}^d \mathbf{W} \cdot \mathbf{h}_{j1}. \quad (13)$$

$\mathbf{W}$  is the weighted matrix, and  $\mathbf{h}_i$  is the column vector constituting matrix  $\mathbf{H}$ . According to the correlation between eigenvalues and eigenvectors, we can get:

$$\mathbf{W}\mathbf{e}_i = \varepsilon \mathbf{e}_i, \quad (14)$$

where  $\varepsilon$  is the eigenvalues corresponding to the vector  $\mathbf{e}_i$ . According to formula (14), formula (13) can be expanded as follows:

$$\arg \min_{\mathbf{G}, \mathbf{H}} \sum_{i=1}^n y_i - \mathbf{H}\mathbf{G}^T \mathbf{y}_i^2 + \lambda \sum_{j=1}^d \mathbf{h}_j^2 + \sum_{j=1}^d \varepsilon_j \mathbf{h}_{j1}, \quad (15)$$

$$\text{s.t. } \mathbf{G}^T \mathbf{G} = \mathbf{I}, \mathbf{H}^T \mathbf{H} = \mathbf{I}.$$

When solving the mathematical model shown in Equation (15), it can be solved by alternating minimization method. The idea of alternating minimization method is to first assume that two initial matrices are given and use these two initial matrices for iterative calculation. During iteration, the matrix generated by the previous iteration is used to solve the matrix of the current iteration. That is, starting from any  $(\mathbf{G}_0, \mathbf{H}_0)$ , matrices  $\mathbf{G}, \mathbf{H}$  are the obtained matrices. The matrix subscript represents the number of iterations. First, an initial matrix  $\mathbf{G}_0$  or  $\mathbf{H}_0$  is given, and then, iterative calculation is carried out. At the  $p$ th iteration, assuming a given matrix  $\mathbf{G}_{(p-1)}$ , the matrix  $\mathbf{G}_{(p-1)}$  is used to solve the matrix  $\mathbf{H}_{(p)}$ . Then, the matrix  $\mathbf{H}_{(p)}$  is used to solve the matrix  $\mathbf{G}_{(p)}$ . Then, repeat the process until the number of iterations meets the preset stop conditions.

First, consider the case that the orthogonal matrix  $\mathbf{G}$  is known. When the orthogonal matrix  $\mathbf{G}$  is known, only the matrix  $\mathbf{H}$  needs to be solved in Equation (15). Therefore, the problem of solving the mathematical model shown in Equation (15) can be transformed into the problem of solving the mathematical model shown in

$$\arg \min_{\mathbf{H}} \mathbf{Y} - \mathbf{Y}\mathbf{H}\mathbf{G}^T + \lambda \|\mathbf{H}\|_F^2 + \|\mathbf{W} \cdot \mathbf{H}\|_1, \quad (16)$$

s.t.  $\mathbf{G}^T \mathbf{G} = \mathbf{I}, \mathbf{H}^T \mathbf{H} = \mathbf{I}$ .

To solve the mathematical model shown in Equation (16), a new matrix  $\mathbf{G}_\perp$  needs to be introduced. The matrix  $\mathbf{G}_\perp$  is an orthogonal matrix. Therefore, matrix  $[\mathbf{G}\mathbf{G}_\perp]$  is an orthogonal matrix of order  $c \times c$ . By projecting the rows of  $\mathbf{Y} - \mathbf{Y}\mathbf{H}\mathbf{G}^T$  onto matrix  $\mathbf{G}$  and matrix  $\mathbf{G}_\perp$ , formula (17) can be get:

$$\mathbf{Y} - \mathbf{Y}\mathbf{H}\mathbf{G}^T = (\mathbf{Y} - \mathbf{Y}\mathbf{H}\mathbf{G}^T)\mathbf{G}_{\perp F}^2 + (\mathbf{Y} - \mathbf{Y}\mathbf{H}\mathbf{G}^T)\mathbf{G}_F^2 = \mathbf{Y}\mathbf{G}_{\perp F}^2 + \|\mathbf{Y}\mathbf{G} - \mathbf{Y}\mathbf{H}\|_F^2. \quad (17)$$

Because  $\mathbf{Y}\mathbf{G}_{\perp F}^2$  is independent of  $\mathbf{H}$ , it is not necessary to consider  $\mathbf{Y}\mathbf{G}_{\perp F}^2$  when solving the matrix  $\mathbf{H}$ . Therefore, formula (15) can be deduced as shown

$$\arg \min_{\mathbf{H}} \|\mathbf{Y}\mathbf{G} - \mathbf{Y}\mathbf{H}\|_F^2 + \lambda \|\mathbf{H}\|_F^2 + \sum_{j=1}^d \varepsilon_j \mathbf{h}_{j1}. \quad (18)$$

Formula (18) is an elastic net regression problem, which can be solved by using LARS-EN (least angle regression-elastic net) algorithm [16]. At this point, when the matrix  $\mathbf{G}$  is given, the matrix  $\mathbf{H}$  can already be solved. At this time, the problem is how to solve the matrix  $\mathbf{G}$  when the matrix  $\mathbf{H}$  is given.

When the orthogonal matrix  $\mathbf{H}$  is given, the orthogonal matrix  $\mathbf{G}$  needs to be solved. Then, the mathematical model shown in formula (15) can be transformed into

$$\arg \min_{\mathbf{G}} \mathbf{Y} - \mathbf{Y}\mathbf{H}\mathbf{G}^T \text{ s.t. } \mathbf{G}^T \mathbf{G} = \mathbf{I}. \quad (19)$$

Formula (19) is the mathematical model of the principal component analysis algorithm, so it can be solved by the solution based on the basis transformation and covariance matrix or by the method based on singular value decomposition. In this paper, the method based on singular value decomposition is used to compute the singular value decomposition of  $\mathbf{Y}^T \mathbf{Y}\mathbf{H}$ . So,  $\mathbf{Y}^T \mathbf{Y}\mathbf{H} = \mathbf{U}\mathbf{\Sigma}\mathbf{V}^T$  gives us the orthogonal matrix  $\mathbf{G} = \mathbf{U}\mathbf{V}^T$ . The final solution can be obtained by repeated iteration using the above method. The solution steps of the model are as follows:

Step 1. Firstly, according to the principal component analysis algorithm model shown in formula (18), the first  $d$  principal component vectors  $[\alpha_1, \alpha_2, \dots, \alpha_k]$  of matrix  $\mathbf{Y}$  are

calculated by singular value decomposition method.  $\mathbf{Y}$  is the matrix of raw data.  $d$  is a constant value set when solving

Step 2. Initializes the matrix  $\mathbf{G}$  to the principal component vector calculated in step 1, where  $\mathbf{G} = [\alpha_1, \alpha_2, \dots, \alpha_k]$

Step 3. According to the given matrix  $\mathbf{G}$ , use LARS-EN algorithm to solve formula (18), and get the matrix  $\mathbf{G} = [\beta_1, \beta_2, \dots, \beta_k]$

Step 4. According to the calculated matrix  $\mathbf{H} = [\alpha_1, \alpha_2, \dots, \alpha_k]$ , update the matrix  $\mathbf{G}$  by singular value decomposition according to formula (19)

Step 5. Repeat steps 3 and 4 until the termination conditions are met, and the final result will be obtained

Word2vec model training sets the dimension of 400, and the obtained word vector is also 400. However, maintaining the congress brings a burden to the training and prediction of deep learning model. In this paper, the reweighted SPCA algorithm is used to reduce the dimension of word vector to reduce the dimension of dataset. Then, the basic features are selected to minimize the information loss while compressing the data.

The relationship between word vector dimension and variance value of principal components is shown in Figure 2, which indicates that the first 100 dimensions can already contain most of the information of the original data, so the first 100 dimensions of word vector data are selected as the input of the model for training.

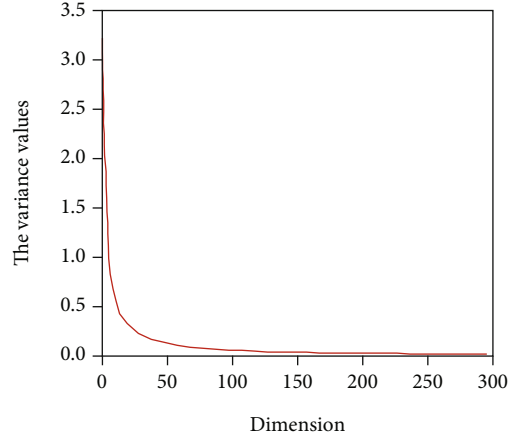


FIGURE 2: Relationship between dimension and reweighted SPCA variance.

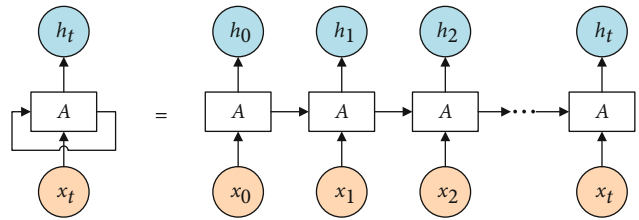


FIGURE 3: Structure of recurrent neural network.

**2.3. Deep Learning Model.** Text is transformed into distributed word vector based on word2vec. Then, the dimension reduced word vector is obtained by reweighting SPCA algorithm as the input data of deep learning model. Text data belongs to time series data, and the emergence of each word depends on its previous word and the latter word. Recurrent neural networks are generally selected for training because of this dependence.

The structure of recurrent neural network (RNN) is different from that of general neural network, which usually consists of input layer, hidden layer, and output layer. There may be multiple hidden layers. On the other hand, the cyclic neural network adds a cyclic structure on the basis of the three-layer structure (see Figure 3). The left side of the equal sign is folded. The right side of the equal sign is an expansion.  $x_t$  is the input layer.  $h_t$  is the output layer.  $A$  is the hidden layer. Each  $A$  can be regarded as a neuron, and each neuron stores the previously input state first. After the operation, some relations between the current input and the previous input are retained, thus having the function of “memory.” In this way, the previously calculated information can be captured, and the influence of the previously input data on the later data can be retained. Good timing is seized.

Long-short-term memory network (LSTM) evolved from RNN. LSTM avoids the problem of long-term dependence by deliberately designing and calculating the hidden layer state. Both RNN and LSTM have a chain structure of repeating artificial neural network modules. However, there are four neural network layers that interact with each other in a special way within each repeating module (see Figure 4).

In LSTM, “memory” is called cell state. The state of cells runs like a conveyor belt on the chain structure, and there is only a small amount of linear operation, which makes the information fidelity when it flows through the chain structure. In addition, LSTM adds information through a structure called a gate, which consists of a single sigmoid neural network layer and a single point multiplication operation, to capture long-term dependencies. The value range is 0~1, and whether the component information passes or not is controlled according to the numerical value. LSTM has three gates for protecting and controlling the cell state. The first gate is the “Forgetting Gate,” which is implemented by the sigmoid layer and selectively forgets the information in the cell state. The second gate is the “input gate,” and the sigmoid layer of the input gate determines which values to update. The candidate vector  $C_t$  created by the subsequent tanh layer selectively records the new information into the cell state. The third gate is the “output gate,” whose object is the hidden layer  $h_t$ , and the output part of the hidden layer is determined through the sigmoid layer. Then, it passes through the tanh layer, gets a value in  $(-1, 1)$ , and multiplies it with the output value of sigmoid layer to determine the information to be output. In the LSTM network, the information in memory is selected to be retained or deleted through three gates. And the previous state, current memory, and input are combined. This structure has proved to be very effective in capturing long-term dependence. Compared with a single LSTM model, Bi-LSTM model utilizes the forward correlation information between the data

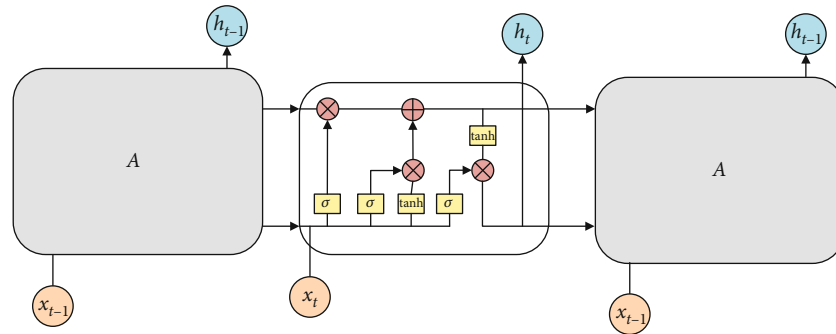


FIGURE 4: Repetitive module structures in LSTM.

at the time before and after the time series. Also, the reverse correlation information of the time before and after is considered. Therefore, it shows superior performance in the classification of time series. In this paper, Bi-LSTM model is selected as the training model.

**2.4. The Emotional Calculation Method of Improve SPCA-LSTM.** The overall framework of the improved SPCA-LSTM emotion calculation method proposed in this paper is shown in Figure 5.

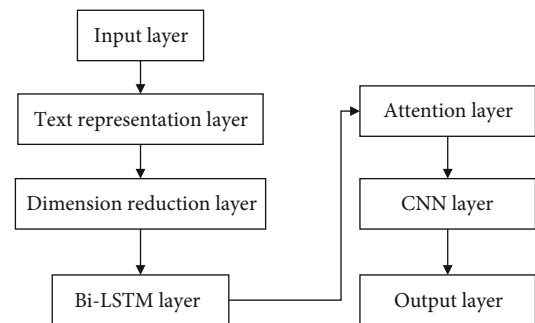


FIGURE 5: The emotional calculation method of improve SPCA-LSTM.

- (1) Input layer: emotional text data of rural tourists
- (2) Text representation layer: it is to embed the words formed by combining Word2vec with TF-IDF-ICP algorithm for vector representation
- (3) Dimension reduction layer: the word vector is reduced in dimension by using the reweighted SPCA algorithm, which is used to reduce the dimension of the dataset. Dimension reduction vector is used as the input of depth model
- (4) Bi-LSTM layer: Bi-LSTM extracts the context semantics of text. Unidirectional LSTM generally captures the past state information and calculates the output of the current time. However, in many problems, the output of the current moment is related not only to past information but also to future information. Therefore, Bi-LSTM structure needs to be used. Bi-LSTM consists of two reverse lstms. The output at each time is determined by the forward output and the reverse output
- (5) Attention layer: the attention network calculates the attention weight of each word and focuses the output features of Bi-LSTM network on the information that is more important for the current task
- (6) CNN layer: put the output feature vectors into convolutional neural network to further extract local features through convolution and pooling operations, in which the convolution kernel is set to several different sizes to extract local features with different granularity
- (7) Output layer: text feature vectors obtained by convolutional neural network layer are classified by softmax function

### 3. Experimental Results and Analysis

**3.1. Experimental Environment and Dataset.** The experimental environment of this paper is Tensorflow2.0 and python3.6. The compilation platform is 64-bit Spider. The hardware environment uses 8 core CPU, 8 G of memory, and NVIDIA (R)GTX (R)1080TI graphics card. Toolkits used include jieba, Scikitlearn, numpy, and gensim. The dataset is the rural tourism comment data captured from the Internet as the dataset of this paper. Among them, there are 6322 positive emotion samples and 1444 negative emotion samples, totaling 7766 samples. 80% of the data was used as training set and 20% as test set. The training set was iterated for 20 times, and the accuracy and loss function values were predicted during the training.

**3.2. Experimental Parameters.** The settings of model parameters in this paper are listed in Table 1 and Table 2.

**3.3. Experimental Results and Comparison.** Firstly, in order to verify the performance of emotion calculation method based on deep neural network proposed in this paper, the text method is compared with emotion calculation method based on emotion dictionary and emotion calculation method based on machine learning. Specific comparison methods are based on emotion dictionary ER (emotion-rules), machine learning SVM (support vector machines), and machine learning NBC (naive Bayesian classifier). The test results of the emotional model are shown in Table 3.

TABLE 1: Setting of word vector training parameters.

Superparameter	Parameter description	Settings
Embedding_size	Word vector dimension	100
Seq Length	Fixed sentence length	600
Num_classes	Number of label categories	10
Vocab_size	Vocabulary	8000
Window	Maximum distance between the current word and the predicted word	5
Min_count	Word frequency	1
Workers	Parallelism number of training	6

TABLE 2: Parameters of deep learning model.

Superparameter	Parameter description	Settings
Num_filters	Number of convolution kernels	128
Filter_sizes	Different convolution kernels	2, 3, 4
Atten_size	Attention layer size	50
Keep_prob	The probability that the neuron is retained	0.5
Learning rate	Learning rate	$1 * 10^{-3}$
Lr_decay	Learning decay rate	0.9
L2 reg lambda	Regularization coefficient	0.01
Batch_size	Training size per batch	64
Hidden_dim	Hidden layer dimension	128
Activation function	Nonlinear function	ReLU

From Table 3, the tourist sentiment calculation method based on machine learning is better than that based on sentiment dictionary. The reason is that machine learning uses statistical methods to extract feature items from text data, and its nonlinear characteristics improve the reliability and accuracy of emotion calculation. In the machine learning method, NBC is better than SVM in all evaluation indexes. And the effect on training set and test set is relatively stable. The reason is that NBC, as a classic classification model in machine learning, has a solid mathematical foundation and stable classification efficiency.

Compared with ER, SVM, and NBC, the accuracy, recall, and *F1* values of the improved SPCA-LSTM algorithm in this paper are greatly improved. The main reason is that Bi-LSTM model with attention mechanism is intelligent in text data feature extraction and learning methods. Deep learning relies on big data and many parameters to automatically fit nonlinear prediction functions, emphasizing the depth of model structure and highlighting the importance of feature learning. At the same time, the feature representation of samples in the original space is transformed into a new feature space by feature transformation layer by layer. Compared with the method of artificial feature construction by machine learning, the algorithm model in this paper fully embodies its advantages of big data.

In addition, word2vec uses high-dimensional vectors to convert words into real vectors and accurately retain their

TABLE 3: Test results of emotion calculation models with different methods.

Evaluation model	Accuracy	Precision	Recall	<i>F1</i>
Emotion dictionary ER	81.0	87.1	73.4	79.6
Machine learning SVM	73.0	76.5	91.6	83.3
Machine learning NBC	83.6	90.2	90.8	90.4
Proposed model	97.4	97.8	97.2	97.5

semantic information. Then, reweighted SPCA is used to reduce the vector dimension and reduce the computation of the deep learning model. The deep learning model not only gives full play to the strong processing ability of deep learning for high-dimensional data but also preserves the good timing of tourism text data. Therefore, the proposed model achieves better results than those based on emotion dictionary and machine learning.

In order to verify the effectiveness of this algorithm, this paper selects several deep learning models for comparison.

- (1) CNN: TextCNN model uses Word2vec model to train word vector as word embedding layer
- (2) LSTM: a network text classification model based on one-way long-short-term memory
- (3) RNN+ Attention: a text classification model based on long-short-term memory based on attention mechanism
- (4) BBGA: Bert model is used to train word vectors as word embedding layer, and Bi-GRU and attention mechanism are used to extract features
- (5) MLCNN: a text classification model combining convolutional neural network and long-short-term memory network
- (6) CTMWT: a convolutional neural network text classification model based on Word2vec and improved TF-IDF
- (7) BGRU-CNN: text classification model based on recurrent neural network variant and convolutional neural network

The experimental results of each model are shown in Table 4.

The accuracy of this model is 5.44% higher than that of the traditional convolutional neural network. The precision rate is 5.0% higher. The recall rate is 5.49% higher. The *F1* value is 5.19% higher. The highest accuracy rate of other text classification models is 96.7%. The highest precision rate is 96.5%. The highest recall rate is 96.6%. The highest *F1* value is 96.6%. The accuracy of this classification model is 0.65% higher. The precision rate is 1.4% higher. The recall rate is 0.59% higher. The *F1* value is 0.89% higher. Experimental data show the superiority of this method.

TABLE 4: Comparison of experimental results of each model.

Evaluation model	Accuracy	Precision	Recall	F1
CNN	92.1	92.9	91.7	92.3
LSTM	90.1	88.0	90.2	89.0
RNN + attention	93.4	93.2	93.3	93.3
BBGA	94.9	94.7	94.7	94.7
MLCNN	96.7	96.5	96.6	96.6
CTMWT	96.2	96.1	96.4	96.2
BGRU-CNN	95.2	94.3	94.5	94.4
ABLNN+TFIDF	95.2	94.1	94.9	94.5
Proposed model	97.4	97.9	97.2	97.5

#### 4. Conclusion

The results of big data analysis of rural tourism are introduced into the development planning of rural tourism, which will provide extremely beneficial strategic guidance for the realization of rural revitalization strategy. In order to realize the big data analysis of rural tourism, this paper proposes a rural tourism sentiment calculation method based on the improved SPCA-LSTM algorithm, which uses the improved TF-IDF+ Word2vec model to represent rural tourism data in vector. Vector dimension is reduced by reweighted SPCA. Then, Bi-LSTM model with attention mechanism is used to extract text features. Finally, SoftMax function is put into practice to calculate the emotion of rural tourists. The experiment demonstrates that the proposed algorithm is feasible and effective for sentiment analysis of rural tourists. In the next step, this paper can consider the construction of tourism-specific emotion dictionary and combine tourism-specific emotion dictionary with machine learning and deep learning methods to study tourist emotion computing.

#### Data Availability

The labeled dataset used to support the findings of this study are available from the corresponding author upon request.

#### Conflicts of Interest

The author declares no competing interests.

#### Acknowledgments

This work was supported in part by the Heilongjiang Art and Science Planning Project “Research on the Integrated Development of Music Culture and Tourism Industry in Heilongjiang Province” (No. 2021B009).

#### References

- [1] J. Yang, R. Yang, M. H. Chen, C. H. (. J.). Su, Y. Zhi, and J. Xi, “Effects of rural revitalization on rural tourism,” *Journal of Hospitality and Tourism Management*, vol. 47, pp. 35–45, 2021.
- [2] Y. Liu, Y. Zang, and Y. Yang, “China’s rural revitalization and development: theory, technology, and management,” *Journal of Geographical Sciences*, vol. 30, no. 12, pp. 1923–1942, 2020.
- [3] W. T. Fang, *Rural Tourism[M]//Tourism in Emerging Economies*, Springer, Singapore, 2020.
- [4] J. M. G. Martínez, J. M. M. Martín, J. A. S. Fernández, and H. Mogorrón-Guerrero, “An analysis of the stability of rural tourism as a desired condition for sustainable tourism,” *Journal of Business Research*, vol. 100, pp. 165–174, 2019.
- [5] H. Zhu and F. Deng, “How to influence rural tourism intention by risk knowledge during COVID-19 containment in China: mediating role of risk perception and attitude,” *International Journal of Environmental Research and Public Health*, vol. 17, no. 10, p. 3514, 2020.
- [6] C. Martínez-Hernández, C. Mínguez, and C. Yubero, “Archaeological sites as peripheral destinations. Exploring big data on fieldtrips for an upcoming response to the tourism crisis after the pandemic,” *Heritage*, vol. 4, no. 4, pp. 3098–3112, 2021.
- [7] X. Zhang, L. Yu, M. Wang, and W. Gao, “Fm-based: algorithm research on rural tourism recommendation combining seasonal and distribution features,” *Pattern Recognition Letters*, vol. 150, pp. 297–305, 2021.
- [8] M. A. Tian and X. I. E. Yanjun, “The study of emotion in tourist experience: current research progress,” *Tourism and Hospitality Prospects*, vol. 3, no. 2, pp. 82–101, 2019.
- [9] J. C. Cuizon and C. G. Agravante, “Sentiment analysis for review rating prediction in a travel journal,” in *Proceedings of the 4th International Conference on Natural Language Processing and Information Retrieval*, pp. 70–74, Seoul, Republic of Korea: ACM, 2020.
- [10] G. Gupta and P. Gupta, “Twitter mining for sentiment analysis in tourism industry,” in *2019 Third World Conference on Smart Trends in Systems Security and Sustainability (WorldS4)*, pp. 302–306, London, UK, 2019.
- [11] C. Song, X. K. Wang, P. Cheng, J. Q. Wang, and L. Li, “SACPC: a framework based on probabilistic linguistic terms for short text sentiment analysis,” *Knowledge-Based Systems*, vol. 194, p. 105572, 2020.
- [12] G. Xu, Z. Yu, H. Yao, F. Li, Y. Meng, and X. Wu, “Chinese text sentiment analysis based on extended sentiment dictionary,” *IEEE Access*, vol. 7, pp. 43749–43762, 2019.
- [13] L. Chen and S. Tang, “Physical-layer security on mobile edge computing for emerging cyber physical systems,” *Computer Communications*, vol. PP, no. 99, pp. 1–12, 2022.
- [14] L. Yang, Y. Li, J. Wang, and R. S. Sherratt, “Sentiment analysis for E-commerce product reviews in Chinese based on sentiment lexicon and deep learning,” *IEEE Access*, vol. 8, pp. 23522–23530, 2020.
- [15] F. Huang, X. Zhang, Z. Zhao, J. Xu, and Z. Li, “Image-text sentiment analysis via deep multimodal attentive fusion,” *Knowledge-Based Systems*, vol. 167, pp. 26–37, 2019.
- [16] J. Lu and M. Tang, “Analytical offloading design for mobile edge computing based smart internet of vehicle,” *EURASIP Journal on Advances in Signal Processing*, vol. PP, 10 pages, 2022.

## Research Article

# A Machine-Assisted Gaze Analysis Method for Students' Psychological Evaluation

Huiling Wang <sup>1</sup> and Yafei Shan <sup>2</sup>

<sup>1</sup>School of Education Science, Henan Vocational University of Science and Technology, Zhoukou 466000, China

<sup>2</sup>Student Affairs Department, Zhoukou Normal University, Zhoukou 466001, China

Correspondence should be addressed to Yafei Shan; 20182028@zkn.edu.cn

Received 6 January 2022; Revised 26 January 2022; Accepted 5 February 2022; Published 21 February 2022

Academic Editor: Wen Zeng

Copyright © 2022 Huiling Wang and Yafei Shan. This is an open access article distributed under the Creative Commons Attribution License, which permits unrestricted use, distribution, and reproduction in any medium, provided the original work is properly cited.

This article combines machine intelligence-assisted gaze analysis to construct a student psychological evaluation system, which provides a basis for solving student psychological evaluation methods. At the same time, by recognizing students' behavioral characteristics and then their psychological characteristics, a PC-side application with multiple functions such as human-computer interaction, user data management, and physiological data display and storage has been developed. In addition, this article constructs an intelligent system structure to evaluate students' psychology through expert diagnosis. Finally, this article evaluates the students' psychology through the system and at the same time uses the comparative test method to evaluate the system. Experimental research shows that the student psychological evaluation system based on machine intelligence-assisted gaze analysis proposed in this paper is very close to the expert diagnosis result of student psychological evaluation.

## 1. Introduction

Educational evaluation can be classified according to different criteria. According to the content of the evaluation, it is divided into condition evaluation, process evaluation, and result evaluation. Moreover, according to the evaluation criteria, it is divided into relative evaluation, absolute evaluation, and intraindividual difference evaluation. According to the subjects participating in the assessment, it is divided into self-assessment and others' assessment. In addition, according to the time and role of evaluation, it is divided into diagnostic evaluation, formative evaluation, and summative evaluation. Finally, according to the method of evaluation, it is divided into quantitative evaluation and qualitative evaluation. Most scholars divide social work evaluation into two basic types: formative evaluation and cumulative evaluation. The former refers to those methods that provide information about project activities [1]. The provision of this type of information can theoretically help the organization develop and improve the project. The latter is to examine the situation in which the project accomplishes

its goals. This type of information is very useful for funding agencies to decide whether to reopen the project or continue to allocate funds to the project. The initial cumulative evaluation may later be transformed into a formative goal, which is used to help the project improve, rather than to summarize the results achieved or no results. The other two concepts are process evaluation and result evaluation. Among them, the process evaluation occurs in the project in the operation stage, and the result evaluation involves the project's results to the client and the community [2].

College students are the successors of the country's future career development, and they are at a critical transition stage from adolescence to adulthood. At this time, their outlook on life, world outlook, and values gradually stabilized, and at the same time, they are in a relatively critical transitional stage. At this stage, college students grow up quickly and start a relatively independent life. Interpersonal relationships with parents, teachers, and peers need to be handled properly, and they are in a stage of high incidence of psychological conflicts. On the one hand, college students are required to have a healthy body, and on the other hand,

they also need to have a good psychological quality to face the pressures of all aspects of society. This makes paying attention to the mental health of college students an indispensable link in higher education [3].

At present, the methods of mental quality assessment include homework method, projection method, and questionnaire method. The homework method is to allow the testee to perform the actual operation, and then, the tester will make a qualitative psychological quality assessment based on his performance in the homework. This method can solve the problem of subject evaluation due to educational and cultural factors, but this method depends on the cognitive level of the tester, and the evaluation results of different testers are quite different and too subjective. The projection method is to respond to ambiguous images, ink stains, or sentences. Subjects are asked to answer freely according to their own understanding and feelings and to understand the subject's internal language and psychological characteristics. This method is the same as the homework method and is not fixed and accurate. Based on the evaluation basis, the individual's psychological quality cannot be accurately evaluated.

This article combines machine intelligence-assisted gaze analysis to construct a student psychological evaluation system and conducts research on the psychological evaluation of college students to improve the effect of college student psychological evaluation.

## 2. Related Work

The standard of mental health is an important basis for evaluating mental health, and it is an evaluative index for connotation and definition. At the same time, mental health evaluation standards are mostly defined around the concept and connotation of mental health [4]. Literature [5] regards mental health as a mental state in terms of emotion, intelligence, and social adaptation, including emotional stability, keen wisdom, and good social adaptation. The mental health standards in the literature [6] are emotional health, personality health, good social adaptation, and harmonious interpersonal relationships. Literature [7] puts forward 6 criteria for mental health: striving for self-growth, treating oneself objectively, unity of outlook on life, establishing harmonious interpersonal relationships, acquiring knowledge and skills necessary for life, and loving life and having empathy. The 6 criteria of mental health proposed in the literature [8] are as follows: positive self-evaluation, moderate control and sense of dominance, realistic optimism, ability to care for others, ability to be happy and satisfying, and ability to be enthusiastic about constructive and creative work. Literature [9] believes that mental health includes six abilities, which are self-knowledge, self-realization, personality integration, autonomy, reality testing, and environmental control. The literature [10] believes that mentally healthy people often have 7 characteristics, which are generally reasonable, have a sense of self-growth, have the ability to love, have good intimacy, adapt to reality, work well, and have the ability to have a better life. Literature [11] puts forward 10 criteria for mental health: adequate self-safety, understand-

ing of one's own abilities, goals are in line with reality, not divorced from society, healthy personality, able to learn from experience, good interpersonal relationships, control one's emotions, give full play to one's own personality, and meet personal needs. Literature [12] believes that a mentally healthy person, that is, a mature person, should possess 15 abilities and characteristics including self-sense, independence, dependence, adaptation, reality testing, the ability to love and be loved, and the ability to control emotions. The literature [13] summarized the evaluation criteria of mental health into four aspects: self-knowledge and self-attitude, interpersonal attitude and social skills, enthusiasm for life and the ability to solve problems effectively, and the internal coordination of personality structure. Literature [14] proposes that the standards of mental health include love of work, good interpersonal relationships, understanding of oneself, and acceptance of the external environment. Literature [15] believes that mentally healthy people should pay attention to self-exploration and discovery, improve self-values and self-esteem, have ideals closely integrated with reality, and be down-to-earth. Literature [16] proposes that three criteria can be used as the basis for judging mental health. One is statistical criteria, which compares individual behavior scores with the average state of the numerical distribution of normal behavior; the other is sociological criteria, which compares individual. The behavior is compared with social norms; the third is medical standards, whether there are mental illnesses. Based on the above standards, it is not difficult to find that the formulation of mental health standards is an extremely comprehensive and complex issue. Combining different standards at home and abroad, the author sums up three levels of mental health standards: first, the physical and mental level, including physical health, no mental illness, able to fully understand self, balance internal psychological conflicts, good at learning and sharing, and having a healthy personality; the second is the level of interpersonal relationships, with good interpersonal interaction, positively accepting others, and being able to get a sense of happiness in communication; the third is at the social level, with good social adaptability, able to actively participate in work, and realize their own value. Comprehensive consideration of these aspects will help to clarify many problems of mental health, so as to play a certain enlightenment role for follow-up related research.

After the mathematical model is established, certain results can be derived through logical reasoning or mathematical operations. If a certain explanation is given to the model, the result can be regarded as a certain prediction of the empirical system [17]. The predicted value is further compared with the actual test value, and the mathematical model can be revised according to the degree of agreement between the two. The advantage of using mathematical models to describe psychological phenomena is not only that it has greater generality, accuracy, deductive power, and predictive power than natural language descriptions, but more importantly, it is convenient for computer simulations and creates for the development of artificial intelligence. Condition: psychological statistics is a branch of applied statistics that studies how to collect, sort, and analyze digital data in





FIGURE 1: Three-dimensional model of intelligent auxiliary gaze analysis platform.

psychological experiments or investigations and how to make scientific inferences based on the information conveyed by these data [18]. Psychological statistics is one of the effective tools for psychological research. The history of the development of psychology proves that scientific psychology is inseparable from scientific experiments or investigations, and psychological experiments or investigations must face the problem of processing digital data. For example: how to collect data to make the numbers most meaningful and reflect the research topics; what methods are used to organize and analyze the data to maximize the information reflected by these data, so as to make a scientific analysis of the results of experiments or investigations. Explain: how can we infer from the partial results obtained to the overall, make general scientific conclusions, and so on. To solve these problems, we must rely on scientific statistical methods [19].

### 3. Machine Intelligence-Assisted Gaze Analysis

The prototype of the machine intelligence auxiliary gaze analysis platform used in this topic is shown in Figure 1. The main intelligent auxiliary platform is composed of a fixed platform, a motion platform, and six motion branches of the same UPU. The 6 UPU branch chains are used as the drive input of the mechanism, and the length of each branch is changed by the expansion and contraction of the electric cylinder to control the pose of the platform. Both the fixed platform and the moving platform are connected to the two ends of each electric cylinder through a Hooke hinge, thus forming a six-degree-of-freedom platform.

The degree of freedom of the intelligent auxiliary platform is calculated:

$$F = 6(n - g - 1) + \sum_{i=1}^g f_i. \quad (1)$$

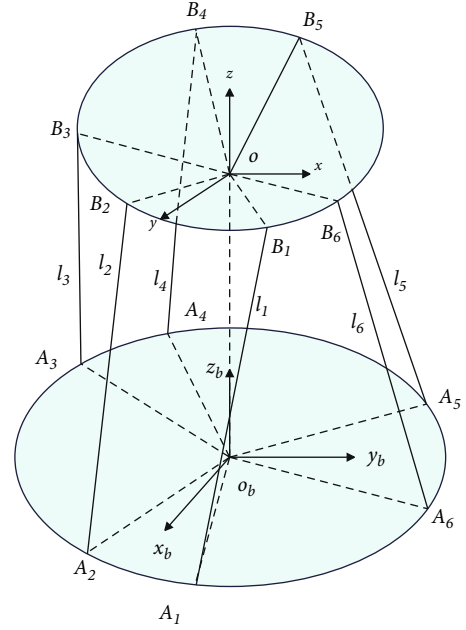


FIGURE 2: The coordinate system of the intelligent auxiliary platform.

TABLE 1: The actual values of the geometric parameters of the prototype (unit: mm).

$R_1$	$R_2$	$h$	$h_1$
800.0	800.0	1000.0	380.0

In the formula,  $n$  is the number of components,  $g$  is the number of motion pairs, and  $f_i$  is the number of degrees of freedom of each motion pair,  $i = 1, 2, \dots, n$ . It can be seen from Figure 1 that the total number of components of the platform is  $n = 14$ , and the number of kinematic pairs is  $g = 18$ , where each drive branch chain kinematic joint is composed of Hooke hinges ( $f = 2$ ) and moving joints ( $f = 1$ ). Substituting it into formula (1), the degree of freedom of the platform can be calculated as 6.

In order to describe the pose of the intelligent auxiliary platform, this paper establishes a spatial rectangular coordinate system, including a fixed coordinate system  $O_b - x_b y_b z_b$  and a moving coordinate system  $O - xyz$ , as shown in Figure 2. Among them, the lower platform is a fixed platform, the upper platform is a moving platform, the Hooke hinge joints of the branch chain connected with the fixed platform and the moving platform are, respectively, denoted as  $A_i, B_i$  ( $i = 1, 2, \dots, 6$ ), and the driving branch chain is denoted by  $f$ . The two coordinate systems are described below [20].

- (1) Inertial coordinate system  $O_b - x_b y_b z_b$  (denoted as  $P$ ): the coordinate origin  $O_b$  is located at the geometric center of the fixed platform, the  $x_b$  axis is perpendicular to the line  $A_1 A_6$ , the  $z_b$  axis is perpendicular to the plane determined by the hinge point  $A_1, A_2, \dots, A_6$ , and the  $y_b$  axis can be determined by the right-hand rule

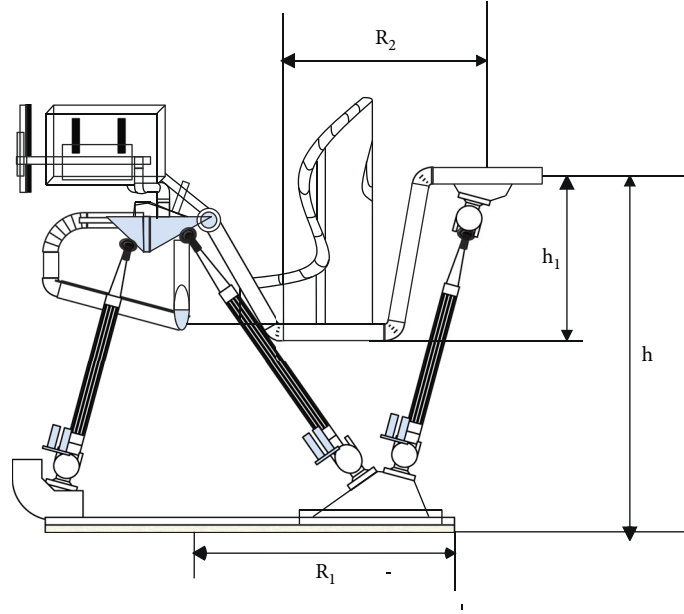


FIGURE 3: Schematic diagram of platform geometric parameters.

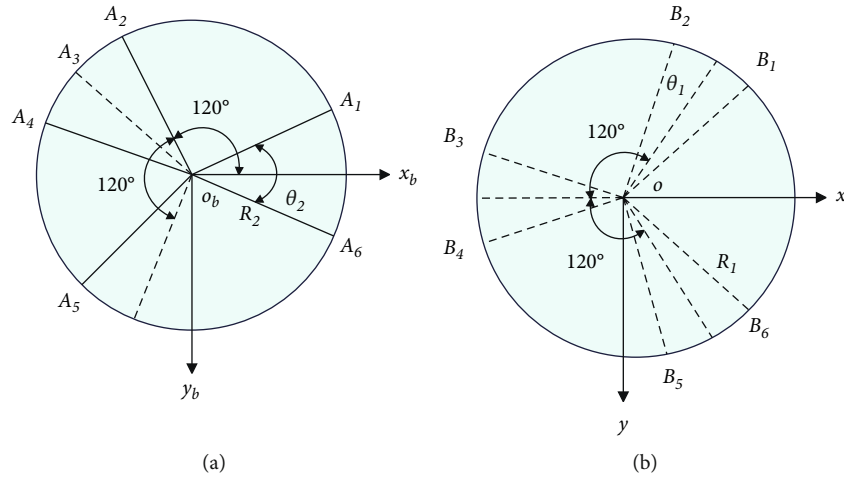


FIGURE 4: Plan view of coordinate system. (a) Coordinate diagram of the fixed platform plan. (b) Coordinate diagram of the dynamic platform plan.

- (2) The moving coordinate system, that is, the upper platform body coordinate system  $O-xyz$  (denoted as  $M$ ): the coordinate origin  $O$  is located at  $h_1$  below the circle where  $B_1, B_2, \dots, B_6$  is located, and this position is the geometric center of the upper platform, the  $x$ -axis is perpendicular to the line  $B_1B_6$ , the  $y$ -axis is perpendicular to the plane determined by  $B_1, B_2, \dots, B_6$  and the plane is straight up, and the  $z$ -axis is determined by the right-hand rule

The geometric parameters of the platform structure are shown in Table 1. Among them,  $R_1$  is the radius of the fixed platform,  $R_2$  is the radius of the circle (circle  $O'_2$ ) where  $B_1, B_2, \dots, B_6$  is located,  $h$  is the distance between the center of the fixed platform and the center of the motion platform,  $h_1$  is the distance between the circle  $O'_2$

and the geometric center of the motion platform, and the geometric meaning of each parameter can be seen in Figure 3.

It can be seen from Figure 3 that there is a vector equation for each branch.

$$\mathbf{A}_i\mathbf{B}_i = \mathbf{O}_1\mathbf{O}_2 + \mathbf{O}_2\mathbf{B}_i - \mathbf{O}_1\mathbf{A}_i \quad (i = 1, 2, \dots, 6). \quad (2)$$

$A_i$  in the fixed coordinate system  $O_b - x_b y_b z_b$  can be expressed as

$$A_i = [R_1 \cos \eta_i \ R_1 \sin \eta_i \ 0]^T \quad (i = 1, 2, \dots, 6). \quad (3)$$

$B_i$  in the moving coordinate system  $O-xyz$  can be expressed as

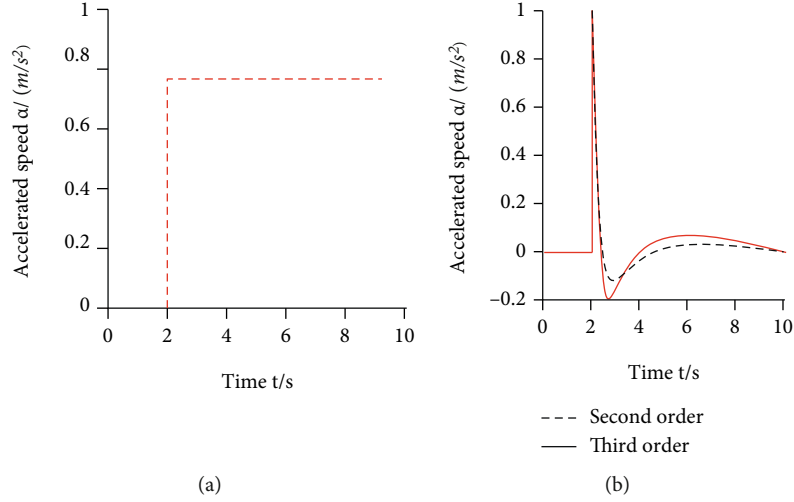


FIGURE 5: Acceleration signal output. (a) Acceleration input signal. (b) Export acceleration of the high-pass filter.

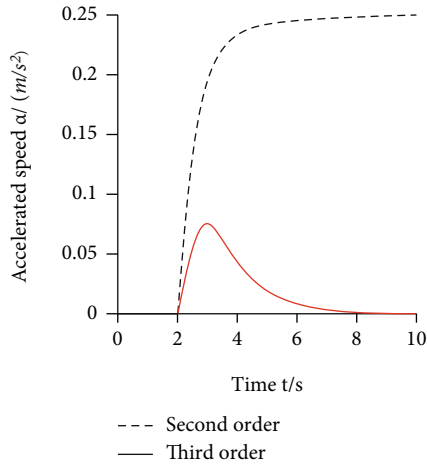


FIGURE 6: Output displacement of the high-pass filter.

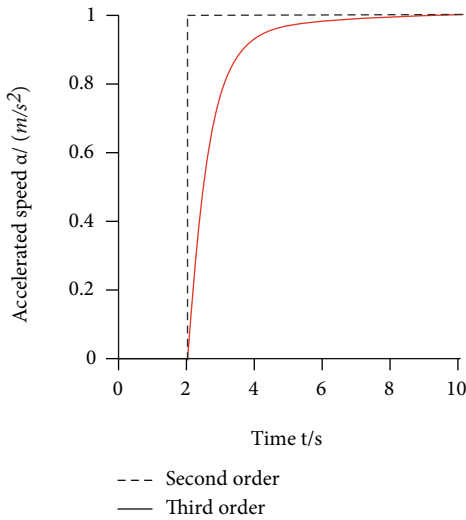


FIGURE 7: Comparison of input and output of low-pass filter.

$$B_i = [R_2 \cos \xi_i \quad R_2 \sin \xi_i \quad 0]^T (i = 1, 2, \dots, 6). \quad (4)$$

In the formula,  $\eta_i$  and  $\xi_i$  are the polar coordinate angles of the plane where each hinge point is located.

$O_b - x_b y_b z_b$  and  $O - xyz$  are projected into the plane determined by the hinge point, and the plane coordinate system is established, as shown in Figures 4(a) and 4(b).

In the plane coordinate system,  $\eta_i$  and  $\xi_i$  are expressed as

$$\begin{cases} \eta_1 = \frac{\theta_2}{2}, \eta_2 = \frac{2\pi}{3} - \frac{\theta_2}{2}, \eta_3 = \frac{2\pi}{3} + \frac{\theta_2}{2}, \\ \eta_4 = \frac{4\pi}{3} - \frac{\theta_2}{2}, \eta_5 = \frac{4\pi}{3} + \frac{\theta_2}{2}, \eta_6 = -\frac{\theta_2}{2}, \\ \xi_1 = \frac{\pi}{3} - \frac{\theta_1}{2}, \xi_2 = \frac{\pi}{3} + \frac{\theta_1}{2}, \xi_3 = \pi - \frac{\theta_1}{2}, \\ \xi_4 = \pi + \frac{\theta_1}{2}, \xi_5 = -\frac{\pi}{3} - \frac{\theta_1}{2}, \xi_6 = -\frac{\pi}{3} + \frac{\theta_1}{2}. \end{cases} \quad (5)$$

When analyzing the movement of the platform, Euler angles are generally used to describe the attitude of the moving platform in the inertial coordinate system. Initially, the initial orientation of the moving coordinate system  $M$  is parallel to the inertial coordinate system  $P$ . First, the algorithm turns  $O - xyz$  around its  $z$ -axis by angle  $\alpha$  to obtain  $O - x^{(1)}y^{(2)}z$  (denoted as  $M^{(1)}$ ) and then rotates around  $M^{(1)}$ 's  $y^{(1)}$ -axis by angle  $\beta$  to obtain  $O - x^{(2)}y^{(1)}z^{(2)}$  (denoted as  $M^{(2)}$ ), and finally, the algorithm rotates  $x^{(2)}$  around  $M^{(2)}$  by angle  $\gamma$  to get  $O - x^{(2)}y^{(3)}z^{(2)}$  (denoted as  $M^{(3)}$ ). Each rotation can be represented by a rotation coefficient matrix, and the above rotation process can be represented as

$$R = \begin{bmatrix} \text{cac}\beta & \text{cas}\beta\text{s}\gamma - \text{sac}\gamma & \text{cas}\beta\text{c}\gamma + \text{sas}\gamma \\ \text{sac}\beta & \text{sas}\beta\text{s}\gamma + \text{cac}\gamma & \text{sas}\beta\text{c}\gamma - \text{cas}\gamma \\ -\text{s}\beta & \text{c}\beta\text{s}\gamma & \text{c}\beta\text{c}\gamma \end{bmatrix}. \quad (6)$$

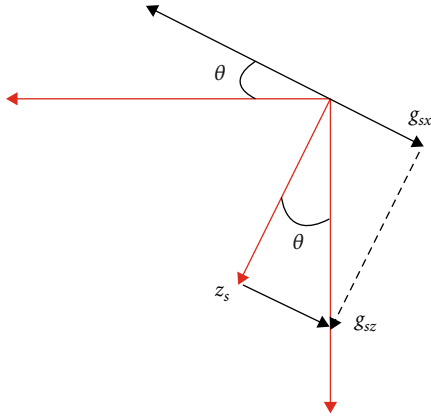


FIGURE 8: Tilt coordination.

In the formula,  $c\alpha = \cos \alpha$ ,  $s\alpha = \sin \alpha$  and others can be deduced by analogy.

The rotation transformation matrix has the following properties:

$$\begin{cases} \mathbf{R}\mathbf{R}^T = \mathbf{E}, \\ \mathbf{R}^T = \mathbf{R}^{-1}. \end{cases} \quad (7)$$

In the formula,  $\mathbf{E}$  is the identity matrix.

The position of  $\mathbf{O}_b\mathbf{B}_i$  in the inertial coordinate system  $O_b - xyz$  can be expressed as

$$\mathbf{O}_b\mathbf{B}_i = \mathbf{R}_3 + \mathbf{R}\mathbf{B}'_i (i = 1, 2, \dots, 6). \quad (8)$$

In the formula,  $\mathbf{R}_3$  is the position vector of the origin  $O$  of the dynamic coordinate system relative to  $O_b$ , that is,  $\mathbf{R}_3 = \mathbf{O}_b\mathbf{O} = [x \ y \ z]^T$ . If it is assumed that each member does not undergo elastic deformation, the inverse solution equation for the drive branch is as follows:

$$\mathbf{l}_i = \mathbf{R}_3 + \mathbf{R}\mathbf{B}'_i - \mathbf{O}_b\mathbf{A}_i (i = 1, 2, \dots, 6). \quad (9)$$

From formula (9), the inverse kinematic solution of the mechanism can be expressed as

$$l_i = |\mathbf{A}_i\mathbf{B}_i| = \sqrt{\|\mathbf{R}_3 + \mathbf{R}\mathbf{B}'_i - \mathbf{O}_b\mathbf{A}_i\|^2} (i = 1, 2, \dots, 6). \quad (10)$$

In the formula,  $l_i$  is the length of the drive branch  $\mathbf{A}_i\mathbf{B}_i$ .

The classic washout algorithm includes comparison calculation, proportional link, coordinate transformation link, acceleration high-pass filter link, acceleration low-pass filter link, angular velocity high-pass filter link, tilt coordination link, angular velocity limiting link, and various integration links. This section will design the main links.

Because students feel the movement of the real intelligent auxiliary platform through the vestibular system of the head, in order to simulate motion, it is necessary to convert the acceleration at the center of mass of the intelligent auxiliary platform into the force of the student's

head. It is necessary to calculate the specific force in the coordinate system of the intelligent auxiliary platform as

$$f_T = a_T - g_T. \quad (11)$$

In the formula,  $a_T$  is the acceleration  $n$  of the real intelligent auxiliary platform in the intelligent auxiliary platform coordinate system ( $\text{m/s}^2$ );  $g_T$  is the acceleration of gravity ( $\text{m/s}^2$ ) in the intelligent auxiliary platform coordinate system, and  $g_T = -g \cdot [\sin \theta, \cos \theta \sin \varphi, \cos \theta \cos \varphi]^T$ ,  $\theta$  and  $\varphi$  are the pitch and roll angles of the intelligent auxiliary platform, respectively.

Taking into account the limited range of motion of the intelligent auxiliary platform, a proportional link (also known as signal reduction link) is added to the washout algorithm to prevent excessive acceleration or angular velocity signals from causing the platform to exceed its range of motion. At present, the most widely used method is the cubic polynomial reduction method, and its general expression is

$$y = -0.001x^3 - 0.03x^2 + x. \quad (12)$$

Since the washout filtering algorithm filters the specific force and angular velocity signals in the inertial coordinate system, it is necessary to perform coordinate transformation on the specific force signal and angular velocity signal of the student's head calculated in the intelligent auxiliary platform coordinate system. It is converted into a signal in the inertial coordinate system, and the process can be realized by formulas (13) and (15).

$$f_2 = \mathbf{L}_s f_1. \quad (13)$$

Among them,  $f_1$  is the specific force in the coordinate system of the intelligent auxiliary platform ( $\text{m/s}^2$ );  $f_2$  is the specific force in the inertial coordinate system ( $\text{m/s}^2$ );  $\mathbf{L}_s$  is the coordinate transformation matrix, and

$$\mathbf{L}_s = \begin{bmatrix} c\theta c\psi & s\varphi s\theta c\psi - c\varphi s\psi & c\varphi s\theta c\psi + s\varphi s\psi \\ c\theta s\psi & s\varphi s\theta s\psi + c\varphi c\psi & c\varphi s\theta s\psi - s\varphi c\psi \\ -s\theta & s\varphi c\theta & c\varphi c\theta \end{bmatrix}. \quad (14)$$

In the formula,  $s\varphi = \sin \varphi$ ,  $c\varphi = \cos \varphi$  and others can be deduced by analogy.

$$\omega_2 = \mathbf{T}_s \omega_1. \quad (15)$$

Among them,  $\omega_1$  is the specific force in the coordinate system of the intelligent auxiliary platform ( $\text{rad/s}$ );  $\omega_2$  is the specific force in the inertial coordinate system ( $\text{rad/s}$ );  $\mathbf{T}_s$  is the coordinate transformation matrix, and

$$\mathbf{T}_s = \begin{bmatrix} 1 & \sin \varphi \tan \theta & \cos \varphi \tan \theta \\ 0 & \cos \varphi & -\sin \varphi \\ 0 & \sin \varphi \sec \theta & \cos \varphi \sec \theta \end{bmatrix}. \quad (16)$$

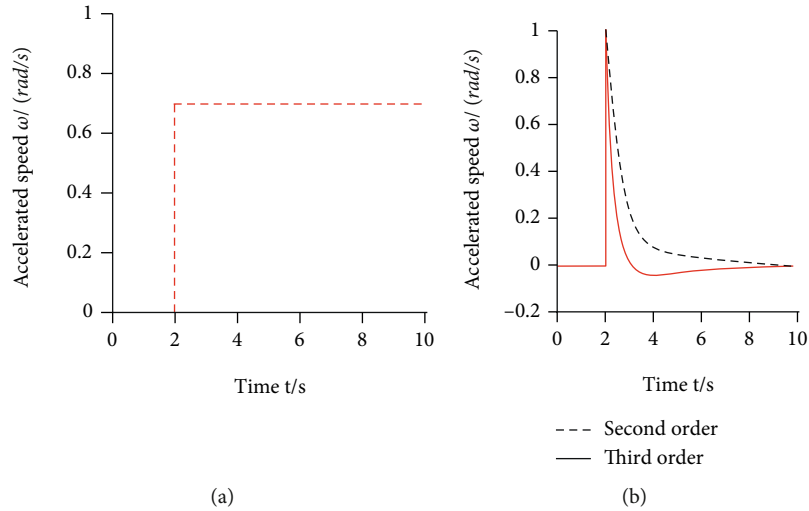


FIGURE 9: Angular velocity signal output. (a) Angular velocity input signal diagram. (b) Comparison of output angular velocity of high-pass filter.

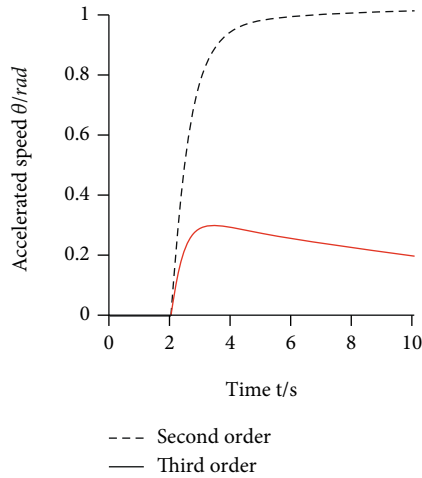


FIGURE 10: Comparison of output angles of high-pass filters.

In order to simulate sudden acceleration and ensure that the platform does not exceed its range of motion, the acceleration high-pass filter is used to filter out the low-frequency signals in the acceleration signal and retain its high-frequency components. The general form of the high-pass filter equation is

$$\frac{Y}{X} = \frac{s^n}{D(s)}. \quad (17)$$

In the formula,  $D(s) = \sum_{i=0}^n a_i s^i$ ,  $a_0 \neq 0$ .

When simulating a certain continuous acceleration, for example, the input is a unit step signal, and after a long enough time, the output displacement is

$$x_{\text{final}} = \lim_{t \rightarrow \infty} x = \lim_{s \rightarrow 0} s \left\{ \frac{1}{s} \left[ \frac{s^n}{D(s)} \frac{1}{s^2} \right] \right\} = \lim_{s \rightarrow 0} \frac{s^{n-2}}{D(s)}. \quad (18)$$

In order to ensure that the platform can return to the neutral position after simulating a certain sudden movement, that is, the high-frequency part of the acceleration,  $x_{\text{find}} = 0$  should be made. When  $n \geq 3$ , the lowest order of the high-pass filter is 3. At this time, the transfer function is

$$H(s) = \frac{s^3}{(s^2 + 2\xi_h \omega_h s + \omega_h^2)(s + \omega_m)}. \quad (19)$$

In the formula,  $\omega_h$  is the second-order natural response frequency (rad/s);  $\omega_m$  is the first-order natural response frequency of the inertial link (rad/s);  $\xi_h$  is the second-order damping ratio.

In order to test the features of the acceleration high-pass filter, the initial input is 0, and a unit step signal is given at time, as shown in Figure 5(a). This signal is input into the second-order and third-order acceleration high-pass filters, respectively, and the filtered acceleration can be obtained, as shown in Figure 5(b). The displacement can be obtained after the acceleration is integrated twice, as shown in Figure 6.

It can be seen from Figure 5(b) that the acceleration output of the two acceleration filters is not much different, and high-frequency acceleration can be obtained. However, it can be found from Figure 6 that the displacements output by the two acceleration filters are significantly different. After a long enough time, the displacement output by the second-order acceleration filter is a nonzero constant value, that is, the platform does not return to the neutral position. In this way, the platform does not have enough space for movement to simulate the next sudden movement. The displacement output by the third-order acceleration filter is finally 0, and the platform will have a sufficient range of motion to simulate the next sudden movement.

Therefore, the acceleration high-pass filters along the  $x$ ,  $y$ , and  $z$  directions all adopt a third-order structure, as shown in

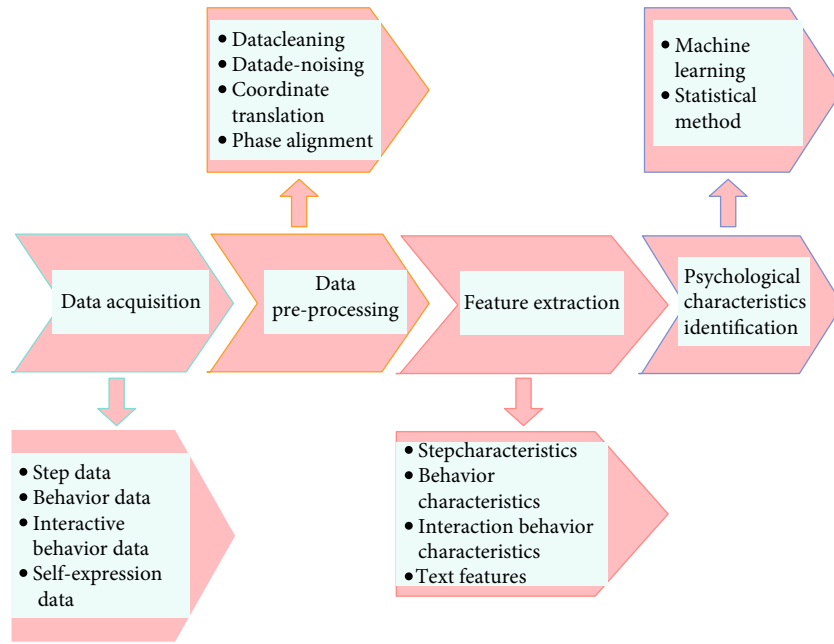


FIGURE 11: The evaluation process of students' psychological features based on machine intelligence-assisted gaze analysis.

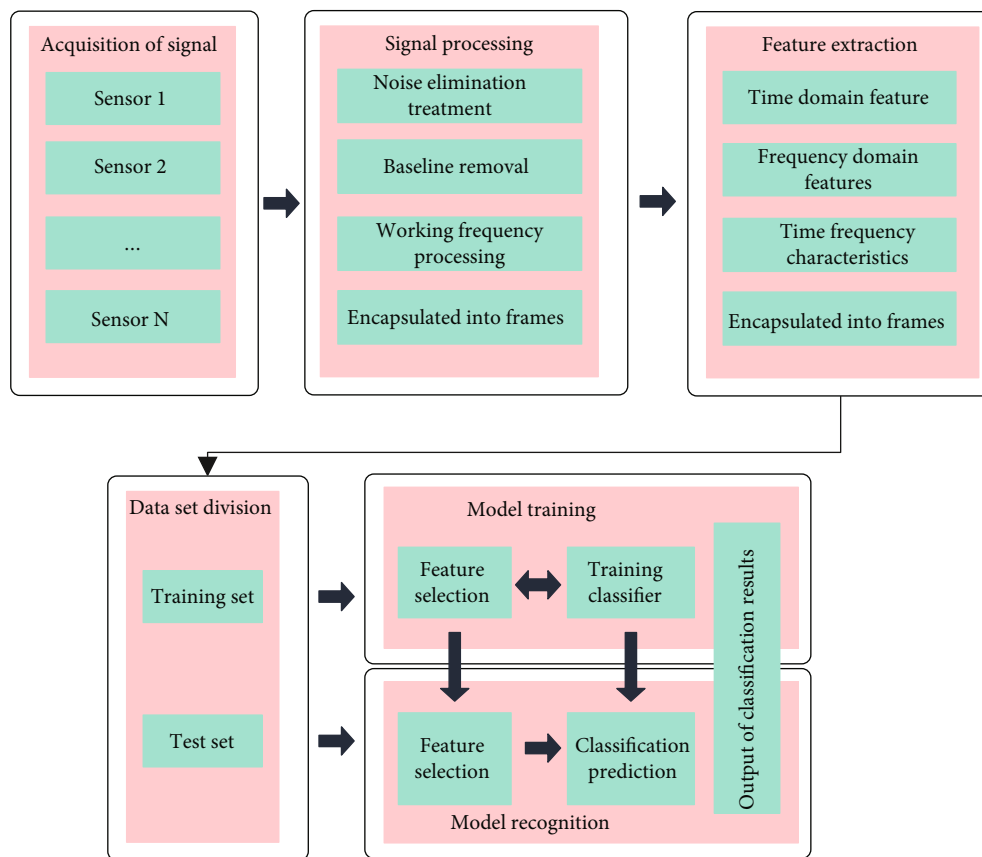


FIGURE 12: Psychological stress evaluation.

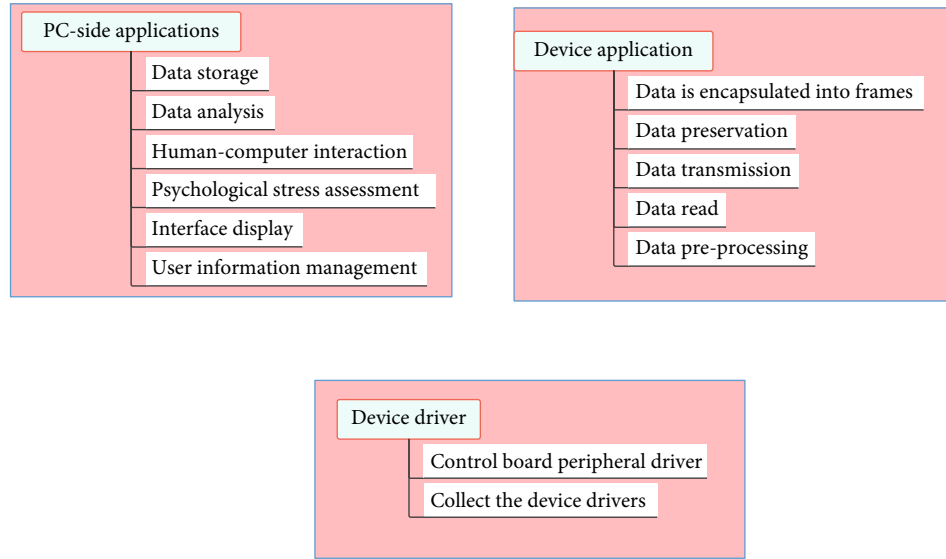


FIGURE 13: The overall software architecture of the system.

$$\begin{cases} H_x(s) = \frac{s^3}{(s^2 + 2\xi_{hx}\omega_{hx}s + \omega_{hx}^2)(s + \omega_{mx})}, \\ H_y(s) = \frac{s^3}{(s^2 + 2\xi_{hy}\omega_{hy}s + \omega_{hy}^2)(s + \omega_{my})}, \\ H_z(z) = \frac{s^3}{(s^2 + 2\xi_{hz}\omega_{hz}s + \omega_{hz}^2)(s + \omega_{mz})}. \end{cases} \quad (20)$$

In order to simulate continuous acceleration, that is, the low-frequency component in the acceleration, the platform needs to be tilted to a certain angle, and the gravity component is used to simulate the continuous acceleration felt by human otoliths. For the vertical force signal, there is no low-pass filter in this direction because the low-frequency component cannot be simulated through tilt coordination.

The low-pass acceleration channel uses a second-order low-pass filter, and the transfer function is

$$\begin{cases} H_x(s) = \frac{\omega_{lx}^2}{s^2 + 2\xi_{lx}\omega_{lx}s + \omega_{lx}^2}, \\ H_y(s) = \frac{\omega_{ly}^2}{s^2 + 2\xi_{ly}\omega_{ly}s + \omega_{ly}^2}. \end{cases} \quad (21)$$

In the formula,  $\omega_{lx}$ ,  $\omega_{ly}$  is the natural cutoff frequency of the second-order low-pass filter (rad/s);  $\xi_{lx}$ ,  $\xi_{ly}$  is the damping ratio.

In order to test the features of the acceleration low-pass filter, the initial input is 0, a unit step signal is given at 2s, and the signal is input to the low-pass filter to obtain the filtered acceleration, as shown in Figure 7. It can be found from Figure 7 that the low-frequency component of acceleration can be obtained through the second-order low-pass filter.

When the simulation platform rotates an angle, a continuous forward or backward specific force can be obtained in the corresponding direction, and the specific force is generated by the gravity component. Since the human body cannot distinguish whether the specific force is generated by acceleration or the gravity component, the specific force can simulate continuous acceleration. As shown in Figure 8, the positive  $x$  direction is the forward direction of the simulation platform, which is consistent with the >forward direction of the real intelligent auxiliary platform. The continuous specific force  $g \sin \theta$  can be obtained by rotating (pitching) the simulation platform around the  $y$ -axis. The magnitude of the specific force is related to the tilt angle.

The Euler angle for continuous acceleration is [21]

$$\begin{cases} \theta_t = \arcsin\left(\frac{f_{lx}}{g}\right), \\ \varphi_t = -\arcsin\left(\frac{f_{ly}}{g \cos \theta}\right). \end{cases} \quad (22)$$

In general, the pitch and roll angles produced by tilt coordination are very small, so formula (22) can be written in the form of

$$\begin{cases} \theta_t = \frac{f_{lx}}{g}, \\ \varphi_t = -\frac{f_{ly}}{g}. \end{cases} \quad (23)$$

When simulating continuous acceleration, the angular velocity of the simulated platform tilt should be less than the human sensory threshold in the previous section to ensure that the process is not noticed by the students, and the purpose of increasing the angular velocity limit link

TABLE 2: Comparison of the results of the student psychological evaluation system based on machine intelligence-assisted gaze and expert diagnosis.

Number	Expert diagnosis	System diagnosis	Number	Expert diagnosis	System diagnosis
1	94.97	94.28	31	76.22	75.39
2	94.90	95.34	32	76.04	78.91
3	94.75	93.92	33	75.22	72.25
4	93.96	96.73	34	74.56	72.66
5	92.89	89.99	35	73.34	76.70
6	92.40	96.84	36	72.90	76.30
7	90.77	94.82	37	72.27	70.62
8	90.53	93.71	38	71.95	73.74
9	90.10	86.45	39	71.66	75.19
10	89.82	90.48	40	71.52	73.47
11	88.75	85.78	41	71.36	74.68
12	88.23	90.67	42	70.99	70.02
13	87.81	83.99	43	70.88	73.13
14	87.56	86.00	44	70.29	72.28
15	86.43	87.21	45	69.53	68.02
16	85.82	82.01	46	69.32	66.14
17	84.31	83.84	47	69.21	70.87
18	83.74	86.15	48	68.44	69.65
19	82.56	84.11	49	66.85	69.20
20	82.55	82.50	50	64.09	64.99
21	80.76	84.00	51	63.53	61.18
22	79.82	83.56	52	63.39	60.57
23	79.48	76.28	53	62.85	60.72
24	79.32	76.13	54	62.70	62.27
25	78.43	79.20	55	62.02	59.15
26	78.05	78.69	56	61.14	63.71
27	77.84	81.33	57	59.37	59.71
28	77.74	77.57	58	59.12	60.37
29	77.13	80.01	59	58.57	58.29
30	76.50	79.92	60	58.43	56.02

comes from this. In addition, tilt coordination relies on a certain angle of tilt to generate gravity components to simulate continuous acceleration. Under normal circumstances, the acceleration of the intelligent auxiliary platform is limited, the corresponding tilt angle is not large, the vertical component of gravity will not decrease too much, and the students will not easily feel the attenuation of the vertical component of gravity. In general, the continuous acceleration simulated by the tilt coordination method cannot exceed  $4 \text{ m/s}^2$ , so the maximum tilt coordination angle cannot exceed  $25^\circ$ .

In order to simulate the situation of sudden angular velocity and to ensure that the platform does not exceed its range of motion, the angular velocity high-pass filter is used to filter out the low-frequency signal in the angular velocity signal and retain its high-frequency components. From the

previous section, we know that the general form of the high-pass filter equation is given by equation (17).

When simulating a certain continuous angular velocity, for example, the input is a unit step signal, and after a long enough time, the output angle is

$$\alpha_{\text{find}} = \lim_{t \rightarrow \infty} \alpha = \lim_{s \rightarrow 0} \left\{ \frac{1}{s} \left[ \frac{s^n}{D(s)} \frac{1}{s} \right] \right\} = \lim_{s \rightarrow 0} \frac{s^{n-1}}{D(s)}. \quad (24)$$

In order to ensure that after simulating a certain sudden movement, that is, the high-frequency part of the angular velocity, the half station can return to the neutral position,  $\alpha_{\text{final}} = 0$  should be made. When  $n \geq 2$ , the lowest order of the high-pass filter is 2. At this time, the transfer function is [22]

$$H(s) = \frac{s^2}{s^2 + 2\xi_h \omega_h s + \omega_h^2}. \quad (25)$$

In the formula,  $\omega_h$  is the second-order natural response frequency (rad/s);  $\xi_h$  is the second-order damping ratio.

In order to test the features of the angular velocity high-pass filter, the initial input is 0, and a unit step signal is given at 2 s, as shown in Figure 9(a). The signal is input into the first-order and second-order angular velocity high-pass filters, respectively, and the filtered angular velocity can be obtained, as shown in Figure 9(b). The angle can be obtained by integrating the angular velocity once, as shown in Figure 10.

It can be seen from Figure 9(b) that the angular velocities output by the two angular velocity filters are not much different, and high-frequency angular velocities can be obtained. However, it can be found from Figure 10 that the output angles of the two angular velocity filters are significantly different. After a long enough time, the output angle of the first-order angular velocity filter is a nonzero constant. In other words, the platform did not return to the median. In this way, the movement range of the platform to simulate the next sudden movement situation will be limited. Moreover, the angle output by the second-order angular velocity filter will eventually be 0, and the platform will have a sufficient range of motion to simulate the next sudden movement.

Therefore, the angular velocity high-pass filters around the  $x$ ,  $y$ , and  $z$  directions all adopt a second-order structure, as shown in

$$\begin{cases} H_x(s) = \frac{s^2}{s^2 + 2\xi_{hx} \omega_{hx} s + \omega_{hx}^2}, \\ H_y(s) = \frac{s^2}{s^2 + 2\xi_{hy} \omega_{hy} s + \omega_{hy}^2}, \\ H_z(s) = \frac{s^2}{s^2 + 2\xi_{hz} \omega_{hz} s + \omega_{hz}^2}. \end{cases} \quad (26)$$



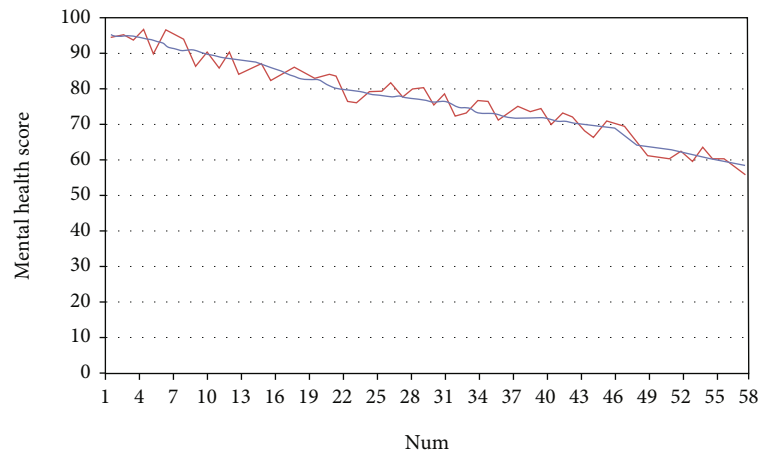


FIGURE 14: Effect analysis of student psychological evaluation system based on machine intelligence-assisted gaze.

#### 4. Psychological Evaluation of Students Based on Machine Intelligence-Assisted Gaze Analysis

The above constructs a student psychological evaluation system based on machine intelligence-assisted gaze. The system mainly recognizes students' behavior features and uses behavior features to recognize students' psychological features. Figure 11 shows the psychological feature evaluation process.

Psychological stress, also known as psychological stress, is the physical and psychological state of physical and mental tension that the human body is stimulated by internal and external environments. Considering that the characteristics of physiological signals cannot be concealed, the psychological stress state of the human body can be objectively and effectively evaluated through the physiological signals of the human body. The psychological stress assessment method of this system is shown in Figure 12, including physiological data collection, preprocessing, feature extraction, data set division, training process, evaluation process, and three types of psychological stress assessment outputs: calm, mild stress, and high pressure.

This system not only completes the design of the software and hardware of the physiological signal acquisition system but also develops a PC-side application with multiple functions such as human-computer interaction, user data management, and physiological data display and storage. The entire software part consists of three parts: device driver, device application, and PC-side application. Figure 13 is the overall software architecture of the system.

Based on the above research, this paper evaluates the student psychological evaluation system based on machine intelligence-assisted gaze built in this paper. This article evaluates students' psychology through expert diagnosis and uses the obtained standards as basic data. After that, the students' psychology is evaluated uniformly through the system of this paper, and the two sets of data are compared, and the results shown in Table 2 and Figure 14 are obtained.

From the above analysis, it can be seen that the evaluation results of student psychological evaluation system based on machine intelligence-assisted gaze proposed in this paper are relatively close to the expert diagnosis results, and the system constructed in this paper can be applied to student psychological evaluation in the future.

#### 5. Conclusion

The most commonly used scale questionnaire method for student psychological evaluation uses structured questions, which allows subjects to answer with "yes" or "no" or a limited number of choices, and scores judgments based on the answer results. The scale method is mostly a questionnaire formulated according to a specific test purpose, and at the same time, a conventional model must be established as a basis for judgment. In view of the shortcomings of the commonly used methods of psychological quality assessment in the past, especially the absolute status of the evaluation of human factors, many psychologists have devoted themselves to studying how to more objectively and accurately assess the individual's psychological quality. In order to explore a reliable method of student psychology evaluation, this paper combines machine intelligence-assisted gaze analysis to analyze student psychology. Through experimental research, it can be known that the evaluation results of the student psychological evaluation system based on machine intelligence-assisted gaze proposed in this paper are relatively close to the expert diagnosis result.

#### Data Availability

The data used to support the findings of this study are available from the corresponding author upon request.

#### Conflicts of Interest

The authors declare that they have no known competing financial interests or personal relationships that could have appeared to influence the work reported in this paper.

## Acknowledgments

This work was supported by the School of Education Science, Henan Vocational University of Science and Technology.

## References

- [1] J. Park, U. G. Kang, and Y. Lee, "Big data decision analysis of stress on adolescent mental health," *Journal of The Korea Society of Computer and Information*, vol. 22, no. 11, pp. 89–96, 2017.
- [2] J. Deckro, T. Phillips, A. Davis, A. T. Hehr, and S. Ochylski, "Big data in the veterans health administration: a nursing informatics perspective," *Journal of Nursing Scholarship*, vol. 53, no. 3, pp. 288–295, 2021.
- [3] F. F. Nastro, D. Croce, S. Schmidt, R. Basili, and F. Schultze-Lutter, "Insideout project: using big data and machine learning for prevention in psychiatry," *European Psychiatry*, vol. 64, no. S1, pp. S343–S343, 2021.
- [4] H. Jung and K. Chung, "Social mining-based clustering process for big-data integration," *Journal of Ambient Intelligence and Humanized Computing*, vol. 12, no. 1, pp. 589–600, 2021.
- [5] M. Gonçalves-Pinho, J. P. Ribeiro, and A. Freitas, "Schizophrenia related hospitalizations—a big data analysis of a national hospitalization database," *Psychiatric Quarterly*, vol. 92, no. 1, pp. 239–248, 2021.
- [6] M. Gonçalves-Pinho, J. P. Ribeiro, A. Freitas, and P. Mota, "The use of big data in psychiatry—the role of pharmacy registries," *European Psychiatry*, vol. 64, no. S1, pp. S793–S793, 2021.
- [7] M. V. Rudorfer, "Psychopharmacology in the age of "big data": the promises and limitations of electronic prescription records," *CNS Drugs*, vol. 31, no. 5, pp. 417–419, 2017.
- [8] A. B. Shatte, D. M. Hutchinson, and S. J. Teague, "Machine learning in mental health: a scoping review of methods and applications," *Psychological Medicine*, vol. 49, no. 9, pp. 1426–1448, 2019.
- [9] W. N. Price and I. G. Cohen, "Privacy in the age of medical big data," *Nature Medicine*, vol. 25, no. 1, pp. 37–43, 2019.
- [10] J. Liu, X. Zhai, and X. Liao, "Bibliometric analysis on cardiovascular disease treated by traditional Chinese medicines based on big data," *International Journal of Parallel, Emergent and Distributed Systems*, vol. 35, no. 3, pp. 323–339, 2020.
- [11] D. Wilfling, A. Hinz, and J. Steinhäuser, "Big data analysis techniques to address polypharmacy in patients—a scoping review," *BMC Family Practice*, vol. 21, no. 1, pp. 1–7, 2020.
- [12] Y. Wang, L. Kung, W. Y. C. Wang, and C. G. Cegielski, "An integrated big data analytics-enabled transformation model: application to health care," *Information & Management*, vol. 55, no. 1, pp. 64–79, 2018.
- [13] A. Hong, B. Kim, and M. Widener, "Noise and the city: leveraging crowdsourced big data to examine the spatio-temporal relationship between urban development and noise annoyance," *Environment and Planning B: Urban Analytics and City Science*, vol. 47, no. 7, pp. 1201–1218, 2020.
- [14] X. Cheng, L. Fang, X. Hong, and L. Yang, "Exploiting mobile big data: sources, features, and applications," *IEEE Network*, vol. 31, no. 1, pp. 72–79, 2017.
- [15] M. Moessner, J. Feldhege, M. Wolf, and S. Bauer, "Analyzing big data in social media: text and network analyses of an eating disorder forum," *International Journal of Eating Disorders*, vol. 51, no. 7, pp. 656–667, 2018.
- [16] J. Miller, R. Atala, D. Sarangarm et al., "Methamphetamine abuse trends in psychiatric emergency services: a retrospective analysis using big data," *Community Mental Health Journal*, vol. 56, no. 5, pp. 959–962, 2020.
- [17] M. Gonçalves-Pinho, J. P. Ribeiro, and A. Freitas, "Schizophrenia hospitalizations—a big data approach," *European Psychiatry*, vol. 64, no. S1, pp. S157–S158, 2021.
- [18] R. T. Perdue, J. Hawdon, and K. M. Thames, "Can big data predict the rise of novel drug abuse?," *Journal of Drug Issues*, vol. 48, no. 4, pp. 508–518, 2018.
- [19] S. Graham, C. Depp, E. E. Lee et al., "Artificial intelligence for mental health and mental illnesses: an overview," *Current Psychiatry Reports*, vol. 21, no. 11, pp. 1–18, 2019.
- [20] J. Popham, J. Lavoie, and N. Coomber, "Constructing a public narrative of regulations for big data and analytics: results from a community-driven discussion," *Social Science Computer Review*, vol. 38, no. 1, pp. 75–90, 2020.
- [21] P. Balthazar, P. Harri, A. Prater, and N. M. Safdar, "Protecting your patients' interests in the era of big data, artificial intelligence, and predictive analytics," *Journal of the American College of Radiology*, vol. 15, no. 3, pp. 580–586, 2018.
- [22] A. Stellbrink and E. Meisenzahl, "Big data market analysis of e-health in medical neuroscience," *European Psychiatry*, vol. 41, no. S1, pp. S39–S39, 2017.